

RECENT ADVANCES IN MOLECULAR TARGETS FOR DRUG DISCOVERY AND DELIVERY IN TUMOR

EDITED BY: Sanjun Shi, Jianxun Ding, Xianjue Chen, Jingxin Mo and
Zhi-xiang Yuan

PUBLISHED IN: Frontiers in Pharmacology and Frontiers in Oncology





frontiers

Frontiers eBook Copyright Statement

The copyright in the text of individual articles in this eBook is the property of their respective authors or their respective institutions or funders. The copyright in graphics and images within each article may be subject to copyright of other parties. In both cases this is subject to a license granted to Frontiers.

The compilation of articles constituting this eBook is the property of Frontiers.

Each article within this eBook, and the eBook itself, are published under the most recent version of the Creative Commons CC-BY licence.

The version current at the date of publication of this eBook is CC-BY 4.0. If the CC-BY licence is updated, the licence granted by Frontiers is automatically updated to the new version.

When exercising any right under the CC-BY licence, Frontiers must be attributed as the original publisher of the article or eBook, as applicable.

Authors have the responsibility of ensuring that any graphics or other materials which are the property of others may be included in the CC-BY licence, but this should be checked before relying on the CC-BY licence to reproduce those materials. Any copyright notices relating to those materials must be complied with.

Copyright and source acknowledgement notices may not be removed and must be displayed in any copy, derivative work or partial copy which includes the elements in question.

All copyright, and all rights therein, are protected by national and international copyright laws. The above represents a summary only. For further information please read Frontiers' Conditions for Website Use and Copyright Statement, and the applicable CC-BY licence.

ISSN 1664-8714

ISBN 978-2-88976-113-5

DOI 10.3389/978-2-88976-113-5

About Frontiers

Frontiers is more than just an open-access publisher of scholarly articles: it is a pioneering approach to the world of academia, radically improving the way scholarly research is managed. The grand vision of Frontiers is a world where all people have an equal opportunity to seek, share and generate knowledge. Frontiers provides immediate and permanent online open access to all its publications, but this alone is not enough to realize our grand goals.

Frontiers Journal Series

The Frontiers Journal Series is a multi-tier and interdisciplinary set of open-access, online journals, promising a paradigm shift from the current review, selection and dissemination processes in academic publishing. All Frontiers journals are driven by researchers for researchers; therefore, they constitute a service to the scholarly community. At the same time, the Frontiers Journal Series operates on a revolutionary invention, the tiered publishing system, initially addressing specific communities of scholars, and gradually climbing up to broader public understanding, thus serving the interests of the lay society, too.

Dedication to Quality

Each Frontiers article is a landmark of the highest quality, thanks to genuinely collaborative interactions between authors and review editors, who include some of the world's best academicians. Research must be certified by peers before entering a stream of knowledge that may eventually reach the public - and shape society; therefore, Frontiers only applies the most rigorous and unbiased reviews.

Frontiers revolutionizes research publishing by freely delivering the most outstanding research, evaluated with no bias from both the academic and social point of view. By applying the most advanced information technologies, Frontiers is catapulting scholarly publishing into a new generation.

What are Frontiers Research Topics?

Frontiers Research Topics are very popular trademarks of the Frontiers Journals Series: they are collections of at least ten articles, all centered on a particular subject. With their unique mix of varied contributions from Original Research to Review Articles, Frontiers Research Topics unify the most influential researchers, the latest key findings and historical advances in a hot research area! Find out more on how to host your own Frontiers Research Topic or contribute to one as an author by contacting the Frontiers Editorial Office: frontiersin.org/about/contact

RECENT ADVANCES IN MOLECULAR TARGETS FOR DRUG DISCOVERY AND DELIVERY IN TUMOR

Topic Editors:

Sanjun Shi, Chengdu University of Traditional Chinese Medicine, China

Jianxun Ding, Changchun Institute of Applied Chemistry, Chinese Academy of Sciences (CAS), China

Xianjue Chen, University of New South Wales, Australia

Jingxin Mo, University of New South Wales, Australia

Zhi-xiang Yuan, Southwest Minzu University, China

Citation: Shi, S., Ding, J., Chen, X., Mo, J., Yuan, Z. -x., eds. (2022). Recent Advances in Molecular Targets for Drug Discovery and Delivery in Tumor. Lausanne: Frontiers Media SA. doi: 10.3389/978-2-88976-113-5

Table of Contents

- 06 Research Progress and Prospect of Nanoplatforms for Treatment of Oral Cancer**
Zhilong Zhao, Dan Li, Ziqi Wu, Qihui Wang, Zhangyu Ma and Congxiao Zhang
- 21 Synthesis, Anti-Tumor Activity and Apoptosis-Inducing Effect of Novel Dimeric Keggin-Type Phosphotungstate**
Yingxue Xue, Yifei Yin, He Li, Mingyu Chi, Jiaxin Guo, Guihua Cui and Wenliang Li
- 31 Doxycycline Inhibits Cancer Stem Cell-Like Properties via PAR1/FAK/PI3K/AKT Pathway in Pancreatic Cancer**
Huijuan Liu, Honglian Tao, Hongqi Wang, Yuyan Yang, Ru Yang, Xintong Dai, Xiujuan Ding, Haidong Wu, Shuang Chen and Tao Sun
- 43 Effect of Micelle-Incorporated Cisplatin With Sizes Ranging From 8 to 40 nm for the Therapy of Lewis Lung Carcinoma**
Zhicheng Wang, Yumin Li, Tong Zhang, Hongxia Li, Zhao Yang and Cheng Wang
- 55 Schiff-Linked PEGylated Doxorubicin Prodrug Forming pH-Responsive Nanoparticles With High Drug Loading and Effective Anticancer Therapy**
Jian Song, Bingbing Xu, Hui Yao, Xiaofang Lu, Yang Tan, Bingyang Wang, Xing Wang and Zheng Yang
- 65 The Tetramethylpyrazine Derivative Statmp-151: A Novel Small Molecule Stat3 Inhibitor With Promising Activity Against Breast Cancer**
Chen Fan, Yijie Wang, Hui Huang, Wenzhen Li, Jialin Ma, Dongping Yao, Zijun Tang, Taixiong Xue, Liyang Ha, Yan Ren, Yiwen Zhang, Qin Wang, Yongmei Xie, Yi Luo, Rui Tan and Jian Gu
- 76 Molecular Targeted Agent and Immune Checkpoint Inhibitor Co-Loaded Thermosensitive Hydrogel for Synergistic Therapy of Rectal Cancer**
Huaiyu Zhang, Jiayu Zhang, Yilun Liu, Yang Jiang and Zhongmin Li
- 86 Targeting PAR2 Overcomes Gefitinib Resistance in Non-Small-Cell Lung Cancer Cells Through Inhibition of EGFR Transactivation**
Yuhong Jiang, Xin Zhuo, Xiujuan Fu, Yue Wu and Canquan Mao
- 97 Photothermal Therapy via NIR II Light Irradiation Enhances DNA Damage and Endoplasmic Reticulum Stress for Efficient Chemotherapy**
Qingduo Kong, Dengshuai Wei, Peng Xie, Bin Wang, Kunyi Yu, Xiang Kang and Yongjun Wang
- 106 Hitchhiking on Controlled-Release Drug Delivery Systems: Opportunities and Challenges for Cancer Vaccines**
Lu Han, Ke Peng, Li-Ying Qiu, Meng Li, Jing-Hua Ruan, Li-Li He and Zhi-Xiang Yuan
- 125 The Role of Tumor Inflammatory Microenvironment in Lung Cancer**
Zhaofeng Tan, Haibin Xue, Yuli Sun, Chuanlong Zhang, Yonglei Song and Yuanfu Qi

- 138 **Targeting Mutated p53 Dependency in Triple-Negative Breast Cancer Cells Through CDK7 Inhibition**
Jingyu Peng, Ming Yang, Ran Bi, Yueyuan Wang, Chunxi Wang, Xue Wei, Zhihao Zhang, Xiao Xie and Wei Wei
- 148 **Development of Store-Operated Calcium Entry-Targeted Compounds in Cancer**
Xiaojing Liang, Ningxia Zhang, Hongming Pan, Jiansheng Xie and Weidong Han
- 166 **Targeting Signaling Pathway Networks in Several Malignant Tumors: Progresses and Challenges**
Hongdan He, Xiaoni Shao, Yanan Li, Ribu Gihu, Haochen Xie, Junfu Zhou and Hengxiu Yan
- 183 **Targeting Tumor-Associated Antigen: A Promising CAR-T Therapeutic Strategy for Glioblastoma Treatment**
Guidong Zhu, Qing Zhang, Junwen Zhang and Fusheng Liu
- 194 **Systems Pharmacology–Based Dissection of Anti-Cancer Mechanism of Traditional Chinese Herb *Saussurea involucreata***
Qian Zhang, Lanyu He, Qingqing Jiang, Hongqing Zhu, Dehua Kong, Hua Zhang, Zhiqiang Cheng, Hongtao Deng, Yaxin Zheng and Xue Ying
- 210 **The Application of Inorganic Nanoparticles in Molecular Targeted Cancer Therapy: EGFR Targeting**
Meng Sun, Ting Wang, Leijiao Li, Xiangyang Li, Yutong Zhai, Jiantao Zhang and Wenliang Li
- 225 **MicroRNA as an Important Target for Anticancer Drug Development**
Zhiwen Fu, Liu Wang, Shijun Li, Fen Chen, Kathy Ka-Wai Au-Yeung and Chen Shi
- 243 **Ginsenoside Rb1 Lessens Gastric Precancerous Lesions by Interfering With β -Catenin/TCF4 Interaction**
Jinhao Zeng, Xiao Ma, Ziyi Zhao, Yu Chen, Jundong Wang, Yanwei Hao, Junrong Yu, Zhongzhen Zeng, Nianzhi Chen, Maoyuan Zhao, Jianyuan Tang and Daoyin Gong
- 256 **Small-Molecule Inhibitors Overcome Epigenetic Reprogramming for Cancer Therapy**
Wenjing Xiao, Qiaodan Zhou, Xudong Wen, Rui Wang, Ruijie Liu, Tingting Wang, Jianyou Shi, Yonghe Hu and Jun Hou
- 277 **Exosome CTLA-4 Regulates PTEN/CD44 Signal Pathway in Spleen Deficiency Internal Environment to Promote Invasion and Metastasis of Hepatocellular Carcinoma**
Yongdan Wang, Pan Li, Shuai Mao, Zhuomao Mo, Zhirui Cao, Jin Luo, Meiling Zhou, Xifeng Liu, Shijun Zhang and Ling Yu
- 290 **Tumor Microenvironment–Responsive Polypeptide Nanogels for Controlled Antitumor Drug Delivery**
Yanhong Liu, Linjiao Chen, Qingyang Shi, Qing Zhao and Hongshuang Ma
- 310 **Functional Nanomedicines for Targeted Therapy of Bladder Cancer**
Chao Tang, Heng Liu, Yanpeng Fan, Jiahao He, Fuqiu Li, Jin Wang and Yuchuan Hou

- 327** *The Inhibitory Effects of 6-Thioguanine and 6-Mercaptopurine on the USP2a Target Fatty Acid Synthase in Human Submaxillary Carcinoma Cells*
Chiao-Pei Cheng, Shu-Ting Liu, Yi-Lin Chiu, Shih-Ming Huang and Ching-Liang Ho
- 339** *From AVATAR Mice to Patients: RC48-ADC Exerted Promising Efficacy in Advanced Gastric Cancer With HER2 Expression*
Zuhua Chen, Jiajia Yuan, Yingying Xu, Cheng Zhang, Zhongwu Li, Jifang Gong, Yanyan Li, Lin Shen and Jing Gao
- 349** *Transmembrane 4 L Six Family Member 1 Suppresses Hormone Receptor--Positive, HER2-Negative Breast Cancer Cell Proliferation*
Jie Chen, Jin Zhu, Shuai-Jun Xu, Jun Zhou, Xiao-Fei Ding, Yong Liang, Guang Chen and Hong-Sheng Lu



Research Progress and Prospect of Nanoplatforms for Treatment of Oral Cancer

Zhilong Zhao^{1†}, Dan Li^{2†}, Ziqi Wu¹, Qihui Wang¹, Zhangyu Ma³ and Congxiao Zhang^{1*}

¹Department of Stomatology, The First Hospital of Jilin University, Changchun, China, ²Department of Cancer Center, The First Hospital of Jilin University, Changchun, China, ³Nanyang Medical College, Nanyang, China

OPEN ACCESS

Edited by:

Sanjun Shi,
Chengdu University of Traditional
Chinese Medicine, China

Reviewed by:

Yi Wang,
Southwest Jiaotong University, China
Jingxiao Chen,
Jiangnan University, China
Qingqing Xiong,
Tianjin Medical University Cancer
Institute and Hospital, China
Baohua Xu,
China-Japan Friendship Hospital,
China

*Correspondence:

Congxiao Zhang
zhangcongxciao@jlu.edu.cn

[†]These authors have contributed
equally to this work.

Specialty section:

This article was submitted to
Pharmacology of Anti-Cancer Drugs,
a section of the journal
Frontiers in Pharmacology

Received: 11 October 2020

Accepted: 30 November 2020

Published: 17 December 2020

Citation:

Zhao Z, Li D, Wu Z, Wang Q, Ma Z and
Zhang C (2020) Research Progress
and Prospect of Nanoplatforms for
Treatment of Oral Cancer.
Front. Pharmacol. 11:616101.
doi: 10.3389/fphar.2020.616101

Oral cancers refer to malignant tumors associated with high morbidity and mortality, and oral squamous cell carcinoma accounts for the majority of cases. It is an important part of head and neck, and oral cancer is one of the six most common cancers in the world. At present, the traditional treatment methods for oral cancer include surgery, radiation therapy, and chemotherapy. However, these methods have many disadvantages. In recent years, nanomedicine, the delivery of drugs through nanoplatforms for the treatment of cancer, has become a promising substitutive therapy. The use of nanoplatforms can reduce the degradation of the drug in the body and accurately deliver it to the tumor site. This minimizes the distribution of the drug to other organs, thereby reducing its toxicity and allowing higher drug concentration at the tumor site. This review introduces polymer nanoparticles, lipid-based nanoparticles, metal nanoparticles, hydrogels, exosomes, and dendrimers for the treatment of oral cancer, and discusses how these nanoplatforms play an anti-cancer effect. Finally, the review gives a slight outlook on the future prospects of nanoplatforms for oral cancer treatment.

Keywords: nanoplatforms, drug delivery system, oral squamous cell carcinoma, treatment of oral cancer, tumor targeted therapy

INTRODUCTION

Oral squamous cell carcinoma (OSCC) is the main type of oral cavity tumor; it is associated with a poor prognosis, and the distant survival rate is <40% (Siegel et al., 2020). The oral cavity is an important site for head and neck tumors, and oral cancer is one of the six most common types of cancer worldwide (Siegel et al., 2013). Approximately two-thirds of patients with head and neck tumors have advanced disease (stages III and IV), and the high metastasis rate is closely related to the low 5-years survival rate (Woolgar et al., 1995; Noguti et al., 2012). Despite important advancements in various treatment modalities, such as surgery, chemotherapy, and radiotherapy, the long-term survival rate of patients with advanced head and neck tumors has not increased significantly over recent decades (Price and Cohen, 2012). In 2018, 354,864 head and neck tumors were diagnosed, and 177,384 individuals worldwide died due to these tumors (Jemal et al., 2011; Bray et al., 2018). The main risk factors for OSCC are shown in **Figure 1**. Smoking and alcoholism are major risk factors (Chi et al., 2015; Li et al., 2016). Oral cancer caused by long-term use of tobacco is largely attributed to tobacco-specific nitrosamines. Alcoholic beverages may contain a variety of carcinogens and aldehydes, which can metabolize to acetaldehyde in the body (a proverbial carcinogen). Innutrition may also increase the risk of head and neck squamous cell carcinoma (HNSCC) in alcoholics. Notably, the combination of smoking and drinking shows a synergistic effect (Chi et al.,

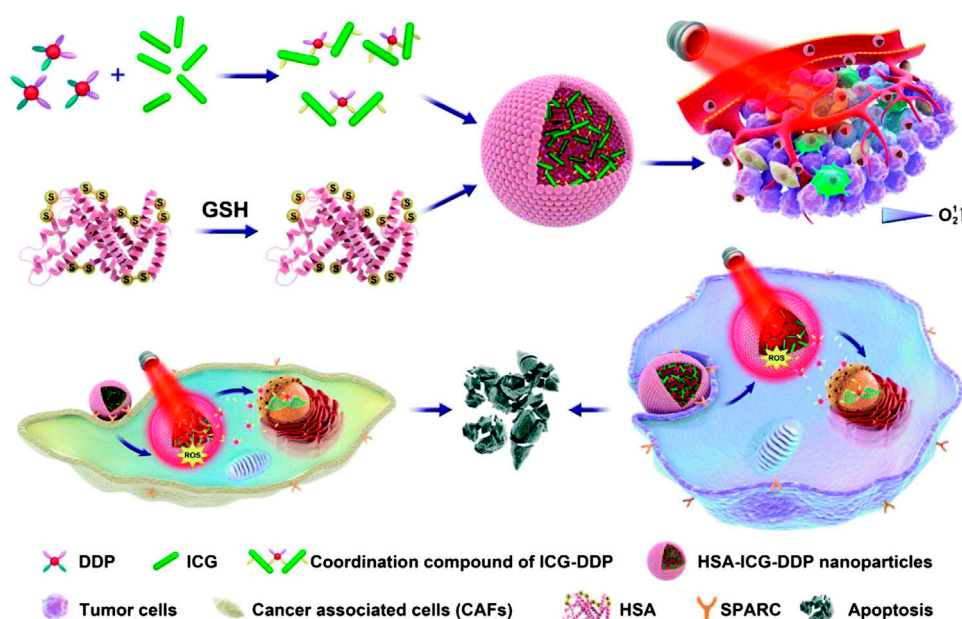


FIGURE 1 | Schematic diagram of PDT/PTT/chemotherapy combination therapy triggered by NIR light. Reproduced from (Wang et al., 2019b) with permission from Biomaterials Science.

2015). Human papillomavirus is also a prime risk factor (Huang et al., 2008). The frequency of traditional risk factors for oral cancer, including tobacco and alcohol consumption, has recently declined (Warnakulasuriya, 2009). However, the incidence of head and neck tumors associated with human papillomavirus infection has increased and continues to rise globally (Chaturvedi et al., 2011; Jemal et al., 2013). Patients with immunosuppression are at the highest risk of developing oral cancer (Petersen, 2009). Immunosuppressive drugs appear to significantly contribute to the development of skin cancer/lip cancer and oral cancer after organ transplantation. This may be the result of immunosuppression or specific carcinogenic mechanisms. Chewing betel nut is also one of the dominant risk factors for oral cancer; of note, the betel nut itself is carcinogenic (Chi et al., 2015). In current clinical practice, the main treatment methods for oral cancer are surgery, chemotherapy, and radiotherapy. However, these methods are characterized by limitations. For example, surgery may cause damage to the shape and function of the patient's head and neck, affecting their quality of life; mandibular resection damages the continuity of the mandible (Shah and Lydiatt, 1995). Radiotherapy may cause permanent xerostomia and radiation caries. Moreover, its therapeutic effect is limited by the development of radioresistance (Ishigami et al., 2007). The disadvantages of chemotherapy include non-specific biodistribution and multidrug resistance (Pérez-Herrero and Fernández-Medarde, 2015; Zhang et al., 2020a).

The current chemotherapeutic drugs used to treat oral cancer are cisplatin (DDP) (Pendleton and Grandis, 2013; Jiang et al.,

2020), fluorouracil (5-FU) (Vodenkova et al., 2020), docetaxel (Cui et al., 2020), paclitaxel (Harada et al., 2014), and methotrexate (Zhu et al., 2017). The oral route is the best approach for the administration of drugs to the body. The advantage of oral administration is that it can improve the compliance of patients and prolong the exposure time of cytotoxic drugs; hence, it is suitable for outpatients (Terwogt et al., 1999). The limitations of oral administration are its poor water solubility, low bioavailability, and high toxicity (Devalapally et al., 2007; Agüeros et al., 2009).

Nanopatform drug delivery systems were developed to overcome these problems. Nanoparticles (NPs) are solid colloidal particles composed of natural, synthetic, or semi-synthetic polymers with sizes ranging 1–1,000 nm (Kaur et al., 2004). Drugs can be dissolved, embedded, wrapped, or attached to the NP matrix, acting as a reservoir for the particle system and as a carrier for the drug delivery system, particularly in oncology (Cho et al., 2008; Couvreur, 2013; Feng et al., 2020). Currently, there are already nanopreparations for oral cancer treatment (Table 1). Compared with the traditional therapy of oral cancer, use of the nanopatform may enhance the bioavailability and biodistribution of drugs in the original tumor site, shorten the treatment duration, and improve drug selectivity, thus reducing medical costs and improving patient compliance (Lu et al., 2018). On the one hand, NPs are passively targeted to the tumor site through their enhanced permeability and retention effect. On the other hand, the modification of active targeting molecules on NPs also helps in achieving effective drug delivery, leading to an improved therapeutic effect

TABLE 1 | The current research and development status of nano-preparations for commonly used oral cancer therapeutics.

Name of drug	Mechanism of action	Marketed preparation	System	Status	References
Cisplatin	Cisplatin can cross-link with DNA, destroy the function of DNA and prevent its repair, and inhibit cell mitosis	Lipoplatin	Liposome	Phase III clinical trial	Dilruba and Kalayda (2016)
Doxorubicin	Intercalation between the base pairs of the DNA strands, thus inhibiting the synthesis of DNA and RNA in tumor cells; production of iron-mediated free radicals, causing oxidative damage to DNA, proteins and cellular membranes	Anti-EGFR immunoliposomes	Liposome	Phase II clinical trial	Mamot et al. (2012), Lee et al. (2017)
Paclitaxel	Paclitaxel promotes mitotic stagnation and cell death by combining with microtubules, accelerating microtubule assembly, and maintaining tubulin polymers unchanged	Abraxane	Polymer NP	Approved internationally	Sofias et al. (2017)
Docetaxel (DTX)	DTX induces apoptosis by promoting the polymerization of microtubules, arresting the transition from metaphase to late stage, and initiating the spindle assembly checkpoint	DTX-SPL8783	Dendrimer	Phase I clinical trial	Kesharwani and Iyer (2015)
Vincristine	Vincristine is a microtubule-destabilizing agent, which affects microtubule dynamics, inducing abnormal mitotic spindle formation and causing cell arrest in the M phase and, subsequently, cell apoptosis	Vincristine sulfate liposome injection (VSLI)	Liposome	Phase II clinical trial	Schiller et al. (2018)

(Matsumura and Maeda, 1986; Chen et al., 2017; Zhang et al., 2018; Feng et al., 2019). For example, Endo et al. studied DDP-loaded polymer NPs NC-6004. Although the inhibitory effect of DDP on tumor cell growth *in vitro* is greater than that of NC-6004, they exert almost the same inhibitory effect on tumor growth *in vivo*. In addition, unlike mice injected with NC-6004, mice treated with DDP showed severe nephrotoxicity. This situation occurs because the polyethylene glycol (PEG)ylated poly(lactic-co-glycolic acid) (PLGA) confers stealth properties to the formulation. This reduces the clearance of NC-6004 by the reticuloendothelial system, thereby prolonging the blood circulation time. The enhanced permeability and retention, as well as the prolonged blood circulation time lead to accumulation of DDP in tumor tissues. Wang et al. developed PEG-stabilized NR7 peptides and DDP-coupled PLGA NPs. NR7-PLGA NP-DDP has good characteristics, namely the targeting tumor cells, stability, high cell uptake rate, lower IC₅₀ than free DDP and PLGA NP, and an excellent apoptotic effect. Compared with non-targeted PLGA NP, targeted PLGA NP can transport more DDP to cancer cells. In short, the NR7-PLGA NP-DDP system can be used as a cell-targeting nanoplatform for the treatment of oral cancer (Wang et al., 2015). Compared with traditional chemotherapeutic drugs, those based on nanoplatforms can achieve higher intra-tumor drug concentration and lower concentration in normal tissues. This has solved numerous problems (e.g., low oral bioavailability, non-specific biological distribution, and significant toxic reactions of traditional chemotherapy), and resulted in innovative changes to the drug treatment of oral cancer (Endo et al., 2013).

In this review, we introduce the nanoplatforms used for the treatment of oral cancer, and comprehensively compare the merits and demerits of these nanoplatforms (Table 2). These nanoplatforms are usually divided into the following categories: Polymer NPs, Lipid-based NPs, Metal NP, Hydrogels, Exosomes, and Dendrimers.

RESEARCH PROGRESS IN NANOPLATFORMS FOR THE TREATMENT OF ORAL CANCER

Polymer Nanoparticles

Polymer-based NPs are submicron-sized polymer colloidal particles in which the therapeutic agent of interest can be embedded or encapsulated in their polymer matrix, or adsorbed or bound to the surface. This type of NPs can improve the efficacy, solubility, toxicity, bioavailability, and pharmacokinetic properties of drug molecules, and deliver biomolecules, drugs, genes, and vaccines to specific targets (Mahapatro and Singh, 2011). Simultaneous application of photodynamic/photothermal therapy (PDT/PTT) can also improve the accuracy of the light position and extend the duration of drug action. Hu et al. synthesized an indocyanine green (ICG)-DDP coordination compound, and encapsulated ICG-DDP into human serum albumin (HSA) to form hybrid NPs (HSA-ICG-DDP NP). Using 808 nm laser irradiation, the coordination bond of ICG and DDP in HSA-ICG-DDP NPs is thermally cleaved, and DDP of HSA-ICG-DDP NPs is released from the cytoplasm (Figure 1). Hence, DDP accumulates in specific tumor sites, reducing the non-specific distribution of platinum. In addition, the coordination bond of ICG-DDP is broken due to the photothermal effect of ICG induced by near-infrared (NIR) radiation. DDP is accurately released at the specific tumor site under 808 nm NIR irradiation, thereby prolonging its action time. Therefore, HSA-ICG-DDP NPs are promising pre-clinical drugs for the PTT/PDT chemotherapy of OSCC (Wang et al., 2019b).

The polymer nanoplatform can reduce the non-specific distribution of chemotherapeutic drugs, and provide targeted drug delivery. The targeting specificity of polymer NPs with active targeting moieties has been previously reported. Wang et al. designed a polymer self-assembled NP. Based on the comparison of the tripeptide motif and the epidermal growth

TABLE 2 | The strengths and limitations, major characteristics, and composition of the nanoplatform in the treatment of oral cancer.

Nanoplatforms	Components	Strengths	Limitations	Characteristic	References
Polymer NPs	Indocyanine green, human serum albumin, cisplatin	Chemotherapy and PTT/PDT synergistic treatment	Low encapsulation rate	Actively target oral cancer with high expression of secreted protein acidic and rich in cysteine (SPARC)	Wang et al. (2019b)
Polymer NPs	PLGA, PEG, NR7 peptide	Core-shell morphology, excellent biodegradability	Early recognition by the immune system and clearance by the liver and kidneys limit its clinical application	Due to NR7 peptide receptor-mediated internalization, cancer cells uptake of nanoparticles increased	Pendleton and Grandis (2013)
Polymer NPs	Fucoidan, PI3K α inhibitor BYL719	Combined with radiotherapy, nanoparticle administration can enhance anti-tumor activity without causing major side effects	Recognition and elimination by the immune system	The cell adhesion molecule P-selectin has nanomolar affinity for fucoidan, so nanoparticles can actively target cancer cells	Mizrachi et al. (2017)
Polymer NPs	HN-1 peptides, PEG, dox	The HNPd nanoplatform has strong tumor targeting performance and penetration efficiency	Low encapsulation rate	The PD nanoparticles synthesized by dox and PEG are a simple and effective nanocarrier	Wang et al. (2017)
NLC	Docetaxel (DTX),NLC	DTX can be well incorporated into NLC with high entrapment efficiency due to its lipophilicity	Lack of ability to actively target target cancer cells	Increase the drug loading efficiency and prolong the half-life of drug	Liu et al. (2011)
Liposome	Cationic liposome, adenoviral vector	Cationic liposomes combined with adenovirus vectors can improve gene transduction efficiency	Immune clearance and clinical application safety still need further research	Suicide gene therapy	Fukuhara et al. (2003)
Liposome	Anionic lipid, cationic lipid, cisplatin	The combined PDT + LPC prolonged the tumor growth inhibition, resulting in the minimal drug administrations	The ability of this nanoplatform to actively target tumor cells needs to be proven	Combined application of liposome-loaded chemotherapy and photodynamic therapy	Gusti-Ngurah-Putu et al. (2019)
Metal NP	Hollow gold nanospheres, aptamer targeted to EGFR	Gold nanospheres have excellent photodetection properties and can be used for imaging. Aptamers that target EGFR have high specificity and low immunogenicity	The phototherapy effect of hollow gold nanospheres is not fully utilized, and the photothermal therapy should be further explored; toxicity	Chemiluminescence optical imaging and RNA aptamer targeting EGFR	Melancon et al. (2014)
Metal NP	PEGylated AuNPs, PDPN Ab, dox	The tumor homing ligand on this nanoplatform can actively target cancer cells, deliver drugs to cancer cells, and cooperate with photothermal therapy to kill cancer cells	The early recognition of the immune system; short blood circulation and toxicity	Application of chemotherapy and photodynamic therapy	Liu et al. (2020)
Metal NP	Super paramagnetic iron oxide,PLGA, folic acid, chitosan	The nanoplatform can rapidly release docetaxel under acidic conditions and can avoid docetaxel leakage under physiological pH	The encapsulation rate of docetaxel in this nanoplatform is not clear	The magnetic iron oxide in the nanoplatform can be used in magnetic resonance imaging	Shanavas et al. (2017)
Metal NP	Polyacrylic acid, hollow mesoporous iron oxide, bleomycin	Magnetic nanoparticles are safe, non-toxic and can actively target cancer cells	The encapsulation efficiency of bleomycin in this nanoplatform is not clear; physiological pH releases more drugs than acidic pH	Surface-engineering polyacrylic acid (PAA) onto the mesoporous iron oxide makes the nanoplatform continuously release bleomycin under the magnetic field	Zhang et al. (2020b)
Hydrogels	Poly (ethylene glycol)-poly (ϵ -caprolactone)-poly (ethylene glycol) (PEG-PCL-PEG, PECE) hydrogel, cisplatin, suberoylanilide hydroxamic acid (SAHA)	The nanoplatform can be administered within a target organ at a predetermined rate and within a predetermined time, which reduces the drug poisonousness and improves the survival quality of patients	Elimination of nanoplatforms by immune cells	Temperature sensitive and injectable	Li et al. (2012)

(Continued on following page)

TABLE 2 | (Continued) The strengths and limitations, major characteristics, and composition of the nanoplatform in the treatment of oral cancer.

Nanoplatforms	Components	Strengths	Limitations	Characteristic	References
Exosomes	Exosomes secreted by menstrual mesenchymal stem cells	Exosomes are nano-sized vesicles that produce therapeutic effects through paracrine action, and have long-term blood circulation and immune escape	The exosome extraction process is complicated and the number of exosomes obtained is limited—a fact that complicates translation of exosome treatments into the clinic	Exosomes are vesicles with a diameter of 40–100 nm, which have the inherent ability to cross biological barriers, even the blood brain barrier	Rosenberger et al. (2019)
Dendrimers	Polyamidoamine (PAMAM) dendrimer, folic acid	The well-defined and highly branched structure of dendrimers provides great flexibility for modification in terms of delivery of a large payload of drug and cell-specific targeting	Large-scale synthesis of functionalized dendrimers is technically challenging and potentially hinders their clinical applications	The surface-functionalized PAMAM dendrimer of folic acid reduces generation-dependent toxicity of PAMAM dendrimer, but it is still more efficient in gene delivery	Xu et al. (2016), Yuan et al. (2019)

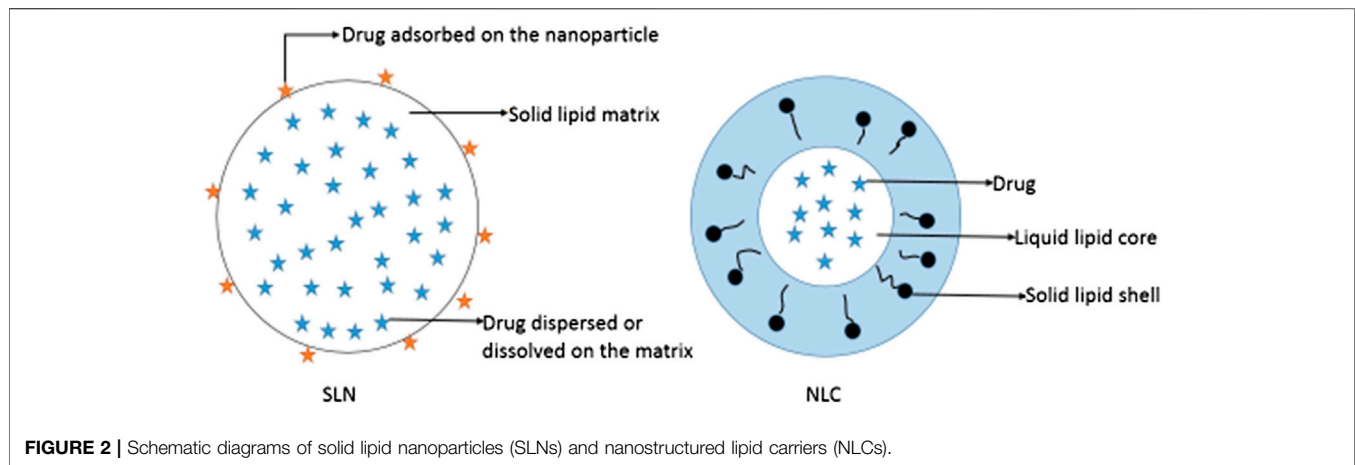
factor receptor (EGFR)-binding domain, the NP uses PLGA-PEG as a carrier and selects the NR7 peptide (NSVRGSR) to actively target specific tumor sites (Wang et al., 2015). DDP forms a cross-strand in DNA, which interferes with the ability of cancer cells to read or copy their genome, leading to programmed cell death (apoptosis) (Pendleton and Grandis, 2013). Although DDP has potential therapeutic effects, it is also linked to numerous serious side effects. The most common ones are gastrointestinal reactions, including nausea, vomiting, diarrhea. The administration of metoclopramide, dexamethasone, or ondansetron during the administration process can inhibit or reduce digestive tract reactions. Nephrotoxicity is the most serious toxic reaction. It is characterized by hematuria and renal damage, increased serum creatinine levels, and decreased clearance (Brillet et al., 1994; Arany and Safirstein, 2003; Wang et al., 2019a). PLGA-PEG nanoplatforms enable the more selective accumulation of DDP in tumors, while reducing its distribution in normal tissues. In addition, the NR7-targeting moiety exists on the surface of the PLGA carrier, which can achieve specific receptor-mediated internalization, while increasing cell uptake and lethality. It has been shown that the uptake rate of HN6 OSCC cancer cells was significantly increased, and a better anti-cancer effect was observed after optimized treatment with specific polymer NPs.

Mizrachi et al. added BYL719 (a PI3K α inhibitor) to P-selectin-targeted NPs, which allowed it to accumulate specifically in cancer cells. The gene phosphatidylinositol-4,5-bisphosphate 3-kinase catalytic subunit alpha (PIK3CA), which encodes the phosphatidylinositol 3-kinase p110 α subunit (PI3K α), is frequently altered in HNSCC. PI3K α inhibitors show good activity in a variety of cancers; however, their use is hindered by the side effects of dose limitation. P-selectin exists on the Weibel–Palade body membrane of vascular endothelial cells and platelet alpha-granule membrane. The cell adhesion molecule P-selectin has nanomolar affinity for fucoidan. Therefore, the embedded nano-PI3K α inhibitor contains a polysaccharide polymer, while reducing the dosage and side effects of the drug. The drug targets specific cancer cells, thereby maintaining a good therapeutic effect (Mizrachi et al., 2017).

Wang et al. developed HN-1-modified PEGylated doxorubicin (HNPD) NPs, which are spherical, uniform in size, and have strong tumor-targeting properties and penetration efficiency. Owing to these characteristics, HNPD NPs specifically accumulate at the tumor site. This can enhance the therapeutic effect of DOX and reduce its toxicity. HNPD NPs can also slowly release DOX, extending its blood circulation time, and have good stability in the body. In addition, they release DOX *in vitro* with pH sensitivity. Compared with the control group, HNPD NPs have a higher cell uptake rate and cytotoxicity. Moreover, the tumor volume of tumor-bearing nude mice injected with HNPD NPs was smaller than that of control mice. Collectively, HNPD NPs can target tumor cells, exert good *in vivo* and *in vitro* therapeutic effects, and are simple to prepare. Hence, these novel nanoplatforms show potential for application in clinical practice (Wang et al., 2017).

Lipid-Based Nanoparticles

Lipid-based NPs include SLNs, NLCs and liposomes. SLNs are a relatively new class of drug carriers. They are particles of submicron size (50–1,000 nm) and composed of lipids that remain in a solid state at room temperature and body temperature; of note, drugs can be dissolved or dispersed in solid lipids (Wong et al., 2007) (Figure 2). SLNs exhibit physical stability, protect unstable drugs from degradation, control drug release, and are associated with good tolerance (Wissing et al., 2004; Souto and Doktorovová, 2009; Mu and Holm, 2018). Pindprolu et al. prepared STAT3 inhibitor niclosamide (Niclo) SLNs (CD133-Niclo-SLNS) modified with CD133 aptamers. Niclo exhibits poor water solubility, it is easily removed, and its low bioavailability limits clinical application. SLNs are suitable for the packaging of poorly soluble drugs and can be used as a carrier for intravenous injection or local administration to achieve targeted positioning and controlled release. Moreover, they can be used for the packaging of Niclo to improve the stability and performance of the drug. In addition, CD133 aptamers can be used as effective targeting ligands to deliver drugs to CD133 cancer stem cells. The prepared SLNs (CD133-Niclo-SLNS) are stable, and can actively target tumor cells to prevent stem cells and epithelial cell-mesenchymal transition-mediated recurrence (Pindprolu and Pindprolu, 2019).

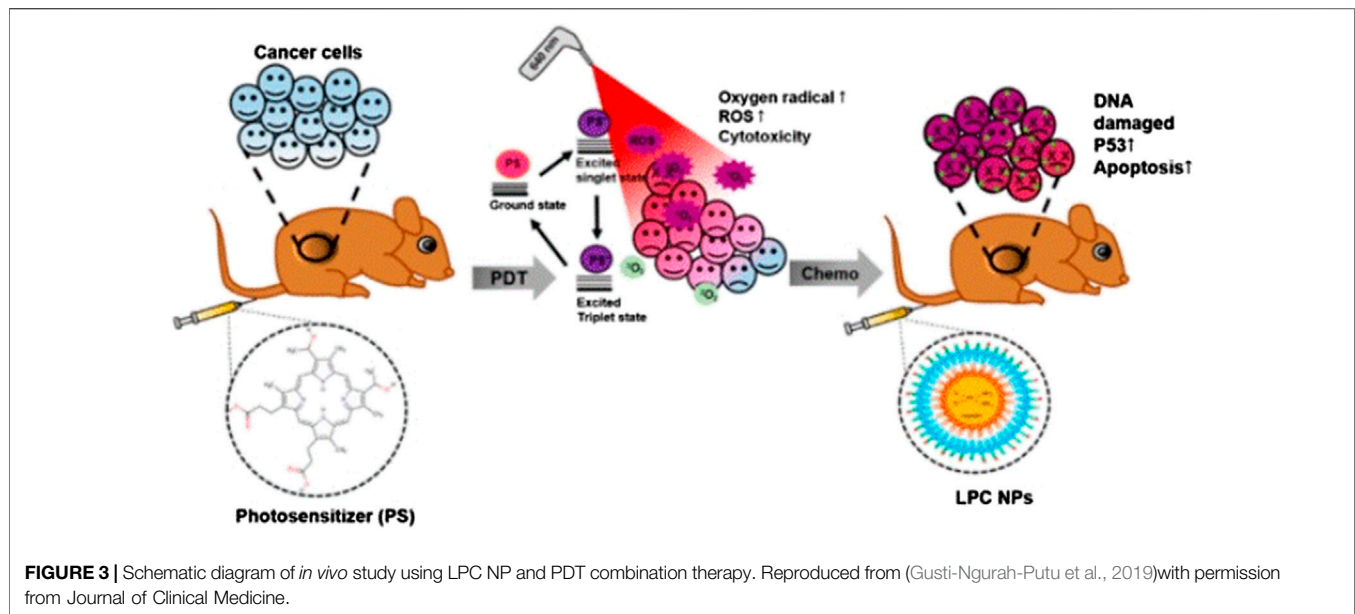


SLNs also have inevitable limitations. High-pressure homogenization is commonly used in the preparation of SLNs. However, the high temperature reached during this process accelerates the degradation rate of drugs and lipids. The coexistence of gelation and other colloidal structures, drug precipitation, particle size growth, and kinetic phenomena are disadvantages of SLNs. Solid lipids are mixed with liquid lipids of different shapes to prepare a new generation of lipid NPs-NLC (Fang et al., 2008; Battaglia and Gallarate, 2012). NLCs are composed of solid lipids enclosing variable liquid lipid nanocompartments (Figure 2). The addition of liquid lipids disrupts the regular lattice structure of solid lipids, increases the proportion of irregular crystal forms in the NP structure, increases the space capacity of the NPs, and improves the drug-carrying capacity. Liquid lipids are controlled by the surrounding solid lipid barrier. Therefore, NLCs can maintain a solid skeleton structure at body temperature to achieve controlled release of NLC drugs (Fang et al., 2008; Lin et al., 2010; Kovacevic et al., 2011). Liu et al. designed DTX-NLC with stearic acid, monoglyceride, soybean lecithin, and oleic acid as the main raw materials, and prepared DTX-NLC using an improved thin-film ultrasonic dispersion method. DTX is fixed in the lipid core of NLCs and can be released for a long time, reducing the number of administrations. In addition, DTX-NLC exhibits a stronger cytotoxic effect than free DTX. This may be because DTX-NLC NPs enter cancer cells through endocytosis, which enhances the accumulation of drugs in cells (Liu et al., 2011). NLCs provide targeted delivery, which improves the treatment efficacy of anti-cancer drugs and reduces their side effects. Therefore, as a carrier, NLCs can provide anti-tumor drug targeting and intracellular administration (Fang et al., 2013).

Liposomes are formed by lipid bilayers and a water core layered by cholesterol. They can encapsulate water-soluble and non-water-soluble drugs in lipid bilayers to form microcapsules with variable sizes (Hu and Zhang, 2012). Liposomes have attracted considerable attention as a valuable carrier and drug delivery system owing to their high drug loading capacity and the flexibility of photosensitizers adapted to different physical and chemical properties.

Compared with free drugs, liposome preparations can be released slowly, reduce the drug's poisonousness on cells, and lengthen the action time of the drug, thereby showing better anti-tumor activity. Liposomes can also encapsulate water-soluble and hydrophobic drugs into selected tissues in a rate-controlled release manner (Derycke and de Witte, 2004; Krajewska et al., 2019). It has been reported that liposomes can mediate gene transduction to treat oral cancer. Konopka et al. used polycationic liposomes as the carrier of DNA for gene therapy of HNSCC. Studies have found that polycationic liposomes can mediate gene transduction under high fetal calf serum conditions, and have a lower carrier immune response. Therefore, in a specific biological environment, polycationic liposomes can be used for gene delivery (Konopka et al., 2005). Fukuhara et al. investigated the treatment of oral cancer by liposomes, and evaluated the effects of a new cationic liposome-coupled adenovirus vector (Ad/SUV) on the gene transduction efficiency of four human oral cancer cell lines and one mouse squamous cell carcinoma cell line. Synthetic Ad/SUV can enhance gene transduction to human oral cancer cells and kill tumor cells. The reason for this phenomenon is that liposomes reduce the neutralization of adenovirus vectors by antibodies. The gene transduction efficiency of Ad/SUV and the killing effect on tumor cells are obviously stronger than that of Ad vector alone. In short, the novel cationic liposome-coupled Ad carrier has strong anti-tumor activity on human OSCC (Fukuhara et al., 2003).

PEGylated adriamycin liposome (Doxil) is a particular dosage form of adriamycin composed of monolayer liposomes. Methoxy PEG is encapsulated on 1,2-distearoylglycerol-3-phosphoethanolamine and exists on the inner and outer surfaces of the lipid bilayer. Owing to its water solubility, doxorubicin (DOX) is stably encapsulated in the water core of liposomes (Mamidi et al., 2010). Doxil is approximately 100 nm in size and can be selectively delivered to tumor sites, permitting it to infiltrate deficient blood vessels in tumor sites. El-Hamid et al. studied the effectiveness of adriamycin and its nanoform (Doxil) to induce apoptosis in oral cancer CAL-27 cells. Compared with the necrosis of cancer cells caused by adriamycin, Doxil mainly



exerts its therapeutic action by inducing apoptosis in cancer cells. Doxil-treated cells showed 3.38-fold higher caspase-3 levels than control cells, while free DOX-treated cells showed 2.72-fold higher caspase-3 levels than control cells. The percentage of C-Myc mRNA inhibition in Doxil-treated was higher than that observed in DOX-treated cells. In summary, Doxil induced apoptosis in CAL-27 cells to a greater degree than DOX (El-Hamid et al., 2019).

Lipid-platinum-chloride (LPC) NP is a nanoplatform formed by liposomes loaded with DDP, and exerts a significant tumor suppressor effect in many types of cancer (Guo et al., 2014a; Guo et al., 2014b; Putra et al., 2016). LPC has unique characteristics, including instantaneous release of platinum for 3–4 h and adjacent effect characteristics (Guo et al., 2013). Eka-Putra et al. reported the therapeutic effect of PDT + LPC on an OSCC xenograft model (Figure 3). The results showed that PDT + LPC can fully reduce the tumor volume by 112%. Tumor volume in the LPC, PDT + DDP, and DDP groups was reduced by 98.8%, 73.1%, and 39.5%, respectively. Histological examination showed that, compared with the DDP or PDT + DDP group, treatment with PDT + LPC or LPC had the least toxic effects on kidneys. Immunohistochemical staining, TUNEL detection, and immunoblotting of tumor suppressor gene p53 verified these findings. Above all, LPC + PDT extended the inhibition of tumor growth, reducing the requirement of chemotherapy. Therefore, treatment with PDT and LPC NPs has a positive therapeutic effect on human oral cancer (Gusti-Ngurah-Putu et al., 2019).

Mohan et al. developed and characterized PEGylated liposome nanocarriers wrapped with *trans*-resveratrol and adriamycin. Both drugs are contained in liposomes, and the supreme encapsulation efficiency of each drug is approximately 80%, when the ratio of resveratrol to DOX is 2:1. The liposome nanoplatform offers slow drug release, decreases the toxicity of the drug to normal tissue, and augments drug concentration at

the tumor site, thus showing higher anti-tumor activity vs. free drugs. In addition, the liposome nanoplatform also regulates the cell cycle and downstream proteins, leading to apoptosis of cancer cells. This study revealed the application prospect of liposomes as nanoplatform carriers in the treatment of oral cancer (Mohan et al., 2016).

Longo et al. found that a liposomal aluminum-chlorophthalocyanine (AlClPc) preparation combined with PDT caused necrosis in Ehrlich tumor cells in the tongue of Swiss mice with strong immunity. The average diameter of liposomal AlClPc is between 120 and 200 nm, easily penetrating into tumor blood vessels. This results in a higher number of passive accumulations of nanoplatforms in tumor tissues vs. normal tissues. The combination of hydrophobic photosensitizers and liposomes preferentially induces cell death through necrosis. The preferred target of this nanoplatform is the phospholipid cell membrane. Photoactivation of the photosensitizer located at this site causes rupture of the cell membrane and destruction of other organelles, leading to cell death. Approximately, 90% of tumor necrosis is attributed to the synergistic effect of liposomal AlClPc-mediated direct toxicity after PDT and tumor vessel closure. Therefore, liposomal AlClPc-mediated PDT is effective in treating oral cancer (Longo et al., 2009).

Metal Nanoparticles

Metal NP includes Au NP and MNP. AuNPs exhibit plasmon resonance and have a highly specific surface area, which enables the modified AuNPs to load drug, thereby improving the solubility, stability, and pharmacokinetic parameters of the drug. Owing to the characteristic photonic properties of AuNPs (surface plasmon resonance absorption and resonance light scattering), their applications in the biological and medical fields are particularly attractive. Preliminary research has investigated the application of nano-gold as a biomedical contrast agent in confocal scanning optical microscopy

(Sokolov et al., 2003), multiphoton plasmon resonance microscopy (Yelin et al., 2003), and optical coherence microscopy (Raub et al., 2004). In addition, AuNPs also have many advantages: ease of detection; inert; lack of toxicity; high scattering intensity; and higher brightness than chemical fluorophores. Due to their supramolecular structure, AuNPs are useful for detecting, diagnosing, and treating tumors. It is an effective reagent used for the determination of heavy metal ions, as well as DNA and protein analysis; it is a chemotherapy carrier for the transport of biomolecules and drug molecules (Kumar et al., 2013).

Coupling antibodies to AuNPs can make NPs actively target cancer cells, which is useful in revealing the internal function of cancer cells and producing better therapies. In addition, by using intelligent bio-coupling technology (Jiao et al., 2011), AuNPs can be functionalized with different molecules. Thus, they are capable of executing targeted, diagnostic, and treatment functions in a single treatment process. This type of multifunctional NP has been used in exciting applications to *in vivo* and *in vitro* therapy experiments (Liang et al., 2014). Biscaglia et al. prepared PEG-bare AuNPs modified with lysine and Ge11. They found that these NPs possess better targeting properties compared with AuNPs modified with cetuximab (C225) (Biscaglia et al., 2017). Melancon et al. prepared hollow gold nanospheres that encapsulate an aptamer targeting EGFR. The hollow gold nanospheres are connected with single-stranded DNA. Subsequently, EGFR-targeting RNA complementary to the single-stranded DNA is added, so that the hollow gold nanospheres have the ability to target EGFR-positive cancer cells. It has been shown that hollow gold nanospheres modified with ^{111}In have a more obvious selective killing effect on EGFR-positive cancer cells than those labeled with an anti-EGFR antibody (C225). Moreover, the physical and chemical properties of the hollow gold nanospheres did not change after modification. This shows that hollow gold nanospheres, as a carrier for a new nanoplatform, can stably and accurately transport the aptamer to EGFR-positive oral cancer cells, providing a promising new direction for the treatment of oral cancer (Melancon et al., 2014).

In another study, Liu et al. prepared PEG-stabilized podoplanin antibody (PDPN Ab) and DOX-coupling AuNPs (**Figure 4**). (PDPN Ab)-AuNP-DOX has good biocompatibility, drug loading capacity, cell uptake efficiency, pH-dependent drug release characteristics, far lower half maximal inhibitory concentration (IC₅₀) than free DOX, and higher photothermal conversion efficiency. Following laser irradiation, (PDPN Ab)-AuNP DOX exerts enhanced anti-tumor effects *in vivo* and *in vitro*. The (PDPN Ab)-AuNP-DOX system serves as a multifunctional combined chemotherapy/PTT nanoplatform for the treatment of oral cancer (Liu et al., 2020).

Reza et al. grafted anti-human epidermal growth factor receptor 2 (anti-HER2) nanoantibodies to gold-silica nanoshells, and used the optical properties of gold to trigger photothermal treatment (PTT) with NIR light for the killing of oral cancer cells. The prepared nanoplatform was co-cultured with KB epithelial cells and HeLa cells (control group) excited with NIR light; this was followed by detection of photothermal

toxicity. It was found that the number of KB tumor cells that died was relatively large, whereas there was almost no cell damage or death noted in the HeLa cells. The higher number of KB tumor cell deaths is mainly related to the positive HER2 on the surface, which makes the nanoplatform selectively accumulate in tumor cells. Thus, labeling NPs with antibodies can improve their targeting properties; this approach has become a new method for the treatment of oral cancer (Fekrazad et al., 2011).

AuNPs can be used as carriers for the delivery of drugs to tumor cells, and have therapeutic effects. Essawy et al. compared two nanostructures coupled with DOX by means of a pH-sensitive and pH-resistant linker. The results of *in vitro* experiments showed that the pH-resistant DOX nanostructure exerted a greater cytotoxic effect in HSC-3 cells compared with pH-sensitive DOX AuNPs. The former has a long-term cytotoxic effect, whereas the latter shows a short-term effect. In addition, the stably connected DOX nanostructure were found to induce cancer cell death through apoptosis, while the DOX AuNPs trigger a necrotic reaction. These results indicate that the stable DOX nanostructure can induce powerful cell death. The results of *in vivo* experiments showed that tumor shrinkage and the survival rate of animals treated with DOX pH-resistant AuNPs were significantly improved compared with those recorded in animals treated with the pH-sensitive type. These *in vitro* and *in vivo* data strongly indicate that AuNPs have greater potency as drug transporters (Essawy et al., 2020).

For superficial tumors (e.g., HNSCC), magnetic drug targeting has achieved a good therapeutic effect. As one of the most promising materials, MNPs are non-toxic to humans, and have been used as a basic platform for imaging, targeted drug delivery, and monitoring efficacy. As one of the most prospective nanomedicine carriers, superparamagnetic NPs (under the control of an external magnetic field) can specifically concentrate the drugs on the lesions, thereby minimizing treatment-related side effects (Laurent et al., 2014; Singh and Sahoo, 2014; Wang and Gu, 2015; Siafaka et al., 2016).

In view of the large number of reports on ferric oxide NPs, folic acid, chitosan, and PLGA in the biomedical field, use of these materials is important for the careful design of NPs to utilize their great advantages and obtain nanomaterials with excellent properties. Using magnetic PLGA nanoparticle as “core” and folic acid-chitosan conjugated as “shell” to modify the surface, Shanavas et al. prepared magnetic core-shell hybrid NPs through the nanoprecipitation method. Using the best molar ratio of folic acid to amine (chitosan), the folic acid-chitosan conjugate was prepared by the carbodiimide cross-linking chemical method, and further coated on the magnetic PLGA NPs encapsulated with docetaxel. The magnetic PLGA nanoplatform modified by folic acid-chitosan is a kind of hybrid NP with a core-shell structure. Folate-positive KB cells can bind to folic acid on their surface and selectively uptake the nanoplatform. The nanoplatform targets cancer cells through folate receptors and plays an anticancer role. In addition, because the protonation of chitosan on nanoparticle surface reduces the resistance of drug release, the nanoplatform can rapidly release docetaxel under acidic conditions. Under physiological pH, folic acid-chitosan can control docetaxel release and avoid drug leakage. The magnetic iron oxide in the

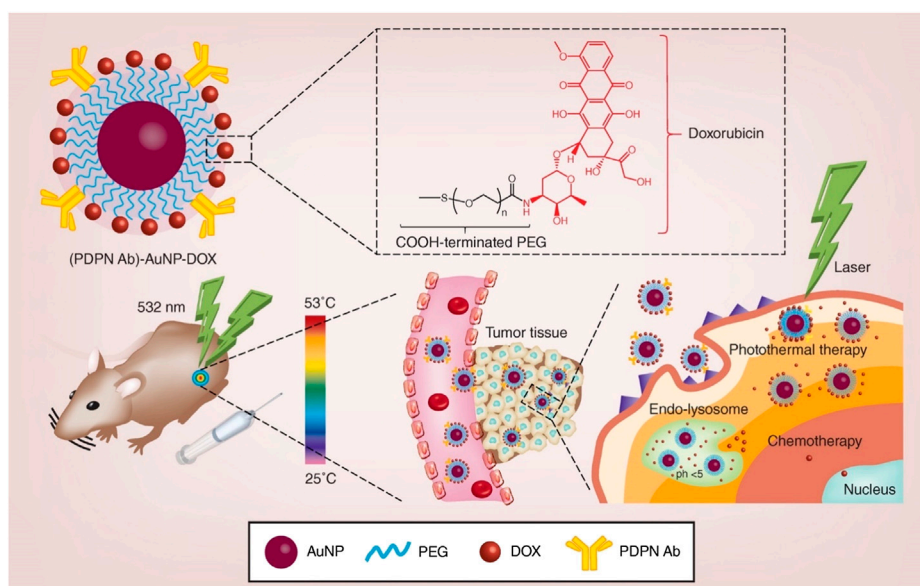


FIGURE 4 | Schematic illustration of the synthesis and application of PDPN antibody-gold nanoparticle-doxorubicin for chemo-photothermal cancer therapy. AuNP: gold nanoparticle; DOX: doxorubicin; PDPN Ab: podoplanin antibody; PEG: polyethylene glycol. Reproduced from (Liu et al., 2020) with permission from *Nanomedicine (Lond)*.

nanoplatfrom can be used in magnetic resonance imaging. It can be observed that the magnetic PLGA hybrid NPs modified by folic acid-chitosan are promising nanoplatfroms with good biocompatibility, and can be used in the magnetic resonance imaging and treatment of cancer (Shanavas et al., 2017).

Zhang et al. announced the preparation and functionalization of biocompatible superparamagnetic hollow mesoporous NPs. The surface engineering of polyacrylic acid is processed on the superparamagnetic NPs that can support bleomycin in the mesoporous structure, and bonded with polyacrylic acid to construct a nanoscale drug delivery system (Figure 5). The drug is targeted through the nanoplatfrom, stays in the focal area under the magnetic field, and is continuously released. Detailed studies have shown that polyacrylic acid functionalized MNPs loaded with bleomycin can stimulate local tumor cell apoptosis. This nanoplatfrom endows anti-cancer drugs with targeting ability *in vitro* and inhibits tumor development *in vivo* (Zhang et al., 2020b). Lu et al. developed a nanoplatfrom composed of pH-dependent β -cyclodextrin and magnetic colloidal NPs. Compared with individual magnetic nanocrystals, β -cyclodextrin and magnetic nanocrystal composites have a higher loading rate of 5-FU (Lv et al., 2014). Anirudhan et al. used chemical precipitation to prepare a maleic anhydride-grafted magnetic cyclodextrin derivative to control the release of 5-FU. The synthetic compound has a good safety profile, high water solubility, and high pH sensitivity. Experimental results regarding the function of this nanoplatfrom in breast cancer therapy showed that the cytotoxicity of cyclodextrin-MNP was markedly enhanced compared with that of the 5-FU control group. The MNP-CD nanoplatfrom has low toxicity and side effects on normal cells (Anirudhan et al., 2015).

Miao et al. combined poly (ethylene imine) (PEI)-modified iron oxide NPs with the human telomerase reverse transcriptase (hTERT) promoter to form a new nanoplatfrom. This nanoplatfrom can deliver the hTERT promoter to tumors, and activate the human tumor necrosis factor-related apoptosis-inducing ligand (TRAIL) gene to cause apoptosis in oral cancer cells. Under the action of a magnetic field, the PEI-modified Fe_3O_4 MNPs are positively charged, whereas the hTERT promoter is negatively charged. Through the combination of the two under the action of a magnetic field, PEI modification can protect DNA from digestion by endosomes and improve the transfection efficiency. In the experimental group, 73% of the tumor cells were positive for TRAIL staining, whereas the tumor cells in the control group were negative. This study showed that PEI-modified iron oxide NPs are promising nanoplatfroms that can be used to deliver gene therapy for oral cancer (Miao et al., 2014).

Hydrogels

Hydrogels have adjustable physical and mechanical properties, and can be widely used in the medical field. In this regard, they have been used as drug delivery systems for several years because they provide a convenient support matrix for the active ingredients (Drury and Mooney, 2003). For example, Li et al. successfully developed a biodegradable thermosensitive hydrogel that can be loaded with succinimidylhydroxamic acid (SAHA) and DDP. The nanoplatfrom can be administered within a target organ at a predetermined rate and within a predetermined time, which overcomes the shortcomings of traditional pharmaceutical preparations. This reduces the drug poisonousness and improves the survival quality of patients. In this study, mice xenotransplanted with HSC-3 cells were classified into six

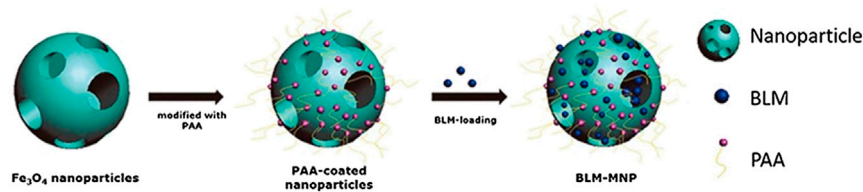


FIGURE 5 | Schematic showing the synthesis of the magnetic nanoparticle with surface-engineering PAA in the outer layer and BLM molecules bonded with PAA. BLM: Bleomycin PAA: Polyacrylic acid Reproduced from (Zhang et al., 2020b) with permission from American journal of cancer research.

groups, and were infected with saline, SAHA, poly (ethylene glycol)-poly (ϵ -caprolactone)-poly (ethylene glycol) (PEG-PCL-PEG, PECE) hydrogel, DDP, SAHA-DDP, or SAHA-DDP/PECE. Compared with other control groups, the two combined treatment groups (particularly the SAHA-DDP/PECE treatment group) had significantly reduced tumor growth. The cell apoptosis rate of the combined treatment group was significantly higher than that of the control group, and the tumor volume was the smallest. These results showed that the SAHA-DDP/PECE nanoplatfrom can effectively inhibit the development of oral tumor cells. Therefore, PECE hydrogel-mediated DDP and SAHA may become a novel and promising chemotherapy for oral cancer (Li et al., 2012).

Exosomes

Exosomes are vesicles with a diameter of 40–100 nm, which can be separated from cell culture supernatants and different biological fluids. They can be captured by neighboring recipient cells through the interaction of vesicle surface ligands and cell receptors, and subsequently fuse with recipient cells through internalization (Théry et al., 2006; Théry et al., 2009). Exosomes include many types of biomolecules; thus, they play a significant role in intercellular communication (Bungulawa et al., 2018). Studies have shown that exosomes belonging to extracellular vesicles can target diseased tissues or organs (Wiklander et al., 2015). Most cells can secrete exosomes, but some cells can actively secrete them, such as macrophages (Bhatnagar et al., 2007), B cells (Clayton et al., 2005), T cells (Nolte-t Hoen et al., 2009), mesenchymal stem (Lai et al., 2015), endothelial (Song et al., 2014), and epithelial cells (Skogberg et al., 2015).

They are highly effective drug carriers that can provide cell-based drug delivery. Exosomes or exosome-like vesicles can passively load small lipophilic molecules and large molecules (e.g., DNA, RNA, and proteins) into exosomes. The surface proteins of exosomes allow their load to easily pass through the cell membrane and deliver their contents in a biologically active form. More importantly, exosomes have the inherent ability to cross biological barriers, even the blood brain barrier (Batrakova and Kim, 2015).

Research studies found that exosomes can be loaded with chemotherapeutic drugs to treat OSCC. Rosenberger et al. investigated the therapeutic effect of menstrual mesenchymal stem cell (MenSC)-derived exosomes on hamster buccal pouch carcinoma, and confirmed that intratumoral injection of

MenSC-exosomes leads to significant anti-tumor effects and tumor blood vessel loss. They found that the biological effects of MenSC-exosomes on endothelial cells and their anti-angiogenic effects may have advantages in the treatment of OSCC. Moreover, they also proposed a method to expand the production of exosomes using the fiber-based microcarrierBioNOC II, which can reduce the production cost. It is established that endothelial cells are responsible for angiogenesis. In this study, following the evaluation of cytotoxicity, they found that exosomes induce endothelial cell death, which may be one of the reasons for tumor blood vessel loss. In addition, they also assessed whether MenSC-exosomes can directly regulate the angiogenic potential of endothelial cells. The results showed that the anti-angiogenic effect of MenSC-exosomes is a unique feature of these exosomes, and is not necessarily attributed to other cell types. More importantly, the anti-angiogenic property of MenSC-exosomes exerts a significant effect on hamster cheek pouch carcinoma. As shown in **Figures 6B,C**, after four injections of exosomes in hamsters with cheek pouch cancer, it was found that the tumor volume and growth were reduced compared with those recorded in the control group. As illustrated in **Figures 6D,E**, compared with the control group, the tumor blood vessel density and blood vessel area of the exosome treatment group were significantly reduced. This evidence shows that exosomes can also inhibit OSCC *in vivo*. In summary, owing to their biological effects on endothelial cells and anti-angiogenesis, exosomes may become a promising nanoplatfrom for the treatment of OSCC (Rosenberger et al., 2019).

Dendrimers

The use of nano-level therapy has many advantages compared with the existing methods for the treatment of human diseases. In these nanoplatfroms, the well-defined and highly branched structure of dendrimers provides great flexibility for modification, especially for cell targeting, high-dose drug loading, gene therapy payloads, or their combinations (Yuan et al., 2019). Dendrimers can couple alternative targeted drugs and therapeutic drugs to a single carrier device. Dendrimer-based methods are exploring many alternative targets, which may allow us to modify therapies (receptor targeting and therapeutic utilization) based on the genetic makeup of tumor characteristics in the future (Ward et al., 2011).

Xu et al. developed a folic acid-modified polyamidoaminodendrimer G4 (G4-FA) nanoplatfrom for the targeted delivery of DNA

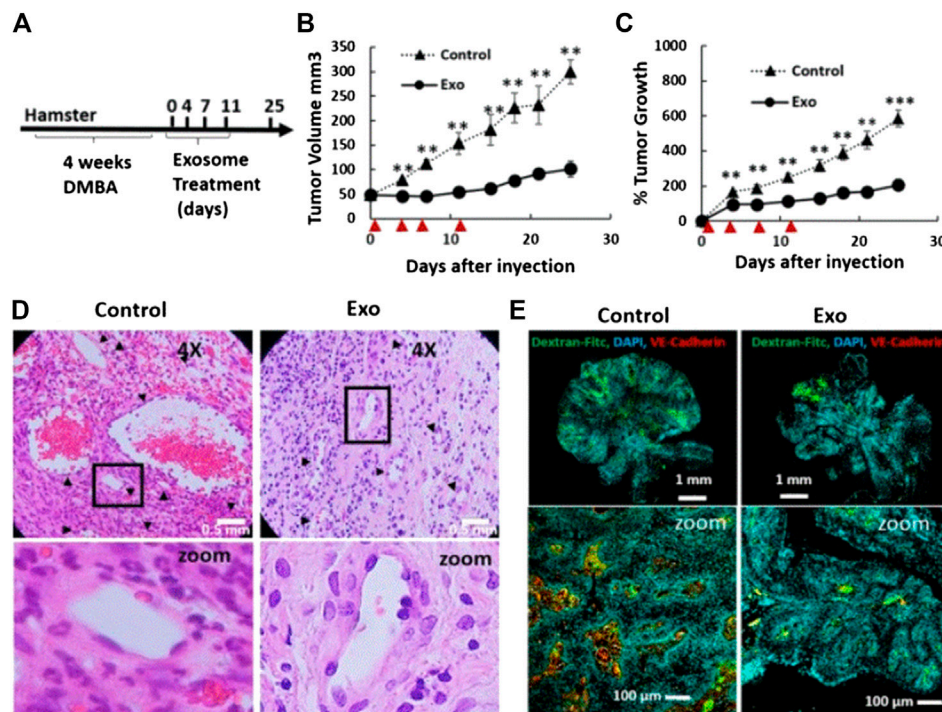


FIGURE 6 | Tumor growth and angiogenesis is conspicuously restrained by exosome therapy. **(A)** Scheme of experimental design. DMBA injection induced tumor production within 4 weeks, and exosomes were injected every 3–4 days for a total of four injections. **(B and C)** Tumor growth and volume of the control and exosomes groups after four injections of exosomes. ▲ indicates days of exosome treatment. **(D)** H&E sections of tumor tissues in the control and exosome treatment group on day 25. **(E)** Histological sections of tumors stained with Hoechst (blue), Dextran-FITC (green), and VE Cadherin (red) at day 25. Reproduced from (Rosenberger et al., 2019) with permission from *Scientific Reports*. DAPI, 4',6-diamidino-2-phenylindole; DMBA, 7,12-dimethylbenzanthracene; FITC, fluorescein; isothiocyanate; H&E, hematoxylin-eosin; VE, vascular endothelial.

plasmids to head and neck cancer cells that highly express folate receptors. G4-FA has good cell compatibility and can contend with free folic acid for identical binding sites on cancer cells. G4-FA can specifically bind to folate receptors to accelerate the uptake of DNA plasmids by cancer cells, and selectively deliver the plasmids to cancer cells with high expression of the folate receptor to increase gene expression (Xu et al., 2016).

Particularly, Xu et al. designed a folic acid-modified polyamidoaminodendrimer as a carrier to deliver siRNA. Following modification of the nanoplatform with folic acid, it can be absorbed by tumor cells that highly express folic acid receptors through endocytosis mediated by these receptors. siRNA targeting vascular endothelial growth factor A enters tumor cells through endocytosis, reducing the molecular targets responsible for tumor cell proliferation and survival, and exerting anti-cancer effects. The G4-FA nanoplatform mainly increases its concentration in tumors through endocytosis, thereby maintaining a high siRNA concentration in the tumor to inhibit growth. According to the evaluation of NIR imaging, G4-FA injected into the tumor showed a high tumor absorption rate and sustained high local retention. Both single-dose and double-dose G4-FA/vascular endothelial growth factor A (siVEGFA) can inhibit tumors. However, the tumor volume increased on day 8 in the single-dose group. This phenomenon disappeared after the application of the double

dose, indicating that the double dose may have a sustained anti-tumor effect. In short, G4-FA is a safe nanoplatform that can specifically deliver siRNA to locally target the treatment of head and neck cancer (Xu et al., 2017).

CONCLUSION

Chemotherapy remains the main treatment strategy for patients with oral cancer. Considering the various shortcomings of this therapeutic approach, nanoplatforms are being developed. In this review, we have summarized a variety of nanoplatforms for the treatment of oral cancer. These nanoplatforms can overcome many shortcomings of chemotherapy, enable drugs to accurately reach tumor cells, reduce side effects on surrounding normal tissues, and bring hope for the discovery of new oral cancer therapies.

However, In order to apply the nanoplatforms for the clinical treatment of oral cancer, several barriers, such as the controversial EPR effect, toxicity and instability, insufficient blood circulation time, need to be overcome (Blanco et al., 2015). Many nanoplatforms target specific tumor cells through the EPR effect. However, studies have shown that the variability of the EPR effect in large animals or humans has rarely been considered (Hansen et al., 2015). The short blood circulation of some

nanoplatfoms makes them cleared by the mononuclear phagocyte system (MPS) and reticulo-endothelial system (RES) (Pérez-Herrero and Fernández-Medarde, 2015). In addition, toxicity and instability also limit the clinical application of nanoplatfoms. AuNPs provoke an imbalance in the oxidative status of the cells, which is accompanied by damage in the genetic, lipid and protein structures. Therefore, it is strongly recommended to conduct a deeper study about the use of AuNPs as drug delivery vehicle in the chronic treatment of diseases as cancer (Lopez-Chaves et al., 2018). Due to the premature release of drugs and serious accumulation or misplaced aggregation, the poor colloidal stability of nanoplatfoms always leads to low drug delivery efficiency (Sang et al., 2019).

In order to improve the performance of nanoplatfoms for oral cancer therapy, some factors should be considered. To start with, the change in the nanoplatfoms' size may lead to a different nanomedicine physiological stability. A suitable size of nanoplatfoms is absolutely necessary to enhance their therapeutic effect (He et al., 2019). Secondary, modifying the surface properties of nanoparticles with cell membranes to

prolong blood circulation time and immune escape (Chen et al., 2016). Meanwhile, the design of appropriate clinical trials is crucial. Furthermore, investigators should also design some nanoplatfoms that are easy to use in the clinic, and design animal models for *in vivo* experiments.

AUTHOR CONTRIBUTIONS

All authors have made a substantial, direct and intellectual contribution to the work, and approved it for publication.

ACKNOWLEDGMENTS

We thank the financial support from the Program of Scientific Development of Jilin Province (20180414043GH and 20190304112YY), the program of Jilin University (3R2201543428), the program of the First Hospital of Jilin University (01032140001, 04023720002 and JDYYJC002).

REFERENCES

- Agüeros, M., Ruiz-Gatón, L., Vauthier, C., Bouchemal, K., Espuelas, S., Ponchel, G., et al. (2009). Combined hydroxypropyl-beta-cyclodextrin and poly(anhydride) nanoparticles improve the oral permeability of paclitaxel. *Eur J Pharm Sci* 38, 405–413. doi:10.1016/j.ejps.2009.09.010
- Anirudhan, T. S., Divya, P. L., and Nima, J. (2015). Synthesis and characterization of silane coated magnetic nanoparticles/glycidylmethacrylate-grafted-maleated cyclodextrin composite hydrogel as a drug carrier for the controlled delivery of 5-fluorouracil. *Mater Sci Eng C Mater Biol Appl* 55, 471–481. doi:10.1016/j.msec.2015.05.068
- Arany, I., and Safirstein, R. L. (2003). Cisplatin nephrotoxicity. *Semin Nephrol* 23, 460–464. doi:10.1016/s0270-9295(03)00089-5
- Batrakova, E. V., and Kim, M. S. (2015). Using exosomes, naturally-equipped nanocarriers, for drug delivery. *J Control Release* 219, 396–405. doi:10.1016/j.jconrel.2015.07.030
- Battaglia, L., and Gallarate, M. (2012). Lipid nanoparticles: state of the art, new preparation methods and challenges in drug delivery. *Expert Opin Drug Deliv* 9, 497–508. doi:10.1517/17425247.2012.673278
- Bhatnagar, S., Shinagawa, K., Castellino, F. J., and Schorey, J. S. (2007). Exosomes released from macrophages infected with intracellular pathogens stimulate a proinflammatory response *in vitro* and *in vivo*. *Blood* 110, 3234–3244. doi:10.1182/blood-2007-03-079152
- Biscaglia, F., Rajendran, S., Conflitti, P., Benna, C., Sommaggio, R., Litti, L., et al. (2017). Enhanced EGFR targeting activity of plasmonic nanostructures with engineered GE11 peptide. *Adv Healthc Mater* 6, 1700596. doi:10.1002/adhm.201700596
- Blanco, E., Shen, H., and Ferrari, M. (2015). Principles of nanoparticle design for overcoming biological barriers to drug delivery. *Nat Biotechnol* 33, 941–951. doi:10.1038/nbt.3330
- Bray, F., Ferlay, J., Soerjomataram, I., Siegel, R. L., Torre, L. A., and Jemal, A. (2018). Global cancer statistics 2018: GLOBOCAN estimates of incidence and mortality worldwide for 36 cancers in 185 countries. *CA Cancer J Clin* 68, 394–424. doi:10.3322/caac.21492
- Brillet, G., Deray, G., Jacquiaud, C., Mignot, L., Bunker, D., Meillet, D., et al. (1994). Long-term renal effect of cisplatin in man. *Am J Nephrol* 14, 81–84. doi:10.1159/000168693
- Bungkulawa, E. J., Wang, W., Yin, T., Wang, N., Durkan, C., Wang, Y., et al. (2018). Recent advancements in the use of exosomes as drug delivery systems. *J Nanobiotechnology* 16, 81. doi:10.1186/s12951-018-0403-9
- Chaturvedi, A. K., Engels, E. A., Pfeiffer, R. M., Hernandez, B. Y., Xiao, W., Kim, E., et al. (2011). Human papillomavirus and rising oropharyngeal cancer incidence in the United States. *J Clin Oncol* 29, 4294–4301. doi:10.1200/JCO.2011.36.4596
- Chen, Z., Zhao, P., Luo, Z., Zheng, M., Tian, H., Gong, P., et al. (2016). Cancer cell membrane-biomimetic nanoparticles for homologous-targeting dual-modal imaging and photothermal therapy. *ACS Nano* 10, 10049–10057. doi:10.1021/acsnano.6b04695
- Chen, J., Ding, J., Wang, Y., Cheng, J., Ji, S., Zhuang, X., et al. (2017). Sequentially responsive shell-stacked nanoparticles for deep penetration into solid tumors. *Adv Mater Weinheim* 29, 1701170. doi:10.1002/adma.201701170
- Chi, A. C., Day, T. A., and Neville, B. W. (2015). Oral cavity and oropharyngeal squamous cell carcinoma--an update. *CA Cancer J Clin* 65, 401–421. doi:10.3322/caac.21293
- Cho, K., Wang, X., Nie, S., Chen, Z., and Shin, D. M. (2008). Therapeutic nanoparticles for drug delivery in cancer. *Clin Cancer Res* 14, 1310–1316. doi:10.1158/1078-0432.CCR-07-1441
- Clayton, A., Turkes, A., Navabi, H., Mason, M. D., and Tabi, Z. (2005). Induction of heat shock proteins in B-cell exosomes. *J Cell Sci* 118, 3631–3638. doi:10.1242/jcs.02494
- Couvreur, P. (2013). Nanoparticles in drug delivery: past, present and future. *Adv Drug Deliv Rev* 65, 21–23. doi:10.1016/j.addr.2012.04.010
- Cui, J., Wang, H., Zhang, X., Sun, X., Zhang, J., and Ma, J. (2020). Exosomal miR-200c suppresses chemoresistance of docetaxel in tongue squamous cell carcinoma by suppressing TUBB3 and PPP2R1B. *Aging* 12, 6756–6773. doi:10.18632/aging.103036
- Derycke, A. S., and De Witte, P. A. (2004). Liposomes for photodynamic therapy. *Adv Drug Deliv Rev* 56, 17–30. doi:10.1016/j.addr.2003.07.014
- Devalapally, H., Chaklam, A., and Amiji, M. M. (2007). Role of nanotechnology in pharmaceutical product development. *J Pharm Sci* 96, 2547–2565. doi:10.1002/jps.20875
- Dilruba, S., and Kalayda, G. V. (2016). Platinum-based drugs: past, present and future. *Cancer Chemother Pharmacol* 77, 1103–1124. doi:10.1007/s00280-016-2976-z
- Drury, J. L., and Mooney, D. J. (2003). Hydrogels for tissue engineering: scaffold design variables and applications. *Biomaterials* 24, 4337–4351. doi:10.1016/s0142-9612(03)00340-5
- El-Hamid, E. S. A., Gamal-Eldeen, A. M., and Sharaf Eldeen, A. M. (2019). Liposome-coated nano doxorubicin induces apoptosis on oral squamous cell carcinoma CAL-27 cells. *Arch Oral Biol* 103, 47–54. doi:10.1016/j.archoralbio.2019.05.011

- Endo, K., Ueno, T., Kondo, S., Wakisaka, N., Muro, S., Ito, M., et al. (2013). Tumor-targeted chemotherapy with the nanopolymer-based drug NC-6004 for oral squamous cell carcinoma. *Cancer Sci* 104, 369–374. doi:10.1111/cas.12079
- Essawy, M. M., El-Sheikh, S. M., Raslan, H. S., Ramadan, H. S., Kang, B., and Talaat, I. M. (2020). Function of gold nanoparticles in oral cancer beyond drug delivery: implications in cell apoptosis. *Oral Dis.* doi:10.1111/odi.13551
- Fang, J. Y., Fang, C. L., Liu, C. H., and Su, Y. H. (2008). Lipid nanoparticles as vehicles for topical psoralen delivery: solid lipid nanoparticles (SLN) versus nanostructured lipid carriers (NLC). *Eur J Pharm Biopharm* 70, 633–640. doi:10.1016/j.ejpb.2008.05.008
- Fang, C. L., Al-Suwayeh, S. A., and Fang, J. Y. (2013). Nanostructured lipid carriers (NLCs) for drug delivery and targeting. *Recent Pat Nanotechnol* 7, 41–55. doi:10.2174/187221013804484827
- Fekrazad, R., Hakimiha, N., Farokhi, E., Rasaei, M. J., Ardestani, M. S., Kalhori, K. A., and Sheikholeslami, F. (2011). Treatment of oral squamous cell carcinoma using anti-HER2 immunonanoshells. *Int J Nanomedicine* 6, 2749–2755. doi:10.2147/IJN.S24548
- Feng, X. R., Xu, W. G., Li, Z. M., Song, W. T., Ding, J. X., and Chen, X. S. (2019). Immunomodulatory nanosystems. *Advanced Science* 6 (17), 39. doi:10.1002/adv.201900101
- Feng, X., Liu, J., Xu, W., Li, G., and Ding, J. (2020). Tackling autoimmunity with nanomedicines. *Nanomedicine* 15 (16), 1585–1597. doi:10.2217/nmm-2020-0102
- Fukuhara, H., Hayashi, Y., Yamamoto, N., Fukui, T., Nishikawa, M., Mitsudo, K., Tohna, I., Ueda, M., Mizuno, M., and Yoshida, J. (2003). Improvement of transduction efficiency of recombinant adenovirus vector conjugated with cationic liposome for human oral squamous cell carcinoma cell lines. *Oral Oncol* 39, 601–609. doi:10.1016/s1368-8375(03)00047-2
- Guo, S., Wang, Y., Miao, L., Xu, Z., Lin, C. M., Zhang, Y., and Huang, L. (2013). Lipid-coated Cisplatin nanoparticles induce neighboring effect and exhibit enhanced anticancer efficacy. *ACS Nano* 7, 9896–9904. doi:10.1021/nn403606m
- Guo, S., Miao, L., Wang, Y., and Huang, L. (2014a). Unmodified drug used as a material to construct nanoparticles: delivery of cisplatin for enhanced anti-cancer therapy. *J. Control Release* 174, 137–142. doi:10.1016/j.jconrel.2013.11.019
- Guo, S., Wang, Y., Miao, L., Xu, Z., Lin, C. H., and Huang, L. (2014b). Turning a water and oil insoluble cisplatin derivative into a nanoparticle formulation for cancer therapy. *Biomaterials* 35, 7647–7653. doi:10.1016/j.biomaterials.2014.05.045
- Gusti-Ngurah-Putu, E. P., Huang, L., and Hsu, Y. C. (2019). Effective combined photodynamic therapy with lipid platinum chloride nanoparticles therapies of oral squamous carcinoma tumor inhibition. *J Clin Med* 8. doi:10.3390/jcm8122112
- Hansen, A. E., Petersen, A. L., Henriksen, J. R., Boerresen, B., Rasmussen, P., Elema, D. R., et al. (2015). Positron emission tomography based elucidation of the enhanced permeability and retention effect in dogs with cancer using copper-64 liposomes. *ACS Nano* 9, 6985–6995. doi:10.1021/acsnano.5b01324
- Harada, K., Ferdous, T., Kobayashi, H., and Ueyama, Y. (2014). Paclitaxel in combination with cetuximab exerts antitumor effect by suppressing NF- κ B activity in human oral squamous cell carcinoma cell lines. *Int J Oncol* 45, 2439–2445. doi:10.3892/ijo.2014.2655
- He, Z., Dai, Y., Li, X., Guo, D., Liu, Y., Huang, X., et al. (2019). Hybrid nanomedicine fabricated from photosensitizer-terminated metal-organic framework nanoparticles for photodynamic therapy and hypoxia-activated cascade chemotherapy. *Small* 15 (4), e1804131. doi:10.1002/sml.201804131
- Hu, C. M., and Zhang, L. (2012). Nanoparticle-based combination therapy toward overcoming drug resistance in cancer. *Biochem Pharmacol* 83, 1104–1111. doi:10.1016/j.bcp.2012.01.008
- Huang, B., Chen, H., and Fan, M. (2008). A postulated role for human papillomavirus (HPV) in the transformation and proliferation of oral squamous cell carcinoma (OSCC). *Med Hypotheses* 70, 1041–1043. doi:10.1016/j.mehy.2007.07.043
- Ishigami, T., Uzawa, K., Higo, M., Nomura, H., Saito, K., Kato, Y., et al. (2007). Genes and molecular pathways related to radioresistance of oral squamous cell carcinoma cells. *Int J Cancer* 120, 2262–2270. doi:10.1002/ijc.22561
- Jemal, A., Bray, F., Center, M. M., Ferlay, J., Ward, E., and Forman, D. (2011). Global cancer statistics. *CA Cancer J Clin* 61, 69–90. doi:10.3322/caac.20107
- Jemal, A., Simard, E. P., Dorell, C., Noone, A. M., Markowitz, L. E., Kohler, B., et al. (2013). Annual Report to the Nation on the Status of Cancer, 1975–2009, featuring the burden and trends in human papillomavirus(HPV)-associated cancers and HPV vaccination coverage levels. *J Natl Cancer Inst* 105, 175–201. doi:10.1093/jnci/djs491
- Jiang, Z.-Y., Feng, X.-R., Xu, W.-G., Zhuang, X.-L., Ding, J.-X., and Chen, X.-S. (2020). Calcium phosphate-cured nanocluster of poly(L-glutamic acid)-cisplatin and arsenic trioxide for synergistic chemotherapy of peritoneal metastasis of ovarian cancer. *Acta Polymerica Sinica* 51 (8), 901–910. doi:10.1177/1389557518666180903150928
- Jiao, P. F., Zhou, H. Y., Chen, L. X., and Yan, B. (2011). Cancer-targeting multifunctionalized gold nanoparticles in imaging and therapy. *Curr Med Chem* 18, 2086–2102. doi:10.2174/092986711795656199
- Kaur, I. P., Garg, A., Singla, A. K., and Aggarwal, D. (2004). Vesicular systems in ocular drug delivery: an overview. *Int J Pharm* 269, 1–14. doi:10.1016/j.ijpharm.2003.09.016
- Kesharwani, P., and Iyer, A. K. (2015). Recent advances in dendrimer-based nanovectors for tumor-targeted drug and gene delivery. *Drug Discov Today* 20, 536–547. doi:10.1016/j.drudis.2014.12.012
- Konopka, K., Fallah, B., Monzon-Duller, J., Overli, N., and Düzgünes, N. (2005). Serum-resistant gene transfer to oral cancer cells by Metafectene and GeneJammer: application to HSV-tk/ganciclovir-mediated cytotoxicity. *Cell Mol Biol Lett* 10, 455–470.
- Kovacevic, A., Savić, S., Vuleta, G., Müller, R. H., and Keck, C. M. (2011). Polyhydroxy surfactants for the formulation of lipid nanoparticles (SLN and NLC): effects on size, physical stability and particle matrix structure. *Int J Pharm* 406, 163–172. doi:10.1016/j.ijpharm.2010.12.036
- Krajewska, J. B., Bartoszek, A., and Fichna, J. (2019). New trends in liposome-based drug delivery in colorectal cancer. *Mini Rev Med Chem* 19 (1), 3–11. doi:10.2174/1389557518666180903150928
- Kumar, D., Saini, N., Jain, N., Sareen, R., and Pandit, V. (2013). Gold nanoparticles: an era in bionanotechnology. *Expert Opin Drug Deliv* 10, 397–409. doi:10.1517/17425247.2013.749854
- Lai, R. C., Yeo, R. W., and Lim, S. K. (2015). Mesenchymal stem cell exosomes. *Semin Cell Dev Biol* 40, 82–88. doi:10.1016/j.semcdb.2015.03.001
- Laurent, S., Saei, A. A., Behzadi, S., Panahifar, A., and Mahmoudi, M. (2014). Superparamagnetic iron oxide nanoparticles for delivery of therapeutic agents: opportunities and challenges. *Expert Opin Drug Deliv* 11, 1449–1470. doi:10.1517/17425247.2014.924501
- Lee, M. S., Dees, E. C., and Wang, A. Z. (2017). Nanoparticle-delivered chemotherapy: old drugs in new packages. *Oncology* 31 (3), 198–208.
- Li, J., Gong, C., Feng, X., Zhou, X., Xu, X., Xie, L., et al. (2012). Biodegradable thermosensitive hydrogel for SAHA and DDP delivery: therapeutic effects on oral squamous cell carcinoma xenografts. *PLoS One* 7, e33860. doi:10.1371/journal.pone.0033860
- Li, H., Shi, L., Wei, J., Zhang, C., Zhou, Z., Wu, L., and Liu, W. (2016). Cellular uptake and anticancer activity of salvianolic acid B phospholipid complex loaded nanoparticles in head and neck cancer and precancer cells. *Colloids Surf B Biointerfaces* 147, 65–72. doi:10.1016/j.colsurfb.2016.07.053
- Liang, R., Wei, M., Evans, D. G., and Duan, X. (2014). Inorganic nanomaterials for bioimaging, targeted drug delivery and therapeutics. *Chem Commun* 50, 14071–14081. doi:10.1039/c4cc03118k
- Lin, Y. K., Huang, Z. R., Zhuo, R. Z., and Fang, J. Y. (2010). Combination of calcipotriol and methotrexate in nanostructured lipid carriers for topical delivery. *Int J Nanomedicine* 5, 117–128. doi:10.2147/ijn.s9155
- Liu, D., Liu, Z., Wang, L., Zhang, C., and Zhang, N. (2011). Nanostructured lipid carriers as novel carrier for parenteral delivery of docetaxel. *Colloids Surf B Biointerfaces* 85, 262–269. doi:10.1016/j.colsurfb.2011.02.038
- Liu, Z., Shi, J., Zhu, B., and Xu, Q. (2020). Development of a multifunctional gold nanopatform for combined chemo-photothermal therapy against oral cancer. *Nanomedicine* 15, 661–676. doi:10.2217/nmm-2019-0415
- Longo, J. P., Lolzi, S. P., Simioni, A. R., Morais, P. C., Tedesco, A. C., and Azevedo, R. B. (2009). Photodynamic therapy with aluminum-chlorophthalocyanine induces necrosis and vascular damage in mice tongue tumors. *J Photochem Photobiol B, Biol* 94, 143–146. doi:10.1016/j.jphotobiol.2008.11.003
- Lopez-Chaves, C., Soto-Alvaredo, J., Montes-Bayon, M., Bettmer, J., Llopis, J., and Sanchez-Gonzalez, C. (2018). Gold nanoparticles: distribution, bioaccumulation and toxicity. *In vitro and in vivo studies. Nanomedicine* 14, 1–12. doi:10.1016/j.nano.2017.08.011

- Lu, Z. R., Steinmetz, N. F., and Zhu, H. (2018). New directions for drug delivery in cancer therapy. *Mol Pharm* 15, 3601–3602. doi:10.1021/acs.molpharmaceut.8b00860
- Lv, S., Zhao, M., Cheng, C., and Zhao, Z. (2014). beta-Cyclodextrin polymer brushes decorated magnetic colloidal nanocrystal clusters for the release of hydrophobic drugs. *Journal of Nanoparticle Research* 16 (5). doi:10.1007/s11051-014-2393-3
- Mahapatro, A., and Singh, D. K. (2011). Biodegradable nanoparticles are excellent vehicle for site directed *in-vivo* delivery of drugs and vaccines. *J Nanobiotechnology* 9, 55. doi:10.1186/1477-3155-9-55
- Mamidi, R. N., Weng, S., Stellar, S., Wang, C., Yu, N., Huang, T., et al. (2010). Pharmacokinetics, efficacy and toxicity of different pegylated liposomal doxorubicin formulations in preclinical models: is a conventional bioequivalence approach sufficient to ensure therapeutic equivalence of pegylated liposomal doxorubicin products?. *Cancer Chemother Pharmacol* 66, 1173–1184. doi:10.1007/s00280-010-1406-x
- Mamot, C., Ritschard, R., Wicki, A., Stehle, G., Dieterle, T., Bubendorf, L., et al. (2012). Tolerability, safety, pharmacokinetics, and efficacy of doxorubicin-loaded anti-EGFR immunoliposomes in advanced solid tumours: a phase 1 dose-escalation study. *Lancet Oncol* 13, 1234–1241. doi:10.1016/S1470-2045(12)70476-X
- Matsumura, Y., and Maeda, H. (1986). A new concept for macromolecular therapeutics in cancer chemotherapy: mechanism of tumorotropic accumulation of proteins and the antitumor agent smancs. *Cancer Res* 46, 6387–6392.
- Melancon, M. P., Zhou, M., Zhang, R., Xiong, C., Allen, P., Wen, X., et al. (2014). Selective uptake and imaging of aptamer- and antibody-conjugated hollow nanospheres targeted to epidermal growth factor receptors overexpressed in head and neck cancer. *ACS Nano* 8, 4530–4538. doi:10.1021/nn406632u
- Miao, L., Liu, C., Ge, J., Yang, W., Liu, J., Sun, W., et al. (2014). Antitumor effect of TRAIL on oral squamous cell carcinoma using magnetic nanoparticle-mediated gene expression. *Cell Biochem Biophys* 69, 663–672. doi:10.1007/s12013-014-9849-z
- Mizrachi, A., Shamay, Y., Shah, J., Brook, S., Soong, J., Rajasekhar, V. K., et al. (2017). Tumour-specific PI3K inhibition via nanoparticle-targeted delivery in head and neck squamous cell carcinoma. *Nat Commun* 8, 14292. doi:10.1038/ncomms14292
- Mohan, A., Narayanan, S., Balasubramanian, G., Sethuraman, S., and Krishnan, U. M. (2016). Dual drug loaded nanoliposomal chemotherapy: a promising strategy for treatment of head and neck squamous cell carcinoma. *Eur J Pharm Biopharm* 99, 73–83. doi:10.1016/j.ejpb.2015.11.017
- Mu, H., and Holm, R. (2018). Solid lipid nanocarriers in drug delivery: characterization and design. *Expert Opin Drug Deliv* 15, 771–785. doi:10.1080/17425247.2018.1504018
- Noguti, J., De Moura, C. F., De Jesus, G. P., Da Silva, V. H., Hossaka, T. A., Oshima, C. T., et al. (2012). Metastasis from oral cancer: an overview. *Cancer Genomics Proteomics* 9, 329–335.
- Nolte-T Hoen, E. N., Buschow, S. I., Anderton, S. M., Stoorvogel, W., and Wauben, M. H. (2009). Activated T cells recruit exosomes secreted by dendritic cells via LFA-1. *Blood* 113, 1977–1981. doi:10.1182/blood-2008-08-174094
- Pendleton, K. P., and Grandis, J. R. (2013). Cisplatin-based chemotherapy options for recurrent and/or metastatic squamous cell cancer of the head and neck. *Clin Med Insights Ther* 5, CMT.S10409. doi:10.4137/CMT.S10409
- Pérez-Herrero, E., and Fernández-Medarde, A. (2015). Advanced targeted therapies in cancer: drug nanocarriers, the future of chemotherapy. *Eur J Pharm Biopharm* 93, 52–79. doi:10.1016/j.ejpb.2015.03.018
- Petersen, P. E. (2009). Oral cancer prevention and control-the approach of the World Health Organization. *Oral Oncol* 45, 454–460. doi:10.1016/j.oraloncology.2008.05.023
- Pindiprolu, S. H., and Pindiprolu, S. K. S. (2019). CD133 receptor mediated delivery of STAT3 inhibitor for simultaneous elimination of cancer cells and cancer stem cells in oral squamous cell carcinoma. *Med Hypotheses* 129, 109241. doi:10.1016/j.mehy.2019.109241
- Price, K. A., and Cohen, E. E. (2012). Current treatment options for metastatic head and neck cancer. *Curr Treat Options Oncol* 13, 35–46. doi:10.1007/s11864-011-0176-y
- Putra, G., Huang, L., and Hsu, Y. C. (2016). “Cisplatin encapsulated nanoparticle as a therapeutic agent for anticancer treatment,” in *Biophotonics and immune responses xi*. Ed W.R. Chen (Bellingham, WA: Spie-Int Soc Optical Engineering). doi:10.1117/12.2214695
- Raub, C. B., Orwin, E. J., Haskell, R., and Ieee (2004). Immunogold labeling to enhance contrast in optical coherence Microscopy of tissue engineered corneal constructs. *Conf Proc IEEE Eng Med Biol Soc* 2, 1210–1213. doi:10.1109/IEMBS.2004.1403386
- Rosenberger, L., Ezquer, M., Lillo-Vera, F., Pedraza, P. L., Ortúzar, M. I., González, P. L., et al. (2019). Stem cell exosomes inhibit angiogenesis and tumor growth of oral squamous cell carcinoma. *Sci Rep* 9, 663. doi:10.1038/s41598-018-36855-6
- Sang, W., Zhang, Z., Dai, Y., and Chen, X. (2019). Recent advances in nanomaterial-based synergistic combination cancer immunotherapy. *Chem Soc Rev* 48, 3771–3810. doi:10.1039/c8cs00896e
- Schiller, G. J., Damon, L. E., Coutre, S. E., Hsu, P., Bhat, G., and Douer, D. (2018). High-dose vincristine sulfate liposome injection, for advanced, relapsed, or refractory philadelphia chromosome-negative acute lymphoblastic leukemia in an adolescent and young adult subgroup of a phase 2 clinical trial. *J Adolesc Young Adult Oncol* 7, 546–552. doi:10.1089/jayao.2018.0041
- Shah, J. P., and Lydiatt, W. (1995). Treatment of cancer of the head and neck. *CA Cancer J Clin* 45, 352–368. doi:10.3322/canjclin.45.6.352
- Shanavas, A., Sasidharan, S., Bahadur, D., and Srivastava, R. (2017). Magnetic core-shell hybrid nanoparticles for receptor targeted anti-cancer therapy and magnetic resonance imaging. *J Colloid Interface Sci* 486, 112–120. doi:10.1016/j.jcis.2016.09.060
- Siafaka, P. I., Üstündağ Okur, N., Karavas, E., and Bikiaris, D. N. (2016). Surface modified multifunctional and stimuli responsive nanoparticles for drug targeting: current status and uses. *Int J Mol Sci* 17. doi:10.3390/ijms17091440
- Siegel, R., Naishadham, D., and Jemal, A. (2013). Cancer statistics, 2013. *CA Cancer J Clin* 63, 11–30. doi:10.3322/caac.21166
- Siegel, R. L., Miller, K. D., Goding Sauer, A., Fedewa, S. A., Butterly, L. F., Anderson, J. C., et al. (2020). Colorectal cancer statistics, 2020. *CA Cancer J Clin* 70, 145–164. doi:10.3322/caac.21601
- Singh, A., and Sahoo, S. K. (2014). Magnetic nanoparticles: a novel platform for cancer theranostics. *Drug Discov Today* 19, 474–481. doi:10.1016/j.drudis.2013.10.005
- Skogberg, G., Lundberg, V., Berglund, M., Gudmundsdottir, J., Telemo, E., Lindgren, S., et al. (2015). Human thymic epithelial primary cells produce exosomes carrying tissue-restricted antigens. *Immunol Cell Biol* 93, 727–734. doi:10.1038/icb.2015.33
- Sofias, A. M., Dunne, M., Storm, G., and Allen, C. (2017). The battle of “nano” paclitaxel. *Adv Drug Deliv Rev* 122, 20–30. doi:10.1016/j.addr.2017.02.003
- Sokolov, K., Follen, M., Aaron, J., Pavlova, I., Malpica, A., Lotan, R., et al. (2003). Real-time vital optical imaging of precancer using anti-epidermal growth factor receptor antibodies conjugated to gold nanoparticles. *Cancer Res* 63 (9), 1999–2004.
- Song, J., Chen, X., Wang, M., Xing, Y., Zheng, Z., and Hu, S. (2014). Cardiac endothelial cell-derived exosomes induce specific regulatory B cells. *Sci Rep* 4, 7583. doi:10.1038/srep07583
- Souto, E. B., and Doktorovová, S. (2009). Chapter 6 - solid lipid nanoparticle formulations pharmacokinetic and biopharmaceutical aspects in drug delivery. *Meth Enzymol* 464, 105–129. doi:10.1016/S0076-6879(09)64006-4
- Terwogt, J. M., Schellens, J. H., Huinink, W. W., and Beijnen, J. H. (1999). Clinical pharmacology of anticancer agents in relation to formulations and administration routes. *Cancer Treat Rev* 25, 83–101. doi:10.1053/ctrv.1998.0107
- Théry, C., Amigorena, S., Raposo, G., and Clayton, A. (2006). Isolation and characterization of exosomes from cell culture supernatants and biological fluids. *Curr Protoc Cell Biol* 30 (1), 22. doi:10.1002/0471143030.cb0322s30
- Théry, C., Ostrowski, M., and Segura, E. (2009). Membrane vesicles as conveyors of immune responses. *Nat Rev Immunol* 9 (8), 581–593. doi:10.1038/nri2567
- Vodenkova, S., Buchler, T., Cervena, K., Veskrnova, V., Vodicka, P., and Vymetalkova, V. (2020). 5-fluorouracil and other fluoropyrimidines in colorectal cancer: past, present and future. *Pharmacol Ther* 206, 107447. doi:10.1016/j.pharmthera.2019.107447
- Wang, Y., and Gu, H. (2015). Core-shell-type magnetic mesoporous silica nanocomposites for bioimaging and therapeutic agent delivery. *Adv Mater Weinheim* 27, 576–585. doi:10.1002/adma.201401124
- Wang, Z., Liu, K., Huo, Z. J., Li, X. C., Wang, M., Liu, P., Pang, B., and Wang, S. J. (2015). A cell-targeted chemotherapeutic nanomedicine strategy for oral

- squamous cell carcinoma therapy. *J Nanobiotechnology* 13, 63. doi:10.1186/s12951-015-0116-2
- Wang, Y., Wan, G., Li, Z., Shi, S., Chen, B., Li, C., et al. (2017). PEGylated doxorubicin nanoparticles mediated by HN-1 peptide for targeted treatment of oral squamous cell carcinoma. *Int J Pharm* 525, 21–31. doi:10.1016/j.ijpharm.2017.04.027
- Wang, Q., Zhang, P., Li, Z., Feng, X., Lv, C., Zhang, H., et al. (2019a). Evaluation of polymer nanoformulations in hepatoma therapy by established rodent models. *Theranostics* 9, 1426–1452. doi:10.7150/thno.31683
- Wang, Y., Xie, D., Pan, J., Xia, C., Fan, L., Pu, Y., et al. (2019b). A near infrared light-triggered human serum albumin drug delivery system with coordination bonding of indocyanine green and cisplatin for targeting photochemistry therapy against oral squamous cell cancer. *Biomater Sci* 7, 5270–5282. doi:10.1039/c9bm01192g
- Ward, B. B., Dunham, T., Majoros, I. J., and Baker, J. R., Jr. (2011). Targeted dendrimer chemotherapy in an animal model for head and neck squamous cell carcinoma. *J Oral Maxillofac Surg* 69, 2452–2459. doi:10.1016/j.joms.2010.12.041
- Warnakulasuriya, S. (2009). Causes of oral cancer—an appraisal of controversies. *Br Dent J* 207, 471–475. doi:10.1038/sj.bdj.2009.1009
- Wiklander, O. P., Nordin, J. Z., O'loughlin, A., Gustafsson, Y., Corso, G., Mäger, I., et al. (2015). Extracellular vesicle *in vivo* biodistribution is determined by cell source, route of administration and targeting. *J Extracell Vesicles* 4, 26316. doi:10.3402/jev.v4.26316
- Wissing, S. A., Kayser, O., and Müller, R. H. (2004). Solid lipid nanoparticles for parenteral drug delivery. *Adv Drug Deliv Rev* 56, 1257–1272. doi:10.1016/j.addr.2003.12.002
- Wong, H. L., Bendayan, R., Rauth, A. M., Li, Y., and Wu, X. Y. (2007). Chemotherapy with anticancer drugs encapsulated in solid lipid nanoparticles. *Adv Drug Deliv Rev* 59, 491–504. doi:10.1016/j.addr.2007.04.008
- Woolgar, J. A., Scott, J., Vaughan, E. D., Brown, J. S., West, C. R., and Rogers, S. (1995). Survival, metastasis and recurrence of oral cancer in relation to pathological features. *Ann R Coll Surg Engl* 77 (5), 325–331.
- Xu, L., Kittrell, S., Yeudall, W. A., and Yang, H. (2016). Folic acid-decorated polyamidoamine dendrimer mediates selective uptake and high expression of genes in head and neck cancer cells. *Nanomedicine* 11, 2959–2973. doi:10.2217/nmm-2016-0244
- Xu, L., Yeudall, W. A., and Yang, H. (2017). Folic acid-decorated polyamidoamine dendrimer exhibits high tumor uptake and sustained highly localized retention in solid tumors: its utility for local siRNA delivery. *Acta Biomater* 57, 251–261. doi:10.1016/j.actbio.2017.04.023
- Yelin, D., Oron, D., Thiberge, S., Moses, E., and Silberberg, Y. (2003). Multiphoton plasmon-resonance microscopy. *Opt Express* 11, 1385–1391. doi:10.1364/oe.11.001385
- Yuan, Q., Yeudall, W. A., Lee, E., and Yang, H. (2019). Targeted inactivation of EPS8 using dendrimer-mediated delivery of RNA interference. *Int J Pharm* 557, 178–181. doi:10.1016/j.ijpharm.2018.12.060
- Zhang, Y., Wang, F., Li, M. Q., Yu, Z. Q., Qi, R. G., Ding, J. X., et al. (2018). Self-stabilized hyaluronate nanogel for intracellular codelivery of doxorubicin and cisplatin to osteosarcoma. *Advanced Science* 5 (6), 12. doi:10.1002/advs.201800811
- Zhang, H., Dong, S., Li, Z., Feng, X., Xu, W., Tuliniao, C. M. S., et al. (2020a). Biointerface engineering nanoplateforms for cancer-targeted drug delivery. *Asian J Pharm Sci* 15, 397–415. doi:10.1016/j.ajps.2019.11.004
- Zhang, Z., Zhuang, L., Lin, Y., Yan, M., Lv, J., Li, X., et al. (2020b). Novel drug delivery system based on hollow mesoporous magnetic nanoparticles for head and neck cancers—targeted therapy *in vitro* and *in vivo*. *Am J Cancer Res* 10 (1), 350–364.
- Zhu, M., Chen, S., Hua, L., Zhang, C., Chen, M., Chen, D., et al. (2017). Self-targeted salinomycin-loaded DSPE-PEG-methotrexate nanomicelles for targeting both head and neck squamous cell carcinoma cancer cells and cancer stem cells. *Nanomedicine (Lond)* 12, 295–315. doi:10.2217/nmm-2016-0382

Conflict of Interest: The authors declare that the research was conducted in the absence of any commercial or financial relationships that could be construed as a potential conflict of interest.

Copyright © 2020 Zhao, Li, Wu, Wang, Ma and Zhang. This is an open-access article distributed under the terms of the Creative Commons Attribution License (CC BY). The use, distribution or reproduction in other forums is permitted, provided the original author(s) and the copyright owner(s) are credited and that the original publication in this journal is cited, in accordance with accepted academic practice. No use, distribution or reproduction is permitted which does not comply with these terms.



Synthesis, Anti-Tumor Activity and Apoptosis-Inducing Effect of Novel Dimeric Keggin-Type Phosphotungstate

Yingxue Xue¹, Yifei Yin¹, He Li², Mingyu Chi¹, Jiaxin Guo¹, Guihua Cui¹ and Wenliang Li^{1,3*}

¹School of Pharmacy, Jilin Medical University, Jilin, China, ²Research and Development Department, NCPC Hebei Lexin Pharmaceutical Co., Ltd., Hebei, China, ³Jilin Collaborative Innovation Center for Antibody Engineering, Jilin Medical University, Jilin, China

OPEN ACCESS

Edited by:

Sanjun Shi,
Chengdu University of Traditional
Chinese Medicine, China

Reviewed by:

Shengnan Li,
Hebei University of Technology, China
Lingyu Zhang,
Northeast Normal University, China

*Correspondence:

Wenliang Li
wenliangl@ciac.ac.cn

Specialty section:

This article was submitted to
Pharmacology of Anti-Cancer Drugs,
a section of the journal
Frontiers in Pharmacology

Received: 24 November 2020

Accepted: 16 December 2020

Published: 27 January 2021

Citation:

Xue Y, Yin Y, Li H, Chi M, Guo J, Cui G
and Li W (2021) Synthesis, Anti-Tumor
Activity and Apoptosis-Inducing Effect
of Novel Dimeric Keggin-
Type Phosphotungstate.
Front. Pharmacol. 11:632838.
doi: 10.3389/fphar.2020.632838

A dimeric Keggin-type phosphotungstate (ODA)₁₀[(PW₁₁FeO₃₉)₂O]₂·9H₂O (abbreviated as ODA₁₀[(PW₁₁Fe)₂], ODA = octadecyltrimethylammonium bromide) was synthesized and investigated comprehensively its antitumor activity on MCF-7 and A549 cells. The dimeric structure and amorphous morphology were characterized by FT-IR, UV-vis-DRS, SEM and XRD. The *in vitro* MTT assay of ODA₁₀[(PW₁₁Fe)₂] showed anticancer activity on MCF-7 and A549 cells in a dose- and time-dependent manner, and the IC₅₀ values for MCF-7 and A549 cells at 48 h were 5.83 μg/ml and 3.23 μg/ml, respectively. The images of the ODA₁₀[(PW₁₁Fe)₂]-treated cells observed by inverted biological microscope exhibited the characteristic morphology of apoptosis. Flow cytometric analysis showed cell apoptosis and cycle arrested at S phase induced by ODA₁₀[(PW₁₁Fe)₂]. The above results illuminated the main mechanism of the antitumor action of ODA₁₀[(PW₁₁Fe)₂] on MCF-7 and A549 cells, indicating that this dimeric phosphotungstate is a promising anticancer drug.

Keywords: anti-tumor, apoptosis, dimeric, Keggin-type, phosphotungstate

INTRODUCTION

With the increasing morbidity and mortality, cancer has become a major killer that leads to health- and life-threatening for humans all over the world (Sun et al., 2019). At present, the main methods for the treatment of cancer are surgery, drug therapy, radiation therapy and cryotherapy. Among them, chemotherapy is also an effective method for cancer treatment (Xiao et al., 2019; Chen et al., 2020; Liu et al., 2020). Many chemotherapeutic agents, such as cisplatin (Weiss and Christian, 1993; Chen et al., 2018), fluorouracil (Arkenau et al., 2003) and capecitabine (Ssif et al., 2008), etc., have shown the potential for alleviating symptoms and curing the cancer (Cao et al., 2020; Geraldi, 2020; Zhao et al., 2020). However, most chemotherapeutic drugs possess inherent disadvantages, such as poor selectivity, severe side effect, low efficiency and drug resistance in cancer cells (Carr et al., 2008; Jonckheere et al., 2014; Hamis et al., 2018). Therefore, it is necessary to design drugs with high efficiency and low toxicity.

Polyoxometalates (abbreviated as POMs) are a series of transition metal oxygen anion clusters, which are mainly composed of molybdenum (Mo^{VI}), tungsten (W^{VI}), vanadium (V^V), niobium (Nb^V), and tantalum (Ta^V) in their highest oxidation state bridged by oxygen atoms (Rhule et al., 1998; Wang et al., 2003). Intriguingly, many other elements can be incorporated into the framework of POMs, leading to the diversity in structures and properties (Dianat et al., 2015), such as redox potential, polarity, thermal stability and electronic properties, etc., making them attractive for

application in the fields of catalysis (Mizuno et al., 2005; Hill, 2007), electrochemistry (Goura et al., 2020), material science (Du et al., 2010) and medicine (Muller et al., 1998). Jasmin et al. (1974) firstly reported the antiviral activity of $(\text{NH}_4)_{17}\text{Na}[\text{NaSb}_9\text{W}_{21}\text{O}_{86}]$ (HPA-23) against sarcoma virus. Since then, more POMs have been found to exhibit antitumor (Boulmier et al., 2017; Bijelic et al., 2019), antibacterial (Ma et al., 2020), antiviral (Qi et al., 2013), and antidiabetic activities (Liu W. J. et al., 2016). It is reported that POMs are significant antitumor drug candidates with high efficiency and low toxicity for curing most types of cancers, such as pancreatic cancer, breast cancer, leukemia, colon cancer, ovarian cancer and so on (Li et al., 2017; Hu et al., 2019).

The unique advantage of POMs over current drugs lies in the fact that the molecular structure and physicochemical properties of POMs are tunable and can be easily synthesized from readily available precursors in a few synthetic steps (Judd et al., 2001; Müller et al., 2006). POMs can be surface modified with synthetic organic compounds or natural molecules to effectively improve the biological activity *in vitro* and/or *in vivo* (Sun et al., 2016; Van Rompuy and Parac-Vogt, 2019). Electrostatic interaction, as a method of surface modification of POMs, combining organic counteranions (such as quaternary ammonium salts) with POM anions together, which makes the formed POMs take advantage of the synergistic effect and enhance the antitumor activity (Yu et al., 2014; Qu et al., 2017; Cheng et al., 2018). Quaternary ammonium salts are widely used as an antibacterial agent against a variety of bacteria, fungi and virus (Diz et al., 2001), which is based on the diversity in properties of low-molecular weight, outstanding cell membrane penetration, extended residence time, low toxicity, good biological activity and environmental stability (Dizman et al., 2006).

On the other hand, Keggin-type POMs were gaining increased interest as antitumor and antiviral agents due to the simple structure, small size and being easily synthesized (Shigeta et al., 2003; Zheng et al., 2009; Liu X. et al., 2016), such as $\text{K}_6\text{H}[\text{CoW}_{11}\text{O}_{39}\text{CpM}]\cdot n\text{H}_2\text{O}$ ($\text{M} = \text{Zr}, \text{Ti}, \text{Fe}, \text{Cp} = \eta^5\text{-C}_5\text{H}_5$), $\text{Ag}_3[\text{PW}_{12}\text{O}_{40}]$, $\text{Ag}_6[\text{SiW}_{10}\text{V}_2\text{O}_{40}]$ and $\text{Ag}_4[\text{SiW}_{12}\text{O}_{40}]$, all exhibiting inhibitory effect on tumor cells and sporotrichosis (Dianat et al., 2013; Mathias et al., 2020), respectively. But the work involving both the synthesis and antitumor effect of dimeric Keggin-type POMs are seldomly reported. Although the synthesis of dimeric $[\text{N}(\text{CH}_3)_4]_{10}[(\text{PW}_{11}\text{FeO}_{39})_2\text{O}]\cdot 12\text{H}_2\text{O}$ (Pichon et al., 2008) and $[\text{Bmim}]_{10}[(\text{PW}_{11}\text{FeO}_{39})_2\text{O}]\cdot 0.5\text{H}_2\text{O}$ (Santos et al., 2012) were reported, the further studies on the antitumor efficacy and mechanism of dimeric Keggin-type phosphotungstate with quaternary ammonium cation are not very frequent.

The exact mechanism of cancer cells death induced by POMs is still unknown, but it is reported that the antitumor activity of POMs correlates with their biological activities, including immunomodulatory (Sun et al., 2010), apoptotic (Cao et al., 2017) and inhibition effects toward enzymes (Prudent et al., 2008). Due to the lack of a comprehensive research on the biological mechanism of POMs, compared to much more common organic drugs, POMs as inorganic drugs are still rarely applied in

pharmacy field (Guo and Sadler, 1999). So, considerable attention has been paid to the cellular and molecular mechanisms between tumor cells and POMs.

In the present work, we have chosen the quaternary ammonium salt with relatively long alkyl chain of octadecyltrimethylammonium bromide (ODAB) as organic counteranion, which is expected to exhibit better biocompatibility and higher cell membrane penetration, because the biological activity of quaternary ammonium salts correlates with their molecular structure and the length of the carbon chain. The longer alkyl chain of the compounds contributes to higher antibacterial activity of theirs (Abel et al., 2002). Herein, it is firstly reported that a dimeric Keggin-type polyoxometalate $(\text{ODA})_{10}[(\text{PW}_{11}\text{FeO}_{39})_2\text{O}]\cdot 9\text{H}_2\text{O}$ ($(\text{ODA})_{10}[(\text{PW}_{11}\text{Fe})_2]$) was synthesized based on electrostatic interaction between octadecyltrimethylammonium cation and $[(\text{PW}_{11}\text{FeO}_{39})_2\text{O}]^{10-}$ anion. The structure and morphological feature of $(\text{ODA})_{10}[(\text{PW}_{11}\text{Fe})_2]$ were characterized. The *in vitro* antitumor activity of $(\text{ODA})_{10}[(\text{PW}_{11}\text{Fe})_2]$ on MCF-7 and A549 cells was investigated. And the morphological changes and cell density of MCF-7 and A549 cells induced by $(\text{ODA})_{10}[(\text{PW}_{11}\text{Fe})_2]$ were detected by inverted biological microscopy. Furthermore, cell apoptosis and cell cycle distribution were analyzed.

MATERIALS AND METHODS

Materials

Sodium tungstate dihydrate ($\text{Na}_2\text{WO}_4\cdot 2\text{H}_2\text{O}$), Sodium phosphate dibasic (Na_2HPO_4), Iron nitrate nonahydrate ($\text{Fe}(\text{NO}_3)_3\cdot 9\text{H}_2\text{O}$), Sodium bicarbonate (NaHCO_3) and octadecyltrimethylammonium bromide (ODAB) were acquired from Sinopharm Chemical Reagent Co. Ltd., China. Cisplatin and carboplatin were purchased from Nanjing Jingzhu Bio-technology Co., Ltd. (Nanjing, China). Trypsin, phosphate buffer saline (PBS), dimethyl sulfoxide (DMSO) and 3-[4,5-dimethylthiazol-2-yl]-2,5-diphenyltetrazolium bromide (MTT) were obtained from Sigma (St. Louis, MO, United States). Fetal bovine serum (FBS), RPMI-1640 Medium and penicillin-streptomycin were purchased from Gibco BRL (Grand Island, NY, United States). Annexin V-FITC apoptosis detection kit and cell cycle kit were obtained from BD Biosciences (San Jose, CA, United States). All chemicals and solvents were used as received from commercial sources without further purification. $(\text{TEA})_{10}[(\text{PW}_{11}\text{FeO}_{39})_2\text{O}]\cdot 3\text{H}_2\text{O}$ and $(\text{TMA})_{10}[(\text{PW}_{11}\text{FeO}_{39})_2\text{O}]\cdot 4\text{H}_2\text{O}$ (TEA = tetraethyl ammonium bromide, TMA = tetramethyl ammonium bromide) were prepared according to the literature (Pichon et al., 2008), and the characteristic data were consistent with previously published values (Pichon et al., 2008; Santos et al., 2012).

General Measurements

The content of P, W, Fe in the phosphotungstate was performed on an ICP-OES Plasma Spec (Thermo iCAP 6000), and the elemental analysis of C, H, N was tested on a CHN elemental analyzer (Perkin-Elmer 2400). Thermogravimetric analysis (TGA) was measured on a Shimadzu DTG-60 instrument using N_2 , with a heating rate of 6°C min^{-1} . Fourier Transform

infrared (FT-IR) spectroscopy was tested by Nicolet-Impact 400 spectrometer using KBr disk. The UV-vis diffuse reflectance spectra (UV-vis DRS) were performed on a UV-Vis-NIR spectrometer (Agilent Technologies Cary Series) using BaSO₄ as reference. X-ray diffraction (XRD) data were tested by a SHIMADZU XRD-6000 X-ray diffractometer with Cu K α radiation ($\lambda = 0.1548$ nm). The morphology of the phosphotungstate was analyzed by scanning electron microscope (SEM) performed on a JSM-6360LV microscope. Particle size distribution was obtained by dynamic light scattering (DLS) using a Mastersizer 2000 laser particle size analyzer.

Synthesis of (ODA)₁₀[(PW₁₁FeO₃₉)₂O]·9H₂O (ODA₁₀[(PW₁₁Fe)₂])

Na₂WO₄·2H₂O (3.3 g) was dissolved in 20 ml of distilled H₂O in a flask. Then Na₂HPO₄ powder (0.13 g) was added to the solution in a molar proportion (Na₂WO₄·2H₂O: Na₂HPO₄) of 11:1. After 1 h of stirring at 80–90°C, conc. HNO₃ was added drop by drop to make the pH of the solution be 4.8. Then, Fe(NO₃)₃·9H₂O (0.49 g, 1.2 mmol) was added and the pH was adjusted to 4.5 by adding NaHCO₃ (1 M) drop by drop. 1.8 g of octadecyltrimethylammonium bromide (ODAB) was added, causing yellow precipitates produced, which were then filtrated, washed twice with distilled water and dried under vacuum. Anal. (%): calcd for (ODA)₁₀[(PW₁₁FeO₃₉)₂O]·9H₂O: P, 0.71; W, 46.14; Fe, 1.28; C, 28.76; H, 5.45; N, 1.60; H₂O, 1.85; found: P, 0.78; W, 48.16; Fe, 1.33; C, 29.21; H, 5.49; N, 1.65; H₂O, 1.91.

Cell Lines and Cell Culture Conditions

Human breast cancer cells MCF-7 and human non-small cell lung cancer cells A549 (ATCC) were incubated in RPMI 1640 medium with penicillin (100 U/ml), streptomycin (100 µg/ml) and FBS (10%) at 37°C with 5% CO₂ in an incubator.

Cell Viability Studies

The anti-proliferation effect of the phosphotungstate was detected by the MTT assay. The stock solution of ODA₁₀[(PW₁₁Fe)₂] with the concentration of 1 mg/ml was prepared in DMSO, and then sterilized by the methyl cellulose ester filter membrane with pore size 0.22 µm. At last, the stock solution was diluted by RPMI 1640 under sterile condition.

Cells were seeded into a 96-well plate at a density of 1×10^4 cells/well. 100 µl/well of RPMI 1640 medium was added to each well to incubate the cells for 24 h, and then the medium was replaced by various concentrations of ODA₁₀[(PW₁₁Fe)₂] (1, 3, 6, 12, 24 µg/ml). Each concentration has four duplicate samples. After 6, 12, 24 and 48 h, 20 µl of MTT (5 mg/ml) was added to each well, and then the plate continued to be incubated for 4 h in the incubator. Next, the formed formazan crystals were dissolved in 150 µl DMSO after removing the MTT medium. Finally, the absorbance was measured at a wavelength of 490 nm by an automatic microplate reader.

Morphological Observation

To observe whether the density and morphology of the tumor cells induced by the phosphotungstate changed or not, cells were seeded into a 6-well plate at a density of 2×10^5 cells/well for 24 h at 37°C, and then treated with different concentration of ODA₁₀[(PW₁₁Fe)₂] (1–24 µg/ml). After 24 h, the cellular density and morphology were observed by the inverted biological microscopy (XDS1C, Shanghai Wanheng Precision Instrument Co. Ltd., China).

Flow Cytometry Analysis of Cell Apoptosis

Cells were seeded into a six-well plate (2×10^5 cells/well) for 24 h, and then exposed to different concentration of ODA₁₀[(PW₁₁Fe)₂] (1–24 µg/ml). After 24 h, the cells were collected, washed thrice with cold PBS and then centrifugated. After discarding the supernatant, the cells were resuspended in Annexin-V-FITC/PI solution and remained in the dark for 15 min at room temperature. The cell apoptosis was determined on a FAC Scanto™ flow cytometer (Becton Dickinson, United States).

Flow Cytometry Analysis of Cell Cycle Distribution

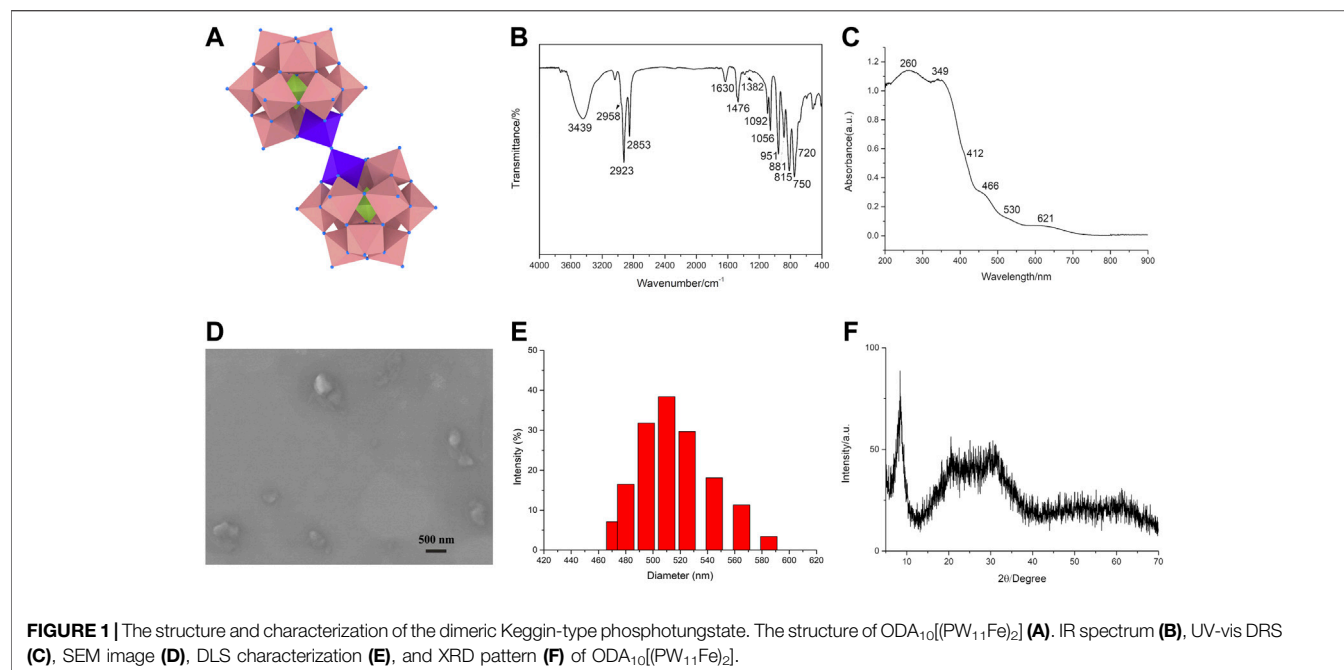
Cells were seeded into a six-well plate (10^6 cells/well) for 24 h at 37°C, and then exposed to different concentration of ODA₁₀[(PW₁₁Fe)₂] (1–24 µg/ml). After 24 h, the cells were collected using trypsin, centrifugated and then washed with PBS for two times. After being fixed by ice-cold 70% ethanol at 4°C overnight, the cells continued to be washed with cold PBS and resuspended in propidium iodide (PI) staining solution in the dark at 37°C for 30 min. Finally, the cell cycle was determined on a FAC Scanto™ flow cytometer (Becton Dickinson, United States).

RESULTS AND DISCUSSION

Synthesis and Characterization of the Dimeric Keggin-Type Phosphotungstate

The adjustment of pH is vital to the synthesis of the dimeric oxo-bridged [(PW₁₁FeO₃₉)₂O]¹⁰⁻ anion, which usually exists at pH = 3–5 (Liu K. et al., 2016). The dimeric phosphotungstate ODA₁₀[(PW₁₁Fe)₂] consists of two phosphotungstate units PW₁₁Fe^{III}O₃₉, which are linked by Fe-O-Fe bond, the structure is shown in **Figure 1A**.

FT-IR spectra provided clear evidence for the successful preparation of the dimeric Keggin-type phosphotungstate ODA₁₀[(PW₁₁Fe)₂] (**Figure 1B**). IR spectrum of ODA₁₀[(PW₁₁Fe)₂] showed characteristic peaks of Keggin-type polyoxometalates (Kuznetsova et al., 1996), which appeared at 1,092, 1,056, 951, 881, 815 cm⁻¹. The peaks at 1,092, 1,056 cm⁻¹ were assigned to asymmetric P-O_a stretching band. The peak at 951 cm⁻¹ corresponded to ν_{as} (W = O_d) vibration. The peaks attributed to ν_{as} (W-O_b-W) and ν_{as} (W-O_c-W) vibrations appeared at 881 and 815 cm⁻¹, respectively. In addition, the asymmetric Fe-O-Fe stretching vibration of dimeric phosphotungstates was observed at 750 cm⁻¹ with a shoulder



around 720 cm⁻¹ (Kuznetsova et al., 1996; Kuznetsova et al., 1997), which illuminated the dimeric structure of ODA₁₀[(PW₁₁Fe)₂]. The IR peaks ascribed to the -CH₂ asymmetric and symmetric stretching bands appeared at 2,923 and 2,853 cm⁻¹, showing the existence of quaternary ammonium in ODA₁₀[(PW₁₁Fe)₂]. The bands attributed to the -CH₃ asymmetric stretching and scissoring modes were observed at 2,958 and 1,382 cm⁻¹, respectively. The peak at 1,476 cm⁻¹ was due to the -CH₂ scissoring modes (Myrzakozha et al., 1999a; Myrzakozha et al., 1999b). The characteristic peaks of water were observed at 3,439 and 1,630 cm⁻¹. The above results illuminated that ODA₁₀[(PW₁₁Fe)₂] was of dimeric Keggin-type structure and prepared by electrostatic interaction between quaternary ammonium cations and heteropoly anions.

UV-vis DRS of the dimeric ODA₁₀[(PW₁₁Fe)₂] is shown in **Figure 1C**. The absorption at 260 nm was due to O→W charge transfer transition. The bands at 349 nm and 412 nm corresponded to O→Fe charge transfer transition of oxo-bridged di-iron complexes (Kurtz, 1990). Another evidence of Fe-O-Fe bond presented the characteristic absorptions at 466, 530 and 621 nm which were attributed to O→Fe charge transfer transitions (Kurtz, 1990). So, the IR and UV-vis DRS results all indicated that ODA₁₀[(PW₁₁Fe)₂] possessed dimeric structure.

The SEM image of the dimeric ODA₁₀[(PW₁₁Fe)₂] is shown in **Figure 1D**. The particles of ODA₁₀[(PW₁₁Fe)₂] were slightly irregular in shape and the particle size was about 510 nm measured by DLS (**Figure 1E**), which was consistent with the result of SEM image. The obtained particles showed amorphous morphology, which might be caused by the relatively long carbon chain of organic counterations, making no crystalline feature observed in ODA₁₀[(PW₁₁Fe)₂], which was also proved by the results of

XRD pattern of ODA₁₀[(PW₁₁Fe)₂] (**Figure 1F**). The spectrum recorded for ODA₁₀[(PW₁₁Fe)₂] indicated an amorphous feature due to the lack of crystallinity caused by ODAB, which had strong diffraction peaks at the 2θ degree of 6.9°–10.3° and a weak broad peak at 14.3°–39.2°. The characteristic diffractions of Keggin-type polyoxometalate were detected at 8.28°, 8.9°, 9.1°, 27.9° and 28.9°, etc (Jalil et al., 2003), so it is concluded that ODA₁₀[(PW₁₁Fe)₂] was of Keggin-type structure. The broad peak at 14.3°–39.2° manifested again that the poor crystallinity of ODA₁₀[(PW₁₁Fe)₂] resulted from the longer carbon chain of quaternary ammonium cations. The above results of SEM and XRD proved that the dimeric ODA₁₀[(PW₁₁Fe)₂] had amorphous morphology and contained Keggin-type structure after quaternary ammonium cations combining with heteropoly anions.

Anticancer Activity Studies

The *in vitro* anti-proliferation activity of ODA₁₀[(PW₁₁Fe)₂] on MCF-7 and A549 cells was evaluated by the MTT assay. Cells were exposed to different concentrations of ODA₁₀[(PW₁₁Fe)₂] (1, 3, 6, 12, 24 μg/ml) for 6, 12, 24 and 48 h. As shown in **Figures 2A,B**, the cell viability decreased with the concentration of ODA₁₀[(PW₁₁Fe)₂] increasing, which illuminated that the anti-proliferative effects of ODA₁₀[(PW₁₁Fe)₂] depended on its concentration. For MCF-7 cells, after treatment with ODA₁₀[(PW₁₁Fe)₂], the cell viability declined to 76.4 at 6, 52.1 at 12, 36.9 at 24 and 14.2% at 48 h. Analogously, for A549 cells, the cell viability was 70.7, 56.8, 26.3 and 4.7% at 6, 12, 24 and 48 h, respectively. The above results indicated that ODA₁₀[(PW₁₁Fe)₂] exhibited inhibitory activity against tumor cells growth in a time-

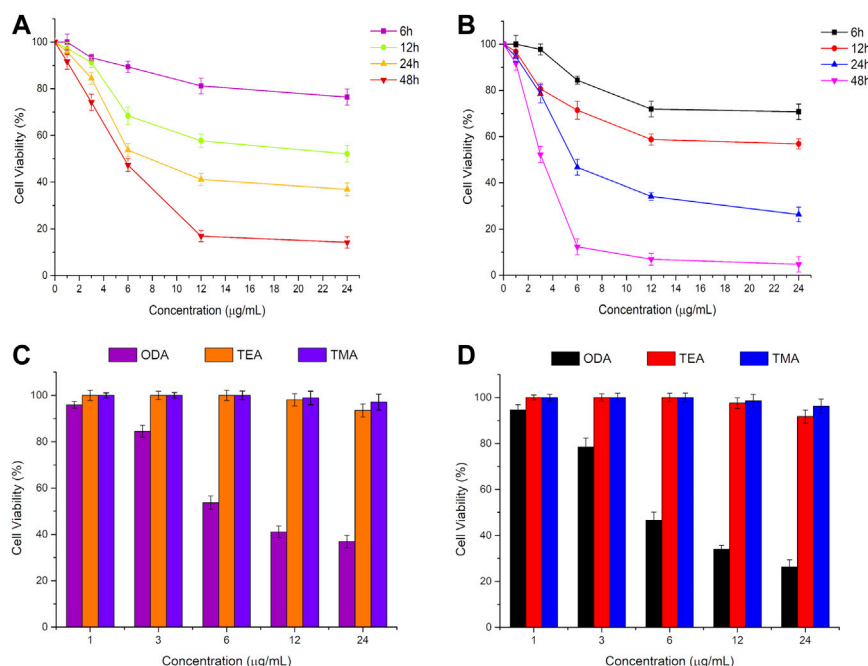


FIGURE 2 | *In vitro* cytotoxicity profiles of ODA₁₀[(PW₁₁Fe)₂] on MCF-7 cells (A) and A549 cells (B) for 6, 12, 24 and 48 h, and different phosphotungstates on MCF-7 cells (C) and A549 cells (D) for 24 h by MTT at different doses. (ODA: ODA₁₀[(PW₁₁Fe)₂]; TEA: (TEA)₁₀[(PW₁₁FeO₃₉)₂O]·3H₂O; TMA: (TMA)₁₀[(PW₁₁FeO₃₉)₂O]·4H₂O).

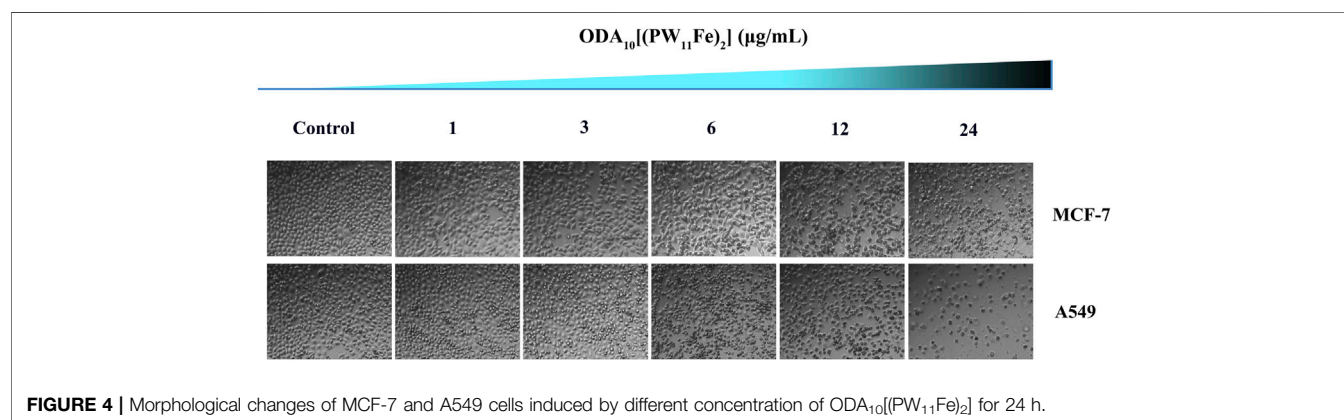
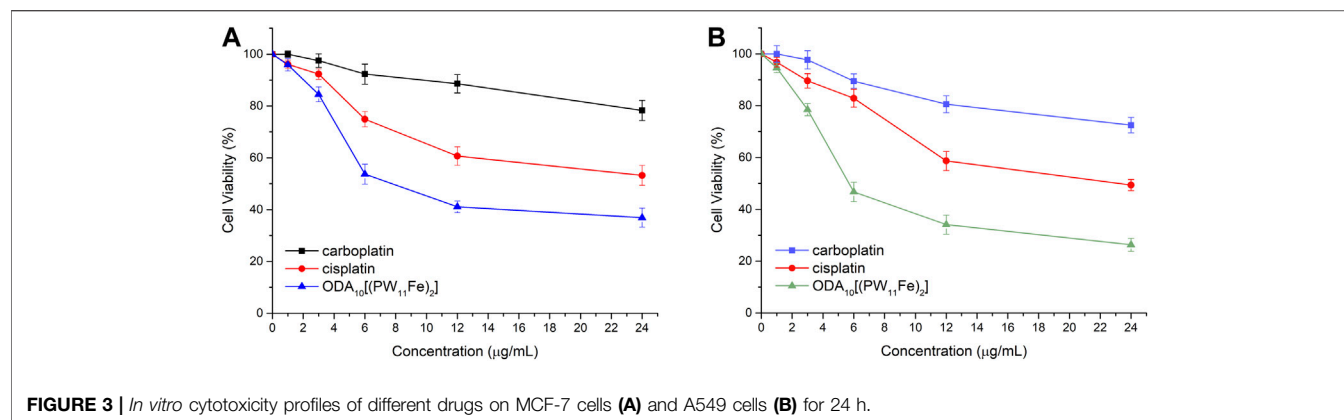
TABLE 1 | IC₅₀ and IC₂₅ values of ODA₁₀[(PW₁₁Fe)₂] against MCF-7 and A549 cells.

Cell line	IC ₅₀ (μg/ml)				IC ₂₅ (μg/ml)			
	6 h	12 h	24 h	48 h	6 h	12 h	24 h	48 h
MCF-7	—	—	8.02	5.83	29.28	5.05	4.13	2.78
A549	—	—	5.75	3.23	10.68	4.71	3.35	1.92

dependent effect during these periods. IC₅₀ values of ODA₁₀[(PW₁₁Fe)₂] against MCF-7 and A549 cells at different time were presented in **Table 1**. The calculated IC₅₀ values in MCF-7 cells for 24 and 48 h were 8.02 μg/ml and 5.83 μg/ml, respectively, and for A549 cells, the IC₅₀ value was observed to be 5.75 μg/ml at 24 h and 3.23 μg/ml at 48 h. For the short treatment time groups, 6 h and 12 h, of MCF-7 and A549 cells, the inhibition rate was lower than 50%, thus IC₅₀ values in MCF-7 and A549 cells for 6 h and 12 h were not obtained in **Table 1**. Nevertheless, IC₂₅ values of ODA₁₀[(PW₁₁Fe)₂] against MCF-7 and A549 cells at different times were calculated and shown in **Table 1**. For MCF-7 cells, IC₂₅ values were 29.28 μg/ml, 5.05 μg/ml, 4.13 μg/ml and 2.78 μg/ml at 6, 12, 24 and 48 h, respectively, and IC₂₅ values in A549 cells for 6, 12, 24 and 48 h were 10.68 μg/ml, 4.71 μg/ml, 3.35 μg/ml and 1.92 μg/ml, respectively. The IC₅₀ and IC₂₅ values were sharply reduced when the drug treatment time prolonged. These data suggested that ODA₁₀[(PW₁₁Fe)₂] could inhibit MCF-7 and A549 cells growth in a time-dependent manner, and the antiproliferation effect on A549 cells was stronger than that on MCF-7 cells.

Moreover, the antitumor activity of ODA₁₀[(PW₁₁Fe)₂] was compared with that of dimeric (TEA)₁₀[(PW₁₁FeO₃₉)₂O]·3H₂O (abbreviated as TEA) and (TMA)₁₀[(PW₁₁FeO₃₉)₂O]·4H₂O (abbreviated as TMA) containing relatively short alkyl chain at the same concentration, which was shown in **Figures 2C,D**. After treatment of the drugs for 24 h, ODA₁₀[(PW₁₁Fe)₂] showed the highest anticancer effect, while nearly no inhibition efficacy against MCF-7 and A549 cells was induced by TEA and TMA, that is because the longer alkyl chain in the quaternary ammonium cation of ODA₁₀[(PW₁₁Fe)₂] possessed better cell membrane penetration (Abel et al., 2002), which is beneficial for ODA₁₀[(PW₁₁Fe)₂] to interact with tumor cells, thus ODA₁₀[(PW₁₁Fe)₂] exhibited excellent antiproliferation effect on MCF-7 and A549 cells. The above results demonstrated that the dimeric Keggin-type POMs modified by quaternary ammonium cation with longer alkyl chain showed higher antitumor activity.

The anticancer activity of ODA₁₀[(PW₁₁Fe)₂] on MCF-7 and A549 cells was further compared with that of the clinical chemotherapeutic agents, such as cisplatin and carboplatin, under the same conditions, which was presented in **Figure 3**. After treatment of the drugs for 24 h, ODA₁₀[(PW₁₁Fe)₂] showed the strongest inhibitory effects against MCF-7 and A549 cells compared to cisplatin and carboplatin. From the above results, it can be demonstrated that ODA₁₀[(PW₁₁Fe)₂] exhibited an anti-proliferation effect on the tumor cells in a dose- and time-dependent manner, and can be utilized as an antitumor drug candidate for the treatment of cancer.



Cell Morphology

The changes of the cellular density and morphology of MCF-7 and A549 cells with the treatment of different doses of ODA₁₀[(PW₁₁Fe)₂] were directly detected using an inverted microscope (Figure 4). After treatment of 24 h, cells of control group were nested distribution, flattened and showed normal cell architecture. The cell shape was regular polygon and few round cells existed. While the morphology of the ODA₁₀[(PW₁₁Fe)₂]-treated cells obviously changed. The cells were becoming round, shrunken, altered adherence, as well as the appearance of a large number of cell membrane blistering, which was the characteristic morphology of apoptosis. Moreover, the density of the cells was reduced with the drug concentration increasing, showing a dose-dependent effect. This phenomenon indicated that ODA₁₀[(PW₁₁Fe)₂] could induce cell apoptosis.

Flow Cytometry Analysis of Cell Apoptosis

The cell apoptosis against MCF-7 and A549 cells induced by different concentrations of ODA₁₀[(PW₁₁Fe)₂] (1, 3, 6, 12, 24 μg/ml) for 24 h was evaluated using Annexin V-FITC/PI double-staining technique. As shown in Figure 5, the apoptotic cells

could be obviously detected by distinct double staining patterns: necrotic (upper left square), viable cells (lower left square), late apoptotic (upper right square) and early apoptotic (lower right square). The results manifested that the ratio of apoptotic (early and late) cells induced by ODA₁₀[(PW₁₁Fe)₂] obviously increased in a dose-dependent manner compared to control group. For MCF-7 cells, after treated with ODA₁₀[(PW₁₁Fe)₂], the proportion of apoptotic cells ranged from 3.69 to 20.78% with the concentration increasing, which was higher than that in control group (2.31%). For A549 cells, the percentage of apoptotic cells in control group was 1.1%, while that in drug-treatment group was 7.88, 15.22, 27.98, 29.68 and 38.26% at the concentration of 1–24 μg/ml, respectively. Taken together, ODA₁₀[(PW₁₁Fe)₂] could inhibit the MCF-7 and A549 cells growth and induce the apoptosis of tumor cells.

Flow Cytometry Analysis of Cell Cycle Distribution

In order to detect whether the antiproliferation effect against MCF-7 and A549 cells of ODA₁₀[(PW₁₁Fe)₂] is caused by cell cycle arrest, MCF-7 and A549 cells were treated with different

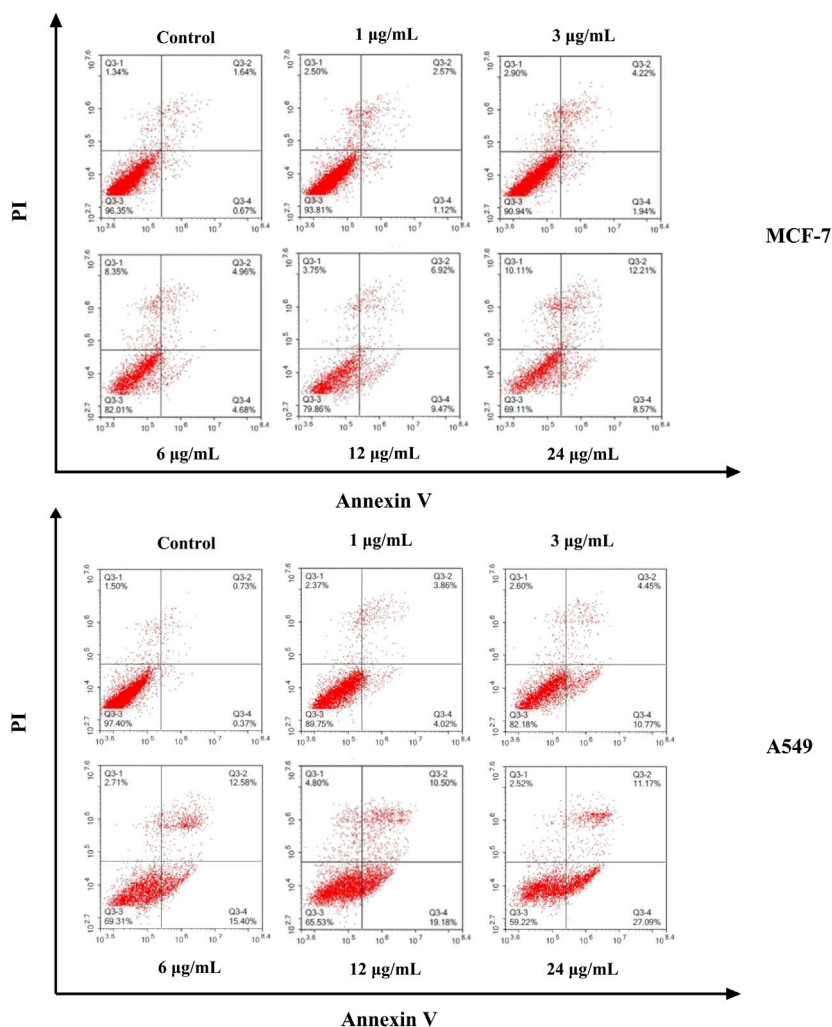


FIGURE 5 | Flow cytometry analysis of MCF-7 and A549 cell apoptosis induced by different concentration of $\text{ODA}_{10}[(\text{PW}_{11}\text{Fe})_2]$ for 24 h.

doses of $\text{ODA}_{10}[(\text{PW}_{11}\text{Fe})_2]$ (1, 3, 6, 12, 24 $\mu\text{g/ml}$) for 24 h with PI staining. The content of DNA was examined by flow cytometry. Generally, the process of cell replication is related to the doubling of DNA and other cellular contents. There are four distinct phases divided from cell cycle distribution: G_1 , S, G_2 and M phase, the entry to which is carefully regulated by different checkpoints. S phase is responsible for the synthesis of DNA. The cell prepares to divide during G_2 phase and division takes place during M phase. Then, the cells continue to divide after passing these checkpoints. Moreover, many external factors such as drugs, radiation and ROS (reactive oxygen species) can induce DNA-damage during S which causes the death of cells (Rodriguez-Vargas et al., 2012; Preya et al., 2017).

The results of cell cycle arrest of MCF-7 and A549 cells induced by different concentrations of $\text{ODA}_{10}[(\text{PW}_{11}\text{Fe})_2]$ from 1 to 24 $\mu\text{g/ml}$ are shown in **Figure 6**. The cell population at S phase of MCF-7 cells in the drug-treatment group increased

from 17.82 to 32.92%, in a dose-dependent effect, which was higher than that in control group (17.71%). The level of G_2 /M phase exhibited no obvious variations after treatment of $\text{ODA}_{10}[(\text{PW}_{11}\text{Fe})_2]$, accompanied by a significant reduction in G_1 phase (**Figure 6A**). Similar to MCF-7 cells, as shown in **Figure 6B**, for A549 cells, the level of S phase increased from 13.8% in the control group to 16.89, 18.47, 36.63, 44.39, and 45.51%, respectively, with the proportions of G_1 and G_2 /M phase decreasing. The ratios of G_1 and G_2 /M phase decreased from 55.74 to 26.7% and 33.08 to 24.19%, respectively. Since DNA replicates during S phase, the above results manifested that DNA damaged at S phase and the antitumor mechanism on MCF-7 and A549 cells was S phase arrest.

CONCLUSION

A novel dimeric Keggin-type polyoxometalate $(\text{ODA})_{10}[(\text{PW}_{11}\text{FeO}_3)_2\text{O}] \cdot 9\text{H}_2\text{O}$ ($\text{ODA}_{10}[(\text{PW}_{11}\text{Fe})_2]$) was firstly

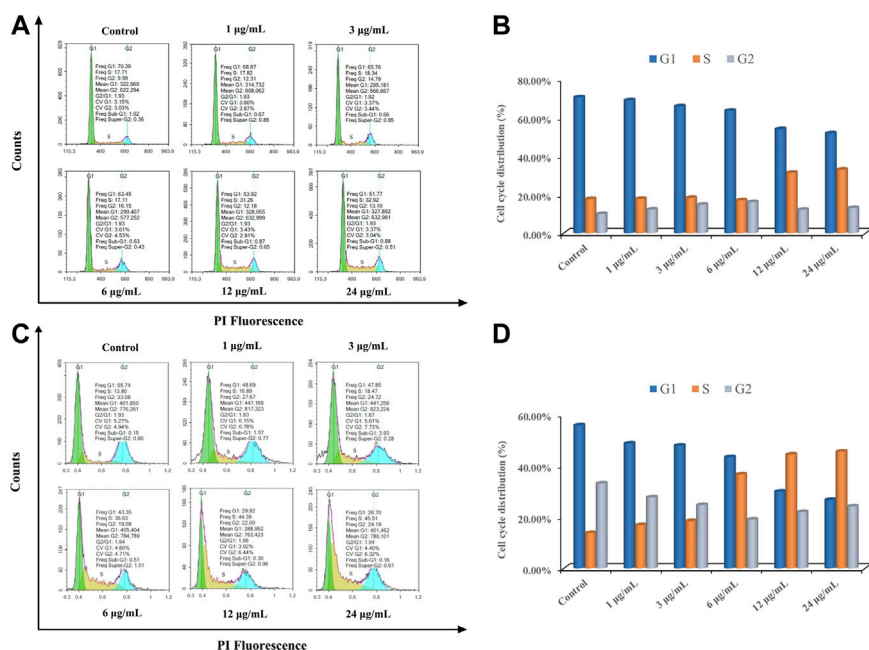


FIGURE 6 | ODA₁₀[(PW₁₁Fe)₂] induces cell cycle arrest in MCF-7 and A549 cells. MCF-7 cells (A) and A549 cells (C) were treated with various concentrations of ODA₁₀[(PW₁₁Fe)₂] for 24 h, and cell cycle arrest was examined by flow cytometry. Quantitative bar graphs of the proportion of MCF-7 cells (B) and A549 cells (D) in different phases.

synthesized with the aid of octadecyltrimethylammonium cation. A comprehensive study on antitumor activity of ODA₁₀[(PW₁₁Fe)₂] against MCF-7 and A549 cells was carried out. ODA₁₀[(PW₁₁Fe)₂] could inhibit MCF-7 and A549 cells growth in a dose- and time-dependent manner, and the IC₅₀ value for MCF-7 and A549 cells was 5.83 µg/ml and 3.23 µg/ml at 48 h, respectively. The higher antitumor activity was due to the better cell membrane penetration of octadecyltrimethylammonium cation with longer alkyl chain. The morphology of MCF-7 and A549 cells treated with ODA₁₀[(PW₁₁Fe)₂] exhibited the characteristics of apoptosis. The Flow cytometry analysis results manifested the fact of the cell apoptosis and cycle arrested at S phase induced by ODA₁₀[(PW₁₁Fe)₂] as the main mechanism for antiproliferation of MCF-7 and A549 cells. Our work has demonstrated that ODA₁₀[(PW₁₁Fe)₂] can be utilized as an antitumor drug candidate for the treatment of cancer.

REFERENCES

- Abel, T., Cohen, J. I., Engel, R., Filshinsky, M., Melkonian, A., and Melkonian, K. (2002). Preparation and investigation of antibacterial carbohydrate-based surfaces. *Carbohydr. Res.* 337, 2495–2499. doi:10.1016/S0008-6215(02)00316-6
- Arkenau, H. T., Bermann, A., Rettig, K., Strohmeyer, G., and Porschen, R. (2003). 5-Fluorouracil plus leucovorin is an effective adjuvant chemotherapy in curatively resected stage III colon cancer: long-term follow-up results of the adjCCA-01 trial. *Ann. Oncol.* 14, 395–399. doi:10.1093/annonc/mdg100
- Bijelic, A., Aureliano, M., and Rompel, A. (2019). Polyoxometalates as potential next-generation metallodrugs in the combat against cancer. *Angew. Chem. Int. Ed. Engl.* 58, 2980–2999. doi:10.1002/anie.201803868

DATA AVAILABILITY STATEMENT

The original contributions presented in the study are included in the article/Supplementary Material, further inquiries can be directed to the corresponding author.

AUTHOR CONTRIBUTIONS

YX and WL designed the experiments. YY, MC, and JG carried out the experiments and wrote the manuscript. GC and HL helped analyzing the experimental results.

FUNDING

This work was financially supported by the Grant of Jilin Province Science & Technology Committee (No. 20180101194JC).

- Boulmier, A., Feng, X. X., Oms, O., Mialane, P., Rivière, E., Shin, C. J., et al. (2017). Anticancer activity of polyoxometalate-bisphosphonate complexes: synthesis, characterization, *in vitro* and *in vivo* results. *Inorg. Chem.* 56, 7558–7565. doi:10.1021/acs.inorgchem.7b01114
- Cao, H., Li, C., Qi, W., Meng, X., Tian, R., Qi, Y., et al. (2017). Synthesis, cytotoxicity and antitumor mechanism investigations of polyoxometalate doped silica nanospheres on breast cancer MCF-7 cells. *PLoS One.* 12, e0181018. doi:10.1371/journal.pone.0181018
- Cao, S. W., Lin, C. H., Liang, S. N., Chee, H. T., Phei, E. S., and Xu, X. D. (2020). Enhancing chemotherapy by RNA interference. *BIO Integration.* 1 (18), 64–81. doi:10.15212/bioi-2020-0003
- Carr, C., Ng, J., and Wigmore, T. (2008). The side effects of chemotherapeutic agents. *Curr. Anaesth. Crit. Care.* 19, 70–79. doi:10.1016/j.cacc.2008.01.004

- Chen, Q., Yang, Y., Lin, X., Ma, W., Chen, G., Li, W., et al. (2018). Platinum(IV) prodrugs with long lipid chains for drug delivery and overcoming cisplatin resistance. *Chem. Commun.* 54, 5369–5372. doi:10.1039/c8cc02791a
- Chen, Y. H., Du, M., Yu, J. S., Rao, L., Chen, X. Y., and Chen, Z. Y. (2020). Nanobiohybrids: a synergistic integration of bacteria and nanomaterials in cancer therapy. *BIO Integration*. 1 (12), 25–36. doi:10.15212/bioi-2020-0008
- Cheng, M., Li, N., Wang, N., Hu, K. H., Xiao, Z. C., Wu, P. F., et al. (2018). Synthesis, structure and antitumor studies of a novel decavanadate complex with a wavelike two-dimensional network. *Polyhedron*. 155, 313–319. doi:10.1016/j.poly.2018.08.052
- Dianat, S., Bordbar, A. K., Tangestaninejad, S., Yadollahi, B., Amiri, R., Zarkesh-Esfahani, S. H., et al. (2015). *In vitro* antitumor activity of free and nano-encapsulated $\text{Na}_5[\text{PMo}_{10}\text{V}_2\text{O}_{40}]\cdot n\text{H}_2\text{O}$ and its binding properties with ctDNA by using combined spectroscopic methods. *J. Inorg. Biochem.* 152, 74–81. doi:10.1016/j.jinorgbio.2015.08.015
- Dianat, S., Bordbar, A. K., Tangestaninejad, S., Yadollahi, B., Zarkesh-Esfahani, S. H., and Habibi, P. (2013). ctDNA binding affinity and *in vitro* antitumor activity of three Keggin type polyoxotungstates. *J. Photochem. Photobiol. B*. 124, 27–33. doi:10.1016/j.jphotobiol.2013.04.001
- Diz, M., Infante, M. R., and Erra, P. (2001). Antimicrobial activity of wool treated with a new thiol cationic surfactant. *Text. Res. J.* 71, 695–700. doi:10.1177/004051750107100808
- Dizman, B., Elasri, M. O., and Mathias, L. J. (2006). Synthesis and antibacterial activities of water-soluble ethacrylate polymers containing quaternary ammonium compounds. *J. Polym. Sci. Part A: Polym. Chem.* 44, 5965–5973. doi:10.1002/pola.21678
- Du, D. Y., Qin, J. S., Li, S. L., Lan, Y. Q., Wang, X. L., and Su, Z. M. (2010). 3d-4f heterometallic complexes for the construction of POM-based inorganic-organic hybrid compounds: from nanoclusters to one-dimensional ladder-like chains. *Aust. J. Chem.* 63, 1389–1395. doi:10.1071/CH10047
- Geraldi, A. (2020). Advances in the production of minor ginsenosides using microorganisms and their enzymes. *BIO Integration*. 1, 15–24. doi:10.15212/bioi-2020-0007
- Goura, J., Bassil, B. S., Bindra, J. K., Rutkowska, I. A., Kulesza, P. J., Dalal, N. S., et al. (2020). $\text{Fe}_{48}^{\text{II}}$ -containing 96-tungsto-16-phosphate: synthesis, structure, magnetism and electrochemistry. *Chem. Eur. J.* 26, 1–5. doi:10.1002/chem.202002832
- Guo, Z. J., and Sadler, P. J. (1999). Medicinal inorganic chemistry. *Adv. Inorg. Chem.* 49, 183–306. doi:10.1016/S0898-8838(08)60271-8
- Hamis, S., Nithiarasu, P., and Powathil, G. G. (2018). What does not kill a tumour may make it stronger: in silico insights into chemotherapeutic drug resistance. *J. Theor. Biol.* 454, 253–267. doi:10.1016/j.jtbi.2018.06.014
- Hill, C. L. (2007). Progress and challenges in polyoxometalate-based catalysis and catalytic materials chemistry. *J. Mol. Catal. A Chem.* 262, 2–6. doi:10.1016/j.molcata.2006.08.042
- Hu, X. K., Wang, H., Huang, B., Li, N., Hu, K. H., Wu, B. L., et al. (2019). A new scheme for rational design and synthesis of polyoxovanadate hybrids with high antitumor activities. *J. Inorg. Biochem.* 193, 130–132. doi:10.1016/j.jinorgbio.2019.01.013
- Jalil, P. A., Faiz, M., Tabet, N., Hamdan, N. M., and Hussain, Z. (2003). A study of the stability of tungstophosphoric acid, $\text{H}_3\text{PW}_{12}\text{O}_{40}$, using synchrotron XPS, XANES, hexane cracking, XRD, and IR spectroscopy. *J. Catal.* 217, 292–297. doi:10.1016/S0021-9517(03)00066-6
- Jasmin, C., Chermann, J., Herve, G., Teze, A., Souchay, P., Boy-Loustau, C., et al. (1974). *In vivo* inhibition of murine leukemia and sarcoma viruses by the heteropolyanion 5-tungsto-2-antimonate. *J. Natl. Cancer. I* 53, 469–474. doi:10.1093/jnci/53.2.469
- Jonckheere, N., Skrypek, N., and Van Seuningen, I. (2014). Mucins and tumor resistance to chemotherapeutic drugs. *Biochim. Biophys. Acta*. 1846, 142–151. doi:10.1016/j.bbcan.2014.04.008
- Judd, D. A., Nettles, J. H., Nevins, N., Snyder, J. P., Liotta, D. C., Tang, J., et al. (2001). Polyoxometalate HIV-1 protease inhibitors. A new mode of protease inhibition. *J. Am. Chem. Soc.* 123, 886–897. doi:10.1021/ja001809e
- Kurtz, D. M., Jr (1990). Oxo- and hydroxo-bridged diiron complexes: a chemical perspective on a biological unit. *Chem. Rev.* 90, 585–606. doi:10.1021/cr00102a002
- Kuznetsova, L. I., Detusheva, L. G., Fedotov, M. A., and Likholobov, V. A. (1996). Catalytic properties of heteropoly complexes containing Fe(III) ions in benzene oxidation by hydrogen peroxide. *J. Mol. Catal. A Chem.* 111, 81–90. doi:10.1016/1381-1169(96)00207-5
- Kuznetsova, L. I., Detusheva, L. G., Kuznetsova, N. I., Fedotov, M. A., and Likholobov, V. A. (1997). Relation between structure and catalytic properties of transition metal complexes with heteropolyanion $\text{PW}_{11}\text{O}_{39}^{7-}$ in oxidative reactions. *J. Mol. Catal. A Chem.* 117, 389–396. doi:10.1016/S1381-1169(96)00294-4
- Li, C. Y., Cao, H. Q., Sun, J. H., Tian, R., Li, D. B., Qi, Y. F., et al. (2017). Antileukemic activity of an arsenomolybdate in the human HL-60 and U937 leukemia cells. *J. Inorg. Biochem.* 168, 67–75. doi:10.1016/j.jinorgbio.2016.12.002
- Liu, J., Xu, M. Z., and Yuan, Z. (2020). Immunoscore guided cold tumors to acquire “temperature” through integrating physicochemical and biological methods. *BIO Integration*. 1, 6–14. doi:10.15212/bioi-2020-0002
- Liu, K., Xu, Y. Q., Yao, Z. X., Miras, H. N., and Song, Y. F. (2016). Polyoxometalate-intercalated layered double hydroxides as efficient and recyclable bifunctional catalysts for cascade reactions. *ChemCatChem*. 8, 929–937. doi:10.1002/cctc.201501365
- Liu, W. J., Al-Oweini, R., Meadows, K., Bassil, B. S., Lin, Z. G., Christian, J. H., et al. (2016). Cr^{III} -substituted heteropoly-16-tungstates $[\text{Cr}_2^{\text{III}}(\beta\text{-X}^{\text{IV}}\text{W}_8\text{O}_{31})_2]^{14-}$ ($\text{X} = \text{Si, Ge}$): magnetic, biological, and electrochemical studies. *Inorg. Chem.* 55, 10936–10946. doi:10.1021/acs.inorgchem.6b01458
- Liu, X., Gan, Q., and Feng, C. G. (2016). Synthesis, characterization and biological activity of 5-fluorouracil derivatives of rare earth (Gd, Dy, Er) substituted phosphotungstate. *Inorg. Chim. Acta*. 450, 299–303. doi:10.1016/j.ica.2015.11.034
- Ma, T., Yang, P., Dammann, I., Lin, Z. G., Mougharbel, A. S., Li, M. X., et al. (2020). Tetra-(p-tolyl)antimony(III)-containing heteropolytungstates, $[(p\text{-tolyl})\text{Sb}^{\text{III}}]_4(\text{A-XW}_9\text{O}_{34})_2]^{10-}$ ($\text{X} = \text{P, As, or Ge}$): synthesis, structure, and study of antibacterial and antitumor activity. *Inorg. Chem.* 59, 2978–2987. doi:10.1021/acs.inorgchem.9b03322
- Mathias, L., Almeida, J., Passoni, L., Gossani, C., Taveira, G., Gomes, V., et al. (2020). Antifungal activity of silver salts of Keggin-type heteropolyacids against *sporothrix* spp. *J. Microbiol. Biotechnol.* 30, 540–551. doi:10.4014/jmb.1907.07064
- Mizuno, N., Yamaguchi, K., and Kamata, K. (2005). Epoxidation of olefins with hydrogen peroxide catalyzed by polyoxometalates. *Coordin. Chem. Rev.* 249, 1944–1956. doi:10.1016/j.ccr.2004.11.019
- Muller, A., Peters, F., Pope, M. T., and Gatteschi, D. (1998). Polyoxometalates: very large clusters—nanoscale magnets. *Chem. Rev.* 98, 239–271. doi:10.1021/cr9603946
- Müller, C. E., Iqbal, J., Baqi, Y., Zimmermann, H., Röllich, A., and Stephan, H. (2006). Polyoxometalates—a new class of potent ecto-nucleoside triphosphate diphosphohydrolase (NTPDase) inhibitors. *Bioorg. Med. Chem. Lett.* 16, 5943–5947. doi:10.1016/j.bmcl.2006.09.003
- Myrzakozha, D. A., Hasegawa, T., Nishijo, J., Imae, T., and Ozaki, Y. (1999a). An infrared study of molecular orientation and structure in one-layer langmuir–blodgett films of octadecyldimethylamine oxide and dioctadecyldimethylammonium chloride: dependence of the structures of the langmuir–blodgett films on substrates, aging, and pH of water subphase. *Langmuir*. 15, 6890–6896. doi:10.1021/la9806294
- Myrzakozha, D. A., Hasegawa, T., Nishijo, J., Imae, T., and Ozaki, Y. (1999b). Structural characterization of langmuir–blodgett films of octadecyldimethylamine oxide and dioctadecyldimethylammonium chloride. 2. thickness dependence of thermal behavior investigated by infrared spectroscopy and wetting measurements. *Langmuir*. 15, 3601–3607. doi:10.1021/la981016u
- Pichon, C., Dolbecq, A., Mialane, P., Marrot, J., Rivière, E., Goral, M., et al. (2008). Fe_2 and Fe_4 clusters encapsulated in vacant polyoxotungstates: hydrothermal synthesis, magnetic and electrochemical properties, and DFT calculations. *Chem. Eur. J.* 14, 3189–3199. doi:10.1002/chem.200700896
- Preya, U. H., Lee, K. T., Kim, N. J., Lee, J. Y., Jang, D. S., and Choi, J. H. (2017). The natural terthiophene alpha-terthienylmethanol induces S phase cell cycle arrest of human ovarian cancer cells via the generation of ROS stress. *Chem. Biol. Interact.* 272, 72–79. doi:10.1016/j.cbi.2017.05.011
- Prudent, R., Moucadel, V., Laudet, B., Barette, C., Lafanechère, L., Hasenknopf, B., et al. (2008). Identification of polyoxometalates as nanomolar noncompetitive inhibitors of protein kinase CK2. *Chem. Biol.* 15, 683–692. doi:10.1016/j.chembiol.2008.05.018

- Qi, Y., Xiang, Y., Wang, J., Qi, Y., Li, J., Niu, J., et al. (2013). Inhibition of hepatitis C virus infection by polyoxometalates. *Antiviral Res.* 100, 392–398. doi:10.1016/j.antiviral.2013.08.025
- Qu, X. S., Feng, H., Ma, C., Yang, Y. Y., and Yu, X. Y. (2017). Synthesis, crystal structure and anti-tumor activity of a novel 3D supramolecular compound constructed from Strandberg-type polyoxometalate and benzimidazole. *Inorg. Chem. Commun.* 81, 22–26. doi:10.1016/j.inoche.2017.04.023
- Rhule, J. T., Hill, C. L., Judd, D. A., and Schinazi, R. F. (1998). Polyoxometalate in medicine. *Chem. Rev.* 98, 327–358. doi:10.1021/cr960396q
- Rodriguez-Vargas, J. M., Ruiz-Magana, M. J., Ruiz-Ruiz, C., Majuelos-Melguizo, J., Peralta-Leal, A., Rodriguez, M. I., et al. (2012). ROS-induced DNA damage and PARP-1 are required for optimal induction of starvation-induced autophagy. *Cell. Res.* 22, 1181–1198. doi:10.1038/cr.2012.70
- Santos, F. M., Brandão, P., Félix, V., Domingues, M. R. M., Amaral, J. S., Amaral, V., et al. (2012). Organic–inorganic hybrid materials based on iron(III)-polyoxotungstates and 1-butyl-3-methylimidazolium cations. *Dalton Trans.* 41, 12145–12155. doi:10.1039/C2DT31206A
- Shigeta, S., Mori, S., Kodama, E., Kodama, J., Takahashi, K., and Yamase, T. (2003). Broad spectrum anti-RNA virus activities of titanium and vanadium substituted polyoxotungstates. *Antiviral Res.* 58, 265–271. doi:10.1016/S0166-3542(03)00009-3
- Ssif, M. W., Katirtzoglou, N. A., and Syrigos, K. N. (2008). Capecitabine: an overview of the side effects and their management. *Anticancer Drugs.* 19, 447–464. doi:10.1097/CAD.0b013e3282f945aa
- Sun, T. D., Cui, W., Yan, M., Qin, G., Guo, W., Gu, H. X., et al. (2016). Target delivery of a novel antitumor organoplatinum(IV)-substituted polyoxometalate complex for safer and more effective colorectal cancer therapy *in vivo*. *Adv. Mater.* 28, 7397–7404. doi:10.1002/adma.201601778
- Sun, X. F., Wu, Y., Gao, W. D., Enjyoji, K., Csizmadia, E., Müller, C. E., et al. (2010). CD39/ENTPD1 expression by CD4⁺Foxp3⁺ regulatory T cells promotes hepatic metastatic tumor growth in mice. *Gastroenterology.* 139, 1030–1040. doi:10.1053/j.gastro.2010.05.007
- Sun, Y. B., Ma, W., Yang, Y. Y., He, M. X., Li, A. M., Bai, L., et al. (2019). Cancer nanotechnology: enhancing tumor cell response to chemotherapy for hepatocellular carcinoma therapy. *Asian. J. Pharm.* 14, 581–594. doi:10.1016/j.ajps.2019.04.005
- Van Rompuy, L. S., and Parac-Vogt, T. N. (2019). Interactions between polyoxometalates and biological systems: from drug design to artificial enzymes. *Curr. Opin. Biotech.* 58, 92–99. doi:10.1016/j.copbio.2018.11.013
- Wang, X. H., Liu, J. F., and Pope, M. T. (2003). New polyoxometalate/starch nanomaterial: synthesis, characterization and antitumoral activity. *Dalton Trans.* (5), 957–960. doi:10.1039/B300920N
- Weiss, R. B., and Christian, M. C. (1993). New cisplatin analogues in development. A review. *Drugs.* 46, 360–377. doi:10.2165/00003495-199346030-00003
- Xiao, Y. F., An, F. F., Chen, J. X., Yu, J., Yu, Z. Q., Ting, R., et al. (2019). The nanoassembly of an intrinsically cytotoxic near-infrared dye for multifunctionally synergistic theranostics. *Small.* 15, 1903121. doi:10.1002/smll.201903121
- Yu, H., Le, S. L., Zeng, X. H., Zhang, J. Y., and Xie, J. L. (2014). Facile synthesis of a novel mono-organoimido functionalized polyoxometalate cluster [(n-C₄H₉)₄N]₂[Mo₆O₁₈(≡NAr)](Ar=p-C₂H₅C₆H₄): crystal structure, spectral characterization and initial antitumor activity. *Inorg. Chem. Commun.* 39, 135–139. doi:10.1016/j.inoche.2013.11.001
- Zhao, Z. J., He, Z. H., Huang, H. Y., Chen, J. W., He, S. S., Yilihamu, A., et al. (2020). Drug-induced interstitial lung disease in breast cancer patients: a lesson we should learn from multi-disciplinary integration. *BIO Integration.* 1 (10), 82–91. doi:10.15212/bioi-2020-0009
- Zheng, L., Ma, Y., Zhang, G. J., Yao, J. N., Bassil, B. S., Kortz, U., et al. (2009). Molecular interaction between a gadolinium–polyoxometalate and human serum albumin. *Eur. J. Inorg. Chem.* 5189–5193. doi:10.1002/ejic.200900610

Conflict of Interest: Author HL was employed by the company NCPC Hebei Lexin Pharmaceutical Co., Ltd.

The remaining authors declare that the research was conducted in the absence of any commercial or financial relationships that could be construed as a potential conflict of interest.

Copyright © 2021 Xue, Yin, Li, Chi, Guo, Cui and Li. This is an open-access article distributed under the terms of the Creative Commons Attribution License (CC BY). The use, distribution or reproduction in other forums is permitted, provided the original author(s) and the copyright owner(s) are credited and that the original publication in this journal is cited, in accordance with accepted academic practice. No use, distribution or reproduction is permitted which does not comply with these terms.



OPEN ACCESS

Edited by:

Zhi-xiang Yuan,
Southwest Minzu University, China

Reviewed by:

Wanxing Duan,
Xi'an Jiaotong University, China
Dongke Yu,
Sichuan Academy of Medical Sciences
and Sichuan Provincial People's
Hospital, China
LianCheng Zhu,
ShengJing Hospital of China Medical
University, China
Kazuhiro Kamada,
Kyoto Prefectural University of
Medicine, Japan

*Correspondence:

Tao Sun
tao.sun@nankai.edu.cn
Huijuan Liu
liuhuijuanxyz@163.com

[†]These authors have contributed
equally to this work

Specialty section:

This article was submitted to
Pharmacology of Anti-Cancer Drugs,
a section of the journal
Frontiers in Oncology

Received: 20 October 2020

Accepted: 24 December 2020

Published: 11 February 2021

Citation:

Liu H, Tao H, Wang H, Yang Y, Yang R,
Dai X, Ding X, Wu H, Chen S and Sun T
(2021) Doxycycline Inhibits Cancer
Stem Cell-Like Properties via
PAR1/FAK/PI3K/AKT
Pathway in Pancreatic Cancer.
Front. Oncol. 10:619317.
doi: 10.3389/fonc.2020.619317

Doxycycline Inhibits Cancer Stem Cell-Like Properties via PAR1/FAK/PI3K/AKT Pathway in Pancreatic Cancer

Huijuan Liu^{1,2,3*†}, Honglian Tao^{1,2†}, Hongqi Wang^{1,2†}, Yuyan Yang^{1,2}, Ru Yang^{1,2},
Xintong Dai^{1,2}, Xiujuan Ding^{1,2}, Haidong Wu², Shuang Chen² and Tao Sun^{1,2,4*}

¹ State Key Laboratory of Medicinal Chemical Biology and College of Pharmacy, Nankai University, Tianjin, China, ² Tianjin Key Laboratory of Early Druggability Evaluation of Innovative Drugs, Tianjin International Joint Academy of Biomedicine, Tianjin, China, ³ Tianjin Key Laboratory of Extracorporeal Life Support for Critical Diseases, Tianjin Third Central Hospital, Tianjin, China, ⁴ Department of Gastroenterology and Hepatology, General Hospital, Tianjin Medical University, Tianjin Institute of Digestive Disease, Tianjin, China

Pancreatic cancer stem cells (CSCs) play an important role in the promotion of invasion and metastasis of pancreatic cancer. Protease activation receptor 1 (PAR1) is closely related to malignant progression of tumors, however, its effects on pancreatic cancer stem cell-like (CSC-like) properties formation have not been reported. In this work, the effects of PAR1 on pancreatic cancer stem cell-like (CSC-like) properties formation were studied. PAR1 overexpression can induce CSC-like properties in Aspc-1 cells, whereas interference of PAR1 in Panc-1 cells showed the contrary results. Data on patients with pancreatic cancer obtained from TCGA showed that high PAR1 expression and focal adhesion kinase (FAK) protein considerably affect the prognosis of patients. Further experiments showed that PAR1 could regulate FAK, PI3K, and AKT phosphorylation and the epithelial–mesenchymal transformation (EMT) in Aspc-1 and Panc-1 cells. Doxycycline, as a PAR1 inhibitor, could effectively inhibit the CSC-like properties of pancreatic cancer cells and the FAK/PI3K/AKT pathway activation. Doxycycline inhibits the growth of pancreatic cancer and enhances the treatment effect of 5-fluorouracil (5-FU) in Panc-1 xenograft mouse model. In conclusion, PAR1 promotes the CSC-like properties and EMT of pancreatic cancer cells via the FAK/PI3K/AKT pathway. Doxycycline inhibits the pancreatic cancer through the PAR1/FAK/PI3K/AKT pathway and enhances the therapeutic effect of 5-FU.

Keywords: protease activation receptor 1, focal adhesion kinase, doxycycline, epithelial–mesenchymal transformation, pancreatic cancer stem cells

INTRODUCTION

Pancreatic cancer is a gastrointestinal disease with high mortality and is usually diagnosed at an advanced stage (1, 2). The prognosis of pancreatic cancer is poor, and its 5-year survival rate is only 9% (3). A small population of cancer stem cells (CSCs) in the tumor has the ability to self-renew and maintain the tumor (4). In 2007, Li et al. were the first to isolate and identify pancreatic CSCs (5). Many pathways, such as the hedgehog (Hh) signaling pathway, were upregulated in pancreatic CSCs (6, 7). Epithelial–mesenchymal transformation (EMT) could result in a CSC-like phenotype (8). EMT activation can possibly generate CSCs and affect cancer cell differentiation and metastasis (9).

Protease-activated receptor 1 (PAR1), also known as thrombin receptor (10), is a G-protein coupled receptor. PAR1 mRNA has a higher expression level in pancreatic cancer cells than in pancreatic tissue (11). PAR1 can mediate the tumor microenvironment remodeling, promoting proliferation ability, angiogenesis ability, and malignant evolution in many kinds of tumor (12–14). However, the effects of PAR1 on the CSC-like properties of pancreatic cancer cells have not been reported.

Focal adhesion kinase (FAK) is a cytoplasmic protein tyrosine kinase that regulates cytoskeleton movement and is essential for cell movement (15). FAK is overexpressed in cancer cells (16) and can be activated by phosphorylation to participate in the transduction of multiple signaling pathways and self-renewal of CSCs (17, 18). PAR1 can regulate the self-phosphorylation of FAK in retinal pigment epithelial cells (19). The effect of PAR1 on FAK pathway has not been reported in pancreatic cancer.

Doxycycline is the third generation of semi-synthetic tetracycline broad-spectrum antibiotics (20). It works by inhibiting bacterial protein synthesis (21). Doxycycline has the anti-tumor effect (22–25). However, its molecular mechanism has not been fully elucidated. In this work, the effect of doxycycline on the CSC-like properties of pancreatic cancer was evaluated.

The effect of PAR1 on the formation of CSC-like properties in pancreatic cancer and the effect of doxycycline on pancreatic cancer were evaluated. PAR1 can promote the CSC-like properties and EMT of pancreatic cancer cells *via* the FAK/PI3K/AKT pathway. Doxycycline inhibits the pancreatic CSC-like properties by targeting PAR1 and enhancing the therapeutic effect of 5-fluorouracil (5-FU).

MATERIALS AND METHODS

Cell Culture

The human pancreatic cancer cell lines Panc-1 and Aspc-1 were purchased from KeyGEN BioTECH, and maintained in media recommended by the vendors. The human pancreatic cancer cell

lines Panc-1 and Aspc-1 were maintained in Dulbecco's modified Eagle's medium (DMEM) supplemented with 10% fetal bovine serum (FBS). The cells were cultured at 37°C with 5% CO₂ in a humidified atmosphere.

Gene Transfection

The PAR1-pCDNA3.1 plasmid and siRNA were used for transfection experiments. For transfection, 2.5 µg of DNA and 75 pmol of siRNA were added to 100 µl of the Opti-MEM medium and mixed with 100 µl of Opti-MEM containing 10 µl of Lipofectamine 2000 for 20 min at room temperature. Before transfection, cells were seeded into a six-well plate and transfected with the abovementioned complex for 48 h.

Western Blot Analysis

The cells were washed with cold PBS, lysed in lysis buffer for 30 min, and centrifuged for 10 min at 4°C. Protein concentration was measured by a BCA (bicinchoninic acid) protein assay kit. Protein samples were separated using 10% SDS-polyacrylamide gel electrophoresis, and electrotransferred onto polyvinylidene difluoride (PVDF) membranes. After blocking the cells with BSA, the PVDF membranes were incubated overnight at 4°C with primary antibodies, including PAR1 (affinity, 1:1000), FAK (Affinity, 1:1000), p-FAK (Affinity, 1:1000), vimentin (VIM, Affinity, 1:1000), E-cadherin (E-Cad, Affinity, 1:500), PI3K (Affinity, 1:500), p-PI3K (Affinity, 1:500), AKT (Affinity, 1:500), p-AKT (Affinity, 1:500), and GAPDH (Affinity, 1:4000), and with secondary HRP-conjugated goat-anti-rabbit antibodies (Invitrogen, 1:5000). The proteins were visualized by enhanced chemiluminescence and analyzed using Image J software.

Flow Cytometry

Panc-1 and Aspc-1 cells were seeded into a six-well plate and treated with doxycycline, PAR1-pCDNA3.1 plasmid, or PAR1-siRNA for 72 h. For flow cytometry, Panc-1 and Aspc-1 cells were digested and washed twice with PBS. After fixing the cells with 70% cold methanol and blocking with 5% BSA, they were incubated with primary antibodies CD133 (Affinity, 1:200). The cells were incubated with green fluorescent secondary antibodies. The green fluorescence was analyzed with FACScan flow cytometer, and the result was analyzed by FlowJo software.

Cell Viability Detection

The viability of pancreatic cancer cells were assessed by MTT assay. Cells (1×10⁴) were seeded in 96-well plates overnight. The experimental groups were treated with doxycycline and combination drugs with different concentrations, and the negative control group was treated with solvent for 48, 72, and 96 h. Then, MTT was added into cells and incubated for 4 h. The synthesized formazan crystals were dissolved using 100 µl of DMSO, and the absorbance was measured at 570 nm. The IC₅₀ of doxycycline was calculated using GraphPad Prism 7.0.

Invasion Assay

The transwell plate was used for invasion assay. Panc-1 and Aspc-1 cells were suspended and plated into the upper portion of the matrigel-coated transwell chambers, and the bottom chamber was

Abbreviations: CSCs, cancer stem cells; Doxy, Doxycycline; PAR1, protease activation receptor 1; FAK, focal adhesion kinase; EMT, epithelial–mesenchymal transformation; 5-FU, 5-fluorouracil; TCGA, the cancer genome atlas; KEGG, The Kyoto Encyclopedia of Genes and Genomes; GO, gene ontology; DMEM, Dulbecco's modified Eagle's medium; FBS, fetal bovine serum; VIM, vimentin; E-cad, E-cadherin; IC₅₀, the half inhibition rate

filled with medium containing 10% FBS. The cells were cultured at 37°C for 48 h. The membranes were fixed using 4% paraformaldehyde and stained with 0.1% crystal violet. Then, the cells on the upper of the membranes were removed gently. Cells that invaded through the membrane were counted under a microscope and compared with different drug concentrations.

Wound Healing Assay

Panc-1 and Aspc-1 cells were seeded into 24-well plate and grown to 70% to 80% confluency. A wound was scratched across each well. The cells were treated with different concentrations doxycycline diluted in non-FBS medium. The wound distance was photographed at 0, 24, and 48 h under a light microscope (Nikon). Three parallel wells were set for each group.

Immunofluorescence

Panc-1 and Aspc-1 cells were seeded into 24-well plate, treated with 30 and 60 μ M of doxycycline, and cultured for 72 h. The cells were washed with PBS, fixed with 4% paraformaldehyde for 20 min, and permeabilized with 0.1% Triton X-100 for 15 min. After blocking the cells with 5% BSA for 30 min, they were immunoblotted overnight with primary antibodies, including E-Cad and VIM (1:200) and fluorescent secondary antibodies (1:200). E-Cad was labeled with green fluorescence, and VIM was labeled with red fluorescence. Finally, the nucleus was stained with DAPI. Cells were photographed under a laser scanning confocal microscope (LSCM, Nikon). All experiments were performed in triplicate.

Cloning Formation Experiment

Panc-1 and Aspc-1 cells were seeded into a six-well plate with a density of approximately 300 cells per well. After 24 h, cells were treated with doxycycline, PAR1-pCDNA3.1 plasmid, or siRNA and cultured for 14 days. The colonies were fixed in 4% paraformaldehyde and stained with 0.1% crystal violet. The colony number was counted and compared in different groups.

Intracellular Ca^{2+} Mobilization Assay

A single cell suspension of pancreatic cancer cells was prepared, and 1.2×10^4 cells per well were seeded into a 384 plate. After cell adherence, the medium was aspirated, and 25 μ l of DMEM containing different concentrations of doxycycline and 25 μ l of Calcium Assay kit Loading were added to each well to ensure that the final concentrations of doxycycline were 0, 5, 10, 30, 60, and 100 μ M. Advance thrombin solution was diluted to 2 U/ml with DMEM medium. The experimental groups were mixed with 12.5 μ l of thrombin solution, whereas the control group was added with 12.5 μ l of DMEM medium. Automatic multi-function microplate reader was used to detect the calcium flux signal.

Animal Studies

Male BALB/C nude mice (5–6 weeks old) were maintained in animal care facilities without specific pathogens. All the animal studies were conducted in accordance with the National Institutes of Health Animal Use Guidelines and current Chinese Regulations and Standards for the Use of Laboratory Animals. All animal procedures were approved according to the guidelines of the

Animal Ethics Committee of Tianjin International Joint Academy of Biotechnology and Medicine. The Panc-1 xenografts of tumors (1×10^6 /ml) suspended in PBS were established by subcutaneous injection into the flank. When the tumor volume reached approximately 50 mm^3 , the experimental mice were given doxycycline and 5-FU by gavage, whereas the model and control mice were given distilled water. The volume of nude mice tumors was monitored every 2 days and calculated using the following equation: tumor volume = $ab^2/2$ (a, tumor length; b, tumor width). After 60 days of treatment, all mice were euthanized. Tumors, livers, and lungs were collected and fixed with 10% formalin.

Immunohistochemical Analysis

The slides of tumors from nude mice were used to examine E-Cad, VIM, and CD133 expression by immunohistochemistry. The slides were deparaffinized and re-hydrated, and the antigen was retrieved with 0.01 M citrate buffer. The slides were placed into a wet box after blocking with serum for 30 min and incubated overnight with primary antibodies, including CD133 (1:100), VIM (1:100), and E-Cad (1:100). The primary antibodies were washed away and added with sensitizer for 20 min. The biotinylated goat-anti-rabbit secondary antibody was added for 30 min. Finally, the slides were stained with DAB and hematoxylin, observed under a microscope, and photographed. Staining intensity was scored as follows: none (0), weak brown (1+), moderate brown (2+), and strong brown (3+). The percentages of the positive cells were divided into five classes on the basis of the percentage of tumor cells stained, namely, 0 for no cells, 1 for 1% to 25%, 2 for 25% to 50%, 3 for 50% to 75%, and 4 for >75%.

Limiting Dilution Assay

Panc-1 cells were diluted to the following densities: 2×10^7 /ml, 2×10^6 /ml, and 2×10^5 /ml. The suspension was injected into the right back of the nude mice at 100 μ l per injection. The growth status of the tumors was observed, and the tumorigenesis rate of each group was calculated after 2 months.

TCGA Data Analysis

The representative images of the immunohistochemical assay were obtained from the Human Protein Atlas (<https://www.proteinatlas.org>). TCGA samples for transcriptional analysis were obtained from UALCAN database (<http://ualcan.path.uab.edu/index.html>). The expression information of PAR1 and FAK in TCGA pancreatic cancer samples was downloaded from the Human Protein Atlas for correlation analysis. Differential analysis of PAR1 in TCGA pancreatic cancer samples was performed in DECenter (Sanger Box). Then, the significantly upregulated genes ($|\log_{2}FC| \geq 1.0$) were analyzed by GO and KEGG enrichment through the Metascape website (<http://metascape.org/>). And the proteins that affected by PAR1 were analyzed by PPI analysis (<https://string-db.org/>).

Statistics

Each experiment was repeated thrice. Data were presented as mean \pm SD and analyzed by GraphPad prism 7. Multiple comparisons were performed by two-way ANOVA. A difference of $P < 0.05$ was considered as statistically significant.

RESULTS

PAR1 Promotes the CSC-like Properties of Pancreatic Cancer Cells

The PAR1 expression in pancreatic cancer cell lines was detected by Western blot. The PAR1 expression level was the highest in the Panc-1 cell line but the lowest in the Aspc-1 cell line (**Figure 1A**). Thus, Panc-1 cells were selected for PAR1 knockdown by using siRNA, and Aspc-1 cells were used for PAR1 overexpression by

using PAR1-pCDNA3.1 plasmid in the next experiment. The effects of PAR1 on pancreatic CSC marker expression and floating mammosphere-formation ability were detected. CD133 expression level and mammosphere formation ability were reduced in PAR1 interference Panc-1 cells. PAR1 overexpression increases the CD133 expression level and enhances the mammosphere-formation ability in Aspc-1 cells (**Figures 1B, C**). The colony formation experiment indicated that PAR1 overexpression promoted the colony formation of Aspc-1 cells, and PAR1 knockdown inhibited the colony

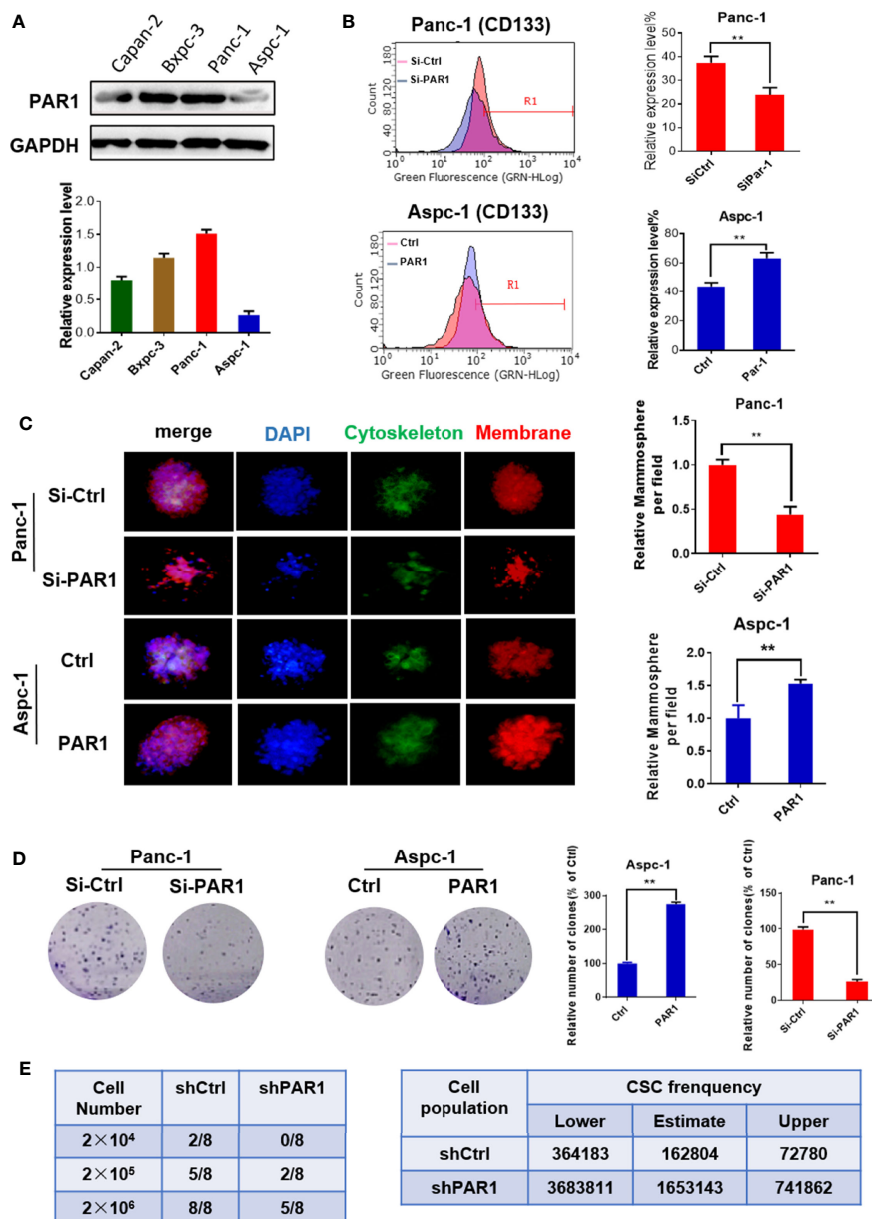


FIGURE 1 | PAR1 promotes the cancer stem cell-like properties of pancreatic cancer cells. **(A)** The expression levels of PAR1 in Panc-1, Bxpc-3, and Aspc-1 cell lines were detected by Western blot analysis. **(B)** Effect of PAR1 on pancreatic cancer stem cell markers CD133 in Panc-1 and Aspc-1 cells. **(C)** Effect of PAR1 on the mammosphere-forming potential of pancreatic cancer cells in PAR1 over-expression and interference experiments. **(D)** Effect of PAR1 on clone formation of Panc-1 and Aspc-1 cells. **(E)** Effect of PAR1 on the tumorigenicity of Panc-1 cells and PAR1 knockdown Panc-1 cells by using limiting dilution assay in node mice ($n = 8$). Cancer stem cell frequency was determined by ELDA (<http://bioinf.wehi.edu.au/software/elda>). Data are shown as the mean \pm SD (** $P < 0.01$).

formation of Panc-1 cells (**Figure 1D**). Limiting dilution analysis (using Panc-1 cells and PAR1 knock down Panc-1 cells) showed that pancreatic CSC frequency was significantly reduced in the sh-PAR1 group compared with the control group (**Figure 1E**).

PAR1 Promotes EMT Progression of Pancreatic Cancer Cells

The stem cell-like features of pancreatic cancer are related to the EMT process of cells. The effect of PAR1 on migration and invasion of pancreatic cancer cells was checked. PAR1 overexpression could promote the migration and invasion ability of Aspc-1 cells (**Figures 2A, B**). PAR1 knockdown could inhibit the migration and invasion ability of Panc-1 cells.

Western blot and immunofluorescence experiments showed that PAR1 overexpression could promote the expression of mesenchymal marker vimentin (VIM) and inhibit the expression of epithelial marker E-cadherin (E-cad) (**Figures 2C, D**) in Aspc-1 cells. PAR1 knockdown could inhibit the expression of VIM and increase the expression of E-cad in Panc-1 cells. These results showed that PAR1 could promote the EMT of pancreatic cancer cells.

PAR1 and FAK Result in the Poor Prognosis of Pancreatic Cancer Patients

The data of patients with pancreatic cancer were obtained from the cancer genome atlas (TCGA) database ((<https://portal.gdc>).

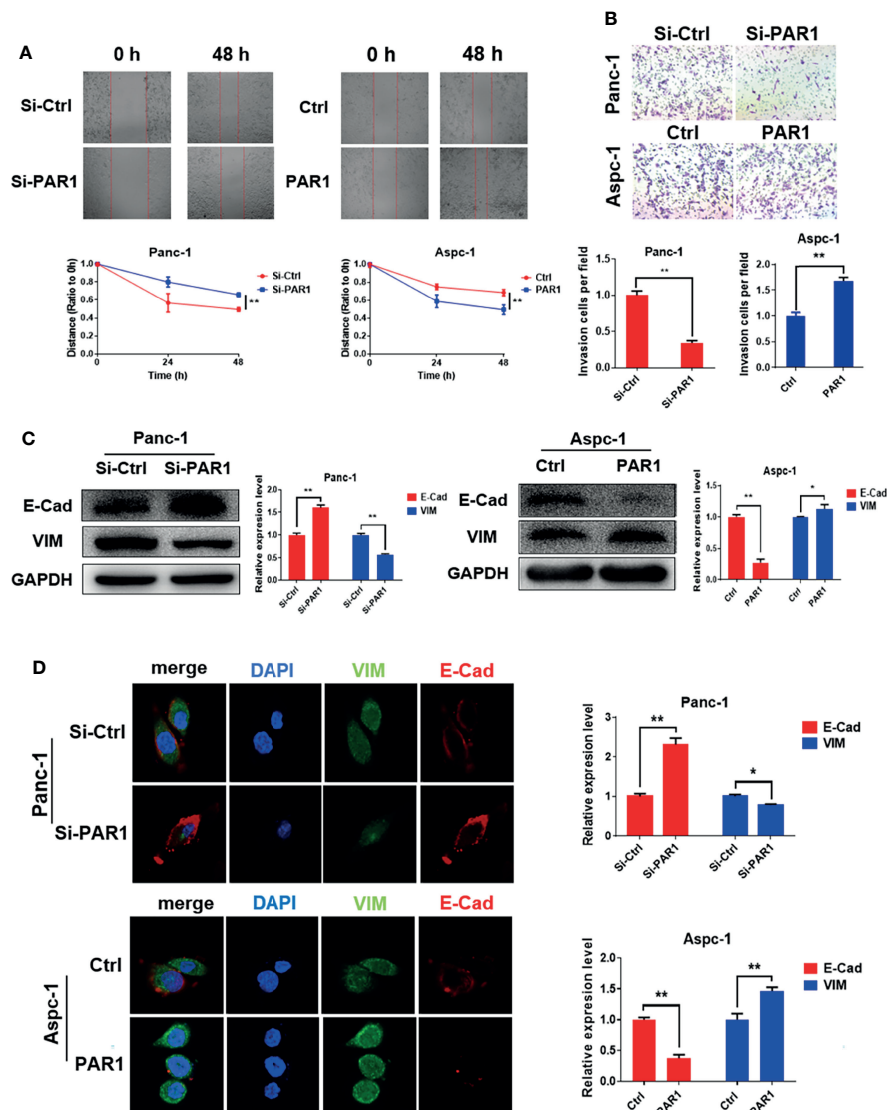


FIGURE 2 | PAR1 promotes EMT progression of pancreatic cancer cells. **(A)** Effect of PAR1 on Panc-1 and Aspc-1 cell migration potential detected using the wound healing assay. **(B)** Effect of PAR1 on pancreatic cancer cell invasion potential by using matrigel-coated transwell assay. **(C)** Effect of PAR1 on the E-Cad and VIM expression detected by Western blot analysis. **(D)** Effect of PAR1 on the E-Cad and VIM expression detected by immunofluorescence. Data are shown as the mean \pm SD (* P < 0.05, ** P < 0.01).

cancer.gov/) and used to evaluate the effect of PAR1 and FAK in patients with pancreatic cancer. Survival analysis revealed that only PAR1 and FAK double positive expression indicated poor prognosis among pancreatic cancer patients (Figure 3A). The immunohistochemical assay from the Human Protein Atlas (<http://www.proteinatlas.org/>) also showed that the PAR1 ($n = 176$) and FAK ($n = 176$) expression in tumors was higher than that of normal pancreatic tissues (Figure 3B). The RNA expression results also showed that PAR1 and FAK expression in tumors was higher than that of normal pancreatic tissues. The expression correlation of PAR1 and FAK, AKT, VIM was analyzed using samples from pancreatic cancer patients from GEPIA (<http://gepia.cancer-pku.cn>). The expression level of PAR1 and FAK ($P < 0.05$, $R = 0.29$), AKT ($P < 0.05$, $R = 0.36$), and VIM ($P < 0.05$, $R = 0.41$) were positively correlated (Figure 3C). Thus, PAR1 may regulate the FAK/PI3K/AKT signaling

pathway and result in the poor prognosis of patients with pancreatic cancer.

PAR1 Could Regulate the FAK/PI3K/AKT Pathway

Based on the abovementioned results, PAR1 may regulate FAK phosphorylation in pancreatic cancer. The effect of PAR1 on FAK phosphorylation was detected, and the results showed that PAR1 activation by thrombin could induce the increase in FAK autophosphorylation at Y397 in PAR1-overexpressing Aspc-1 cells (Figure 4A). FAK can modulate the PI3K/AKT signaling pathway and promote EMT and CSC formation (26). Thus, the effect of PAR1 on PI3K/AKT phosphorylation was further detected. PAR1 activation by thrombin enhanced PI3K and AKT phosphorylation in PAR1-overexpressing Aspc-1 cells. PAR1 interference could inhibit PI3K and AKT phosphorylation

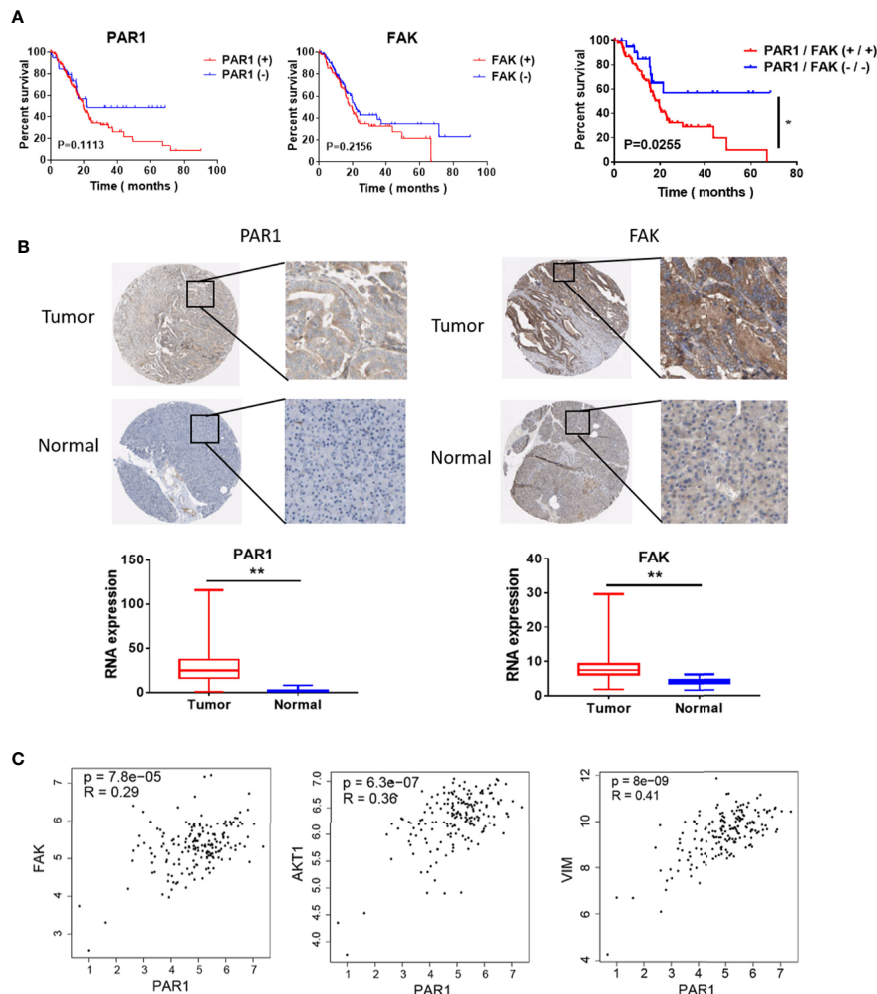


FIGURE 3 | Effect of PAR1 on the pancreatic cancer prognosis. **(A)** Effect of PAR1 and FAK on pancreatic cancer prognosis. Data were obtained from TCGA database. **(B)** PAR1 and FAK expression levels in normal pancreatic tissues and pancreatic cancer tissues. Data were obtained from the Human Protein Atlas online database. **(C)** The correlation analysis between PAR1 and FAK, AKT, and VIM expression of TCGA pancreatic cancer samples from GEPIA (<http://gepia.cancer-pku.cn/>). Data are shown as the mean \pm SD (* $P < 0.05$, ** $P < 0.01$).

in Panc-1 cells (**Figure 4B**). And the statistics results of phosphorylation PI3K/AKT were shown in **Figure 4C**. After the pancreatic cancer data from TCGA was clustered on the basis of the PAR1 expression level, the differentially expressed genes between the high- and low-expression groups were analyzed. The Kyoto Encyclopedia of Genes and Genomes (KEGG) and Gene Ontology (GO) enrichment analysis results showed that PAR1 affected the ECM-receptor interaction, the calcium signaling pathway, the PI3K/AKT signaling pathway, and focal adhesion in pancreatic cancer cells (**Figure 4D**). PPI analysis result showed that PAR1 affected the function of calcium signaling pathways, cell migration,

G-protein coupling receptors, and cell junction (**Figure 4E**). The differential genes involved in cell migration, proliferation, CSCs, and apoptosis were further analyzed (**Figure 4F**). Thus, PAR1 could affect cancer cell invasion, metastasis, proliferation, and CSC formation through FAK/PI3K/AKT pathways in pancreatic cancer.

Doxycycline Inhibits the CSC-Like Properties of Pancreatic Cancer Cells

The Ca^{2+} mobilization assay of doxycycline in pancreatic cancer cells showed that doxycycline (Doxy) inhibited intracellular calcium

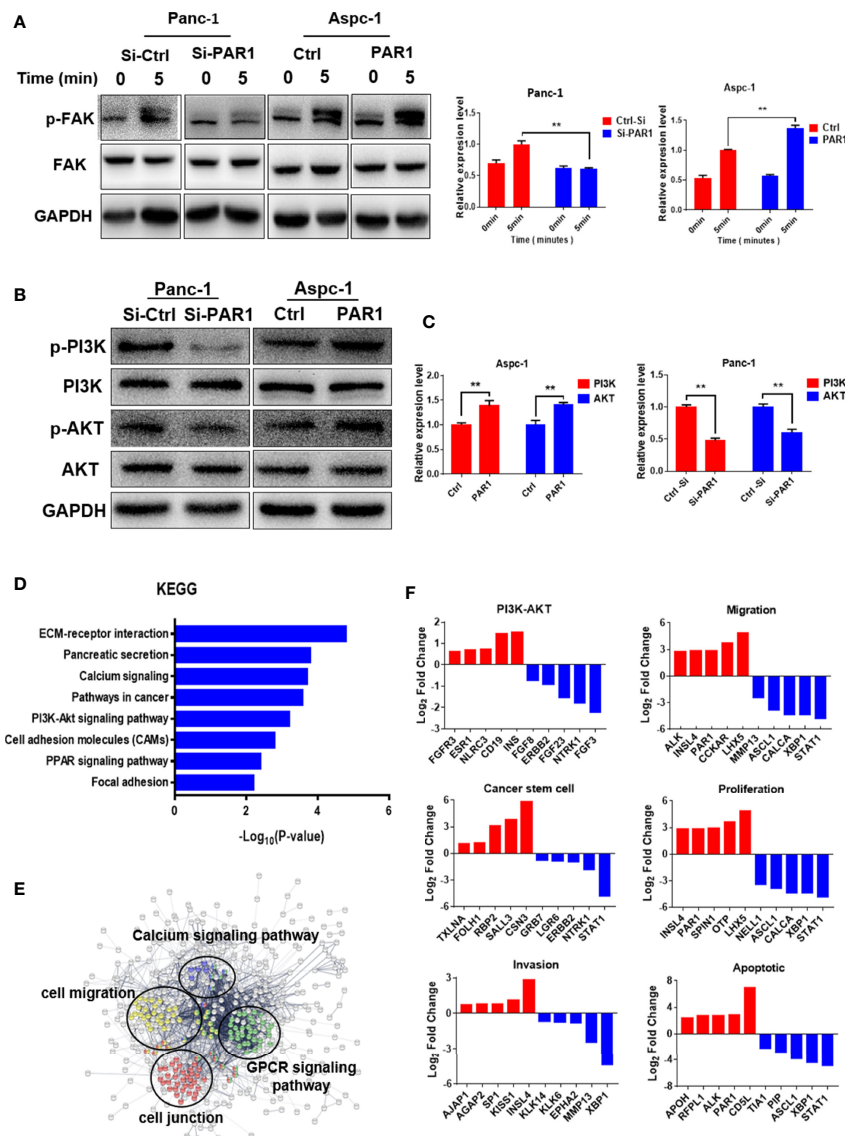


FIGURE 4 | PAR1 can activate the FAK/PI3K/AKT signaling pathways. **(A)** PAR1 activation by thrombin can induce FAK autophosphorylation at Y397 in Panc-1 and Aspc-1 cells. **(B)** Effect of PAR1 on PI3K and AKT phosphorylation in Panc-1 and Aspc-1 cells. **(C)** The statistics results of p-PI3K and p-AKT expression in Panc-1 and Aspc-1 cells. **(D)** The key pathways affected by PAR1 in pancreatic cancer cells. The genomic data for patients with pancreatic cancer were clustered by PAR1 expression level, and the differentially expressed genes were analyzed by GO and KEGG. **(E)** PPI analysis of proteins involved in the pathways affected by PAR1. **(F)** Differentially expressed genes in PI3K/AKT pathway, migration, cancer stem cell, proliferation, invasion, and apoptosis pathways. Data are shown as the mean \pm SD (** $P < 0.01$).

mobilization signals induced by thrombin in a dose-dependent manner (**Figure 5A**). MTT assay results showed that doxycycline inhibited the pancreatic cancer cell activity in a time- and dose-dependent manner (**Figure 5B**). The half inhibition rate (IC₅₀) of doxycycline was 987.5, 99.64, and 50.02 μ M after the drug was added for 48, 72, and 96 h, respectively. The effects of doxycycline

on pancreatic CSC marker expression and mammosphere formation were examined. The expression levels of CD133 and balloon-formation ability were inhibited by doxycycline in Panc-1 cells (**Figures 5C, D**). The effects of doxycycline on migration and invasion in pancreatic cancer cells were determined. Doxycycline significantly inhibited migration and invasion ability of pancreatic

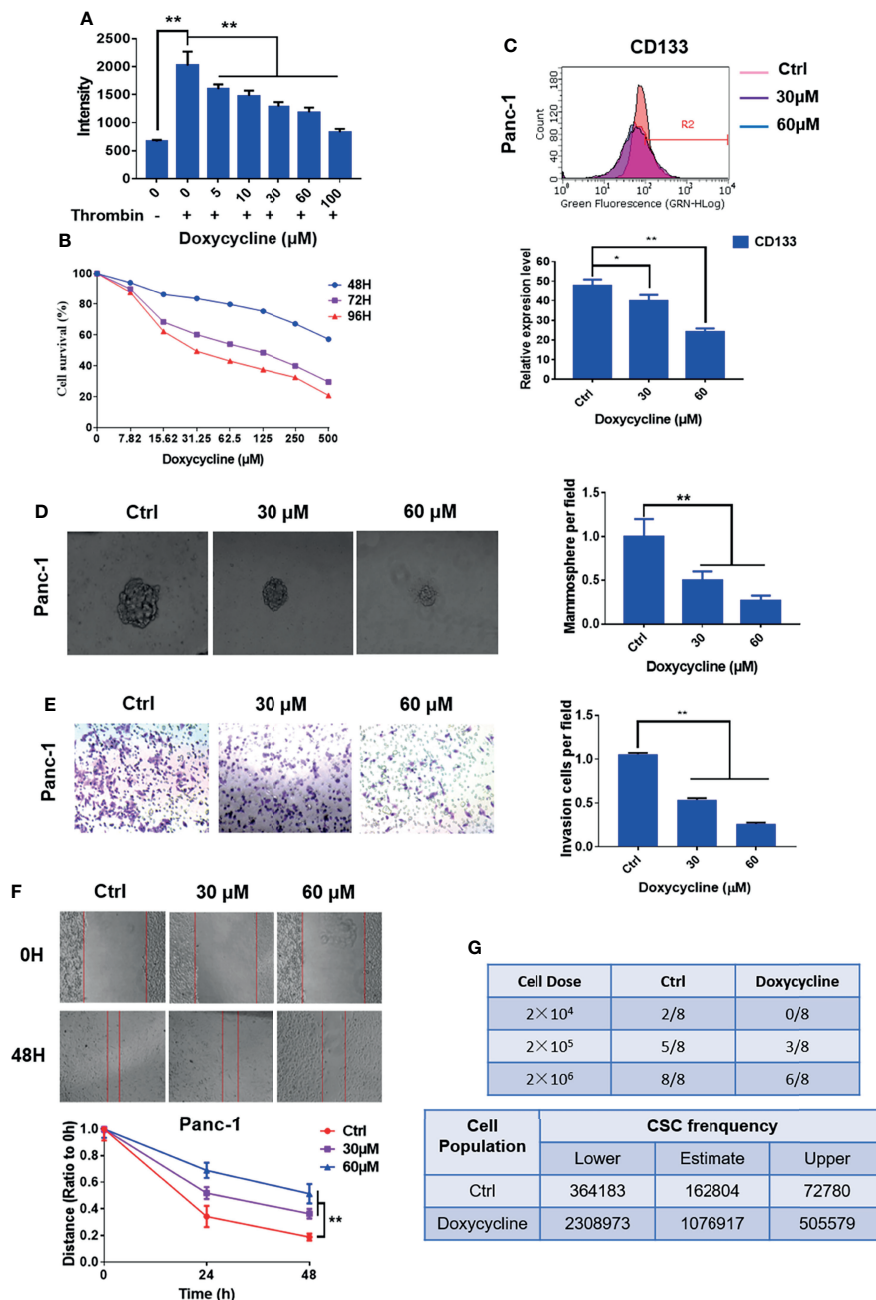


FIGURE 5 | Doxycycline inhibits the cancer stem cell-like properties of pancreatic cancer cells. **(A)** Effect of doxycycline on PAR1 activation stimulated by thrombin in pancreatic cancer cells detected by the Ca^{2+} -mobilization assay. **(B)** Effect of doxycycline on pancreatic cancer cell viability after 48, 72, and 96 h treatment. **(C)** Effect of doxycycline on pancreatic cancer stem cell marker CD133 in Panc-1 cells. **(D)** Effect of doxycycline on the mammosphere formation of Panc-1 cells. **(E)** Effect of doxycycline on pancreatic cancer cell invasion ability. **(F)** Effect of doxycycline on pancreatic cancer cells migration ability. **(G)** Limiting dilution assay of pancreatic cancer stem cell from Panc-1 cells after treatment with doxycycline in nude mice ($n = 8$). Cancer stem cell frequency was determined by ELDA. Data are shown as the mean \pm SD (* $P < 0.05$, ** $P < 0.01$).

cancer cells (**Figures 5E, F**). In vivo limiting dilution assay also showed that the pancreatic CSC frequency of Panc-1 was significantly reduced in doxycycline-treated group compared with that of the control group (**Figure 5G**). Doxycycline significantly inhibited the CSC-like properties of pancreatic cancer cells.

Doxycycline Inhibits the FAK/PI3K/AKT Pathway

Western blot results showed that the levels of phosphorylated FAK, PI3K, and AKT in Panc-1 cells decreased after treatment with doxycycline (**Figures 6A, B**). Immunofluorescence results showed that doxycycline increased E-Cad expression in Panc-1 cell expression and decreased VIM expression (**Figure 6C**).

Thus, doxycycline could inhibit the FAK/PI3K/AKT pathway and EMT of pancreatic cancer cells.

Doxycycline Inhibits Pancreatic Cancer Growth and Enhances the Therapeutic Effect of 5-FU

The effects of doxycycline on the viability of Panc-1 cells treated with cisplatin, oxaliplatin, 5-FU, sorafenib, and gemcitabine were detected by MTT assay to determine the sensitization of doxycycline to chemotherapeutic drugs. Treatment with doxycycline effectively enhanced the effect of chemotherapy drugs in comparison with the results obtained when only chemotherapy drugs were used. Doxycycline had synergistic effects with cisplatin,

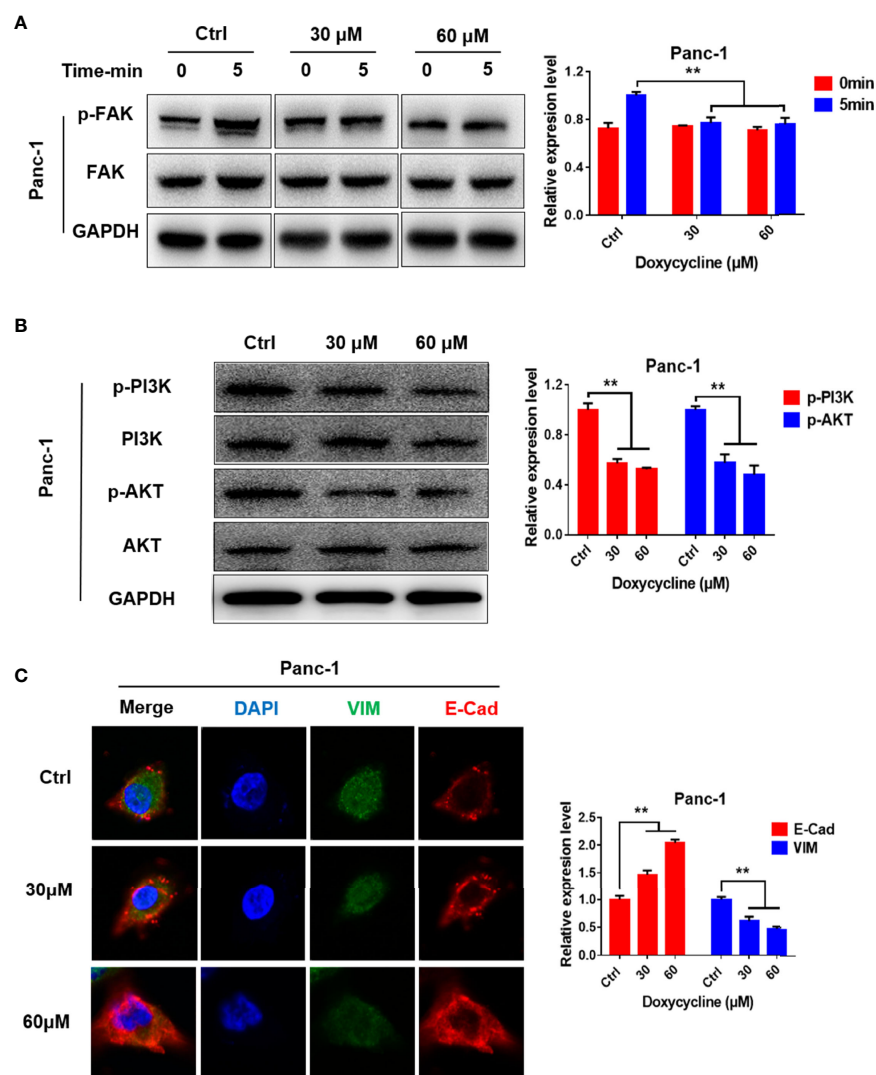


FIGURE 6 | Doxycycline inhibits the FAK/PI3K/AKT signaling pathways. **(A)** Panc-1 cells were treated with doxycycline and stimulated by thrombin for indicated time intervals, and the FAK phosphorylation changes were detected by Western blot analysis. **(B)** Effect of doxycycline on PI3K and AKT phosphorylation in Panc-1 cells detected by Western blot analysis. **(C)** Effect of doxycycline on the E-Cad and VIM expression levels in Panc-1 cells. Data are shown as the mean \pm SD (** P < 0.01).

oxaliplatin, 5-FU, sorafenib, and gemcitabine (**Figures 7A–E**). Doxycycline combination with 5-FU showed the best synergistic effect.

Panc-1 subcutaneous xenografts were used to detect the effect of doxycycline and 5-FU to verify the treatment effect of doxycycline and 5-FU on pancreatic cancer *in vivo*. Tumor growth was significantly inhibited in the doxycycline, 5-FU,

and the combination treatment group compared with the model group. 5-FU combined with doxycycline had the best inhibitory effect, and the tumor inhibition rate was 80.5% (**Figures 7F, G**). The immunohistochemical assay also revealed that under doxycycline treatment, VIM and CD133 expressions decreased, whereas E-Cad expression increased (**Figure 7H**).

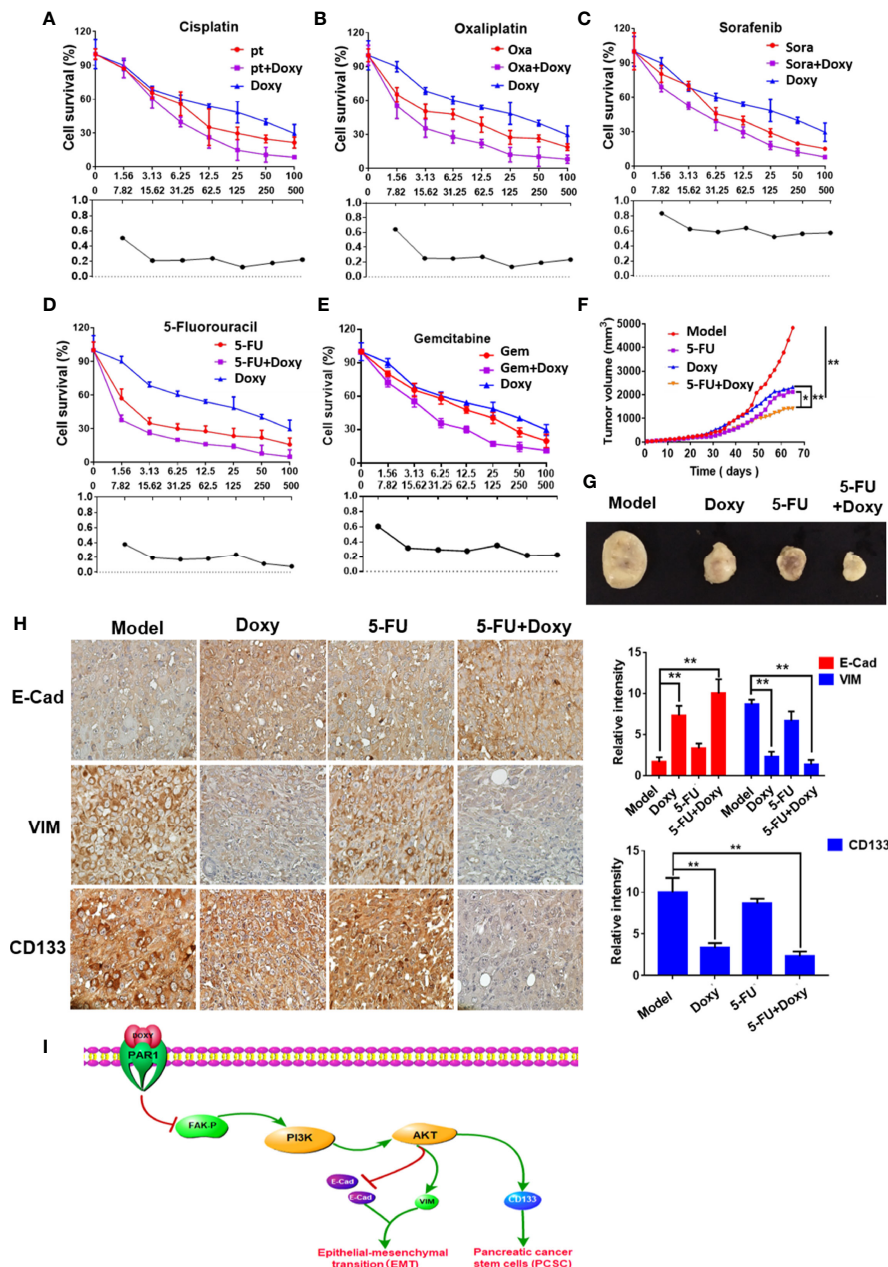


FIGURE 7 | Doxycycline inhibits pancreatic cancer growth and enhances the therapeutic effect of 5-FU. (**A–E**) The sensitization effect of doxycycline for chemotherapeutic drugs in Panc-1 cells after 72 h treatment. (**F, G**) The tumor volume change of Panc-1 subcutaneous xenografts in doxycycline, 5-FU, and the combination treatment group. (**H**) Immunohistochemical staining for E-cad, VIM, and CD133 in tumor tissues. Data are shown as the mean \pm SD (* $P < 0.05$, ** $P < 0.01$). (**I**) Molecular mechanism of doxycycline inhibits cancer stem cell-like properties of pancreatic cancer.

DISCUSSION

Pancreatic cancer is a disease with high mortality and increasing incidence (27). CSCs can promote cancer invasion, metastasis, and cancer tolerance to chemotherapy (28). The CSC in pancreatic cancer was isolated and identified by Li et al. in 2007. The PAR1 expression level is closely related to the cancer malignant evolution in breast cancer (29). After PAR1 is activated by thrombin, it can mediate cancer cell biological behavior, including the remodeling of tumor microenvironment, and it can promote cancer malignant evolution through downstream molecule and cytokine regulator. The effect of PAR1 on pancreatic cancer cells has not been reported. The effects of PAR1 on the CSC-like properties of pancreatic cancer cells were determined in the present work. PAR1 can promote the expression of pancreatic CSC marker CD133, the microsphere formation ability, and CSC-like characteristics of pancreatic cancer cells. PAR1 can also promote the migration, invasion and EMT of pancreatic cancer cells. Thus, PAR1 can promote the CSC-like properties and EMT of pancreatic cancer cells.

PAR1 can induce FAK phosphorylation in retinal pigment epithelial cells after activation by thrombin, which has not been reported in pancreatic cancer. PI3K is one of the main downstream signaling molecules of the FAK pathway (30). The PI3K/AKT signaling pathway is closely related to cancer cell proliferation, migration, and invasion, and its abnormal activation may result in cancer malignant evolution. FAK may induce EMT (31) and CSC formation through the PI3K/AKT signaling pathway. In the present study, the mechanism underlying the effect of PAR1 on pancreatic CSC formation was investigated by overexpressing and interfering with PAR1 in pancreatic cancer cell lines. FAK, PI3K, and AKT phosphorylation were inhibited after PAR1 interference. PAR1 can activate the FAK/PI3K/AKT signaling pathway in pancreatic cancer cells. It can mediate the occurrence of EMT and the CSC-like properties of pancreatic cancer cells.

In our previous studies, we found that doxycycline is a PAR1 inhibitor. Doxycycline can combine with the PAR1 key amino acid residues of Val257, Leu258, His336, His164, and Leu167, which inhibit PAR1 activity (25). In the present work, we showed that doxycycline can target PAR1 and inhibit the FAK/PI3K/AKT signaling pathway activation in pancreatic cancer cells, EMT, and the CSC-like properties of pancreatic cancer cells. The synergistic effects of doxycycline with chemotherapeutic drugs, such as cisplatin, oxaliplatin, gemcitabine and 5-FU, were evaluated. Doxycycline combined with 5-FU showed the best synergistic effect. Besides, doxycycline and 5-FU can inhibit the growth of the Panc-1 subcutaneous xenografts in nude mice. The immunohistochemical analysis showed a significant increase in

E-Cad expression, whereas VIM and CD133 expression levels were significantly decreased. Thus, doxycycline inhibited EMT and the CSC-like properties of pancreatic cancer *in vivo*.

In conclusion, this work showed that PAR1 can promote the CSC-like properties of pancreatic cancer by activating the FAK/PI3K/AKT pathway. As a PAR1 inhibitor, doxycycline can inhibit the CSC-like properties of pancreatic cancer cells targeting the PAR1/FAK/PI3K/AKT pathway and can enhance the therapeutic effect of 5-FU (Figure 7I). This work showed that PAR1 may be a therapeutic target of pancreatic cancer and provided insights into pancreatic cancer therapeutic strategies.

DATA AVAILABILITY STATEMENT

The original contributions presented in the study are included in the article/supplementary materials. Further inquiries can be directed to the corresponding authors.

ETHICS STATEMENT

The animal study was reviewed and approved by the guidelines of the Animal Ethics Committee of the Tianjin International Joint Academy of Biotechnology and Medicine.

AUTHOR CONTRIBUTIONS

TS and HL conceived and designed the projects. HL, HT, and HQW wrote the manuscript. HL, HT, HQW, YY, and RY performed the experiments. HL, HT, HQW, XTD, XJD, and SC provided technical and material support. All authors contributed to the article and approved the submitted version.

FUNDING

This study was financially supported by the National Natural Science Funds of China (grant nos. 81872374, 81703581, 81972746, 81871972, and 81972629), the Tianjin Science and Technology Project (grant nos. 19JCJC63200, 18PTSJC00060), the Chinese National Major Scientific and Technological Special Project for "Significant New Drugs Development" (grant no. 2018ZX09736-005), and the National Key Research and Development Program of China (grant no. 2018YFA0507203).

REFERENCES

- Vincent A, Herman J, Schulick R, Hruban RH, Goggins M. Pancreatic cancer. *Lancet* (2011) 378(9791):607–20. doi: 10.1016/S0140-6736(10)62307-0
- Drouillard A, Manfredi A, Lepage C, Bouvier AM. [Epidemiology of pancreatic cancer]. *Bull Cancer* (2018) 105(1):63–9. doi: 10.1016/j.bulcan.2017.11.004
- Siegel RL, Miller KD, Jemal A. Cancer statistics, 2019. *CA: A Cancer J Clin* (2019) 69(1):7–34. doi: 10.3322/caac.21551
- Dietrich F, Martins JP, Kaiser S, Silva RBM, Rockenbach L, Edelweiss MIA, et al. The Quinovic Acid Glycosides Purified Fraction from *Uncaria tomentosa* Protects against Hemorrhagic Cystitis Induced by Cyclophosphamide in Mice. *PLoS One* (2015) 10(7):e0131882. doi: 10.1371/journal.pone.0131882
- Li C, Heidt DG, Dalerba P, Burant CF, Zhang L, Adsay V, et al. Identification of pancreatic cancer stem cells. *Cancer Res* (2007) 67(3):1030–7. doi: 10.1158/0008-5472.CAN-06-2030

6. Dai L, Li C, Shedden KA, Lee CJ, Li C, Quoc HV, et al. Quantitative proteomic profiling studies of pancreatic cancer stem cells. *J Proteome Res* (2010) 9(7):3394–402. doi: 10.1021/pr100231m
7. Song L, Chen X, Gao S, Zhang C, Qu C, Wang P, et al. Ski modulate the characteristics of pancreatic cancer stem cells via regulating sonic hedgehog signaling pathway. *Tumour Biol* (2016) 37:16115–25. doi: 10.1007/s13277-016-5461-8
8. Shibue T, Weinberg RA. EMT, CSCs, and drug resistance: the mechanistic link and clinical implications. *Nat Rev Clin Oncol* (2017) 14(10):611–29. doi: 10.1038/nrclinonc.2017.44
9. Tanabe S, Quader S, Cabral H, Ono R. Interplay of EMT and CSC in Cancer and the Potential Therapeutic Strategies. *Front Pharmacol* (2020) 11:904–4. doi: 10.3389/fphar.2020.00904
10. Zhang C, Srinivasan Y, Arlow DH, Fung JJ, Palmer D, Zheng Y, et al. High-resolution crystal structure of human protease-activated receptor 1. *Nature* (2012) 492(7429):387–92. doi: 10.1038/nature11701
11. Yang Y, Stang A, Schweickert PG, Lanman NA, Paul EN, Monia BP, et al. Thrombin Signaling Promotes Pancreatic Adenocarcinoma through PAR-1-Dependent Immune Evasion. *Cancer Res* (2019) 79(13):3417–30. doi: 10.1158/0008-5472.CAN-18-3206
12. Wang Q, Tang Y, Wang T, Yang HL, Wang X, Ma H, et al. EPCR promotes MGC803 human gastric cancer cell tumor angiogenesis in vitro through activating ERK1/2 and AKT in a PAR1-dependent manner. *Oncol Lett* (2018) 16(2):1565–70. doi: 10.3892/ol.2018.8869
13. Nguyen QD, Wever OD, Bruyneel E, Hendrix A, Xie WZ, Lombet A, et al. Commutators of PAR-1 signaling in cancer cell invasion reveal an essential role of the Rho-Rho kinase axis and tumor microenvironment. *Oncogene* (2005) 24(56):8240–51. doi: 10.1038/sj.onc.1208990
14. Tekin C, Shi K, Daalhuisen JB, Brink MST, Bijlsma MF, Spek CA. PAR1 signaling on tumor cells limits tumor growth by maintaining a mesenchymal phenotype in pancreatic cancer. *Oncotarget* (2018) 9(62):32010–23. doi: 10.18632/oncotarget.25880
15. Thennes T, Mehta D. Heterotrimeric G proteins, focal adhesion kinase, and endothelial barrier function. *Microvasc Res* (2012) 83(1):31–44. doi: 10.1016/j.mvr.2011.05.004
16. Golubovskaya VM, Virnig C, Cance WG. TAE226-induced apoptosis in breast cancer cells with overexpressed Src or EGFR. *Mol Carcinog* (2008) 47(3):222–34. doi: 10.1002/mc.20380
17. Parsons JT. Focal adhesion kinase: the first ten years. *J Cell Sci* (2003) 116(Pt 8):1409–16. doi: 10.1242/jcs.00373
18. Thakur R, Trivedi R, Rastogi N, Singh M, Mishra DP. Inhibition of STAT3, FAK and Src mediated signaling reduces cancer stem cell load, tumorigenic potential and metastasis in breast cancer. *Sci Rep* (2015) 5:10194. doi: 10.1038/srep10194
19. Aguilar-Solis ED, Lee-Rivera I, Álvarez-Arce A, López E, López-Colomé AM. FAK phosphorylation plays a central role in thrombin-induced RPE cell migration. *Cell Signal* (2017) 36:56–66. doi: 10.1016/j.cellsig.2017.04.016
20. Syapin PJ, Martinez JM, Curtis DC, Marquardt PC, Allison CL, Groot JA, et al. Effective Reduction in High Ethanol Drinking by Semisynthetic Tetracycline Derivatives. *Alcohol Clin Exp Res* (2016) 40(12):2482–90. doi: 10.1111/acer.13253
21. Carmena D, Benito-Perez de Mendiola A, Sanchez-Serrano LP. Reporting of human cystic echinococcosis in Spain: how effective is the epidemiological surveillance system? *Enferm Infecc Microbiol Clin* (2010) 28(2):135–6. doi: 10.1016/j.eimc.2009.03.013
22. Carmena D, Benito-Perez de Mendiola A, Sanchez-Serrano LP. Doxycycline Inducible Melanogenic Vaccinia Virus as Theranostic Anti-Cancer Agent. *Theranostics* (2015) 5(10):1045–57. doi: 10.7150/thno.12533
23. Bendeck MP, Conte M, Zhang M, Nili N, Strauss BH, Farwell SM. Doxycycline modulates smooth muscle cell growth, migration, and matrix remodeling after arterial injury. *Am J Pathol* (2002) 160(3):1089–95. doi: 10.1016/S0002-9440(10)64929-2
24. Zhong W, Chen S, Qin Y, Zhang H, Wang H, Meng J, et al. Doxycycline inhibits breast cancer EMT and metastasis through PAR-1/NF-kappaB/miR-17/E-cadherin pathway. *Oncotarget* (2017) 8(62):104855–66. doi: 10.18632/oncotarget.20418
25. Zhong W, Chen S, Zhang Q, Xiao T, Qin Y, Gu J, et al. Doxycycline directly targets PAR1 to suppress tumor progression. *Oncotarget* (2017) 8(10):16829–42. doi: 10.18632/oncotarget.15166
26. Cao X-Y, Zhang XX, Zhang MW, Hu LP, Jiang SH, Tian GA, et al. Aberrant upregulation of KLK10 promotes metastasis via enhancement of EMT and FAK/SRC/ERK axis in PDAC. *Biochem Biophys Res Commun* (2018) 499(3):584–93. doi: 10.1016/j.bbrc.2018.03.194
27. Ohlund D, Handly-Santana A, Biffi G, Elyada E, Almeida AS, Ponz-Sarvise M, et al. Distinct populations of inflammatory fibroblasts and myofibroblasts in pancreatic cancer. *J Exp Med* (2017) 214(3):579–96. doi: 10.1084/jem.20162024
28. Seymour T, Nowak A, Kakulas F. Targeting Aggressive Cancer Stem Cells in Glioblastoma. *Front Oncol* (2015) 5:159. doi: 10.3389/fonc.2015.00159
29. Ray T, Pal A. PAR-1 mediated apoptosis of breast cancer cells by V. cholerae hemagglutinin protease. *Apoptosis* (2016) 21(5):609–20. doi: 10.1007/s10495-016-1229-2
30. Fu QF, Liu Y, Fan Y, Hua SN, Qu HY, Dong SW, et al. Alpha-enolase promotes cell glycolysis, growth, migration, and invasion in non-small cell lung cancer through FAK-mediated PI3K/AKT pathway. *J Hematol Oncol* (2015) 8:22. doi: 10.1186/s13045-015-0117-5
31. Zhang PF, Li KS, Shen YH, Gao PT, Dong ZR, Cai JB, et al. Galectin-1 induces hepatocellular carcinoma EMT and sorafenib resistance by activating FAK/PI3K/AKT signaling. *Cell Death Dis* (2016) 7:e2201. doi: 10.1038/cddis.2015.324

Conflict of Interest: The authors declare that the research was conducted in the absence of any commercial or financial relationships that could be construed as a potential conflict of interest.

Copyright © 2021 Liu, Tao, Wang, Yang, Yang, Dai, Ding, Wu, Chen and Sun. This is an open-access article distributed under the terms of the Creative Commons Attribution License (CC BY). The use, distribution or reproduction in other forums is permitted, provided the original author(s) and the copyright owner(s) are credited and that the original publication in this journal is cited, in accordance with accepted academic practice. No use, distribution or reproduction is permitted which does not comply with these terms.



Effect of Micelle-Incorporated Cisplatin With Sizes Ranging From 8 to 40nm for the Therapy of Lewis Lung Carcinoma

Zhicheng Wang¹, Yumin Li^{1,2}, Tong Zhang¹, Hongxia Li¹, Zhao Yang^{2*} and Cheng Wang^{1,3*}

¹Key Laboratory of Marine Drugs, Chinese Ministry of Education, School of Medicine and Pharmacy, Ocean University of China, Qingdao, China, ²Qingdao Institute for Food and Drug Control, Qingdao, China, ³Laboratory for Marine Drugs and Bioproducts of Qingdao National Laboratory for Marine Science and Technology, Qingdao, China

OPEN ACCESS

Edited by:

Sanjun Shi,
Chengdu University of Traditional
Chinese Medicine, China

Reviewed by:

Shuai Shi,
Wenzhou Medical University, China
Ke Wang,
Xi'an Jiaotong University, China

*Correspondence:

Chen Wang
cheng13980029671@163.com
Zhao Yang
yangzhaosyy@qd.shandong.cn

Specialty section:

This article was submitted to
Pharmacology of Anti-Cancer Drugs,
a section of the journal
Frontiers in Pharmacology

Received: 24 November 2020

Accepted: 07 January 2021

Published: 08 March 2021

Citation:

Wang Z, Li Y, Zhang T, Li H, Yang Z
and Wang C (2021) Effect of Micelle-
Incorporated Cisplatin With Sizes
Ranging From 8 to 40 nm for the
Therapy of Lewis Lung Carcinoma.
Front. Pharmacol. 12:632877.
doi: 10.3389/fphar.2021.632877

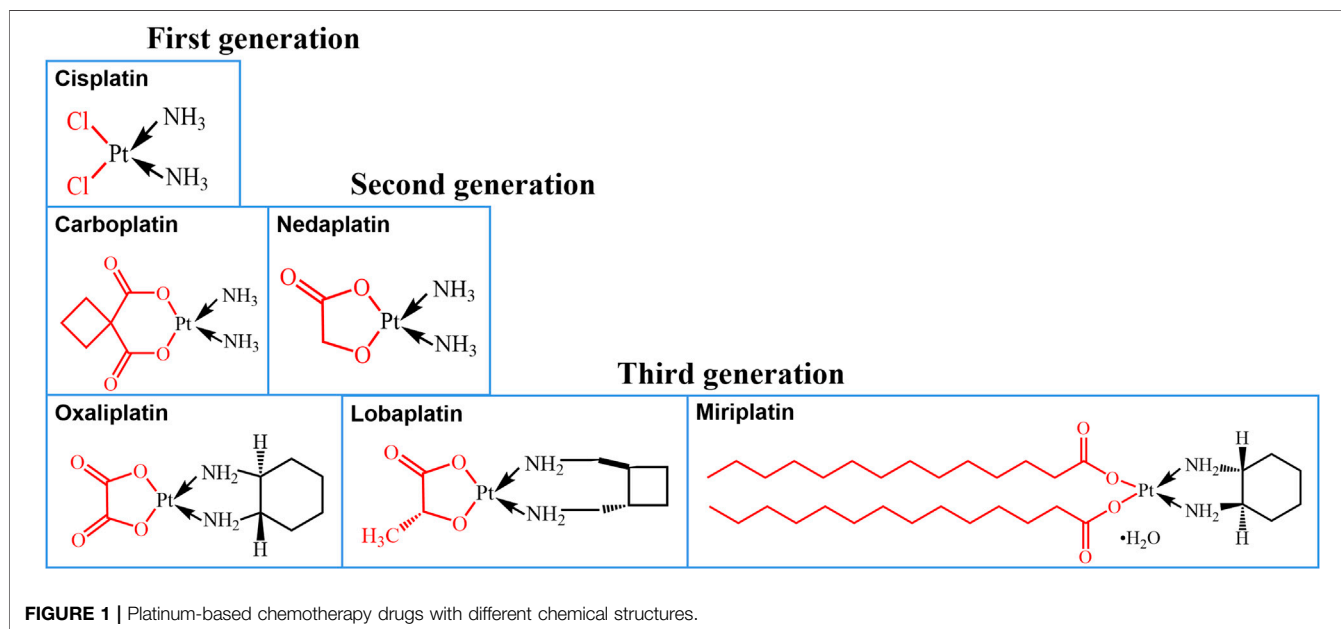
Insufficient transport of therapeutic cargo into tumor bed is a bottleneck in cancer nanomedicine. Block copolymers are promising carriers with smaller particle size by ratio modification. Here, we constructed cisplatin nanoparticles with sizes ranging from 8 to 40 nm to study the permeability and therapy of Lewis lung carcinoma. We synthesized methoxypoly(ethylene glycol)₂₀₀₀-block poly(L-glutamic acid sodium salt)₁₉₇₉ loading cisplatin through complexation reaction. The cisplatin nanomedicine has high drug loading and encapsulation efficiency. *In vitro* data demonstrated that cisplatin nanoparticles had equivalent growth-inhibiting effects on Lewis lung carcinoma cells compared to free cisplatin. *In vivo* evidences showed cisplatin nanoparticles had superior antitumor effects on the Lewis lung carcinoma mouse model with no obvious side effects. All results indicated that optimizing the ratio of block copolymers to obtain smaller sized nanomedicine could act as a promising strategy for overcoming the inadequate accumulation in poorly vascularized tumors.

Keywords: cisplatin, nanomedicine, block copolymers, nanoparticles, lung cancer, drug delivery

INTRODUCTION

Nonspecific distribution and inadequate accumulation of therapeutic cargo are the main challenges in nanomedicine (Poon et al., 2020). Wilhelm et al. reported that conventional nanoparticles, only 0.7% injected dose, could accumulate in the tumor and that exploiting new strategies for overcoming the poor delivery efficiency is a formidable challenge to drug developers (Wilhelm et al., 2016).

Lung cancer is difficult to be cured due to its poor penetration ascribing to its complex microenvironment (Gao et al., 2014; Bussard et al., 2016; Pautu et al., 2017; Shen et al., 2018). Cisplatin (CISP, **Figure 1**, trade name is Nuoxin[®]), a first-line chemotherapy agent for lung cancer since its launch in 1978 (Guo et al., 2018; Wiltshaw, 1979), causes interstrand and intrastrand crosslinking of nuclear DNA, leading to DNA damage and cell apoptosis (Xu et al., 2019). However, the high activity of the chloride ion as the leaving group leads to considerable nephrotoxicity and neurotoxicity, as well as other adverse reactions, resulting in limited clinical application (Ghosh, 2019). For this reason, in the subsequent design of platinum-based drugs, the chloride ion was replaced with the relatively stable cyclobutanecarboxylic acid and glycolic acid, respectively, to derive carboplatin (Calvert et al., 1982) and nedaplatin (Kuwahara et al., 2010). However, the commercial introduction of next-generation platinum drugs has been followed by a new challenge of high levels



of cross-resistance between platinum agents. Further research revealed that the primary reason for the high degree of cross-resistance was that the platinum ion was liganded on the same side as the amino group. Consequently, in the tertiary development of platinum-based drugs, oxaliplatin (Wheate et al., 2010) and miriplatin (Liu et al., 2015) were generated by replacing the amino group with cyclohexane, and cyclobutane modification gave rise to lobaplatin (Martinez-Balibrea et al., 2015), whereas the more stable oxalic, lactic, and myristic acids substitute for the leaving group (**Figure 1**). Although the deleterious effects of the structurally modified platinum drugs were reduced, the antitumor spectrum of the drugs was narrowed and their efficacy diminished (Ghosh, 2019). As a result, CISP remains among the most effective chemotherapeutic agents used alone or in combination for the treatment of many neoplasms (Ghosh, 2019).

In addition, the particles smaller than 4–6 nm are filtered out of the blood and eventually passed in the urine (Dai et al., 2017), so only larger particles could escape kidney clearance. Kataoka and coworkers reported that particles below 30 nm have a superior penetration into poorly vascularized tumors (Cabral et al., 2011). Chauhan et al. also demonstrated that nanoparticles with diameters 12 nm are of ideal sizes for deeply penetrating tumor (Chauhan et al., 2012). NC-6004 was prepared through complexation of ionized carboxylic group of the polymer with CISP, and the efficacy of NC-6004 is being assessed in Phase III of the clinical trial in the United States (Plummer et al., 2011; Varela-Moreira et al., 2017). However, 80% of the nanoparticles formed from the hydrophilic fragments of methoxypoly(ethylene glycol)₁₂₀₀₀ and hydrophobic fragment of poly(L-glutamic acid sodium salt)₆₀₀₀ of the carrier are larger than 20 nm, and the particle

size is not optimal (Nishiyama et al., 2003). Furthermore, methoxy-PEG is synthesized by ring opening polymerization of ethylene oxide using methanol as initiator. The polydispersity of MPEG < 5,000 Da can reach 1.01, which can ensure the MPEG derivative has lower polydispersity. Besides, its body clearance depends upon its molecular weight. The higher the molecular weight of PEG becomes, the slower it is cleared, and the liver clearance becomes more dominant (Pasut and Veronese, 2007). Of utmost importance is the molar mass of PEG affecting the composition of the proteins coating the nanoparticle surface (Schöttler et al., 2016), and the presence of distinct protein will influence the cellular uptake (Poon et al., 2020). In light of above considerations, it is essential to optimize the carrier to construct optimal cisplatin nanomedicine.

In this research, we successfully synthesized methoxypoly(ethylene glycol)₂₀₀₀-poly(L-glutamic acid sodium salt)₁₉₇₉ [MPEG₂₀₀₀-P(Glu)₁₉₇₉] block copolymers. The molecular weight ratio of MPEG to P(Glu) was according to the carrier of methoxypoly(ethylene glycol)₂₀₀₀-poly(DL-lactide)₁₇₅₀ (MPEG₂₀₀₀-PDLLA₁₇₅₀), which has been applied in the commercial production of Genexol-PM. Schöttler et al. also demonstrated that PEG₂₀₀₀ has a better effect of inhibiting the protein adsorption on particle compared to PEG₆₀₀₀ (Schöttler et al., 2016). To sum up, we have the following hypothesis that cisplatin nanoparticles (CISP-NPs) composed of MPEG₂₀₀₀-P(Glu)₁₉₇₉ should have smaller particle size with 8–40 nm and excellent tumor penetration leading to superior antitumor effect. To test the hypothesis, CISP-NPs were developed and characterized *in vitro*. Furthermore, we preliminarily evaluate its antitumor efficacy in a xenograft mouse model of Lewis lung carcinoma to provide more evidence toward new drug registration. Finally, the results confirmed that the strategy is applicable.

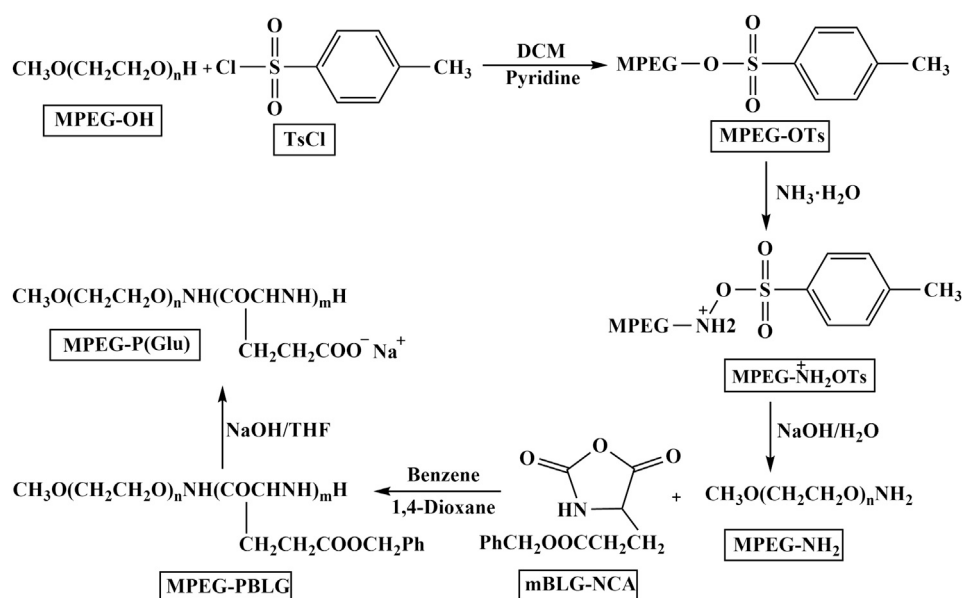


FIGURE 2 | The route of synthesis sodium salt of MPEG-P(Glu).

MATERIALS AND METHODS

Materials

Methoxypoly(ethylene glycol) (MPEG, $M_n = 2000$, Aldrich, United States), γ -benzyl-L-glutamate-N-carboxy anhydride (BLG-NCA), dichloromethane, pyridine, *p*-toluene sulfonyl chloride (TsCl), absolute ether, ammonium hydroxide, benzene, dimethylsulfoxide (DMSO) and 1,4-dioxane were purchased from Sinopharm Chemical Reagent Co., Ltd. (Shanghai, China). Petroleum ether was obtained from Fuyu Chemical Corp. (Shanghai, China). Simethicone was purchased from Yongda Chemical Corp. (Tianjin, China). Sodium bicarbonate was purchased from Dingshengxin Chemical Corp. (Tianjin, China). Tetrahydrofuran and sodium hydrate were purchased from Huirui Chemicals Corp. (Tianjin, China) and Jinshan Pharmaceutical Corp. (Sichuan, China), respectively. Spectrographic grade potassium bromide (KBr) was obtained from Sinopharm Chemical Reagent Co., Ltd. (Shanghai, China). HPLC-grade acetonitrile was purchased from Anaqua Chemical Supply (Houston, TX, United States). *Cis*-platinum was purchased from Meryer (Shanghai, China).

Dulbecco's Modified Eagle's Medium (DMEM) High Glucose and fetal bovine serum (FBS) were purchased from Gibco (Shanghai, China). Penicillin/streptomycin and 0.25% (w/v) trypsin-0.1% (w/v) Ethylenediaminetetraacetic acid (EDTA) were bought from Solarbio (Beijing, China). 3-(4,5-Dimethylthiazol-2-yl)-2,5-diphenyl-tetrazolium bromide (MTT) was purchased from Sigma (Shanghai, China). Culture flasks and dishes were obtained from Corning (NY, United States).

Lewis lung carcinoma (LLC) cell line, derived from the C57BL/6 mouse, was purchased from the Type Culture Collection of the Chinese Academy of Sciences (Shanghai, China). LLC cells were maintained in DMEM with 10% FBS in the humidified atmosphere containing 5% CO₂ at 37°C.

Healthy, six-to-eight-week-old male C57BL/6 mice were purchased from Qingdao Daren Fortune Animal Technology Co., Ltd. (Qingdao, China). Food and water were given to all mice *ad libitum*. Feeding temperature was controlled at 20–22°C, relative humidity 50–60%, light and dark cycles for 12 h. All experiments were conducted in accordance with the guidelines of the Institutional Animal Care and Use Committee, Ocean University of China.

Synthesis of MPEG-P(Glu) Block Copolymer

MPEG-P(Glu) block copolymer was synthesized as previously reported (Cabral et al., 2007) (Figure 2). First, methoxypoly(ethylene glycol) amine (MPEG₂₀₀₀-NH₂) was prepared by the method of toluene sulfonate esterification. MPEG₂₀₀₀ (40 g, 20 mmol) and CH₂Cl₂ (200 ml) were added in a 3-neck round-bottomed flask (500 ml), stirred for 5 min. Subsequently, pyridine (150 ml, 1.89 mol) and TsCl (7.6 g, 40 mmol) were added into the solution above and stirred for 24 h under nitrogen protection at 30°C and then cooled to 0°C. The reaction mixture was poured into hydrochloric acid solution stirred for 15 min and the CH₂Cl₂ layer was collected. The aqueous phase was extracted from 200 ml dichloromethane (three times). The combined organic layer was washed with brine, aqueous sodium bicarbonate, and brine successively, dried over anhydrous sodium sulfate overnight. Next, tetrahydrofuran was added and stirred for 5 min. Then, the acquired white powder (MPEG₂₀₀₀-OTs) was washed 2–3 times with diethyl ether and dried under vacuum at 25°C for 4 h. After MPEG₂₀₀₀-OTs (7 g, 3.25 mmol) was dissolved in aqueous ammonia and stirred for 8.5 h at 135°C, MPEG₂₀₀₀-NH₂ was obtained by isolation and purification, dried for 4 h. The following steps were applied to generate methoxypoly(ethylene glycol)-poly(γ -benzyl-L-glutamate) (MPEG-PBLG) block

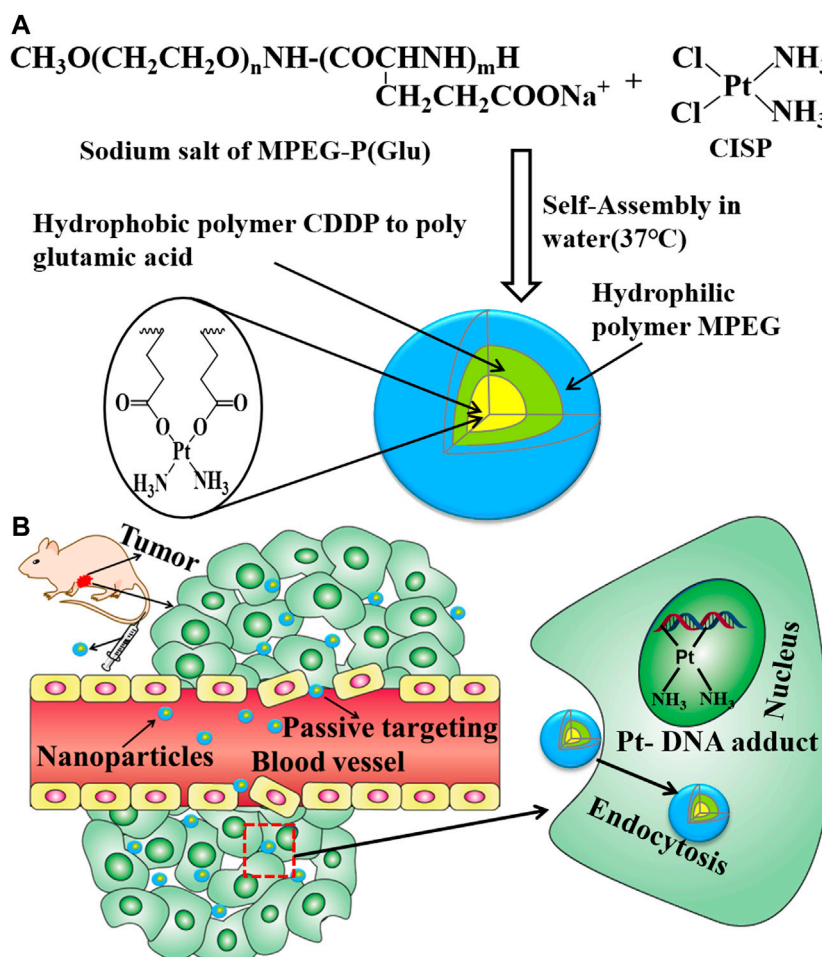


FIGURE 3 | (A) Preparative procedure of CISP-NPs. **(B)** The intracorporal process of CISP-NPs after administration.

copolymer. MPEG-PBLG was synthesized by ring-opening polymerization of BLG-NCA monomer using MPEG₂₀₀₀-NH₂ as macro initiator, and then the benzyl group was deprotected following the literature procedure (Song et al., 2012). BLG-NCA (4 g, 15.2 mmol) was suspended in a mixed solution of benzene (64 ml) and dioxane (16 ml) and then MPEG₂₀₀₀-NH₂ (1.2 g, 0.6 mmol) was added. The reaction mixture was reacted under nitrogen protection at ambient temperature for 4 days. After the reaction, the mixture was poured into a large volume of anhydrous ethanol and stirred for 1 h, rested for 30 min, suction filtration, and washed with little ethanol. The precipitated product was dried under vacuum at 30°C for 12 h. At last, the benzyl group was removed from protection by blending with 0.025 N NaOH at ambient temperature to produce MPEG-P(Glu).

Characterization of MPEG-NH₂, MPEG-PBLG, and MPEG-P(Glu)

The structure of MPEG-OH, MPEG-NH₂, and MPEG-PBLG was confirmed by Fourier-transform infrared (FT-IR) analyzer

(Nexus 470 by Nicolet Instruments America). 2% (w/w) of the sample was dispersed in KBr and then compressed it into slices. Each slice was scanned between 400 and 4,000 cm⁻¹.

The structure and purity of MPEG₂₀₀₀-PBLG and MPEG₂₀₀₀-P(Glu) were determined by ¹H nuclear magnetic resonance spectroscopy (¹H-NMR) instrument (JNM-ECP600, JEOL TMS, Tokyo, Japan) at 25°C. MPEG₂₀₀₀-PBLG and MPEG₂₀₀₀-P(Glu) were dissolved in deuterated dimethyl sulfoxide (DMSO-d₆, 500 MHz), D₂O to a concentration of approximately 10 mg/ml, respectively.

Preparation and Characterization of CISP-NPs

Preparation of CISP-NPs

CISP-NPs were prepared according to the procedure described previously with slight modifications (Nishiyama et al., 2003; Uchino et al., 2005). Figure 3A was the preparation scheme of CISP-NPs. MPEG₂₀₀₀-P(Glu)₁₉₇₉ and CISP (CISP)/(Glu) = 1.0) were dissolved in distilled water and shaken at 37°C for 72 h in the dark until the mixture was dissolved completely. The hydrophilic

chain of the block copolymer, MPEG, made up the outer shell of the micelles. Poly(glutamic acid) and CISP were hydrophobic chains, a polymer-metal complex-forming chain, which formed the inner core of the micelles. Once the micelle was formed, free CISP was eliminated by dialysis with a membrane of the molecular cut-off of 1 kDa. The water was freshened every 2 h during the previous 8 h. After dialysis for 12 h, the micelle solution was filtered with 0.22 μm filters (Millipore).

Characterization of CISP-NPs

The morphological characteristics of CISP-NPs were investigated by transmission electron microscope (TEM, EOL JEM-1200EX, Ltd., Japan) (Weng et al., 2017). Briefly, the micelle solution was dropped onto a 200-mesh copper grid coated with a Formvar-carbon support film and stained with 2% phosphotungstic acid. Extra liquid was wiped with filter paper and then slowly dried at room temperature prior to measurement. Moreover, the mean diameter of the CISP-NPs was measured by Malvern Zetasizer Nano ZS90 (Malvern, Worcestershire, United Kingdom) particle size analyzer, as well as polydispersity index (PDI). Acquisition of three-dimensional images of the sample used atomic force microscopy (AFM, Agilent) (Zhu et al., 2013). Briefly, a droplet of 0.5 mg/ml polymer samples was spread on the polyethyleneimine-coated glass cap and dried naturally. Scanning was done with a probe tip, then the sample was imaged with Nano-scope III (Digital Instrument VEECO).

To identify whether CISP was encapsulated in MPEG-P(Glu), samples analyzed by the powder X-ray diffractometer (XRD, Bruker D8 ADVANCE) of which the voltage and current employed were 40 kV and 30 mA, respectively (Pansini et al., 2017). X-ray diffraction (XRD) patterns of MPEG-P(Glu), CISP, and CISP-NPs lyophilized powder and physical mixture of CISP and MPEG-P(Glu) (30:70) were obtained from 5° to 60° at a 0.02° step and 5°/min scan speed.

Drug Loading and Encapsulation Efficiency of CISP-NPs

Drug loading (DL) and encapsulation efficiency (EE) of the CISP-NPs were determined as follows: briefly, lyophilized CISP-NPs was dissolved in double distilled water and then hydrochloric acid (2 mol/L) was used to disrupt the structure of micelles. Afterwards, the solution was filtered by 0.22 μm syringe filter. The subsequent filtrate was measured by high performance liquid chromatography (HPLC) and inductively coupled plasma atomic emission spectroscopy (ICP-AES), respectively. According to the following formulas, DL and EE of CISP-NPs were calculated:

$$DL = \frac{\text{weight of CISP in micelle}}{\text{weight of the polymer and CISP}} \times 100\%, \quad (1)$$

$$EE = \frac{\text{weight of CISP in micelle}}{\text{weight of the feeding CISP}} \times 100\%. \quad (2)$$

Determination of CISP concentration by HPLC (Shimadzu, Kyoto, Japan) is performed with the LC-20AT solvent delivery unit, the SPD-20A UV/VIS detector, the plus manual sampler, and the HT-230A column heater (Tianjin Hengao Technology,

Tianjin, China). The chromatographic analysis was conducted on a Hypersil NH₂ (250 mm \times 4.6 mm, 5 μm , Elite, Dalian, China) with the detection wave length at 310 nm. The flow rate of mobile phase, ethyl acetate-methanol-dimethyl formamide-deionized water (25:16:5:5, v/v), was 0.8 ml/min whilst the column temperature was maintained at 25°C. The standard curve equation is $A = 696.37 \times C - 913.69$ (A for the area of peak; C for the concentration of CISP-NPs) and the correlation coefficient is 0.9999.

Another test method, the metal ions standard solution, was the configuration at concentrations of 8 $\mu\text{g/L}$, 16 $\mu\text{g/L}$, 24 $\mu\text{g/L}$, 32 $\mu\text{g/L}$, and 48 $\mu\text{g/L}$ to obtain standard curve. After the nanoparticles were nitrated with nitric acid (5 mg/ml), the manganese content of solution was measured with optima 8000 ICP-AES.

Cytotoxicity Evaluation

Cytotoxicity of free CISP, CISP-NPs, and MPEG-P(Glu) polymer was determined by the MTT assay on LLC cells. LLC cells were seeded in 96-well culture plates (Jet Biofil) at a density of 6×10^3 cells/well and incubated for 24 h. Cells were then treated with a series of drugs at different concentrations of free CISP (DMSO <0.5%), CISP-NPs, and MPEG-P(Glu) polymers for 24, 48, and 72 h, respectively. Tests were repeated for 6 times. Briefly, at the determined incubation-time, 20 μl of 5 mg/ml MTT was added per well of the plate. After incubation for another 4 h at 37°C, purple formazan crystals were observed. The supernatant was aspirated off gently, and 150 μl /well of DMSO was added into each well and the plate was gently shaken for 10 min at room temperature to dissolve the formazan crystals, and the absorbance of the resulting DMSO solution at 490 nm was measured with a SPECTRA-max M5 microplate reader (Molecular Devices, United States). Cells without drug treatment were served as a negative control with a 100% survival rate, while cells without MTT were used as a blank control to calibrate the spectrometer meter. Relative cell viability (%) in comparison to control cells was calculated as $(\text{Abs}_{\text{sample}}/\text{Abs}_{\text{control}}) \times 100\%$, expressed as the mean \pm SD of six measures.

Flow Cytometry Analysis for Cell Cycle

Cell cycle analysis was evaluated as described below (Wang et al., 2013). In brief, LLC cells were seeded at a density of 5×10^5 cells in each well in a six-well plate (NEST Biotechnology) followed by incubation for 12 h. Then, culture media was substituted with fresh medium containing free CISP or CISP-NPs formulations at dosage of 12.55 $\mu\text{g/ml}$ of CISP and cultivated for 48 h, with untreated cells as the negative control. At the end of the incubation, the collected cells (1×10^6) were centrifuged at 1,000 rpm for 5 min, resuspended and washed twice with ice-cold PBS, and then fixed with 75% cold ethanol. After storage for 24 h at 4°C, the cell suspension was centrifuged again and washed twice with cold PBS and then incubated with the freshly prepared staining solution containing propidium iodide (PI) and RNase (Beyotime, Haimen, China) at 37°C under light-proof conditions for 30 min. Subsequently, the DNA content was determined by Cytomics FC500 MPL flow cytometry system (Beckman Coulter, United States). The percentage of cell populations in each stage of the cell cycle,

including G0/G1, S, and G2/M phases, was assessed using MultiCycle AV software (San Diego, CA).

Antitumor Activity

Antineoplastic activity of CISP-NPs was elucidated in the mouse xenograft model. 1×10^6 LLC cells were inoculated subcutaneously into the right axillary space of the C57BL/6 mice. Briefly, the treatment was initiated when the tumor size reached an average of 7–9 mm and randomly divided into four groups ($n = 6$ for per group). Mice were separately injected with saline and MPEG-P (Glu) polymer, free CISP (6 mg/kg), CISP-NPs (6 mg/kg CISP or 12 mg/kg CISP) via the tail vein on days 7, 10, 13, 16, and 19, respectively. On day 21, three mice in each group were executed by cervical dislocation, followed by the tumor, heart, liver, spleen, and kidney which were excised with histopathological examination by Hematoxylin-Eosin (H&E) staining. The remaining three mice in each group were further used for survival experiments.

Histopathology Evaluation

Histopathological impairment evaluated by hematoxylin and eosin (H&E) assay according to manufacturer's instruction. Liver, heart, spleen, and kidney from treated mice were stained with hematoxylin-eosin for assessment of toxicity. Briefly, tumor, heart, liver and spleen and kidney tissues in different groups were harvested and then fixed in 10% neutral buffered formalin. The fixed tissues were subsequently embedded in paraffin and sectioned in 3- μ m increments. The sections were dewaxed by dipping them in xylene and then placed on glass slides and stained with H&E. Observations were made by optical microscopy (OLYMPUS BX60, Japan) with corresponding image analysis software (OLYMPUS DP25, Japan).

Statistical Analysis

All statistical data were expressed as means \pm standard deviation (SD) and total experiments were performed at least three replicates. The significant difference between the groups were examined by Student's *t*-test. * $p < 0.05$, ** $p < 0.01$, and *** $p < 0.001$ were deemed statistically significant.

RESULTS AND DISCUSSION

Preparation and Characterization of MPEG-NH₂, MPEG-PBLG, and MPEG-P(Glu)

The FTIR spectra of MPEG₂₀₀₀-OH, MPEG₂₀₀₀-NH₂, and MPEG₂₀₀₀-PBLG were shown in **Figure 4**. The characteristic peak of amine bond appearing at 1,648 and 1,548 cm^{-1} indicated the N-H stretch of MPEG₂₀₀₀-NH₂ [**Figure 4**(2)]. The characteristic IR absorption frequencies for MPEG₂₀₀₀-PBLG [**Figure 4**(3)] were 3,300 (OH, NH Str), 2,885 (CH₂ Str), 1,734 (C = O Str), 1,654 and 1,542 (CONH Str), and 778 (CH bend aromatic). The ¹H-NMR spectra (**Figure 5**) also showed that MPEG₂₀₀₀-PBLG and MPEG₂₀₀₀-P(Glu) block copolymers were successfully synthesized. In the ¹H NMR spectrum (**Figure 5A**), five major signals were observed at 3.50 (**Figure 5A-a**), 3.90–4.4

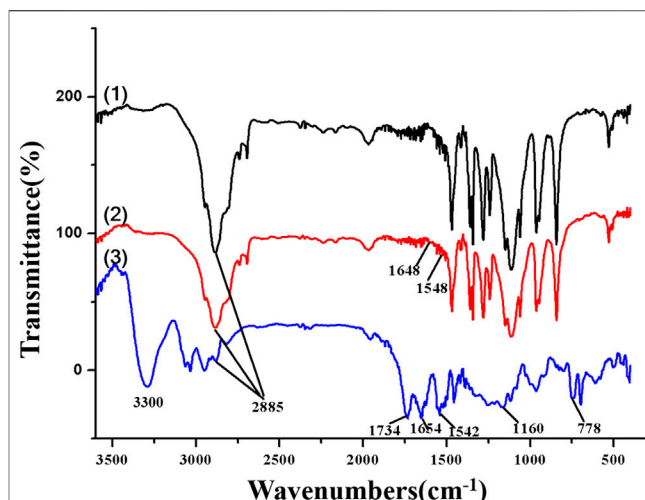


FIGURE 4 | The FTIR spectra of (1) MPEG-OH, (2) MPEG-NH₂, and (3) MPEG-PBLG.

(**Figure 5A-b**), 1.791–2.180 (**Figure 5A-c**), 2.364 (**Figure 5A-d**), 5.034 (**Figure 5A-e**), and 7.256 (**Figure 5A-f**) ppm, which represented the carbons of (CH₃O–, 3H), (–CH₂CH₂O–, 4H), (–CH₂CH₂COO[–]Na⁺, 2H), (–CH₂CH₂COO[–]Na⁺, 2H), (C₆H₅CH₂–, 2H), and (C₆H₅–, 5H), respectively. Taking above mentioned results into consideration, it's proved MPEG₂₀₀₀-PBLG was successfully synthesized. The deprotection of the benzyl group was performed by mixing with 0.025 N NaOH at ambient temperature to obtain MPEG₂₀₀₀-P(Glu), the peak of which at δ 5.034 and 7.256 ppm disappeared, confirming the complete deprotection (**Figure 5B**). The peak of 3.630 (**Figure 5B-a**), 4.24 (**Figure 5B-b**), 2.17 (**Figure 5B-c**), and 1.85–1.95 (**Figure 5B-d**) ppm represented the carbons of (CH₃O–, 3H), (–CH₂CH₂O–, 4H), (–CH₂CH₂COO[–]Na⁺, 2H), and (–CH₂CH₂COO[–]Na⁺, 2H), respectively. The whole average molecular weight of MPEG₂₀₀₀-P(Glu)₁₉₇₉ was 3,979 Da, while the number of units of the P(Glu) was 13.

Characterization of CISP-NPs

As CISP is widely used for chemotherapy drug in clinical trials, it still has a lot of side effects, especially nephrotoxicity, which make many patients suffered. In order to resolve this problem, nanotechnology-based delivery systems were devised to be capable of loading all sorts of drugs in recent decades (Xu et al., 2017). In this study, the biocompatible methoxypoly(ethylene glycol)-*b*-poly(L-glutamic acid) (MPEG-P(Glu)) was used to encapsulate CISP. The typical XRD patterns of pure MPEG₂₀₀₀-P(Glu)₁₉₇₉ material (1), CISP crystalline powder (2), CISP-NPs lyophilized powder (DL = 31.7%) (3), and the mixture of CISP and MPEG₂₀₀₀-P(Glu)₁₉₇₉ (4) were illustrated in **Figure 6A**. The XRD spectrum of free CISP showed many sharp peaks confirming that CISP was a crystalline compound, where narrow peaks represented some paracrystalline phases. While blank carrier was amorphous, the mixture of CISP and MPEG₂₀₀₀-P(Glu)₁₉₇₉ presented some peaks (in the 2θ range of 10–30°) suggesting crystallizability of

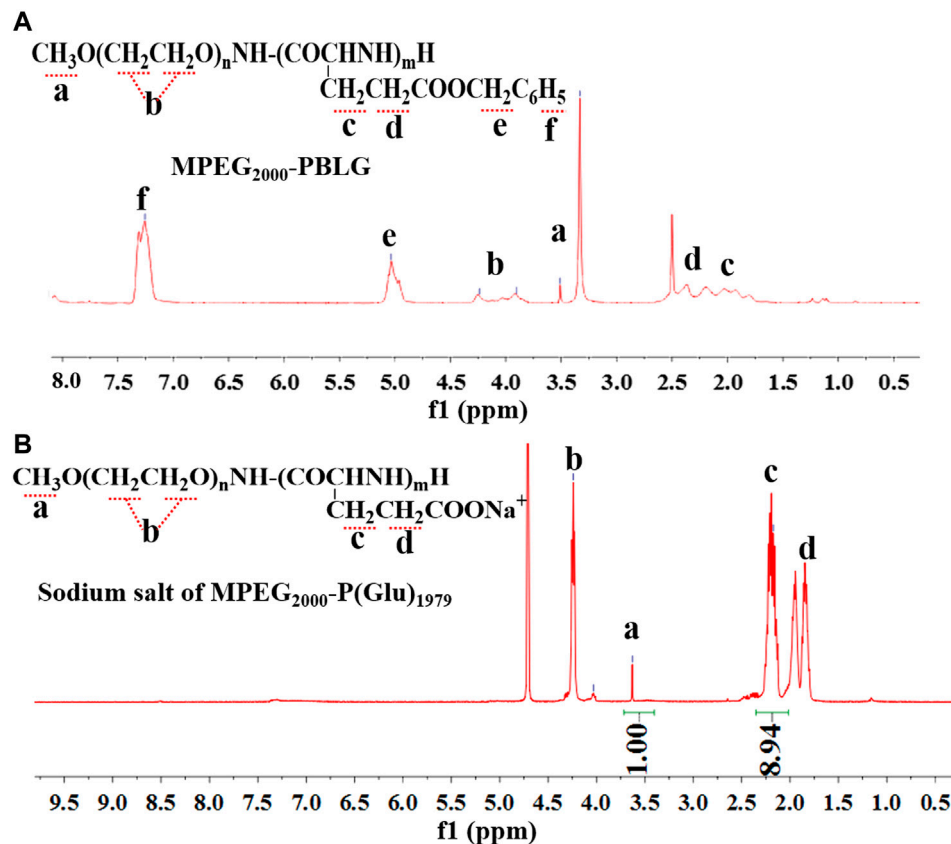


FIGURE 5 | The ¹H NMR spectra for MPEG₂₀₀₀-PBLG (A) and sodium salt of MPEG₂₀₀₀-P(Glu)₁₉₇₉ (B).

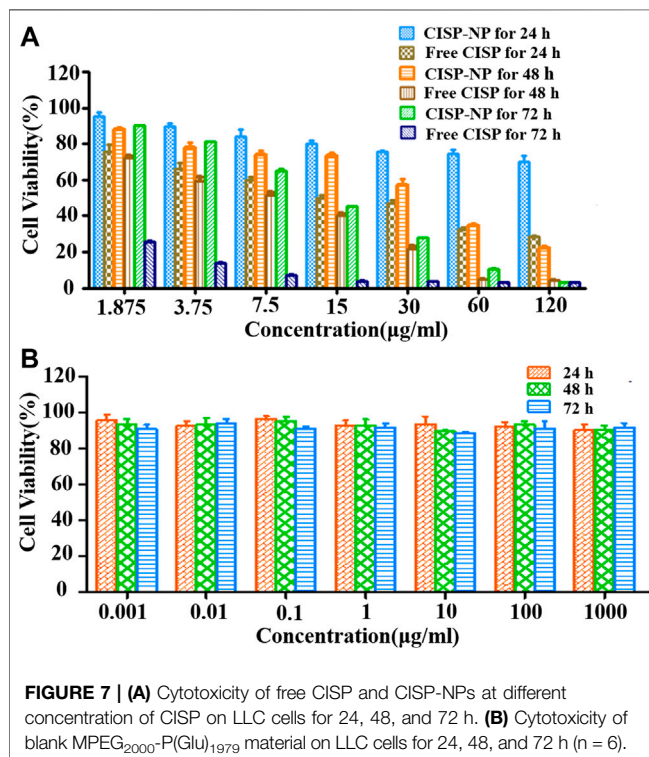
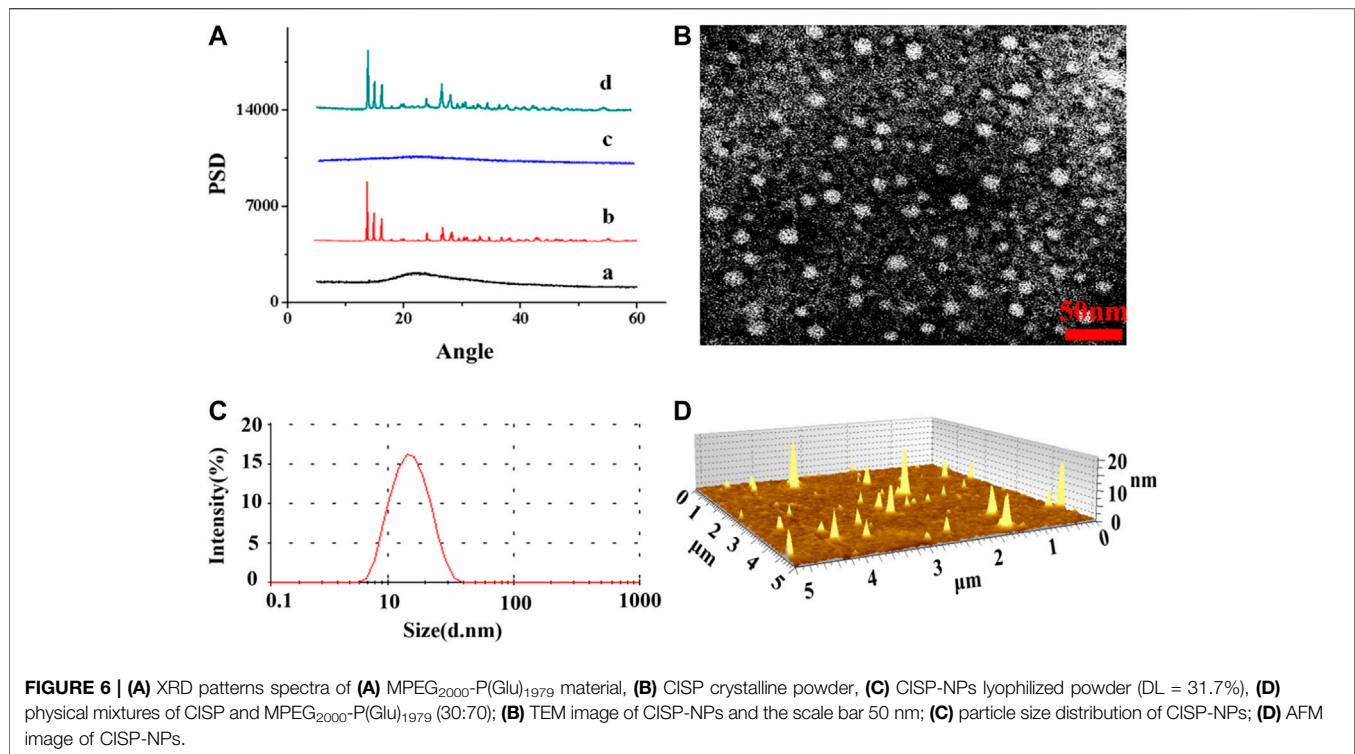
CISP. However, CISP-NPs lyophilized powder was not detected with crystalline peaks, and the crystalline diffraction peaks of CISP disappeared or were masked since the CISP was encapsulated into CISP-NPs in an amorphous form. Furthermore, it was reported that the change of XRD patterns was due to the possible inhibition of CISP crystallization by polymer matrices. Compared with free CISP, CISP-NPs showed superior dissolution rate and water solubility through transforming a crystalline drug into its amorphous form (Hancock and Zografi, 1997; Lobmann et al., 2011). The amorphous crystalline form of CISP inside the MPEG₂₀₀₀-P(Glu)₁₉₇₉ contributes to its sustained release (Ji et al., 2016). The drug-polymer amorphous system could reach the goal of improving solubility and bioavailability of poorly soluble drugs and the stability of the amorphous could be improved by distributing the drug in an amorphous state in highly dispersed carrier materials (Li and Huang, 2008).

The drug loading (DL) and encapsulated efficiency (EE) of CISP-NPs were (28.54, 27.82%) and (85.63, 83.74%), which were measured by HPLC and ICP-AES, respectively. Optimizing nanocarrier MPEG₂₀₀₀-P(Glu)₁₉₇₉ and the particle size of nanodrug, the average size of CISP-NPs obtained in this study was (18 ± 1.33) nm (Figure 6C), with PDI of 0.185 and zeta potential of -21 mV, which could enhance tumor accumulation

and aggregation via the EPR effect and achieve longer blood circulation. The TEM (Figure 6B) and AFM (Figure 6D) image revealed that CISP-NPs was spherical in shape and uniformly distributed without significant agglomeration. The particle size of CISP-NPs ranged from 8 to -40 nm with an average size of 18 ± 1.33 nm, which not only could evade renal clearance but also advance the penetration of nanodrugs into tumor tissues.

Cytotoxicity Assay

To evaluate whether free CISP and CISP-NPs bring into play antineoplastic effect against lung carcinoma, MTT assay was performed to evaluate the cell viability in response to drug treatment in LLC cell lines. Accordingly, both the free CISP and CISP-NPs displayed time-dependent and dose-dependent manner against LLC cells (Figure 7A). Fifty percent growth inhibitory concentration (IC₅₀) was used as the measure of relative cytotoxicity. The IC₅₀ (μg/ml) values of the free CISP group vs. CISP-NPs group were (17.9 vs. 908), (6.789 vs. 33.2), and (3.538 vs. 4.55), at 24, 48, and 72 h, respectively. CISP-NPs showed remarkably lower cytotoxicity than free CISP at 24 and 48 h. CISP-NPs could slightly inhibit the proliferation of LLC cells with cells viability greater than 80%, which were incubated in CISP at a concentration of 15 μg/ml for 24 h. This indicated that most of the Pt complexes came out of the micelle through a ligand



exchange reaction and kept active. Then, the conjugation of CISP to the CISP-NPs polymer reduced its *in vitro* cytotoxic activity, but it retained its antitumor activity. However, there was no

significant difference between the CISP-NPs group and free CISP group according to the IC₅₀ values at 72 h.

The viabilities of LLC cells treated with MPEG₂₀₀₀-P(Glu)₁₉₇₉ polymer with concentrations from 0.001 to 1,000 μg/ml after 24, 48, and 72 h incubation were also evaluated (Figure 7B). The blank copolymer micelles were found to be almost nondeleterious, and even if the concentration of the copolymer was up to 1,000 μg/ml, the cell viabilities were still higher than 85.82%. These results indicated that MPEG₂₀₀₀-P(Glu)₁₉₇₉ polymer was biocompatible with no cytotoxicity and suitably served as a drug delivery vehicle.

Flow Cytometry Analysis for Cell Cycle

As shown in Figure 8, after 48 h incubation with different formulations, the results of distribution of LLC cells in the five phases of the cell cycle clearly illustrated that both the group of free CISP and the group of CISP-NPs induced a typical G₂/M phase arrest in LLC cells. Specifically, the G₂/M proportions, in quantitative analysis of the cell cycle distribution, were 36.23 and 70.94% for the free CISP group and CISP-NPs group, while the G₂/M proportion of control group (NS) was only 9.28%. Obviously, LLC tumor cells after CISP-NPs treating displayed a better arrest than the free-CISP-treated group, in terms of the G₂/M phase. Moreover, cells cycle arrest in the G₀/G₁ phase decreased significantly and this would result in enhanced cancer cells death.

Histopathology Evaluation

To further evaluate the safety of CISP-NPs, the analyses of pathology were performed. Cell nucleus was dyed blue by

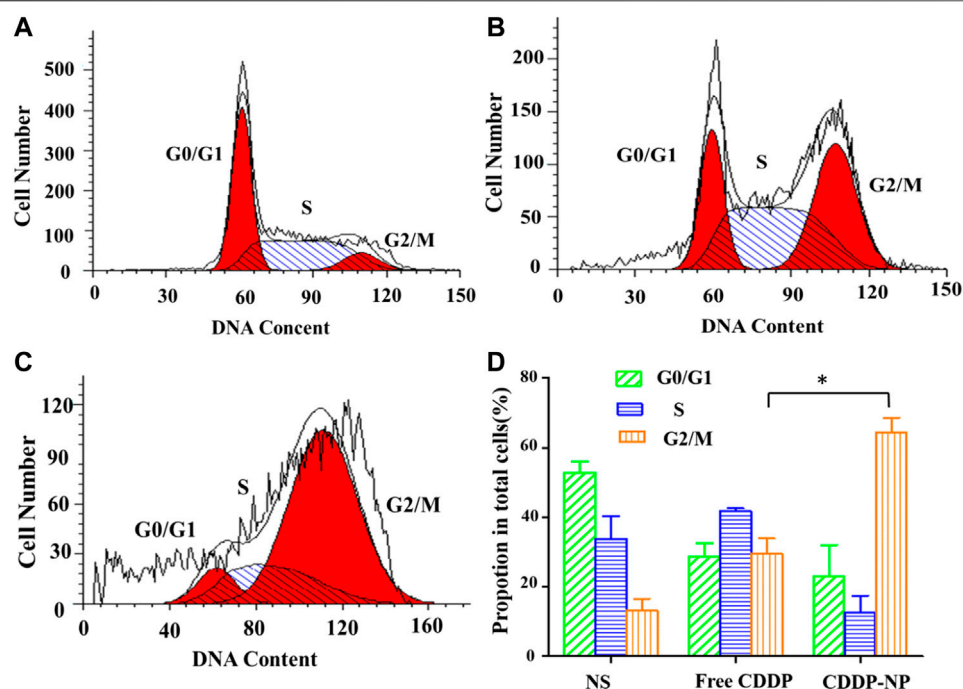


FIGURE 8 | (A–C) The cycle kinetics of LLC cells incubated in negative control group (NS) and free CISP, CISP-NPs group at 12.55 $\mu\text{g}/\text{ml}$ of CISP for 48 h, respectively. **(D)** Quantitative analysis of cell cycle distribution by flow cytometry of the NS group, free CISP and CISP-NPs group. ($n = 3$, $*p < 0.05$).

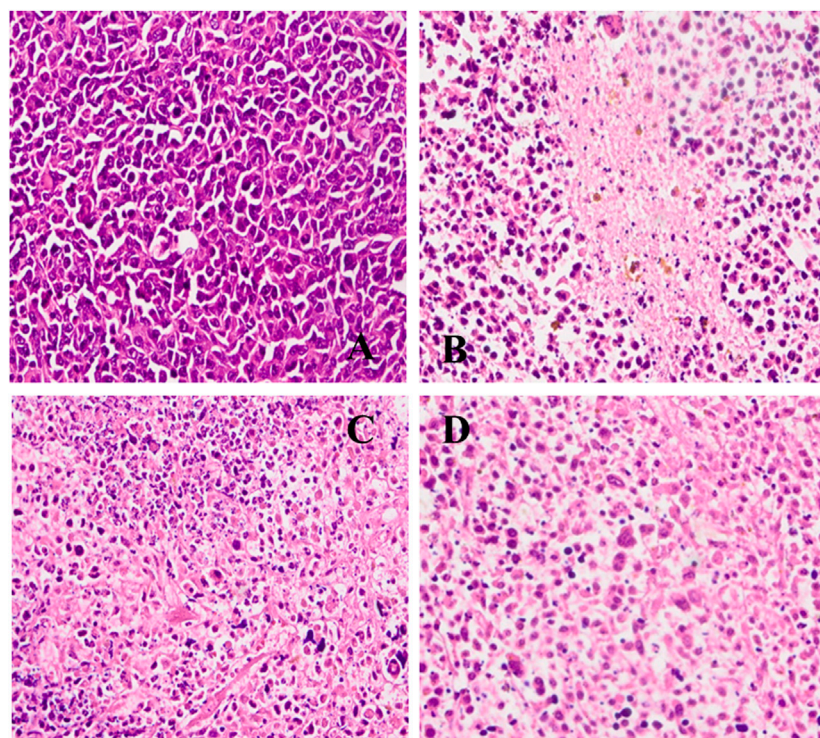


FIGURE 9 | H&E staining of tumor tissue image collected from **(A)** NS group; **(B)** free CISP group; **(C)** CISP-NPs group (6 mg/kg); **(D)** CISP-NPs group (12 mg/kg) ($\times 400$).

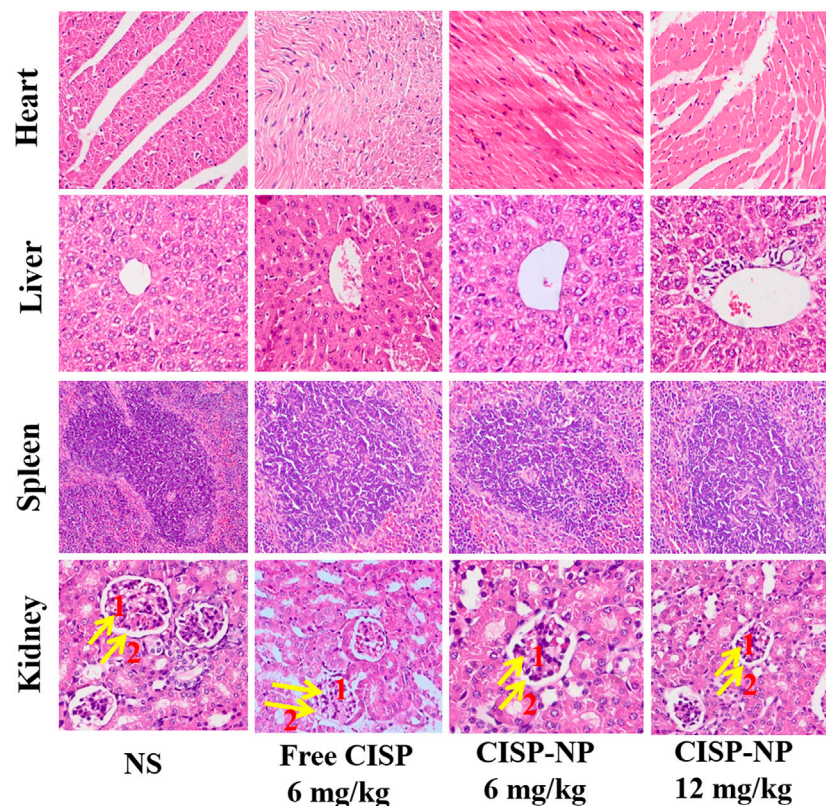


FIGURE 10 | H&E staining of heart, liver, spleen, and kidney tissue excised from LLC tumor-bearing mice following 5 times at 2-day treatment with NS, Free CISP, CISP-NPs (6 mg/kg) and CISP-NPs (12 mg/kg) (yellow arrows one and two represent the glomerular and glomerular wall, respectively, $\times 400$).

staining with hematoxylin, and, meanwhile, both cytoplasm and extracellular matrix were dyed red by staining with eosin in H&E staining. The cell morphology was not clear, and the chromatin deepened or diffused out of the cell if cell necrosis happened. It was seen that the cells had a large nucleus with a spherical or spindle shape in the tumor tissue of the NS group. At the same time, high nucleocytoplasmic ratio and the soakage of inflammatory cells were seen, which illustrated a fast-growing tumor (**Figure 9A**). By comparison, in the groups of both CISP-NPs, the tissue is in a state of necrosis to varying degrees, concentrated chromatin was distributed around the edge, and the nuclei of the tumor cells of CISP-NPs (12 mg/kg) group (**Figure 9D**) were extremely shrinking, fragmented or absent. Of all the tested groups, the CISP-NPs (12 mg/kg) group has the largest necrosis area, whereas CISP-NPs (6 mg/kg) (**Figure 9C**) administration groups at the same dose levels as free CISP (6 mg/kg) (**Figure 9B**) showed no significant difference in the degree of necrotic tissue. In addition, PEG could improve the circulation time of the nanoparticles in the bloodstream (Roberts et al., 2012), and CISP-NPs usually had remarkably prolonged blood circulation time in comparison with free CISP.

As shown in **Figure 10**, free CISP groups showed obvious damage to kidney, while the groups treated with CISP-NPs were normal. In addition, it was seen that these organs, like heart, liver, spleen, and kidney, had no damage in both CISP-NPs groups.

Free CISP disappeared rapidly from circulation and was distributed to each organ. Especially, rapid and high accumulation was observed in the kidney, which was illustrated by the yellow arrows in the figure. NS groups showed a small amount of inflammatory cell infiltration. As for free CISP group (6 mg/kg), tubular epithelial cells in the convoluted proximal tubule became swollen and enlarged. The disappearance of the tubular lumen, cell edema, glomerular wall hyperplasia, nuclear atrophy, and glomerular inflammatory cells infiltration occurred, while CISP-NPs groups (6 mg/kg) were normal. For the CISP-NPs groups (12 mg/kg), due to the larger dose, a small amount of inflammatory cells infiltration was observed, indicating that the CISP-NPs could significantly reduce the nephrotoxicity caused by CISP. Therefore, our results showed that the efficacy of CISP-NPs was statistically equivalent to that of free CISP at the same dosage. However, CISP-NPs have successfully reduced the nephrotoxicity that hampers the clinical application of CISP. Furthermore, the higher concentration of CISP-NPs not only reduced the side effects but also had a better antitumor activity.

The key factors influencing the effect of cellular internalization were the size and composition of particles. PEGylation could enhance the stability and solubility of the drug in plasma and reduce the toxicity of the drug (Saravanan et al., 2017). The renal filtration threshold was about 4–5 nm, and particles with size

more than 50 nm were mostly sequestered by the reticuloendothelial system (RES) of the liver, lungs, kidney, and spleen (Li and Huang, 2008; Dai et al., 2017). The average size of CISP-NPs was (18 ± 1.33) nm, which could efficiently avoid renal clearance for reducing nephrotoxicity and nonselective RES scavenge as well as showing enhanced permeability and retention (EPR) effects of passive targeted drug at solid tumor sites (**Figure 3B**) (Yang et al., 2014). There are two main factors which contributed to the hypoxia in the tumor microenvironment. The entire tissue was incapable of getting sufficient oxygen due to the abnormal vascular network in the solid tumor, especially for the poorly vascularized internal area. At the same time, the overproliferation of tumor cells further accelerated the consumption of oxygen. Therefore, in the tumor microenvironment, the regions far from the blood vessels were typically hypoxic, which was not conducive to the large size, low penetration of nanoparticles in deep tissues. Jain and coworkers proved that nanoparticles with a 12-nm size had a better tumor penetration than larger sized nanoparticles (Cabral et al., 2011; Chen et al., 2017). To this end, CISP-NPs exhibited significantly superior efficacy in impeding tumor growth with no obvious side effects than that of free CISP in a mouse model of LLC cell line.

CONCLUSION

In this study, the CISP-NPs, which was able to reduce side effects obviously and display excellent drug efficacy, were successfully developed. The characterization of CISP-NPs demonstrated that cisplatin was encapsulated in CISP-NPs mostly. Meanwhile, the size distribution of CISP-NPs had a narrow and appropriate distribution, from 8 nm to 40 nm, which contributed to evade renal excretion, prolong systemic circulation, cross tumor blood vessels, and accumulate in tumor tissues due to enhanced permeability and retention effect. The statistics *in vitro* cellular studies revealed that CISP-NPs could release drug slowly so that the duration of action was extended. In addition, MPEG₂₀₀₀-P(Glu)₁₉₇₉ polymer possessed fine biological compatibility but no

systemic cytotoxicity. In further histology evaluation, compared with free cisplatin, CISP-NPs exhibited not only outstanding antitumor activity, but tremendously diminished tissue injury, especially renal toxicity. In conclusion, the present data show that CISP-NPs, reducing nephrotoxicity, are a safe and effective formulation and might be a promising measure to overcome tissue toxicity in antitumor therapy.

DATA AVAILABILITY STATEMENT

The original contributions presented in the study are included in the article/Supplementary Material; further inquiries can be directed to the corresponding authors.

ETHICS STATEMENT

The animal study was examined and approved by the Ethics Committee of Ocean University of China.

AUTHOR CONTRIBUTIONS

ZW and CW devised the study. HL, ZW, and TZ performed the majority of experiments. YL and ZY analyzed data and were involved in several experiments. ZW and HL drafted the original manuscript, as well as figures. CW revised the manuscript. All authors have reviewed and agreed to the final version of the manuscript.

FUNDING

This work was financially supported by the Qingdao Program for Original Innovation and Fundamental Research (18-2-2-73-jch), Fundamental Research Funds for the Central Universities (201964018), and National Natural Science Foundation of China (NSFC31872754).

REFERENCES

- Bussard, K. M., Mutkus, L., Stumpf, K., Gomez-Manzano, C., and Marini, F. C. (2016). Tumor-associated stromal cells as key contributors to the tumor microenvironment. *Breast Cancer Res.* 18 (1), 84. doi:10.1186/s13058-016-0740-2
- Cabral, H., Matsumoto, Y., Mizuno, K., Chen, Q., Murakami, M., Kimura, M., et al. (2011). Accumulation of sub-100 nm polymeric micelles in poorly permeable tumours depends on size. *Nat. Nanotechnol.* 6 (12), 815–823. doi:10.1038/nnano.2011.166
- Cabral, H., Nishiyama, N., and Kataoka, K. (2007). Optimization of (1,2-diamino-cyclohexane)platinum(II)-loaded polymeric micelles directed to improved tumor targeting and enhanced antitumor activity. *J. Contr. Release* 121 (3), 146–155. doi:10.1016/j.jconrel.2007.05.024
- Calvert, A. H., Harland, S. J., Newell, D. R., Siddik, Z. H., Jones, A. C., McElwain, T. J., et al. (1982). Early clinical studies with cis-diammine-1,1-cyclobutane dicarboxylate platinum II. *Cancer Chemother. Pharmacol.* 9 (3), 140–147. doi:10.1007/BF00257742
- Chauhan, V. P., Stylianopoulos, T., Martin, J. D., Popović, Z., Chen, O., Kamoun, W. S., et al. (2012). Normalization of tumour blood vessels improves the delivery of nanomedicines in a size-dependent manner. *Nat. Nanotechnol.* 7 (6), 383–388. doi:10.1038/nnano.2012.45
- Chen, B., Dai, W., He, B., Zhang, H., Wang, X., Wang, Y., et al. (2017). Current multistage drug delivery systems based on the tumor microenvironment. *Theranostics* 7 (3), 538–558. doi:10.7150/thno.16684
- Dai, Y., Xu, C., Sun, X., and Chen, X. (2017). Nanoparticle design strategies for enhanced anticancer therapy by exploiting the tumour microenvironment. *Chem. Soc. Rev.* 46 (12), 3830–3852. doi:10.1039/c6cs00592f
- Gao, H., Yang, Z., Zhang, S., Pang, Z., Liu, Q., and Jiang, X. (2014). Study and evaluation of mechanisms of dual targeting drug delivery system with tumor microenvironment assays compared with normal assays. *Acta Biomater.* 10 (2), 858–867. doi:10.1016/j.actbio.2013.11.003
- Ghosh, S. (2019). Cisplatin: the first metal based anticancer drug. *Bioorg. Chem.* 88, 102925. doi:10.1016/j.bioorg.2019.102925
- Guo, J., Xu, B., Han, Q., Zhou, H., Xia, Y., Gong, C., et al. (2018). Ferroptosis: a novel anti-tumor action for cisplatin. *Cancer Res. Treat.* 50 (2), 445–460. doi:10.4143/crt.2016.572

- Hancock, B. C., and Zografi, G. (1997). Characteristics and significance of the amorphous state in pharmaceutical systems. *J. Pharm. Sci.* 86 (1), 1–12. doi:10.1021/js9601896
- Ji, P., Yu, T., Liu, Y., Jiang, J., Xu, J., Zhao, Y., et al. (2016). Naringenin-loaded solid lipid nanoparticles: preparation, controlled delivery, cellular uptake, and pulmonary pharmacokinetics. *Drug Des. Dev. Ther.* 10, 911–925. doi:10.2147/DDDT.S97738
- Kuwahara, A., Yamamori, M., Nishiguchi, K., Okuno, T., Chayahara, N., Miki, I., et al. (2010). Effect of dose-escalation of 5-fluorouracil on circadian variability of its pharmacokinetics in Japanese patients with Stage III/IVa esophageal squamous cell carcinoma. *Int. J. Med. Sci.* 7 (1), 48–54. doi:10.7150/ijms.7.48
- Li, S. D., and Huang, L. (2008). Pharmacokinetics and biodistribution of nanoparticles. *Mol. Pharm.* 5 (4), 496–504. doi:10.1021/mp800049w
- Liu, F., Gou, S., Chen, F., Fang, L., and Zhao, J. (2015). Study on antitumor platinum(II) complexes of chiral diamines with dicyclic species as steric hindrance. *J. Med. Chem.* 58 (16), 6368–6377. doi:10.1021/jm501952r
- Löbmann, K., Laitinen, R., Grohgan, H., Gordon, K. C., Strachan, C., and Rades, T. (2011). Coamorphous drug systems: enhanced physical stability and dissolution rate of indomethacin and naproxen. *Mol. Pharm.* 8 (5), 1919–1928. doi:10.1021/mp2002973
- Martínez-Balibrea, E., Martínez-Cardús, A., Ginés, A., Ruiz de Porras, V., Moutinho, C., Layos, L., et al. (2015). Tumor-related molecular mechanisms of oxaliplatin resistance. *Mol. Cancer Ther.* 14 (8), 1767–1776. doi:10.1158/1535-7163.MCT-14-0636
- Nishiyama, N., Okazaki, S., Cabral, H., Miyamoto, M., Kato, Y., Sugiyama, Y., et al. (2003). Novel cisplatin-incorporated polymeric micelles can eradicate solid tumors in mice. *Cancer Res.* 63 (24), 8977–8983. doi:10.1002/cncr.11858
- Pansini, M., Dell'Agli, G., Marocco, A., Netti, P. A., Battista, E., Lettera, V., et al. (2017). Preparation and characterization of magnetic and porous metal-ceramic nanocomposites from a zeolite precursor and their application for DNA separation. *J. Biomed. Nanotechnol.* 13 (3), 337–348. doi:10.1166/jbn.2017.2345
- Pasut, G., and Veronese, F. M. (2007). Polymer–drug conjugation, recent achievements and general strategies. *Prog. Polym. Sci.* 32 (8-9), 933–961. doi:10.1016/j.progpolymsci.2007.05.008
- Pautu, V., Leonetti, D., Lepeltier, E., Clere, N., and Passirani, C. (2017). Nanomedicine as a potent strategy in melanoma tumor microenvironment. *Pharmacol. Res.* 126, 31–53. doi:10.1016/j.phrs.2017.02.014
- Plummer, R., Wilson, R. H., Calvert, H., Boddy, A. V., Griffin, M., Sludden, J., et al. (2011). A Phase I clinical study of cisplatin-incorporated polymeric micelles (NC-6004) in patients with solid tumours. *Br. J. Cancer* 104 (4), 593–598. doi:10.1038/bjc.2011.6
- Poon, W., Kingston, B. R., Ouyang, B., Ngo, W., and Chan, W. C. W. (2020). A framework for designing delivery systems. *Nat. Nanotechnol.* 15 (10), 819–829. doi:10.1038/s41565-020-0759-5
- Roberts, M. J., Bentley, M. D., and Harris, J. M. (2012). Chemistry for peptide and protein PEGylation. *Adv. Drug Delivery Rev.* 64, 116–127. doi:10.1016/j.addr.2012.09.025
- Saravanan, S., Malathi, S., Sesh, P. S. L., Selvasubramanian, S., Balasubramanian, S., and Pandiyan, V. (2017). Hydrophilic poly (ethylene glycol) capped poly (lactic-co-glycolic) acid nanoparticles for subcutaneous delivery of insulin in diabetic rats. *Int. J. Biol. Macromol.* 95, 1190–1198. doi:10.1016/j.ijbiomac.2016.11.009
- Schöttler, S., Becker, G., Winzen, S., Steinbach, T., Mohr, K., Landfester, K., et al. (2016). Protein adsorption is required for stealth effect of poly(ethylene glycol)- and poly(phosphoester)-coated nanocarriers. *Nat. Nanotechnol.* 11 (4), 372–377. doi:10.1038/nnano.2015.330
- Shen, F., Gai, J., Xing, J., Guan, J., Fu, L., and Li, Q. (2018). Dynasore suppresses proliferation and induces apoptosis of the non-small-cell lung cancer cell line A549. *Biochem. Biophys. Res. Commun.* 495 (1), 1158–1166. doi:10.1016/j.bbrc.2017.11.109
- Song, W., Li, M., Tang, Z., Li, Q., Yang, Y., Liu, H., et al. (2012). Methoxypoly(ethylene glycol)-block-poly(L-glutamic acid)-loaded cisplatin and a combination with iRGD for the treatment of non-small-cell lung cancers. *Macromol. Biosci.* 12 (11), 1514–1523. doi:10.1002/mabi.201200145
- Uchino, H., Matsumura, Y., Negishi, T., Koizumi, F., Hayashi, T., Honda, T., et al. (2005). Cisplatin-incorporating polymeric micelles (NC-6004) can reduce nephrotoxicity and neurotoxicity of cisplatin in rats. *Br. J. Cancer* 93 (6), 678–687. doi:10.1038/sj.bjc.6602772
- Varela-Moreira, A., Shi, Y., Fens, M. H. A. M., Lammers, T., Hennink, W. E., and Schiffelers, R. M. (2017). Clinical application of polymeric micelles for the treatment of cancer. *Mater. Chem. Front.* 1 (8), 1485–1501. doi:10.1039/c6qm00289g
- Wang, S., Li, W., Xue, Z., Lu, Y., Narsinh, K., Fan, W., et al. (2013). Molecular imaging of p53 signal pathway in lung cancer cell cycle arrest induced by cisplatin. *Mol. Carcinog.* 52 (11), 900–907. doi:10.1002/mc.21930
- Weng, Y. H., Che, J., Ma, X. W., Guo, H. B., Xue, X. D., Chen, S. Z., et al. (2017). Contrast enhancement method of transmission electron microscopy in visualization of polymeric micelles by fluoride addition and staining. *J. Biomed. Nanotechnol.* 13 (5), 534–543. doi:10.1166/jbn.2017.2375
- Wheate, N. J., Walker, S., Craig, G. E., and Oun, R. (2010). The status of platinum anticancer drugs in the clinic and in clinical trials. *Dalton Trans.* 39 (35), 8113–8127. doi:10.1039/c0dt00292e
- Wilhelm, S., Tavares, A. J., Dai, Q., Ohta, S., Audet, J., Dvorak, H. F., et al. (2016). Analysis of nanoparticle delivery to tumours. *Nat. Rev. Mater.* 1 (5), 16014. doi:10.1038/natrevmats.2016.14
- Wiltshaw, E. (1979). Cisplatin in the treatment of cancer. *Platin. Met. Rev.* 23 (3), 90–98.
- Xu, C., Tian, H., and Chen, X. (2017). Recent progress in cationic polymeric gene carriers for cancer therapy. *Sci. China Chem.* 60 (3), 319–328. doi:10.1007/s11426-016-0466-x
- Xu, Y., Han, X., Li, Y., Min, H., Zhao, X., Zhang, Y., et al. (2019). Sulforaphane mediates glutathione depletion via polymeric nanoparticles to restore cisplatin chemosensitivity. *ACS Nano* 13 (11), 13445–13455. doi:10.1021/acsnano.9b07032
- Yang, X. L., Luo, Y. L., Xu, F., and Chen, Y. S. (2014). Thermosensitive mPEG-b-PA-g-PNIPAM comb block copolymer micelles: effect of hydrophilic chain length and camptothecin release behavior. *Pharm. Res.* 31 (2), 291–304. doi:10.1007/s11095-013-1160-y
- Zhu, L., Li, Q., Gong, F.-L., Yan, X.-F., Li, X.-Q., Ma, G.-H., et al. (2013). An insight into structure regulation of uniform polystyrene micro/nano-particles by porogen in premix membrane emulsification process. *J. Membr. Sci.* 448, 248–255. doi:10.1016/j.memsci.2013.08.002

Conflict of Interest: The authors declare that the research was conducted in the absence of any commercial or financial relationships that could be construed as a potential conflict of interest.

Copyright © 2021 Wang, Li, Zhang, Li, Yang and Wang. This is an open-access article distributed under the terms of the Creative Commons Attribution License (CC BY). The use, distribution or reproduction in other forums is permitted, provided the original author(s) and the copyright owner(s) are credited and that the original publication in this journal is cited, in accordance with accepted academic practice. No use, distribution or reproduction is permitted which does not comply with these terms.



Schiff-Linked PEGylated Doxorubicin Prodrug Forming pH-Responsive Nanoparticles With High Drug Loading and Effective Anticancer Therapy

OPEN ACCESS

Edited by:

Jianxun Ding,
Chinese Academy of Sciences, China

Reviewed by:

Zhigang Xu,
Southwest University, China
Jianfeng Liu,
Chinese Academy of Medical
Sciences and Peking Union Medical
College, China
Yunlong Yang,
Fudan University, China

*Correspondence:

Xing Wang
wangxing@iccas.ac.cn
Zheng Yang
yangzh25@mail.sysu.edu.cn

[†]These authors have contributed
equally to this work

Specialty section:

This article was submitted to
Pharmacology of
Anti-Cancer Drugs,
a section of the journal
Frontiers in Oncology

Received: 21 January 2021

Accepted: 05 March 2021

Published: 25 March 2021

Citation:

Song J, Xu B, Yao H, Lu X, Tan Y,
Wang B, Wang X and Yang Z (2021)
Schiff-Linked PEGylated Doxorubicin
Prodrug Forming pH-Responsive
Nanoparticles With High Drug Loading
and Effective Anticancer Therapy.
Front. Oncol. 11:656717.
doi: 10.3389/fonc.2021.656717

Jian Song^{1†}, Bingbing Xu^{2†}, Hui Yao^{3†}, Xiaofang Lu¹, Yang Tan¹, Bingyang Wang¹,
Xing Wang^{4,5*} and Zheng Yang^{1*}

¹ Department of Pathology, The Seventh Affiliated Hospital of Sun Yat-Sen University, Shenzhen, China, ² Department of Sports Medicine, Peking University Third Hospital, Institute of Sports Medicine of Peking University, Beijing, China, ³ Eye Hospital, China Academy of Chinese Medical Sciences, Beijing, China, ⁴ Beijing National Laboratory for Molecular Sciences, Institute of Chemistry, Chinese Academy of Sciences, Beijing, China, ⁵ University of Chinese Academy of Sciences, Beijing, China

Developing efficacious drug delivery systems for targeted cancer chemotherapy remains a major challenge. Here we demonstrated a kind of pH-responsive PEGylated doxorubicin (DOX) prodrug via the effective esterification and Schiff base reactions, which could self-assemble into the biodegradable micelles in aqueous solutions. Owing to low pH values inside the tumor cells, these PEG-Schiff-DOX nanoparticles exhibited high drug loading ability and pH-responsive drug release behavior within the tumor cells or tissues upon changes in physical and chemical environments, but they displayed good stability at physiological conditions for a long period. CCK-8 assay showed that these PEGylated DOX prodrugs had a similar cytotoxicity to the MCF-7 tumor cells as the free DOX drug. Moreover, this kind of nanoparticle could also encapsulate small DOX drugs with high drug loading, sufficient drug release and enhanced therapeutic effects toward MCF-7 cells, which will be benefited for developing more drug carriers with desirable functions for clinical anticancer therapy.

Keywords: pH-responsive nanoparticles, prodrug, Schiff base, control release, drug delivery

INTRODUCTION

Biodegradable nanoparticles have been intensively utilized as promising candidates for targeted cancer therapy over a long period, because they possess the increased drug solubility, prolonged circulation time, improved pharmacokinetic properties, good bioavailability, enhanced tumor accumulation at the tumor sites, high therapeutic effects and low systemic side effects (1–8). Among these various nanomedicines such as nanoparticles, polymeric micelles, vesicles, nanogels, liposomes and polymer conjugates, prodrug-based nanoparticles have drawn much more attention due to their simple structure, feasible preparation and great potential in clinical translation (9–11).

Doxorubicin (DOX) is a most widely used anticancer drug approved by FDA, which has been applied to the treatment of many neoplasms, but its severe toxic side effects, low bioavailability and high doses requirement greatly limit its clinical use (12, 13). Therefore, significant progress has been made towards the fabrication of ideal DOX delivery system with improved drug utilization at the action sites and reduced side effects in non-target tissues. Although the liposomal formulations of DOX have been approved for clinical use and many polymeric nanoparticles loading DOX molecules are being evaluated in clinical trials (14–18), these DOX-loaded nanocarriers have some inherent drawbacks like low drug loading, premature burst release and inactive carriers to patients, which may ascribe to the high polarity and hydrophilicity of DOX molecules. To overcome this unintended and undesirable leakage, chemically-linked drug carriers offer an alternative for the effective anti-tumor treatment. For example, Wen et al. had prepared a high-density DOX component *via* covalent decoration on the nanocarrier, which could be effectively released in the acidic tumor tissue and significantly improved chemotherapy efficacy (19).

Polyethylene glycol (PEG) is one of the most widely used hydrophilic polymer approved by FDA with negligible toxicity and low immunogenicity, which has been expected to effectively reduce the non-specific uptake by the reticuloendothelial system (RES), prolong circulation time and allow for specific tumor-targeting *via* the enhanced permeability and retention (EPR) effect (20–24). Thus, PEGylated doxorubicin prodrugs have shown distinctly therapeutic advantages including better antitumor activity and fewer side effects than free drugs. However, many reported PEG-DOX prodrugs presented some inherent drawbacks like relatively low drug loading capacity,

incomplete drug release and insensitive manipulation (25–27). To ensure the high-effective intracellular drug release, it is important to design and develop more stimuli-responsive prodrugs that can possess precise target ability and controllable drug release inside the target cells upon changes in physical and chemical environments. Wherein, the significance of pH change in the tumor cell environment is recognized as a most popular chemical stimuli to tailor drug release in aqueous solutions. For example, Ding et al. developed a cRGD-decorated pH-responsive polyion complex (PIC) micelle for intracellular targeted delivery of DOX to upregulate tumor inhibition and reduce toxicity (28–33). Although Sui et al. had reported a PEG-DOX prodrug with an acid-labile hydrazone bond for cancer chemotherapy, this drug system displayed a weak pH response with approximately 12% release content at pH 5.0 even for 3 days, which may induce the antitumor efficiency in the first place and lose the opportunity for early treatment (26).

In this study, we designed and prepared an amphiphilic polymer drug conjugate (PEG-Schiff-DOX) *via* an acid-sensitive Schiff base bond, which could self-assemble into pH-responsive nanoparticles in solutions. These PEGylated nanoparticles had a well-defined structure, suitable architecture and size, high and fixed DOX loading content, good biocompatibility, stability and storage (**Figure 1**). The bridged Schiff bases could keep the structural integrity at normal physiological condition but endow the aggregates disassembly in response to faintly acidic environment. CCK-8 assays showed that these PEG-Schiff-DOX nanoparticles demonstrated outstanding antitumor activity compared to free DOX against human breast cancer cells (MCF-7). Additionally, benefiting from the drug carrier with the encapsulation ability, a new DOX-based PEG-Schiff-DOX polymer with programmed DOX release behavior was obtained, which may result in high drug

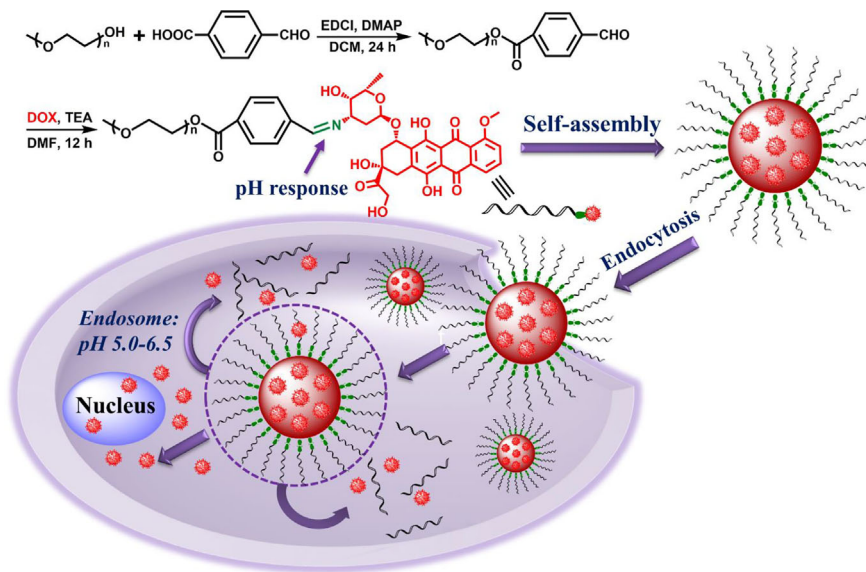


FIGURE 1 | Synthetic route of pH-responsive PEG-Schiff-DOX polymer and activated intracellular drug release from the pH-sensitive self-assembled nanoparticles.

concentration, long treatment period and enhanced therapeutic effect. Thus, we believe that these prodrug nanomedicines will hold promise to an alternative translational DOX formulations for cancer chemotherapy.

MATERIALS AND METHODS

Materials

Poly(ethylene glycol) methyl ether (PEG-OH, $M_n = 750$ g/mol, Alfa Aesar), 4-carboxybenzaldehyde (98%, J&K), 4-(dimethyl-amino)-pyridine (DMAP, 99%, Aldrich), 1-(3-dimethylaminopropyl)-3-ethylcarbodiimide hydrochloride (EDCI, 99%, Energy Chemical), triethylamine (TEA, 99%, Beijing Chemical Works), hydrochloric acid, sodium sulfate, sodium bicarbonate, n-hexane and ether were purchased from Beijing Chemical Works. Doxorubicin-HCl (DOX-HCl) was purchased from Beijing Zhongshuo Pharmaceutical Technology Development Co., Ltd. Dichloromethane (DCM) and dimethylformamide (DMF) were purified by stirring over calcium hydride for 24 h followed by distillation. All other reagents were purchased from Sigma-Aldrich and used as received without further purification. Cells were supplied by China Infrastructure of Cell Line Resource.

Characterizations

Nuclear magnetic resonance (NMR) spectra were recorded on a Bruker 400 MHz spectrometer with tetramethylsilane (TMS) as the internal reference. Transmission electron microscopy (TEM) images were obtained on a JEM-2200FS microscope (JEOL, Japan). A 5 μ l droplet of self-assembled solution was dropped onto a copper grid (300 mesh) coated with a carbon film, followed by drying at room temperature. Dynamic light scattering (DLS) spectra were obtained on a commercial laser light scattering spectrometer (ALV/DLS/SLS-5022F) equipped with a multi- τ digital time correlator (ALV5000) and a cylindrical 22 mW UNIPHASE He-Ne laser ($\lambda_0 = 632.8$ nm) was used. All data were averaged over three time. The laser light scattering cell was held in a thermostat index matching vat filled with purified and dust-free toluene, with the temperature controlled to within 0.1°C. Fluorescence measurement was carried on a Hitachi F4600 photo-luminescent spectrometer with a xenon lamp as a light source. Confocal laser scanning microscopy (CLSM) images were obtained on a Zeiss LSM 510 microscope.

Synthesis of the PEG-CHO Polymer

PEG-OH (0.75 g, 1 mmol), 4-carboxybenzaldehyde (0.18 g, 1.2 mmol), EDCI (0.24 g, 1.2 mmol) and DMAP (25 mg, 0.2 mmol) were added into a 50 ml round-bottomed flask equipped with a magnetic stirring bar, followed by the addition of 20 ml of freshly dried DCM to fully dissolve all the solids. After the stirring for 24 h at room temperature, the organic phase was collected and washed with 2 M HCl aqueous solution, saturated sodium bicarbonate solution, saturated NaCl aqueous solution and DI water for several times and dried over anhydrous Na_2SO_4 .

The final product was precipitated into ether/hexane for three times to afford the white powder with 90.1% yields.

Synthesis of the PEG-Schiff-DOX Polymer

PEG-CHO (0.27 g, 0.31 mmol), DOX-HCl (0.15 g, 0.25 mmol) and TEA (70 μ l, 0.5 mmol) were dissolved in 10 ml of DMF solution under a nitrogen atmosphere. The mixture was refluxed with vigorous stirring for 12 h. After removing the solvent under the vacuum, the crude products were resolved in DCM and washed with saturated NaCl aqueous solution and DI water for several times and dried over anhydrous Na_2SO_4 . The final product was precipitated into ether/hexane for three times to afford the dark-red powder with 66.4% yields.

Formation and Self-Assembly of the Polymeric PEG-Schiff-DOX Nanoparticles

A typical self-assembly solution was prepared as following: PEG-Schiff-DOX (5 mg) was first dissolved in DMF (1 ml), then the deionized water (4 ml) was added dropwise into the solution at the rate of 0.05 ml/min *via* a syringe pump. The colloidal dispersion was further stirred for another 2 h at room temperature during the self-assembling process. The organic solvent was removed by dialysis (MW cutoff, 1 kDa) against deionized water for 3 days. These PEG-Schiff-DOX nanoparticles were obtained and characterized by TEM and DLS measurement.

Stability and pH-Responsive Degradation of the PEG-Schiff-DOX Nanoparticles

In PBS (pH 7.4) and fetal bovine serum (FBS) solutions, we measured the transformation of size distributions for PEG-Schiff-DOX nanoparticles in order to study the stability and resisting protein adsorption ability. First of all, the self-assembled nanoparticles were dispersed in PBS and 20 wt% of FBS solutions with the concentration of 1 mg/mL, respectively. For maintaining the constant temperature of 37°C, the size distributions were recorded by DLS for each 12 h.

For determining the pH response of PEG-Schiff-DOX nanoparticles, a certain amount of phosphate buffered saline (PBS) with different pH values (5.0 and 7.4) was added into 10 ml of PEG-Schiff-DOX nanoparticles (1 mg/ml) under mildly stirring at 37°C. After 4 h, morphological and dimensional changes of nanoparticles were characterized by TEM and DLS measurement.

In vitro DOX Release From the PEG-Schiff-DOX Nanoparticles

pH-triggered DOX release measurement was conducted as below: dispersed PEG-Schiff-DOX nanoparticles were added into a dialysis membrane tube (MW cutoff, 1 kDa), which was then incubated in 30 ml of PBS (pH 5.0 and 7.4) solutions at 37°C in a shaking water bath. pH-triggered DOX release profiles were determined by measuring the UV-vis absorbance of solutions at 480 nm. All DOX-release experiments were conducted in triplicate and the results were expressed as average data with standard deviations.

Cellular Uptake and Intracellular Localization of MCF-7 Cells Incubated With PEG-Schiff-DOX Nanoparticles and Free DOX Drug

MCF-7 cells were plated on microscope slides in a 96-well plate (5×10^4 cells/well) using Dulbecco's Modified Eagle Medium (DMEM) containing 10% FBS. After incubation for 24 h, the cells were incubated with prescribed amounts of free DOX (8 $\mu\text{g}/\text{ml}$) and PEG-Schiff-DOX nanoparticles (equivalent to 8 $\mu\text{g}/\text{ml}$ DOX) for 1 and 4 h at 37°C and 5% CO_2 . Then the culture medium was removed and the cells on microscope plates were washed for three times with PBS. After fixing with 4% paraformaldehyde overnight, the MCF-7 cells were observed under a confocal laser scanning microscopy (CLSM) with excitation at 488 nm for DOX.

CCK-8 Assay

The cytotoxicity of PEG-Schiff-DOX and DOX-encapsulated PEG-Schiff-DOX nanoparticles was studied by CCK-8 assay using MCF-7 cells. Cells were seeded onto a 96-well plate at a density of 1×10^4 cells per well in 200 μl of DMEM containing 10% FBS and further incubated for 24 h (37°C , 5% CO_2). The medium was replaced by 90 μl of fresh DMEM medium containing 10% FBS, and then various concentrations (10^{-3} – 10 $\mu\text{g}/\text{ml}$) of micelle suspensions in PBS (pH 7.4) solutions were added. After incubation for another 24 h and removal of culture media from cell culture plates, 100 μl of fresh culture media and 10 μl of CCK-8 kit solutions were immediately added and homogeneously mixed and then

incubated for 4 h in a CO_2 incubator. Finally, 100 μl of solutions were put into 96-well plate. The optical density of each well at 450 nm was read by a microplate reader. Cells cultured in DMEM medium containing 10% FBS (without exposure to nanoparticles) were used as controls.

RESULTS AND DISCUSSION

Synthesis and Characterization of PEG-Schiff-DOX Prodrugs

The Schiff-linked PEGylate DOX prodrug was prepared following the synthetic route as shown in **Figure 1**. Previously, Sui et al. reported that DOX was conjugated into the PEG *via* an acid-cleavable hydrazone bond, but this doxorubicin prodrug system displayed the insensitive pH response, which exhibited a small DOX release with only 12% drug content within 72 h at pH 5.0. In this study, by means of the simple esterification reaction of 4-carboxybenzaldehyde and sequentially high-effective Schiff base reaction of DOX, the PEG-Schiff-DOX was feasibly obtained and confirmed by the ^1H NMR spectra. **Figure 2A** clearly presented the assignments of PEG-CHO polymer. The signals at δ 8.0–8.3 ppm were attributed to the benzene components and the resonance peak of δ 10.2 ppm belonged to the proton of aldehyde group. Taking consideration of the intricate peaks for DOX, there was no clear peak attribution in **Figure 2B**. **Figure 2C** proved the successful conjugation of PEG with DOX, presenting the integrated assignments of PEG

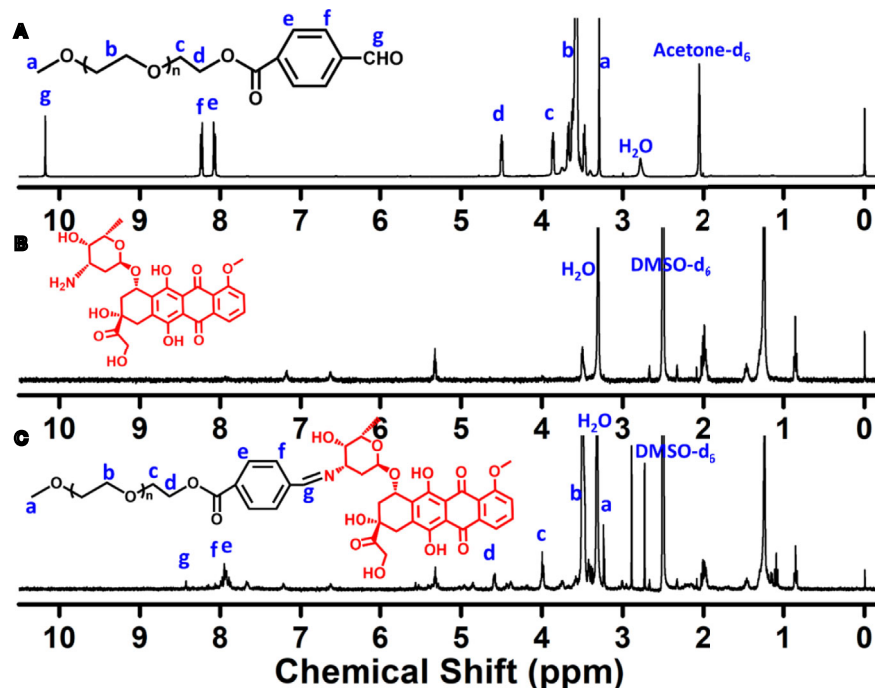


FIGURE 2 | ^1H NMR spectra of (A) PEG-CHO, (B) DOX and (C) PEG-Schiff-DOX. The newly generated peak of Schiff base bond and the intricate peaks of DOX components fully testify the successful preparation of PEG-Schiff-DOX polymer.

(δ 3.3 ppm and 3.5–4.1 ppm) and DOX moieties. The newly generated peak at δ 8.4 ppm for Schiff base bond and the completely disappeared signal of aldehyde group fully testified the successful preparation of PEG-Schiff-DOX polymer. Especially, the integration ratio of representative characteristic peaks further certified its exact and identical structure. The DOX content in the PEG-Schiff-DOX prodrug was calculated to be 38.1 wt%, higher than most of other reported DOX prodrugs, which was sufficient for therapeutic usage.

Preparation, Stability and pH-Responsive Degradation of the Nanoparticles

The obtained PEG-Schiff-DOX could self-assemble into micellar nanoparticles in solutions because of its amphiphilic structure

and high uniformity, which was well demonstrated by TEM image in **Figure 3A-a**. These nanoparticles had a z-average particle size of ca. 85 nm and a polydispersity index (PDI) of 0.22 by DLS result in **Figure 3B-a**. On account of the appropriate diameters (less than 200 nm) to keep lowered level of RES uptake, minimal renal excretion and efficient EPR effect for the passive tumor-targeting, PEG-Schiff-DOX prodrugs could be used as suitable drug carriers for tumor treatment.

These polymeric nanoparticles possessed outstanding storage stability that was important for the drug formulations. The acid-labile Schiff base linker between the hydrophobic DOX and the hydrophilic PEG made the PEG-Schiff-DOX nanoparticles susceptible to disassemble even under faintly acidic condition. The pH-responsive degradation behaviors of these nanoparticles

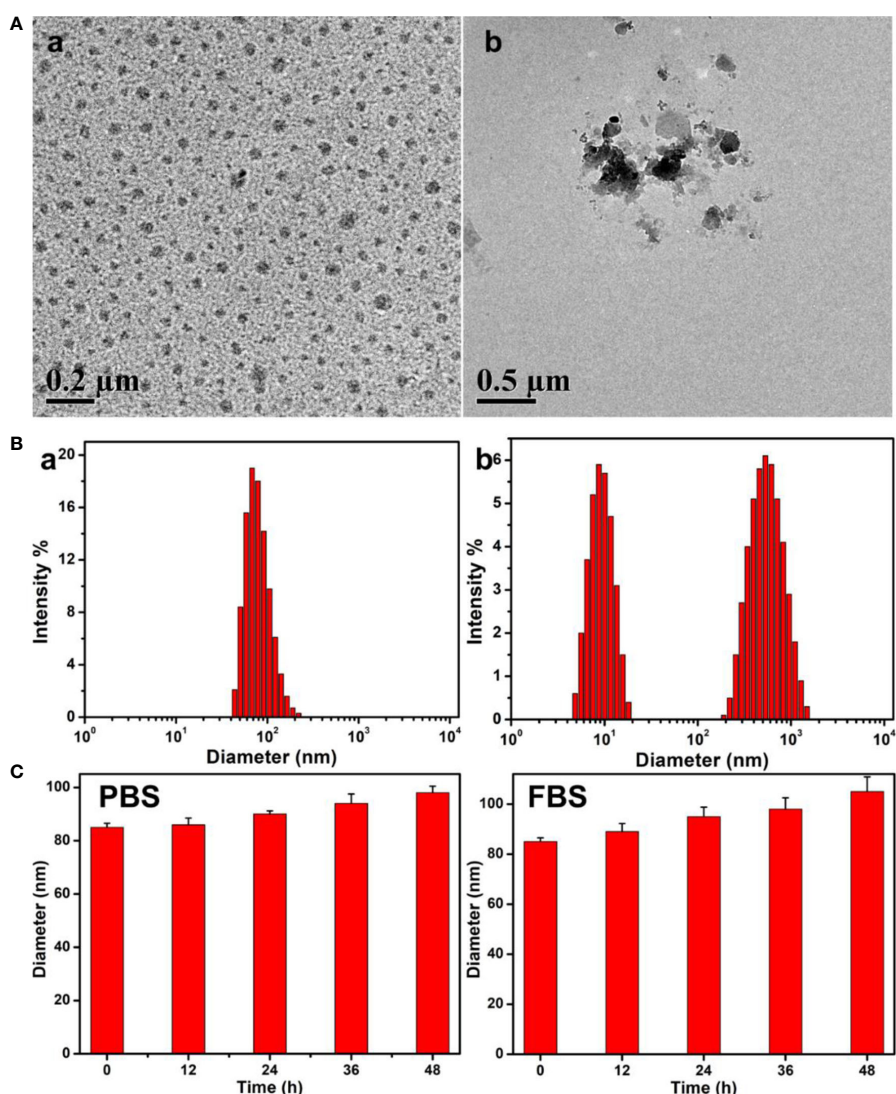


FIGURE 3 | (A) TEM images and **(B)** Size changes of the PEG-Schiff-DOX nanoparticles before (a) and after (b) treatment of pH 5.0 PBS solutions for 4 h. **(C)** Size variations of the PEG-Schiff-DOX nanoparticles after incubation in PBS (pH = 7.4) and 20 wt% FBS solutions. These PEG-Schiff-DOX nanoparticles possessed pH-responsive drug release behavior within the tumor cells or tissues upon changes in physical and chemical environments, but they displayed good stability at physiological conditions for a long period.

at pH 5.0 solutions were monitored by DLS as summarized in **Figure 3B-b**. After incubated at pH 5.0 for 4 h, small molecules and aggregates were found, indicating the disassembly of polymeric nanoparticles. **Figure 3A-b** showed the degradation of micellar nanoparticles in the presence of pH 5.0 solutions, further confirming pH-induced cleavage of Schiff base bonds and dissociation of the aggregates. In addition, the diameter variations of PEG-Schiff-DOX micelles in PBS and FBS solutions were characterized using DLS, revealing their better storage stability in **Figure 3C**, which partly ascribed to the low CMC (0.018 mg/ml) of the prodrug. Besides, PEGylated prodrug nanoparticles themselves were negatively charged that could prevent aggregation by electrostatic repulsion and resistant protein absorption (8). Therefore, these kinds of pH-sensitive nanoparticles could keep stable at normal physiological conditions and degradable in response to acidic solutions, which may be used as the intelligent drug carriers in biomedical fields.

In Vitro Drug Release of the Nanoparticles

The drug release profile of PEG-DOX nanoparticles was assessed under the physiological (PBS, pH 7.4) and acidic conditions (PBS, pH 5.0) to simulate the endo-lysosomal environment at 37°C. As depicted in **Figure 4**, a negligible DOX was released from the PEG-Schiff-DOX nanoparticles at pH 7.4 solutions while a much faster release of DOX at pH 5.0 solutions, thus achieving a high release content of 82.2%, which was attributed to the cleavage of Schiff base bonds to accelerate the DOX release. This pH change from extracellular environment (pH 7.4) to the endosomal compartments (pH 5.0) suggested that the PEG-

Schiff-DOX nanoparticles would maintain stable and eliminate the premature burst release in blood circulation, while effectively promoting DOX release from its prodrug in the process of intracellular trafficking. In contrast to the conventional liposomal DOX formulations with poor stability and premature drug burst release, these pH-responsive nanoparticles exhibited the favorable stability, passive target capacity and tailored DOX release behavior could significantly promote the tumor endocytosis and enhance therapeutic effect.

Cellular Uptake and Intracellular Localization of the Nanoparticles

To determine the prodrugs internalized by tumors with therapeutic effects, cellular uptake process and intracellular drug release behavior were investigated using MCF-7 cells, because PEG-Schiff-DOX with inherent red fluorescence were directly observed with CLSM. As illustrated in **Figure 5A**, red fluorescence was apparently observed at the cytoplasm within the cells after incubation for 1 h, suggesting that these nanoparticles had been internalized easily internalized by the cells and concentrated in the endosome *via* the endocytosis. Along with the prolonged incubation time for 4 h, the intracellular fluorescence intensities tended to be stronger as observed in **Figure 5B**, suggesting the payload of the nanoparticles were gradually released into the nuclei. These findings indicated that the PEG-Schiff-DOX nanoparticles were successfully internalized by MCF-7 cells with efficient release of DOX from the nanoparticles and their further escape from the endosome/lysosome to the nucleus, revealing the applicability and practicability of this smart drug delivery system.

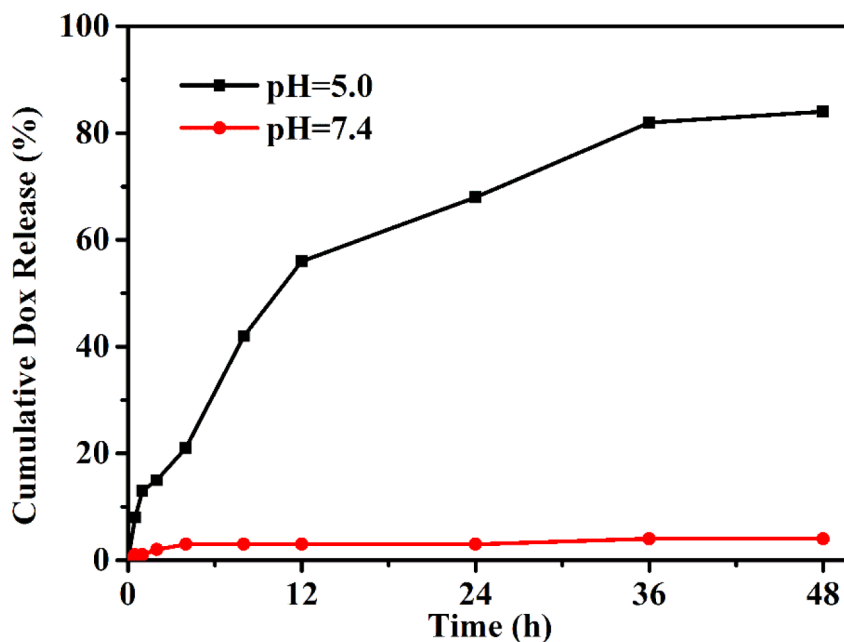


FIGURE 4 | pH-triggered DOX release from PEG-Schiff-DOX nanoparticles at 37°C. The drug release profile reflects the pH responsivity of these nanoparticles that would maintain stable in neutral environment and quickly disassemble in acidic conditions.

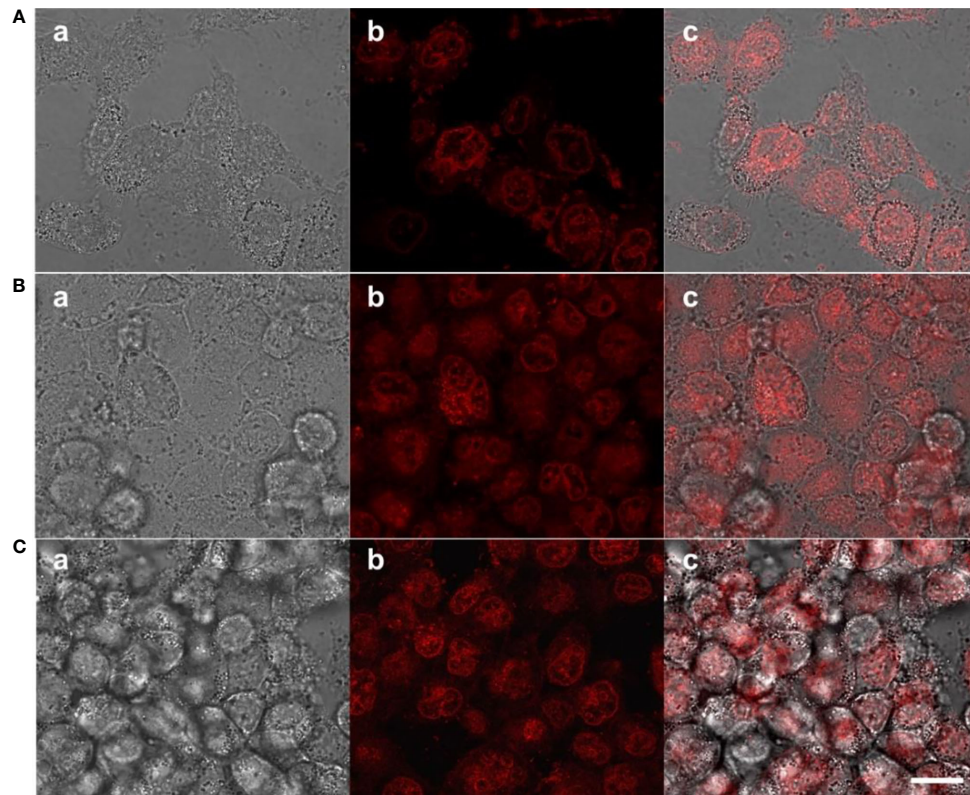


FIGURE 5 | CLSM of MCF-7 cells after incubation with PEG-Schiff-DOX nanoparticles for (A) 1 h and (B) 4 h and free DOX drugs for (C) 1 h. a: bright field image, b: red fluorescence image and c: overlap of bright field and fluorescence images. Scale bars are 20 μ m.

In Vitro Antitumor Activity of the Nanoparticles

The biocompatibility of the nanoparticles is an important issue in the fabrication of drug delivery system. Compared to the free DOX drug, PEG-Schiff-DOX nanoparticles could greatly enhance the drugs' water solubility and stability, prolong their circulation in blood compartments, target cancerous tissues by passive accumulation *via* tumor's EPR effect. Moreover, PEG is a well-known and widely used polymer carrier for drug delivery since it has been approved for clinical use. Therefore, PEGylated doxorubicin prodrugs have shown distinctly therapeutic advantages including better antitumor activity and fewer side effects than free drugs. *In vitro* cytotoxicity to MCF-7 cells of the nanoparticles was determined by CCK-8 assay. **Figure 6** showed high efficiency of antitumor activity toward MCF-7 cells after the incubation for 24 h. The viability of MCF-7 cells was relative to the DOX concentration. In a low concentration, PEG-Schiff-DOX nanoparticles had a similar toxicity as free DOX in a low concentration. While in a high concentration, DOX molecules could easily permeate the cellular and nuclear membranes by passive diffusion into cells, whereas PEG-Schiff-DOX nanoparticles were expected to be endocytosed to locate at the cells followed by endo-lysosomal escape and subsequent drug distribution in the cytosol and nucleus. In addition, **Figure 5C** showed that after incubation with free DOX at 1 h, the

fluorescent intensity was obviously higher than that of PEG-Schiff-DOX nanoparticles incubated for 4 h, indicating the high concentration of free DOX internalized into the cells. In this case, the passive diffusion of free DOX molecules were much quicker than the above internalization processes of polymeric nanoparticles (34–38), demonstrating the relatively higher efficient antitumor capacity.

Although we have not performed the *in vivo* antitumor activity and cardiotoxicity, it is reasonable to conclude that the tumor growth can be effectively inhibited after DOX treatment. On account of the severe toxic side effects of free DOX drug, the body weight of animals can sharply decrease. In contrast, PEG-Schiff-DOX nanoparticles have significantly increased *in vivo* safety and exerted excellent therapeutic activity in animal models, which deserves further preclinical and clinical studies.

Fabrication of DOX-Encapsulated PEG-Schiff-DOX Nanoparticles

Recent developments in nanomedicine for the cancer therapy have enabled programmable delivery of therapeutics by exploiting the stimuli-responsive properties of smart drug carriers. These therapeutic systems are designed with the relevant chemical and physical properties that respond to different triggers for enhanced anticancer efficacy, including the reduced development of drug-resistance, lower therapeutic dose, specific tumor target transport

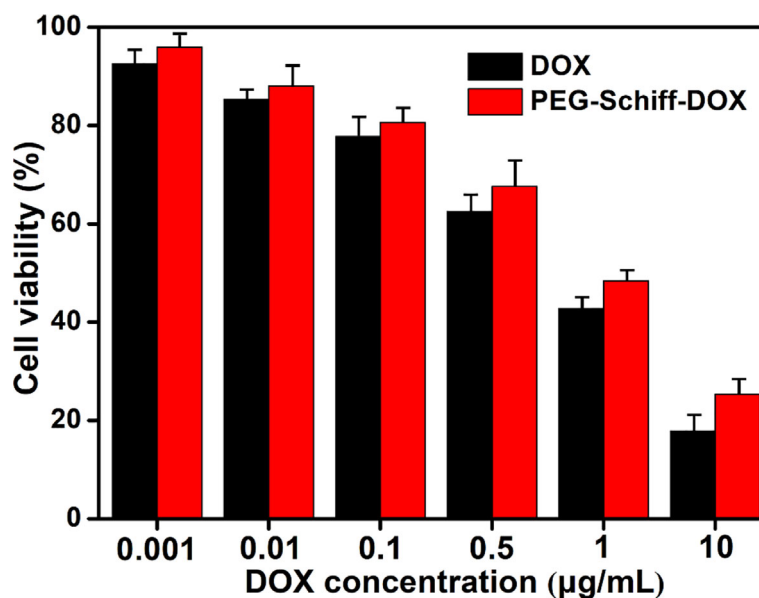


FIGURE 6 | Cytotoxicity of MCF-7 cells following 24 h incubation with PEG-Schiff-DOX nanoparticles and free DOX molecules as a function of DOX dosages. All the data are presented as the average \pm standard deviation.

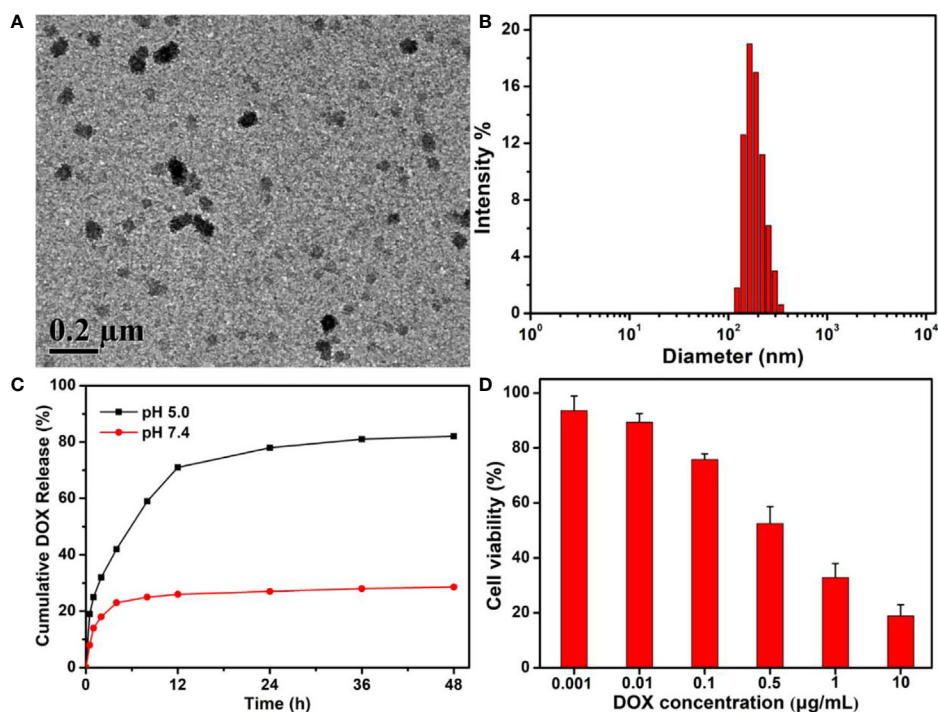


FIGURE 7 | (A) TEM image, (B) DLS result and (C) *In vitro* drug release profile of DOX-encapsulated PEG-Schiff-DOX aggregates. (D) Cytotoxicity of MCF-7 cells following 24 h incubation with DOX-encapsulated PEG-Schiff-DOX aggregates as a function of DOX dosages. All the data are presented as the average \pm standard deviation. These DOX-encapsulated PEG-Schiff-DOX nanoparticles possessed suitable structures and capacities with high drug loading, sufficient drug release and enhanced therapeutic effects of antitumor activity toward MCF-7 cells.

and spatiotemporally controlled release. Therefore, development of programmable nanocarriers for cancer therapy with particular emphasis on synergistic and sequential drug delivery systems is urgent (39, 40). Drug release kinetics are always associated with the intracellular drug concentration, drug action time and therapeutic effects. To actually simulate the tumor environment and maximum tumor growth inhibition, it is necessary to keep effective drug concentration for a time period as long as possible, especially at various requirement periods. Therefore, it is greatly desired to construct an ideal criterion that the designed drug delivery system should be able to reach high drug concentration to kill the tumor cells at an early period and exert an environmental responsive effect whenever needed over a long period. So, incorporation of encapsulated DOX and conjugated DOX in one drug delivery system would achieve a programmed drug release, which acquired the rapid release of encapsulated DOX to enhance intracellular drug concentration at first stage within a short time, and then responsive release of conjugated DOX to continue the effective treatment over a longer period, thereby resulting in the intelligent therapeutic effect.

Using the traditional self-assembly strategy, free DOX drugs could be easily encapsulated into the PEG-Schiff-DOX nanoparticles due to the amphiphilic structures in solutions. The morphology, size and drug release behavior were clearly seen in **Figures 7A–C**. On account of the micellar structures, suitable hydrodynamic sizes, high drug loading and reasonable drug release capacity, these DOX-based nanoparticles with integrating physical encapsulation and chemical linkage can exhibit a two-phase programmed drug release behavior, namely, that the encapsulated DOX released rapidly at an early period to achieve high drug concentration to kill the tumors, and the conjugated DOX provided a responsive release requirement and longer release period to prolong the treatment time. However, an effective and practical carrier had not been required for the excessive drug content, because the instability of nanoparticles may lead to the undesirable drug release and induce the potential side effects. In fact, compared to the free DOX and PEG-Schiff-DOX nanoparticles, these DOX-encapsulated PEG-Schiff-DOX aggregates possessed more superior capacities with high drug loading, sufficient drug release and enhanced therapeutic effects of antitumor activity toward MCF-7 cells after the incubation of 24 h (**Figure 7D**), which can fully satisfy the clinical requirements with reducing drug leakage in the neutral environment of blood circulation and fast drug release in the acidic environment of tumor tissues and intracellular endosomal/lysosomal compartments.

CONCLUSIONS

In summary, we developed a self-assembling PEGylated doxorubicin prodrug of PEG-Schiff-DOX *via* the conjugating hydrophobic DOX into a short PEG chain. This prodrug possessed good storage stability, high drug loading capacity and controlled release behavior. Incorporation of Schiff base into the polymeric architectures furnished the PEG-Schiff-DOX nanoparticles with pH responsiveness that maintained the structural integrity at neutral conditions and quickly disassembled in acidic conditions. Cytotoxicity assay indicated a fast internalization and a high cellular proliferation inhibition to MCF-7 cells, demonstrating excellent antitumor activities. In addition, this kind of nanoparticle could also encapsulate small free DOX drugs with high drug loading, sufficient drug release and enhanced therapeutic effects of antitumor activity toward MCF-7 cells, which may provide a promising option for developing translational DOX formulations and construction of multifunctional drug delivery systems in future.

DATA AVAILABILITY STATEMENT

The original contributions presented in the study are included in the article/supplementary material. Further inquiries can be directed to the corresponding authors.

AUTHOR CONTRIBUTIONS

JS, BX, and HY contributed equally to this reviewed paper. XW and ZY initiated the project. JS, BX, XL, YT, HY, and BW searched the data base, wrote, and finalized the manuscript. XW and ZY made important suggestions and helped in revising the paper. All authors reviewed and commented on the entire manuscript. All authors contributed to the article and approved the submitted version.

FUNDING

This work was supported by National Natural Science Foundation of China (grant no. 51973226), Shenzhen Science and Technology Innovation Committee (grant no. JCYJ20180228163446770), and Youth Innovation Promotion Association CAS (grant no. 2019031).

REFERENCES

1. Wei H, Zhuo RX, Zhang XZ. Design and development of polymeric micelles with cleavable links for intracellular drug delivery. *Prog Polym Sci* (2013) 38:503–35. doi: 10.1016/j.progpolymsci.2012.07.002
2. Wang X, Gao PY, Yang YY, Guo HX, Wu DC. Dynamic and programmable morphology and size evolution via a living hierarchical self-assembly strategy. *Nat Commun* (2018) 9:2772. doi: 10.1038/s41467-018-05142-3
3. Kemp JA, Shim MS, Heo CY, Kwon YJ. “Combo” nanomedicine: Co-delivery of multi-modal therapeutics for efficient, targeted, and safe cancer therapy. *Adv Drug Deliv Rev* (2016) 98:3–18. doi: 10.1016/j.addr.2015.10.019
4. Ulbrich K, Hola K, Subr V, Bakandritsos A, Tucek J, Zboril R. Targeted drug delivery with polymers and magnetic nanoparticles: covalent and noncovalent approaches, release control, and clinical studies. *Chem Rev* (2016) 116:5338–431. doi: 10.1021/acs.chemrev.5b00589

5. Fan LF, Wang X, Cao QC, Yang YY, Wu DC. POSS-based supramolecular amphiphilic zwitterionic complexes for drug delivery. *Biomater Sci* (2019) 7:1984–94. doi: 10.1039/C9BM00125E
6. Sun GF, Liu JH, Wang X, Li M, Cui X, Zhang LC, et al. Fabrication of dual-sensitive poly(β -hydroxyl amine) micelles for controlled drug delivery. *Eur Polym J* (2019) 114:338–45. doi: 10.1016/j.eurpolymj.2019.02.048
7. Al-Musawi S, Albukhaty S, Al-Karagoly H, Almalki F. Design and synthesis of multi-functional superparamagnetic core-gold shell nanoparticles coated with chitosan and folate for targeted antitumor therapy. *Nanomaterials* (2021) 11:32. doi: 10.3390/nano11010032
8. Huang D, Zhuang YP, Shen H, Yang F, Wang X, Wu DC. Acetal-linked PEGylated paclitaxel prodrugs forming free-paclitaxel-loaded pH-responsive micelles with high drug loading capacity and improved drug delivery. *Mater Sci Eng C* (2018) 82:60–8. doi: 10.1016/j.msec.2017.08.063
9. Li GP, Pei ML, Liu P. pH/Reduction dual-responsive comet-shaped PEGylated CQD-DOX conjugate prodrug: Synthesis and self-assembly as tumor nanotheranostics. *Mater Sci Eng C* (2020) 110:110653. doi: 10.1016/j.msec.2020.110653
10. An L, Zhang P, Shen W, Yi X, Yin WY, Jiang RH, et al. A sulfur dioxide polymer prodrug showing combined effect with doxorubicin in combating subcutaneous and metastatic melanoma. *Bioact Mater* (2021) 6:1365–74. doi: 10.1016/j.bioactmat.2020.10.027
11. Murad AM, Santiago FF, Petroianu A, Rocha PRS, Rodrigues MAG, Rausch M. Modified therapy with 5-fluorouracil, doxorubicin and methotrexate in advanced gastric cancer. *Cancer* (1993) 72:37–41. doi: 10.1002/1097-0142(19930701)72:1<37::AID-CNCR2820720109>3.0.CO;2-P
12. Minotti G, Menna P, Salvatorelli E, Cairo G, Gianni L. Anthracyclines: molecular advances and pharmacologic developments in antitumor activity and cardiotoxicity. *Pharmacol Rev* (2004) 56:185–229. doi: 10.1124/pr.56.2.6
13. Lyass O, Uziely B, Ben-Yosef R, Tzemach D, Heshing NI, Lotem M, et al. Correlation of toxicity with pharmacokinetics of pegylated liposomal doxorubicin (Doxil) in metastatic breast carcinoma. *Cancer* (2000) 89:1037–47. doi: 10.1002/1097-0142(20000901)89:5<1037::AID-CNCR13>3.0.CO;2-Z
14. Zhou N, Zhang N, Zhi Z, Jing XN, Liu DM, Shao YP, et al. One-pot synthesis of acid-degradable polyphosphazene prodrugs for efficient tumor chemotherapy. *J Mater Chem B* (2020) 8:10540–8. doi: 10.1039/D0TB01992E
15. Zhu XH, Li C, Lu Y, Liu YJ, Wan D, Zhu DW, et al. Tumor microenvironment-activated therapeutic peptide-conjugated prodrug nanoparticles for enhanced tumor penetration and local T cell activation in the tumor microenvironment. *Acta Biomater* (2021) 119:337–48. doi: 10.1016/j.actbio.2020.11.008
16. Wen W, Guo C, Guo J. Acid-responsive adamantane-cored amphiphilic block polymers as platforms for drug delivery. *Nanomaterials* (2021) 11:188. doi: 10.3390/nano11010188
17. Cytryniak A, Nazaruk E, Bilewicz R, Górzynska E, Żelechowska-Matysiak K, Walczak R, et al. lipidic cubic-phase nanoparticles (cubosomes) loaded with doxorubicin and labeled with ¹⁷⁷Lu as a potential tool for combined chemo and internal radiotherapy for cancers. *Nanomaterials* (2020) 10:2272. doi: 10.3390/nano10112272
18. Li DW, Bu YZ, Zhang LN, Wang X, Yang YY, Zhuang YP, et al. Facile construction of pH- and redox-responsive micelles from a biodegradable poly(β -hydroxyl amine) for drug delivery. *Biomacromolecules* (2016) 17:291–300. doi: 10.1021/acs.biomac.5b01394
19. Zhang XL, Zhang T, Ma XB, Wang YJ, Lu Y, Jia D, et al. The design and synthesis of dextran-doxorubicin prodrug-based pH-sensitive drug delivery system for improving chemotherapy efficacy. *Asian J Pharm Sci* (2020) 15:605–16. doi: 10.1016/j.ajps.2019.10.001
20. Wang X, Yang YY, Zhuang YP, Gao PY, Yang F, Shen H, et al. Fabrication of pH-responsive nanoparticles with an AIE feature for imaging intracellular drug delivery. *Biomacromolecules* (2016) 17:2920–9. doi: 10.1021/acs.biomac.6b00744
21. Li JG, Li XM, Pei ML, Liu P. Acid-labile anhydride-linked doxorubicin-doxorubicin dimer nanoparticles as drug self-delivery system with minimized premature drug leakage and enhanced anti-tumor efficacy. *Colloids Surf B* (2020) 192:111064. doi: 10.1016/j.colsurfb.2020.111064
22. Greenwald RB. PEG drugs: an overview. *J Control Release* (2001) 74:159–71. doi: 10.1016/S0168-3659(01)00331-5
23. Harris JM, Chess RB. Effect of PEGylation on pharmaceuticals. *Nat Rev Drug Discov* (2003) 2:214–21. doi: 10.1038/nrd1033
24. Wu YH, Zhong D, Li YH, Wu HY, Xu XH, Yang J, et al. Tumor-oriented telomerase-terminated nanoplatfrom as versatile strategy for multidrug resistance reversal in cancer treatment. *Adv Healthc Mater* (2020) 9:1901739. doi: 10.1002/adhm.201901739
25. Veronese FM, Pasut G. PEGylation, successful approach to drug delivery. *Drug Discov Today* (2005) 10:1451–8. doi: 10.1016/S1359-6446(05)03575-0
26. Gou PF, Liu WW, Mao WW, Tang JB, Shen YQ, Sui MH. Self-assembling doxorubicin prodrug forming nanoparticles for cancer chemotherapy: synthesis and anticancer study in vitro and in vivo. *J Mater Chem B* (2013) 1:284–92. doi: 10.1039/C2TB00004K
27. Greenwald RB, Choe YH, McGuire J, Conover CD. Effective drug delivery by PEGylated drug conjugates. *Adv Drug Deliv Rev* (2003) 55:217–50. doi: 10.1016/S0169-409X(02)00180-1
28. Wang YQ, Huang D, Wang X, Yang F, Shen H, Wu DC. Fabrication of zwitterionic and pH-responsive polyacetal dendrimers for anticancer drug delivery. *Biomater Sci* (2019) 7:3238–48. doi: 10.1039/C9BM00606K
29. Li DA, Song Y, He JL, Zhang MZ, Ni PH. Polymer-doxorubicin prodrug with biocompatibility, pH response, and main chain breakability prepared by catalyst-free click reaction. *ACS Biomater Sci Eng* (2019) 5:2307–15. doi: 10.1021/acsbomaterials.9b00301
30. Song Y, Li D, He JL, Zhang MZ, Ni PH. Facile preparation of pH-responsive PEGylated prodrugs for activated intracellular drug delivery. *Chin Chem Lett* (2019) 30:2027–31. doi: 10.1016/j.ccllet.2019.04.052
31. Ko NR, Van SY, Hong SH, Kim S-Y, Kim M, Lee JS, et al. Dual pH- and GSH-responsive degradable PEGylated graphene quantum dot-based nanoparticles for enhanced HER2-positive breast cancer therapy. *Nanomaterials* (2020) 10:91. doi: 10.3390/nano10010091
32. Zhang PF, Wang JQ, Chen H, Zhao L, Chen BB, Chu CC, et al. Tumor microenvironment-responsive ultrasmall nanodrug generators with enhanced tumor delivery and penetration. *J Am Chem Soc* (2018) 140:14980–9. doi: 10.1021/jacs.8b09396
33. Chen J, Jiang Z, Xu W, Sun T, Zhuang X, Ding J, et al. Spatiotemporally targeted nanomedicine overcomes hypoxia-induced drug resistance of tumor cells after disrupting neovasculature. *Nano Lett* (2020) 20:6191–8. doi: 10.1021/acs.nanolett.0c02515
34. Zheng P, Liu Y, Chen JJ, Xu WG, Li G, Ding JX. Targeted pH-responsive polyion complex micelle for controlled intracellular drug delivery. *Chin Chem Lett* (2020) 31:1178–82. doi: 10.1016/j.ccllet.2019.12.001
35. Tang N, Du GJ, Wang N, Liu CC, Hang HY, Liang W. Improving penetration in tumors with nanoassemblies of phospholipids and doxorubicin. *J Natl Cancer Inst* (2007) 99:1347. doi: 10.1093/jnci/djm027
36. Higgins CF. Multiple molecular mechanisms for multidrug resistance transporters. *Nature* (2007) 446:749–57. doi: 10.1038/nature05630
37. Gottesman MM, Fojo T, Bates SE. Multidrug resistance in cancer: role of ATP-dependent transporters. *Nat Rev Cancer* (2002) 2:48–58. doi: 10.1038/nrc706
38. Ding J, Chen J, Gao L, Jiang Z, Zhang Y, Li M, et al. Engineered nanomedicines with enhanced tumor penetration. *Nano Today* (2019) 29:100800. doi: 10.1016/j.nantod.2019.100800
39. Zhang H, Dong S, Li Z, Feng X, Xu W, Tulinao CMS, et al. Biointerface engineering nanoplatfroms for cancer-targeted drug delivery. *Asian J Pharm Sci* (2020) 15:397–415. doi: 10.1016/j.ajps.2019.11.004
40. Pacardo DB, Ligler FS, Gu Z. Programmable nanomedicine: synergistic and sequential drug delivery systems. *Nanoscale* (2015) 7:3381–91. doi: 10.1039/C4NR07677J

Conflict of Interest: The authors declare that the research was conducted in the absence of any commercial or financial relationships that could be construed as a potential conflict of interest.

Copyright © 2021 Song, Xu, Yao, Lu, Tan, Wang, Wang and Yang. This is an open-access article distributed under the terms of the Creative Commons Attribution License (CC BY). The use, distribution or reproduction in other forums is permitted, provided the original author(s) and the copyright owner(s) are credited and that the original publication in this journal is cited, in accordance with accepted academic practice. No use, distribution or reproduction is permitted which does not comply with these terms.



The Tetramethylpyrazine Derivative Statmp-151: A Novel Small Molecule Stat3 Inhibitor With Promising Activity Against Breast Cancer

Chen Fan^{1†}, Yijie Wang^{2†}, Hui Huang^{3†}, Wenzhen Li², Jialin Ma², Dongping Yao², Zijun Tang², Taixiong Xue², Liyang Ha¹, Yan Ren¹, Yiwen Zhang², Qin Wang², Yongmei Xie², Yi Luo^{2*}, Rui Tan^{4*} and Jian Gu^{1*}

OPEN ACCESS

Edited by:

Sanjun Shi,
Chengdu University of Traditional
Chinese Medicine, China

Reviewed by:

Nadiah Abu,
National University of Malaysia,
Malaysia
Wukun Liu,
Nanjing University of Chinese
Medicine, China

*Correspondence:

Yi Luo
orthop_luoyi@163.com
Rui Tan
tanrui@swjtu.edu.cn
Jian Gu
gujiancd@163.com

[†]These authors have contributed
equally to this work

Specialty section:

This article was submitted to
Pharmacology of Anti-Cancer Drugs,
a section of the journal
Frontiers in Pharmacology

Received: 11 January 2021

Accepted: 23 March 2021

Published: 15 April 2021

Citation:

Fan C, Wang Y, Huang H, Li W, Ma J,
Yao D, Tang Z, Xue T, Ha L, Ren Y,
Zhang Y, Wang Q, Xie Y, Luo Y, Tan R
and Gu J (2021) The
Tetramethylpyrazine Derivative
Statmp-151: A Novel Small Molecule
Stat3 Inhibitor With Promising Activity
Against Breast Cancer.
Front. Pharmacol. 12:651976.
doi: 10.3389/fphar.2021.651976

¹College of Pharmacy, Southwest Minzu University, Chengdu, China, ²State Key Laboratory of Biotherapy and Cancer Center, Department of Orthopedics, West China Hospital, Sichuan University, Chengdu, China, ³Department of Oncology, The Fifth Hospital of Wuhan, Wuhan, China, ⁴College of Life Science and Engineering, Southwest Jiaotong University, Chengdu, China

Breast cancer is the most common malignancy in women and is a molecularly heterogeneous disease. Signal transducer and activator of transcription 3 (Stat3) is overexpressed and hyperactivated in a variety of human tumours, including breast cancer, thus representing a promising target for breast cancer treatment. In the present study, we evaluated the activities of a novel Stat3 inhibitor named Statmp-151 in the human breast cancer cell lines MCF-7 and MDA-MB-231 and the murine mammary carcinoma cell line 4T1. The *in vitro* results showed that Statmp-151 inhibited the proliferation of breast cancer cell lines in a dose- and time-dependent manner and suppressed the phosphorylation of Stat3 in a dose-dependent manner. Flow cytometry (FCM) assays revealed that Statmp-151 affected mitochondrial membrane potential and reactive oxygen species (ROS) production. Furthermore, Statmp-151 inhibited cell migration, as shown by analysis of the matrix metalloproteinases MMP2 and MMP9. Finally, in a 4T1 tumour-bearing mouse model, intraperitoneal injection of 30 mg/kg/day Statmp-151 significantly suppressed the growth of tumours without obvious toxicity. These results indicated that Statmp-151 might be a potential candidate for the treatment of breast cancer.

Keywords: breast cancer, tetramethylpyrazine derivatives, stat3, statmp-151, apoptosis

INTRODUCTION

Breast cancer is a major cause of cancer-related mortality as one of the most common cancers in females. The strong metastatic potential of this disease accounts for most deaths from breast cancer. Treatment for breast cancer is multidisciplinary, including locoregional surgery and radiotherapy as well as systemic treatment (Harbeck et al., 2019). Triple-negative breast cancer (TNBC) is the most aggressive type and has much higher recurrence and metastasis rates than other types (Waks and Winer, 2019). When patients are diagnosed with TNBC at the early stage, a combination of chemotherapeutic agents with radiotherapy or no radiotherapy is used as the standard nonsurgical treatment; unfortunately, the efficacy is limited (Sharma and Priyanka, 2018). In addition to chemotherapy and surgery, molecular-targeted therapy has been one of the hotspots in the field of breast cancer research in recent years (Lu and Liu, 2020).

Stat3 regulates tyrosinase gene expression and transcript activity and thus plays a pivotal role in promoting breast cancer growth and metastasis (Federica et al., 2018). The Stat3 protein consists of an N-terminal domain, a coiled-coil domain (CCD), a DNA binding domain (DBD), a linker domain, an SRC homology 2 (SH2) domain for phosphorylation and dimerization, and a C-terminal transactivation domain (TAD) (Furtek et al., 2016). The SH2 domain is a very important domain of Stat3 and is related to many important physiological functions of Stat3. When extracellular signals are transmitted to the cell membrane, through a series of cascade amplification reactions, tyrosine 705 (Tyr705) of the SH2 domain is finally phosphorylated to activate the entire Stat3. The activated Stat3 monomer dimerizes through the SH2 domain and enters the nucleus, binding with DNA and promoting the expression of downstream genes (Schust et al., 2006; Chen et al., 2013).

Therefore, targeted inhibitors of the SH2 domain may have potential to treat breast cancer. However, targeted inhibitors of the SH2 domain possess many disadvantages, such as high toxicity, low activity and poor selectivity. Tetramethylpyrazine (TMP) is an alkaloid isolated from the rhizome of *Ligusticum chuanxiong* Hort. TMP has been reported to have several significant biological effects, such as antioxidative, antifibrotic, calcium antagonist and antitumour effects (Zhao et al., 2016). TMP could also inhibit the viability of MDA-MB-231 breast cancer cells (Shen et al., 2018). However, the anticancer activity is relatively weak. Hence, it is necessary to enhance its effects *via* reasonable structural modification. In this study, we synthesized Statmp-151 to improve TMP's anti-breast cancer activity; this molecule combined the classic SH2 domain targeting inhibitor Stattic with TMP (Zeng et al., 2013; Furtek et al., 2016). Finally, the potential anti-breast cancer mechanisms were explored by a series of experiments.

MATERIALS AND METHODS

Cell Culture

The breast cancer cell lines MCF-7, MDA-MB-231 and 4T1 were purchased from the American Type Culture Collection (Rockville, MD, United States). Cells were maintained in DMEM or RPMI 1640 medium supplemented with 10% foetal bovine serum (Si Ji Qin Bioengineering, China) and 1% antibiotics (penicillin and streptomycin) at 37°C in a 5% CO₂ incubator.

Cell Viability and Colony Formation Assays

The cells ($1-5 \times 10^3$ cells per well) were incubated in 96-well plates overnight and then treated with different concentrations of Statmp-151 for 24, 48, and 72 h. Afterward, 5 mg/ml MTT (20 µl) was added to each well for 3 h. Finally, the supernatant was removed, and 150 µl of DMSO was added to each well. The optical density values were determined at 490 or 570 nm by a SpectraMAX M5 Microplate Spectrophotometer. All experiments were performed three times with three replicates.

Colony formation was measured by seeding cells in 6-well plates at 500–800 cells per well and treating the cells with various

concentrations of Statmp-151 after approximately 24 h of incubation. The culture medium containing Statmp-151 was replaced every three days. All cells were fixed and stained with 0.5% crystal violet after 12 days.

Apoptosis Analysis

For determination of the effect of Statmp-151 on tumour apoptosis, apoptosis detection kits were used. The cells (1×10^5 cells per well) were incubated in 6-well plates overnight and then treated with different concentrations of Statmp-151. After 24 h, the cells were harvested and washed twice with cold PBS. Following the manufacturer's instructions, the cells were stained with FITC-conjugated Annexin V and PI (Propidium Iodide) and detected by FCM.

Mitochondrial Membrane Potential ($\Delta\psi$ m)

The cells (1×10^5 cells per well) were incubated in 6-well plates overnight, and treated with Statmp-151 for another 24 h. Then, the cells were harvested and washed twice with cold PBS, stained with JC-1 according to the instructions, and finally detected by FCM.

Reactive Oxygen Species Level in Cells

The cells (1×10^5 cells per well) were incubated in 6-well plates overnight and then treated with different concentrations of Statmp-151. After 24 h, the cells were harvested and washed twice with cold PBS. The ROS levels were monitored using 10 µM DCFH-DA for 30 min and then detected by FCM.

Western Blotting

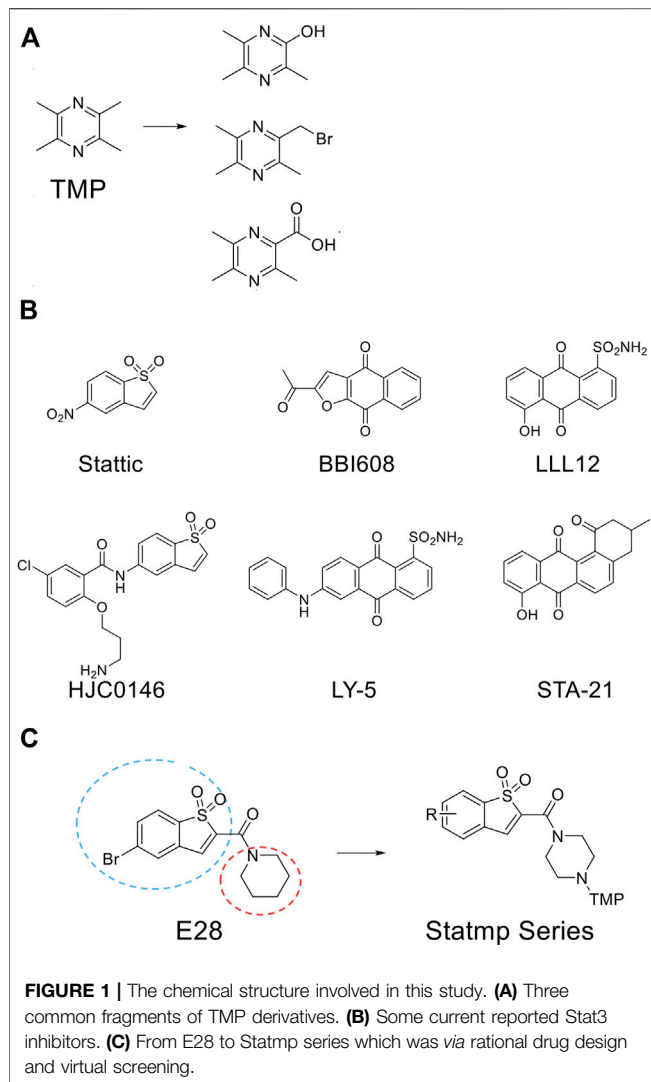
For analysis of the expression of the corresponding proteins in MDA-MB-231 and 4T1 cells after incubation with Statmp-151 for 24 h, harvested cells were lysed with RIPA buffer for 1 h. Then, the protein concentrations were measured and equalized. SDS-PAGE with the optimal concentration of proteins selected according to their molecular weight was performed, and then, the proteins were transferred onto polyvinylidene difluoride nitrocellulose membranes. After incubation with 5% skim milk for 1 h, the target protein was incubated with the corresponding primary antibodies overnight at 4°C. The next day, the cells were washed several times and then incubated with the corresponding secondary antibodies, followed by washing several times. Finally, the protein bands were visualized using an enhanced chemiluminescence kit. Monoclonal β -actin proteins were used as a reference.

Wound-Healing Migration Assays

A wound-healing migration assay was performed to evaluate cell migration. When cells grew to 80% confluence in 6-well plates, they were renewed with 2% FBS containing different concentrations of Statmp-151. Images were taken at 0 and 24 h by an inverted microscope.

The Anticancer Effect of Statmp-151 *In Vivo*

All animal experiments were conducted in accordance with the principles and procedures approved by the Committee on the Ethics of Animal Experiments of State Key Laboratory of Biotherapy, Sichuan University. BALB/c mice aged 6–8 weeks



were purchased from the experimental Animal Centre of Sichuan University. Approximately 1×10^6 4T1 cells were inoculated into the right lower limb of the mice. We randomly divided the mice into 4 groups ($n = 5$) when the tumours reached an average volume of 100 mm^3 . Statmp-151 (10, 20, and 30 mg/kg) or vehicle was intraperitoneally injected once a day for 15 days. After administration, the body weights and tumour sizes of the mice were measured every 3 days. At the end of the animal experiment, the weight of the tissue and tumour was recorded, and then, the tumour volume was measured and photographed. The tumour tissue was stored in paraformaldehyde for further analysis.

Toxicity Evaluation

For evaluation of the safety of Statmp-151 during the treatment, all the mice were observed continuously for general conditions, such as body weight, appetite, mental state and other clinical features. Blood was obtained from the eyeball for biochemistry analysis. Haematoxylin and eosin staining was performed of paraffin sections of lung, liver, spleen, heart and kidney tissues of the mice treated with Statmp-151.

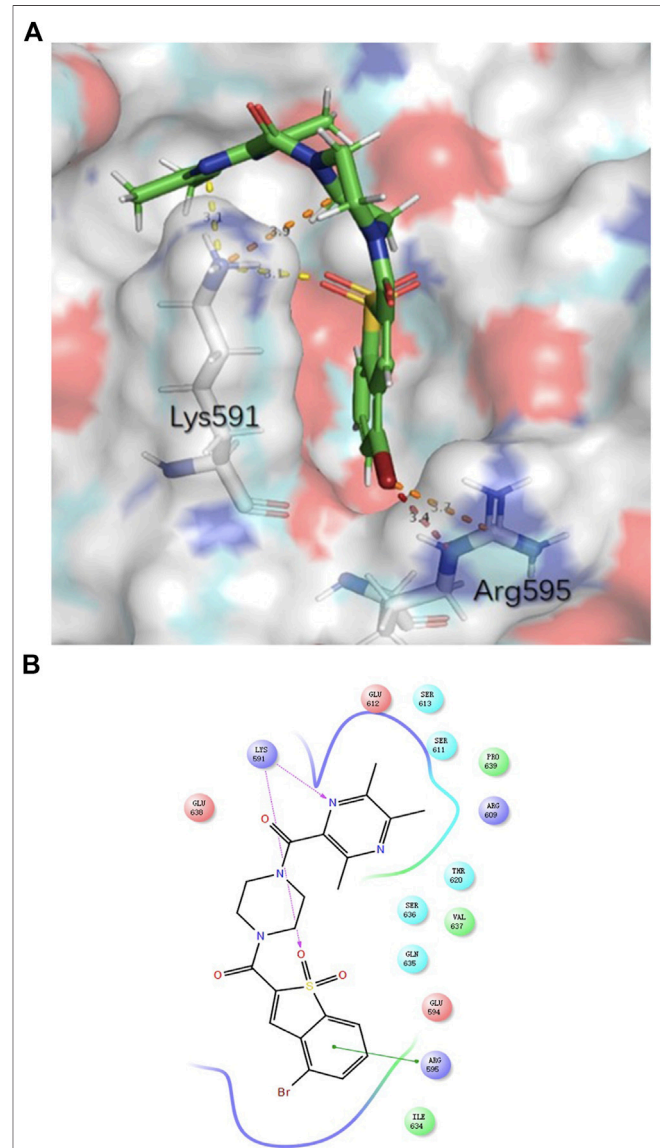
Statistical Analysis

The results are presented as the mean and standard deviation ($M \pm SD$). Statistically significant p values were labelled as follows: $*p < 0.05$; $**p < 0.01$; $***p < 0.001$. All statistical workflows were performed in GraphPad Prism (version 7.0).

RESULTS

Drug Design of Statmp-151

TMP was reported to possess multiple activities, as described above. For chemical structure modification, there are three common fragments of TMP to utilize (**Figure 1A**). Carboxyl, bromo and hydroxyl groups are operable reactive groups for



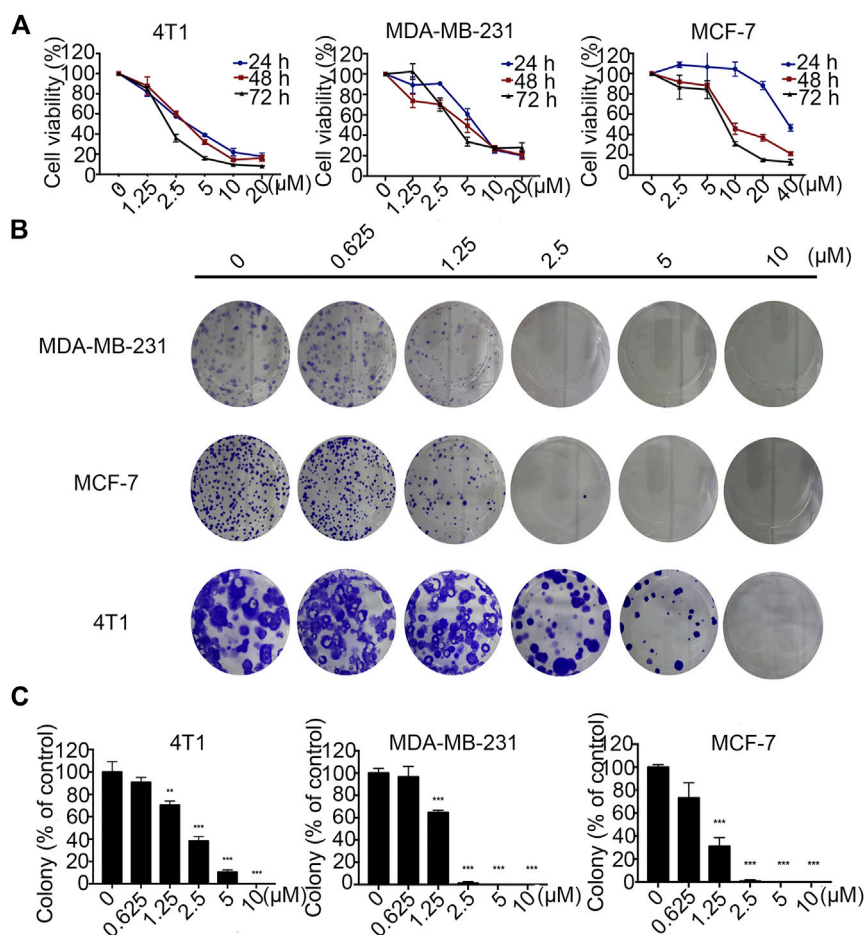


FIGURE 3 | Statmp-151 inhibited the growth of breast cancer cells *in vitro*. **(A)** Breast cancer cell lines 4T1, MDA-MB-231 and MCF-7 were treated with different concentrations of Statmp-151 for 24, 48 and 72 h, respectively. **(B)** The effects of statmp-151 on the colony formation in three breast cancer cell lines for 10 days. **(C)** The statistical results were presented using vehicle control at 100%. Each point represents the mean \pm SD for at least 3 independent experiments (* $p < 0.05$, ** $p < 0.01$ and *** $p < 0.001$ vs. control group).

various modification strategies. Stat3-targeted inhibitors, such as Stattic, BBI608, LLL12, HJC0146, LY-5 and STA-21, are listed in **Figure 1B**. Among them, Stattic was the first small molecule inhibitor of Stat3 activation and dimerization (Schust et al., 2006). This compound is often used for further development to discover Stat3 inhibitors (Ji et al., 2015). In this study, we used (5-bromo-1,1-dioxidobenzo[b]thiophen-2-yl) (piperidin-1-yl) methanone (E28) (Ji et al., 2015) as the lead compound to discover Stat3 inhibitors containing TMP. We replaced the piperazine ring of E28 with a piperazine ring for further modification (in blue circle) and explored the group linking TMP with the piperazine ring. In terms of the scaffold of Stattic, we also explored the substituents on the benzene ring (in red circle), and a total of 38 compounds were designed (**Figure 1C**). We employed the Glide docking program to conduct a virtual screening against these 38 rationally designed Statmp series and finally found that Statmp-151 could exhibit potent activity against Stat3, had the best docking score and showed a more favourable conformation (**Figure 2**). Binding mode analysis indicated that the pyrazine ring and sulfone form hydrogen

bonds with Lys591, while the bromo substituent forms halogen bonds with Arg595. Then, wet laboratory experiments were conducted to explore whether Statmp-151 was consistent with the primary drug design. The synthesis and characterization of Statmp-151 are shown in the supporting information.

Statmp-151 Inhibited the Growth of Breast Cancer Cells *In Vitro*

The effects of Statmp-151 on the proliferation of MCF-7, MDA-MB-231 and 4T1 cells were detected by MTT assays (Liu et al., 2019). In 4T1 and MDA-MB-231 cells where Statmp-151 was used at concentrations of 0–20 μ M, and in MCF-7 cells where Statmp-151 was used at concentrations of 0–40 μ M for 24, 48 and 72 h. The results showed that the IC_{50} at 72 h was 2.20 ± 0.01 μ M in 4T1 cells, 4.75 ± 0.39 μ M in MDA-MB-231 cells, and 8.06 ± 0.08 μ M in MCF-7 cells (**Figure 3A**). Pan J reported the anti-tumour activity of TMP which is not ideal. The ligustrazine IC_{50} results showed it is about 10 mmol/l in breast cancer. The above results significantly improved the anti-tumour activity of maternal TMP (Pan et al., 2015).

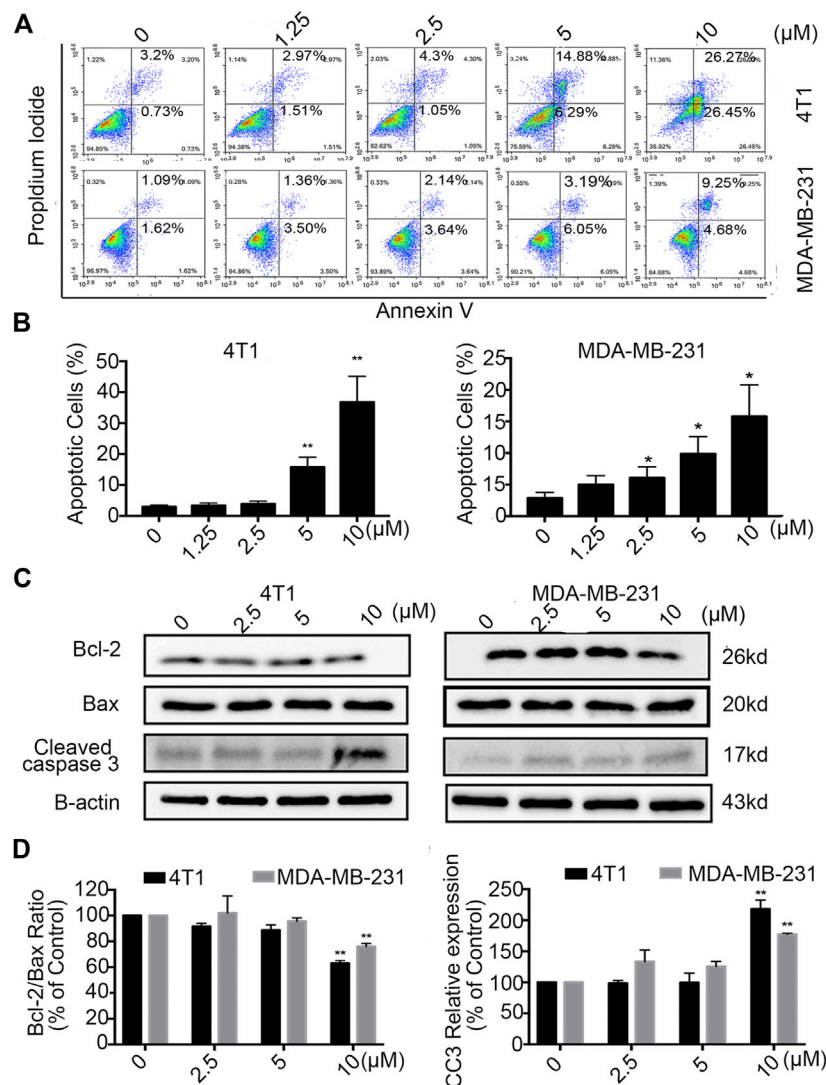


FIGURE 4 | Statmp-151 induced apoptosis in breast cancer cells. **(A)** 4T1 and MDA-MB-231 cells were treated with different concentrations of Statmp-151 for 24 h and then analyzed by FCM using Annexin V/PI dual staining. **(B)** The apoptosis data analysis is presented in a histogram. **(C)** After treated with Statmp-151 for 24 h in 4T1 and MDA-MB-231 cells, the expressions of cleaved caspase-3, Bcl-2 and Bax were obtained, with β -actin used as a standard control. **(D)** The gray level statistics were quantified with ImageJ (* $p < 0.05$, ** $p < 0.01$ and *** $p < 0.001$ vs. the control group).

A clone formation experiment was utilized to further verify the effects of Statmp-151 on the proliferation of MDA-MB-231, MCF-7 and 4T1 cells. As shown in **Figure 3B,C**, cancer cell proliferation was reduced in a concentration-dependent manner, which was consistent with the results of the MTT assay.

Statmp-151 Induced Apoptosis of Breast Cancer Cells

For further analysis of the effect of Statmp-151, we performed Annexin V and PI double dye detection of MDA-MB-231 and 4T1 cells (Zhu et al., 2016). As shown in **Figure 4A,B**, Statmp-151 was able to induce breast cancer cell apoptosis in a dose-dependent manner after treatment for 24 h compared to that in the control group.

To confirm the apoptotic effect of Statmp-151 on breast cancer cells, we determined the expression of Bcl-2, Bax and Cleaved caspase-3 (CC3) in MDA-MB-231 and 4T1 cells after treatment with Statmp-151 for 24 h. As shown in **Figure 4C,D**, the expression level of Bcl-2 was strongly decreased in 4T1 cells, Bax expression was not changed, and CC3 expression was significantly increased. This treatment showed no effect on Bcl-2/Bax ratio expression and increased CC3 expression in MDA-MB-231 cells. Collectively, these results showed that Statmp-151 could induce breast cancer cell apoptosis.

The Effect of Statmp-151 on Mitochondrial Membrane Potential and ROS

Mitochondrial membrane potential is a marker of the early apoptotic pathway. During mitochondrial pathway-mediated

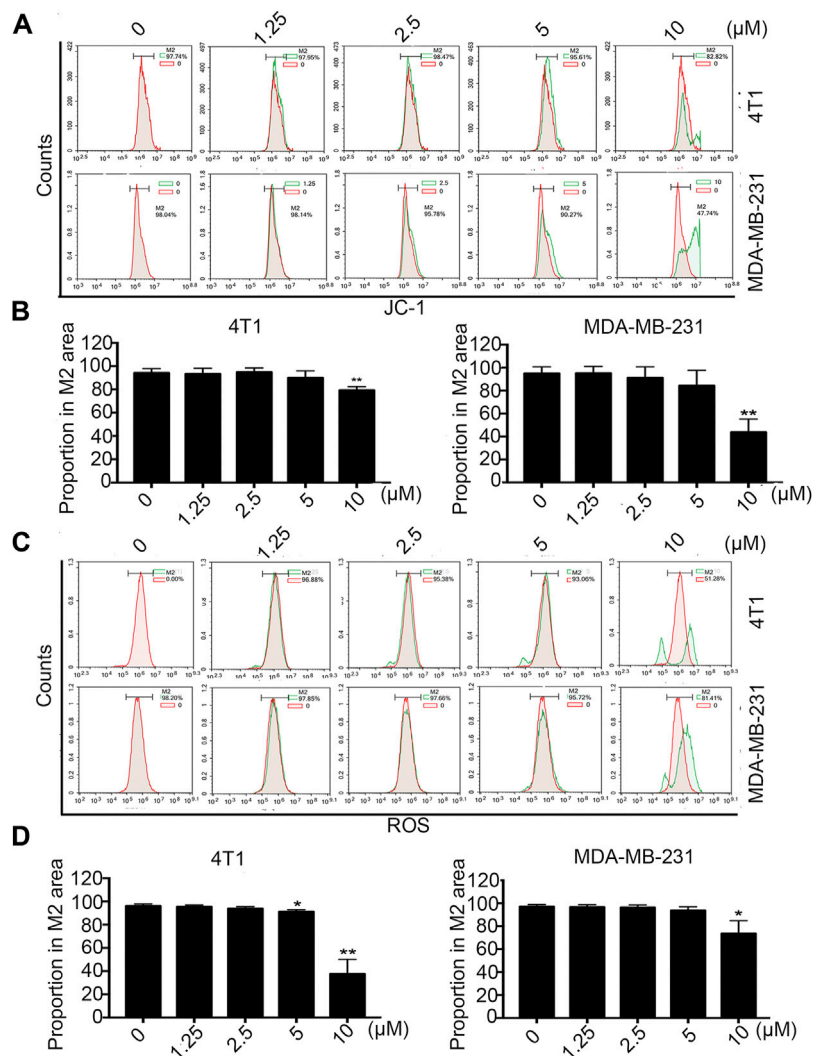


FIGURE 5 | The effect of Statmp-151 on mitochondrial $\Delta\Psi_m$ and ROS. **(A)** Statmp-151 decreased the mitochondrial membrane potential in 4T1 and MDA-MB-231 cells. **(B)** The mitochondrial $\Delta\Psi_m$ results were presented using quantified. **(C)** The levels of ROS were decreased after treatment with Statmp-151. The harvested 4T1 and MDA-MB-231 cells were measured by FCM. **(D)** The ROS data is presented in a histogram. Data are present as mean \pm SD for at least three independent experiments (* $p < 0.05$, ** $p < 0.01$ and *** $p < 0.001$ vs. control group).

apoptosis, mitochondrial membrane permeability increases, stromal calcium outflow and mitochondrial membrane rupture occur, and apoptotic induction factor (AIF) and cytochrome C are released, thus initiating a cascade reaction to activate the caspase family and ultimately induce apoptosis (Reed, 1997). Mitochondrial membrane potential and intracellular ROS level jointly have a marker effect on the growth and development of cancer cells. When the mitochondrial membrane potential changes or the ROS level changes, it often indicates the loss of homeostasis of cancer cells. Once a compound has an inhibitory effect on cancer cells, these two indicators usually change (Zhao et al., 2016; Burke, 2017).

According to this knowledge, we detected the changes in mitochondrial membrane potential ($\Delta\Psi_m$) by FCM after treatment with different concentrations of Statmp-151 in

breast cancer cells. As shown in **Figure 5A,B**, treatment with 10 μM Statmp-151 led to a 17.28% loss of $\Delta\Psi_m$ for 4T1 cells. The loss was 52.26% in MDA-MB-231 cells under the same conditions.

Tumor cells are often in an environment with a high level of reactive oxygen species (ROS), and intracellular ROS levels are closely related to the stability of the mitochondrial membrane potential (Li et al., 2011). The effect of Statmp-151 on membrane potential was identified in previous experiments, and the ligustrazine structure of Statmp-151 has been reported to reduce intracellular reactive oxygen species (Zhang et al., 2010). In view of this, we also determined the effect of Statmp-151 on ROS by FCM using DCFH-DA. The results indicated that Statmp-151 led to increased ROS levels in a dose-dependent manner. As shown in **Figure 5C,D**, the results showed that after 24 h of treatment with 10 μM Statmp-151

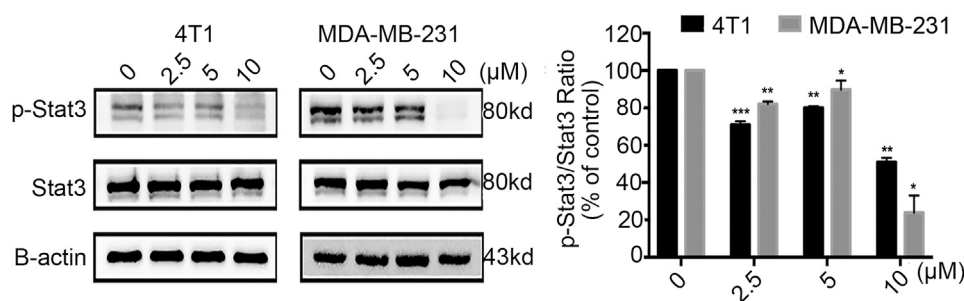


FIGURE 6 | Statmp-151 inhibited phosphorylation of Stat3. The cells treated with Statmp-151 for 24 h were used, and the expression levels of Stat3 and p-Stat3^{Tyr705} were measured by western blotting and the protein expression was quantified.

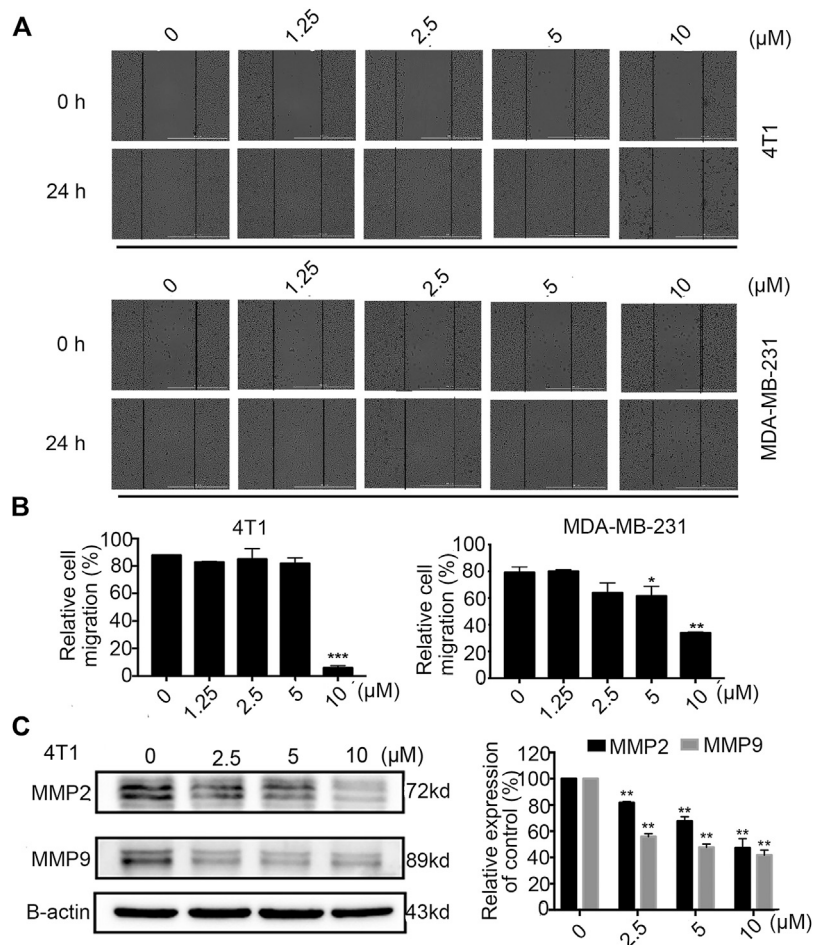


FIGURE 7 | Statmp-151 inhibited cell migration of 4T1 and MDA-MB-231 cells. **(A)** The images were taken after treating with Statmp-151 for 0 and 24 h with the lines indicating the area occupied by the initial scraping. **(B)** The migrated cells were quantified in a histogram. **(C)** The cells treated with Statmp-151 for 24 h were harvested, and the expression levels of MMP-2 and MMP-9 were measured by western blotting and quantified.

in 4T1 and MDA-MB-231 cells, ROS levels were 18.89 and 48.72%, respectively. These results confirmed that Statmp-151 induced cell apoptosis *via* the mitochondrial-mediated apoptotic pathway.

Statmp-151 Inhibited Stat3 Phosphorylation
Phosphorylation by Jak kinase is a key step in the activation of Stat3 (Li et al., 2019); therefore, we detected whether Statmp-151 could influence the expression of p-Stat3. The results confirmed

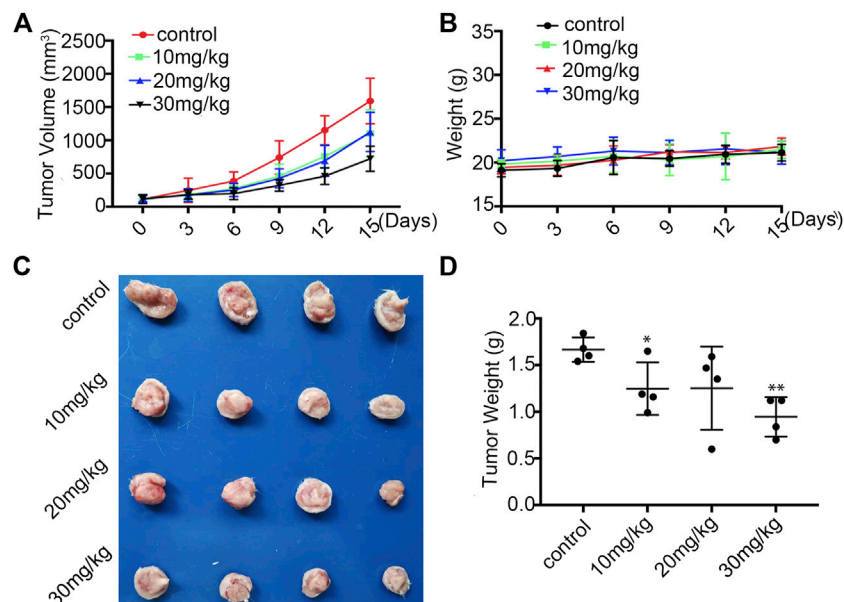


FIGURE 8 | Statmp-151 inhibited tumor growth *in vivo*. **(A)** In 4T1 mice model, the mice were treated with Statmp-151 (10, 20, and 30 mg/kg) or Control. Tumor volumes were measured every 3 days. **(B)** The body weight of 4T1 tumour mice was measured every 3 days. **(C)** Tumours from mice treated with indicated Statmp-151 on the final day (Day 15). **(D)** Tumors weight treated with Statmp-151 at the 15 days.

that Statmp-151 could decrease the expression of p-Stat3 but had no effect on total Stat3 in MDA-MB-231 and 4T1 cells **Figure 6**. The results implied that Statmp-151 inhibited the phosphorylation of Stat3 proteins, consistent with the original drug design.

Stamp-151 Inhibited the Migration of Breast Cancer Cells

Tumour cell migration is one of the committed steps in cancer metastasis (Li et al., 2016). We conducted wound healing assays on 4T1 and MDA-MB-231 cells to explore the therapeutic potential of Statmp-151. As shown in **Figure 7A,B**, the results indicated that Statmp-151 significantly inhibited the migration of both 4T1 and MDA-MB-231 cells in a concentration-dependent manner. The migration of these cells to the wound area was significantly inhibited after incubation with Statmp-151 for 24 h at 10 μ M.

To further verify the mechanism of the antimigratory effects of Statmp-151, we determined the MMP-9 and MMP-2 levels by western blotting. The results suggested that Statmp-151 could significantly inhibit the expression levels of MMP-2 and MMP-9 in 4T1 cells **Figure 7C**. These results suggested that Statmp-151 possessed a potent ability to inhibit breast cancer cell migration.

In Vivo Anti-breast Cancer Activity of Statmp-151

To evaluate the anti-tumour efficacy of Statmp-151 *in vivo* (Yang et al., 2015), we established a 4T1 tumour-bearing mouse model. The mice were administered Statmp-151 daily at doses of 10, 20

and 30 mg/kg for 15 days (Heppner et al., 2000; Zeng et al., 2020). There was a significant reduction in tumour growth, while the body weight of mice had no significant changes (**Figure 8A,B**). On the final day, there were significant reductions in tumor size and tumour weight compared with the control group (**Figure 8C,D**). These results suggested that Statmp-151 had potent anti-tumour activity *in vivo*.

As mentioned above, the body weights of the mice were not significantly changed. To further evaluate the safety of Statmp-151, we determined the serum biochemical indexes and weights of the heart, liver, spleen, lung and kidney. Paraffin sections of the lung, liver, spleen, heart and kidney were stained with haematoxylin and eosin. As shown in **Figure 9A,B**, there were no obvious differences in organ weight or serum biochemical indexes. Furthermore, no pathologic changes were observed in the lung, liver, spleen, heart or kidney compared with those in the control group **Figure 9C**. Therefore, Statmp-151 was considered to be a relatively safe small molecule compound.

DISCUSSION

Breast cancer is the most common malignancy in females and is a heterogeneous disease at the molecular level (Harbeck et al., 2019). Accumulating evidence has shown that Stat3 signalling is involved in breast cancer initiation and progression. Inhibition of the activity of Stat3 has become a popular therapeutic strategy (Zhang et al., 2010; Li et al., 2011; Alshaer et al., 2019; Xie et al., 2019). Therefore, the aim of this study was to explore the mechanisms of a novel small molecule inhibitor, Statmp-151,

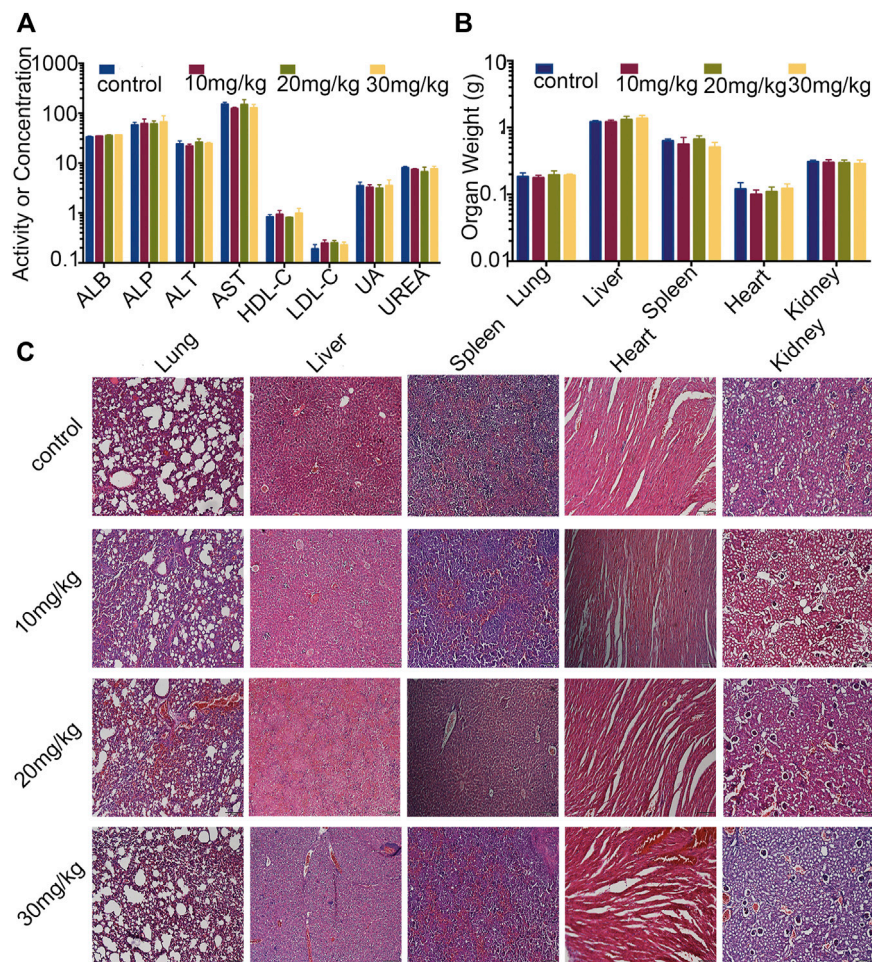


FIGURE 9 | Evaluation of side effects of Statmp-151 in mice. **(A)** Blood biochemical indexes of mice (ALB, ASP unite is g/L, ALT, AST unite is U/L, HDL-C, LDL-C, UREA unite is mmol/L, UA unite is mg/dl). **(B)** The weight of lung, liver, spleen, heart, and kidney. **(C)** Haematoxylin and eosin stained of paraffin sections of lung, liver, spleen, heart and kidney of mice treated with Statmp-151.

in breast cancer cells and provide support for the treatment of breast cancer.

Stattic is one of the classic inhibitors of Stat3 but is limited by low activity, low selectivity and high toxicity (Zhang et al., 2010). Ligustrazine is an alkaloid found in nature whose structure is simple and easy to modify (Alshaer et al., 2019; Xie et al., 2019). Ligustrazine has good pharmacokinetic properties, fast absorption, broad distribution and no cumulative toxicity (Cheng et al., 2007; Wu et al., 2013; Zeng et al., 2013; Han et al., 2015). In this study, we synthesized a new compound, Statmp-151, by combining ligustrazine and Stattic with the aid of virtual screening and rational drug design.

First, we evaluated the anti-tumour activity of Statmp-151 *in vitro* by MTT assays and colony formation assays. In both tests, Statmp-151 inhibited the proliferation of 4T1, MDA-MB-231, and MCF-7 breast cancer cells in a dose-dependent manner. Then, we verified the apoptosis-inducing effect of Stamp-151 on tumour cells. Our results showed that Stamp-151 induced mitochondrial membrane potential loss and reduced Bcl-2 expression. The steady state of ROS is correlated with the

stability of the membrane potential. In view of this, we found that Statmp-151 significantly changed the ROS levels, suggesting that the effect of Statmp-151 on inducing apoptosis was related to changes in ROS levels and mitochondrial membrane potential. Furthermore, we found that Statmp-151 has an anti-tumour effect by inhibiting the phosphorylation of Stat3. Next, we evaluated the effect of Stamp-151 on the migration of breast cancer cells. Wound-healing migration assays confirmed that Statmp-151 could significantly inhibit cell migration. MMP2 and MMP9 are considered to be transport-related proteins, and protein analysis of 4T1 cells showed significant inhibition of MMP2 and MMP9 protein expressions. Our experiments confirmed that Statmp-151 significantly inhibited tumour growth, and there was no significant change in body weight, organ weight, serum biochemistry or haematoxylin-eosin staining in mice, suggesting that Statmp-151 may have no toxic effects *in vivo*.

In summary, Statmp-151 is a small molecule compound that was confirmed to inhibit the growth of breast cancer cells *in vitro* and *in vivo* by blocking Stat3 activation in this study. Based on

our preliminary investigations on the various pharmacological properties of Statmp-151, it has good anti-tumour activity and is relatively safe. Additionally, Statmp-151 can undergo continued chemical optimization and pharmacological exploration. Therefore, Statmp-151 is worthy of continued development and is a drug candidate for the treatment of breast cancer.

DATA AVAILABILITY STATEMENT

The raw data supporting the conclusions of this article will be made available by the authors, without undue reservation.

ETHICS STATEMENT

The animal study was reviewed and approved by the Committee on the Ethics of Animal Experiments of Sichuan University.

REFERENCES

- Alshaer, W., Alqudah, D. A., Wehaibi, S., Abuarqoub, D., Zihlif, M., Hatmal, M. M., et al. (2019). Downregulation of STAT3, β -catenin, and notch-1 by single and combinations of siRNA treatment enhance chemosensitivity of wild type and doxorubicin resistant MCF7 breast cancer cells to doxorubicin. *Int J Mol Sci.* 20 (15), 3696. doi:10.3390/ijms20153696
- Burke, P. J. (2017). Mitochondria, bioenergetics and apoptosis in cancer. *Trends Cancer* 3 (12), 857–870. doi:10.1016/j.trecan.2017.10.006
- Chen, H., Yang, Z., Ding, C., Chu, L., Zhang, Y., Terry, K., et al. (2013). Fragment-based drug design and identification of HJC0123, a novel orally bioavailable STAT3 inhibitor for cancer therapy. *Eur. J. Med. Chem.* 62, 498–507. doi:10.1016/j.ejmech.2013.01.023
- Cheng, X., Zhang, L. J., Sun, L., and Du, G. (2007). Neuroprotective effects of tetramethylpyrazine on hydrogen peroxide-induced apoptosis in PC12 cells. *Cel Biol. Int.* 31 (5), 438–443. doi:10.1016/j.cellbi.2006.10.001
- Federica, L., Fabio, C., Giovanni, M., and Carmine, S. (2018). STAT3 Interactors as potential therapeutic targets for cancer treatment. *Int. J. Mol. Sci.* 19 (6), 1787. doi:10.3390/ijms19061787
- Furtek, S. L., Backos, D. S., Matheson, C. J., and Reigan, P. (2016). Strategies and approaches of targeting STAT3 for cancer treatment. *ACS Chem. Biol.* 11 (2), 308–318. doi:10.1021/acscchembio.5b00945
- Han, J., Song, J., Li, X., Zhu, M., Guo, W., Xing, W., et al. (2015). Ligustrazine suppresses the growth of HRPC cells through the inhibition of cap-dependent translation via both the mTOR and the MEK/ERK pathways. *Anticancer Agents Med Chem.* 15 (6), 764–772. doi:10.2174/1871520615666150305112120
- Harbeck, N., Penault-Llorca, F., Cortes, J., Gnant, M., Houssami, N., Poortmans, P., et al. (2019). Breast cancer. *Nat. Rev. Dis. Primers.* 5 (1), 66. doi:10.1038/s41572-019-0111-2
- Heppner, G. H., Miller, F. R., and Shekhar, P. M. (2000). Nontransgenic models of breast cancer. *Breast Cancer Res.* 2 (5), 331–334. doi:10.1186/bcr77
- Ji, P., Xu, X., Ma, S., Fan, J., Zhou, Q., Mao, X., et al. (2015). Novel 2-carbonylbenzo [b]thiophene 1,1-dioxide derivatives as potent inhibitors of STAT3 signaling pathway. *ACS Med. Chem. Lett.* 6 (9), 1010–1014. doi:10.1021/acsmchemlett.5b00228
- Li, S., Chen, H., Wang, X., Wu, J., Jiang, J., and Wang, Y. (2011). Pharmacokinetic study of a novel stroke therapeutic, 2-[[[(1,1-dimethylethyl)oxidoimino]methyl]-3,5,6-trimethylpyrazine, by a simple HPLC-UV method in rats. *Eur. J. Drug Metab. Pharmacokinet.* 36 (2), 95–101. doi:10.1007/s13318-011-0032-2
- Li, Y., Gan, C., Zhang, Y., Yu, Y., Fan, C., Deng, Y., et al. (2019). Inhibition of Stat3 signaling pathway by natural product pectolinarigenin attenuates breast cancer metastasis. *Front. Pharmacol.* 10, 1195. doi:10.3389/fphar.2019.01195

AUTHOR CONTRIBUTIONS

CF, YW, HH, WL, JM, DY, ZT, and TX: Experiment and Data analysis. LH and YR: Data analysis. YZ, QW, and YX: Writing. YL, RT, and JG: Conception, design, data analysis and writing. All authors contributed to the article and approved the submitted version.

FUNDING

This work was supported by the International Cooperation Project of Science and Technology Department of Sichuan Province (2019YFH0119, 2021YFH0173), Chengdu Science and Technology Bureau International Cooperation Project (No. 2019-GH02-00036-HZ).

- Li, Y., Yang, F., Zheng, W., Hu, M., Wang, J., Ma, S., et al. (2016). Punica granatum (pomegranate) leaves extract induces apoptosis through mitochondrial intrinsic pathway and inhibits migration and invasion in non-small cell lung cancer *in vitro*. *Biomed. Pharmacother.* 80, 227–235. doi:10.1016/j.biopha.2016.03.023
- Liu, Z., Ge, X., Gu, Y., Huang, Y., and Liu, Y. (2019). Small molecule STAT3 inhibitor, 6Br-6a suppresses breast cancer growth *in vitro* and *in vivo*. *Biom Pharmacother.* 121, 109502. doi:10.1016/j.biopha.2019.109502
- Lu, Y., and Liu, W. (2020). Selective estrogen receptor degraders (SERDs): a promising strategy for estrogen receptor positive endocrine-resistant breast cancer. *J. Med. Chem.* 63 (24), 15094–15114. doi:10.1021/acs.jmedchem.0c00913
- Pan, J., Shang, J. F., Jiang, G. Q., and Yang, Z. X. (2015). Ligustrazine induces apoptosis of breast cancer cells *in vitro* and *in vivo*. *J. Cancer Res. Ther.* 11 (2), 454–458. doi:10.4103/0973-1482.147378
- Reed, J. C. (1997). Cytochrome c: can't live with it-can't live without it. *Cell.* 91 (5), 559–562. doi:10.1016/s0092-8674(00)80442-0
- Schust, J., Sperl, B., Hollis, A., Mayer, T. U., and Berg, T. (2006). Stattic: a small-molecule inhibitor of STAT3 activation and dimerization. *Chem. Biol.* 13 (11), 1235–1242. doi:10.1016/j.chembiol.2006.09.018
- Sharma, P. (2018). Update on the treatment of early-stage. Triple-negative breast cancer. *Curr. Treat. Options. Oncol.* 19 (5), 22. doi:10.1007/s11864-018-0539-8
- Shen, J., Zeng, L., Pan, L., Yuan, S., Wu, M., and Kong, X. (2018). Tetramethylpyrazine regulates breast cancer cell viability, migration, invasion and apoptosis by affecting the activity of Akt and caspase-3. *Oncol. Lett.* 15(4): 4557–4563. doi:10.3892/ol.2018.7851
- Waks, A. G., and Winer, E. P. (2019). Breast cancer treatment. *JAMA* 321 (3), 288–300. doi:10.1001/jama.2018.19323
- Wu, W., Yu, X., Luo, X.-P., Yang, S.-H., and Zheng, D. (2013). Tetramethylpyrazine protects against scopolamine-induced memory impairments in rats by reversing the cAMP/PKA/CREB pathway. *Behav. Brain Res.* 253 (18), 212–216. doi:10.1016/j.bbr.2013.07.052
- Xie, Q., Yang, Z., Huang, X., Zhang, Z., and Ma, J. (2019). Ilamycin C induces apoptosis and inhibits migration and invasion in triple-negative breast cancer by suppressing IL-6/STAT3 pathway. *J. Hematol. Oncol.* 12(1), 60. doi:10.1186/s13045-019-0744-310.1186/s13045-019-0744-3
- Yang, F., Hu, M., Lei, Q., Xia, Y., Zhu, Y., Song, X., et al. (2015). Nifuroxazide induces apoptosis and impairs pulmonary metastasis in breast cancer model. *Cell Death Dis.* 6 (3), e1701. doi:10.1038/cddis.2015.63
- Zeng, L., Li, W., and Chen, C. S. (2020). Breast cancer animal models and applications. *Zool Res.* 41 (5), 477–494. doi:10.24272/j.issn.2095-8137.2020.095
- Zeng, M., Pan, L., Qi, S., Cao, Y., Zhu, H., Guo, L., et al. (2013). Systematic review of recent advances in pharmacokinetics of four classical Chinese medicines used for the treatment of cerebrovascular disease. *Fitoterapia* 88, 50–75. doi:10.1016/j.fitote.2013.04.006

- Zhang, X., Yue, P., Fletcher, S., Zhao, W., Gunning, P. T., and Turkson, J. (2010). A novel small-molecule disrupts Stat3 SH2 domain-phosphotyrosine interactions and Stat3-dependent tumor processes. *Biochem. Pharmacol.* 79 (10), 1398–1409. doi:10.1016/j.bcp.2010.01.001
- Zhao, Y., Liu, Y., and Chen, K. (2016). Mechanisms and clinical application of tetramethylpyrazine (an interesting natural compound isolated from *ligusticum wallichii*): current status and perspective. *Oxidative Med. Cell Longevity*. 2016, 1. doi:10.1155/2016/2124638
- Zhu, Y., Wei, W., Ye, T., Liu, Z., Liu, L., Luo, Y., et al. (2016). Small molecule TH-39 potentially targets Hec1/Nek2 interaction and exhibits antitumor efficacy in K562 cells via G0/G1 cell cycle arrest and apoptosis induction. *Cell Physiol Biochem* 40 (1-2), 297–308. doi:10.1159/000452546

Conflict of Interest: The authors declare that the research was conducted in the absence of any commercial or financial relationships that could be construed as a potential conflict of interest.

Copyright © 2021 Fan, Wang, Huang, Li, Ma, Yao, Tang, Xue, Ha, Ren, Zhang, Wang, Xie, Luo, Tan and Gu. This is an open-access article distributed under the terms of the Creative Commons Attribution License (CC BY). The use, distribution or reproduction in other forums is permitted, provided the original author(s) and the copyright owner(s) are credited and that the original publication in this journal is cited, in accordance with accepted academic practice. No use, distribution or reproduction is permitted which does not comply with these terms.



Molecular Targeted Agent and Immune Checkpoint Inhibitor Co-Loaded Thermosensitive Hydrogel for Synergistic Therapy of Rectal Cancer

Huaiyu Zhang, Jiayu Zhang, Yilun Liu, Yang Jiang* and Zhongmin Li*

Department of Gastrointestinal Colorectal and Anal Surgery, China-Japan Union Hospital of Jilin University, Changchun, China

OPEN ACCESS

Edited by:

Sanjun Shi,
Chengdu University of Traditional
Chinese Medicine, China

Reviewed by:

Zhiyu Zhang,
Fourth Affiliated Hospital of China
Medical University, China
Ning Wei,
University of Pittsburgh, United States

*Correspondence:

Yang Jiang
jiangyang@jlu.edu.cn
Zhongmin Li
lizhongmin1211@jlu.edu.cn

Specialty section:

This article was submitted to
Pharmacology of Anti-Cancer Drugs,
a section of the journal
Frontiers in Pharmacology

Received: 24 February 2021

Accepted: 26 March 2021

Published: 16 April 2021

Citation:

Zhang H, Zhang J, Liu Y, Jiang Y and
Li Z (2021) Molecular Targeted Agent
and Immune Checkpoint Inhibitor Co-
Loaded Thermosensitive Hydrogel for
Synergistic Therapy of Rectal Cancer.
Front. Pharmacol. 12:671611.
doi: 10.3389/fphar.2021.671611

Molecular targeted therapy has been proved effective in treatment of rectal cancer. Up-regulated expression of programmed death ligand-1 (PD-L1) was observed after the management of molecular targeted therapy, which made the therapeutic effect discounted. Tumors with higher PD-L1 expression were more sensitive and responsive to treatment of PD-L1 inhibitor. Therefore, the combination of molecular targeted therapy and immune checkpoint blockade makes sense. In this study, the copolymers of poly (ethylene glycol)-block-poly (L-leucine) (PEG-PLLeu) were synthesized as a thermosensitive hydrogel composite for consecutive release of regorafenib (REG) and BMS202. The mechanical properties of PEG-PLLeu were investigated, confirming that PEG-PLLeu (5 wt.%) was suitable for *in situ* injection as drug-delivery composite at low temperature and stable after sol-gel transition at body temperature. Importantly, the double drug loaded hydrogel showed superior antitumor activity over single drugs in an orthotopic rectal cancer model (CT26-Luc). Further analysis of the tumor tissues suggested that REG upregulated the expression of PD-L1 in tumor tissues. In addition, the immunosuppressive tumor microenvironment of CT26-Luc tumor was distinctly relieved under the effect of BMS202, as characterized by increased infiltration of CD8⁺ T cells in tumors and enhanced secretion of antitumor cytokines (IFN- γ and TNF- α). Moreover, the drug-loaded composite showed no obvious toxicity in histological analysis. Taken together, the administration of REG and BMS202 in the PEG-PLLeu composite could induce a synergistic effect in *in situ* treatment of rectal cancer without obvious toxicity, and thus represented a potential strategy for enhanced *in situ* therapeutic modality.

Keywords: molecular targeted therapy, immunotherapy, immune checkpoint blockade, thermosensitive hydrogel, cancer treatment, rectal cancer

INTRODUCTION

Globally, rectal cancer is a common malignant tumor with high morbidity and mortality (Bray et al., 2018). So far, surgery remains preferred for therapy in cases of rectal cancer. Besides, chemotherapy and radiotherapy are also the most common methods of cancer treatment including rectal cancer. These adjuvant therapies reduce local recurrence around the tumor bed and suppress distant

metastasis after surgical resection. In recent years, preoperative chemoradiotherapy for patients with locally advanced rectal cancer is also an alternative to improve surgical resection rate and sphincter preservation rate (Weiser et al., 2009; Sauer et al., 2012); however, when a rectal tumor deteriorates after conventional treatment, molecular targeted therapy and checkpoint blockade immunotherapy are preeminent candidates for interdicting tumor advancement (Tokumaru et al., 2019; Jung et al., 2020).

Normally, molecular targeted agents mainly take effect in two ways: 1) Monoclonal antibodies competitively bind the ligands involved in tumor angiogenesis or the paired receptors in tumor microenvironment (TME), such as vascular endothelial growth factor (VEGF) and vascular endothelial growth factor receptor (VEGFR), and then interrupt their integration and signal transduction (Hurwitz et al., 2004); 2) Kinase inhibitors interdict the phosphorylation and signal transduction downwards (Wilhelm et al., 2011; Jang et al., 2019). Regorafenib (REG) is a type of multi-kinase inhibitor and has been approved in treatment of advanced colorectal cancer (Skarderud et al., 2018). A primary function of REG is that it blocks the phosphorylation of VEGFR-2 after binding with VEGF in TME, and then influences tumour-induced pathologic angiogenesis (Wilhelm et al., 2011). Once uncontrolled angiogenesis is ceased, the abnormal blood vessels in TME tend to be normalized to cope with sufficient oxygen supply, increased migration of antitumour immune cells, and enhanced penetration of antitumour agents into the tumor which contributed to the suppression thereof; however, it was found that molecular targeted therapy boosted upregulation of programmed death ligand-1 (PD-L1) in tumor tissues (Liu et al., 2015). This immune accommodation of a tumor may hamper the molecular targeted agent-based antitumour efficiency. Therefore, how to counteract immunosuppression involved with PD-L1 up-regulation is key to improving therapeutic responses of molecular targeted therapy. Those types of tumor with higher PD-L1 expression were more sensitive and responsive to treatment of PD-L1 inhibitor (Ribas and Tumei, 2014; Patel and Kurzrock, 2015). Therefore, the combination of molecular targeted therapy and checkpoint blockade immunotherapy makes sense.

Checkpoint blockade immunotherapy is a burgeoning strategy for cancer solution which targets the T-cell co-inhibitory signaling pathways (Song et al., 2018). Nowadays, several monoclonal antibodies have been approved for immune checkpoint blockade, such as nivolumab (Halmos et al., 2020), pembrolizumab (Halmos et al., 2020), avelumab (Verschraegen et al., 2020), etc. The monoclonal antibodies competitively bind and block PD-1 on T-cells or PD-L1 on tumor cells. This checkpoint blockade immunotherapy neutralizes incapacitation of T cells triggered by pairing of PD-1/PD-L1 and promotes antitumour immunity of tumor infiltrating lymphocytes (TILs). Apart from monoclonal antibodies, small-molecule compounds have also been investigated for use in checkpoint blockade immunotherapy (Bailly and Vergoten, 2020). Compared with anti-PD-1/PD-L1 monoclonal antibodies, the chemical constructions of small-molecule drugs are more stable, which

guarantees that they are easy to store. In addition, the cost and selling price of small-molecule drugs is normally low. As a result of that, more patients can be treated with small-molecule anticancer drugs. BMS202 is a type of PD-L1 inhibitor which propels aggregation of PD-L1 on tumor cells into the dimer structure (Zak et al., 2017; Bailly and Vergoten, 2020). This hinders the integration between PD-1 and PD-L1 which shields immunosuppressive signals from tumor cells and enhances recognition and killing from TILs. In this way, BMS202 counteracts immunosuppression triggered by PD-L1 upregulation and promotes antitumour immune responses, thus may boost therapeutic responses of molecular targeted agents.

To address this, we constructed an orthotopic rectal cancer model, and proved that BMS202 would boost tumor responses to treatment of REG. To reduce anticancer drug-associated side-effects and improve treatment efficacy, various polymer-based carriers have been designed by researchers and employed in drug delivery (Ding et al., 2019a; Ding et al., 2019b; Sun et al., 2019; Zheng et al., 2020; Ma et al., 2021). In addition to the popular nanoparticle-based drug carriers (Wang et al., 2018; Chen et al., 2020; Feng et al., 2020; Jiang et al., 2020; Zhang et al., 2020), hydrogels were also designed and optimized in drug delivery nowadays (Guo et al., 2020). In this study, we designed an injectable thermosensitive hydrogel and performed peritumoral injection of the antitumour-agent-loaded hydrogel. Various amino acids are essential nutrients for the body's metabolism. Therefore, the hydrogel prepared from amino acids as raw materials not only has obvious advantages in biocompatibility, but also can be degraded into neutral products under the action of various proteases in the body. Besides, this process does not produce acidic metabolism to change the pH value of microenvironment at tumor site, which is very important for the treatment of tumors. The L-leucine based thermosensitive hydrogel in this study exhibited superior biocompatibility and step-by-step degradation which avoided repeated administration of REG and BMS202. Moreover, the combination of REG and BMS202 resulted in coadjuvant antitumour activities with no obvious side-effects. We propose that the combination of locally applied molecular targeted therapy and checkpoint blockade immunotherapy may be meaningful as a therapy for rectal cancer.

MATERIALS AND METHODS

Materials

The amino-terminated poly (ethylene glycol) (mPEG₄₅-NH₂) was synthesized through the protocol described in our previous work (Chen et al., 2015). L-Leucine N-carboxyanhydride (L-Leu NCA) was obtained from Chengdu Enlai Biological Technology Co., Ltd. (Chengdu, China). Penicillin, streptomycin, trypsin-EDTA (0.05% trypsin and 0.02% EDTA) solution, RPMI 1640 medium, and new-born calf serum (NBCS) were bought from Gibco (Grand Island, NY, United States). Toluene, N,N-dimethylformamide (DMF; anhydrous), diethyl ether, elastase, and chymotrypsin were obtained from Aladdin Reagent Co., Ltd. (Shanghai, China). Hematoxylin and eosin (H&E) staining solution was

purchased from Sigma-Aldrich (Shanghai, China). BMS202 was purchased from Selleck Chemicals (United States). PD-L1 antibody and Phospho-VEGF Receptor 2 antibody used for western blot (WB) were purchased from eBioscience (San Diego, CA, United States). PE-cy7-anti-CD45, FITC-anti-CD3, PerCP-cy5.5-anti-CD4, and Pacific Blue-anti-CD8 used for flow cytometry were purchased from eBioscience (San Diego, CA, United States). Enzyme-linked immunosorbent assay (ELISA) kits were purchased from Shanghai Lengton Bioscience Co., Ltd. (Shanghai, China). All the other chemicals were purchased from Beijing Chemical Industry Group Co., Ltd. (China).

Preparation of Poly (Ethylene Glycol)-Block-Poly (α -Leucine) Copolymers

The PEG-PLLeu copolymers were prepared by the ring-opening polymerization (ROP) of α -Leu NCA initiated by mPEG₄₅-NH₂ (Ding et al., 2015; Liu et al., 2020). In brief, 2.0 g of mPEG₄₅-NH₂ was added into toluene and dewatered by azeotropic distillation. The anhydrous mPEG₄₅-NH₂ was dissolved in 45.0 ml of anhydrous DMF. After that, 2.78 g of α -Leu NCA was added and stirred with the solution. After reaction for 3 days at room temperature and under an N₂ atmosphere, the resulting solution was placed into 500 ml of diethyl ether by pre-freezing, and the precipitate was then collected. The collected precipitate was then dissolved in anhydrous DMF and dialyzed against water. The final products were obtained by lyophilisation.

Characterization of Poly (Ethylene Glycol)-Block-Poly (α -Leucine) Copolymers

The chemical structure of PEG-PLLeu copolymers was investigated by using proton nuclear magnetic resonance (¹H NMR) and Fourier-transform infrared (FT-IR) spectra as in our previous study (Ding et al., 2015). Typical ¹H NMR spectra of PEG-PLLeu copolymers dissolved in deuterated trifluoroacetic acid (TFA-*d*) were determined on a Bruker AV 400 NMR spectrometer (Ettlingen, Germany). According to the potassium bromide (KBr) method, FT-IR spectra of the PEG-PLLeu copolymers were detected on a Bio-Rad Win-IR instrument (Cambridge, MA, United States).

Phase Diagrams

The phase diagrams of the polymers were determined by a test tube inverting method. In brief, these polymers were dissolved in PBS with a concentration of 3–7 wt.% and stirred for 24 h on an ice bath. Next, 200.0 μ L of each sample with the given concentration was added to a 2-ml cylindrical vial and transferred into a thermostat at the pre-set temperature. The temperature rise was programmed to be 2°C per 10 min. The temperature corresponding to the sol–gel transition when that at which no liquid flow was noticed within 30 s after inverting the cylindrical vial.

Rheological Analyses

Dynamic mechanical characteristics of the PEG-PLLeu copolymers were investigated by rheological analyses on an

MCR 301 Rheometer (Anton Paar, GmbH, Germany). The pre-set temperature interval was between 5 and 60°C, and the temperature was increased at 0.5°C/min. Samples dissolved in PBS (350.0 μ L) were titrated onto a 25.0 mm sample-maintained plate with a gap of 0.5 mm between the plates, and maintained for 5 min before structural recovery. Meanwhile, a thin layer of silicone oil was dropwise dripped onto the edge of the samples for evaporation limitation. The final data pertaining to storage modulus (G') and loss modulus (G'') were collected under a strain and frequency of 1% and 1 rad s⁻¹.

Scanning Electron Microscopy

The morphology of PEG-PLLeu copolymers was identified by SEM examination which was performed on a Philips XL30 instrument (Eindhoven, Netherlands). In brief, the PEG-PLLeu copolymers were dissolved in phosphate-buffered saline (PBS) and stirred for 24 h on an ice bath. Thereafter, the samples were placed in a thermostatically controlled water bath for 10 min at the pre-set temperature of 37°C to allow gel formation. Then, the samples were frozen in liquid nitrogen for 30 s before lyophilization under vacuum. Finally, the cross sections of lyophilized samples were investigated by SEM under an acceleration voltage of 10 kV.

In Vitro Degradation

Briefly, the PEG-PLLeu polymers were premixed in PBS (5 wt.%) and stirred for 24 h on an ice bath. After that, 0.5 ml of the copolymer solution was added to each 3-ml tube whose masses were recorded beforehand. The solution was then located into a thermostat for 12 min with the pre-set temperature of 37°C for gel formation. The mass of the gel loaded tube was recorded again. Then, 2.0 ml of PBS with or without elastase or chymotrypsin was dripped to the surface of the gel, and the glass tube was transferred into a shaking incubator at 37°C and 70 rpm. The supernatant was removed every day before accurately weighing the gel-loaded tube. After that, an equal dosage of fresh solution was supplemented for the next measurement. The mass loss of the PEG-PLLeu gel was monitored for 30 days, and the data were used to analyze the degradation.

Cell Line and Animal Model Establishment

CT26-Luc cell line stably expressing luciferase was purchased from Golden Tran Co., Ltd. (Changchun, China). Four-week-old female BALB/c mice (18–20 g) were obtained from Vital River Laboratory Animal Center (Beijing, China). Animals used in this study were fed and handled following the guidelines of the Institutional Animal Care and Use Committee of Jilin University. For establishment of the orthotopic rectal tumor model, mice were subjected to fasting for 12 h and anesthetized using 2% pentobarbital sodium. The mice were bodily fixed in a supine position. The anal tube was exposed by hook tweezers. CT26-Luc cells (1×10^5 cells in 50 μ L of PBS) were submucosally injected into the posterior wall of the rectum with an insulin-gauge syringe. The puncture site was approximately 2 mm proximal to the anal edge. Light pressure was exerted at the puncture site to avoid leakage of the cell suspensions. Tumor formation and burden were monitored

through bioluminescent detection using BRUKER Xtreme II. Under anesthesia, the bioluminescent detection was conducted 10 min after intraperitoneal (i.p.) injection of 100 μ L solution of D-luciferin (10 mg mL^{-1}) (Song et al., 2018).

In Vivo Antitumour Assay

Two weeks after inoculation of CT26-Luc cells, the tumour-bearing mice were subjected to the first detection of bioluminescence, and randomly allocated into different treatment groups ($n = 5$). The PEG-PLLeu copolymers were then prepared into injectable gel with or without antitumour agents and maintained in an ice bath. After that, CT26-Luc tumour-bearing mice were given an *in situ* pericarcinomatous injection of 100 μ L PBS, Gel, Gel/REG, Gel/BMS, and Gel/(BMS + REG) c. CT26-Luc tumor burdens were monitored through bioluminescent detection using BRUKER Xtreme II every 5 days. The enlargement of tumor burdens was calculated as bioluminescent intensities over the initial values thereof. Tumor suppression rate (TSR %) = $(I_c - I_x)/I_c \times 100\%$, where I_c represents the bioluminescent intensity of the PBS group, and I_x denotes the bioluminescent intensity of other treatment groups. The body mass of all groups was recorded every other day. Mice in different groups were sacrificed at the given time points. Tumors were obtained for immunohistochemistry staining, flow cytometry analysis, ELISA, and WB assay. Spleens and sentinel lymph nodes were obtained for flow cytometry analysis. Major organs (heart, liver, spleen, lung, and kidney) were obtained for H&E staining.

Histopathological and Immunohistochemistry Analyses

The mice were sacrificed the next day after the last bioluminescent detection. After collection of the tumor tissues or organs, the samples were immersed into 4% (W/V) PBS-buffered paraformaldehyde for 12 h and embedded in paraffin. Then the paraffin-embedded samples were sliced for further H&E staining and immunohistochemistry analyses (Ki-67 and caspase-3). The H&E staining and immunohistochemistry results were investigated using a microscope (Nikon Eclipse Ti, Optical Apparatus Co., Ardmore, PA, United States).

Flow Cytometry Assay

Briefly, tissues of tumor, sentinel lymph nodes, and spleen were harvested and digested with lysate buffer (collagenase A and dnaase) at 37°C for 40 min. After the digestion of ACK buffer, lysis of red blood cells was completed, then, the remaining cells were obtained and fabricated into single-cell suspensions. After staining with fluorescence conjugated antibodies, disparate cells in single-cell suspensions were fixed with 4% PFA and quantitatively analyzed via fluorescent-activated cell sorting (FACS).

Western Blot Analysis

Tumor tissues of different groups were collected after sacrificing the mice. The samples were then prepared and lyzed to obtain the whole protein. After centrifugation, quantification, and boiling for 10 min, samples were loaded onto 12% SDS-PAGE gel and

electrophoretically transferred to PVDF membranes. The membranes were then blocked with 5% (W/V) bovine serum albumin in Tris-buffered saline plus 0.1% Tween 20. After incubating with primary antibody on a shaker at 4°C overnight, the membranes were washed, incubated for 1 h with a secondary antibody. Finally, after washing to remove superfluous antibodies, the proteins then detected were visualized (GAPDH was utilized as an internal reference).

Enzyme-Linked Immunosorbent Assay Detection

Cytokine analysis including IFN- γ and TNF- α was performed using the corresponding ELISA kits (Shanghai Lengton Bioscience Co., Ltd., Shanghai, China) according to the standard protocols provided by the manufacturer.

Statistical Analyses

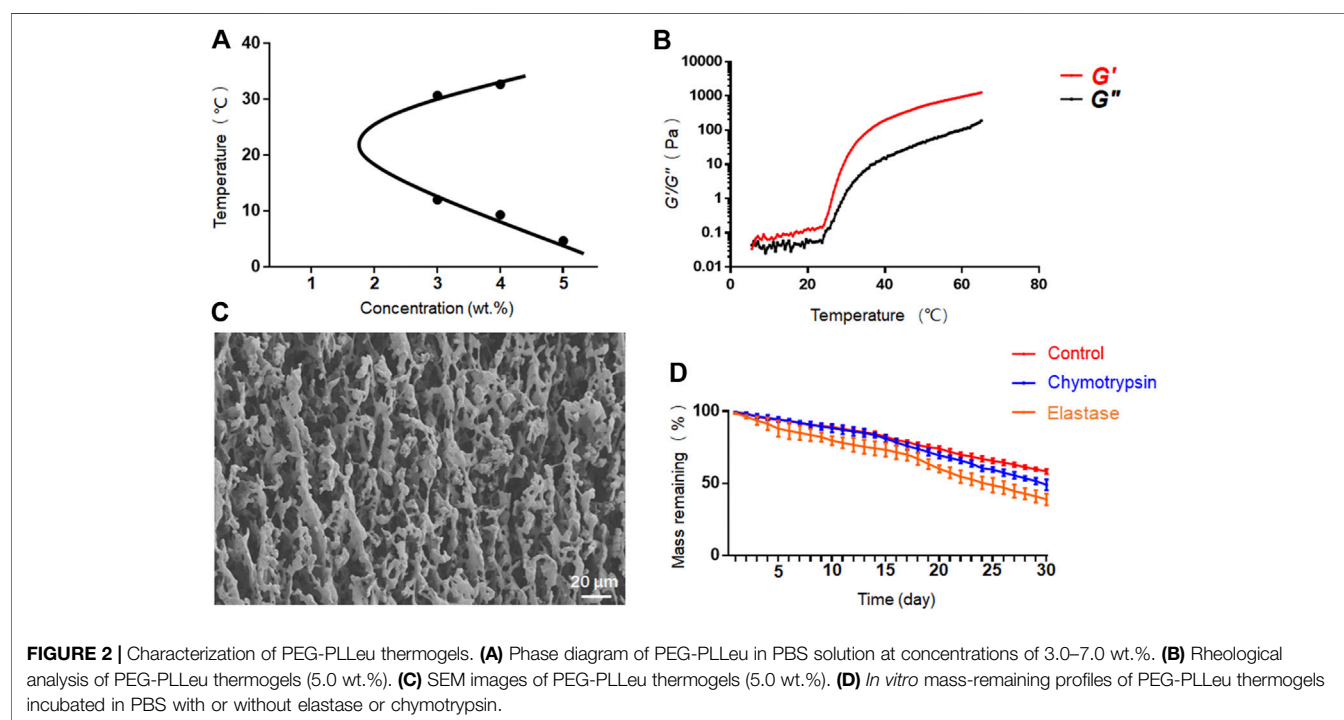
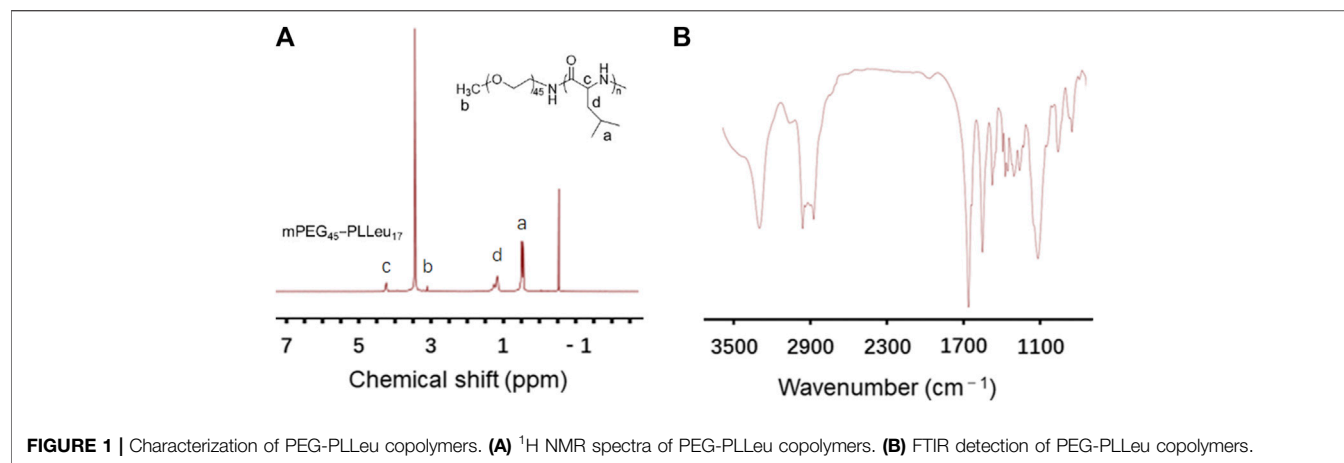
Data analyzed in this manuscript are presented as means \pm standard deviations. Differences between each group were determined by Student's t-test with SPSS 17.0 (SPSS Inc., Chicago, IL, United States). Statistical significance was defined as $*p < 0.05$, and $**p < 0.01$ and $***p < 0.001$ were regarded as highly significant.

RESULTS AND DISCUSSION

Preparation and Characterization of Poly (Ethylene Glycol)-Block-Poly (L -Leucine) Copolymers

The PEG-PLLeu copolymers in this study were prepared by ROP of L -Leu NCA initiated by mPEG₄₅-NH₂ as mentioned. ^1H NMR and FTIR detections were employed for analyzing the chemical structure of PEG-PLLeu. As shown in **Figure 1A**, all the peak signals of protons in PEG and polymerized L -Leu block were assigned in the ^1H NMR spectra, which illustrated the successful manufacture of PEG-PLLeu copolymers. The degrees of polymerization (DPs) of L -Leu units in PEG-PLLeu copolymer block were analyzed based on the integrated area assigned to the side methyl protons ($-\text{CH}_2\text{CH}(\text{CH}_3)_2$) and that assigned to the methylene proton in PEG: the calculated DPs value of L -Leu units in PEG-PLLeu copolymers was 17. As displayed in **Figure 1B**, the outcome of FTIR spectra also proved the successful generation of L -Leu blocks based on the appearance of the typical amide bands at $1,548\text{ cm}^{-1}$ ($\nu_{\text{C(O)-NH}}$) and $1,653\text{ cm}^{-1}$ ($\nu_{\text{C=O}}$).

We further investigated the phase diagram of PEG-PLLeu in PBS solution at concentrations of 3.0–7.0 wt.%. As shown in **Figure 2A**, phase transition appeared only at concentrations of 3.0–5.0 wt.%. The average sol-gel transition temperatures were 12.00/30.67°C at 3.0 wt.% and 9.33/32.67°C at 4.0 wt.%, suggesting that PEG-PLLeu at these concentrations would not gelatinize at body temperature. At the concentration of 5.0 wt.%, PEG-PLLeu copolymer gelatinized at 4.67°C and was stable as the temperature increased. Herein, 5.0 wt.% PEG-PLLeu was suitable for *in situ* injection as drug container when manipulation at low



temperature was guaranteed. This screened concentration (5.0 wt.%) was chosen for all further characterisations.

Rheological analysis of PEG-PLLeu was then conducted in which G' referred to the stiffness of PEG-PLLeu and G'' represented its viscosity. As shown in **Figure 2B**, the value of G'' exceeded G' below 6°C , and then G' exceeded G'' as the temperature increased, implying the gelation of PEG-PLLeu. This outcome was consistent with that inference drawn from the phase diagram. Besides, the maximum G' value of PEG-PLLeu hydrogel exceeded 1,200 Pa, indicating the proper mechanical intensity of PEG-PLLeu hydrogel as an *in situ* drug release composite (Zhang et al., 2018). The microscopic morphology of PEG-PLLeu cross section was further investigated by SEM detection: the outcome revealed an interconnected porous microstructure of the PEG-PLLeu hydrogel (**Figure 2C**).

The favourable biodegradability is a vital factor for biomedical application of various thermogels. The *in vitro* degradation behavior of PEG-PLLeu thermogel was investigated in PBS with or without elastase or chymotrypsin over a 30-day period. As displayed in **Figure 2D**, degradation of PEG-PLLeu thermogels was faster in PBS with elastase or chymotrypsin than that in pure PBS due to the enzymolysis of polypeptides by elastase and chymotrypsin. This degradation property of PEG-PLLeu thermogel exhibited suitable biodegradability kinetics and could afford the long-term effect of the loading agents.

Antitumour Performance *In Vivo*

Regarding the unique anti-angiogenic mechanism of REG and immune regulation property of BMS202, we directly conducted the antitumour assay *in vivo*. Besides, in the light of the various

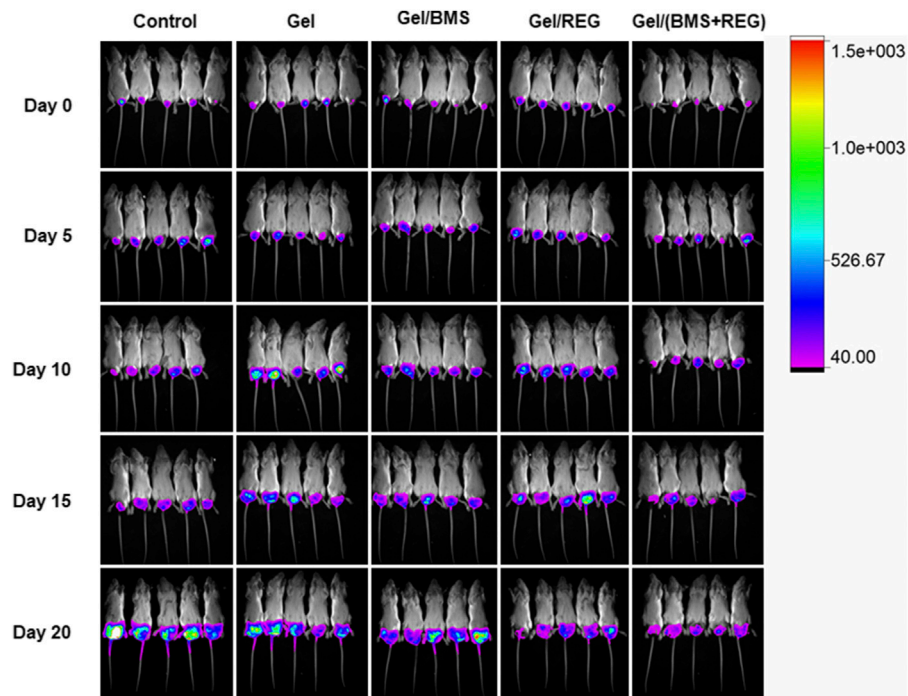


FIGURE 3 | Bioluminescent detection of the PBS, Gel, Gel/REG, Gel/BMS, and Gel/(BMS + REG) groups, from the day before treatment to 20 days after *in situ* treatment.

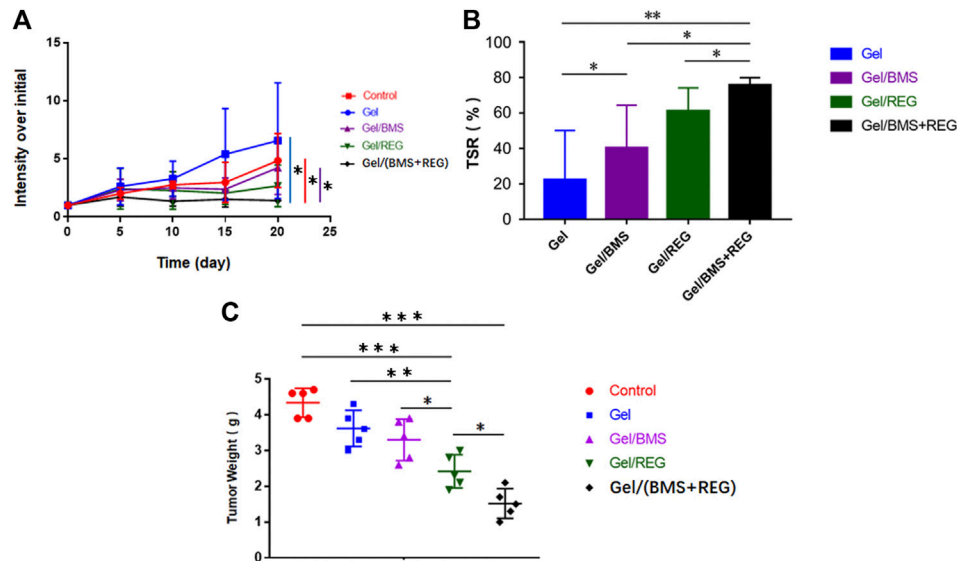
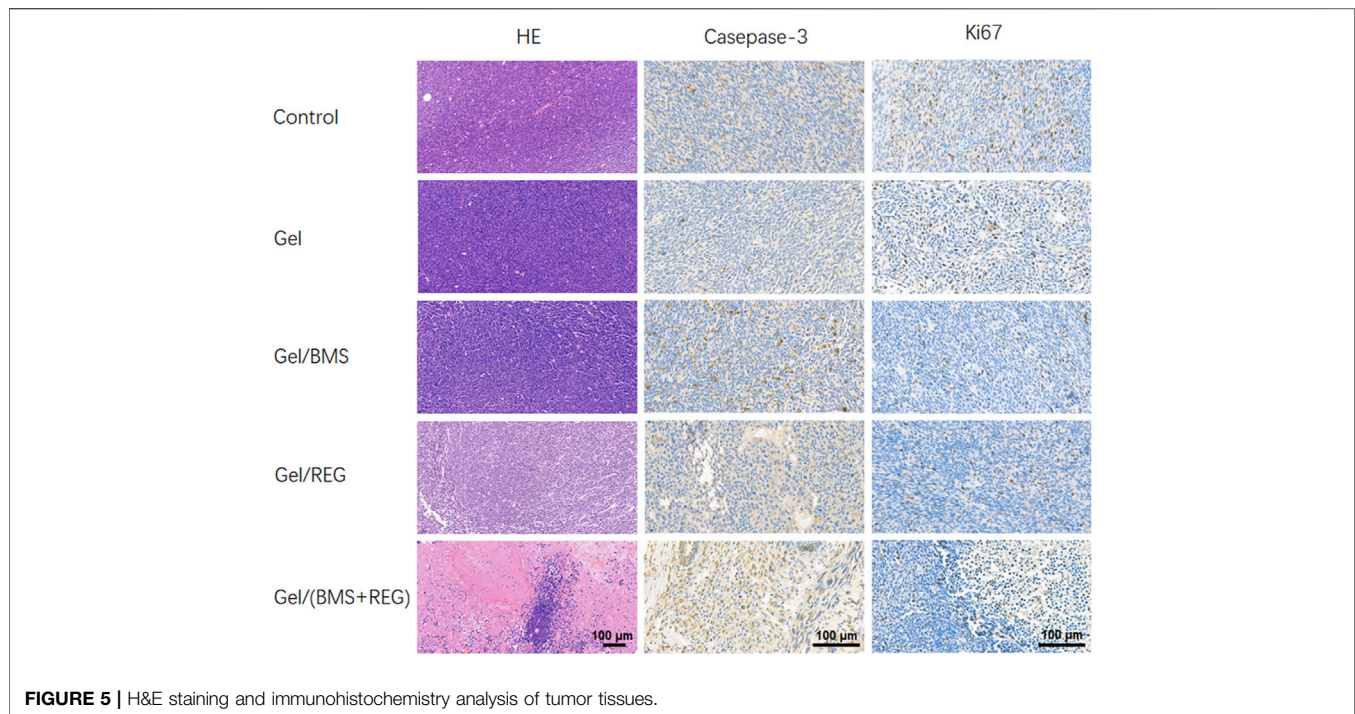


FIGURE 4 | *In vivo* anticancer efficacy of different groups (REG: 45 mg/kg, BMS202: 50 mg/kg). **(A)** Tumor growth curves of orthotopic CT26-Luc tumors in PBS, Gel, Gel/REG, Gel/BMS, and Gel/(BMS + REG) groups ($n = 5$). **(B)** TSR% results on day 20. **(C)** Tumor masses of different groups. Data are represented as the mean \pm SD (* $p < 0.05$, ** $p < 0.01$, and *** $p < 0.001$).

properties of PEG-PLLeu thermogel, 5.0 wt.% PEG-PLLeu was programmed to be carrier of REG and/or BMS202 for the *in vivo* inhibition against CT26-Luc tumor. BALB/c mice first received

inoculation of CT26-Luc cells. Two weeks after the inoculation, the inoculation-accepted mice were subjected to bioluminescence, and randomly allocated into different



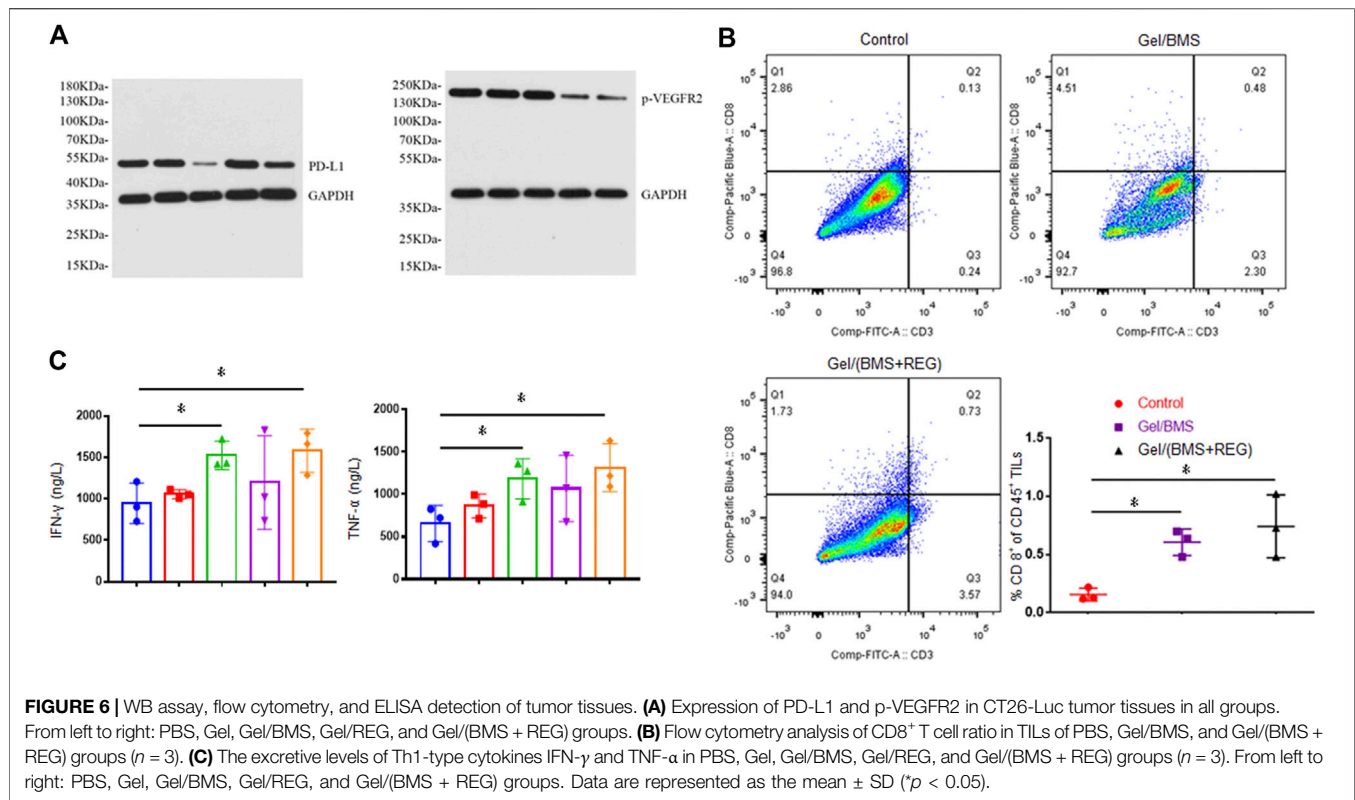
treatment groups. Mice of different groups were then subjected to pericarcinomatous injection with PBS, Gel, Gel/REG, Gel/BMS, and Gel/(BMS + REG), and bioluminescent detection was conducted every 5 days until 20 days after the treatment (**Figure 3**). In order to investigate the anticancer efficacy of each group, we draw a curve of tumor inhibition on the basis of bioluminescent detection. As shown in **Figure 4A**, Gel/REG showed potent tumor inhibition. On the contrary, the treatment efficacy of Gel/BMS was not obvious. However, there was the most significant tumor inhibition observed in Gel/(BMS + REG) treatment group. This indicated that BMS202, as a PD-L1 inhibitor, was synergistic with molecular targeted agent such as REG. But the treatment efficacy of BMS202 alone was quite limited. Apart of that, TSR% of Gel, Gel/REG, Gel/BMS, and Gel/(BMS + REG) on day 20 were 22.33 ± 27.79 , 61.09 ± 13.07 , 40.38 ± 23.97 , and $75.76 \pm 4.21\%$, respectively, implying the synergistic suppressive efficiency of combining molecular targeted agent and checkpoint inhibitor in CT26-Luc rectal cancer therapy (**Figure 4B**). Moreover, with the consideration of deviation relevant to bioluminescent detection, the whole tumors of each mouse were obtained and compared on day 21 after sacrificing the mice. Tumor masses of PBS, Gel, Gel/REG, Gel/BMS, and Gel/(BMS + REG) groups were 4.34 ± 0.40 , 3.62 ± 0.51 , 2.42 ± 0.47 , 3.30 ± 0.58 , and 1.52 ± 0.41 g, respectively (**Figure 4C**). Obviously, tumor masses in the Gel/(BMS + REG) group were significantly lower than those in the other treatment groups, consistent with the bioluminescent analysis.

H&E staining of tumor tissues and immunohistochemistry staining of caspase-3 and ki67 were then performed to demonstrate the histological variation, apoptosis, and proliferation of CT26-Luc tumors in various groups. As shown in **Figure 5**, single application of REG could achieve considerable

therapeutic outcomes and was more efficient in terms of tumor inhibition compared with BMS202. On the contrary, single utilization of BMS202 was slightly influential in apoptosis and proliferation of CT26-Luc cells, with minor morphological changes to CT26-Luc cells via H&E staining; however, there were the significant cytological variation of H&E slides, the highest caspase-3 expression, and the lowest ki67 expression in Gel/(BMS + REG) group, matching the therapeutic efficiency of this synergistic style of treatment.

Researchers found that the types of tumors with higher PD-L1 expression were more sensitive and responsive to treatment of PD-L1 inhibitor (Ribas and Tumei, 2014; Patel and Kurzrock, 2015). Besides, tumor tissue of renal cell carcinoma patients treated with molecular targeted therapy was found to display increased PD-L1 expression (Liu et al., 2015). Herein, WB assay was performed in this study to verify the expression of PD-L1 in CT26-Luc tumor influenced by treatment of REG. As shown in **Figure 6A**, tumor samples in the Gel/BMS group displayed the lowest expression of PD-L1. By contrast, the samples in the Gel/REG group displayed the highest expression of PD-L1. Moreover, PD-L1 expression of Gel/(BMS + REG) group was notably up-regulated compared with that of Gel/BMS group, which reflected the effect of REG treatment on PD-L1 expression of CT26-Luc tumors. The expression of phosphorylated VEGFR-2 (p-VEGFR2) was also examined via WB, which demonstrated the prime anti-angiogenic mechanism of REG.

To further explore whether BMS202 relieved the deteriorative TME involved with PD-L1 upregulation and its potential mechanism, we conducted flow cytometry assay and examined the CD8⁺ T cell in TILs. As shown in **Figure 6B**, treatment including BMS202 significantly improved recruitment of CD8⁺ T cell into tumors, fulfilling their mission of tumor cell elimination. The ratio of



CD8⁺ T cell in spleen and tumour-draining lymph nodes was also examined, and no significant difference was discovered between Gel/BMS, Gel/(BMS + REG), and the control group (**Supplementary Figures S1, S2**). This indicated that *in situ* application of BMS202 only relieved the immunological condition of local TME. The variational secretion of IFN- γ and TNF- α in TME is always relevant to the recruitment of CD8⁺ T cell. IFN- γ and TNF- α not only inhibit the growth of tumor cells directly, they also promote recognizing and killing of tumor cells from tumour-associated antigen-specific CD8⁺ T cells. As a result, excretive levels of Th1-type cytokines IFN- γ and TNF- α were further detected via ELISA assay. As shown in **Figure 6C**, the utilization of BMS202 specifically boosted secretion of IFN- γ and TNF- α and revoked the immunosuppressive TME of CT26-Luc tumor, thus resulting in the activation of CD8⁺ T cells and consequently enhanced efficacy of this synergistic therapy.

Safety Assessment of Poly (Ethylene Glycol)-Block-Poly (L-Leucine) Copolymers *In Vivo*

As a promising drug delivery system for *in situ* therapy of rectal cancer, the systematic toxicity and safety of the PEG-PLLeu thermogel is a primary concern. Besides, toxicity of REG and BMS202 should also to be monitored. We supervised specific parameters in mice as safety indexes. As shown in **Supplementary Figure S3**, the body mass of mice in all groups was monitored, and no obvious loss of mass was observed between each group, suggesting that implantation of the PEG-PLLeu

thermogel with or without REG/BMS202 did not influence the overall health of the mice. H&E staining and analysis was further introduced to investigate the potential histopathological microlesions. As shown in **Figure 7**, no prominent histopathological abnormalities or microlesions were noticed in the main organs. Overall, results in this study demonstrated the potential use of the REG/BMS202-loaded PEG-PLLeu thermogel as an efficient drug delivery system for synergistic treatment of rectal malignancies while alleviating the adverse effects thereof.

CONCLUSION

In summary, the PEG-PLLeu thermogels were successfully prepared by ROP. The thermogels displayed favourable mechanical properties and biodegradability because of the unique properties of the polypeptide copolymers. In addition, the local delivery system for *in situ* release of REG and BMS202 facilitated synergetic suppression on orthotopic CT26-Luc rectal tumors. Regardless of the upregulation of PD-L1 attributed to REG, the immunosuppressive TME of CT26-Luc tumor was distinctly relieved of the effects of BMS202, characterized by the increased infiltration of CD8⁺ T cell in CT26-Luc tumor and enhanced secretion of antitumour cytokines (IFN- γ and TNF- α). Moreover, the drug delivery composite exhibited no obvious toxicity in histopathological analysis. Taken together, the allied administration of molecular targeted therapy and checkpoint blockade immunotherapy by virtue of PEG-PLLeu hydrogel represented a potential strategy for enhanced *in situ* therapeutic modality for rectal cancer.

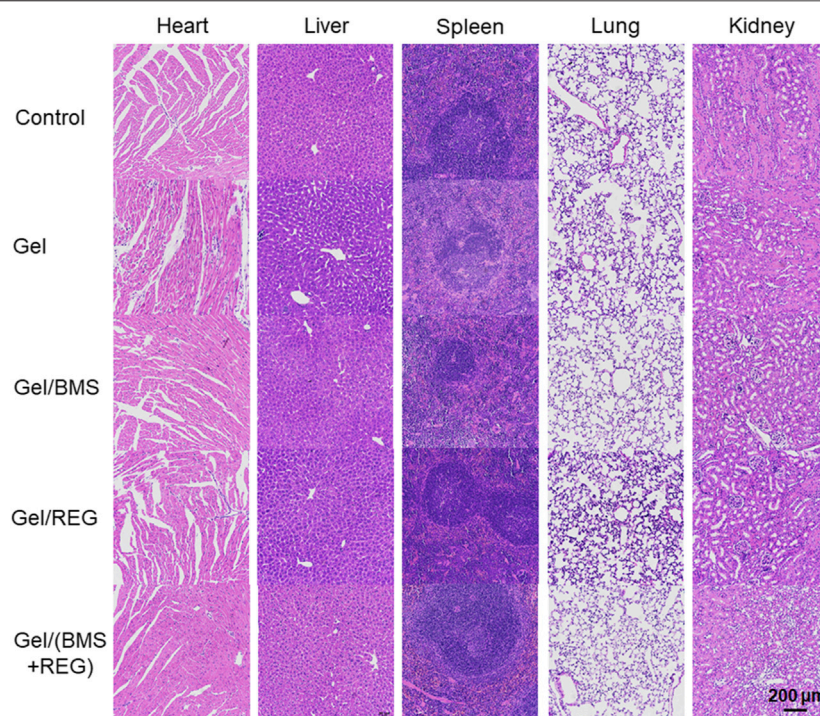


FIGURE 7 | Representative images of H&E staining for major organs obtained from mice in various treatment groups.

DATA AVAILABILITY STATEMENT

The original contributions presented in the study are included in the article/**Supplementary Material**, further inquiries can be directed to the corresponding authors.

ETHICS STATEMENT

The animal study was reviewed and approved by the Institutional Animal Care and Use Committee of Jilin University.

AUTHOR CONTRIBUTIONS.

YJ and ZL designed the experiments together. HZ carried out the experiments in company with ZL and YL. HZ analyzed the data

and drafted the manuscript. JZ, ZL, and YJ revised the manuscript.

FUNDING

This research was financially supported by the Medical and Health Program of Jilin Province (20190304047YY), Jilin Provincial Science and Technology Department (20200201430JC), Jilin Province Development and Reform Commission (2021C043-9), and Education Department of Jilin Province (JJKH20201034KJ).

SUPPLEMENTARY MATERIAL

The Supplementary Material for this article can be found online at: <https://www.frontiersin.org/articles/10.3389/fphar.2021.671611/full#supplementary-material>.

REFERENCES

- Bailly, C., and Vergoten, G. (2020). Protein homodimer sequestration with small molecules: focus on PD-L1. *Biochem. Pharmacol.* 174, 113821. doi:10.1016/j.bcp.2020.113821
- Bray, F., Ferlay, J., Soerjomataram, I., Siegel, R. L., Torre, L. A., and Jemal, A. (2018). Global cancer statistics 2018: GLOBOCAN estimates of incidence and mortality worldwide for 36 cancers in 185 countries. *CA: A Cancer J. Clinicians* 68 (6), 394–424. doi:10.3322/caac.21492
- Chen, J., Ding, J., Zhang, Y., Xiao, C., Zhuang, X., and Chen, X. (2015). Polyion complex micelles with gradient pH-sensitivity for adjustable intracellular drug delivery. *Polym. Chem.* 6 (3), 397–405. doi:10.1039/c4py01149j
- Chen, J., Jiang, Z., Xu, W., Sun, T., Zhuang, X., Ding, J., et al. (2020). Spatiotemporally targeted nanomedicine overcomes hypoxia-induced drug resistance of tumor cells after disrupting neovasculature. *Nano Lett.* 20 (8), 6191–6198. doi:10.1021/acs.nanolett.0c02515
- Ding, J., Chen, J., Gao, L., Jiang, Z., Zhang, Y., Li, M., et al. (2019a). Engineered nanomedicines with enhanced tumor penetration. *Nano Today* 29, 100800. doi:10.1016/j.nantod.2019.100800

- Ding, J., Feng, X., Jiang, Z., Xu, W., Guo, H., Zhuang, X., et al. (2019b). Polymer-mediated penetration-independent cancer therapy. *Biomacromolecules* 20 (12), 4258–4271. doi:10.1021/acs.biomac.9b01263
- Ding, J., Li, C., Zhang, Y., Xu, W., Wang, J., and Chen, X. (2015). Chirality-mediated polypeptide micelles for regulated drug delivery. *Acta Biomater.* 11, 346–355. doi:10.1016/j.actbio.2014.09.043
- Feng, X., Xu, W., Xu, X., Li, G., Ding, J., and Chen, X. (2020). Cystine proportion regulates fate of polypeptide nanogel as nanocarrier for chemotherapeutics. *Sci. China Chem.* 64 (2), 293–301. doi:10.1007/s11426-020-9884-6
- Guo, H., Li, F., Qiu, H., Xu, W., Li, P., Hou, Y., et al. (2020). Synergistically enhanced mucoadhesive and penetrable polypeptide nanogel for efficient drug delivery to orthotopic bladder cancer. *Research* 2020, 1. doi:10.34133/2020/8970135
- Halmos, B., Burke, T., Kalyvas, C., Insinga, R., Vandormael, K., Frederickson, A., et al. (2020). A matching-adjusted indirect comparison of Pembrolizumab plus chemotherapy vs. Nivolumab plus ipilimumab as first-line therapies in patients with PD-L1 TPS \geq 1% metastatic NSCLC. *Cancers* 12 (12), 3648. doi:10.3390/cancers12123648
- Hurwitz, H., Fehrenbacher, L., Novotny, W., Cartwright, T., Hainsworth, J., Heim, W., et al. (2004). Bevacizumab plus irinotecan, fluorouracil, and leucovorin for metastatic colorectal cancer. *N. Engl. J. Med.* 350 (23), 2335–2342. doi:10.1056/NEJMoa032691
- Jang, J. Y., Kim, H.-J., and Han, B. W. (2019). Structural basis for the regulation of PPAR γ activity by imatinib. *Molecules* 24 (19), 3562. doi:10.3390/molecules24193562
- Jiang, Z.-y., Feng, X.-r., Xu, W.-g., Zhuang, X.-l., Ding, J.-x., and Chen, X.-s. (2020). Calcium phosphate-cured nanocluster of poly(L-glutamic acid)-cisplatin and arsenic trioxide for synergistic chemotherapy of peritoneal metastasis of ovarian cancer. *Acta Polym. Sin.* 51 (8), 901–910. doi:10.11777/j.issn1000-3304.2020.20053
- Jung, G., Benítez-Ribas, D., Sánchez, A., and Balaguer, F. (2020). Current treatments of metastatic colorectal cancer with immune checkpoint inhibitors-2020 update. *JCM* 9 (11), 3520. doi:10.3390/jcm9113520
- Liu, X.-D., Hoang, A., Zhou, L., Kalra, S., Yetil, A., Sun, M., et al. (2015). Resistance to antiangiogenic therapy is associated with an immunosuppressive tumor microenvironment in metastatic renal cell carcinoma. *Cancer Immunol. Res.* 3 (9), 1017–1029. doi:10.1158/2326-6066.Cir-14-0244
- Liu, Y., Li, D., Ding, J., and Chen, X. (2020). Controlled synthesis of polypeptides. *Chin. Chem. Lett.* 31 (12), 3001–3014. doi:10.1016/j.ccl.2020.04.029
- Ma, W., Chen, Q., Xu, W., Yu, M., Yang, Y., Zou, B., et al. (2021). Self-targeting visualizable hyaluronate nanogel for synchronized intracellular release of doxorubicin and cisplatin in combating multidrug-resistant breast cancer. *Nano Res.* 14 (3), 846–857. doi:10.1007/s12274-020-3124-y
- Patel, S. P., and Kurzrock, R. (2015). PD-L1 expression as a predictive biomarker in cancer immunotherapy. *Mol. Cancer Ther.* 14 (4), 847–856. doi:10.1158/1535-7163.Mct-14-0983
- Ribas, A., and Tume, P. C. (2014). The future of cancer therapy: selecting patients likely to respond to PD1/L1 blockade. *Clin. Cancer Res.* 20 (19), 4982–4984. doi:10.1158/1078-0432.Ccr-14-0933
- Sauer, R., Liersch, T., Merkel, S., Fietkau, R., Hohenberger, W., Hess, C., et al. (2012). Preoperative versus postoperative chemoradiotherapy for locally advanced rectal cancer: results of the German CAO/ARO/AIO-94 randomized phase III trial after a median follow-up of 11 years. *JCO* 30 (16), 1926–1933. doi:10.1200/jco.2011.40.1836
- Skarderud, M. R., Polk, A., Vistisen, K. K., Larsen, F. O., and Nielsen, D. L. (2018). Efficacy and safety of regorafenib in the treatment of metastatic colorectal cancer: a systematic review. *Cancer Treat. Rev.* 62, 61–73. doi:10.1016/j.ctrv.2017.10.011
- Song, W., Shen, L., Wang, Y., Liu, Q., Goodwin, T. J., Li, J., et al. (2018). Synergistic and low adverse effect cancer immunotherapy by immunogenic chemotherapy and locally expressed PD-L1 trap. *Nat. Commun.* 9, 2237. doi:10.1038/s41467-018-04605-x
- Sun, Y., Shan, H., Wang, J., Wang, X., Yang, X., and Ding, J. (2019). Laden nanofiber capsules for local malignancy chemotherapy. *J Biomed. Nanotechnol.* 15 (5), 939–950. doi:10.1166/jbn.2019.2745
- Tokumaru, Y., Matsushashi, N., Takahashi, T., Tanahashi, T., Matsui, S., Imai, H., et al. (2019). Efficacy of combination therapy with zoledronic acid and cetuximab for unresectable rectal cancer with bone metastases: a case report. *Mol. Clin. Onc.* 10 (6), 571–574. doi:10.3892/mco.2019.1836
- Verschraegen, C. F., Jerusalem, G., McClay, E. F., Iannotti, N., Redfern, C. H., Bennaoui, J., et al. (2020). Efficacy and safety of first-line avelumab in patients with advanced non-small cell lung cancer: results from a phase Ib cohort of the JAVELIN Solid Tumor study. *J. Immunother. Cancer* 8 (2), e001064. doi:10.1136/jitc-2020-001064
- Wang, J., Xu, W., Li, S., Qiu, H., Li, Z., Wang, C., et al. (2018). Poly(lactide-cholesterol) stereocomplex micelle encapsulating chemotherapeutic agent for improved antitumor efficacy and safety. *J Biomed. Nanotechnol.* 14 (12), 2102–2113. doi:10.1166/jbn.2018.2624
- Weiser, M. R., Quah, H.-M., Shia, J., Guillem, J. G., Paty, P. B., Temple, L. K., et al. (2009). Sphincter preservation in low rectal cancer is facilitated by preoperative chemoradiation and intersphincteric dissection. *Ann. Surg.* 249 (2), 236–242. doi:10.1097/SLA.0b013e318195e17c
- Wilhelm, S. M., Dumas, J., Adnane, L., Lynch, M., Carter, C. A., Schütz, G., et al. (2011). Regorafenib (BAY 73-4506): a new oral multikinase inhibitor of angiogenic, stromal and oncogenic receptor tyrosine kinases with potent preclinical antitumor activity. *Int. J. Cancer* 129 (1), 245–255. doi:10.1002/ijc.25864
- Zak, K. M., Grudnik, P., Magiera, K., Dömling, A., Dubin, G., and Holak, T. A. (2017). Structural biology of the immune checkpoint receptor PD-1 and its ligands PD-L1/PD-L2. *Structure* 25 (8), 1163–1174. doi:10.1016/j.str.2017.06.011
- Zhang, H., Dong, S., Li, Z., Feng, X., Xu, W., Tulinao, C. M. S., et al. (2020). Biointerface engineering nanoplateforms for cancer-targeted drug delivery. *Asian J. Pharm. Sci.* 15 (4), 397–415. doi:10.1016/j.ajps.2019.11.004
- Zhang, W., Ning, C., Xu, W., Hu, H., Li, M., Zhao, G., et al. (2018). Precision-guided long-acting analgesia by hydrogel-immobilized bupivacaine-loaded microsphere. *Theranostics* 8 (12), 3331–3347. doi:10.7150/thno.25276
- Zheng, P., Liu, Y., Chen, J., Xu, W., Li, G., and Ding, J. (2020). Targeted pH-responsive polyion complex micelle for controlled intracellular drug delivery. *Chin. Chem. Lett.* 31 (5), 1178–1182. doi:10.1016/j.ccl.2019.12.001

Conflict of Interest: The authors declare that the research was conducted in the absence of any commercial or financial relationships that could be construed as a potential conflict of interest.

Copyright © 2021 Zhang, Zhang, Liu, Jiang and Li. This is an open-access article distributed under the terms of the Creative Commons Attribution License (CC BY). The use, distribution or reproduction in other forums is permitted, provided the original author(s) and the copyright owner(s) are credited and that the original publication in this journal is cited, in accordance with accepted academic practice. No use, distribution or reproduction is permitted which does not comply with these terms.



Targeting PAR2 Overcomes Gefitinib Resistance in Non-Small-Cell Lung Cancer Cells Through Inhibition of EGFR Transactivation

Yuhong Jiang*, Xin Zhuo, Xiujuan Fu, Yue Wu and Canquan Mao*

School of Life Science and Engineering, Southwest Jiaotong University, Chengdu, China

OPEN ACCESS

Edited by:

Xianjue Chen,
University of New South Wales,
Australia

Reviewed by:

Xiaofeng Lu,
Sichuan University, China
Bin Li,
Army Medical University, China

*Correspondence:

Yuhong Jiang
yuh.jiang@foxmail.com
Canquan Mao
maocq@swjtu.edu.cn

Specialty section:

This article was submitted to
Pharmacology of Anti-Cancer Drugs,
a section of the journal
Frontiers in Pharmacology

Received: 02 November 2020

Accepted: 25 March 2021

Published: 22 April 2021

Citation:

Jiang Y, Zhuo X, Fu X, Wu Y and Mao C
(2021) Targeting PAR2 Overcomes
Gefitinib Resistance in Non-Small-Cell
Lung Cancer Cells Through Inhibition
of EGFR Transactivation.
Front. Pharmacol. 12:625289.
doi: 10.3389/fphar.2021.625289

Drug resistance can notably restrict clinical applications of gefitinib that is a commonly used EGFR-tyrosine kinase inhibitors (EGFR-TKIs) for non-small cell lung cancer (NSCLC). The attempts in exploring novel drug targets and reversal strategies are still needed, since gefitinib resistance has not been fully addressed. Protease-activated receptor 2 (PAR2), a G protein-coupled receptor, possesses a transactivation with EGFR to initiate a variety of intracellular signal transductions, but there is a lack of investigations on the role of PAR2 in gefitinib resistance. This study established that protease-activated receptor 2 (PAR2), actively participated in NSCLC resistant to gefitinib. PAR2 expression was significantly up-regulated when NSCLC cells or tumor tissues became gefitinib resistance. PAR2 inhibition notably enhanced gefitinib to modulate EGFR transactivation, cell viability, migration and apoptosis in gefitinib-sensitive and-resistant NSCLC cells, suggesting its reversal effects in gefitinib resistance. Meanwhile, the combination of a PAR2 inhibitor (P2pal-18S) and gefitinib largely blocked ERK phosphorylation and epithelial-mesenchymal transition (EMT) compared to gefitinib alone. Importantly, we probed its underlying mechanism and uncovered that PAR2 blockade sensitized gefitinib and reversed its resistance mainly via β -arrestin-EGFR-ERK signaling axis. These effects of PAR2 inhibition were further confirmed by the *in vivo* study which showed that P2pal-18S reactivated gefitinib to inhibit tumor growth via restricting ERK activation. Taken together, this study could not only reveal a new mechanism of receptor-mediated transactivation to modulate drug resistance, but also provide a novel drug target and direction for overcoming gefitinib resistance in NSCLC.

Keywords: protease-activated receptor 2, epidermal growth factor receptor-tyrosine kinase inhibitors, drug resistance, non-small-cell lung cancer cells, transactivation

INTRODUCTION

Non-small cell lung cancer (NSCLC) accounts for approximately 85% of lung cancers which is the leading cause of cancer-related death worldwide (Gridelli et al., 2015; Herbst et al., 2018). Since an epidermal growth factor receptor (EGFR) activating mutation has been identified as one of the most common gene mutations in lung cancer, EGFR-tyrosine kinase inhibitors (EGFR-TKIs) became first-line molecular targeted therapies for EGFR-mutated NSCLC patients (Network, 2014). Gefitinib as the first-generation EGFR-TKI has markedly prolonged the overall survival of NSCLC patients;

however, drug resistance has been eventually harboured leading to the ultimate failure of clinical treatments (Hirsch et al., 2016). There are a variety of resistance mechanisms, including second-site mutations (e.g., EGFR-T790M gatekeeper mutation) (Yun et al., 2008), compensatory downstream signaling activation (e.g., MEK/ERK, PI3K/AKT) (Shou et al., 2016; Rotow and Bivona, 2017), parallel bypass signaling activation (other receptor tyrosine kinases, RTKs, e.g., MET, FGFR, IGFR) (Rotow and Bivona, 2017; Raoof et al., 2019) and histological transformation (e.g., epithelial-to-mesenchymal transition, EMT) (Marcucci et al., 2016; Weng et al., 2019). Although the third-generation EGFR-TKI, osimertinib, has been successfully developed to overcome EGFR-T790M mutated resistance to gefitinib (Jänne et al., 2015), other resistance mechanisms have not been clinically well-addressed due to its diverse and complicated characteristics. Thus, it is an urgent need for exploring novel drug strategies targeting NSCLC resistant to gefitinib depending on other receptors, signaling pathways or histological changes.

G protein-coupled receptors (GPCRs) as the most widely studied drug targets have been reported to exhibit a transactivation with EGFR, i.e., GPCR ligands can activate EGFR to stimulate downstream signaling 2 decades ago (Daub et al., 1996). Protease-activated receptor 2 (PAR2) as a GPCR itself can facilitate Ca^{2+} , MEK/ERK, AKT, PI3K and mTOR signaling pathways to promote a variety of tumor cell functions (Huang et al., 2013; Jiang et al., 2018; Tsai et al., 2018; Pawar et al., 2019). Meanwhile, PAR2 can transactivate EGFR and subsequently trigger MEK/ERK or AKT signaling, cooperatively modulating cell migration, apoptosis or proliferation in colon (Darmoul et al., 2004), pancreatic (Shi et al., 2013), gastric (Caruso et al., 2006), lung (Michel et al., 2014) and ovarian cancers (Jiang et al., 2020). PAR2 blockade can significantly impair cell migration and EMT via ERK signaling in lung cancer (Tsai et al., 2018) whereas the dysregulation of ERK signaling and EMT are considered as molecular mechanisms of gefitinib resistance in NSCLC (Tricker et al., 2015; Becker et al., 2019; Weng et al., 2019), suggesting the potential involvement of PAR2-mediated signaling in lung tumor progression and drug resistance. Notably, mutational activations of other RTKs have also been identified to initiate gefitinib resistance since these receptors can exhibit parallel signaling pathways required for NSCLC cell survival (Rotow and Bivona, 2017). Similarly, PAR2-mediated EGFR transactivation can regulate EGFR-related signaling and therefore we hypothesized that this transactivation might also bypass gefitinib-induced EGFR blockade to modulate NSCLC resistant to gefitinib. A study on expression analysis of 384 GPCRs in gefitinib resistance has also showed that the level of PAR2 expression was largely higher in gefitinib-resistant NSCLC cells than sensitive cells (Kuzumaki et al., 2012), further indicating that PAR2 might be positively related to the development of gefitinib resistance. However, classical strategies mainly focus on modulation of resistance-related EGFR mutations, RTKs and compensatory signaling pathways, and few literatures reported about the role of other receptor families, including PAR2, in gefitinib resistance upon EGFR transactivation.

In this study, we aimed to investigate whether inhibition of PAR2 could overcome gefitinib resistance in NSCLCs as well as its underlying mechanism *in vitro* and *in vivo*. Here, we first showed that combination of a PAR2 antagonist, P2pal-18S, and gefitinib can cooperatively impair phosphorylation of EGFR to confirm the transactivation between PAR2 and EGFR. Furthermore, inhibition of PAR2 augmented the effect of gefitinib in cell proliferation, migration and apoptosis in gefitinib-sensitive and -resistant NSCLC cells while targeting PAR2 promoted gefitinib to modulate ERK signaling and EMT. PAR2 blockade potentiated gefitinib in attenuating NSCLC cell functions via β -arrestin-ERK signalling axis upon EGFR transactivation. Alternatively, *in vivo* xenograft study of combination of P2pal-18S and gefitinib confirmed the effect and mechanism of targeting PAR2 in gefitinib resistance. Taken together, our study revealed the promising role of PAR2 in NSCLC cell resistant to gefitinib and targeting PAR2 maybe as a potential therapeutic strategy for reversing gefitinib resistance and improving EGFR-TKI therapy in NSCLC patients.

MATERIALS AND METHODS

Materials

Gefitinib (99%) was obtained from Aladdin (Shanghai, China) and P2pal-18S (palmitate-RSSAMDENSEKKRKAISK-NH₂, 98%) was custom-made by Apeptides (Shanghai, China). Mitomycin C (99%) and FR180204 (100%) were purchased from Selleckchem (Houston, TX, United States) while Barbadin (99%) were obtained from MedChemExpress (Monmouth Junction, NJ, United States). The primary antibodies used against PAR2, total or phospho-EGFR, total or phospho-ERK as well as the secondary antibodies, HRP-conjugated anti-rabbit IgG, were purchased from Cell Signaling Technology (Boston, MA, United States). The primary antibodies used against Bcl-2, Bax, E-cadherin and vimentin were obtained from Abcam (Cambridge, MA, United States).

Cell Cultures and Construction of Gefitinib-Resistant Cells

Human non-small lung cancer cell line PC-9 (KeyGEN BioTech, Nanjing, China) and A549 (the Cell Bank of the Chinese Academy of Science, Shanghai, China) were cultured at 37°C in DMEM or RPMI-1640 medium (Invitrogen, Carlsbad, CA, United States) containing 10% FBS and 1% penicillin/streptomycin in a humidified 5% CO₂ incubator. To establish the gefitinib-resistant cells, PC-9 cells was exposed to gradually increasing concentrations of gefitinib as described previously (Shou et al., 2016). The gefitinib-resistant PC-9 cells (PC-9-GR) can proliferate normally in the presence of 5 mM gefitinib. The resistance index (RI) was calculated using formula: $\text{RI} = \text{IC}_{50}(\text{PC-9-GR cells})/\text{IC}_{50}(\text{PC-9 cells})$.

Cell Viability CCK8 Assays

Cells (5×10^4 cells/mL) were seeded overnight and were then treated with compounds for 48 h. After that, Cells were incubated with $10 \mu\text{L}$ CCK-8 solution (KeyGEN BioTECH, Nanjing, China) for another 4 h. The absorbance was measured at 450 nm by using a microplate reader (Synergy H1, Biotek, United States).

In vitro Scratch Assay

Cells (3×10^5 cells/well) were seeded at 24 well-plate overnight and a scratch was created in the center of the well using a P200 micropipette tip. Cells were washed with PBS three times to remove floating cells and incubated with compounds. Scratch size were photographed at 0 and 48 h, using an inverted microscope (IX71, Olympus, Japan). The scratch gap size was measured using ImageJ software and was defined as the scratch size at 48 h divided by the initial gap area at 0 h.

Transwell Migration Assay

Cell migration was measured by a transwell system (polycarbonate filter insert with $8 \mu\text{m}$ pore size membrane, Corning Inc., NY, United States). Cells were seeded at 5×10^5 /insert in the upper chamber of transwell overnight. Compounds were added to the upper chamber while medium with 2% FBS were added to the bottom chamber. After 24 h, cells on the top membrane were removed gently using cotton swabs and washed with PBS. Cells on the underside of the membrane were fixed in 4% paraformaldehyde and was then stained with 0.1% crystal violet. Migrated cells was photographed by an inverted brightfield microscope (BX53, Olympus, Japan) and was counted using ImageJ software.

AO/EB Fluorescence Staining

Cells (5×10^5 cells/well) were seeded at six well-plate and treated with P2pal-18S or gefitinib in serum-free medium for 48 h at 37°C . After that, the mixed AO/EB solutions (Solarbio, Beijing, China) were added to cells and incubated for 5 min in dark. Cell morphology was examined under a fluorescence microscope (IX71, Olympus).

mRNA Isolation and Real Time-PCR

RNA was isolated using Trizol reagent (Invitrogen). Total RNA ($1 \mu\text{g}$) was reverse-transcribed by Revert PrimeScript RT Enzyme Kit (TaKaRa, Shiga, Japan). RT-PCR was then performed by a Lightcycler96 instrument (Roche Diagnostics, Switzerland). Genes were amplified for 40 cycles. The cycling conditions were 94°C for 10 min, followed by 40 cycles of 94°C for 30 s, 60°C for 40 s and 72°C for 20 s. Relative-gene expression was normalized against *Actin*. All primer sequences are described in **Supplementary Table S1**.

Western Blot

Cells (5×10^5 cells/well) were seeded overnight and then stimulated with compounds after serum-starve. Whole-cell lysates were prepared using RIPA lysis buffer (Beyotime, Shanghai, China) supplemented with 1% PMSF (Sigma).

Each sample with equal loading was separated by 6–12% PAGE gel and then transferred to a nitrocellulose filter membrane. After blocked with 5% skim milk for 2 h, membranes were incubated with the primary antibodies (1:1000) and secondary antibodies conjugated to HRP (1:3000). Exposure times were varied to eliminate signal saturation while GAPDH, total EGFR or ERK was loading control. Densitometric analysis of bands was calculated with ImageJ software.

Animal Experiments

All animals were kept in a specific pathogen-free facility and treated with humane care with approval from the Animal Use and Care Committee of Southwest Jiaotong University. For the xenograft studies, PC-9-GR cells (5×10^6) were injected subcutaneously into the back of the right forelimbs of five-week-old male Balb/c nude mice (Chengdu Dashuo Laboratory Animal Technology, China). Once the tumor size reached $\sim 200 \text{ mm}^3$, mice were randomized to four groups treated with vehicle, P2pal-18S (i.m., every two days), gefitinib (p.o., daily), or P2pal-18S and gefitinib. The tumor volume of mice was monitored twice a week and calculated using the formula $V = (\text{length} \times \text{width}^2)/2$. At indicated time points, mice were sacrificed, and tumor tissues were isolated. After fixed with 4% paraformaldehyde and embedded in paraffin, tumor tissues were detected by H&E staining for histopathological examination while levels of PAR2, total or phospho-ERK in tumor were detected by immunohistochemistry assay and observed under a light microscope (BX53, Olympus, Japan). mRNA and protein expressions of PAR2, total or phospho-ERK, E-cadherin or vimentin were also analyzed by RT-PCR and Western blot, respectively.

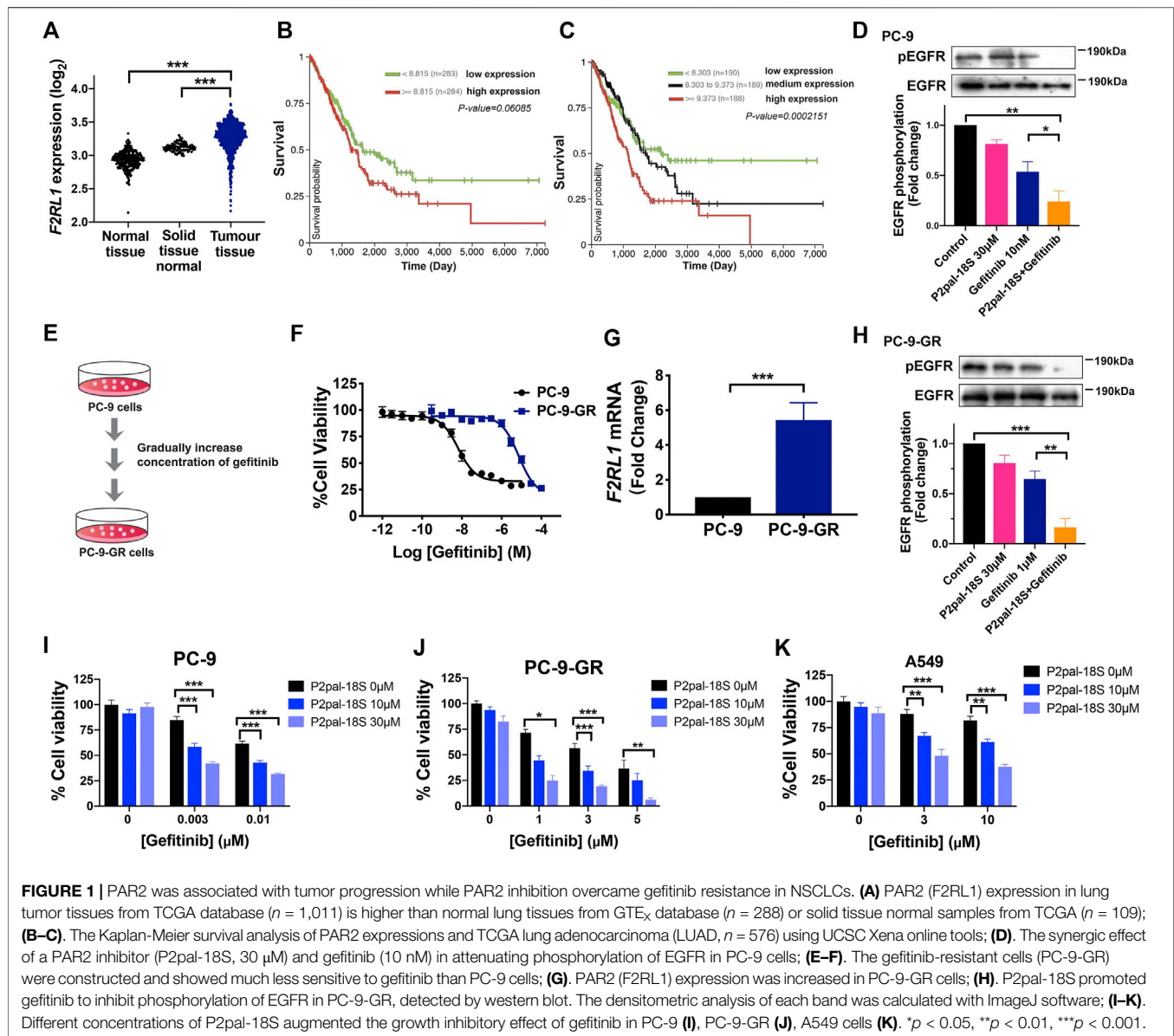
Statistical Analysis

Data were plotted and analyzed using GraphPad Prism 8.0 (GraphPad Software, San Diego, CA, United States). Data point represents mean \pm SEM ($n \geq 3$) unless otherwise stated. Statistical significance of intergroup differences was calculated using one-way ANOVA analysis ($*p < 0.05$, $**p < 0.01$, $***p < 0.001$).

RESULTS

Protease-Activated Receptor 2 Inhibition Sensitized Non-Small Cell Lung Cancer Cells to Gefitinib Upon Epidermal Growth Factor Receptor Transactivation

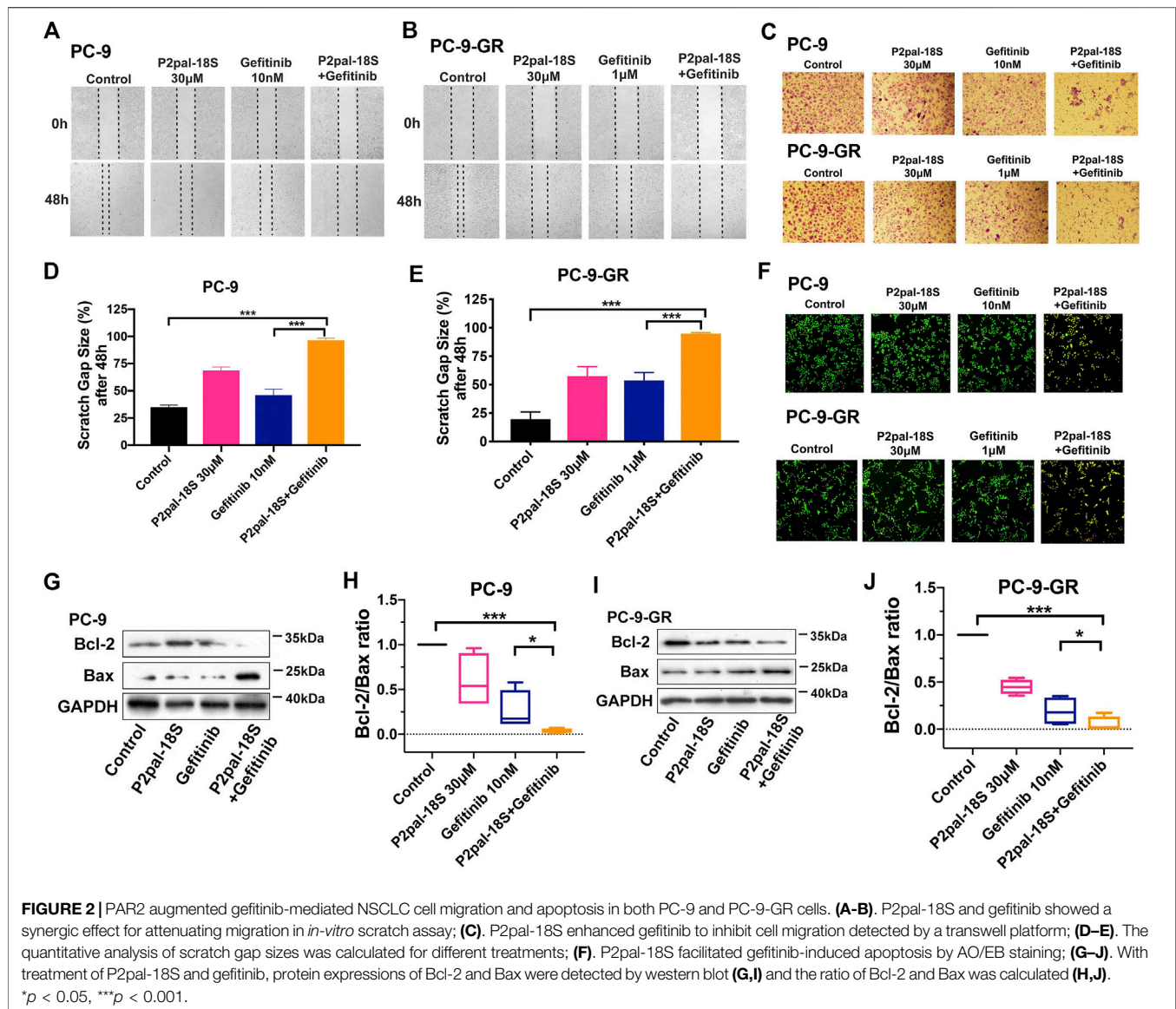
To probe the role of PAR2 in human NSCLC, we first compared the expression level of PAR2 (F2RL1) in human lung tumor tissues and normal lung tissues from The Cancer Genome Atlas (TCGA) and The Genotype-Tissue Expression (GTEx) databases using online analysis tools (Goldman et al., 2018). PAR2 expression was notably higher in human lung tumor tissues than that in normal lung tissues samples derived from peri-tumour tissues or lung tissues of persons without



cancer (Figure 1A). Similarly, in the Gene Expression Omnibus (GEO) databases, lung tumor tissues exhibited up-regulation of PAR2 expression compared to normal tissues (Supplementary Figure S1). As shown in Figures 1B,C, there was a highly positive correlation between PAR2 expression and tumor progression of lung adenocarcinoma patients in Kaplan-Meier survival plots, revealing its active participations in lung cancer. It has also been discovered that PAR2 could not only itself mediate tumor progression but also transactivate EGFR to cooperatively modulate cancer cell functions (Michel et al., 2014; Pawar et al., 2019). Consistent with previous findings, a PAR2 inhibitor, P2pal-18S, and gefitinib cooperatively attenuating EGFR activation in PC-9 cells (Figure 1D), indicating a transactivation between PAR2 and EGFR in NSCLC cells. We hypothesized that targeting PAR2 could reverse

NSCLC cells resistance to gefitinib upon the receptor transactivation.

To test this hypothesis, we constructed a gefitinib-resistant NSCLC cells, PC-9-GR, by gradually increasing concentration of gefitinib in PC-9 cells (Figures 1E,F). PC-9-GR cells (IC_{50} 9.5 μ M, pIC_{50} 5.2 \pm 0.1) possessed more resistance (RI = 872) to gefitinib than PC-9 cells (IC_{50} 10.9 nM, pIC_{50} 7.8 \pm 0.1), while A549 cells showed its primary resistance to gefitinib (IC_{50} 2.1 μ M, pIC_{50} 5.0 \pm 0.1) (Supplementary Figure S2A). Similar to our prior patient data analysis, the expression level of PAR2 was significantly elevated in PC-9-GR cells with increasing gefitinib resistance (Figure 1G). Due to drug resistance, gefitinib almost lost its capacity of blocking EGFR activation in PC-9-GR whereas addition of P2pal-18S largely promoted gefitinib to inhibit phosphorylation of EGFR (~3-fold increase, Figure 1H). To further test whether PAR2 sensitize NSCLC cells to gefitinib,



PC-9, PC-9-GR and A549 cells were treated with gefitinib at different concentrations in the presence of P2pal-18S at 10 μM or 30 μM . The incubation time of compound incubation was also studied and 48 h was selected as the optimal time point (Supplementary Figures S2B,C). As shown in Figures 1I–K, P2pal-18S significantly augmented gefitinib inhibition (~70–90%) in sensitive cells PC-9, acquired resistant cells PC-9-GR and primary resistant cells A549 in dose-dependent manner, revealing the synergic effect between PAR2 and EGFR inhibitors. Importantly, no matter what concentrations of inhibitors were in Figures 1I,J, the inhibitory effect by the combination of P2pal-18S and gefitinib was ~2-fold more than gefitinib alone in PC-9, while addition of P2pal-18S into gefitinib treatment triggered nearly a 3-fold increase in attenuating cell viability of PC-9-GR. It indicated that the sensitization effect of PAR2 blockade was more potent in PC-9-GR cells than in PC-9

cells. Therefore, with overexpression of PAR2 in NSCLC cells, PAR2 blockade sensitized gefitinib to attenuate EGFR activation and lung cancer cell viability.

Protease-Activated Receptor 2 Inhibition Potentiated Gefitinib to Modulate Non-Small Cell Lung Cancer Cell Migration and Apoptosis

Apart from cell ability, we tested the reversal effect of PAR2 inhibition in cell migration and apoptosis. We found that there was a strong synergic effect of P2pal-18S and gefitinib in PC-9 and PC-9-GR cells by *in-vitro* scratch wound healing and transwell migration assay (Figures 2A–E), indicating that PAR2 inhibition exerted a significant enhancement of gefitinib in inhibiting NSCLC cell migration. Furthermore,

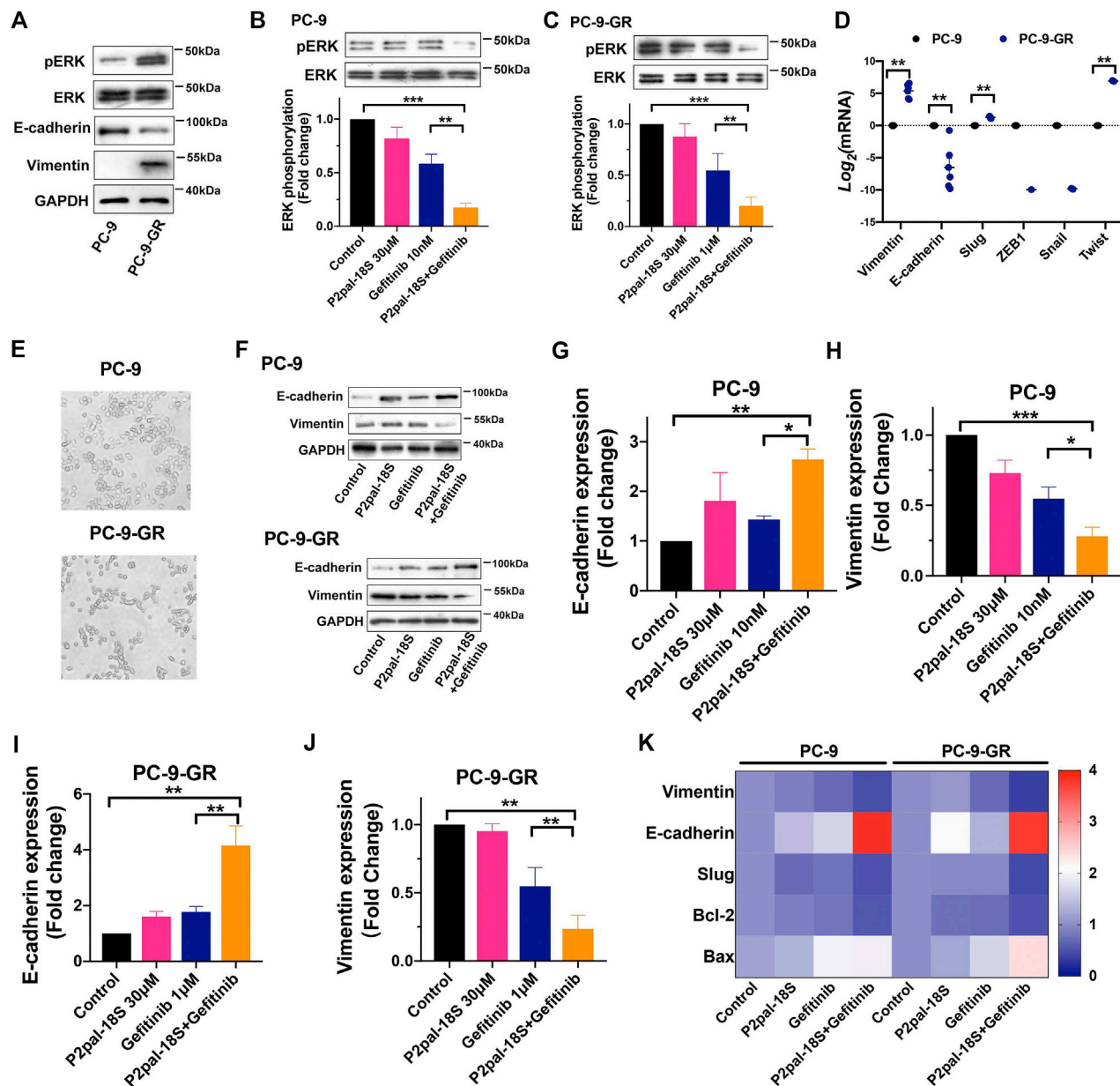


FIGURE 3 | Targeting PAR2 enhanced gefitinib inhibition in ERK phosphorylation and EMT. (A). Protein expressions of total or phosph-ERK, E-cadherin and vimentin were increased in PC-9-GR cells; (B–C). P2pal-18S promoted gefitinib to inhibit phosphorylation of ERK in PC-9 (B) and PC-9-GR cells (C); (D). EMT-related gene expressions were detected and compared in gefitinib-sensitive and -resistant cells; (E). The morphology of PC-9 and PC-9-GR cells was observed; (F–J). P2pal-18S facilitated gefitinib to increase expressions of E-cadherin and decrease expressions of vimentin; (K). The heat map of gene expressions of vimentin, E-cadherin, Slug, Bcl-2 and Bax by different treatments compared with control group (value = 1) in PC-9 and PC-9-GR cells, respectively. * $p < 0.05$, ** $p < 0.01$, *** $p < 0.001$.

as shown in **Figure 2F**, the increasing numbers of yellow-green or orange stained apoptotic/dead cells were observed in cells treated with combination of P2pal-18S and gefitinib whereas there were a large number of live cells (green) in the gefitinib treatment determined by the AO/EB fluorescence staining (Liu et al., 2015; Qi et al., 2020; Zhang et al., 2018). This effect of PAR2 blockade in NSCLC cell apoptosis was further confirmed by detection of Bcl-2 and Bax expressions (**Figures 2G–J**).

Bcl-2/Bax ratio has been considered as a marker for cell apoptosis, since the decrease of Bcl-2 expression and increase of Bax expression represent cancer cells under apoptosis process. P2pal-18S largely promoted gefitinib to up-regulate Bax expression and down-regulate Bcl-2 expression in PC-9 and PC-9-GR cells, and therefore the Bcl-2/Bax ratio was notably reduced in NSCLC cells treated with P2pal-18S and gefitinib. Additionally, Annexin-FITC/PI staining results further

confirmed that P2pal-18S could significantly enhance gefitinib to stimulate early or late apoptosis of PC-9 and PC-9-GR cells (**Supplementary Figure S3**). Thus, it indicated that PAR2 inhibition also facilitated gefitinib to limit NSCLC cell functions vs modulating cell migration and apoptosis.

Protease-Activated Receptor 2 Inhibition Reversed EMT to Sensitize Non-Small Cell Lung Cancer Cells to Gefitinib

It has been reported that the EMT phenotype and dysregulation of bypass signaling could initiate gefitinib resistance in NSCLC (Weng et al., 2019), which are also highly associated with PAR2 activation (Tsai et al., 2018). Therefore, we studied cell signaling pathway and EMT in P2pal-18S and gefitinib-treated cells for exploring the underlying mechanism of PAR2 inhibition in sensitizing NSCLC cells to gefitinib. With increasing resistance to gefitinib, there was a rising trend in phosphorylation of ERK (**Figure 3A**), suggesting the participation of ERK signaling in EGFR-TKI resistance. Furthermore, ERK signaling has been revealed to be modulated by the transactivation between PAR2 and EGFR in cancer cells (Darmoul et al., 2004; Shi et al., 2013). Our results further showed that P2pal-18S potentiated gefitinib inhibition in phosphorylation of ERK, suggesting that targeting PAR2 may inhibit EGFR transactivation and ERK activation to reverse gefitinib resistance in NSCLC (**Figures 3B,C**).

Alternatively, at mRNA and protein expression levels, E-cadherin was suppressed and vimentin was elevated in PC-9-GR cells, indicating the occurrence of EMT when gefitinib resistance were generated (**Figures 3A,D**). Meanwhile, we screened the gene expressions of EMT-related transcription factors, Slug, ZEB1, Snail and Twist, showing an enhancement in Slug and Twist expressions in PC-9-GR compared to PC-9 cells. Moreover, PC-9-GR cells possessed more spindle mesenchymal-like phenotypes whereas most of PC-9 cells were round epithelial-like cells, confirming EMT during the development of gefitinib resistance (**Figure 3E**). Importantly, our results uncovered that the cooperative effect of PAR2 and EGFR inhibitors in reversing EMT (**Figures 3F–J**). P2pal-18S markedly potentiated gefitinib to increase the protein expression of E-cadherin and decrease vimentin (~2-fold) in both sensitive and resistant cells whereas gefitinib alone did not trigger such effects, suggesting PAR2 antagonism could assist gefitinib to inhibit EMT. The gene expression changes of vimentin, E-cadherin, Slug, Bcl-2 and Bax induced by P2pal-18S and gefitinib were also plotted and compared in the heat map, which revealed that the combination of PAR2 and EGFR blockade significantly prevented Slug-mediated EMT and apoptosis, compared to gefitinib alone (**Figure 3K**). Therefore, inhibition of PAR2 may suppress ERK activation and Slug-mediated EMT to overcome gefitinib resistance in NSCLC cells.

Protease-Activated Receptor 2-Mediated β -Arrestin-Epidermal Growth Factor Receptor-ERK Signaling Axis Was Critical for Overcoming Gefitinib Resistance in Non-Small Cell Lung Cancer Cells

For deeply understanding of its molecular mechanism, we looked into the role of the receptor transactivation-mediated signaling

pathway in NSCLC cell functions related to gefitinib resistance. β -arrestin is considered as a crucial factor regulating EGFR transactivation while PAR2 could promote β -arrestin to drive EGFR transactivation and downstream ERK signaling (Köse, 2017). Similar to previous studies, barbadin as a β -arrestin1/2 inhibitor effectively facilitated gefitinib to impair phosphorylation of EGFR and ERK, uncovering the participation of β -arrestin in EGFR transactivation (**Figures 4A–D**). We then combined gefitinib with barbadin or an ERK inhibitor (FR180204) to treat PC-9 and PC-9-GR cells, in order to investigate participations of PAR2-mediated β -arrestin and ERK signaling in gefitinib resistance. As shown in **Figures 4E–H** and **Supplementary Figure S4**, either barbadin or FR180204 notably enhanced gefitinib inhibition in NSCLC cell viability and migration (~2-fold) compared to gefitinib alone, indicating potential roles of β -arrestin and ERK signaling in reversing resistance to gefitinib. Furthermore, with inhibition of β -arrestin or ERK, EMT was suppressed by gefitinib treatments since there were increased expression of E-cadherin and decreased expression of vimentin (**Figures 4I,K,M,O**, **Supplementary Figure S5**). The bcl-2/bax ratio were also largely down-regulated when addition of barbadin or FR180204 into gefitinib in PC-9 and PC-9-GR cells, revealing participations of β -arrestin or ERK in reactivating gefitinib inhibition in apoptosis (**Figures 4I–P**). Thus, it suggested that PAR2 inhibition may reverse NSCLCs resistant to gefitinib through the β -arrestin-EGFR-ERK signaling.

Protease-Activated Receptor 2 Inhibition Augmented Gefitinib to Attenuate Tumor Growth by Preventing ERK Activation *in vivo*

The therapeutic benefit of PAR2 antagonism in reversing gefitinib resistance was further investigated in a PC-9-GR xenograft model. The combination treatment of P2pal-18S and gefitinib notably augmented the *in vivo* antitumor effect whereas gefitinib itself exhibited little therapeutic ability for 15 days (**Figure 5A**). P2pal-18S largely facilitated gefitinib to slow down and inhibit tumor growth with ~3-fold decrease of tumor volume (**Supplementary Figure S6**, **Figure 5B**, *** $p < 0.001$). Moreover, H&E staining results showed that combination of P2pal-18S and gefitinib triggered abundant cell necrosis (~90%, green arrow) in tumor tissues compared to negative control and gefitinib alone (**Figure 5C**). Cells in the tumor tissues from combination treatment group were loosely arranged with disintegration, lyzed nuclei and eosinophilic cell fragments, whereas there were only a small number of non-necrotic tumor cells.

To confirm the underlying mechanism of PAR2 inhibition *in vivo*, we studied the key regulatory factor, ERK, in tumor tissues from drug-treated xenograft mice. Unsurprisingly, the combination of P2pal-18S and gefitinib notably restricted protein levels of phospho-ERK (~2.5 fold) in PC-9-GR tumors compared to gefitinib alone detected by western blot analysis (**Figure 5D**), suggesting that PAR2 inhibition may reactivate gefitinib to block PC-9-GR tumor growth via limiting ERK activation, which consistent with previous *in vitro* results.

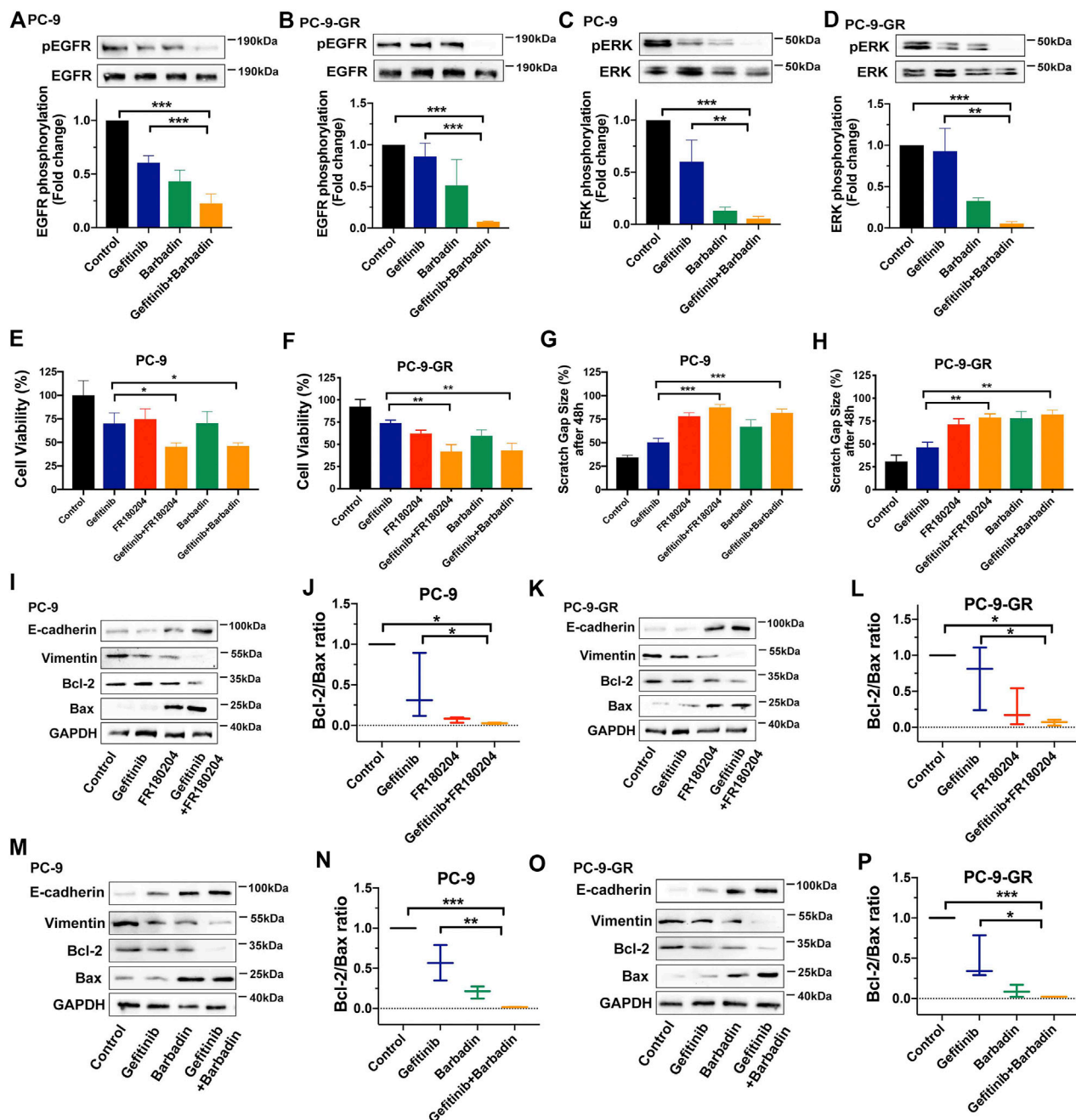


FIGURE 4 | PAR2 reversed NSCLC cell resistant to gefitinib via β -arrestin-EGFR-ERK signaling. (A–D). A β -arrestin inhibitor (Barbadin, 30 μ M) facilitated gefitinib to block phosphorylation of EGFR and ERK in PC-9 (A, C) and PC-9-GR cells (B, D); (E–F). Either barbadin or ERK inhibitor (FR180204, 10 μ M) largely enhanced inhibitory effects of gefitinib in cell viability of PC-9 (E) and PC-9-GR (F); (G–H). Barbadin or FR180204 also promoted gefitinib to attenuate cell migration of PC-9 (G) and PC-9-GR (H); (I–L). Addition of FR180204 assisted gefitinib to up-regulate or down-regulate expressions of E-cadherin, vimentin, bcl-2 and bax, suggesting β -arrestin and ERK related to PAR2-mediated EMT and apoptosis (I, K). The bcl-2/bax ratios were also calculated (J, L); (M–P). Barbadin also enhanced gefitinib to modulate EMT- or apoptosis-related gene expressions in PC-9 (M) and PC-9-GR cells (O), while bcl-2/bax ratios were presented (M, P). * $p < 0.05$, ** $p < 0.01$, *** $p < 0.001$.

DISCUSSION

GPCRs are the largest membrane receptor family and widely investigated drug targets, which exhibit a crosstalk with RTKs family including EGFR. Although GPCR-mediated EGFR

transactivation was identified as a crucial mechanism in modulating a variety of tumor cell signaling and functions (Köse, 2017), therapeutic potentials of GPCRs have been rarely probed in EGFR-TKI resistance. A recent study showed that a GPCR membrane receptor, CXCR7, could facilitate NSCLC

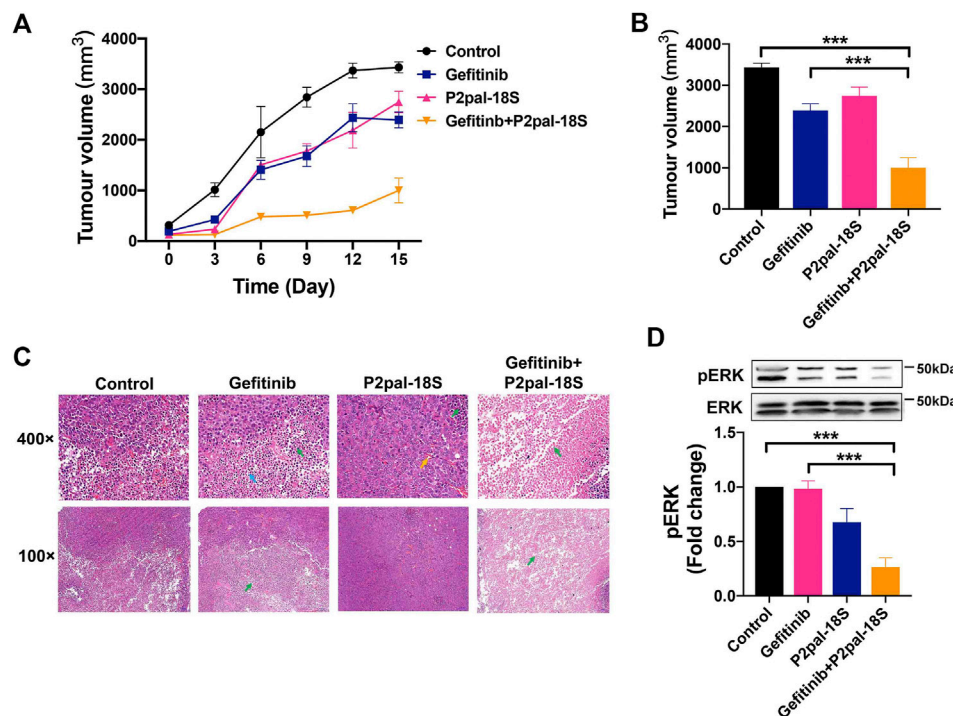


FIGURE 5 | PAR2 inhibition reactivated gefitinib to inhibit tumor growth via ERK signaling *in vivo*. **(A)** The combination of P2pal-18S and gefitinib significantly attenuated PC-9-GR tumor growth; **(B)** P2pal-18S promoted gefitinib to decrease tumor growth whereas gefitinib exhibited little inhibitory effects; **(C)** The H&E staining analysis of tumor tissues with different treatments were detected; **(D)** P2pal-18S facilitated gefitinib to inhibit phosphorylation of ERK in PC-9-GR tumor tissues. Tumor cell necrosis (green), blood capillary (yellow), neutrophil (blue), *** $p < 0.001$.

resistant to gefitinib via reactivating ERK signaling (Becker et al., 2019), but the possible participation of receptor transactivation in molecular mechanism has not been extensively reported. We found overexpression of PAR2 that belongs to GPCRs in lung tumor tissues from patients compared to normal controls while PAR2 expression was highly related to overall survival of patients, indicating a promising role of PAR2 in lung tumor progression (Figures 1A–C, Supplementary Figure S1). More importantly, we found that PAR2 expression was notably elevated in NSCLC cells during the generation of gefitinib resistance (Figure 1G) and this was consistent with a previous multiple analysis of GPCRs expressions in gefitinib-resistant NSCLC cells (Kuzumaki et al., 2012). PAR2 can transactivate EGFR (Kawao et al., 2005; Huang et al., 2013; Michel et al., 2014), and P2pal-18S as a PAR2 inhibitor cooperatively augmented gefitinib to attenuate phosphorylation of EGFR in both gefitinib-sensitive and -resistant NSCLC cells (Figures 1D,H), which suggested that the inhibition of receptor transactivation may affect drug resistance. Moreover, several studies have been reported that PAR2 could modulate numerous cancer cell functions, such as proliferation, migration and apoptosis, by EGFR transactivation or itself (Darmoul et al., 2004; Michel et al., 2014; Arakaki et al., 2018; Pawar et al., 2019). It is not hard to speculate that PAR2 inhibition may attenuate tumor cell signaling pathways and functions to reverse gefitinib resistance in NSCLC, but there is a lack of such investigations. Our findings showed that a synergic effect of the PAR2 inhibitor and gefitinib in preventing cell

viability in gefitinib-sensitive cell PC-9, acquired resistant cell PC-9-GR and primary resistant cell A549 (Figures 1I–K), revealing targeting PAR2 could sensitive NSCLC responses to gefitinib. Moreover, PAR2 blockade exhibited a stronger sensitization effect in PC-9-GR cells than in PC-9 cells. This reversal effect of PAR2 inhibition was further uncovered in enhancing gefitinib to modulate NSCLC cell migration and apoptosis (Figure 2, Supplementary Figure S3). Moreover, a PAR2 inhibitor markedly reactivated gefitinib to prevent tumor growth in PC-9-GR xenograft mice (Figure 5), confirming that PAR2 inhibition could overcome gefitinib resistance *in vivo*.

Moreover, it has been reported that some cell signaling pathways and histological changes not only involved in transactivation of PAR2 and EGFR, but also promoted gefitinib resistance in NSCLC (Michel et al., 2014; Rotow and Bivona, 2017). However, rare studies attempted to linking signaling pathways in EGFR-TKI resistance to PAR2 regulation. ERK signaling as a compensatory downstream signaling promotes the development of gefitinib resistance whereas combination of MEK/ERK and EGFR inhibitors could prevent EGFR-TKI resistance (Tricker et al., 2015). Our results uncovered the involvement of ERK signaling upon EGFR transactivation in targeting PAR2 overcoming gefitinib, since phosphorylation of ERK was largely increased in gefitinib-resistant cells and PAR2 blockade promoted gefitinib to attenuate ERK activation (Figures 3A–C). Furthermore, we observed a loss of E-cadherin and an increase of vimentin,

which are the hallmark of EMT, in gefitinib-resistant NSCLC cells compared to sensitive cells (**Figures 3A,D**). This is in accordance with previous reports on the existence of EMT as a histological transformation during generation of EGFR-TKI resistance (Weng et al., 2019). There are numerous attempts in exploring therapeutic approaches for targeting EMT to overcome EGFR-TKI resistance, e.g., metformin, gene knockout or pharmacological inhibition of FGFR or a transcription factor, Twist1 (Li et al., 2014; Raoof et al., 2019; Yochum et al., 2019). Meanwhile, EMT can be triggered by PAR2 activation in lung cancer cells and inhibition of PAR2 can stimulate prevention of EMT and cell migration (Sun et al., 2018; Tsai et al., 2018). When NSCLC became resistance to gefitinib, EMT could not be blocked by gefitinib whereas addition of a PAR2 inhibitor notably sensitized gefitinib to up-regulate E-cadherin and down-regulate vimentin, consequently overcoming EMT-related drug resistance (**Figures 3F–K**). Furthermore, a transcription factor Slug, but not ZEB1, Snail or Twist, actively involved in this PAR2-mediated EMT in gefitinib resistance (**Figures 3D,K**).

Alternatively, GPCRs have been discovered to stimulate key mediators, such as β -arrestin, SRC or MMP, to transactivate EGFR and downstream signaling (Bhola and Grandis, 2008; Köse, 2017). Our work also uncovered that β -arrestin mediated transactivation between PAR2 and EGFR in gefitinib-resistant NSCLC since inhibition of β -arrestin immediately impaired phosphorylation of EGFR and ERK (**Figures 4A–D**). Moreover, previous studies reported that a variety of PAR2-mediated cancer cell functions were depending on ERK signaling pathways (Yau et al., 2013; Michel et al., 2014; Jiang et al., 2017). Inhibition of either β -arrestin or ERK augmented gefitinib to impair EMT, migration and proliferation in PC-9-GR cells (**Figure 4E–P**), revealing β -arrestin-ERK signaling as a principal pathway for targeting PAR2 in reversing gefitinib-resistant NSCLC cells. The inhibition of PAR2 also notably facilitated gefitinib to slow down and block PC-9-GR tumor growth, while phosphorylation of ERK was markedly attenuated in tumor tissues from the combination treatment group, *in vivo* confirming targeting PAR2 could overcome gefitinib in NSCLC via ERK signaling pathway (**Figure 5**).

In summary, we first revealed that the novel therapeutic potential of PAR2 inhibition in reversing NSCLC resistance to gefitinib resistance and its molecular mechanism. PAR2 expression was markedly elevated in NSCLC tumor progression and gefitinib resistance, indicating the participation of PAR2 in NSCLC resistant to gefitinib. Targeting PAR2 facilitated the effect of gefitinib in EMT, cell proliferation, migration and apoptosis in gefitinib-sensitive and -resistant NSCLC cells through blocking β -arrestin-ERK signaling upon EGFR transactivation. The combination of a PAR2 inhibitor and gefitinib in PC-9-GR xenograft model exhibited larger inhibition of tumor growth

and phosphorylation of ERK, confirming that the reversal effect of PAR2 inhibition as well as the underlying mechanism *in vivo*. This study not only suggested PAR2 as a novel therapeutic target for gefitinib resistance but also uncovered a new receptor-mediated mechanism for overcoming NSCLC resistant to gefitinib. Meanwhile, we provided a preclinical evidence for the combination of a PAR2 inhibitor and gefitinib as a promising approach to reverse drug resistance and improve the overall survival of NSCLC patients.

DATA AVAILABILITY STATEMENT

The original contributions presented in the study are included in the article/**Supplementary Material**. Further inquiries can be directed to the corresponding authors.

ETHICS STATEMENT

The animal study was reviewed and approved by the Animal Use and Care Committee of Southwest Jiaotong University.

AUTHOR CONTRIBUTIONS

YJ and CM participated in research design; YJ and XZ conducted experiments; YJ performed data analysis and wrote the original manuscript; XF, YW and CM contributed to the writing of the manuscript.

FUNDING

This work was supported by the National Natural Science Foundation of China (No. 82003784, No. 81872789); the Fundamental Research Funds for the Central Universities (No. 2682019CX73); Sichuan Science and Technology Program (No. 2021JDRC0145); Scientific Research Foundation for the Returned Overseas Chinese Scholars by Ministry of Personnel of Sichuan Province; and the Program for “Qingmiao” Excellent Talents in Southwest Jiaotong University.

SUPPLEMENTARY MATERIAL

The Supplementary Material for this article can be found online at: <https://www.frontiersin.org/articles/10.3389/fphar.2021.625289/full#supplementary-material>.

REFERENCES

- Arakaki, A., Pan, W.-A., and Trejo, J. (2018). GPCRs in Cancer: protease-activated receptors, endocytic adaptors and signaling. *Ijms* 19, 1886–1924. doi:10.3390/ijms19071886
- Becker, J. H., Gao, Y., Soucheray, M., Pulido, I., Kikuchi, E., Rodríguez, M. L., et al. (2019). CXCR7 reactivates ERK signaling to promote resistance to EGFR kinase inhibitors in NSCLC. *Cancer Res.* 79, 4439–4452. doi:10.1158/0008-5472.can-19-0024
- Bhola, N. E., and Grandis, J. R. (2008). Crosstalk between G-protein-coupled receptors and epidermal growth factor receptor in cancer. *Front. Biosci.* 13, 1857–1865. doi:10.2741/2805

- Caruso, R., Pallone, F., Fina, D., Gioia, V., Peluso, I., Caprioli, F., et al. (2006). Protease-activated receptor-2 activation in gastric cancer cells promotes epidermal growth factor receptor trans-activation and proliferation. *Am. J. Pathol.* 169, 268–278. doi:10.2353/ajpath.2006.050841
- Darmoul, D., Gratio, V., Devaud, H., and Laburthe, M. (2004). Protease-activated receptor 2 in colon cancer. *J. Biol. Chem.* 279, 20927–20934. doi:10.1074/jbc.m401430200
- Daub, H., Ulrich Weiss, F., Wallasch, C., and Ullrich, A. (1996). Role of transactivation of the EGF receptor in signalling by G-protein-coupled receptors. *Nature* 379, 557–560. doi:10.1038/379557a0
- Goldman, M., Craft, B., Brooks, A., Zhu, J., and Haussler, D. (2018). The UCSC Xena Platform for cancer genomics data visualization and interpretation. Available at: <https://www.biorxiv.org/content/10.1101/326470v3#>.
- Gridelli, C., Rossi, A., Carbone, D. P., Guarize, J., Karachaliou, N., Mok, T., et al. (2015). Non-small-cell lung cancer. *Nat. Rev. Dis. Primers.* 1, 15009 1–15. doi:10.1038/nrdp.2015.9
- Herbst, R. S., Morgensztern, D., and Boshoff, C. (2018). The biology and management of non-small cell lung cancer. *Nature* 553, 446–454. doi:10.1038/nature25183
- Hirsch, F. R., Suda, K., Wiens, J., and Bunn, P. A., Jr (2016). New and emerging targeted treatments in advanced non-small-cell lung cancer. *The Lancet* 388, 1012–1024. doi:10.1016/s0140-6736(16)31473-8
- Huang, S. H., Li, Y., Chen, H. G., Rong, J., and Ye, S. (2013). Activation of proteinase-activated receptor 2 prevents apoptosis of lung cancer cells. *Cancer Invest.* 31, 578–581. doi:10.3109/07357907.2013.845674
- Jänne, P. A., Yang, J. C. H., Kim, D. W., Planchard, D., Ohe, Y., Ramalingam, S. S., et al. (2015). AZD9291 in EGFR inhibitor-resistant non-small-cell lung cancer. *N. Engl. J. Med.* 372, 1689–1699. doi:10.1056/nejmoa1411817
- Jiang, Y., Lim, J., Wu, K. C., Xu, W., Suen, J. Y., and Fairlie, D. P. (2020). PAR2 induces ovarian cancer cell motility by merging three signalling pathways to transactivate EGFR. *Br. J. Pharmacol.* 178, 913. doi:10.1111/bph.15332
- Jiang, Y., Yau, M. K., Kok, W. M., Lim, J., Wu, K. C., Liu, L., et al. (2017). Biased signaling by agonists of protease activated receptor 2. *ACS Chem. Biol.* 12, 1217–1226. doi:10.1021/acscchembio.6b01088
- Jiang, Y., Yau, M.-K., Lim, J., Wu, K.-C., Xu, W., Suen, J. Y., et al. (2018). A potent antagonist of protease-activated receptor 2 that inhibits multiple signaling functions in human cancer cells. *J. Pharmacol. Exp. Ther.* 364, 246–257. doi:10.1124/jpet.117.245027
- Kawao, N., Nagataki, M., Nagasawa, K., Kubo, S., Cushing, K., Wada, T., et al. (2005). Signal transduction for proteinase-activated receptor-2-triggered prostaglandin E2 formation in human lung epithelial cells. *J. Pharmacol. Exp. Ther.* 315, 576–589. doi:10.1124/jpet.105.089490
- Köse, M. (2017). GPCRs and EGFR - cross-talk of membrane receptors in cancer. *Bioorg. Med. Chem. Lett.* 27, 3611–3620. doi:10.1016/j.bmcl.2017.07.002
- Kuzumaki, N., Suzuki, A., Narita, M., Hosoya, T., Nagasawa, A., Imai, S., et al. (2012). Multiple analyses of G-protein coupled receptor (GPCR) expression in the development of gefitinib-resistance in transforming non-small-cell lung cancer. *PLoS One* 7, e44368. doi:10.1371/journal.pone.0044368
- Li, L., Han, R., Xiao, H., Lin, C., Wang, Y., Liu, H., et al. (2014). Metformin sensitizes EGFR-TKI-resistant human lung cancer cells in vitro and in vivo through inhibition of IL-6 signaling and EMT reversal. *Clin. Cancer Res.* 20, 2714–2726. doi:10.1158/1078-0432.ccr-13-2613
- Liu, K., Liu, P. C., Liu, R., and Wu, X. (2015). Dual AO/EB staining to detect apoptosis in osteosarcoma cells compared with flow cytometry. *Med. Sci. Monit. Basic Res.* 21, 15–20.
- Marcucci, F., Stassi, G., and De Maria, R. (2016). Epithelial-mesenchymal transition: a new target in anticancer drug discovery. *Nat. Rev. Drug Discov.* 15, 311–325. doi:10.1038/nrd.2015.13
- Michel, N., Heuzé-Vourc'h, N., Lavergne, E., Parent, C., Jourdan, M. L., Vallet, A., et al. (2014). Growth and survival of lung cancer cells: regulation by kallikrein-related peptidase 6 via activation of proteinase-activated receptor 2 and the epidermal growth factor receptor. *Biol. Chem.* 395, 1015–1025. doi:10.1515/hsz-2014-0124
- Network, C. G. A. R. (2014). Comprehensive molecular profiling of lung adenocarcinoma. *Nature* 511, 543–550. doi:10.1038/nature13385
- Pawar, N. R., Buzza, M. S., and Antalis, T. M. (2019). Membrane-anchored serine proteases and protease-activated receptor-2-mediated signaling: Co-conspirators in cancer progression. *Cancer Res.* 79, 301–310. doi:10.1158/0008-5472.can-18-1745
- Qi, W., Zhou, X., Wang, J., Zhang, K., Zhou, Y., Chen, S., et al. (2020). Cordyceps sinensis polysaccharide inhibits colon cancer cells growth by inducing apoptosis and autophagy flux blockage via mTOR signaling. *Carbohydr. Polym.* 237, 116113. doi:10.1016/j.carbpol.2020.116113
- Raouf, S., Mulford, I. J., Frisco-Cabanas, H., Nangia, V., Timonina, D., Labrot, E., et al. (2019). Targeting FGFR overcomes EMT-mediated resistance in EGFR mutant non-small cell lung cancer. *Oncogene* 38, 6399–6413. doi:10.1038/s41388-019-0887-2
- Rotow, J., and Bivona, T. G. (2017). Understanding and targeting resistance mechanisms in NSCLC. *Nat. Rev. Cancer* 17, 637–658. doi:10.1038/nrc.2017.84
- Shi, K., Queiroz, K. C. S., Stap, J., Richel, D. J., and Spek, C. A. (2013). Protease-activated receptor-2 induces migration of pancreatic cancer cells in an extracellular ATP-dependent manner. *J. Thromb. Haemost.* 11, 1892–1902. doi:10.1111/jth.12361
- Shou, J., You, L., Yao, J., Xie, J., Jing, J., Jing, Z., et al. (2016). Cyclosporine a sensitizes human non-small cell lung cancer cells to gefitinib through inhibition of STAT3. *Cancer Lett.* 379, 124–133. doi:10.1016/j.canlet.2016.06.002
- Sun, L., Li, P. B., Yao, Y. F., Xiu, A. Y., Peng, Z., Bai, Y. H., et al. (2018). Proteinase-activated receptor 2 promotes tumor cell proliferation and metastasis by inducing epithelial-mesenchymal transition and predicts poor prognosis in hepatocellular carcinoma. *Wjg* 24, 1120–1133. doi:10.3748/wjg.v24.i10.1120
- Tricker, E. M., Xu, C., Uddin, S., Capelletti, M., Ercan, D., Ogino, A., et al. (2015). Combined EGFR/MEK inhibition prevents the emergence of resistance in EGFR-mutant lung cancer. *Cancer Discov.* 5, 960–971. doi:10.1158/2159-8290.cd-15-0063
- Tsai, C.-C., Chou, Y.-T., and Fu, H.-W. (2018). Protease-activated receptor 2 induces migration and promotes Slug-mediated epithelial-mesenchymal transition in lung adenocarcinoma cells. *BBA-Mol. Cell Res.* 1866, 486–503.
- Weng, C.-H., Chen, L.-Y., Lin, Y.-C., Shih, J.-Y., Lin, Y.-C., Tseng, R.-Y., et al. (2019). Epithelial-mesenchymal transition (EMT) beyond EGFR mutations per se is a common mechanism for acquired resistance to EGFR TKI. *Oncogene* 38, 455–468.
- Yau, M. K., Liu, L., and Fairlie, D. P. (2013). Toward drugs for protease-activated receptor 2 (PAR2). *J. Med. Chem.* 56, 7477–7497.
- Yochum, Z. A., Cades, J., Wang, H., Chatterjee, S., Simons, B. W., O'Brien, J. P., et al. (2019). Targeting the EMT transcription factor twist1 overcomes resistance to EGFR inhibitors in EGFR-mutant non-small-cell lung cancer. *Oncogene* 38, 656–670.
- Yun, C. H., Mengwasser, K. E., Toms, A. V., Woo, M. S., Greulich, H., Wong, K. K., et al. (2008). The T790M mutation in EGFR kinase causes drug resistance by increasing the affinity for ATP. *Proc. Natl. Acad. Sci. U. S. A.* 105, 2070–2075.
- Zhang, R. J., Shi, Y., Zheng, J., Mao, X. M., Liu, Z. Y., Chen, Q. X., et al. (2018). Effects of polysaccharides from abalone viscera (*Haliotis discus hannai* Ito) on MGC 803 cells proliferation. *Int. J. Biol. Macromol.* 106, 587–595.

Conflict of Interest: The authors declare that the research was conducted in the absence of any commercial or financial relationships that could be construed as a potential conflict of interest.

Copyright © 2021 Jiang, Zhuo, Fu, Wu and Mao. This is an open-access article distributed under the terms of the Creative Commons Attribution License (CC BY). The use, distribution or reproduction in other forums is permitted, provided the original author(s) and the copyright owner(s) are credited and that the original publication in this journal is cited, in accordance with accepted academic practice. No use, distribution or reproduction is permitted which does not comply with these terms.



Photothermal Therapy *via* NIR II Light Irradiation Enhances DNA Damage and Endoplasmic Reticulum Stress for Efficient Chemotherapy

Qingduo Kong^{1,2,3}, Dengshuai Wei³, Peng Xie³, Bin Wang³, Kunyi Yu^{3*}, Xiang Kang^{4*} and Yongjun Wang^{1*}

OPEN ACCESS

Edited by:

Jianxun Ding,
Changchun Institute of Applied
Chemistry, Chinese Academy of
Sciences, China

Reviewed by:

Haihua Xiao,
Chinese Academy of Sciences (CAS),
China
Zhiqiang Yu,
Southern Medical University, China
Ping'an Ma,
Changchun Institute of Applied
Chemistry, Chinese Academy of
Sciences, China
Yunlu Dai,
University of Macau, China

*Correspondence:

Kunyi Yu
yuky14@tsinghua.org.cn
Xiang Kang
kchigo@163.com
Yongjun Wang
wyongjunhys@sina.com

Specialty section:

This article was submitted to
Pharmacology of Anti-Cancer Drugs,
a section of the journal
Frontiers in Pharmacology

Received: 20 February 2021

Accepted: 01 April 2021

Published: 29 April 2021

Citation:

Kong Q, Wei D, Xie P, Wang B, Yu K,
Kang X and Wang Y (2021)
Photothermal Therapy *via* NIR II Light
Irradiation Enhances DNA Damage
and Endoplasmic Reticulum Stress for
Efficient Chemotherapy.
Front. Pharmacol. 12:670207.
doi: 10.3389/fphar.2021.670207

¹Department of Obstetrics and Gynecology, Peking University International Hospital, Beijing, China, ²Clinical Medical College, Weifang Medical University, Weifang, China, ³Beijing National Laboratory for Molecular Sciences, State Key Laboratory of Polymer Physics and Chemistry, Institute of Chemistry, Chinese Academy of Sciences, Beijing, China, ⁴Department of Obstetrics and Gynecology, Union Hospital, Tongji Medical College, Huazhong University of Science and Technology, Wuhan, China

Ovarian cancer has the highest death rate in gynecologic tumors and the main therapy for patients with advanced is chemotherapy based on cisplatin. Additionally, hyperthermic intraperitoneal has been used in clinic to obtain better efficacy for patients. Hence, combined photothermal therapy with platinum drugs in a new delivery system might bring new hope for ovarian cancer. A reduction sensitive polymer encapsulating a Pt (IV) prodrug and a near infrared II (NIR II) photothermal agent IR1048 to form nanoparticles were reported to enhance the efficacy of ovarian cancer treatment. At the same time, endoplasmic reticulum stress indicates an imbalance in proteostasis which probably caused by extrinsic stress such as chemotherapy and the temperature changed. The efficacy of nanoparticles containing Pt (IV) and IR1048 under NIR II light might be caused *via* increased DNA damage and endoplasmic reticulum (ER) stress.

Keywords: chemotherapy, photothermal therapy, mild hyperthermia, NIR II light, DNA damage, endoplasmic reticulum stress key

INTRODUCTION

Ovarian cancer is one of the most common malignant tumors in gynecology. Once diagnosed, 70% of ovarian cancer patients are in advanced stage, and nearly no targeted drugs are available (Wright et al., 2016; Grossman et al., 2018). The main treatment of ovarian cancer is still chemotherapy based on cisplatin (Konner et al., 2011). However, cisplatin resistance as well as its serious side effects hindered its application (Rottenberg et al., 2021). To this end, the development of platinum drugs with high efficiency and low toxicity combined with a new delivery system might bring new hope (Wang et al., 2019; Xiaoxu et al., 2019).

Extensive progress has been made on photothermal therapy (PTT) recently (Yang et al., 2020; Wen et al., 2021). The mechanism of PTT is to convert light energy into local heat energy through photothermal agents, which can be used to eradicate tumor through thermal ablation (Meng et al., 2018). The advantages such as non-invasive operation, high specificity, make it a promising candidate for cancer therapy (Liu et al., 2011; Ruan et al., 2019; Jędrzak et al., 2020). Numerous PTT agents with high photo conversion efficiency (PCE) have been reported. However, the temperature over 50°C might lead to side effect such as skin burns. Hence, in comparison to conventional PTT which focuses on the high operation temperature, mild hyperthermia lower than

45°C is more desirable for clinical application. Furthermore, PTT with excitation light in NIR II window (1000–1700 nm) has drawn tremendous attention due to the reduced absorption and tissue scattering. It is able to penetrate deep tumor tissue, which is more suitable for the clinic practice (Chen et al., 2020; Yang et al., 2021). In practical clinical scenario, hyperthermic intraperitoneal has already been included in the guideline of 2019 NCCN Guidelines Insights for ovarian cancer (Armstrong et al., 2019).

The ability of cancer cells to respond to extrinsic stress such as chemotherapy or mild hyperthermia depends on their ability to activate appropriate adaptive pathways. In the endoplasmic reticulum (ER), ER stress indicates an imbalance in proteostasis which probably caused by extrinsic stress (Rubio-Patiño et al., 2018). Studies showed that ER stress might be a pathway which caused cell apoptosis (Madden et al., 2019). X-Box binding protein 1 (XBP1), which is an important protein in ER stress pathway, was significantly reduced under this combinational therapy (Chen et al., 2016; Lhomond et al., 2018).

Herein, we hypothesize that mild hyperthermia relying on NIR II laser combined with cisplatin chemotherapy could become a promising strategy to tackle with ovarian cancer (Balakrishnan et al., 2020; Xi et al., 2020). To achieve this, a reduction sensitive block polymer (P1) was firstly synthesized, which is characterized by the presence of numerous disulfide bonds (S-S) in the polymer main chain. Secondly, a hydrophobic Pt (IV) prodrug with aliphatic chains was prepared. Subsequently, P1 and Pt (IV) prodrug were mixed to self-assemble into nanoparticles with Pt (IV) prodrugs (NP-1). To obtain the final nanoparticles with photothermal effect, P1 and Pt (IV) prodrug as well as a IR1048 were mixed to self-assemble into nanoparticles with both Pt (IV) prodrugs and photothermal dyes (NP-2). After NP-2 enter cancer cells *via* endocytosis, they could then be dissociated to release toxic cisplatin in the reductive microenvironment, leading to DNA replication and transcription dysfunction (Mortensen et al., 2020; Zhang et al., 2020). At the same time, the released photothermal IR1048 can be irradiated under 1064 nm laser, resulting in photothermal effect which could further sensitize cisplatin *via* enhanced DNA damage and ER stress. We found here the combination of mild hyperthermia and cisplatin chemotherapy leads to decreased expression of X-Box binding protein 1 (XBP1), an important protein in ER stress pathway. Therefore, the combination of mild hyperthermia with platinum drugs in nanoparticles is of great significance and brings a new perspective to clinical treatment for ovarian cancer.

ARTICLE TYPES

Original Research.

MANUSCRIPT FORMATTING

Materials and Methods

Materials

Cisplatin were purchased from Shangdong Boyuan Chemical Company. 3- (4,5-dimethyl-2-thiazolyl)-2,5-diphenyl-2-H-

tetrazolium bromide (MTT), 2- (4-amidinophenyl)-1H-indole-6-carboxamide (DAPI), methyl sulfoxide (DMSO), ethanol, sodium azide (NaN₃), IR1048 were purchased from Sigma-Aldrich (Shanghai, China). RPMI 1640, fetal bovine serum (FBS), penicillin-streptomycin solution, trypsin, Annexin V-FITC/PI apoptosis detection kit and cell cycle detection kit were purchased from Keygen Biotech. Hydrogen peroxide, N, N-Dimethyl formamide (DMF) and methoxyl-poly (ethylene glycol) (molecular weight = 5000) were purchased from Beijing chemical works.

Preparation of Pt(IV)-OH

Cisplatin (1.67 mmol, 0.5 g) was suspended in H₂O₂. The mixture was stirred at 40°C overnight and clear solution was produced. After the mixture down to the room temperature, much of needle-like crystal was precipitated. The product was washed many times with acetone and dried in vacuum oven. The yield rate was 80%. ESI-MS (positive mode) for Cl₂H₈N₂O₂Pt: *m/z* [M + H]⁺ Calcd: 332.96, Found: 333.0.

Preparation of C₈-Pt(IV)-C₈ [Pt(IV)]

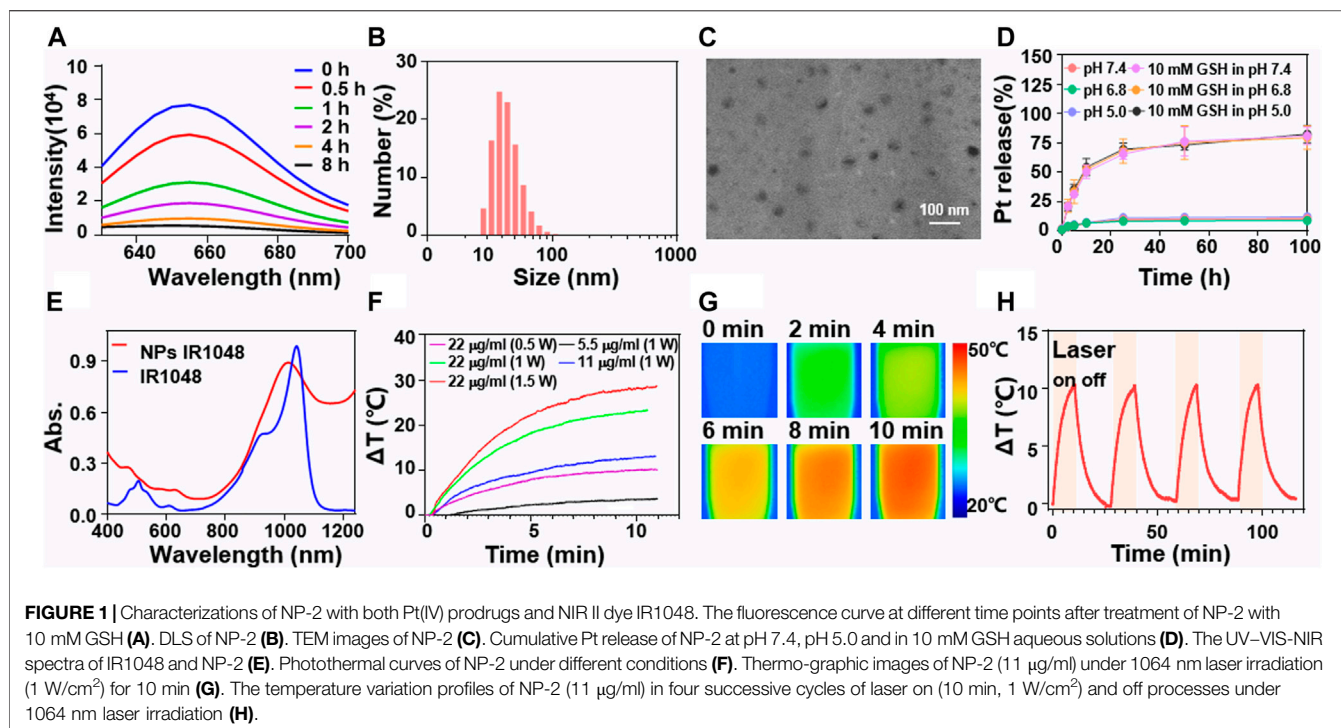
Pt (IV)-OH (1.2 mmol, 400 mg) and 1-isocyanatoctane (2.4 mmol, 0.744 ml) were suspended in 5 ml anhydrous DMF. The solution is stirred at 70°C for 8 h. The solvent is evaporated, the residual substance is dissolved by a small amount of methanol, and the methanol solution is added with ice ethyl ether under stirring to collect the precipitate products. Products were dried under the vacuum to obtain C₈-Pt (IV)-C₈ [Pt (IV)] (28%) as light yellow solid. ¹H NMR (300 MHz, DMSO) 6.61 (7 H, d, J 43.6), 2.88 (2 H, d, J 6.0), 1.29 (12 H, d, J 31.9), 0.86 (3 H, t, J 6.5). ESI-MS (positive mode) for C₁₈H₄₃C₁₂N₄O₄Pt⁺: *m/z* [M + H]⁺ Calcd: 644.23, Found: 644.24.

Preparation of P1

DSB ((2,2'-disulfanediy)bis (ethan-1-ol), 0.20 mmol, 30.8 mg) and CHTA (hexahydro-1H, 3H-benzo [1,2-c:4,5-c']difuran-1,3,5,7-tetraone, 0.21 mmol, 44.8 mg) were added in 5 ml anhydrous DMF. After magnetic stirring for 24 h, mPEG₅₀₀₀-OH (2 mmol, 110 mg) was added in the reaction system. After magnetic stirring for another 24 h, under sonication, 5 ml mixture was added in 15 ml deionized water, followed by dialysis in a dialysis bag (molecular weight cut-off, 5000 Da). After 72 h, the solution was freeze-dried under reduced pressure to obtained 112 mg polymer named P1.

Preparation of NP-1 and NP-2

20 mg P1 and 2 mg Pt (IV) were weighed and fully dissolved in 1 ml DMF. This mixture was stirred for 5 min. Then 10 ml water was added to the above solution in dropwise. After stirring for 10 min, it was subjected to dialysis for 12 h using dialysis bag (molecular weight cut-off, 3500 Da). The product was named NP-1. At the same time, 20 mg P1, 2 mg Pt (IV) and 1 mg IR1048 were weighed and fully dissolved in 1 ml DMF. This mixture was stirred for 5 min. Then 10 ml water was added to the above solution in dropwise. After stirring for 10 min, it was subjected to dialysis for 12 h using dialysis bag (molecular weight cut-off, 3500 Da). The product was named NP-2.



Drug Release of NP-2

Drug release of NP-2 was arisen at pH 7.4, pH 5.0 and in the presence of 10 mmol GSH, respectively. Different pH solutions were prepared in PBS. 1ml of nanoparticles solution was taken into dialysis bag (molecular weight cut-off, 3500 Da) and then immersed in those solutions of different pH as soon as possible. Then, the systems were placed into an incubator shaking at 37°C. At each specific point in time, 1 ml of sample solution was collected and replenish a considerable volume of solution immediately. All the samples were examined by ICP-MS.

Dissociation Kinetics of NP-2

The dissociation kinetics of NP-2 was performed according to report with minor modifications. In brief, P1 (10 mg) were dissolved in 1 ml DMF. 10 μl of Nile Red stock solution (0.05 mg/ml) in THF were added into the mixture. After that, with gentle stirring, 9 ml deionized water were added dropwise to prepare the new nanoparticle. The change in fluorescence curves were recorded at an excitation wavelength of 550 nm and the emission wavelength from 620 to 720 nm by adding 10 mM GSH at different time points. The half-life time ($t_{1/2}$) was calculated based on the fluorescence measurements.

Hyperthermia Effect of NP-2

The hyperthermia effect of NP-2 was monitored under near-infrared light irradiation. Specifically, 1 ml of NP-2 at three different concentration (5.5, 11 and 22 $\mu\text{g/ml}$) was irradiated with 1064 nm near-infrared laser at three different powers (0.5, 1.0 and 1.5 W) respectively. The FLUKE thermal imager was used to determine the solution temperature and the temperature rise curve was recorded.

Cell Lines and Cell Incubation Conditions

A2780 and A2780 DDP cells were gifted from the Medical Department of Jilin University in China. A2780, A2780 DDP cells were incubated in RPMI 1640 media. Culture medium were supplemented with 10% fetal bovine serum, 1% penicillin-streptomycin solution. The cell lines were cultured in 37°C with 5% CO_2 atmosphere.

Nanoparticles Uptake in the Cells

Fluorescent dye Rh B was encapsulated with the P1 to assemble new nanoparticles (termed NPs@Rh B). Cell slides were placed on the bottom of the wells in advance, then A2780 cells at a density of 2×10^4 per well were seeded and incubated at 37°C overnight. The cells were exposed to NPs@Rh B with a final concentration of 2 $\mu\text{g/ml}$ of Rh B for 1, 3 and 6 h. After that, cells were washed with cold PBS and fixed with paraformaldehyde. For cell colocalization, the nuclei were stained with DAPI (blue) and filamentous actin cytoskeleton were strained with phalloidin (green), respectively. Finally, images were immediately captured by confocal laser scanning microscopy (CLSM) at a $\times 100$ magnification.

The intracellular uptake studies of NPs@Rh B were also performed by using flow cytometry. In particular, A2780 cells were seeded in 6-well plates with a density of 2×10^5 cells per well. After incubation overnight, cells were exposed to the above synthesized NPs@Rh B for another 1, 3 and 6 h at 37°C. Next, cells were washed with PBS and harvested by trypsin, and the mean fluorescence intensity (MFI) of cells was detected by flow cytometry.

Cell Relative Viability Studies

MTT assay was used to examine the cell relative viability. A2780, A2780 DDP cells were seeded in 96-well plates with a density of

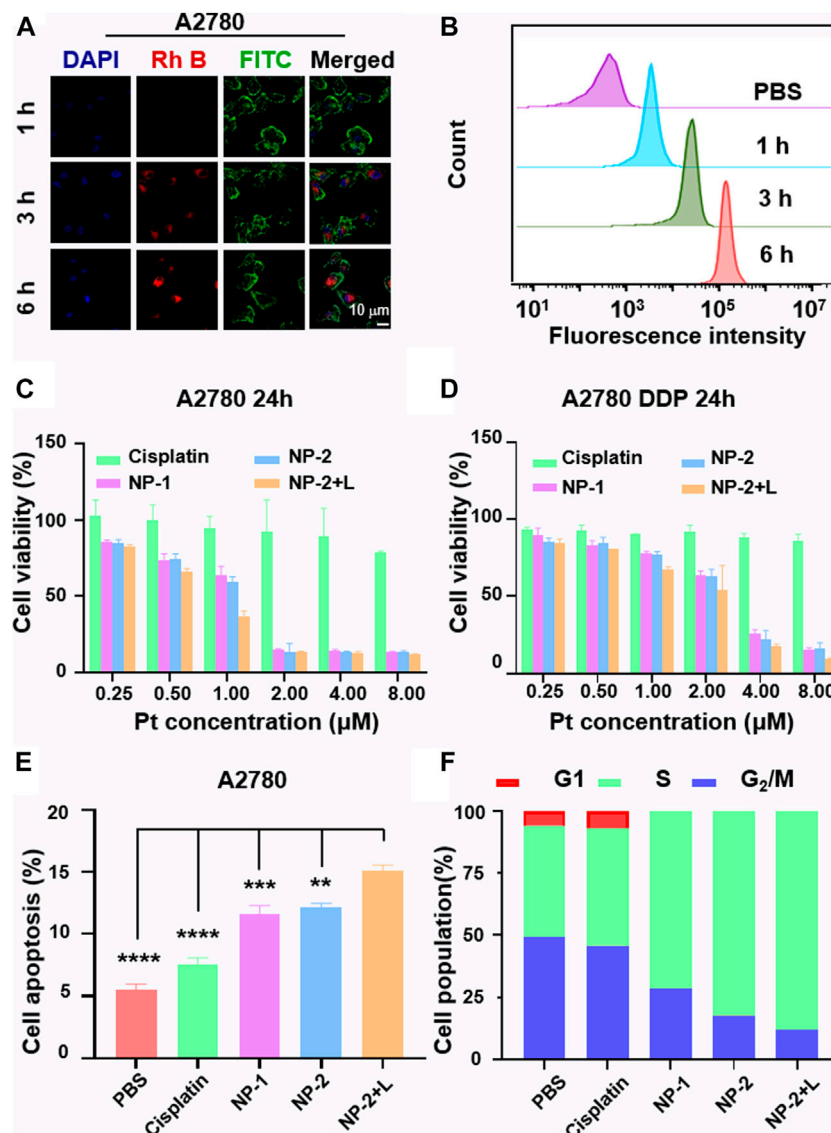


FIGURE 2 | The intracellular uptake of NP-2 and the anticancer activity evaluation. CLSM images of A2780 cells incubated with nanoparticles labelled with Rh B for 1, 3 and 6 h respectively. The blue fluorescence comes from a nuclear dye DAPI. The red fluorescence comes from Rh B in the nanoparticles. The green fluorescence comes from a filamentous actin cytoskeleton dye FITC. The scale bar is 10 μ m (A). Quantification of the intracellular uptake of NP-2 on A2780 via flow cytometry (B). The anticancer activity study of Cisplatin, NP-1, NP-2, NP-2 + L on A2780 and A2780 DDP cells via MTT assay (C) and (D). Cell apoptosis rate induced by Cisplatin, NP-1, NP-2, NP-2 + L on A2780 cells (E). Significance is defined as ** $p < 0.01$, *** $p < 0.001$, **** $p < 0.0001$. Cell cycles of Cisplatin, NP-1, NP-2, NP-2 + L in A2780 cells (F).

8×10^3 per well and cultured at 37 C for 12 h. Cells were treated with cisplatin, NP-1, NP-2 and NP-2 with NIR II irradiation (after treatment for 18 h) with final concentrations (μ M) of 0.25, 0.5, 1, 2, 4, 8 with Pt. After treatment for 24 h, 10% MTT diluted with 1640 was added in the wells. After incubation in 37 C for 4 h, 10% SDS was added in the wells and cells were incubated in 37 C for 12 h in the dark. The results were performed with Molecular Devices.

Apoptosis Studies

A2780 cells were seeded in twelve-well plates at a density of 2×10^5 per well and incubated at 37 C for 12 h. Cisplatin, NP-1,

NP-2, NP-2 with NIR II irradiation (after treatment for 6 h) were added in the wells at the final concentration 1 μ M of Pt. After treatment for 12 h, the media was removed and the cells were washed Three times with cold PBS. Then the cells were harvested and strained with 5 μ l FITC and 5 μ l PI for 10 min in the dark at room temperature respectively. Finally, all the samples were performed with flow cytometry in 1 h.

Cell Cycle Studies

A2780 cells were seeded in twelve-well plates at a density of 2×10^5 per well and incubated at 37 C for 12 h. Cisplatin, NP-1,

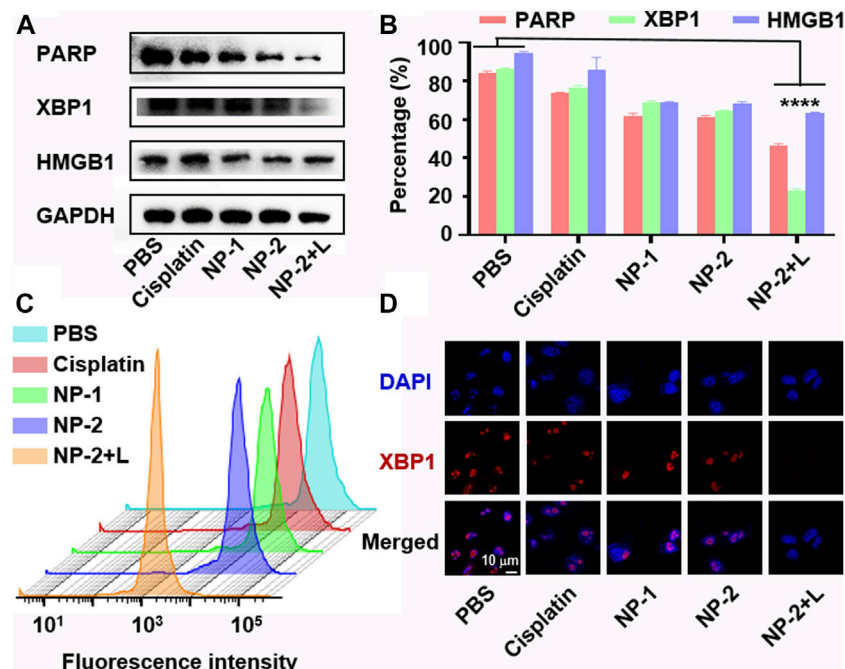


FIGURE 3 | Increased DNA damage and ER stress in cells treated with NP-2 under NIR II light irradiation. Expression of PARP, XBP1, HMGB1 protein in cells treated with Cisplatin, NP-1, NP-2, NP-2+L (A). Quantification of PARP, XBP1, and HMGB1 level in A (B). Quantification of the XBP1 level in A2780 cells via flow cytometry (C). CLSM images showing translocation of XBP1 in A2780 cells treated with Cisplatin, NP-1, NP-2, and NP-2+L respectively (D). Significance is defined as **** $p < 0.0001$.

NP-2, NP-2 with NIR II irradiation (after treatment for 6 h) were added in the wells at the final concentration of $1 \mu\text{M}$ of Pt. After treatment for 12 h, the media was removed and the cells were washed three times with cold PBS. After fixed with 50% ethanol at 4°C for 12 h, the cells were harvested and treated with RNase (100 $\mu\text{g}/\text{ml}$) and propidium iodide (100 $\mu\text{g}/\text{ml}$) at 4°C for 30 min. Finally, all the samples were performed with flow cytometry in 1 h.

Western Blot Assay

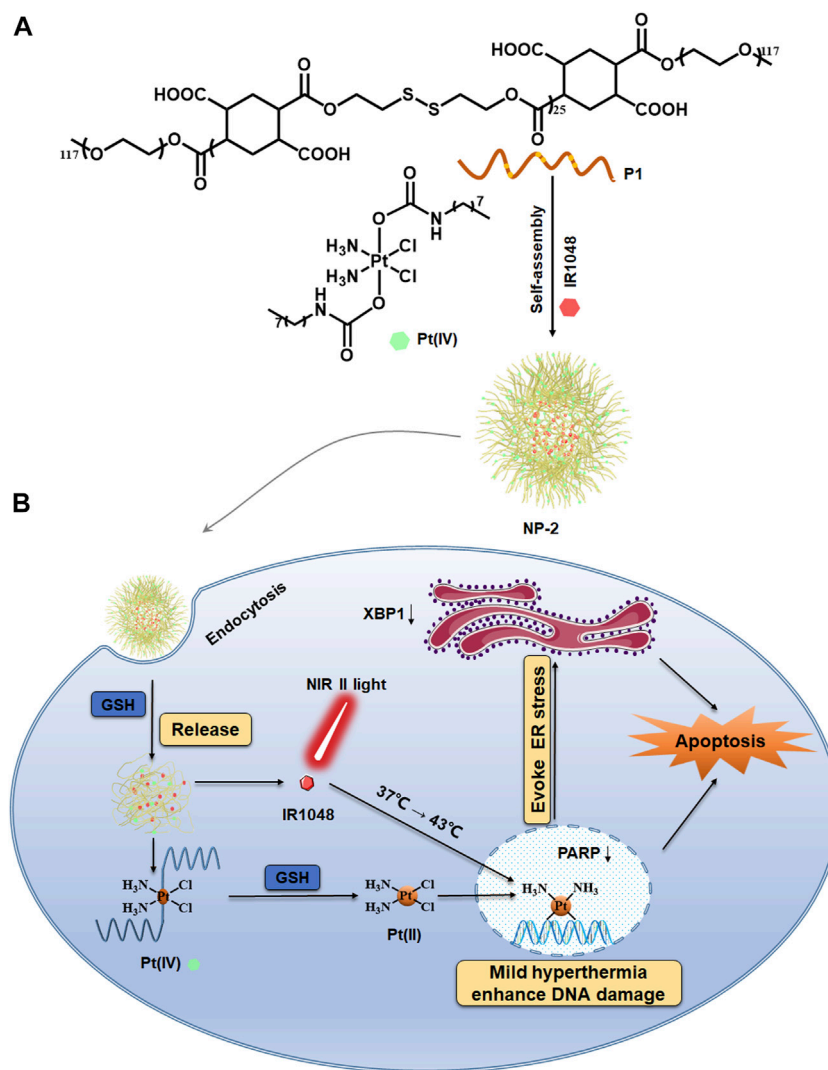
In this study, the following primary antibodies were used: anti-PARP (# 9542, CST), XBP1 (# 40435, CST), HMGB1 (# 3935, CST) and GAPDH (# 5174, CST). Typically, A2780 cells were seeded in 6-well plates at a density of 6×10^5 per well and incubated at 37°C for 12 h. Cisplatin, NP-1, NP-2, NP-2 with NIR II irradiation (after treatment for 18 h) at the final concentration of $1 \mu\text{M}$ of Pt for 24 h separately. Cells were harvested and the lysates were homogenized in RIPA lysis buffer followed by centrifugation (Beyotime, Beijing, China). A total of 30 μg protein was separated by SDS-PAGE and transferred onto a PVDF membrane. Following incubation with the primary antibodies overnight at 4°C , the membranes were washed with TBST and subsequently incubated with horse radish peroxidase (HRP)-conjugated anti-rabbit secondary antibody for 1 h. Bands of interest were analyzed by using image analysis system (Bio-rad, United States of America) according to the manufacturer's instructions. The lysates from the xenografts with different treatments were also homogenized in RIPA for western blot assay. GAPDH was used as the internal control.

Immunofluorescence of XBP1

Cell slides were placed on the bottom of the wells in advance, A2780 cells were seeded in 24-well plates at density of 1×10^5 per well and incubated at 37°C for 12 h. Cisplatin, NP-1, NP-2, NP-2 with NIR II irradiation (after treatment for 18 h) at the final concentration of $1 \mu\text{M}$ of Pt were added. After treatment of 24 h, absorb liquid, and cover cells to a depth of 2–3 mm with 4% formaldehyde diluted in PBS. Cells were fixed for 15 min at room temperature. Then washed three times in PBS for 5 min each. Cells were blocked in blocking buffer for 60 min. Then they were applied diluted primary antibody. They were incubated overnight at 4°C . They were washed three times in PBS for 5 min each. And they were incubated specimen in fluorochrome-conjugated secondary antibody diluted in antibody dilution buffer for 2 h at room temperature in the dark. They were washed three times in PBS for 5 min each. Coverslip slides with DAPI. In the end, images were performed with CLSM.

Flow Cytometry of XBP1

A2780 cells were seeded in 6-well plates with a density of 2×10^5 cells per well. After incubation overnight, incubated with Cisplatin, NP-1, NP-2, NP-2 with NIR II irradiation (after treatment for 18 h) at the final concentration of $1 \mu\text{M}$ of Pt. After treatment, 1 million cells in approximately were in 100 μl 4% formaldehyde. They were fixed for 15 min at room temperature. They were washed by centrifugation with excess PBS. Then, they were added 1 ml PBS and added ice-cold 100% methanol slowly to pre-chilled cells, while gently vortexed, to a



SCHEME 1 | Mild hyperthermia induced by NIR II light irradiation enhancing platinum drug-based chemotherapy via increased DNA damage and ER stress. Chemical structure of the reductive polymer P1 and the Pt(IV) prodrug (A). NP-2 were taken in by the cancer cells and the mild hyperthermia for enhancing chemotherapy via increased DNA damage as well as ER stress (B).

final concentration of 90% methanol for 10 min on ice. And they were washed by centrifugation in excess PBS to remove methanol. They were added 100 μ l of diluted primary antibody and incubated for 1 h at room temperature. They were washed by centrifugation in PBS for three times and added 100 μ l of diluted fluorochrome-conjugated secondary antibody. And they were incubated for 30 min at room temperature with dark and washed by PBS for three times. They were added 500 μ l PBS and analyzed on flow cytometer.

Statistical Analysis

Results are presented as mean \pm standard deviation (S.D.). Statistical analysis is subjected to t testing and means are assessed for significance by using Student's t-test. Differences are considered significant for p value less than 0.01 ($*p < 0.01$) and very significant for p value less than 0.01 ($****p < 0.0001$). Unless

especially mentioned, all assays were conducted in triplicate in three independent experiments. All statistical analysis are performed by using SPSS.

Results

Characterizations of NP-2

The combination of mild hyperthermia with platinum drugs in nanoparticles is of great significance and brings a new perspective to clinical treatment for ovarian cancer. P1 was successfully synthesized and characterized. Its molecular weight is about 15000 Da (Supplementary Figure S1). The Pt(IV) prodrug with axial octyl groups was then characterized by ¹H NMR (Supplementary Figure S2). To confirm the responsiveness of NP-1 and NP-2 to GSH, Nile red dye was encapsulated. The results showed that the fluorescence intensity of the polymer containing Nile red gradually decreased with a half-life of 0.8 h

(Figure 1A). Desirable NP-2 with both Pt (IV) prodrug and IR1048 were obtained at a feed ratio of Pt (IV), IR1048 and polymer was 2:1:20. Dynamic light scattering (DLS) showed that the size of NP-2 was 45 nm in diameter (Figure 1B). Transmission electron microscopy (TEM) showed that NP-2 were spherical with a mean diameter 40 nm (Figure 1C). Meanwhile, *in vitro* release profile of NP-2 showed that the cumulative platinum release was different at pH 7.4, pH 5.0 and in 10 mM GSH solutions. Specifically, the cumulative release was only 20% under pH 7.4 and pH 5.0, while the cumulative Pt release reached 80% in 10 mmol GSH (Figure 1D). The ultraviolet-visible-near-infrared (UV-VIS-NIR) absorption spectrum was further applied to study the optical properties and the potential for photothermal conversion. The UV-VIS-NIR absorption spectrum showed that NP-2 had an absorption peak at 1028 nm (Figure 1E). Thereafter, the photothermal effect of NP-2 with various concentration (5.5, 11 and 22 µg/ml) under different powers (0.5, 1.0 and 1.5 W/cm²) was studied under the irradiation of 1064 nm laser. NP-2 can induce obvious photothermal effect, and the highest temperature increase (delta T) can reach 30°C (Figure 1F). Additionally, the temperature of NP-2 with the concentration of 11 µg/ml increased nearly 10°C which might be an appropriate temperature for mild hyperthermia under the stable light irradiation of 1064 nm for 10 min in Figure 1F. To visualize the increasing temperature, thermal imaging of NP-2 under the stable light irradiation of 1064 nm for 10 min were shown (Figure 1G). In addition, NP-2 had little photo-bleach effect during the four heating processes, indicating its excellent photothermal stability (Figure 1H).

Intracellular Uptake of NP-2 and Anticancer Activity Evaluation

To visualize and quantify cell uptake of NP-2, P1 were labeled with rhodamine B (Rh B) (NPs@Rh B). NPs@Rh B was co-incubated with A2780 cells for 1, 3 and 6 h respectively. Subsequently, confocal laser scanning microscopy (CLSM) revealed that the red fluorescence in the cells increased with longer culture time (Figure 2A). In addition, flow cytometry quantitatively proved that the fluorescence intensity in A2780 cells increased with longer culture time which was nearly ten times at 6 h compared with PBS group indicating a rapid uptake of nanoparticles (Figure 2B and Supplementary Figure S3). Secondly, MTT assay was used to evaluate the cytotoxicity of cisplatin, NP-1 and NP-2 on A2780 and A2780 DDP cells *in vitro*. The results showed that NP-2 under NIR II light irradiation on A2780 cells and A2780 DDP cells were most potent (IC₅₀ = 0.8 µM, IC₅₀ = 2.2 µM). However, cisplatin was less potent on A2780 cells and A2780 DDP cells (IC₅₀ >> 8 µM, IC₅₀ >> 8 µM, Figures 2C,D). Similarly, NP-2 induced an apoptosis rate up to 14.61% on A2780 cells under the NIR II laser irradiation (Figure 2E and Supplementary Figure S4). Moreover, the S-phase arrest of cells treated with NP-2 under NIR II light was significantly higher than other treatment groups, suggesting that NP-2 may enhance DNA damage and induce more apoptosis (Figure 2F and Supplementary Figure S5).

DNA Damage and ER Stress in Cells Treated With NP-2 Under NIR II Light Irradiation

Platinum drugs inhibit cancer cell proliferation by increasing DNA damage (Yang et al., 2019). As a DNA damage repair enzyme, PARP is involved in the DNA damaging repair process (Shao et al., 2020). The expression of PARP might be closely related to apoptosis. As shown in Figures 3A,B, the expression of PARP in cells treated with NP-2 under NIR II irradiation significantly decreased, suggesting that NP-2 induced apoptosis by increasing DNA damage. At the same time, ER stress is a downstream mechanism of DNA damage which could promote cell apoptosis (Chen et al., 2018). As a biomarker of ER stress, XBP1 might be another reason for anticancer activity of NP-2 under 1064 nm laser irradiation. Western blot results further showed that the expression of XBP1 was significantly reduced in cells treated with NP-2 under NIR II light irradiation, suggesting an ER stress related pathway (Figures 3A,B).

High mobility group box one (HMGB1) is a nearly discovered inflammatory cytokine with immune stimulation. Studies showed that HMGB1 might induce cell apoptosis (Liu et al., 2021). Thereafter, we showed that HMGB1 levels in A2780 cells treated with NP-2 group under NIR II light irradiation decreased (Figures 3A,B). This suggested that mild hyperthermia by NIR II light might inhibited cell growth through immune-related responses. Moreover, flow cytometry analysis showed that cells treated with NP-2 under NIR II light irradiation had two times less XBP1 than other treatment groups (Figures 3C; Supplementary Figure S6). What's more, CLSM showed that the XBP1 expression level of cells treated with NP-2 was very low under NIR II light irradiation, while the red signal of XBP1 expression was obvious in other treatment groups (Figure 3D).

Conclusion

In conclusion, a reduction sensitive polymer was designed to encapsulate Pt (IV) prodrugs and NIR II photothermal dyes for nanoparticle-based drug delivery system. The nanoparticles can be dissociated in response to intracellular concentration of GSH, which could then effectively release cisplatin and IR1048. Moreover, the cancer cells can uptake the nanoparticles which were then heated under NIR II light irradiation, resulting in the enhanced DNA damage of platinum drugs, inducing ER stress, finally resulting in cell apoptosis, and possibly causing inflammatory and immune responses. Therefore, we found that mild hyperthermia under NIR II light irradiation could increase DNA damage and induce ER stress to enhance chemotherapy effect.

DATA AVAILABILITY STATEMENT

The original contributions presented in the study are included in the article/Supplementary Material, further inquiries can be directed to the corresponding authors.

AUTHOR CONTRIBUTIONS

YW, XK, and KY designed this experiment. QK, DW, and KY performed experiment. QK, YW and XK wrote the main

manuscript, PX and BW prepared the figures. All authors reviewed the manuscript.

FUNDING

This research was supported by Capital's Funds for Health Improvement and Research (No. 2020-2-8022) in China and the National Natural Science Foundation of China (No. 81602629).

REFERENCES

- Armstrong, D. K., Alvarez, R. D., Bakkum-Gamez, J. N., Barroilhet, L., Behbakht, K., Berchuck, A., et al. (2019). NCCN Guidelines Insights: Ovarian Cancer, Version 1.2019. *J. Natl. Compr. Canc. Netw.* 17 (8), 896–909. doi:10.6004/jnccn.2019.0039
- Balakrishnan, P. B., Silvestri, N., Fernandez-Cabada, T., Marinaro, F., Fernandes, S., Fiorito, S., et al. (2020). Exploiting Unique Alignment of Cobalt Ferrite Nanoparticles, Mild Hyperthermia, and Controlled Intrinsic Cobalt Toxicity for Cancer Therapy. *Adv. Mater.* 32 (45), 2003712. doi:10.1002/adma.202003712
- Chen, G., Yang, Y., Xu, Q., Ling, M., Lin, H., Ma, W., et al. (2020). Self-Amplification of Tumor Oxidative Stress with Degradable Metallic Complexes for Synergistic Cascade Tumor Therapy. *Nano Lett.* 20 (11), 8141–8150. doi:10.1021/acs.nanolett.0c03127
- Chen, L., Li, Q., She, T., Li, H., Yue, Y., Gao, S., et al. (2016). IRE1 α -XBP1 Signaling Pathway, a Potential Therapeutic Target in Multiple Myeloma. *Leuk. Res.* 49, 7–12. doi:10.1016/j.leukres.2016.07.006
- Chen, O. I., Bobak, Y. P., Stasyk, O. V., and Kunz-Schughart, L. A. (2018). A Complex Scenario and Underestimated Challenge: The Tumor Microenvironment, ER Stress, and Cancer Treatment. *Curr. Med. Chem.* 25 (21), 2465–2502. doi:10.2174/0929867325666180117110259
- Grossman, D. C., Grossman, D. C., Curry, S. J., Owens, D. K., Barry, M. J., Davidson, K. W., et al. (2018). Screening for Ovarian Cancer: US Preventive Services Task Force Recommendation Statement. *JAMA* 319 (6), 588–594. doi:10.1001/jama.2017.21926
- Jędrzak, A., Grześkowiak, B. F., Golba, K., Coy, E., Synoradzki, K., Jurga, S., et al. (2020). Magnetite Nanoparticles and Spheres for Chemo- and Photothermal Therapy of Hepatocellular Carcinoma in vitro. *Int. J. Nanomed.* 15, 7923–7936. doi:10.2147/IJN.S257142
- Konner, J. A., Grabon, D. M., Gerst, S. R., Iasonos, A., Thaler, H., Pezzulli, S. D., et al. (2011). Phase II Study of Intraperitoneal Paclitaxel Plus Cisplatin and Intravenous Paclitaxel Plus Bevacizumab as Adjuvant Treatment of Optimal Stage II/III Epithelial Ovarian Cancer. *J. Clin. Oncol.* 29 (35), 4662–4668. doi:10.1200/JCO.2011.36.1352
- Lhomond, S., Avril, T., Dejeans, N., Voutetakis, K., Doultinos, D., McMahon, M., et al. (2018). Dual IRE1 RNase Functions Dictate Glioblastoma Development. *EMBO Mol. Med.* 10 (3), e7929. doi:10.15252/emmm.201707929
- Liu, H., Chen, D., Li, L., Liu, T., Tan, L., Wu, X., et al. (2011). Multifunctional Gold Nanoshells on Silica Nanorattles: a Platform for the Combination of Photothermal Therapy and Chemotherapy with Low Systemic Toxicity. *Angew. Chem. Int. Ed.* 50 (4), 891–895. doi:10.1002/anie.201002820
- Liu, L., Zhang, J., Zhang, X., Cheng, P., Liu, L., Huang, Q., et al. (2021). HMGB1: an Important Regulator of Myeloid Differentiation and Acute Myeloid Leukemia as Well as a Promising Therapeutic Target. *J. Mol. Med.* 99 (1), 107–118. doi:10.1007/s00109-020-01998-5

ACKNOWLEDGMENTS

We would like to thank all authors who provided published data for our study.

SUPPLEMENTARY MATERIAL

The Supplementary Material for this article can be found online at: <https://www.frontiersin.org/articles/10.3389/fphar.2021.670207/full#supplementary-material>.

- Madden, E., Logue, S. E., Healy, S. J., Manie, S., and Samali, A. (2019). The Role of the Unfolded Protein Response in Cancer Progression: From Oncogenesis to Chemoresistance. *Biol. Cell* 111 (1), 1–17. doi:10.1111/boc.201800050
- Meng, X., Zhang, J., Sun, Z., Zhou, L., Deng, G., Li, S., et al. (2018). Hypoxia-triggered Single Molecule Probe for High-Contrast NIR II/PA Tumor Imaging and Robust Photothermal Therapy. *Theranostics* 8 (21), 6025–6034. doi:10.7150/thno.26607
- Mortensen, A. C. L., Mohajershojai, T., Hariri, M., Pettersson, M., and Spiegelberg, D. (2020). Overcoming Limitations of Cisplatin Therapy by Additional Treatment with the HSP90 Inhibitor Onalespib. *Front. Oncol.* 10, 532285. doi:10.3389/fonc.2020.532285
- Rottenberg, S., Disler, C., and Perego, P. (2021). The Rediscovery of Platinum-Based Cancer Therapy. *Nat. Rev. Cancer* 21 (1), 37–50. doi:10.1038/s41568-020-00308-y
- Ruan, C., Liu, C., Hu, H., Guo, X.-L., Jiang, B.-P., Liang, H., et al. (2019). NIR-II Light-Modulated Thermosensitive Hydrogel for Light-Triggered Cisplatin Release and Repeatable Chemo-Photothermal Therapy. *Chem. Sci.* 10 (17), 4699–4706. doi:10.1039/c9sc00375d
- Rubio-Patiño, C., Bossowski, J. P., Chevet, E., and Ricci, J.-E. (2018). Reshaping the Immune Tumor Microenvironment through IRE1 Signaling. *Trends Mol. Med.* 24 (7), 607–614. doi:10.1016/j.molmed.2018.05.005
- Shao, Z., Lee, B. J., Rouleau-Turcotte, É., Langelier, M.-F., Lin, X., Estes, V. M., et al. (2020). Clinical PARP Inhibitors Do Not Abrogate PARP1 Exchange at DNA Damage Sites in vivo. *Nucleic Acids Res.* 48 (17), 9694–9709. doi:10.1093/nar/gkaa718
- Wang, B., Wang, S., Zhang, Q., Deng, Y., Li, X., Peng, L., et al. (2019). Recent Advances in Polymer-Based Drug Delivery Systems for Local Anesthetics. *Acta Biomater.* 96, 55–67. doi:10.1016/j.actbio.2019.05.044
- Wen, M., Qiling, C., Weiguo, X., et al. (2021). Self-targeting Visualizable Hyaluronate Nanogel for Synchronized Intracellular Release of Doxorubicin and Cisplatin in Combating Multidrug-Resistant Breast Cancer. *Nano Res.* 14 (3), 846–857. doi:10.1007/s12274-020-3124-y
- Wright, A. A., Bohlke, K., Armstrong, D. K., Bookman, M. A., Cliby, W. A., Coleman, R. L., et al. (2016). Neoadjuvant Chemotherapy for Newly Diagnosed, Advanced Ovarian Cancer: Society of Gynecologic Oncology and American Society of Clinical Oncology Clinical Practice Guideline. *J. Clin. Oncol.* 34 (28), 3460–3473. doi:10.1200/JCO.2016.68.6907
- Xi, D., Xiao, M., Cao, J., Zhao, L., Xu, N., Long, S., et al. (2020). NIR Light-Driving Barrier-free Group Rotation in Nanoparticles with an 88.3% Photothermal Conversion Efficiency for Photothermal Therapy. *Adv. Mater.* 32 (11), e1907855. doi:10.1002/adma.201907855
- Xiaoxu, K., Yingjie, Y., Zhigang, C., Yixin, W., Dengshuai, W., Yao, Z., et al. (2019). A Negatively Charged Pt(IV) Prodrug for Electrostatic Complexation with Polymers to Overcome Cisplatin Resistance. *J. Mater. Chem. B* 7, 3346–3350. doi:10.1039/C9TB00155G
- Yang, X., Yu, Y., Huang, X., Chen, Q., Wu, H., Wang, R., et al. (2019). Delivery of Platinum (II) Drugs with Bulky Ligands in Trans-geometry for Overcoming

- Cisplatin Drug Resistance. *Mater. Sci. Eng. C* 96, 96–104. doi:10.1016/j.msec.2018.10.092
- Yang, Y., Liu, X., Ma, W., Xu, Q., Chen, G., Wang, Y., et al. (2021). Light-activatable Liposomes for Repetitive On-Demand Drug Release and Immunopotential in Hypoxic Tumor Therapy. *Biomaterials* 265, 120456. doi:10.1016/j.biomaterials.2020.120456
- Yang, Y., Yu, Y., Chen, H., Meng, X., Ma, W., Yu, M., et al. (2020). Illuminating Platinum Transportation while Maximizing Therapeutic Efficacy by Gold Nanoclusters via Simultaneous Near-Infrared-I/II Imaging and Glutathione Scavenging. *ACS Nano* 14 (10), 13536–13547. doi:10.1021/acsnano.0c05541
- Zhang, Y., Song, Y., Li, C., Ren, J., Fang, M., Fang, J., et al. (2020). Brother of Regulator of Imprinted Sites Inhibits Cisplatin-induced DNA Damage in Non-small Cell Lung Cancer. *Oncol. Lett.* 20 (5), 1. doi:10.3892/ol.2020.12114

Conflict of Interest: The authors declare that the research was conducted in the absence of any commercial or financial relationships that could be construed as a potential conflict of interest.

The handling editor and the reviewer (PM) declared a shared affiliation with the authors at time of review.

Copyright © 2021 Kong, Wei, Xie, Wang, Yu, Kang and Wang. This is an open-access article distributed under the terms of the Creative Commons Attribution License (CC BY). The use, distribution or reproduction in other forums is permitted, provided the original author(s) and the copyright owner(s) are credited and that the original publication in this journal is cited, in accordance with accepted academic practice. No use, distribution or reproduction is permitted which does not comply with these terms.



Hitchhiking on Controlled-Release Drug Delivery Systems: Opportunities and Challenges for Cancer Vaccines

Lu Han¹, Ke Peng², Li-Ying Qiu¹, Meng Li¹, Jing-Hua Ruan^{3*}, Li-Li He^{1*} and Zhi-Xiang Yuan^{1*}

¹College of Pharmacy, Southwest Minzu University, Chengdu, China, ²School of pharmacy, Queen's University Belfast, Belfast, United Kingdom, ³The First Affiliated Hospital, Guizhou University of Traditional Chinese Medicine, Guiyang, China

OPEN ACCESS

Edited by:

Peixin Dong,
Hokkaido University, Japan

Reviewed by:

Guangbao Yang,
Soochow University, China
Thomas Kieber-Emmons,
University of Arkansas for Medical
Sciences, United States
Jian You,
Zhejiang University, China

*Correspondence:

Jing-Hua Ruan
1438274952@qq.com
Li-Li He
lililhes@163.com; lililhes@163.com
Zhi-Xiang Yuan
Zhixiang-yuan@hotmail.com

Specialty section:

This article was submitted to
Pharmacology of Anti-Cancer Drugs,
a section of the journal
Frontiers in Pharmacology

Received: 12 March 2021

Accepted: 28 April 2021

Published: 10 May 2021

Citation:

Han L, Peng K, Qiu L-Y, Li M,
Ruan J-H, He L-L and Yuan Z-X (2021)
Hitchhiking on Controlled-Release
Drug Delivery Systems: Opportunities
and Challenges for Cancer Vaccines.
Front. Pharmacol. 12:679602.
doi: 10.3389/fphar.2021.679602

Cancer vaccines represent among the most promising strategies in the battle against cancers. However, the clinical efficacy of current cancer vaccines is largely limited by the lack of optimized delivery systems to generate strong and persistent antitumor immune responses. Moreover, most cancer vaccines require multiple injections to boost the immune responses, leading to poor patient compliance. Controlled-release drug delivery systems are able to address these issues by presenting drugs in a controlled spatiotemporal manner, which allows co-delivery of multiple drugs, reduction of dosing frequency and avoidance of significant systemic toxicities. In this review, we outline the recent progress in cancer vaccines including subunit vaccines, genetic vaccines, dendritic cell-based vaccines, tumor cell-based vaccines and *in situ* vaccines. Furthermore, we highlight the efforts and challenges of controlled or sustained release drug delivery systems (e.g., microparticles, scaffolds, injectable gels, and microneedles) in ameliorating the safety, effectiveness and operability of cancer vaccines. Finally, we briefly discuss the correlations of vaccine release kinetics and the immune responses to enlighten the rational design of the next-generation platforms for cancer therapy.

Keywords: cancer vaccine, *in situ* vaccination, drug delivery system, controlled release, sustained release, hydrogel, microneedle

INTRODUCTION

Immunotherapy was first introduced by Dr. William Coley to treat malignant tumors using intratumoral injections of live bacteria and bacterial toxins in the 1890s (Coley, 1991). Nowadays, immunotherapy has been fully embraced by the oncologists for the treatment of various tumors. Chimeric antigen receptor (CAR) T cell-based therapies as well as immune checkpoint inhibitors (ICIs), including antibodies targeting programmed cell death protein-1 (PD-1), programmed death-ligand 1 (PD-L1) and cytotoxic T-lymphocyte-associated antigen-4 (CTLA-4), have revolutionized the cancer treatments and have been approved by the U.S. Food and Drug Administration (FDA) for tackling many tumors (Allison, 2015; Sharma and Allison, 2015; Labanieh et al., 2018). However, the response rate to ICIs varies dramatically among cancers. Growing evidence supports the idea that patients lacking pre-existing tumor-infiltrating CD8⁺ T cells have a low response rate to ICIs, suggesting the hypothesis that ICIs need to be combined with other therapies that can stimulate potent tumor-specific T cell responses to improve the clinic outcomes (Hu et al., 2018; van der Burg, 2018; Shae et al., 2019).

One attractive strategy to mount effective antitumor responses is vaccination. Cancer vaccines can provoke antigen-specific immunity or reactivate pre-existing but quiescent tumor-reactive T cells by

delivering the antigens and immunoadjuvants with the aim to prevent cancers or fight against established tumor burdens (Lybaert et al., 2018). Two prophylactic vaccines, namely the human papilloma virus (HPV) vaccine and the hepatitis B virus (HBV) vaccine, have been successfully approved for preventing cervical cancer and liver cancer, respectively (Stanley, 2017). Whereas, only one antigen-loaded therapeutic cancer vaccine, termed Sipuleucel-T (Provenge), has received FDA approval for the treatment of advanced prostate cancer so far (Shae et al., 2019). Although cancer vaccines have generated acceptable therapeutic effects in some clinic trials, their overall clinical efficacy is not encouraging especially in solid tumors (Jacobs et al., 2014; Bouzid et al., 2020). The main reasons for these disappointing outcomes include: 1) the use of suboptimal vaccine delivery systems which compromise the vaccine immunogenicity and efficacy; 2) the rapid clearance of antigens at the injection site and the inadequate delivery to lymph nodes; 3) the choice of weakly immunogenic antigens that lack variety and specificity (e.g., overexpressed self-antigens); 4) the inefficient controlling of the immunosuppressive tumor microenvironment (van der Burg, 2018; Shae et al., 2019; Bouzid et al., 2020). On the other hand, cancer vaccines usually require multiple injections to elicit effective immune responses, resulting in poor patient compliance. To surmount these issues, numerous controlled drug release technologies, which are effective in a single shot, have been developed to improve the delivery efficiency and potency of cancer vaccines. Controlled-release platforms can prolong the spatiotemporal presentation of antigens and immunomodulators to immune cells or mimic the prime-boost effect of the traditional multi-bolus vaccination schedules, thereby stimulating stronger antitumor immune responses (Ali et al., 2009b; Korupalli et al., 2019; Irvine et al., 2020). Moreover, the controlled-release systems can also improve patient compliance by eliminating the booster shots, minimize the toxic side effects by reducing drug dose and avoiding rapid drug clearance, as well as improve outcomes by integrating the synergistic effect of multiple therapeutics within one platform (Huang et al., 2019; Riley et al., 2019). Especially for *in situ* cancer vaccines that require intratumoral injections, this single-dose vaccine technology can improve the antitumor immunity and increase the operational feasibility by a local and sustained release of immunomodulators *in vivo*.

Below, we will present recent advances in the engineering of controlled-release delivery platforms for improving the safety and efficacy of cancer vaccines. Firstly, we introduce the advantages and challenges of various types of cancer vaccines. Secondly, an overview of the controlled-release drug delivery systems is provided and the limitations that should be addressed to improve the safety, effectiveness and operability of cancer vaccines are enlightened. Finally, we briefly discuss the possible relevancy between the release kinetics of controlled-release vaccines and the type and magnitude of the immune responses.

CONVENTIONAL CANCER VACCINES

Conventional vaccines are composed of antigens and adjuvants. The selection of an immunogenic antigen plays a critical role in

implementing the vaccine effectiveness and specificity. Tumor antigens can be broadly divided into two categories: tumor-associated antigens (TAAs) and neoantigens. TAAs are overexpressed self-antigens that are shared among many tumors and can also be found in some normal cells. TAAs have been widely used in cancer vaccines for decades but they are not tumor-specific antigens and can only trigger weak immune responses owing to thymic tolerance (Hu et al., 2018). In contrast, neoantigens are highly tumor-specific immunogens derived from somatic mutations and they are more immunogenic due to the lack of central tolerance (Chu et al., 2018). With the rapid development of next-generation sequencing and peptide immunogenicity prediction technologies, neoantigens represent the most promising candidates for the preparation of personalized cancer vaccines and the diagnosis of ICI therapy response (Desrichard et al., 2016). Tumor antigens can be presented in various forms ranging from defined proteins, peptides, protein-encoding DNA or RNA, recombinant viral or bacterial vectors, tumor cell-based preparations, to antigen-pulsed dendritic cells (DCs).

The other crucial component of a vaccine is the adjuvant that can strengthen the magnitude of the immune responses or skew the immune responses toward Th1 or Th2 immunity. There are several types of vaccine adjuvants, including toll-like receptor (TLR) agonists, e.g. unmethylated cytosine-phosphate-guanine (CpG), imiquimod and polyinosinic:polycytidylic acid (poly(I:C)); cytokines, e.g. interferon (IFN)- α and interleukin (IL)-12; bacterial derivatives, e.g. monophosphoryl lipid A (MPLA) and Bacille Calmette-Guerin (BCG); depot-like adjuvants, e.g. aluminum salts, incomplete Freund's adjuvant (IFA) and Montanide; particle adjuvants, e.g., liposomes, virus-like particles and polymeric particles (Sivakumar et al., 2011; Pilla et al., 2018). However, only aluminum salts, three emulsions (MF59, AS03, AF03), virosomes and MPLA are approved for human vaccines (Lybaert et al., 2018). Therefore, exploring potent and safe adjuvants and identifying the optimal adjuvants for vaccines are also appealing areas of research.

Subunit Vaccines

Subunit vaccines are defined by the use of purified proteins, peptides or polysaccharides as the antigens to stimulate the immune responses. Subunit vaccines usually contain one or several well-structured antigenic components, making them easier to manufacture and much safer than live pathogen vaccines, as well as avoiding the side effects from antigen-induced unrelated immune responses (Table 1) (Riley et al., 2019). However, these vaccines can hardly conquer the tumor heterogeneity between and within tumors as a consequence of lacking antigen variety. One strategy is mixing multiple antigens in one formulation to benefit the antitumor immune responses (Fennemann et al., 2019; Noguchi et al., 2020). In comparison of whole protein-based vaccines, peptide vaccines only contain one or several epitopes, which can be easily processed by DCs (Rosalia et al., 2013). Peptide vaccines are composed of TAA peptides or neoantigen peptides which are presented in the form of short peptides (<15 amino acids) or long peptides (15–40 amino acids), and the difference between the short peptides and the long

TABLE 1 | Characteristics of conventional cancer vaccines and *in situ* cancer vaccines.

Therapy	Classification	Advantages	Disadvantages
Subunit vaccines	Protein vaccines Peptide vaccines	Easy for mass production Cheap Safe to use Long peptides: not HLA-restricted Neoantigen peptides can be personalized	Weak immunogenicity Lacking antigen variety Short peptides: HLA-restricted
Genetic vaccines	DNA vaccines RNA vaccines	Easy for mass production Cheap Can encode multiple antigens Not HLA-restricted	Weak immunogenicity Rapid degradation Limited cellular transfection DNA vaccines have the risk of integration into the host genome
Tumor cell-based vaccines	Autologous tumor cell vaccines Allogeneic tumor cell vaccines	Contain the whole tumor antigens Autologous vaccines: not HLA-restricted Allogeneic vaccines have a broader target population	Complex preparation process Weak immunogenicity May have immunosuppressive effects May induce autoimmunity Autologous vaccines need tumor biopsies or operation
DC vaccines	Exogenous DC vaccines Endogenous DC-targeting vaccines Artificial DC vaccines	Exogenous DCs: safe; measurable maturation Endogenous DC vaccines: easy to fabricate; can program a large scale of DC subsets Artificial DCs: long shelf-life; not vulnerable to the tumor immunosuppressive conditions	Exogenous DCs: costly; complex preparation process; short shelf-life Not fully activated DCs may induce immune tolerance
In situ cancer vaccines	—	Simple, personalized and off-the-shelf No need for identification and isolation of tumor antigens Contain the whole tumor antigens	Need intratumoral injections Weak immunogenicity (need combination therapies)

peptides has been elucidated in detail elsewhere (Lybaert et al., 2018; Bouzid et al., 2020).

Despite these excellent features, the major challenge that hinders the broad application of subunit vaccines is the low immune efficacy, which is partially due to the poor uptake of antigens and adjuvants in lymph nodes (Pilla et al., 2018; Riley et al., 2019). To overcome this issue, vaccines need to be exquisitely engineered using the following strategies. 1) Increasing the accumulation of antigens and adjuvants in lymph nodes. This can be achieved by a direct intra-lymph node injection (Ribas et al., 2011), especially when immunogenic cargos are loaded in sustained-release platforms that allow extended retention in lymph nodes (Shae et al., 2019). Another approach is the use of albumin-hitchhiking vaccines which can be constructed through conjugating an antigen (or an adjuvant) to a lipophilic albumin-binding tail (Liu et al., 2014) or to a derivative of Evans Blue (Zhu et al., 2017). Besides, nanoparticles with optimized size, surface charge and composition are more likely to be drained into lymph nodes (Jiang et al., 2017). 2) Promoting antigen uptake by DCs, such as using anchoring endocytosis molecules (e.g., mannose, fucose and N-acetylglucosamine)-decorated nanoparticles (Koerner et al., 2019) or antibody-antigen conjugates (Keler et al., 2007). 3) Improving the adjuvant effect of vaccines. This can be implemented by adding more powerful adjuvant reagents or using delivery vehicles with adjuvant activity, such as liposomes or nanoparticles (Vartak and Suchek, 2016). 4) Promoting cross-presentation of the antigens to potentiate the Th1 immune responses. For example, pH-responsive cationic polymers can

facilitate endosomal antigen escape by the “proton sponge” effect (Shae et al., 2019).

Genetic Vaccines

Genetic vaccines have emerged as promising alternatives to subunit vaccines by exploiting tumor antigen-encoding DNA or RNA sequences that require intracellular delivery into DCs to express targeted antigens (Pardi et al., 2018). Genetic vaccines have many merits (Table 1), such as cost-effectiveness, easy for mass production, allowing the delivery of multiple antigens in one platform, and avoiding human leukocyte antigen (HLA) restriction (Lybaert et al., 2018). In spite of these promising features, the clinical results of plasmid DNA vaccines for treating solid tumors have been disappointing mainly due to the barriers for nuclear delivery, low immunogenicity and the immunosuppressive factors within the tumor (Lopes et al., 2019; Riley et al., 2019). Alternatively, mRNA-based vaccines only require to cross the cell membranes to be translated in the cytoplasm, which avoids the risk of integration into the host genome (McNamara et al., 2015). Moreover, the *in vivo* half-life and immunogenicity of mRNA can be regulated by modification and delivery strategies (Pardi et al., 2018). However, the rapid degradation of mRNA by nucleases and the limited translocation into the cytoplasm still challenge the development of RNA-based vaccines (Lybaert et al., 2018; Lin et al., 2020).

Based on the characteristics of genetic vaccines, delivery systems with the ability to increase the drug delivery into lymph nodes, promote intracellular uptake of nucleic acids,

facilitate protein translation and reduce nucleic acid degradation will greatly prompt the clinical application of genetic vaccines. These vaccines can be delivered in diverse ways, for instance, by gene gun, electroporation, ultrasound, laser, viral or bacterial vectors, liposomes, nanoparticles, autologous DCs or other carrier modalities (Guo et al., 2013). The safety and efficacy of various viral vectors, such as pox and adenovirus, have been tested in clinical trials, but the high immunogenicity of viral vectors can, on the contrary, lead to the secretion of neutralizing antibodies (Pilla et al., 2018). A heterologous prime-boost regimen can handle this dilemma. For example, PROSTVAC was a promising viral cancer vaccine, composed of a vaccinia priming vector and a fowlpox boosting vector carrying transgenes for human prostate-specific antigen (PSA) along with three costimulatory molecules (CD80, CD58, and CD54), but it failed to benefit the patients in a phase III study (Gulley et al., 2019; Zhao et al., 2019). Cationic materials are commonly used to condense nucleic acids. For example, a lipid nanoparticle with ionizable lipids was allowed to form complexation with negatively charged mRNA encoding two TAAs (gp100 and TRP2) at low pH, and this formulation could induce a strong CD8⁺ T cell response and remarkable tumor shrinkage (Oberli et al., 2017). Moreover, a local gene depot made of mRNA polyplex-loaded implantable porous scaffolds showed superior sustained delivery and higher local transgene expression than a bolus injection (Chen et al., 2018). This indicates that sustained delivery of mRNA may potentiate the antitumor immunity. Furthermore, the combination of immunoadjuvants or other cancer therapies may further boost the therapeutic effects of genetic vaccines.

Tumor Cell-Based Vaccines

In addition to neoantigens, another class of patient-individualized antigens is whole tumor cell derivatives including the live attenuated tumor cells, killed tumor cells, tumor lysates, tumor-derived exosomes, tumor-derived whole RNAs, tumor cell membrane-based particles, and fusions of tumor cells and DCs (Browning, 2013; Fang et al., 2014; Chiang et al., 2015). Autologous tumor cell vaccines based on patient individual-derived cancer tissues, contain the complete antigen repertoire of the tumor, thereby avoiding the costly and complex identification procedure needed for neoantigens (Table 1). Even more importantly, they are not restricted to HLA type. However, the preparation of whole tumor cell vaccines requires multiple steps: 1) obtaining the patient's tumor cells by surgery or biopsy, 2) processing them *in vitro* to acquire tumor cell derivatives, 3) then loading the tumor antigens into delivery systems. These complex procedures may hinder the clinical practicality of tumor cell-based vaccines. Moreover, this autologous vaccine technology is only feasible for the patients with selected tumor types and stages that are capable of tumor biopsies or operation (Schlom et al., 2014). Alternatively, allogeneic tumor cell vaccines can benefit more patients with homologous tumors because they are prepared from two or three specific tumor cell lines which have been established and characterized (Schlom et al., 2014). In one example of this, Canvaxin containing three irradiated melanoma cell lines showed excellent therapeutic results in phase II clinical trials,

but it did not meet the expectation in phase III trials (Ozao-Choy et al., 2014). This probably resulted from the use of suboptimal dosage, schedule and adjuvant. Tumor stroma-associated antigens are another kind of attractive targets for cancer vaccines as they are genetically more stable and less subjected to tumor immune evasion mechanisms in contrast to tumor cells (Chiang et al., 2015).

Although tumor cell-based vaccines have attracted enormous attention in recent years, two of the most important challenges for whole tumor cell vaccines remain the low accumulation in lymph nodes and low immunogenicity. Numerous strategies have been developed to handle these issues, such as cloaking nanoparticles with tumor cell membranes or fused cytomembranes derived from tumor cells and DCs (Liu et al., 2019b; Gan et al., 2020), or loading the immunogenically dying tumor cells with adjuvants (e.g., BCG) or adjuvant-loaded nanoparticles (Fan et al., 2017). For example, the sustained release of adjuvants and tumor cell membrane-coated nanoparticles from thermosensitive hydrogels could recruit DCs and induce a strong CD8⁺ T cell response, and the combination with antibodies targeting PD-1 could further prolong the survival time of tumor-bearing mice (Ye et al., 2019). It is worth noting that the immune properties of tumor-derived exosomes can be immune-activating or immunosuppressive depending on the physiological state of donor cells and exogenous factors (Théry et al., 2009; Greening et al., 2015). Fortunately, the immunosuppressive role of tumor-derived exosomes can be switched to promote the antitumor immune responses by using heat treatment, adding strong adjuvant components or using transgenic tumor cells expressing IL-2 or IL-18 (Cho et al., 2009; Théry et al., 2009). Besides, the whole tumor cell-based vaccines also contain abundant normal self-proteins which may induce autoimmunity as well as diminish the vaccine effectiveness by the dilution of the most immunogenic tumor antigens (Obeid et al., 2015; Hu et al., 2018). Using autologous induced pluripotent stem cells as the antigen resource may provide new insights to tackle these obstacles (Ouyang et al., 2019).

DC Vaccines

DCs, as the most potent professional antigen-presenting cells (APCs), play a pivotal role in initiating and bridging the innate and adaptive immune responses. The ultimate goal of many delivery strategies of cancer vaccines is to target DCs and fully activate them. One approach for this is exogenous DC vaccines which usually rely on the isolation and differentiation of peripheral blood autologous DC precursor cells into immature DCs, followed by loading these immature DCs with a proper form of antigens (such as peptides, proteins, nucleic acids or tumor cell derivatives), then maturing these DCs with different stimuli, and finally reinfusing the manipulated DCs to the patient to implement the cancer immunotherapy (Bol et al., 2016; Sabado et al., 2017). Sipuleucel-T, prepared from autologous DCs loaded with a fusion protein (PA2024) of prostatic acid phosphatase (PAP) and granulocyte-macrophage colony-stimulating factor (GM-CSF), was approved in 2010 to treat metastatic prostate cancer on the basis of a survival benefit (Gardner et al., 2012). Although substantial clinical studies have demonstrated the

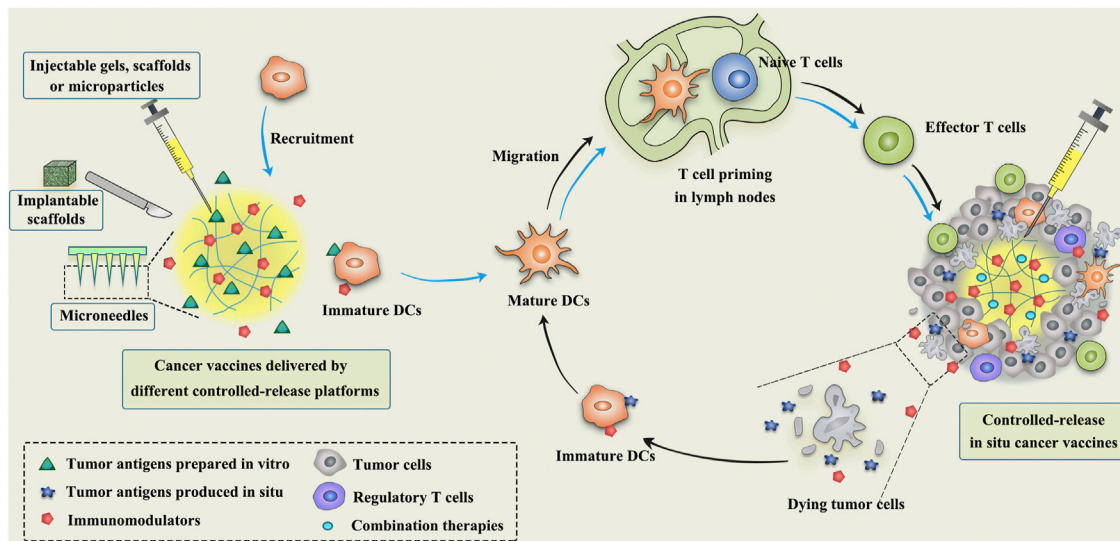


FIGURE 1 | Schematic illustration of the mechanism of controlled-release cancer vaccines for cancer therapy. The blue arrows indicate the antitumor process of conventional cancer vaccines, while the black arrows indicate the mechanism of *in situ* cancer vaccines.

safety and immunogenicity of exogenous DC vaccines, the clinical outcomes are not encouraging (Perez and De Palma, 2019). Many factors affect the efficacy of exogenous DC vaccines, including a suboptimal choice of DC subsets, limited migration to the lymph nodes and negative immune regulation within tumors. Hence, DC vaccines can be further improved by optimizing, for instance, the choice of DC type and antigen type, activation method, the design of drug delivery system, the number of DCs for injection, the vaccination schedule and the administration route (Sabado et al., 2017). Another approach to exploit natural DCs in cancer vaccines is targeting and modulating the endogenous DC subpopulations *in vivo*. This targeting goal can be implemented by various strategies involving GM-CSF-secreting irradiated tumor cells, conjugation of antigens or antigen-loaded nanoparticles to ligands directing against DC surface receptors (e.g., CD40, DEC205, Langerin or Clec9A), or using injectable controlled-release platforms that are engineered to release chemokines, tumor antigens and adjuvants (Sabado et al., 2017; Calmeiro et al., 2019). These *in vivo* targeting technologies allow to program a large scale of DC subsets without the need for a costly and labor-intensive extracorporeal training of exogenous DCs (Table 1; Sabado et al., 2017). However, the endogenous DC-targeting vaccines cannot control the extent of antigen loading and DC activation as the exogenous DC vaccines do, and DCs that are not fully activated may induce immune tolerance (Bouzid et al., 2020). Recently, artificial DCs, such as nanoparticles coated with tumor lysate-primed DC membranes or scaffolds carrying T cell activation cues and peptide antigens, can directly stimulate the activation and expansion of antigen-specific T cells (Cheung et al., 2018; Cheng et al., 2020). These artificial DCs can circumvent the short shelf-life concerns of exogenous DC vaccines and they are not vulnerable to the

tumor immunosuppressive conditions (Cheng et al., 2020). Furthermore, DC vaccine-based combination therapies may provide better control over cancers (Bol et al., 2016; Tanyi et al., 2018), thus many clinical trials are exploring the synergistic effect of DC vaccines and ICI therapies (Sprooten et al., 2019).

IN SITU CANCER VACCINES

Despite the fact that the substantial improvement achieved by conventional cancer vaccines, the risk of undetected contaminations during the elaborate preparation process and the high costs associated with preparation and storage remain bottlenecks limiting their broad clinical implementation (Duong et al., 2020a). *In situ* vaccination (ISV), without the need for previous identification and isolation of tumor antigens, is raising great attention in cancer immunotherapy. ISV is a simple, personalized and off-the-shelf cancer vaccine by *in vivo* transforming tumors into “antigen factories” (Table 1). As depicted in Figure 1, ISV can activate systemic antitumor immune responses by simply delivering immunomodulators (Hammerich et al., 2015; Sheen and Fiering, 2019). Taking advantage of the complete antigenic repertoire of a tumor, including all mutated antigens and unmutated antigens, ISV potentiates the immune system to recognize the evolving tumor antigen arrays, thereby overcoming the weak immunogenicity of single-antigen vaccines and minimizing immune escape.

Broadly speaking, any approach that employs TAAs available at the tumor site to elicit antitumor immune responses can be termed as ISV (Hammerich et al., 2015). ISV usually refers to the approaches using intratumoral administration of immunomodulators to activate immune cells or reverse the

immunosuppressive microenvironment within the tumor. The most extensively studied immunomodulators include bacteria and its derivatives (Janku et al., 2021), oncolytic viruses (Oh et al., 2017; Russell and Barber, 2018), TLR agonists (Wei et al., 2019), monoclonal antibodies (e.g., anti-PD-1, anti-CTLA-4 and anti-CD40) (Rahimian et al., 2015; Wang et al., 2016; Knorr et al., 2018), immunomodulatory cytokines (e.g., IL-2 and IL-12) (Jackaman and Nelson, 2012; Hwang et al., 2020), and immune cells (e.g., DCs) (Subbiah et al., 2018). In an example of successful ISVs, Talimogene laherparepvec (T-VEC), a genetically modified herpes simplex virus that can replicate selectively within tumors and express GM-CSF, is the first intratumoral oncolytic viral therapy approved by the FDA in 2015 for local treatment of unresectable advanced melanoma (Rehman et al., 2016).

However, a single regimen of immunomodulators is generally difficult to surmount the complexity and compensatory evolution of tumors, especially since many types of tumor cell death are nonimmunogenic, thus leading to suboptimal clinic outcomes (Sheen and Fiering, 2019). Local treatment with radiotherapy, phototherapy, oncolytic viruses, cryoablation, sonodynamic therapy, or some chemotherapeutic drugs (e.g., anthracyclines, taxane, cyclophosphamide, gemcitabine and oxaliplatin) can induce significant immunogenic cell death (ICD) of tumor cells when administrated at appropriate doses and schemes (Pol et al., 2015; Galluzzi et al., 2017; Min et al., 2017; Twumasi-Boateng et al., 2018; Yakkala et al., 2019; Zhao et al., 2020; Zhu et al., 2020). ICD can expose calreticulin on the surface of dying tumor cells to provide an “eat-me” signal for APCs, and release a large number of damage-associated molecular patterns (DAMPs) to provide adjuvant stimuli to activate APCs (Galluzzi et al., 2017). Therefore, the combination of ICD-inducing therapies with immunomodulators, such as chemoimmunotherapy, radioimmunotherapy and photoimmunotherapy, can not only directly kill tumor cells, but also turn ‘cold’ tumors into ‘hot’ tumors to elicit potent immune responses against a broad spectrum of cancers. In an elegant example of this, Patel et al. combined bacterial membrane-coated nanoparticles (BNP) with radiotherapy to treat syngeneic melanoma or neuroblastoma in mice (Patel et al., 2019). This multifunctional BNP consisted of an immunostimulatory PC7A/CpG polyplex nanocore coated with bacterial membrane and imide groups. After radiotherapy, BNP could capture TAAs released by ICD, followed by promoting the antigen uptake and cross presentation. Subsequently, a strong antitumor T-cell response was induced, leading to remarkable tumor regression alongside immunological memory.

Although ISV and its combinatorial therapies are gaining rising attention among researchers, the magnitude and durability of antitumor immune responses induced by ISV could be unfortunately impeded by the immunosuppressive tumor microenvironment (van der Burg et al., 2016). One appealing strategy is to introduce CAR-T, ICIs or other immunosuppressive signal inhibitors in the combinatorial therapies to improve the outcomes (Wang et al., 2018; Chen et al., 2019a; Song et al., 2019; Chen et al., 2020a). Moreover, approaches that loosen the desmoplastic stroma or target the

tumor vasculature would help to augment the antitumor immunity of ISV by facilitating immune infiltration (Galluzzi et al., 2018). Furthermore, identifying the optimal immunoadjuvants and applying the most suitable delivery system may maximize the safety and effectiveness of ISV. Although intratumoral injection technology is widely used in accessible superficial tumors, such as skin, head and neck, and breast tumors, it remains a challenge for those deep tumors, such as brain, liver and pancreas tumors (Sheen and Fiering, 2019). Fortunately, with the help of modern imaging technologies such as ultrasound, computed tomography guidance and laparoscopy, safe and accurate injections can be performed for tumors in various locations (Sheen and Fiering, 2019). Moreover, one should take full account of the effects of injection pressure, volume, viscosity, frequency, etc. on tumor bulk, therapeutic effect and patient tolerance. Collectively, combinatorial ISV therapies have great potential to provide a comprehensive approach to treat heterogeneous cancers.

CONTROLLED-RELEASE DRUG DELIVERY SYSTEMS

Early depot-like adjuvants, such as aluminum salts and IFA, are effective in promoting protective humoral immunity against pathogens, but they are not excellent candidates for cancer vaccines that rely on cellular immunity (Brito and O’Hagan, 2014; Shae et al., 2019). Therefore, the next generation of controlled-release cancer vaccines should be able to elicit efficient and durable antitumor cellular immune responses. To date, numerous controlled-release delivery platforms, such as polymeric microspheres, scaffolds, hydrogels and microneedles (MNs) have been designed for local and controlled release of multiple immunotherapeutic agents to improve antitumor efficacy and reduce off-target toxicities (Figure 1; Table 2).

Microparticles

Peris and Langer proposed in 1979 for the first time that the release of antigens could be controlled using polymeric materials to stimulate immune responses (Peris and Langer, 1979). Numerous natural and synthetic biodegradable polymeric materials including chitosan, alginate, gelatin, poly(lactic-co-glycolic acid) (PLGA), Poly(lactic acid) (PLA), poly(ϵ -caprolactone) (PCL), poly(β -amino esters) (PBAE) and poly(methyl methacrylate) (PMMA), etc., as well as some inorganic materials (such as silica) have been widely used in the field of controlled release of antigens and immunomodulatory agents (Lin et al., 2015; Zhu et al., 2018; Huang et al., 2019; Koerner et al., 2019; Hou et al., 2021). Polymeric microparticles (MPs) or microspheres can induce potent antigen-specific immunity by controlling the release of antigens or mimicking the size of pathogens, but they are much safer than live pathogens (Huang et al., 2019). Different forms of antigens as mentioned above (e.g., purified proteins, peptides, nucleic acids, and cell lysates) have been successfully formulated in MPs (Joshi et al., 2014; Pradhan et al., 2014; Guarecuco et al., 2018; Zhu et al., 2018) (Table 2). As compared to bolus injections, MPs can protect the

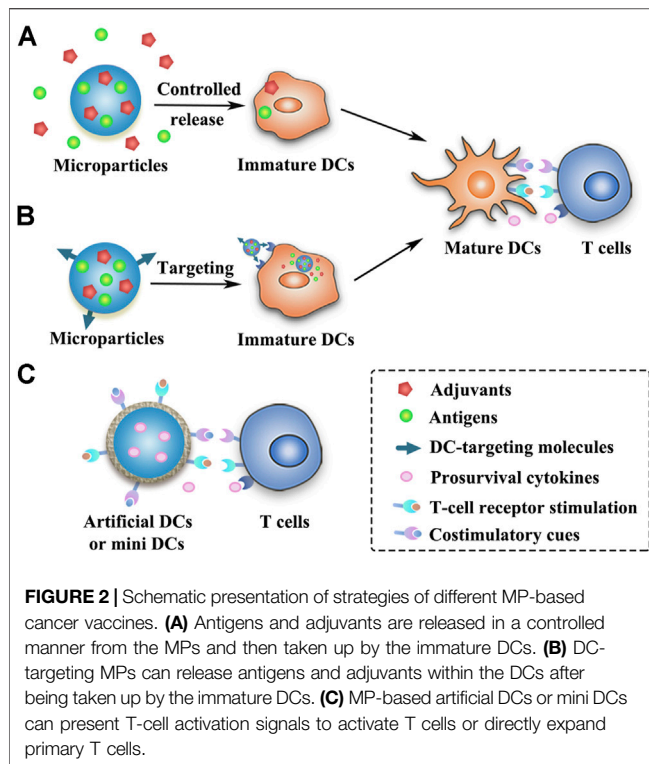
TABLE 2 | Representative examples of cancer vaccines delivered by controlled-release platforms (from 2017 to 2021).

Delivery system	Composition	Antigens	Adjuvants and combination therapies	Tumor model	Reference
1. Subunit vaccines					
MPs	Mesoporous silicon vector	TRP2 peptide	CpG and MPLA	C57BL/6 mice with B16 tumor	Zhu et al. (2018)
Injectable Scaffolds	PEI-coated Mesoporous silica rods	OVA or neoantigen peptides	GM-CSF, CpG and anti-CTLA4	C57BL/6 mice with E7-TC-1, B16F10, or CT26 tumor	Li et al. (2018)
Injectable hydrogels	Comp.1 peptides	OVA	—	C57BL/6 mice with EG7-OVA or B16-OVA tumor	Wang et al. (2020b)
MNs	Pluronic F127	OVA	Resiquimod	C57BL/6 mice with EG7-OVA tumor	Kim et al. (2018)
2. Genetic vaccines					
Scaffolds	Mesoporous silica microrods	DNA polyplexes encoding OVA	GM-CSF, PEI, CpG and anti-PD-1	C57BL/6 mice with B16-OVA tumor	Nguyen et al. (2020)
Injectable hydrogels	HA-PCLA	DNA polyplexes encoding OVA	GM-CSF and PEI	C57BL/6 mice with B16-OVA tumor	Duong et al. (2020a)
MNs	PVA	RALA/pDNA nanoparticles encoding PSCA	—	C57BL/6 mice with TRAMP-C1 tumor	Cole et al. (2019)
3. Tumor cell-based vaccines					
MPs	Yeast derived β -glucan	Tumor cell lysate	CpG	C57BL/6 mice with MC38 tumor	Hou et al. (2021)
Scaffolds	Collagen and HA	Tumor cell lysate	Nanogel-based poly (I:C) and gemcitabine	BALB/c mice with 4T1 tumor	Phuengkham et al. (2018)
Injectable hydrogels	Tumor-penetrable peptides	Dead tumor cells	ICG and JQ1	BALB/c mice with 4T1 tumor or EMT6 tumor	Wang et al. (2018)
Injectable hydrogels	HA and Pluronic F-127	Tumor cell membrane-coated BPQD nanovesicles	GM-CSF, LPS, anti-PD-1 and NIR irradiation	BALB/c mice with 4T1 tumor and C57BL/6 mice with B16F10 tumor	Ye et al. (2019)
MNs	HA	Tumor cell lysate	GM-CSF, melanin and NIR irradiation	C57BL/6J mice with B16F10 or BPD6 tumor; BALB/cJ mice with 4T1 tumor	Ye et al. (2017)
4. DC-based vaccines					
Injectable hydrogel	RADA16 peptide	OVA-pulsed DCs + free OVA or tumor cell lysate-pulsed DCs + tumor cell lysate	anti-PD-1	C57BL/6 mice with EG7-OVA tumor	Yang et al. (2018)
Scaffold	Mesoporous silica micro-rods	APC-mimetic scaffold presenting tumor peptides, CD28 and IL-2	19BBz CAR-T cells	NSG mice with Raji xenograft tumor	Cheung et al. (2018)
5. In situ cancer vaccines					
MPs	Poly(lactide acid)	—	IL-12 and stereotactic body radiation	C57BL/6J and KPC mice with KOKC or Pan02 tumor	Mills et al. (2019)
Injectable hydrogels	Alginate	—	GM-CSF, CpG and doxorubicin-iRGD conjugate	BALB/c mice with 4T1 tumor	Wang et al. (2020a)
Injectable hydrogels	Gelatin-hydroxyphenyl propionic acid	—	Exogenous DCs and oncolytic adenovirus co-expressing IL-12 and GM-CSF	C57BL/6 mice with LLC tumor	Oh et al. (2017)
MNs	PVA and PVP	—	1-methyl-tryptophan, chitosan nanoparticles containing ICG and NIR irradiation	C57BL/6 mice with B16 tumor	Chen et al. (2020a)

—, not performed; MPs, microparticles; TRP2, tyrosinase related protein 2; CpG, unmethylated cytosine-phosphate-guanine; MPLA, monophosphoryl lipid A; OVA, ovalbumin; GM-CSF, granulocyte-macrophage colony-stimulating factor; PEI, polyethyleneimine; anti-CTLA-4, cytotoxic T-lymphocyte-associated antigen-4 antibody; MNs, microneedles; PLGA, poly(lactide-co-glycolide); IL, interleukin; DNA, deoxyribonucleic acid; anti-PD-1, programmed cell death protein-1 antibody; HA-PCLA, levodopa- and poly(ϵ -caprolactone-co-lactide)ester-functionalized hyaluronic acid; poly(I:C), polyinosinic:polycytidylic acid; PVA, poly(vinyl pyrrolidone); pDNA, plasmid DNA; RALA, cationic peptide consists of arginine/alanine/leucine/alanine repeats; HA, hyaluronic acid; APC, antigen-presenting cell; PSCA, prostate stem cell antigen; TRAMP-C1, transgenic adenocarcinoma mouse prostate cell line 1; LPS, lipopolysaccharides; anti-PD-L1, programmed death-ligand 1 antibody; BPQD, black phosphorus quantum dot; NIR, near-infrared; DC, dendritic cell; CAR-T cells, chimeric antigen receptor T cells; iRGD, an internalizing cyclic peptide containing an Arg-Gly-Asp (RGD) motif; PVP, poly(vinyl alcohol); ICG, indocyanine green.

antigens and adjuvants from degradation with slow release at the injection site to prolong antigen presentation and allow simultaneous delivery of antigens and adjuvants to the same APC (Lin et al., 2015; Huang et al., 2019) (**Figure 2**). By modulating the polymer molecular weight, composition, preparation method, particle size and additives, etc., MPs can provide sustained or pulsatile release of entrapped antigens over

periods lasting weeks to months (Sivakumar et al., 2011). Furthermore, the modification of surface physicochemical properties or decoration with ligands or antibodies can lead to different functionalized MPs (**Figure 2**), such as APCs-targeting MPs, immune cell-engaging particles (artificial DCs) or MPs for intranasal vaccination (Mata et al., 2011; Li et al., 2016b; Jung et al., 2019; Koerner et al., 2019; Huang et al., 2020).



Among the most extensively exploited synthetic polymers in many areas, PLGA has been approved by the FDA for human use in drug delivery and biomedical devices due to its biodegradability and biocompatibility (Koerner et al., 2019). PLGA micro- or nanoparticles are promising carriers with remarkable application prospects for cancer vaccines. For example, tumor lysates alongside with TLR agonists (CpG-ODN) were co-encapsulated into PLGA microspheres to induce cytotoxic T cell responses and mediate tumor shrinkage in a transgenic mouse model of prostate cancer, and these particles could be sterilized by γ -irradiation without impairing their antitumor efficacy (Mueller et al., 2012). Recently, PLGA microspheres loaded with antigens and photosensitizers facilitated an active transport of microsphere-containing APCs to draining lymph nodes after illumination, resulting in strong CD8⁺ T cell responses (Schineis et al., 2021). Moreover, combination therapies that attack tumors from all sides can further augment the antitumor effects of MPs-based vaccines. PLGA nanoparticles that co-deliver doxorubicin, two immune adjuvants (poly(I:C) and R848), and one chemokine (CCL20) generated superior antitumor effects than separate compounds, as demonstrated on two treatment-resistant lung and colon cancer models (Silva et al., 2019). However, the prolonged survival time requires four repeated intratumoral injections of the PLGA nanoparticles, indicating that MPs may be a preferable platform for the sustained delivery of multiple drugs.

In spite of these promising features of PLGA MPs, the encapsulation efficiency and loading efficiency of hydrophilic drugs in PLGA MPs are usually low, and antigens, especially the

macromolecular proteins, have high risks of aggregation or degradation in the presence of organic solvents and high shear stresses during the preparation process, leading to impaired antigenicity and immunogenicity. Many strategies have been developed to maintain the integrity of proteins. Bailey et al. developed a “self-healing encapsulating” method to load protein antigens into pre-made porous PLGA microspheres with minimal impact on the antigens (Bailey et al., 2017). Besides, before encapsulated into the PLGA MPs, protein antigens can be previously loaded into polysaccharide (dextran) glassy particles through freezing-induced phase separation to protect antigen’s integrity (Geng et al., 2008). In another example, antigens and other immunomodulators can be efficiently and intactly loaded on the surface of PLGA MPs by conjugating short synthetic DNA scaffolds to the surface (Huang et al., 2020). More importantly, many advanced manufacturing processes, such as spray drying technology and supercritical carbon dioxide, are able to greatly improve the drug loading, protein stability, reproducibility and scaling-up production of PLGA MPs (Han et al., 2016a; Koerner et al., 2019). Another challenge limiting the broad application of PLGA MPs as vaccine carriers is high initial burst release that often consumes about 25% of the total drug in the first day (Park et al., 2019). This initial burst release, mainly resulted from the quick dissolution of adsorbed or weakly bound drugs on the surface of PLGA MPs, may lead to unintentional toxicity (Koerner et al., 2019). The release kinetics of PLGA MPs can be modulated by many approaches including multi-layered microparticles, nanoparticles-in-microparticles, hydrogel templates, coaxial electrospray and microfluidic fabrication, etc. (Han et al., 2016a). Interestingly, the initial burst can be advantageous to produce pulsatile-release MPs that mimic the prime-boost effect of conventional vaccines, showing the potential to make single-injection vaccines (Guarecuco et al., 2018). After administration, the bulk degrading PLGA MPs can generate acidic degradation products which may affect both antigen stability and release kinetics (McHugh et al., 2015). These pH issues may be alleviated by preparation of small PLGA particles which facilitate the diffusion of acidic degradation products and by addition of insoluble buffers to maintain a stable interior pH (McHugh et al., 2015).

Scaffolds

The scaffold system is commonly used in tissue engineering as the artificial extracellular matrix for the proliferation and differentiation of seeded cells or as the sustained delivery vehicles for therapeutic substances (Bessa et al., 2008; Shafiee and Atala, 2017). Nowadays, scaffolds or implants are also implemented in the field of cancer therapy (Table 2), providing new insights into the design of cancer vaccines. In order to modulate the antitumor immunity, scaffolds can be surgically implanted or low-invasively injected into the body to form localized immune niches or reservoirs for the controlled delivery of engineered immunocytes or cancer vaccines (Figures 3A–C). Various organic or inorganic materials can be used to fabricate scaffolds, such as alginate, collagen, hyaluronic acid, PLGA, and silica rods (Ali et al., 2009b; Kim et al., 2015; Stephan

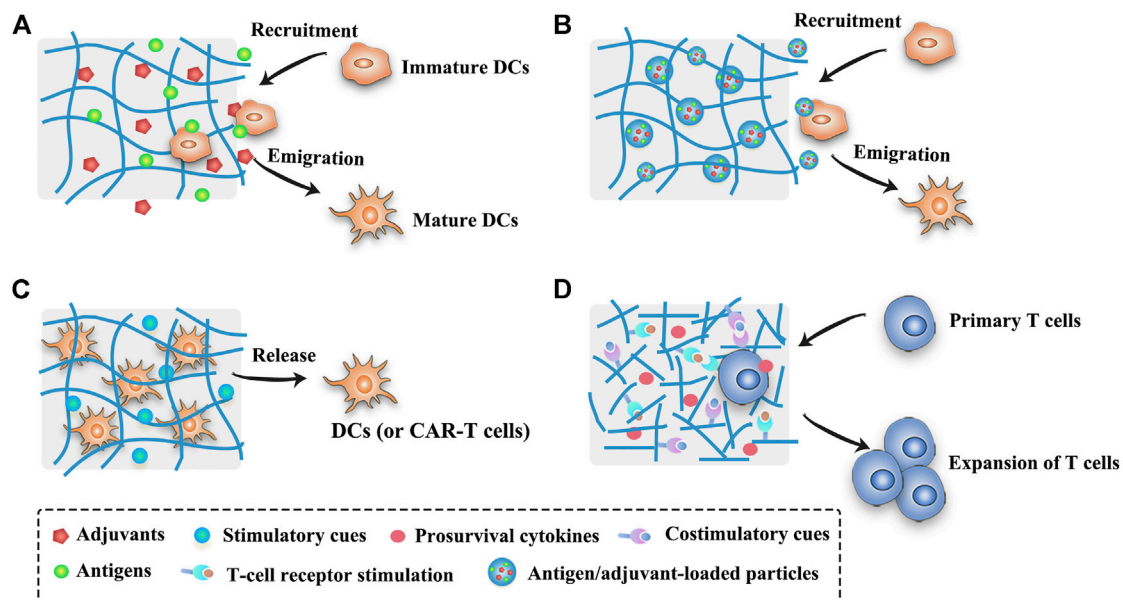


FIGURE 3 | Schematic illustration of strategies of scaffold- or hydrogel-based cancer vaccines. **(A)** Scaffold- or hydrogel-based cancer vaccines can recruit immature DCs into the injection site and subsequently activate them into mature DCs. **(B)** Nanocomposite hydrogel/scaffold systems can co-deliver antigens and adjuvants into the same DCs. **(C)** Scaffold- or hydrogel-based adoptive cell transfer can release mature DCs or CAR-T cells in a sustained manner and maintain the viability of cells. **(D)** Functionalized scaffolds can mimic APCs to directly expand primary T cells.

et al., 2015; Phuengkham et al., 2018). Early implants require surgical procedures to place the pre-formed scaffolds into the body to concentrate drug release for a long period of time at the target site. These pre-formed implantable scaffolds have a defined size and shape and can be fabricated in various sophisticated and functionalized structures to meet the needs of different medical applications. In addition, they usually exhibit an interconnected porous architecture, facilitating the diffusion of encapsulated immunomodulatory cues and providing space for the expansion and interaction of encapsulated immune cells or the incoming immune cells (Weiden et al., 2018) (**Figure 3**). Moreover, the release profiles of the biomolecules or immunocytes in the scaffolds can be fine-tuned to modulate the immune cell function (Ali et al., 2011b; Weiden et al., 2018). The pioneering work of scaffold vaccine was done by the Mooney group, who designed macroporous PLGA scaffolds. These scaffolds released GM-CSF in a sustained manner to recruit host DCs and subsequently presented tumor cell lysates and CpG to activate the incoming DCs (Ali et al., 2009a; Ali et al., 2009b). Implantation of this scaffold vaccine generated strong tumor-specific T cell responses, resulting in significant tumor regression and survival improvement in both melanoma and glioma mouse models (Ali et al., 2009a; Ali et al., 2009b; Ali et al., 2011a). Various chemokines, immunoadjuvants and cytokines can be also incorporated into this flexible scaffold to direct the recruitment of DC subset and augment the therapeutic activity in combination with checkpoint antibodies (Ali et al., 2013; Ali et al., 2014; Ali et al., 2016). Encouragingly, a human version of the PLGA scaffold vaccine (designated as WDVAX) is currently being evaluated in a phase I clinical trial for metastatic

melanoma (US National Library of Medicine, 2021). Although the implantable scaffolds have the ability to control their structure shape and rigidity as well as prevent the diffusion of scaffold materials, the invasive surgical implantation is quite cumbersome, causing patient discomfort and increasing the infection risk (Li and Mooney, 2016; Weiden et al., 2018). These implanted scaffolds cannot be placed in areas that are surgically inaccessible or volume-sensitive due to their stiffness (Leach et al., 2019). In addition, the function of normal organs may be affected if the scaffolds are placed into the tumor resection bed or near the tumor (Leach et al., 2019).

Moving forward, the injectable scaffolds that gel or self-assemble in the body have presented highly deformable and self-organizing abilities, thus avoiding the risks associated with implant surgery. Mooney et al. designed a fascinating injectable and self-assembling scaffold vaccine which was based on mesoporous silica rods (MSRs) with high-aspect-ratio to reprogram the immune cells and enhance the vaccine efficacy (Kim et al., 2015; Li et al., 2018). Upon subcutaneous injection in mice, these MSRs spontaneously assembled themselves into three-dimensional (3D) macroporous structures for the influx and efflux of immune cells. Analogous to previous studies, this injectable inorganic scaffold extended the release of the embedded GM-CSF, CpG and model antigens to recruit and educate host immune cells, leading to significant production of systemic antibodies and cytotoxic T cells that effectively delayed the tumor growth (Kim et al., 2015). The adsorption of cationic polymer polyethyleneimine (PEI) in the previous MSR vaccine could greatly enhance the immunogenicity of neoantigens and eradicate three different established tumors (Li et al., 2018).

Besides, surface modifications with poly(ethylene glycol) (PEG) or integrin-binding ligand RGD on MSR scaffolds could also regulate immune cell infiltration and activation (Li W. A. et al., 2016). Notably, these MSR scaffolds were demonstrated to be a promising platform for the delivery of DNA-based cancer vaccines (Nguyen et al., 2020). Different to those macroscopic scaffolds aiming to reprogram the incoming DCs, scaffolds that were composed of lipid bilayer-coated micro-MSRs and functionalized with T cell activation cues (anti-CD3, anti-CD28 and IL-2) could mimic APCs to directly expand primary T cells (Cheung et al., 2018) (**Figure 3D**). These inorganic scaffolds showed great potential in the delivery of personalized cancer vaccines, however, the biocompatibility, biodegradability and safety of injected materials need to be further evaluated before their clinical use. Other administration methods apart from surgical implantation and syringe injection are waited to be explored to broaden the application of controlled-release vaccines. In an example of this, an *in situ* formed fibrin gel was sprayed into the post-surgery tumor site to control the release of therapeutic antibodies (Chen et al., 2019b). In addition to these PLGA and MSR scaffolds, injectable biomaterials including hydrogels, cryogels, and other *in situ* forming platforms can also form the porous matrix *in vivo* to modulate the immune system. The opportunities and challenges of these injectable biomaterials are described below.

Injectable Gels

Injectable gels are widely applied in many areas including wound healing, bone regeneration, diabetes treatment and cosmetic surgery (Li et al., 2021). Recently, macroscopic injectable gels, especially intelligent hydrogels with the size ranging from millimetres to centimetres, have attracted enormous attention as biocompatible carriers for the spatiotemporal control over cancer vaccines involving antigens, immunomodulators and engineered immunocytes (**Table 2**). Injectable gels are flowable fluid before or at the time of injection. Once injected into the body, they immediately undergo “sol-to-gel” phase transition by means of chemical or physical crosslink (Li and Mooney, 2016), loss of shear force (Shear-thinning hydrogels) (Yan et al., 2010), mechanical collapse and recover (such as cryogels) (Bencherif et al., 2015), or solvent exchange (such as phospholipid-based gels) (Han et al., 2016b) to form gels. Consequently, injectable gels can be localized almost anywhere in the body by a syringe without the complicated surgical procedures of implantable scaffolds. More importantly, injectable gels have a highly deformable ability to fit the spatial structure of the injection site before they form into a persisting implant (Leach et al., 2019).

Hydrogels are crosslinked 3D polymeric networks containing a large amount of water (typically 70–99%) which enables them to mimic the extracellular matrix (Li and Mooney, 2016). Due to the excellent biocompatibility and tunable release kinetics, hydrogels are the most extensively explored gel carriers in the delivery of cancer vaccines. In addition, hydrogels have high loading capacity for hydrophilic drugs, and they are harmless to the integrity of antigens because the encapsulation process is usually carried out under mild aqueous conditions. Moreover, antigens can be

protected in the hydrogels from degradation by the *in vivo* enzymes during the extended periods of antigen presentation. Hydrogels can be made from a variety of materials including peptides (Wang et al., 2018; Wang Z. et al., 2020), proteins (e.g., silk fibroin and gelatin) (Wu et al., 2016; Oh et al., 2017), polysaccharides (e.g., alginate, hyaluronic acid and chitosan) (Hori et al., 2009; Kordalivand et al., 2019; Ye et al., 2019), nucleic acids (e.g., DNA) (Li et al., 2020) and synthetic polymers (e.g., poloxamers and polyesters) (Cirillo et al., 2019; Leach et al., 2019). To form hydrogels, these materials can be crosslinked through different mechanisms, mainly by physical noncovalent interactions (such as hydrogen bonding, host-guest interactions, hydrophobic interactions, electrostatic interactions, etc.) and by chemical covalent bonds (such as click chemistry, Diels-Alder reactions, Michael addition, enzymatic reactions, etc.) (Yu and Ding, 2008; Li and Mooney, 2016; Lei and Tang, 2019).

Many macroscopic hydrogels seek to recruit and activate the endogenous DCs by prolonging the presentation of the antigens and immunomodulators (**Figure 3A**) (Bencherif et al., 2015; Ye et al., 2019; Duong et al., 2020a). In one representative study, irradiated tumor cells, GM-CSF and CpG were co-encapsulated in sponge-like macroporous cryogels which were fabricated by alginate with RGD peptide modification (Bencherif et al., 2015). After subcutaneously injected into the mice bearing melanoma, these cryogels released the immunomodulators in a sustained and localized manner to facilitate the influx of DCs and subsequently induce robust and durable tumor-specific T cell responses. In addition, hydrogels are excellent delivery vehicles for adoptive cell therapies (such as DC vaccines and CAR-T cells, **Figure 3C**) due to the concentration of the engineered immunocytes at the desired site as well as the maintenance of cell viability for a long time (Hori et al., 2009; Yang et al., 2018). Furthermore, hydrogels can easily co-deliver diverse drugs using one platform for a combination of cancer treatments (Wang et al., 2018; Song et al., 2019; Wang et al., 2020b). For example, Wang et al. developed a personalized cancer vaccine (termed PVAX) by integrating JQ1 (an inhibitor of PD-L1 expression) and indocyanine green (ICG, a photosensitizer) co-loaded autologous tumor cells into a hydrogel matrix composed of tumor-penetrable peptides (Wang et al., 2018). After intratumoral administration, the PVAX was triggered by near-infrared (NIR) irradiation to release tumor antigens and JQ1, causing the full activation of the postoperative antitumor immunity that efficiently prevented tumor recurrence and metastasis.

Numerous studies are striving to develop methods for on-demand control over the release kinetics of injectable gels to improve the spatiotemporal delivery of cancer vaccines. Various intelligent hydrogels have been designed to respond to intrinsic or extrinsic stimuli such as low pH, temperature, enzymes, redox, photoirradiation, magnetic fields and ultrasound (Lu et al., 2017; Kanwar and Sinha, 2019). Duong et al. developed an injectable thermosensitive smart hydrogel by conjugating thermo-responsive poly(ϵ -caprolactone-co-lactide) ester and levodopa to hyaluronic acid (Duong et al., 2020a). This hydrogel exhibited sol-to-gel transition in response to the body temperature, and the levodopa moieties were introduced to

strengthen the stability of the hydrogel during implantation. The sustained degradation of this smart hydrogel led to a controlled release of GM-CSF and nano-sized polyplexes expressing model protein antigen ovalbumin (OVA), and then effective inhibition of B16/OVA melanoma tumors by a single injection was observed. Furthermore, many dual-sensitive hydrogels have gained enormous attention in more precisely controlling the release profiles of drugs, such as thermo-pH dual-sensitive hydrogels (Liu et al., 2019a), thermo-reactive oxygen species (ROS) dual-sensitive hydrogels (Yu et al., 2018) and electric field-pH double-sensitive hydrogels (Qu et al., 2018). Interestingly, Brudno et al. developed a replenishable and injectable hydrogel depot system which could capture systemically administrated prodrug refills and then release them locally in a sustained manner (Brudno et al., 2018). This repeatedly refillable hydrogel can be used to prepare precisely controlled-release or pulsatile-release cancer vaccines.

The lag time during the sol to gel transformation may induce a severe initial burst release effect which is responsible for the toxic side effects of immunomodulators and even immune tolerance (Wang and Mooney, 2018; Kanwar and Sinha, 2019). Many strategies are conceived to settle this issue, for example, burst release can be alleviated by optimizing the molecular weight and the concentration of polymers, by using appropriate solvents, and by adding plasticizers or surfactants (Kanwar and Sinha, 2019). The prompt interactions of antigens (and adjuvants) with polymers can also regulate the release profiles, such as by electrostatic interaction or covalent binding (Umeki et al., 2015; Yu et al., 2018; Kordalivand et al., 2019). In one representative study, cationic OVA or cationic OVA peptide were bound to anionic CpG DNA hydrogel by electrostatic interaction, resulting in significantly slower drug release and better tumor inhibition in the group of cationic OVA hydrogel than the group of unmodified OVA hydrogel (Umeki et al., 2015). Another strategy to mitigate the burst effect is to use nanocomposite hydrogel systems (Figure 3B). For example, the incorporation of OVA and two adjuvants (MPLA and Quil A)-loaded PLGA nanoparticles into thermoresponsive pentablock copolymer (PEG-PCL-PLA-PCL-PEG) hydrogels could greatly reduce the burst release of antigens and adjuvants (Bobbala et al., 2016). In another study, OVA was encapsulated into cationic chitosan nanoparticles and then incorporated in hyaluronic acid-based hydrogels in order to achieve a prime-boost regimen (Korupalli et al., 2019). This nanocomposite hydrogel system could rapidly release the nanoparticles that had no specific interactions with the hydrogels for a priming dose, and retain the nanoparticles that were bonded to the hydrogels by covalent or electrostatic interactions for a booster dose. With the minimal burst effect, these chitosan nanoparticles could promote antigen uptake and DC activation, thus inducing higher antibody responses than soluble antigens. Moreover, an onion-structure multilayer hydrogel capsules may be another promising approach to effectively inhibit the burst release of therapeutic cargos (Zhang et al., 2019).

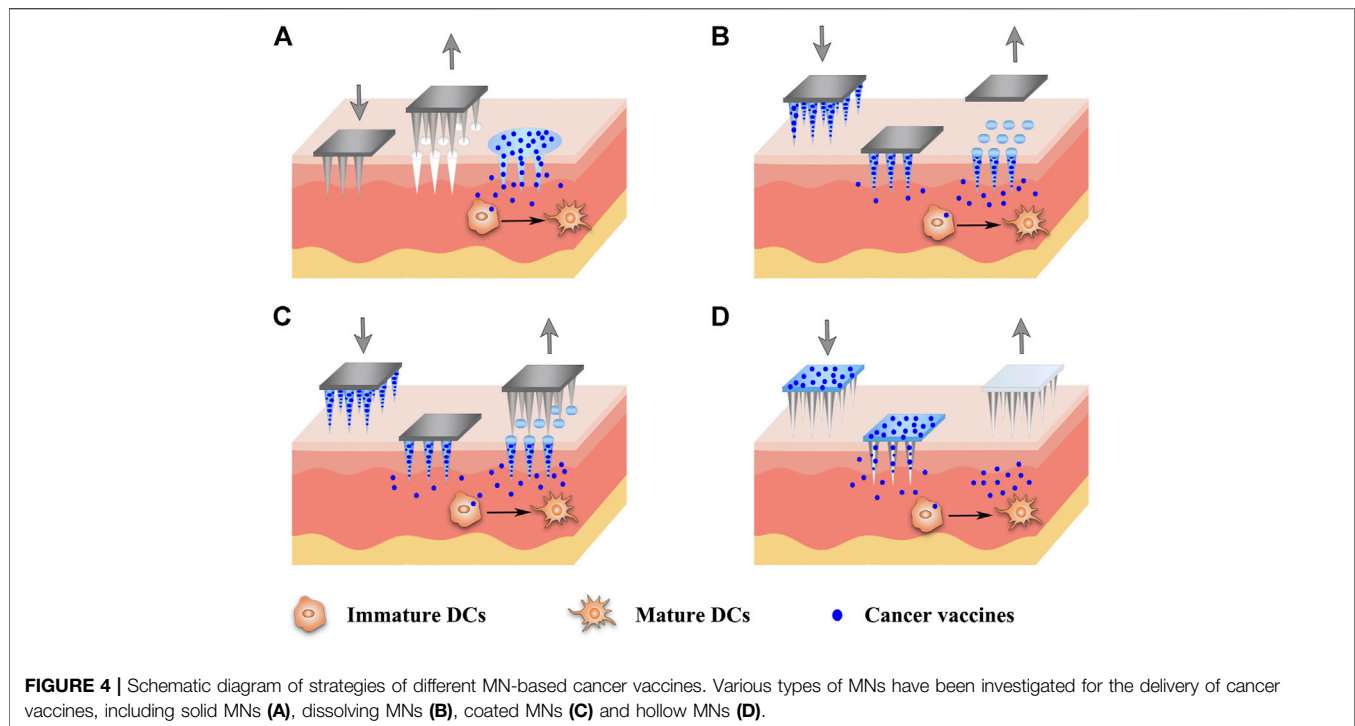
Despite these encouraging progresses, there still exist many hurdles lying on the road to the broad clinical application of hydrogels, including safety concerns about the elaborate materials and solvents, the difficulty in the highly precise control of the release kinetics, the inconsistent drug release resulted from the

inconsistent shape of the gels formed, the challenge of *in situ* injectability to deep tumors, the complexity of scaling-up manufacturing, and the difficulty in storage and terminal sterilization (Kanwar and Sinha, 2019). Consequently, the influence of the polymer composition, gel stiffness, network density, porosity and drug-polymer interactions on the release kinetics, as well as the influence of combination therapies, drug doses, administration routes and times on the immune system, should be better understood and these factors should be optimized to exert the maximum efficacy of hydrogel-based cancer vaccines.

Microneedles

Most vaccines are administrated *via* intramuscular (IM), subcutaneous (SC) and intradermal (ID) inoculation using conventional hypodermic needles. Although the relative immunogenicity of vaccines by these three routes (IM, SC and ID) varies among individual vaccines, ID immunization usually induces more robust immune responses than IM or SC immunizations in clinical studies. This is partly because the different skin layers host a tight semi-contiguous network of immune cells that can interact with the antigens administered to direct drastically different immune responses compared to subcutaneous fat and muscle tissue (Al-Zahrani et al., 2012). The development of MNs is a great achievement to take advantage of skin immunization and to address the issues associated with vaccination by conventional needles (e.g., pain, needle-stick injuries or needle re-use) (Leone et al., 2017). MNs, arrays of sharp tiny needles at lengths varying from 100 to 2,000 μm , are designed to pierce the *stratum corneum* of the skin to deliver both small molecular and macromolecular drugs or even nanoparticles (NPs) to the epidermal and the dermal or even deeper layers in a safe and controlled manner (Alimardani et al., 2021). As a painless transcutaneous administration platform, MNs have been extensively explored for cancer vaccines, antiviral immunotherapies, and diabetes (Jin et al., 2018b; Chen et al., 2020b; Uppu et al., 2020). MNs can promote the deposition of the vaccines by creating micropores in the skin, facilitating vaccine transport, and hence reducing the necessary dose of antigens/vaccines for the immunological responses. A significant number of MNs mediated vaccine candidates have shown encouraging results in preclinical and clinical trials (Hossain et al., 2020).

The minimally invasive and cost-effective features of MNs have aroused their rapid development and extensive exploration in cancer vaccine delivery recently (Table 2). Various types of MNs have been investigated for cancer vaccine delivery, as depicted in Figure 4, including solid MNs (Bhowmik et al., 2011; Chablani et al., 2019), dissolving MNs (Zaric et al., 2013; Gala et al., 2018; Kim et al., 2018; Cole et al., 2019; Kim et al., 2019), coated MNs (Zeng et al., 2017; Duong et al., 2018) and hollow MNs (van der Maaden et al., 2018; Niu et al., 2019). Novel design to utilize parallel circular blades with MN on edge as electrodes was also studied for their ability to deliver siRNA targeting PD-L1 alone, or combined with anti-PD-1 antibody and immunoadjuvant CpG 2395 (Yang et al., 2021). This immunotherapy treatment has been tested in two tumor xenograft murine models and produced robust T cell immune



responses and significant tumor growth inhibition as well as excellent safety profiles. Various vaccine formulations, including microparticles (Bhowmik et al., 2011), nanoparticles (Zaric et al., 2013), nanopolyplex (Duong et al., 2020b), liposomes (van der Maaden et al., 2018), and *in situ* generating nanomicelles (Kim et al., 2018) to ensure efficient co-encapsulation of antigens and adjuvants within the nanovaccine platforms have been delivered using MNs to improve cancer vaccine therapy. Du et al. used hollow MNs to administer a range of nanoparticle vaccine formulations loaded with OVA and poly(I:C) (Du et al., 2017). PLGA nanoparticles, liposomes, mesoporous silica nanoparticles, and gelatin nanoparticles were compared. The co-encapsulation of OVA and poly(I:C) using those formulations yielded a similar IgG1 response, but a surprisingly higher IgG2a response than OVA/poly(I:C) solution in a murine model. Particularly, PLGA nanoparticles and especially cationic liposomes, which presented sustained release profiles of both OVA and poly(I:C), elicited better immune responses (Du et al., 2017). The antigens and adjuvants were co-encapsulated in some vaccine formulations through electrostatic interaction, hydrophobic interaction as well as covalent linking interaction (Chen et al., 2021). However, when these formulations are loaded into the MNs, especially adding some excipients to form the MNs, the electrostatic interaction between the antigen and adjuvant is hampered. As a good example to address this issue, an *in situ* generating nanomicelle including hydrophilic tumor model antigen (OVA), hydrophobic adjuvant TLR 7/8 agonist (R848) and amphiphilic triblock copolymer has been delivered using dissolving MNs platform to form nanomicelles *in situ* with a size of 30–40 nm after cutaneous application (Kim et al., 2018). Antigen-specific humoral and cellular immunity protection were found to be elicited after administration, leading to a significant

antitumor activity in the EG7-OVA tumor-xenograft mice. Since MNs are usually applied topically on the surface of the skin, they are very suitable to be combined with phototherapy (Ye et al., 2017; Chen et al., 2020a). One example of such combination therapies was based on the tumor lysates, melanin and GM-CSF were loaded into hyaluronic acid-based MNs that allowed sustained release of the lysates (Ye et al., 2017). After administration, the melanin converted the NIR irradiation into heat, which facilitated tumor-antigen uptake by DCs and boosted the antitumor immune responses in both B16F10 and 4T1 tumor models.

Collectively, MNs have offered a unique set of properties for cancer vaccine delivery with improved vaccination efficacy, compliance, and coverage. The use of MNs instead of a needle injection can not only avoid pain for the patients but also provide the promise of self-vaccination as well as release the assistance from professional healthcare, which is especially suitable for mass vaccination in the case of a pandemic (Zaric et al., 2013). Although the use of MNs could be more effective than a single-needle injection as the antigens might be more evenly distributed after injection and have a more targeted delivery to APCs in the dermis and epidermis layers under the skin, MNs-based delivery may cause more frequent local reactions due to the shallow penetration (Zhang et al., 2015). MNs can be fabricated in different shapes using various materials, including stainless steel, titanium, silicon, ceramic and polymers (Alimardani et al., 2021). However, there is a possibility of needle breakage within the skin after the application of metal, silicon or glass MNs, triggering unintentional safety concerns (Jin et al., 2018a). In addition, some materials such as nickel may cause allergic reactions. Biodegradable polymeric MNs can minimize the risk of inflammation induced by undissolving materials, because they

can degrade to metabolizable objects in the body (Jin et al., 2018a). On the other hand, MNs should have enough mechanical strength and sharpness to pierce the skin for transdermal applications. However, the incorporation of drugs and nanoparticles may compromise the mechanical strength of MNs (Kim et al., 2018). Therefore, the design of MNs-based cancer vaccines should be optimized with the full consideration of balancing the pain, mechanical strength, drug doses and drug release profiles for therapeutic efficacy. For a cancer vaccine, the efficacy is closely associated with the distance from the injection site to the cancer site. Most of the studies for MN-based cancer vaccines were conducted in malignant melanoma. Although they can provide invaluable information about other cancers as well, more cancer models will need testing for evaluating the systemic immune protections of MNs (Zhang et al., 2015).

CORRELATIONS OF THE IMMUNE RESPONSES AND THE RELEASE KINETICS OF CANCER VACCINES

It has been widely reported that controlled or sustained release of antigens and adjuvants is beneficial to generate antigen-specific antibodies, T cell responses and immunological memory responses (Kanchan et al., 2009; Ali et al., 2011b; Demento et al., 2012; Han et al., 2016b; Irvine et al., 2020). The mechanisms underlying these benefits of controlled-release vaccines may be complex and multifactorial. Herein, we describe four major mechanisms as follows. Firstly, controlled-release platforms usually form an *in situ* drug depot in which antigens can maintain their intact conformation for a considerable period of time. Antigens and adjuvants can be released in a continuous or pulsatile manner to extend the antigen exposure or to mimic the traditional prime-boost regimen of vaccination (Sivakumar et al., 2011; Brito and O'Hagan, 2014). Secondly, owing to the heterogeneity and immunostimulatory activity of materials or the effect of encapsulated chemokines, most depot-like controlled-release systems can stimulate the accumulation of inflammatory cells or recruit APCs to the injection sites (Ali et al., 2009b; Brito and O'Hagan, 2014; Han et al., 2016b). Subsequently, cytokines secreted by inflammatory cells can stimulate the activation, proliferation and differentiation of immune cells. On the other hand, the antigen depot is surrounded or infiltrated by the recruited APCs, thus increasing the chance of antigen uptake. Thirdly, controlled-release systems, especially when loaded with immunoadjuvants, can further motivate the maturation of APCs and then direct the Th1 or Th2 immune responses (Li et al., 2018; Song et al., 2018). Last, but not least, some polymeric micro- or nanoparticles mimicking the size and surface characteristics of pathogens or functionalized with targeting ligands can accumulate in lymph nodes or target the specific immunocytes (Mata et al., 2011; Silva et al., 2016), thereby reducing the antigen dose and improving the magnitude of immune responses.

Although controlled-release systems have the potential to augment the vaccine efficacy with minimal toxicity, the effect

of release kinetics on immune responses is complex and unclear. It is worth noting that antigen stimulation can be either immunologically activating or immunologically tolerant. For example, intravenous injection of low-dose antigens could induce immune activation, whereas intravenous injection of high-dose antigens might cause T cell exhaustion (Zinkernagel et al., 1997). Although the slow and sustained release of vaccines is demonstrated to favor the antitumor immunity, the extremely long periods of antigen presentation may, in turn, hamper the antitumor immunity by exhausting and deleting tumor-specific T cells or directing T cells to the antigen depot rather than to the target tumor (Iezzi et al., 1998; Hailemichael et al., 2013; Shae et al., 2019). On the other hand, a particularly fast release of antigens may result in rapid clearance of antigens from the lymph nodes (Shae et al., 2019; Irvine et al., 2020), necessitating repeated injections to boost the immune responses. Moreover, the release rate of adjuvants seems necessary to be coincident with that of antigens, because a fast release of adjuvants leads to early exhaustion of adjuvants, while an extremely slow release of adjuvants cannot provide sufficient activation cues to the immature DCs, thereby promoting T cell anergy and immune tolerance (Audiger et al., 2017; Wang and Mooney, 2018; Leach et al., 2019). Therefore, the release kinetics of antigens and adjuvants from the controlled-release platforms has a significant influence on the type and magnitude of immune responses. An interesting study showed that a “dose escalation” regimen with an exponentially increasing antigen dose elicited a superior CD8⁺ T cell response than a single bolus injection or constantly repeated dose regimen (Johansen et al., 2008). Another opinion suggested that an appropriate burst release followed by a sustained vaccine release was optimal to induce fast and powerful immune responses (Zhang et al., 2014). Consequently, a highly precisely controlled vaccine delivery system with on-demand drug release is believed to maximize the immune efficacy. Nevertheless, the optimal vaccine release kinetics for inducing the most potent and durable immunity is still not clear. It may vary among different types of controlled-release vaccines which have distinct adjuvant properties, antigen types, disease types and administration routes (Bruto and O'Hagan, 2014; McHugh et al., 2015). Moreover, antigens and adjuvants can hardly share consistent release profiles due to their different physicochemical properties. Therefore, The release kinetics of antigens and adjuvants should be screened and optimized to augment the antitumor immunity. Fortunately, the release kinetics can be modulated by numerous factors, including material properties (such as chemical composition, molecular weight, hydrophobicity, crystallinity, glass transition temperature and degradation products), depot geometry (such as size, shape, porosity and network density), antigenic factors (such as antigen size, position and loading amount), and others (such as antigen-polymer interactions, additives and administration route) (McHugh et al., 2015; Li and Mooney, 2016). Furthermore, strategies that guarantee the simultaneous presentation of antigens and adjuvants to the same APCs during the long period of release may exert stronger antigen-specific CD8⁺ T cell responses. For example, antigens and adjuvants can be linked together by covalent or ionic bonds

before loaded into controlled-release platforms, or antigens and adjuvants can be pre-encapsulated into nano- or microparticles followed by incorporating these particles into a macroscopic matrix.

Depiction of the drug release profiles is the inevitable step to study the controlled-release vaccines. However, most studies contain only the *in vitro* release data, which may not be coincident with the *in vivo* release due to the different release environment inside and outside the body. Unfortunately, the accurate quantitative data of *in vivo* release kinetics are difficult to acquire owing to the low antigen loading amount and long duration of release (McHugh et al., 2015). *In vivo* imaging is now commonly used to semi-quantitate the *in vivo* vaccine kinetics by measuring the remaining fluorescence intensity of fluorescently labeled antigens in the vaccine depot over time. However, it is unable to determine the actual amount and stability of the antigens because fluorescence quenches easily. Therefore, both the exploration of more accurate *in vivo* measuring technologies and the in-depth understanding of *in vitro-in vivo* correlations are needed to spur the development of controlled-release vaccines. By far, many controlled-release vaccine delivery systems have been using model antigens (such as OVA) and model tumors (such as immortalized tumor cell lines) to study the release kinetics and antitumor immune responses (Kim et al., 2015; Umeki et al., 2015; Han et al., 2016b; Niu et al., 2019). However, these model antigens and the model tumors cannot recapitulate the complex challenges facing the real therapeutic antigens and patient individualized tumors (Day et al., 2015; McHugh et al., 2015). For example, the model antigen ovalbumin for mouse studies is exceptionally immunogenic and may lead to overestimating vaccine efficacy. Moreover, subcutaneous injection of B16F10 cell lines into the mice is widely used to establish melanoma, but these *in vitro* cultured murine cancer cells cannot simulate the cancer heterogeneity and are not physiologically relevant to human cancers. Moreover, the immune system of a healthy mouse differs significantly from that of a human in both innate and adaptive immunity (Mestas and Hughes, 2004). Therefore, more data on the immune efficacy of controlled-release vaccines that are tested using clinically relevant antigens and using suitable tumor and animal models should be assessed in the future.

CONCLUSIONS AND OUTLOOK

Cancer vaccines represent the most promising and cost-effective antitumor strategy which engages the immunity of patients to target malignancies. Depending on the form and source of antigens, cancer vaccines can be briefly categorized into five types, including subunit vaccines, genetic vaccines, DC-based vaccines, tumor cell-based vaccines and *in situ* cancer vaccines. The pros and cons of these vaccines have been outlined in this review. Local and sustained delivery of vaccines at lower doses shows higher effectiveness and lower toxicity than bolus injections. Recently, the controlled-release drug delivery systems, such as polymeric MPs, scaffolds, hydrogels and

MNs, have attracted enormous attention in the spatiotemporal delivery of cancer vaccines. However, there are still many obstacles limiting the broad application of controlled-release cancer vaccines, including the instability of antigens and adjuvants during the preparation and release period, the challenge of precisely controlling over release kinetics, safety concerns, and the difficulties in scaling-up manufacturing, storage and terminal sterilization. The mechanisms and patterns of the action of controlled-release vaccines need to be studied in-depth to develop potent, persistent, non-toxic and easily available single-shot cancer vaccines.

Despite the fact that immunotherapy have been widely studied and applied on hematological tumors and melanoma, the effect of current immunotherapies on solid tumors remains faint because of the immunosuppressive tumor microenvironments, low tumor immunogenicity and low infiltration of immune cells into tumors (Kuol et al., 2017; Galluzzi et al., 2018). Based on the unique advantages of these controlled-release systems as mentioned above, the combination of multiple cancer therapies with controlled-release cancer vaccines may be the most promising approach to treat solid tumors as well as to prevent tumor metastasis and recurrence. For example, many clinical available strategies, such as chemotherapy, radiotherapy, phototherapy, oncolytic viruses and immune checkpoint antibodies, show great therapeutic potential in combination with cancer vaccines. Moreover, targeting the microbiome in the intestine or the tumor may have a synergistic antitumor effect with cancer vaccines (Matson et al., 2018; Nejman et al., 2020). More work should be done to explore the synergistic therapeutic effects of controlled-release vaccines and other therapies. In conclusion, the next generation of cancer vaccines should focus on the following aspects: 1) the choice of antigens with high immunogenicity; 2) co-delivering antigens and appropriate adjuvants to the same APCs; 3) modulating the optimal release kinetics of the antigens and adjuvants from delivery systems to augment subsequent immune responses; 4) reshaping the immunosuppressive environment to maximize the specific cytotoxic function of T cells; 5) adopting optimal combinatorial therapeutic regimens to improve the outcomes and avoid tumor evade.

AUTHOR CONTRIBUTIONS

All authors listed have made a substantial, direct, and intellectual contribution to the work and approved it for publication.

FUNDING

This work was supported by the National Natural Science Foundation of China (no. 82003683), the Science and Technology Plan of Guizhou province ((2018)2821) and the Fundamental Research Funds for the Central Universities, Southwest Minzu University (2019NQ57).

REFERENCES

- Al-Zahrani, S., Zaric, M., McCrudden, C., Scott, C., Kissenpfennig, A., and Donnelly, R. F. (2012). Microneedle-mediated Vaccine Delivery: Harnessing Cutaneous Immunobiology to Improve Efficacy. *Expert Opin. Drug Deliv.* 9 (5), 541–550. doi:10.1517/17425247.2012.676038
- Ali, O. A., Doherty, E., Bell, W. J., Fradet, T., Hudak, J., Laliberte, M.-T., et al. (2011a). The Efficacy of Intracranial PLG-Based Vaccines Is Dependent on Direct Implantation into Brain Tissue. *J. Controlled Release* 154 (3), 249–257. doi:10.1016/j.jconrel.2011.06.021
- Ali, O. A., Doherty, E., Mooney, D. J., and Emerich, D. (2011b). Relationship of Vaccine Efficacy to the Kinetics of DC and T-Cell Responses Induced by PLG-Based Cancer Vaccines. *Biomater* 1 (1), 66–75. doi:10.4161/biom.1.1.16277
- Ali, O. A., Emerich, D., Dranoff, G., and Mooney, D. J. (2009a). *In situ* regulation of DC Subsets and T Cells Mediates Tumor Regression in Mice. *Sci. Translational Med.* 1 (8), 8ra19. doi:10.1126/scitranslmed.3000359
- Ali, O. A., Huebsch, N., Cao, L., Dranoff, G., and Mooney, D. J. (2009b). Infection-mimicking Materials to Program Dendritic Cells *In Situ*. *Nat. Mater* 8 (2), 151–158. doi:10.1038/nmat2357
- Ali, O. A., Lewin, S. A., Dranoff, G., and Mooney, D. J. (2016). Vaccines Combined with Immune Checkpoint Antibodies Promote Cytotoxic T-Cell Activity and Tumor Eradication. *Cancer Immunol. Res.* 4 (2), 95–100. doi:10.1158/2326-6066.Cir-14-0126
- Ali, O. A., Tayalia, P., Shvartsman, D., Lewin, S., and Mooney, D. J. (2013). Inflammatory Cytokines Presented from Polymer Matrices Differentially Generate and Activate DCs *In Situ*. *Adv. Funct. Mater.* 23 (36), 4621–4628. doi:10.1002/adfm.201203859
- Ali, O. A., Verbeke, C., Johnson, C., Sands, R. W., Lewin, S. A., White, D., et al. (2014). Identification of Immune Factors Regulating Antitumor Immunity Using Polymeric Vaccines with Multiple Adjuvants. *Cancer Res.* 74 (6), 1670–1681. doi:10.1158/0008-5472.CAN-13-0777
- Alimardani, V., Abolmaali, S. S., Tamaddon, A. M., and Ashfaq, M. (2021). Recent Advances on Microneedle Arrays-Mediated Technology in Cancer Diagnosis and Therapy. *Drug Deliv. Transl. Res.* 11, 788–816. doi:10.1007/s13346-020-00819-z
- Allison, J. P. (2015). Immune Checkpoint Blockade in Cancer Therapy. *JAMA* 314 (11), 1113–1114. doi:10.1001/jama.2015.11929
- Audiger, C., Rahman, M. J., Yun, T. J., Tarbell, K. V., and Lesage, S. (2017). The Importance of Dendritic Cells in Maintaining Immune Tolerance. *J.I.* 198 (6), 2223–2231. doi:10.4049/jimmunol.1601629
- Bailey, B. A., Ochyl, L. J., Schwendeman, S. P., and Moon, J. J. (2017). Toward a Single-Dose Vaccination Strategy with Self-Encapsulating PLGA Microspheres. *Adv. Healthc. Mater.* 6 (12), 1601418. doi:10.1002/adhm.201601418
- Bencherif, S. A., Warren Sands, R., Ali, O. A., Li, W. A., Lewin, S. A., Braschler, T. M., et al. (2015). Injectable Cryogel-Based Whole-Cell Cancer Vaccines. *Nat. Commun.* 6, 7556. doi:10.1038/ncomms8556
- Bessa, P. C., Casal, M., and Reis, R. L. (2008). Bone Morphogenetic Proteins in Tissue Engineering: the Road from Laboratory to Clinic, Part II (BMP Delivery). *J. Tissue Eng. Regen. Med.* 2 (2-3), 81–96. doi:10.1002/term.74
- Bhowmik, T., D'Souza, B., Shashidharamurthy, R., Oettinger, C., Selvaraj, P., and D'Souza, M. J. (2011). A Novel Microparticulate Vaccine for Melanoma Cancer Using Transdermal Delivery. *J. Microencapsulation* 28 (4), 294–300. doi:10.3109/02652048.2011.559287
- Bobbala, S., Tamboli, V., McDowell, A., Mitra, A. K., and Hook, S. (2016). Novel Injectable Pentablock Copolymer Based Thermoresponsive Hydrogels for Sustained Release Vaccines. *AAPS J.* 18 (1), 261–269. doi:10.1208/s12248-015-9843-4
- Bol, K. F., Schreiber, G., Gerritsen, W. R., de Vries, I. J. M., and Figdor, C. G. (2016). Dendritic Cell-Based Immunotherapy: State of the Art and beyond. *Clin. Cancer Res.* 22 (8), 1897–1906. doi:10.1158/1078-0432.CCR-15-1399
- Bouzd, R., Peppelenbosch, M., and Buschow, S. I. (2020). Opportunities for Conventional and *In Situ* Cancer Vaccine Strategies and Combination with Immunotherapy for Gastrointestinal Cancers, a Review. *Cancers* 12 (5), 1121. doi:10.3390/cancers12051121
- Brito, L. A., and O'Hagan, D. T. (2014). Designing and Building the Next Generation of Improved Vaccine Adjuvants. *J. Controlled Release* 190, 563–579. doi:10.1016/j.jconrel.2014.06.027
- Browning, M. J. (2013). Antigen Presenting Cell/Tumor Cell Fusion Vaccines for Cancer Immunotherapy. *Hum. Vaccin. Immunother.* 9 (7), 1545–1548. doi:10.4161/hv.24235
- Brudno, Y., Pezone, M. J., Snyder, T. K., Uzun, O., Moody, C. T., Aizenberg, M., et al. (2018). Replenishable Drug Depot to Combat Post-resection Cancer Recurrence. *Biomaterials* 178, 373–382. doi:10.1016/j.biomaterials.2018.05.005
- Calmeiro, J., Carrascal, M., Gomes, C., Falcão, A., Cruz, M. T., and Neves, B. M. (2019). Biomaterial-based Platforms for *In Situ* Dendritic Cell Programming and Their Use in Antitumor Immunotherapy. *J. Immunotherapy Cancer* 7 (1), 238. doi:10.1186/s40425-019-0716-8
- Chablani, L., Tawde, S. A., Akalkotkar, A., and D'Souza, M. J. (2019). Evaluation of a Particulate Breast Cancer Vaccine Delivered via Skin. *AAPS J.* 21 (2), 12. doi:10.1208/s12248-018-0285-7
- Chen, F., Wang, Y., Gao, J., Saeed, M., Li, T., Wang, W., et al. (2021). Nanobiomaterial-based Vaccination Immunotherapy of Cancer. *Biomaterials* 270, 120709. doi:10.1016/j.biomaterials.2021.120709
- Chen, M., Quan, G., Wen, T., Yang, P., Qin, W., Mai, H., et al. (2020a). Cold to Hot: Binary Cooperative Microneedle Array-Amplified Photoimmunotherapy for Eliciting Antitumor Immunity and the Abscopal Effect. *ACS Appl. Mater. Inter.* 12 (29), 32259–32269. doi:10.1021/acsami.0c05090
- Chen, Q., Chen, J., Yang, Z., Xu, J., Xu, L., Liang, C., et al. (2019a). Nanoparticle-enhanced Radiotherapy to Trigger Robust Cancer Immunotherapy. *Adv. Mater.* 31 (10), e1802228. doi:10.1002/adma.201802228
- Chen, Q., Wang, C., Zhang, X., Chen, G., Hu, Q., Li, H., et al. (2019b). *In situ* sprayed Bioresponsive Immunotherapeutic Gel for Post-surgical Cancer Treatment. *Nat. Nanotech* 14 (1), 89–97. doi:10.1038/s41565-018-0319-4
- Chen, R., Zhang, H., Yan, J., and Bryers, J. D. (2018). Scaffold-mediated Delivery for Non-viral mRNA Vaccines. *Gene Ther.* 25 (8), 556–567. doi:10.1038/s41434-018-0040-9
- Chen, S.-X., Ma, M., Xue, F., Shen, S., Chen, Q., Kuang, Y., et al. (2020b). Construction of Microneedle-Assisted Co-delivery Platform and its Combining Photodynamic/immunotherapy. *J. Controlled Release* 324, 218–227. doi:10.1016/j.jconrel.2020.05.006
- Cheng, S., Xu, C., Jin, Y., Li, Y., Zhong, C., Ma, J., et al. (2020). Artificial Mini Dendritic Cells Boost T Cell-Based Immunotherapy for Ovarian Cancer. *Adv. Sci.* 7 (7), 1903301. doi:10.1002/advs.201903301
- Cheung, A. S., Zhang, D. K. Y., Koshy, S. T., and Mooney, D. J. (2018). Scaffolds that Mimic Antigen-Presenting Cells Enable *Ex Vivo* Expansion of Primary T Cells. *Nat. Biotechnol.* 36 (2), 160–169. doi:10.1038/nbt.4047
- Chiang, C., Coukos, G., and Kandalaft, L. (2015). Whole Tumor Antigen Vaccines: where Are We? *Vaccines* 3 (2), 344–372. doi:10.3390/vaccines3020344
- Cho, J.-a., Lee, Y.-S., Kim, S.-H., Ko, J.-K., and Kim, C.-W. (2009). MHC Independent Anti-tumor Immune Responses Induced by Hsp70-Enriched Exosomes Generate Tumor Regression in Murine Models. *Cancer Lett.* 275 (2), 256–265. doi:10.1016/j.canlet.2008.10.021
- Chu, Y., Liu, Q., Wei, J., and Liu, B. (2018). Personalized Cancer Neoantigen Vaccines Come of Age. *Theranostics* 8 (15), 4238–4246. doi:10.7150/thno.24387
- Cirillo, G., Curcio, U. G., Nicoletta, M., Iemma, F. P., and Iemma, F. (2019). Injectable Hydrogels for Cancer Therapy over the Last Decade. *Pharmaceutics* 11 (9), 486. doi:10.3390/pharmaceutics11090486
- Cole, G., Ali, A. A., McErlan, E., Mulholland, E. J., Short, A., McCrudden, C. M., et al. (2019). DNA Vaccination via RALA Nanoparticles in a Microneedle Delivery System Induces a Potent Immune Response against the Endogenous Prostate Cancer Stem Cell Antigen. *Acta Biomater.* 96, 480–490. doi:10.1016/j.actbio.2019.07.003
- Coley, W. B. (1991). The Classic. *Clin. Orthopaedics Relat. Res.* 262, 3–11. doi:10.1097/00003086-199101000-00002
- Da Silva, C. G., Camps, M. G. M., Li, T. M. W. Y., Zerrillo, L., Löwik, C. W., Ossendorp, F., et al. (2019). Effective Chemimmunotherapy by Co-delivery of Doxorubicin and Immune Adjuvants in Biodegradable Nanoparticles. *Theranostics* 9 (22), 6485–6500. doi:10.7150/thno.34429
- Day, C.-P., Merlino, G., and Van Dyke, T. (2015). Preclinical Mouse Cancer Models: a Maze of Opportunities and Challenges. *Cell* 163 (1), 39–53. doi:10.1016/j.cell.2015.08.068
- Demento, S. L., Cui, W., Criscione, J. M., Stern, E., Tulipan, J., Kaech, S. M., et al. (2012). Role of Sustained Antigen Release from Nanoparticle Vaccines in Shaping the T Cell Memory Phenotype. *Biomaterials* 33 (19), 4957–4964. doi:10.1016/j.biomaterials.2012.03.041
- Desrichard, A., Snyder, A., and Chan, T. A. (2016). Cancer Neoantigens and Applications for Immunotherapy. *Clin. Cancer Res.* 22 (4), 807–812. doi:10.1158/1078-0432.CCR-14-3175

- Du, G., Hathout, R. M., Nasr, M., Nejadnik, M. R., Tu, J., Koning, R. I., et al. (2017). Intradermal Vaccination with Hollow Microneedles: a Comparative Study of Various Protein Antigen and Adjuvant Encapsulated Nanoparticles. *J. Controlled Release* 266, 109–118. doi:10.1016/j.jconrel.2017.09.021
- Duong, H. T. T., Thambi, T., Yin, Y., Kim, S. H., Nguyen, T. L., Phan, V. H. G., et al. (2020a). Degradation-regulated Architecture of Injectable Smart Hydrogels Enhances Humoral Immune Response and Potentiates Antitumor Activity in Human Lung Carcinoma. *Biomaterials* 230, 119599. doi:10.1016/j.biomaterials.2019.119599
- Duong, H. T. T., Yin, Y., Thambi, T., Kim, B. S., Jeong, J. H., and Lee, D. S. (2020b). Highly Potent Intradermal Vaccination by an Array of Dissolving Microneedle Polypeptide Cocktails for Cancer Immunotherapy. *J. Mater. Chem. B* 8 (6), 1171–1181. doi:10.1039/c9tb02175b
- Duong, H. T. T., Yin, Y., Thambi, T., Nguyen, T. L., Giang Phan, V. H., Lee, M. S., et al. (2018). Smart Vaccine Delivery Based on Microneedle Arrays Decorated with Ultra-pH-responsive Copolymers for Cancer Immunotherapy. *Biomaterials* 185, 13–24. doi:10.1016/j.biomaterials.2018.09.008
- Fan, Y., Kuai, R., Xu, Y., Ochyl, L. J., Irvine, D. J., and Moon, J. J. (2017). Immunogenic Cell Death Amplified by Co-localized Adjuvant Delivery for Cancer Immunotherapy. *Nano Lett.* 17 (12), 7387–7393. doi:10.1021/acs.nanolett.7b03218
- Fang, R. H., Hu, C.-M. J., Luk, B. T., Gao, W., Copp, J. A., Tai, Y., et al. (2014). Cancer Cell Membrane-Coated Nanoparticles for Anticancer Vaccination and Drug Delivery. *Nano Lett.* 14 (4), 2181–2188. doi:10.1021/nl500618u
- Fennemann, F. L., de Vries, I. J. M., Figdor, C. G., and Verdoes, M. (2019). Attacking Tumors from All Sides: Personalized Multiplex Vaccines to Tackle Intratumor Heterogeneity. *Front. Immunol.* 10, 824–832. doi:10.3389/fimmu.2019.00824
- Gala, R., Zaman, R., D'Souza, M., and Zughaier, S. (2018). Novel Whole-Cell Inactivated neisseria Gonorrhoeae Microparticles as Vaccine Formulation in Microneedle-Based Transdermal Immunization. *Vaccines* 6 (3), 60. doi:10.3390/vaccines6030060
- Galluzzi, L., Buqué, A., Kepp, O., Zitvogel, L., and Kroemer, G. (2017). Immunogenic Cell Death in Cancer and Infectious Disease. *Nat. Rev. Immunol.* 17 (2), 97–111. doi:10.1038/nri.2016.107
- Galluzzi, L., Chan, T. A., Kroemer, G., Wolchok, J. D., and López-Soto, A. (2018). The Hallmarks of Successful Anticancer Immunotherapy. *Sci. Transl. Med.* 10 (459), eaat7807. doi:10.1126/scitranslmed.aat7807
- Gan, J., Du, G., He, C., Jiang, M., Mou, X., Xue, J., et al. (2020). Tumor Cell Membrane Enveloped Aluminum Phosphate Nanoparticles for Enhanced Cancer Vaccination. *J. Controlled Release* 326, 297–309. doi:10.1016/j.jconrel.2020.07.008
- Gardner, T., Elzey, B., and Hahn, N. M. (2012). Sipuleucel-T (Provenge) Autologous Vaccine Approved for Treatment of Men with Asymptomatic or Minimally Symptomatic Castrate-Resistant Metastatic Prostate Cancer. *Hum. Vaccin. Immunother.* 8 (4), 534–539. doi:10.4161/hv.19795
- Geng, Y., Yuan, W., Wu, F., Chen, J., He, M., and Jin, T. (2008). Formulating Erythropoietin-Loaded Sustained-Release PLGA Microspheres without Protein Aggregation. *J. Controlled Release* 130 (3), 259–265. doi:10.1016/j.jconrel.2008.06.011
- Greening, D. W., Gopal, S. K., Xu, R., Simpson, R. J., and Chen, W. (2015). Exosomes and Their Roles in Immune Regulation and Cancer. *Semin. Cell Dev. Biol.* 40, 72–81. doi:10.1016/j.semcdb.2015.02.009
- Guarecuco, R., Lu, J., McHugh, K. J., Norman, J. J., Thapa, L. S., Lydon, E., et al. (2018). Immunogenicity of Pulsatile-Release PLGA Microspheres for Single-Injection Vaccination. *Vaccine* 36 (22), 3161–3168. doi:10.1016/j.vaccine.2017.05.094
- Gulley, J. L., Borre, M., Vogelzang, N. J., Ng, S., Agarwal, N., Parker, C. C., et al. (2019). Phase III Trial of PROSTVAC in Asymptomatic or Minimally Symptomatic Metastatic Castration-Resistant Prostate Cancer. *Jco* 37 (13), 1051–1061. doi:10.1200/jco.18.02031
- Guo, C., Manjili, M. H., Subjeck, J. R., Sarkar, D., Fisher, P. B., and Wang, X.-Y. (2013). Therapeutic Cancer Vaccines. *Adv. Cancer Res.* 119, 421–475. doi:10.1016/B978-0-12-407190-2.00007-1
- Hailemichael, Y., Dai, Z., Jaffarzad, N., Ye, Y., Medina, M. A., Huang, X.-F., et al. (2013). Persistent Antigen at Vaccination Sites Induces Tumor-specific CD8+ T Cell Sequestration, Dysfunction and Deletion. *Nat. Med.* 19 (4), 465–472. doi:10.1038/nm.3105
- Hammerich, L., Binder, A., and Brody, J. D. (2015). In Situ Vaccination: Cancer Immunotherapy Both Personalized and Off-The-Shelf. *Mol. Oncol.* 9 (10), 1966–1981. doi:10.1016/j.molonc.2015.10.016
- Han, F. Y., Thurecht, K. J., Whittaker, A. K., and Smith, M. T. (2016a). Bioerodable PLGA-Based Microparticles for Producing Sustained-Release Drug Formulations and Strategies for Improving Drug Loading. *Front. Pharmacol.* 7, 185. doi:10.3389/fphar.2016.00185
- Han, L., Xue, J., Wang, L., Peng, K., Zhang, Z., Gong, T., et al. (2016b). An Injectable, Low-Toxicity Phospholipid-Based Phase Separation Gel that Induces Strong and Persistent Immune Responses in Mice. *Biomaterials* 105, 185–194. doi:10.1016/j.biomaterials.2016.08.007
- Hori, Y., Stern, P. J., Hynes, R. O., and Irvine, D. J. (2009). Engulfing Tumors with Synthetic Extracellular Matrices for Cancer Immunotherapy. *Biomaterials* 30 (35), 6757–6767. doi:10.1016/j.biomaterials.2009.08.037
- Hossain, M. K., Ahmed, T., Bhusal, P., Subedi, R. K., Salahshoori, I., Soltani, M., et al. (2020). Microneedle Systems for Vaccine Delivery: the Story So Far. *Expert Rev. Vaccin.* 19 (12), 1153–1166. doi:10.1080/14760584.2020.1874928
- Hou, Y., Liu, R., Hong, X., Zhang, Y., Bai, S., Luo, X., et al. (2021). Engineering a Sustained Release Vaccine with a Pathogen-Mimicking Manner for Robust and Durable Immune Responses. *J. Controlled Release* 333, 162–175. doi:10.1016/j.jconrel.2021.03.037
- Hu, Z., Ott, P. A., and Wu, C. J. (2018). Towards Personalized, Tumour-specific, Therapeutic Vaccines for Cancer. *Nat. Rev. Immunol.* 18 (3), 168–182. doi:10.1038/nri.2017.131
- Huang, P., Wang, X., Liang, X., Yang, J., Zhang, C., Kong, D., et al. (2019). Nano-, Micro-, and Macroscale Drug Delivery Systems for Cancer Immunotherapy. *Acta Biomater.* 85, 1–26. doi:10.1016/j.actbio.2018.12.028
- Huang, X., Williams, J. Z., Chang, R., Li, Z., Burnett, C. E., Hernandez-Lopez, R., et al. (2020). DNA Scaffolds Enable Efficient and Tunable Functionalization of Biomaterials for Immune Cell Modulation. *Nat. Nanotechnol.* 16 (2), 214–223. doi:10.1038/s41565-020-00813-z
- Hwang, M. P., Fecek, R. J., Qin, T., Storkus, W. J., and Wang, Y. (2020). Single Injection of IL-12 Coacervate as an Effective Therapy against B16-F10 Melanoma in Mice. *J. Controlled Release* 318, 270–278. doi:10.1016/j.jconrel.2019.12.035
- Iezzi, G., Karjalainen, K., and Lanzavecchia, A. (1998). The Duration of Antigenic Stimulation Determines the Fate of Naive and Effector T Cells. *Immunity* 8 (1), 89–95. doi:10.1016/s1074-7613(00)80461-6
- Irvine, D. J., Aung, A., and Silva, M. (2020). Controlling Timing and Location in Vaccines. *Adv. Drug Deliv. Rev.* 158, 91–115. doi:10.1016/j.addr.2020.06.019
- Jackaman, C., and Nelson, D. J. (2012). Intratumoral Interleukin-2/agonist CD40 Antibody Drives CD4+-independent Resolution of Treated Tumors and CD4+-dependent Systemic and Memory Responses. *Cancer Immunol. Immunother.* 61 (4), 549–560. doi:10.1007/s00262-011-1120-5
- Jacobs, J. J., Snackey, C., Geldof, A. A., Characiejus, D., Van Moerselaar, R. J., and Den Otter, W. (2014). Inefficacy of Therapeutic Cancer Vaccines and Proposed Improvements. *Casus of Prostate Cancer. Anticancer Res.* 34 (6), 2689–2700.
- Janku, F., Zhang, H. H., Pezeshki, A., Goel, S., Murthy, R., Wang-Gillam, A., et al. (2021). Intratumoral Injection of *Clostridium* Novyi-NT Spores in Patients with Treatment-Refractory Advanced Solid Tumors. *Clin. Cancer Res.* 27 (1), 96–106. doi:10.1158/1078-0432.CCR-20-2065
- Jiang, H., Wang, Q., and Sun, X. (2017). Lymph Node Targeting Strategies to Improve Vaccination Efficacy. *J. Controlled Release* 267, 47–56. doi:10.1016/j.jconrel.2017.08.009
- Jin, X., Zhu, D. D., Chen, B. Z., Ashfaq, M., and Guo, X. D. (2018a). Insulin Delivery Systems Combined with Microneedle Technology. *Adv. Drug Deliv. Rev.* 127, 119–137. doi:10.1016/j.addr.2018.03.011
- Jin, X., Zhu, D. D., Chen, B. Z., Ashfaq, M., and Guo, X. D. (2018b). Insulin Delivery Systems Combined with Microneedle Technology. *Adv. Drug Deliv. Rev.* 127, 119–137. doi:10.1016/j.addr.2018.03.011
- Johansen, P., Storni, T., Rettig, L., Qiu, Z., Der-Sarkissian, A., Smith, K. A., et al. (2008). Antigen Kinetics Determines Immune Reactivity. *Pnas* 105 (13), 5189–5194. doi:10.1073/pnas.0706296105
- Joshi, V. B., Geary, S. M., Gross, B. P., Wongrakpanich, A., Norian, L. A., and Salem, A. K. (2014). Tumor Lysate-Loaded Biodegradable Microparticles as Cancer Vaccines. *Expert Rev. Vaccin.* 13 (1), 9–15. doi:10.1586/14760584.2014.851606
- Jung, H., Jang, H.-E., Kang, Y. Y., Song, J., and Mok, H. (2019). PLGA Microspheres Coated with Cancer Cell-Derived Vesicles for Improved

- Internalization into Antigen-Presenting Cells and Immune Stimulation. *Bioconjug. Chem.* 30 (6), 1690–1701. doi:10.1021/acs.bioconjchem.9b00240
- Kanchan, V., Kataré, Y. K., and Panda, A. K. (2009). Memory Antibody Response from Antigen Loaded Polymer Particles and the Effect of Antigen Release Kinetics. *Biomaterials* 30 (27), 4763–4776. doi:10.1016/j.biomaterials.2009.05.075
- Kanwar, N., and Sinha, V. R. (2019). *In situ* forming Depot as Sustained-Release Drug Delivery Systems. *Crit. Rev. Ther. Drug Carrier Syst.* 36 (2), 93–136. doi:10.1615/CritRevTherDrugCarrierSyst.2018025013
- Keler, T., He, L., Ramakrishna, V., and Champion, B. (2007). Antibody-targeted Vaccines. *Oncogene* 26 (25), 3758–3767. doi:10.1038/sj.onc.1210375
- Kim, H., Seong, K.-Y., Lee, J. H., Park, W., Yang, S. Y., and Hahn, S. K. (2019). Biodegradable Microneedle Patch Delivering Antigenic Peptide-Hyaluronate Conjugate for Cancer Immunotherapy. *ACS Biomater. Sci. Eng.* 5 (10), 5150–5158. doi:10.1021/acsbomaterials.9b00961
- Kim, J., Li, W. A., Choi, Y., Lewin, S. A., Verbeke, C. S., Dranoff, G., et al. (2015). Injectable, Spontaneously Assembling, Inorganic Scaffolds Modulate Immune Cells in vivo and Increase Vaccine Efficacy. *Nat. Biotechnol.* 33 (1), 64–72. doi:10.1038/nbt.3071
- Kim, N. W., Kim, S.-Y., Lee, J. E., Yin, Y., Lee, J. H., Lim, S. Y., et al. (2018). Enhanced Cancer Vaccination by In Situ Nanomicelle-Generating Dissolving Microneedles. *ACS Nano* 12 (10), 9702–9713. doi:10.1021/acsnano.8b04146
- Knorr, D. A., Dahan, R., and Ravetch, J. V. (2018). Toxicity of an Fc-Engineered Anti-CD40 Antibody Is Abrogated by Intratumoral Injection and Results in Durable Antitumor Immunity. *Proc. Natl. Acad. Sci. USA* 115 (43), 11048–11053. doi:10.1073/pnas.1810566115
- Koerner, J., Horvath, D., and Groettrup, M. (2019). Harnessing Dendritic Cells for Poly (D,L-lactide-co-glycolide) Microspheres (PLGA MS)-mediated Antitumor Therapy. *Front. Immunol.* 10, 707. doi:10.3389/fimmu.2019.00707
- Kordalivand, N., Tondini, E., Lau, C. Y. J., Vermonden, T., Mastrobattista, E., Hennink, W. E., et al. (2019). Cationic Synthetic Long Peptides-Loaded Nanogels: an Efficient Therapeutic Vaccine Formulation for Induction of T-Cell Responses. *J. Controlled Release* 315, 114–125. doi:10.1016/j.jconrel.2019.10.048
- Korupalli, C., Pan, W.-Y., Yeh, C.-Y., Chen, P.-M., Mi, F.-L., Tsai, H.-W., et al. (2019). Single-injecting, Bioinspired Nanocomposite Hydrogel that Can Recruit Host Immune Cells In Situ to Elicit Potent and Long-Lasting Humoral Immune Responses. *Biomaterials* 216, 119268. doi:10.1016/j.biomaterials.2019.119268
- Kuol, N., Stojanovska, L., Nurgali, K., and Apostolopoulos, V. (2017). The Mechanisms Tumor Cells Utilize to Evade the Host's Immune System. *Maturitas* 105, 8–15. doi:10.1016/j.maturitas.2017.04.014
- Labanieh, L., Majzner, R. G., and Mackall, C. L. (2018). Programming CAR-T Cells to Kill Cancer. *Nat. Biomed. Eng.* 2 (6), 377–391. doi:10.1038/s41551-018-0235-9
- Leach, D. G., Young, S., and Hartgerink, J. D. (2019). Advances in Immunotherapy Delivery from Implantable and Injectable Biomaterials. *Acta Biomater.* 88, 15–31. doi:10.1016/j.actbio.2019.02.016
- Lei, K., and Tang, L. (2019). Surgery-free Injectable Macroscale Biomaterials for Local Cancer Immunotherapy. *Biomater. Sci.* 7 (3), 733–749. doi:10.1039/c8bm01470a
- Leone, M., Mönkäre, J., Bouwstra, J. A., and Kersten, G. (2017). Dissolving Microneedle Patches for Dermal Vaccination. *Pharm. Res.* 34 (11), 2223–2240. doi:10.1007/s11095-017-2223-2
- Li, A. W., Sobral, M. C., Badrinath, S., Choi, Y., Graveline, A., Stafford, A. G., et al. (2018). A Facile Approach to Enhance Antigen Response for Personalized Cancer Vaccination. *Nat. Mater.* 17 (6), 528–534. doi:10.1038/s41563-018-0028-2
- Li, F., Lyu, D., Liu, S., and Guo, W. (2020). DNA Hydrogels and Microgels for Biosensing and Biomedical Applications. *Adv. Mater.* 32 (3), e1806538. doi:10.1002/adma.201806538
- Li, J., and Mooney, D. J. (2016). Designing Hydrogels for Controlled Drug Delivery. *Nat. Rev. Mater.* 1 (12), 16071. doi:10.1038/natrevmats.2016.71
- Li, W. A., Lu, B. Y., Gu, L., Choi, Y., Kim, J., and Mooney, D. J. (2016a). The Effect of Surface Modification of Mesoporous Silica Micro-rod Scaffold on Immune Cell Activation and Infiltration. *Biomaterials* 83, 249–256. doi:10.1016/j.biomaterials.2016.01.026
- Li, Y., Yang, H. Y., and Lee, D. S. (2021). Advances in Biodegradable and Injectable Hydrogels for Biomedical Applications. *J. Controlled Release* 330, 151–160. doi:10.1016/j.jconrel.2020.12.008
- Li, Z., Xiong, F., He, J., Dai, X., and Wang, G. (2016b). Surface-functionalized, pH-Responsive Poly(lactic-Co-Glycolic Acid)-Based Microparticles for Intranasal Vaccine Delivery: Effect of Surface Modification with Chitosan and Mannan. *Eur. J. Pharmaceutics Biopharmaceutics* 109, 24–34. doi:10.1016/j.ejpb.2016.08.012
- Lin, C.-Y., Lin, S.-J., Yang, Y.-C., Wang, D.-Y., Cheng, H.-F., and Yeh, M.-K. (2015). Biodegradable Polymeric Microsphere-Based Vaccines and Their Applications in Infectious Diseases. *Hum. Vaccin. Immunother.* 11 (3), 650–656. doi:10.1080/21645515.2015.1009345
- Lin, Y.-X., Wang, Y., Blake, S., Yu, M., Mei, L., Wang, H., et al. (2020). RNA Nanotechnology-Mediated Cancer Immunotherapy. *Theranostics* 10 (1), 281–299. doi:10.7150/thno.35568
- Liu, H., Moynihan, K. D., Zheng, Y., Szeto, G. L., Li, A. V., Huang, B., et al. (2014). Structure-based Programming of Lymph-Node Targeting in Molecular Vaccines. *Nature* 507 (7493), 519–522. doi:10.1038/nature12978
- Liu, H., Shi, X., Wu, D., Kahsay Khshen, F., Deng, L., Dong, A., et al. (2019a). Injectable, Biodegradable, Thermosensitive Nanoparticles-Aggregated Hydrogel with Tumor-specific Targeting, Penetration, and Release for Efficient Postsurgical Prevention of Tumor Recurrence. *ACS Appl. Mater. Inter.* 11 (22), 19700–19711. doi:10.1021/acsmi.9b01987
- Liu, W.-L., Zou, M.-Z., Liu, T., Zeng, J.-Y., Li, X., Yu, W.-Y., et al. (2019b). Cytomembrane Nanovaccines Show Therapeutic Effects by Mimicking Tumor Cells and Antigen Presenting Cells. *Nat. Commun.* 10 (1), 3199. doi:10.1038/s41467-019-11157-1
- Lopes, A., Vandermeulen, G., and Préat, V. (2019). Cancer DNA Vaccines: Current Preclinical and Clinical Developments and Future Perspectives. *J. Exp. Clin. Cancer Res.* 38 (1), 146. doi:10.1186/s13046-019-1154-7
- Lu, Y., Aimetti, A. A., Langer, R., and Gu, Z. (2017). Bioresponsive Materials. *Nat. Rev. Mater.* 2, 16075. doi:10.1038/natrevmats.2016.75
- Lybaert, L., Vermaelen, K., De Geest, B. G., and Nuhn, L. (2018). Immunoen지니어링 through Cancer Vaccines - A Personalized and Multi-step Vaccine Approach towards Precise Cancer Immunity. *J. Controlled Release* 289, 125–145. doi:10.1016/j.jconrel.2018.09.009
- Mata, E., Igartua, M., Patarroyo, M. E., Pedraz, J. L., and Hernández, R. M. (2011). Enhancing Immunogenicity to PLGA Microparticulate Systems by Incorporation of Alginate and RGD-Modified Alginate. *Eur. J. Pharm. Sci.* 44 (1–2), 32–40. doi:10.1016/j.ejps.2011.05.015
- Matson, V., Fessler, J., Bao, R., Chongsuwan, T., Zha, Y., Alegre, M.-L., et al. (2018). The Commensal Microbiome Is Associated with Anti-PD-1 Efficacy in Metastatic Melanoma Patients. *Science* 359 (6371), 104–108. doi:10.1126/science.aao3290
- McHugh, K. J., Guarecuco, R., Langer, R., and Jaklenec, A. (2015). Single-injection Vaccines: Progress, Challenges, and Opportunities. *J. Controlled Release* 219, 596–609. doi:10.1016/j.jconrel.2015.07.029
- McNamara, M. A., Nair, S. K., and Holl, E. K. (2015). RNA-based Vaccines in Cancer Immunotherapy. *J. Immunol. Res.* 2015, 794528. doi:10.1155/2015/794528
- Mestas, J., and Hughes, C. C. W. (2004). Of Mice and Not Men: Differences between Mouse and Human Immunology. *J. Immunol.* 172 (5), 2731–2738. doi:10.4049/jimmunol.172.5.2731
- Mills, B. N., Connolly, K. A., Ye, J., Murphy, J. D., Uccello, T. P., Han, B. J., et al. (2019). Stereotactic Body Radiation and Interleukin-12 Combination Therapy Eradicates Pancreatic Tumors by Repolarizing the Immune Microenvironment. *Cel Rep.* 29 (2), 406–421. e405. doi:10.1016/j.celrep.2019.08.095
- Min, Y., Roche, K. C., Tian, S., Eblan, M. J., McKinnon, K. P., Caster, J. M., et al. (2017). Antigen-capturing Nanoparticles Improve the Abscopal Effect and Cancer Immunotherapy. *Nat. Nanotech.* 12 (9), 877–882. doi:10.1038/nnano.2017.113
- Mueller, M., Reichardt, W., Koerner, J., and Groettrup, M. (2012). Coencapsulation of Tumor Lysate and CpG-ODN in PLGA-Microspheres Enables Successful Immunotherapy of Prostate Carcinoma in TRAMP Mice. *J. Controlled Release* 162 (1), 159–166. doi:10.1016/j.jconrel.2012.06.015
- Nejman, D., Livyatan, I., Fuks, G., Gavert, N., Zwang, Y., Geller, L. T., et al. (2020). The Human Tumor Microbiome Is Composed of Tumor Type-specific Intracellular Bacteria. *Science* 368 (6494), 973–980. doi:10.1126/science.aay9189
- Nguyen, T. L., Yin, Y., Choi, Y., Jeong, J. H., and Kim, J. (2020). Enhanced Cancer DNA Vaccine via Direct Transfection to Host Dendritic Cells Recruited in Injectable Scaffolds. *ACS Nano* 14 (9), 11623–11636. doi:10.1021/acsnano.0c04188
- Niu, L., Chu, L. Y., Burton, S. A., Hansen, K. J., and Panyam, J. (2019). Intradermal Delivery of Vaccine Nanoparticles Using Hollow Microneedle Array Generates

- Enhanced and Balanced Immune Response. *J. Controlled Release* 294, 268–278. doi:10.1016/j.jconrel.2018.12.026
- Noguchi, M., Arai, G., Egawa, S., Ohyama, C., Naito, S., Matsumoto, K., et al. (2020). Mixed 20-peptide Cancer Vaccine in Combination with Docetaxel and Dexamethasone for Castration-Resistant Prostate Cancer: a Randomized Phase II Trial. *Cancer Immunol. Immunother.* 69 (5), 847–857. doi:10.1007/s00262-020-02498-8
- Obeid, J., Hu, Y., and Slingluff, C. L., Jr. (2015). Vaccines, Adjuvants, and Dendritic Cell Activators-Current Status and Future Challenges. *Semin. Oncol.* 42 (4), 549–561. doi:10.1053/j.seminoncol.2015.05.006
- Oberli, M. A., Reichmuth, A. M., Dorkin, J. R., Mitchell, M. J., Fenton, O. S., Jaklenec, A., et al. (2017). Lipid Nanoparticle Assisted mRNA Delivery for Potent Cancer Immunotherapy. *Nano Lett.* 17 (3), 1326–1335. doi:10.1021/acs.nanolett.6b03329
- Oh, E., Oh, J.-E., Hong, J., Chung, Y., Lee, Y., Park, K. D., et al. (2017). Optimized Biodegradable Polymeric Reservoir-Mediated Local and Sustained Co-delivery of Dendritic Cells and Oncolytic Adenovirus Co-expressing IL-12 and GM-CSF for Cancer Immunotherapy. *J. Controlled Release* 259, 115–127. doi:10.1016/j.jconrel.2017.03.028
- Ouyang, X., Telli, M. L., and Wu, J. C. (2019). Induced Pluripotent Stem Cell-Based Cancer Vaccines. *Front. Immunol.* 10, 1510. doi:10.3389/fimmu.2019.01510
- Ozao-Choy, J., Lee, D. J., and Faries, M. B. (2014). Melanoma Vaccines. *Surg. Clin. North America* 94 (5), 1017–1030. doi:10.1016/j.suc.2014.07.005
- Pardi, N., Hogan, M. J., Porter, F. W., and Weissman, D. (2018). mRNA Vaccines - a New Era in Vaccinology. *Nat. Rev. Drug Discov.* 17 (4), 261–279. doi:10.1038/nrd.2017.243
- Park, K., Skidmore, S., Hadar, J., Garner, J., Park, H., Otte, A., et al. (2019). Injectable, Long-Acting PLGA Formulations: Analyzing PLGA and Understanding Microparticle Formation. *J. Controlled Release* 304, 125–134. doi:10.1016/j.jconrel.2019.05.003
- Patel, R. B., Ye, M., Carlson, P. M., Jaquish, A., Zangl, L., Ma, B., et al. (2019). Development of an *In Situ* Cancer Vaccine via Combinational Radiation and Bacterial-Membrane-Coated Nanoparticles. *Adv. Mater.* 31 (43), e1902626. doi:10.1002/adma.201902626
- Perez, C. R., and De Palma, M. (2019). Engineering Dendritic Cell Vaccines to Improve Cancer Immunotherapy. *Nat. Commun.* 10 (1), 5408. doi:10.1038/s41467-019-13368-y
- Peris, I., and Langer, R. S. (1979). A Single-step Immunization by Sustained Antigen Release. *J. Immunol. Methods* 28 (1), 193–197. doi:10.1016/0022-1759(79)90341-7
- Phuengkham, H., Song, C., Um, S. H., and Lim, Y. T. (2018). Implantable Synthetic Immune Niche for Spatiotemporal Modulation of Tumor-Derived Immunosuppression and Systemic Antitumor Immunity: Postoperative Immunotherapy. *Adv. Mater.* 30 (18), e1706719. doi:10.1002/adma.201706719
- Pilla, L., Ferrone, S., and MacCalli, C. (2018). Methods for Improving the Immunogenicity and Efficacy of Cancer Vaccines. *Expert Opin. Biol. Ther.* 18 (7), 765–784. doi:10.1080/14712598.2018.1485649
- Pol, J., Vacchelli, E., Aranda, F., Castoldi, F., Eggermont, A., Cremer, I., et al. (2015). Trial Watch: Immunogenic Cell Death Inducers for Anticancer Chemotherapy. *Oncoimmunol.* 4 (4), e1008866. doi:10.1080/2162402X.2015.1008866
- Pradhan, P., Qin, H., Leleux, J. A., Gwak, D., Sakamaki, I., Kwak, L. W., et al. (2014). The Effect of Combined IL10 siRNA and CpG ODN as Pathogen-Mimicking Microparticles on Th1/Th2 Cytokine Balance in Dendritic Cells and Protective Immunity against B Cell Lymphoma. *Biomaterials* 35 (21), 5491–5504. doi:10.1016/j.biomaterials.2014.03.039
- Qu, J., Zhao, X., Ma, P. X., and Guo, B. (2018). Injectable Antibacterial Conductive Hydrogels with Dual Response to an Electric Field and pH for Localized "smart" Drug Release. *Acta Biomater.* 72, 55–69. doi:10.1016/j.actbio.2018.03.018
- Rahimian, S., Fransen, M. F., Kleinovink, J. W., Amidi, M., Ossendorp, F., and Hennink, W. E. (2015). Polymeric Microparticles for Sustained and Local Delivery of antiCD40 and antiCTLA-4 in Immunotherapy of Cancer. *Biomaterials* 61, 33–40. doi:10.1016/j.biomaterials.2015.04.043
- Rehman, H., Silk, A. W., Kane, M. P., and Kaufman, H. L. (2016). Into the Clinic: Talimogene Laherparepvec (T-VEC), a First-In-Class Intratumoral Oncolytic Viral Therapy. *J. Immunotherapy Cancer* 4, 53. doi:10.1186/s40425-016-0158-5
- Ribas, A., Weber, J. S., Chmielowski, B., Comin-Anduix, B., Lu, D., Douek, M., et al. (2011). Intra-lymph Node Prime-Boost Vaccination against Melan A and Tyrosinase for the Treatment of Metastatic Melanoma: Results of a Phase I Clinical Trial. *Clin. Cancer Res.* 17 (9), 2987–2996. doi:10.1158/1078-0432.Ccr-10-3272
- Riley, R. S., June, C. H., Langer, R., and Mitchell, M. J. (2019). Delivery Technologies for Cancer Immunotherapy. *Nat. Rev. Drug Discov.* 18 (3), 175–196. doi:10.1038/s41573-018-0006-z
- Rosalía, R. A., Quakkelaar, E. D., Redeker, A., Khan, S., Camps, M., Drijfhout, J. W., et al. (2013). Dendritic Cells Process Synthetic Long Peptides Better Than Whole Protein, Improving Antigen Presentation and T-Cell Activation. *Eur. J. Immunol.* 43 (10), 2554–2565. doi:10.1002/eji.201343324
- Russell, S. J., and Barber, G. N. (2018). Oncolytic Viruses as Antigen-Agnostic Cancer Vaccines. *Cancer Cell* 33 (4), 599–605. doi:10.1016/j.ccell.2018.03.011
- Sabado, R. L., Balan, S., and Bhardwaj, N. (2017). Dendritic Cell-Based Immunotherapy. *Cell Res* 27 (1), 74–95. doi:10.1038/cr.2016.157
- Schineis, P., Kotkowska, Z. K., Vogel-Kindgen, S., Friess, M. C., Theisen, M., Schwyter, D., et al. (2021). Photochemical Internalization (PCI)-mediated Activation of CD8 T Cells Involves Antigen Uptake and CCR7-Mediated Transport by Migratory Dendritic Cells to Draining Lymph Nodes. *J. Controlled Release* 332, 96–108. doi:10.1016/j.jconrel.2021.02.014
- Schlom, J., Hodge, J. W., Palena, C., Tsang, K.-Y., Jochems, C., Greiner, J. W., et al. (2014). Therapeutic Cancer Vaccines. *Adv. Cancer Res.* 121, 67–124. doi:10.1016/B978-0-12-800249-0.00002-0
- Shae, D., Baljon, J. J., Wehbe, M., Becker, K. W., Sheehy, T. L., and Wilson, J. T. (2019). At the Bench: Engineering the Next Generation of Cancer Vaccines. *J. Leukoc. Biol.* 108 (4), 1435–1453. doi:10.1002/jlb.5b10119-016r
- Shafiee, A., and Atala, A. (2017). Tissue Engineering: toward a New Era of Medicine. *Annu. Rev. Med.* 68, 29–40. doi:10.1146/annurev-med-102715-092331
- Sharma, P., and Allison, J. P. (2015). Immune Checkpoint Targeting in Cancer Therapy: toward Combination Strategies with Curative Potential. *Cell* 161 (2), 205–214. doi:10.1016/j.cell.2015.03.030
- Sheen, M. R., and Fiering, S. (2019). *In situ* vaccination: Harvesting Low Hanging Fruit on the Cancer Immunotherapy Tree. *WIREs Nanomed Nanobiotechnol* 11 (1), e1524. doi:10.1002/wnan.1524
- Silva, A. L., Soema, P. C., Slütter, B., Ossendorp, F., and Jiskoot, W. (2016). PLGA Particulate Delivery Systems for Subunit Vaccines: Linking Particle Properties to Immunogenicity. *Hum. Vaccin. Immunother.* 12 (4), 1056–1069. doi:10.1080/21645515.2015.1117714
- Sivakumar, S. M., Safhi, M. M., Kannadasan, M., and Sukumaran, N. (2011). Vaccine Adjuvants - Current Status and Prospects on Controlled Release Adjuvancity. *Saudi Pharm. J.* 19 (4), 197–206. doi:10.1016/j.jsps.2011.06.003
- Song, C., Phuengkham, H., Kim, Y. S., Dinh, V. V., Lee, I., Shin, I. W., et al. (2019). Syringeable Immunotherapeutic Nanogel Reshapes Tumor Microenvironment and Prevents Tumor Metastasis and Recurrence. *Nat. Commun.* 10 (1), 3745. doi:10.1038/s41467-019-11730-8
- Song, H., Huang, P., Niu, J., Shi, G., Zhang, C., Kong, D., et al. (2018). Injectable Polypeptide Hydrogel for Dual-Delivery of Antigen and TLR3 Agonist to Modulate Dendritic Cells in vivo and Enhance Potent Cytotoxic T-Lymphocyte Response against Melanoma. *Biomaterials* 159, 119–129. doi:10.1016/j.biomaterials.2018.01.004
- Sprooten, J., Ceusters, J., Coosemans, A., Agostinis, P., De Vleeschouwer, S., Zitvogel, L., et al. (2019). Trial Watch: Dendritic Cell Vaccination for Cancer Immunotherapy. *Oncoimmunol.* 8 (11), e1638212. doi:10.1080/2162402x.2019.1638212
- Stanley, M. (2017). Tumour Virus Vaccines: Hepatitis B Virus and Human Papillomavirus. *Phil. Trans. R. Soc. B* 372 (1732), 20160268. doi:10.1098/rstb.2016.0268
- Stephan, S. B., Taber, A. M., Jileeva, I., Pegues, E. P., Sentman, C. L., and Stephan, M. T. (2015). Biopolymer Implants Enhance the Efficacy of Adoptive T-Cell Therapy. *Nat. Biotechnol.* 33 (1), 97–101. doi:10.1038/nbt.3104
- Subbiah, V., Murthy, R., Hong, D. S., Prins, R. M., Hosing, C., Hendricks, K., et al. (2018). Cytokines Produced by Dendritic Cells Administered Intratumorally Correlate with Clinical Outcome in Patients with Diverse Cancers. *Clin. Cancer Res.* 24 (16), 3845–3856. doi:10.1158/1078-0432.CCR-17-2707
- Tanyi, J. L., Bobisse, S., Ophir, E., Tuyaerts, S., Roberti, A., Genolet, R., et al. (2018). Personalized Cancer Vaccine Effectively Mobilizes Antitumor T Cell Immunity in Ovarian Cancer. *Sci. Transl. Med.* 10 (436), ea05931. doi:10.1126/scitranslmed.a05931

- Théry, C., Ostrowski, M., and Segura, E. (2009). Membrane Vesicles as Conveyors of Immune Responses. *Nat. Rev. Immunol.* 9 (8), 581–593. doi:10.1038/nri2567
- Twumasi-Boateng, K., Pettigrew, J. L., Kwok, Y. Y. E., Bell, J. C., and Nelson, B. H. (2018). Oncolytic Viruses as Engineering Platforms for Combination Immunotherapy. *Nat. Rev. Cancer* 18 (7), 419–432. doi:10.1038/s41568-018-0009-4
- Umeki, Y., Mohri, K., Kawasaki, Y., Watanabe, H., Takahashi, R., Takahashi, Y., et al. (2015). Induction of Potent Antitumor Immunity by Sustained Release of Cationic Antigen from a DNA-Based Hydrogel with Adjuvant Activity. *Adv. Funct. Mater.* 25 (36), 5758–5767. doi:10.1002/adfm.201502139
- Uppu, D. S. S. M., Turvey, M. E., Sharif, A. R. M., Bidet, K., He, Y., Ho, V., et al. (2020). Temporal Release of a Three-Component Protein Subunit Vaccine from Polymer Multilayers. *J. Controlled Release* 317, 130–141. doi:10.1016/j.jconrel.2019.11.022
- US National Library of Medicine (2021). Dendritic Cell Activating Scaffold in Melanoma. [Online]. Available: <https://clinicaltrials.gov/ct2/show/NCT01753089> (Accessed March 10, 2021).
- van der Burg, S. H., Arens, R., Ossendorp, F., van Hall, T., and Melief, C. J. M. (2016). Vaccines for Established Cancer: Overcoming the Challenges Posed by Immune Evasion. *Nat. Rev. Cancer* 16 (4), 219–233. doi:10.1038/nrc.2016.16
- van der Burg, S. H. (2018). Correlates of Immune and Clinical Activity of Novel Cancer Vaccines. *Semin. Immunol.* 39, 119–136. doi:10.1016/j.smim.2018.04.001
- van der Maaden, K., Heuts, J., Camps, M., Pontier, M., Terwisscha van Scheltinga, A., Jiskoot, W., et al. (2018). Hollow Microneedle-Mediated Micro-injections of a Liposomal HPV E743-63 Synthetic Long Peptide Vaccine for Efficient Induction of Cytotoxic and T-Helper Responses. *J. Controlled Release* 269, 347–354. doi:10.1016/j.jconrel.2017.11.035
- Vartak, A., and Sucheck, S. (2016). Recent Advances in Subunit Vaccine Carriers. *Vaccines* 4 (2), 12. doi:10.3390/vaccines4020012
- Wang, C., Ye, Y., Hochu, G. M., Sadeghifar, H., and Gu, Z. (2016). Enhanced Cancer Immunotherapy by Microneedle Patch-Assisted Delivery of Anti-PD1 Antibody. *Nano Lett.* 16 (4), 2334–2340. doi:10.1021/acs.nanolett.5b05030
- Wang, H., and Mooney, D. J. (2018). Biomaterial-assisted Targeted Modulation of Immune Cells in Cancer Treatment. *Nat. Mater* 17 (9), 761–772. doi:10.1038/s41563-018-0147-9
- Wang, H., Najibi, A. J., Sobral, M. C., Seo, B. R., Lee, J. Y., Wu, D., et al. (2020a). Biomaterial-based Scaffold for In Situ Chemo-Immunotherapy to Treat Poorly Immunogenic Tumors. *Nat. Commun.* 11 (1), 5696. doi:10.1038/s41467-020-19540-z
- Wang, T., Wang, D., Yu, H., Feng, B., Zhou, F., Zhang, H., et al. (2018). A Cancer Vaccine-Mediated Postoperative Immunotherapy for Recurrent and Metastatic Tumors. *Nat. Commun.* 9 (1), 1532. doi:10.1038/s41467-018-03915-4
- Wang, Z., Shang, Y., Tan, Z., Li, X., Li, G., Ren, C., et al. (2020b). A Supramolecular Protein Chaperone for Vaccine Delivery. *Theranostics* 10 (2), 657–670. doi:10.7150/thno.39132
- Wei, X., Liu, L., Li, X., Wang, Y., Guo, X., Zhao, J., et al. (2019). Selectively Targeting Tumor-Associated Macrophages and Tumor Cells with Polymeric Micelles for Enhanced Cancer Chemo-Immunotherapy. *J. Controlled Release* 313, 42–53. doi:10.1016/j.jconrel.2019.09.021
- Weiden, J., Tel, J., and Figdor, C. G. (2018). Synthetic Immune Niches for Cancer Immunotherapy. *Nat. Rev. Immunol.* 18 (3), 212–219. doi:10.1038/nri.2017.89
- Wu, H., Liu, S., Xiao, L., Dong, X., Lu, Q., and Kaplan, D. L. (2016). Injectable and pH-Responsive Silk Nanofiber Hydrogels for Sustained Anticancer Drug Delivery. *ACS Appl. Mater. Inter.* 8 (27), 17118–17126. doi:10.1021/acsami.6b04424
- Yakkala, C., Chiang, C. L.-L., Kandalaft, L., Denys, A., and Duran, R. (2019). Cryoablation and Immunotherapy: an Enthralling Synergy to Confront the Tumors. *Front. Immunol.* 10, 2283. doi:10.3389/fimmu.2019.02283
- Yan, C., Altunbas, A., Yucel, T., Nagarkar, R. P., Schneider, J. P., and Pochan, D. J. (2010). Injectable Solid Hydrogel: Mechanism of Shear-Thinning and Immediate Recovery of Injectable β -hairpin Peptide Hydrogels. *Soft Matter* 6 (20), 5143–5156. doi:10.1039/c0sm00642d
- Yang, P., Song, H., Qin, Y., Huang, P., Zhang, C., Kong, D., et al. (2018). Engineering Dendritic-Cell-Based Vaccines and PD-1 Blockade in Self-Assembled Peptide Nanofibrous Hydrogel to Amplify Antitumor T-Cell Immunity. *Nano Lett.* 18 (7), 4377–4385. doi:10.1021/acs.nanolett.8b01406
- Yang, T., Huang, D., Li, C., Zhao, D., Li, J., Zhang, M., et al. (2021). Rolling Microneedle Electrode Array (RoMEA) Empowered Nucleic Acid Delivery and Cancer Immunotherapy. *Nano Today* 36, 101017. doi:10.1016/j.nantod.2020.101017
- Ye, X., Liang, X., Chen, Q., Miao, Q., Chen, X., Zhang, X., et al. (2019). Surgical Tumor-Derived Personalized Photothermal Vaccine Formulation for Cancer Immunotherapy. *ACS Nano* 13 (3), 2956–2968. doi:10.1021/acsnano.8b07371
- Ye, Y., Wang, C., Zhang, X., Hu, Q., Zhang, Y., Liu, Q., et al. (2017). A Melanin-Mediated Cancer Immunotherapy Patch. *Sci. Immunol.* 2 (17), eaan5692. doi:10.1126/sciimmunol.aan5692
- Yu, L., and Ding, J. (2008). Injectable Hydrogels as Unique Biomedical Materials. *Chem. Soc. Rev.* 37 (8), 1473–1481. doi:10.1039/b713009k
- Yu, S., Wang, C., Yu, J., Wang, J., Lu, Y., Zhang, Y., et al. (2018). Injectable Bioresponsive Gel Depot for Enhanced Immune Checkpoint Blockade. *Adv. Mater.* 30 (28), e1801527. doi:10.1002/adma.201801527
- Zaric, M., Lyubomska, O., Touzelet, O., Poux, C., Al-Zahrani, S., Fay, F., et al. (2013). Skin Dendritic Cell Targeting via Microneedle Arrays Laden with Antigen-Encapsulated Poly-D,L-Lactide-Co-Glycolide Nanoparticles Induces Efficient Antitumor and Antiviral Immune Responses. *ACS Nano* 7 (3), 2042–2055. doi:10.1021/nn304235j
- Zeng, Q., Gammon, J. M., Tostanoski, L. H., Chiu, Y.-C., and Jewell, C. M. (2017). *In vivo* expansion of Melanoma-specific T Cells Using Microneedle Arrays Coated with Immune-Polyelectrolyte Multilayers. *ACS Biomater. Sci. Eng.* 3 (2), 195–205. doi:10.1021/acsbomaterials.6b00414
- Zhang, L., Wang, W., and Wang, S. (2015). Effect of Vaccine Administration Modality on Immunogenicity and Efficacy. *Expert Rev. Vaccin.* 14 (11), 1509–1523. doi:10.1586/14760584.2015.1081067
- Zhang, W., Jin, X., Li, H., Wei, C.-x., and Wu, C.-w. (2019). Onion-structure Bionic Hydrogel Capsules Based on Chitosan for Regulating Doxorubicin Release. *Carbohydr. Polym.* 209, 152–160. doi:10.1016/j.carbpol.2019.01.028
- Zhang, W., Wang, L., Liu, Y., Chen, X., Liu, Q., Jia, J., et al. (2014). Immune Responses to Vaccines Involving a Combined Antigen-Nanoparticle Mixture and Nanoparticle-Encapsulated Antigen Formulation. *Biomaterials* 35 (23), 6086–6097. doi:10.1016/j.biomaterials.2014.04.022
- Zhao, H., Zhao, B., Li, L., Ding, K., Xiao, H., Zheng, C., et al. (2020). Biomimetic Decoy Inhibits Tumor Growth and Lung Metastasis by Reversing the Drawbacks of Sonodynamic Therapy. *Adv. Healthc. Mater.* 9 (1), e1901335. doi:10.1002/adhm.201901335
- Zhao, J., Chen, Y., Ding, Z.-Y., and Liu, J.-Y. (2019). Safety and Efficacy of Therapeutic Cancer Vaccines Alone or in Combination with Immune Checkpoint Inhibitors in Cancer Treatment. *Front. Pharmacol.* 10, 1184. doi:10.3389/fphar.2019.01184
- Zhu, G., Lynn, G. M., Jacobson, O., Chen, K., Liu, Y., Zhang, H., et al. (2017). Albumin/vaccine Nanocomplexes that Assemble in vivo for Combination Cancer Immunotherapy. *Nat. Commun.* 8 (1), 1954. doi:10.1038/s41467-017-02191-y
- Zhu, M., Ding, X., Zhao, R., Liu, X., Shen, H., Cai, C., et al. (2018). Co-delivery of Tumor Antigen and Dual Toll-like Receptor Ligands into Dendritic Cell by Silicon Microparticle Enables Efficient Immunotherapy against Melanoma. *J. Controlled Release* 272, 72–82. doi:10.1016/j.jconrel.2018.01.004
- Zhu, Y., Xue, J., Chen, W., Bai, S., Zheng, T., He, C., et al. (2020). Albumin-biomimetic Nanoparticles to Synergize Phototherapy and Immunotherapy against Melanoma. *J. Controlled Release* 322, 300–311. doi:10.1016/j.jconrel.2020.03.045
- Zinkernagel, R. M., Ehl, S., Aichele, P., Oehen, S., Kündig, T., and Hengartner, H. (1997). Antigen Localisation Regulates Immune Responses in a Dose- and Time-dependent Fashion: a Geographical View of Immune Reactivity. *Immunol. Rev.* 156, 199–209. doi:10.1111/j.1600-065x.1997.tb00969.x

Conflict of Interest: The authors declare that the research was conducted in the absence of any commercial or financial relationships that could be construed as a potential conflict of interest.

Copyright © 2021 Han, Peng, Qiu, Li, Ruan, He and Yuan. This is an open-access article distributed under the terms of the Creative Commons Attribution License (CC BY). The use, distribution or reproduction in other forums is permitted, provided the original author(s) and the copyright owner(s) are credited and that the original publication in this journal is cited, in accordance with accepted academic practice. No use, distribution or reproduction is permitted which does not comply with these terms.



The Role of Tumor Inflammatory Microenvironment in Lung Cancer

Zhaofeng Tan^{1,2†}, Haibin Xue^{3†}, Yuli Sun², Chuanlong Zhang¹, Yonglei Song² and Yuanfu Qi^{2*}

¹First Clinical Medical College, Shandong University of Traditional Chinese Medicine, Jinan, China, ²Departments of Oncology Affiliated Hospital of Shandong University of Traditional Chinese Medicine, Jinan, China, ³Eighth Medical Center of the General Hospital of the Chinese People's Liberation Army, Beijing, China

OPEN ACCESS

Edited by:

Jianxun Ding,
Changchun Institute of Applied
Chemistry (CAS), China

Reviewed by:

Jun Dong,
Sun Yat-sen University Cancer Center
(SYSUCC), China
Xiaodan Zhang,
Shandong University, China
Ke-Fei Xue,
Tsinghua University, China

*Correspondence:

Yuanfu Qi
m13793132317@163.com

[†]These authors have contributed
equally to this work

Specialty section:

This article was submitted to
Pharmacology of Anti-Cancer Drugs,
a section of the journal
Frontiers in Pharmacology

Received: 31 March 2021

Accepted: 29 April 2021

Published: 17 May 2021

Citation:

Tan Z, Xue H, Sun Y, Zhang C, Song Y
and Qi Y (2021) The Role of Tumor
Inflammatory Microenvironment in
Lung Cancer.
Front. Pharmacol. 12:688625.
doi: 10.3389/fphar.2021.688625

Lung cancer is the most common and fatal malignant tumor in the world. The tumor microenvironment (TME) is closely related to the occurrence and development of lung cancer, in which the inflammatory microenvironment plays an important role. Inflammatory cells and inflammatory factors in the tumor inflammatory microenvironment promote the activation of the NF- κ B and STAT3 inflammatory pathways and the occurrence, development, and metastasis of lung cancer by promoting immune escape, tumor angiogenesis, epithelial-mesenchymal transition, apoptosis, and other mechanisms. Clinical and epidemiological studies have also shown a strong relationship among chronic infection, inflammation, inflammatory microenvironment, and lung cancer. The relationship between inflammation and lung cancer can be better understood through the gradual understanding of the tumor inflammatory microenvironment, which is advantageous to find more therapeutic targets for lung cancer.

Keywords: tumor microenvironment, inflammation, lung cancer, metastasis, immune escape

INTRODUCTION

Tumor diseases are increasingly becoming a major disease that seriously endangers human health all over the world. Among all tumors, lung cancer has the greatest prevalence and mortality (Barta et al., 2019). Studies on tumor diseases have shown that the tumor microenvironment (TME), which consists of tumor-related cells and stromal cells, interacts with tumor cells and plays an important role in tumor growth, invasion, and metastasis (Huang et al., 2021). With the rise of precision therapy, the importance of the TME is becoming increasingly significant. In chronic inflammatory diseases and smoldering inflammation caused by tumors, inflammation has a great impact on the composition of the TME, especially on the plasticity of tumors and stromal cells (Greten and Grivnik, 2019). With the deepening of research on lung cancer and the TME, a close relationship between inflammation and lung cancer has been found, and considerable attention has been paid to the role of inflammation and the inflammatory microenvironment in lung cancer. In addition, some reports indicate that the intervention of tumor inflammatory microenvironment can reduce the development of lung cancer in animal models and patients of lung cancer (Caetano et al., 2016; Weichand et al., 2017).

The TME was first proposed by Lord et al., through the tumor model system *in vitro*, the interaction between lymphoid host cells and multicellular spheres was studied, and the effect of host cells on tumor cells was verified (Lord et al., 1979). In recent years, the TME has become one of the fastest-growing areas of cancer research, which is widely considered to be closely related to the occurrence and development of tumors, and is a hot spot in current cancer research. It mainly includes tumor cells, tumor-associated fibroblasts, immune cells, vascular endothelial cells,

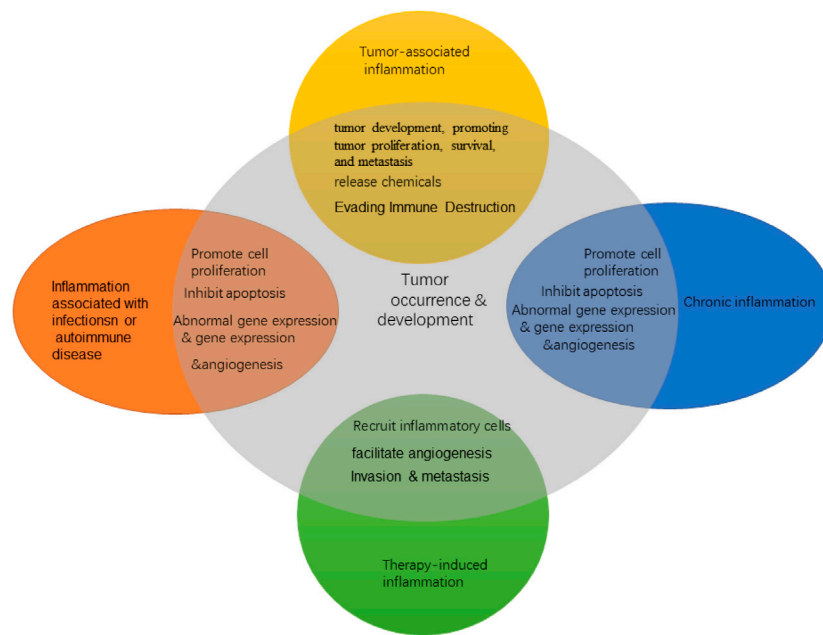


FIGURE 1 | Inflammatory types in cancer.

extracellular matrix (ECM) and its degrading enzymes, various growth factors, and inflammatory factors. Moreover, it has special physical and chemical characteristics (e.g., hypoxia, low pH) (Wang et al., 2016; Wang et al., 2019; Jiang et al., 2020; Zheng et al., 2020; Liu et al., 2021; Song et al., 2021; Zheng et al., 2021). The TME has multiple effects on tumor initiation, development, and progression, and the mechanism is complex. Therefore, in the treatment of tumors and targeted control of cytokines and related factors in the TME, studying the role of the TME and its related molecular mechanisms will provide a new and important target for cancer therapy. This review mainly focused on inflammatory cells and inflammatory factors in the tumor inflammatory microenvironment and the principal mechanisms that govern the effects of inflammation on lung cancer development.

INFLAMMATION AND LUNG CANCER: A MULTIFACETED LINK

The persistence of chronic inflammation is one of the important characteristics of malignant tumors. The TME is largely regulated by inflammatory cells and is an indispensable component in tumor development, promoting tumor proliferation, survival, and metastasis. In the 19th century, German pathologist Rudolf Virchow found infiltrating white blood cells in tumor tissue, which suggested for the first time that there may be some relationship between inflammation and tumors. With the development of epidemiology and molecular biology, the close relationship between inflammation and tumors has attracted considerable attention. In 2011, famous cancer scholars Hanahan and Weinberg listed “promoting tumor

inflammation” as one of the 10 characteristics of cancer and proposed that inflammation can promote a variety of tumor landmark functions by providing bioactive molecules to the TME (Hanahan and Weinberg, 2011). Inflammation is involved in all stages of tumorigenesis, from malignant transformation and tumor initiation to established tumor invasion and metastasis (Figure 1). Although the mechanism by which inflammation promotes cancer is not fully understood, two interrelated hypotheses have emerged: one is the internal pathway driven by genetic changes that lead to tumors and inflammation; the other is the external pathway driven by inflammatory conditions that increase tumor risk (Conway et al., 2016).

Inflammation promotes the emergence of multiple cancer markers by providing essential molecules to the TME. Several studies have shown that the inflammatory microenvironment may predate tumor formation. Inflammation can lead to tumor formation and development through epigenetics and subsequent abnormal gene expression, vascular abnormalities, and tumor neovascularization and by promoting cell proliferation, inhibiting apoptosis, adjusting genomic stability, and promoting metastasis and other mechanisms. In addition, inflammatory cells can release chemicals such as ROS that promote carcinogenic evolution, and many factors released by inflammatory cells may directly or indirectly lead to significant inhibition of immune response (Hanahan and Weinberg, 2011). Inflammation, especially chronic inflammation, is related to the occurrence and development of various tumors. The inflammatory TME is a common feature of solid tumors. The interaction between inflammatory microenvironment and tumor cells has a profound impact on tumor growth, metastasis, and drug resistance (Kitamura et al., 2015).

Inflammation can easily lead to the development of cancer and promote all stages of tumorigenesis. Clinical and epidemiological

studies have shown a strong correlation among chronic infection, inflammation, and lung cancer. Epidemiological studies have shown that people prone to chronic inflammatory diseases have an increased risk of cancer, and potential infections and inflammation are associated with 15–20% of cancer deaths worldwide (Bremnes et al., 2011). The lung is an open organ, where gas exchange occurs. Due to its unique physiological structure, it is easily affected by a large number of pathogens, pollutants, oxidants, gases, and poisons inhaled from the air. Long-term exposure to inhalable silica dust, mineral fibers, air particulate matter, and smoke and chronic inflammation caused by bronchitis, chronic obstructive pulmonary disease (COPD), and bronchial asthma can induce lung cancer (Houghton, 2013; Valavanidis et al., 2013). The vast majority of lung cancer cases are due to continued exposure to tobacco smoke (Gandini et al., 2008). Smoking is the main cause of chronic pulmonary inflammation and lung injury. At the same time, its carcinogens increase the oxidative stress of tissues and cause tissue inflammation. The comprehensive analysis results of Brenner et al. showed that the prevalence of past lung diseases (chronic bronchitis, emphysema, pneumonia, and tuberculosis) independently affects the development of lung cancer in non-smokers and may be related to disease-related inflammation and pathogenesis (Brenner et al., 2012). Inflammation can cause lung tissue damage. During inflammation, the cell division rate, DNA damage, and cell mutation rate in lung tissue are increased. In addition, inflammation increases the likelihood of lung cancer by acting as an initiator or promoter of antiapoptotic signals. It can also cause angiogenesis (the formation of new blood vessels) and provide nutrients for the growth and spread of tumor cells (Azad et al., 2008).

Continuous inflammation will cause a large number of inflammatory cell infiltration, which in turn floods the microenvironment with a large number of inflammatory cytokines and active mediators (such as ROS, TNF- α , etc.) (Azad et al., 2008; Kundu and Surh, 2008). The inflammatory TME plays many roles in tumor progression and metastasis, including creating a hypoxic environment, increasing angiogenesis and invasion, altering the expression of microRNA, and increasing stem cell phenotype, thereby promoting epithelial–mesenchymal transition (EMT) (Heinrich et al., 2012). Hypoxia and decreased tissue oxygen tension are the basic characteristics of the cancer microenvironment. Chronic inflammation also leads to local hypoxia due to the combined effect of reduced circulation at the site of inflammation and increasing metabolic demand for infiltrating immune cells. Hypoxia can lead to increased resistance to conventional radiation and chemotherapy, which further induces the EMT (Semenza, 2010). In non-small cell lung cancer (NSCLC) cell lines, the activation of HIF-1 α by cMet stimulates the HGF of tumor cells, which leads to ECM degradation, cell dissociation, and increased cell migration through tissue parenchyma (Yoo et al., 2011). Inflammatory cells in the inflammatory microenvironment can secrete vascular endothelial growth factor (VEGF) in large quantity to promote tumor angiogenesis (Gomes et al., 2014).

Inflammation and the inflammatory microenvironment affect numerous aspects of malignant tumors, including the

proliferation and survival of malignant cells, angiogenesis, tumor metastasis, and tumor response to chemotherapy drugs and hormones (Greten and Grivennikov, 2019). In the occurrence of lung cancer, inflammation caused by infection increases the likelihood of lung cancer and affects the prognosis of lung cancer to a certain extent. Preventing and controlling inflammation and finding targets in the inflammatory microenvironment are one of the critical ways to prevent and control lung cancer.

INFLAMMATORY CELLS, CYTOKINES, AND PATHWAYS ASSOCIATED WITH LUNG CANCER

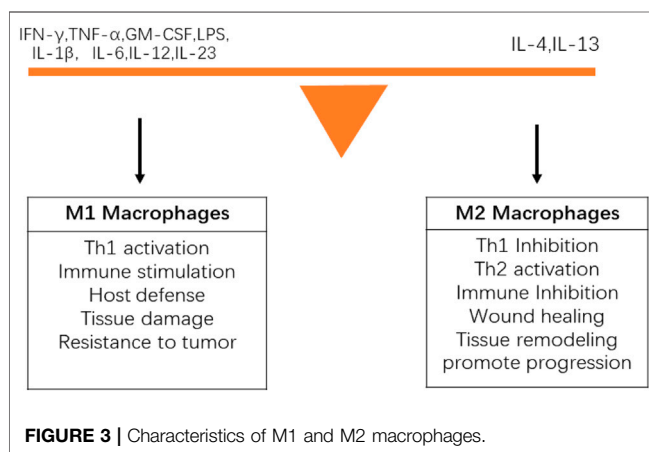
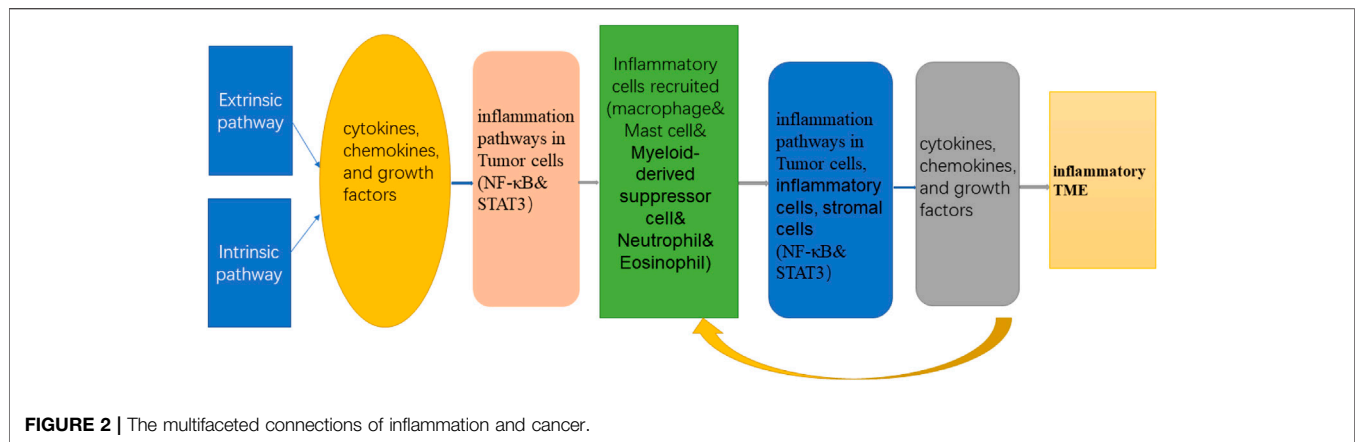
From the perspective of the TME, the occurrence and progression of lung cancer should be the outcome of problems in the entire body tissue, not just tumor cells. The inflammatory microenvironment is an essential component of the occurrence and metastasis of lung cancer and a key factor in regulating invasion and metastasis.

The neutrophils, macrophages, and myeloid-derived suppressor cells contained in the tumor inflammatory microenvironment and their secreted cytokines, chemokines, and growth factors together affect the progression and metastasis of tumors. Among them, tumor-related cytokines, oxygen metabolites, proteases, inflammatory factors, and other inflammatory mediators can cause mutations in cell genes and induce inflammatory reactions. The inflammatory factors produced in the inflammatory response, such as interleukin (IL-1) and TNF- α , can also promote the activation of NF- κ B and STAT3 inflammation pathways, cause damage to cellular genes, induce gene mutations, and ultimately lead to the formation of tumors. At the same time, the activation of NF- κ B and STAT3 can increase the production of inflammatory factors, maintain the tumor inflammatory microenvironment, and form a vicious circle of “inflammation–tumor–inflammation” (Figure 2). The following sections mainly introduce the focal inflammatory cells, factors, and inflammatory pathways in the inflammatory microenvironment.

Inflammatory Cells Associated With Lung Cancer

When the cause of inflammation persists, acute inflammation can be converted into chronic inflammation with significant white blood cell infiltration in the lung tissue. Inflammatory cells associated with lung cancer include T cells, myelogenic suppressor cells, natural killer cells, mast cells, tumor-associated neutrophils (TAN) and macrophages, etc. At present, macrophages are the most studied inflammatory cells.

Macrophages are innate immune cells that not only play a critical role in improving the immune response to foreign cells, bacteria, and viruses, but also mediate tissue repair after injury. Macrophages have various physiological functions, including non-specific immune defense, non-specific immune surveillance, processing and presenting antigens to initiate an



adaptive immune response, immunomodulatory effects, and participation in inflammation. Macrophages can participate in and promote inflammation by secreting chemokines and inflammatory factors such as MIP, monocyte chemoattractant protein-1 (MCP-1), IL-1, and IL-8. There are at least two types of tumor-associated macrophages (TAMs). (I) Classic M1 macrophages have the following characteristics: efficient antigen presentation function; massive secretion of IL-12 and IL-23; and ability to activate Th1 immune response, eliminate infectious microorganisms, and kill tumor cells. The phenotype is characterized by high IL-12 and IL-23 and low IL-10. (II) Tumor-promoting mutant M2 macrophages participate in the formation of tumor stroma; promote tumor growth, metastasis, and tumor angiogenesis; and lead to tumor immunosuppression. The phenotype is characterized by low IL-12 and IL-23 and high IL-10. Macrophages constitute the main cells of tumor inflammatory infiltration. There is a lineage of activated macrophages, and the difference between M1 and M2 phenotypes represents the extreme of this lineage (Mantovani et al., 2002). The polarization of M1 or M2 phenotype depends on the precise combination of signals in the local microenvironment. Macrophages change their functions and the expression of surface markers according to these changing signals (Figure 3). During persistent inflammation or in the TME,

TAMs in established tumors are usually biased toward the M2 phenotype, which promotes the survival, development and spread of tumors by promoting angiogenesis, EMT and immunosuppression (Ye et al., 2015). The various tumor-prone functions of M2 macrophages create a microenvironment to support cell growth and immune evasion/inhibition, and promote the growth and development of tumors. Macrophages are closely linked and aggregated by activating key transcription factors in tumor cells, such as NF-κB, STAT3, and HIF-1α. Together, they lead to increased tumor cell proliferation, inhibition of apoptosis, neovascularization, ECM remodeling, migration, and invasion. Because macrophages are involved in multiple pathways of tumorigenesis, treatments for different stages of macrophages can be designed by inhibiting the recruitment, differentiation, and activation of macrophages, such as CCL2, COX-2, M-CSF, and GM-CSF, downregulating the PGE2/IL-6/STAT3 activation loop, and blocking the NF-κB signaling pathway (Hagemann et al., 2008; Coussens et al., 2013; Gutschalk et al., 2013; Mizuno et al., 2019; Piotrowski et al., 2020).

Inflammatory Cytokines Associated With Lung Cancer

Cytokines link inflammation to tumor, and they are activated in both inflammatory cells and tumor cells. Cytokines play an important role in maintaining chronic inflammation, promoting the transformation of malignant epithelial cells, inhibiting tumor immune surveillance, and promoting tumor metastasis. The inflammatory factors closely related to lung cancer are IL-1β, IL-4, IL-6, IL-11, IL-12, TNF-α, MCP-1, and transforming growth factor (TGF)-β.

IL-1β: IL-1β is a member of the IL-1 cytokine family and is an important mediator of inflammatory response. It participates in a variety of cellular activities, including cell proliferation, differentiation, and apoptosis; the expression of IL-1 targets that promote tumor angiogenesis in chronic inflammation, and the expression of soluble mediators in cancer-related fibroblasts (CAFs) that cause antiapoptotic signals in tumor cells, thus promoting tumor progression (Bent et al., 2018). *In vitro* experiments showed that IL-1β induces angiogenesis and

lymphatic angiogenesis *in vitro* (Nakao et al., 2011). IL-1 β can increase tumor invasion and metastasis mainly by promoting angiogenic factors produced by stromal cells in the TME to induce tumor angiogenesis, endothelial cell activation, and immunosuppressive cells (Apte et al., 2006; Mantovani et al., 2018; Steel et al., 2018). Lee et al. found that IL-1 β induces the expression of actin-binding protein fascin to promote tumor metastasis through the ERK1/2, JNK, NF- κ B and CREB signal pathways (Lee et al., 2018). Weichand et al. found S1PR1 inflammatory bodies on TAMs promote lymph angiogenesis and metastasis through NLRP3/IL-1 β (Weichand et al., 2017).

TNF- α : TNF- α is one of the most important cytokines produced by macrophages, the main mediator of cancer-related inflammation, and the key factor of inflammatory response, which was first proposed by Carswell et al. (Helson et al., 1975). Many pathogenic factors can induce TNF- α , which further induces other inflammatory mediators and proteases. During chronic inflammation, the imbalance and persistent production of TNF may promote carcinogenesis, and, in some cases, TNF may even be a carcinogen. An increasing number of evidences shows that a small amount of TNF- α produced by tumor cells and stromal cells is an endogenous tumor promoter (Balkwill, 2002). Tumor production of TNF- α is associated with poor prognosis, loss of hormone response, and cachexia (Kim et al., 2013). The NF- κ B signal pathway is the bridge between TNF and tumor promotion (Greten et al., 2004). TNF produced by malignant cells can also cause excessive permeability of existing blood vessels, thus stimulating pleural effusion in lung cancer models (Stathopoulos et al., 2007). Preclinical studies have shown that the anti-tumor effect of TNF is due to the destruction of tumor vascular system (Daniel and Wilson, 2008). Outside the field of cancer, especially in rheumatism, TNF has been identified as a major regulator of inflammation and a key participant in the cytokine network, which has led to the development of antagonists of its role and revolutionized the treatment of rheumatoid arthritis and other inflammatory diseases (Tracey et al., 2008; Billmeier et al., 2016; Green et al., 2019). With the progress of research in patients with chronic inflammatory diseases, many mechanisms of TNF antagonist therapy in inhibiting TNF-enhanced cancer development have been found: angiogenesis, leukocyte infiltration, and stimulation of other cytokines and chemokines (Charles et al., 1999). TNF antagonists are safe for cancer patients (Madhusudan et al., 2004; Brown et al., 2008).

IL-6: IL-6, a powerful multipotent proinflammatory cytokine, plays a key role in host defense against pathogens and acute stress (Yao et al., 2014). IL-6–Janus kinase 2 (JAK)–signal transduction and transcriptional activator (STAT) signaling pathway plays an important role in various tumorigenesis models, including lung, breast, colon, ovarian, prostate, and multiple myeloma (Jin et al., 2013; Eskiler et al., 2019). CAFs isolated from human lung cancer tissue secrete IL-6, which stimulates JAK2 and STAT3 signal transduction in human lung cancer cells, thereby increasing metastasis (Wang L. et al., 2017). The combination of IL-6 blocking and other signal pathway inhibition has been widely studied in lung cancer. Caetano et al. found that IL-6 is overexpressed in a mouse model of K-ras mutant lung cancer

and human lung cancer. The use of monoclonal anti-IL-6 antibody to block IL-6 can significantly reduce the promoting effect of COPD-like airway inflammation on lung tumor cell proliferation and tumor angiogenesis and bias the precursor immunosuppressive environment to anti-tumor phenotype, indicating that IL-6 is a potential drug target for the prevention and treatment of K-ras-mutant lung tumors. The study found that 8 (53%) of the 15 lung cancer cell lines expressed IL-6 mRNA and protein, suggesting that the overexpression of IL-6 may disrupt the cytokine balance and weaken the anti-tumor immunity of patients with lung cancer (Yamaji et al., 2004).

TGF- β : TGF- β is an evolutionarily conserved multipotent factor, which regulates many biological processes such as development, tissue regeneration, immune response, and tumorigenesis (Saito et al., 2018). It can promote tumor development by regulating certain microenvironmental pathways in a certain environment. It plays multiple roles in tumor biology and is often overexpressed in many tumors, including NSCLC (Bruno et al., 2013). High expression of TGF- β is a characteristic of NSCLC and a poor prognostic factor (Teixeira et al., 2011). High expression levels of TGF- β are related to lymph node metastasis and tumor angiogenesis in NSCLC (Hasegawa et al., 2001). William et al. found that the expression of TGF- β in lung adenocarcinoma is higher than that of other histological subtypes, which is the only independent immunological parameter with prognostic significance (Sterlacci et al., 2012). TGF- β also plays a role in the polarization of immune cells in the TME, including macrophages, neutrophils, and NK cells associated with tumor immune escape (Flavell et al., 2010). Some studies have shown that TGF- β -mediated EMT in cancer cells is related to antiapoptosis, acquisition of stem cell characteristics, chemotherapy resistance, and other invasive characteristics (Hao et al., 2019). TGF- β participates in the maintenance of T cell homeostasis and induces Treg cells that limit tumor immune response (Chen et al., 2003). Blocking TGF- β signal transduction with TGF- β -blocking antibodies or TGF- β receptor I kinase inhibitors can enhance anti-tumor immunity and show therapeutic benefits (Tauriello et al., 2018).

IL-10: IL-10 is a multifunctional cytokine with immunosuppressive and anti-angiogenesis functions that is mainly secreted by M2 macrophages, Treg cells, and Th2 cells. Polymorphisms in the IL-10 gene promoter region are associated with susceptibility to a variety of cancers (including lung cancer) (Namazi et al., 2018). Many patients with malignant tumors, including lung cancer, have elevated serum and peritumoral IL-10 levels (Vahl et al., 2017). Increased IL-10 mRNA expression is associated with the advanced lung cancer (Wang et al., 2011). The expression of IL-10 is a prognostic factor of NSCLC, and high IL-10 expression of TAMs is an important independent predictor of advanced tumor stage. Thus, it is related to poor overall survival rate. The local expression of IL-10 may promote tumor progression through the immunosuppression (Zeni et al., 2007).

MCP-1: MCP-1 is a chemokine that regulates monocyte chemotaxis and lymphocyte differentiation by binding to CC chemokine receptor 2 and plays a vital role in the pathogenesis of

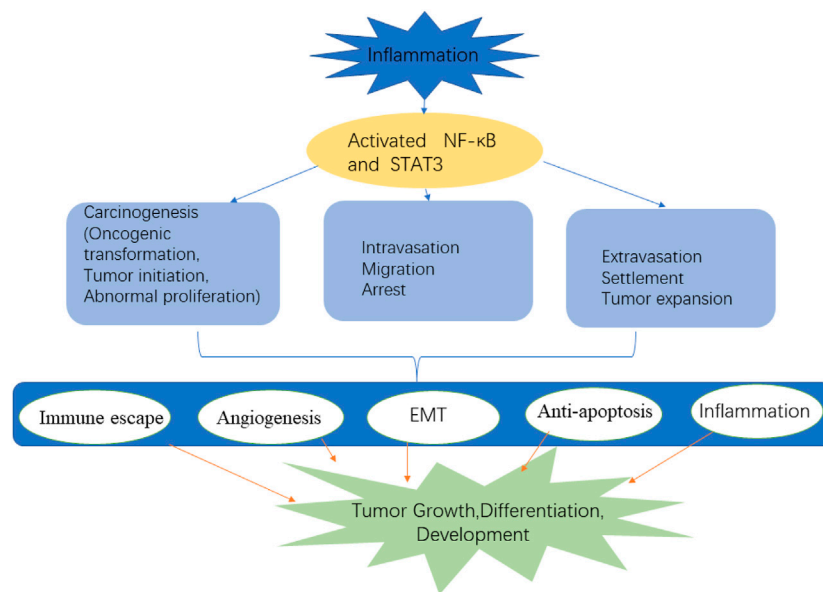


FIGURE 4 | The multifaceted role of NF- κ B and STAT3 in tumor.

inflammatory diseases, atherosclerosis, and cancer (Bianconi et al., 2018). Many tumor lines and different non-tumor stromal cells in the TME, including fibroblasts, endothelial cells, and inflammatory cells, produce MCP-1, which can promote the proliferation, migration, and survival of tumor cells (Yoshimura, 2017). A meta-analysis evaluated the prognostic value of MCP-1 expression in patients with solid tumors, and the results showed that increased MCP-1 levels were associated with decreased overall survival (hazard ratio 1.95, 95% CI 1.32–2.88) (Wang et al., 2014). Studies have found that MCP-1 induces the interaction between tumor-derived factors and host-derived chemokines, thereby promoting bone metastasis (Mulholland et al., 2019).

Inflammation-Related Signal Pathways of Associated With Lung Cancer

The signal pathways related to the inflammatory microenvironment mainly include NF- κ B signal pathway and STAT3 signal pathway. Both pathways are involved in the process of inflammation and tumor production and are extremely active in various tumor cells. Thus, they are considered to be the most important participants in the tumor signal pathway.

NF- κ B: NF- κ B is a positive regulator of cell growth and proliferation, which is often activated by proinflammatory cytokines such as IL-1 β and TNF- α . In most cases, NF- κ B remains active in cancer cells through mutations in upstream signal molecules or in response to extracellular stimuli in the TME (Karin et al., 2002). NF- κ B is structurally activated in a variety of solid tumors, including prostate cancer, breast cancer, cervical cancer, pancreatic cancer, and lung cancer. The NF- κ B pathway is an important tumor signal pathway that plays an important role in the inflammatory response induced by lung

cancer gene mutation (Lin et al., 2010). NF- κ B promotes the key steps of tumor cell invasion and EMT, which is closely related to tumor apoptosis and angiogenesis (Figure 4). NF- κ B increases the expression of several factors related to cell cycle progression, such as cyclin D and E (Chen et al., 2011). The upregulation of cyclin D1 expression by NF- κ B is related to the increased transition from G1 phase to S phase. In addition, NF- κ B negatively regulates the expression of growth arrest and DNA damage-inducible protein 45 (GADD45). GADD45 is a checkpoint protein of the cell cycle, which causes cells to transition in the G2/M phase. In addition, the interaction between NF- κ B and proinflammatory cytokines such as TNF- α and IL-1 β is also involved in stimulating cancer cell proliferation, especially during chronic inflammation (Rius et al., 2008). Although lung cancer is histologically heterogeneous, tumor samples obtained from lung cancer patients show a high level of NF- κ B activation in both small cell lung cancer and NSCLC, which is significantly correlated with TNM stage and poor prognosis in these patients. The inhibition of NF- κ B by siRNA, IKK inhibitors, and I κ B super inhibitors can inhibit the survival and proliferation of lung cancer cells (Chen et al., 2011).

STAT3: Among the seven members of the STAT protein family (STAT1, STAT2, STAT3, STAT4, STAT5a, STAT5b, and STAT6), STAT3 and STAT5 are the most important factors for tumor progression (Yu and Jove, 2004). STAT3 plays a key role in the process of cell surface receptors transmitting extracellular signals to the nucleus. It is an important regulator of immunity, inflammation, and tumorigenesis and is the convergence point of a variety of signal transduction pathways (Dutta et al., 2014). The structural activation of STAT3 is involved in many cellular processes, including proliferation, survival, inflammation,

invasion, metastasis, and angiogenesis, all of which are conducive to tumor initiation and progression (Siveen et al., 2014). In addition to its established role as a transcription factor in cancer, STAT3 regulates mitochondrial function and gene expression through epigenetic mechanisms (Yu et al., 2014). The activation of STAT3 is also an effective immune checkpoint for a variety of anti-tumor immune responses (Yu et al., 2009). Abnormal STAT3 signals promote the occurrence and development of a variety of human cancers by inhibiting apoptosis or inducing cell proliferation, angiogenesis, invasion, and metastasis (Grivennikov and Karin, 2010). STAT3 has been shown to prolong the survival of human PC-13 large cell lung cancer cells after serum deprivation (Akca et al., 2006). The structural activation of STAT3 is a common feature of NSCLC, and it is also considered to play an important role in tumor resistance to conventional and targeted small molecule therapy, especially the rich mutations in the JAK/STAT pathway (Govindan et al., 2012; Looyenga et al., 2012; You et al., 2014). In NSCLC cells, IL-6 neutralizing antibodies have been shown to inhibit tumor growth in mouse transplanted tumor models by inhibiting JAK1/STAT3 signaling (Song et al., 2011).

The NF- κ B family and STAT3 are widely expressed, which can be activated rapidly under the stimulation of stress and cytokines. Once activated, NF- κ B and STAT3 control the expression of antiapoptosis, proliferation, and immune response genes (Grivennikov and Karin, 2010). The activation and interaction of STAT3 and NF- κ B play a key role in controlling the dialogue between tumor cells and their microenvironment, especially in inflammatory/tumor-infiltrating immune cells. They are powerful activators of malignant tumor state, affect the persistence of inflammation, and promote the production of tumor cytokines. They play an important role as a bridge between tumor cells and peripheral inflammatory cells. In the tumor inflammatory microenvironment, the activation of these two signal pathways can promote the release of corresponding cytokines, chemokines, and active substances, as well as the malignant proliferation and adhesion of tumor cells (Figure 4). Antiapoptotic genes are the main targets of NF- κ B and STAT3, and Bcl-xL, B-cell lymphoma 2 (Bcl-2), Mcl-1, and other genes are activated by these two factors, especially can promote the expression of anti-apoptotic genes, such as Bcl-2 and so on (Rebouissou et al., 2009; Siveen et al., 2014). In addition, they can further chemotactic inflammatory cells by promoting the release of enzymes related to cytokines, chemokines, and prostaglandin synthesis and inducible nitric oxide synthase, thus forming an inflammatory microenvironment conducive to tumor production. In short, these two pathways play a key role in tumor cell production, survival, EMT, invasion, metastasis, inhibition of adaptive immunity and drug resistance.

MECHANISMS OF TUMOR INFLAMMATORY MICROENVIRONMENT IN PROMOTING THE DEVELOPMENT AND METASTASIS OF LUNG CANCER

The TME has been considered as a major factor in tumor progression and metastasis (Hanahan and Coussens, 2012). Its

composition is heterogeneous. The coordinated heterogeneous interaction between genetically altered tumor epithelial cells and tumor stromal cells regulates the main characteristics of the tumor, including immune escape, angiogenesis, EMT, and metastasis. Myeloid cells (monocytes, macrophages, and neutrophils) also secrete VEGF, basic fibroblast growth factor, platelet-derived growth factor, placental growth factor, and Bv8, all of which contribute to vascular remodeling during tumor progression (Shojaei et al., 2007). The major mechanisms of the inflammatory microenvironment in promoting lung cancer metastasis are as follows.

Immune Escape

More and more attention has been paid to the role of the immune system in tumorigenesis, and immune escape is now regarded as one of the markers of cancer. Abnormalities in the structure and function of the immune system are closely related to the occurrence and development of tumors. There are complex interactions between immune cells and malignant cells in the tumor stroma. The immune system can not only promote the tumor, but also inhibit it. On the one hand, the body's immune system can sense the existence of tumors and kill or eliminate tumor cells through a variety of immune mechanisms. On the other hand, tumor cells can also escape or resist the killing and clearance of tumor cells by the immune system through a variety of mechanisms. Burnet put forward the concept of immune surveillance in 1970: the immune system spontaneously recognizes and eliminates cancer cells, thus preventing tumor development (Burnet, 1970). Inflammatory cells and inflammatory factors can help tumor cells escape immune surveillance. Many factors released by inflammatory cells may directly or indirectly lead to significant inhibition of immune response (Ben-Baruch, 2006). For example, chronic tumor cells secrete cytokines and other soluble factors and subsequently induce, expand, and recruit Treg cells to tumor sites. A high proportion of Treg cells produce an immunosuppressive microenvironment, which inhibits anti-tumor immunity and promotes tumor growth. TAMs further induce immunosuppression by activating immune checkpoint PD-L1 and increasing the expression of specific metabolic pathways arginase-1 and indoleamine 2,3-dioxygenase (Johnson and Munn, 2012).

Tumor Angiogenesis

Angiogenesis plays a key role in the growth, proliferation, and metastasis of various solid tumors (Rivas-Fuentes et al., 2015). Pathological angiogenesis is a hallmark of cancer and various ischemic and inflammatory diseases, and tumor tissues of lung cancer show active angiogenesis. Chronic inflammation is related to angiogenesis, which is a process that helps cancer cells grow. Studies have shown that different types of cells in the TME can affect angiogenesis, participate in the regulation of secreted local concentrations of pro-angiogenic factors and anti-angiogenic factors, and change the local insoluble matrix surrounding blood vessels. Among them, inflammatory infiltrating cells (including monocytes, macrophages, mast cells) and inflammatory factors are involved in the regulation of

angiogenesis. Inflammation-related chemokines (including CC, CXC, CX3C, and XC family) play a central role as tumor angiogenesis regulators. In turn, the endothelial cells that form the vascular system actively participate in and regulate the inflammatory response of normal and diseased tissues (Pober and Sessa, 2007).

Epithelial-To-Mesenchymal Transition

The concept of EMT comes from the study of events related to development (Shook and Keller, 2003). Tumor metastasis begins when cancer cells infiltrate from the epithelial layer to adjacent tissues and at least temporarily acquire the EMT phenotype, which enables cancer cells to move and penetrate the basement membrane, invade the tissues, and reach the lymphatics or blood vessels for further spread (Varga and Greten, 2017). Inflammation is an effective cause of EMT in tumors, and the EMT program can also stimulate cancer cells to produce proinflammatory factors. Therefore, inflammation and EMT are inseparable factors in cancer progression (Suarez-Carmona et al., 2017). In the TME, TGF- β , CXCL4/12, IL-6, and TNF- α can enhance EMT. At the same time, tumor cells secrete more epithelial growth factors, fibroblast growth factors, and insulin-like growth factor, which lead to low oxygen, acidity, and high interstitial fluid pressure state in the microenvironment and activates CAFs to produce more matrix metalloproteinases and reshape the tumor ECM (Jung et al., 2015). A previous study found the weighted score of tumor inflammatory signals and the genetic characteristics of EMT can accurately predict the response of lung cancer patients to immune checkpoint blockade (Thompson et al., 2019). In lung cancer cells, erlotinib-induced autocrine IL-8 production can induce EMT and trigger the drug resistance of erlotinib through the p38MAP kinase pathway (Fernando et al., 2016).

Anti-apoptosis

Apoptosis is the most common form of programmed cell death in vertebrates and one of the key determinants in regulating the efficiency of tumor metastasis. It is generally considered to be an important mechanism for negative regulation of cancer development. Apoptotic pathways include external apoptotic pathways (dependent on death receptors) and internal apoptotic pathways (dependent on mitochondria). The intrinsic pathway is closely regulated by the intracellular protein Bcl-2 family. The exogenous apoptosis pathway is initiated by the binding of ligands (Fas-related death domains) to death receptors (death-inducing signal complexes) that contain intracellular death domains. Intrinsic pathways are activated by physical or chemical stimuli, such as hypoxia, growth factor deprivation, cell detachment, or stress signals (Millimouno et al., 2014).

Toshiko et al. found that granatin A and granatin B, ellagitannins isolated from pomegranate leaves, and geraniin, their structural analog, could selectively suppress mPGES-1 expression without affecting COX-2 in non-small

cell lung carcinoma A549 cells (**Figure 5**). The ellagitannins also downregulated TNF- α , inducible nitric oxide synthase, and antiapoptotic factor Bcl-2, and induced A549 cells to undergo apoptosis (Toda et al., 2020). Padwad et al. found that berberine can induce dose-dependent resting and apoptosis of A549 cancer cells by regulating cyclin and inflammation independent of the mTOR pathway (Kumar et al., 2020). The IL-33/ST2 axis can modify the TME to support malignant proliferation or enhance anti-tumor immunity by recruiting immune cells. It is also responsible for the release of NF- κ B, thus increasing the expression of GLUT1 in NSCLC. The administration of anti-IL-33 and anti-ST2 drugs effectively limit this process and reduce the presence of Treg cells in cancer sites (Wang K. et al., 2017).

PROGRESS IN THE TREATMENT OF LUNG CANCER BASED ON INFLAMMATION AND INFLAMMATORY MICROENVIRONMENT

The treatment of lung cancer has developed from specific cytotoxic drugs to more specific molecular targeted drugs. Although great progress has been made in the treatment of lung cancer with the development of targeted therapy and immune therapy, the 5-years survival rate of NSCLC is still about 15%, and most lung cancer patients do not show targeted gene mutations (Gettinger et al., 2018). Traditional surgery, radiotherapy, and chemotherapy are still the only treatment options for most advanced NSCLC patients, but these treatments are unsatisfactory (Choi et al., 2010). Consequently, more and more studies have begun to investigate lung cancer from the perspective of the TME, especially inflammation; actively explore targets related to anti-angiogenesis, immune regulation, and EMT in the microenvironment; and develop more therapeutic targets (Blumenschein, 2012). For example, Logsdon et al. found that in the presence of carcinogenic Ras, inflammatory stimulation initiates a positive feedback loop involving NF- κ B, which further amplifies the activity of Ras to the pathological level (**Figure 6**). The effect of these inflammatory stimuli can be blocked through the deletion of NF- κ B kinase 2 inhibitor or the inhibition of COX-2. Because a large number of lung cancer patients have Ras gene mutations, blocking this positive feedback loop may be an important strategy for cancer prevention (Daniluk et al., 2012).

Epidemiological research and meta-analysis showed that long-term use of aspirin, a non-steroidal anti-inflammatory drug (NSAID), can reduce the risk of various solid tumors including lung cancer, and taking NSAIDs every day for 1 or 2 years can reduce the relative risk of lung cancer by 60–68% (Smith et al., 2006). The chemoprevention characteristics of the long-term use of NSAIDs are based on their cyclooxygenase inhibitory activity, and the ability to inhibit COX-1 and COX-2 is the basis of NSAIDs' chemoprevention mechanism. In some cancers (e.g., NSCLC), the overexpression of COX-2 is associated with

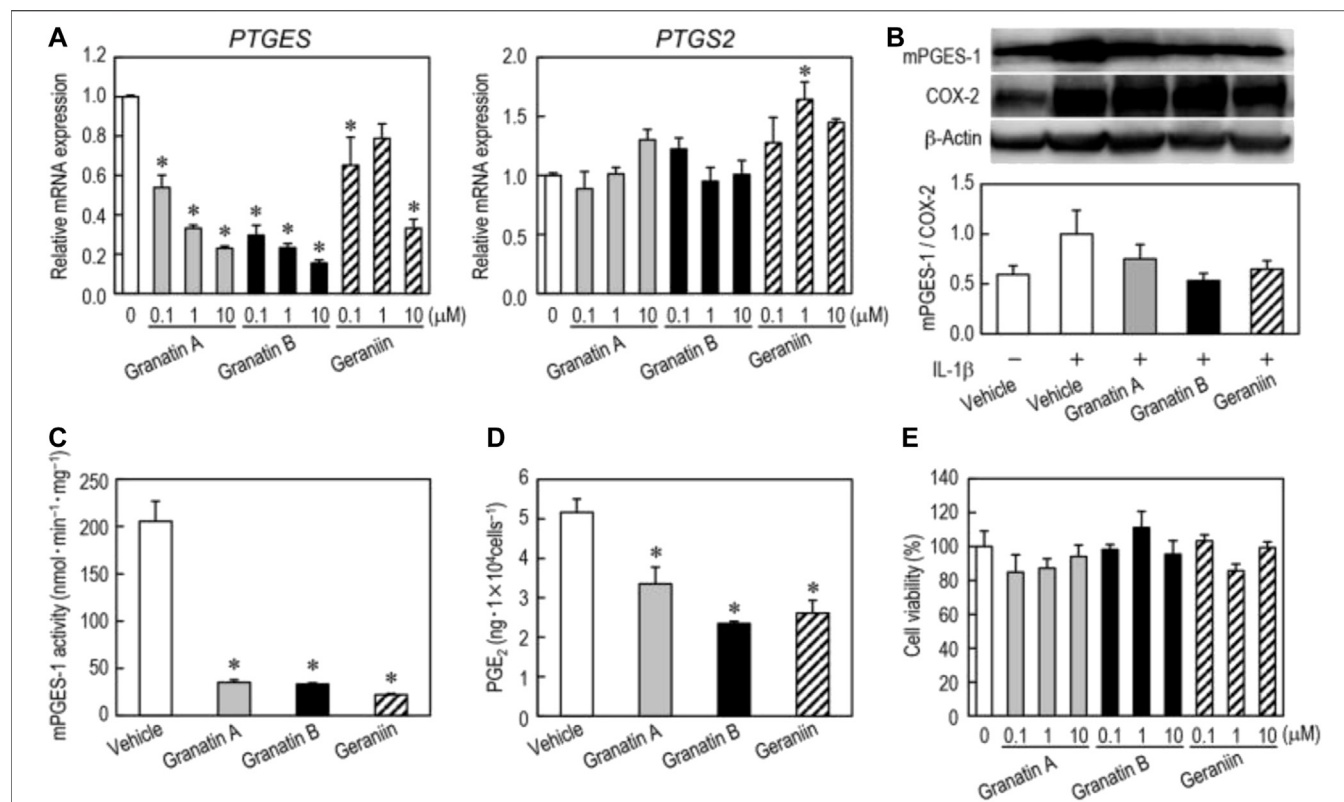


FIGURE 5 | Effects of granatin A, granatin B, and geraniin on mPGES-1 and COX-2 expression. Changes in mRNA and protein levels of mPGES-1 and COX-2 by treatment with granatin A, granatin B, and geraniin were analyzed by real-time PCR and western blotting. Reproduced from Toda et al., 2020 with permission from Taylor and Francis Ltd. Copyright 2019.

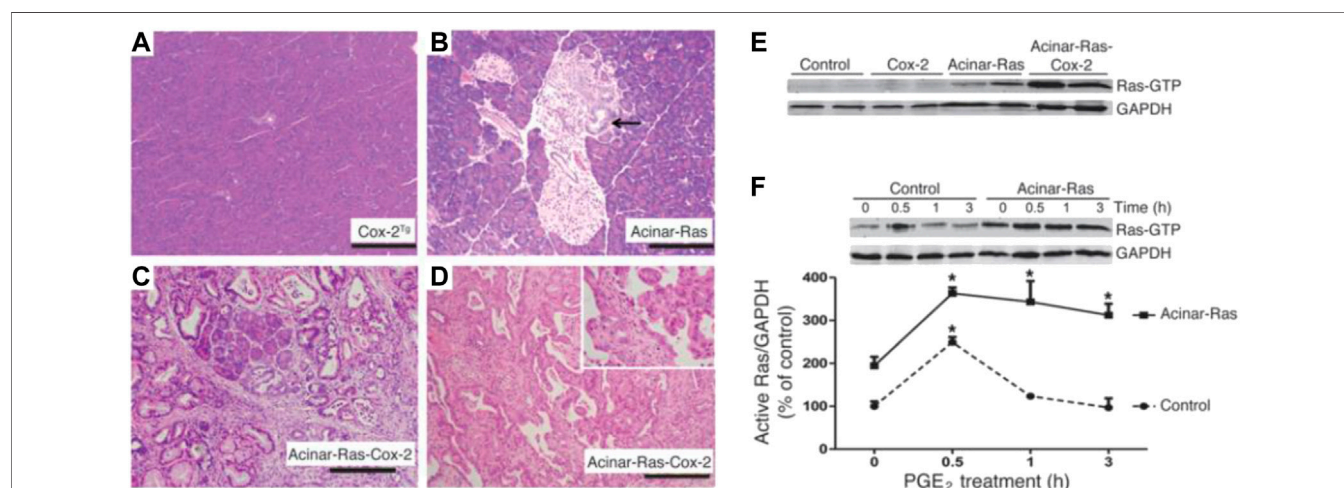


FIGURE 6 | COX-2 and oncogenic K-Ras synergized to promote the development of chronic inflammation and cancer. Reproduced from Daniluk et al., 2012 with permission from JCI. Copyright 2012.

poor prognosis (Lee et al., 2008). COX-2 is closely related to apoptosis resistance, angiogenesis, decreased host immune function, invasion, and metastasis and plays a key role in the occurrence and development of tumors. However, many

NSAIDs, especially those that selectively inhibit COX-2, can cause life-threatening adverse effects such as gastric ulcers, heart attacks, and stroke in a number of patients (Singh et al., 2019).

FUTURE OUTLOOK AND CONCLUSION

Signal molecules in the inflammatory microenvironment have extensive effects on the maintenance and development of lung cancer. More and more animal and human experiments have revealed that lung cancer can be regulated by interfering with inflammation and inflammatory signal pathway. The in-depth understanding of the molecular mechanisms of inflammatory cells and tumor growth, angiogenesis, and progression in the TME will help to identify new therapeutic targets and design new drugs without serious side effects. It will also help promote the development of anti-tumor vaccines and other therapeutic strategies.

REFERENCES

- Akca, H., Tani, M., Hishida, T., Matsumoto, S., and Yokota, J. (2006). Activation of the AKT and STAT3 Pathways and Prolonged Survival by a Mutant EGFR in Human Lung Cancer Cells. *Lung Cancer* 54 (1), 25–33. doi:10.1016/j.lungcan.2006.06.007
- Apte, R. N., Krelm, Y., Song, X., Dotan, S., Recih, E., Elkabets, M., et al. (2006). Effects of Micro-environment- and Malignant Cell-Derived Interleukin-1 in Carcinogenesis, Tumour Invasiveness and Tumour-Host Interactions. *Eur. J. Cancer* 42 (6), 751–759. doi:10.1016/j.ejca.2006.01.010
- Azad, N., Rojanasakul, Y., and Vallyathan, V. (2008). Inflammation and Lung Cancer: Roles of Reactive Oxygen/nitrogen Species. *J. Toxicol. Environ. Health B* 11 (1), 1–15. doi:10.1080/10937400701436460
- Balkwill, F. (2002). Tumor Necrosis Factor or Tumor Promoting Factor?. *Cytokine Growth Factor Rev.* 13 (2), 135–141. doi:10.1016/s1359-6101(01)00020-x
- Barta, J. A., Powell, C. A., and Wisnivesky, J. P. (2019). Global Epidemiology of Lung Cancer. *Ann. Glob. Health* 85 (1), 8. doi:10.5334/aogh.2419
- Ben-Baruch, A. (2006). The Multifaceted Roles of Chemokines in Malignancy. *Cancer Metastasis Rev.* 25 (3), 357–371. doi:10.1007/s10555-006-9003-5
- Bent, R., Moll, L., Grabbe, S., and Bros, M. (2018). Interleukin-1 β -A Friend or Foe in Malignancies?. *Int. J. Mol. Sci.* 19 (8), 2155. doi:10.3390/ijms19082155
- Bianconi, V., Sahebkar, A., Atkin, S. L., and Pirro, M. (2018). The Regulation and Importance of Monocyte Chemoattractant Protein-1. *Curr. Opin. Hematol.* 25 (1), 44–51. doi:10.1097/moh.0000000000000389
- Billmeier, U., Dieterich, W., Neurath, M. F., and Atreya, R. (2016). Molecular Mechanism of Action of Anti-tumor Necrosis Factor Antibodies in Inflammatory Bowel Diseases. *World J Gastroenterol.* 22, 9300–9313. doi:10.3748/wjg.v22.i42.9300
- Blumenschein, G. R. (2012). Developmental Antiangiogenic Agents for the Treatment of Non-small Cell Lung Cancer (NSCLC). *Invest. New Drugs* 30 (4), 1802–1811. doi:10.1007/s10637-011-9750-1
- Bremnes, R. M., Al-Shibli, K., Donnem, T., Sirera, R., Al-Saad, S., Andersen, S., et al. (2011). The Role of Tumor-Infiltrating Immune Cells and Chronic Inflammation at the Tumor Site on Cancer Development, Progression, and Prognosis: Emphasis on Non-small Cell Lung Cancer. *J. Thorac. Oncol.* 6 (4), 824–833. doi:10.1097/jto.0b013e3182037b76
- Brenner, D. R., Boffetta, P., Duell, E. J., Bickeböller, H., Rosenberger, A., McCormack, V., et al. (2012). Previous Lung Diseases and Lung Cancer Risk: a Pooled Analysis from the International Lung Cancer Consortium. *Am. J. Epidemiol.* 176 (7), 573–585. doi:10.1093/aje/kws151
- Brown, E. R., Charles, K. A., Hoare, S. A., Rye, R. L., Jodrell, D. I., Aird, R. E., et al. (2008). A Clinical Study Assessing the Tolerability and Biological Effects of Infliximab, a TNF- α Inhibitor, in Patients with Advanced Cancer. *Ann. Oncol.* 19 (7), 1340–1346. doi:10.1093/annonc/mdn054
- Bruno, A., Focaccetti, C., Pagani, A., Imperatori, A. S., Spagnoletti, M., Rotolo, N., et al. (2013). The Proangiogenic Phenotype of Natural Killer Cells in Patients with Non-small Cell Lung Cancer. *Neoplasia* 15 (2), 133–IN7. doi:10.1593/neo.121758
- Burnet, M. (1970). Introductory Conspectus. *Prog. Exp. Tumor Res.* 13, 1–28. doi:10.1016/b978-0-08-017481-5.50005-5
- Caetano, M. S., Zhang, H., Cumpian, A. M., Gong, L., Unver, N., Ostrin, E. J., et al. (2016). IL6 Blockade Reprograms the Lung Tumor Microenvironment to Limit the Development and Progression of K-Ras-Mutant Lung Cancer. *Cancer Res.* 76 (11), 3189–3199. doi:10.1158/0008-5472.can-15-2840
- Charles, P., Elliott, M. J., Davis, D., Potter, A., Kalden, J. R., Antoni, C., et al. (1999). Regulation of Cytokines, Cytokine Inhibitors, and Acute-phase Proteins Following Anti-TNF- α Therapy in Rheumatoid Arthritis. *J. Immunol.* 163, 1521–1528.
- Chen, G., Qiao, Y., Yao, J., Jiang, Q., Lin, X., Chen, F., et al. (2011). Construction of NF-K β -Targeting RNAi Adenovirus Vector and the Effect of NF-K β Pathway on Proliferation and Apoptosis of Vascular Endothelial Cells. *Mol. Biol. Rep.* 38 (5), 3089–3094. doi:10.1007/s11033-010-9977-5
- Chen, W., Jin, W., Hardegen, N., Lei, K.-j., Li, L., Marinos, N., et al. (2003). Conversion of Peripheral CD4+CD25– Naive T Cells to CD4+CD25+ Regulatory T Cells by TGF- β Induction of Transcription Factor Foxp3. *J. Exp. Med.* 198 (12), 1875–1886. doi:10.1084/jem.20030152
- Chen, W., Li, Z., Bai, L., and Lin, Y. (2011). NF-kappaB in Lung Cancer, a Carcinogenesis Mediator and a Prevention and Therapy Target. *Front. Biosci.* 16, 1172–1185. doi:10.2741/3782
- Choi, Y. L., Soda, M., Yamashita, Y., Ueno, T., Takashima, J., Nakajima, T., et al. (2010). EML4-ALK Mutations in Lung Cancer that Confer Resistance to ALK Inhibitors. *N. Engl. J. Med.* 363 (18), 1734–1739. doi:10.1056/nejmoa1007478
- Conway, E. M., Pikor, L. A., Kung, S. H. Y., Hamilton, M. J., Lam, S., Lam, W. L., et al. (2016). Macrophages, Inflammation, and Lung Cancer. *Am. J. Respir. Crit. Care Med.* 193 (2), 116–130. doi:10.1164/rccm.201508-1545ci
- Coussens, L. M., Zitvogel, L., and Palucka, A. K. (2013). Neutralizing Tumor-Promoting Chronic Inflammation: a Magic Bullet?. *Science* 339 (6117), 286–291. doi:10.1126/science.1232227
- Daniel, D., and Wilson, N. (2008). Tumor Necrosis Factor: Renaissance as a Cancer Therapeutic?. *Curr. Cancer Drug Target.* 8 (2), 124–131. doi:10.2174/15680908783769346
- Daniluk, J., Liu, Y., Deng, D., Chu, J., Huang, H., Gaiser, S., et al. (2012). An NF-K β Pathway-Mediated Positive Feedback Loop Amplifies Ras Activity to Pathological Levels in Mice. *J. Clin. Invest.* 122 (4), 1519–1528. doi:10.1172/jci59743
- Dutta, P., Sabri, N., Li, J., and Li, W. X. (2014). Role of STAT3 in Lung Cancer. *JAKSTAT* 3 (4), e999503. doi:10.1080/21623996.2014.999503
- Eskiler, G. G., Bezdegumeli, E., Ozman, Z., Ozkan, A. D., Bilir, C., Kucukakca, B. N., et al. (2019). IL-6 Mediated JAK/STAT3 Signaling Pathway in Cancer Patients with Cachexia. *Bratisl Lek Listy.* 120 (11), 819–826. doi:10.4149/blil_2019_136
- Fernando, R. I., Hamilton, D. H., Dominguez, C., David, J. M., McCampbell, K. K., and Palena, C. (2016). IL-8 Signaling Is Involved in Resistance of Lung Carcinoma Cells to Erlotinib. *Oncotarget* 7 (27), 42031–42044. doi:10.18632/oncotarget.9662
- Flavell, R. A., Sanjabi, S., Wrzesinski, S. H., and Licona-Limón, P. (2010). The Polarization of Immune Cells in the Tumour Environment by TGF β . *Nat. Rev. Immunol.* 10 (8), 554–567. doi:10.1038/nri2808
- Gandini, S., Botteri, E., Iodice, S., Boniol, M., Lowenfels, A. B., Maisonneuve, P., et al. (2008). Tobacco Smoking and Cancer: a Meta-Analysis. *Int. J. Cancer* 122 (1), 155–164. doi:10.1002/ijc.23033

AUTHOR CONTRIBUTIONS

ZT and YQ initiated the project. ZT, HX, SY, CZ, and YS searched the data base. ZT, HX, and YQ wrote, revised and finalized the manuscript.

FUNDING

This work was supported by Chinese Medicine Science and Technology Development Project of Shandong Province (2019-0091).

- Gettinger, S., Horn, L., Jackman, D., Spigel, D., Antonia, S., Hellmann, M., et al. (2018). Five-year Follow-Up of Nivolumab in Previously Treated Advanced Non-small-cell Lung Cancer: Results from the CA209-003 Study. *J Clin Oncol.* 36 (17), 1675–1684. doi:10.1200/jco.2017.77.0412
- Gomes, M., Teixeira, A. L., Coelho, A., Araújo, A., and Medeiros, R. (2014). *The Role of Inflammation in Lung Cancer*. Porto, Portugal: Springer Basel. doi:10.5772/58252
- Govindan, R., Ding, L., Griffith, M., Subramanian, J., Dees, N. D., Kanchi, K. L., et al. (2012). Genomic Landscape of Non-small Cell Lung Cancer in Smokers and Never-Smokers. *Cell* 150 (6), 1121–1134. doi:10.1016/j.cell.2012.08.024
- Green, L. J., Yamauchi, P. S., and Kircik, L. H. (2019). Comparison of the Safety and Efficacy of Tumor Necrosis Factor Inhibitors and Interleukin-17 Inhibitors in Patients with Psoriasis. *J. Drugs Dermatol.* 18 (8), 776–788.
- Greten, F. R., Eckmann, L., Greten, T. F., Park, J. M., Li, Z.-W., Egan, L. J., et al. (2004). IKK β Links Inflammation and Tumorigenesis in a Mouse Model of Colitis-Associated Cancer. *Cell* 118 (3), 285–296. doi:10.1016/j.cell.2004.07.013
- Greten, F. R., and Grivnickov, S. I. (2019). Inflammation and Cancer: Triggers, Mechanisms, and Consequences. *Immunity* 51 (1), 27–41. doi:10.1016/j.immuni.2019.06.025
- Grivnickov, S. I., and Karin, M. (2010). Dangerous Liaisons: STAT3 and NF-Kb Collaboration and Crosstalk in Cancer. *Cytokine Growth Factor. Rev.* 21 (1), 11–19. doi:10.1016/j.cytogfr.2009.11.005
- Gutschalk, C. M., Yanamandra, A. K., Linde, N., Meides, A., Depner, S., and Mueller, M. M. (2013). GM-CSF Enhances Tumor Invasion by Elevated MMP -2, -9, and -26 Expression. *Cancer Med.* 2 (2), 117–129. doi:10.1002/cam4.20
- Hagemann, T., Lawrence, T., Mcneish, I., Charles, K. A., Kulbe, H., Thompson, R. G., et al. (2008). "Re-educating" Tumor-Associated Macrophages by Targeting NF-Kb. *J. Exp. Med.* 205 (6), 1261–1268. doi:10.1084/jem.20080108
- Hanahan, D., and Coussens, L. M. (2012). Accessories to the Crime: Functions of Cells Recruited to the Tumor Microenvironment. *Cancer Cell* 21 (3), 309–322. doi:10.1016/j.ccr.2012.02.022
- Hanahan, D., and Weinberg, R. A. (2011). Hallmarks of Cancer: the Next Generation. *Cell* 144 (5), 646–674. doi:10.1016/j.cell.2011.02.013
- Hao, Y., Baker, D., and Ten Dijke, P. (2019). TGF- β -Mediated Epithelial-Mesenchymal Transition and Cancer Metastasis. *Int. J. Mol. Sci.* 20 (11), 2767. doi:10.3390/ijms20112767
- Hasegawa, Y., Takanashi, S., Kanehira, Y., Tsushima, T., Imai, T., and Okumura, K. (2001). Transforming Growth Factor- β Level Correlates with Angiogenesis, Tumor Progression, and Prognosis in Patients with Nonsmall Cell Lung Carcinoma. *Cancer* 91 (5), 964–971. doi:10.1002/1097-0142(20010301)91:5<964:aid-cncl1086>3.0.co;2-o
- Heinrich, E. L., Walsler, T. C., Krysan, K., Liclican, E. L., Grant, J. L., Rodriguez, N. L., et al. (2012). The Inflammatory Tumor Microenvironment, Epithelial Mesenchymal Transition and Lung Carcinogenesis. *Cancer Microenvironment* 5 (1), 5–18. doi:10.1007/s12307-011-0089-0
- Helson, L., Green, S., Carswell, E., and Old, L. J. (1975). Effect of Tumour Necrosis Factor on Cultured Human Melanoma Cells. *Nature* 258 (5537), 731–732. doi:10.1038/258731a0
- Houghton, A. M. (2013). Mechanistic Links between COPD and Lung Cancer. *Nat. Rev. Cancer* 13 (4), 233–245. doi:10.1038/nrc3477
- Huang, X., Ding, L., Liu, X., Tong, R., Ding, J., Qian, Z., et al. (2021). Regulation of Tumor Microenvironment for Pancreatic Cancer Therapy. *Biomaterials* 270, 120680. doi:10.1016/j.biomaterials.2021.120680
- Jiang, Z. Y., Feng, X. R., Xu, W. G., and Zhuang, X. L., Ding, J. X., and Chen, X. S. (2020). Calcium Phosphate-Cured Nanocluster of Poly(L-Glutamic Acid)-Cisplatin and Arsenic Trioxide for Synergistic Chemotherapy of Peritoneal Metastasis of Ovarian Cancer. *Acta Polymerica Sinica* 51 (8), 901–910.
- Jin, S., Mutvei, A. P., Chivukula, I. V., Andersson, E. R., Ramsköld, D., Sandberg, R., et al. (2013). Non-canonical Notch Signaling Activates IL-6/JAK/STAT Signaling in Breast Tumor Cells and Is Controlled by P53 and IKK α /IKK β . *Oncogene* 32 (41), 4892–4902. doi:10.1038/onc.2012.517
- Johnson, T. S., and Munn, D. H. (2012). Host Indoleamine 2,3-dioxygenase: Contribution to Systemic Acquired Tumor Tolerance. *Immunol. Invest.* 41 (6–7), 765–797. doi:10.3109/08820139.2012.689405
- Jung, H.-Y., Fattet, L., and Yang, J. (2015). Molecular Pathways: Linking Tumor Microenvironment to Epithelial-Mesenchymal Transition in Metastasis. *Clin. Cancer Res.* 21 (5), 962–968. doi:10.1158/1078-0432.ccr-13-1373
- Karin, M., Cao, Y., Greten, F. R., and Li, Z.-W. (2002). NF- κ B in Cancer: from Innocent Bystander to Major Culprit. *Nat. Rev. Cancer* 2 (4), 301–310. doi:10.1038/nrc780
- Kim, J.-W., Koh, Y., Kim, D.-W., Ahn, Y.-O., Kim, T. M., Han, S.-W., et al. (2013). Clinical Implications of VEGF, TGF- β 1, and IL-1 β in Patients with Advanced Non-small Cell Lung Cancer. *Cancer Res. Treat.* 45 (4), 325–333. doi:10.4143/crt.2013.45.4.325
- Kitamura, T., Qian, B.-Z., and Pollard, J. W. (2015). Immune Cell Promotion of Metastasis. *Nat. Rev. Immunol.* 15 (2), 73–86. doi:10.1038/nri3789
- Kumar, R., Awasthi, M., Sharma, A., Padwad, Y., and Sharma, R. (2020). Berberine Induces Dose-dependent Quiescence and Apoptosis in A549 Cancer Cells by Modulating Cell Cyclins and Inflammation Independent of mTOR Pathway. *Life Sci.* 244, 117346. doi:10.1016/j.lfs.2020.117346
- Kundu, J. K., and Surh, Y. J. (2008). Inflammation: Gearing the Journey to Cancer. *Mutat. Res.* 659 (1–2), 15–30. doi:10.1016/j.mrrev.2008.03.002
- Lee, J. M., Yanagawa, J., Peebles, K. A., Sharma, S., Mao, J. T., and Dubinett, S. M. (2008). Inflammation in Lung Carcinogenesis: New Targets for Lung Cancer Chemoprevention and Treatment. *Crit. Rev. Oncology/Hematology* 66 (3), 208–217. doi:10.1016/j.critrevonc.2008.01.004
- Lee, M. K., Park, J. H., Gi, S. H., and Hwang, Y. S. (2018). IL-1 β Induces Fascin Expression and Increases Cancer Invasion. *Anticancer Res.* 38 (11), 6127–6132. doi:10.21873/anticancer.12964
- Lin, Y., Bai, L., Chen, W., and Xu, S. (2010). The NF-Kb Activation Pathways, Emerging Molecular Targets for Cancer Prevention and Therapy. *Expert Opin. Ther. Targets* 14 (1), 45–55. doi:10.1517/14728220903431069
- Liu, J., Li, Z., Zhao, D., Feng, X., Wang, C., Li, D., et al. (2021). Immunogenic Cell Death-Inducing Chemotherapeutic Nanoformulations Potentiate Combination Chemoimmunotherapy. *Mater. Des.* 202, 109465. doi:10.1016/j.matdes.2021.109465
- Looyenga, B. D., Hutchings, D., Cherni, I., Kingsley, C., and Weiss, C. G. and Mackeigan, J. P. (2012). STAT3 Is Activated by JAK2 Independent of Key Oncogenic Driver Mutations in Non-small Cell Lung Carcinoma. *PLoS One* 7 (2), e30820. doi:10.1371/journal.pone.0030820
- Lord, E. M., Penney, D. P., Sutherland, R. M., and Cooper, R. A., Jr. (1979). Morphological and Functional Characteristics of Cells Infiltrating and Destroying Tumor Multicellular Spheroids In Vivo. *Virchows Arch. B Cell Pathol Incl Mol Pathol.* 31 (2), 103–116. doi:10.1007/bf02889928
- Madhusudan, S., Foster, M., Muthuramalingam, S. R., Braybrooke, J. P., Wilner, S., Kaur, K., et al. (2004). A Phase II Study of Etencept (Enbrel), a Tumor Necrosis Factor α Inhibitor in Patients with Metastatic Breast Cancer. *Clin. Cancer Res.* 10 (19), 6528–6534. doi:10.1158/1078-0432.ccr-04-0730
- Mantovani, A., Barajon, I., and Garlanda, C. (2018). IL-1 and IL-1 Regulatory Pathways in Cancer Progression and Therapy. *Immunol. Rev.* 281 (1), 57–61. doi:10.1111/imr.12614
- Mantovani, A., Sozzani, S., Locati, M., Allavena, P., and Sica, A. (2002). Macrophage Polarization: Tumor-Associated Macrophages as a Paradigm for Polarized M2 Mononuclear Phagocytes. *Trends Immunol.* 23 (11), 549–555. doi:10.1016/s1471-4906(02)02302-5
- Millimouno, F. M., Dong, J., Yang, L., Li, J., and Li, X. (2014). Targeting Apoptosis Pathways in Cancer and Perspectives with Natural Compounds from Mother Nature. *Cancer Prev. Res.* 7 (11), 1081–1107. doi:10.1158/1940-6207.capr-14-0136
- Mizuno, R., Kawada, K., and Sakai, Y. (2019). Prostaglandin E2/EP Signaling in the Tumor Microenvironment of Colorectal Cancer. *Int. J. Mol. Sci.* 20 (24), 6254. doi:10.3390/ijms20246254
- Mulholland, B. S., Forwood, M. R., and Morrison, N. A. (2019). Monocyte Chemoattractant Protein-1 (MCP-1/CCL2) Drives Activation of Bone Remodelling and Skeletal Metastasis. *Curr. Osteoporos. Rep.* 17 (6), 538–547. doi:10.1007/s11914-019-00545-7
- Nakao, S., Noda, K., Zandi, S., Sun, D., Taher, M., Schering, A., et al. (2011). VAP-1-Mediated M2 Macrophage Infiltration Underlies IL-1 β - but Not VEGF-A-Induced Lymph- and Angiogenesis. *Am. J. Pathol.* 178 (4), 1913–1921. doi:10.1016/j.ajpath.2011.01.011
- Namazi, A., Forat-Yazdi, M., Jafari, M., Farahnak, S., Nasiri, R., Foroughi, E., et al. (2018). Association of Interleukin-10 -1082 A/g (Rs1800896) Polymorphism with Susceptibility to Gastric Cancer: Meta-Analysis of 6,101 Cases and 8,557 Controls. *Arq. Gastroenterol.* 55 (1), 33–40. doi:10.1590/s0004-2803.201800000-18

- Piotrowski, I., Kulcenty, K., and Suchorska, W. (2020). Interplay between Inflammation and Cancer. *Rep. Pract. Oncol. Radiother.* 25 (3), 422–427. doi:10.1016/j.rpor.2020.04.004
- Pober, J. S., and Sessa, W. C. (2007). Evolving Functions of Endothelial Cells in Inflammation. *Nat. Rev. Immunol.* 7 (10), 803–815. doi:10.1038/nri2171
- Rebouissou, S., Amessou, M., Couchy, G., Poussin, K., Imbeaud, S., Pilati, C., et al. (2009). Frequent In-Frame Somatic Deletions Activate Gp130 in Inflammatory Hepatocellular Tumours. *Nature* 457 (7226), 200–204. doi:10.1038/nature07475
- Rius, J., Guma, M., Schachtrup, C., Akassoglou, K., Zinkernagel, A. S., Nizet, V., et al. (2008). NF- κ B Links Innate Immunity to the Hypoxic Response through Transcriptional Regulation of HIF-1 α . *Nature* 453 (7196), 807–811. doi:10.1038/nature06905
- Rivas-Fuentes, S., Salgado-Aguayo, A., Pertuz Belloso, S., Gorocica Rosete, P., Alvarado-Vásquez, N., and Aquino-Jarquín, G. (2015). Role of Chemokines in Non-small Cell Lung Cancer: Angiogenesis and Inflammation. *J. Cancer* 6 (10), 938–952. doi:10.7150/jca.12286
- Saito, A., Horie, M., and Nagase, T. (2018). TGF- β Signaling in Lung Health and Disease. *Int J Mol Sci.* 19 (8), 2460. doi:10.3390/ijms19082460
- Semenza, G. L. (2010). Defining the Role of Hypoxia-Inducible Factor 1 in Cancer Biology and Therapeutics. *Oncogene* 29 (5), 625–634. doi:10.1038/onc.2009.441
- Shojaei, F., Wu, X., Zhong, C., Yu, L., Liang, X.-H., Yao, J., et al. (2007). Bv8 Regulates Myeloid-cell-dependent Tumour Angiogenesis. *Nature* 450 (7171), 825–831. doi:10.1038/nature06348
- Shook, D., and Keller, R. (2003). Mechanisms, Mechanics and Function of Epithelial-Mesenchymal Transitions in Early Development. *Mech. Develop.* 120 (11), 1351–1383. doi:10.1016/j.mod.2003.06.005
- Singh, N., Baby, D., Rajguru, J., Patil, P., Thakkannavar, S., and Pujari, V. (2019). Inflammation and Cancer. *Ann. Afr. Med.* 18 (3), 121–126. doi:10.4103/aam.aam_56_18
- Siveen, K. S., Sikka, S., Surana, R., Dai, X., Zhang, J., Kumar, A. P., et al. (2014). Targeting the STAT3 Signaling Pathway in Cancer: Role of Synthetic and Natural Inhibitors. *Biochim. Biophys. Acta (Bba) - Rev. Cancer* 1845 (2), 136–154. doi:10.1016/j.bbcan.2013.12.005
- Smith, C. J., Perfetti, T. A., and King, J. A. (2006). Perspectives on Pulmonary Inflammation and Lung Cancer Risk in Cigarette Smokers. *Inhalation Toxicol.* 18 (9), 667–677. doi:10.1080/08958370600742821
- Song, J., Xu, B. B., Yao, H., Lu, X., Tan, Y., Wang, B., et al. (2021). Schiff-linked PEGylated Doxorubicin Prodrug Forming pH-Responsive Nanoparticles with High Drug Loading and Effective Anticancer Therapy. *Front. Oncol.* 11, 656717. doi:10.3389/fonc.2021.656717
- Song, L., Rawal, B., Nemeth, J. A., and Haura, E. B. (2011). JAK1 Activates STAT3 Activity in Non-small-cell Lung Cancer Cells and IL-6 Neutralizing Antibodies Can Suppress JAK1-STAT3 Signaling. *Mol. Cancer Ther.* 10 (3), 481–494. doi:10.1158/1535-7163.mct-10-0502
- Stathopoulos, G. T., Kollintza, A., Moschos, C., Psallidas, I., Sherrill, T. P., Pitsinos, E. N., et al. (2007). Tumor Necrosis Factor- α Promotes Malignant Pleural Effusion. *Cancer Res.* 67 (20), 9825–9834. doi:10.1158/0008-5472.can-07-1064
- Steel, J. L., Terhorst, L., Collins, K. P., Geller, D. A., Vodovotz, Y., Kim, J., et al. (2018). Prospective Analyses of Cytokine Mediation of Sleep and Survival in the Context of Advanced Cancer. *Psychosom Med.* 80 (5), 483–491. doi:10.1097/psy.0000000000000579
- Sterlacci, W., Wolf, D., Savic, S., Hilbe, W., Schmid, T., Jamnig, H., et al. (2012). High Transforming Growth Factor β Expression Represents an Important Prognostic Parameter for Surgically Resected Non-small Cell Lung Cancer. *Hum. Pathol.* 43 (3), 339–349. doi:10.1016/j.humpath.2011.05.017
- Suarez-Carmona, M., Lesage, J., Cataldo, D., and Gilles, C. (2017). EMT and Inflammation: Inseparable Actors of Cancer Progression. *Mol. Oncol.* 11 (7), 805–823. doi:10.1002/1878-0261.12095
- Tauriello, D. V. F., Palomo-Ponce, S., Stork, D., Berenguer-Llgero, A., Badiarmentol, J., Iglesias, M., et al. (2018). TGF β Drives Immune Evasion in Genetically Reconstituted Colon Cancer Metastasis. *Nature* 554 (7693), 538–543. doi:10.1038/nature25492
- Teixeira, A. L., Araújo, A., Coelho, A., Ribeiro, R., Gomes, M., Pereira, C., et al. (2011). Influence of TGF β 1+869T>C Functional Polymorphism in Non-small Cell Lung Cancer (NSCLC) Risk. *J. Cancer Res. Clin. Oncol.* 137 (3), 435–439. doi:10.1007/s00432-010-0896-6
- Thompson, J. C., Hwang, W. T., Davis, C., Deshpande, C., Jeffries, S., Rajpurohit, Y., et al. (2019). Gene Signatures of Tumor Inflammation and Epithelial-To-Mesenchymal Transition (EMT) Predict Responses to Immune Checkpoint Blockade in Lung Cancer with High Accuracy. *Lung Cancer* 139, 1–8. doi:10.1016/j.lungcan.2019.10.012
- Toda, K., Ueyama, M., Tanaka, S., Tsukayama, I., Mega, T., Konoike, Y., et al. (2020). Ellagitannins from Punica Granatum Leaves Suppress Microsomal Prostaglandin E Synthase-1 Expression and Induce Lung Cancer Cells to Undergo Apoptosis. *Biosci. Biotechnol. Biochem.* 84 (4), 757–763. doi:10.1080/09168451.2019.1706442
- Tracey, D., Klareskog, L., Sasso, E. H., Salfeld, J. G., and Tak, P. P. (2008). Tumor Necrosis Factor Antagonist Mechanisms of Action: a Comprehensive Review. *Pharmacol. Ther.* 117 (2), 244–279. doi:10.1016/j.pharmthera.2007.10.001
- Vahl, J. M., Friedrich, J., Mittler, S., Trump, S., Heim, L., Kachler, K., et al. (2017). Interleukin-10-regulated Tumour Tolerance in Non-small Cell Lung Cancer. *Br. J. Cancer* 117 (11), 1644–1655. doi:10.1038/bjc.2017.336
- Valavanidis, A., Vlachogianni, T., Fiotakis, K., and Loidas, S. (2013). Pulmonary Oxidative Stress, Inflammation and Cancer: Respirable Particulate Matter, Fibrous Dusts and Ozone as Major Causes of Lung Carcinogenesis through Reactive Oxygen Species Mechanisms. *Int J Environ Res Public Health.* 10 (9), 3886–3907. doi:10.3390/ijerph10093886
- Varga, J., and Greten, F. R. (2017). Cell Plasticity in Epithelial Homeostasis and Tumorigenesis. *Nat. Cell Biol.* 19 (10), 1133–1141. doi:10.1038/ncb3611
- Wang, H., Zhang, Q., Kong, H., Zeng, Y., Hao, M., Yu, T., et al. (2014). Monocyte Chemotactic Protein-1 Expression as a Prognostic Biomarker in Patients with Solid Tumor: a Meta Analysis. *Int. J. Clin. Exp. Pathol.* 7 (7), 3876–3886.
- Wang, K., Shan, S., Yang, Z., Gu, X., Wang, Y., Wang, C., et al. (2017). IL-33 Blockade Suppresses Tumor Growth of Human Lung Cancer through Direct and Indirect Pathways in a Preclinical Model. *Oncotarget* 8 (40), 68571–68582. doi:10.18632/oncotarget.19786
- Wang, L., Cao, L., Wang, H., Liu, B., Zhang, Q., Meng, Z., et al. (2017). Cancer-associated Fibroblasts Enhance Metastatic Potential of Lung Cancer Cells through IL-6/STAT3 Signaling Pathway. *Oncotarget* 8 (44), 76116–76128. doi:10.18632/oncotarget.18814
- Wang, R., Lu, M., Zhang, J., Chen, S., Luo, X., Qin, Y., et al. (2011). Increased IL-10 mRNA Expression in Tumor-Associated Macrophage Correlated with Late Stage of Lung Cancer. *J. Exp. Clin. Cancer Res.* 30 (1), 62. doi:10.1186/1756-9966-30-62
- Wang, X., Yang, Y., Zhuang, Y., Gao, P., Yang, F., Shen, H., et al. Fabrication of pH-Responsive Nanoparticles with an Aie Feature for Imaging Intracellular Drug Delivery. *Biomacromolecules*, 2016, 17, 2920–2929. doi:10.1021/acs.biomac.6b00744
- Wang, Y., Huang, D., Wang, X., Yang, F., Shen, H., and Wu, D. (2019). Fabrication of Zwitterionic and pH-Responsive Polyacetal Dendrimers for Anticancer Drug Delivery. *Biomater. Sci.* 7, 3238–3248. doi:10.1039/c9bm00606k
- Weichand, B., Popp, R., Dziubla, S., Mora, J., Strack, E., Elwakeel, E., et al. (2017). S1PR1 on Tumor-Associated Macrophages Promotes Lymphangiogenesis and Metastasis via NLRP3/IL-1 β . *J. Exp. Med.* 214 (9), 2695–2713. doi:10.1084/jem.20160392
- Yamaji, H., Iizasa, T., Koh, E., Suzuki, M., Otsuji, M., Chang, H., et al. (2004). Correlation between Interleukin 6 Production and Tumor Proliferation in Non-small Cell Lung Cancer. *Cancer Immunol. Immunother.* 53 (9), 786–792. doi:10.1007/s00262-004-0533-9
- Yao, X., Huang, J., Zhong, H., Shen, N., Faggioni, R., Fung, M., et al. (2014). Targeting Interleukin-6 in Inflammatory Autoimmune Diseases and Cancers. *Pharmacol. Ther.* 141 (2), 125–139. doi:10.1016/j.pharmthera.2013.09.004
- Ye, X., Tam, W. L., Shibue, T., Kaygusuz, Y., Reinhardt, F., Ng Eaton, E., et al. (2015). Distinct EMT Programs Control Normal Mammary Stem Cells and Tumour-Initiating Cells. *Nature* 525 (7568), 256–260. doi:10.1038/nature14897
- Yoo, Y.-G., Christensen, J., and Huang, L. E. (2011). HIF-1 α Confers Aggressive Malignant Traits on Human Tumor Cells Independent of its Canonical Transcriptional Function. *Cancer Res.* 71 (4), 1244–1252. doi:10.1158/0008-5472.can.10-2360
- Yoshimura, T. (2017). The Production of Monocyte Chemoattractant Protein-1 (MCP-1)/CCL2 in Tumor Microenvironments. *Cytokine* 98, 71–78. doi:10.1016/j.cyto.2017.02.001

- You, S., Li, R., Park, D., Xie, M., Sica, G. L., Cao, Y., et al. (2014). Disruption of STAT3 by Niclosamide Reverses Radioresistance of Human Lung Cancer. *Mol. Cancer Ther.* 13 (3), 606–616. doi:10.1158/1535-7163.mct-13-0608
- Yu, H., and Jove, R. (2004). The STATs of Cancer - New Molecular Targets Come of Age. *Nat. Rev. Cancer* 4 (2), 97–105. doi:10.1038/nrc1275
- Yu, H., Lee, H., Herrmann, A., Buettner, R., and Jove, R. (2014). Revisiting STAT3 Signalling in Cancer: New and Unexpected Biological Functions. *Nat. Rev. Cancer* 14 (11), 736–746. doi:10.1038/nrc3818
- Yu, H., Pardoll, D., and Jove, R. (2009). STATs in Cancer Inflammation and Immunity: a Leading Role for STAT3. *Nat. Rev. Cancer* 9 (11), 798–809. doi:10.1038/nrc2734
- Zeni, E., Mazzetti, L., Miotto, D., Lo Cascio, N., Maestrelli, P., Querzoli, P., et al. (2007). Macrophage Expression of Interleukin-10 Is a Prognostic Factor in Nonsmall Cell Lung Cancer. *Eur. Respir. J.* 30 (4), 627–632. doi:10.1183/09031936.00129306
- Zheng, P., Ding, B., Jiang, Z., Xu, W., Li, G., Ding, J., et al. (2021). Ultrasound-augmented Mitochondrial Calcium Ion Overload by Calcium Nanomodulator to Induce Immunogenic Cell Death. *Nano Lett.* 21 (5), 2088–2093. doi:10.1021/acs.nanolett.0c04778
- Zheng, P., Liu, Y., Chen, J., Xu, W., Li, G., and Ding, J. (2020). Targeted pH-Responsive Polyion Complex Micelle for Controlled Intracellular Drug Delivery. *Chin. Chem. Lett.* 31 (5), 1178–1182. doi:10.1016/j.cclet.2019.12.001

Conflict of Interest: The authors declare that the research was conducted in the absence of any commercial or financial relationships that could be construed as a potential conflict of interest.

Copyright © 2021 Tan, Xue, Sun, Zhang, Song and Qi. This is an open-access article distributed under the terms of the Creative Commons Attribution License (CC BY). The use, distribution or reproduction in other forums is permitted, provided the original author(s) and the copyright owner(s) are credited and that the original publication in this journal is cited, in accordance with accepted academic practice. No use, distribution or reproduction is permitted which does not comply with these terms.



Targeting Mutated p53 Dependency in Triple-Negative Breast Cancer Cells Through CDK7 Inhibition

Jingyu Peng^{1,2}, Ming Yang^{1*}, Ran Bi^{2,3}, Yueyuan Wang^{1,2}, Chunxi Wang³, Xue Wei¹, Zhihao Zhang¹, Xiao Xie¹ and Wei Wei^{2*}

¹ Department of Breast Surgery, The First Hospital of Jilin University, Changchun, China, ² Key Laboratory of Organ Regeneration & Transplantation of the Ministry of Education, Institute of Translational Medicine, The First Hospital of Jilin University, Changchun, China, ³ Department of Urology, The First Hospital of Jilin University, Changchun, China

OPEN ACCESS

Edited by:

Sanjun Shi,
Chengdu University of Traditional
Chinese Medicine, China

Reviewed by:

Qiyang Shou,
Zhejiang Chinese
Medical University, China
Hebao Yuan,
University of Michigan,
United States
Mingqiang Li,
Sun Yat-Sen University, China
Di Li,
Changchun Institute of Applied
Chemistry (CAS), China

*Correspondence:

Ming Yang
yangming@jlu.edu.cn
Wei Wei
wwwei6@jlu.edu.cn

Specialty section:

This article was submitted to
Pharmacology of
Anti-Cancer Drugs,
a section of the journal
Frontiers in Oncology

Received: 06 February 2021

Accepted: 07 May 2021

Published: 24 May 2021

Citation:

Peng J, Yang M, Bi R, Wang Y,
Wang C, Wei X, Zhang Z, Xie X and
Wei W (2021) Targeting Mutated p53
Dependency in Triple-Negative Breast
Cancer Cells Through CDK7 Inhibition.
Front. Oncol. 11:664848.
doi: 10.3389/fonc.2021.664848

Background: Cyclin-dependent kinase 7 (CDK7) is crucial for cell cycle progression and gene expression transcriptional regulation, which are often not assessed in cancer developing process. CDK7 inhibitors have emerged as promising drugs for treating diverse cancers, including breast cancer. However, the mechanism behind its anticancer effect has not been well investigated. Here, the possible mechanism of CDK7 inhibitors for treating human triple-negative breast cancer (TNBC) has been studied.

Methods: The effects of CDK7 inhibitors on breast cancer cells have been identified by measuring cell viability (Cell Counting Kit-8) and cell proliferation and calculating colony formation. The short hairpin RNA and short interfering RNA were used for the construction of knockdown cells. To assess the expression of associated proteins, western blot was used.

Results: This study confirmed that, compared to hormone receptor-positive breast cancer cells, TNBC cells were more sensitive to THZ1, a novel CDK7 inhibitor. THZ1 treatment specifically downregulated mutated p53 in a dose- and time-dependent manner in TNBC cells with p53 mutation. Another CDK7 inhibitor, LDC4297, also potentially interfered with the expression of mutated p53. Furthermore, endogenous CDK7 expression was positively correlated with the levels of mutated p53 in TNBC cells with p53 mutation. Downregulating mutated p53 expression significantly suppressed the proliferation of TNBC cells with p53 mutation.

Conclusion: Our findings demonstrated that targeting CDK7 was an effective approach for the treatment of TNBC with p53 mutation.

Keywords: CDK7 inhibition, THZ1, triple-negative breast cancer, mutated p53, targeted therapy, cancer treatment

INTRODUCTION

Triple-negative breast cancer (TNBC), a heterogeneous breast cancer subtype, lacks endocrine estrogen receptor (ER) and progesterone receptor (PR) and human epidermal growth factor receptor 2 (HER2, encoded by ERBB2) (1, 2). When comparing to other breast cancer subtypes, TNBC is more likely to recur and develop resistance to endocrine or anti-HER2 therapy (1, 3).

Unfortunately, although targeted drugs such as poly (ADP)-ribose polymerase inhibitors have been applied for TNBC therapy, the scope and efficacy of its application are limited. Currently, chemotherapy is still the main systemic treatment for TNBC patients. Although it initially responds well to chemotherapy, TNBC remains to have a poorer prognosis than non-TNBC. For stage I triple-negative tumors, the 5-year breast cancer-specific survival rate is 85%, while that of ERBB2 and hormone receptor-positive cancer ranges from 94% to 99% (4). Hence, there is an urgent need for therapeutic approaches against TNBC.

Pharmacological blockade of transcription is a potential anticancer strategy. Some members of the cyclin-dependent kinases (CDKs), such as CDK7, CDK9, CDK12, and CDK13, which regulate transcription by phosphorylating RNA polymerase (RNAP) II, are possible drug targets (5). CDK7, an essential component of CDK-activating kinase (CAK) and the general transcription factor IIH (TFIIH), modulates cell division cycle and transcription (6). CDK7 binds with two other subunits (cyclin-H and MAT1) to form the complex CAK mediating the activation of other CDKs, including CDK1, CDK2, CDK4, and CDK6 (7). Besides, CDK7 is also one component of TFIIH that phosphorylates RNAP II or other transcription factors, such as androgen receptor and ER (8). Thus far, accumulating studies have demonstrated that CDK7 is frequently overexpressed in diverse tumor tissues including gastric cancer, oral squamous cell carcinoma, and breast cancer (9–12). Preclinical studies have confirmed that covalent CDK7 inhibitors selectively induce apoptosis in certain cancers, but not in normal human cells (13–18).

THZ1 is a phenylamino-pyrimidine that covalently targets CDK7 by covalently binding to its adenosine triphosphate (ATP) site allosterically with strong antitumor activity against TNBC cells (19). However, its effects on ER/PR+ breast cancer cells still remain controversial (19, 20). Moreover, the mechanism behind its anticancer activity has not yet been described. In this study, we investigated whether TNBC cells were more susceptible than ER/PR+ breast cancer cells to THZ1 therapy. Our results indicated that THZ1 selectively downregulated endogenous mutant p53 levels in TNBC cells with p53 mutation, but not in other breast cancer cells. Another CDK7 inhibitor treatment (LDC4297, a competitive inhibitor of ATPase) or silencing of CDK7 expression also decreased mutant p53 in TNBC cells with p53 mutation. Direct downregulation of mutant p53 expression levels effectively suppressed the proliferation of TNBC cells with p53 mutation. These results indicate the potential usage of CDK7 inhibitors in the treatment of TNBCs with p53 mutant by downregulating the content of endogenous mutant p53.

MATERIALS AND METHODS

Cell Culture and Compound Preparation

Hs-578T (TNBC cells with mutant-type p53) and MCF-7 (non-TNBC cells with wild-type p53) were 10% fetal bovine serum cultivated in Dulbecco's Modified Eagle's medium (Biological Industries, USA) from the Type Culture Set of the Chinese Academy of Sciences (Shanghai, China). DU4475 (TNBC cells

with wild-type p53) were 10% fetal bovine serum cultivated in 1640 medium (Biological Industries, USA) from the FuHeng BioLogY (Shanghai, China). Under normal incubator conditions (37°C and 5% carbon dioxide), all cells were developed. THZ1 (HY-80013) and LDC4297 (HY-126p53) were obtained from MedChemExpress (Monmouth Junction, NJ, USA). All drugs we used in this article were dissolved in a stock solution of 10 mM dimethyl sulfoxide (DMSO).

Assay of Cell Viability

To detect cell viability, we chose the Cell Counting Kit-8 (CCK-8, TransGen Biotech) and performed the assay following the manufacturer's instructions. Nearly 8,000 cells were seeded onto 96-well plates per well and incubated until detection for 24 h. We established three parallel groups for each test group. Cells were subsequently treated with different THZ1 concentrations for 48 h. The cells were then incubated in 100 μ L of cell culture medium containing 10 μ L CCK-8 for 2 h at 37°C. The absorbance was observed using the BioTek ELISA reader (Winooski, VT, USA) at a wavelength of 450 nm. Cell inhibitory ratio was calculated using the following formula:

$$100 \times \text{cell growth inhibitory ratio}(\%)$$

$$= 100 \times \left(\frac{[A \times 450 \text{ control} - A_{450 \text{ sample}}]}{[A \times 450 \text{ control} - A_{450 \text{ blank}}]} \right)$$

Microscopy Images

Cells (approximately 1×10^5) were planted in 12-well plates and treated for 48 h at different concentrations of THZ1 or vehicle control (DMSO) or treated with short interfering RNAs (siRNAs) (si-889) that target the human p53 gene and negative control siRNAs (si-con) for 48 h. Static bright-field images were photographed using OLYMPUS cellSens Standard software (Olympus).

Cell Proliferation Assay

For growth assays, Hs-578T (4×10^4), DU4475 (8×10^4), or MCF-7 (5×10^4) cells were seeded into 12-well plates and were then treated for 24 h and 48 h with THZ1 or DMSO (as control) or treated with siRNAs (si-889) that target the human p53 gene and negative control siRNAs (si-con) for 24 h and 48 h. We established three parallel groups for each test group. Cells were counted using the cell counting chamber (Shanghai Precision Instruments Co., Ltd., Shanghai, China) at specified time points and staining with trypan blue. We repeated all of the tests three times.

Cell Colony Formation Assays

In colony formation assays, approximately 5000 cells/well were plated with 2-mL medium in 6-well plates, treated with THZ1 or DMSO (as control) in different concentrations or treated with siRNAs (si-889) that target the human p53 gene and negative control siRNAs (si-con), and incubated for 7 days. Cells were fixed with 100% methanol for 30 min and stained with 20% ethanol with 0.2 g/mL crystal violet solution after washing with cold phosphate-buffered solution (PBS) twice. Phase-contrast microscopy (Olympus) was used to detect colonies, and colonies

not less than 50 cells were counted. We repeated all of the tests three times. Because DU4475 cells are cells that grow in suspension, it is inconvenient to perform colony formation assays; thus, this experiment did not involve corresponding content.

Western Blot

Until lysing cells in the RIPA buffer (Beyotime, China), cells were washed twice with cold PBS, followed by incubation for 10 min at 4°C. At 12,000 g at 4°C, the whole-cell lysate was centrifuged and the supernatant was collected, mixing with the loading buffer. Then, it was denatured for 10 min at 100°C, followed by electrophoresis of 12% sodium dodecyl sulfate polyacrylamide gel. The isolated proteins were transferred to membranes of nitrocellulose (Bio-Rad, USA). The membranes were probed overnight with sufficiently diluted primary antibodies after being blocked with 5% nonfat milk. After washing the membranes, they were incubated for 1 h at room temperature with alkaline phosphatase-conjugated secondary antibodies. The protein bands were visualized by 5-bromo-4-chloro-3-indolyl phosphate and nitro blue tetrazolium (Millipore). Western blotting images were acquired on a scanner (Epson Perfection V330 Photo) using Scan-n-Stitch Deluxe software (version 1.1.9, ArcSoft). Quantification analysis of protein expression was analyzed using ImageJ software (version 1.8.0, National Institutes of Health, Bethesda, MD, USA).

The primary antibodies included CDK7 (cat# 2916T, Cell Signaling Technology), p53 (cat# 10442-1-AP, Proteintech), GAPDH (cat# 10494-1-AP, Proteintech), and tubulin (cat# 11224-1-AP, Proteintech). Secondary antibodies included anti-rabbit IgG (cat# 7054) and anti-mouse IgG (cat# 7056) (Cell Signaling Technology, USA). All experiments were repeated three times.

Preparation of Lentiviruses

pRSV-Rev (122p53), pMDLg/pRRE (12251), and pCMV-VSV-G (8454) were bought from Addgene (Cambridge, MA, USA). The short hairpin RNAs (shRNAs) (5'-CCGGGCTGTAGAAGTGAGTTTGTAACTCGAGTTACAACTCACTTCTACAGCTTTT-3') that target human CDK7 (sh-CDK7) were purchased from Sigma-Aldrich (USA). Viruses were produced by 293T cells. After transfection, the supernatant of 293T cells was collected for 48 h and then purified through 0.45- μ m membranes. Puromycin (1.5 μ g/mL) was used for 2 days to pick cells for selection.

Short Interfering RNAs for Knockdown Cell Building

The siRNAs (si-889) (5'-CCACCAUCCACUACAACUATT-3'), which target the human p53 gene, and negative control siRNAs (si-con) were obtained from GenePharma (Shanghai, China). Lipofectamine 3000 (Thermo Fisher Scientific, USA) was used to conduct the cellular delivery of siRNA into Hs-578T and MCF-7 cells. jetPRIME (Polyplus-transfection, France) was used to conduct the cellular delivery of siRNA into DU4475 cells. Approximately 6000 Hs-578T and MCF-7 cells/well and 15000 DU4475 cells/well, as instructed by the manufacturer, were seeded into 12 wells after transfection with siRNAs or negative

control. After 48 h, a part of the cells was collected for testing the gene interference ability of siRNA, and the other part of the cells was used for subsequent proliferation assay and clone formation assay.

Statistical Analyses

Using GraphPad Prism 6 (GraphPad Software, CA, USA), all data were analyzed and presented as the mean \pm standard deviation. The differences between the two groups were compared by t-test, and the difference between multiple groups was compared using analysis of variance. $P < 0.05$ was considered statistically significant.

RESULTS

Distinct Efficiency of THZ1 on the Growth Inhibition of Triple-Negative Breast Cancer (TNBC) and Estrogen Receptor+ Breast Cancer Cells

Recent mRNA expression profiling and immunohistochemistry studies have documented elevated CDK7 expression in breast cancer tumors (10). Previous studies have investigated the correlations between CDK7 RNA expression and relapse-free survival (RFS) in breast cancer using a microarray database of 3,951 breast cancer patients and found that high expression levels of CDK7 are closely associated with worse RFS in all breast cancer subtypes (20). To illustrate the effect of THZ1 on breast cancer, we profiled several groups of cell lines representing various subtypes of breast cancer. The cell viability assay indicated that the 50% inhibitory concentration values of THZ1 in Hs-578T (TNBCs with mutant-type p53), DU4475 (TNBCs with wild-type p53), and MCF-7 (ER+) cells were 30.54 nM, 139.7 nM, and 209.3 nM, respectively (**Figure 1A**). This indicated that different breast cancer cells had variable sensitivity to THZ1. This was further supported by the results showing that 50 nM of THZ1 did not cause significant suppression of DU4475 cell and MCF7 cell proliferation (**Figures 1B, C**). Next, we performed colony formation assays, and the results showed that THZ1 inhibited breast cancer proliferation chronically and effectively. ER+ MCF-7 cells were significantly less sensitive to THZ1 compared to TNBC cells (**Figure 1D**). These findings demonstrated that THZ1 was effective in multiple subtypes of breast cancer, but its efficiency varies depending on the subtype.

THZ1 Selectively Suppressed The Expression of Mutated p53 in TNBC Cells With p53 Mutation

The exact mechanism of the determinants of the sensitivity of cancer cells to THZ1 has not yet been characterized. We observed that TNBC cells bearing genetic p53 mutations were more sensitive to THZ1. Interestingly, we found that THZ1 potentially decreased p53 protein expression in TNBC cells with p53 mutations (Hs-578T cells) in a dose-dependent manner. However, this effect was not observed in TNBC cell lines with wild-type p53 (DU4475 cells) or ER-positive MCF-7 cells with

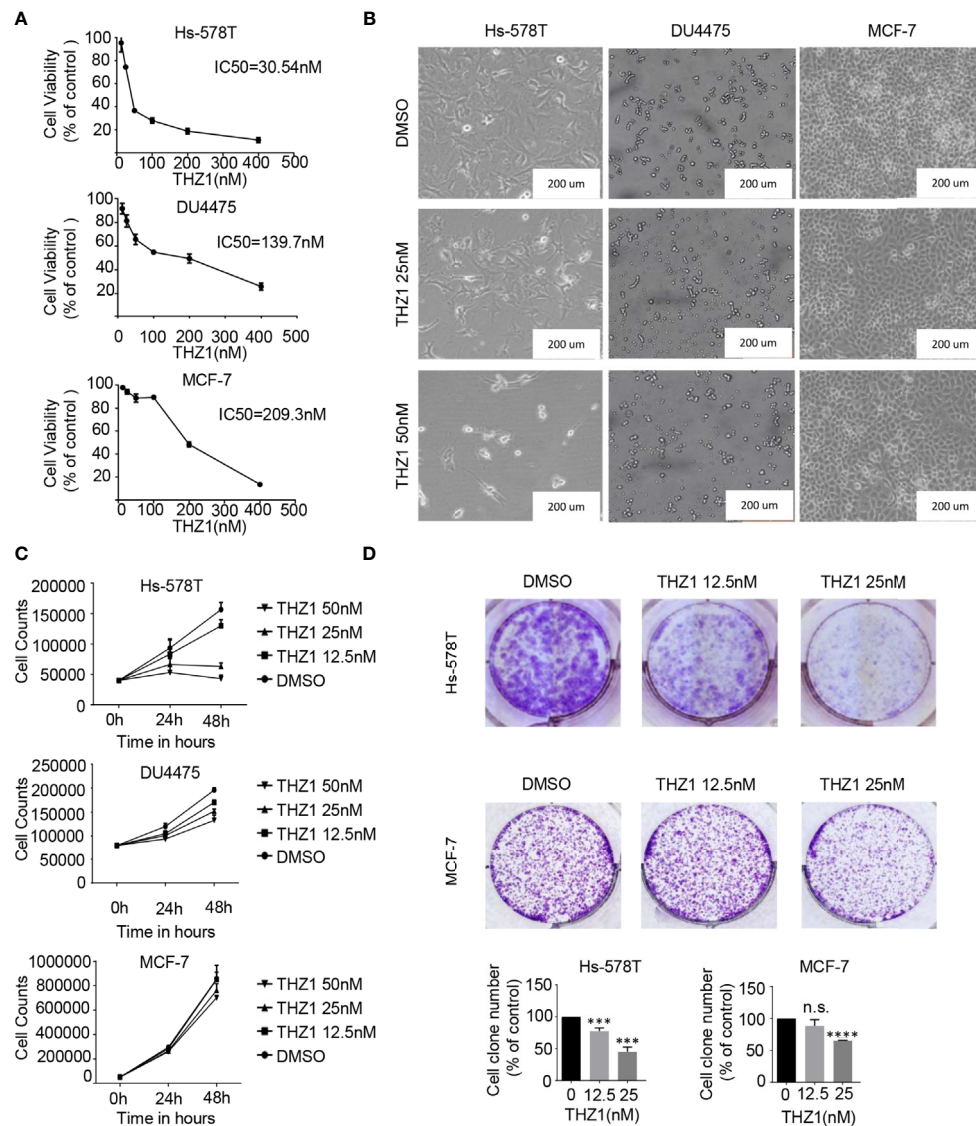


FIGURE 1 | THZ1 inhibits cell proliferation in breast cancer cells. **(A)** Cell Counting Kit-8 assays have determined the proliferation of breast cancer cells after treatment with dimethyl sulfoxide (DMSO) (control) or indicated concentrations of THZ1 (12.5, 25, 50, 100, 200, and 400 nM) for 48 h. **(B)** Images (200×) show Hs-578T, DU4475, and MCF-7 cells following THZ1 treatment for 48 h. **(C)** Effects of THZ1 treatment on breast cancer cell proliferation curve. Verification was performed by cell counting. **(D)** Impact of treatment with THZ1 on the development of breast cancer cells in the colony. Cells have been treated with either DMSO (control) or indicated THZ1 concentrations (12.5, 25, and 50 nM) for 7 days. With an inverted microscope, cell colonies (>50 cells) were counted. The mean \pm standard deviation reflects the data. (n.s., non significant, $P > 0.05$; *** $P < 0.001$, **** $P < 0.0001$, $n = 3$).

wild-type p53 (**Figures 2A, B**). We also confirmed that the suppression of mutated p53 expression in TNBC cells by THZ1 was time-dependent (**Figures 2C, D**). Next, we used another CDK7 inhibitor, LDC4297, to further verify the effect of CDK7 inhibitors on p53 protein expression. Similarly, LDC4297 treatment effectively downregulated p53 expression in TNBC cells with mutant-type p53 (Hs-578T), but not in TNBC cell lines with wild-type p53 (DU4475 cells) or ER-positive MCF-7 cells with wild-type p53. Moreover, the manner of its suppressive effect was dependent on dose and time (**Figure 3**). Hence, we found that CDK7 inhibitors selectively interfered with mutated p53 expression

in TNBC cells with p53 mutation, but they did not influence the expression of wild-type p53 in other breast cancer cells.

Cyclin-Dependent Kinase 7 Is Critical for the Expression of Mutated p53 in TNBC Cells With p53 Mutation

Since CDK7 inhibitors interfered with mutated p53 expression, we proceeded to investigate the effects of CDK7 proteins on the regulation of mutated p53 in breast cancer cells. We generated CDK7 stable knockdown Hs-578T, DU4475, and MCF-7 cells using shRNA targeting CDK7 (**Figures 4A, C**). The immunoblotting data

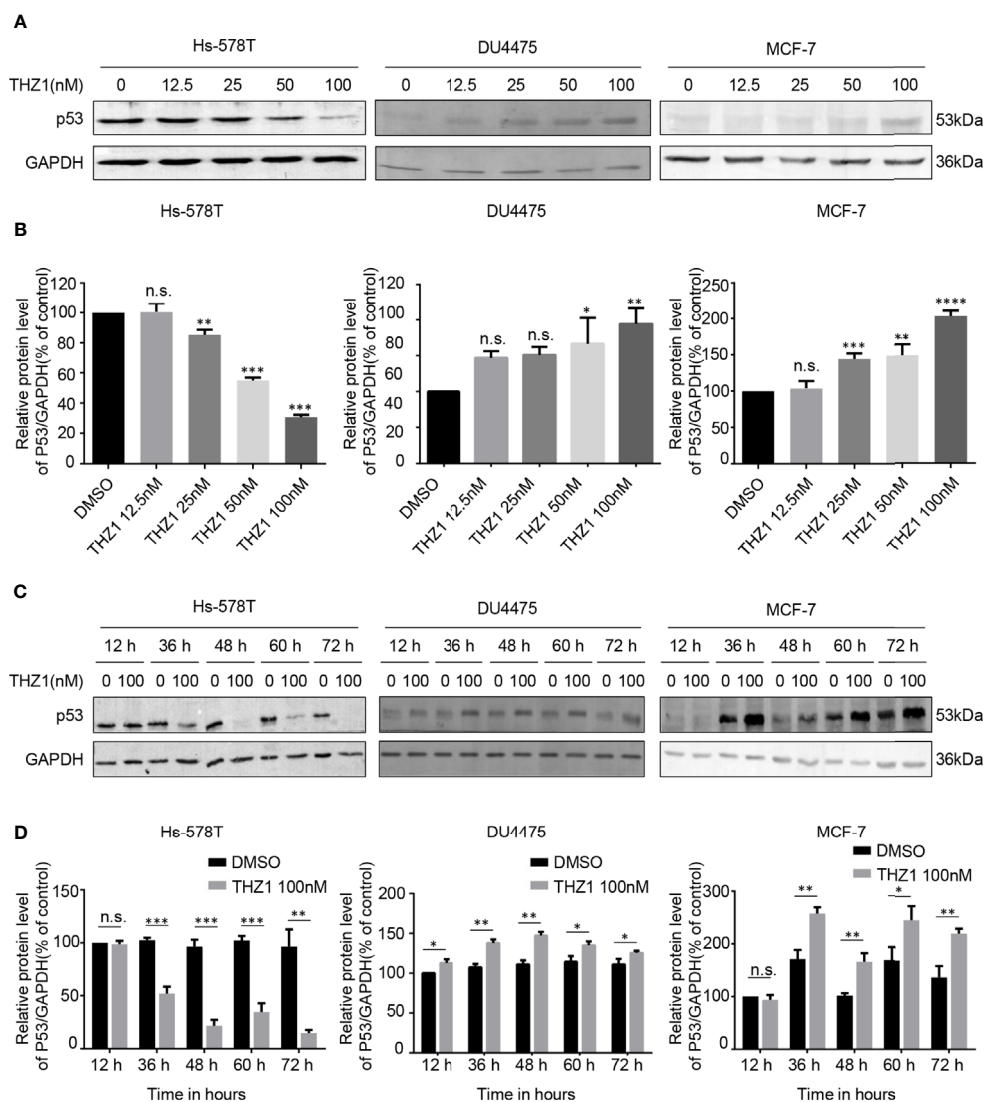


FIGURE 2 | THZ1 downregulates the expression of mutant-type p53 rather than wild-type p53 in breast cancer cells. **(A)** Western blot was used to detect relative p53 protein expression in breast cancer cells after treatment with dimethyl sulfoxide (DMSO) (control) or specified concentrations of THZ1 (12.5, 25, 50, and 100 nM) for 48 h. **(B)** Quantification analysis of p53 protein expression after treatment with DMSO (control) or indicated concentrations of THZ1 (12.5, 25, 50, and 100 nM) for 48 h. **(C)** Western blot analysis of relative p53 expression levels in breast cancer cells was performed at different times (12 h, 36 h, 48 h, 60 h, and 72 h) following treatment with DMSO (control) or the same THZ1 concentration. **(D)** Quantification analysis of p53 protein expression after treatment with DMSO (control) or the same concentration of THZ1 (100 nM) for different durations (12 h, 36 h, 48 h, 60 h, and 72 h). The mean \pm standard deviation reflects the data. (n.s., non significant, $P > 0.05$; * $P < 0.05$, ** $P < 0.01$, *** $P < 0.001$, **** $P < 0.0001$, $n = 3$).

indicated that p53 expression levels were dramatically downregulated in CDK7 knockdown Hs-578T cells, but not in sh-CDK7 DU4475 and MCF7 cells (**Figure 4**). These results confirmed that CDK7 supported mutant p53 expression in TNBC cells with p53 mutation.

Mutated p53 Proteins Support the Proliferation of TNBC Cells With p53 Mutation

THZ1 specifically decreased mutant p53 expression in TNBC cells with p53 mutation. This suggested that the growth inhibitory activity of THZ1 in TNBC cells with p53 mutation relied on

mutated p53 downregulation. We used RNA interference to downregulate endogenous p53 expression in TNBC or ER+ breast cancer cells (**Figures 5A, B**). Morphological changes in si-p53 and control cells suggested that mutant p53 proteins were essential for the survival of Hs-578T cells, but not DU4475 and MCF-7 cells (**Figure 5C**). Cell proliferation and colony formation assays further supported the fact that knockdown p53 inhibited the proliferation of TNBC cells with mutant p53, but not TNBC or ER+ cells with wild-type p53 (**Figures 5D, E**). Our data clarified the determinant roles of p53 mutant for the maintenance of cell survival of p53-mutated TNBCs.

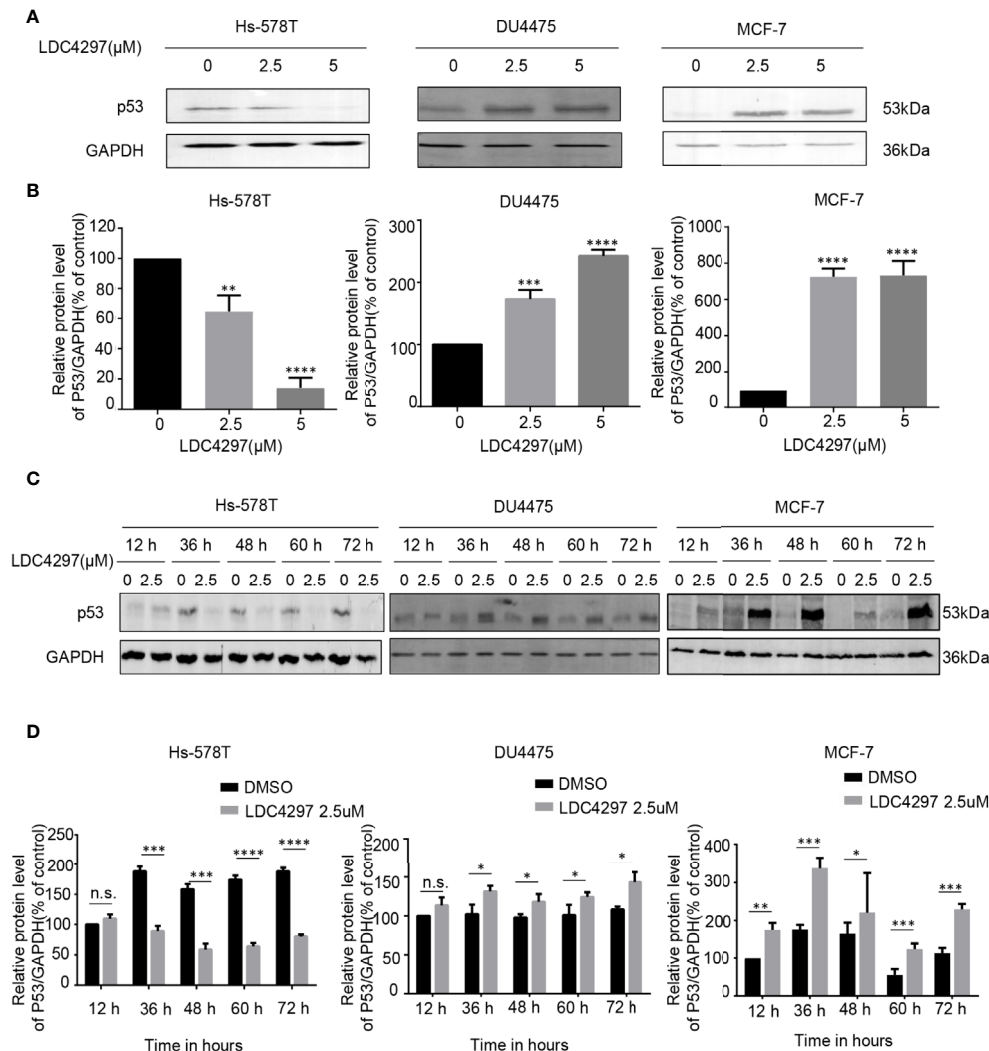


FIGURE 3 | The expression of mutant-type p53 instead of wild-type p53 is downregulated after the expression of cyclin-dependent kinase 7 is blocked by LDC4297.

(A) Western blot was used to detect relative p53 protein expression in breast cancer cells after treatment with dimethyl sulfoxide (DMSO) (control) or specified concentrations of LDC4297 (2.5 and 5 μM) for 48 h. **(B)** Quantification analysis of p53 protein expression after treatment with DMSO (control) or indicated concentrations of LDC4297 (2.5 and 5 μM) for 48 h. **(C)** The relative expression levels of p53 in breast cancer cells were analyzed by Western blot after treatment with DMSO (control) or the same concentration of LDC4297 (2.5 μM) for different times (12–72 h). **(D)** Quantification analysis of p53 protein expression after treatment with DMSO (control) or the same concentration of LDC4297 (2.5 μM) for different times (12–72 h). The mean ± standard deviation reflects the data. (n.s., non significant, $P > 0.05$; * $P < 0.05$, ** $P < 0.01$, *** $P < 0.001$, **** $P < 0.0001$, $n = 3$).

DISCUSSION

CDK7 plays a dual role in driving cell cycle progression and modulating transcription (6). Its expression frequently increases in many cancers and is important for tumor development (10, 12). A number of CDK7 inhibitors are considered to be potential drug candidates for cancer therapy because they are highly cytotoxic to tumor cells only (13, 21, 22). One main concern regarding the application of CDK7 inhibitors in cancer therapy is the variable sensitivity of different cancer types to CDK7 inhibition, which has been found in preclinical studies. In this study, we selected drugs affected through different pathways to inhibit CDK7 and established adenovirus containing vectors with CDK7-shRNA to interfere its

expression. Fortunately, we identified TNBC cells with p53 mutations as most sensitive to CDK7 inhibitors because mutated p53-dependent cancer cell proliferation was selectively inhibited.

Previous studies have demonstrated that TNBC cells particularly rely on CDK7 due to a group of CDK7 kinase-controlled TNBC-specific genes (19). Other experiments have shown that no apparent selectivity between different subtypes of breast cancer under CDK7 treatment was detected (20). In addition, not only recent mRNA expression profiling but also immunohistochemistry studies have demonstrated that the expression of CDK7 in ER+ breast cancer was elevated (10). By comparing the results after adding varied THZ1 concentrations to different cell lines of breast cancer, we confirmed that THZ1 has a

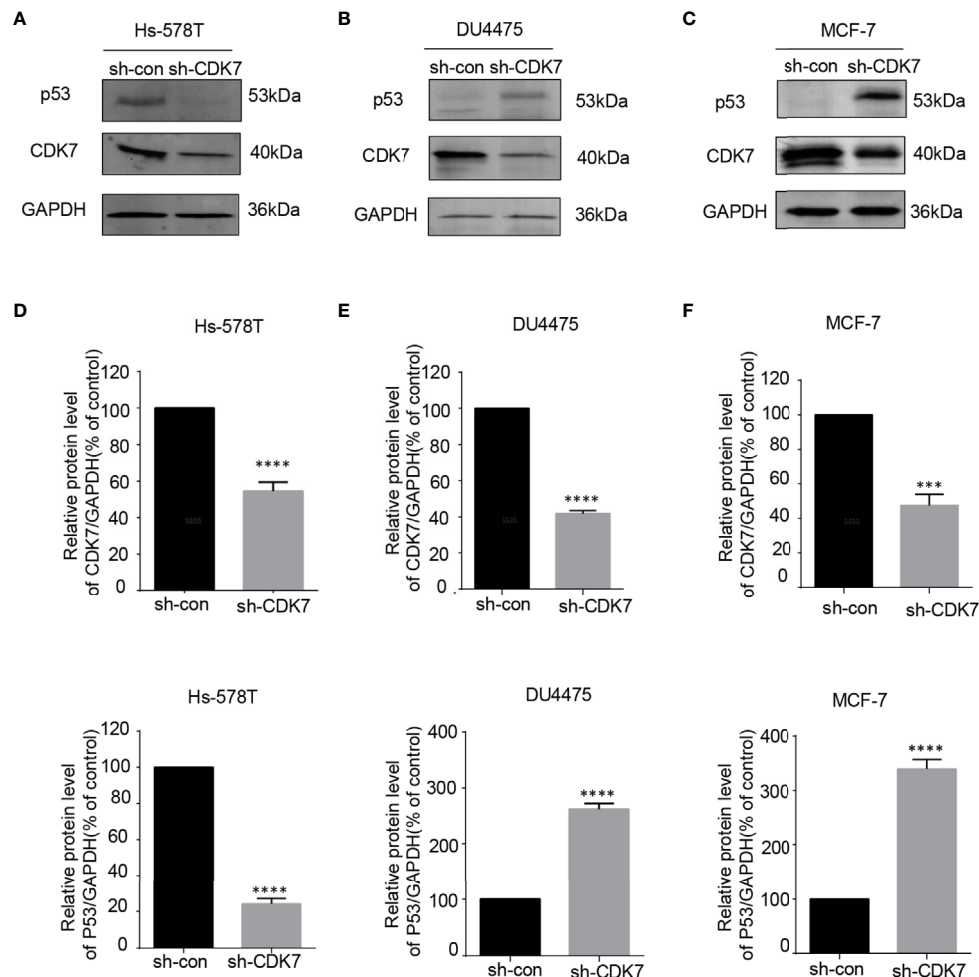


FIGURE 4 | The expression of mutant-type p53 instead of wild-type p53 is downregulated after the expression of cyclin-dependent kinase 7 (CDK7) is blocked by sh-CDK7. **(A–C)** The relative expression of CDK7 and p53 protein detected by western blot in Hs-578T, DU4475, and MCF-7 cells, with CDK7 being knocked down by short hairpin RNA. **(D–F)** Quantification analysis of CDK7 and p53 protein expression. The mean \pm standard deviation reflects the data. (*** $P < 0.001$, **** $P < 0.0001$, $n = 3$).

broad antitumor activity with diverse sensitivities. We further explored the mechanisms that contributed to the different sensitivities of different breast cancer cells to CDK7 inhibition. This study also emphasized the importance of p53 status in breast cancer cells for CDK7 inhibitor treatment.

TNBC has a greater level of genetic sophistication compared to the other breast cancer subtypes, as shown by its higher prevalence of point mutation, gene amplification, and deletion (3). Since TNBC is ER/PR- and HER2-negative, common drugs used for breast cancer therapies such as tamoxifen; letrozole, which targets hormone receptors; and trastuzumab, which aims to destroy HER2 overexpression in breast cancer cells, are inapplicable in TNBC treatment. Researchers are consistently identifying several drugs designed to suppress TNBC development. A mutated p53 tumor suppressor gene is found in over 80% of TNBC cells (23–25). Previous studies have focused on reactivating mutant p53 and converting it into a wild-type mutant *via* small molecule

inhibitors. Their results showed that this approach efficiently suppressed TNBC cell growth (26, 27). However, there are a variety of mutation sites and multiple mutation forms for mutant p53; thus, reactivating p53 might not lead to a satisfied cost performance. Hence, we suggest that decreased mutant-type p53 protein expression would be a distinct idea for TNBC with mutant-type p53 treatment. This study shows that the use of CDK7 inhibitors to directly downregulate the content of endogenous mutant-type p53 protein can inhibit the proliferation of p53 mutant-type TNBC cells. These findings support the fact that mutated p53 is a determinant factor for the survival of TNBC cells with p53 mutation.

Cell cycle progression by CDKs T-loop phosphorylation is guided by the CAK, comprising CDK7, cyclin H, and MAT1. CDK7 is also a vital member of the general TFIIF (6). In contrast to the specific downregulation of intracellular accumulation of mutated p53 by CDK7 inhibition in TNBC cells, our data also

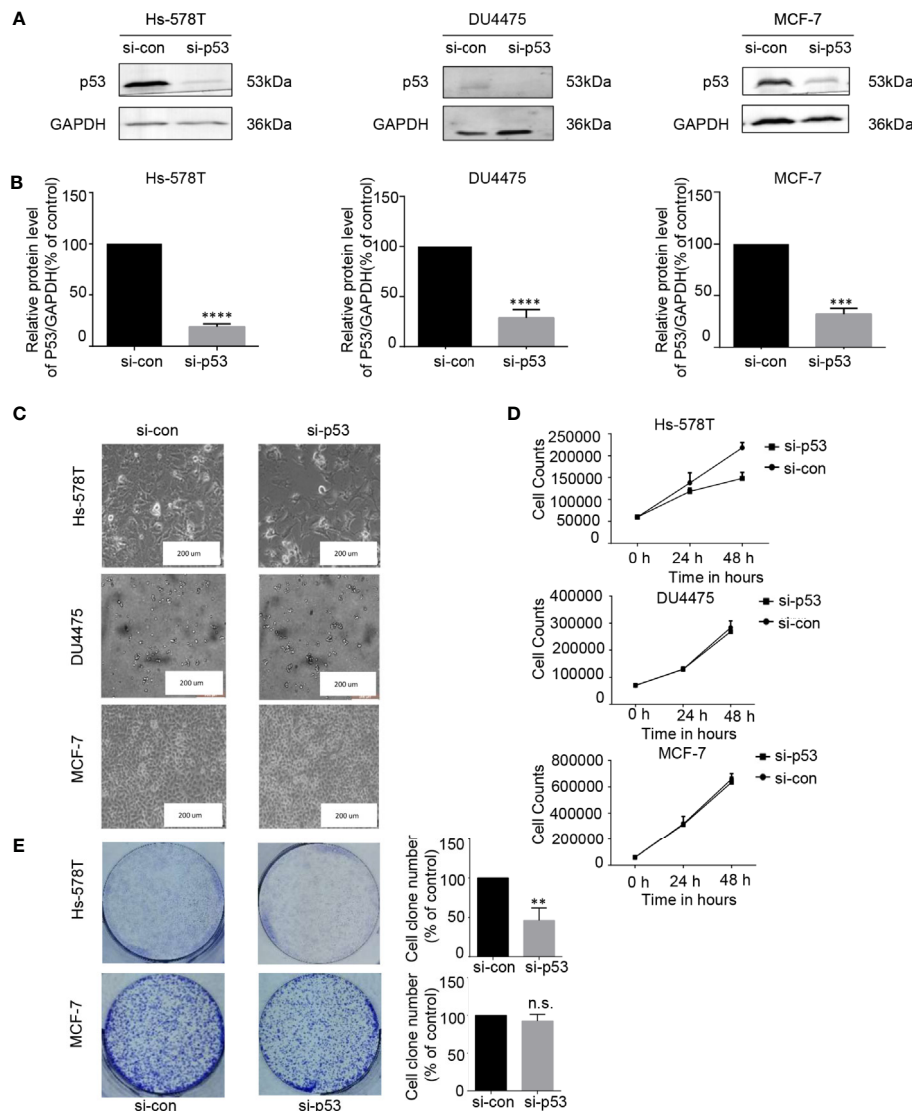


FIGURE 5 | The proliferation of breast cancer cell lines was inhibited after the expression of p53 protein was downregulated. **(A, B)** Effects of p53 knockdown using short interfering RNA (siRNA) in breast cancer cell lines. **(C)** Images (200x) show breast cancer cells after 48 h of siRNA treatment **(D)** Effects of siRNA treatment on breast cancer cell line proliferation curve. Verification by cell counting. **(E)** Impact of treatment with p53 knockdown on the colony formation of breast cancer cells. Cell colonies (>50 cells) were counted. The mean \pm standard deviation reflects the data. (n.s., non significant, $P > 0.05$; ** $P < 0.01$, *** $P < 0.001$, **** $P < 0.0001$, $n = 3$).

show that CDK7 inhibitor treatment could elevate the expression of p53 in breast cancer cells with wild-type p53 (Figures 2, 3). Recent studies have observed that CDK inhibition elevated the expression of p53 proteins in human colon cancer-derived cells (28). p53 is recognized and phosphorylated by CDK7-cyclinH-p36 trimeric complex (29). Posttranslational phosphorylation of p53 regulates its transcriptional activity and stability. The roles of CDK7, cyclin H, and p36 mediated by p53 phosphorylation on the intracellular accumulation of wild-type and mutant-type p53 in breast carcinoma cells need further investigation in future studies. Besides, all our conclusions are based on the *in vitro* results from the immortalized breast carcinoma-derived cell

lines. Relevant experiments that determine the effects of CDK7 inhibitors on the stability and function of mutated p53 *in vivo* are equally important to evaluate the potential usage of CDK7 inhibitors in the therapeutic treatment of TNBC patients with p53 mutant.

In summary, our results suggested that CDK7 facilitates the proliferative activity of TNBC cells with p53 mutation by maintaining high expression of mutated p53. This established a regulatory association between CDK7 kinase activity and mutated p53 expression. Downregulation of p53 by CDK7 inhibition is an optimal drug target for TNBC or even for other carcinomas bearing a p53 mutation.

DATA AVAILABILITY STATEMENT

The datasets presented in this study can be found in online repositories. The names of the repository/repositories and accession number(s) can be found in the article/**Supplementary Material**.

AUTHOR CONTRIBUTIONS

Manuscript writing: JP, WW, MY. Data analysis: YW, ZZ. Study design: JP, RB, CW. Data collection: XW, XX. All authors contributed to the article and approved the submitted version.

REFERENCES

1. Cancer Genome Atlas, Network. Comprehensive Molecular Portraits of Human Breast Tumors. *Nature* (2012) 490(7418):61–70. doi: 10.1038/nature11412
2. Wang, W, Zhang B, Mani AM, Wu Z, Fan Y, Li W, et al. Survivin Inhibitors Mitigate Chemotherapeutic Resistance in Breast Cancer Cells by Suppressing Genotoxic Nuclear Factor- κ B Activation. *J Pharmacol Exp Ther* (2018) 366(1):184–93. doi: 10.1124/jpet.118.249151
3. Giampaolo B, Balko JM, Mayer IA, Sanders ME, Gianni L. Triple-Negative Breast Cancer: Challenges and Opportunities of a Heterogeneous Disease. *Nat Rev Clin Oncol* (2016) 13(11):674–90. doi: 10.1038/nrclinonc.2016.66
4. Waks AG, Winer EP. Breast Cancer Treatment. *Jama* (2019) 321(3):288–300. doi: 10.1001/jama.2018.19323
5. Chou, J., D. A., Quigley TM, Robinson F, Feng Y, Ashworth A. Transcription-Associated Cyclin-Dependent Kinases as Targets and Biomarkers for Cancer Therapy. *Cancer Discovery* (2020) 10(3):351–70. doi: 10.1158/2159-8290.CD-19-0528
6. Malumbres M. Cyclin-Dependent Kinases. *Genome Biol* (2014) 15:122. doi: 10.1186/gb4184
7. Fisher RP. The CDK Network: Linking Cycles of Cell Division and Gene Expression. *Genes Cancer* (2012) 3:731–8. doi: 10.1177/1947601912473308
8. Patel H, Abduljabbar R, Lai CF, Periyasamy M, Harrod A, Gemma C, et al. Expression of CDK7, Cyclin H, and MAT1 Is Elevated in Breast Cancer and Is Prognostic in Estrogen Receptor-Positive Breast Cancer. *Clin Cancer Res* (2016) 22(23):5929–38. doi: 10.1158/1078-0432.CCR-15-1104
9. Li B, Ni Chonghaile T, Fan Y, Madden SF, Klinger R, O'Connor AE, et al. Therapeutic Rationale to Target Highly Expressed Cdk7 Conferring Poor Outcomes in Triple-Negative Breast Cancer. *Cancer Res* (2017) 77(14):3834–45. doi: 10.1158/0008-5472.Can-16-2546
10. Patel H, Abduljabbar R, Lai CF, Periyasamy M, Harrod A, Gemma C, et al. Expression of CDK7, Cyclin H, and MAT1 Is Elevated in Breast Cancer and Is Prognostic in Estrogen Receptor-Positive Breast Cancer. *Clin Cancer Res* (2016) 22(23):5929–38. doi: 10.1158/1078-0432.CCR-15-1104
11. Diab S, Yu M, Wang S. Cdk7 Inhibitors in Cancer Therapy: The Sweet Smell of Success? *J Med Chem* (2020) 63(14):7458–74. doi: 10.1021/acs.jmedchem.9b01985
12. Kim J, Cho YJ, Ryu JY, Hwang I, Han HD, Ahn HJ, et al. CDK7 Is a Reliable Prognostic Factor and Novel Therapeutic Target in Epithelial Ovarian Cancer. *Gynecol Oncol* (2020) 156(1):211–21. doi: 10.1016/j.ygyno.2019.11.004
13. Kwiatkowski N, Tinghu Z, Peter B, Rahl B, Abraham J, Reddy J, et al. Targeting Transcription Regulation in Cancer With a Covalent CDK7 Inhibitor. *Nature* (2014) 511(7511):616–+. doi: 10.1038/nature13393
14. Greenall SA, Lim YC, Mitchell CB, Ensby KS, Stringer BW, Wilding AL, et al. Cyclin-Dependent Kinase 7 Is a Therapeutic Target in High-Grade Glioma. *Oncogenesis* (2017) 6(5):e336. doi: 10.1038/onc.2017.33
15. Cheng ZJ, Miao DL, Su QY, Tang XL, Wang XL, Deng LB, et al. THZ1 Suppresses Human non-Small-Cell Lung Cancer Cells In Vitro Through Interference With Cancer Metabolism. *Acta Pharmacol Sin* (2019) 40(6):814–22. doi: 10.1038/s41401-018-0187-3
16. Lu, P, Geng J, Zhang L, Wang Y, Niu N, Fang Y, et al. THZ1 Reveals CDK7-dependent Transcriptional Additions in Pancreatic Cancer. *Oncogene* (2019) 38(20):3932–45. doi: 10.1038/s41388-019-0701-1
17. Lei G, Li J, Zeng H, Guzman AG, Li T, Lee M, et al. A Combination Strategy Targeting Enhancer Plasticity Exerts Synergistic Lethality Against BET-resistant Leukemia Cells. *Nat Commun* (2020) 11(1):740–55. doi: 10.1038/s41467-020-14604-6
18. Huang T, Ding X, Xu G, Chen G, Cao Y, Peng C, et al. CDK7 Inhibitor THZ1 Inhibits MCL1 Synthesis and Drives Cholangiocarcinoma Apoptosis in Combination With BCL2/BCL-XL Inhibitor ABT-263. *Cell Death Dis* (2019) 10(8):602. doi: 10.1038/s41419-019-1831-7
19. Wang Y, Zhang T, Kwiatkowski N, Abraham BJ, Lee TI, Xie S, et al. CDK7-Dependent Transcriptional Addiction in Triple-Negative Breast Cancer. *Cell* (2015) 163(1):174–86. doi: 10.1016/j.cell.2015.08.063
20. McDermott MSJ, Sharko AC, Munie J, Kassler S, Melendez T, Lim CU, et al. Cdk7 Inhibition Is Effective in All the Subtypes of Breast Cancer: Determinants of Response and Synergy With EGFR Inhibition. *Cells* (2020) 9(3):638–55. doi: 10.3390/cells9030638
21. Sava GP, Fan H, Coombes RC, Buluwela L, Ali S. CDK7 Inhibitors as Anticancer Drugs. *Cancer Metastasis Rev* (2020) 39(3):805–23. doi: 10.1007/s10555-020-09885-8
22. Olson CM, Liang Y, Leggett A, Park WD, Li L, Mills CE, et al. Development of a Selective Cdk7 Covalent Inhibitor Reveals Predominant Cell-Cycle Phenotype. *Cell Chem Biol* (2019) 26(6):792–803.e10. doi: 10.1016/j.chembiol.2019.02.012
23. Lawrence MS, Stojanov P, Mermel CH, Robinson JT, Garraway LA, Golub TR, et al. Discovery and Saturation Analysis of Cancer Genes Across 21 Tumour Types. *Nature* (2014) 505(7484):495–501. doi: 10.1038/nature12912
24. Nik-Zainal S, Davies H, Staaf J, Ramakrishna M, Glodzik D, Zou X, et al. Landscape of Somatic Mutations in 560 Breast Cancer Whole-Genome Sequences. *Nature* (2016) 534(7605):47–54. doi: 10.1038/nature17676
25. Silwal-Pandit L, Vollen HK, Chin SF, Rueda OM, McKinney S, Osako T, et al. TP53 Mutation Spectrum in Breast Cancer Is Subtype Specific and has Distinct Prognostic Relevance. *Clin Cancer Res* (2014) 20(13):3569–80. doi: 10.1158/1078-0432.CCR-13-2943
26. Synnott NC, Bauer MR, Madden S, Murray A, Klinger R, O'Donovan N, et al. Mutant p53 as a Therapeutic Target for the Treatment of Triple-Negative Breast Cancer: Preclinical Investigation With the Anti-p53 Drug, PK11007. *Cancer Lett* (2018) 414:99–106. doi: 10.1016/j.canlet.2017.09.053
27. Synnott NC, Murray A, McGowan PM, Kiely M, Kiely PA, O'Donovan N, et al. Mutant p53: A Novel Target for the Treatment of Patients With Triple-Negative Breast Cancer? *Int J Cancer* (2017) 140(1):234–46. doi: 10.1002/ijc.30425
28. Kalan S, Amat R, Schachter MM, Kwiatkowski N, Abraham BJ, Liang Y, et al. Activation of the P53 Transcriptional Program Sensitizes Cancer Cells to Cdk7 Inhibitors. *Cell Rep* (2017) 21(2):467–81. doi: 10.1016/j.celrep.2017.09.056
29. Lu H, Fisher RP, Bailey P, Levine AJ. The CDK7-cycH-p36 Complex of Transcription Factor IIH Phosphorylates p53, Enhancing Its Sequence-

ACKNOWLEDGMENTS

We thank Dr. Haoran Guo and Guanchen Liu for technical assistance. This work was partially funded by funding from the National Natural Science Foundation of China (81772183), the Department of Science and Technology of Jilin Province (20190304033YY and 20180101127JC and 3D5204177428).

SUPPLEMENTARY MATERIAL

The Supplementary Material for this article can be found online at: <https://www.frontiersin.org/articles/10.3389/fonc.2021.664848/full#supplementary-material>

Specific DNA Binding Activity In Vitro. *Mol Cell Biol* (1997) 17(10):5923–34. doi: 10.1128/mcb.17.10.5923

Conflict of Interest: The authors declare that the research was conducted in the absence of any commercial or financial relationships that could be construed as a potential conflict of interest.

Copyright © 2021 Peng, Yang, Bi, Wang, Wang, Wei, Zhang, Xie and Wei. This is an open-access article distributed under the terms of the Creative Commons Attribution License (CC BY). The use, distribution or reproduction in other forums is permitted, provided the original author(s) and the copyright owner(s) are credited and that the original publication in this journal is cited, in accordance with accepted academic practice. No use, distribution or reproduction is permitted which does not comply with these terms.



Development of Store-Operated Calcium Entry-Targeted Compounds in Cancer

Xiaojing Liang^{1†}, Ningxia Zhang^{1†}, Hongming Pan¹, Jiansheng Xie^{1,2*} and Weidong Han^{1*}

¹Department of Medical Oncology, Sir Run Run Shaw Hospital, College of Medicine, Zhejiang University, Hangzhou, China,

²Laboratory of Cancer Biology, Institute of Clinical Science, Sir Run Run Shaw Hospital, College of Medicine, Zhejiang University, Hangzhou, China

OPEN ACCESS

Edited by:

Zhi-Xiang Yuan,
Southwest Minzu University, China

Reviewed by:

Raphaël Courjaret,
Weill Cornell Medicine- Qatar, Qatar
Yih-Fung Chen,
Kaohsiung Medical University, Taiwan
Zhi Qi,
Nankai University, China
Jianjie Ma,
The Ohio State University,
United States

*Correspondence:

Jiansheng Xie
xjs85@126.com
Weidong Han
hanwd@zju.edu.cn

[†]These authors have contributed
equally to this work

Specialty section:

This article was submitted to
Pharmacology of Anti-Cancer Drugs,
a section of the journal
Frontiers in Pharmacology

Received: 30 March 2021

Accepted: 17 May 2021

Published: 28 May 2021

Citation:

Liang X, Zhang N, Pan H, Xie J and
Han W (2021) Development of Store-
Operated Calcium Entry-Targeted
Compounds in Cancer.
Front. Pharmacol. 12:688244.
doi: 10.3389/fphar.2021.688244

Store-operated Ca^{2+} entry (SOCE) is the major pathway of Ca^{2+} entry in mammalian cells, and regulates a variety of cellular functions including proliferation, motility, apoptosis, and death. Accumulating evidence has indicated that augmented SOCE is related to the generation and development of cancer, including tumor formation, proliferation, angiogenesis, metastasis, and antitumor immunity. Therefore, the development of compounds targeting SOCE has been proposed as a potential and effective strategy for use in cancer therapy. In this review, we summarize the current research on SOCE inhibitors and blockers, discuss their effects and possible mechanisms of action in cancer therapy, and induce a new perspective on the treatment of cancer.

Keywords: SOCE, cancer, inhibitor, pharmacodynamics, therapy

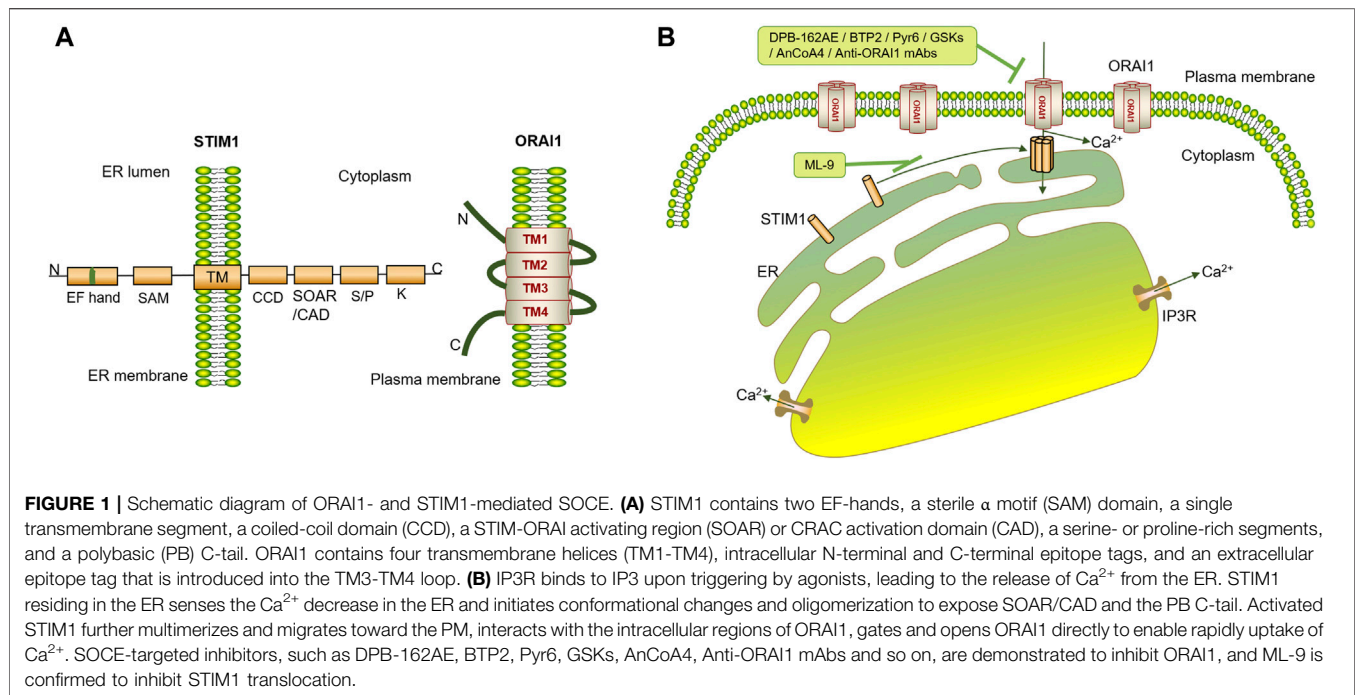
INTRODUCTION

The Overview of Store-Operated Calcium Entry

Store-operated calcium entry (SOCE) is typically activated by ligands of cell surface receptors such as G proteins that activate phospholipase C (PLC) to cleave phosphatidylinositol 4, 5-bisphosphate (PIP2) and produce inositol 1, 4, 5-trisphosphate (IP3). IP3 binds to IP3 receptors (IP3R) on the endoplasmic reticulum (ER) membrane, leading to the release of Ca^{2+} from the ER. Cells respond to this depletion of ER intraluminal Ca^{2+} by opening Ca^{2+} channels to allow cellular influx, which is also the provenance of “SOCE.” Researchers have been exploring the mechanisms and functions of SOCE since its discovery and definition, and it has been found that stromal interaction molecules (STIMs) and ORAI family proteins are the two major participants in SOCE (Hogan et al., 2010; Prakriya and Lewis, 2015).

STIM proteins (STIM1 and STIM2) are located on the ER membrane and are essential for SOCE (Williams et al., 2001; Liou et al., 2005; Roos et al., 2005). STIM1 contains an ER-luminal portion (containing two EF-hands and a sterile α -motif (SAM) domain), a single transmembrane segment, and a cytoplasmic portion (containing a coiled-coil domain (CCD), a STIM-Orai-activating region (SOAR) or CRAC activation domain (CAD), a serine- or proline-rich segments and a polybasic (PB) C-tail) (Hogan et al., 2010; Xie et al., 2016). STIM2 has a structure similar to STIM1 but a critical residue difference in the SOAR domain, which endows STIM2 with partial agonist properties and competitive inhibiting functions in STIM1-mediated Ca^{2+} entry, thereby maintaining basal cytoplasmic Ca^{2+} levels by preventing uncontrolled activation of ORAI proteins (Brandman et al., 2007; Wang et al., 2014).

ORAI proteins are plasma membrane (PM) channels that can be gated by STIMs for Ca^{2+} entry during SOCE. Three homologs of ORAI have been identified in humans, namely, ORAI1, ORAI2, and ORAI3 (also called CRACM1-3), among which, ORAI1 is the most potent and has been extensively studied. ORAI1 contains four transmembrane helices (TM1-TM4), an intracellular



location domain (including N-terminal and C-terminal epitope tags) and an extracellular location domain (including an epitope tag introduced into the TM3-TM4 loop). The N-terminus and C-terminus of ORAI1 intracellular sites are essential for the interaction with STIM1 and the opening of the ORAI1 channel (Peinelt et al., 2006; Vig et al., 2006; Hogan et al., 2010; Xie et al., 2016). The homologs, ORAI2 and ORAI3 primarily differ in cytosolic N-terminal, C-terminal and 3–4 loop sequences (Amcheslavsky et al., 2015), and they mediate SOCE in a manner similar to that of ORAI1, but they differ in permeability properties and inactivation (Lis et al., 2007), leading to augmented SOCE efficacy in the order ORAI1 > ORAI2 > ORAI3 (Mercer et al., 2006).

When STIM1 residing in the ER lumen senses a Ca^{2+} decrease in the ER, it initiates conformational changes and oligomerization, overcoming the intracellular autoinhibition mediated by CC1 to expose SOAR/CAD and the PB C-tail. Activated STIM1 multimerizes and migrates toward the PM, where it interacts with the intracellular regions of ORAI1, resulting in ORAI1 activation and Ca^{2+} influx (Figure 1) (Liou et al., 2005; Park et al., 2009; Yuan et al., 2009; Zhou et al., 2010).

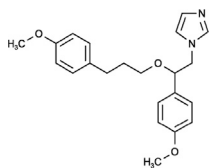
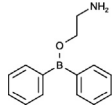
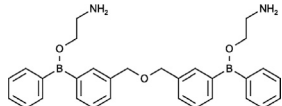
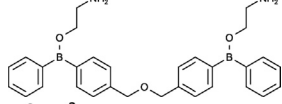
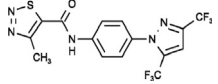
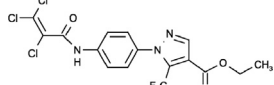
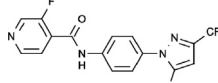
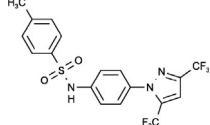
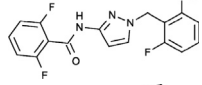
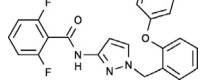
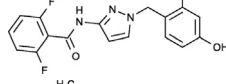
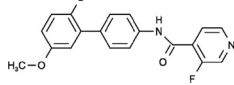
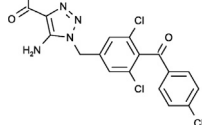
Transient receptor potential proteins (TRPs) contain similar structures, consisting of six transmembrane-helical domains (TM1-TM6) with a loop between TM5 and TM6 and cytoplasmic N- and C-termini (Venkatachalam and Montell, 2007). TRP channels, especially TRPC channels, have been proposed as candidate components of SOCE, although this assignment is still disputed, under certain conditions, several TRPC channels can function in SOCE pathways (Prakriya and Lewis, 2015). For example, in

HEK-293 cells, the knockdown of TRPC1, TRPC3 or TRPC7 dramatically reduced the SOCE activated by passive Ca^{2+} store depletion, while inhibition of TRPC4 or TRPC6 had no effect on SOCs activity (Zagranichnaya et al., 2005). However, in human corneal epithelial cells, mouse endothelial cells and mouse mesangial cells, TRPC4 deficiency decreased SOCE (Tiruppathi et al., 2002; Wang et al., 2004; Yang et al., 2005). Furthermore, TRPC3 and TRPC7 effects on SOCE depend on their expression levels. At low expression levels, they are activated by passive Ca^{2+} store depletion and act as SOCE, while at high expression levels, they behave as Ca^{2+} store-independent Ca^{2+} influx channels (Worley et al., 2007). Therefore, it is necessary to continue to explore the function of TRPCs in SOCE.

Role of Store-Operated Calcium Entry in Cancer

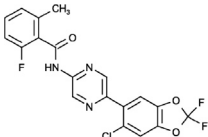
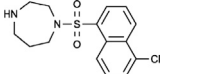
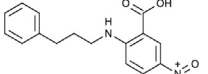
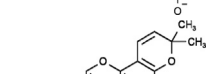
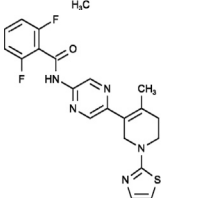
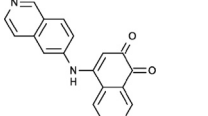
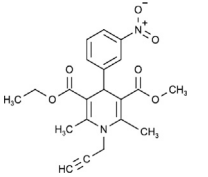
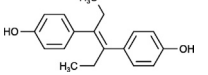
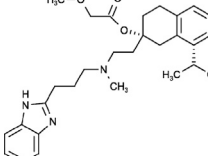
Accumulating evidence has revealed that many cancers, such as breast, liver, lung, gastric, colon, and ovarian cancer, exhibit augmented SOCE and overexpression of STIM1 or ORAI1. SOCE inhibition through STIM1 or ORAI1 knockdown inhibits the proliferation and metastasis of cancer cells, suggesting that SOCE may act as an oncogenic pathway (Yang et al., 2009; Chen et al., 2011; Yoshida et al., 2012; Motiani et al., 2013; Yang et al., 2013; Zhang et al., 2013; Kim et al., 2014; Umemura et al., 2014; Wang et al., 2015; Xu et al., 2015; Schmid et al., 2016; Xia et al., 2016; Goswamee et al., 2018; Wang Y. et al., 2018; Zang et al., 2019; Huang et al., 2020). In addition, SOCE is believed to promote tumor angiogenesis through the increased secretion of VEGF by

TABLE 1 | Structures and IC₅₀ of compounds.

Compound	Structure	IC ₅₀ of SOCE inhibition	References
SKF96365		IC ₅₀ = 10.2 ± 1.2 μM in VSMCs IC ₅₀ = 12 μM in Jurkat T cells IC ₅₀ = 1.2 μM in arterioles IC ₅₀ = 60 μM in PLP-B lymphocyte cells	Zhang et al. (1999) Chung et al. (1994) McGahon et al. (2012) Dago et al. (2018)
2-APB		IC ₅₀ = 4.8 ± 0.6 μM in DT40 cells IC ₅₀ = 3.7 μM as inhibitor, >100 μM as activator in arterioles IC ₅₀ = 3 μM in CHO cells IC ₅₀ = 17 ± 1 μM in human platelets IC ₅₀ = 15 μM in Jurkat T cells	Goto et al. (2010) McGahon et al. (2012) Ozaki et al. (2013) Giambelluca and Gende (2007) Suzuki et al. (2010)
DPB-162AE		IC ₅₀ = 27 ± 2 nM in DT40 cells IC ₅₀ = 190 ± 6 nM in CHO cells IC ₅₀ = 200 nM in HEK293 cells IC ₅₀ = 0.32 μM in Jurkat T cells	Goto et al. (2010) Goto et al. (2010) Hendron et al. (2014) Suzuki et al. (2010)
DPB-163AE		IC ₅₀ = 42 ± 3 nM in DT40 cells IC ₅₀ = 210 ± 20 nM in CHO cells IC ₅₀ = 600 nM in HEK293 cells IC ₅₀ = 0.43 μM in Jurkat T cells	Goto et al. (2010) Goto et al. (2010) Hendron et al. (2014) Suzuki et al. (2010)
BTP2		IC ₅₀ = 100 nM in Jurkat T cells IC ₅₀ = ~10 nM in peripheral blood T-lymphocytes IC ₅₀ = 0.1–0.3 μM in HEK293 cells, DT40 B cells and A7r5 smooth muscle cells IC ₅₀ = 0.59 μM in RBL-2H3 cells	Ishikawa et al. (2003) Zitt et al. (2004) He et al. (2005) Schleifer et al. (2012)
Pyr3		IC ₅₀ = 0.5 μM in E13 cortical neurons IC ₅₀ = 0.54 μM in RBL-2H3 cells	Gibon et al. (2010) Schleifer et al. (2012)
Pyr6		IC ₅₀ = 0.49 μM in RBL-2H3 cells	Schleifer et al. (2012)
Pyr10		IC ₅₀ = 13.08 μM in RBL-2H3 cells	Schleifer et al. (2012)
GSK-5498A		IC ₅₀ = ~1 μM in human embryonic kidney cells IC ₅₀ = 3.7 μM in ASMCs	Rice et al. (2013) Chen and Sanderson (2017)
GSK-5503A		IC ₅₀ = ~4 μM in HEK cells	Derler et al. (2013)
GSK-7975A		IC ₅₀ = ~4 μM in HEK cells IC ₅₀ = 4.1 μM in ASMCs IC ₅₀ = 0.34 μM in HLMCs	Derler et al. (2013) Chen and Sanderson (2017) Ashmole et al. (2012)
Synta66		IC ₅₀ = ~1 μM in Jurkat T cells IC ₅₀ = 3 μM in RBL-1 mast cells IC ₅₀ = 0.25 μM in HLMCs	Di Sabatino et al. (2009) Ng et al. (2008) Ashmole et al. (2012)
CAI		IC ₅₀ = 2~5 μM in Huh-7 cells	Enfissi et al. (2004)

(Continued on following page)

TABLE 1 | (Continued) Structures and IC₅₀ of compounds.

Compound	Structure	IC ₅₀ of SOCE inhibition	References
CM4620		IC ₅₀ = 120 nM for ORAI1/STIM1-mediated SOCE in HEK 293 cells IC ₅₀ = 900 nM for ORAI2/STIM1-mediated SOCE in HEK 293 cells	Wen et al. (2015); Waldron et al. (2019)
ML-9		IC ₅₀ = ~16 μM in HEK293 cells	Smyth et al. (2008)
NPPB		IC ₅₀ = 5 μM in Jurkat T cells	Li et al. (2000)
AnCoA4		Not found	Not found
RO2959		IC ₅₀ = 402 ± 129 nM in RBL-2H3 cells IC ₅₀ = 265 ± 16 nM in CD4 ⁺ T cells	Chen G. et al. (2013) Chen G. et al. (2013)
YZ129		IC ₅₀ = 820 ± 130 nM in HeLa cells	Liu et al. (2019)
MRS-1845		IC ₅₀ = 1.7 μM in HL-60 cells	Harper et al. (2003)
DES		IC ₅₀ = ~1 μM in GBM cells	Liu et al. (2011)
Mibefradil		IC ₅₀ = 52.6, 14.1, and 3.8 μM for ORAI1, ORAI2, and ORAI3 respectively in HEK-293 T-REx cells	Li et al. (2019)

endothelial and cancer cells. For example, in cervical cancer, STIM1 regulates the production of VEGF to control the formation of blood vessels, and the formation of tumor could be impaired by inhibiting STIM1 (Chen et al., 2011). In addition, the potential therapeutic value of targeting SOCE in cancer has further been supported by the fact that STIM- and ORAI- mediated SOCE is essential for the secretion of cytokines and chemokines from T cells, mast cells, and macrophages, as well as in the differentiation and functions of CD4⁺ and CD8⁺ T cells. For example, the inhibition of SOCE by genetic deletion of ORAI1, STIM1, or STIM2 in

murine CD4⁺ T cells impaired Th17 cell function, causing a decrease in the production of IL-17, which is believed to be proinflammatory factor important for tumor progression (Ma et al., 2010; Shaw et al., 2014; Mehrotra et al., 2019). Moreover, as candidate components of SOCE, TRP channels have been found to affect the survival, proliferation, and invasion of cancer cells (Shapovalov et al., 2016). For example, TRPC1 was confirmed to play different roles in tumorigenesis, inhibition of TRPC1 by siRNA or SOCE inhibitors could suppress the proliferation and invasion of cancer cells including nasopharyngeal carcinoma, malignant glioma and

TABLE 2 | Targeting channels of compounds.

Compound	Channel	Mechanism	References
SKF96365	SOCE	Inhibitor	Iwamuro et al. (1999)
	RMCE	Inhibitor	Merritt et al. (1990); Cabello and Schilling (1993)
	TRP channels	Inhibitor	Bennett et al. (2001)
	CCE	Inhibitor	Wu et al. (1999)
2-APB	SOCE IP3R channel	Activator-Low concentration	Peinelt et al. (2008)
	TRP channels	Inhibitor-high concentration inhibitor	Peinelt et al. (2008)
		Activator-TRPV1 TRPV2 TRPV3 TRPM6 TRPC3	Maruyama et al. (1997)
		Inhibitor-TRPC1 TRPC3 TRPC4 TRPC5 TRPC6	Ma et al. (2003); Chung et al. (2004); Hu et al. (2004); Li et al. (2006); Colton and Zhu (2007)
		TRPC7 TRPM2 TRPM3 TRPM7 TRPM8 TRPV3 TRPV6	
			Hu et al. (2004); Poburko et al. (2004); Li et al. (2006); Colton and Zhu (2007); Chokshi et al. (2012)
DPB-162AE	SOCE	Specific inhibitor	Goto et al. (2010); Hendron et al. (2014); Bittremieux et al. (2017)
DPB-163AE	SOCE	Activator-Low concentration	Goto et al. (2010); Hendron et al. (2014)
		Inhibitor-high contraction	Goto et al. (2010); Hendron et al. (2014)
BTP2	SOCE	Inhibitor	Ishikawa et al. (2003)
	CRAC	Inhibitor	Zitt et al. (2004)
	TRPC1	Inhibitor	Oláh et al. (2011)
	TRPC6	Inhibitor	Wu et al. (2017)
	TRPC3	Inhibitor	He et al. (2005)
	TRPC5	Inhibitor	He et al. (2005)
	TRPM4	Activator	Takezawa et al. (2006)
Pyr3	SOCE	Inhibitor	Schleifer et al. (2012)
	TRPC3	Inhibitor	Kiyonaka et al. (2009); Oda et al. (2017); Wang et al. (2019)
Pyr6	SOCE	Inhibitor	Schleifer et al. (2012); Chauvet et al. (2016)
	TRPC3	Inhibitor	Schleifer et al. (2012); Chauvet et al. (2016)
Pyr10	TRPC3	Inhibitor	Schleifer et al. (2012)
GSK (GSK-5503A/GSK-7975A/GSK-5498A)	SOCE	Inhibitor	Yamashita et al. (2007); Derler et al. (2013); Jairaman and Prakriya (2013); Rice et al. (2013); Chen and Sanderson (2017)
	TRPV6	Inhibitor	Owsianik et al. (2006); Jairaman and Prakriya (2013)
Synta66	SOCE	Specific inhibitor	Li et al. (2011)
mAbs	Oral1	Inhibitor	Cox et al. (2013); Lin et al. (2013)
CAI	SOCE	Inhibitor	Sjaastad et al. (1996)
	RMCE	Inhibitor	Hu et al. (1991); Kohn et al. (1994)
	VDCE	Inhibitor	Hu et al. (1991); Kohn et al. (1994)
RP4010	SOCE	Inhibitor	Cui et al. (2018)
CM4620	SOCE	Inhibitor	Wen et al. (2015)
ML-9	Myosin light chain kinases	Inhibitor	Saitoh et al. (1987)
	SOCE	Inhibitor	Smyth et al. (2008); Cui et al. (2017)
	CRAC	Inhibitor	Smyth et al. (2008)
	TRPC5	Inhibitor	Shimizu et al. (2006)
NPPB	CCE	Inhibitor	Gericke et al. (1994)
	CRAC	Inhibitor	Li et al. (2000)
AnCoA4	SOCE	Inhibitor	Sadaghiani et al. (2014)
RO2959	SOCE	Inhibitor	Chen G. et al. (2013)
YZ129	NFAT	Inhibitor	Liu et al. (2019)
MRS-1844/MRS-1845	SOCE	Inhibitor	Harper et al. (2003); van Kruchten et al. (2012)
	L-type channels	Inhibitor	Harper et al. (2003)
DES	SOCE	Inhibitor	Zakharov et al. (2004); Ohana et al. (2009); Dobrydneya et al. (2010)
NSAIDs	SOCE	Inhibitor	Núñez et al. (2006)
Mibefradil	SOCE	Inhibitor	Li et al. (2019)

non-small-cell lung carcinoma (Bomben and Sontheimer, 2010; He et al., 2012; Tajeddine and Gailly, 2012).

In summary, SOCE promotes the proliferation and metastasis of cancer cells, and enhances tumor angiogenesis and the formation of a tumor-promoting inflammatory environment.

Inhibition of SOCE may be a potential and effective therapy for cancers. In this review, we summarize the available inhibitors of SOCE (Tables 1, 2), discuss their effects and possible mechanisms (Table 3), and introduce a new viewpoint on the treatment of cancer.

TABLE 3 | SOCE inhibitors in cancer research.

Compound	Cancer type	Cell lines	Major effect	Possible mechanisms	References
SKF96365	MG astrocytoma	U373	Inhibition of cell growth	Promotes the accumulation of [3H] IP1 and inhibits the mobilization of intracellular Ca^{2+}	Lee et al. (1993); Arias-Montaña et al. (1998)
	Cervical cancer	Hela	Inhibition of cell growth and cell migration	Promotes the accumulation of [3H]IP1	Arias-Montaña et al. (1998); Chen Y.-T. et al. (2013)
		SiHa		Inhibits the activation of non-muscle myosin II and the formation of actomyosin via blocking SOCE channel	
	Neuroblastoma	SK-N-MC	Inhibition of cell growth	Inhibits the mobilization of intracellular Ca^{2+}	Lee et al. (1993)
	Gastric cancer	AGS and MKN45	Inhibition of cell growth and tumor formation	Arrests cell cycle in G2/M phase	Cai et al. (2009)
	Nasopharyngeal carcinoma	CNE2 and HONE1	Inhibition of cell proliferation and colony formation, promotion of apoptosis and cell-cycle	Distracts the transduction of oncogenic Ca^{2+} signaling	Zhang et al. (2015)
	Colorectal cancer	HCT116 and HT29	Inhibition of cell growth and tumor formation, inducement of apoptosis, cell-cycle and autophagy	Inhibits the calcium/CaMKII γ /AKT-mediated pathway	Jing et al. (2016)
	Prostate cancer	DU145 and PC3	Inhibition of the survival and proliferation	Inhibits AKT/mTOR pathway and induces autophagy	Selvaraj et al. (2016)
	Multiple myeloma	KM3 and U266	Inhibition of cell viability and proliferation, inducement of apoptosis	Arrests cell cycle in G2/M phase. Induces the reduction of $[Ca^{2+}]_i$	Wang W. et al. (2018)
	Ovarian cancer	SKOV3	Inhibition of cell proliferation	Arrests cell cycle in G2/M phase through inhibiting TRPC channels	Zeng et al. (2013)
	Glioma and glioblastoma	U251, U87, D54MG, LN-229, T98G, U373	Inhibition of cell growth and colony formation. Increase in the sensitivity to irradiation	Inhibits TRPC channels. Arrests cell cycle in G2/M phase	Bomben and Sontheimer (2008); Ding et al. (2010); Song et al. (2014)
	Breast tumor	MDA-MB-231	Inhibition of cell migration, inhibition of tumor Metastasis in mice	Impairs the assembly and disassembly of focal adhesions	Yang et al. (2009)
	Melanoma	WM793	Inhibition of cell invasion	Blocks the formation, activity of invadopodium	Sun et al. (2014)
	Non-small cell lung cancer	A549	Inhibition of cell migration and proliferation	Inhibits TRPC channels and SOCE channel	Wang Y. et al. (2018)
2-APB	Rhabdomyosarcoma (RMS)	RD, RH30	Inhibition of cell proliferation, migration and invasion	Inhibits SOCE channel	Schmid et al. (2016)
	Melanoma	WM793	Inhibition of cell invasion and lung metastasis	Blocks the formation, activity and maturation of invadopodium	Sun et al. (2014)
	Cervical cancer	SiHa	Inhibition of cell migration	Inhibits actomyosin formation and cellular contractile force via blocking SOCE channel	Chen Y.-T. et al. (2013)
	Ovarian cancer	SKOV3	Inhibition of cell proliferation	Inhibits TRPC channels	Zeng et al. (2013)
	Breast cancer	MDA-MB-231, AU565, T47D	Inhibition of cell viability and proliferation	Arrests cell cycle in S phase	Liu et al. (2020)
	Prostate cancer	DU145, PC3	Inhibition of cell migration	Inhibits EMT via blocking TRPM7 channel activity	Sun et al. (2018)
	Glioma and glioblastoma	D54MG, U87	Inhibition of cell development, migration and invasion	Inhibits SOCE channel and TRPC channels (TRPC1, TRPC3, TRPC5, TRPC6)	Bomben and Sontheimer (2008); Shi et al. (2015)
	GBM (Glioblastoma multiforme)	A172	Inhibition of cell proliferation, migration and invasion	Inhibits TRPM7 channel	Leng et al. (2015)
	Nasopharyngeal carcinoma	CNE2, 5-8F, 6-10B	Inhibition of cell migration and invasion	Inhibits TRPC1 and TRPM7 channel	Chen et al. (2010); He et al. (2012)
		HK1	Inhibition of angiogenesis	Inhibits VEGF production and endothelial tube formation by blocking SOCE	Ye et al. (2018)
	Non-small-cell lung cancer (NSCLC)	H1975, A549, LLC-1	Inhibition of primary and metastatic Lewis lung cancer	Inhibits intracellular Ca^{2+} mobilization	Qu et al. (2018)

(Continued on following page)

TABLE 3 | (Continued) SOCE inhibitors in cancer research.

Compound	Cancer type	Cell lines	Major effect	Possible mechanisms	References
BTP2	Colon cancer	HT29	Inhibition of cell growth	Inhibits SOCE channel and transcription cycling of topoisomerase-II α	Núñez et al. (2006)
	Cervical cancer	SiHa	Inhibition of cell migration	Inhibits actomyosin formation and cellular contractile force via blocking SOCE channel	Chen Y.-T. et al. (2013)
	Rhabdomyosarcoma (RMS)	RD, RH30	Inhibition of cell proliferation, migration and invasion	Inhibits SOCE channel	Schmid et al. (2016)
	Breast cancer	MDA-MB-468	Inhibition of cell proliferation, migration and invasion	Inhibits SOCE channel	Azimi et al. (2018)
	Prostate cancer	PC-3	Inhibition of cell invasion	Inhibits drebrin to bind to actin filaments	Dart et al. (2017)
Pyr3	triple negative breast cancer	MDA-MB-231	Inhibition of cell proliferation, inducement of apoptosis and cell death	Affects the TRPC3/RASA4/MAPK Pathway	Wang et al. (2019)
	Melanoma	C8161	Inhibition of cell proliferation and migration	Inhibits TRPC3 channel	Oda et al. (2017)
	Glioblastoma multiforme	LN229, U87	Inhibition of cell proliferation, migration and invasion	Dephosphorylates focal adhesion kinase and myosin light chain via inhibiting TRPC3 channel	Chang et al. (2018)
CAI	Melanoma	A2058	Inhibition of cell proliferation, adhesion and motility Inhibition growth and metastasis of transplanted xenografts	Inhibits the receptor-mediated stimulation of effector enzymes Inhibits calcium fluxes, arachidonic acid release, and phosphoinositides generation	Kohn and Liotta (1990); Kohn et al. (1992)
	Breast cancer	MDA-MB-231	Inhibition of cell proliferation, adhesion and motility	Inhibits the receptor-mediated stimulation of effector enzymes	Kohn and Liotta. (1990)
	Ovarian cancer	OVCAR-3	Inhibition of cell proliferation, adhesion and motility Inhibition growth and metastasis of transplanted xenografts	Inhibits the receptor-mediated stimulation of effector enzymes Inhibits calcium fluxes, arachidonic acid release, and phosphoinositides generation	Kohn and Liotta (1990); Kohn et al. (1992)
	Colon cancer	HT-29	Inhibition of the formation and growth of experimental pulmonary metastases in nude mice	Inhibits calcium fluxes, arachidonic acid release, and phosphoinositides generation	Kohn et al. (1992)
	Prostate cancer	DU-145, PPC-1, PC3, LNCaP	Inhibition of cell proliferation	Inhibits calcium fluxes and PSA production	Wasilenko et al. (1996)
	Glioblastoma	A172, T98G, U87, H4, U251	Inhibition of cell proliferation and adhesion	Inhibits calcium fluxes and calcium-sensitive signal transduction pathways	Jacobs et al. (1997)
	Head and neck squamous cell carcinoma	EVSCC14/17M, EVSCC19M, EVSCC18, UMSSC10A, FaDu	Inhibition of cell growth and invasion	Inhibits calcium fluxes	Wu et al. (1997)
	Hepatoma	Hep G2, Huh-7	Inhibition of cell proliferation	Inhibits calcium entry	Enfissi et al. (2004)
	Small cell lung cancer	NCI-H209, NCI- H345	Inhibition of cell growth, inhibition of xenograft proliferation in nude mice	Inhibits calcium fluxes Inhibits the angiogenesis	Moody et al. (2003)
	Chronic myeloid leukemia	32D P210, 32D E255K	Inhibition of cell growth and decrease of BCR-ABL	Inhibits calcium influxes and signal transduction	Corrado et al. (2011)
	Liver metastases from B16F1 melanoma	B16F1	Decrease of the volume size and angiogenesis of tumor	Reduces the number of microvessels/mm ² and microvessel size	Luzzi et al. (1998)
	Lewis lung carcinoma	LLC cell	Inhibition of cell growth	Inhibits production of pro-inflammatory cytokines in TAMs	Ju et al. (2012)
	Melanoma	OVA-B16	Inhibition of tumor growth	Activates the CD8 ⁺ T cells and stimulates IDO1-Kyn metabolic circuitry	Shi et al. (2019)
	Esophageal cancer	KYSE-30, KYSE-150, KYSE-790, KYSE-190	Inhibition of cell proliferation and tumor growth	Inhibits SOCE channel-mediated Ca ²⁺ oscillations	Cui et al. (2018)
	Pancreatic ductal adenocarcinoma	L3.6pl, BxPC-3, MiaPaCa-2	Inhibition of cell proliferation and colony formation	Inhibits CRAC channel	Khan et al. (2020)

(Continued on following page)

TABLE 3 | (Continued) SOCE inhibitors in cancer research.

Compound	Cancer type	Cell lines	Major effect	Possible mechanisms	References
ML-9	Pancreatic cancer	MIA PaCa-2, Panc1, BxPC3	Inhibition of cell invasion and adhesion	Inhibits MLCK to decrease the activity of cytoskeleton	Kaneko et al. (2002)
	Prostate cancer	LNCaP, PC3, DU-145	Inducement of prostate cell death	Stimulates autophagy via modulating Ca^{2+} homeostasis	Kondratskiy et al. (2014)
NPPB	Ovarian cancer	A2780	Inhibition of cell adhesion and invasion	Inhibits chloride channels leading to inhibition of $[\text{Ca}^{2+}]_i$	Li et al. (2009)
YZ129	Glioblastoma	U87	Inhibition of cell proliferation, migration and mobility	Inhibits calcineurin-NFAT pathway	Liu et al. (2019)
NSAIDs	Colon cancer	HT29	Inhibition of cell growth	Inhibits SOCE channel and COX-2 expression	Núñez et al. (2006); Wang et al. (2015)

STORE-OPERATED CALCIUM ENTRY-TARGETED COMPOUNDS IN THE APPLICATION OF CANCER TREATMENT

SKF 96365

(1-[2-(4-Methoxyphenyl)-2-[3-(4-Methoxyphenyl)propoxy]ethyl]imidazole;hydrochloride)

SKF 96365 is structurally distinct from classic Ca^{2+} antagonists, drugs or compounds that inhibit Ca^{2+} entry by directly inhibiting Ca^{2+} channels or affecting Ca^{2+} pools. It shows selectivity in blocking receptor-mediated Ca^{2+} entry (RMCE), the Ca^{2+} influx that is independent of depolarization and caused by receptor occupation, leading to a significant increase in $[\text{Ca}^{2+}]_i$ biologically, with no impact on internal Ca^{2+} release in platelets, neutrophils or endothelial cells (Spedding, 1982; Merritt et al., 1990; Cabello and Schilling, 1993), and the inhibition of RMCE exerted by SKF 96365 could inhibit $[\text{3H}]$ -thymidine incorporation, interleukin-2 (IL-2) synthesis and cell proliferation of peripheral blood lymphocytes (Chung et al., 1994). It was also found that SKF 96365 could block store-independent TRP channels in osteoclasts and capacitative Ca^{2+} entry (CCE) in astrocytes (Wu et al., 1999; Bennett et al., 2001).

Iwamuro et al. found, for the first time, that SKF 96365 sensitively inhibited the SOCE activated by ET-1 at high concentrations (Iwamuro et al., 1999). As a SOCE inhibitor, SKF 96365 was reported to inhibit cell proliferation in many cancers by inducing cell apoptosis and cell cycle arrest in G2/M phase (Nordström et al., 1992; Lee et al., 1993; Arias-Montaña et al., 1998; Cai et al., 2009; Zeng et al., 2013; Zhang et al., 2015; Jing et al., 2016; Wang W. et al., 2018). Autophagy seems to play different roles in the pharmacological mechanism of SKF 96365. Inhibition of SOCE by SKF 96365 inhibited the AKT/mTOR pathway, induced autophagic cell death and decreased the survival, and proliferation of PC3 and DU145 prostate cancer cells (Selvaraj et al., 2016), while in colorectal cancer cells, SKF 96365 was reported to induce cytoprotective autophagy to delay apoptosis through the inhibition of calcium/calmodulin-dependent protein kinase II γ (CaMKII γ)/AKT signaling cascade, and autophagy inhibition could significantly augment the anticancer effect of SFK 96365 in mouse xenograft models (Jing et al., 2016).

In addition, SKF 96365 could also effectively inhibit the metastasis of cancers. It could impair the assembly and

disassembly of focal adhesions of breast cancer cells (Yang et al., 2009), block the formation and activity of invadopodium in melanoma cells (Sun et al., 2014), and it could also inhibit cell migration by inactivating non-muscle myosin II and reducing actomyosin formation and contractile force in cervical and non-small cell lung cancer (NSCLC) cells (Chen Y.-T. et al., 2013; Wang Y. et al., 2018). In addition to inhibiting growth and colony formation independently through the blockage of Ca^{2+} channels, for example, through the blockage of TRPC channels in glioma cells (Bomben and Sontheimer, 2008; Ding et al., 2010; Song et al., 2014), SKF 96365 could also enhance the sensitivity of glioma cell lines to irradiation (Ding et al., 2010), suggesting that SKF 96365 may be developed not only as an anti-chemotherapy, but also as an adjuvant drug for radiotherapy.

In summary, the antineoplastic effects of SKF 96345 are universal. However, it has been confirmed that its effects are nonspecific (Franzius et al., 1994), and therefore it is necessary to conduct more studies to clearly delineate its specific mechanisms.

2-Aminoethoxydiphenyl Borate and Analogs

2-APB (2-Diphenylboranyloxyethanamine)

Initial studies reported that 2-APB, as a novel membrane-penetrable modulator, inhibited Ca^{2+} release induced by IP_3 without affecting IP_3 binding to IP_3R ($\text{IC}_{50} = 42 \mu\text{M}$) (Maruyama et al., 1997). Subsequently, 2-APB was found to be a reliable blocker of SOCE but an inconsistent inhibitor of IP_3 -induced Ca^{2+} release. With further study, it was found that 2-APB could exert both stimulatory and inhibitory effects on Ca^{2+} influx through CRAC channels: at low concentrations (1–5 μM), it activated SOCE pathway, while at high concentrations ($\geq 10 \mu\text{M}$), it blocked SOCE pathway completely (Prakriya and Lewis, 2001). The mechanisms of the dual effects of 2-APB on SOCE are also complicated: 2-APB could inhibit STIM1 directly by facilitating the coupling between CC1 (coiled-coil 1) and SOAR (STIM-ORAI-activating region) of STIM1. On the other hand, 2-APB could also impair the functions of STIM1 indirectly by interrupting the coupling between STIM1 and the mutant, ORAI1-V102C (Peinelt et al., 2008; Wei et al., 2016). Moreover, 2-APB could directly gate and dilate the pore diameter

of ORAI1 and ORAI3 to regulate SOCE pathway without affecting STIM1 (DeHaven et al., 2008; Peinelt et al., 2008; Schindl et al., 2008; Yamashita et al., 2011; Amcheslavsky et al., 2014; Xu et al., 2016; Kappel et al., 2020). 2-APB also exerts multifaceted effects on transient receptor potential (TRP) channels (Colton and Zhu, 2007). It was reported that 2-APB could act as an agonist of TRPV1, TRPV2, TRPV3, TRPM6, and TRPC3 channels (Ma et al., 2003; Chung et al., 2004; Hu et al., 2004; Li et al., 2006), however, it exerted inhibitory roles on TRPC1, TRPC3, TRPC4, TRPC5, TRPC6, TRPC7, TRPM2, TRPM3, TRPM7, TRPM8, TRPV3, and TRPV6 channels (Hu et al., 2004; Poburko et al., 2004; Lievreumont et al., 2005; Xu et al., 2005; Li et al., 2006; Bomben and Sontheimer, 2008; Togashi et al., 2008; Chokshi et al., 2012; Kovacs et al., 2012; Singh et al., 2018). Among these TRP channels, 2-APB could close the TRPV6 channel through protein–lipid interactions by binding to TRPV6 directly, and TRPV3 also was found to undergo similar structural changes triggered by 2-APB (Singh et al., 2018; Zubcevic et al., 2018).

When used as a blocker of SOCE at high concentrations, 2-APB displayed anticancer effects on rhabdomyosarcoma (RMS), nasopharyngeal carcinoma (NPC), prostate cancer, ovarian cancer, breast cancer, glioblastoma, lung cancer, melanoma, and cervical cancer (Bomben and Sontheimer, 2008; Chen Y.-T. et al., 2013; Zeng et al., 2013; Sun et al., 2014; Leng et al., 2015; Shi et al., 2015; Schmid et al., 2016; Sun et al., 2018; Liu et al., 2020). For instance, in breast cancer, 2-APB inhibited cell viability, and proliferation through inhibiting TRPM7 channel by arresting cell cycle in S phase not by promoting cell death (Liu et al., 2020). In melanoma and cervical cancer, 2-APB could reduce migration and invasion by inhibiting actomyosin formation, invadopodium assembly and maturation, through mechanisms similar to those of SKF 96365 action (Chen Y.-T. et al., 2013; Sun et al., 2014). 2-APB in NPC could also attenuate adhesive and invasive abilities by inhibiting TRPC1 and TRPM7 (Chen et al., 2010; He et al., 2012). Furthermore, it was reported that 2-APB could effectively antagonize the angiogenesis of NPC *in vivo* by inhibiting VEGF production and endothelial tube formation through the blockage of SOCE (Ye et al., 2018). In another study, 2-APB sensitized NSCLC cells to the antitumor effect of bortezomib (BZM) via suppression of Ca²⁺-mediated autophagy (Qu et al., 2018).

These effects suggest that 2-APB is attractive as a potentially potent therapy for primary cancer and metastatic cancer.

2-Aminoethoxydiphenyl Borate and Analogs

As 2-APB is a promising but not entirely specific SOCE inhibitor, Goto et al. explored two novel 2-APB structurally isomeric analogs in order to develop more specific and potent SOCE inhibitors: DPB-162AE and DPB-163AE (Goto et al., 2010). These two diphenylborinate (DPB) compounds are 100-fold more potent than 2-APB, and they are able to inhibit the clustering of STIM1 and block the ORAI1 or ORAI2 activity induced by STIM1 by inactivating the SOAR domain in STIM1. In particular, DPB-162 AE could consistently inhibit endogenous

SOCE regardless of whether the concentration was high or low and exerted little effect on L-type Ca²⁺ channels, TRPC channels, or Ca²⁺ pumps when exerting maximal inhibitory effect on Ca²⁺ entry (Goto et al., 2010; Hendron et al., 2014; Bittremieux et al., 2017). However, the actions of DPB-163AE are more complex, showing a similar pattern to 2-APB by activating SOCE at low concentrations and inhibiting SOCE at higher levels (Goto et al., 2010).

Moreover, similar to 2-APB, at low concentrations (~100 nM), both DPB-162AE and DPB-163AE could facilitate Orai3 currents, and at high concentrations (>300 nM), they transiently activated ORAI3 currents and then deactivated them. DPB compounds have been proven to activate ORAI3 in a STIM1-dependent manner, but they could not change the pore diameter of ORAI3, which is different from the mechanisms of 2-APB. It is speculated that because they are larger than 2-APB, DPB compounds are unable to enter the pore of ORAI3 (Goto et al., 2010; Hendron et al., 2014). In addition, DPB-162AE was reported to provoke leakage of Ca²⁺ from the ER into the cytosol in HeLa and SU-DHL-4 cells at concentrations required for adequate SOCE inhibition (Hendron et al., 2014; Bittremieux et al., 2017).

Although there have been no studies on DPB compounds with respect to cancer treatment to date, considering the specific inhibition of SOCE, DPB compounds are expected to be developed as potential anticancer drugs.

Pyrazole Derivatives

Pyr2 (N-[4-[3,5-Bis(trifluoromethyl)pyrazol-1-yl]phenyl]-4-Methylthiadiazole-5-Carboxamide)

Pyr2, also known as BTP2 or YM-58483, was initially found to be able to inhibit SOCE, leading to impaired IL-2 production and NFAT dephosphorylation in Jurkat cells without affecting the T cell receptor (TCR) signal transduction cascade (Ishikawa et al., 2003). BTP2 also showed complicated effects on TRP channels, TRPC1, TRPC3, TRPC5, and TRPC6 channels were inhibited effectively; however, TRPM4 was activated by BTP2 at low concentrations in a dose-dependent manner. BTP-mediated facilitation of TRPM4, which is a Ca²⁺-activated cation channel that decreases Ca²⁺ influx by depolarizing lymphocytes, is the main mechanism for the suppression of cytokine release. Furthermore, it has been reported that the mechanism of inhibiting TRP channels, such as TRPC3 and TRPC5, involved in reducing their open probability rather than changing their pore properties without affecting the other Ca²⁺ signals in T cells including Ca²⁺ pumps, mitochondrial Ca²⁺ signaling and ER Ca²⁺ release (Zitt et al., 2004; He et al., 2005; Schwarz et al., 2006; Takezawa et al., 2006; Oláh et al., 2011; Wu et al., 2017).

BTP2 has exhibited inhibitory effects on several types of allergic inflammation, including autoimmune and antigen induced diseases through the suppression of cytokine release (IL-2, IL-4, IL-5, TNF- α , and IFN- γ) and T cell proliferation (Ohga et al., 2008; Law et al., 2011; Geng et al., 2012). Although many studies have indicated that BTP2 affects cancer through the modulation of immune cells, previous reports have mainly focused on the direct inhibition of cell proliferation, migration, and invasion of cancer cells themselves. For example, in colon cancer, BTP2 obviously decreased cell growth through direct

SOCE inhibition (Núñez et al., 2006). BTP2 could also inhibit cell migration of cervical cancer, rhabdomyosarcoma (RMS), and breast cancer via blockage of SOCE (Chen Y.-T. et al., 2013; Schmid et al., 2016; Azimi et al., 2018); furthermore, the inhibition of cell migration in cervical cancer was due to the inhibition of actomyosin reorganization and contraction forces, similar to the effects of SKF96365 and 2-APB (Chen Y.-T. et al., 2013). It was also found that BTP2 could inhibit the proliferation and tubulogenesis of endothelial progenitor cells (EPCs), which are essential for the vascularization and metastatic switching of solid tumors (Dragoni et al., 2011; Lodola et al., 2012). On the other hand, BTP2 could inhibit the invasion of prostate cancer cells by impeding the binding of drebrin to actin filaments, with a SOCE independent mechanism (Dart et al., 2017).

In summary, the mechanism and effect of BTP2 on cancer are multi-aspect, and it is necessary to carry out further research on them for clarification.

Pyr3 (Ethyl-1-(4-(2,3,3-Trichloroacrylamido)phenyl)-5-(Trifluoromethyl)-1h-Pyrazole-4-Carboxylate)

Pyr3 has mainly been recognized for directly and selectively inhibiting TRPC3 with attenuated activation of Ca^{2+} -dependent signaling pathways, and structure-function relationship studies showed that the trichloroacrylic amide group is important for the TRPC3 selectivity of Pyr3 (Kiyonaka et al., 2009). The blockade of TRPC3-mediated Ca^{2+} signaling pathways by Pyr3 reduced cell proliferation, induced cell apoptosis and sensitized cell death to chemotherapeutic agents in triple-negative breast cancer through the inhibition of TRPC3-Ras GTPase-activating protein 4 (RASA4)-MAPK signaling cascade (Wang et al., 2019). In melanoma, Pyr3 also decreased the cell proliferation and migration *in vitro* and inhibited tumor growth *in vivo* by inhibiting TRPC3 and its downstream JAK/STAT5 and AKT pathways (Oda et al., 2017). Chang et al. reported that Pyr3 could inhibit the migration and invasion of glioblastoma multiforme (GBM) cells and reduce the size of tumor xenografts significantly by dephosphorylating focal adhesion kinase and myosin light chain (Chang et al., 2018). Subsequently, Pyr3 was found to effectively inhibit ORAI1-mediated SOCE in HEK293 cells and mast cells (RBL-2H3) in a dose dependent manner, and the amid-bond linked side-group pivotal for TRPC subtype selectivity was also proposed as a potential structural determinant for the SOCE inhibitory action (Schleifer et al., 2012).

Pyr6 and Pyr10 (N-[4-[3,5-Bis(trifluoromethyl)pyrazol-1-yl]phenyl]-3-Fluoropyridine-4-Carboxamide), (N-[4-[3,5-Bis(trifluoromethyl)pyrazol-1-yl]phenyl]-4-Methylbenzenesulfonamide)

It was reported that Pyr6 could inhibit both ORAI1-mediated SOCE and TRPC3 channels in mast cells leading to the suppression of mast cell activation, however, its effect on SOCE inhibition was 37-fold times that of TRPC3 inhibition, and it differed from the effect of Pyr10, which could specifically inhibit TRPC3 and had no effect on SOCE (Schleifer et al., 2012; Chauvet et al., 2016), thereby suggesting that Pyr6 and Pyr10 can be used as valuable tools to distinguish SOCE and TRPC3 channels.

GSK-5503A, GSK-7975A and GSK-5498A (2,6-Difluoro-N-[1-[(2-Phenoxyphenyl)methyl]pyrazol-3-yl]benzamide), (2,6-Difluoro-N-[1-[[4-Hydroxy-2-(trifluoromethyl)phenyl]methyl]pyrazol-3-yl]benzamide), (2,6-Difluoro-N-[1-[[2-Fluoro-6-(trifluoromethyl)phenyl]methyl]pyrazol-3-yl]benzamide)

Several novel pyrazole compounds including GSK-5503A, GSK-7975A, and GSK-5498A have been developed by GlaxoSmithKline as specific blockers of SOCE. GSK-5503A and GSK-7975A could inhibit STIM1-mediated ORAI1 and ORAI3 currents potentially via an allosteric effect on the selectivity filter of ORAI with a slow onset of action that did not have effects on STIM1-STIM1 oligomerization or STIM1-ORAI1 coupling (Yamashita et al., 2007; Derler et al., 2013). GSK-7975A could also efficiently inhibit the TRPV6 channel, possibly due to its architectural similarities to the selectivity filters of ORAI channels (Owsianik et al., 2006; Derler et al., 2013; Jairaman and Prakriya, 2013). GSK-5498A and GSK-7975A have been used to inhibit mediator and cytokine release from mast cells and T cells (such as IFN- γ and IL2) in multiple human and rat preparations by completely inhibiting SOCE (Rice et al., 2013). Although the roles of immune cells and cytokines are complicated in the tumor microenvironment, these compounds are expected to be applied as cancer treatments that function through anticancer immunity processes under certain circumstances.

Synta66 (N-[4-(2,5-Dimethoxyphenyl)phenyl]-3-Fluoropyridine-4-Carboxamide)

Synta66, also known as GSK1349571A, has garnered extensive attention in recent years because of its ability to selectively inhibit CRAC channels without affecting on PDGF- or ATP-evoked Ca^{2+} release, overexpressed TRPC5 channels, native TRPC1/5-containing channels, STIM1 clustering or nonselective store-operated cationic currents (Li et al., 2011). It has been confirmed that the potency of SOCE inhibition is directed against Orail in the order of Synta66 > 2-APB > GSK-7975A > SKF96365 > MRS1845 in human platelets (van Kruchten et al., 2012). By inhibiting SOCE effectively and specifically, Synta66 could inhibit the receptor-triggered mutual activation between Syk activation and Ca^{2+} influx in the RBL mast cell line, reduce the release of histamine, leukotriene C_4 (LTC_4), and cytokines (such as IL-5, IL-8, IL-13, and TNF- α) in human lung mast cells (HLMCs), and inhibit the expression of T-bet and the production of IL-2, IL17, and IFN- γ in lamina propria mononuclear cells (LPMCs) and biopsy specimens obtained from inflammatory bowel disease (IBD) patients (Ng et al., 2008; Di Sabatino et al., 2009; Ashmole et al., 2012). Azimi et al. compared the pharmacological inhibitory effects of Synta66 and BTP2 on SOCE pathway in breast cancer cell lines. They found that both Synta66 and BTP2 could inhibit the protease activated receptor 2 (PAR2) activator, and trypsin and EGF produced Ca^{2+} influx and serum-activated migration of MDA-MB-468 cells (Azimi et al., 2018). However, interestingly, Synta66, but not BTP2, had no effect on proliferation or EGF-activated cell migration, which are realized through unexplored mechanisms (Azimi et al., 2018). To date, no study has investigated whether Synta66 has anti-tumor effects in other cancers, nevertheless, Synta66 still has great potential to be

developed as an available therapy for tumor treatment due to its specific and effective inhibition of SOCE.

Monoclonal Antibodies

Anti-ORAI1 Monoclonal Antibodies

Lin et al. developed high-affinity fully human mAbs to human ORAI1, that bind to amino acid residues 210–217 of the human ORAI1 extracellular loop 2 domain (ECL2). These mAbs potently inhibited the SOCE, NFAT translocation and cytokine secretion from Jurkat T cells and in human whole blood (Lin et al., 2013). Another mAb to human native ORAI1, generated by Cox, also binds to ECL2 and could block the function of T cells both *in vitro* and *in vivo*, including the inhibition of T cell proliferation and cytokine production in immune cells isolated from rheumatoid arthritis patients and showed efficacy on an anti-ORAI1 human T cell-mediated graft-versus host disease (GvHD) mouse model (Cox et al., 2013), suggesting that mAb may be a novel treatment for humans with autoimmune diseases. Taken together, since anti-ORAI1 mAbs could impact on the autoimmune response, we speculate that they also show great potential to be used as cancer therapy by modulating of the tumor immune microenvironment.

Inhibitors in Clinical Trials

Carboxyamidotriazole (5-Amino-1-[[3,5-Dichloro-4-(4-Chlorobenzoyl)phenyl]methyl]triazole-4-Carboxamide) CAI (carboxyamidotriazole), also called L-651582, is one of the SOCE inhibitors that has been evaluated in clinical trials. It was initially developed as a coccidiostat and was confirmed to inhibit calcium influx, including SOCE, RMCE and VDCE (Hupe et al., 1991; Kohn et al., 1994; Sjaastad et al., 1996). Through the inhibition of Ca^{2+} influx and related signaling processes, such as receptor-associated tyrosine phosphorylation, arachidonic acid generation, and nucleotide biosynthesis, CAI displayed effective anticancer effects, including antiproliferative, antimigratory, antiangiogenic and antimetastatic properties, in a broad range of human tumors, including melanoma, glioblastoma, head and neck squamous cell carcinoma (HNSCC), hepatoma, small cell lung cancer (SCLC), chronic myelogenous leukemia (CML), and ovarian, breast, colon and prostate cancer (Kohn and Liotta, 1990; Kohn et al., 1992; Wasilenko et al., 1996; Jacobs et al., 1997; Wu et al., 1997; Luzzi et al., 1998; Moody et al., 2003; Enfissi et al., 2004; Corrado et al., 2011). Moreover, CAI could exert its anti-tumor activity through modulation of the tumor immune microenvironment by inhibiting proinflammatory cytokine production (such as $\text{TNF-}\alpha$) in tumor-associated macrophages (TAMs), promoting $\text{IFN-}\gamma$ release from activated CD8^+ T cells or stimulating the IDO1-Kyn metabolic circuitry (Ju et al., 2012; Shi et al., 2019).

As a potential anticancer drug, CAI has been tested in phase I/II/III clinical trials, some of which showing that CAI could stabilize and improve the condition of patients with pancreaticobiliary carcinomas, melanoma, non-small cell lung cancer, epithelial ovarian cancer, prostate cancer, glioblastoma and other anaplastic gliomas while exhibiting a limited toxicity profile (Figg et al., 1995; Kohn et al., 1996; Bauer et al., 1999; Hussain et al., 2003; Hillman et al., 2010; Das, 2018; Omuro et al., 2018). However, its performance was barely satisfactory in many

clinical trials, preventing it from being a first-line chemotherapy drug (Stadler et al., 2005).

RP4010

RP4010 was developed by Rhizen Pharmaceuticals. It was confirmed to block SOCE and SOCE-mediated Ca^{2+} oscillations in a dose-dependent manner, leading to the inhibition of NF- κ B/p65 translocation to nuclei, thus impeding the proliferation and in ESCC xenograft tumor growth (Cui et al., 2018). In pancreatic ductal adenocarcinoma, RP4010 inhibited cancer cell proliferation and colony formation by reducing Akt/mTOR and Ca^{2+} influx-mediated NFAT signaling. Furthermore, RP4010 combined with gemcitabine and nab-paclitaxel could enhance anticancer activities in PDAC cells and patient-derived xenografts, indicating the potential of RP4010 as an anticancer chemotherapy (Khan et al., 2020). Indeed, RP4010 is in phase I/IB clinical trials currently.

CM4620 (N-[5-(6-Chloro-2,2-Difluoro-1,3-Benzodioxol-5-yl)pyrazin-2-yl]-2-Fluoro-6-Methylbenzamide)

CM4620, also called CM-128, was developed by CalciMedica and tested in phase I/II clinical trials to reduce pancreatitis. It could inhibit cell death pathway activation by SOCE inhibition in pancreatic acinar cells, thus leading to markedly reduced acute pancreatitis in mouse models (Wen et al., 2015). A recent study further demonstrated that in acute pancreatitis, CM4620 could not only inhibit the necrosis of parenchymal pancreatic acinar cells but could also prevent the activation of immune cells to reduce inflammation (Waldron et al., 2019). Although the effect of CM4620 on cancer cells is still unknown, it has the potential to be developed as a cancer therapy through its regulation of tumor immune cells.

Other Small Molecular Inhibitors

ML-9 (1-(5-chloronaphthalen-1-yl)sulfonyl-1,4-diazepane) was initially described as an inhibitor of myosin light chain kinases (MLCKs) that binds at or near the ATP-binding site at the active center of kinases with or without Ca^{2+} calmodulin (Saitoh et al., 1987). Shortly thereafter, ML-9 was found to inhibit agonist-stimulated Ca^{2+} entry in endothelial cells without affecting the release of intracellular Ca^{2+} stores (Watanabe et al., 1996), and it was confirmed to inhibit SOCE in a dose-dependent manner by blocking rearrangement and puncta formation of STIM1 without inhibiting MLCKs. Thus far, ML-9 is the only inhibitor of STIM1 translocation (Smyth et al., 2008). Furthermore, ML-9 could also inhibit the activity of TRPC5 channel by impairing its plasma membrane localization through MLCK inhibition (Shimizu et al., 2006), causing apoptosis in both untransformed and transformed epithelial cells, retarding the growth of mammary and prostate cancer cells and blocking the invasion and adhesion of human pancreatic cancer cells (Kaneko et al., 2002). In another study, ML-9 reduced SOCE and induced Ca^{2+} -dependent autophagy to promote the death of prostate cancer cells, but the effect of ML-9 on autophagy was independent of STIM1 and SOCE inhibition, suggesting that ML-9 may exert its effects on cancer cells through multiple mechanisms. Moreover, ML-9 combined with docetaxel could enhance the cell death of LNCaP, PC3 and DU-145 cells,

suggesting that ML-9 may be developed as an adjuvant to anticancer chemotherapy (Kondratskyi et al., 2014).

NPPB (5-nitro-2-(3-phenylpropylamino)-benzoic acid), frequently used as a blocker of chloride channels, could also reduce CCE in endothelial cells (Gericke et al., 1994). It was also confirmed that NPPB could directly interact with CRAC to reversibly inhibit Ca^{2+} influx in Jurkat cells in a dose-dependent manner (Li et al., 2000). In ovarian cancer, NPPB could significantly inhibit A2780 cell adhesion and invasion (Li et al., 2009).

AnCoA4 (3-(6-methoxy-1,3-benzodioxol-5-yl)-8,8-dimethylpyrano[2,3-f]chromen-4-one) was identified by screening small-molecule microarray (SMM) using minimal functional domains of STIM1 and ORAI1, and it was found to inhibit Ca^{2+} influx by binding to the C-terminus of ORAI1 directly to perturb the interaction between STIM1 and ORAI1 by reducing the affinity of ORAI1 for STIM1. Through SOCE inhibition, AnCoA4 blocked T cell activation and inhibited the T cell-mediated immune response *in vitro* and *in vivo*, indicting the possibility that it can be used in therapeutic areas, including immunomodulation, inflammation and cancer (Sadaghiani et al., 2014).

RO2959 (2,6-difluoro-N-[5-[4-methyl-1-(1,3-thiazol-2-yl)-3,6-dihydro-2H-pyridin-5-yl]pyrazin-2-yl]benzamide) could specifically block SOCE by inhibiting the IP3-dependent CRAC current in native RBL-2H3 cells, CHO cells with STIM1/ORAI1 overexpression and human primary CD4⁺ T cells, resulting in a decrease in TCR-triggered gene expression, cell proliferation and cytokine production in T cells (Chen G. et al., 2013).

YZ129 (4-(isoquinolin-6-ylamino)-naphthalene-1,2-dione) was identified because of its inhibition of thapsigargin-triggered Ca^{2+} influx and NFAT nuclear entry through an automated high-content screening platform and it was found to exhibit potent anti-tumor activity against glioblastoma. It could bind to HSP90 directly and antagonize its calcineurin-chaperoning effect to reduce NFAT nuclear translocation and inhibit other key proto-oncogenic pathways, including hypoxic and glycolytic pathways and the PI3K/AKT/mTOR axis, thus leading to cell cycle arrest in G2/M phase of glioblastoma and promoting apoptosis and inhibition of tumor cell proliferation and migration (Liu et al., 2019).

MRS-1844 (DHPs-32) and **MRS-1845** (DHPs-35) are compounds in the 1,4-dihydropyridine (DHP) family, and they were confirmed to inhibit store-operated calcium channels and reduce voltage-dependent L-type calcium channels. In addition, their potency in SOCE inhibition was much smaller than that of common SOCE inhibitors (the reported order is Synta66 > 2-APB > GSK-7975A > SKF96365 > MRS1845) (Harper et al., 2003; van Kruchten et al., 2012).

Repurposing FDA-Approved Drugs

In addition to the abovementioned compounds targeting SOCE, other compounds that have been approved for clinical use in corresponding diseases were confirmed to inhibit SOCE. The ability of these compounds to inhibit Ca^{2+} influx through SOCE indicates the importance of learning more about their

pharmacological properties and mechanisms, and the potential to extend their clinical indications.

Diethylstilbestrol (DES), 4-[(E)-4-(4-hydroxyphenyl)-hex-3-en-3-yl]-phenol) is a potent synthetic estrogen used for estrogen therapy in prostate and breast cancer. It was reported to inhibit SOCE and Ca^{2+} influx in a variety of cell types without affecting the whole-cell monovalent cation current mediated by TRPM7 channels. Trans-stilbene, a close structural analog of DES that lacks hydroxyl and ethyl groups, had no effect on CRAC current, further suggesting the specificity of DES for SOCE (Zakharov et al., 2004; Ohana et al., 2009; Dobrydyneva et al., 2010).

Nonsteroidal anti-inflammatory drugs (NSAIDs) are commonly used to relieve pain, fever and inflammation. Epidemiological studies worldwide have demonstrated that NSAIDs also have cancer-protective effects, as these drugs are associated with a reduced risk of various types of cancer. In colon cancer, it has been reported that NSAIDs could exert antiproliferative effects through SOCE inhibition, and salicylate, the main aspirin metabolite, is considered a mild mitochondrial uncoupler that prevents mitochondrial Ca^{2+} uptake and promotes the Ca^{2+} -dependent inactivation of SOCE, thus inhibiting the proliferation of HT29 cells (Núñez et al., 2006). Another study suggested that STIM1 overexpression promoted colorectal cancer progression through an increase in the expression of the pro-inflammatory and pro-metastatic enzyme cyclooxygenase-2 (COX-2). The inhibition of COX-2 with two NSAIDs, ibuprofen and indomethacin, abrogated STIM1-induced colorectal cancer (CRC) progression (Wang et al., 2015).

Mibefradil ([1S,2S)-2-[2-[3-(1H-benzimidazol-2-yl)propyl-methylamino]ethyl]-6-fluoro-1-propan-2-yl-3,4-dihydro-1H-naphthalen-2-yl]2-methoxyacetate), a T-type Ca^{2+} channel blocker that was initially developed as a cardiovascular drug, was recently found to inhibit SOCE by blocking ORAI channels in a dose-dependent and reversible manner to significantly inhibit cell proliferation, induce cell apoptosis and arrest cell cycle in S and G2/M phases in HEK-293T-REx cells (Li et al., 2019).

CONCLUSION AND PERSPECTIVES

Ca^{2+} signaling is involved in almost all cellular activities in organisms. As a major route of Ca^{2+} entry in mammalian cells for replenishing the depleted intracellular Ca^{2+} store, SOCE regulates a diverse array of biological processes. Accumulating evidence has shown that STIM/ORAI-mediated SOCE is excessive in cancer tissues, and it is becoming clear that augmented SOCE promotes the malignant behavior of cancer cells, including tumor growth, angiogenesis, and metastasis. Therefore, SOCE could be a potential therapeutic target for the treatment of cancer.

As we summarized above, multiple compounds targeting SOCE have been developed and their efficiency in the inhibition of proliferation and migration of cancer cells has been evaluated. However, rare SOCE inhibitors have

been approved for clinical use in cancer treatment due to their poor selectivity, which urgently needs to be addressed. In addition, as SOCE is not the only channel for Ca^{2+} entry, cells could adopt other ways to obtain sufficient Ca^{2+} even after complete SOCE inhibition. Under this condition, drug combinations could be considered. Furthermore, due to the universal roles of Ca^{2+} signaling in cells, the cytotoxicity of SOCE inhibitors on normal cells and some anticancer immune cell inhibitors should also be considered in clinical anticancer applications. Developing SOCE inhibitors that could specifically target tumor tissues in certain circumstances is a hopeful therapeutic orientation toward cancer in the future.

REFERENCES

- Amcheslavsky, A., Safrina, O., and Cahalan, M. D. (2014). State-Dependent Block of Orai3 TM1 and TM3 Cysteine Mutants: Insights Into 2-APB Activation. *J. Gen. Physiol.* 143 (5), 621–631. doi:10.1085/jgp.201411171
- Amcheslavsky, A., Wood, M. L., Yeromin, A. V., Parker, I., Freites, J. A., Tobias, D. J., et al. (2015). Molecular Biophysics of Orai Store-Operated Ca^{2+} Channels. *Biophys. J.* 108 (2), 237–246. doi:10.1016/j.bpj.2014.11.3473
- Arias-Montano, J.-A., Gibson, W. J., and Young, J. M. (1998). SK&F 96365 (1-[3-(4-Methoxyphenyl)propoxy]-4-Methoxyphenylethyl]-1H-Imidazole Hydrochloride) Stimulates Phosphoinositide Hydrolysis in Human U373 MG Astrocytoma Cells. *Biochem. Pharmacol.* 56 (8), 1023–1027. doi:10.1016/s0006-2952(98)00125-7
- Ashmole, I., Duffy, S. M., Leyland, M. L., Morrison, V. S., Begg, M., and Bradding, P. (2012). CRAC/Orai Ion Channel Expression and Function in Human Lung Mast Cells. *J. Allergy Clin. Immunol.* 129 (6), 1628–1635. doi:10.1016/j.jaci.2012.01.070
- Azimi, I., Bong, A. H., Poo, G. X. H., Armitage, K., Lok, D., Roberts-Thomson, S. J., et al. (2018). Pharmacological Inhibition of Store-Operated Calcium Entry in MDA-MB-468 Basal A Breast Cancer Cells: Consequences on Calcium Signalling, Cell Migration and Proliferation. *Cell. Mol. Life Sci.* 75 (24), 4525–4537. doi:10.1007/s00018-018-2904-y
- Bauer, K. S., Figg, W. D., Hamilton, J. M., Jones, E. C., Premkumar, A., Steinberg, S. M., et al. (1999). A Pharmacokinetically Guided Phase II Study of Carboxyamido-Triazole in Androgen-Independent Prostate Cancer. *Clin. Cancer Res.* 5 (9), 2324–2329.
- Bennett, B. D., Alvarez, U., and Hruska, K. A. (2001). Receptor-Operated Osteoclast Calcium Sensing. *Endocrinology* 142 (5), 1968–1974. doi:10.1210/endo.142.5.8125
- Bittremieux, M., Gerasimenko, J. V., Schuermans, M., Luyten, T., Stapleton, E., Alzayady, K. J., et al. (2017). DPB162-AE, An Inhibitor of Store-Operated Ca^{2+} Entry, Can Deplete the Endoplasmic Reticulum Ca^{2+} Store. *Cell Calcium* 62, 60–70. doi:10.1016/j.ceca.2017.01.015
- Bomben, V. C., and Sontheimer, H. W. (2008). Inhibition of Transient Receptor Potential Canonical Channels Impairs Cytokinesis in Human Malignant Gliomas. *Cell Prolif.* 41 (1), 98–121. doi:10.1111/j.1365-2184.2007.00504.x
- Bomben, V. C., and Sontheimer, H. (2010). Disruption of Transient Receptor Potential Canonical Channel 1 Causes Incomplete Cytokinesis and Slows the Growth of Human Malignant Gliomas. *Glia* 58 (10), 1145–1156. doi:10.1002/glia.20994
- Brandman, O., Liou, J., Park, W. S., and Meyer, T. (2007). STIM2 is a Feedback Regulator that Stabilizes Basal Cytosolic and Endoplasmic Reticulum Ca^{2+} Levels. *Cell* 131 (7), 1327–1339. doi:10.1016/j.cell.2007.11.039
- Cabello, O. A., and Schilling, W. P. (1993). Vectorial Ca^{2+} Flux From the Extracellular Space to the Endoplasmic Reticulum via a Restricted Cytoplasmic Compartment Regulates Inositol 1,4,5-Trisphosphate-Stimulated Ca^{2+} Release From Internal Stores in Vascular Endothelial Cells. *Biochem. J.* 295 (Pt 2), 357–366. doi:10.1042/bj2950357
- Cai, R., Ding, X., Zhou, K., Shi, Y., Ge, R., Ren, G., et al. (2009). Blockade of TRPC6 Channels Induced G2/M Phase Arrest and Suppressed Growth in Human Gastric Cancer Cells. *Int. J. Cancer* 125 (10), 2281–2287. doi:10.1002/ijc.24551
- Chang, H.-H., Cheng, Y.-C., Tsai, W.-C., Tsao, M.-J., and Chen, Y. (2018). Pyr3 Induces Apoptosis and Inhibits Migration in Human Glioblastoma Cells. *Cell Physiol. Biochem.* 48 (4), 1694–1702. doi:10.1159/000492293
- Chauvet, S., Jarvis, L., Chevallet, M., Shrestha, N., Groschner, K., and Bouron, A. (2016). Pharmacological Characterization of the Native Store-Operated Calcium Channels of Cortical Neurons From Embryonic Mouse Brain. *Front. Pharmacol.* 7, 486. doi:10.3389/fphar.2016.00486
- Chen, J., and Sanderson, M. J. (2017). Store-Operated Calcium Entry is Required for Sustained Contraction and Ca^{2+} Oscillations of Airway Smooth Muscle. *J. Physiol.* 595 (10), 3203–3218. doi:10.1113/JP272694
- Chen, J.-P., Luan, Y., You, C.-X., Chen, X.-H., Luo, R.-C., and Li, R. (2010). TRPM7 Regulates the Migration of Human Nasopharyngeal Carcinoma Cell by Mediating Ca^{2+} Influx. *Cell Calcium* 47 (5), 425–432. doi:10.1016/j.ceca.2010.03.003
- Chen, Y.-F., Chiu, W.-T., Chen, Y.-T., Lin, P.-Y., Huang, H.-J., Chou, C.-Y., et al. (2011). Calcium Store Sensor Stromal-Interaction Molecule 1-Dependent Signaling Plays an Important Role in Cervical Cancer Growth, Migration, and Angiogenesis. *Proc. Natl. Acad. Sci.* 108 (37), 15225–15230. doi:10.1073/pnas.1103315108
- Chen, G., Panicker, S., Lau, K.-Y., Apparsundaram, S., Patel, V. A., Chen, S.-L., et al. (2013). Characterization of a Novel CRAC Inhibitor that Potently Blocks Human T Cell Activation and Effector Functions. *Mol. Immunol.* 54 (3–4), 355–367. doi:10.1016/j.molimm.2012.12.011
- Chen, Y.-T., Chen, Y.-F., Chiu, W.-T., Wang, Y.-K., Chang, H.-C., and Shen, M.-R. (2013). The ER Ca^{2+} Sensor STIM1 Regulates Actomyosin Contractility of Migratory Cells. *J. Cell Sci.* 126 (Pt 5), 1260–1267. doi:10.1242/jcs.121129
- Chokshi, R., Fruasaha, P., and Kozak, J. A. (2012). 2-Aminoethyl Diphenyl Borinate (2-APB) Inhibits TRPM7 Channels through an Intracellular Acidification Mechanism. *Channels* 6 (5), 362–369. doi:10.4161/chan.21628
- Chung, S. C., McDonald, T. V., and Gardner, P. (1994). Inhibition by SK&F 96365 of Ca^{2+} Current, IL-2 Production and Activation in T Lymphocytes. *Br. J. Pharmacol.* 113 (3), 861–868. doi:10.1111/j.1476-5381.1994.tb17072.x
- Chung, M.-K., Lee, H., Mizuno, A., Suzuki, M., and Caterina, M. J. (2004). 2-Aminoethoxydiphenyl Borate Activates and Sensitizes the Heat-Gated Ion Channel TRPV3. *J. Neurosci.* 24 (22), 5177–5182. doi:10.1523/jneurosci.0934-04.2004
- Colton, C. K., and Zhu, M. X. (2007). 2-Aminoethoxydiphenyl Borate as a Common Activator of TRPV1, TRPV2, and TRPV3 Channels. *Handb. Exp. Pharmacol.* 179, 173–187. doi:10.1007/978-3-540-34891-7_10
- Corrado, C., Raimondo, S., Flugy, A. M., Fontana, S., Santoro, A., Stassi, G., et al. (2011). Carboxyamidotriazole Inhibits Cell Growth of Imatinib-Resistant Chronic Myeloid Leukaemia Cells Including T315I Bcr-Abl Mutant by a Redox-Mediated Mechanism. *Cancer Lett.* 300 (2), 205–214. doi:10.1016/j.canlet.2010.10.007
- Cox, J. H., Hussell, S., Søndergaard, H., Roepstorff, K., Bui, J.-V., Deer, J. R., et al. (2013). Antibody-Mediated Targeting of the Orai1 Calcium Channel Inhibits T Cell Function. *PLoS One* 8 (12), e82944. doi:10.1371/journal.pone.0082944
- Cui, C., Merritt, R., Fu, L., and Pan, Z. (2017). Targeting Calcium Signaling in Cancer Therapy. *Acta Pharm. Sin. B* 7 (1), 3–17. doi:10.1016/j.apsb.2016.11.001

AUTHOR CONTRIBUTIONS

All authors listed have made a substantial, direct, and intellectual contribution to the work and approved it for publication.

FUNDING

This work was supported by the National Natural Science Foundation of China (81972745, 81872238, and 81572361), Ten Thousand Plan Youth Talent Support Program of Zhejiang Province (ZJWR0108009), and Zhejiang Medical Innovative Discipline Construction Project-2016.

- Cui, C., Chang, Y., Zhang, X., Choi, S., Tran, H., Penmetsa, K. V., et al. (2018). Targeting Orai1-Mediated Store-Operated Calcium Entry by RP4010 for Anti-Tumor Activity in Esophagus Squamous Cell Carcinoma. *Cancer Lett.* 432, 169–179. doi:10.1016/j.canlet.2018.06.006
- Dago, C., Maux, P., Roisnel, T., Brigaudeau, C., Bekro, Y.-A., Mignen, O., et al. (2018). Preliminary Structure-Activity Relationship (SAR) of a Novel Series of Pyrazole SKF-96365 Analogues as Potential Store-Operated Calcium Entry (SOCE) Inhibitors. *Int. J. Mol. Sci.* 19 (3), 856. doi:10.3390/ijms19030856
- Dart, A. E., Worth, D. C., Muir, G., Chandra, A., Morris, J. D., McKee, C., et al. (2017). The Drebrin/EB3 Pathway Drives Invasive Activity in Prostate Cancer. *Oncogene* 36 (29), 4111–4123. doi:10.1038/ncr.2017.45
- Das, M. (2018). Carboxyamidotriazole Orotate in Glioblastoma. *Lancet Oncol.* 19 (6), e292. doi:10.1016/s1470-2045(18)30347-4
- DeHaven, W. I., Smyth, J. T., Boyles, R. R., Bird, G. S., and Putney, J. W., Jr. (2008). Complex Actions of 2-Aminoethyldiphenyl Borate on Store-Operated Calcium Entry. *J. Biol. Chem.* 283 (28), 19265–19273. doi:10.1074/jbc.M801535200
- Derler, I., Schindl, R., Fritsch, R., Heftberger, P., Riedl, M. C., Begg, M., et al. (2013). The Action of Selective CRAC Channel Blockers is Affected by the Orai Pore Geometry. *Cell Calcium* 53 (2), 139–151. doi:10.1016/j.ceca.2012.11.005
- Di Sabatino, A., Rovedatti, L., Kaur, R., Spencer, J. P., Brown, J. T., Morisset, V. D., et al. (2009). Targeting Gut T Cell Ca²⁺ Release-Activated Ca²⁺ Channels Inhibits T Cell Cytokine Production and T-Box Transcription Factor T-Bet in Inflammatory Bowel Disease. *J. Immunol.* 183 (5), 3454–3462. doi:10.4049/jimmunol.0802887
- Ding, X., He, Z., Zhou, K., Cheng, J., Yao, H., Lu, D., et al. (2010). Essential Role of TRPC6 Channels in G2/M Phase Transition and Development of Human Glioma. *J. Natl. Cancer Inst.* 102 (14), 1052–1068. doi:10.1093/jnci/djq217
- Dobryden, Y., Williams, R. L., and Blackmore, P. F. (2010). Diethylstilbestrol and Other Nonsteroidal Estrogens: Novel Class of Store-Operated Calcium Channel Modulators. *J. Cardiovasc. Pharmacol.* 55 (5), 522–530. doi:10.1097/FJC.0b013e3181d64b33
- Dragoni, S., Laforenza, U., Bonetti, E., Lodola, F., Bottino, C., Berra-Romani, R., et al. (2011). Vascular Endothelial Growth Factor Stimulates Endothelial colony Forming Cells Proliferation and Tubulogenesis by Inducing Oscillations in Intracellular Ca²⁺ Concentration. *Stem Cells* 29 (11), 1898–1907. doi:10.1002/stem.734
- Enfissi, A., Prigent, S., Colosetti, P., and Capiod, T. (2004). The Blocking of Capacitative Calcium Entry by 2-Aminoethyl Diphenylborate (2-APB) and Carboxyamidotriazole (CAI) Inhibits Proliferation in Hep G2 and Huh-7 Human Hepatoma Cells. *Cell Calcium* 36 (6), 459–467. doi:10.1016/j.ceca.2004.04.004
- Figg, W. D., Cole, K. A., Reed, E., Steinberg, S. M., Piscitelli, S. C., Davis, P. A., et al. (1995). Pharmacokinetics of Orally Administered Carboxyamido-Triazole, an Inhibitor of Calcium-Mediated Signal Transduction. *Clin. Cancer Res.* 1 (8), 797–803.
- Franz, D., Hoth, M., and Penner, R. (1994). Non-Specific Effects of Calcium Entry Antagonists in Mast Cells. *Pflügers Arch.* 428 (5–6), 433–438. doi:10.1007/bf00374562
- Geng, S., Gao, Y.-d., Yang, J., Zou, J.-j., and Guo, W. (2012). Potential Role of Store-Operated Ca²⁺ Entry in Th2 Response Induced by Histamine in Human Monocyte-Derived Dendritic Cells. *Int. Immunopharmacol.* 12 (2), 358–367. doi:10.1016/j.intimp.2011.12.008
- Gericke, M., Oike, M., Droogmans, G., and Nilius, B. (1994). Inhibition of Capacitative Ca²⁺ Entry by a Cl[−] Channel Blocker in Human Endothelial Cells. *Eur. J. Pharmacol. Mol. Pharmacol.* 269 (3), 381–384. doi:10.1016/0922-4106(94)90046-9
- Giambelluca, M. S., and Gende, O. A. (2007). Selective Inhibition of Calcium Influx by 2-Aminoethoxydiphenyl Borate. *Eur. J. Pharmacol.* 565 (1–3), 1–6. doi:10.1016/j.ejphar.2007.02.017
- Gibson, J., Tu, P., and Bouron, A. (2010). Store-Depletion and Hyperforin Activate Distinct Types of Ca²⁺-Conducting Channels in Cortical Neurons. *Cell Calcium* 47 (6), 538–543. doi:10.1016/j.ceca.2010.05.003
- Goswamee, P., Pounardjian, T., and Giovannucci, D. R. (2018). Arachidonic Acid-Induced Ca²⁺ Entry and Migration in a Neuroendocrine Cancer Cell Line. *Cancer Cell Int.* 18, 30. doi:10.1186/s12935-018-0529-8
- Goto, J.-I., Suzuki, A. Z., Ozaki, S., Matsumoto, N., Nakamura, T., Ebisui, E., et al. (2010). Two Novel 2-Aminoethyl Diphenylborinate (2-APB) Analogues Differentially Activate and Inhibit Store-Operated Ca²⁺ Entry via STIM Proteins. *Cell Calcium* 47 (1), 1–10. doi:10.1016/j.ceca.2009.10.004
- Harper, J. L., Camerini-Otero, C. S., Li, A.-H., Kim, S.-A., Jacobson, K. A., and Daly, J. W. (2003). Dihydropyridines as Inhibitors of Capacitative Calcium Entry in Leukemic HL-60 Cells. *Biochem. Pharmacol.* 65 (3), 329–338. doi:10.1016/s0006-2952(02)01488-0
- He, L.-P., Hewavitharana, T., Soboloff, J., Spassova, M. A., and Gill, D. L. (2005). A Functional Link Between Store-Operated and TRPC Channels Revealed by the 3,5-Bis(trifluoromethyl)pyrazole Derivative, BTP2. *J. Biol. Chem.* 280 (12), 10997–11006. doi:10.1074/jbc.M411797200
- He, B., Liu, F., Ruan, J., Li, A., Chen, J., Li, R., et al. (2012). Silencing TRPC1 Expression Inhibits Invasion of CNE2 Nasopharyngeal Tumor Cells. *Oncol. Rep.* 27 (5), 1548–1554. doi:10.3892/or.2012.1695
- Hendron, E., Wang, X., Zhou, Y., Cai, X., Goto, J.-I., Mikoshiba, K., et al. (2014). Potent Functional Uncoupling Between STIM1 and Orai1 by Dimeric 2-Aminodiphenyl Borinate Analogs. *Cell Calcium* 56 (6), 482–492. doi:10.1016/j.ceca.2014.10.005
- Hillman, S. L., Mandrekar, S. J., Bot, B., DeMatteo, R. P., Perez, E. A., Ballman, K. V., et al. (2010). Evaluation of the Value of Attribution in the Interpretation of Adverse Event Data: A North Central Cancer Treatment Group and American College of Surgeons Oncology Group Investigation. *J. Clin. Oncol.* 28 (18), 3002–3007. doi:10.1200/jco.2009.27.4282
- Hogan, P. G., Lewis, R. S., and Rao, A. (2010). Molecular Basis of Calcium Signaling in Lymphocytes: STIM and ORAI. *Annu. Rev. Immunol.* 28, 491–533. doi:10.1146/annurev.immunol.021908.132550
- Hu, H.-Z., Gu, Q., Wang, C., Colton, C. K., Tang, J., Kinoshita-Kawada, M., et al. (2004). 2-Aminoethoxydiphenyl Borate is a Common Activator of TRPV1, TRPV2, and TRPV3. *J. Biol. Chem.* 279 (34), 35741–35748. doi:10.1074/jbc.M404164200
- Huang, H.-K., Lin, Y.-H., Chang, H.-A., Lai, Y.-S., Chen, Y.-C., Huang, S.-C., et al. (2020). Chemoresistant Ovarian Cancer Enhances its Migration Abilities by Increasing Store-Operated Ca²⁺ Entry-Mediated Turnover of Focal Adhesions. *J. Biomed. Sci.* 27 (1), 36. doi:10.1186/s12929-020-00630-5
- Hupe, D. J., Boltz, R., Cohen, C. J., Felix, J., Ham, E., Miller, D., et al. (1991). The Inhibition of Receptor-Mediated and Voltage-Dependent Calcium Entry by the Antiproliferative I-651,582. *J. Biol. Chem.* 266 (16), 10136–10142. doi:10.1016/s0021-9258(18)99200-8
- Hussain, M. M., Kotz, H., Minasian, L., Premkumar, A., Sarosy, G., Reed, E., et al. (2003). Phase II Trial of Carboxyamidotriazole in Patients With Relapsed Epithelial Ovarian Cancer. *J. Clin. Oncol.* 21 (23), 4356–4363. doi:10.1200/jco.2003.04.136
- Ishikawa, J., Ohga, K., Yoshino, T., Takezawa, R., Ichikawa, A., Kubota, H., et al. (2003). A Pyrazole Derivative, YM-58483, Potently Inhibits Store-Operated Sustained Ca²⁺ Influx and IL-2 Production in T Lymphocytes. *J. Immunol.* 170 (9), 4441–4449. doi:10.4049/jimmunol.170.9.4441
- Iwamuro, Y., Miwa, S., Zhang, X.-F., Minowa, T., Enoki, T., Okamoto, Y., et al. (1999). Activation of Three Types of Voltage-Independent Ca²⁺ Channel in A7r5 Cells by Endothelin-1 as Revealed by a Novel Ca²⁺-channel Blocker LOE 908. *Br. J. Pharmacol.* 126 (5), 1107–1114. doi:10.1038/sj.bjp.0702416
- Jacobs, W., Mikkelsen, T., Smith, R., Nelson, K., Rosenblum, M. L., and Kohn, E. C. (1997). Inhibitory Effects of CAI in Glioblastoma Growth and Invasion. *J. Neurooncol.* 32 (2), 93–101. doi:10.1023/a:1005777711567
- Jairaman, A., and Prakriya, M. (2013). Molecular Pharmacology of Store-Operated CRAC Channels. *Channels* 7 (5), 402–414. doi:10.4161/chan.25292
- Jing, Z., Sui, X., Yao, J., Xie, J., Jiang, L., Zhou, Y., et al. (2016). SKF-96365 Activates Cytoprotective Autophagy to Delay Apoptosis in Colorectal Cancer Cells Through Inhibition of the Calcium/CaMKII γ /AKT-Mediated Pathway. *Cancer Lett.* 372 (2), 226–238. doi:10.1016/j.canlet.2016.01.006
- Ju, R., Wu, D., Guo, L., Li, J., Ye, C., and Zhang, D. (2012). Inhibition of Pro-Inflammatory Cytokines in Tumour Associated Macrophages is a Potential Anti-Cancer Mechanism of Carboxyamidotriazole. *Eur. J. Cancer* 48 (7), 1085–1095. doi:10.1016/j.ejca.2011.06.050
- Kaneko, K., Satoh, K., Masamune, A., Satoh, A., and Shimosegawa, T. (2002). Myosin Light Chain Kinase Inhibitors Can Block Invasion and Adhesion of Human Pancreatic Cancer Cell Lines. *Pancreas* 24 (1), 34–41. doi:10.1097/00006676-200201000-00005
- Kappel, S., Kilch, T., Baur, R., Lochner, M., and Peinelt, C. (2020). The Number and Position of Orai3 Units Within Heteromeric Store-Operated Ca²⁺ Channels

- Alter the Pharmacology of ICRAC. *Int. J. Mol. Sci.* 21 (7), 2458. doi:10.3390/ijms21072458
- Khan, H. Y., Mpilla, G. B., Sexton, R., Viswanadha, S., Penmetsa, K. V., Aboukameel, A., et al. (2020). Calcium Release-Activated Calcium (CRAC) Channel Inhibition Suppresses Pancreatic Ductal Adenocarcinoma Cell Proliferation and Patient-Derived Tumor Growth. *Cancers* 12 (3), 750. doi:10.3390/cancers12030750
- Kim, J.-H., Lkhagvadorj, S., Lee, M.-R., Hwang, K.-H., Chung, H. C., Jung, J. H., et al. (2014). Orai1 and STIM1 are Critical for Cell Migration and Proliferation of Clear Cell Renal Cell Carcinoma. *Biochem. Biophys. Res. Commun.* 448 (1), 76–82. doi:10.1016/j.bbrc.2014.04.064
- Kiyonaka, S., Kato, K., Nishida, M., Mio, K., Numaga, T., Sawaguchi, Y., et al. (2009). Selective and Direct Inhibition of TRPC3 Channels Underlies Biological Activities of a Pyrazole Compound. *Proc. Natl. Acad. Sci.* 106 (13), 5400–5405. doi:10.1073/pnas.0808793106
- Kohn, E. C., and Liotta, L. A. (1990). L651582: A Novel Antiproliferative and Antimetastasis Agent. *J. Natl. Cancer Inst.* 82 (1), 54–61. doi:10.1093/jnci/82.1.54
- Kohn, E. C., Sandeen, M. A., and Liotta, L. A. (1992). *In Vivo* Efficacy of a Novel Inhibitor of Selected Signal Transduction Pathways Including Calcium, Arachidonate, and Inositol Phosphates. *Cancer Res.* 52 (11), 3208–3212.
- Kohn, E. C., Felder, C. C., Jacobs, W., Holmes, K. A., Day, A., Freer, R., et al. (1994). Structure-Function Analysis of Signal and Growth Inhibition by Carboxyamido-Triazole, CAI. *Cancer Res.* 54 (4), 935–942.
- Kohn, E. C., Reed, E., Sarosy, G., Christian, M., Link, C. J., Cole, K., et al. (1996). Clinical Investigation of a Cytostatic Calcium Influx Inhibitor in Patients With Refractory Cancers. *Cancer Res.* 56 (3), 569–573.
- Kondratskyi, A., Yassine, M., Slomianny, C., Kondratska, K., Gordienko, D., Dewailly, E., et al. (2014). Identification of ML-9 as a Lysosomotropic Agent Targeting Autophagy and Cell Death. *Cell Death Dis.* 5 (4), e1193. doi:10.1038/cddis.2014.156
- Kovacs, G., Montalbetti, N., Simonin, A., Danko, T., Balazs, B., Zsembery, A., et al. (2012). Inhibition of the Human Epithelial Calcium Channel TRPV6 by 2-Aminoethoxydiphenyl Borate (2-APB). *Cell Calcium* 52 (6), 468–480. doi:10.1016/j.ceca.2012.08.005
- Law, M., Morales, J. L., Mottram, L. F., Iyer, A., Peterson, B. R., and August, A. (2011). Structural Requirements for the Inhibition of Calcium Mobilization and Mast Cell Activation by the Pyrazole Derivative BTP2. *Int. J. Biochem. Cell Biol.* 43 (8), 1228–1239. doi:10.1016/j.biocel.2011.04.016
- Lee, Y. S., Sayeed, M. M., and Wurster, R. D. (1993). Inhibition of Human Brain Tumor Cell Growth by a Receptor-Operated Ca²⁺ Channel Blocker. *Cancer Lett.* 72 (1–2), 77–81. doi:10.1016/0304-3835(93)90014-z
- Leng, T.-D., Li, M.-H., Shen, J.-F., Liu, M.-L., Li, X.-B., Sun, H.-W., et al. (2015). Suppression of TRPM7 Inhibits Proliferation, Migration, and Invasion of Malignant Human Glioma Cells. *CNS Neurosci. Ther.* 21 (3), 252–261. doi:10.1111/cns.12354
- Li, J. H., Spence, K. T., Dargis, P. G., and Christian, E. P. (2000). Properties of Ca²⁺ Release-Activated Ca²⁺ Channel Block by 5-Nitro-2-(3-Phenylpropylamino)-Benzoic Acid in Jurkat Cells. *Eur. J. Pharmacol.* 394 (2–3), 171–179. doi:10.1016/s0014-2999(00)00144-8
- Li, M., Jiang, J., and Yue, L. (2006). Functional Characterization of Homo- and Heteromeric Channel Kinases TRPM6 and TRPM7. *J. Gen. Physiol.* 127 (5), 525–537. doi:10.1085/jgp.200609502
- Li, M., Wang, Q., Lin, W., and Wang, B. (2009). Regulation of Ovarian Cancer Cell Adhesion and Invasion by Chloride Channels. *Int. J. Gynecol. Cancer* 19 (4), 526–530. doi:10.1111/IGC.0b013e3181a3d6d2
- Li, J., McKeown, L., Ojelabi, O., Stacey, M., Foster, R., O'Regan, D., et al. (2011). Nanomolar Potency and Selectivity of a Ca²⁺ Release-Activated Ca²⁺ Channel Inhibitor Against Store-Operated Ca²⁺ Entry and Migration of Vascular Smooth Muscle Cells. *Br. J. Pharmacol.* 164 (2), 382–393. doi:10.1111/j.1476-5381.2011.01368.x
- Li, P., Rubaiy, H. N., Chen, G. L., Hallett, T., Zaibi, N., Zeng, B., et al. (2019). Mibefradil, a T-Type Ca²⁺ Channel Blocker Also Blocks Orai Channels by Action at the Extracellular Surface. *Br. J. Pharmacol.* 176 (19), 3845–3856. doi:10.1111/bph.14788
- Lievremont, J.-P., Bird, G. S., and Putney, J. W., Jr. (2005). Mechanism of Inhibition of TRPC Cation Channels by 2-Aminoethoxydiphenylborane. *Mol. Pharmacol.* 68 (3), 758–762. doi:10.1124/mol.105.012856
- Lin, F.-F., Elliott, R., Colombero, A., Gaida, K., Kelley, L., Moksa, A., et al. (2013). Generation and Characterization of Fully Human Monoclonal Antibodies Against Human Orai1 for Autoimmune Disease. *J. Pharmacol. Exp. Ther.* 345 (2), 225–238. doi:10.1124/jpet.112.202788
- Liou, J., Kim, M. L., Do Heo, W., Jones, J. T., Myers, J. W., Ferrell, J. E., Jr., et al. (2005). STIM is a Ca²⁺ Sensor Essential for Ca²⁺-Store-Depletion-Triggered Ca²⁺ Influx. *Curr. Biol.* 15 (13), 1235–1241. doi:10.1016/j.cub.2005.05.055
- Lis, A., Peinelt, C., Beck, A., Parvez, S., Monteilh-Zoller, M., Fleig, A., et al. (2007). CRACM1, CRACM2, and CRACM3 are Store-Operated Ca²⁺ Channels With Distinct Functional Properties. *Curr. Biol.* 17 (9), 794–800. doi:10.1016/j.cub.2007.03.065
- Liu, H., Hughes, J. D., Rollins, S., Chen, B., and Perkins, E. (2011). Calcium Entry via ORAI1 Regulates Glioblastoma Cell Proliferation and Apoptosis. *Exp. Mol. Pathol.* 91 (3), 753–760. doi:10.1016/j.yexmp.2011.09.005
- Liu, Z., Li, H., He, L., Xiang, Y., Tian, C., Li, C., et al. (2019). Discovery of Small-Molecule Inhibitors of the HSP90-Calcineurin-NFAT Pathway Against Glioblastoma. *Cel Chem. Biol.* 26 (3), 352–365. doi:10.1016/j.chembiol.2018.11.009
- Liu, H., Dilger, J. P., and Lin, J. (2020). The Role of Transient Receptor Potential Melastatin 7 (TRPM7) in Cell Viability: A Potential Target to Suppress Breast Cancer Cell Cycle. *Cancers* 12 (1), 131. doi:10.3390/cancers12010131
- Lodola, F., Laforenza, U., Bonetti, E., Lim, D., Dragoni, S., Bottino, C., et al. (2012). Store-Operated Ca²⁺ Entry is Remodelled and Controls *In Vitro* Angiogenesis in Endothelial Progenitor Cells Isolated From Tumoral Patients. *PLoS One* 7 (9), e42541. doi:10.1371/journal.pone.0042541
- Luzzi, K. J., Varghese, H. J., MacDonald, I. C., Schmidt, E. E., Kohn, E. C., Morris, V. L., et al. (1998). Inhibition of Angiogenesis in Liver Metastases by Carboxyamidotriazole (CAI). *Angiogenesis* 2 (4), 373–379. doi:10.1023/a:1009259521092
- Ma, H.-T., Venkatachalam, K., Rys-Sikora, K. E., He, L.-P., Zheng, F., and Gill, D. L. (2003). Modification of Phospholipase C- γ -Induced Ca²⁺ Signal Generation by 2-Aminoethoxydiphenyl Borate. *Biochem. J.* 376 (Pt 3), 667–676. doi:10.1042/bj20031345
- Ma, J., McCarl, C.-A., Khalil, S., Lüthy, K., and Feske, S. (2010). T-Cell-Specific Deletion of STIM1 and STIM2 Protects Mice From EAE by Impairing the Effector Functions of Th1 and Th17 Cells. *Eur. J. Immunol.* 40 (11), 3028–3042. doi:10.1002/eji.201040614
- Maruyama, T., Kanaji, T., Nakade, S., Kanno, T., and Mikoshiba, K. (1997). 2APB, 2-Aminoethoxydiphenyl Borate, a Membrane-Penetrable Modulator of Ins(1,4,5)P₃-Induced Ca²⁺ Release. *J. Biochem.* 122 (3), 498–505. doi:10.1093/oxfordjournals.jbchem.a021780
- McGahon, M. K., McKee, J., Dash, D. P., Brown, E., Simpson, D. A., Curtis, T. M., et al. (2012). Pharmacological Profiling of Store-Operated Ca²⁺ Entry in Retinal Arteriolar Smooth Muscle. *Microcirculation* 19 (7), 586–597. doi:10.1111/j.1549-8719.2012.00192.x
- Mehrotra, P., Sturek, M., Neyra, J. A., and Basile, D. P. (2019). Calcium Channel Orai1 Promotes Lymphocyte IL-17 Expression and Progressive Kidney Injury. *J. Clin. Invest.* 129 (11), 4951–4961. doi:10.1172/jci.126108
- Mercer, J. C., Dehaven, W. L., Smyth, J. T., Wedel, B., Boyles, R. R., Bird, G. S., et al. (2006). Large Store-Operated Calcium Selective Currents Due to Co-expression of Orai1 or Orai2 With the Intracellular Calcium Sensor, Stim1. *J. Biol. Chem.* 281 (34), 24979–24990. doi:10.1074/jbc.M604589200
- Merritt, J. E., Armstrong, W. P., Benham, C. D., Hallam, T. J., Jacob, R., Jaxa-Chamiec, A., et al. (1990). SK&F 96365, a Novel Inhibitor of Receptor-Mediated Calcium Entry. *Biochem. J.* 271 (2), 515–522. doi:10.1042/bj2710515
- Moody, T. W., Chiles, J., Moody, E., Sieczkiewicz, G. J., and Kohn, E. C. (2003). CAI Inhibits the Growth of Small Cell Lung Cancer Cells. *Lung Cancer* 39 (3), 279–288. doi:10.1016/s0169-5002(02)00525-1
- Motiani, R. K., Hyzinski-García, M. C., Zhang, X., Henkel, M. M., Abdullaev, I. F., Kuo, Y.-H., et al. (2013). STIM1 and Orai1 Mediate CRAC Channel Activity and are Essential for Human Glioblastoma Invasion. *Pflugers Arch.* 465 (9), 1249–1260. doi:10.1007/s00424-013-1254-8
- Ng, S. W., di Capite, J., Singaravelu, K., and Parekh, A. B. (2008). Sustained Activation of the Tyrosine Kinase Syk by Antigen in Mast Cells Requires Local Ca²⁺ Influx through Ca²⁺ Release-Activated Ca²⁺ Channels. *J. Biol. Chem.* 283 (46), 31348–31355. doi:10.1074/jbc.M804942200

- Nordström, T., Nevanlinna, H. A., and Andersson, L. C. (1992). Mitosis-Arresting Effect of the Calcium Channel Inhibitor SK&F 96365 on Human Leukemia Cells. *Exp. Cell Res.* 202 (2), 487–494. doi:10.1016/0014-4827(92)90103-f
- Núñez, L., Valero, R. A., Senovilla, L., Sanz-Blasco, S., García-Sancho, J., and Villalobos, C. (2006). Cell Proliferation Depends on Mitochondrial Ca²⁺ Uptake: Inhibition by Salicylate. *J. Physiol.* 571 (Pt 1), 57–73. doi:10.1113/jphysiol.2005.100586
- Oda, K., Umemura, M., Nakakaji, R., Tanaka, R., Sato, I., Nagasako, A., et al. (2017). Transient Receptor Potential Cation 3 Channel Regulates Melanoma Proliferation and Migration. *J. Physiol. Sci.* 67 (4), 497–505. doi:10.1007/s12576-016-0480-1
- Ohana, L., Newell, E. W., Stanley, E. F., and Schlichter, L. C. (2009). The Ca²⁺ Release-Activated Ca²⁺ Current (ICRAC) Mediates Store-Operated Ca²⁺ Entry in Rat Microglia. *Channels* 3 (2), 129–139. doi:10.4161/chan.3.2.8609
- Ohga, K., Takezawa, R., Arakida, Y., Shimizu, Y., and Ishikawa, J. (2008). Characterization of YM-58483/BTP2, a Novel Store-Operated Ca²⁺ Entry Blocker, on T Cell-Mediated Immune Responses *In Vivo*. *Int. Immunopharmacol.* 8 (13–14), 1787–1792. doi:10.1016/j.intimp.2008.08.016
- Oláh, T., Fodor, J., Ruzsnavszky, O., Vincze, J., Berbey, C., Allard, B., et al. (2011). Overexpression of Transient Receptor Potential Canonical Type 1 (TRPC1) Alters Both Store Operated Calcium Entry and Depolarization-Evoked Calcium Signals in C2C12 Cells. *Cell Calcium* 49 (6), 415–425. doi:10.1016/j.ceca.2011.03.012
- Omuro, A., Beal, K., McNeill, K., Young, R. J., Thomas, A., Lin, X., et al. (2018). Multicenter Phase IB Trial of Carboxyamidotriazole Orotate and Temozolomide for Recurrent and Newly Diagnosed Glioblastoma and Other Anaplastic Gliomas. *J. Clin. Oncol.* 36 (17), 1702–1709. doi:10.1200/jco.2017.76.9992
- Owsianik, G., D'hoedt, D., Voets, T., and Nilius, B. (2006). Structure-Function Relationship of the TRP Channel Superfamily. *Rev. Physiol. Biochem. Pharmacol.* 156, 61–90.
- Ozaki, S., Suzuki, A. Z., Bauer, P. O., Ebisui, E., and Mikoshiba, K. (2013). 2-Aminoethyl Diphenylborinate (2-APB) Analogues: Regulation of Ca²⁺ Signaling. *Biochem. Biophysical Res. Commun.* 441 (2), 286–290. doi:10.1016/j.bbrc.2013.08.102
- Park, C. Y., Hoover, P. J., Mullins, F. M., Bachhawat, P., Covington, E. D., Raunser, S., et al. (2009). STIM1 Clusters and Activates CRAC Channels via Direct Binding of a Cytosolic Domain to Orai1. *Cell* 136 (5), 876–890. doi:10.1016/j.cell.2009.02.014
- Peinelt, C., Vig, M., Koomoa, D. L., Beck, A., Nadler, M. J. S., Koblan-Huberson, M., et al. (2006). Amplification of CRAC Current by STIM1 and CRACM1 (Orai1). *Nat. Cell Biol.* 8 (7), 771–773. doi:10.1038/ncb1435
- Peinelt, C., Lis, A., Beck, A., Fleig, A., and Penner, R. (2008). 2-Aminoethoxydiphenyl Borate Directly Facilitates and Indirectly Inhibits STIM1-Dependent Gating of CRAC Channels. *J. Physiol.* 586 (13), 3061–3073. doi:10.1113/jphysiol.2008.151365
- Poburko, D., Lhote, P., Szado, T., Behra, T., Rahimian, R., McManus, B., et al. (2004). Basal Calcium Entry in Vascular Smooth Muscle. *Eur. J. Pharmacol.* 505 (1–3), 19–29. doi:10.1016/j.ejphar.2004.09.060
- Prakriya, M., and Lewis, R. S. (2001). Potentiation and Inhibition of Ca(2+) Release-Activated Ca(2+) Channels by 2-Aminoethoxydiphenyl Borate (2-APB) Occurs Independently of IP(3) Receptors. *J. Physiol.* 536 (Pt 1), 3–19. doi:10.1111/j.1469-7793.2001.t01-1-00003.x
- Prakriya, M., and Lewis, R. S. (2015). Store-Operated Calcium Channels. *Physiol. Rev.* 95 (4), 1383–1436. doi:10.1152/physrev.00020.2014
- Qu, Y. Q., Gordillo-Martinez, F., Law, B. Y. K., Han, Y., Wu, A., Zeng, W., et al. (2018). 2-Aminoethoxydiphenylborane Sensitizes Anti-Tumor Effect of Bortezomib via Suppression of Calcium-Mediated Autophagy. *Cell Death Dis.* 9 (3), 361. doi:10.1038/s41419-018-0397-0
- Rice, L. V., Bax, H. J., Russell, L. J., Barrett, V. J., Walton, S. E., Deakin, A. M., et al. (2013). Characterization of Selective Calcium-Release Activated Calcium Channel Blockers in Mast Cells and T-Cells From Human, Rat, Mouse and Guinea-Pig Preparations. *Eur. J. Pharmacol.* 704 (1–3), 49–57. doi:10.1016/j.ejphar.2013.02.022
- Roos, J., DiGregorio, P. J., Yeromin, A. V., Ohlsen, K., Lioudyno, M., Zhang, S., et al. (2005). STIM1, an Essential and Conserved Component of Store-Operated Ca²⁺ Channel Function. *J. Cell Biol.* 169 (3), 435–445. doi:10.1083/jcb.200502019
- Sadaghiani, A. M., Lee, S. M., Odegaard, J. I., Leveson-Gower, D. B., McPherson, O. M., Novick, P., et al. (2014). Identification of Orai1 Channel Inhibitors by Using Minimal Functional Domains to Screen Small Molecule Microarrays. *Chem. Biol.* 21 (10), 1278–1292. doi:10.1016/j.chembiol.2014.08.016
- Saitoh, M., Ishikawa, T., Matsushima, S., Naka, M., and Hidaka, H. (1987). Selective Inhibition of Catalytic Activity of Smooth Muscle Myosin Light Chain Kinase. *J. Biol. Chem.* 262 (16), 7796–7801. doi:10.1016/s0021-9258(18)47638-7
- Schindl, R., Bergsmann, J., Frischauf, I., Derler, I., Fahrner, M., Muik, M., et al. (2008). 2-Aminoethoxydiphenyl Borate Alters Selectivity of Orai3 Channels by Increasing Their Pore Size. *J. Biol. Chem.* 283 (29), 20261–20267. doi:10.1074/jbc.M803101200
- Schleifer, H., Doleschal, B., Lichtenegger, M., Oppenrieder, R., Derler, I., Frischauf, I., et al. (2012). Novel Pyrazole Compounds for Pharmacological Discrimination Between Receptor-Operated and Store-Operated Ca²⁺ Entry Pathways. *Br. J. Pharmacol.* 167 (8), 1712–1722. doi:10.1111/j.1476-5381.2012.02126.x
- Schmid, E., Stagno, M. J., Yan, J., Stournaras, C., Lang, F., Fuchs, J., et al. (2016). Store-Operated Ca²⁺ Entry in Rhabdomyosarcoma Cells. *Biochem. Biophys. Res. Commun.* 477 (1), 129–136. doi:10.1016/j.bbrc.2016.06.032
- Schwarz, E. C., Wissenbach, U., Niemeyer, B. A., Strauss, B., Philipp, S. E., Flockerzi, V., et al. (2006). TRPV6 Potentiates Calcium-Dependent Cell Proliferation. *Cell Calcium* 39 (2), 163–173. doi:10.1016/j.ceca.2005.10.006
- Selvaraj, S., Sun, Y., Sukumaran, P., and Singh, B. B. (2016). Resveratrol Activates Autophagic Cell Death in Prostate Cancer Cells via Downregulation of STIM1 and the mTOR Pathway. *Mol. Carcinog.* 55 (5), 818–831. doi:10.1002/mc.22324
- Shapovalov, G., Ritaine, A., Skryma, R., and Prevarskaia, N. (2016). Role of TRP Ion Channels in Cancer and Tumorigenesis. *Semin. Immunopathol.* 38 (3), 357–369. doi:10.1007/s00281-015-0525-1
- Shaw, P. J., Weidinger, C., Vaeth, M., Luethy, K., Kaech, S. M., and Feske, S. (2014). CD4+ and CD8+ T Cell-Dependent Antiviral Immunity Requires STIM1 and STIM2. *J. Clin. Invest.* 124 (10), 4549–4563. doi:10.1172/JCI76602
- Shi, Z.-x., Rao, W., Wang, H., Wang, N.-d., Si, J.-W., Zhao, J., et al. (2015). Modeled Microgravity Suppressed Invasion and Migration of Human Glioblastoma U87 Cells Through Downregulating Store-Operated Calcium Entry. *Biochem. Biophys. Res. Commun.* 457 (3), 378–384. doi:10.1016/j.bbrc.2014.12.120
- Shi, J., Chen, C., Ju, R., Wang, Q., Li, J., Guo, L., et al. (2019). Carboxyamidotriazole Combined With IDO1-Kyn-AhR Pathway Inhibitors Profoundly Enhances Cancer Immunotherapy. *J. Immunother. Cancer* 7 (1), 246. doi:10.1186/s40425-019-0725-7
- Shimizu, S., Yoshida, T., Wakamori, M., Ishii, M., Okada, T., Takahashi, M., et al. (2006). Ca²⁺-Calmodulin-Dependent Myosin Light Chain Kinase is Essential for Activation of TRPC5 Channels Expressed in HEK293 Cells. *J. Physiol.* 570 (Pt 2), 219–235. doi:10.1113/jphysiol.2005.097998
- Singh, A. K., Saotome, K., McGoldrick, L. L., and Sobolevsky, A. I. (2018). Structural Bases of TRP Channel TRPV6 Allosteric Modulation by 2-APB. *Nat. Commun.* 9 (1), 2465. doi:10.1038/s41467-018-04828-y
- Sjaastad, M. D., Lewis, R. S., and Nelson, W. J. (1996). Mechanisms of Integrin-Mediated Calcium Signaling in MDCK Cells: Regulation of Adhesion by IP₃- and Store-Independent Calcium Influx. *Mol. Biol. Cell* 7 (7), 1025–1041. doi:10.1091/mbc.7.7.1025
- Smyth, J. T., Dehaven, W. I., Bird, G. S., and Putney, J. W., Jr. (2008). Ca²⁺-Store-Dependent and -Independent Reversal of Stim1 Localization and Function. *J. Cell Sci.* 121 (Pt 6), 762–772. doi:10.1242/jcs.023903
- Song, M., Chen, D., and Yu, S. P. (2014). The TRPC Channel Blocker SKF 96365 Inhibits Glioblastoma Cell Growth by Enhancing Reverse Mode of the Na⁺/Ca²⁺ Exchanger and Increasing Intracellular Ca²⁺. *Br. J. Pharmacol.* 171 (14), 3432–3447. doi:10.1111/bph.12691
- Spedding, M. (1982). Assessment of “Ca²⁺ -Antagonist” Effects of Drugs in K⁺-Depolarized Smooth Muscle. Differentiation of Antagonist Subgroups. *Naunyn Schmiedeberg's Arch. Pharmacol.* 318 (3), 234–240. doi:10.1007/bf00500485
- Stadler, W. M., Rosner, G., Small, E., Hollis, D., Rini, B., Zaentz, S. D., et al. (2005). Successful Implementation of the Randomized Discontinuation Trial Design: An Application to the Study of the Putative Antiangiogenic Agent Carboxyaminoimidazole in Renal Cell Carcinoma-CALGB 69901. *J. Clin. Oncol.* 23 (16), 3726–3732. doi:10.1200/jco.2005.44.150

- Sun, J., Lu, F., He, H., Shen, J., Messina, J., Mathew, R., et al. (2014). STIM1- and Orai1-Mediated Ca²⁺ Oscillation Orchestrates Invadopodium Formation and Melanoma Invasion. *J. Cell Biol.* 207 (4), 535–548. doi:10.1083/jcb.201407082
- Sun, Y., Schaar, A., Sukumaran, P., Dhasarathy, A., and Singh, B. B. (2018). TGF β -Induced Epithelial-to-Mesenchymal Transition in Prostate Cancer Cells is Mediated via TRPM7 Expression. *Mol. Carcinog.* 57 (6), 752–761. doi:10.1002/mc.22797
- Suzuki, A. Z., Ozaki, S., Goto, J.-I., and Mikoshiba, K. (2010). Synthesis of Bisboron Compounds and Their Strong Inhibitory Activity on Store-Operated Calcium Entry. *Bioorg. Med. Chem. Lett.* 20 (4), 1395–1398. doi:10.1016/j.bmcl.2009.12.108
- Tajeddine, N., and Gailly, P. (2012). TRPC1 Protein Channel is Major Regulator of Epidermal Growth Factor Receptor Signaling. *J. Biol. Chem.* 287 (20), 16146–16157. doi:10.1074/jbc.M112.340034
- Takezawa, R., Cheng, H., Beck, A., Ishikawa, J., Launay, P., Kubota, H., et al. (2006). A Pyrazole Derivative Potently Inhibits Lymphocyte Ca²⁺ Influx and Cytokine Production by Facilitating Transient Receptor Potential Melastatin 4 Channel Activity. *Mol. Pharmacol.* 69 (4), 1413–1420. doi:10.1124/mol.105.021154
- Tirupathi, C., Freichel, M., Vogel, S. M., Paria, B. C., Mehta, D., Flockerzi, V., et al. (2002). Impairment of Store-Operated Ca²⁺ Entry in TRPC4(–/–) Mice Interferes With Increase in Lung Microvascular Permeability. *Circ. Res.* 91 (1), 70–76. doi:10.1161/01.res.0000023391.40106.a8
- Togashi, K., Inada, H., and Tominaga, M. (2008). Inhibition of the Transient Receptor Potential Cation Channel TRPM2 by 2-Aminoethoxydiphenyl Borate (2-APB). *Br. J. Pharmacol.* 153 (6), 1324–1330. doi:10.1038/sj.bjp.0707675
- Unemura, M., Baljinnayam, E., Feske, S., De Lorenzo, M. S., Xie, L.-H., Feng, X., et al. (2014). Store-Operated Ca²⁺ Entry (SOCE) Regulates Melanoma Proliferation and Cell Migration. *PLoS One* 9 (2), e89292. doi:10.1371/journal.pone.0089292
- van Kruchten, R., Braun, A., Feijge, M. A. H., Kuijpers, M. J. E., Rivera-Galdos, R., Kraft, P., et al. (2012). Antithrombotic Potential of Blockers of Store-Operated Calcium Channels in Platelets. *Arterioscler Thromb. Vasc. Biol.* 32 (7), 1717–1723. doi:10.1161/atvbaha.111.243907
- Venkatachalam, K., and Montell, C. (2007). TRP Channels. *Annu. Rev. Biochem.* 76, 387–417. doi:10.1146/annurev.biochem.75.103004.142819
- Vig, M., Peinelt, C., Beck, A., Koomoa, D. L., Rabah, D., Koblan-Huberson, M., et al. (2006). CRACM1 is a Plasma Membrane Protein Essential for Store-Operated Ca²⁺ Entry. *Science* 312 (5777), 1220–1223. doi:10.1126/science.1127883
- Waldron, R. T., Chen, Y., Pham, H., Go, A., Su, H. Y., Hu, C., et al. (2019). The Orai Ca²⁺ Channel Inhibitor CM4620 Targets Both Parenchymal and Immune Cells to Reduce Inflammation in Experimental Acute Pancreatitis. *J. Physiol.* 597 (12), 3085–3105. doi:10.1113/jp277856
- Wang, X., Pluznick, J. L., Wei, P., Padanilam, B. J., and Sansom, S. C. (2004). TRPC4 Forms Store-Operated Ca²⁺ Channels in Mouse Mesangial Cells. *Am. J. Physiol. Cell Physiol.* 287 (2), C357–C364. doi:10.1152/ajpcell.00068.2004
- Wang, X., Wang, Y., Zhou, Y., Hendron, E., Mancarella, S., Andrade, M. D., et al. (2014). Distinct Orai-Coupling Domains in STIM1 and STIM2 Define the Orai-Activating Site. *Nat. Commun.* 5, 3183. doi:10.1038/ncomms4183
- Wang, J.-Y., Sun, J., Huang, M.-Y., Wang, Y.-S., Hou, M.-F., Sun, Y., et al. (2015). STIM1 Overexpression Promotes Colorectal Cancer Progression, Cell Motility and COX-2 Expression. *Oncogene* 34 (33), 4358–4367. doi:10.1038/onc.2014.366
- Wang, W., Ren, Y., Wang, L., Zhao, W., Dong, X., Pan, J., et al. (2018). Orai1 and Stim1 Mediate the Majority of Store-Operated Calcium Entry in Multiple Myeloma and Have Strong Implications for Adverse Prognosis. *Cel. Physiol. Biochem.* 48 (6), 2273–2285. doi:10.1159/000492645
- Wang, Y., He, J., Jiang, H., Zhang, Q., Yang, H., Xu, X., et al. (2018). Nicotine Enhances Store Operated Calcium Entry by Upregulating HIF 1 α and SOCC Components in Non Small Cell Lung Cancer Cells. *Oncol. Rep.* 40 (4), 2097–2104. doi:10.3892/or.2018.6580
- Wang, Y., Qi, Y. X., Qi, Z., and Tsang, S. Y. (2019). TRPC3 Regulates the Proliferation and Apoptosis Resistance of Triple Negative Breast Cancer Cells Through the TRPC3/RASA4/MAPK Pathway. *Cancers* 11 (4), 558. doi:10.3390/cancers11040558
- Wasilenko, W. J., Palad, A. J., Somers, K. D., Blackmore, P. F., Kohn, E. C., Rhim, J. S., et al. (1996). Effects of the Calcium Influx Inhibitor Carboxyamido-Triazole on the Proliferation and Invasiveness of Human Prostate Tumor Cell Lines. *Int. J. Cancer* 68 (2), 259–264. doi:10.1002/(SICI)1097-0215(19961009)68:2<259::AID-IJC20>3.0.CO;2-4
- Watanabe, H., Takahashi, R., Zhang, X.-X., Kakizawa, H., Hayashi, H., and Ohno, R. (1996). Inhibition of Agonist-Induced Ca²⁺ Entry in Endothelial Cells by Myosin Light-Chain Kinase Inhibitor. *Biochem. Biophys. Res. Commun.* 225 (3), 777–784. doi:10.1006/bbrc.1996.1250
- Wei, M., Zhou, Y., Sun, A., Ma, G., He, L., Zhou, L., et al. (2016). Molecular Mechanisms Underlying Inhibition of STIM1-Orai1-Mediated Ca²⁺ Entry Induced by 2-Aminoethoxydiphenyl Borate. *Pflugers Arch.* 468 (11–12), 2061–2074. doi:10.1007/s00424-016-1880-z
- Wen, L., Voronina, S., Javed, M. A., Awais, M., Szatmary, P., Latawiec, D., et al. (2015). Inhibitors of ORAI1 Prevent Cytosolic Calcium-Associated Injury of Human Pancreatic Acinar Cells and Acute Pancreatitis in 3 Mouse Models. *Gastroenterology* 149 (2), 481–492. doi:10.1053/j.gastro.2015.04.015
- Williams, R. T., Manji, S. S. M., Parker, N. J., Hancock, M. S., Van Stekelenburg, L., Eid, J.-P., et al. (2001). Identification and Characterization of the STIM (Stromal Interaction Molecule) Gene Family: Coding for a Novel Class of Transmembrane Proteins. *Biochem. J.* 357 (Pt 3), 673–685. doi:10.1042/0264-6021:3570673
- Worley, P. F., Zeng, W., Huang, G. N., Yuan, J. P., Kim, J. Y., Lee, M. G., et al. (2007). TRPC Channels as STIM1-Regulated Store-Operated Channels. *Cell Calcium* 42 (2), 205–211. doi:10.1016/j.ceca.2007.03.004
- Wu, Y., Palad, A. J., Wasilenko, W. J., Blackmore, P. F., Pincus, W. A., Schechter, G. L., et al. (1997). Inhibition of Head and Neck Squamous Cell Carcinoma Growth and Invasion by the Calcium Influx Inhibitor Carboxyamido-Triazole. *Clin. Cancer Res.* 3 (11), 1915–1921.
- Wu, M. L., Chen, W. H., Liu, I. H., Tseng, C. D., and Wang, S. M. (1999). A Novel Effect of Cyclic AMP on Capacitative Ca²⁺ Entry in Cultured Rat Cerebellar Astrocytes. *J. Neurochem.* 73 (3), 1318–1328. doi:10.1046/j.1471-4159.1999.0731318.x
- Wu, Y.-L., Xie, J., An, S.-W., Oliver, N., Barrezaeta, N. X., Lin, M.-H., et al. (2017). Inhibition of TRPC6 Channels Ameliorates Renal Fibrosis and Contributes to Renal protection by Soluble Klotho. *Kidney Int.* 91 (4), 830–841. doi:10.1016/j.kint.2016.09.039
- Xia, J., Wang, H., Huang, H., Sun, L., Dong, S., Huang, N., et al. (2016). Elevated Orai1 and STIM1 Expressions Upregulate MACC1 Expression to Promote Tumor Cell Proliferation, Metabolism, Migration, and Invasion in Human Gastric Cancer. *Cancer Lett.* 381 (1), 31–40. doi:10.1016/j.canlet.2016.07.014
- Xie, J., Pan, H., Yao, J., Zhou, Y., and Han, W. (2016). SOCE and Cancer: Recent Progress and New Perspectives. *Int. J. Cancer* 138 (9), 2067–2077. doi:10.1002/ijc.29840
- Xu, S.-Z., Zeng, F., Boulay, G., Grimm, C., Harteneck, C., and Beech, D. J. (2005). Block of TRPC5 Channels by 2-Aminoethoxydiphenyl Borate: a Differential, Extracellular and Voltage-Dependent Effect. *Br. J. Pharmacol.* 145 (4), 405–414. doi:10.1038/sj.bjp.0706197
- Xu, Y., Zhang, S., Niu, H., Ye, Y., Hu, F., Chen, S., et al. (2015). STIM1 Accelerates Cell Senescence in a Remodeled Microenvironment But Enhances the Epithelial-to-Mesenchymal Transition in Prostate Cancer. *Sci. Rep.* 5, 11754. doi:10.1038/srep11754
- Xu, X., Ali, S., Li, Y., Yu, H., Zhang, M., Lu, J., et al. (2016). 2-Aminoethoxydiphenyl Borate Potentiates CRAC Current by Directly Dilating the Pore of Open Orai1. *Sci. Rep.* 6, 29304. doi:10.1038/srep29304
- Yamashita, M., Navarro-Borelly, L., McNally, B. A., and Prakriya, M. (2007). Orai1 Mutations Alter Ion Permeation and Ca²⁺-Dependent Fast Inactivation of CRAC Channels: Evidence for Coupling of Permeation and Gating. *J. Gen. Physiol.* 130 (5), 525–540. doi:10.1085/jgp.200709872
- Yamashita, M., Somasundaram, A., and Prakriya, M. (2011). Competitive Modulation of Ca²⁺ Release-Activated Ca²⁺ Channel Gating by STIM1 and 2-Aminoethoxydiphenyl Borate. *J. Biol. Chem.* 286 (11), 9429–9442. doi:10.1074/jbc.M110.189035
- Yang, H., Mergler, S., Sun, X., Wang, Z., Lu, L., Bonanno, J. A., et al. (2005). TRPC4 Knockdown Suppresses Epidermal Growth Factor-Induced Store-Operated Channel Activation and Growth in Human Corneal Epithelial Cells. *J. Biol. Chem.* 280 (37), 32230–32237. doi:10.1074/jbc.M504553200
- Yang, S., Zhang, J. J., and Huang, X.-Y. (2009). Orai1 and STIM1 are Critical for Breast Tumor Cell Migration and Metastasis. *Cancer Cell* 15 (2), 124–134. doi:10.1016/j.ccr.2008.12.019
- Yang, N., Tang, Y., Wang, F., Zhang, H., Xu, D., Shen, Y., et al. (2013). Blockade of Store-Operated Ca²⁺ Entry Inhibits Hepatocarcinoma Cell Migration and

- Invasion by Regulating Focal Adhesion Turnover. *Cancer Lett.* 330 (2), 163–169. doi:10.1016/j.canlet.2012.11.040
- Ye, J., Huang, J., He, Q., Zhao, W., Zhou, X., Zhang, Z., et al. (2018). Blockage of Store-Operated Ca²⁺ Entry Antagonizes Epstein-Barr Virus-Promoted Angiogenesis by Inhibiting Ca²⁺ Signaling-Regulated VEGF Production in Nasopharyngeal Carcinoma. *Cancer Manag. Res.* 10, 1115–1124. doi:10.2147/cmar.S159441
- Yoshida, J., Iwabuchi, K., Matsui, T., Ishibashi, T., Masuoka, T., and Nishio, M. (2012). Knockdown of Stromal Interaction Molecule 1 (STIM1) Suppresses Store-Operated Calcium Entry, Cell Proliferation and Tumorigenicity in Human Epidermoid Carcinoma A431 Cells. *Biochem. Pharmacol.* 84 (12), 1592–1603. doi:10.1016/j.bcp.2012.09.021
- Yuan, J. P., Zeng, W., Dorwart, M. R., Choi, Y.-J., Worley, P. F., and Muallem, S. (2009). SOAR and the Polybasic STIM1 Domains Gate and Regulate Orai Channels. *Nat. Cell Biol.* 11 (3), 337–343. doi:10.1038/ncb1842
- Zagranichnaya, T. K., Wu, X., and Villereal, M. L. (2005). Endogenous TRPC1, TRPC3, and TRPC7 Proteins Combine to Form Native Store-Operated Channels in HEK-293 Cells. *J. Biol. Chem.* 280 (33), 29559–29569. doi:10.1074/jbc.M505842200
- Zakharov, S. I., Smani, T., Dobrydneva, Y., Monje, F., Fichandler, C., Blackmore, P. F., et al. (2004). Diethylstilbestrol is a Potent Inhibitor of Store-Operated Channels and Capacitative Ca(2+) Influx. *Mol. Pharmacol.* 66 (3), 702–707. doi:10.1124/mol.66.310.1124/mol.66.3
- Zang, J., Zuo, D., Zuo, D., L. Shogren, K., T. Gustafson, C., Zhou, Z., et al. (2019). STIM1 Expression is Associated With Osteosarcoma Cell Survival. *Chin. J. Cancer Res.* 31 (1), 203–211. doi:10.21147/j.issn.1000-9604.2019.01.15
- Zeng, B., Yuan, C., Yang, X., L. Atkin, S., and Xu, S.-Z. (2013). TRPC Channels and Their Splice Variants are Essential for Promoting Human Ovarian Cancer Cell Proliferation and Tumorigenesis. *Curr. Cancer Drug Targets* 13 (1), 103–116. doi:10.2174/156800913804486629
- Zhang, X.-F., Iwamuro, Y., Enoki, T., Okazawa, M., Lee, K., Komuro, T., et al. (1999). Pharmacological Characterization of Ca²⁺ Entry Channels in Endothelin-1-Induced Contraction of Rat Aorta Using LOE 908 and SK&F 96365. *Br. J. Pharmacol.* 127 (6), 1388–1398. doi:10.1038/sj.bjp.0702661
- Zhang, J., Wei, J., Kanada, M., Yan, L., Zhang, Z., Watanabe, H., et al. (2013). Inhibition of Store-Operated Ca²⁺ Entry Suppresses EGF-Induced Migration and Eliminates Extravasation From Vasculature in Nasopharyngeal Carcinoma Cell. *Cancer Lett.* 336 (2), 390–397. doi:10.1016/j.canlet.2013.03.026
- Zhang, J., He, Q., Ye, J., Zhang, Z., Li, Y., Wei, J., et al. (2015). SKF95365 Induces Apoptosis and Cell-Cycle Arrest by Disturbing Oncogenic Ca²⁺ Signaling in Nasopharyngeal Carcinoma Cells. *Onco. Targets Ther.* 8, 3123–3133. doi:10.2147/ott.S92005
- Zhou, Y., Meraner, P., Kwon, H. T., Machnes, D., Oh-hora, M., Zimmer, J., et al. (2010). STIM1 Gates the Store-Operated Calcium Channel ORAI1 *In Vitro*. *Nat. Struct. Mol. Biol.* 17 (1), 112–116. doi:10.1038/nsmb.1724
- Zitt, C., Strauss, B., Schwarz, E. C., Spaeth, N., Rast, G., Hatzelmann, A., et al. (2004). Potent Inhibition of Ca²⁺ Release-Activated Ca²⁺ Channels and T-Lymphocyte Activation by the Pyrazole Derivative BTP2. *J. Biol. Chem.* 279 (13), 12427–12437. doi:10.1074/jbc.M309297200
- Zubcevic, L., Herzik, M. A., Jr., Wu, M., Borschel, W. F., Hirschi, M., Song, A. S., et al. (2018). Conformational Ensemble of the Human TRPV3 Ion Channel. *Nat. Commun.* 9 (1), 4773. doi:10.1038/s41467-018-07117-w

Conflict of Interest: The authors declare that the research was conducted in the absence of any commercial or financial relationships that could be construed as a potential conflict of interest.

Copyright © 2021 Liang, Zhang, Pan, Xie and Han. This is an open-access article distributed under the terms of the Creative Commons Attribution License (CC BY). The use, distribution or reproduction in other forums is permitted, provided the original author(s) and the copyright owner(s) are credited and that the original publication in this journal is cited, in accordance with accepted academic practice. No use, distribution or reproduction is permitted which does not comply with these terms.



Targeting Signaling Pathway Networks in Several Malignant Tumors: Progresses and Challenges

Hongdan He¹, Xiaoni Shao², Yanan Li², Ribu Gihu², Haochen Xie¹, Junfu Zhou² and Hengxiu Yan^{2*}

¹Qinghai Tibet Plateau Research Institute, Southwest Minzu University, Chengdu, China, ²Immunotherapy Laboratory, College of Pharmacology, Southwest Minzu University, Chengdu, China

OPEN ACCESS

Edited by:

Jingxin Mo,
University of New South Wales,
Australia

Reviewed by:

Chunjie Jiang,
University of Pennsylvania,
United States
Gang Sun,
Tumor Hospital of Xinjiang Medical
University, China

*Correspondence:

Hengxiu Yan
719306512@qq.com

Specialty section:

This article was submitted to
Pharmacology of Anti-Cancer Drugs,
a section of the journal
Frontiers in Pharmacology

Received: 03 March 2021

Accepted: 18 May 2021

Published: 31 May 2021

Citation:

He H, Shao X, Li Y, Gihu R, Xie H,
Zhou J and Yan H (2021) Targeting
Signaling Pathway Networks in Several
Malignant Tumors: Progresses
and Challenges.
Front. Pharmacol. 12:675675.
doi: 10.3389/fphar.2021.675675

Malignant tumors remain the health problem of highest concern among people worldwide due to its high mortality and recurrence. Lung, gastric, liver, colon, and breast cancers are among the top five malignant tumors in terms of morbidity and mortality. In cancer biology, aberrant signaling pathway regulation is a prevalent theme that drives the generation, metastasis, invasion, and other processes of all malignant tumors. The Wnt/ β -catenin, PI3K/AKT/mTOR, Notch and NF- κ B pathways are widely concerned and signal crosstalks exist in the five solid tumors. This review provides an innovative summary of the recent progress in research on these signaling pathways, the underlying mechanism of the molecules involved in these pathways, and the important role of some miRNAs in tumor-related signaling pathways. It also presents a brief review of the antitumor molecular drugs that target these signaling pathways. This review may provide a theoretical basis for the study of the molecular biological mechanism of malignant tumors and vital information for the development of new treatment strategies with a focus on efficacy and the reduction of side effects.

Keywords: malignant tumors, signaling pathway, miRNA, targeted therapy, antitumor molecular drugs

INTRODUCTION

Malignant tumors are a public health problem of worldwide concern and a leading cause of death for people in the world. According to a 2017 report by the American Cancer Society, lung cancer (LC), gastric cancer (GC), liver cancer, colorectal cancer, and breast cancer (BC) remain the top five causes of cancer deaths (Siegel et al., 2020). The highly invasive nature of cancer cells is the main cause of high cancer mortality and often leads to cancer progression and metastasis. Therefore, determining the mechanism underlying the occurrence and development of malignant tumors is of great importance.

The numerous studies that have been performed in recent decades suggest that signaling pathways are implicated in the development of cancer. Abnormal pathways drive the generation, metastasis, invasion, and other processes of all malignant tumors. Among the five tumors that received the most attention and emerged as crosstalk pathways were Wnt/ β -catenin pathway, PI3K/AKT/mTOR, Notch and NF- κ B pathway (Rogers et al., 2008; Ahmed et al., 2013; Collu et al., 2014; Zheng et al., 2017). Four signaling pathways play important roles in the occurrence, development and spread of malignant tumors. These pathways include the secretory glycoprotein (Wnt)/ β -serial protein (β -catenin) signaling pathway (Holstein, 2012), the phosphatidylinositol-3-kinase (PI3K)/protein kinase B (AKT)/mammalian rapamycin

target protein (mTOR) signaling pathway (Engelman et al., 2006), the Notch signaling pathway (Kopan and Ilagan, 2009), and the nuclear factor kappa beta (NF- κ B) signaling pathway (Karin, 2006). The Wnt/ β -catenin signaling pathway is engaged in cell multiplication, migration, genetic stability, and apoptosis, as well as participates in maintaining the pluripotent state of adult stem cells, which is associated with tumor generation and development (Holstein, 2012). PI3K/AKT/mTOR signal transduction pathway can not only control cell metabolism, movement, survival and proliferation, but also can affect the growth and spread of cancer cells. The PI3K/AKT/mTOR pathway dysregulation are often observed in human cancers (Engelman et al., 2006). In addition, the Notch signaling pathway has been detected in human BC, indicating that it acts an indispensable part in BC occurrence as a result of its participation in cell growth process (Kopan and Ilagan, 2009). Furthermore, the NF- κ B signaling pathway has been increasingly considered to be a key factor in many steps of cancer occurrence and development (Karin, 2006). Therefore, all of these signaling pathways are frequently seen in malignant tumors. Meanwhile, an increasing number of new drugs that target these signaling pathways have been used in the gene therapy of malignant tumors (Polivka and Janku, 2014). Therefore, an improved understanding of the above signaling pathways may improve oncologists' prognosis ability and prediction accuracy for treatment response.

MicroRNAs are a group of very conservative small single-stranded noncoding RNA molecules that, by pairing with complementary RNA molecules, negatively regulate the expression patterns of different genes at the post-transcriptional or translational level, thereby inhibiting translation through RNA degradation. MiRNAs participate in many cellular processes, such as transcription, cell growth, proliferation, inflammation, cell movement, differentiation, and apoptosis, as well as in the cell cycle (Iqbal et al., 2019). MiRNA can as a tumor suppressor gene (TSG) or oncogene by regulating the expression levels of several proteins, so that the abnormal expression patterns of microRNA-related signaling pathways are associated with the occurrence and development of human malignant tumors. The miRNA-based therapies of tumors have been widely reported. Given that miRNAs are effective modulators of resistance, they could be a beneficial strategy of therapy, especially for resistant phenotypes, in conjunction with chemotherapy or radiotherapy (Yu et al., 2015; Arab et al., 2017). MiRNA-based therapeutic strategies targeting signaling pathways have been made to decrease the level of expression of specific miRNAs and supplement the deficiency in miRNAs that develops during disease progression.

This review provides an innovative summary of several signaling pathways that have been associated with the occurrence and progression of malignant tumors with high morbidity and mortality worldwide in recent years (Leake et al., 2012; Rapp et al., 2017; Stotz et al., 2015). Notably, we describe some key signaling molecules involved in the pathogenesis of malignant tumors and the drugs targeting

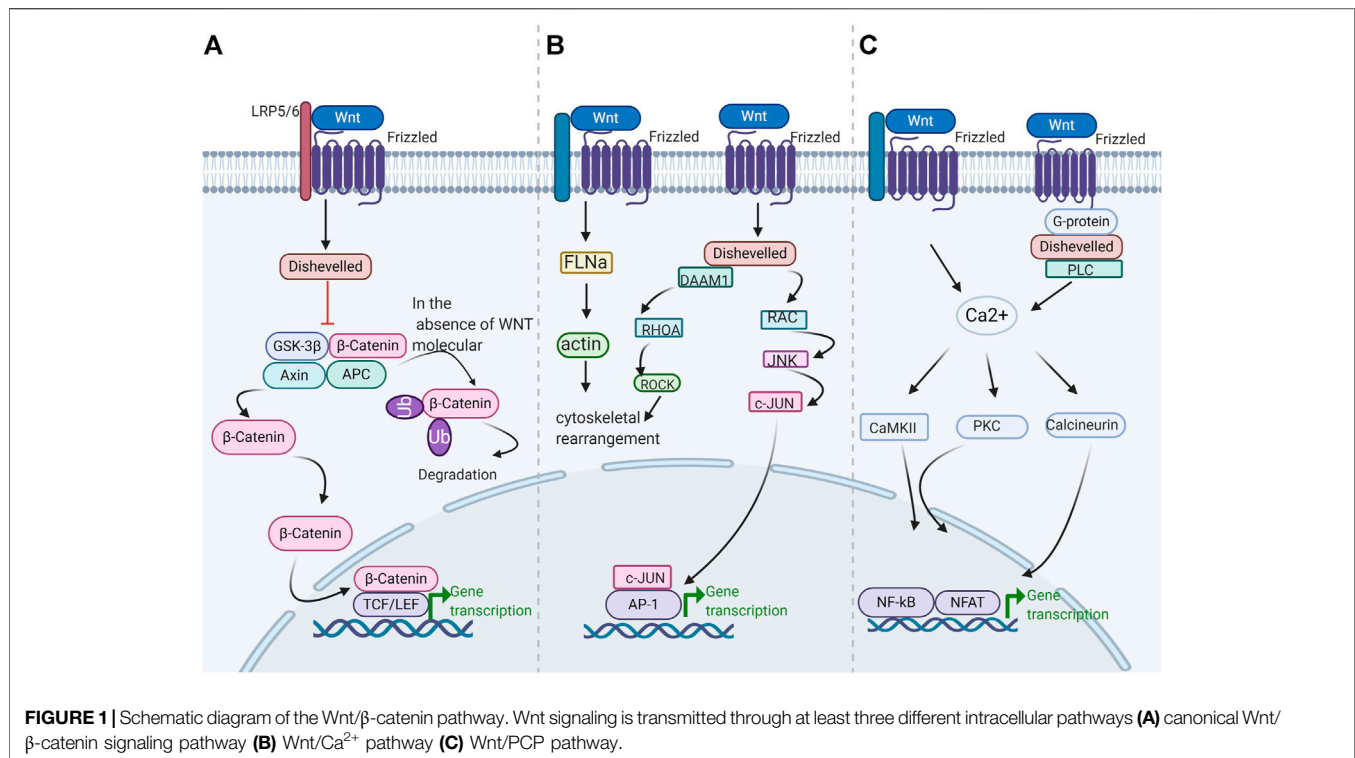
these pathways that have been marketed (Lagadec et al., 2008; Rakha and Green, 2017). In addition, this article presents an analysis of the current research related to the role of miRNAs in cancer invasion and metastasis with the expectation that the further exploration of miRNA-targeted therapy may help establish a new spectrum of cancer treatments. The goal of our study is to help develop and design new drugs that will extend the lives of patients with the five top-ranked malignancies and reduce side effects, risks, and drug resistance.

TARGETING WNT/ β -CATENIN PATHWAY FOR CANCER

Wnt/ β -Catenin Pathway

The Wnt family is a class of proteins involved in many functions, including cell survival, stem cell renewal, and organ formation (Holstein, 2012). The name Wnt is determined by the *Drosophila* gene *Wingless* and the mouse proto-oncogene *Int1* (Katoh and Katoh, 2005). At present, researchers have discovered nearly a hundred Wnt genes in different species. In humans, 19 Wnt proteins have amino acid sequence homologies of 27–83% and the conservative pattern of 23 or 24 cysteine residues. Cysteine-rich glycoproteins in the Wnt family act as ligands for up to 15 receptors or coreceptors (Li et al., 2006).

Wnt signals transduction through three distinct cellular pathways, including the Wnt/ β -catenin-dependent or canonical pathway and the Wnt/ β -catenin-independent or noncanonical pathway. The β -Catenin independent pathway includes the Wnt/ Ca^{2+} pathway and the planar cell polarity (PCP) pathway. The β -catenin-dependent signaling pathway is initiated by the binding of the Wnt ligand to lipoprotein receptor-related protein (LRP)-5/6 receptors, which activate disheveled (DVL) and in turn induce the recruitment of the receptor axis inhibition protein Axin, glycogen synthase kinase-3 β (GSK-3 β), casein kinase 1 (CK1), and adenomatous polyposis *Escherichia coli* (APC) in the form of a complex (Macdonald et al., 2009). The Wnt-Frizzled-Axin-LRP-5/6 complex sequesters cytosolic GSK-3 β , preventing it from phosphorylating β -catenin. Unphosphorylated β -Catenin accumulates in the cytosol migrating to the nucleus, where it interacts with the T cell-specific factor (TCF) lymph enhancer-binding factor and coactivators, such as pygopus and B-cell lymphoma 9, to turn on Wnt target genes, such as *c-myc*, *cyclin D1*, and cyclin-dependent kinase inhibitor 1. In the lack of the Wnt molecule, β -catenin in the cytosol is phosphorylated by GSK-3 β and subsequently isolated from the β -catenin destruction complex (Wu and Pan, 2010). Phosphorylated compounds enhance β -catenin ubiquitination and lead to subsequent proteasome degradation. In the atypical Wnt pentachlorophenol or PCP pathway, the Wnt protein binds to the frizzled transmembrane receptor on the cell surface, subsequently activates RHO/RAC small GTPase and Jun N-terminal kinase (JNK) through DVL, and then assists in the regulation of the cytoskeleton and gene expression (Gordon and Nusse, 2006). DVL connects to the



downstream effector ras homolog family member A and RHO-associated kinase through the DVL-associated activator of morphogenesis-1 (Fumoto and Kikuchi, 2019). In the Wnt/Ca²⁺ pathway, Wnt proteins are mainly composed of Wnt1, Wnt5a, and Wnt11. They bind to frizzled transmembrane receptors and participate in several cellular processes. These processes involve the stimulation of the heterodimer G protein to further activate phospholipase-C (PLC) (Okamoto et al., 2014). PLC increases intracellular Ca²⁺ release, decreases cGMP levels, and activates calcineurin and protein kinase-C or Ca²⁺-calmodulin-dependent protein kinase-II (Macdonald and He, 2012; Jiang et al., 2015). These processes may spur the nuclear factor of activated T cells and other transcription factors, such as cAMP response element-binding protein-1 (Jernigan et al., 2010) (Figure 1). The Wnt signaling pathway is activated in various cancers, and these molecules are closely related to its activation.

Wnt signals are activated in the crypt floor, which are crucial for cell repair and the optimal maintenance of stem cells. Numerous of evidence indicates that colorectal cancer is under the effect of Wnt signaling pathway activation, which is related to the loss-of-function of the tumor regulator APC (Krishnamurthy and Kurzrock, 2018). The Wnt pathways can cross-talk with the Notch pathway. This phenomenon provides a reliable idea for cancer treatment and intervention. Nonetheless, considerable challenges are encountered in targeting the Wnt pathway. These challenges include the search for drugs that are effective in cell repair and tissue homeostasis without impairing the functional system of normal stem cells (Yang et al., 2016; Li

et al., 2018a; Xing et al., 2019). Next, we retrospect the Wnt/β-catenin pathway in different cancers. Moreover, we will introduce the status of research on the effectors and inhibitors of the Wnt/β-catenin signaling pathway.

Wnt/β-Catenin Pathway and Lung Cancer

The abnormal Wnt/β-catenin pathway drives the generation, metastasis, invasion, and other processes of LC and plays an active role in the formation of LC angiogenesis and the stability of LC stem cells. Abnormalities in the Wnt/β-catenin pathway involve gene mutations in the Wnt pathway, molecular modifications, and protein molecular changes in transcription and translation (Ullah et al., 2013; Santana et al., 2020). Therefore, targeting the Wnt/β-catenin pathway has become an effective means to treat LC.

Given that APC is part of the degradation scaffold for β-catenin, mutations in APC, including cyclin D1 and c-myc, lead to decreased degradation and increased nuclear accumulation (Yedid et al., 2016). Studies have shown that loss of heterozygosity on chromosome 5q and increased levels of β-catenin at the APC locus have occurred in LC types. However, LC types are characterized mainly by transcriptional dysregulation of Wnt ligands rather than specific site mutations in the APC or β-catenin genes (Wang et al., 2019). For example, a common feature of certain LC cell lines is the loss of Wnt7a mRNA (Ohgaki et al., 2004; Nakayama et al., 2014). Elevated levels of Wnt1 and Wnt2 in some other NSCLCs also have been reported. The inhibition of Wnt2-induced signaling results in the down-regulation of the antiapoptotic gene and consequently initiates apoptosis (Winn et al., 2005; Chen et al., 2018). The

SRY-like HMG box 2 (*Sox2*) gene codes for the SOX2 transcription factor which is expressed in the main histological types of LC (Chen et al., 2012). By inhibiting the expression of SOX2 in lung cancer, the expression of *Wnt1/2*, *Notch1* and *c-myc* genes can be down-regulated and tumor cell apoptosis can be induced (Nakatsugawa et al., 2011). By contrast, the sustained β -catenin signaling hinders the differentiation of clara cells into ciliated cells, whereas the Knockout of β -catenin in basal cells can inhibit proliferation and prompts apoptosis (Yedid et al., 2016). Besides, *Wnt7b* is up-regulated in adenocarcinoma, and *Wnt5a* is up-regulated in primary squamous cell carcinoma (Ghosh et al., 2013). In lung metastasis, the overexpression of *Wnt5a* in the noncanonical pathway also regulates the expression of fibroblast growth factor (FGF) 10 and sonic hedgehog and epithelial-mesenchymal transition (EMT). Matrix metalloproteinases are the targets of canonical and noncanonical Wnt signaling pathways and are critical for tissue remodeling; they are increased in spread tumors (Mao et al., 2018). In addition to Wnt *in vitro*, other molecules in the Wnt/ β -catenin pathway are abnormally regulated in LC. For instance, the overexpression of DVL-3, a signal converter molecule and a positive regulator of the Wnt/ β -catenin signaling pathway, has been reported in NSCLC. Moreover, the Wnt pathway antagonists Dickkopf-3, WNT inhibitor (Mao et al., 2018), and secreted crimped protein-related proteins have been reported in different subtypes of LCs (Lee et al., 2004).

In addition to the genetic studies described above, epigenetic research has grown rapidly over the past period, especially for miRNAs (Lee et al., 2004). Increasingly miRNAs have been discovered that related with various types of LCs. Several β -catenin interacting proteins have also been found among the miR-214 targets in lung adenocarcinomas (Qi et al., 2015), and β -catenin itself is rather affected by miR-3619-5p. Mir-3619-5p has been reported to inhibit tumor cell growth of A549 and H460 NSCLC by binding to the 3'-UTR region of the β -catenin gene. In addition, miR-374a targets *Wnt5a*, and miR-487b can reduce *Wnt5a* activity (Qi et al., 2015). The type 2B sodium dependent phosphate transporter (NaPi-IIB) is situated in the apical membrane of ATII cells (Qi et al., 2015; Zhang et al., 2016). MiR-410 can activate the Wnt/ β -catenin pathway by decreasing NaPi-IIB levels (Zhang et al., 2016), thus improving the ability of tumor growth and invasion.

Wnt/ β -Catenin Pathway and Liver Cancer

The inhibitors of the Wnt/ β -catenin signaling pathway might be effective in the hepatocellular carcinoma (HCC) intervention therapy (Taciak et al., 2018). In a HepG2 cell line, the knockout of β -catenin under the mediation of RNA interference decreases proliferation and growth *in vitro*. Evidence showing that miRNAs correlated with the expression of Wnt/ β -catenin pathway related genes, such as *c-myc*, *APC*, *cyclin D1*, and *DKK1*, are increasing. Ashmawy held that miR-106b, miR-10a, miR-99a, miR-148a, miR-215, miR-199a, miR-30e, miR-199a3p, miR-24, miR-122, and miR-125b, are down-regulated in patients with HCC (Ashmawy et al., 2017). Liu thought that miR-18a expression is up-regulated relative to that

in adjacent nontumoral liver tissue in human HCC. Up-regulation of miR-18a expression level improved the spread and migration ability of HCC cell lines by suppressing krüppel-like factor4, a factor that negatively regulates β -catenin expression. Other than miR-18a, Liu also concluded that upon induction by *c-myc* silencing, miR-320a expression levels were upregulated in HCC tissues relative to paired adjacent non tumorous liver tissues, and the ability to inhibit HCC cell proliferation and invasion would be enhanced (Lu et al., 2017; Xie et al., 2017). These data suggest that miR-320a may be exploited as a target for HCC therapy. Moreover, *wnt3* is a target of miR-1247-5p, and its expression is significantly down-regulated by miR-1247-5p overexpression. This restrains the invasion and proliferation of HepG2 cells, induces cell apoptosis *in vitro* (Chu et al., 2017). Thus, miR-1247-5p may serve as a target for HCC therapy (Table 1).

Wnt/ β -Catenin Pathway and CRC

Wnt/ β -catenin pathway dysregulation also occurs frequently in CRC. The abnormal activation of this pathway is related to cell proliferation, invasion behavior, and drug resistance, suggesting the potential value of targeting Wnt/ β -catenin pathway as an intervention method for CRC. Most CRC patients have at least one mutation in a Wnt signaling cascade gene such as *APC* and β -catenin protein. Gene mutations in β -catenin, *GSK-3 β* , *Axin*, or *APC* leads to abnormal activation of the Wnt/ β -catenin pathway, and simultaneous Wnt overexpression causes abnormal activation of this pathway (Schmalhofer et al., 2009). The Wnt/ β -catenin pathway regulates *E-cadherin* by enhancing the expression level of repressors of this adhesion molecule, involving the transcriptional factors recombinant snail homolog (*SNAI1*), zinc finger E-box binding homeobox 1 and *SNAI2*. This action therefore leads to metastasis and invasiveness.

Abnormal expression of miRNA is related to the disorder of cancer-related signaling pathways, Wnt/ β -catenin pathway is included. Further research showed that Smad7 is a protein necessary for nuclear accumulation of β -catenin. MiR-93 inhibits the Wnt/ β -catenin pathway by targeting Smad7 (Tang et al., 2015). Similarly, miR-185 (Dong-Xu et al., 2015) and miR-320a expression levels in CRC cells are significantly down-regulated compared with those in normal colon cells. Consistently, the enforced expression of miR-101 (Strillacci et al., 2009) attenuates the promalignant features of CRC, including cell growth, invasion and hypoxic survival, which means that miR-101 can be an effective cancer suppressor for CRC patients. Moreover, several agents targeting this pathway have been developed for CRC treatment (Table 2). These agents include retinoic acid and vitamin D. Retinoic acid can suppress Wnt signaling via interaction with β -catenin or via competing with TCF. The active form of vitamin D encourages β -catenin binding to the vitamin D receptor, and reducing the level of β -catenin. Besides, several monomers of Chinese traditional herbs, including quercetin and resveratrol, and the green tea polyphenol epigallocatechin-3-gallate are observed to inhibit Wnt inhibitory activity (Roa et al., 2019). The inhibitors of Wnt production are a new type of Porcupine-targeted Wnt antagonists. For example, LGK974 can bind to and block

TABLE 1 | miRNAs regulate Wnt/ β -catenin pathway in liver cancer.

miRNA	Regulation	Pathway	References
miR-18a	Upregulating and promoting the proliferation and migration of HCC cell lines by inhibiting KLF4	Wnt/ β -catenin pathway	Lu et al. (2017)
miR-320a	Inhibiting it can up-regulation of the expression levels of β -catenin, c-myc, cyclin D1 and DKK-1	Wnt/ β -catenin pathway	Xie et al. (2017)
miR-1247-5p	Inhibiting the invasion and proliferation of HepG2 cells by targeting Wnt3	Wnt/ β -catenin pathway	Chu et al. (2017)

TABLE 2 | Some agents target Wnt/ β -catenin pathway in colon cancer.

Agents	Regulation	Reference
Retinoic acid	Inhibit Wnt signaling by direct interaction with β -catenin/competition for TCF binding	Roa et al. (2019)
Vitamin D	Encourages the β -catenin binding to the vitamin D receptor and decreases the amount of β -catenin	Roa et al. (2019)
Quercetin	Suppresses Wnt inhibiting activity	Roa et al. (2019)
Resveratrol	Suppresses Wnt inhibiting activity	Roa et al. (2019)
Green tea polyphenol epigallocatechin-3-gallate	Suppresses Wnt inhibiting activity	Roa et al. (2019)
LGK974	Binds and blocks the porcupine enzyme	Liu et al. (2013)
PRI-724	Increase p300/ β -catenin binding and stem-cell differentiation	Lenz and Kahn (2014)
BBI608	Not only inhibits signal transducer and activator of Stat3 but also suppresses β -catenin signaling	Ciombor et al. (2015)

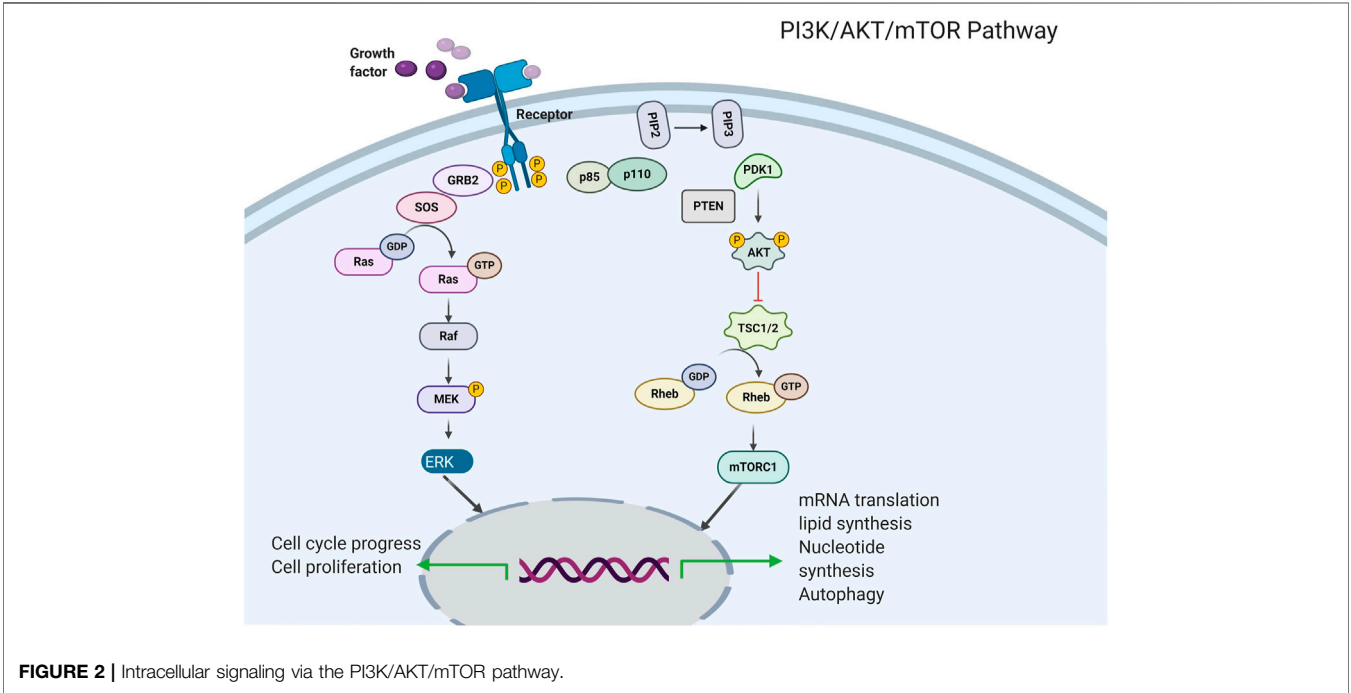


FIGURE 2 | Intracellular signaling via the PI3K/AKT/mTOR pathway.

porcupine enzymes. LGK974 inhibits the expansion of the murine tumor xenograft model via ectopic Wnt1 expression originating from the mouse mammary tumor virus (MMTV) (Liu et al., 2013). PRI-724, a second generation β -catenin antagonist, increases p300/ β -catenin binding and stem-cell differentiation. BBI608 is another small molecule that not only inhibits the signal transducer and activator of transcription-3 but

also suppresses β -catenin signaling to treat colorectal cancer (Lenz and Kahn, 2014). BBI608 can be combined with chemotherapy agents (such as cisplatin, gemcitabine, paclitaxel, temozolomide, sorafenib and pemetrexed) to treat patients with CRC. However, when BBI608 was used in the phase III trial of metastatic CRC, its expected efficacy was not achieved in the short-term analysis (Ciombor et al., 2015).

TARGETING THE PHOSPHATIDYLINOSITOL-3-KINASE/PROTEIN KINASE B/MAMMALIAN RAPAMYCIN TARGET PROTEIN PATHWAY FOR CANCER

Phosphatidylinositol-3-Kinase/Protein Kinase B/Mammalian Rapamycin Target Protein Pathway

The PI3K enzyme mainly participates in the phosphorylation of the inositol lipid membrane and mediates signal transduction (Figure 2, Costa et al., 2018). Two receptor tyrosine kinases (RTKs) and non-RTKs lead to the activation of PI3K, consequently leading to the formation of a second messenger, phosphatidylinositol 3, 5-triphosphate, from phosphatidylinositol 4, 5-diphosphate. PI3K activation recruits pleckstrin homology domain-containing proteins, including AKT/PKB kinases (Engelman et al., 2006) to the cell membrane, therefore driving conformational changes and resulting in phosphorylation at threonine 308 and at serine 473, which via the active phosphoinositide-dependent kinase 1 and via phosphoinositide-dependent kinase 2, respectively. Activated AKT kinases are capable of phosphorylating tuberous sclerosis protein 1 (TSC1) and tuberous sclerosis protein 2 (TSC2) (Kwiatkowski et al., 2016). In addition, the activity of the kinase mTOR is negatively regulated by the TSC1/TSC2 complex, therefore, AKT leads to that the mTOR complex 1 (mTORC1) are activated, this effect ultimately leads to lipid synthesis and increased protein and decreased autophagy, thereby supporting cell expansion and cell development (Cheng et al., 2015). Particularly, mTORC1 participates in a negative feedback route that prevents AKT over-activation. The PI3K/AKT/mTOR pathway could be up-regulated via the activation of molecular alterations in AKT subunits, PI3K, and mTOR or via inhibiting the PI3K regulatory subunit gene of phosphate and tension homology deleted on chromosome ten (PTEN), TSC1, TSC2, and serine/threonine protein kinase LKB1 (Moulder et al., 2015).

The therapeutic targeting of the PI3K/AKT/mTOR pathway has led to the advancement of some different kinds of drugs, PI3K and AKT inhibitors, as well as catalytic and allosteric mTOR kinase inhibitors are included. For example, the mTOR inhibitors Temsirolimus and Everolimus and the PI3K inhibitors Idelalisib and Copanlisib have been accepted by the FDA for Clinical treatment of patients with cancer (Janku et al., 2011; Moulder et al., 2011; Janku et al., 2014). However, many questions related to the inhibitors of the PI3K/AKT/mTOR pathway remain unanswered. They include which drugs or kinds of drugs are ought to be used in a specific cancer environment and whether the formulation of a reasonable combination strategy will improve the efficacy of tumor treatment.

Phosphatidylinositol-3-Kinase/Protein Kinase B/Mammalian Rapamycin Target Protein and Lung Cancer

Dysregulated PI3K/AKT/mTOR pathway also contributes to LC initiation and progression, and eukaryotic translation initiation

factor 4E (eIF4E), one of its downstream effectors (Mamane et al., 2004), has been recognized to function as an oncogene in many studies. It is not only able to transform cells that are overexpressed in adenocarcinoma, but also can cause poor prognosis factors. Increasing evidence supports that the mTOR pathway plays a part in lung carcinogenesis by binding to eIF4E. The mTOR pathway is involved in the occurrence and development of lung cancer. Negative regulators of mTOR signaling, such as LKB1 and PTEN, are frequently mutated in LC and are considered tumor suppressors (Phillips et al., 2005). Studies have shown that the mTOR signaling pathway act a significant role in behaviors such as aggressiveness and metastasis of LC. Exposure of NSCLC cells to epidermal growth factors or hypoxia causes the activation of hypoxia inducible factor-1 (HIF-1), which ultimately leads to the significant upregulation of C-X-C motif chemokine receptor 4 (CXCR4) expressions and chemotactic behavior. Fortunately, activation of HIF-1 α was inhibited by mTOR inhibitor rapamycin as well as PI3K inhibitors wortmannin and LY294002, and consequently upregulation of CXCR4 expression was inhibited (Sarkaria et al., 2007).

MTOR pathway agents become tempting targets for LC treatment. For example, many models *in vitro* and *in vivo* have demonstrated the antiproliferative and antitumor effects of rapamycin (Phillips et al., 2005). CCI-779 is a water-soluble ester of sirolimus, whereas everolimus is an oral sirolimus analogue, and studies have suggested that both could be used to treat lung cancer. And is used for the advanced renal cell carcinoma therapy (Pandya et al., 2007). PI3K inhibitors have also emerged as effective agents to inhibit the mTOR pathway. Although many PI3K inhibitors exhibit preclinical antitumor activity, they fail to achieve estimated efficacy at the time of clinical evaluation. For example, the PI3K inhibitors wortmannin and LY2994002 have been proven to be unable for clinical treatment in spite of preclinical anticancer ability. Novel PI3K inhibitors have been developed for the treatment of LC and other solid tumors, including BKM120, XL147, and GDC-0941, are ongoing, data regarding LC remain pending (Ekman et al., 2012, Table 3).

Phosphatidylinositol-3-Kinase/Protein Kinase B/Mammalian Rapamycin Target Protein and Gastric Cancer

The molecular characterization of gastric cancers has revealed that PI3K/AKT/mTOR pathway abnormalities are associated with a high recurrence rate of gastric cancer, suggesting that these molecules are potential therapeutic targets (2014). Aberrant PI3K pathway activation is mediated by mechanisms including altered genes for AKT and PIK3CA, decreased upstream RTK, PTEN expression, and other less frequent events. PIK3CA with mutations and amplification has been seen frequently in gastric cancer. PTEN negatively regulates PI3K activity under physiological conditions. It is a TSG located on chromosome 10q23.3 (Markman et al., 2010). The Akt family of genes consists of the AKT1, AKT2, and AKT3 genes. Different isoform gene expression leads to difference in function. For example, AKT1

TABLE 3 | PI3K/AKT/mTOR inhibitors in cancers.

Compound	Target	Cancer	Clinical symptoms	Reference
Wortmannin	PI3K	Lung cancer and breast cancer and other solid tumors	Poor solubility, instability, and high toxicity	Ekman et al. (2012)
LY2994002	PI3K	Lung cancer and breast cancer and other solid tumors	Poor solubility, instability, and high toxicity	Ekman et al. (2012)
BKM120	PI3K	Gastric cancer	Well tolerated, high toxicity	Yang et al. (2018b)
PX-886	PI3K	Gastric cancer	Instability, and high toxicity	Yang et al. (2018a)
XL147	PI3K	Gastric cancer	Poor solubility, instability, and high toxicity	Gravina et al. (2016)
WX-037	PI3K	Gastric cancer		Haagensen et al. (2016)
BYL719	PI3K	Gastric cancer	Poor solubility, instability, and high toxicity	Juric et al. (2018)
GDC0032	PI3K	Gastric cancer		Juric et al. (2018)
P7170	PI3K/mTOR	Gastric cancer, lung cancer		Jalota-Badhwar et al. (2015)
BEZ235	PI3K/mTOR	Gastric cancer	Well tolerated, gastrointestinal toxicity	Kim et al. (2019)
XL765	PI3K/mTOR	Gastric cancer		Gravina et al. (2016)
GDC-0980	PI3K/mTOR	Gastric cancer, breast cancer	Poor solubility, instability, and high toxicity	Kim et al. (2019)
GDC-0941	PI3K/mTOR	Gastric cancer	Poor solubility, instability, and high toxicity	Ekman et al. (2012)
SF1126	PI3K/mTOR	Gastric cancer	Poor solubility, instability, and high toxicity	Kim et al. (2019)
PF-05212384	PI3K/mTOR	Gastric cancer		Kim et al. (2019)
PF-4691502	PI3K/mTOR	Gastric cancer		Kim et al. (2019)
VS-558	PI3K/mTOR	Gastric cancer		Kim et al. (2019)
MK-2206	Allosteric AKT	Gastric cancer	Well tolerated, high toxicity	Hirai et al. (2010)
AZD5363	Catalytic AKT	Gastric cancer		Brown and Banerji (2017)
GSK690693	Catalytic AKT	Gastric cancer	Poor solubility, instability, and high toxicity	Brown and Banerji (2017)
Everolimus	mTOR	Breast cancer	Tends to have an infection, including bacterial, fungal, and viral infections, as well as reactivation of hepatitis B virus/increased incidence of fatigue, asthenia, and anorexia	Janku et al. (2014)

enhances cellular survival and proliferation ability, the loss of *AKT1* can increase invasiveness. Paradoxically, *AKT2* promotes mesenchymal transformation and cellular invasive behavior, and the loss of *AKT2* expression might weaken ability of metastatic (Cariaga-Martinez et al., 2013).

Consequently, four major kinds of drugs that target the PI3K/AKT/mTOR pathway have been identified (Table 3): PI3K, AKT, PI3K/mTOR, and mTOR inhibitors. The PI3K inhibitors BKM120 (Yang et al., 2018a), PX-886 (Yang et al., 2018b), XL147 (Gravina et al., 2016), WX-037 (Haagensen et al., 2016), BYL719 (Juric et al., 2018), and GDC0032 (Juric et al., 2018) were designed treat gastric cancer. PI3K/mTOR inhibitors include P7170 (Jalota-Badhwar et al., 2015), BEZ235 (Kim et al., 2019), XL765 (Gravina et al., 2016), GDC-0980 (Kim et al., 2019), SF1126 (Kim et al., 2019), PF-05212384 (Kim et al., 2019), PF-4691502 (Kim et al., 2019), and VS-558 (Kim et al., 2019). AKT inhibitors include MK-2206 (Hirai et al., 2010), AZD5363, and GSK690693 (Brown and Banerji, 2017). Although PI3K signaling inhibitors appear promising, several theoretical shortcomings raise concerns regarding their clinical efficacy (Engelman, 2009). PI3K inhibitors exhibit obvious antitumor effect when used alone. Unfortunately, relevant studies have shown that gastric cancer may become resistance to combination therapy, so combination therapy with PI3K signaling pathway inhibitors is unlikely to be useful for gastric cancer.

Phosphatidylinositol-3-Kinase/Protein Kinase B/Mammalian Rapamycin Target Protein and Breast Cancer

Recent life science studies have proposed that aberrant PI3K/AKT/mTOR signaling pathway activation is the key to the shortened life cycle of cancer patients and that aberrant activation of this pathway is a vital mechanism of resistance to targeted therapies (Droog et al., 2013). It is estimated that aberrant activation of the mTOR pathway occurs in 70% of all BC cases. In BC, the genes that encode several process of the mTOR pathway are altered. On the one hand, mutations or amplifications of some genes become activated, including those encoding insulin-like growth factor 1 receptor, PIK3CA, RAC- α , AKT1, and human epidermal growth factor receptor 2 (HER2). On the other hand, the expression of genes encoding PTEN and LKB156 are decreased or even no function (Wu et al., 2015; Luey and May, 2016). Breast cancer growth depends on a certain level of estrogen; this conclusion is because nearly 75% of BC cases are ER+. The mechanism of selective estrogen receptor modulators in the treatment of patients with ER + BC is to block the binding of nuclear ER α to estrogen by binding to nuclear ER α , thereby blocking receptor activation. Tamoxifen is such a drug. However, the problem of resistance to the drugs is still widespread in patients with ER + BC (Droog et al., 2013). MTOR pathway is the primary factor of drug resistance in ER + BC patients. This is because the estrogen-independent estrogen receptor (ER)

transcriptional activity is activated by this pathway, making the ER highly sensitive to activation, so that the possibility of tamoxifen binding to nuclear ER α was reduced. HER2 expression is closely correlated with enhanced aggressiveness and significantly worse prognosis in BC and it is a key biomarker for BC. This is because mTOR signaling can be activated by HER family receptors, in particular, HER2 expression is critical for over activation of mTOR pathway in BC. mTOR signaling is associated with tolerance to HER2 therapeutic mechanisms in BC, the case in point is the dual epidermal growth factor receptors HER1 and HER2, the antibody-based agent trastuzumab, and the inhibitor lapatinib (Luey and May, 2016).

Apamycin was the first available mTOR inhibitor for BC therapy and was originally developed as an immunosuppressant for transplant recipients. Researchers classified the new generation of mTOR inhibitors into PI3K/mTOR inhibitors and mTORC1/2 inhibitors. Besides, more and more compounds that block the upstream of the mTOR pathway have been developed. These compounds include AKT and PI3K inhibitors (Table 3). LY294002 and Wortmannin are the earliest and most widely studied PI3K pathway inhibitors (Verret et al., 2019). BC cell model experiments have proved that the inhibitors have strong anti-tumor effects, and also confirmed that they can inhibit the PI3K pathway, but unfortunately they have the disadvantages of poor solubility, instability and high toxicity, so they are limited to pre-clinical studies (Fruman et al., 2017; Liu et al., 2017). In the future research, the main issues need to be paid attention to include whether a relational treatment combination can completely block or partially inhibit mTOR pathway, and whether subtype specific or pan-PI3K inhibition can provide additional benefits for BC patients.

Phosphatidylinositol-3-Kinase/Protein Kinase B/Mammalian Rapamycin Target Protein Pathway and Liver Cancer

In cell lines, miR-758-3P repair inhibits cell proliferation, migration, and invasion. Jiang and his colleagues showed that miR-758-3P significantly down-regulates the expression of murine double minute 2 (MDM2) and mTOR while up-regulating the expression of p53, AKT, and PRAS40 (Jiang et al., 2017). In addition, effector AKT can regulate downstream mTOR and inhibits PRAS40, thus eliminating the inhibitory effect on mTORC1. IGF-1R can regulate behaviors such as cell progress, migration and invasion in HCC and is activated via the mTOR pathway. MiR-187 (Han et al., 2017), miR-497 (Cheng et al., 2017), miR-99a (Han et al., 2017) and miR-592 (Wang et al., 2017) are targeted IGF1R. Han found that miR-187 is down-regulated in HCC tissues and cell lines and reported that the recovery of miR-187 will lead to a significant halt in the growth of HCC (Han et al., 2017). Moreover, miR-497 and miR-99a could target not only IGF-1R but also 3'-UTR of mTOR, and their down-regulation was observed in HCC human tissues and cell lines (Cheng et al., 2017). Wang confirmed that miR-592 was lowly expressed in HCC cell lines, and affected metastasis to lymph nodes (Wang et al., 2017). It has been

demonstrated that miR-2965p inhibits HCC cell proliferation, migration and invasion through targeting AKT2 (Ma et al., 2017). These findings show that the miR-187, miR-497, miR-99a, miR-592 and miR2965p can be an effective target for HCC treatment. Yu showed that miR-142 can directly target transforming growth factor β (TGF- β), and mTOR is one of the effector pathways of TGF- β signaling. Additionally, TGF- β signaling also controls cell viability, growth, EMT, and neoangiogenesis. On the whole, miR-142 can act as a TSG in HCC, being able to increase TGF- β -induced HCC development (Yu et al., 2017). Moreover, miR-23b has been demonstrated to regulate ST7L, a suppressor of the AKT/GSK-3 β / β -catenin signaling in HCC cells (Jiang et al., 2017). MiR-181A (Han et al., 2017), miR-155-5p (Cheng et al., 2017), and miR-25 (Wang et al., 2017) are up-regulated in HCC tissues. HCC plays a carcinogenic part in HCC through targeting PTEN (Table 4).

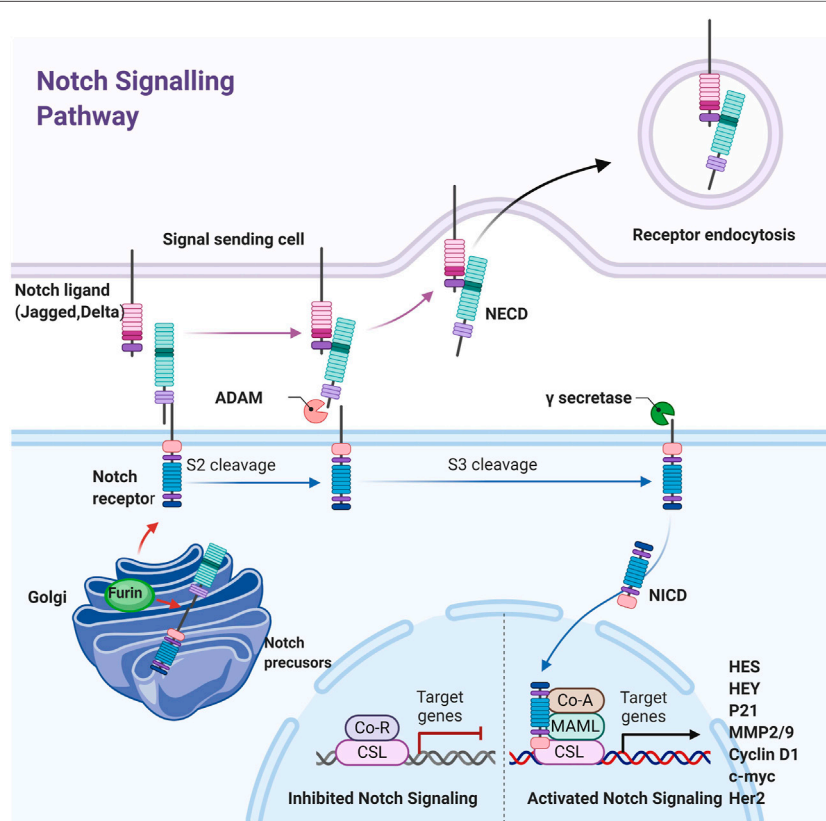
TARGETING THE NOTCH PATHWAY FOR CANCER

Notch Pathway

The Notch signaling pathway is evolutionarily conservative and was originally thought to have a vital role in all kinds of developmental processes (Zardawi et al., 2010; Danza et al., 2013). It is found in the gap that appears on fruit fly wings and acts an indispensable role in embryonic development (Ai et al., 2012). The signaling pathway is composed of these parts: Notch receptor, Notch ligand, and the DNA-binding sequence CSL (CBF1/Su(H)/lag-1. The Notch pathway in humans possesses five ligands (*Jagged-1*, *Jagged-2*, *DLL-1*, *DLL-3*, and *DLL-4*) and four receptors (*Notch-1*, *Notch-2*, *Notch-3*, and *Notch-4*) (Reichrath and Reichrath, 2020). The Notch ligand is also a type I transmembrane protein that contains extracellular repeat sequences similar to the EGF, a Delta/serrate/lag2 motif that accounts for Notch interplay, and short and highly dispersed intracellular domains. When a ligand combine with Notch receptors between two nearby cells, the Notch signaling pathway is activated to control cell growth and regulate organogenesis and morphogenesis (Figure 3). Total three steps of proteolytic cleavage are required in canonical Notch activation process (Teodorczyk and Schmidt, 2014). First, the Notch single-chain precursor is cut by Furin protease in the Golgi complex to form large fragments containing extracellular domains and small fragments containing intracellular and transmembrane regions. Mature heterodimer receptors are formed through Ca²⁺-dependent noncovalent bonding and transferred to the cell membrane. When the mature receptor binds to a ligand, it performs a second cleavage with TACE or a member of the ADAM de-integrin and metalloproteinase family to release extracellular fragments. The remaining fragment, which consists of transmembrane and intracellular regions, is dissected for the third time by γ -secretase for the release of the soluble Notch intracellular region (NICD) and transfer to the nucleus (Suresh and Irvine, 2015). CSL is bound with NCID and lead to specific gene expression. The Notch signaling pathway exhibits CSL nondependent activation in addition to CSL-

TABLE 4 | MicroRNAs regulate PI3K/AKT/mTOR pathway in liver cancer.

miRNA	Regulation	Pathway	References
miR-758-3P	Down-regulated the expression of MDM2 and mTOR/Upregulated the expression of p53, AKT and PRAS40	PI3K/AKT/mTOR pathway	Jiang et al. (2017)
miR-187	Leads to a significant halt in the growth of HCC.	PI3K/AKT/mTOR pathway	Han et al. (2017)
miR-497	Target the 3'-UTR of IGF-1R and mTOR, decrease tumor proliferation and tumor growth	PI3K/AKT/mTOR pathway	Cheng et al. (2017)
miR-99a	Target the 3'-UTR of IGF-1R and mTOR, decrease tumor proliferation and tumor growth	PI3K/AKT/mTOR pathway	Han et al. (2017)
miR-592	Down-regulated in HCC tissues and cell lines, and was associated with lymph node metastasis	PI3K/AKT/mTOR pathway	Wang et al. (2017)
miR2965p	Inhibited HCC cell proliferation, migration and invasion <i>in vitro</i> by targeting AKT2	PI3K/AKT/mTOR pathway	Yu et al. (2017)
miR-142	Controls cell vitality, proliferation, (EMT) and neo-angiogenesis target TGF- β	PI3K/AKT/mTOR pathway	Yu et al. (2017)
miR-23b	As a suppressor of the AKT/GSK3 β / β -catenin pathway in HCC cells by regulating ST7L	PI3K/AKT/mTOR pathway	Jiang et al. (2017)
miR-181A	Plays a carcinogenic role targeting PTEN	PI3K/AKT/mTOR pathway	Han et al. (2017)
miR-155-5p	Plays a carcinogenic role targeting PTEN	PI3K/AKT/mTOR pathway	Cheng et al. (2017)
miR-25	Plays a carcinogenic role targeting PTEN	PI3K/AKT/mTOR pathway	Wang et al. (2017)

**FIGURE 3 |** Schematic diagram of the Notch pathway. The Notched mono-precursors are furin-cut in Golgi bodies to form mature Notched receptors and transferred to the plasma membrane. The Notch is activated when Notch ligands on adjacent cells combined with them, leading to second and third cut by ADAM and γ -secretases, releasing Notch intracellular domain NICD, which is transferred into the nucleus and combined with CSL to initiate downstream gene expression.

dependent activation. However, a great majority Notch target genes exist CSL binding sites. The signal transduction receives signals from neighboring cells and transfers them to the nucleus, thus spurring the expression of transcription factors (Uzhachenko and Shanker, 2016) (**Figure 3**).

Although Notch signaling does not amplify signals, the cell differentiation is precisely controlled (Kopan and Ilagan, 2009). Notch target genes include members of the HES and HEY families, *MMP-2*, *MMP-9*, *cyclin D1*, *Her2*, *c-myc*, and apoptosis-related genes (Wu et al., 2010; Ranganathan et al., 2011; Li et al., 2014; De Francesco et al., 2018; Krishna et al., 2019). The Notch pathway may regulate cell growth, differentiation, and tumor metastasis exactly through regulating the expression of these genes (Zardawi et al., 2009; Zhou et al., 2013). Dysregulated Notch signaling due to mutations, amplification, or ligand and/or receptor overexpression is associated with many malignancies. Given that Notch signaling plays a critical role in cancer genesis and prognosis, it is a promising approach for cancer therapy to block Notch pathway.

Notch Pathway and BC

Notch has been identified as an oncogene in mice infected with MMTV in the past few years. It has also been detected in human BC and likely plays a significant part in BC development (Reichrath and Reichrath, 2020). The American Cancer Association states that BC can be classified into four BC molecular subtypes with prognostic differences in terms of patient outcome on the basis of the presence or absence of the expression of specific biological markers: ERs, progesterone receptors, and HER2. The Notch system, in cooperation with the VEGF pathway, engages in the adjusting of angiogenesis and sprouting in BC (Zhang et al., 2019). Notch expression is controlled by hypoxia and inflammatory cytokines (IL-1, IL-6, and leptin). Endothelial cells can develop into tip or stalk cellular norm under pro-angiogenic signal (Zhang et al., 2019). The acquisition of the high expression of Notch ligands is indisputably related to the aggressive clinical behavior of tumors. BC clinical symptom is accompanied by the high expression of the *Notch-1*, *Notch-3*, and *Notch-4* pathways, and *Notch-2* has been considered to be a tumor suppressor in previous research (Shen and Reedijk, 2021). The evidence of the essential role of the Notch system in BC originates from MMTV, wherein *Notch-1* and *Notch-4* genes have been detected. The genes *Notch-1* and *Notch-4* are the major targets of MMTV. Mutations that induce epithelial mammary oncogenesis are created through insertion and rearrangement (Guo et al., 2011).

In view of the key role of Notch in BC cell proliferation, differentiation, invasion, and drug resistance, this pathway has become a potential target for BC prevention and treatment. Notch targeting agents have been widely used in clinical trials, including γ -secretase inhibitors and monoclonal antibodies. γ -secretase inhibitors are small agent that used frequently (Suresh and Irvine, 2015; Uzhachenko and Shanker, 2016). GSI is one of γ -secretase inhibitors, which achieves anti-tumor effects by reducing the levels of activated Notch and several other substrate proteins in cells. GSI MK-0752 has been proven to have

a good anti-BC effect in clinical trials (Krishna et al., 2019). Unfortunately, continuous use of GSI drugs can cause serious side effects to the body of BC patients. Therefore, GSI drugs are generally not used alone but combined with chemotherapy to treat BC. Monoclonal antibody is also a biological drug that can effectively resist BC. For example, trastuzumab and pertuzumab have been successfully used to treat patients with metastatic BC overexpressing HER2 by targeting Notch receptors (Shen and Reedijk, 2021).

TARGETING THE NF- κ B PATHWAY FOR CANCER

NF- κ B Pathway

The NF- κ B signaling pathway in cancer has been studied for decades. The abnormal activation of NF- κ B transcription factors is frequently seen in various solid tumors, such as CRC and gastric cancer (Lawrence, 2009). NF- κ B pathway members and their regulatory genes response control cancer cell blood vessel formation, growth, metastasis, and tolerance to drug (Mitchell et al., 2016).

NF- κ B is a Rel family transcription factor composed of RelA (p65), RelB, Rel (c-Rel), NF- κ B1 (p50/p105), and NF- κ B2 (p52/p100) (Oeckinghaus et al., 2011). There are three pathways of NF- κ B signal transduction. NF- κ B signaling could be activated by canonical and alternate pathways via an I κ B kinase (IKK)-dependent manner. In the typical pathway, after activating β -subunit of IKK, the negative regulator of the NF- κ B inhibitor of kappa B- α (I κ B α) protein are phosphorylated and subsequent results in the ubiquitination and proteasome-mediated degradation of I κ B α (Baud and Jacque, 2008; Perkins, 2012). The event results in the release of the p65/p50 heterodimer and makes the translocation of the NF- κ B complex into the nucleus. The alternative pathway results in the specific activation of p52: RelB heterodimers and is not required for the activation of the highly ubiquitous p50: RelA dimers. The alternative pathway is distinguished from the classical pathway on the basis of IKK- α homodimers rather than reliance on IKK- γ and IKK- β activity, the preferred substrate of which is the precursor of p52-p100/NF- κ B2. The activation of IKK- α dimers results in the degradation of the latter and the nuclear entry of p52: RelB dimers (Gilmore, 2006). Another pathway that can make NF- κ B activation is based on the activation of casein kinase 2, which can phosphorylate carboxyl-terminal sites and thereby make I κ B α degradation, independently of IKK. This pathway is activated only when the skin is exposed to carcinogenic ultraviolet radiation (Karin, 2006, **Figure 4**).

NF- κ B is an activator of antiapoptotic genes. It could also monitor tumor angiogenesis and metastatic invasiveness, the signaling pathways that mediate its activation have shed new light on chemotherapy and prevention of cancer (Didonato et al., 2012).

NF- κ B Pathway and CRC

NF- κ B is related to angiogenesis and EMT formation in CRC and controls the CRC cells to migrate and invade. Angiogenesis

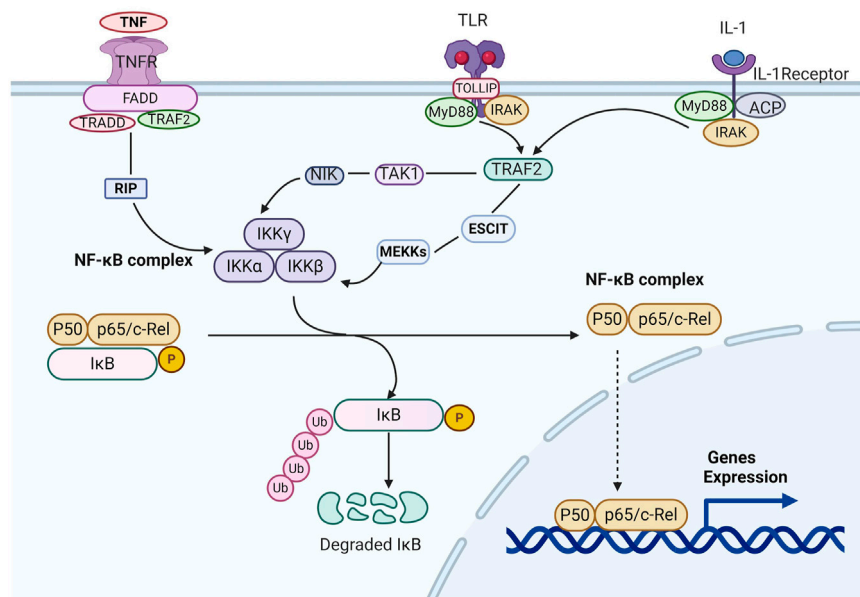


FIGURE 4 | Schematic diagram of the NF- κ B pathway. When the inflammatory factors such as tumor necrosis factor α /interleukin-1/Toll-like Receptors combine with the related receptors, they cause the configuration changes of the latter receptors, like RIP, NIK, or MEKKs. Then IKKs are activated, which can phosphorylate I κ B α , and ubiquitination under the action of the ubiquitin ligase p-trap. The ubiquitin ligase p-trap can be recognized and degraded by 26S proteasome. Therefore, NF- κ B can be released from the cytoplasm of NF- κ B/I κ B α complex, activate and expose the activate site domain, and rapidly transfer nucleus. Through P50 subunit binding with target genes, the expression of target genes such as TNF- α , IL-1.

represents the occurrence of cancer. Vascular endothelial growth factor (VEGF) drives the formation of some angiogenesis regulators, which include the angiogenesis regulator cyclooxygenase-2, CXCL1, CXCL8, and IL-8 in the NF- κ B pathway. Monoclonal antibodies against VEGF are widely exploited for CRC therapy. VEGF is also inducible under HIF (D'ignazio et al., 2016). The HIF pathway regulates immune responses through cross-talk with NF- κ B (Kwon et al., 2010). This cross-talk was proposed by numerous scholars and also proved that HIF-1 α is inhibited by the NF- κ B inhibitor parthenolide, which results in the down-regulation of hypoxia-dependent angiogenesis in human umbilical vein endothelial cells (Thiery et al., 2009). Moreover, in CRC tissues, histological evidence indicates that the expression of NF- κ B (p65) is correlated with the expression of HIF-1 α , VEGF, and vascular invasion. The role of NF- κ B in the angiogenesis of CRC and its interactions with other signaling pathways provide important insights into the targeted therapy of CRC (Chu et al., 2012). Furthermore, NF- κ B participates in the EMT of tumor cells. EMT leads to epithelial mesenchymal cells invasion and metastasis and is thus significant in advancing CRC metastasis. Matrix metalloproteinases (MMPs) are proteolytic enzymes that are capable of degrading the extracellular matrix and promoting tumor invasion. MMP is overexpressed in CRC and is involved in the poor prognosis and spread of CRC. The connection of mechanism between NF- κ B and MMP-9 was studied in consideration of the absence of the β subunit of the IKK complex in CRC cells (Fukuyama et al., 2007). MMP-9 gene expression requires the involvement of NF- κ B (p65 and IKK

activity). The NIK- and IKK- β -binding protein (NIBP) has taken part in the regulation of cytokine-induced canonical NF- κ B signaling. Activin A is overexpressed in human CRC, particularly tumors in stage IV disease, implying that activin A might play a part in advanced CRC (Patel et al., 2018; Soleimani et al., 2020). Related reports have pointed out that activin A induces NF- κ B activation with an increase in MDM2 ubiquitin ligase and the degradation of p21. In general, these findings further indicate that the NF- κ B pathway is a key point of CRC processes involving EMT and the angiogenic process.

According to the report, Approximately 760 natural and synthetic molecular inhibitors of the NF- κ B pathway have been developed (Vaiopoulos et al., 2013). A wide array of IKK inhibitors has been reported, but none have put into clinical practice. Until now, owing to the broad spectrum of the inhibitors, the nature of NF- κ B inhibitors remains incompletely defined. However, first-in-class IKK- α -specific inhibitors are available. NF- κ B activity is associated with chemoresistance and radioresistance, and curcumin was able to block this NF- κ B activity (Sandur et al., 2009).

CONCLUSION AND FUTURE CONSIDERATIONS

In addition to the above four signaling pathways, there are other important signaling pathways in the process of tumor development, such as p53 signaling pathway, Hippo signaling pathway, Hedgehog pathway, TGF- β pathway and JAK-STAT

pathway. P53 signaling pathway is a typical pathway of abnormal disorder in tumors. Due to the complexity of p53 pathway, imperfect drug design methods and other restrictive conditions. Although some drugs targeting p53 have entered the clinical stage, including APG-115 and UBX-0101, no drugs are on the market. Hippo signaling pathway is closely related to tumor immunity. YAP in the Hippo pathway is highly expressed and functions in the generation of regulatory T cells and plays a certain role in anti-tumor immunosuppression. On the other hand, the Hippo pathway can regulate the immune checkpoint molecule PD-L1, thereby enhancing the body's immunity (Ma et al., 2017). Inhibitors targeting the Hedgehog pathway Vismodegib and Sonidegib were approved by the US Food and Drug Administration (FDA) in 2012 and 2015, respectively, for the treatment of basal cell carcinoma (BCC) and associated blastoma (MB), but to date there is no evidence that inhibitors of the Hedgehog pathway can treat the five cancers described above. A variety of TGF- β inhibitors have been developed to kill tumor cells. Fresolimumab, an inhibitor of TGF- β , has entered phase I clinical trials in breast cancer. Galunisertib has also entered phase II clinical trials in HCC. The JAK-STAT pathway is also involved in the genesis, progression, metastasis and drug resistance of tumors, especially STAT3 and STAT5 can continuously activate the survival, proliferation and invasion of tumor cells, which are of great interest in cancer biology. Ruxolitinib and Cucurbitacin I (JSI-24) inhibitors of JAK and STAT have been reported to treat solid tumors.

In addition to miRNAs, noncoding RNAs, such as long non-coding RNAs (lncRNAs) and circular RNAs (circRNAs), have also attracted extensive attention due to their important regulatory roles in tumor development involving in Wnt/ β -catenin, PI3K/AKT/mTOR, Notch and NF- κ B pathways (Anastasiadou et al., 2018). lncRNAs are currently considered to regulate gene expression mainly at transcriptional and post transcriptional levels. At the transcriptional level, the most common mechanism of lncRNAs regulating gene transcription is the direct interaction between lncRNAs and transcriptional complexes or DNA elements. At the post transcriptional level, lncRNAs regulates gene expression through the regulation of mRNA stability, mRNA splicing and modification, mRNA translation, protein stability and subcellular localization. Besides, CircRNAs and lncRNAs act as miRNA sponges to participate in the regulation of gene splicing, transcription and gene expression. As competitive endogenous ribonucleic acids (ceRNAs), circRNAs and lncRNAs can compete for miRNA binding to its response elements (MREs), thus affecting the expression of miRNA. In the Wnt/ β -catenin pathway, lnc01133 regulates APC expression by acting as a miR-106a-3p ceRNA to affect Wnt/ β -catenin pathway (Yang et al., 2018a). The researchers found that lncRNA CCAL regulates the progression of CRC through inhibiting activator protein APC2 α activate Wnt/ β -catenin signaling pathway. In addition, lncRNA BCAR4 has been found to directly interact with and stabilize β -catenin protein, which promote the progress of CRC. Interaction between β -catenin and lncRNAs can also influence its cellular localization, CYTOR by favoring the nuclear localization

of β -catenin to promote CRC metastasis (Schwarzmueller et al., 2020). Other malignant tumors are no exception, lncRNA CCAT2 and UCA1 can activate Wnt and promote the development, migration and invasion of BC. The up regulation of lnc00968 promotes the growth, migration and invasion of non-small cell lung cancer cells by activating Wnt/ β -catenin signaling pathway (Hu et al., 2018). A large number of studies have found that lncRNAs play an important role in PI3K/AKT/mTOR pathway. Importantly, lncRNAs are involved in the occurrence, development, metastasis and drug resistance of solid tumors, lncRNA-SNHG7 can target miR-34a and regulate PI3K/AKT/mTOR pathway to promote the occurrence and development of CRC. lncRNA TM4SF1-AS1 promotes the migration and invasion of LC cells by activating PI3K/AKT/mTOR signaling pathway. lncRNA-HNF1A-AS1, as a ceRNA, can activate PI3K/AKT/mTOR signal pathway by competitively binding miR-30b-3p to promote GC metastasis. This indicates that TM4SF1-ASS1, lncRNA-SNHG7 and lncRNA-HNF1A-AS1 may be a new target for molecular therapy of tumors. lncRNA PICSAR appears to function as miR-588 sponge in HCC cells, activating PI3K/AKT/mTOR signaling pathway and plays a carcinogenic role. It can be used as a potential prognostic biomarker and therapeutic target of HCC. lncRNA HOTAIR enhances the drug resistance of GC cells by regulating PI3K/AKT signaling pathway (Liu et al., 2020). In the Notch signaling pathway, lncRNA FAM83H-AS1 and lncRNA FOXD2-AS1 can regulate the Notch signaling pathway and promote the development of CRC (Li et al., 2018b). In the NF- κ B signaling pathway, lncRNA NKILA can interact with NF- κ B, participating in the negative feedback regulation of NF- κ B, and acts as a tumor suppressor gene in BC.

CircRNAs also plays an important role in the occurrence, migration and invasion of malignant tumors by affecting Wnt/ β -catenin, PI3K/AKT/mTOR and Notch pathways. In HCC, circRNA DEND4C enhances the expression of TCF4 through activating Wnt/ β -catenin pathway and regulates the malignant behavior of HCC cells. Overexpression of circ0067934 increases FZD5 expression by activating miR-1324, which leads to Wnt/ β -catenin pathway is activated. There is evidence that circ_001946 up-regulates SIRT1 expression, SIRT1 exerts promotive effects on Wnt/ β -catenin cascade by targeting miR-135a-5p promotes the proliferation of LC cells. Circ_0006427 up regulates the expression of DKK1 and Wnt/ β -catenin signaling pathway is inactivated (Li et al., 2019). Overexpression of circ103809 accelerates the progression of BC by regulating PI3K/AKT/mTOR signaling pathway *in vivo* and *in vitro*. CircRNA APLP2 can activate Notch signaling pathway in CRC by targeting miR 101-3p to promote proliferation and metastasis (Arab et al., 2017). In view of the importances of lncRNAs and circRNAs in signaling pathways, it suggests that lncRNAs and circRNAs may be potential targets for cancer treatment and diagnostic indicators for predicting therapeutic response.

Currently, scientists have designed an increasing number of drugs targeting signaling molecules. In clinical practice, molecular targeted therapy does reduce the toxic side effects of

drugs to greatly improve the quality of patient survival, and can substantially prolong the survival time of patients, which brings new hope to many patients with cancer (Alzahrani, 2019). But targeted drugs still have certain limitations. First, not all patients are suitable for the use of targeted agents, only those patients with appropriate genetic mutations will respond to the targeted drug. And, there are many rare mutations that have not yet been developed for drugs. In addition, there is a subset of patients no responding to the targeted drugs, even if they have the corresponding mutation. The most common in the clinical is the rapid development of resistance in tumor cells to targeted drugs (Alzahrani, 2019), and its mechanisms are various, for example, crosstalk between signaling pathways, reactivation of downstream signals, and activation of alternative pathways and so on. The establishment of compensatory cell signaling pathway is an important mechanism that is, after one signaling pathway inhibited by drug; another signaling pathway is possibly activated to stimulate cell proliferation. Therefore, several molecularly targeted drugs are often used in combination or with other therapeutic modalities in clinical practice to improve drug efficacy and circumvent drug resistance. For example, Rapamycin inhibitors of PI3K/AKT/mTOR signaling pathway and SMO inhibitors of hedgehog signaling pathway significantly delayed the development of drug resistance in Medulloblastoma (Krishnamurthy and kurzrock, 2018; Buonamici et al., 2010). It has also been shown that the combination of drugs targeting signaling pathways and drugs interfering with autophagy to treat tumors can also achieve better therapeutic outcomes. Preclinical studies have found that the combination of the autophagy inhibitor hydrochloroquine (HCQ) and the targeting AKT drug MK2206 can treat solid tumors. In addition, the combination of signaling pathway targeted drugs with immunotherapy drugs is also an effective way to circumvent drug resistance (Alzahrani, 2019).

REFERENCES

- Ahmed, I., Roy, B., Chandrasekaran, P., Venugopal, A., Xia, L., Jensen, R., et al. (2013). Evidence of Functional Cross Talk between the Notch and NF- κ B Pathways in Nonneoplastic Hyperproliferating Colonic Epithelium. *Am. J. Physiology-Gastrointestinal Liver Physiol.* 304, G356–G370. doi:10.1152/ajpgi.00372.2012
- Ai, Q., Ma, X., Huang, Q., Liu, S., Shi, T., Zhang, C., et al. (2012). High-level Expression of Notch1 Increased the Risk of Metastasis in T1 Stage clear Cell Renal Cell Carcinoma. *PLoS One* 7, e35022. doi:10.1371/journal.pone.0035022
- Alzahrani, A. S. (2019). PI3K/Akt/mTOR Inhibitors in Cancer: At the Bench and Bedside. *Semin. Cancer Biol.* 59, 125–132. doi:10.1016/j.semcancer.2019.07.009
- Anastasiadou, E., Jacob, L. S., and Slack, F. J. (2018). Non-coding RNA Networks in Cancer. *Nat. Rev. Cancer* 18, 5–18. doi:10.1038/nrc.2017.99
- Arab, A., Karimipour, M., Irani, S., Kiani, A., Zeinali, S., Tafsiri, E., et al. (2017). Potential Circulating miRNA Signature for Early Detection of NSCLC. *Cancer Genet.* 216–217, 150–158. doi:10.1016/j.cancergen.2017.07.006
- Ashmawy, A. M., Elgeshy, K. M., Abdel Salam, E.-S. T., Ghareeb, M., Kobaisi, M. H., Amin, H. A. A., et al. (2017). Crosstalk between Liver-Related microRNAs and Wnt/ β -Catenin Pathway in Hepatocellular Carcinoma Patients. *Arab J. Gastroenterol.* 18, 144–150. doi:10.1016/j.ajg.2017.09.001
- In fact humans have an extremely limited knowledge of signaling pathways. At present, in the internet age, big data is considered to be a powerful tool to broaden and deepen people's understanding of targeted drugs. We guess, if gene sequences of every cancer patient in the world and the therapeutic effects by drugs targeting one or more genes mutations are documented and shared, for patients with the same genetic mutation, the key genetic mutations will be more quickly identified and the best treatment to the patient will be formulated. In addition, by big data, scientists could further understand the molecular mechanisms in the genesis and development of tumors, which is very helpful for developing a new generation of targeted drugs. Thus, it seems a powerful measure for pushing molecular targeting research, which has shown great promise but has always been hard to see in practice. At that, as the cost of gene sequencing drops, more cancer patients are willing to have their genes sequenced, the explosion of genomic data makes this idea a reality.

AUTHOR CONTRIBUTIONS

HH drafted the Manuscript and edited the manuscript. XS and YL participated in preparing the figures. RG, HX, and JZ contributed to the data collection. HY contributed to revisions of the manuscript.

FUNDING

This work was supported by the National Natural Science Foundation of China (Grant No. 81801086), the Applied basic research project of Sichuan Science Technology Department (2021YJ0256), “The Fundamental Research Funds for the Central Universities”, Southwest Minzu University (2018NZD16)

- Baud, V., and Jacque, E. (2008). Voie alternative d'activation de NF- κ B et cancer. *Med. Sci. (Paris)* 24, 1083–1088. doi:10.1051/medsci/200824121083
- Brown, J. S., and Banerji, U. (2017). Maximising the Potential of AKT Inhibitors as Anti-cancer Treatments. *Pharmacol. Ther.* 172, 101–115. doi:10.1016/j.pharmthera.2016.12.001
- Buonamici, S., Williams, J., Morrissey, M., Wang, A., Guo, R., Vattay, A., et al. (2010). Interfering with Resistance to Smoothed Antagonists by Inhibition of the PI3K Pathway in Medulloblastoma. *Sci. Translational Med.* 2, 51ra70. doi:10.1126/scitranslmed.3001599
- Cariaga-Martinez, A. E., López-Ruiz, P., Nombela-Blanco, M. P., Motiño, O., González-Corpas, A., Rodríguez-Ubreva, J., et al. (2013). Distinct and Specific Roles of AKT1 and AKT2 in Androgen-Sensitive and Androgen-independent Prostate Cancer Cells. *Cell Signal.* 25, 1586–1597. doi:10.1016/j.cellsig.2013.03.019
- Chen, S., Xu, Y., Chen, Y., Li, X., Mou, W., Wang, L., et al. (2012). SOX2 Gene Regulates the Transcriptional Network of Oncogenes and Affects Tumorigenesis of Human Lung Cancer Cells. *PLoS One* 7, e36326. doi:10.1371/journal.pone.0036326
- Chen, L., Wang, X., Zhu, Y., Zhu, J., and Lai, Q. (2018). miR-200b 3p Inhibits Proliferation and Induces Apoptosis in Colorectal Cancer by Targeting Wnt1. *Mol. Med. Rep.* 18, 2571–2580. doi:10.3892/mmr.2018.9287
- Cheng, H., Zou, Y., Ross, J. S., Wang, K., Liu, X., Halmos, B., et al. (2015). RICTOR Amplification Defines a Novel Subset of Patients with Lung Cancer Who May

- Benefit from Treatment with mTORC1/2 Inhibitors. *Cancer Discov.* 5, 1262–1270. doi:10.1158/2159-8290.cd-14-0971
- Cheng, H., Xue, J., Yang, S., Chen, Y., Wang, Y., Zhu, Y., et al. (2017). Co-targeting of IGF1R/mTOR Pathway by miR-497 and miR-99a Impairs Hepatocellular Carcinoma Development. *Oncotarget* 8, 47984–47997. doi:10.18632/oncotarget.18207
- Chu, D., Zhao, Z., Zhou, Y., Li, Y., Li, J., Zheng, J., et al. (2012). Matrix Metalloproteinase-9 Is Associated with Relapse and Prognosis of Patients with Colorectal Cancer. *Ann. Surg. Oncol.* 19, 318–325. doi:10.1245/s10434-011-1686-3
- Chu, Y., Fan, W., Guo, W., Zhang, Y., Wang, L., Guo, L., et al. (2017). miR-1247-5p Functions as a Tumor Suppressor in Human Hepatocellular Carcinoma by Targeting Wnt3. *Oncol. Rep.* 38, 343–351. doi:10.3892/or.2017.5702
- Ciombor, K. K., Wu, C., and Goldberg, R. M. (2015). Recent Therapeutic Advances in the Treatment of Colorectal Cancer. *Annu. Rev. Med.* 66, 83–95. doi:10.1146/annurev-med-051513-102539
- Collu, G. M., Hidalgo-Sastre, A., and Brennan, K. (2014). Wnt-Notch Signalling Crosstalk in Development and Disease. *Cell. Mol. Life Sci.* 71, 3553–3567. doi:10.1007/s00018-014-1644-x
- Costa, R. L. B., Han, H. S., and Gradishar, W. J. (2018). Targeting the PI3K/AKT/mTOR Pathway in Triple-Negative Breast Cancer: a Review. *Breast Cancer Res. Treat.* 169, 397–406. doi:10.1007/s10549-018-4697-y
- Danza, G., Di Serio, C., Ambrosio, M. R., Sturli, N., Lonetto, G., Rosati, F., et al. (2013). Notch3 Is Activated by Chronic Hypoxia and Contributes to the Progression of Human Prostate Cancer. *Int. J. Cancer* 133, 2577–2586. doi:10.1002/ijc.28293
- De Francesco, E. M., Maggolini, M., and Musti, A. M. (2018). Crosstalk between Notch, HIF-1 α and GPER in Breast Cancer EMT. *Int. J. Mol. Sci.* 19, 2011. doi:10.3390/ijms19072011
- Didonato, J. A., Mercurio, F., and Karin, M. (2012). NF- κ B and the Link between Inflammation and Cancer. *Immunol. Rev.* 246, 379–400. doi:10.1111/j.1600-065x.2012.01099.x
- D'ignazio, L., Bandarra, D., and Rocha, S. (2016). NF- κ B and HIF Crosstalk in Immune Responses. *Febs j* 283, 413–424. doi:10.1111/febs.13578
- Dong-Xu, W., Jia, L., and Su-Juan, Z. (2015). MicroRNA-185 Is a Novel Tumor Suppressor by Negatively Modulating the Wnt/ β -Catenin Pathway in Human Colorectal Cancer. *Indian J. Cancer* 52 (Suppl. 3), E182–E185. doi:10.4103/0019-509x.186576
- Droog, M., Beelen, K., Linn, S., and Zwart, W. (2013). Tamoxifen Resistance: from Bench to Bedside. *Eur. J. Pharmacol.* 717, 47–57. doi:10.1016/j.ejphar.2012.11.071
- Ekman, S., Wynes, M. W., and Hirsch, F. R. (2012). The mTOR Pathway in Lung Cancer and Implications for Therapy and Biomarker Analysis. *J. Thorac. Oncol.* 7, 947–953. doi:10.1097/jto.0b013e31825581bd
- Engelman, J. A., Luo, J., and Cantley, L. C. (2006). The Evolution of Phosphatidylinositol 3-kinases as Regulators of Growth and Metabolism. *Nat. Rev. Genet.* 7, 606–619. doi:10.1038/nrg1879
- Engelman, J. A. (2009). Targeting PI3K Signalling in Cancer: Opportunities, Challenges and Limitations. *Nat. Rev. Cancer* 9, 550–562. doi:10.1038/nrc2664
- Fruman, D. A., Chiu, H., Hopkins, B. D., Bagrodia, S., Cantley, L. C., and Abraham, R. T. (2017). The PI3K Pathway in Human Disease. *Cell* 170, 605–635. doi:10.1016/j.cell.2017.07.029
- Fukuyama, R., Ng, K. P., Cicek, M., Kelleher, C., Nicolaita, R., Casey, G., et al. (2007). Role of IKK and Oscillatory NF κ B Kinetics in MMP-9 Gene Expression and Chemoresistance to 5-fluorouracil in RKO Colorectal Cancer Cells. *Mol. Carcinog.* 46, 402–413. doi:10.1002/mc.20288
- Fumoto, K., and Kikuchi, A. (2019). [Canonical Wnt Signaling Pathway and Current issues]. *Clin. Calcium* 29, 283–289. doi:10.20837/4201903283
- Ghosh, M. C., Gorantla, V., Makena, P. S., Luellen, C., Sinclair, S. E., Schwingshackl, A., et al. (2013). Insulin-like Growth Factor-I Stimulates Differentiation of ATII Cells to ATI-like Cells through Activation of Wnt5a. *Am. J. Physiology-Lung Cell Mol. Physiol.* 305, L222–L228. doi:10.1152/ajplung.00014.2013
- Gilmore, T. D. (2006). Introduction to NF- κ B: Players, Pathways, Perspectives. *Oncogene* 25, 6680–6684. doi:10.1038/sj.onc.1209954
- Gordon, M. D., and Nusse, R. (2006). Wnt Signaling: Multiple Pathways, Multiple Receptors, and Multiple Transcription Factors. *J. Biol. Chem.* 281, 22429–22433. doi:10.1074/jbc.r600015200
- Gravina, G. L., Mancini, A., Scarsella, L., Colapietro, A., Jitariu, A., Vitale, F., et al. (2016). Dual PI3K/mTOR Inhibitor, XL765 (SAR245409), Shows superior Effects to Sole PI3K [XL147 (SAR245408)] or mTOR [rapamycin] Inhibition in Prostate Cancer Cell Models. *Tumor Biol.* 37, 341–351. doi:10.1007/s13277-015-3725-3
- Guo, S., Liu, M., and Gonzalez-Perez, R. R. (2011). Role of Notch and its Oncogenic Signaling Crosstalk in Breast Cancer. *Biochim. Biophys. Acta (Bba) - Rev. Cancer* 1815, 197–213. doi:10.1016/j.bbcan.2010.12.002
- Haagensen, E. J., Thomas, H. D., Schmalix, W. A., Payne, A. C., Kevorkian, L., Allen, R. A., et al. (2016). Enhanced Anti-tumour Activity of the Combination of the Novel MEK Inhibitor WX-554 and the Novel PI3K Inhibitor WX-037. *Cancer Chemother. Pharmacol.* 78, 1269–1281. doi:10.1007/s00280-016-3186-4
- Han, X., Wang, X., Zhao, B., Chen, G., Sheng, Y., Wang, W., et al. (2017). MicroRNA-187 Inhibits Tumor Growth and Metastasis via Targeting of IGF-1R in Hepatocellular Carcinoma. *Mol. Med. Rep.* 16, 2241–2246. doi:10.3892/mmr.2017.6788
- Hirai, H., Sootome, H., Nakatsuru, Y., Miyama, K., Taguchi, S., Tsujioka, K., et al. (2010). MK-2206, an Allosteric Akt Inhibitor, Enhances Antitumor Efficacy by Standard Chemotherapeutic Agents or Molecular Targeted Drugs *In Vitro* and *In Vivo*. *Mol. Cancer Ther.* 9, 1956–1967. doi:10.1158/1535-7163.mct-09-1012
- Holstein, T. W. (2012). The Evolution of the Wnt Pathway. *Cold Spring Harbor Perspect. Biol.* 4, a007922. doi:10.1101/cshperspect.a007922
- Hu, X.-Y., Hou, P.-F., Li, T.-T., Quan, H.-Y., Li, M.-L., Lin, T., et al. (2018). The Roles of Wnt/ β -Catenin Signaling Pathway Related lncRNAs in Cancer. *Int. J. Biol. Sci.* 14, 2003–2011. doi:10.7150/ijbs.27977
- Iqbal, M. A., Arora, S., Prakasam, G., Calin, G. A., and Syed, M. A. (2019). MicroRNA in Lung Cancer: Role, Mechanisms, Pathways and Therapeutic Relevance. *Mol. Aspects Med.* 70, 3–20. doi:10.1016/j.mam.2018.07.003
- Jalota-Badwar, A., Bhatia, D. R., Boreddy, S., Joshi, A., Venkatraman, M., Desai, N., et al. (2015). P7170: A Novel Molecule with Unique Profile of mTORC1/C2 and Activin Receptor-like Kinase 1 Inhibition Leading to Antitumor and Antiangiogenic Activity. *Mol. Cancer Ther.* 14, 1095–1106. doi:10.1158/1535-7163.mct-14-0486
- Janku, F., Tsimberidou, A. M., Garrido-Laguna, I., Wang, X., Luthra, R., Hong, D. S., et al. (2011). PIK3CA Mutations in Patients with Advanced Cancers Treated with PI3K/AKT/mTOR axis Inhibitors. *Mol. Cancer Ther.* 10, 558–565. doi:10.1158/1535-7163.mct-10-0994
- Janku, F., Hong, D. S., Fu, S., Piha-Paul, S. A., Naing, A., Falchook, G. S., et al. (2014). Assessing PIK3CA and PTEN in Early-phase Trials with PI3K/AKT/mTOR Inhibitors. *Cel Rep.* 6, 377–387. doi:10.1016/j.celrep.2013.12.035
- Jernigan, K. K., Cselenyi, C. S., Thorne, C. A., Hanson, A. J., Tahinci, E., Hajicek, N., et al. (2010). G Activates GSK3 to Promote LRP6-Mediated -Catenin Transcriptional Activity. *Sci. Signaling* 3, ra37. doi:10.1126/scisignal.2000647
- Jiang, X., Charlat, O., Zamponi, R., Yang, Y., and Cong, F. (2015). Dishevelled Promotes Wnt Receptor Degradation through Recruitment of ZNRF3/RNF43 E3 Ubiquitin Ligases. *Mol. Cell* 58, 522–533. doi:10.1016/j.molcel.2015.03.015
- Jiang, D., Cho, W. C., Li, Z., Xu, X., Qu, Y., Jiang, Z., et al. (2017). MiR-758-3p Suppresses Proliferation, Migration and Invasion of Hepatocellular Carcinoma Cells via Targeting MDM2 and mTOR. *Biomed. Pharmacother.* 96, 535–544. doi:10.1016/j.biopha.2017.10.004
- Juric, D., Rodon, J., Tabernero, J., Janku, F., Burris, H. A., Schellens, J. H. M., et al. (2018). Phosphatidylinositol 3-Kinase α -Selective Inhibition with Alpelisib (BYL719) in PIK3CA-Altered Solid Tumors: Results from the First-In-Human Study. *Jco* 36, 1291–1299. doi:10.1200/jco.2017.72.7107
- Karin, M. (2006). Nuclear Factor- κ B in Cancer Development and Progression. *Nature* 441, 431–436. doi:10.1038/nature04870
- Katoh, M., and Katoh, M. (2005). Comparative Genomics on Wnt5a and Wnt5b Genes. *Int. J. Mol. Med.* 15, 749–753.
- Kim, M. Y., Kruger, A. J., Jeong, J. Y., Kim, J., Shin, P. K., Kim, S. Y., et al. (2019). Combination Therapy with a PI3K/mTOR Dual Inhibitor and Chloroquine Enhances Synergistic Apoptotic Cell Death in Epstein-Barr Virus-Infected Gastric Cancer Cells. *Mol. Cell* 42, 448–459. doi:10.14348/molcells.2019.2395
- Kopan, R., and Ilagan, M. X. G. (2009). The Canonical Notch Signaling Pathway: Unfolding the Activation Mechanism. *Cell* 137, 216–233. doi:10.1016/j.cell.2009.03.045
- Krishna, B. M., Jana, S., Singhal, J., Horne, D., Awasthi, S., Sargia, R., et al. (2019). Notch Signaling in Breast Cancer: From Pathway Analysis to Therapy. *Cancer Lett.* 461, 123–131. doi:10.1016/j.canlet.2019.07.012

- Krishnamurthy, N., and Kurzrock, R. (2018). Targeting the Wnt/beta-Catenin Pathway in Cancer: Update on Effectors and Inhibitors. *Cancer Treat. Rev.* 62, 50–60. doi:10.1016/j.ctrv.2017.11.002
- Kwiatkowski, D. J., Choueiri, T. K., Fay, A. P., Rini, B. I., Thorner, A. R., De Velasco, G., et al. (2016). Mutations in TSC1, TSC2, and mTOR Are Associated with Response to Rapalogs in Patients with Metastatic Renal Cell Carcinoma. *Clin. Cancer Res.* 22, 2445–2452. doi:10.1158/1078-0432.ccr-15-2631
- Kwon, H.-C., Kim, S. H., Oh, S. Y., Lee, S., Kwon, K. A., Lee, J. H., et al. (2010). Clinicopathological Significance of Nuclear Factor-Kappa B, HIF-1 Alpha, and Vascular Endothelial Growth Factor Expression in Stage III Colorectal Cancer. *Cancer Sci.* 101, 1557–1561. doi:10.1111/j.1349-7006.2010.01553.x
- Lagade, P., Griessinger, E., Nawrot, M. P., Fenouille, N., Colosetti, P., Imbert, V., et al. (2008). Pharmacological Targeting of NF-Kb Potentiates the Effect of the Topoisomerase Inhibitor CPT-11 on colon Cancer Cells. *Br. J. Cancer* 98, 335–344. doi:10.1038/sj.bjc.6604082
- Lawrence, T. (2009). The Nuclear Factor NF-kappaB Pathway in Inflammation. *Cold Spring Harb Perspect. Biol.* 1, a001651. doi:10.1101/cshperspect.a001651
- Leake, P. A., Cardoso, R., Seevaratnam, R., Lourenco, L., Helyer, L., Mahar, A., et al. (2012). A Systematic Review of the Accuracy and Indications for Diagnostic Laparoscopy Prior to Curative-Intent Resection of Gastric Cancer. *Gastric Cancer* 15 (Suppl. 1), S38–S47. doi:10.1007/s10120-011-0047-z
- Lee, A. Y., He, B., You, L., Dadfaray, S., Xu, Z., Mazieres, J., et al. (2004). Expression of the Secreted Frizzled-Related Protein Gene Family Is Downregulated in Human Mesothelioma. *Oncogene* 23, 6672–6676. doi:10.1038/sj.onc.1207881
- Lenz, H. J., and Kahn, M. (2014). Safely Targeting Cancer Stem Cells via Selective Catenin Coactivator Antagonism. *Cancer Sci.* 105, 1087–1092. doi:10.1111/cas.12471
- Li, F., Chong, Z. Z., and Maiese, K. (2006). Winding through the WNT Pathway during Cellular Development and Demise. *Histol. Histopathol* 21, 103–124. doi:10.14670/HH-21.103
- Li, D., Masiero, M., Banham, A. H., and Harris, A. L. (2014). The Notch Ligand JAGGED1 as a Target for Anti-tumor Therapy. *Front. Oncol.* 4, 254. doi:10.3389/fonc.2014.00254
- Li, X., Meng, Y., Xie, C., Zhu, J., Wang, X., Li, Y., et al. (2018a). Dialyl Trisulfide Inhibits Breast Cancer Stem Cells via Suppression of Wnt/beta-catenin Pathway. *J. Cell. Biochem.* 119, 4134–4141. doi:10.1002/jcb.26613
- Li, Y., Zeng, C., Hu, J., Pan, Y., Shan, Y., Liu, B., et al. (2018b). Long Non-coding RNA-SNHG7 Acts as a Target of miR-34a to Increase GALNT7 Level and Regulate PI3K/Akt/mTOR Pathway in Colorectal Cancer Progression. *J. Hematol. Oncol.* 11, 89. doi:10.1186/s13045-018-0632-2
- Li, Y.-F., Zhang, J., and Yu, L. (2019). Circular RNAs Regulate Cancer Onset and Progression via Wnt/beta-Catenin Signaling Pathway. *Yonsei Med. J.* 60, 1117–1128. doi:10.3349/ymj.2019.60.12.1117
- Liu, J., Pan, S., Hsieh, M. H., Ng, N., Sun, F., Wang, T., et al. (2013). Targeting Wnt-Driven Cancer through the Inhibition of Porcupine by LGK974. *Proc. Natl. Acad. Sci.* 110, 20224–20229. doi:10.1073/pnas.1314239110
- Liu, J., Li, H. Q., Zhou, F. X., Yu, J. W., Sun, L., and Han, Z. H. (2017). Targeting the mTOR Pathway in Breast Cancer. *Tumour Biol.* 39, 1010428317710825. doi:10.1177/1010428317710825
- Liu, Z., Mo, H., Sun, L., Wang, L., Chen, T., Yao, B., et al. (2020). Long Noncoding RNA PICSA/miR-588/EIF6 axis Regulates Tumorigenesis of Hepatocellular Carcinoma by Activating PI3K/AKT/mTOR Signaling Pathway. *Cancer Sci.* 111, 4118–4128. doi:10.1111/cas.14631
- Lu, C., Liao, Z., Cai, M., and Zhang, G. (2017). MicroRNA-320a Downregulation Mediates Human Liver Cancer Cell Proliferation through the Wnt/beta-Catenin Signaling Pathway. *Oncol. Lett.* 13, 573–578. doi:10.3892/ol.2016.5479
- Luey, B. C., and May, F. E. (2016). Insulin-like Growth Factors Are Essential to Prevent Anoikis in Oestrogen-Responsive Breast Cancer Cells: Importance of the Type I IGF Receptor and PI3-kinase/Akt Pathway. *Mol. Cancer* 15, 8. doi:10.1186/s12943-015-0482-2
- Ma, X., Zhuang, B., and Li, W. (2017). MicroRNA-296-5p Downregulated AKT2 to Inhibit Hepatocellular Carcinoma Cell Proliferation, Migration and Invasion. *Mol. Med. Rep.* 16, 1565–1572. doi:10.3892/mmr.2017.6701
- Macdonald, B. T., and He, X. (2012). Frizzled and LRP5/6 Receptors for Wnt/beta-Catenin Signaling. *Cold Spring Harb Perspect. Biol.* 4, a007880. doi:10.1101/cshperspect.a007880
- Macdonald, B. T., Tamai, K., and He, X. (2009). Wnt/beta-Catenin Signaling: Components, Mechanisms, and Diseases. *Dev. Cell* 17, 9–26. doi:10.1016/j.devcel.2009.06.016
- Mamane, Y., Petroulakis, E., Rong, L., Yoshida, K., Ler, L. W., and Sonenberg, N. (2004). eIF4E - from Translation to Transformation. *Oncogene* 23, 3172–3179. doi:10.1038/sj.onc.1207549
- Mao, X., Tong, J., Wang, Y., Zhu, Z., Yin, Y., and Wang, Y. (2018). Triptolide Exhibits Antitumor Effects by Reversing Hypermethylation of WIF-1 in L-ung C-ancer C-ells. *Mol. Med. Rep.* 18, 3041–3049. doi:10.3892/mmr.2018.9263
- Markman, B., Atzori, F., Pérez-García, J., Tabernero, J., and Baselga, J. (2010). Status of PI3K Inhibition and Biomarker Development in Cancer Therapeutics. *Ann. Oncol.* 21, 683–691. doi:10.1093/annonc/mdp347
- Mitchell, S., Vargas, J., and Hoffmann, A. (2016). Signaling via the NFkB System. *Wiley Interdiscip. Rev. Syst. Biol. Med.* 8, 227–241. doi:10.1002/wsbm.1331
- Moulder, S., Moroney, J., Helgason, T., Wheler, J., Booser, D., Albarracín, C., et al. (2011). Responses to Liposomal Doxorubicin, Bevacizumab, and Temsirolimus in Metaplastic Carcinoma of the Breast: Biologic Rationale and Implications for Stem-Cell Research in Breast Cancer. *Jco* 29, e572–e575. doi:10.1200/jco.2010.34.0604
- Moulder, S., Helgason, T., Janku, F., Wheler, J., Moroney, J., Booser, D., et al. (2015). Inhibition of the Phosphoinositide 3-kinase Pathway for the Treatment of Patients with Metastatic Metaplastic Breast Cancer. *Ann. Oncol.* 26, 1346–1352. doi:10.1093/annonc/mdv163
- Nakatsugawa, M., Takahashi, A., Hirohashi, Y., Torigoe, T., Inoda, S., Murase, M., et al. (2011). SOX2 Is Overexpressed in Stem-like Cells of Human Lung Adenocarcinoma and Augments the Tumorigenicity. *Lab. Invest.* 91, 1796–1804. doi:10.1038/labinvest.2011.140
- Nakayama, S., Sng, N., Carretero, J., Welner, R., Hayashi, Y., Yamamoto, M., et al. (2014). beta-Catenin Contributes to Lung Tumor Development Induced by EGFR Mutations. *Cancer Res.* 74, 5891–5902. doi:10.1158/0008-5472.can-14-0184
- Oeckinghaus, A., Hayden, M. S., and Ghosh, S. (2011). Crosstalk in NF-Kb Signaling Pathways. *Nat. Immunol.* 12, 695–708. doi:10.1038/ni.2065
- Ohgaki, H., Kros, J. M., Okamoto, Y., Gaspert, A., Huang, H., and Kurrer, M. O. (2004). APC Mutations Are Infrequent but Present in Human Lung Cancer. *Cancer Lett.* 207, 197–203. doi:10.1016/j.canlet.2003.10.020
- Okamoto, M., Udagawa, N., Uehara, S., Maeda, K., Yamashita, T., Nakamichi, Y., et al. (2014). Noncanonical Wnt5a Enhances Wnt/beta-Catenin Signaling during Osteoblastogenesis. *Sci. Rep.* 4, 4493. doi:10.1038/srep04493
- Pandya, K. J., Dahlberg, S., Hidalgo, M., Cohen, R. B., Lee, M. W., Schiller, J. H., et al. (2007). A Randomized, Phase II Trial of Two Dose Levels of Temsirolimus (CCI-779) in Patients with Extensive-Stage Small-Cell Lung Cancer Who Have Responding or Stable Disease after Induction Chemotherapy: a Trial of the Eastern Cooperative Oncology Group (E1500). *J. Thorac. Oncol.* 2, 1036–1041. doi:10.1097/jto.0b013e318155a439
- Patel, M., Horgan, P. G., Mcmillan, D. C., and Edwards, J. (2018). NF-kB Pathways in the Development and Progression of Colorectal Cancer. *Translational Res.* 197, 43–56. doi:10.1016/j.trsl.2018.02.002
- Perkins, N. D. (2012). The Diverse and Complex Roles of NF-Kb Subunits in Cancer. *Nat. Rev. Cancer* 12, 121–132. doi:10.1038/nrc3204
- Phillips, R. J., Mestas, J., Gharaee-Kermani, M., Burdick, M. D., Sica, A., Belperio, J. A., et al. (2005). Epidermal Growth Factor and Hypoxia-Induced Expression of CXCR4 Chemokine Receptor 4 on Non-small Cell Lung Cancer Cells Is Regulated by the Phosphatidylinositol 3-Kinase/PTEN/AKT/Mammalian Target of Rapamycin Signaling Pathway and Activation of Hypoxia Inducible Factor-1a. *J. Biol. Chem.* 280, 22473–22481. doi:10.1074/jbc.m500963200
- Polivka, J., Jr., and Janku, F. (2014). Molecular Targets for Cancer Therapy in the PI3K/AKT/mTOR Pathway. *Pharmacol. Ther.* 142, 164–175. doi:10.1016/j.pharmthera.2013.12.004
- Qi, W., Chen, J., Cheng, X., Huang, J., Xiang, T., Li, Q., et al. (2015). Targeting the Wnt-Regulatory Protein CTNNBIP1 by microRNA-214 Enhances the Stemness and Self-Renewal of Cancer Stem-like Cells in Lung Adenocarcinomas. *Stem Cells* 33, 3423–3436. doi:10.1002/stem.2188
- Rakha, E. A., and Green, A. R. (2017). Molecular Classification of Breast Cancer: what the Pathologist Needs to Know. *Pathology* 49, 111–119. doi:10.1016/j.pathol.2016.10.012

- Ranganathan, P., Weaver, K. L., and Capobianco, A. J. (2011). Notch Signalling in Solid Tumours: a Little Bit of Everything but Not All the Time. *Nat. Rev. Cancer* 11, 338–351. doi:10.1038/nrc3035
- Rapp, J., Jaromi, L., Kvell, K., Miskei, G., and Pongracz, J. E. (2017). WNT Signaling - Lung Cancer Is No Exception. *Respir. Res.* 18, 167. doi:10.1186/s12931-017-0650-6
- Reichrath, J., and Reichrath, S. (2020). Notch Signaling and Tissue Patterning in Embryology: An Introduction. *Adv. Exp. Med. Biol.* 1218, 1–7. doi:10.1007/978-3-030-34436-8_1
- Roa, L. A., Bloemen, M., Carels, C. E. L., Wagener, F. A. D. T. G., and Von Den Hoff, J. W. (2019). Retinoic Acid Disrupts Osteogenesis in Pre-osteoblasts by Down-Regulating WNT Signaling. *Int. J. Biochem. Cell Biol.* 116, 105597. doi:10.1016/j.biocel.2019.105597
- Rogers, R., Ouellet, G., Brown, C., Moyer, B., Rasoulpour, T., and Hixon, M. (2008). Cross-talk between the Akt and NF-Kb Signaling Pathways Inhibits MEHP-Induced Germ Cell Apoptosis. *Toxicol. Sci.* 106, 497–508. doi:10.1093/toxsci/kfn186
- Sandaru, S. K., Deorukhkar, A., Pandey, M. K., Pabón, A. M., Shentu, S., Guha, S., et al. (2009). Curcumin Modulates the Radiosensitivity of Colorectal Cancer Cells by Suppressing Constitutive and Inducible NF-Kb Activity. *Int. J. Radiat. Oncology*Biophysics* 75, 534–542. doi:10.1016/j.ijrobp.2009.06.034
- Santana, N. O., Lerario, A. M., Schmerling, C. K., Marui, S., Alves, V. A. F., Hoff, A. O., et al. (2020). Molecular Profile of Hürthle Cell Carcinomas: Recurrent Mutations in the Wnt/ β -Catenin Pathway. *Eur. J. Endocrinol.* 183, 647–656. doi:10.1530/eje-20-0597
- Sarkaria, J. N., Schwinger, P., Schild, S. E., Grogan, P. T., Mladek, A. C., Mandrekar, S. J., et al. (2007). Phase I Trial of Sirolimus Combined with Radiation and Cisplatin in Non-small Cell Lung Cancer. *J. Thorac. Oncol.* 2, 751–757. doi:10.1097/jto.0b013e3180cc2587
- Schmalhofer, O., Brabletz, S., and Brabletz, T. (2009). E-cadherin, β -catenin, and ZEB1 in Malignant Progression of Cancer. *Cancer Metastasis Rev.* 28, 151–166. doi:10.1007/s10555-008-9179-y
- Schwarzmueller, L., Bril, O., Vermeulen, L., and Léveillé, N. (2020). Emerging Role and Therapeutic Potential of lncRNAs in Colorectal Cancer. *Cancers (Basel)* 12, 3843. doi:10.3390/cancers12123843
- Shen, Q., and Reedijk, M. (2021). Notch Signaling and the Breast Cancer Microenvironment. *Adv. Exp. Med. Biol.* 1287, 183–200. doi:10.1007/978-3-030-55031-8_12
- Siegel, R. L., Miller, K. D., and Jemal, A. (2020). Cancer Statistics, 2020. *CA Cancer J. Clin.* 70, 7–30. doi:10.3322/caac.21590
- Soleimani, A., Rahmani, F., Ferns, G. A., Ryzhikov, M., Avan, A., and Hassani, S. M. (2020). Role of the NF-Kb Signaling Pathway in the Pathogenesis of Colorectal Cancer. *Gene* 726, 144132. doi:10.1016/j.gene.2019.144132
- Stotz, M., Gerger, A., Haybaeck, J., Kiesslich, T., Bullock, M. D., and Pichler, M. (2015). Molecular Targeted Therapies in Hepatocellular Carcinoma: Past, Present and Future. *Anticancer Res.* 35, 5737–5744.
- Strillacci, A., Griffoni, C., Sansone, P., Paterini, P., Piazzi, G., Lazzarini, G., et al. (2009). MiR-101 Downregulation Is Involved in Cyclooxygenase-2 Overexpression in Human colon Cancer Cells. *Exp. Cell Res.* 315, 1439–1447. doi:10.1016/j.yexcr.2008.12.010
- Suresh, S., and Irvine, A. E. (2015). The NOTCH Signaling Pathway in normal and Malignant Blood Cell Production. *J. Cell Commun. Signal.* 9, 5–13. doi:10.1007/s12079-015-0271-0
- Taciak, B., Pruszyńska, I., Kiraga, L., Bialasek, M., and Krol, M. (2018). Wnt Signaling Pathway in Development and Cancer. *J. Physiol. Pharmacol.* 69, 185–196. doi:10.26402/jpp.2018.2.07
- Tang, Q., Zou, Z., Zou, C., Zhang, Q., Huang, R., Guan, X., et al. (2015). MicroRNA-93 Suppress Colorectal Cancer Development via Wnt/ β -Catenin Pathway Downregulating. *Tumor Biol.* 36, 1701–1710. doi:10.1007/s13277-014-2771-6
- Teodorczyk, M., and Schmidt, M. H. H. (2014). Notching on Cancer's Door: Notch Signaling in Brain Tumors. *Front. Oncol.* 4, 341. doi:10.3389/fonc.2014.00341
- Thiery, J. P., Acloque, H., Huang, R. Y. J., and Nieto, M. A. (2009). Epithelial-mesenchymal Transitions in Development and Disease. *Cell* 139, 871–890. doi:10.1016/j.cell.2009.11.007
- Ullah, E., Nagi, A., and Ashraf, M. (2013). Angiogenesis and Mast Cell Density as Predictors of Patient Survival in Squamous Cell Carcinoma of Lung. *J. Can. Res. Ther.* 9, 701–705. doi:10.4103/0973-1482.126487
- Uzhachenko, R., and Shanker, A. (2016). Notching Tumor: Signaling through Notch Receptors Improves Antitumor T Cell Immunity. *Oncoimmunology* 5, e1122864. doi:10.1080/2162402x.2015.1122864
- Vaiopoulos, A. G., Athanasoula, K. C., and Papavassiliou, A. G. (2013). NF- κ B in Colorectal Cancer. *J. Mol. Med.* 91, 1029–1037. doi:10.1007/s00109-013-1045-x
- Verret, B., Cortes, J., Bachelot, T., Andre, F., and Arnedos, M. (2019). Efficacy of PI3K Inhibitors in Advanced Breast Cancer. *Ann. Oncol.* 30 (Suppl. 10), x12–x20. doi:10.1093/annonc/mdz381
- Wang, W., Zhang, H., Tang, M., Liu, L., Zhou, Z., Zhang, S., et al. (2017). MicroRNA-592 Targets IGF-1R to Suppress Cellular Proliferation, Migration and Invasion in Hepatocellular Carcinoma. *Oncol. Lett.* 13, 3522–3528. doi:10.3892/ol.2017.5902
- Wang, D., Gao, Y., Zhang, Y., Wang, L., and Chen, G. (2019). Glypican-3 Promotes Cell Proliferation and Tumorigenesis through Up-Regulation of β -catenin Expression in Lung Squamous Cell Carcinoma. *Biosci. Rep.* 39, BSR20181147. doi:10.1042/bsr20181147
- Winn, R. A., Marek, L., Han, S.-Y., Rodriguez, K., Rodriguez, N., Hammond, M., et al. (2005). Restoration of Wnt-7a Expression Reverses Non-small Cell Lung Cancer Cellular Transformation through Frizzled-9-Mediated Growth Inhibition and Promotion of Cell Differentiation. *J. Biol. Chem.* 280, 19625–19634. doi:10.1074/jbc.m409392200
- Wu, D., and Pan, W. (2010). GSK3: a Multifaceted Kinase in Wnt Signaling. *Trends Biochem. Sci.* 35, 161–168. doi:10.1016/j.tibs.2009.10.002
- Wu, Y., Cain-Hom, C., Choy, L., Hagenbeek, T. J., De Leon, G. P., Chen, Y., et al. (2010). Therapeutic Antibody Targeting of Individual Notch Receptors. *Nature* 464, 1052–1057. doi:10.1038/nature08878
- Wu, V. S., Kanaya, N., Lo, C., Mortimer, J., and Chen, S. (2015). From Bench to Bedside: What Do We Know about Hormone Receptor-Positive and Human Epidermal Growth Factor Receptor 2-positive Breast Cancer? *J. Steroid Biochem. Mol. Biol.* 153, 45–53. doi:10.1016/j.jsbmb.2015.05.005
- Xie, F., Yuan, Y., Xie, L., Ran, P., Xiang, X., Huang, Q., et al. (2017). miRNA-320a Inhibits Tumor Proliferation and Invasion by Targeting C-Myc in Human Hepatocellular Carcinoma. *Ott* 10, 885–894. doi:10.2147/ott.s122992
- Xing, M., Li, P., Wang, X., Li, J., Shi, J., Qin, J., et al. (2019). Overexpression of p62/IMP2 Can Promote Cell Migration in Hepatocellular Carcinoma via Activation of the Wnt/ β -Catenin Pathway. *Cancers (Basel)* 12, 7. doi:10.3390/cancers12010007
- Yang, J., Chen, J., He, J., Li, J., Shi, J., Cho, W. C., et al. (2016). Wnt Signaling as Potential Therapeutic Target in Lung Cancer. *Expert Opin. Ther. Targets* 20, 999–1015. doi:10.1517/14728222.2016.1154945
- Yang, L., Yang, G., Ding, Y., Huang, Y., Liu, S., Zhou, L., et al. (2018a). Combined Treatment with PI3K Inhibitor BKM120 and PARP Inhibitor Olaparib Is Effective in Inhibiting the Gastric Cancer Cells with ARID1A Deficiency. *Oncol. Rep.* 40, 479–487. doi:10.3892/or.2018.6445
- Yang, X. Z., Cheng, T. T., He, Q. J., Lei, Z. Y., Chi, J., Tang, Z., et al. (2018b). LINC01133 as ceRNA Inhibits Gastric Cancer Progression by Sponging miR-106a-3p to Regulate APC Expression and the Wnt/ β -Catenin Pathway. *Mol. Cancer* 17, 126. doi:10.1186/s12943-018-0874-1
- Yedid, N., Kalma, Y., Malcov, M., Amit, A., Kariv, R., Caspi, M., et al. (2016). The Effect of a Germline Mutation in the APC Gene on β -catenin in Human Embryonic Stem Cells. *BMC Cancer* 16, 952. doi:10.1186/s12885-016-2809-9
- Yu, P., Fan, S., Huang, L., Yang, L., and Du, Y. (2015). MIR210 as a Potential Molecular Target to Block Invasion and Metastasis of Gastric Cancer. *Med. Hypotheses* 84, 209–212. doi:10.1016/j.mehy.2014.12.024
- Yu, Q., Xiang, L., Yin, L., Liu, X., Yang, D., and Zhou, J. (2017). Loss-of-function of miR-142 by Hypermethylation Promotes TGF- β -Mediated Tumour Growth and Metastasis in Hepatocellular Carcinoma. *Cell Prolif* 50, e12384. doi:10.1111/cpr.12384
- Zardawi, S. J., O'toole, S. A., Sutherland, R. L., and Musgrove, E. A. (2009). Dysregulation of Hedgehog, Wnt and Notch Signalling Pathways in Breast Cancer. *Histol. Histopathol* 24, 385–398. doi:10.14670/HH-24.385

- Zardawi, S. J., Zardawi, I., Mcneil, C. M., Millar, E. K. A., Mcleod, D., Morey, A. L., et al. (2010). High Notch1 Protein Expression Is an Early Event in Breast Cancer Development and Is Associated with the HER-2 Molecular Subtype. *Histopathology* 56, 286–296. doi:10.1111/j.1365-2559.2009.03475.x
- Zhang, X., Ke, X., Pu, Q., Yuan, Y., Yang, W., Luo, X., et al. (2016). MicroRNA-410 Acts as Oncogene in NSCLC through Downregulating SLC34A2 via Activating Wnt/ β -Catenin Pathway. *Oncotarget* 7, 14569–14585. doi:10.18632/oncotarget.7538
- Zhang, Y., Xie, Z. Y., Guo, X. T., Xiao, X. H., and Xiong, L. X. (2019). Notch and Breast Cancer Metastasis: Current Knowledge, New Sights and Targeted Therapy. *Oncol. Lett.* 18, 2743–2755. doi:10.3892/ol.2019.10653
- Zheng, M. L., Zhou, N. K., Huang, D. L., and Luo, C. H. (2017). Pathway Cross-Talk Network Strategy Reveals Key Pathways in Non-small Cell Lung Cancer. *J. Buon* 22, 1252–1258.
- Zhou, W., Wang, G., and Guo, S. (2013). Regulation of Angiogenesis via Notch Signaling in Breast Cancer and Cancer Stem Cells. *Biochim. Biophys. Acta (Bba) - Rev. Cancer* 1836, 304–320. doi:10.1016/j.bbcan.2013.10.003

Conflict of Interest: The authors declare that the research was conducted in the absence of any commercial or financial relationships that could be construed as a potential conflict of interest.

Copyright © 2021 He, Shao, Li, Gihu, Xie, Zhou and Yan. This is an open-access article distributed under the terms of the Creative Commons Attribution License (CC BY). The use, distribution or reproduction in other forums is permitted, provided the original author(s) and the copyright owner(s) are credited and that the original publication in this journal is cited, in accordance with accepted academic practice. No use, distribution or reproduction is permitted which does not comply with these terms.



Targeting Tumor-Associated Antigen: A Promising CAR-T Therapeutic Strategy for Glioblastoma Treatment

Guidong Zhu^{1,2,3,4†}, Qing Zhang^{1,2,3†}, Junwen Zhang^{1,2,3} and Fusheng Liu^{1,2,3*}

¹Brain Tumor Research Center, Beijing Neurosurgical Institute, Capital Medical University, Beijing, China, ²Department of Neurosurgery, Beijing Tiantan Hospital Affiliated to Capital Medical University, Beijing, China, ³Beijing Laboratory of Biomedical Materials, Beijing, China, ⁴Shandong Second Provincial General Hospital, Shandong Provincial ENT Hospital, Jinan, China

OPEN ACCESS

Edited by:

Jianxun Ding,
Changchun Institute of Applied
Chemistry (CAS), China

Reviewed by:

Ajay Sharma,
University of Texas Health Science
Center at Houston, United States

Jin Zhang,
Fuzhou University, China

*Correspondence:

Fusheng Liu
liufusheng@ccmu.edu.cn

[†]These authors have contributed
equally to this work

Specialty section:

This article was submitted to
Pharmacology of Anti-Cancer Drugs,
a section of the journal
Frontiers in Pharmacology

Received: 31 January 2021

Accepted: 09 June 2021

Published: 24 June 2021

Citation:

Zhu G, Zhang Q, Zhang J and Liu F
(2021) Targeting Tumor-Associated
Antigen: A Promising CAR-T
Therapeutic Strategy for
Glioblastoma Treatment.
Front. Pharmacol. 12:661606.
doi: 10.3389/fphar.2021.661606

Chimeric antigen receptor T cells (CAR-T) therapy is a prospective therapeutic strategy for blood cancers tumor, especially leukemia, but it is not effective for solid tumors. Glioblastoma (GBM) is a highly immunosuppressive and deadly malignant tumor with poor responses to immunotherapies. Although CAR-T therapeutic strategies were used for glioma in preclinical trials, the current proliferation activity of CAR-T is not sufficient, and malignant glioma usually recruit immunosuppressive cells to form a tumor microenvironment that hinders CAR-T infiltration, depletes CAR-T, and impairs their efficacy. Moreover, specific environments such as hypoxia and nutritional deficiency can hinder the killing effect of CAR-T, limiting their therapeutic effect. The normal brain lack lymphocytes, but CAR-T usually can recognize specific antigens and regulate the tumor immune microenvironment to increase and decrease pro- and anti-inflammatory factors, respectively. This increases the number of T cells and ultimately enhances anti-tumor effects. CAR-T therapy has become an indispensable modality for glioma due to the specific tumor-associated antigens (TAAs). This review describes the characteristics of CAR-T specific antigen recognition and changing tumor immune microenvironment, as well as ongoing research into CAR-T therapy targeting TAAs in GBM and their potential clinical application.

Keywords: car-t, glioblastoma, tumor-associated antigen, targeted therapy, immunotherapy, tumor microenvironment

INTRODUCTION

Glioblastoma is the most common and highly vascular malignant brain tumor that accounts for more than 50% of diagnosed intracranial glioma; it carries a poor prognosis, with a mean survival of ~15 months (Zhang and Liu, 2020). The current first-line GBM treatments include surgery in combination with radiotherapy (RT) and temozolomide (TMZ) (Zhang Q. et al., 2018; Chen and Hambardzumyan, 2018). The dismal prognosis of GBM patients is due to the extreme proliferation,

Abbreviations: CAR-T: chimeric antigen receptor T cells, CTLA-4: cytotoxic T lymphocyte-associated protein 4, GBM: glioblastoma, EGFR: epidermal growth factor receptor, EGFRvIII: epidermal growth factor receptor mutant variant III, HER2: human epidermal growth factor receptor 2, IL13Ra2: interleukin-13 receptor α 2, MET: mesenchymal-epithelial transition factor, NKG2D: natural killer group 2 member D, OV: oncolytic virus, PBMC: peripheral blood mononuclear cell, PD-1: programmed death 1, PDGFR α : platelet-derived growth factor receptor A, PTEN: phosphatase and tensin homolog, TAA: tumor-associated antigen, TME: tumor microenvironment.

malignant invasion, immunosuppressive nature, intra- and intertumoral heterogeneity, and therapeutic resistance of GBM, as well as our limited understanding of the disease's molecular characteristics and delayed diagnoses (Cheng et al., 2020; Zhang and Liu, 2020). It is therefore important to clarify the mechanisms of GBM pathogenesis and identify dependable and applicable molecular biomarkers.

GBM is widely recognized as an intractable disease. However, recent genomic studies have revealed that it undergoes continual mutation (Chen and Hambardzumyan, 2018). In view of gene expression differences, GBMs are further divided into three subgroups: proneural (PN), classical (CL), and mesenchymal (MES) (Chen and Hambardzumyan, 2018). The PN subclass is subdivided into two distinct types. The first is characterized by up-regulation of platelet-derived growth factor receptor A (PDGFR α) and deletion of the p53 gene, and the second has repeated mutations in the genes that encode isocitrate dehydrogenase (IDH1 and IDH2) (Boussiotis and Charest, 2018). The CL subtype has abnormal expression of wild-type or mutant epidermal growth factor receptor (EGFR) that is related to homozygous deficiency or mutation of the INK4a/ARF (CDKN2A) site and loss of phosphatase and tensin homolog (PTEN) function (Brennan et al., 2013). Finally, the MES subtype features loss of the neurofibromatosis type1 (NF1) gene function, and the driving nature of this change in GBM has been verified in NF1-deficient mouse models (Zhu et al., 2005). Understanding the molecular landscapes of GBM microenvironments can provide promising evidence and insight into specific gene treatments.

The GBM microenvironment consists of extremely intricate factors that lead to therapeutic resistance and disease progression (Zhang and Liu, 2020). Despite our improved understanding of the molecular characteristics of GBM, treatments targeting specific molecular pathways remain limited (Boussiotis and Charest, 2018). In recent years, tumor-associated antigens (TAAs) have gradually become a GBM research hotspot. TAAs can be over-expressed or down-regulated and regulate many features of GBM such as proliferation, migration, vascularization, immune evasion, and therapeutic limitation. For example, hepatocyte growth factor (HGF)/mesenchymal-epithelial transition factor (MET) expression results in enhanced proliferation, migration, and invasion due to phosphoinositide 3-kinase (PI3K)/protein kinase B (Akt) and focal adhesion kinase (FAK)/signal transducer and activator of transcription 3 (STAT3) signaling, while glioma cell invasion and increased angiogenesis share mechanisms of extracellular matrix (ECM) degradation through up-regulation of ECM-degrading proteases and activation of aberrant signaling (De Bacco et al., 2012; Joo et al., 2012; Cruickshanks et al., 2017; Keller and Schmidt, 2017). Moreover, programmed death ligand 1 (PD-L1) expression in the tumor microenvironment (TME) can induce T cell dysfunction and apoptosis by binding to programmed death protein 1 (PD-1), which works to promote tumor immune evasion (Sharpe and Pauken, 2018; Zamarin et al., 2018). Notably, tumor-specific receptors are only expressed on tumor cell surfaces, not in normal tissues (Liu et al., 2004). TAAs can produce ligand-independent component activity signals that

enhance proliferation, accelerate tumor formation, decrease apoptosis, and promote GBM vascularization and invasion (Friese et al., 2004; Keller and Schmidt, 2017; Cheng and Guo, 2019).

Despite progress in understanding the molecular underpinnings and developing new treatments, the therapeutic outcomes are still poor; the life expectancy of patients with GBM is just 15 months (Zhang and Liu, 2020). The therapeutic modalities targeting TAAs are considerable and have yielded promising results in preclinical and clinical trials. A growing body of research shows that targeted therapies offer significant benefits. Moreover, CAR-T therapy has been approved for clinical trials for several solid tumors and showed good therapeutic safety and efficacy (O'Rourke et al., 2017; Tchou et al., 2017; Zhang et al., 2017). Currently, CAR-T therapy is of extreme interest for glioma treatment because it can specifically recognize and kill tumor cells and generate an anti-tumor immune microenvironment characterized by increased pro-inflammatory factors and decreased anti-inflammatory factors (Jin et al., 2018; O'Rourke et al., 2017). This review summarizes the biological characteristics and current research of TAAs in GBM, as well as their potential clinical application.

TUMOR-ASSOCIATED ANTIGENS IN GBM

TAAs have been widely used as biomarkers for a variety of cancers and show differential expression in several GBM subtypes. Antigen expression can vary depending on the origin, stage, and grade of tumor, and even the examination method (Boussiotis and Charest, 2018). Many kinds of molecules have been found in GBM, including tumor-suppressing and -promoting proteins. Increasing evidence suggests that GBM-associated antigens with various functional proteins are abundant and play crucial roles in glioma initiation, progression, and recurrence (De Bacco et al., 2012; Liu et al., 2015; Avril et al., 2017). This review summarizes the biological characteristics of antigens in GBM.

EGFR/EGFRVIII

Epidermal growth factor receptor (EGFR) is a tyrosine kinase receptor binds EGF, which belongs to the ErbB family, so it is also called human epidermal growth factor receptor-1 (HER1) or ErbB1. This family contains four receptors (ErbB1-4 or HER1-4), but EGFR is the best characterized (An et al., 2018). Genomic analyses revealed that more than half of the EGFR genes are changed in rat GBM due to amplifications and mutations (Eskilsson et al., 2018). EGFR gene alterations include point mutations or deletions that can lead to constitutive activation of the receptor independently of the ligand (Liu et al., 2015; An et al., 2018; Eskilsson et al., 2018). The most common deletion is exons 2–7 of the EGFR extracellular domain, leading to truncated mutant III (EGFRVIII) (Furnari et al., 2015). The cellular processes activated by EGFR or receptor mutations may depend on specific cell types (Liu et al., 2015). Activated

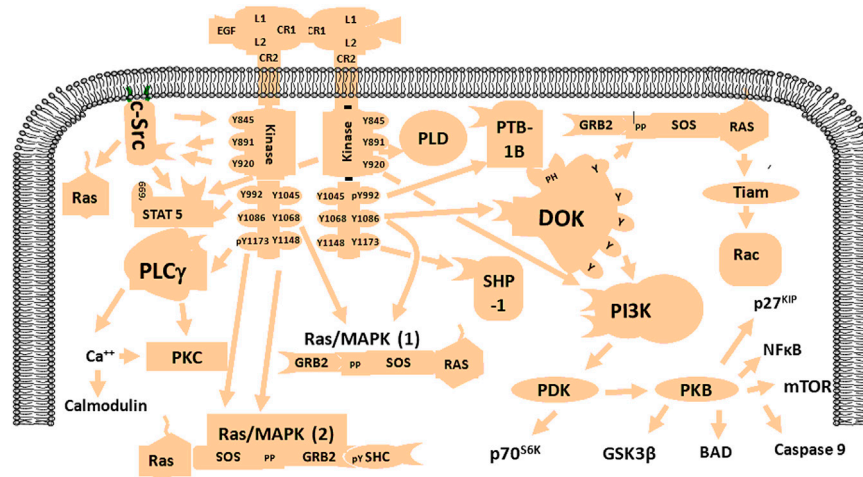


FIGURE 1 | Schematic diagram of the EGFR signaling network. EGFR is activated by specific factors that induce different signaling pathways such as PI3K/Akt, Ras/MAPK, NF- κ B, and mTOR with various biological functions including enhancement of proliferation, invasion, angiogenesis, and resistance to apoptosis.

EGFR may be involved in multiple signaling pathways, (e.g. PI3K/Akt, Ras/Raf/MEK/ERK, STAT3, and phospholipase C [PLC]) with various functional roles including proliferation, invasiveness, vascularization, and apoptotic resistance (Liu et al., 2015; An et al., 2018; Eskilsson et al., 2018). The EGFR signaling pathway is shown in **Figure 1**.

EGFRVIII mutants are found in GBM but not in normal brain tissue (Yang et al., 2017). The kinase activity of EGFRVIII is essential for enhancing the signaling pathway. EGFRVIII signals differ from those of wild-type EGFR in both quantity and quality. EGFRVIII has a low level of constitutive kinase activity due in part to impaired endocytosis and degradation (An et al., 2018). EGFRVIII can transduce signals through the traditional EGFR pathway and is regulated by RAS/mitogen-activated protein kinase (MAPK), PI3K/Akt, and JAK/Stat. EGFR/EGFRVIII may take part in the genesis and development of glioma, including proliferation, migration, tube formation, and drug resistance (Liu et al., 2015; Eskilsson et al., 2016; Keller and Schmidt, 2017). Therefore, EGFR/EGFRVIII could serve as diagnostic and prognostic biomarkers for patients with GBM.

PDGFRA

PDGFRA is a transmembrane receptor containing five immunoglobulin-like domains and one tyrosine kinase domain. Ligand-receptor binding activates key downstream signal transduction pathways that promote tumorigenesis, including MAPK, PI3K/Akt, JAK/Stat, and PLC-protein kinase C (Alentorn et al., 2012). Although PDGFRA amplification is not as common as EGFR amplification, it is found in 11% of GBMs, making it the second most common tyrosine kinase receptor gene amplification in this tumor family (Ozawa et al., 2010; Alentorn et al., 2012). In 2013, Phillips et al. showed that PDGFRA amplification increased with grade and was associated with poor prognosis in IDH1-mutant GBMs (Phillips et al., 2013).

Amplification or activation mutations in PDGFRA represent a significant subset of PN GBM, and up-regulation of PDGFRA promotes GBM initiation and progression (Silber et al., 2012). Previous work showed that the PDGFRA gene is rearranged in GBM (Ozawa et al., 2010). PDGFRA gene expression is mediated by various mechanisms in patients with high-grade glioma, and its amplification may be a prognostic biomarker.

IL13Ra2

Interleukin-13Ra2 (IL-13 receptor α 2) is a monomeric high-affinity receptor that is up-regulated by more than 50% in GBM; it is a prognostic marker of poor survival in patients but is not significantly expressed in normal brain tissue (Brown et al., 2013; Thaci et al., 2014). In high-grade gliomas, IL13RA2 expression was closely correlated with the MES GBM, which may reflect its association with the pro-inflammatory features of this subtype (Brown et al., 2015). IL13Ra2 plays a crucial role in GBM invasiveness and progression. Moreover, IL-13Ra2 is an inhibitor of IL-4-dependent signal transduction and gene expression in the STAT6 response. This restriction may be controlled by an interaction between the short intracellular domain of the IL-13Ra2 protein and the cytoplasmic domain of the IL-4Ra chain (Rahaman et al., 2002). Early clinical research supports the safety and tolerability of vaccine therapies targeting IL13Ra2 and IL-13 immunotoxin for GBM (Brown et al., 2015).

NKG2D

Natural Killer Group 2 member D (NKG2D) is a C-type lectin-like homodimeric receptor expressed on human NK, $\gamma\delta$ T, and CD8⁺ $\alpha\beta$ T cells (Friesen et al., 2004). The NKG2D ligand (NKG2DL) is a key element of tumor immune surveillance. NKG2DL can trigger self-ligands, and such markers mediate

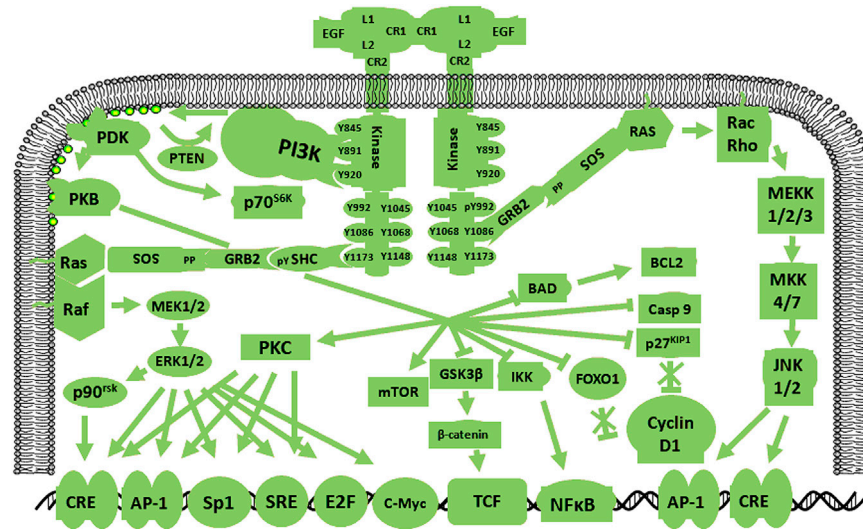


FIGURE 2 | Schematic diagram of the HER2 signaling pathway. HER2 amplification in human GBM is limited by the *EGFR* gene, indicating that HER2 expression in GBM is closely related to the EGFR. HER2 pathway activation gives rise to cascades of specific signals.

the killing effect of NK and CD8⁺ T cells. In 2018, Fluh et al. demonstrated that NKG2DL was positively expressed in glioma stem cells (GSCs) *in vivo* and *in vitro* (Fluh et al., 2018). The over-expression of NKG2D in CD8⁺ T and NK cells could enhance the immune response to hinder glioma cell migration and invasion and eradicate tumors (Friese et al., 2004). NKG2D also mediates the innate reactivity of V γ 9V δ 2 T lymphocytes and targets GBM cells by recognizing pathways involved in the innate identification of the MES subtype (Chauvin et al., 2019). These results underscore the utility of novel targeted immunotherapies in GBM treatment.

HER2

Human epidermal growth factor receptor 2 (HER2), also known as HER2/neu or ErbB2, is a 185-kDa transmembrane protein that is broadly homologous to the EGFR in structure and sequence. HER2 gene magnification and up-regulation frequently occur in many human malignancies (Koka et al., 2003; Liu et al., 2004). HER2 expression in GBM cells and the identification of peptide-specific, major histocompatibility complex-limited CTL production in GBM cells lay the foundation for the use of relevant alternative assays to measure antigen-specific cytotoxicity (Liu et al., 2004). Moreover, ErbB gene amplification is limited to the EGFR gene in human GBM, indicating that ErbB2 expression in GBM is closely associated with EGFR levels (Schlegel et al., 1994). HER2 signaling pathways are shown in **Figure 2**. Previous work showed a relationship between HER2/neu expression in GBM and survival time. Specifically, HER2/neu over-expression in the early stage of GBM is used to predicting mortality (Koka et al., 2003). These results indicate that HER2 may be a poor prognostic indicator for patients with GBM.

MET

MET and HGF are located on chromosome 7q31 and 7q21.1, respectively (Cruickshanks et al., 2017). The HGF receptor MET is a high-affinity tyrosine kinase composed of α and β subunits. The extracellular domain consists of an α -subunit and amino-terminal region of the β -subunit. The other β -chain regions span the cell membrane to create a cytoplasmic region with tyrosine kinase activity (Cheng and Guo, 2019). In 2012, Joo et al. demonstrated that MET signaling plays vital roles in the maintenance, migration, and radiation resistance of GSCs (Joo et al., 2012). The mutual effect of MET and HGF induces autophosphorylation at various tyrosine remainders, which generates stimulation of a few signaling molecules such as Gab1, Grb2, Src, Shc, PLC- γ , and c-Cbl that are subsequently phosphorylated to induce downstream transduction including STAT3 and Ras/MAPK/ERK, (De Bacco et al., 2012; Joo et al., 2012; Cruickshanks et al., 2017; Cheng and Guo, 2019). MET and HGF signaling pathways are shown in **Figure 3**. Some studies confirmed that the interaction between MET and its ligand HGF plays an important role in GBM proliferation, invasion, survival, vascularization, treatment resistance, and recurrence (Hu H. et al., 2018; Cheng and Guo, 2019). In addition, glioma expressing PTPRZ1-MET (ZM) gene fusions show potent invasiveness and sensitivity to chemotherapy drugs (International Cancer Genome Consortium PedBrain Tumor Project, 2016; Hu H. et al., 2018). In summary, MET is a functional marker and a candidate target for novel GBM treatments.

IMMUNE CHECKPOINT PROTEINS

GBM is a highly immunosuppressive malignant brain tumor. Immune checkpoint proteins—especially PD-1, PD-L1, cytotoxic T lymphocyte-associated protein 4 (CTLA-4), and B7 homolog 3

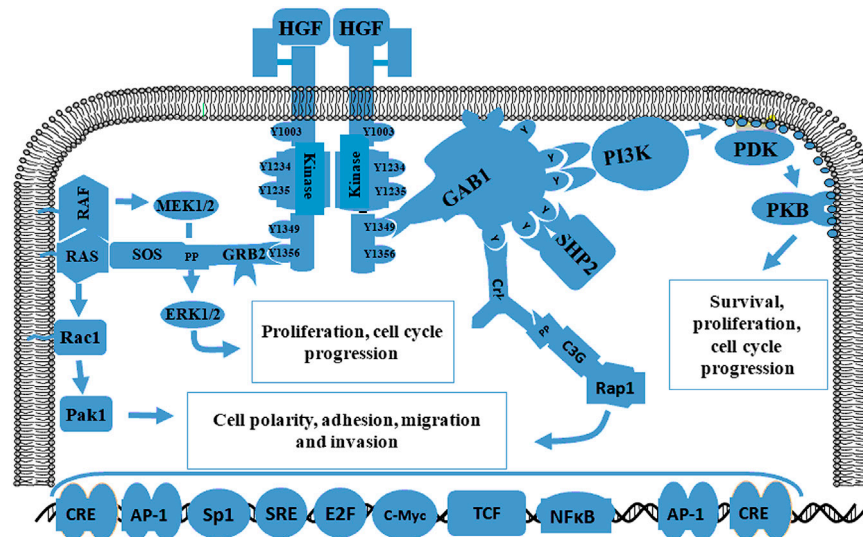


FIGURE 3 | Schematic diagram of the MET signaling pathway related to proliferation, migration, and invasion. The initiation of MET signaling activates several signals including Gab1, Grb2, Ras, SOS and Shp2 and the subsequent phosphorylation of downstream molecules such as STAT3 and Ras/MAPK/ERK. The interaction between MET and HGF plays a crucial role in proliferation, survival, migration, invasion, treatment resistance, and GBM recurrence.

(B7-H3) —have immunosuppressive characteristics that are up-regulated in the GBM TME, which contribute to tumor cell immune escape (Berghoff et al., 2015; Nduom et al., 2016; Saha et al., 2017; Wang et al., 2018). CTLA-4 is an immune checkpoint co-inhibitory receptor expressed on T cells that competes with the co-stimulatory receptor CD28 for binding by their ligands CD80 and CD86; this reduces the number of T helper cells and effector T cells while increasing regulatory T cells (Tregs) (Liu F. et al., 2020). PD-1 is another immune inhibitor expressed on T cells, B cells, and NK cells. Its ligand PD-L1 is up-regulated in GBM cells. PD-L1 binds PD-1 and induces immune cell dysfunction (Litak et al., 2019). The well-studied immune checkpoints including CTLA-4, PD-1, and PD-L1 play crucial roles in the tumor immunoreaction process (Fong et al., 2012; Wang et al., 2019). Moreover, higher expression of immune checkpoint proteins is related to poor prognosis in patients with GBM. Various clinical studies targeting PD-1/PD-L1 and CTLA-4 have been carried out in patients with GBM to promote powerful antitumor immune responses (Fong et al., 2012; Litak et al., 2019; Liu F. et al., 2020).

B7-H3 is another immune checkpoint protein that belongs to the immunoglobulin superfamily and is considered to be involved in mediating the T cell immune response (Picarda et al., 2016; Wang et al., 2018). Previous research described its biological characteristics in malignant brain gliomas and found that its expression was closely correlated with cell cycle, immune response, and angiogenesis in glioma. Moreover, B7-H3 levels were higher in high-grade compared to low-grade tumor tissues. Elevated B7-H3 expression is associated with extremely poor prognosis. It is up-regulated in wild-type IDH gliomas and the MES subtype (Zhang C. et al., 2018). In 2020, Zhong et al. demonstrated that B7-H3 contributed to epithelial-mesenchymal transition (EMT) development via E-cadherin

down-regulation and MMP2/9 up-regulation and promoted glioma progression and invasion through JAK2/STAT3/Slug-dependent signaling (Zhong et al., 2020). Moreover, the collaboration of B7-H3 with other checkpoint members may result in T cell dysfunction. Further research into B7-H3 will provide promising insights to further optimize GBM immunotherapies.

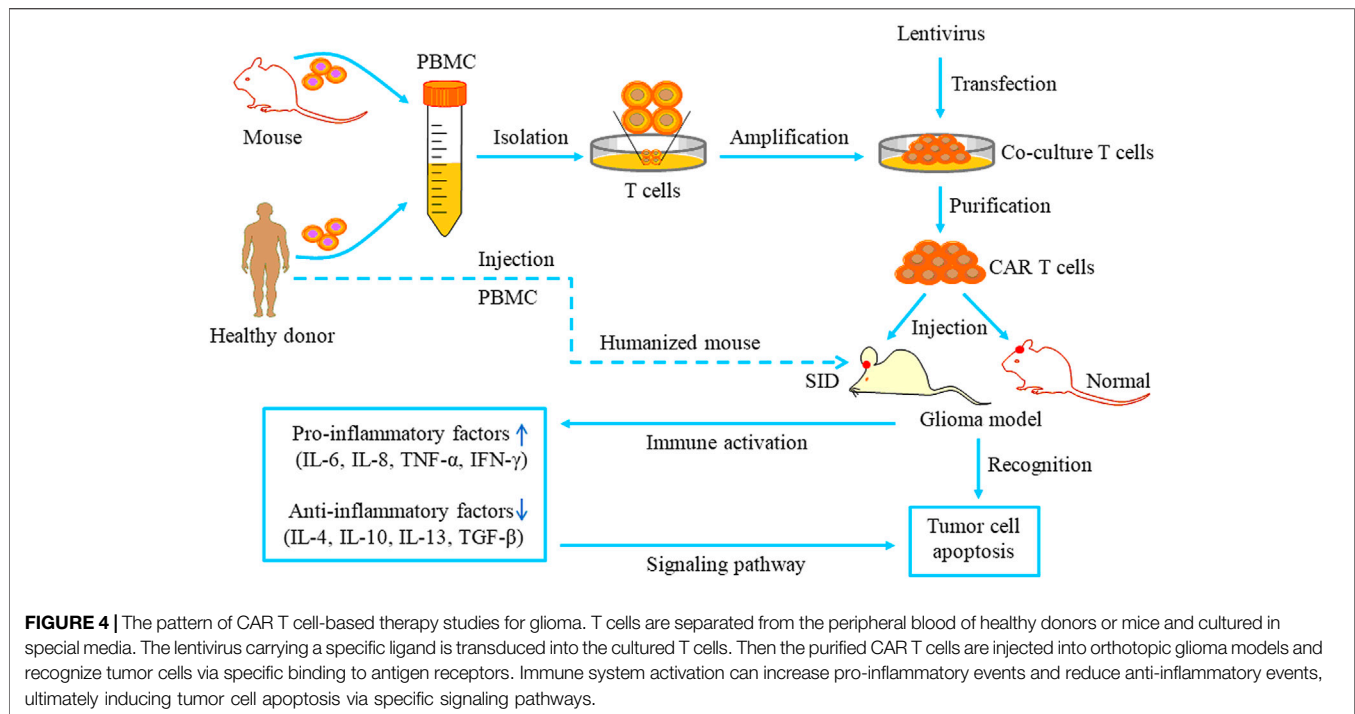
TUMOR SUPPRESSOR PROTEINS

It is well known that tumor suppressor genes play vital roles in tumorigenesis. Here we mainly summarize PTEN and P53 because mutations in these genes contribute to tumorigenesis. Previous studies showed that PTEN and P53 mutations occurred in GBM patients with extremely poor prognosis (Wiencke et al., 2007; Benitez et al., 2017; Ham et al., 2019). PTEN is a candidate gene for inactivating mutations in GBM. Deletions and mutations in PTEN in GBM are frequent events that are related to treatment resistance. Benitez et al. found that PTEN could regulate tumorigenesis through chromatin-associated complexes of death-domain associated protein and histone H3.3 (Benitez et al., 2017). P53 is another tumor suppressor that participates in different aspects of cell cycle regulation and conversion inhibition (Ham et al., 2019). TP53 mutations are related to poor prognosis and EMT characteristics in malignant gliomas (Cho et al., 2017).

CAR-T RESEARCH ADVANCES IN GBM

Targeting TAAs

GBM is a highly intractable disease. Despite great progress in molecular research and treatments, the clinical outcomes



remained extremely poor, and the survival of patients with GBM has not been significantly improved. Developing targeted GBM therapies has increasingly become a research hotspot. Several preclinical and clinical studies on CAR-T immunotherapy for malignant gliomas have yielded positive results (Ahmed et al., 2017; Schneider et al., 2017; Thistlethwaite et al., 2017; Haydar et al., 2020). The therapeutic patterns of CAR-T cells targeting TAAs for GBM treatment are depicted in **Figure 4**. CAR-T therapy can specifically recognize and kill tumors and create an anti-tumor immune microenvironment. These targeted therapies will be gradually developed to provide therapeutic approaches for gliomas.

Targeting EGFRvIII

Exploration of glioma-specific antigens identified many CAR-T strategies for glioma. A clinical study confirmed that CAR-T targeting EGFRvIII can specifically kill GBM cells by releasing cytokines and induced glioma cell toxicity in a dose- and time-dependent manner for patients with recurrent GBM (O'Rourke et al., 2017). Another group showed a close correlation between CAR-T activity and the concentration of small molecules that increased the safety of CAR-T treatment (Zheng et al., 2018). Bispecific T-cell engager (BiTEs) have an anti-EGFR effect, and Choi et al. found that EGFR-targeted BiTEs generated by CAR-T can generate powerful and specific antitumor activity that mitigates the effect of EGFRvIII antigen loss (Choi et al., 2019). The combination of EGFRvIII-CAR-T and PD-1 down-regulation has potent anti-glioma efficacy and prolongs survival in mice. Furthermore, PD-1 knockout significantly enhances lysis of CAR-T cells targeting EGFRvIII for PD-L1⁺ EGFRvIII⁺ GBM cells (Song et al., 2020; Zhu et al., 2020a; Zhu et al., 2020b). Importantly, intratumoral IL-12 administration effectively

reshapes the TME (i.e., increased pro-inflammatory CD4⁺ T cells and decreased Tregs), thus improving CAR-T cell immunotherapy in a preclinical model (Agliardi et al., 2021). These results provide insight into developing new CAR-T strategies for GBM therapy in future.

Targeting IL13Ra2

IL13Ra2-CAR-T is a promising immunotherapy strategy for GBM. In 2015, a clinical trial was performed to evaluate effectiveness and safety of IL13Ra2-redirected CAR-CD8⁺ T cells in patients with recurrent GBM (Brown et al., 2015). This clinical experience in the intracranial treatment of GBM with IL13Ra2-specific CAR-T lays the foundation for the future application of modified CAR-T therapies. This approach creates a pro-inflammatory immune microenvironment in a syngeneic model of GBM by generating obvious increases in CD4⁺ and CD8⁺ T cells, while decreasing the number of myeloid-derived suppressor cells and producing cytokines such as interferon (IFN)- γ and tumor necrosis factor- α , thus further enhancing anti-glioma effects (Pituch et al., 2018). Brown and colleagues designed a 4-1BB (CD137) co-stimulatory CAR (IL13BB ζ) and a manufacturing platform using enriched central memory T cells to confirm that IL13Ra2-targeted CAR-T enhanced anti-tumor effect in patient-derived tumor models (Brown et al., 2016; Brown et al., 2018). In a clinical trial, CAR-T cells targeting IL13Ra2 had potent antitumor effects in patients with malignant glioma (Brown et al., 2016). In addition, human IL13Ra2-CAR-T therapy improves the GBM immune microenvironment and induces the activation of host immune cells that enhance the antitumor efficacy of CAR-T (Alizadeh et al., 2021). These findings will contribute to the clinical application of CAR-T for malignant gliomas.

Targeting NKG2D

A previous study demonstrated that chemotherapy and RT enhanced NKG2DL expression for all GBM models, and tissue samples from GBM patients show up-regulation of NKG2DL expression after treatment with TMZ or RT (Weiss et al., 2018a). This suggests improved glioma cell immunogenicity and provides a theoretical basis for combining NKG2D-based immunotherapy with TMZ and RT. In 2019, Yang et al. showed that NKG2D specific-CAR T effectively eradicated GBM cells and GSCs *in vitro* and induced cytokine over-expression (Yang et al., 2019). CAR-T significantly inhibited tumor growth *in vivo* and did not show obvious treatment toxicity in GBM-bearing animals. CAR-T targeting NKG2D combined with RT exerts synergistic efficacy in mouse glioma models (Weiss et al., 2018b). The findings described above provide a basis to develop rationale immunotherapeutic strategies to treat human glioma patients in the future.

Targeting B7-H3

B7-H3 is a new target of CAR-T cells for GBM therapy. Tang et al. evaluated the antitumor activities of CAR-T targeting B7-H3 in both primary glioma cells and GBM cell lines; they also observed significantly longer median survival in the CAR-T group compared to the control group in an orthotopic GBM model (Tang et al., 2019). In 2019, Nehama et al. verified that CAR-T targeting B7-H3 release effective factors such as IFN- γ and IL-2 and control the growth of B7-H3⁺ human GBM cell lines and neurospheres (Nehama et al., 2019). CAR-T targeting B7-H3 has potent antitumor activities in patient-derived orthotopic xenograft and immune-competent animal models (Haydar et al., 2020). Dual CAR-T target antigens exhibit enhanced antitumor activities and improve the heterogeneity and variation of antigens in treating multiple types of solid tumors (Yang et al., 2020). These lines of evidence suggest that B7-H3 may be a promising target for CAR-T treatment for GBM.

POTENTIAL CLINICAL APPLICATIONS

TAA's Are Promising Molecular Biomarkers

TAA's have been used as targets for glioma therapy in basic studies and clinical trials. These results hold great promise for patients with refractory disease. Several GBM-associated biological molecules have been extensively studied. An important indicator is how representative they are in the overall tumor or at least reflect the tumor's major biological characteristics. Variable expression in GBM is one of the main causes of tumor heterogeneity, which contributes to treatment resistance and poor efficacy. A growing number of studies have confirmed a key role of TAA's in glioma initiation and development. Targeted GBM therapy is increasingly researched due to limitations of traditional therapeutic strategies. Hence, TAA-specific targeted therapies have a good prospect of clinical application in glioma treatment and are receiving more attention.

Molecular detection is widely used for clinically monitoring patients with brain malignant tumors. One study reported up-regulation of glioma-associated antigens and found that their

expression correlated with histological grade and patient prognosis (Brown et al., 2013; Jin et al., 2018). Therefore, TAA's have potential as diagnostic and prognostic markers. Acquired drug resistance is an important issue that restricts treatment. Timely detection of potential drug-resistant patients who may require alternative treatment is very important to improve prognosis. Collectively, the existing evidence indicates that TAA's in GBM show great potential as biomarkers, and their clinical application is worthy of further investigation.

TAA's in GBM Treatment

Considering the important roles of TAA's in glioma, therapies that target TAA's will be important treatment options. In 2018, Hu et al. reported that the MET kinase inhibitor PLB1001 demonstrated significant ability to selectively inhibit tumor cells with MET mutations in an animal model. Moreover, the drug was able to pass through the blood-brain barrier (BBB) and was used in a phase I clinical trial of patients with chemo-resistant glioma (Hu H. et al., 2018). We designed a novel Ki67-expressing oncolytic adenovirus to target glioma and showed potent oncolytic efficacy (Zhang Q. et al., 2020). These studies underscore the possibility of targeting specific antigens for GBM therapy.

Administering chemotherapy for GBM faces great challenges and limitations because of the BBB (Moesta et al., 2017). However, modified CAR-T have special features such as high proliferation, rapid onset, high remission rate, and long remission time that can overcome dominant biological barriers such as the BBB. In 2018, Samaha et al. modified CAR-T cells to successfully cross the BBB and spread tumor sites, which contributed to glioma eradication and significantly extended animal survival (Samaha et al., 2018). Therefore, CAR-T could be a promising glioma therapy delivery system.

Compared with T cells, CAR-NK (natural killer) cells have a few advantages such as their safety in clinical trials, their mechanism for recognizing tumor cells, and high levels in clinical specimens (Hu Y. et al., 2018). EGFR-CAR-NK cells induce potent cell lysis and increase IFN- γ production when co-cultured with GBM cells, and intracranial NK-EGFR-CAR cell injection can effectively inhibit tumor growth and significantly extend the life expectancy of orthotopic GBM animal models (Han et al., 2015). In addition, human CAR-NK cells expressing a HER2-specific show potent antitumor immunity in NSG GBM models (Schonfeld et al., 2015; Zhang et al., 2016). Many modalities have been exploited to increase the safety and efficacy of CAR-based immunotherapies. These given findings suggest TAA's-specific-CAR cells represent a prospective strategy for GBM treatment.

Oncolytic Virus in Combination With CAR-T for GBM Treatment

In recent years, characterizing complex TMEs has become a research hotspot in tumor therapy (Gutmann, 2015; Wang et al., 2017; Xie et al., 2019). GBM is a highly immunosuppressive tumor, which results in immunotherapy resistance and limitation (Saha et al., 2017). Immunotherapy is

an emerging therapeutic strategy for solid tumors. Although CAR-T therapy shows potential advantages compared to other immunotherapies, they cannot function effectively because of the immunosuppressive TME of GBM. The TME can be regulated by oncolytic viruses (OVs) that stimulate antitumor immunity (Kurozumi et al., 2007; De Silva et al., 2010; Moncayo et al., 2018; Meng et al., 2019; Liu et al., 2020b), but the potential mechanisms remain unclear. Researchers have exploited the advantages of OVs to improve CAR-T for solid tumor therapy. For example, mice treated with a combined injection of OVs and CAR-T cells show long-term antitumor immune protection.

OVS have therapeutic capacity for cancer treatment. During infections, viruses hijack host cells replication mechanisms, promote their own genetic expression, and unavoidably cause the death of host cells, allowing viral offspring to reach and infect neighboring host cells (Martinez-Velez et al., 2019). OVs can specifically infect and kill tumor cells and have become an attractive treatment choice (Fang et al., 2014; Martikainen and Essand, 2019; Zhang W. et al., 2020). Our research team has showed that OVs have potent therapeutic efficacy and safety to treat malignant brain glioma and uveal melanoma (Zhang J. et al., 2020; Liu et al., 2020a; Zhang Q. et al., 2020; Liu et al., 2020b; Liu et al., 2021). Previous studies confirm that intratumoral OV injection can enhance anti-tumor immunity and eliminate contralateral tumors (Lun et al., 2005; Saha et al., 2018; Martinez-Velez et al., 2019; Liu et al., 2021). Moreover, OV-mediated tumor tissue destruction is closely associated with innate immune responses and adaptive T-cell immune responses (Hellums et al., 2005; Stephenson et al., 2012). Immune checkpoint molecules such as PD-1 and CTLA-4 are often up-regulated in the TME and induce T cell dysfunction (Saha et al., 2017; Boussiotis and Charest, 2018). However, OVs direct immune cells into tumor regions, further regulating the TME and generating antitumor immune responses. OVs equipped with immunomodulatory factors deliver therapeutic genes and further induce immune cell activation and proliferation (Lei et al., 2009; Lun et al., 2010; Jiang et al., 2017). For example, IL-15 enhances the activities of macrophages and neutrophils, accelerates the production and activation of NK cells and CD8⁺ T cells, and regulates memory T cell survival and proliferation (Stephenson et al., 2012). A recent study revealed that combining CD19-CAR-T cells and OVs encoding for truncated CD19 (OV19t) achieved a >50% cure rate in a mouse tumor model

by inducing local immunity characterized by tumor T cell infiltration; CAR T cell-mediated tumor killing also promoted viral release from dying tumor cells, further propagating CD19t tumor expression (Park et al., 2020). Combination treatment overcomes the limitation of targeting CAR T to solid tumors and helps normalize the TME, and these effects will improve CAR-T therapeutic efficacy in GBM.

CONCLUSION

As new targeted therapies are developed, an increasing number of novel therapeutic strategies have achieved many beneficial outcomes, such as CAR-T immunotherapy that can specifically recognize and target tumor cells. In GBM treatment, second- and third-generation CAR-T therapies have shown promising therapeutic efficacy to prolong patient survival. However, there have been no phase III clinical trial results due to the challenging location and particular characteristics of GBM. Further studies are needed to optimally modify CAR-T cells and their targets to improve efficacy. The current dilemmas that must be addressed are selecting the best delivery approach, comprehending the TME, exploiting new targets, and improving therapeutic efficacy. As we learn more about these issues, we expect a bright future for CAR-T therapy for GBM.

AUTHOR CONTRIBUTIONS

GZ and QZ were mainly responsible for the conception, draft, modification of the paper and the production of diagram, JZ contributed to the modification of the manuscript, literature collection; FL contributes to language polish and revision of the manuscript for significant intellectual content. All authors read and agreed the final manuscript.

FUNDING

This work was supported by Capital's Funds for Health Improvement and Research (CFH, 2020-1-1071), National Natural Science Foundation of China (No. 81972344), Beijing Natural Science Foundation (No. 7202020) and Beijing Laboratory of Biomedical Materials Foundation.

REFERENCES

- Agliardi, G., Liuzzi, A. R., Hotblack, A., De Feo, D., Núñez, N., Stowe, C. L., et al. (2021). Intratumoral IL-12 Delivery Empowers CAR-T Cell Immunotherapy in a Pre-clinical Model of Glioblastoma. *Nat. Commun.* 12, 444. doi:10.1038/s41467-020-20599-x
- Ahmed, N., Brawley, V., Hegde, M., Bielamowicz, K., Kalra, M., Landi, D., et al. (2017). HER2-Specific Chimeric Antigen Receptor-Modified Virus-specific T Cells for Progressive Glioblastoma. *JAMA Oncol.* 3, 1094–1101. doi:10.1001/jamaoncol.2017.0184
- Alentorn, A., Marie, Y., Carpentier, C., Boisselier, B., Giry, M., Labussiere, M., et al. (2012). Prevalence, Clinico-Pathological Value, and Co-occurrence of PDGFRA Abnormalities in Diffuse Gliomas. *Neuro-Oncology* 14, 1393–1403. doi:10.1093/neuonc/nos217
- Alizadeh, D., Wong, R. A., Gholamin, S., Maker, M., Aftabzadeh, M., Yang, X., et al. (2021). IFN γ Is Critical for CAR T Cell Mediated Myeloid Activation and Induction of Endogenous Immunity. *Cancer Discov.* 11, candisc.1661.2020. doi:10.1158/2159-8290.CD-20-1661
- An, Z., Aksoy, O., Zheng, T., Fan, Q.-W., and Weiss, W. A. (2018). Epidermal Growth Factor Receptor and EGFRvIII in Glioblastoma: Signaling Pathways and Targeted Therapies. *Oncogene* 37, 1561–1575. doi:10.1038/s41388-017-0045-7
- Avril, T., Etcheverry, A., Pineau, R., Obacz, J., Jegou, G., Jouan, F., et al. (2017). CD90 Expression Controls Migration and Predicts Dasatinib Response in Glioblastoma. *Clin. Cancer Res.* 23, 7360–7374. doi:10.1158/1078-0432.CCR-17-1549

- Benitez, J. A., Ma, J., D'Antonio, M., Boyer, A., Camargo, M. F., Zanca, C., et al. (2017). PTEN Regulates Glioblastoma Oncogenesis through Chromatin-Associated Complexes of DAXX and Histone H3.3. *Nat. Commun.* 8, 15223. doi:10.1038/ncomms15223
- Berghoff, A. S., Kiesel, B., Widhalm, G., Rajky, O., Ricken, G., Wöhrer, A., et al. (2015). Programmed Death Ligand 1 Expression and Tumor-Infiltrating Lymphocytes in Glioblastoma. *Neuro Oncol.* 17, 1064–1075. doi:10.1093/neuonc/nou307
- Boussiotis, V. A., and Charest, A. (2018). Immunotherapies for Malignant Glioma. *Oncogene* 37, 1121–1141. doi:10.1038/s41388-017-0024-z
- Brennan, C. W., Verhaak, R. G., McKenna, A., Campos, B., Nounshmehr, H., Salama, S. R., et al. (2013). The Somatic Genomic Landscape of Glioblastoma. *Cell* 155, 462–477. doi:10.1016/j.cell.2013.09.034
- Brown, C. E., Aguilár, B., Starr, R., Yang, X., Chang, W.-C., Weng, L., et al. (2018). Optimization of IL13Ra2-Targeted Chimeric Antigen Receptor T Cells for Improved Anti-tumor Efficacy against Glioblastoma. *Mol. Ther.* 26, 31–44. doi:10.1016/j.ymthe.2017.10.002
- Brown, C. E., Alizadeh, D., Starr, R., Weng, L., Wagner, J. R., Naranjo, A., et al. (2016). Regression of Glioblastoma after Chimeric Antigen Receptor T-Cell Therapy. *N. Engl. J. Med.* 375, 2561–2569. doi:10.1056/NEJMoa1610497
- Brown, C. E., Badie, B., Barish, M. E., Weng, L., Ostberg, J. R., Chang, W.-C., et al. (2015). Bioactivity and Safety of IL13Ra2-Redirected Chimeric Antigen Receptor CD8+ T Cells in Patients with Recurrent Glioblastoma. *Clin. Cancer Res.* 21, 4062–4072. doi:10.1158/1078-0432.CCR-15-0428
- Brown, C. E., Warden, C. D., Starr, R., Deng, X., Badie, B., Yuan, Y.-C., et al. (2013). Glioma IL13Ra2 Is Associated with Mesenchymal Signature Gene Expression and Poor Patient Prognosis. *PLoS One* 8, e77769. doi:10.1371/journal.pone.0077769
- Chauvin, C., Joalland, N., Perroteau, J., Jarry, U., Lafrance, L., Willem, C., et al. (2019). NKG2D Controls Natural Reactivity of V γ 9V δ 2 T Lymphocytes against Mesenchymal Glioblastoma Cells. *Clin. Cancer Res.* 25, 7218–7228. doi:10.1158/1078-0432.CCR-19-0375
- Chen, Z., and Hambardzumyan, D. (2018). Immune Microenvironment in Glioblastoma Subtypes. *Front. Immunol.* 9, 1004. doi:10.3389/fimmu.2018.01004
- Cheng, F., and Guo, D. (2019). MET in Glioma: Signaling Pathways and Targeted Therapies. *J. Exp. Clin. Cancer Res.* 38, 270. doi:10.1186/s13046-019-1269-x
- Cheng, J., Meng, J., Zhu, L., and Peng, Y. (2020). Exosomal Noncoding RNAs in Glioma: Biological Functions and Potential Clinical Applications. *Mol. Cancer* 19, 66. doi:10.1186/s12943-020-01189-3
- Cho, S.-Y., Park, C., Na, D., Han, J. Y., Lee, J., Park, O.-K., et al. (2017). High Prevalence of TP53 Mutations Is Associated with Poor Survival and an EMT Signature in Gliosarcoma Patients. *Exp. Mol. Med.* 49, e317. doi:10.1038/emmm.2017.9
- Choi, B. D., Yu, X., Castano, A. P., Bouffard, A. A., Schmidts, A., Larson, R. C., et al. (2019). CAR-T Cells Secreting BiTEs Circumvent Antigen Escape without Detectable Toxicity. *Nat. Biotechnol.* 37, 1049–1058. doi:10.1038/s41587-019-0192-1
- Cruickshanks, N., Zhang, Y., Yuan, F., Pahuski, M., Gibert, M., and Abounader, R. (2017). Role and Therapeutic Targeting of the HGF/MET Pathway in Glioblastoma. *Cancers* 9, 87. doi:10.3390/cancers9070087
- De Bacco, F., Casanova, E., Medico, E., Pellegatta, S., Orzan, F., Albano, R., et al. (2012). The MET Oncogene Is a Functional Marker of a Glioblastoma Stem Cell Subtype. *Cancer Res.* 72, 4537–4550. doi:10.1158/0008-5472.CAN-11-3490
- De Silva, N., Atkins, H., Kirn, D. H., Bell, J. C., and Breitbach, C. J. (2010). Double Trouble for Tumours: Exploiting the Tumour Microenvironment to Enhance Anticancer Effect of Oncolytic Viruses. *Cytokine Growth Factor. Rev.* 21, 135–141. doi:10.1016/j.cytogfr.2010.02.007
- Eskilsson, E., Røslund, G. V., Solecki, G., Wang, Q., Harter, P. N., Graziani, G., et al. (2018). EGFR Heterogeneity and Implications for Therapeutic Intervention in Glioblastoma. *Neuro Oncol.* 20, 743–752. doi:10.1093/neuonc/now191
- Eskilsson, E., Røslund, G. V., Talasila, K. M., Knappskog, S., Keunen, O., Sottoriva, A., et al. (2016). EGFRvIII Mutations Can Emerge as Late and Heterogenous Events in Glioblastoma Development and Promote Angiogenesis through Src Activation. *Neuonc* 18, 1644–1655. doi:10.1093/neuonc/now113
- Fang, L., Cheng, Q., Li, W., Liu, J., Li, L., Xu, K., et al. (2014). Antitumor Activities of an Oncolytic Adenovirus Equipped with a Double siRNA Targeting Ki67 and hTERT in Renal Cancer Cells. *Virus. Res.* 181, 61–71. doi:10.1016/j.virusres.2013.12.021
- Flüh, C., Chitadze, G., Adamski, V., Hattermann, K., Synowitz, M., Kabelitz, D., et al. (2018). NKG2D Ligands in Glioma Stem-like Cells: Expression *In Situ* and *In Vitro*. *Histochem. Cel Biol* 149, 219–233. doi:10.1007/s00418-018-1633-5
- Fong, B., Jin, R., Wang, X., Safaei, M., Lisiero, D. N., Yang, I., et al. (2012). Monitoring of Regulatory T Cell Frequencies and Expression of CTLA-4 on T Cells, before and after DC Vaccination, Can Predict Survival in GBM Patients. *PloS one* 7, e32614. doi:10.1371/journal.pone.0032614
- Frieze, M. A., Wischhusen, J., Wick, W., Weiler, M., Eisele, G., Steinle, A., et al. (2004). RNA Interference Targeting Transforming Growth Factor- β Enhances NKG2D-Mediated Antiglioma Immune Response, Inhibits Glioma Cell Migration and Invasiveness, and Abrogates Tumorigenicity *In Vivo*. *Cancer Res.* 64, 7596–7603. doi:10.1158/0008-5472.CAN-04-1627
- Furnari, F. B., Cloughesy, T. F., Cavenee, W. K., and Mischel, P. S. (2015). Heterogeneity of Epidermal Growth Factor Receptor Signalling Networks in Glioblastoma. *Nat. Rev. Cancer* 15, 302–310. doi:10.1038/nrc3918
- Gutmann, D. H. (2015). Microglia in the Tumor Microenvironment: Taking Their TOLL on Glioma Biology. *Neuro-Oncology* 17, 171–173. doi:10.1093/neuonc/nou346
- Ham, S. W., Jeon, H.-Y., Jin, X., Kim, E.-J., Kim, J.-K., Shin, Y. J., et al. (2019). TP53 Gain-Of-Function Mutation Promotes Inflammation in Glioblastoma. *Cell Death Differ* 26, 409–425. doi:10.1038/s41418-018-0126-3
- Han, J., Chu, J., Keung Chan, W., Zhang, J., Wang, Y., Cohen, J. B., et al. (2015). CAR-engineered NK Cells Targeting Wild-type EGFR and EGFRvIII Enhance Killing of Glioblastoma and Patient-Derived Glioblastoma Stem Cells. *Sci. Rep.* 5, 11483. doi:10.1038/srep11483
- Haydar, D., Houke, H., Chiang, J., Yi, Z., Odé, Z., Caldwell, K., et al. (2020). Cell-surface Antigen Profiling of Pediatric Brain Tumors: B7-H3 Is Consistently Expressed and Can Be Targeted via Local or Systemic CAR T-Cell Delivery. *Neuro Oncol.* 23, 999–1011. doi:10.1093/neuonc/noaa278
- Hellums, E. K., Markert, J. M., Parker, J. N., He, B., Perbal, B., Roizman, B., et al. (2005). Increased Efficacy of an Interleukin-12-Secreting Herpes Simplex Virus in a Syngeneic Intracranial Murine Glioma Model. *Neuro Oncol.* 7, 213–224. doi:10.1215/S1152851705000074
- Hu, H., Mu, Q., Bao, Z., Chen, Y., Liu, Y., Chen, J., et al. (2018). Mutational Landscape of Secondary Glioblastoma Guides MET-Targeted Trial in Brain Tumor. *Cell* 175, 1665–1678.e18. doi:10.1016/j.cell.2018.09.038
- Hu, Y., Tian, Z.-g., and Zhang, C. (2018). Chimeric Antigen Receptor (CAR)-transduced Natural Killer Cells in Tumor Immunotherapy. *Acta Pharmacol. Sin* 39, 167–176. doi:10.1038/aps.2017.125
- International Cancer Genome Consortium PedBrain Tumor Project (2016). Recurrent MET Fusion Genes Represent a Drug Target in Pediatric Glioblastoma. *Nat. Med.* 22, 1314–1320. doi:10.1038/nm.4204
- Jiang, H., Rivera-Molina, Y., Gomez-Manzano, C., Clise-Dwyer, K., Bover, L., Vence, L. M., et al. (2017). Oncolytic Adenovirus and Tumor-Targeting Immune Modulatory Therapy Improve Autologous Cancer Vaccination. *Cancer Res.* 77, 3894–3907. doi:10.1158/0008-5472.CAN-17-0468
- Jin, L., Ge, H., Long, Y., Yang, C., Chang, Y., Mu, L., et al. (2018). CD70, a Novel Target of CAR T-Cell Therapy for Gliomas. *Neuro Oncol.* 20, 55–65. doi:10.1093/neuonc/now116
- Joo, K. M., Jin, J., Kim, E., Ho Kim, K., Kim, Y., Gu Kang, B., et al. (2012). MET Signaling Regulates Glioblastoma Stem Cells. *Cancer Res.* 72, 3828–3838. doi:10.1158/0008-5472.CAN-11-3760
- Keller, S., and Schmidt, M. (2017). EGFR and EGFRvIII Promote Angiogenesis and Cell Invasion in Glioblastoma: Combination Therapies for an Effective Treatment. *Ijms* 18, 1295. doi:10.3390/ijms18061295
- Koka, V., Potti, A., Forseen, S. E., Pervez, H., Fraiman, G. N., Koch, M., et al. (2003). Role of Her-2/neu Overexpression and Clinical Determinants of Early Mortality in Glioblastoma Multiforme. *Am. J. Clin. Oncol.* 26, 332–335. doi:10.1097/01.COC.0000020922.66984.E7
- Kurozumi, K., Hardcastle, J., Thakur, R., Yang, M., Christoforidis, G., Fulci, G., et al. (2007). Effect of Tumor Microenvironment Modulation on the Efficacy of Oncolytic Virus Therapy. *J. Natl. Cancer Inst.* 99, 1768–1781. doi:10.1093/jnci/djm229
- Lei, N., Shen, F. B., Chang, J. H., Wang, L., Li, H., Yang, C., et al. (2009). An Oncolytic Adenovirus Expressing Granulocyte Macrophage colony-stimulating

- Factor Shows Improved Specificity and Efficacy for Treating Human Solid Tumors. *Cancer Gene Ther.* 16, 33–43. doi:10.1038/cgt.2008.46
- Litak, J., Mazurek, M., Grochowski, C., Kamieniak, P., and Roliński, J. (2019). PD-L1/PD-1 Axis in Glioblastoma Multiforme. *Ijms* 20, 5347. doi:10.3390/ijms20215347
- Liu, F., Hon, G. C., Villa, G. R., Turner, K. M., Ikegami, S., Yang, H., et al. (2015). EGFR Mutation Promotes Glioblastoma through Epigenome and Transcription Factor Network Remodeling. *Mol. Cell* 60, 307–318. doi:10.1016/j.molcel.2015.09.002
- Liu, F., Huang, J., Liu, X., Cheng, Q., Luo, C., and Liu, Z. (2020). CTLA-4 Correlates with Immune and Clinical Characteristics of Glioma. *Cancer Cell Int* 20, 7. doi:10.1186/s12935-019-1085-6
- Liu, G., Ying, H., Zeng, G., Wheeler, C. J., Black, K. L., and Yu, J. S. (2004). HER-2, Gp100, and MAGE-1 Are Expressed in Human Glioblastoma and Recognized by Cytotoxic T Cells. *Cancer Res.* 64, 4980–4986. doi:10.1158/0008-5472.CAN-03-3504
- Liu, S., Liu, F., Zhao, M., and Zhang, J. (2020a). Antitumor Efficacy of Oncolytic Herpes Virus Type 1 Armed with GM-CSF in Murine Uveal Melanoma Xenografts. *Cmar* 12, 11803–11812. doi:10.2147/CMAR.S274605
- Liu, S., Zhang, J., Fang, S., Su, X., Zhang, Q., Zhu, G., et al. (2020b). Antitumor Efficacy of Oncolytic HSV-1 Expressing Cytosine Deaminase Is Synergistically Enhanced by DPD Down-Regulation and EMT Inhibition in Uveal Melanoma Xenograft. *Cancer Lett.* 495, 123–134. doi:10.1016/j.canlet.2020.09.013
- Liu, S., Zhang, J., Fang, S., Zhang, Q., Zhu, G., Tian, Y., et al. (2021). Macrophage Polarization Contributes to the Efficacy of an Oncolytic HSV-1 Targeting Human Uveal Melanoma in a Murine Xenograft Model. *Exp. Eye Res.* 202, 108285. doi:10.1016/j.exer.2020.108285
- Lun, X., Chan, J., Zhou, H., Sun, B., Kelly, J. J., Stechishin, O. O., et al. (2010). Efficacy and Safety/toxicity Study of Recombinant Vaccinia Virus JX-594 in Two Immunocompetent Animal Models of Glioma. *Mol. Ther.* 18, 1927–1936. doi:10.1038/mt.2010.183
- Lun, X., Yang, W., Alain, T., Shi, Z.-Q., Muzik, H., Barrett, J. W., et al. (2005). Myxoma Virus Is a Novel Oncolytic Virus with Significant Antitumor Activity against Experimental Human Gliomas. *Cancer Res.* 65, 9982–9990. doi:10.1158/0008-5472.Can-05-1201
- Martikainen, M., and Essand, M. (2019). Virus-Based Immunotherapy of Glioblastoma. *Cancers* 11, 186. doi:10.3390/cancers11020186
- Martínez-Vélez, N., García-Moure, M., Marigil, M., González-Huarriz, M., Puigdelloses, M., Gallego Pérez-Larraya, J., et al. (2019). The Oncolytic Virus Delta-24-RGD Elicits an Antitumor Effect in Pediatric Glioma and DIPG Mouse Models. *Nat. Commun.* 10, 2235. doi:10.1038/s41467-019-10043-0
- Meng, X., Duan, C., Pang, H., Chen, Q., Han, B., Zha, C., et al. (2019). DNA Damage Repair Alterations Modulate M2 Polarization of Microglia to Remodel the Tumor Microenvironment via the P53-Mediated MDK Expression in Glioma. *EBioMedicine* 41, 185–199. doi:10.1016/j.ebiom.2019.01.067
- Moesta, A. K., Cooke, K., Piasecki, J., Mitchell, P., Rottman, J. B., Fitzgerald, K., et al. (2017). Local Delivery of OncoVEXmGM-CSF Generates Systemic Antitumor Immune Responses Enhanced by Cytotoxic T-Lymphocyte-Associated Protein Blockade. *Clin. Cancer Res.* 23, 6190–6202. doi:10.1158/1078-0432.CCR-17-0681
- Moncayo, G., Grzmil, M., Smirnova, T., Zmarz, P., Huber, R. M., Hynx, D., et al. (2018). SYK Inhibition Blocks Proliferation and Migration of Glioma Cells and Modifies the Tumor Microenvironment. *Neuro Oncol.* 20, 621–631. doi:10.1093/neuonc/noy008
- Nduom, E. K., Wei, J., Yaghi, N. K., Huang, N., Kong, L.-Y., Gabrusiewicz, K., et al. (2016). PD-L1 Expression and Prognostic Impact in Glioblastoma. *Neuro Oncol.* 18, 195–205. doi:10.1093/neuonc/nov172
- Nehama, D., Di Ianni, N., Musio, S., Du, H., Patané, M., Pollo, B., et al. (2019). B7-H3-redirected Chimeric Antigen Receptor T Cells Target Glioblastoma and Neurospheres. *EBioMedicine* 47, 33–43. doi:10.1016/j.ebiom.2019.08.030
- O'Rourke, D. M., Nasrallah, M. P., Desai, A., Melenhorst, J. J., Mansfield, K., Morrisette, J. J. D., et al. (2017). A Single Dose of Peripherally Infused EGFRvIII-Directed CAR T Cells Mediates Antigen Loss and Induces Adaptive Resistance in Patients with Recurrent Glioblastoma. *Sci. Transl. Med.* 9, eaaa0984. doi:10.1126/scitranslmed.aaa0984
- Ozawa, T., Brennan, C. W., Wang, L., Squatrito, M., Sasayama, T., Nakada, M., et al. (2010). PDGFRA Gene Rearrangements Are Frequent Genetic Events in PDGFRA-Amplified Glioblastomas. *Genes Dev.* 24, 2205–2218. doi:10.1101/gad.1972310
- Park, A. K., Fong, Y., Kim, S.-I., Yang, J., Murad, J. P., Lu, J., et al. (2020). Effective Combination Immunotherapy Using Oncolytic Viruses to Deliver CAR Targets to Solid Tumors. *Sci. Transl. Med.* 12, eaaz1863. doi:10.1126/scitranslmed.aaz1863
- Phillips, J. J., Aranda, D., Ellison, D. W., Judkins, A. R., Croul, S. E., Brat, D. J., et al. (2013). PDGFRA Amplification Is Common in Pediatric and Adult High-Grade Astrocytomas and Identifies a Poor Prognostic Group in IDH1 Mutant Glioblastoma. *Brain Pathol.* 23, 565–573. doi:10.1111/bpa.12043
- Picarda, E., Ohaegbulam, K. C., and Zang, X. (2016). Molecular Pathways: Targeting B7-H3 (CD276) for Human Cancer Immunotherapy. *Clin. Cancer Res.* 22, 3425–3431. doi:10.1158/1078-0432.CCR-15-2428
- Pituch, K. C., Miska, J., Krenciute, G., Panek, W. K., Li, G., Rodriguez-Cruz, T., et al. (2018). Adoptive Transfer of IL13Ra2-Specific Chimeric Antigen Receptor T Cells Creates a Pro-inflammatory Environment in Glioblastoma. *Mol. Ther.* 26, 986–995. doi:10.1016/j.ymthe.2018.02.001
- Rahaman, S. O., Sharma, P., Harbor, P. C., Aman, M. J., Vogelbaum, M. A., and Haque, S. J. (2002). IL-13R(alpha)2, a Decoy Receptor for IL-13 Acts as an Inhibitor of IL-4-dependent Signal Transduction in Glioblastoma Cells. *Cancer Res.* 62, 1103–1109.
- Saha, D., Martuza, R. L., and Rabkin, S. D. (2017). Macrophage Polarization Contributes to Glioblastoma Eradication by Combination Immunovirotherapy and Immune Checkpoint Blockade. *Cancer Cell* 32, 253–267.e5. doi:10.1016/j.ccell.2017.07.006
- Saha, D., Martuza, R. L., and Rabkin, S. D. (2018). Oncolytic Herpes Simplex Virus Immunovirotherapy in Combination with Immune Checkpoint Blockade to Treat Glioblastoma. *Immunotherapy* 10, 779–786. doi:10.2217/imt-2018-0009
- Samaha, H., Pignata, A., Fousek, K., Ren, J., Lam, F. W., Stossi, F., et al. (2018). A Homing System Targets Therapeutic T Cells to Brain Cancer. *Nature* 561, 331–337. doi:10.1038/s41586-018-0499-y
- Schlegel, J. r., Stumm, G., Brändle, K., Merdes, A., Mechttersheimer, G., Hynes, N. E., et al. (1994). Amplification and Differential Expression of Members of theerbB-Gene Family in Human Glioblastoma. *J. Neuro-oncol* 22, 201–207. doi:10.1007/BF01052920
- Schneider, J. R., Kwan, K., and Boockvar, J. A. (2017). Use of HER2-specific Chimeric Antigen Receptor-Modified Virus-specific T Cells as a Potential Therapeutic for Progressive HER2-Positive Glioblastoma. *Neurosurgery* 81, N42–N43. doi:10.1093/neuros/nyx449
- Schönfeld, K., Sahm, C., Zhang, C., Naundorf, S., Brendel, C., Odendahl, M., et al. (2015). Selective Inhibition of Tumor Growth by Clonal NK Cells Expressing an ErbB2/HER2-specific Chimeric Antigen Receptor. *Mol. Ther.* 23, 330–338. doi:10.1038/mt.2014.219
- Sharpe, A. H., and Pauken, K. E. (2018). The Diverse Functions of the PD1 Inhibitory Pathway. *Nat. Rev. Immunol.* 18, 153–167. doi:10.1038/nri.2017.108
- Silber, J., Jacobsen, A., Ozawa, T., Harinath, G., Pedraza, A., Sander, C., et al. (2012). miR-34a Repression in Proneural Malignant Gliomas Upregulates Expression of its Target PDGFRA and Promotes Tumorigenesis. *PloS one* 7, e33844. doi:10.1371/journal.pone.0033844
- Song, Y., Liu, Q., Zuo, T., Wei, G., and Jiao, S. (2020). Combined Antitumor Effects of Anti-EGFR Variant III CAR-T Cell Therapy and PD-1 Checkpoint Blockade on Glioblastoma in Mouse Model. *Cell Immunol.* 352, 104112. doi:10.1016/j.cellimm.2020.104112
- Stephenson, K. B., Barra, N. G., Davies, E., Ashkar, A. A., and Lichty, B. D. (2012). Expressing Human Interleukin-15 from Oncolytic Vesicular Stomatitis Virus Improves Survival in a Murine Metastatic colon Adenocarcinoma Model through the Enhancement of Anti-tumor Immunity. *Cancer Gene Ther.* 19, 238–246. doi:10.1038/cgt.2011.81
- Tang, X., Zhao, S., Zhang, Y., Wang, Y., Zhang, Z., Yang, M., et al. (2019). B7-H3 as a Novel CAR-T Therapeutic Target for Glioblastoma. *Mol. Ther. - Oncolytics* 14, 279–287. doi:10.1016/j.omto.2019.07.002
- Tchou, J., Zhao, Y., Levine, B. L., Zhang, P. J., Davis, M. M., Melenhorst, J. J., et al. (2017). Safety and Efficacy of Intratumoral Injections of Chimeric Antigen Receptor (CAR) T Cells in Metastatic Breast Cancer. *Cancer Immunol. Res.* 5, 1152–1161. doi:10.1158/2326-6066.CIR-17-0189
- Thaci, B., Brown, C. E., Binello, E., Werbaneth, K., Sampath, P., and Sengupta, S. (2014). Significance of Interleukin-13 Receptor Alpha 2-targeted Glioblastoma Therapy. *Neuro-Oncology* 16, 1304–1312. doi:10.1093/neuonc/nou045

- Thistlethwaite, F. C., Gilham, D. E., Guest, R. D., Rothwell, D. G., Pillai, M., Burt, D. J., et al. (2017). The Clinical Efficacy of First-Generation Carcinoembryonic Antigen (CEACAM5)-specific CAR T Cells Is Limited by Poor Persistence and Transient Pre-conditioning-dependent Respiratory Toxicity. *Cancer Immunol. Immunother.* 66, 1425–1436. doi:10.1007/s00262-017-2034-7
- Wang, Q., Hu, B., Hu, X., Kim, H., Squatrito, M., Scarpacci, L., et al. (2017). Tumor Evolution of Glioma-Intrinsic Gene Expression Subtypes Associates with Immunological Changes in the Microenvironment. *Cancer Cell* 32, 42–56.e6. doi:10.1016/j.ccell.2017.06.003
- Wang, X., Guo, G., Guan, H., Yu, Y., Lu, J., and Yu, J. (2019). Challenges and Potential of PD-1/pd-L1 Checkpoint Blockade Immunotherapy for Glioblastoma. *J. Exp. Clin. Cancer Res.* 38, 87. doi:10.1186/s13046-019-1085-3
- Wang, Z., Wang, Z., Zhang, C., Liu, X., Li, G., Liu, S., et al. (2018). Genetic and Clinical Characterization of B7-H3 (CD276) Expression and Epigenetic Regulation in Diffuse Brain Glioma. *Cancer Sci.* 109, 2697–2705. doi:10.1111/cas.13744
- Weiss, T., Schneider, H., Silginer, M., Steinle, A., Pruschy, M., Polić, B., et al. (2018a). NKG2D-Dependent Antitumor Effects of Chemotherapy and Radiotherapy against Glioblastoma. *Clin. Cancer Res.* 24, 882–895. doi:10.1158/1078-0432.CCR-17-1766
- Weiss, T., Weller, M., Guckenberger, M., Sentman, C. L., and Roth, P. (2018b). NKG2D-Based CAR T Cells and Radiotherapy Exert Synergistic Efficacy in Glioblastoma. *Cancer Res.* 78, 1031–1043. doi:10.1158/0008-5472.CAN-17-1788
- Wiencke, J. K., Zheng, S., Jelluma, N., Tihan, T., Vandenberg, S., Tamgüney, T., et al. (2007). Methylation of the PTEN Promoter Defines Low-Grade Gliomas and Secondary Glioblastoma. *Neuro Oncol.* 9, 271–279. doi:10.1215/15228517-2007-003
- Xie, T., Liu, B., Dai, C.-G., Lu, Z.-H., Dong, J., and Huang, Q. (2019). Glioma Stem Cells Reconstruct Similar Immunoinflammatory Microenvironment in Different Transplant Sites and Induce Malignant Transformation of Tumor Microenvironment Cells. *J. Cancer Res. Clin. Oncol.* 145, 321–328. doi:10.1007/s00432-018-2786-2
- Yang, D., Sun, B., Dai, H., Li, W., Shi, L., Zhang, P., et al. (2019). T Cells Expressing NKG2D Chimeric Antigen Receptors Efficiently Eliminate Glioblastoma and Cancer Stem Cells. *J. Immunotherapy Cancer* 7, 171. doi:10.1186/s40425-019-0642-9
- Yang, J., Yan, J., and Liu, B. (2017). Targeting EGFRvIII for Glioblastoma Multiforme. *Cancer Lett.* 403, 224–230. doi:10.1016/j.canlet.2017.06.024
- Yang, M., Tang, X., Zhang, Z., Gu, L., Wei, H., Zhao, S., et al. (2020). Tandem CAR-T Cells Targeting CD70 and B7-H3 Exhibit Potent Preclinical Activity against Multiple Solid Tumors. *Theranostics* 10, 7622–7634. doi:10.7150/thno.43991
- Zamarin, D., Ricca, J. M., Sadekova, S., Oseledchik, A., Yu, Y., Blumenschein, W. M., et al. (2018). PD-L1 in Tumor Microenvironment Mediates Resistance to Oncolytic Immunotherapy. *J. Clin. Invest.* 128, 1413–1428. doi:10.1172/JCI98047
- Zhang, C., Burger, M. C., Jennewein, L., Genssler, S., Schönfeld, K., Zeiner, P., et al. (2016). ErbB2/HER2-Specific NK Cells for Targeted Therapy of Glioblastoma. *J. Natl. Cancer Inst.* 108. doi:10.1093/jnci/djv375
- Zhang, C., Wang, Z., Yang, Z., Wang, M., Li, S., Li, Y., et al. (2017). Phase I Escalating-Dose Trial of CAR-T Therapy Targeting CEA + Metastatic Colorectal Cancers. *Mol. Ther.* 25, 1248–1258. doi:10.1016/j.jymthe.2017.03.010
- Zhang, C., Zhang, Z., Li, F., Shen, Z., Qiao, Y., Li, L., et al. (2018). Large-scale Analysis Reveals the Specific Clinical and Immune Features of B7-H3 in Glioma. *Oncoimmunology* 7, e1461304. doi:10.1080/2162402X.2018.1461304
- Zhang, J., Fang, S., Song, W., Zhang, B., Fan, W., Jin, G., et al. (2020). Biological Characterization and Therapeutics for Subscalp Recurrent in Intracranial Glioblastoma. *Ott* 13, 9085–9099. doi:10.2147/ott.s265322
- Zhang, Q., and Liu, F. (2020). Advances and Potential Pitfalls of Oncolytic Viruses Expressing Immunomodulatory Transgene Therapy for Malignant Gliomas. *Cell Death Dis.* 11, 485. doi:10.1038/s41419-020-2696-5
- Zhang, Q., Xiang, W., Yi, D.-y., Xue, B.-z., Wen, W.-w., Abdelmaksoud, A., et al. (2018). Current Status and Potential Challenges of Mesenchymal Stem Cell-Based Therapy for Malignant Gliomas. *Stem Cell Res. Ther.* 9, 228. doi:10.1186/s13287-018-0977-z
- Zhang, Q., Zhang, J., Tian, Y., Zhu, G., Liu, S., and Liu, F. (2020). Efficacy of a Novel Double-Controlled Oncolytic Adenovirus Driven by the Ki67 Core Promoter and Armed with IL-15 against Glioblastoma Cells. *Cell Biosci* 10, 124. doi:10.1186/s13578-020-00485-1
- Zhang, W., Zhang, C., Tian, W., Qin, J., Chen, J., Zhang, Q., et al. (2020). Efficacy of an Oncolytic Adenovirus Driven by a Chimeric Promoter and Armed with Decorin against Renal Cell Carcinoma. *Hum. Gene Ther.* 31, 651–663. doi:10.1089/hum.2019.352
- Zheng, Y., Gao, N., Fu, Y.-L., Zhang, B.-Y., Li, X.-L., Gupta, P., et al. (2018). Generation of Regulable EGFRvIII Targeted Chimeric Antigen Receptor T Cells for Adoptive Cell Therapy of Glioblastoma. *Biochem. Biophysical Res. Commun.* 507, 59–66. doi:10.1016/j.bbrc.2018.10.151
- Zhong, C., Tao, B., Chen, Y., Guo, Z., Yang, X., Peng, L., et al. (2020). B7-H3 Regulates Glioma Growth and Cell Invasion through a JAK2/STAT3/Slug-dependent Signaling Pathway. *Ott* 13, 2215–2224. doi:10.2147/OTT.S237841
- Zhu, H., You, Y., Shen, Z., and Shi, L. (2020a). EGFRvIII-CAR-T Cells with PD-1 Knockout Have Improved Anti-glioma Activity. *Pathol. Oncol. Res.* 26, 2135–2141. doi:10.1007/s12253-019-00759-1
- Zhu, H., You, Y., Shen, Z., and Shi, L. (2020b). EGFRvIII-CAR-T Cells with PD-1 Knockout Have Improved Anti-glioma Activity. *Pathol. Oncol. Res.* 26, 2135–2141. doi:10.1007/s12253-019-00759-1
- Zhu, Y., Guignard, F., Zhao, D., Liu, L., Burns, D. K., Mason, R. P., et al. (2005). Early Inactivation of P53 Tumor Suppressor Gene Cooperating with NF1 Loss Induces Malignant Astrocytoma. *Cancer Cell* 8, 119–130. doi:10.1016/j.ccr.2005.07.004

Conflict of Interest: The authors declare that the research was conducted in the absence of any commercial or financial relationships that could be construed as a potential conflict of interest.

Copyright © 2021 Zhu, Zhang, Zhang and Liu. This is an open-access article distributed under the terms of the Creative Commons Attribution License (CC BY). The use, distribution or reproduction in other forums is permitted, provided the original author(s) and the copyright owner(s) are credited and that the original publication in this journal is cited, in accordance with accepted academic practice. No use, distribution or reproduction is permitted which does not comply with these terms.



Systems Pharmacology–Based Dissection of Anti-Cancer Mechanism of Traditional Chinese Herb *Saussurea involucrata*

OPEN ACCESS

Edited by:

Zhi-xiang Yuan,
Southwest Minzu University, China

Reviewed by:

Qilong Chen,
Independent Researcher, Shanghai,
China
Xiaoxia Liang,
Sichuan Agricultural University, China

*Correspondence:

Hongtao Deng
denghtshzu@163.com
Yaxin Zheng
zhengyaxinxyz@163.com
Xue Ying
yingxueshzu@163.com

[†]These authors have contributed
equally to this work and share first
authorship

Specialty section:

This article was submitted to
Pharmacology of Anti-Cancer Drugs,
a section of the journal
Frontiers in Pharmacology

Received: 09 March 2021

Accepted: 26 May 2021

Published: 25 June 2021

Citation:

Zhang Q, He L, Jiang Q, Zhu H,
Kong D, Zhang H, Cheng Z, Deng H,
Zheng Y and Ying X (2021) Systems
Pharmacology–Based Dissection of
Anti-Cancer Mechanism of Traditional
Chinese Herb *Saussurea involucrata*.
Front. Pharmacol. 12:678203.
doi: 10.3389/fphar.2021.678203

Qian Zhang^{1†}, Lanyu He^{1†}, Qingqing Jiang¹, Hongqing Zhu², Dehua Kong², Hua Zhang¹, Zhiqiang Cheng³, Hongtao Deng^{1*}, Yaxin Zheng^{2*} and Xue Ying^{1,2*}

¹School of Pharmacy/Key Laboratory of Xinjiang Phytomedicine Resources and Utilization, Ministry of Education, Shihezi University, Xinjiang, China, ²School of Pharmaceutical Sciences/Key Laboratory of Sichuan Province for Specific Structure of Small Molecule Drugs, Chengdu Medical College, Chengdu, China, ³Department of Pharmacology and Molecular Sciences, Johns Hopkins School of Medicine, Baltimore, MD, United States

Cancer has the highest mortality in humans worldwide, and the development of effective drugs remains a key issue. Traditional Chinese medicine *Saussurea involucrata* (SI) exhibits a series of effects, such as anti-cancer, but the action mechanisms are still unclear. Here, systems pharmacology was applied to reveal its anti-cancer mechanism. First, we screened the active compounds of SI. Then, the compound–target network, target–disease network, and target–pathway network were constructed. DAVID was applied for GOBP analysis and KEGG pathway enrichment analysis on cancer-related targets. Seven potential compounds and 187 targets were identified. The target–disease classification network showed that compounds mainly regulated proteins related to cancer, nervous system diseases, and cardiovascular system diseases. Also, SI anti-tumor effect mainly associated with the regulation of NO production, angiogenesis, MAPK, and PKB from GOBP enrichment. Additionally, KEGG pathway enrichment indicated that targets involved in anti-inflammatory action, inhibiting angiogenesis and anti-proliferation or inducing apoptosis. Experimental validation showed that four active compounds could inhibit cell proliferation and promote apoptosis in A549 (except for kaempferol), PC-3, and C6 cells. This study not only provides experimental evidence for further research on SI in cancer treatment but also promotes the development of potential drugs of SI in modern medicine.

Keywords: systems pharmacology, *Saussurea involucrata*, cancer, action mechanism, active compounds

Abbreviations: DAVID, the Database for Annotation, Visualization and Integrated Discovery; DL, drug likeness; GO, Gene Ontology; KEGG, Kyoto Encyclopedia of Genes and Genomes; OB, oral bioavailability; PTGS2, prostaglandin G/H synthase 2; PGI2, prostaglandin I2; SI, *Saussurea involucrata*; TCM, traditional Chinese medicine; TCMSP, Traditional Chinese Medicine Systems Pharmacology Database; TNFR1, tumor necrosis factor receptor 1.

INTRODUCTION

Cancer has become one of the major diseases that threaten human health globally (Siegel et al., 2020) and brought a huge economic burden to the world until now. According to the statistics, lung cancer is a leading cause of cancer death with the highest morbidity and on the rise gradually. Breast cancer, prostate cancer, and colorectal cancer are next only to lung cancer (Bray et al., 2018). Currently, conventional cancer treatment is the combination of surgery, radiotherapy, and chemotherapy. As one of the main methods, chemotherapy is indispensable in cancer treatment, but the serious adverse effects of chemotherapeutic drugs limit its further development and application (Zhai et al., 2019). Facing such situations, it is urgently necessary to explore effective drugs and study new therapies. In recent years, traditional Chinese medicine (TCM) is rich in various chemical components and can regulate multiple cancer-related signaling pathways and targets. Besides, it has the advantages of alleviating side effects, providing high safety, and prolonging the survival time of patients (Liu Y. T. et al., 2019; Ma et al., 2019). Consequently, TCM plays an increasingly important role in the process of new anti-cancer drug research. And it is increasingly beneficial to apply TCM for cancer treatment.

Saussurea involucrata Kar. et Kir. (SI) is a perennial herbaceous plant that is distributed in high altitude areas of Xinjiang, China (Guo et al., 2019). In traditional Chinese medicine theory, SI has the functions of dispersing cold and removing dampness, activating blood circulation to promote menstruation, strengthening the bones and muscles, warming the kidney, restoring yang, etc. SI is already used for the symptoms of cough due to lung cold, wind-cold-dampness arthralgia, rheumatoid arthritis, and irregular menstruation (Gong et al., 2020b). In modern pharmacology, SI has multiple pharmacological effects such as anti-oxidant, anti-fatigue, analgesic, anti-inflammatory (Wang et al., 2018), and anti-tumor (breast cancer, prostate cancer, etc.) (Gong et al., 2020a), most of which are closely related to its traditional usage. Recently, researchers turned their attention to the anti-tumor effect of SI. However, there are few studies on the connection between specific chemical components and anti-tumor activity. The relationship among active components, potential targets, and related pathways of SI has not been systematically explored.

Confronting with such issues, it is particularly needful to investigate the action mechanism of SI by systems pharmacology. Systems pharmacology (Chen et al., 2018; LUO et al., 2018) is an emerging discipline that can be used as a powerful method for the systematic research on SI. And systems pharmacology breaks the traditional framework of “one drug, one target, one disease” and integrates multi-disciplinary technology and content such as system biology, computational biology, and network topology. Meanwhile, systems pharmacology constructs a multi-level network and systematically explores the relationship between drugs and diseases from an overall perspective. For this reason, it is of great significance to clarify the complex mechanism of traditional Chinese medicine (Zheng et al., 2016).

In this study, active compounds of SI were screened by systems pharmacology. Then, the compound–target network,

target–disease network, and target–pathway network were constructed through the data obtained above. Furthermore, Gene Ontology analysis and KEGG pathway enrichment analysis were applied to analyze the anti-cancer molecular mechanism of SI molecules. Finally, *in vitro* experimental validation proved the regulation of targets by several important compounds (as shown in Figure 1).

MATERIALS AND METHODS

The Screening of Active Compounds of *Saussurea involucrata*

In this study, the Traditional Chinese Medicine Systems Pharmacology Database (TCMSP, <http://lsp.nwu.edu.cn/tcmsp.php>) was employed to summarize the chemical constituents of *Saussurea involucrata*. Then, drug likeness (DL) and oral bioavailability (OB) were adopted for obtaining active compounds with the keywords of “*Saussurea involucrata*.”

Drug likeness (DL) refers to a molecule that contains specific functional groups and/or has physical characteristics consistent with most of the drugs. In the early stages of drug development, DL was widely used to screen leading compounds (Hu et al., 2018). In order to calculate the drug likeness of these compounds, the Tanimoto coefficient and molecular descriptors were utilized in this database. The formula is as follows:

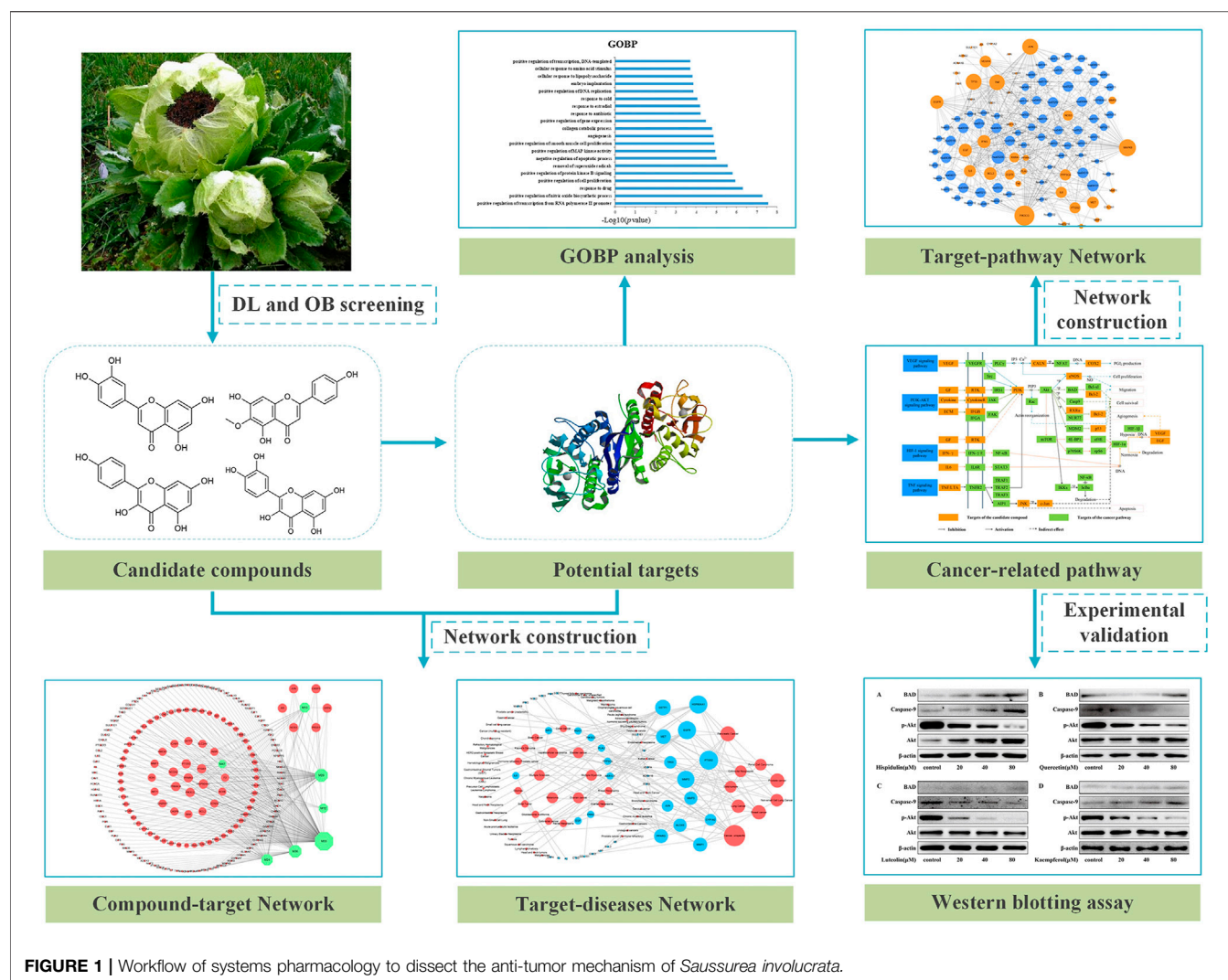
$$T(X, Y) = \frac{x \cdot y}{|x|^2 + |y|^2 - x \cdot y}, \quad (1)$$

where x is the molecular descriptor index of SI that is calculated by Dragon and y is defined as the average drug likeness index of all compound descriptors in the DrugBank database. The threshold of the DL value is determined by DrugBank's average DL value (0.18). Therefore, the active compounds of *Saussurea involucrata* were screened with $DL \geq 0.18$ in this study.

Oral bioavailability (OB) is the relative amount of a drug absorbed into the circulatory system through extravascular administration. OB is one of the vital indicators to reflect drug efficacy (Yang et al., 2020). In general, drugs with poor oral bioavailability might not be able to reach the minimum effective concentration to achieve therapeutic effect even if they have a strong effect on pharmacological targets *in vitro* (Aungst, 2017). So, compounds with $OB \geq 30\%$ were utilized for subsequent analysis in this work.

Construction of Compound–Target Network and Target–Disease Network

After the screening procedure mentioned above, seven active compound–related targets were obtained from the TCMSP. And UniProt (<https://www.uniprot.org/>) was utilized to convert targets into corresponding genes and defined the species as “human.” In order to further analyze the complex relationship between compounds, targets, and diseases, Cytoscape 3.7.1 (Ou et al., 2020) software was used to construct the active compound–target network (C–T network), target–disease



network (T-D network), and target-pathway network (T-P network). The plug-in network analyzer of Cytoscape analyzed the degree, which is a critical parameter of these networks.

Gene Ontology Analysis and KEGG Pathway Enrichment Analysis

For exploring the related biological processes of potential targets, DAVID 6.8 (the Database for Annotation, Visualization and Integrated Discovery, <https://david.ncifcrf.gov/>) was used for Gene Ontology analysis and KEGG pathway enrichment analysis. Firstly, the target gene list was input to DAVID 6.8, which defined the species as “*Homo sapiens*.” Then, the target gene was modified to the “office gene symbol.” Each GO term had a *p*-value, and the threshold $p \leq 0.05$ was set, which indicated that target genes were significantly enriched in this biological process.

Experimental Validation

In vitro experiments were performed to validate the integrated anti-cancer pathway of SI. The cancer target-cancer network

displayed that SI is associated with multiple cancers, including pancreatic cancer, lung cancer, prostate cancer, breast cancer, colorectal cancer, and renal cell cancer. In this study, A549 cells, C6 cells, and PC-3 cells were cultured and treated with various concentrations of four monomeric active compounds separately. And four proteins of Akt, p-Akt, caspase-9, and BAD were selected to verify the integrated pathway.

Cell Culture

Human non-small-cell lung adenocarcinoma A549 cells (Procell Life Science and Technology Co., Ltd., Wuhan, China) were cultured in an RPMI-1640 medium (Gibco, United States) containing 10% fetal bovine serum (Biological Industries, Israel), 100 µg/ml streptomycin, and 100U/mL penicillin (Gibco, United States). The cells were incubated in a saturated humidity incubator (37°C, 5% CO₂) (Thermo Fisher Scientific, United States).

Rat glioma C6 cells and human prostate cancer PC-3 cells (Procell Life Science and Technology Co., Ltd.) were cultured in a DMEM/F12 (Gibco) medium complemented with 10% fetal

TABLE 1 | Information on candidate compounds in *Saussurea involucrata*.

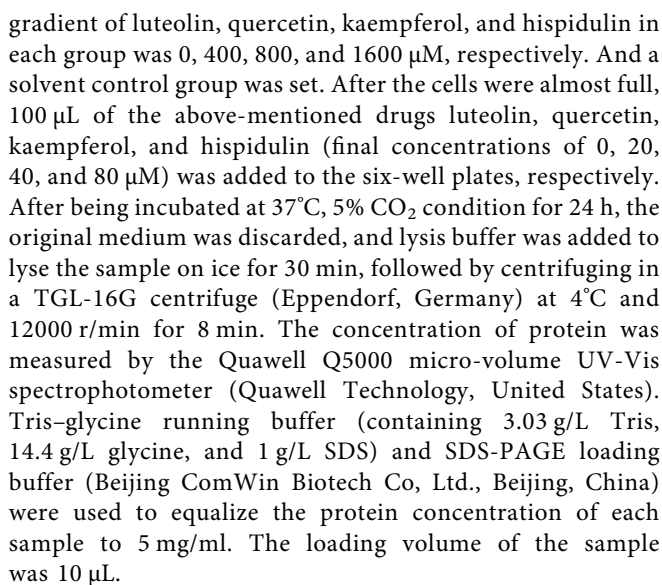
No.	Compounds	Degree	OB	DL	Structure
M10	Hispidulin	17	30.97	0.27	
M12	Alloisioimperatorin	6	34.8	0.22	
M24	β-Sitosterol	36	36.91	0.75	
M29	Kaempferol	60	41.88	0.24	
M36	Luteolin	55	36.16	0.25	
M47	Flazin	3	94.28	0.39	
M55	Quercetin	145	46.43	0.28	

bovine serum, 100 µg/ml streptomycin, and 100 U/mL penicillin and incubated in a saturated humidity incubator.

Cell Protein Extraction

In the logarithmic growth phase, A549, C6, and PC-3 cells (5 × 10⁵/well) were seeded in six-well plates (Corning incorporated Costar, United States), at 1.9 ml per well, and continued to be

cultured at 37°C, 5% CO₂ condition. Then, a series of concentrations of luteolin (Chengdu Biopurify Phytochemicals Co., Ltd., Chengdu, China), quercetin (Chengdu Biopurify Phytochemicals Co., Ltd., Chengdu, China), kaempferol (Chengdu Biopurify Phytochemicals Co., Ltd., Chengdu, China), and hispidulin (Tauto Biotech Co., Ltd., Shanghai, China) solutions were prepared, and the final concentration



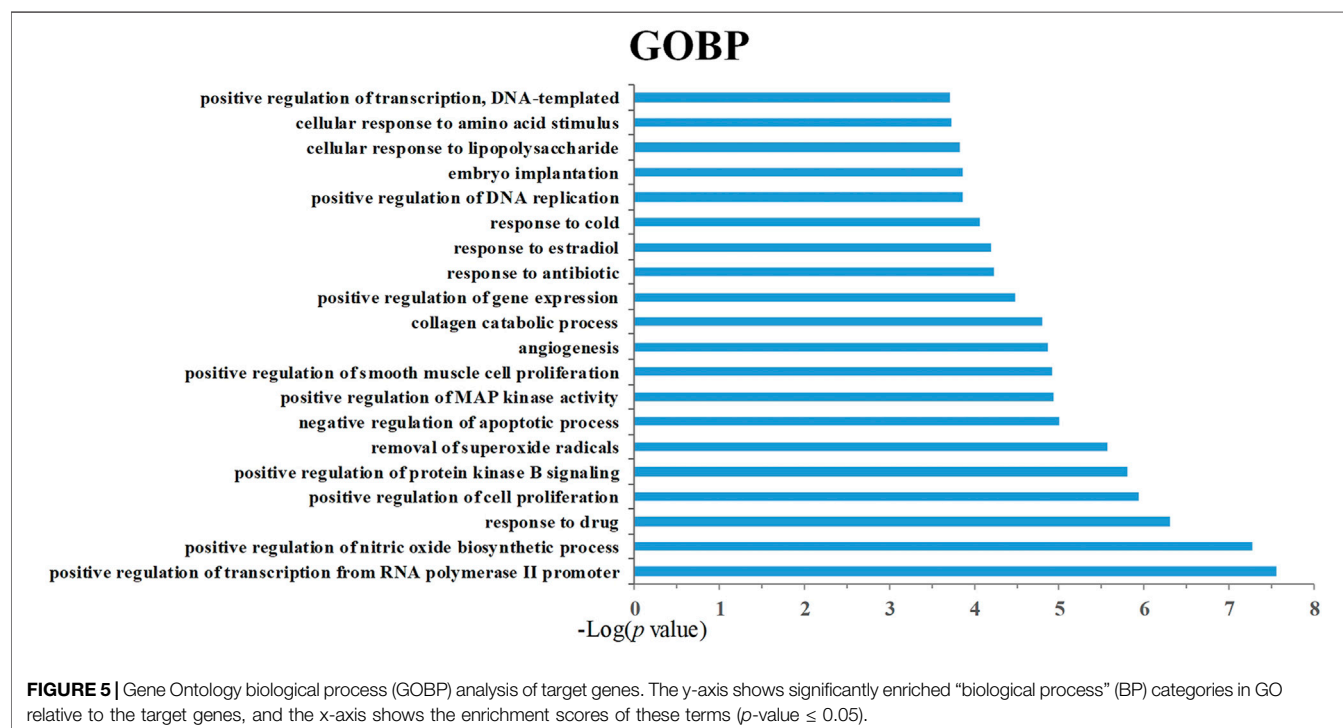
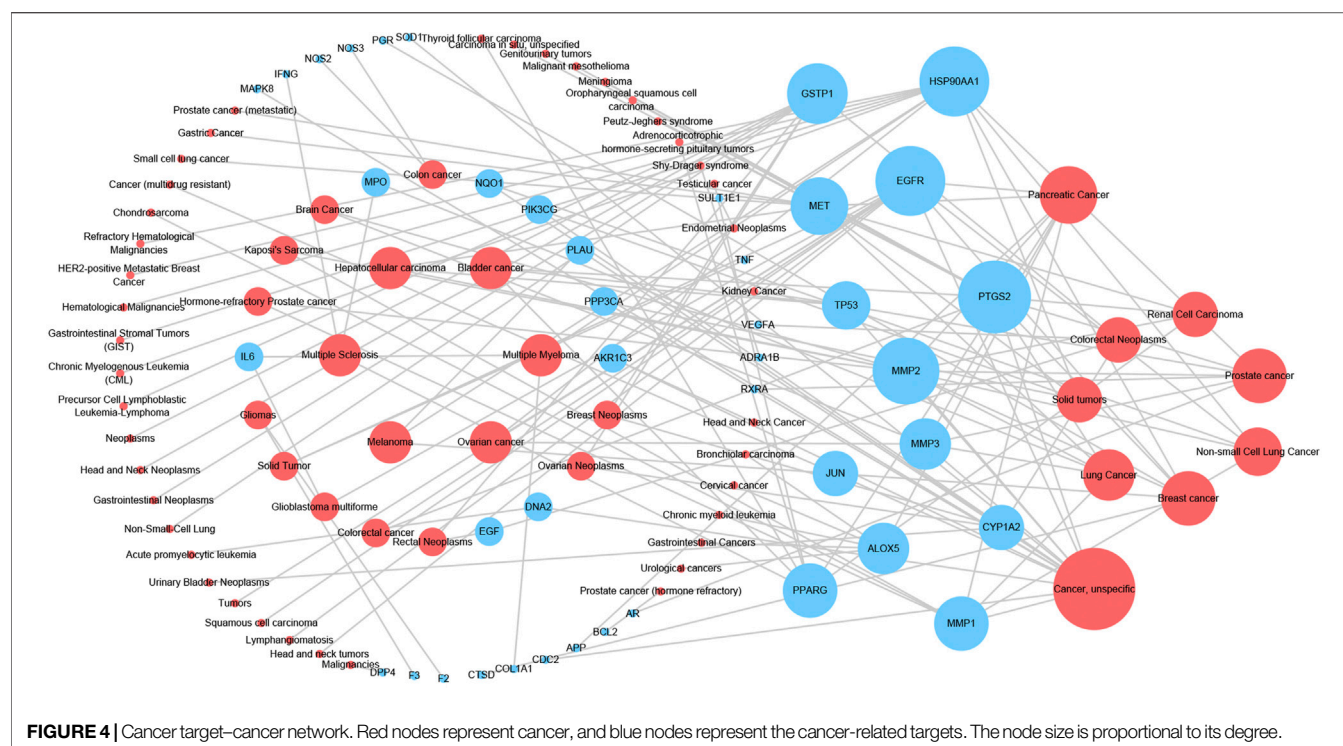
After SDS-PAGE gel electrophoresis, protein bands were transferred to PVDF membranes (Merck Millipore, Germany) in an ice bath. The membranes were blocked in 5% skim milk powder for 1 h at room temperature, washed with TBST four times, and incubated with the primary antibody at 4°C overnight. Then, the membranes were washed with TBST, conjugated with the secondary antibody (1: 10000) at room temperature for 2 h, and then washed with TBST buffer to remove the residual secondary antibody. Akt (Cell Signaling Technology, United States), p-Akt (Cell Signaling Technology), BAD (Abcam, United Kingdom), caspase-9 (Abcam), and β -actin (Beijing Jinqiao Biotechnology Co, Ltd., Beijing, China) were the primary antibodies conjugated with the membranes. The membranes were detected by the SuperSignalTM West Femto Maximum Sensitivity Substrate (Thermo Fisher Scientific) and imaged by the EC3TM 510 Imaging System (Ultra-Violet Products Ltd., Cambridge, United Kingdom). ImageJ software was used for data analysis to semi-quantitate the expression level of protein.



Data are expressed as mean \pm SD. The significance of results was determined based on one-way analysis of variance using Prism 6 (GraphPad, San Diego, CA, United States). $p < 0.05$ was considered significant. All experiments were repeated at least three times.

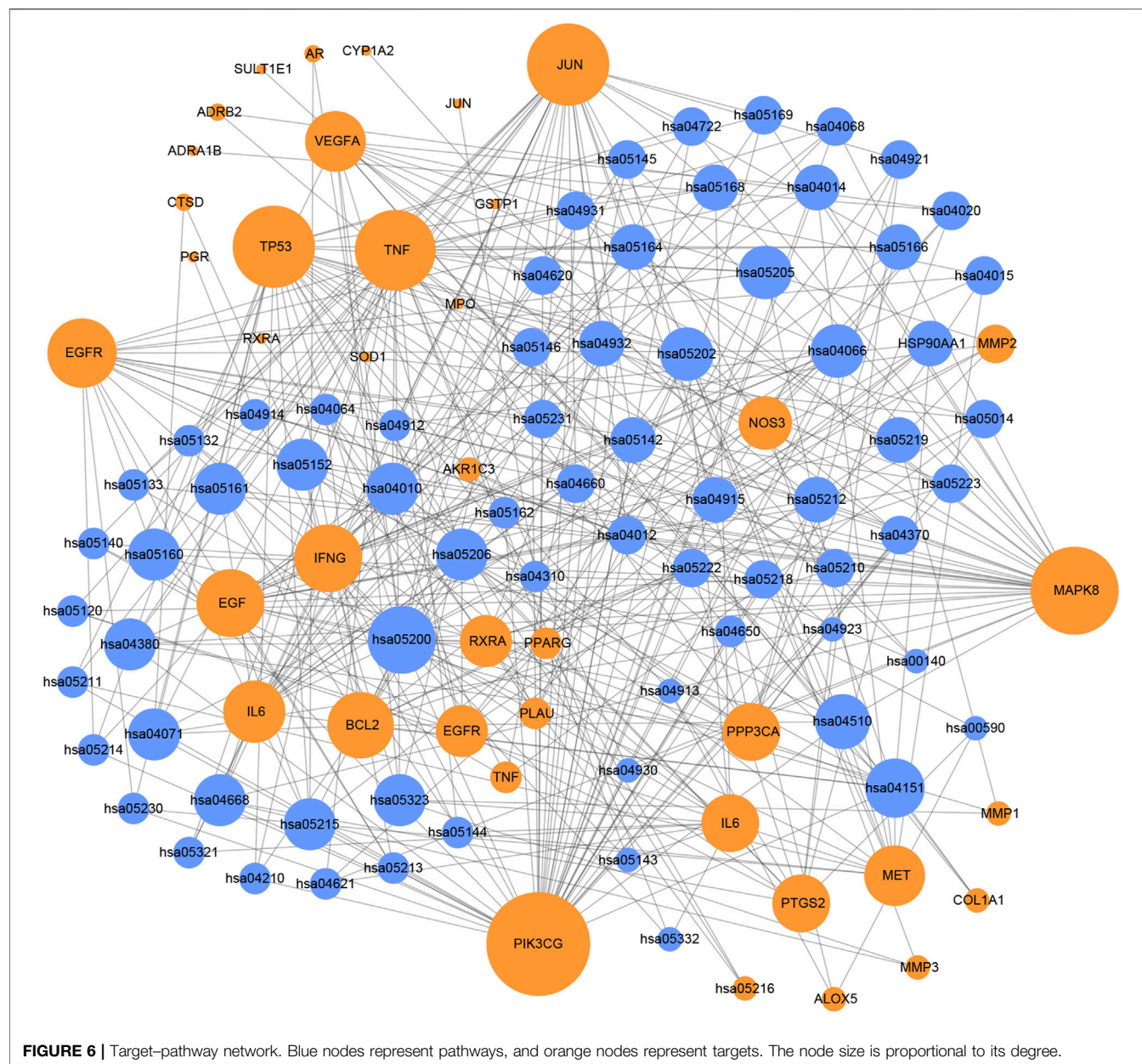
The 55 compounds of SI were collected from the TCMSP, including flavonoids, alkaloids, and sterols. As a result, seven compounds were screened out with the condition of $OB \geq 30\%$ and $DL \geq 0.18$, which were hispidulin, alloisioimperatorin, β -sitosterol, kaempferol, luteolin, flazin, and quercetin. The detailed information on these compounds is shown in **Table 1**.

In this study, compounds' targets were obtained from the TCMSP and UniProt was used to query target information (**Supplementary Table S1**). Then, the C-T network of SI was constructed by Cytoscape 3.7.1 to visualize the interactions between compounds and targets. As shown in **Figure 2**, nodes represent the active compounds and their corresponding targets of SI, while edges represent the relationship between them. Besides, the degree of the node is defined as the number of edges connected to the node, which is proportional to the importance of the node in the network. The C-T network of candidate compounds consists of 194 nodes and 322 edges. Among them, five compounds showed high degree (degree ≥ 10), indicating that they play a key role in the network. At the same time, each active compound is associated with multiple targets, and targets partly are the same. These suggest the multi-target characteristics of the active ingredients and the potential synergistic effects among compounds.



In order to illustrate the action mechanism of SI, the target–disease classification network was constructed based on 95 nodes and 194 edges. As shown in **Figure 3**, active compounds mainly regulate the proteins related to cancer, nervous system diseases, and cardiovascular system diseases. Subsequently, the

cancer target–cancer network was built to deeply explore the relationship between cancer targets and cancer. As shown in **Figure 4**, the average degree of the potential cancer target is 3.38. It is supposed that active compounds vitally have positive effects on pancreatic cancer, lung cancer, prostate cancer, and breast

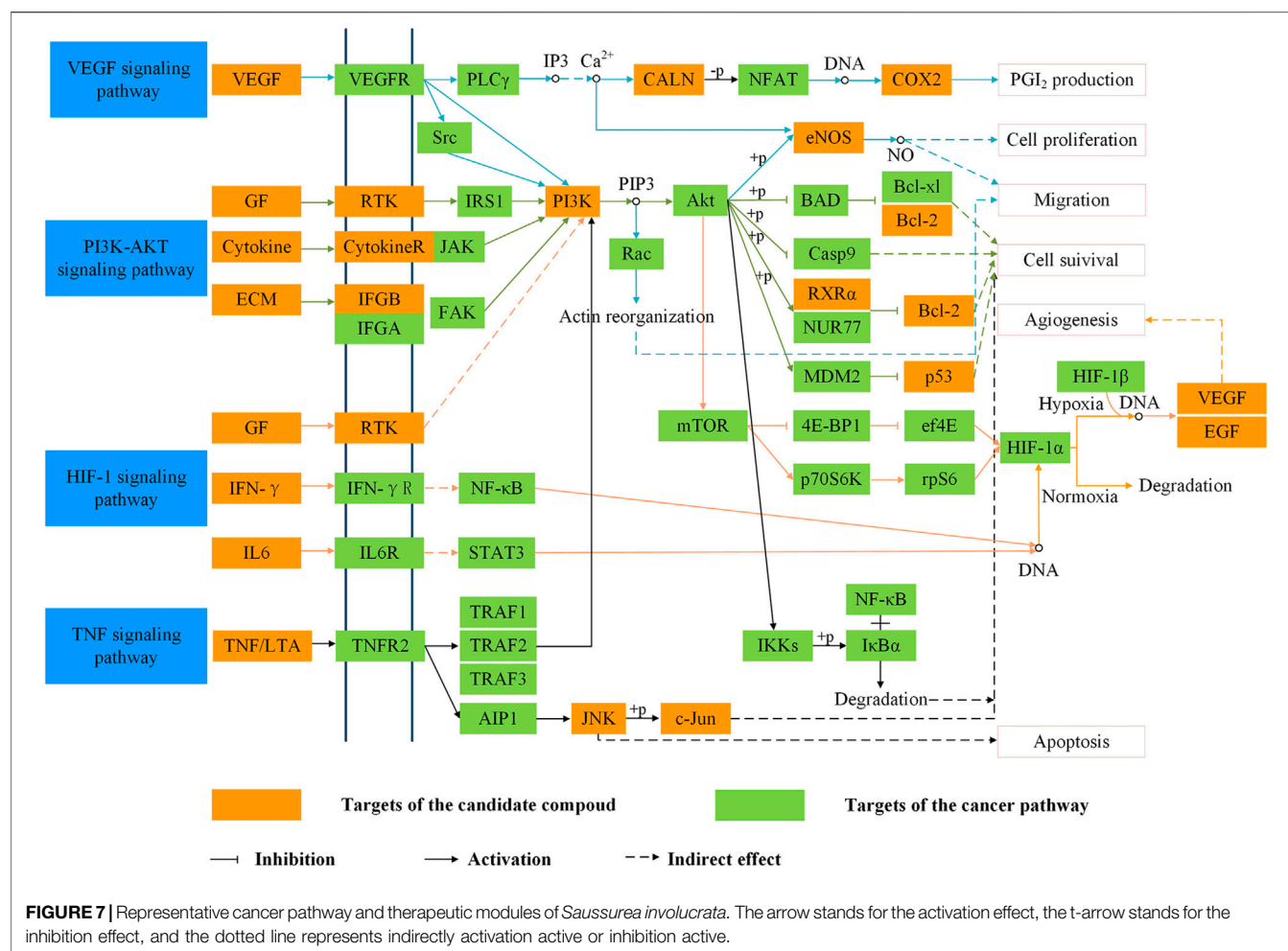


cancer. Prostaglandin G/H synthase 2 (PTGS2) exhibits the highest degree and regulates 13 types of cancers, followed by HSP90AA1 (degree = 12), EGFR (degree = 12), and MMP2 (degree = 11). The result displays that active ingredients can exert the anti-cancer cumulative therapeutic effect through multiple targets. Hence, we hypothesize that the anti-tumor effect of SI can be achieved by regulating multiple systems.

Gene Ontology Analysis and KEGG Pathway Enrichment Analysis

In order to analyze the corresponding relationship between target genes and biological processes, 43 candidate cancer genes were mapped to DAVID for GOBP enrichment. A total of 157 important biological processes were obtained,

and the top 20 biological processes in terms of enrichment degree were mapped (Figure 5). The results showed that targets were closely related to multiple biological processes, including positive regulation of transcription from RNA polymerase II promoter, positive regulation of nitric oxide biosynthetic process, response to drug, positive regulation of cell proliferation, and positive regulation of protein kinase B signaling. “Positive regulation of nitric oxide biosynthetic process” may play a crucial role in exerting anti-cancer effects. NO is a unique gas chemical molecule that can directly damage cell DNA with high concentration and lead a variety of cancer cells to death (Liu L. et al., 2019; Sinha et al., 2019; Sung et al., 2019). “Positive regulation of MAP kinase activity” and “positive regulation of protein kinase B signaling” are related to cancer proliferation, migration, and invasion,



which can be used as one of the potential strategies for cancer treatment (Wen et al., 2019). Tumor growth is usually accompanied by neovascularization, and “angiogenesis” is an important cause of tumor growth and hematogenous metastasis. These biological processes indicate that SI can treat cancer by inhibiting cell proliferation and migration. Meanwhile, the target-pathway network was constructed. Firstly, targets were mapped to DAVID for KEGG pathway enrichment. After that, the T-P network was drawn based on the enrichment results. As shown in **Figure 6**, the T-P network was composed of 40 targets and 70 pathways (**Supplementary Table S2**) (110 nodes and 378 edges). The results showed that SI is highly correlated with four pathways, including the HIF-1 signaling pathway (hsa04066), PI3K-Akt signaling pathway (hsa04151), TNF signaling pathway (hsa04668), and VEGF signaling pathway (hsa04370). As shown in **Figure 7**, SI can integrate multiple signaling pathways to inhibit cancer proliferation, promote apoptosis, and inhibit angiogenesis.

In Vitro Experimental Validation

In this study, based on the analysis of systemic pharmacology, *Saussurea involucrata* can integrate multiple pathways to play

an anti-tumor role. In order to further verify the integrated anti-cancer pathway of *Saussurea involucrata*, we selected three cancer cells and four active compounds with high correlation and most representative. And we also selected the PI3K-Akt pathway, which basically converged with the other three pathways, to carry out *in vitro* verification experiments.

A549 Cell Pathway Validation

After being treated with hispidulin for 24 h, the results of western blot on A549 cells are shown in **Figure 8**. Hispidulin increased the expression of BAD and caspase-9 and reduced p-Akt expression. Quercetin significantly increased the expression of p-Akt ($p < 0.001$), caspase-9, and BAD in A549 cells. Luteolin inhibited the expression of p-Akt and caspase-9 in A549 cells and increased the expression of BAD. Kaempferol enhanced the expression of p-Akt and suppressed the levels of caspase-9 and BAD. These data showed that hispidulin, luteolin, and quercetin had good anti-tumor effects on A549 cells, while kaempferol was beneficial to the proliferation of A549 cells.

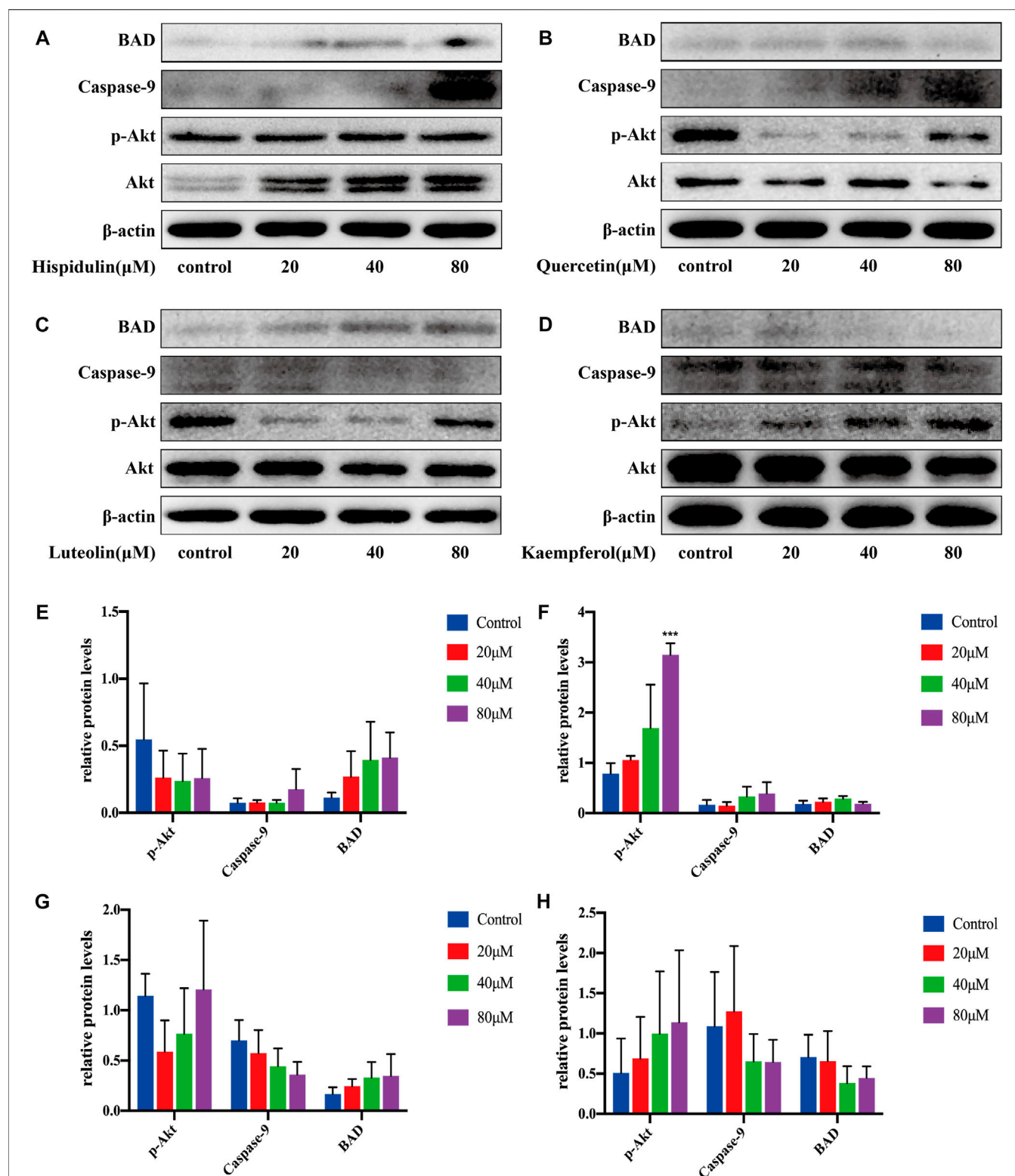


FIGURE 8 | Western blot analysis of Akt, p-Akt, caspase-9, and BAD expressions in A549 cells. **(A)** Cells were treated with or without hispidulin (0, 20, 40, or 80 μ M) for 24 h. **(B)** Cells were treated with or without quercetin (0, 20, 40, or 80 μ M) for 24 h. **(C)** Cells were treated with or without luteolin (0, 20, 40, or 80 μ M) for 24 h. **(D)** Cells were treated with or without kaempferol (0, 20, 40, or 80 μ M) for 24 h. **(E)** Quantification data of western blot in group A. **(F)** Quantification data of western blot in group B. **(G)** Quantification data of western blot in group C. **(H)** Quantification data of western blot in group D. Experimental values are expressed as mean \pm SD for each group ($n = 3$, *** $p < 0.001$ with the control group).

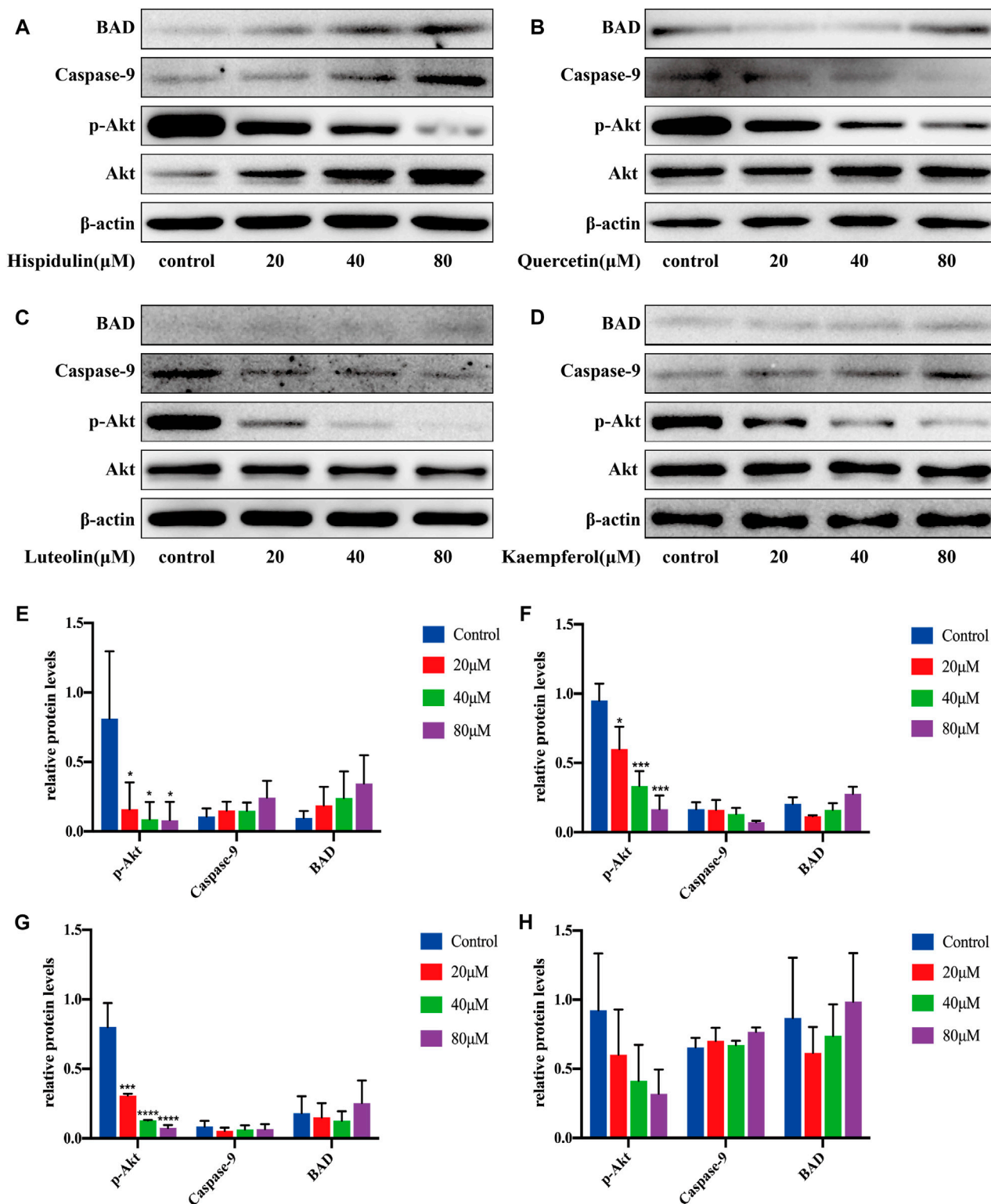


FIGURE 9 | Western blot analysis of Akt, p-Akt, caspase-9, and BAD expressions in PC-3 cells. **(A)** Cells were treated with or without hispidulin (0, 20, 40, or 80 μ M) for 24 h. **(B)** Cells were treated with or without quercetin (0, 20, 40, or 80 μ M) for 24 h. **(C)** Cells were treated with or without luteolin (0, 20, 40, or 80 μ M) for 24 h. **(D)** Cells were treated with or without kaempferol (0, 20, 40, or 80 μ M) for 24 h. **(E)** Quantification data of western blot in group A. **(F)** Quantification data of western blot in group B. **(G)** Quantification data of western blot in group C. **(H)** Quantification data of western blot in group D. Experimental values are expressed as mean \pm SD for each group ($n = 3$, * $p < 0.05$, *** $p < 0.001$, and **** $p < 0.0001$ with the control group).

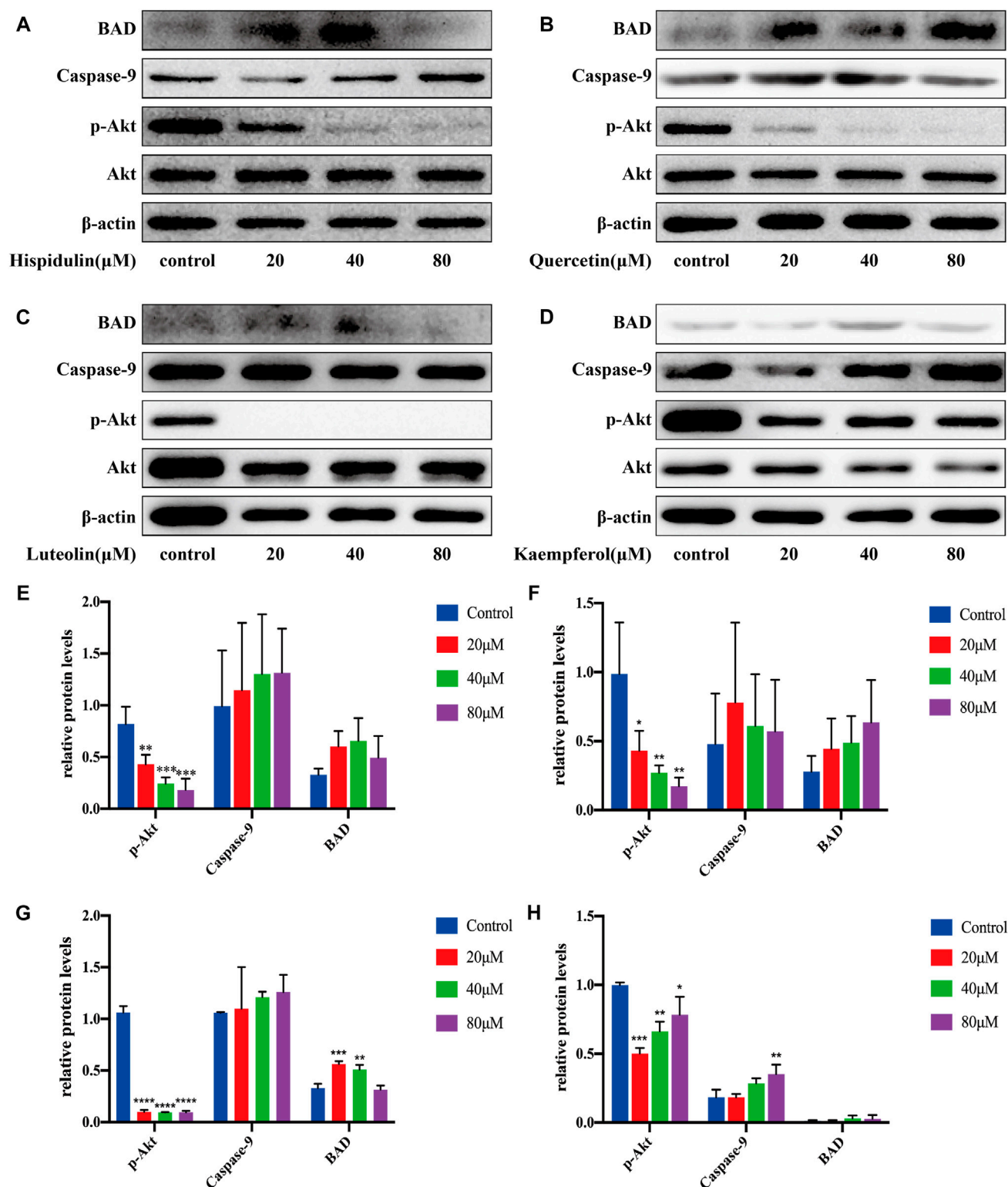


FIGURE 10 | Western blot analysis of Akt, p-Akt, caspase-9, and BAD expressions in C6 cells. **(A)** Cells were treated with or without hispidulin (0, 20, 40, or 80 μM) for 24 h. **(B)** Cells were treated with or without quercetin (0, 20, 40, or 80 μM) for 24 h. **(C)** Cells were treated with or without luteolin (0, 20, 40, or 80 μM) for 24 h. **(D)** Cells were treated with or without kaempferol (0, 20, 40, or 80 μM) for 24 h. **(E)** Quantification data of western blot in group A. **(F)** Quantification data of western blot in group B. **(G)** Quantification data of western blot in group C. **(H)** Quantification data of western blot in group D. Experimental values are expressed as mean \pm SD for each group ($n = 3$, $*p < 0.05$, $**p < 0.01$, $***p < 0.001$, and $****p < 0.0001$ with the control group).

PC-3 Cell Pathway Validation

As shown in **Figure 9**, hispidulin significantly reduced p-Akt expression ($p < 0.05$) and augmented the expression of BAD and caspase-9. Quercetin significantly decreased the expression of p-Akt ($p < 0.05$, $p < 0.001$, and $p < 0.001$, respectively), increased the expression of BAD, and inhibited the expression of caspase-9 protein. Luteolin significantly downregulated the expression of p-Akt with the increase in drug concentration ($p < 0.001$, $p < 0.0001$, and $p < 0.0001$, respectively), increased the expression of BAD, and decreased caspase-9 expression. Kaempferol decreased the expression of p-Akt and promoted the expression of BAD and caspase-9.

These data showed that, in PC-3 cells, hispidulin, luteolin, quercetin, and kaempferol had good anti-tumor effects.

The Validation of C6 Cell Pathway

As shown in **Figure 10**, hispidulin significantly reduced p-Akt expression ($p < 0.001$) and increased caspase-9 expression. Quercetin significantly downregulated the expression of p-Akt with the increase in drug concentration ($p < 0.05$, $p < 0.01$, and $p < 0.01$, respectively) and improved the expression of BAD and caspase-9 in C6 cells. Luteolin significantly lowered the expression of p-Akt ($p < 0.0001$) and improved the expression of BAD ($p < 0.001$ and $p < 0.01$, respectively) and caspase-9. Kaempferol significantly decreased the expression of p-Akt ($p < 0.001$, $p < 0.01$, and $p < 0.05$, respectively) and enhanced the expression of BAD and caspase-9 ($p < 0.01$). These data showed that hispidulin, luteolin, quercetin, and kaempferol inhibited the proliferation and promoted the apoptosis of C6 cells.

DISCUSSION

At present, cancer is increasingly harmful to human health, and the number of deaths still accounts for a large proportion of global deaths. It remains a critical issue for anti-cancer drugs as chemotherapy frequently causes severe side effects. In recent years, traditional Chinese medicine has played a critical role in clinical cancer therapy. SI has various physiological activities such as anti-tumor, but its systemic mechanism of action is still unclear. Therefore, this study employed systems pharmacology to screen active ingredients, analyze networks and pathways by combining with corresponding targets, diseases, and pathways, and explore the mechanism of *Saussurea involucrata* in cancer treatment.

In this study, seven active compounds and 187 related targets were obtained under the conditions of drug likeness and oral bioavailability based on systems pharmacology. The results explained that SI could have therapeutic effect through multiple compounds and multiple targets. In the C-T network, quercetin (M55) displays the highest degree and interacts with 145 target proteins such as HSP90AA1, PTGS2, and PRKACA, which indicates that active ingredients have multi-target characteristics. At the same time, HSP90AA1 is corresponding to seven active compounds, suggesting SI may act on a target through multiple components. Among the seven active ingredients, quercetin can induce apoptosis of various

cancer cells, such as colon cancer (Pang et al., 2019), prostate cancer, and gastric cancer (Shang et al., 2018). As a natural flavonoid, kaempferol (M29, degree = 60) has anti-oxidant, anti-inflammatory (Imran et al., 2019), and anti-cancer activities (Mao et al., 2019). In addition, luteolin (M36, degree = 55) is one of the active ingredients of flavonoids in SI, which can control cell apoptosis by regulating the mitochondrial membrane potential (Seydi et al., 2018). Therefore, we speculated that these ingredients are the key ingredients for SI to have an anti-tumor effect.

Furthermore, the target-disease classification network was constructed in order to further analyze the interaction between targets and diseases. And the network indicated that targets mainly regulate proteins related to cancer, nervous system diseases, and cardiovascular system diseases. The cancer target-cancer network indicates that targets have principal effects on pancreatic cancer, lung cancer, and prostate cancer. Besides, SI displays positive effects on PTGS2, HSP90AA1, and other targets to produce anti-inflammatory, anti-proliferative, and anti-angiogenic effects. In detail, PTGS2 is the rate-limiting enzyme in prostaglandin synthesis, which induces the inflammatory environment to promote cancer development and progression (Peng et al., 2018). It is reported that prostaglandins are capable of stimulating cancer proliferation, promoting angiogenesis (Prima et al., 2017), inhibiting cell apoptosis, and enhancing its metastatic function (Kobayashi et al., 2018). Therefore, the effect of pivotal targets on cancer is worthy of further investigation.

The data of GOBP enrichment display that targets are strongly associated with various biological processes such as NO synthesis, MAPK signaling pathway, PKB signaling pathway, and angiogenesis. NO has a variety of cellular biological functions such as vasodilation, inflammation, immunity, and cell vitality regulation, and high concentrations of NO can be toxic to cells (Edholm et al., 2017). While mitogen-activated protein kinase (MAPK) is critical for cell proliferation, survival, and migration and inflammation regulation (Wei et al., 2017), abnormal MAPK signaling plays an important role in cancer occurrence and progression and the determination of response to cancer treatment (Wang et al., 2017). Besides, the abnormal activation of Akt/PKB is also related to human cancer, and PKB is able to enhance the metabolism and viability of cancer cells (Tang et al., 2018). Therefore, PKB signaling pathway inhibition may be a promising strategy for cancer therapy (Shariati and Meric-Bernstam, 2019). In the development of cancer, tumor cells generally secrete high levels of angiogenic factors that contribute to the formation of abnormal blood vessel networks. Due to the fact that blood vessel networks have characteristics of confusion, immaturity, and permeability, resulting in poor blood perfusion of tumors, the abnormal blood perfusion at the tumor site can reduce the efficiency of chemotherapy drug delivery and radiation therapy (Viallard and Larrivée, 2017). Therefore, active components can regulate related targets to impact on cell proliferation and differentiation, participating in inflammation and angiogenesis processes and thus affecting the development and progression of tumors.

The T-P network and integrated SI cancer-related pathway demonstrate that compounds inhibit the proliferation of cancer cells, promote apoptosis, are anti-inflammatory, and inhibit angiogenesis by regulating the HIF-1 signaling pathway, PI3K-Akt signaling pathway, TNF signaling pathway, and VEGF signaling pathway. Moreover, the PI3K-Akt signaling pathway, TNF signaling pathway, and HIF-1 signaling pathway are involved in the cell proliferation and apoptosis module. Activated PI3K can convert PIP2 to PIP3, which induces Akt phosphorylation. Phosphorylated Akt can not only inhibit the activity of BAD, caspase-9, and Bcl-2 to induce cell proliferation and migration but also activate eNOS to generate NO and promote cell proliferation. Hence, SI might have an anti-cancer effect by regulating BAD, caspase-9, Bcl-2, and eNOS. In the inflammatory module, there are the PI3K-Akt signaling pathway and TNF signaling pathway. Inflammation is a physiological response to infection, injury, or chemical stimulation. Chronic inflammation can induce a variety of diseases like cancer. Tumor necrosis factor receptor 1 (TNFR1) activates the transcription factor NF- κ B, mediates apoptosis, and acts as an inflammation regulator. The VEGF, PI3K-Akt, TNF, and HIF-1 signaling pathways were involved in the migration module. The VEGF signaling pathway activates PI3K, which can further activate eNOS to generate NO and promote cancer proliferation and metastasis. In addition, the VEGF signaling pathway can activate PLC γ , promote the production of IP3, induce the release of Ca²⁺, then activate COX-2, and increase prostaglandin I₂ (PGI₂) production. PGI₂ has the effects of anti-platelet formation, anti-inflammatory, anti-proliferation, and tumor migration inhibition. The above four pathways basically converge on the PI3K-Akt pathway, so that this pathway is selected as the verification pathway.

In order to further verify the results of systematic pharmacology, we selected the PI3K-Akt signaling pathway for *in vitro* validation experiments. It is well known that the PI3K-Akt signaling pathway is one of the main intracellular signal transduction pathways, which plays a very important role in the pathogenesis of many cancers. Abnormal activation of the PI3K-Akt signaling pathway will lead to abnormal expression of a series of downstream proteins and eventually lead to excessive proliferation of cancer cells. Therefore, the PI3K-Akt signaling pathway is a key target in cancer treatment. Akt, the key protein in the PI3K-Akt signaling pathway, is a serine/threonine kinase that regulates cell survival, proliferation, and apoptosis, angiogenesis, and glucose uptake (Song et al., 2019). Overexpression or overactivation of Akt often leads to abnormal signal transduction and uncontrolled proliferation of related diseases, which is an important feature of many human cancers. When Akt is activated on the cell membrane, it can phosphorylate the serine and threonine in the specific part of the substrate protein, thereby exerting extensive anti-apoptosis effect and promoting cell survival. BAD and caspase-9 are two vital direct downstream substrates of Akt. The Bcl-2 agonist of cell death (BAD) is a pro-apoptotic protein (Wan et al., 2018), which can be inactivated by its phosphorylation in many cancers (Bui et al., 2018), so blocking BAD phosphorylation can promote cell

apoptosis. Comparably, caspase-9 is a key protease in the mitochondrial apoptosis pathway, which is located at the top of cascade activation. Activated caspase-9 activates various downstream caspase molecules, causing a series of cascade reactions that induce apoptosis. Our results indicate that hispidulin and quercetin could inhibit p-Akt activation in A549 cells and promote the expression of BAD and caspase-9, respectively. Luteolin is capable of downregulating p-Akt and caspase-9, as well as upregulating BAD simultaneously. But kaempferol enhances the p-Akt level and lowers the expression of caspase-9 and BAD, which is beneficial to A549 cell proliferation and plays an antagonistic role with other drugs. For PC-3 cells, the expression of p-Akt is decreased, while BAD and caspase-9 are increased after being treated with kaempferol and hispidulin. On the contrary, luteolin and quercetin can downregulate p-Akt and caspase-9 and upregulate BAD, indicating that they can inhibit the growth of PC-3 cells and induce their apoptosis. In C6 cells, four compounds could contribute to the phosphorylation of Akt downregulation and BAD and caspase-9 upregulation, manifesting that these compounds play a synergistic role in inhibiting cell proliferation and promoting apoptosis. Consequently, the active compounds in SI can adjust the integrated cancer pathway proteins to display an anti-tumor effect.

In summary, systems pharmacology provides a new and effective method for SI anti-tumor mechanism research in this work. *In vitro* experimental validation manifests that four active ingredients can act on the same target in A549 cells, PC-3 cells, and C6 cells, which proves that the anti-tumor effect of SI has the properties of multiple components. Meanwhile, there are synergistic or antagonistic pharmacological effects among four active ingredients in the same type of cancer, but the strength of anti-tumor effect may be different for unlike tumors. Further experiments are needed to investigate the regulation of this pathway with the complex mixed system of SI in the future.

CONCLUSION

In this study, systems pharmacology was used to explore the mechanism of SI in cancer treatment. Firstly, we screened SI active compounds. Secondly, the C-T network, T-D network, and T-P network were constructed. Finally, target enrichment was applied to analyze the relevant targets. It is revealed that quercetin, luteolin, hispidulin, and kaempferol can inhibit the PI3K-Akt pathway, which is closely related to the anti-tumor property of *Saussurea involucrata*. As a result, *Saussurea involucrata* shows therapeutic effect through multiple components acting on the same target. Our study provides a basis for the research and development of novel anti-cancer drugs.

DATA AVAILABILITY STATEMENT

The original contributions presented in the study are included in the article/**Supplementary Material**, and further inquiries can be directed to the corresponding authors.

AUTHOR CONTRIBUTIONS

QZ, LH and XY conceived and designed the study. QZ, LH and QJ performed the experiment *in vitro*. All authors participated in writing and revision of the manuscript before final submission.

FUNDING

This work was supported by grants from the National Science Foundation of China (No. 81760421 and No. 81460540), the

Foundation of Chengdu Medical College (No. CYZ19-17 and No. CYZ17-03), the program of innovation and entrepreneurship training for college students in Sichuan Province (No. S201913705131 and No. S202013705112), and the project of 2019 science and technology activities for returned students.

SUPPLEMENTARY MATERIAL

The Supplementary Material for this article can be found online at: <https://www.frontiersin.org/articles/10.3389/fphar.2021.678203/full#supplementary-material>

REFERENCES

- Aungst, B. J. (2017). Optimizing Oral Bioavailability in Drug Discovery: An Overview of Design and Testing Strategies and Formulation Options. *J. Pharm. Sci.* 106, 921–929. doi:10.1016/j.xphs.2016.12.002
- Bray, F., Ferlay, J., Soerjomataram, I., Siegel, R. L., Torre, L. A., and Jemal, A. (2018). Global Cancer Statistics 2018: GLOBOCAN Estimates of Incidence and Mortality Worldwide for 36 Cancers in 185 Countries. *CA: A Cancer J. Clinicians* 68, 394–424. doi:10.3322/caac.21492
- Bui, N. L. C., Pandey, V., Zhu, T., Ma, L., Basappaandand Lobie, P. E. (2018). Bad Phosphorylation as a Target of Inhibition in Oncology. *Cancer Lett.* 415, 177–186. doi:10.1016/j.canlet.2017.11.017
- Chen, Y.-L., Zhang, Y.-L., Dai, Y.-C., and Tang, Z.-P. (2018). Systems Pharmacology Approach Reveals the Antiinflammatory Effects of Ampelopsis Grossedentata on Dextran Sodium Sulfate-Induced Colitis. *Wjg* 24, 1398–1409. doi:10.3748/wjg.v24.i13.1398
- Edholm, E.-S., Rhoo, K. H., and Robert, J. (2017). Evolutionary Aspects of Macrophages Polarization. *Macrophages Orig. Funct. Biointervention* 62, 3–22. doi:10.1007/978-3-319-54090-0_1
- Gong, G., Huang, J., Yang, Y., Qi, B., Han, G., Zheng, Y., et al. (2020a). *Saussurea Involucratae Herba* (Snow Lotus): Review of Chemical Compositions and Pharmacological Properties. *Front. Pharmacol.* 10, 1–11. doi:10.3389/fphar.2019.01549
- Gong, G., Xie, F., Zheng, Y., Hu, W., Qi, B., He, H., et al. (2020b). The Effect of Methanol Extract from *Saussurea Involucrata* in the Lipopolysaccharide-Stimulated Inflammation in Cultured RAW 264.7 Cells. *J. Ethnopharmacol.* 251, 112532. doi:10.1016/j.jep.2019.112532
- Guo, X., Zhang, L., Dong, G., Xu, Z., Li, G., Liu, N., et al. (2019). A Novel Cold-Regulated Protein Isolated from *Saussurea Involucrata* Confers Cold and Drought Tolerance in Transgenic Tobacco (*Nicotiana Tabacum*). *Plant Sci.* 289, 110246. doi:10.1016/j.plantsci.2019.110246
- Hu, Q., Feng, M., Lai, L., and Pei, J. (2018). Prediction of Drug-Likeness Using Deep Autoencoder Neural Networks. *Front. Genet.* 9, 1–8. doi:10.3389/fgene.2018.00585
- Imran, M., Salehi, B., Sharifi-Rad, J., Aslam Gondal, T., Saeed, F., Imran, A., et al. (2019). Kaempferol: A Key Emphasis to its Anticancer Potential. *Molecules* 24, 2277–2316. doi:10.3390/molecules24122277
- Kobayashi, K., Omori, K., and Murata, T. (2018). Role of Prostaglandins in Tumor Microenvironment. *Cancer Metastasis Rev.* 37, 347–354. doi:10.1007/s10555-018-9740-2
- Liu, L., Chen, J., Cao, M., Wang, J., and Wang, S. (2019). NO Donor Inhibits Proliferation and Induces Apoptosis by Targeting PI3K/AKT/mTOR and MEK/ERK Pathways in Hepatocellular Carcinoma Cells. *Cancer Chemother. Pharmacol.* 84, 1303–1314. doi:10.1007/s00280-019-03965-5
- Liu, Y.-T., Hsiao, C.-H., Tzang, B.-S., and Hsu, T.-C. (2019). *In Vitro* and *In Vivo* Effects of Traditional Chinese Medicine Formula T33 in Human Breast Cancer Cells. *BMC Complement. Altern. Med.* 19, 1–9. doi:10.1186/s12906-019-2630-5
- Luo, Y.-X., Wang, X.-Y., Huang, Y.-J., Fang, S.-H., Wu, J., Zhang, Y.-B., et al. (2018). Systems Pharmacology-Based Investigation of Sanwei Ganjiang Foundation of Chengdu Medical College (No. CYZ19-17 and No. CYZ17-03), the program of innovation and entrepreneurship training for college students in Sichuan Province (No. S201913705131 and No. S202013705112), and the project of 2019 science and technology activities for returned students.
- Prescription: Related Mechanisms in Liver Injury. *Chin. J. Nat. Medicines* 16, 756–765. doi:10.1016/S1875-5364(18)30115-8
- Ma, Z., Fan, Y., Wu, Y., Kebebe, D., Zhang, B., Lu, P., et al. (2019). Traditional Chinese Medicine-Combination Therapies Utilizing Nanotechnology-Based Targeted Delivery Systems: A New Strategy for Antitumor Treatment. *Ijn* 14, 2029–2053. doi:10.2147/IJN.S197889
- Mao, Z., Shen, X., Dong, P., Liu, G., Pan, S., Sun, X., et al. (2019). Fucosterol Exerts Antiproliferative Effects on Human Lung Cancer Cells by Inducing Apoptosis, Cell Cycle Arrest and Targeting of Raf/MEK/ERK Signalling Pathway. *Phytomedicine* 61, 152809–152981. doi:10.1016/j.phymed.2018.12.032
- Ou, C., Geng, T., Wang, J., Gao, X., Chen, X., Luo, X., et al. (2020). Systematically Investigating the Pharmacological Mechanism of Dazhu Hongjingtian in the Prevention and Treatment of Acute Mountain Sickness by Integrating UPLC/Q-TOF-MS/MS Analysis and Network Pharmacology. *J. Pharm. Biomed. Anal.* 179, 113028. doi:10.1016/j.jpba.2019.113028
- Pang, B., Xu, X., Lu, Y., Jin, H., Yang, R., Jiang, C., et al. (2019). Prediction of New Targets and Mechanisms for Quercetin in the Treatment of Pancreatic Cancer, colon Cancer, and Rectal Cancer. *Food Funct.* 10, 5339–5349. doi:10.1039/c9fo01168d
- Peng, Y., Wang, Y., Tang, N., Sun, D., Lan, Y., Yu, Z., et al. (2018). Andrographolide Inhibits Breast Cancer through Suppressing COX-2 Expression and Angiogenesis via Inactivation of P300 Signaling and VEGF Pathway. *J. Exp. Clin. Cancer Res.* 37, 1–14. doi:10.1186/s13046-018-0926-9
- Prima, V., Kaliberova, L. N., Kaliberov, S., Curiel, D. T., and Kusmartsev, S. (2017). COX2/mPGES1/PGE2 pathway Regulates PD-L1 Expression in Tumor-Associated Macrophages and Myeloid-Derived Suppressor Cells. *Proc. Natl. Acad. Sci. USA* 114, 1117–1122. doi:10.1073/pnas.1612920114
- Seydi, E., Salimi, A., Rasekh, H. R., Mohsenifar, Z., and Pourahmad, J. (2018). Selective Cytotoxicity of Luteolin and Kaempferol on Cancerous Hepatocytes Obtained from Rat Model of Hepatocellular Carcinoma: Involvement of ROS-Mediated Mitochondrial Targeting. *Nutr. Cancer* 70, 594–604. doi:10.1080/01635581.2018.1460679
- Shang, H.-S., Lu, H.-F., Lee, C.-H., Chiang, H.-S., Chu, Y.-L., Chen, A., et al. (2018). Quercetin Induced Cell Apoptosis and Altered Gene Expression in AGS Human Gastric Cancer Cells. *Environ. Toxicol.* 33, 1168–1181. doi:10.1002/tox.22623
- Shariati, M., and Meric-Bernstam, F. (2019). Targeting AKT for Cancer Therapy. *Expert Opin. Investig. Drugs* 28, 977–988. doi:10.1080/13543784.2019.1676726
- Siegel, R. L., Miller, K. D., and Jemal, A. (2020). Cancer Statistics, 2020. *CA A. Cancer J. Clin.* 70, 7–30. doi:10.3322/caac.21590
- Sinha, B. K., Perera, L., and Cannon, R. E. (2019). Reversal of Drug Resistance by JS-K and Nitric Oxide in ABCB1- and ABCG2-Expressing Multi-Drug Resistant Human Tumor Cells. *Biomed. Pharmacother.* 120, 109468. doi:10.1016/j.biopha.2019.109468
- Song, M., Bode, A. M., Dong, Z., and Lee, M.-H. (2019). AKt as a Therapeutic Target for Cancer. *Cancer Res.* 79, 1019–1031. doi:10.1158/0008-5472.CAN-18-2738
- Sung, Y.-C., Jin, P.-R., Chu, L.-A., Hsu, F.-F., Wang, M.-R., Chang, C.-C., et al. (2019). Delivery of Nitric Oxide with a Nanocarrier Promotes Tumour Vessel Normalization and Potentiates Anti-cancer Therapies. *Nat. Nanotechnol.* 14, 1160–1169. doi:10.1038/s41565-019-0570-3

- Tang, F., Wang, Y., Hemmings, B. A., Rüegg, C., and Xue, G. (2018). PKB/Akt-dependent Regulation of Inflammation in Cancer. *Semin. Cancer Biol.* 48, 62–69. doi:10.1016/j.semcancer.2017.04.018
- Viallard, C., and Larrivée, B. (2017). Tumor Angiogenesis and Vascular Normalization: Alternative Therapeutic Targets. *Angiogenesis* 20, 409–426. doi:10.1007/s10456-017-9562-9
- Wan, H., Tang, B., Liao, X., Zeng, Q., Zhang, Z., and Liao, L. (2018). Analysis of Neuronal Phosphoproteome Reveals PINK1 Regulation of BAD Function and Cell Death. *Cell Death Differ.* 25, 904–917. doi:10.1038/s41418-017-0027-x
- Wang, C., Li, P., Xuan, J., Zhu, C., Liu, J., Shan, L., et al. (2017). Cholesterol Enhances Colorectal Cancer Progression via ROS Elevation and MAPK Signaling Pathway Activation. *Cell. Physiol. Biochem.* 42, 729–742. doi:10.1159/000477890
- Wang, X., Chu, L., Liu, C., Wei, R., Xue, X., Xu, Y., et al. (2018). Therapeutic Effects of *Saussurea Involucrata* Injection against Severe Acute Pancreatitis- Induced Brain Injury in Rats. *Biomed. Pharmacother.* 100, 564–574. doi:10.1016/j.biopha.2018.02.044
- Wei, C.-H., Wu, G., Cai, Q., Gao, X.-C., Tong, F., Zhou, R., et al. (2017). RETRACTED ARTICLE: MicroRNA-330-3p Promotes Cell Invasion and Metastasis in Non-small Cell Lung Cancer through GRIA3 by Activating MAPK/ERK Signaling Pathway. *J. Hematol. Oncol.* 10, 1–19. doi:10.1186/s13045-017-0493-0
- Wen, S., Hou, Y., Fu, L., Xi, L., Yang, D., Zhao, M., et al. (2019). Cancer-associated Fibroblast (CAF)-derived IL32 Promotes Breast Cancer Cell Invasion and Metastasis via Integrin β 3-p38 MAPK Signalling. *Cancer Lett.* 442, 320–332. doi:10.1016/j.canlet.2018.10.015
- Yang, S., Zhang, J., Yan, Y., Yang, M., Li, C., Li, J., et al. (2020). Network Pharmacology-Based Strategy to Investigate the Pharmacologic Mechanisms of *Atractylodes Macrocephala* Koidz. For the Treatment of Chronic Gastritis. *Front. Pharmacol.* 10, 1–13. doi:10.3389/fphar.2019.01629
- Zhai, B., Zhang, N., Han, X., Li, Q., Zhang, M., Chen, X., et al. (2019). Molecular Targets of β -elemene, a Herbal Extract Used in Traditional Chinese Medicine, and its Potential Role in Cancer Therapy: A Review. *Biomed. Pharmacother.* 114, 108812. doi:10.1016/j.biopha.2019.108812
- Zheng, C., Pei, T., Huang, C., Chen, X., Bai, Y., Xue, J., et al. (2016). A Novel Systems Pharmacology Platform to Dissect Action Mechanisms of Traditional Chinese Medicines for Bovine Viral Diarrhea Disease. *Eur. J. Pharm. Sci.* 94, 33–45. doi:10.1016/j.ejps.2016.05.018

Conflict of Interest: The authors declare that the research was conducted in the absence of any commercial or financial relationships that could be construed as a potential conflict of interest.

Copyright © 2021 Zhang, He, Jiang, Zhu, Kong, Zhang, Cheng, Deng, Zheng and Ying. This is an open-access article distributed under the terms of the Creative Commons Attribution License (CC BY). The use, distribution or reproduction in other forums is permitted, provided the original author(s) and the copyright owner(s) are credited and that the original publication in this journal is cited, in accordance with accepted academic practice. No use, distribution or reproduction is permitted which does not comply with these terms.



The Application of Inorganic Nanoparticles in Molecular Targeted Cancer Therapy: EGFR Targeting

Meng Sun¹, Ting Wang², Leijiao Li^{1*}, Xiangyang Li¹, Yutong Zhai¹, Jiantao Zhang^{2*} and Wenliang Li^{3*}

¹School of Chemistry and Environmental Engineering, Changchun University of Science and Technology, Changchun, China, ²Department of Colorectal and Anal Surgery, The First Hospital of Jilin University, Changchun, China, ³Jilin Collaborative Innovation Center for Antibody Engineering, Jilin Medical University, Jilin, China

OPEN ACCESS

Edited by:

Jianxun Ding,
Changchun Institute of Applied
Chemistry (CAS), China

Reviewed by:

Hamed Barabadi,
Shahid Beheshti University of Medical
Sciences, Iran
Ruogu Qi,
Nanjing University of Chinese
Medicine, China
Li Quan,
Huaiyin Institute of Technology, China

*Correspondence:

Leijiao Li
lileijiao@cust.edu.cn
Jiantao Zhang
zjt@jlu.edu.cn
Wenliang Li
wenliangl@ciac.ac.cn

Specialty section:

This article was submitted to
Pharmacology of Anti-Cancer Drugs,
a section of the journal
Frontiers in Pharmacology

Received: 29 April 2021

Accepted: 26 May 2021

Published: 12 July 2021

Citation:

Sun M, Wang T, Li L, Li X, Zhai Y,
Zhang J and Li W (2021) The
Application of Inorganic Nanoparticles
in Molecular Targeted Cancer Therapy:
EGFR Targeting.
Front. Pharmacol. 12:702445.
doi: 10.3389/fphar.2021.702445

Epidermal growth factor receptor (EGFR) is an anticancer drug target for a number of cancers, such as non-small cell lung cancer. However, unsatisfying treatment effects, terrible side-effects, and development of drug resistance are current insurmountable challenges of EGFR targeting treatments for cancers. With the advancement of nanotechnology, an increasing number of inorganic nanomaterials are applied in EGFR-mediated therapy to improve those limitations and further potentiate the efficacy of molecular targeted cancer therapy. Given their facile preparation, easy modification, and biosecurity, inorganic nanoparticles (iNPs) have been extensively explored in cancer treatments to date. This review presents an overview of the application of some typical metal nanoparticles and nonmetallic nanoparticles in EGFR-targeted therapy, then discusses and summarizes the relevant advantages. Moreover, we also highlight future perspectives regarding their remaining issues. We hope these discussions inspire future research on EGFR-targeted iNPs.

Keywords: inorganic nanoparticles (iNPs), epidermal growth factor receptor (EGFR), molecular targeted, multifunctional nanotherapeutics, cancer treatment

INTRODUCTION

Cancer is a major public health problem worldwide (Li et al., 2021a). The incidence and mortality rates are on the rise year by year all over the world (Bray et al., 2018; Li et al., 2021b; Siegel et al., 2021). As we know, the conventional treatment methods for malignant tumors are surgery, chemotherapy, and radiotherapy. However, the finite antineoplastic effects also associate with some serious side effects for patients with cancer due to the destructiveness generated by the conventional treatment strategies, such as pain, partial loss of bodily function, and complications (Pearce et al., 2017; McGhee and Steele, 2020). Molecular targeted therapy is an emerging cancer therapy strategy that possesses specific anticancer effects at cellular and molecular levels (Lee et al., 2018; Goyal et al., 2021). It could be used to identify specific cancerogenic targets of tumor cells or microenvironment (TME) and thereby provide negative control of the signaling pathways associated with cell proliferation and metastasis (Yang et al., 2021). On the one hand, the significant inhibition of tumor cells' growth and metastasis is accomplished. On the other hand, the immune response could be simultaneously activated by molecular targeted drugs (Liu et al., 2020). Therefore, molecular targeted therapy has become the standard cancer treatment strategy for many malignant tumors due to it being more effective for tumor cells and having fewer side effects for normal cells (La Salvia et al., 2021).

Tumor tissue is mainly composed of parenchyma and stroma. Tumor parenchyma essentially refers to carcinoma cells, which has specificity in relation to tissue. Carcinoma cells are characterized by intense proliferation due to the insensitiveness to apoptotic signal, escaping from apoptosis and so on. The tumor stroma, namely TME, provides survival necessity and conditions for tumor cell growth and metastasis (Wu and Dai, 2017). TME consists mainly of stromal cells, extracellular matrix, and other extracellular regulatory factors. Cell tumor-associated fibroblasts, immune cells, and vascular endothelial cells are all belong to stromal cells, which provide multifarious specific targets for molecular targeted agents. Due to the said factors, the conventional molecular targeted agents aim at targeting tumor cells and TME prevalently.

Epidermal growth factor receptor (EGFR) is a transmembrane protein that widely distributes in epithelial cells, fibroblasts, spongocytes, and keratinocytes. EGFR plays a crucial role in cell growth metastasis and angiogenesis (Mendelsohn and Baselga, 2000). Frequent abnormalities in the expression of EGFR and EGFR-mediated activation of downstream signaling pathways have been detected in many human malignancies. Anti-EGFR targeted therapy has been brought into focus in recent years (Chen et al., 2020a; Fasano et al., 2021). To date, two primary species of EGFR targeted agents include monoclonal antibodies (McAb) and small molecule tyrosine kinase inhibitors (TKI). McAb act on the extracellular region of the receptor, while TKI act on the intracellular region of the receptor. The most commonly used McAb is cetuximab (C225) (Van Cutsem et al., 2009). Moreover, several EGFR-TKI have been approved by the FDA to date including gefitinib, erlotinib, icotinib, afatinib, lapatinib, osimertinib, and vandetanib (Westover et al., 2018). Unfortunately, the present preclinical and clinical data show a low cure rate, easy recurrence, and adverse events (Paez et al., 2004). For example, EGFR inhibitor brings various awful gastrointestinal, hematologic, and endocrine disorders, arthritis, mucositis, and rash, restricting their wide application (Vermorken et al., 2007; Bar-Ad et al., 2016). Drug resistance is another common problem in the treatment of EGFR-targeted drugs, such as the changes of miRNA and gene profiles (Holohan et al., 2013). As reported, a second point mutation happens in the DNA sequence of the EGFR gene in patients with non-small-cell lung cancer at relapse due to the obvious gefitinib resistance (Kobayashi et al., 2005). In addition, resistant subclones containing an additional EGFR mutation has been observed in cancer patients bearing erlotinib-sensitive EGFR mutations (Pao et al., 2005). More importantly, poor water solubility and insufficient accumulation of EGFR inhibitors at the tumor site limit their application. Therefore, all kinds of new methods and ways are explored actively so as to solve the above problems.

The use of modern nanoscience and material science has provided new approaches to conquer cancer (Chen et al., 2020b; Er Saw and Jiang, 2020; Zhao et al., 2020). Novel nanoparticle engineering is considered as a major innovative impetus in combining diagnosis and treatment into an integrated nanoplatform known as “nanotherapeutics.” INPs, important carriers, can lower the drug dose, prolong retention time, and achieve targeted delivery, thus increasing the cure rate and

reducing complications. Moreover, iNPs could change the immunosuppressive environment. Therefore, iNPs could effectively deliver and extensively accumulate EGFR-targeted drugs in tumor tissue, reducing the accumulation of drugs in normal tissues. The interaction between EGFR and karyopherin- β does not interfere with the EGFR-bonded nanoparticles. Combining inorganic nanoparticles with EGFR-targeting can improve the effectiveness and compatibility, change drug resistance of EGFR-targeting drugs, and combine multiple therapeutic approaches on a single nanoplatform to achieve synergistic therapeutic effects. In this review, some bioactive iNPs, such as the McAb and EGFR-TKI drug deliveries, are focused on and summarized with emphasis on their applications in tumor therapy (Table 1 and Figure 1), in order to provide new ideas for subsequent research.

METALLIC NANOPARTICLES

Recent years have witnessed the wide application of oncotherapy of iNPs. Due to their particular physico-chemical properties, metallic NPs (MNP) have been explored in EGFR-targeted therapy to achieve synergistic treatment, improve therapeutic effects, and delay the development of drug resistance. These multifarious adopted strategies in EGFR-targeted therapy are summarized as follows.

Gold Nanoparticles

Gold NPs (Au NPs) are one of the most studied diagnosis and treatment agents for the treatment of cancer due to their ease of functionalization, good stability, low toxicity, and high biocompatibility. Au NPs-based targeted nanomedicine, such as AurImmune™ (CYT-6091, Au-rhTNF), has entered clinical trials. Au NPs have been demonstrated as EGFR antibodies and KTIs' vehicles in molecule targeted therapy because of their large surface area for attachment of targeting drugs. For example, EGF-tagged Au NPs, as a versatile delivery, was bound to indium-111 to form an ^{111}In -labelled EGF-targeted agent (^{111}In -EGF-Au-PEG) (Song et al., 2017). The outcomes showed that ^{111}In -EGF-Au-PEG could effectively and specifically target EGFR-positive cancer cells (MDA-MB-468), enhance the tumor uptake, and reduce liver uptake compared to the unlabeled ^{111}In -Au-PEG NPs. Au NPs are also qualified for the delivery of EGFR antibodies and cetuximab is the most widely used and reliable EGFR antibody. Groybeck et al. conjugated water-soluble thiolate-protected Au NPs with cetuximab (AuNP-Cetuximab) against EGFR expressing glioblastoma cells. The obvious inhibition of EGFR autophosphorylation was observed (Groybeck et al., 2019). The conjugated Au NPs endowed their electronic properties without any influence on the biological behavior of cetuximab. Additionally, the antineoplastic activity of cetuximab-conjugated cubic gold nanocages (Au NCs) for EGFR targeting in triple-negative breast cancer cells have been studied by Prosperi's group (Avvakumova et al., 2019). The improved permeability and retention effect of AuNCs resulted in active targeting. They concluded that the conjugation strategy of binding AuNPs to

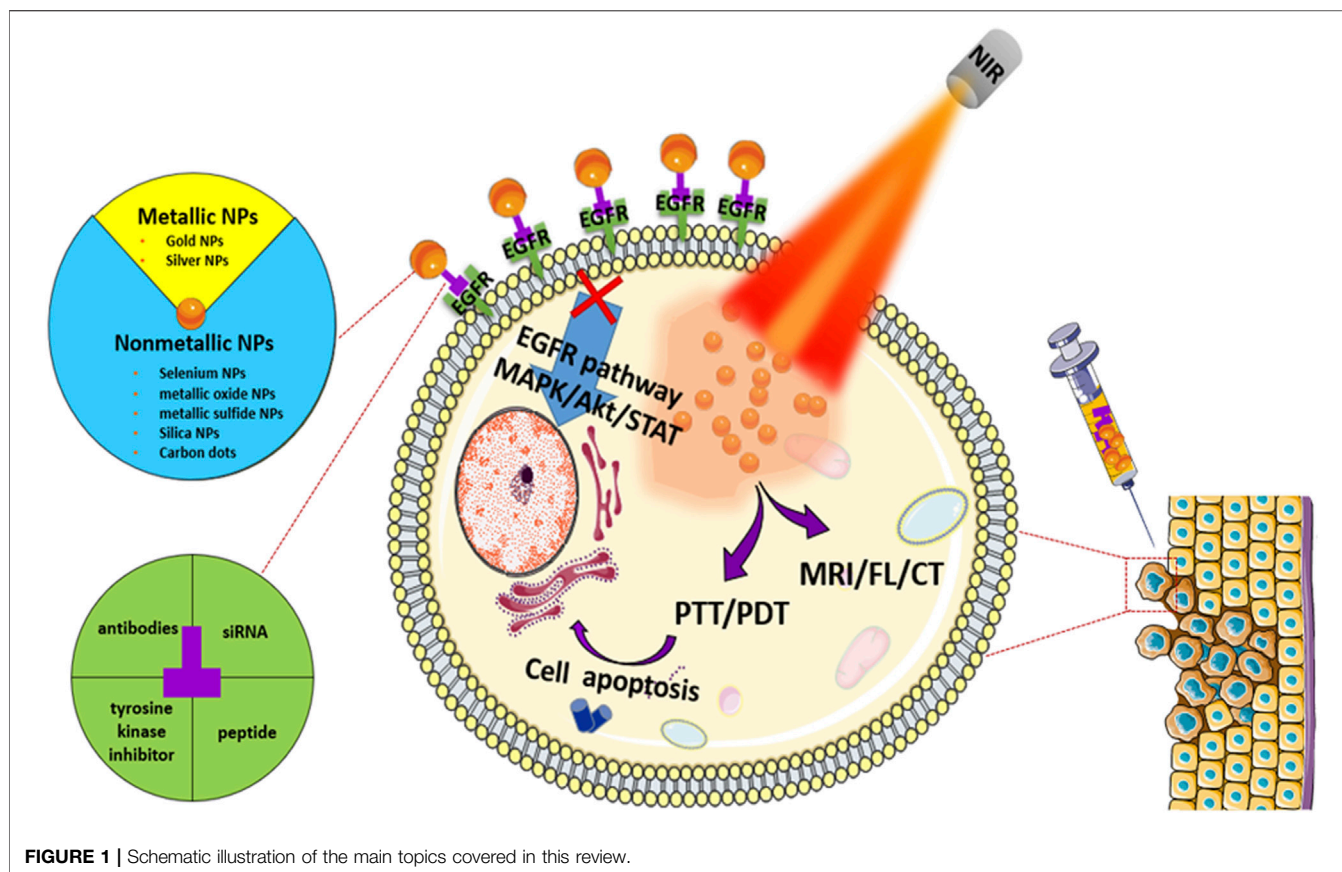
TABLE 1 | Summary of the Inorganic nanoparticle for EGFR-targeted therapeutic strategies.

Nanoparticles	Targeted therapy strategies	Strengths	References
Au NPs	1) Au NPs as vehicles for EGFR antibodies and KTIS.	AuNPs are easily functionalized, stable, low toxic, biocompatible, possess a large surface area for drug attachment, and enable fluorescence and photoacoustic chromatography imaging, controlled drug release, and photothermal therapy. EGFR inhibitors and tumor-targeting peptides can target cancer cells and block signaling pathway	25–31
Ag NPs	2) AuNPs conjugate with tumor targeting peptides	AgNPs has the effect of radiosensitization. EGFR-specific small molecules or EGFR mAb can target tumor cells and inhibit EGFR signal	32–33
Se NPs	Incorporation of the EGFR-specific small molecules or EGFR mAb into Ag NPs	SeNPs has the functions of anticancer, immunomodulatory and drug carrier. EGFR-targeted elements make nanoparticles EGFR targeted, increase SeNPs uptake and inhibit tumor cell growth/survival, metastasis and angiogenesis	34–36
IONPs	Combination of Se NPs and various EGFR-targeted elements (siRNA, peptides, antibody)	IONPs has unique optical and magnetic properties and can be used in drug delivery, laser hyperthermia, MRI, radiotherapy and PDT.	39–44
MxS or MxSe (x = 1–2)	1) EGFR-conjugated IONPs	EGFR antibody provides specific targeting. Composite platform combines multiple treatment modalities. Novel carbon materials have a considerable specific surface area can be used as drug carriers	45–50
Metallic oxideare	2) EGFR-targeted composite nanoplatfoms	ZnS QDs, AgS QDs, CdSe QDs can be used as fluorescent probes, and CuS NPs can be used for photothermal treatment. EGFR antibody provides specific targeting. Their combination can achieve EGFR targeted imaging or photothermal synergistic therapy	56
SNs	3) Novel carbon materials participate in the construction of multifunctional therapeutic agents	ZnO is pH sensitive and allows for controlled release of Zn ²⁺ and loaded drugs in the tumor microenvironment. EGFR antibody or EGFR KTI provides specific targeting and inhibition. Nanotheranostic platforms can realize synergistic therapy	59–73
CQDs	1) Metal sulfide combined with EGFR antibody (ZnS, CuS, AgS)	SNs can be used as nanocarriers due to their excellent biodegradability, high porosity and surface area. EGFR-targeted SNs further realize targeted delivery. Specific drug can be used for chemotherapy. siRNA can silence tumor-related genes and reverse multidrug resistance of cancer. Nano-contrast agents can be used for real-time tumor detection	80–84
	2) Metal selenide combined with EGFR antibody (CdSe)	CQDs has photostability, chemical stability and low toxicity, so it can be used for biological imaging. EGFR antibody modification provides specific targeting. The addition of CT or MRI reagents can improve the spatial resolution of fluorescence imaging and enhance tissue penetration	
	Metallic oxideare establish nanotheranostic platforms combining with EGFR antibody or EGFR KTI (ZnO)		
	1) EGFR-targeted SNs delivery specific drug		
	2) EGFR-targeted MSNs deliver siRNA.		
	3) EGFR-labeled MSNs used as directional carriers of nano-contrast agents		
	Construction of multifunctional nano-platform based on EGFR-targeted CQDs combined contrast agent, SFN, MIP.		

EGFR antibody was an important factor that affected the effectiveness of cellular uptake and the active feature of AuNPs in cancer cells. Wu et al. used bovine serum albumin (BSA) stabilized Au nanocluster (AuCluster@BSA for short) as an EGFR inhibitor delivery. This strategy was not restricted to transfer erlotinib directionally, but could realize whole-body multispectral optoacoustic tomography imaging and photothermal therapy with the aid of Au cluster (Zhan et al., 2019) (Figures 2A–C).

Moreover, recent research showed that AuNPs could conjugate with some peptide resulting in fascinating EGFR-targeting functionality, such as artificial peptide GE11 decorate AuNPs. Yu et al. conjugated Au NPs with different functional polypeptides for tumor-targeting gene therapy (Yan et al., 2020). These composite nanosystems (AuNPPs) consisted of Au NPs, targeting peptide GE11, cell-penetrating peptide octaarginine (R8), and polyhistidine. The resultant AuNPPs

were endowed with tumor targeting and redox-responsive features. The vitro and vivo experiment results showed that AuNPPs possess great tumor cell-targeting ability, transfection efficiency, and tumor growth suppression. Au cluster could further be modified by both the specific GE11 peptide (YHWYGYTPQNVI) and peptide (Au₁₀Peptide₅-GE11: CCYKKKYHWYGYTPQNVI) to achieve cancer inhibition through dual pathways. On one hand, the designed Au₁₀Peptide₅-GE11 could target EGFRs in both active and inactive states, and then induce the oxidative stress mediated apoptosis in the active EGFR mediated endocytosis process. On the other hand, the inactive state of EGFR at the membrane of tumor cells could be maintained by binding Au₁₀Peptide₅-GE11 to avoid the dimerization and further inhibit the activities of tumor cells. Therefore, employing Au₁₀Peptide₅ as EGFR TKIs delivery results in inhibiting cancer cells through dual pathways (Zhang et al., 2018a).



Silver Nanoparticles

In addition to Au NPs, silver nanoparticles (Ag NPs) have been recognized as useful tools for diagnosis and treatment in anticancer and antimicrobial fields. Ag NPs were found to have potential utility as radiosensitizers to improve the outcomes of cancer radiotherapy. Therefore, the incorporation of the EGFR-specific small molecules (e.g. gefitinib) or humanized McAb targeting EGFR (e.g. Erbitux; C225) into Ag NPs is an alternative strategy. For instance, C225-coated Ag NPs (Ag/C225) have been tested for their enhanced radiosensitization in nasopharyngeal carcinoma epithelial cell lines (Yu et al., 2017). The anti-EGFR antibody activity was well maintained in Ag/C225 nanocomposite with the average preserved activity of about 82%. More importantly, Ag/C225 nanocomposites were not cytotoxic alone for normal cell lines without X-ray irradiation. According to the half maximal inhibitory concentration values (IC_{50}), Ag/C225 nanocomposites cause irreversible cell growth inhibition. Therefore, Ag/C225 nanocomposites, as a specific radiosensitizer, exhibited better anti-proliferative effects in nasopharyngeal carcinoma cell lines by assistive EGFR-targeting of C225. Cho et al. developed a targeted Au/Ag drug delivery (AuHNS-EGFR-DOX) for near-infrared (NIR) light induced thermo-chemotherapy (Noh et al., 2015). The Au/Ag hollow nanoshells were prepared on PEGylation silica NPs (AuHNS) to further conjugate EGFR antibody. There is a hollow interior between the Au/Ag shell and the silica core particle with the distance of about 16 nm to load doxorubicin

(DOX). The DOX loading capacity was about 3×10^6 DOX molecules per single nanoparticle. The targeted-drug delivery was relatively stable at pH7.4, while the DOX release rate was 12% over 24 h at pH5.0. Moreover, DOX release could be triggered by the NIR-induced hyperthermia. This EGFR-targeted thermo-chemotherapeutic agent was approved to be a pH-sensitive and thermo-sensitive drug release system. Additionally, the A549 cell viability was much lower in AuHNS-EGFR-DOX group under NIR irradiation than that in AuHNS-DOX group, indicating the marked availability of EGFR-mediated endocytosis compared to non-specific cellular uptake. These works indicated that metallic nanoparticles, such as McAb or EGFR-KTI deliveries, extended the application of metallic nanoparticles in targeting therapy for tumor (Figure 2D).

NON-METALLIC NANOPARTICLES

In this section, we selectively present various typical nanometallic nanoparticles that have been synthesized and conjugated to EGFR-targeted small molecule drugs for numerous oncotherapies in recent years. The applications in oncotherapy of non-metallic nanomaterials consisting mainly of selenium (Se), iron-based nanomaterials, metallic chalcogenide, metallic oxide, silicon, and carbon-based materials have been described in the following sections.

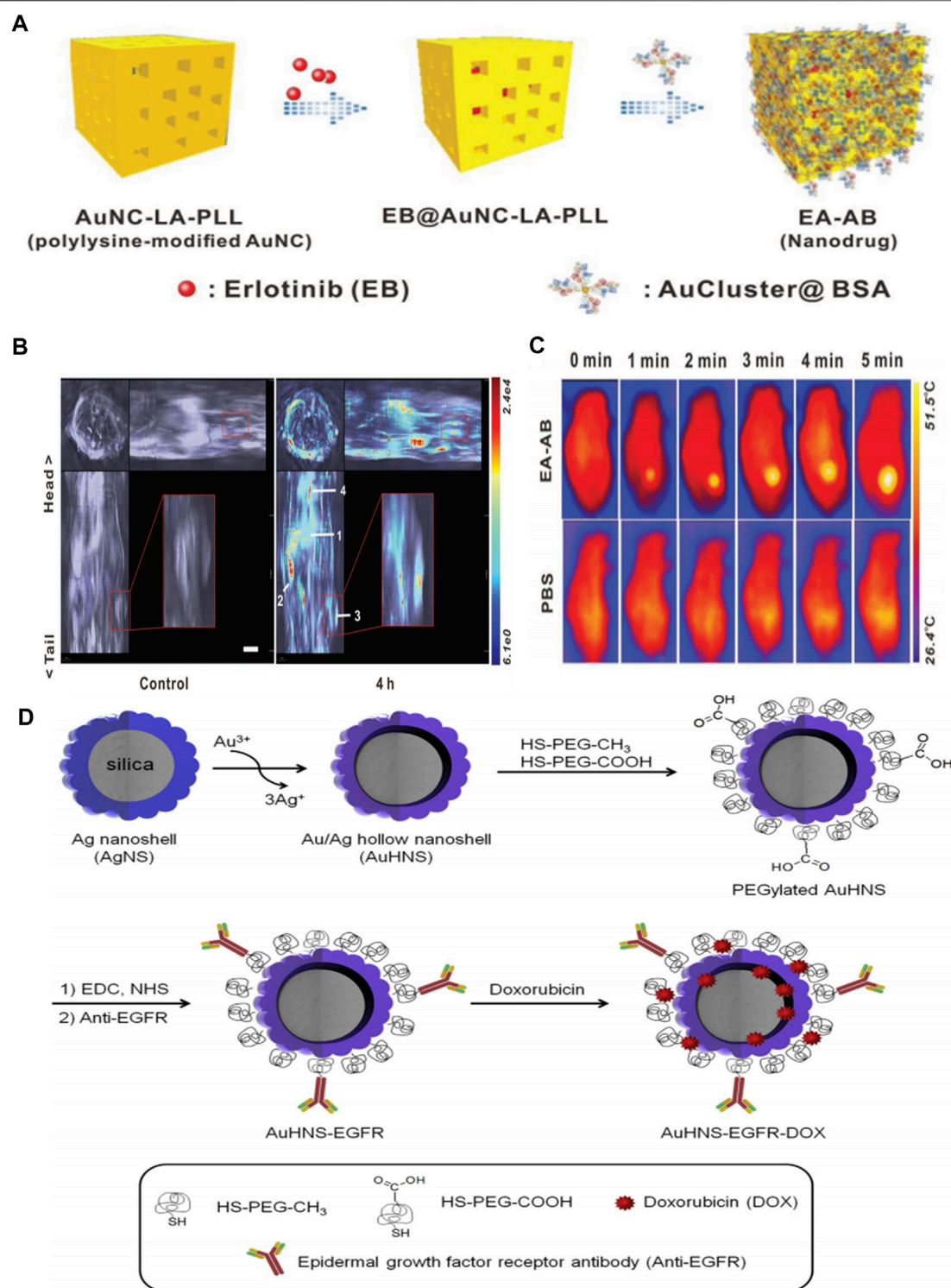


FIGURE 2 | (A) Schematic illustration for fabrication of EA-AB **(B)** *In vivo* orthogonal 3D MSOT view of 4T1 tumor-bearing mice before and after tail vein injection of the EA-AB dispersion (AuNC content: 80 mg kg⁻¹). The numbers indicate different organs and tumor regions: 1) liver, 2) spleen, 3) tumor, and 4) lung **(C)** Infrared thermal images of 4T1 tumor-bearing mice intravenously injected with 200 μL PBS (the control) or EA-AB dispersion (AuNC content: 80 mg kg⁻¹) and 12 h later subject to 5 min of NIR laser irradiation (808 nm at 1.5 W cm⁻²). Reproduced from (Avvakumova et al., 2019) with permission from Wiley **(D)** Schematic illustration for the preparation of anti-EGFR-conjugated and doxorubicin-loaded Au/Ag hollow nanoshell (AuHNS-EGFR-DOX). Reproduced from (Yu et al., 2017) with permission from Elsevier.

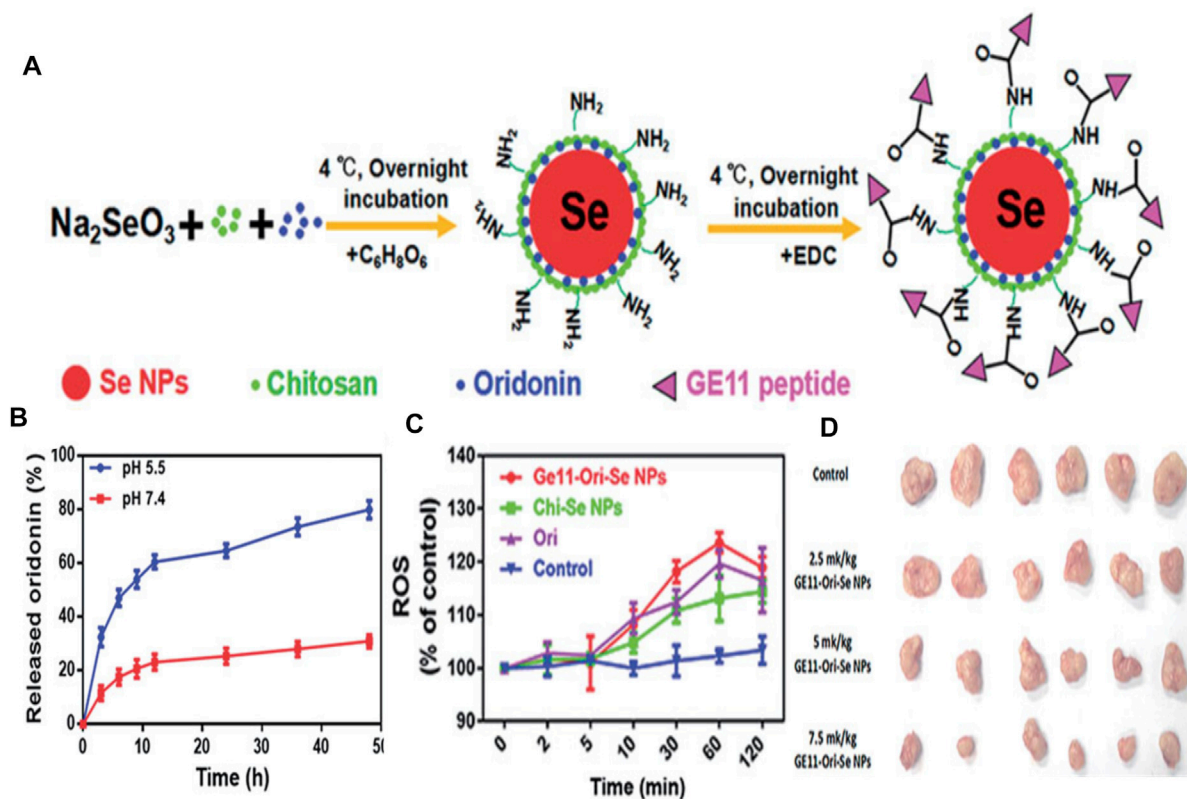


FIGURE 3 | (A) The formation process of GE11-Ori-Se NPs **(B)** *In vitro* release of oridonin from GE11-Ori-Se NPs at pH 5.5 and 7.4 **(C)** Effects of GE11-Ori-Se NPs, and the same dosage of oridonin or Chi-Se NPs on the production of ROS in KYSE-150 cells **(D)** Images of the tumor from control and GE11-Ori-Se NPs treated xenograft KYSE-150 cancer nude mice. Reproduced from (Kong et al., 2011) with permission from Informa.

Selenium Nanoparticles

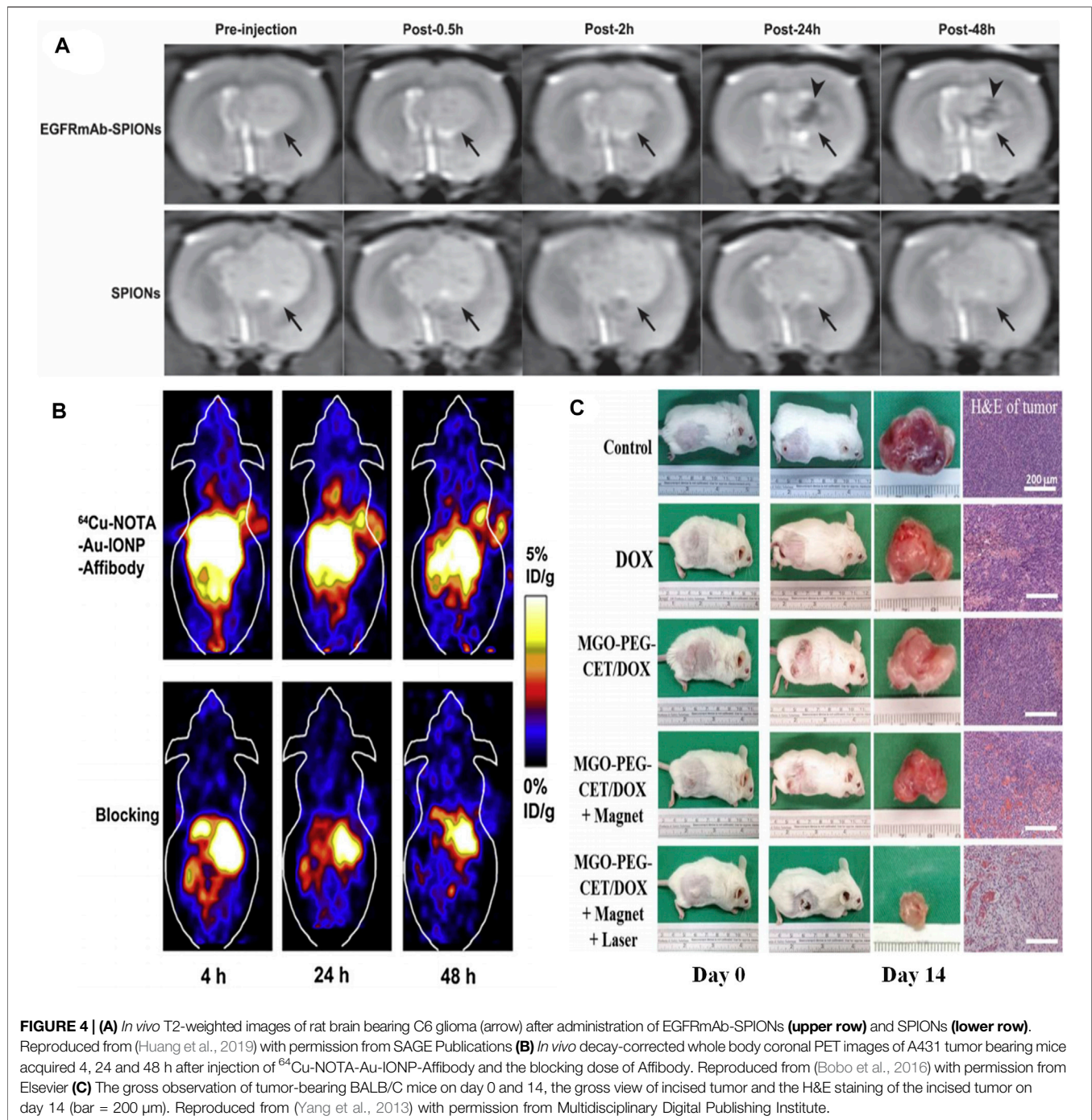
Se elements with anticancer and immunoregulation properties are indispensable and necessary in humans. Gao's team found that selenium nanoparticles could inhibit the growth of prostate cancer cells in part through cysteine mediated apoptosis and Ahmadrzashahverdi's team demonstrated that Se nanoparticles could significantly induce the immune response of 4T1 breast cancer tumors in mice (Kong et al., 2011; Yazdi et al., 2012). Consequently, the combination of Se NPs and various EGFR-targeted elements have been used recently. For instance, Jebal et al. synthesized hexagonal selenium nanoparticles and then endowed them with EGFR-targeting abilities by modifying SiRNA (HSNM-SiRNA) (Moghaddam et al., 2016). HSNM-SiRNA was found to be able to change the structure of EGFR and destroy its activity when NSCLC cells were exposed to HSNM-SiRNA. Besides, GE11 peptide-conjugated Se NPs (GE11-Ori-Se NPs) were applied as oridonin delivery to inhibit growth and metastasis of EGFR over-expressed cancer cells and reduce the toxicity against normal cells (Pi et al., 2017). Substantial oridonin molecules could release in a tumor acidic microenvironment and thus enter into the lysosomes and cytoplasm of cancer cells. Impressively, GE11-Ori-Se NPs could trigger reactive oxygen species (ROS) production. And GE11-Ori-Se NPs further killed cancer cells by disrupting the function of mitochondria, specifically inhibiting EGFR-mediated

PI3K/AKT and Ras/Raf/MEK/ERK pathways (**Figures 3A–D**). Chen and co-workers recently performed anti-EGFR therapy against nasopharyngeal carcinoma by combining Se NPs with gefitinib, which is a human-mouse chimeric antibody blocking EGFR. This strategy effectively increased intracellular accumulation in nasopharyngeal carcinoma cells with the help of selenium nano-platform and thus sheds light on its application in anti-EGFR therapy (Huang et al., 2019).

Iron Oxide Nanoparticles

Iron is another indispensable microelement in the human body. Iron is required in multitudinous biological processes such as composition of hemoglobin to deliver oxygen around the body. Importantly, iron-based nanomaterials have been approved by the FDA in inorganic nanomedicines (Bobo et al., 2016). Iron oxide nanoparticles (IONPs) are well established nano-therapeutic platforms in clinical trials against several types of cancer. Because of the peculiar optical and magnetic properties, IONPs are widely used in laser-induced thermotherapy, magnetic resonance imaging (MRI), radiotherapy, and photodynamic therapy (PDT) (Zhang et al., 2016).

As for MRI agents, EGFR-conjugated superparamagnetic Fe_3O_4 (EGFRmAb-SPIONs) were synthesized and served as a targeted MRI contrast agent for the EGFR-positive detection *in vitro* and *in vivo*. The MRI results suggested that the brain



glioma cells treated with EGFRmAb-SPIONs exhibited a more significant negative contrast enhancement even at low concentrations than that observed in the tumor cells incubated only with SPIONs (Mu et al., 2015). The dramatic reduction of T_2 relaxation time was found as a result of the treatment of EGFRmAb-SPIONs. According to the *in vivo* experimental results, T_2 -weighted MRI exhibited an obvious hypointense region within glioma after intravenous administration of EGFRmAb-SPIONs. The maximal negative enhancement within the tumor was

reached at 24 h after injection along with the increasing R_2 value (Figure 4A).

A number of EGFR-targeted composite nanoplateforms with IONPs as the main component for targeting MRI and therapy have been studied so far. Cheng's group developed a hetero-nanostructural trimodality nanoprobe, which was composed of Fe_3O_4 , Au, and anti-EGFR Affibody protein (Au-IONPs) (Yang et al., 2013). In this hetero-nanostructural nanoprobe, EGFR-targeted IONPs played a major role as T_2 reporter for MRI. Additionally, Au component was used as positron emission

tomography (PET) probe for imaging of EGFR positive tumor cells. The outcomes indicated that Au-IONPs nanoprobe provided significant specificity and high sensitivity for both PET and MRI imaging in the human EGFR-expressing tumor cells (**Figure 4B**). Moreover, $\text{Fe}_3\text{O}_4/\text{Au}$ nanoparticle was conjugated with a single-chain antibody (scFv) to obtain an EGFR-specific MRI bioprobe (scFv@ $\text{Fe}_3\text{O}_4/\text{Au}$). The *in vivo* results showed that scFv@ $\text{Fe}_3\text{O}_4/\text{Au}$ could specifically transfer $\text{Fe}_3\text{O}_4/\text{Au}$ to detect EGFR-positive non-small cell lung cancer through MRI method. The scFv@ $\text{Fe}_3\text{O}_4/\text{Au}$ immunonanoparticles were detected in the cell cytoplasm of EGFR-overexpressing SPC-A1 cells, while very little scFv@ $\text{Fe}_3\text{O}_4/\text{Au}$ could be detected in EGFR-deficient H69 cells. Therefore, these IONPs-based MRI agents are potential strategies for both selective imaging and cell screening. C225-encapsulated core-shell $\text{Fe}_3\text{O}_4/\text{Au}$ were fabricated as a therapeutic nano-system ($\text{Fe}_3\text{O}_4/\text{Au}$ -C225) to conduct targeted magneto-photothermal therapy against glioma cells (Lu et al., 2018a). $\text{Fe}_3\text{O}_4/\text{Au}$ -C225 integrated magnetic fluid hyperthermia, NIR-induced hyperthermia, and significant specificity was generated by EGFR inhibitor, allowing the glioma specific hyperthermic treatment. $\text{Fe}_3\text{O}_4/\text{Ag}$ conjugated with C225 ($\text{Fe}_3\text{O}_4/\text{Ag}$ /C225) was fabricated to realize radiation therapy (Zhao et al., 2012). Herein, Fe_3O_4 component served as an MRI reporter, while the Ag component assumed the role of a radiotherapy sensitizer. The composite nanoplatfrom ($\text{Fe}_3\text{O}_4/\text{Ag}$ /C225) was used to be an EGFR-targeted tumor tracer for radiation therapy. The *in vitro* experimental results revealed that the enhanced inhibition of human nasopharyngeal carcinoma cell combined with X-ray treatment was found. In a word, this multifunctional nanocomposite $\text{Fe}_3\text{O}_4/\text{Ag}$ /C225 might be a potential EGFR-targeted radiosensitizer for treating human nasopharyngeal carcinoma tumor.

Some novel carbon materials are chosen as auxiliaries to construct multifunctional therapeutic agents. Chen et al. took graphene oxide (GO) as a carrier to delivery IONPs and doxorubicin (DOX), and further modified this magnetic graphene oxide with cetuximab (MGO-PEG-CET) (Lu et al., 2018b). This EGFR-targeted magnetic thermo-chemotherapy system could enter high EGFR-expressing CT26 murine colorectal cells by receptor-mediated endocytosis. The *in vivo* and *in vitro* results all demonstrated that EGFR-targeted nanosystems could effectively ablate tumor tissue by synergistic treatment of chemotherapy and photothermal therapy (**Figure 4C**). In addition, magnetic Fe-filled carbon nanotubes binding with mAb cetuximab could selectively remove EGFR-positive cells from a mixed population of healthy cell lines in about 10 min (Marega et al., 2013). A two-fold increased selective suppression of the EGFR-positive cells was detected compared with EGFR-deficient cells by *in vivo* experiment through an electromagnetic radiation inducing magnetic fluid hyperthermia.

Metallic Sulfide and Metallic Selenide

In addition, some metallic sulfides and metallic selenides (MxS or MxSe , $x = 1-2$) have been intensely studied. Herein, some recent reports about zinc sulfide (ZnS), copper sulfide (CuS), silver

sulfide (AgS), and cadmium selenide (CdSe) as subjects for EGFR-targeting oncotherapy are summarized in the next section.

For example, poly (lactic-co-glycolic acid) coated ZnS:Mn^{2+} (PLGA-ZnS) conjugated with cetuximab was used to accomplish targeted imaging and delivery of anti-cancer drugs. As the cell uptake results showed, the uptake of targeted NPs was over 80%, while that of the nontargeted NPs was only 40% (Deepagan et al., 2012). Gong et al. designed a type of QD with core shell structure, in which indium phosphate (InP) and ZnS acted as core and shell, respectively (Wang et al., 2017). The prepared InP/ZnS QDs were endowed with hydrophilia via modifying with amphiphilic block copolymer polylactide-b-poly (ethylene glycol) (PLA-PEG). InP/ZnS@ PLA-PEG micelles were further embellished with an anti-EGFR nanobody (7D12 Nbs) to assess the therapeutic effect of triple-negative breast tumor. As we know, CuS have been demonstrated as potent theranostic nanotool with promising outcomes in the past decade (Yun et al., 2020; Dong et al., 2020). The cetuximab-modified CuS NPs (CuS-Ab NPs) were constructed as a synergistic anti-cancer agent, which could successfully suppress the tumor spread and growth (Li et al., 2018). With the help of cetuximab, CuS NPs were accumulated in tumors rather than in normal tissues. Superior photothermal effect could be obtained under NIR irradiation even at a low power level (0.2 W/cm^2). Therefore, the designed CuS-Ab NPs fully exploit higher local tumoricidal effect and lower nephric and systemic toxicity by EGFR-targeting with cetuximab (**Figure 5A**). Additionally, silica coated cadmium selenide quantum dots (CdSe-Silica QDs) conjugated with McAb successfully achieve the specific recognition of EGFR-positive tumor cell lines (Vibin et al., 2017). The resultant QD-Ab finally turned out to be an excellent tumor targeting fluorescent probe, which exhibited much higher internalization efficiency than non-targeted QDs. Over 90% EGFR-targeted QD-Ab probe could enter in the cytoplasm by endocytosis, yet non-targeted QDs showed only 67% internalization. After 4 h of intravenous injection, EGFR-targeted QD-Ab probe specifically accumulated in tumor tissue. Ag₂S QDs exhibit fluorescence emission maximum within the scope of 650–1,200 nm, making it a promising targeted bioprobe for imaging in neoplastic tissues. In order to solve the lack of specific tumor-targeting capability, anti-EGFR Affibody (ZEGFR:1907)-based Ag₂S QD (ZEGFR:1907-Ag₂S QDs) nanoprobe have been successfully synthesized and used for targeted photoacoustic imaging of EGFR-overexpressed tumor (Zhang et al., 2018b). The prepared ZEGFR:1907-Ag₂S QDs exhibited a sharp and strong absorbance peak at 800 nm along with a weak shoulder absorbance peak in the range of 900–1,100 nm. Two kinds of cell lines with different expression levels of EGFR were chosen to test the targeting specificity cell uptake of ZEGFR:1907-Ag₂S QDs, including A431 (EGFR-overexpressed) and Bxpc3 with β -actin (EGFR-negative). The uptake of ZEGFR:1907-Ag₂S QDs was up to 80% in A431 cells due to the prominent targeting and specificity endowed by ZEGFR:1907. In one word, the photoacoustic imaging results showed that ZEGFR:1907-Ag₂S QDs could detect EGFR-positive tumor cell lines perfectly.

Metallic Oxideare

In addition, some familiar metallic oxides are also established nanotheranostic platforms combined with EGFR antibody or

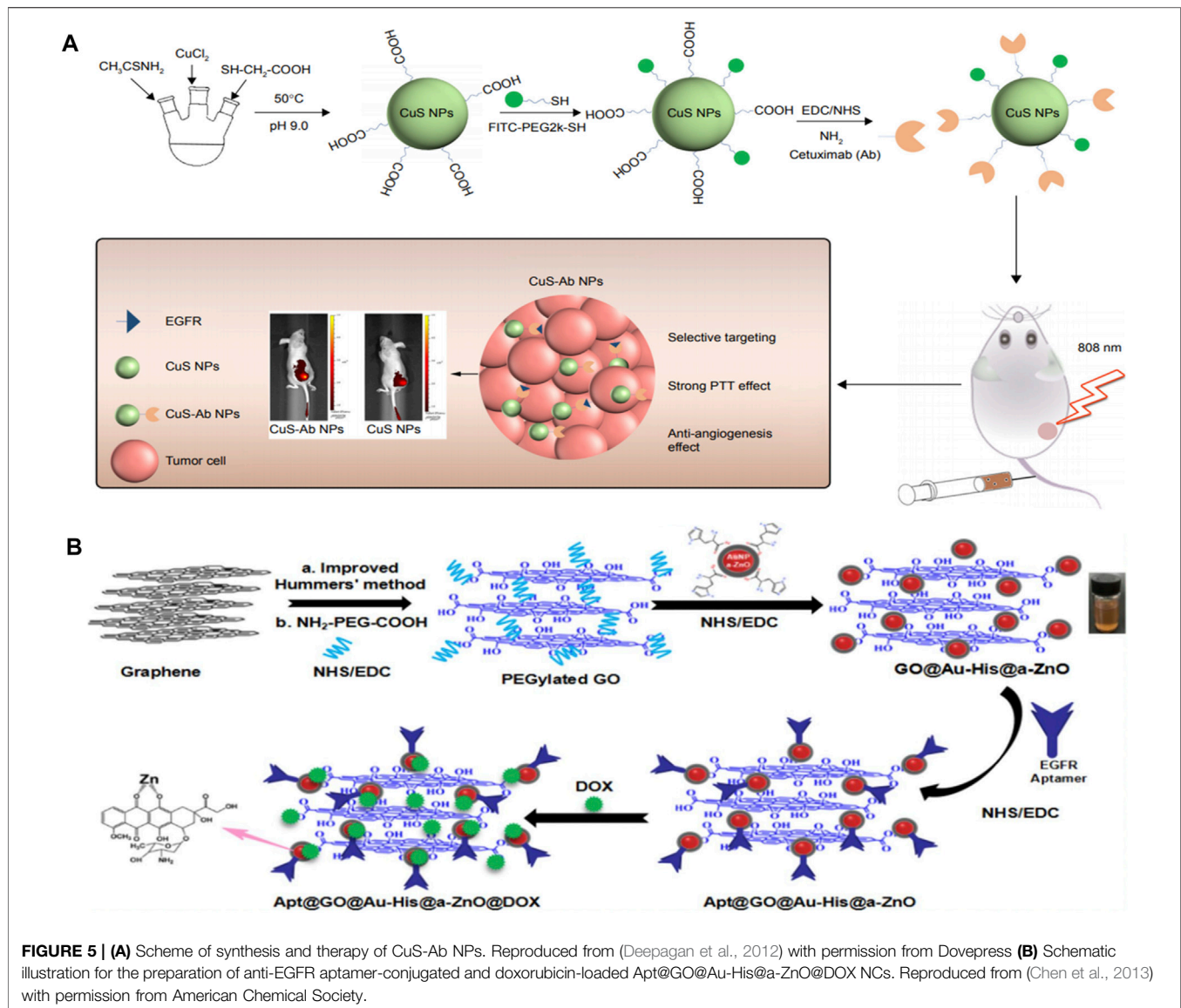


FIGURE 5 | (A) Scheme of synthesis and therapy of CuS-Ab NPs. Reproduced from (Deepagan et al., 2012) with permission from Dovepress **(B)** Schematic illustration for the preparation of anti-EGFR aptamer-conjugated and doxorubicin-loaded Apt@GO@Au-His@a-ZnO@DOX NCs. Reproduced from (Chen et al., 2013) with permission from American Chemical Society.

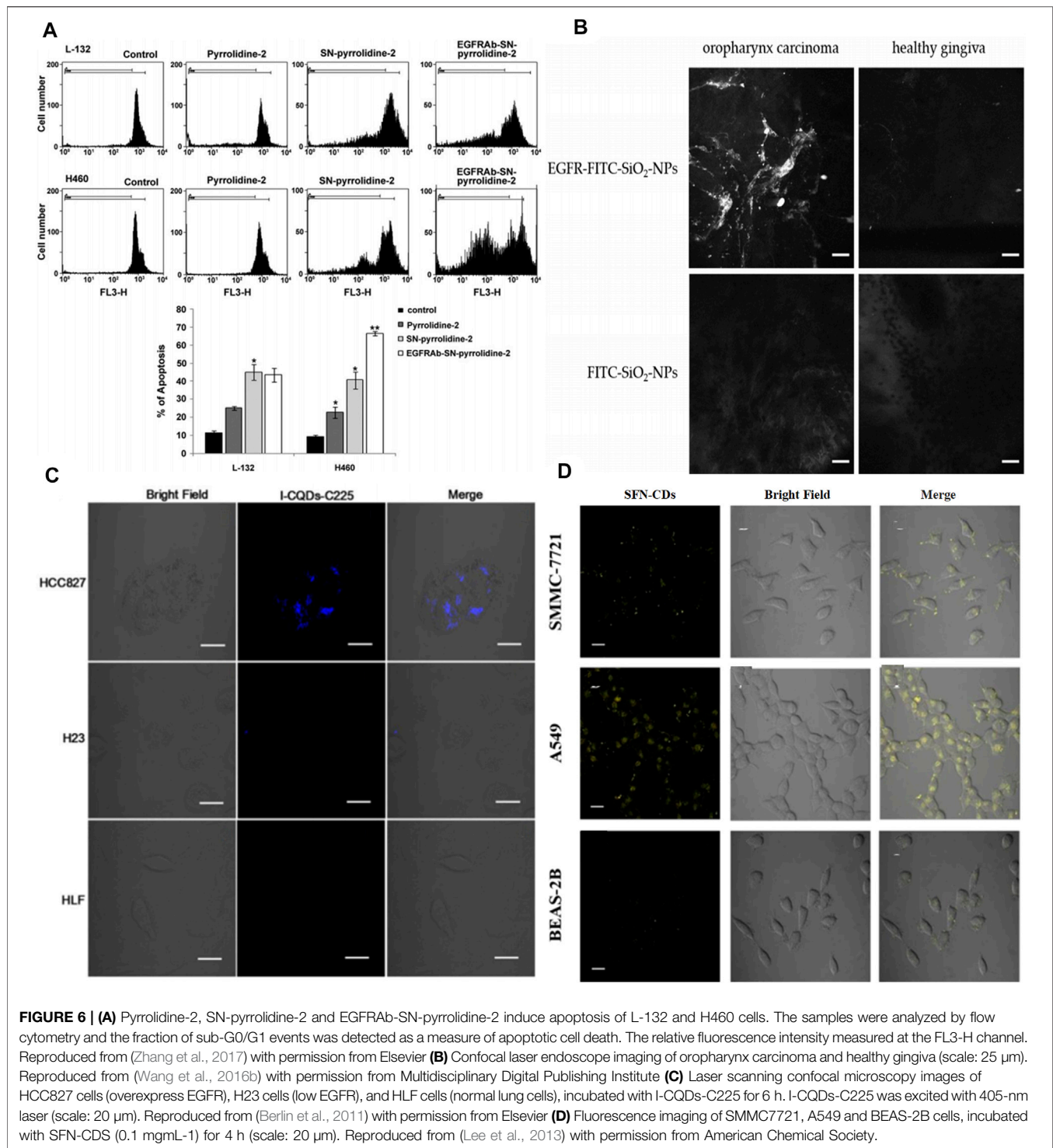
EGFR KTI against several types of cancer (eg. ZnO NPs) (Muhammad et al., 2011; Chen et al., 2013; Cai et al., 2016; Zhang et al., 2017; Zhou et al., 2017). For example, Wu's group integrated the histidine-mediate amorphous zinc oxide shells coated Au NPs on graphene oxide to obtain the multifunctional nanocomposites (GO@Au-His@a-ZnO) (Zhang et al., 2019a). The novel nanocomposites were further conjugated with antibody of EGFR aptamer and DOX to accomplish targeting, photothermal, and chemotherapy (Apt@GO@Au-His@a-ZnO@DOX NCs). The maximum loading capacity of DOX was 250 mg/g and the accumulative DOX release rate was 75.4% in PBS pH5.5 under NIR irradiation (808 nm, 1.5 W/cm^2). Apt@GO@Au-His@a-ZnO@DOX NCs was demonstrated as an excellent photothermal nanomaterial with high photothermal conversion efficiency ($\eta = 38\%$). The resultant Apt@GO@Au-His@a-ZnO@DOX NCs could release antitumor Zn^{2+} ions in the acidic endosome/lysosome of

tumor tissue simultaneously. Importantly, Apt@GO@Au-His@a-ZnO@DOX NCs exhibited much higher targeting efficacy and tumor inhibition to EGFR-positive A549 cells than that of $\text{GO@Au-His@a-ZnO@DOX}$ NCs according to the laser scanning confocal microscope (LSCM) images for cellular uptake and *in vivo* experiments (Figure 5B).

Silica Nanoparticles

Except for the above mentioned metallic chalcogenide, silica nanoparticles (SNs) exhibit excellent biodegradability and thus were always chosen as the nanocarriers due to their high porosity and surface area (Wang et al., 2016; Zhang et al., 2019b). Herein, we summarized some recent applications of EGFR-targeted SNs including specific drug delivery, targeted gene therapy, and targeted imaging.

As for SN-based specific drug delivery, some progress has been made. For instance, polyethylenimine modified mesoporous SNs



were conjugated with EGFR antibody (EGFRAb-SN-pyrrolidine-2) to use as a targeted prodrug delivery for effective lung cancer therapy (Sundarraj et al., 2014). According to the flow cytometry results, about 44.57% of EGFRAb-SN-pyrrolidine-2 could be internalized in H460 cells. EGFRAb-SN-pyrrolidine-2 convincingly suppressed H460 cell proliferation compared with EGFR-deficient L-132 cells at the same concentration of

100 μ g ml⁻¹. And the inhibition rate in EGFRAb-SN-pyrrolidine-2 treated group reached 64% (**Figure 6A**). Kong et al. synthesized hollow mesoporous silica nanoparticles (HMSNs) and then dressed up HMSNs with amine groups to conjugate with EGF. According to the principal component analysis, the quantity and density of the EGF attachments could be controlled by tuning the EGF concentration at grafting stages (She et al., 2015a; She et al.,

2015b). Impressively, they further confirmed that using HMSNs grafted with EGF to deliver 5-FU could overcome acquired 5-fluorouracil (5-FU) resistance. The constructed EGFR-targeted 5-FU nanocarrier (EGF-HMSNs-5-FU) could be specifically internalized in acquired 5-fluorouracil (5-FU) resistance colorectal cell line (SW480/DAR) abundantly through a receptor-mediated endocytosis, thus resulting in cell death through S phase arrest (Chen et al., 2015).

More interestingly, EGFR-targeted MNs also could deliver small interfering RNA (siRNA) to directly silence the gene expression with complementary messenger RNA (mRNA) sequence, particularly the reversal of drug resistance (Chen et al., 2018; Cao et al., 2020; Tieu et al., 2021). The inhibition ratio was up to $74 \pm 6\%$ when incubated with EGFR-pSiNPs through the dual treatments of chemotherapy and genetic therapy. EGFR-pSiNPs were further used as an efficient vehicle to deliver camptothecin to solve its poor water-soluble and toxic side effects (Landgraf et al., 2020). Shao et al. developed a targeted gene-drug co-delivery system based on polyamidoamine (PAMAM) mediated HMSNs (Zhang et al., 2020a). CRISPR/Cas9 was chosen to provide gene therapy, meanwhile, Sorafenib acts as molecular target by specifically inhibiting EGFR or VEGFR2 on hepatocellular carcinoma. Importantly, the co-delivery therapeutic systems caused 85% specific targeting tumor inhibition *in vivo* models. Furthermore, the nanocomplex showed high accumulation at the tumor site *in vivo* and exhibited good safety with no damage to major organs. Ji et al. also proved that using MSNs to deliver cetuximab and DOX could accomplish effective management of EGFR-mutant lung cancer and overcome acquired drug resistance (PC9-DR). The resultant MSNs have the specific surface area of $887.9 \text{ m}^2/\text{g}$ and the pore size of 2.5 nm, which is suitable to carry cetuximab, gefitinib, and DOX into cells with high EGFR expression by endocytosis. Significant effect upon inhibiting PC9-DR xenograft tumor growth was observed; the weight of the xenograft tumors decreased to 0.1 g, indicating the potential ability to solve drug resistance (Wang et al., 2016). Brinker et al. recently synthesized the mesoporous silica nanoparticles-supported lipid bilayers conjugating of gemcitabine to endow active EGFR targeting (Durfee et al., 2016). They emphasized on the factors influencing size uniformity and long-term stability in complex biological media. As expected, compared with EGFR-negative control cells, significant bonding specificity was observed and the maximal binding was realized at 30 min of incubation by flow cytometry combined with fluorescence microscopy. Additionally, Brennan et al. proved the ultrasmall SNs (<8 nm) as drug delivery to improve the biological characteristics and therapeutic properties of gefitinib. The ultrasmall size of SNs was conducive to increase tumor accumulation and dominant renal excretion (Weissleder et al., 2014; Bregoli et al., 2016).

EGFR-labeled MSNs were also used as directional carriers of nano-contrast agents for real-time tumor detection. Gadolinium (Gd^{3+}) is well known as an exogenous contrast agent with strong T1-weighted image signal intensity, however, high doses and indiscriminate accumulation result in terrible side-effects for normal tissues. Therefore, EGFR antibody conjugated SNs

were utilized for geometric confinement of small molecule Gd-chelate (Sinha et al., 2017). The longitudinal MR relaxivity (r_1) value of before and after EGFR antibody conjugation on Gd-chelate grafted MSNs were calculated as 22.19 and $19.39 \text{ mM}^{-1}\text{S}^{-1}$, respectively. Besides, the fluorophore fluorescein (FITC) is an important auxiliary to implement contrast enhancement. FITC-labeled SNs with the attachment of anti-EGF-receptor-antibodies (Alexa Fluor® 555) were built as a novel contrast agent (AF555-EGFR-FITC- SiO_2 -NPs) (Watermann et al., 2019). It could real-time define tumor borders, contributing to easier surgical intervention in the treatment of carcinoma of the head and neck (Figure 6B). Moreover, Nonell et al. provided a strategy of combining EGFR-targeted MSNs and zinc phthalocyanine (ZnPcOBP) for selective photodynamic therapy (Er et al., 2018). The C225-labeled MSNs were applied as a photosensitizer carrier. The quantum yield of singlet oxygen production of undecorated ZnPcOBP was about 0.60 in toluene. Comfortingly, the fatality rate of ZnPcOBP-loaded-MSNs coated with PEG and C225 (ZnPcOBP-loaded-MSN5) on MIA PaCa-2 cells reached 80%, indicating that abundant photosensitizer molecules were delivering into intracellular membranes via EGFR-targeted cell uptake. This strategy based on EGFR-targeted MSNs could avoid unwanted photo-induced damage to normal tissue cells.

Carbon Dots

The fabrication and bioimaging applications of carbon dots (CQDs) have rapidly advanced in recent years because of their photostability and chemical stability. Importantly, CQDs contain no heavy metals, suggesting lower biotoxicity than semiconductor QDs (Bhirde et al., 2009; Berlin et al., 2011; Sano et al., 2012; Lee et al., 2013; Rungrim et al., 2016; Sengupta et al., 2015). When CQDs were modified with EGF antibody, the functionalized CQDs have been invested with specific targeting. To improve spatial resolution and enhance tissue penetration of fluorescence imaging, the incorporations of CT or MRI agents into EGFR-targeted CQDs could obtain the multimode imaging nanoplatforms. In the clinic, iodine and Gd-chelates are traditional CT and MRI contrast agents that are always chosen to combine with novel nanomaterials. For instance, Zhu et al. prepared the cetuximab-conjugated iodine doped CQDs ((I-CQDs-C225) by a “one-pot” hydrothermal method to construct dual fluorescent/CT bioprobe for targeted imaging (Su et al., 2018). I-CQDs-C225 showed bright blue fluorescence with the quantum yield of 18%, which was similar to that of I-CQDs without antibodies. The CT image brightness of I-CQDs-C225 was nearly equal to or brighter than those iodixanol (commercial contrast agents) at the same concentration. I-CQDs-C225 were abundantly internalized into the lysosomes of HCC827 cells (EGFR-overexpression non-small lung cells) and showed a strong blue fluorescence after incubation for 6 h (Figure 6C). Gd(III)-encapsulated CQDs were conjugated with Ac-Cys-ZEGFR:1907 (a kind of EGFR antibodies) forming an effective MRI contrast agent (Wu et al., 2020). This ideal bioprobe maintained the optimal T1 relaxivity without obvious cellular toxicity. Dong's group constructed sulforaphane-functionalized carbon dots (SFN-

CDs) for EGFR-overexpressing cancer cell targeted imaging and inhibition (Lu et al., 2019). SFN-CDs showed a strong yellow fluorescence at 547 nm, which could effectively avoid the influence of autologous fluorescence in organisms. The results of *in vitro* experiments, targeted imaging, and effective apoptosis of cancer cells were caused by the specific internalization of SFN-CDs (Figure 6D). Interestingly, Zhang et al. recently prepared red-emitting CDs-embedded epitope imprinted polymer (C-MIP) for fluorescence imaging and EGFR-positive tumor cell identification (Zhang et al., 2020b). The fluorescence of C-MIP was quenched with the determination limit of $0.73 \mu\text{g ml}^{-1}$, when C-MIP specifically bonded to the epitopes of EGFR through their imprinted cavities. Erlotinib mediated nitrogen doped CDs (NCDs) also proved that this nanosystem possessed an effective capability for targeted fluorescence imaging of pancreatic cancer cells (Devi et al., 2020). It is worth noting that nitrogen doped content had an effect on photoluminescence of NCDs, and thus NCDs (citric acid: urea = 1:1 by mass) exhibited the strongest fluorescence intensity. EGFR-NCDs by coating bovine serum albumin (BSA) retained their fluorescence even with increased fluorescence intensity to a small extent.

FUTURE PERSPECTIVES AND CONCLUSION

The rapid advance of nanotechnology in recent years has provided progressive strategies for cancer therapy. Various advantages of novel iNPs have been identified as multifunctional nanotherapeutics, especially molecular targeted therapy for cancers. Metal nanoparticles and nonmetallic nanoparticles have unique properties, such as easy accumulation in tumor cells, fluorescence imaging, enhanced Raman scattering, photothermal, and antimicrobial properties. A large number of biomedical applications have been successfully demonstrated *in vitro*. But there is still room for further improvement so that the nanoparticles can be suitable for clinical trials and applications. Some of the challenges that still need to be addressed include improving the stability of nanoparticles in a variety of complex *in vivo* environments, designing proper functionalization to improve biocompatibility and reducing cytotoxicity, effective cost control, and optimization of synthesis protocols. This paper sums up the description and the benefits of different EGFR-loaded nanotechnological platforms based on iNPs.

As we previously described, EGFR-targeted iNPs have a solid role in imaging diagnosis and cancer therapy. However, these

EGFR-targeted antineoplastic agents still have a great distance from nanomedicine in lab to clinical reality and there are many unresolved issues to be elucidated. First of all, regarding the synthesis, the controllable preparation of iNPs with uniform size, high crystallinity, and good morphology is important. Second, combining EGFR-mediated iNPs with the guidance of fluorescence, CT, or MRI imaging has a great perspective to achieve more satisfying therapeutic effect. Therefore, the construction of imaging-guided and EGFR-targeted therapy in one nanoplatform still needs to be further explored to achieve drug delivery monitoring, tumor localization, and treatment effect monitoring. Additionally, whether and why the combination of iNPs with EGFR-KIT or McAb could overcome the drug resistance to a certain extent and suppress the progression of point mutation in the DNA sequence is an urgent issue to understand. Moreover, the pharmacodynamic and pharmacokinetic properties of inorganic nanoparticles are immature. As a consequence, numerous comprehensive studies need to be carried out to scrutinize the pharmacokinetic, biodistribution, and safety profiles of iNPs. Given the interactions between iNPs and immune system in body, the immunotoxicity of iNPs should be further assessed in future.

In a word, great efforts are required to meet the challenges in implementing the transformation from nanomedicine to clinical trials. With profound exploration, iNPs will revolutionize molecular targeted cancer therapy in the near future.

AUTHOR CONTRIBUTIONS

MS and TW designed and wrote the manuscript under LL and WL's supervision. XL and YZ searched articles relating to the subject. JZ helped in final editing. All authors contributed to the article and approved the submitted version.

FUNDING

Financial support by National Natural Science Foundation of China (No. 21871246), the Grant of Jilin Province Science and Technology Committee (No. 20200201082JC), the Science and Technology Innovation and Development projects of Jilin City (No. 20190601178), Jilin Province Education Department the Science and Technology development project (No. JJKH20200741KJ and JJKH20200449KJ) are acknowledged.

REFERENCES

- Avvakumova, S., Pandolfi, L., Soprano, E., Moretto, L., Bellini, M., Galbiati, E., et al. (2019). Does Conjugation Strategy Matter? Cetuximab-Conjugated Gold Nanocages for Targeting Triple-Negative Breast Cancer Cells. *Nanoscale Adv.* 1, 3626–3638. doi:10.1039/c9na00241c
- Bar-Ad, V., Zhang, Q., Harari, P. M., Axelrod, R., Rosenthal, D. I., and Trotti, A. (2016). Correlation between the Severity of Cetuximab-Induced Skin Rash and Clinical Outcome for Head and Neck Cancer Patients: The RTOG Experience. *Int. J. Mol. Sci.* 21, 2956. doi:10.3390/ijms21082956
- Berlin, J. M., Pham, T. T., Sano, D., Mohamedali, K. A., Marcano, D. C., Myers, J. N., et al. (2011). Noncovalent Functionalization of Carbon Nanovectors with an Antibody Enables Targeted Drug Delivery. *ACS Nano* 5, 6643–6650. doi:10.1021/nn2021293
- Bhirde, A. A., Patel, V., Gavard, J., Zhang, G., Sousa, A. A., Masedunskas, A., et al. (2009). Targeted Killing of Cancer Cells *In Vivo* and *In Vitro* with EGF-Directed Carbon Nanotube-Based Drug Delivery. *ACS Nano* 3, 307–316. doi:10.1021/nn800551s
- Bobo, D., Robinson, K. J., Islam, J., Thurecht, K. J., and Corrie, S. R. (2016). Nanoparticle-Based Medicines: A Review of FDA-Approved Materials and Clinical Trials to Date. *Pharm. Res.* 33, 2373–2387. doi:10.1007/s11095-016-1958-5

- Bray, F., Ferlay, J., Soerjomataram, I., Siegel, R. L., Torre, L. A., and Jemal, A. (2018). Global Cancer Statistics 2018: GLOBOCAN Estimates of Incidence and Mortality Worldwide for 36 Cancers in 185 Countries. *CA: A Cancer J. Clinicians* 68, 394–424. doi:10.3322/caac.21492
- Bregoli, L., Movia, D., Gavigan-Imedio, J. D., Lysaght, J., Reynolds, J., and Prina-Mello, A. (2016). Nanomedicine Applied to Translational Oncology: A Future Perspective on Cancer Treatment. *Nanomedicine: Nanotechnology, Biol. Med.* 12, 81–103. doi:10.1016/j.nano.2015.08.006
- Cai, X., Luo, Y., Zhang, W., Du, D., and Lin, Y. (2016). pH-Sensitive ZnO Quantum Dots-Doxorubicin Nanoparticles for Lung Cancer Targeted Drug Delivery. *ACS Appl. Mater. Inter.* 8, 22442–22450. doi:10.1021/acsami.6b04933
- Cao, S., Lin, C., Liang, S., Tan, C. H., Er Saw, P., and Xu, X. (2020). Enhancing Chemotherapy by RNA Interference. *BIO. Integration.* 1, 64–81. doi:10.15212/bioi-2020-0003
- Chen, L., She, X., Wang, T., He, L., Shigdar, S., Duan, W., et al. (2015). Overcoming Acquired Drug Resistance in Colorectal Cancer Cells by Targeted Delivery of 5-FU with EGF Grafted Hollow Mesoporous Silica Nanoparticles. *Nanoscale* 7, 14080–14092. doi:10.1039/c5nr03527a
- Chen, L., She, X., Wang, T., Shigdar, S., Duan, W., and Kong, L. (2018). Mesoporous Silica Nanorods toward Efficient Loading and Intracellular Delivery of siRNA. *J. Nanopart. Res.* 20, 37. doi:10.1007/s11051-017-4115-0
- Chen, T., Zhao, T., Wei, D., Wei, Y., Li, Y., and Zhang, H. (2013). Core-shell Nanocarriers with ZnO Quantum Dots-Conjugated Au Nanoparticle for Tumor-Targeted Drug Delivery. *Carbohydr. Polym.* 92, 1124–1132. doi:10.1016/j.carbpol.2012.10.022
- Chen, X., Liang, R., and Zhu, X. (2020). Anti-EGFR Therapies in Nasopharyngeal Carcinoma. *Biomed. Pharmacother.* 131, 110649. doi:10.1016/j.biopha.2020.110649
- Chen, Y., Du, M., Yu, J., Rao, L., Chen, X., and Chen, Z. (2020). Nanobiohybrids: a Synergistic Integration of Bacteria and Nanomaterials in Cancer Therapy. *BIO. Integration.* 1, 25–36. doi:10.15212/bioi-2020-0008
- Deepagan, V. G., Sarmento, B., Menon, D., Nascimento, A., Jayasree, A., Sreeranganathan, M., et al. (2012). *In Vitro* targeted Imaging and Delivery of Camptothecin Using Cetuximab-Conjugated Multifunctional PLGA-ZnS Nanoparticles. *Nanomedicine* 7, 507–519. doi:10.2217/nnm.11.139
- Devi, J. S. A., Aparna, R. S., Anjana, R. R., Anju, S. M., and George, S. (2020). Erlotinib Conjugated Nitrogen Doped Carbon Nanodots for Targeted Fluorescence Imaging of Human Pancreatic Cancer Cells. *Chemistryselect* 5, 9269–9276. doi:10.1002/slct.202002095
- Dong, C., Feng, W., Xu, W., Yu, L., Xiang, H., Chen, Y., et al. (2020). The Copper Age: Copper (Cu)-Involved Nanotheranostics. *Adv. Sci.* 7, 2001549. doi:10.1002/advs.202001549
- Durfee, P. N., Lin, Y.-S., Dunphy, D. R., Muñoz, A. J., Butler, K. S., Humphrey, K. R., et al. (2016). Mesoporous Silica Nanoparticle-Supported Lipid Bilayers (Protocells) for Active Targeting and Delivery to Individual Leukemia Cells. *ACS Nano* 10, 8325–8345. doi:10.1021/acsnano.6b02819
- Er, Ö., Colak, S., Ocakoglu, K., Ince, M., Bresoli-Obach, R., Mora, M., et al. (2018). Selective Photokilling of Human Pancreatic Cancer Cells Using Cetuximab-Targeted Mesoporous Silica Nanoparticles for Delivery of Zinc Phthalocyanine. *Molecules* 23, 2749. doi:10.3390/molecules23112749
- Er Saw, P., and Jiang, S. (2020). The Significance of Interdisciplinary Integration in Academic Research and Application. *BIO Integration.* 1, 2–5. doi:10.15212/bioi-2020-0005
- Fasano, M., Della Corte, C. M., Viscardi, G., Di Liello, R., Paragliola, F., Sparano, F., et al. (2021). Head and Neck Cancer: the Role of Anti-EGFR Agents in the Era of Immunotherapy. *Ther. Adv. Med. Oncol.* 13, 175883592094941. doi:10.1177/1758835920949418
- Goyal, L., Kongpetch, S., Crolley, V. E., and Bridgewater, J. (2021). Targeting FGFR Inhibition in Cholangiocarcinoma. *Cancer Treat. Rev.* 95, 102170. doi:10.1016/j.ctrv.2021.102170
- Groybeck, N., Stoessel, A., Donzeau, M., da Silva, E. C., Lehmann, M., Strub, J.-M., et al. (2019). Synthesis and Biological Evaluation of 2.4 Nm Thiolate-Protected Gold Nanoparticles Conjugated to Cetuximab for Targeting Glioblastoma Cancer Cells via the EGFR. *Nanotechnology* 30, 184005. doi:10.1088/1361-6528/aaff0a
- Holohan, C., Van Schaeybroeck, S., Longley, D. B., and Johnston, P. G. (2013). Cancer Drug Resistance: an Evolving Paradigm. *Nat. Rev. Cancer* 13, 714–726. doi:10.1038/nrc3599
- Huang, J., Huang, W., Zhang, Z., Lin, X., Lin, H., Peng, L., et al. (2019). Highly Uniform Synthesis of Selenium Nanoparticles with EGFR Targeting and Tumor Microenvironment-Responsive Ability for Simultaneous Diagnosis and Therapy of Nasopharyngeal Carcinoma. *ACS Appl. Mater. Inter.* 11, 11177–11193. doi:10.1021/acsami.8b22678
- Kobayashi, S., Boggan, T. J., Dayaram, T., Jänne, P. A., Kocher, O., Meyerson, M., et al. (2005). EGFR Mutation and Resistance of Non-small-cell Lung Cancer to Gefitinib. *N. Engl. J. Med.* 352, 786–792. doi:10.1056/NEJMoa044238
- Kong, L., Yuan, Q., Zhu, H., Li, Y., Guo, Q., Wang, Q., et al. (2011). The Suppression of Prostate LNCaP Cancer Cells Growth by Selenium Nanoparticles through Akt/Mdm2/AR Controlled Apoptosis. *Biomaterials* 32, 6515–6522. doi:10.1016/j.biomaterials.2011.05.032
- La Salvia, A., Espinosa-Olarte, P., Riesco-Martinez, M. D. C., Anton-Pascual, B., and Garcia-Carbonero, R. (2021). Targeted Cancer Therapy: What's New in the Field of Neuroendocrine Neoplasms? *Cancers (Basel)* 13, 1701. doi:10.3390/cancers13071701
- Landgraf, M., Lahr, C. A., Kaur, I., Shafiee, A., Sanchez-Herrero, A., Janowicz, P. W., et al. (2020). Targeted Camptothecin Delivery via Silicon Nanoparticles Reduces Breast Cancer Metastasis. *Biomaterials* 240, 119791. doi:10.1016/j.biomaterials.2020.119791
- Lee, P.-C., Chiou, Y.-C., Wong, J.-M., Peng, C.-L., and Shieh, M.-J. (2013). Targeting Colorectal Cancer Cells with Single-Walled Carbon Nanotubes Conjugated to Anticancer Agent SN-38 and EGFR Antibody. *Biomaterials* 34, 8756–8765. doi:10.1016/j.biomaterials.2013.07.067
- Lee, Y. T., Tan, Y. J., and Oon, C. E. (2018). Molecular Targeted Therapy: Treating Cancer with Specificity. *Eur. J. Pharmacol.* 834, 188–196. doi:10.1016/j.ejphar.2018.07.034
- Li, B., Jiang, Z., Xie, D., Wang, Y., and Lao, X. (2018). Cetuximab-modified CuS Nanoparticles Integrating Near-Infrared-II-Responsive Photothermal Therapy and Anti-vessel Treatment. *Int. J. Nanomedicine.* Vol. 13, 7289–7302. doi:10.2147/IJN.S175334
- Li, N., Wu, P., Shen, Y. B., Yang, C. H., Zhang, L. W., Chen, Y. L., et al. (2021). WORLD CANCER RESEARCH DAY: A Call to Action for a Coordinated International Research Effort to Prevent, Diagnose, and Treat Cancer. *Clin. Cancer Res.* 27, 963–966. doi:10.1158/1078-0432.CCR-20-2978
- Li, N., Wu, P., Shen, Y., Yang, C., Zhang, L., Chen, Y., et al. (2021). Predictions of Mortality Related to Four Major Cancers in China, 2020 to 2030. *Cancer Commun.* 41, 404–413. doi:10.1002/cac2.12143
- Liu, J., Xu, M., and Yuan, Z. (2020). Immunoscore Guided Cold Tumors to Acquire “Temperature” through Integrating Physicochemical and Biological Methods. *BIO. Integration.* 1, 6–14. doi:10.15212/bioi-2020-0002
- Lu, Q., Dai, X., Zhang, P., Tan, X., Zhong, Y., Yao, C., et al. (2018). Fe₃O₄@Au Composite Magnetic Nanoparticles Modified with Cetuximab for Targeted Magneto-Photothermal Therapy of Glioma Cells. *Int. J. Nanomedicine.* Vol. 13, 2491–2505. doi:10.2147/IJN.S157935
- Lu, W., Du, F., Zhao, X., Shi, L., Shuang, S., Cui, X. T., et al. (2019). Sulfuraphane-Conjugated Carbon Dots: A Versatile Nanosystem for Targeted Imaging and Inhibition of EGFR-Overexpressing Cancer Cells. *ACS Biomater. Sci. Eng.* 5, 4692–4699. doi:10.1021/acsbomaterials.9b00690
- Lu, Y.-J., Lin, P.-Y., Huang, P.-H., Kuo, C.-Y., Shalumon, K. T., Chen, M.-Y., et al. (2018). Magnetic Graphene Oxide for Dual Targeted Delivery of Doxorubicin and Photothermal Therapy. *Nanomaterials* 8, 193. doi:10.3390/nano8040193
- Marega, R., De Leo, F., Pineux, F., Sgrignani, J., Magistrato, A., Naik, A. D., et al. (2013). Functionalized Fe-Filled Multiwalled Carbon Nanotubes as Multifunctional Scaffolds for Magnetization of Cancer Cells. *Adv. Funct. Mater.* 23, 3173–3184. doi:10.1002/adfm.201202898
- McGhee, D. E., and Steele, J. R. (2020). Physical Side-Effects Following Breast Reconstructive Surgery Impact Physical Activity and Function. *Support Care Cancer* 29, 787–794. doi:10.1007/s00520-020-05534-6
- Mendelsohn, J., and Baselga, J. (2000). The EGF Receptor Family as Targets for Cancer Therapy. *Oncogene* 19, 6550–6565. doi:10.1038/sj.onc.1204082
- Moghaddam, L. K., Paschepari, S. R., Zaimy, M. A., Abdalaian, A., and Jebali, A. (2016). The Inhibition of Epidermal Growth Factor Receptor Signaling by Hexagonal Selenium Nanoparticles Modified by siRNA. *Cancer Gene Ther.* 23, 321–325. doi:10.1038/cgt.2016.38
- Mu, K., Zhang, S., Ai, T., Jiang, J., Yao, Y., Jiang, L., et al. (2015). Monoclonal Antibody-Conjugated Superparamagnetic Iron Oxide Nanoparticles for Imaging of Epidermal Growth Factor Receptor-Targeted Cells and Gliomas. *Mol. Imaging* 14, 7290.2015.00002. doi:10.2310/7290.2015.00002

- Muhammad, F., Guo, M., Qi, W., Sun, F., Wang, A., Guo, Y., et al. (2011). pH-Triggered Controlled Drug Release from Mesoporous Silica Nanoparticles via Intracellular Dissolution of ZnO Nanolids. *J. Am. Chem. Soc.* 133, 8778–8781. doi:10.1021/ja200328s
- Noh, M. S., Lee, S., Kang, H., Yang, J.-K., Lee, H., Hwang, D., et al. (2015). Target-specific Near-IR Induced Drug Release and Photothermal Therapy with Accumulated Au/Ag Hollow Nanoshells on Pulmonary Cancer Cell Membranes. *Biomaterials* 45, 81–92. doi:10.1016/j.biomaterials.2014.12.036
- Paez, J. G., Janne, P. A., Lee, J. C., Tracy, S., Greulich, H., Gabriel, S., et al. (2004). EGFR Mutations in Lung Cancer: Correlation with Clinical Response to Gefitinib Therapy. *Science* 304, 1497–1500. doi:10.1126/science.1099314
- Pao, W., Miller, V. A., Politi, K. A., Riely, G. J., Somwar, R., Zakowski, M. F., et al. (2005). Acquired Resistance of Lung Adenocarcinomas to Gefitinib or Erlotinib Is Associated with a Second Mutation in the EGFR Kinase Domain. *PLoS Med* 2, e73. doi:10.1371/journal.pmed.0020073
- Pearce, A., Haas, M., Viney, R., Pearson, S.-A., Haywood, P., Brown, C., et al. (2017). Incidence and Severity of Self-Reported Chemotherapy Side Effects in Routine Care: A Prospective Cohort Study. *Plos One* 12, e0184360. doi:10.1371/journal.pone.0184360
- Pi, J., Jiang, J., Cai, H., Yang, F., Jin, H., Yang, P., et al. (2017). GE11 Peptide Conjugated Selenium Nanoparticles for EGFR Targeted Oridonin Delivery to Achieve Enhanced Anticancer Efficacy by Inhibiting EGFR-Mediated PI3K/AKT and Ras/Raf/MEK/ERK Pathways. *Drug Deliv.* 24, 1549–1564. doi:10.1080/10717544.2017.1386729
- Rungnim, C., Rungrotmongkol, T., Kungwan, N., and Hannongbua, S. (2016). Protein-protein Interactions between SWCNT/chitosan/EGF and EGF Receptor: a Model of Drug Delivery System. *J. Biomol. Struct. Dyn.* 34, 1919–1929. doi:10.1080/07391102.2015.1095114
- Sano, D., Berlin, J. M., Pham, T. T., Marcano, D. C., Valdecana, D. R., Zhou, G., et al. (2012). Noncovalent Assembly of Targeted Carbon Nanovectors Enables Synergistic Drug and Radiation Cancer Therapy *In Vivo*. *ACS Nano* 6, 2497–2505. doi:10.1021/nl204885f
- Sengupta, A., Mezenec, R., McDonald, J. F., and Prausnitz, M. R. (2015). Delivery of siRNA to Ovarian Cancer Cells Using Laser-Activated Carbon Nanoparticles. *Nanomedicine* 10, 1775–1784. doi:10.2217/nnm.15.27
- She, X., Chen, L., Velleman, L., Li, C., He, C., Denman, J., et al. (2015). The Control of Epidermal Growth Factor Grafted on Mesoporous Silica Nanoparticles for Targeted Delivery. *J. Mater. Chem. B* 3, 6094–6104. doi:10.1039/c5tb00790a
- She, X., Chen, L., Velleman, L., Li, C., Zhu, H., He, C., et al. (2015). Fabrication of High Specificity Hollow Mesoporous Silica Nanoparticles Assisted by Eudragit for Targeted Drug Delivery. *J. Colloid Interf. Sci.* 445, 151–160. doi:10.1016/j.jcis.2014.12.053
- Siegel, R. L., Miller, K. D., Fuchs, H. E., and Jemal, A. (2021). Cancer Statistics, 2021. *CA A. Cancer J. Clin.* 71, 7–33. doi:10.3322/caac.21654
- Sinha, S., Tong, W. Y., Williamson, N. H., McInnes, S. J. P., Puttick, S., Cifuentes-Rius, A., et al. (2017). Novel Gd-Loaded Silicon Nanohybrid: A Potential Epidermal Growth Factor Receptor Expressing Cancer Cell Targeting Magnetic Resonance Imaging Contrast Agent. *ACS Appl. Mater. Inter.* 9, 42601–42611. doi:10.1021/acsami.7b14538
- Song, L., Able, S., Johnson, E., and Vallis, K. A. (2017). Accumulation of ¹¹¹In-Labelled EGF-Au-PEG Nanoparticles in EGFR-Positive Tumours Is Enhanced by Coadministration of Targeting Ligand. *Nanotheranostics* 1, 232–243. doi:10.7150/ntno.19952
- Su, H., Liao, Y., Wu, F., Sun, X., Liu, H., Wang, K., et al. (2018). Cetuximab-conjugated Iodine Doped Carbon Dots as a Dual Fluorescent/CT Probe for Targeted Imaging of Lung Cancer Cells. *Colloids Surf. B: Biointerfaces* 170, 194–200. doi:10.1016/j.colsurfb.2018.06.014
- Sundarraj, S., Thangam, R., Sujitha, M. V., Vimala, K., and Kannan, S. (2014). Ligand-conjugated Mesoporous Silica Nanorattles Based on Enzyme Targeted Prodrug Delivery System for Effective Lung Cancer Therapy. *Toxicol. Appl. Pharmacol.* 275, 232–243. doi:10.1016/j.taap.2014.01.012
- Tieu, T., Wojnilowicz, M., Huda, P., Thurecht, K. J., Thissen, H., Voelcker, N. H., et al. (2021). Nanobody-displaying Porous Silicon Nanoparticles for the Co-delivery of siRNA and Doxorubicin. *Biomater. Sci.* 9, 133–147. doi:10.1039/d0bm01335h
- Van Cutsem, E., Köhne, C.-H., Hitt, R., Salazar, J., Chang Chien, C.-R., Makhson, A., et al. (2009). Cetuximab and Chemotherapy as Initial Treatment for Metastatic Colorectal Cancer. *N. Engl. J. Med.* 360, 1408–1417. doi:10.1056/NEJMoa0805019
- Vermorken, J. B., Trigo, J., Hitt, R., Koralewski, P., Diaz-Rubio, E., Rolland, F., et al. (2007). Open-Label, Uncontrolled, Multicenter Phase II Study to Evaluate the Efficacy and Toxicity of Cetuximab as a Single Agent in Patients with Recurrent And/or Metastatic Squamous Cell Carcinoma of the Head and Neck Who Failed to Respond to Platinum-Based Therapy. *J. Clin. Oncol.* 25, 2171–2177. doi:10.1200/JCO.2006.06.7447
- Vibin, M., Vinayakan, R., Fernandez, F. B., John, A., and Abraham, A. (2017). A Novel Fluorescent Quantum Dot Probe for the Rapid Diagnostic High Contrast Imaging of Tumor in Mice. *J. Fluoresc.* 27, 669–677. doi:10.1007/s10895-016-1996-8
- Wang, Y., Huang, H.-Y., Yang, L., Zhang, Z., and Ji, H. (2016). Cetuximab-modified Mesoporous Silica Nano-Medicine Specifically Targets EGFR-Mutant Lung Cancer and Overcomes Drug Resistance. *Sci. Rep.* 6, 25468. doi:10.1038/srep25468
- Wang, Y., Wang, Y., Chen, G., Li, Y., Xu, W., and Gong, S. (2017). Quantum-Dot-Based Theranostic Micelles Conjugated with an Anti-EGFR Nanobody for Triple-Negative Breast Cancer Therapy. *ACS Appl. Mater. Inter.* 9, 30297–30305. doi:10.1021/acsami.7b05654
- Watermann, A., Gieringer, R., Bauer, A.-M., Kurch, S., Kiesslich, R., Tremel, W., et al. (2019). Fluorescein- and EGFR-Antibody Conjugated Silica Nanoparticles for Enhancement of Real-Time Tumor Border Definition Using Confocal Laser Endomicroscopy in Squamous Cell Carcinoma of the Head and Neck. *Nanomaterials* 9, 1378. doi:10.3390/nano9101378
- Weissleder, R., Nahrendorf, M., and Pittet, M. J. (2014). Imaging Macrophages with Nanoparticles. *Nat. Mater.* 13, 125–138. doi:10.1038/nmat3780
- Westover, D., Zugazagoitia, J., Cho, B. C., Lovly, C. M., and Paz-Ares, L. (2018). Mechanisms of Acquired Resistance to First- and Second-Generation EGFR Tyrosine Kinase Inhibitors. *Ann. Oncol.* 29, 110–119. doi:10.1093/annonc/mdx703
- Wu, T., and Dai, Y. (2017). Tumor Microenvironment and Therapeutic Response. *Cancer Lett.* 387, 61–68. doi:10.1016/j.canlet.2016.01.043
- Wu, Y., Li, H., Yan, Y., Wang, K., Cheng, Y., Li, Y., et al. (2020). Affibody-Modified Gd@C-Dots with Efficient Renal Clearance for Enhanced MRI of EGFR Expression in Non-small-cell Lung Cancer. *Int. J. Nanomedicine*. Vol. 15, 4691–4703. doi:10.2147/IJN.S244172
- Yan, X., Li, S., Qu, Y., Wang, W., Chen, B., Liu, S., et al. (2020). Redox-Responsive Multifunctional Polypeptides Conjugated with Au Nanoparticles for Tumor-Targeting Gene Therapy and Their 1 + 1 > 2 Synergistic Effects. *ACS Biomater. Sci. Eng.* 6, 463–473. doi:10.1021/acsbomaterials.9b01581
- Yang, M., Cheng, K., Qi, S., Liu, H., Jiang, Y., Jiang, H., et al. (2013). Affibody Modified and Radiolabeled Gold-Iron Oxide Hetero-Nanostructures for Tumor PET, Optical and MR Imaging. *Biomaterials* 34, 2796–2806. doi:10.1016/j.biomaterials.2013.01.014
- Yang, M., Li, J., Gu, P., and Fan, X. (2021). The Application of Nanoparticles in Cancer Immunotherapy: Targeting Tumor Microenvironment. *Bioactive Mater.* 6, 1973–1987. doi:10.1016/j.bioactmat.2020.12.010
- Yazdi, M. H., Mahdavi, M., Varastehmoradi, B., Faramarzi, M. A., and Shahverdi, A. R. (2012). The Immunostimulatory Effect of Biogenic Selenium Nanoparticles on the 4T1 Breast Cancer Model: an *In Vivo* Study. *Biol. Trace Elem. Res.* 149, 22–28. doi:10.1007/s12011-012-9402-0
- Yu, D., Zhang, Y., Lu, H., and Zhao, D. (2017). Silver Nanoparticles Coupled to Anti-EGFR Antibodies Sensitize Nasopharyngeal Carcinoma Cells to Irradiation. *Mol. Med. Rep.* 16, 9005–9010. doi:10.3892/mmr.2017.7704
- Yun, B., Zhu, H., Yuan, J., Sun, Q., and Li, Z. (2020). Synthesis, Modification and Bioapplications of Nanoscale Copper Chalcogenides. *J. Mater. Chem. B* 8, 4778–4812. doi:10.1039/d0tb00182a
- Zhan, C., Huang, Y., Lin, G., Huang, S., Zeng, F., and Wu, S. (2019). A Gold Nanocage/Cluster Hybrid Structure for Whole-Body Multispectral Photoacoustic Tomography Imaging, EGFR Inhibitor Delivery, and Photothermal Therapy. *Small* 15, 1900309. doi:10.1002/smll.201900309
- Zhang, B.-C., Luo, B.-Y., Zou, J.-J., Wu, P.-Y., Jiang, J.-L., Le, J.-Q., et al. (2020). Co-delivery of Sorafenib and CRISPR/Cas9 Based on Targeted Core-Shell Hollow Mesoporous Organosilica Nanoparticles for Synergistic HCC Therapy. *ACS Appl. Mater. Inter.* 12, 57362–57372. doi:10.1021/acsami.0c17660
- Zhang, C., Bu, W., Ni, D., Zhang, S., Li, Q., Yao, Z., et al. (2016). Synthesis of Iron Nanometallic Glasses and Their Application in Cancer Therapy by a Localized Fenton Reaction. *Angew. Chem. Int. Ed.* 55, 2101–2106. doi:10.1002/anie.201510031

- Zhang, M., Wang, J., Wang, W., Zhang, J., and Zhou, N. (2017). Magnetofluorescent Photothermal Micelles Packaged with GdN@CQDs as Photothermal and Chemical Dual-Modal Therapeutic Agents. *Chem. Eng. J.* 330, 442–452. doi:10.1016/j.cej.2017.07.138
- Zhang, M., Wu, F., Wang, W., Shen, J., Zhou, N., and Wu, C. (2019). Multifunctional Nanocomposites for Targeted, Photothermal, and Chemotherapy. *Chem. Mater.* 31, 1847–1859. doi:10.1021/acs.chemmater.8b00934
- Zhang, P., Zhai, J., Gao, X., Zhao, H., Su, W., and Zhao, L. (2018). Targeted Peptide-Au Cluster Binds to Epidermal Growth Factor Receptor (EGFR) in Both Active and Inactive States: a Clue for Cancer Inhibition through Dual Pathways. *Sci. Bull.* 63, 349–355. doi:10.1016/j.scib.2018.02.007
- Zhang, X., Li, Y., Wei, M., Liu, C., Yu, T., and Yang, J. (2019). Cetuximab-modified Silica Nanoparticle Loaded with ICG for Tumor-Targeted Combinational Therapy of Breast Cancer. *Drug Deliv.* 26, 129–136. doi:10.1080/10717544.2018.1564403
- Zhang, Y., Li, S., Ma, X.-T., He, X.-W., Li, W.-Y., and Zhang, Y.-K. (2020). Carbon Dots-Embedded Epitope Imprinted Polymer for Targeted Fluorescence Imaging of Cervical Cancer via Recognition of Epidermal Growth Factor Receptor. *Microchim Acta* 187, 228. doi:10.1007/s00604-020-4198-7
- Zhang, Y., Zhao, N., Qin, Y., Wu, F., Xu, Z., Lan, T., et al. (2018). Affibody-functionalized Ag₂S Quantum Dots for Photoacoustic Imaging of Epidermal Growth Factor Receptor Overexpressed Tumors. *Nanoscale* 10, 16581–16590. doi:10.1039/c8nr02556h
- Zhao, D., Sun, X., Tong, J., Ma, J., Bu, X., Xu, R., et al. (2012). A Novel Multifunctional Nanocomposite C225-Conjugated Fe₃O₄/Ag Enhances the Sensitivity of Nasopharyngeal Carcinoma Cells to Radiotherapy. *Acta Biochim. Biophys. Sinica* 44, 678–684. doi:10.1093/abbs/gms051
- Zhao, Z., He, Z., Huang, H., Chen, J., He, S., Yilihamu, A., et al. (2020). Drug-induced Interstitial Lung Disease in Breast Cancer Patients: a Lesson We Should Learn from Multi-Disciplinary Integration. *BIO. Integration.* 1, 82–91. doi:10.15212/bioi-2020-0009
- Zhou, Y., Fang, X., Gong, Y., Xiao, A., Xie, Y., Liu, L., et al. (2017). The Interactions between ZnO Nanoparticles (NPs) and α -Linolenic Acid (LNA) Complexed to BSA Did Not Influence the Toxicity of ZnO NPs on HepG2 Cells. *Nanomaterials* 7, 91. doi:10.3390/nano7040091

Conflict of Interest: The authors declare that the research was conducted in the absence of any commercial or financial relationships that could be construed as a potential conflict of interest.

Copyright © 2021 Sun, Wang, Li, Li, Zhai, Zhang and Li. This is an open-access article distributed under the terms of the Creative Commons Attribution License (CC BY). The use, distribution or reproduction in other forums is permitted, provided the original author(s) and the copyright owner(s) are credited and that the original publication in this journal is cited, in accordance with accepted academic practice. No use, distribution or reproduction is permitted which does not comply with these terms.



MicroRNA as an Important Target for Anticancer Drug Development

Zhiwen Fu^{1,2}, Liu Wang^{1,2}, Shijun Li^{1,2}, Fen Chen^{1,2}, Kathy Ka-Wai Au-Yeung^{3*} and Chen Shi^{1,2*}

¹Department of Pharmacy, Union Hospital, Tongji Medical College, Huazhong University of Science and Technology, Wuhan, China, ²Hubei Province Clinical Research Center for Precision Medicine for Critical Illness, Wuhan, China, ³St. Boniface Hospital Research Centre, Winnipeg, MB, Canada

OPEN ACCESS

Edited by:

Sanjun Shi,
Chengdu University of Traditional
Chinese Medicine, China

Reviewed by:

Khalil Hajiasgharzadeh,
Tabriz University of Medical
Sciences, Iran
Alfredo Garcia Venzor,
Instituto Nacional de Medicina
Genómica (INMEGEN), Mexico
Ping Sun,
University of Pittsburgh, United States
Saravanakumar Marimuthu,
University of Nebraska Medical
Center, United States
Ipek Erdogan,
Izmir Institute of Technology, Turkey

*Correspondence:

Kathy Ka-Wai Au-Yeung
KAuYeung@sbrc.ca
Chen Shi
219136909@qq.com

Specialty section:

This article was submitted to
Pharmacology of Anti-Cancer Drugs,
a section of the journal
Frontiers in Pharmacology

Received: 05 July 2021

Accepted: 10 August 2021

Published: 25 August 2021

Citation:

Fu Z, Wang L, Li S, Chen F,
Au-Yeung KK-W and Shi C (2021)
MicroRNA as an Important Target for
Anticancer Drug Development.
Front. Pharmacol. 12:736323.
doi: 10.3389/fphar.2021.736323

Cancer has become the second greatest cause of death worldwide. Although there are several different classes of anticancer drugs that are available in clinic, some tough issues like side-effects and low efficacy still need to dissolve. Therefore, there remains an urgent need to discover and develop more effective anticancer drugs. MicroRNAs (miRNAs) are a class of small endogenous non-coding RNAs that regulate gene expression by inhibiting mRNA translation or reducing the stability of mRNA. An abnormal miRNA expression profile was found to exist widely in cancer cell, which induces limitless replicative potential and evading apoptosis. MiRNAs function as oncogenes (oncomiRs) or tumor suppressors during tumor development and progression. It was shown that regulation of specific miRNA alterations using miRNA mimics or antagomirs can normalize the gene regulatory network and signaling pathways, and reverse the phenotypes in cancer cells. The miRNA hence provides an attractive target for anticancer drug development. In this review, we will summarize the latest publications on the role of miRNA in anticancer therapeutics and briefly describe the relationship between abnormal miRNAs and tumorigenesis. The potential of miRNA-based therapeutics for anticancer treatment has been critically discussed. And the current strategies in designing miRNA targeting therapeutics are described in detail. Finally, the current challenges and future perspectives of miRNA-based therapy are conferred.

Keywords: microRNA, anticancer therapeutics, drug target, MiRNA mimics, antagomirs, oncomirs, tumor suppressor miRNAs

INTRODUCTION

When researchers first discovered miRNAs in 1993, they did not realize the importance of these miRNAs. Because the first miRNAs gene Lin-4 found from the *C. elegans* that controls the timing development in its life cycle is considered to be unique in the *C. elegans*. (Lee et al., 1993). However, hundreds of miRNAs were found in different species including mammals by traditional cloning and bioinformatics methods, which attracted the attention of scientists in various fields, especially for let-7 (Reinhart et al., 2000). Up to present, a total of 38,589 miRNAs have been recorded in miRBase (v222018, www.mirbase.org), an online miRNA database. MiRNA is a single chain non-coding endogenous RNA with a length of around 22 nucleotides, which is a post-transcription regulatory factor. It plays an important regulatory role mainly by inhibiting mRNA translation or reducing the stability of mRNA. More than 90% of miRNA is in the region of encoding protein genes or introns of the gene, and few of them are in the exon region of the gene. miRNAs located in intergenic regions

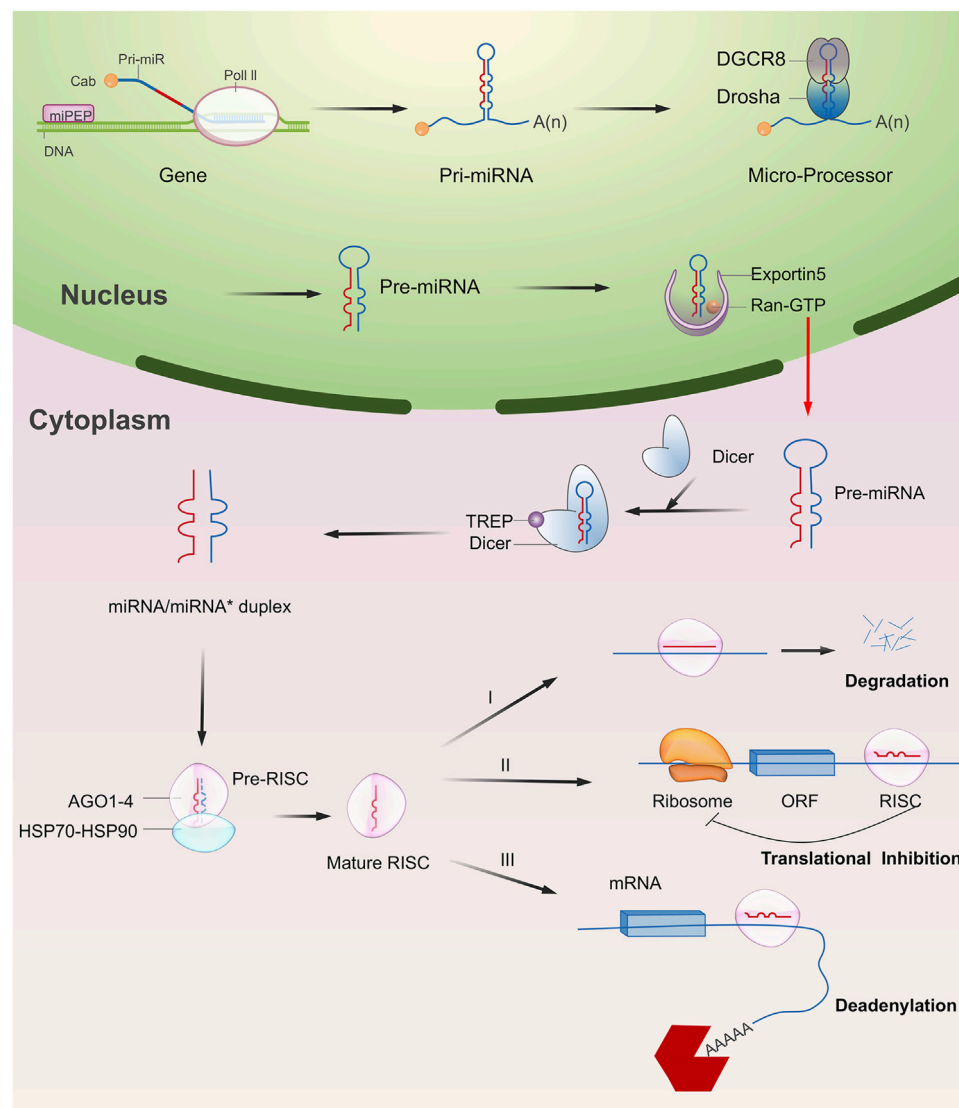


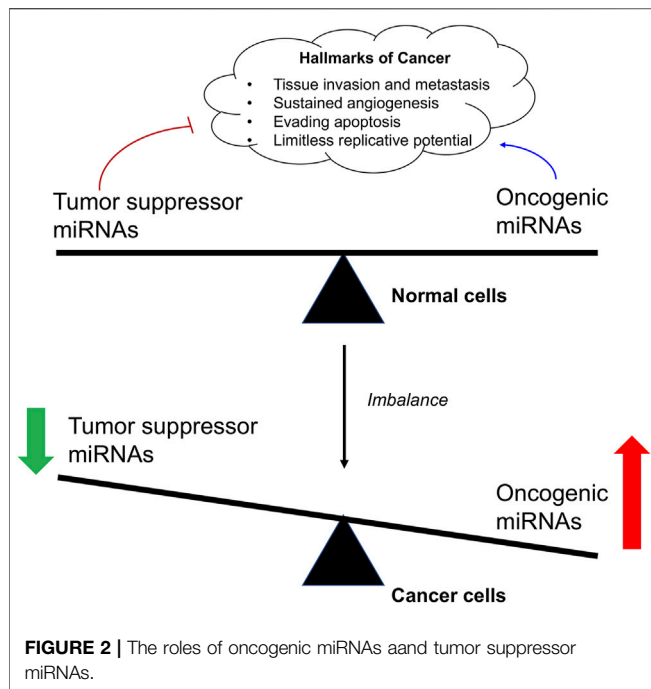
FIGURE 1 | Overview of miRNA biogenesis and functions. Typically, miRNA begins with a transcription to generate the pri-miRNA. It was next processed into pre-miRNA with hairpin structure by Drosha and DGCR8 enzymes (microprocessor complex). The pre-miRNA is then exported to the cytoplasm and forms a double stranded miRNA under the processing of Dicer enzyme. A single stranded RNA that is cleaved from the double stranded miRNA is transported and assembled into a protein complex composed of Argonaute to form a RNA induced silencing complex (RISC). In most cases, RISC binds to target mRNAs to induce translational repression, deadenylation, and degradation.

have independent promoter elements, while those located in coding protein genes can share specific promoter elements with host genes in addition to their own independent promoters (Bartel, 2009).

The biosynthesis pathway of miRNA in animal cells is a complex process starting from nucleus to cytoplasm (Figure 1). For most of miRNAs, a primitive miRNA (pri-miRNA) is first formed from DNA sequences, and then processed into pre-miRNA with hairpin structure by Drosha and DGCR8 enzymes. Under the action of transporters composed of Ran-GTP and Exportin-5, pre-miRNA is transported to the cytoplasm and forms a double stranded miRNA under the processing of Dicer enzyme. A single stranded RNA that is

cleaved from the double stranded miRNA is transported and assembled into a protein complex composed of Argonaute to form a RNA induced silencing complex (RISC), which can recognize the target gene and play an inhibitory role (Peng and Croce, 2016; Lou et al., 2018). A single miRNA could regulate the mRNA of more than one target gene, and each target gene mRNA could also be regulated by multiple miRNAs. The miRNA binding to the target mainly plays a regulatory role by post transcriptional inhibition of mRNA translation, or through a cleavage or degradation of mRNA (Wu, 2020a).

Although most of the miRNAs are located in the cytoplasm, some of them are located in the nucleus, directly regulating the transcription process at the DNA level (Pu et al., 2019). For



example, miRNA-373 could up-regulate the expression level of E-cadherin after binding to the E-cadherin promoter (Wang et al., 2018a). MiRNA-mediated gene regulation is a basic post transcriptional regulatory pathway in human beings, which regulates 90% of protein-coding genes and participates in many cell biological processes (Makarova and Kramerov, 2007; Czimmerer et al., 2013). In cancer cells, mature miRNAs were found to play a crucial role in the cancer pathogenesis as an oncogenic or tumor suppressor agent because imbalance of miRNA regulation seem to be markedly associated to cancer cell proliferation, invasion, migration and metastasis, as well as apoptosis (He et al., 2020). The restoration of abnormal miRNA alterations in cancer cells using miRNA mimics or antagomirs could normalize the gene regulatory network and signaling pathways, and even reverse the phenotype (He et al., 2020; Otoukesh et al., 2020). Therefore, miRNA-based therapy provides a promising anti-cancer strategy for cancer therapy and miRNA could be also regarded as a good target for the development of anticancer drugs. In this review paper, we will summarize the latest research on the miRNA-based therapeutics for cancer and the development of anticancer drugs targeting miRNA.

MICRORNA AND CANCERS

Cancer is a genetic disease characterized by the uncontrollable cell proliferation and apoptosis with the tumor suppressor gene mutation (He et al., 2020). Since the emergence of recombinant DNA technology, to identify the underlying mutated genes that contributes to the development of a cancer has been the central goal of cancer research. For example, the transcription factors (myc genes), Src-family, epidermal growth factor receptor (EGFR),

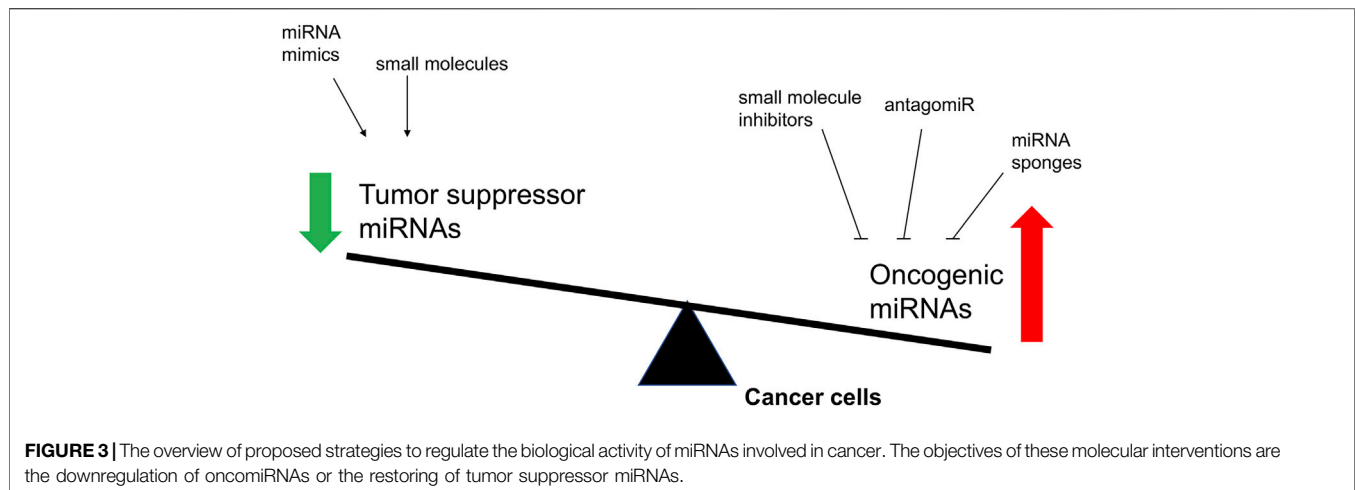
and Raf kinase have been performed extensive researches in cancer research (Elbadawy et al., 2019; Parkin et al., 2019). In recent years, emerging evidence has shown that miRNA is also closely related to the occurrence of various types of cancers (Song and Meltzer, 2012; Chen et al., 2015a; Takasaki, 2015; Gao et al., 2018). Studies have shown that a single miRNA may bind to up to 200 targets with different functions, including transcription factors, receptors and vectors. MiRNA may control about 30% of human mRNA expression involved in cell growth, differentiation and apoptosis (Figure 2). Moreover, the expression of some types of miRNAs is found to be significantly different between normal tissues and tumor tissues, suggesting its important role in tumor occurrence, development, invasion, and metastasis (Gaur et al., 2007; Lee et al., 2008).

Based on their differential roles in the regulation of mRNA in cancer cells, miRNA are divided into oncogenic miRNAs, also known as oncomiRs, and tumor suppressor miRNAs (Table 1). For examples, the miR-15a and miR-16 were identified as the first tumor-suppressive miRNA, which negatively regulate bcl-2 (Cimmino et al., 2005). Bcl-2 is an anti-apoptotic gene, which is overexpressed in a variety of tumors, including leukemia and lymphoma (Warren et al., 2019). Therefore, the deletion or down-regulation of these two miRNAs leads to the increase of bcl-2 expression and promotes the occurrence of leukemia and lymphoma. Let-7, as one of the first identified miRNAs, is found to inhibit the expression of oncogene Ras (Johnson et al., 2005; Chirshv et al., 2019). About 15–30% of human tumors contain Ras mutation, it would cause cell transformation when the Ras mutation is activated with increased protein expression of bcl-2 (Kapoor et al., 2020). The analysis of 21 patients with different types of tumor showed that the expression of let-7 decreased significantly in twelve lung cancer patients, but only partially decreased in other tumor patients. *In vitro* tissue culture test also showed that the transient increase of let-7 in human lung cancer cells could inhibit the proliferation of cancer cells, which also indicated that let-7 might be a tumor suppressor gene in lung tissue (Takamizawa et al., 2004; Huang et al., 2020). It is also interesting to note that overall miRNA expression is lower in cancer cells than in normal cells. This suggests that a subgroup of miRNAs play a role in tumor inhibition, and the loss of their function may promote tumor occurrence. He et al. reported that three miRNAs encoded by miR-34 (miR-34 a-c) were found in human tumors by *in vivo* and *in vitro* tests, which were induced in p53 dependent cell cycle stress response or DNA damage (He et al., 2007). Among them, miR-34a is located on chromosome 1p36, and the deletion of this region could be observed in a variety of tumors (such as neurofibroma). The abnormal expression of these miRNAs down-regulates a variety of cell cycle regulatory genes, such as anti-apoptotic factor Bcl-2, resulting in cell cycle arrest and even apoptosis. Therefore, miR-34 plays an important role in the regulation of cell proliferation and apoptosis and may be used as a tumor suppressor gene.

Alternatively, oncogenic miRNAs that promote tumorigenesis with a highly expressed in tumor tissues have also been identified. The discovery of miR-17-92 provided the first functional evidence of such an oncomiR (Gruszka and Zakrzewska, 2018). In B-cell lymphoma and cell lines, the pri-miRNA and

TABLE 1 | Aberrant expression of miRNA in cancers.

Tumor suppressor miRs (Down-regulation)		Reference	OncomiRs (Up-regulation)		Reference
miR-1	bladder, colon, lung, breast, liver, prostate, gastric cancer	Yoshino et al. (2011), Hudson et al. (2012), Reid et al. (2012), Liu et al. (2015a), Han et al. (2017)	miR-10b	esophageal cancer, gastric cancer	Tian et al. (2010), Wang et al. (2013a)
miR-7	pancreatic and colorectal cancer	Xu et al. (2014a), Xia et al. (2018)	miR-17	Neuroblastoma	Fontana et al. (2008)
let-7	breast, lung, colon, ovarian cancer	Esquela-Kerscher et al. (2008), Chirshv et al. (2019)	miR-21	Breast, colon, pancreatic, lung, prostate, liver and stomach cancer	Chan et al. (2005), Volinia et al. (2006), Zhu et al. (2007)
miR-9	ovarian cancer	Tang et al. (2013)	miR-23b	Renal cancer	Liu et al. (2010)
miR-15a	chronic lymphocytic	qeilan et al. (2010)	miR-27a	Prostate cancer	Fletcher et al. (2012)
miR-16	leukemia, prostate cancers,	Kang et al. (2015), Pekarsky and Croce (2015)	miR-100	Myeloid leukemia, glioma	Ng et al. (2010)
family	gastric cancer				
miR-18a	colorectal cancer	Humphreys et al. (2014)	miR-155	Lymphoma, leukemia, breast, colon, lung, pancreatic, thyroid brain cancer, diffuse large B-cell lymphoma	Jiang et al. (2010), Ling et al. (2013)
miR-25	prostate cancer	Zoni et al. (2015)	miR-222	osteosarcoma, glioma, breast cancer, follicular thyroid carcinoma, digestive system carcinoma	Quintavalle et al. (2012), Chen et al. (2013a), Matsuzaki and Suzuki (2015)
miR-27a	prostate cancer	Scheibner et al. (2012)	miR-296	Brain tumors	Würdinger et al. (2008)
miR-29	nasopharyngeal carcinoma, lung cancer, cervical	Sengupta et al. (2008), Garzon et al. (2009), Ugalde et al. (2011)	miR-301	Breast cancer	Shi et al. (2011)
family					
miR-30b	laryngeal carcinoma	Li and Wang, (2014)	miR-372	Testicular tumors	Voorhoeve et al. (2006)
miR-31	breast cancer, lung adenocarcinoma	Barrett-Lee (2009), Hou et al. (2016)	miR-375	Gastric cancer	Xu et al. (2014b)
miR-33	chronic myelogenous leukemia, colon carcinoma, breast cancer	Ibrahim et al. (2011), Thomas et al. (2012), Lin et al. (2015)	miR-378	Breast carcinoma	Lee et al. (2007)
family	lung metastasis, osteosarcoma				
miR-34	breast, lung, colon, kidney, prostate, bladder, pancreatic, bone and lung cancer, and melanoma	Bommer et al. (2007), Fujita et al. (2008), Saito et al. (2015)	miR-519a	Hepatocellular carcinoma, breast cancer	Shao et al. (2015), Tu et al. (2016)
family					
miR-124	intrahepatic, bladder, colorectal and lung cancer, osteosarcoma, neuroblastoma, glioma	Huang et al. (2011), Kato et al. (2014), Taniguchi et al. (2015)	miR-675	Colorectal cancer	Tsang et al. (2010)
miR-126	non-small cell lung cancer cells, breast, thyroid, liver, colorectal cancer, osteosarcoma	Sun et al. (2010), Wang et al. (2015), Wen et al. (2015), Xiong et al. (2015)	miR-182	Melanoma	Segura et al. (2009)
miR-128	glioblastoma, hepatocellular carcinoma, acute lymphoblastic leukemia	Zhang et al. (2009), Wuchty et al. (2011), Shi et al. (2012)	miR-483	esophageal cancer, prostate cancer	Ma et al. (2016), Yang et al. (2017)
miR-145	esophageal squamous cell carcinoma, colon carcinoma, gastric cancer, neuroblastoma	Kano et al. (2010), Ibrahim et al. (2011), Gao et al. (2013)	miR-9	Breast cancer, cervical cancer, leukemias	Selcuklu et al. (2012), Chen et al. (2013b), Azizmohammadi et al. (2017)
miR-193b	breast cancer, pancreatic ductal adenocarcinoma	Gambari et al. (2016), Yang et al. (2016)	miR-132		
miR-198	hepatocellular carcinoma	Tan et al. (2011)			
miR-204	neuroblastoma, glioma	Bao et al. (2013), Xia et al. (2015)			
miR-205	prostate cancer	Gandellini et al. (2009)			
miR-206	breast cancer	Chen et al. (2015b)			
miR-302	breast and liver cancer	Wang et al. (2013b), Liang et al. (2013)			
miR-335	breast cancer	Tavazoie et al. (2008)			
miR-383	medulloblastoma	Li et al. (2013)			
miR-449	gastric cancer, non- small cell lung cancer	Bou Kheir et al. (2011), Luo et al. (2013)			
miR-493	colon, lung cancer	Okamoto et al. (2012), Gu et al. (2014)			
miR-504	hypopharyngeal squamous cell carcinoma	Kikkawa et al. (2014)			
miR-545	pancreatic ductal adenocarcinoma, lung cancer cells	Du et al. (2014), Song et al. (2014)			
miR-596	oral squamous cell carcinoma	Endo et al. (2013)			



mature miRNAs of miR-17-92 were found to be significantly overexpressed (Mihailovich et al., 2015). *In vivo* examination confirmed that enhanced miR-17-92 expression would promote the formation of myc-induced B cell lymphoma and the incidence rate of lymphoma is faster and higher. Furthermore, the expression of miR-17-92 was found to be regulated by myc protein. Myc activates its expression by directly binding to miR-17-92 site on chromosome 13 to down-regulate the expression of transcription factor E2F1 protein, which could induce apoptosis. When a single member of miR-17-92 family was induced to co-express with c-myc, it did not promote the formation of tumor, indicating that the tumorigenic effect of miR-17 family may be caused by the interaction of all members of miR-17 family (Fuziwara and Kimura, 2015). All above suggest that miR-17-92 gene cluster is a potential human oncogene. Another oncomiR, miR-21, is found to be a significant up-regulation in several types of solid tumors, such as lung, breast, prostate, and malignant glioma, supporting its oncogenic role in cancer pathogenesis (Meq, 2013; Amani-Shalamzari et al., 2020; Shakeri et al., 2021). When miR-21 inhibitor was transfected into gastric cancer cell line HEK-293, the proliferation of cancer cells was inhibited, and the apoptosis of cancer cells was induced. It also increased the proportion of G1/S phase of cancer cells, which made the cells to be more sensitive to radiotherapy and chemotherapy (Zhang et al., 2011a). In animal models, when the nude mice were injected the MCF-7 cells transfected with oligonucleotides complementary to miR-21, the tumor volume was significantly decreased as 50% compared with that of control groups, and the inhibition effect on tumor growth lasted for 2 weeks (Si et al., 2007). Some studies have also revealed that miR-483 family could significantly inhibit the expression of PDGFB and directly down regulate the proliferation, migration and other malignant behaviors of human umbilical vein endothelial like cells. It was also showed that miR-483 family was shown to down-regulate the phosphorylation of Akt protein in PI3K/Akt signaling pathway after negatively regulating PDGFB (Bertero et al., 2013).

From the above, the rise of miRNA research has made scientists gradually realize that miRNA plays an irreplaceable role in the complex molecular network of oncogenes and tumor suppressor

genes. The expression of miRNAs in tumors could be reduced, deleted or increased, and its expression changes are related to gene deletion, translocation, amplification or virus infection. As miRNA is a regulatory molecule in the process of gene expression and protein translation, and it plays a pivotal role in the regulation of tumor occurrence. With the breakthrough of important theories on cancer pathogenesis and the solution of difficult problems in diagnosis and treatment, it will be possible to effectively control and treat cancer in extensive research in the future.

POTENTIAL OF MICRORNA-BASED THERAPEUTICS FOR ANTICANCER TREATMENT

As the imbalance of miRNA expression level is associated with tumorigenesis, restoring miRNA function and inhibition of overexpressed miRNAs in cancer represent the two major approaches to develop miRNA-based cancer therapies (He et al., 2020) (Figure 3). Restoring miRNA function usually applied the miRNA mimics and some small molecules, which could enhance the function of endogenous miRNAs and restore the expression of tumor suppressive miRNAs, while inhibition of overexpressed miRNAs included the small molecule inhibitors, antagomiRs, and miRNA sponges, that specifically target oncomiRs which are overexpressed in cancer cells.

Restoring miRNA Function in Cancer

Since those miRNAs play the role as tumor suppressors, restoration of reduced tumor suppressor miRNA function to normal level by miRNA mimics represents a promising cancer treatment strategy (To et al., 2020). Indeed, the gene therapy methods were applied to restore the gene function in cancer cells before the discovery of miRNAs. However, it achieved limited success because of the limitations of DNA plasmids and viral vectors (Roma-Rodrigues et al., 2020). In recent decades, the rapid development of miRNA technology has provided an alternative tools. The size of miRNA are considerably small than that of protein so that it could permeate into cell easily by some techniques. Esquela-Kerscher et al.

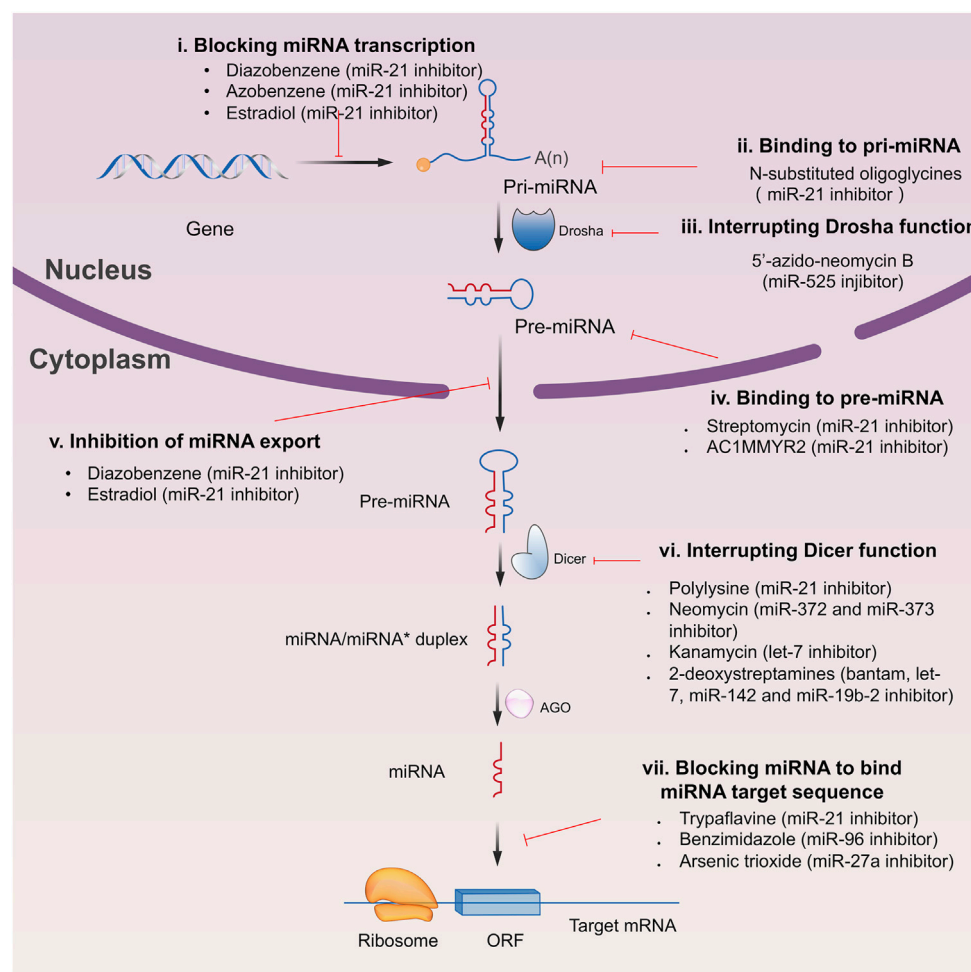


FIGURE 4 | Schematic illustration of different inhibition mechanisms of miRNA specific small molecule inhibitors.

demonstrated that a restoration of the miRNA let-7 could observably inhibit the tumor growth on mice models (Esquela-Kerscher et al., 2008). It was the first time for this study to confirm the tumor suppressor role of let-7 and its potential to use as the targets for cancer therapy. Since then, the therapy of restoring miRNA function by miRNA mimics has rapidly gained interest. The miRNA mimics used for restoring miRNA function are summarized in **Table 2**. Among them, the let-7 and miR-34 families were two members to be the most studied.

Studies have shown that let-7 family miRNAs inhibit well-known oncogenes, like N1RF, myc, HMGA, STAT3, and Ras, and the low expression of let-7 is found to be associated with poor prognosis in lung adenocarcinoma (Esquela-Kerscher et al., 2008). Hence, recovery of its activity may be a feasible strategy for lung cancer therapeutic. On the mouse lung cancer models, the effect of let-7 was examined using different delivery methods. The results showed that the let-7 mimics could reduce tumor growth, induce necrosis and de-repression of the direct let-7 targets Ras and CDK6 (Trang et al., 2010). As for miR-34 family, it was shown to be transcriptionally regulated by the tumor suppressor p53, and depletion or down-regulation of miR-34 has been found in

several cancers (Hermeking, 2010). Through targeting CD44, miR-34a was shown to inhibit metastasis and reduce the growth of tumor (Wiggins et al., 2010). Similar with the supplement by let-7 mimics, when treated with the lipid-complexed miR-34a mimic on the mouse lung cancer models, the tumor volumes were significantly inhibited with a well-tolerated dose range (Wiggins et al., 2010). In the myc-driven liver cancer cells, the expression level of miR-26a was lower than in the normal health cells (Ji et al., 2009). With the replacement of miR-26a mimics to increase miR-26a levels, it would induce the cell cycle arrest through the inhibition of cyclin D2 and E2 (Kota et al., 2009). *In vivo* animals models, the tumor volumes were shown a sensitive response to the administration of miR-26a (Kota et al., 2009). All these above suggest that restoring miRNA function by miRNA mimics could provide a promising strategy for the cancer therapeutics.

Inhibition of Overexpressed miRNAs in Cancer

As for those overexpressed oncomiRs in cancer cells, the suppression of oncomiRs has been widely studied for the

TABLE 2 | Restoring miRNA function by miRNA mimics in cancer.

Target miRNAs	Cancer types	Reference
let-7	lung cancer	Trang et al. (2010), Trang et al. (2011)
miR-34	lung cancer, prostate cancer	Wiggins et al. (2010), Trang et al. (2011)
miR-15	prostate cancer	Bonci et al. (2008)
miR-16	prostate cancer	Takeshita et al. (2010)
miR-145	colon cancer	Ibrahim et al. (2011)
miR-33	colon cancer	Ibrahim et al. (2011)

TABLE 3 | Inhibition of overexpressed miRNAs in cancer.

Target miRNAs	Cancer types	Reference
miR-10b	breast cancer, colorectal cancer	Sun et al. (2013), Song and Li (2019)
miR-132	breast cancer, lung cancer, liver cancer	Li et al. (2015), Zhang et al. (2014), Liu et al. (2015b)
miR-296	breast cancer, colorectal cancer	Savi et al. (2014), He et al. (2017)
miR-222	breast cancer, lung cancer	Shen et al. (2017), Yamashita et al. (2015)
miR-9	ovarian cancer	Tang et al. (2013)
miR-17	kidney cancer, ovarian cancer	Lichner et al. (2015), Gong et al. (2016)

development of novel miRNA-based therapeutics (Table 3). The main inhibitors of miRNA included the small molecule inhibitors and the complementary oligonucleotides, such as anti-miRNA oligonucleotide (AMOS), locked nuclear acid (LNA)-AMOS, antagomirs and miRNA sponge. AMOS is the first miRNA inhibitor based on the principle of complementary with target miRNA sequence to neutralize the function of miRNA (Weiler et al., 2006). AMOS, in the form of a short DNA oligonucleotide strand, specifically combines with complementary endogenous miRNA or its precursor molecules to form stable DNA:RNA, which makes the endogenous miRNA occupied by AMO instead of binding to its target mRNA. miRNA is thus degraded by nuclease to achieve the effect of inhibiting miRNA (Garbett et al., 2010). A series of modified AMOS, such as 2'-O-methyl AMOS, 2'-O-methoxyethyl AMOS and LNA-AMOS, have emerged in the follow-up studies. LNA-AMOS are modified on the structure of AMOS. In detail, it forms a rigid ring through a connection of methylene at the positions of the 2'-oxygen and 4'-position of multiple nucleotides, which is embedded in the C3 position of sugar group. LNA-AMOS are more stable than AMOS, and it has higher selectivity and sensitivity (Weiler et al., 2006). Similar to antagomirs, miRNA sponges could be applied to inhibit miRNA functions by preventing stable binding to their targets. Instead of short oligonucleotide strands, these agents are longer nucleic acids, usually DNA plasmids or transcribed RNA, with several miRNA binding motives.

For example, miR-10b is associated with the metastatic properties with a overexpression in breast and esophagus tumors. Through the inhibition of miR-10b, treatment of mice with the cholesterol-conjugated antagomir-10b resulted in significantly reduced levels of tumor volumes compared with the vehicle group. It is well known that tumor angiogenesis significantly enhances the invasion and metastasis of tumor cells (De Ieso and Yool, 2018; Wang et al., 2018b). With the development of technology for miRNA research, the relationship

between miRNA and tumor angiogenesis becomes more evidently. High expression of miRNA-132 in the endothelium of human tumors could promote pathological angiogenesis (Zhang et al., 2011b). By reducing the expression of miRNA-132, 2'-O-Me modified antimiR-132 was demonstrated a significant decrease in tumor burden and angiogenesis, indicating the potential for miR-132 as a target in anti-angiogenesis therapeutics. In glioma, miR-9 was found an up-regulation compared with normal cells and could promote the tumorigenesis and angiogenesis. It suggested that miR-9 is crucial for glioma pathogenesis and can be treated as a potential therapeutic target for glioma.

MIRNA AS AN IMPORTANT TARGET FOR THE DEVELOPMENT OF ANTICANCER DRUGS

The investigation of drug targets has always been one of the most important contents in the research and development of new drugs. As a molecule widely involved in the regulation of gene expression, miRNA is undoubtedly an important object in the research of drug targets (Schmidt, 2014). Traditional drugs are mainly small chemical molecules targeting single protein in cancer which have certain limitations in clinical use. In contrast, miRNA has the natural characteristics of regulating multiple target genes, and is at the center of the multi-target regulatory network (Wang, 2011a). Moreover, the generation of miRNA is strictly regulated by signal pathway, which involves different important enzymes. MiRNA has such a complex and fine regulatory mechanism that the whole signal pathway has become a promising therapeutic drug or drug therapeutic targets in cancer (Vishnoi and Rani, 2017). Furthermore, miRNA-based drugs target molecules that cannot be target molecules that cannot be targeted by chemical drugs or antibody drugs,

which is expected to make a breakthrough in diseases with poor efficacy of traditional drugs, especially cancer (Yu et al., 2020). Therefore, as drug targets, multi-target regulatory molecular miRNA has attracted more and more attention in the research and development of new drugs used in clinic.

Restoring miRNA by Small Molecules

The down-regulated expression of miRNA can be restored by some small molecular compounds, such as the hypomethylating agents (Galm et al., 2006). Decitabine or 5-azacytidine are two drugs for the treatment of myelodysplastic and they were found to increase the expression of several miRNAs (Lujambio et al., 2007). In addition, enoxacin was also demonstrated to promote the biosynthesis of several miRNAs. In the cell-cultured tests, an overall upregulation of miRNA expression was induced by the treatment of enoxacin (Melo et al., 2011). Moreover, enoxacin reduced the tumor growth by the upregulated expression of 24 mature miRNAs on the mice xenograft models (Melo et al., 2011). All these examples suggested the feasible role of restoring miRNA by small molecules for the anticancer therapeutics.

Restoring miRNA by Oligonucleotides

Another more specific approach for restoring miRNA is miRNA mimics. MiRNA mimics are chemically synthesized double stranded RNA molecules which regulate the function of miRNA by a simulation of endogenous miRNAs (Wang, 2011b). Because of the unstable status of miRNA mimics in the biological system, the core obstacle of the application is to develop an effective delivery system, like the nanoparticles, lipid emulsions, atelocollagen formulations, and adeno-associated virus. It was shown that the target delivery of miR-34a and let-7 mimics using the lipid emulsions could significantly inhibit the cancer progression on a colon xenograft mouse model (Trang et al., 2011). Using the adeno-associated virus as the carrier, the administration of miR-26a was demonstrated an inhibition of cancer cell proliferation and reducing tumor volume (Kota et al., 2009). Importantly, the strategy for restoring miRNA by the liposome-formulated miR-34 mimic (MRX34) has been developed to the clinical trials for the patients with liver cancer (Bader, 2012). The detailed information of MRX34 would be discussed in the subsequent sections.

Inhibiting miRNA by Oligonucleotides

Recent decades, the most frequently used approaches to block the function of miRNA are belongs to antisense oligonucleotides (ASO) and miRNA sponges (Roberts et al., 2020). The former includes the locked nucleic acids (LNAs) and antagomirs. LNA is a synthetic nucleic acid analogue containing bridged, bicyclic sugar moiety. As a novel nucleotide derivative, it has attracted extensive attention in the field of pharmaceutical research and is expected to become a new breakthrough in the treatment of various diseases at the molecular level (Papargyri et al., 2020). It is a special bicyclic nucleotide derivative with one or more 2'-O, 4'-C-methylene in its structure. β -D-furan ribonucleic acid monomer, the 2'-O position and 4'-C position of ribose form oxygen methylene bridge, sulfur methylene bridge or amine

methylene bridge through different shrinkage which are connected into a ring. This ring bridge locks the N configuration of furan sugar C3'- endotype and reduces the flexibility of ribose structure. Since LNA and DNA/RNA have the same phosphate skeleton in structure, it has good recognition ability and strong affinity for DNA and RNA. A higher expression of miR-21 was associated with the cancer initiation and progression of melanoma (Javanmard et al., 2020). *In vitro* studies using B16F10 cell line, a significant reduction was found in the number of transfected cells with LNA-anti-miR-21 and the transfected cells were shown an observable apoptosis. Moreover, the treatment of anti-miR-21 could inhibit the tumor growth in the xenograft mouse models (Javanmard et al., 2020).

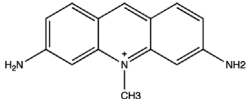
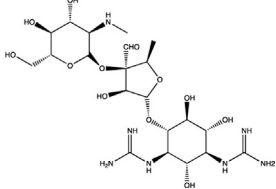
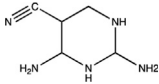
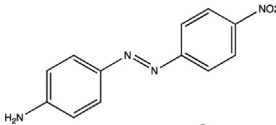
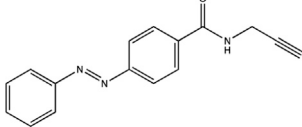
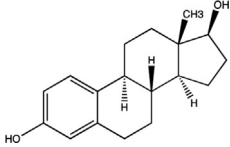
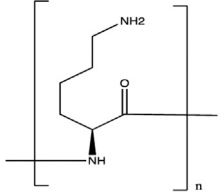
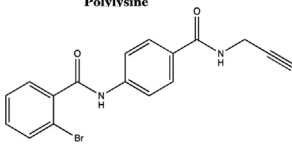
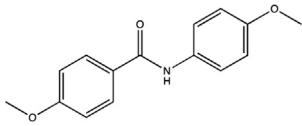
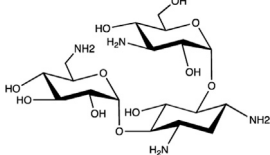
Antagomir is a single stranded small RNA designed according to the mature sequence of microRNA and specially labeled and chemically modified (Scherr et al., 2007). It is an efficient blocker specially used to inhibit endogenous microRNA. Antagomirs often use thiophosphate instead of phosphate to covalently bind with cholesterol at the 3'-end of oligomer to prevent the complementary matching between miRNA and its target gene mRNA by competitive binding with mature miRNA *in vivo*, and inhibit the function of miRNA (Scherr et al., 2007). It has higher stability and inhibition effect *in vivo* and *in vitro*. Arefeh Kardani et al. reported that an inhibition of miR-155 in MCF-7 breast cancer cell lines was induced by the treatment of gold nanoparticles functionalized with antagomir-155 (Kardani et al., 2020). In another study, the inhibition of miR-194 by antagomir-194 significantly reduced the proliferation of MCF-7 and MDA-MB-231 breast cancer cells (Chen et al., 2018).

As for miRNA sponge, it is another effective inhibitor of miRNA. It contains multiple miRNA binding sites (RBS) and can adsorb corresponding miRNA molecules like a sponge. After adsorption, miRNA cannot bind to its target molecules, which affects the function of miRNA (Kluiver et al., 2012). At present, it is found that the molecules that can act as miRNA sponge include long non coding RNA (lncrna) and circular RNA (circular RNA, circrna), these two RNAs can bind miRNA or compete for miRNA target molecules and play a negative regulatory role in miRNA. For example, Shu et al. developed a system to express circular inhibitors of miRNA targeting miR-223 and miR-21 as a sponge. It was shown a more potent suppression of miRNA functions than their linear counterparts for the inhibition of cancer cell growth (Shu et al., 2018).

Small Molecule Inhibitors of microRNA

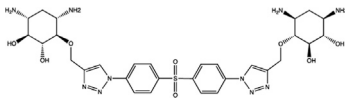
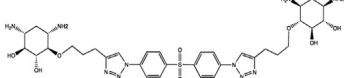
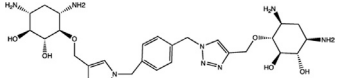
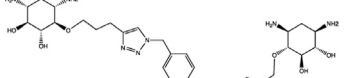

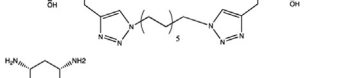
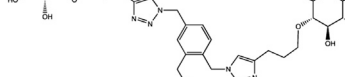
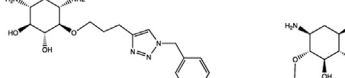
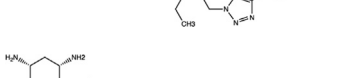
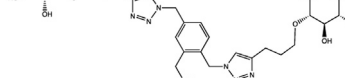
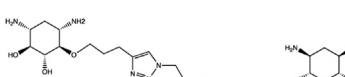
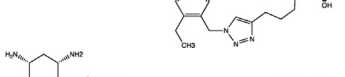
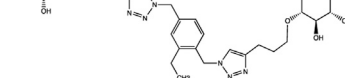
Since the biggest challenge for ASO applied in clinic is the poor cell-permeability for drug delivery, the recent trend is moving toward to the development of small-molecule drugs in the regulation of miRNA. Small molecules could cross the cell membrane by free diffusion, they modulate the function of miRNA like a microRNA mimic. Furthermore, small molecule inhibitors of microRNA are chemical compounds and thus traditional drug development can be applied (Wu, 2020b). At present, there are many kinds of miRNA specific chemical small molecule inhibitors, and their mechanisms are different. The target sites of inhibition and interference are throughout the whole process of miRNA gene expression, processing, maturation

TABLE 4 | The summary of some representative small-molecule miRNA inhibitors.

Target miRNAs	Inhibitors	Structures	Possible mechanisms of action
miR-21	Trypaflavine		Blocking the assembly of miR-21 with Ago2 Watashi et al. (2010)
miR-21/ miR-27a	Streptomycin		Blocking the cleavage of pre-miR-21 by Dicer Bose et al. (2012)
miR-21	AC1MMYR2		Blocking the cleavage of pre-miR-21 to produce mature miR-21 Shi et al. (2013)
miR-21	Diazobenzene		Inhibition the transcription of miR-21 gene Gumireddy et al. (2008)
miR-21	Azobenzene		Inhibition the transcription of miR-21 gene Gumireddy et al. (2008)
miR-21	Estradiol		Inhibition the transcription of miR-21 gene Wickramasinghe et al. (2009)
miR-21	Polylysine		Blocking the formation of mature of pre-miR-21 by the inhibition of Dicer Watashi et al. (2010)
miR-21	4-benzoylamino-N-(prop-2-yn-1-yl)benzamides		Up-regulation of PDCD4, the function target of miR-21 Jiang et al. (2015)
miR-21	Arylamide derivatives		Blocking the mature of pre-miR-21 Naro et al. (2015)
Let-7/ miR-27a	Kanamycin A		Binding to pre-let-7 and blocking the function of Dicer Davies (2008)

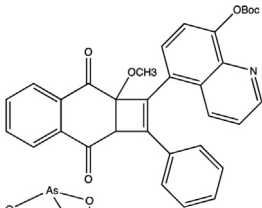
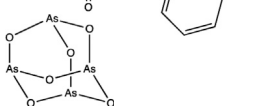
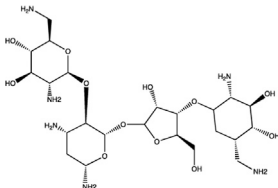
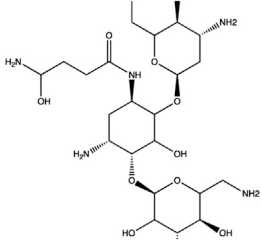
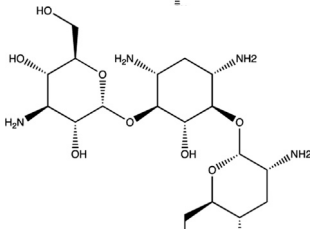
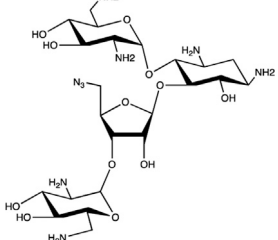
(Continued on following page)

TABLE 4 | (Continued) The summary of some representative small-molecule miRNA inhibitors.

Target miRNAs	Inhibitors	Structures	Possible mechanisms of action
Let-7	2-DOS Compound 1		Binding to pre-let-7 and blocking the function of Dicer Davies (2008)
Let-7	2-DOS Compound 2		Binding to pre-let-7 and blocking the function of Dicer Davies (2008)
Let-7	2-DOS Compound 3		Binding to pre-let-7 and blocking the function of Dicer Davies (2008)
Let-7	2-DOS Compound 4		Binding to pre-let-7 and blocking the function of Dicer Davies (2008)
Let-7	2-DOS Compound 5		Binding to pre-let-7 and blocking the function of Dicer Davies (2008)
Let-7	2-DOS Compound 6		Binding to pre-let-7 and blocking the function of Dicer Davies (2008)
Bantam	2-DOS Compound 7		Binding to pre-bantam and blocking the function of Dicer Davies (2008)
miR-142	2-DOS Compound 8		Binding to pre-miR-142 and blocking the function of Dicer Davies (2008)
miR-19b-2	2-DOS Compound 9		Binding to pre-miR-19b-2 and blocking the function of Dicer Davies (2008)
miR-122	NSC 158959		Inhibition of the transcription of miR-122 Young et al. (2010)
miR-122	NSC 5476		Inhibition of the transcription of miR-122 Young et al. (2010)
miR-96	Benzimidazole		Up-regulation of FOXO1, the function target of miR-21 Velagapudi et al. (2014)
miR-1	2-methoxy-1,4-naphthalenequin		Down-regulation the expression level of miR-1 Tan et al. (2013)

(Continued on following page)

TABLE 4 | (Continued) The summary of some representative small-molecule miRNA inhibitors.

Target miRNAs	Inhibitors	Structures	Possible mechanisms of action
miR-27a	Arsenic trioxide		Down-regulation the expression level of miR-27a Zhang et al. (2016)
miR-27a	Neomycin		Blocking the mature of miR-27a by the inhibition of Dicer Bose et al. (2013)
miR-27a	Amikacin		Blocking the mature of miR-27a by the inhibition of Dicer Bose et al. (2013)
miR-27a	Tobramycin		Blocking the mature of miR-27a by the inhibition of Dicer Bose et al. (2013)
miR-525	5''-azido-neomycin B		Binding to the processing site of Drosha to block the generation of pre-miR-525 Childs-Disney and Disney (2016)
miR-21	N-substituted oligoglycines		A specific ligand binding with pri-miR-21. Diaz et al. (2014)

and function (Figure 4). The chemical structures of representative small molecule inhibitors were listed in Table 4.

For example, miR-21 is one of the tumor-associated microRNAs (oncomiR) that was discovered earlier and recognized. It has been confirmed in a variety of tumor cells, including breast cancer, ovarian cancer, colon cancer, pancreatic cancer, thyroid cancer, *etc.* There is high expression in cancer which are closely related to the occurrence and development of tumor (Volinia et al., 2006; Tetzlaff et al., 2007; Asangani et al., 2008; Pan et al., 2010). At present, there are abundant literatures

on the chemical small molecule inhibitors. Trypaflavine (TPF), a small molecule compound, was reported by Jiang Research Group in 2010, which significantly down-regulated the expression level of miR-21 (Watashi et al., 2010). Further experiments showed that TPF could inhibit the formation of RISC by blocking the assembly of miR-21 and Argonaute 2 (ago2) protein, leading to the down-regulation of the expression level of miR-21. Davies et al. found that kanamycin A could inhibit the expression of let-7 by binding to pre-let-7 and interfering with Dicer (Davies and Arenz, 2006). In addition, experiments showed that the inhibition

rate reached $69 \pm 3\%$ after 2 h with the treatment of 100 μM of kanamycin A.

MIR-122 is a liver specific miRNA, which is highly expressed in the liver, accounting for about 72% of the total miRNA in adult liver. It is one of the earliest miRNAs with tissue-specific and high abundance expression (Girard et al., 2008). At present, it has been found that miR-122 plays an important role in regulating liver physiological functions such as the growth cycle of hepatocytes and fat metabolism (Esau et al., 2006). It also plays a key role in the occurrence and development of liver diseases such as acute and chronic liver injury, liver cirrhosis, alcoholic hepatitis, liver tumor and hepatitis C virus (HCV) infection (Jopling et al., 2005). Deiters's group performed the research work on the discovery of small-molecule inhibitors of miR-122 and they successfully obtained two small-molecule inhibitors (NSC 158959 and NSC 5476) with specificity towards miR-122 (Young et al., 2010). Its target may be resulted from the transcription of miR-122 gene to pri-miR-122. As for miR-1, it is highly expressed in skeletal muscle cells, which has been proved to regulate the formation of skeletal muscle cells and the development of muscle and is closely related to the development of heart (Thum et al., 2008; Wystub et al., 2013). Using 4-naphthalenequinone as the basic skeleton, dozens of derivatives were obtained by photocyclization reaction (Tan et al., 2013). The 2-methoxy-1,4-naphthalenequin, which exerted specific inhibitory effect on miR-1, was screened out from these compounds. It was confirmed that 2-methoxy-1,4-naphthalenequin could significantly down-regulate the expression level of mature miR-1 in cells. However, the specific mechanism of this compound remains to be further studied.

Clinical Research Progress of miRNA-Related Drugs

In recent 20 years, the field of miRNA has made rapid progress and made great achievements in all directions. The three main discoverers, Victor Ambros, Gary Ruvkun and David Baulcombe won the Lasker Basic Medicine Award in 2008 and became hot candidates for the Nobel Prize in physiology and medicine for many years. At present, cooperated with academic laboratories, several pharmaceutical companies were launched miRNA clinical researches for anticancer therapeutics.

MRX34, a liposomal injection of miRNA-34a, developed by Mirnax Therapeutics, Inc., entered the Phase I clinical trials in 2013 to evaluate the safety in patients with primary liver cancer or other selected solid tumors or hematologic malignancies (ClinicalTrials.gov, NCT number: 01829971) (Zhou et al., 2019). miRNA-34a is generally downregulated and acted as tumor suppressor in most of cancer cells by affecting more than 20 oncogenes to induce the cell apoptosis and cell cycle arrest (Welch et al., 2007). It has been shown that an increase of miRNA-34a in cancer cells would significantly inhibit the cell proliferation, suggesting a potential therapeutic strategy for cancer treatment (Yu et al., 2014). The AODNS is not permeable to enter cell by diffusion, a liposomal nanoparticle was thus employed to carry the miRNA-34a for cancer treatment. The MRX34 is given intravenously for 5 days in a

row and then 2 weeks off (total of 21 days). The trials was finally terminated as the occurrence of five immune related serious adverse events involving death of patients (Beg et al., 2017). However, the development of MRX34 indicated a feasible approach in miRNA drug discovery by using advanced formulations such as liposomal nanoparticles to increase the permeability of AODNS into the cell.

In 2014, the TargomiRs, a miR-16 based microRNA mimic, was developed by EnGeneIC Limited and underwent phase I clinical trial in patients as second or third line treatment for patients with recurrent malignant pleural mesothelioma and non-small cell lung cancer (ClinicalTrials.gov, NCT number: 02369198) (Reid et al., 2016). Several family members of miR-16 were found to be as tumor suppressors, showing a down-regulation in the broad variety of cancer cells. A restore of expression of miR-16 by a miR-16 based microRNA mimic could induce a significant inhibition of cell proliferation of some cancer cells *in vitro* models (Liu et al., 2008). As for the *in vivo* nude mice models, the miR-16 mimic need to be loaded by the nonliving bacterial minicells for the intravenous injection (Viteri and Rosell, 2018). Preliminary data revealed that the treatment of TargomiRs is controllable when the patients were exposed to five billion nanoparticles loaded with miR-16 once a week (van Zandwijk et al., 2017). The results from the phase I study were encouraging and no adverse effects were observed, therefore, TargomiR is expected to perform the phase II clinical trials in next.

MiR-155 plays a crucial role in promoting the growth and survival of the cancer cells because it is found to be highly expressed in certain lymphomas and leukemias (Poltronieri et al., 2013). In 2016, a phase I clinical trial of cobomarsen, an inhibitor of miR-155, was carried out to evaluate its safety, tolerability, pharmacokinetics and potential efficacy on the patients with cutaneous T-cell lymphoma (CTCL), chronic lymphocytic leukemia (CLL), diffuse large B-cell lymphoma (DLBCL), and adult T-cell leukemia/lymphoma (ATLL) (Anastasiadou et al., 2021). The preliminary data revealed that intratumoral injections of cobomarsen over a period of up to 15 days could improve the cutaneous lesions and without any observable adverse effects (Foss et al., 2018). Therefore, a phase II clinical trial was continued to study the efficacy and safety of cobomarsen for the treatment of CTCL and mycosis fungoides (MF) subtype in 2018 (ClinicalTrials.gov, NCT number: 03713320) (Anastasiadou et al., 2021). Although the study was terminated in December, 2020 because of some business reasons, it also encouraged to develop the microRNA as the cancer therapy.

A high expression level of miR-10b was found in glioblastoma patients by the analysis of the Cancer Genome Atlas data, indicating the oncogenic effects of miR-10b. Guessous et al confirmed that miR-10b is upregulated in human glioblastoma tissues, glioblastoma cell and stem cell lines while inhibition of miR-10b would reduce the cancer cell proliferation and inhibited invasion and migration, as well (Guessous et al., 2013). Hence, targeting miR-10b might be a good strategy for glioblastoma treatment. Furthermore, based on the critical function of anti-miR-10b in inhibition of glioblastoma growth, a clinical trial was performed for evaluating the expression Levels of microRNA-10b

in patients with gliomas (clinicaltrials.gov, NCT number: 01849952). The estimated primary completion date would be May 2022. More studies are needed for confirming the effects of anti-glioblastoma in clinic.

CHALLENGES AND PERSPECTIVES OF MIRNA-BASED THERAPY

Since developing miRNA as new drug candidates is the ultimate aim in clinical settings, the most important issue is to ensure its safety and effectiveness. Although miRNA-based therapeutics has made some progresses, there are still some barriers that limit the further application of miRNA from bench to bedside. The first limitation is delivery efficiency. The miRNA delivery systems currently used are chemically synthesized with poor cellular uptake properties (Bader et al., 2011). To make use of their medicinal effects, the miRNA should be able to across the complicated circulatory systems and the cell membranes of different tissues (Cheng et al., 2015). Since it was difficult for the miRNAs to access target cells, the second obstacle is the specificity and off-target effects of miRNA. Different from siRNA, the property of “multi-targeting” of miRNA is double-edged sword. It could help to cure the diseases by affecting as many targets correlated with pathogenesis as possible. In the meantime, it caused the off-target effects. While targeting is sequence specific rather than gene specific, it is more challenging to specifically target since the off target effect only requires partial complementary binding of miRNA and target mRNA (Singh et al., 2011). The third concern is the miRNA-induced toxicity. Studies showed that some miRNAs could transcriptionally regulate the expression of drug metabolizing enzymes, such as cytochrome P450s (CYPs) and bile acid synthase CYP7A1 (Takagi et al., 2010). Deregulating the expression of CYPs by specific miRNA may weaken the metabolism of drug to induce drug accumulation, and eventually lead to toxicity. The fourth challenge is to overcome the issue of rapid clearance in blood system (Fortunato and Iorio, 2020). For the naked nucleotide based drugs, the biggest obstacle for their function *in vivo* are the quick degradation by nuclease and the drug escape from endosome during endocytosis.

Despite the mentioned limitations, miRNA still has broad application prospects in cancer treatment. Some miRNAs may be directly related to cancer by controlling cell proliferation, differentiation and apoptosis, while others may be indirectly related to cancer by targeting oncogenes and tumor suppressor genes. Research on the role of miRNA in the occurrence and development of malignant tumor has become a hot spot. With the development of molecular biology, the detection methods of miRNA have been improved, more and more miRNAs related to cancer has been identified, and the correlation between miRNA and target mRNA has been increasingly identified. The change of miRNA expression profile is an important factor in tumorigenesis and development. Detection of miRNA in tumor patients is advantageous for tumor diagnosis, treatment and prognosis, therefore miRNA may become a new biomarker of tumor. As miRNAs are involved in the main biological behaviors of tumors by regulating target genes, new research-based therapies based on miRNAs will bring positive application prospects in the future. The clinical application of miRNA is based on high efficiency, high sensitivity and low-cost detection methods. However, the current detection methods of miRNA have certain limitations, which hinder the wide use in clinic. After overcoming these problems, miRNA detection and treatment will be expected to smoothly enter the clinic and become a new target for cancer therapeutics.

AUTHOR CONTRIBUTIONS

Conceptualization, KK-WA-Y and ZF; collected and reviewed the literature, ZF, LW, and FC; Data analysis and figure preparation, ZF and SL; writing-original draft preparation, ZF and KK-WA-Y; writing-review and final editing, KK-WA-Y and CS; funding acquisition, CS. All authors have read and agreed to the published version of the manuscript.

FUNDING

This study was supported by the National Natural Science Foundation of China (Grant No. 82073402).

REFERENCES

- Amani-Shalamzari, S., Agha Alinejad, H., Shahbazi, S., and Alizadeh, S. (2020). The Effect of Endurance Training on Expression of miR-21 and its Downstream in Breast Cancer Bearing Mice. *J. Basic Res. Med. Sci.* 7, 47–57.
- Anastasiadou, E., Seto, A. G., Beatty, X., Hermreck, M., Gilles, M.-E., Stroopinsky, D., et al. (2021). Cobomarsen, an Oligonucleotide Inhibitor of miR-155, Slows DLBCL Tumor Cell Growth *In Vitro* and *In Vivo*. *Clin. Cancer Res.* 27, 1139–1149. doi:10.1158/1078-0432.ccr-20-3139
- Aqeilan, R. I., Calin, G. A., and Croce, C. M. (2010). miR-15a and miR-16-1 in Cancer: Discovery, Function and Future Perspectives. *Cell Death Differ* 17, 215–220. doi:10.1038/cdd.2009.69
- Asangani, I. A., Rasheed, S. A., Nikolova, D. A., Leupold, J. H., Colburn, N. H., Post, S., et al. (2008). MicroRNA-21 (miR-21) post-transcriptionally Downregulates Tumor Suppressor Pdc4 and Stimulates Invasion, Intravasation and Metastasis in Colorectal Cancer. *Oncogene* 27, 2128–2136. doi:10.1038/sj.onc.1210856
- Azizmohammadi, S., Safari, A., Azizmohammadi, S., Kaghazian, M., Sadrkhanlo, M., Yahaghi, E., et al. (2017). Molecular Identification of miR-145 and miR-9 Expression Level as Prognostic Biomarkers for Early-Stage Cervical Cancer Detection. *QJM* 110, 11–15. doi:10.1093/qjmed/hcw101
- Bader, A. G., Brown, D., Stoudemire, J., and Lammers, P. (2011). Developing Therapeutic microRNAs for Cancer. *Gene Ther.* 18, 1121–1126. doi:10.1038/gt.2011.79
- Bader, A. G. (2012). miR-34 - a microRNA Replacement Therapy Is Headed to the Clinic. *Front. Genet.* 3, 120. doi:10.3389/fgene.2012.00120
- Bao, W., Wang, H. H., Tian, F. J., He, X. Y., Qiu, M. T., Wang, J. Y., et al. (2013). A TrkB-STAT3-miR-204-5p Regulatory Circuitry Controls Proliferation and Invasion of Endometrial Carcinoma Cells. *Mol. Cancer* 12, 1–19. doi:10.1186/1476-4598-12-155
- Barrett-Lee, P. (2009). A Pleiotropically Acting microRNA, miR-31, Inhibits Breast Cancer Metastasis. *Adv. Breast Cancer* 6, 24–25.
- Bartel, D. P. (2009). MicroRNAs: Target Recognition and Regulatory Functions. *Cell* 136, 215–233. doi:10.1016/j.cell.2009.01.002

- Beg, M. S., Brenner, A. J., Sachdev, J., Borad, M., Kang, Y. K., Stoudemire, J., et al. (2017). Phase I Study of MRX34, a Liposomal miR-34a Mimic, Administered Twice Weekly in Patients with Advanced Solid Tumors. *Invest. New Drugs* 35, 180–188. doi:10.1007/s10637-016-0407-y
- Bertero, T., Bourget-Ponzio, I., Puissant, A., Loubat, A., Mari, B., Meneguzzi, G., et al. (2013). Tumor Suppressor Function of miR-483-3p on Squamous Cell Carcinomas Due to its Pro-apoptotic Properties. *Cell Cycle* 12, 2183–2193. doi:10.4161/cc.25330
- Bommer, G. T., Gerin, I., Feng, Y., Kaczorowski, A. J., Kuick, R., Love, R. E., et al. (2007). p53-mediated Activation of miRNA34 Candidate Tumor-Suppressor Genes. *Curr. Biol.* 17, 1298–1307. doi:10.1016/j.cub.2007.06.068
- Bonci, D., Coppola, V., Musumeci, M., Addario, A., Biffoni, M., Labbaye, C., et al. (2008). The miR-15a/miR-16-1 Cluster Controls Prostate Cancer Progression by Targeting Multiple Oncogenic Activities. *Nat. Med.* 14, 1271–1277. doi:10.1038/nm.1880
- Bose, D., Jayaraj, G., Suryawanshi, H., Agarwala, P., Pore, S. K., Banerjee, R., et al. (2012). The Tuberculosis Drug Streptomycin as a Potential Cancer Therapeutic: Inhibition of miR-21 Function by Directly Targeting its Precursor. *Angew. Chem. Int. Ed. Engl.* 51, 1019–1023. doi:10.1002/anie.201106455
- Bose, D., Jayaraj, G. G., Kumar, S., and Maiti, S. (2013). A molecular-beacon-based Screen for Small Molecule Inhibitors of miRNA Maturation. *ACS Chem. Biol.* 8, 930–938. doi:10.1021/cb300650y
- Bou Kheir, T., Futoma-Kazmierczak, E., Jacobsen, A., Krogh, A., Bardram, L., Hother, C., et al. (2011). miR-449 Inhibits Cell Proliferation and Is Down-Regulated in Gastric Cancer. *Mol. Cancer* 10, 29–12. doi:10.1186/1476-4598-10-29
- Chan, J. A., Krichevsky, A. M., and Kosik, K. S. (2005). MicroRNA-21 Is an Antiapoptotic Factor in Human Glioblastoma Cells. *Cancer Res.* 65, 6029–6033. doi:10.1158/0008-5472.CAN-05-0137
- Chen, J., Sun, D., Chu, H., Gong, Z., Zhang, C., Gong, B., et al. (2015). Screening of Differential microRNA Expression in Gastric Signet Ring Cell Carcinoma and Gastric Adenocarcinoma and Target Gene Prediction. *Oncol. Rep.* 33, 2963–2971. doi:10.3892/or.2015.3935
- Chen, P., Price, C., Li, Z., Li, Y., Cao, D., Wiley, A., et al. (2013). miR-9 Is an Essential Oncogenic microRNA Specifically Overexpressed in Mixed Lineage Leukemia-Rearranged Leukemia. *Proc. Natl. Acad. Sci. U S A.* 110, 11511–11516. doi:10.1073/pnas.1310144110
- Chen, Q. Y., Jiao, D. M., Yan, L., Wu, Y. Q., Hu, H. Z., Song, J., et al. (2015). Comprehensive Gene and microRNA Expression Profiling Reveals miR-206 Inhibits MET in Lung Cancer Metastasis. *Mol. Biosyst.* 11, 2290–2302. doi:10.1039/c4mb00734d
- Chen, W. X., Hu, Q., Qiu, M. T., Zhong, S. L., Xu, J. J., Tang, J. H., et al. (2013). miR-221/222: Promising Biomarkers for Breast Cancer. *Tumour Biol.* 34, 1361–1370. doi:10.1007/s13277-013-0750-y
- Chen, Y., Wei, H., Liu, Y., and Zheng, S. (2018). Promotional Effect of microRNA-194 on Breast Cancer Cells via Targeting F-Box/WD Repeat-Containing Protein 7. *Oncol. Lett.* 15, 4439–4444. doi:10.3892/ol.2018.7842
- Cheng, C. J., Bahal, R., Babar, I. A., Pincus, Z., Barrera, F., Liu, C., et al. (2015). MicroRNA Silencing for Cancer Therapy Targeted to the Tumour Microenvironment. *Nature* 518, 107–110. doi:10.1038/nature13905
- Childs-Disney, J. L., and Disney, M. D. (2016). Small Molecule Targeting of a MicroRNA Associated with Hepatocellular Carcinoma. *ACS Chem. Biol.* 11, 375–380. doi:10.1021/acscmbio.5b00615
- Chirshv, E., Oberg, K. C., Ioffe, Y. J., and Unternaehrer, J. J. (2019). Let-7 as Biomarker, Prognostic Indicator, and Therapy for Precision Medicine in Cancer. *Clin. Transl. Med.* 8, 24–14. doi:10.1186/s40169-019-0240-y
- Cimmino, A., Calin, G. A., Fabbri, M., Iorio, M. V., Ferracin, M., Shimizu, M., et al. (2005). miR-15 and miR-16 Induce Apoptosis by Targeting BCL2. *Proc. Natl. Acad. Sci. U S A.* 102, 13944–13949. doi:10.1073/pnas.0506654102
- Czimmerer, Z., Hulvely, J., Simandi, Z., Varallyay, E., Havelda, Z., Szabo, E., et al. (2013). A Versatile Method to Design Stem-Loop Primer-Based Quantitative PCR Assays for Detecting Small Regulatory RNA Molecules. *PLoS one* 8, e55168. doi:10.1371/journal.pone.0055168
- Davies, B. P., and Arenz, C. (2006). A Homogenous Assay for Micro RNA Maturation. *Angew. Chem. Int. Ed. Engl.* 45, 5550–5552. doi:10.1002/anie.200601332
- Davies, B. P. (2008). *A Homogenous Fluorescence Assay of Micro RNA Maturation*. Dissertation
- De Ieso, M. L., and Yool, A. J. (2018). Mechanisms of Aquaporin-Facilitated Cancer Invasion and Metastasis. *Front. Chem.* 6, 135. doi:10.3389/fchem.2018.00135
- Diaz, J. P., Chirayil, R., Chirayil, S., Tom, M., Head, K. J., and Luebke, K. J. (2014). Association of a Peptoid Ligand with the Apical Loop of Pri-miR-21 Inhibits Cleavage by Drosha. *RNA* 20, 528–539. doi:10.1261/rna.042911.113
- Du, B., Wang, Z., Zhang, X., Feng, S., Wang, G., He, J., et al. (2014). MicroRNA-545 Suppresses Cell Proliferation by Targeting Cyclin D1 and CDK4 in Lung Cancer Cells. *PLoS one* 9, e88022. doi:10.1371/journal.pone.0088022
- Elbadawy, M., Usui, T., Yamawaki, H., and Sasaki, K. (2019). Emerging Roles of C-Myc in Cancer Stem Cell-Related Signaling and Resistance to Cancer Chemotherapy: a Potential Therapeutic Target against Colorectal Cancer. *Int. J. Mol. Sci.* 20, 2340. doi:10.3390/ijms20092340
- Endo, H., Muramatsu, T., Furuta, M., Uzawa, N., Pimkhakham, A., Amagasa, T., et al. (2013). Potential of Tumor-Suppressive miR-596 Targeting LGALS3BP as a Therapeutic Agent in Oral Cancer. *Carcinogenesis* 34, 560–569. doi:10.1093/carcin/bgs376
- Esau, C., Davis, S., Murray, S. F., Yu, X. X., Pandey, S. K., Pear, M., et al. (2006). miR-122 Regulation of Lipid Metabolism Revealed by *In Vivo* Antisense Targeting. *Cell Metab* 3, 87–98. doi:10.1016/j.cmet.2006.01.005
- Esquela-Kerscher, A., Trang, P., Wiggins, J. F., Patrawala, L., Cheng, A., Ford, L., et al. (2008). The Let-7 microRNA Reduces Tumor Growth in Mouse Models of Lung Cancer. *Cell cycle* 7, 759–764. doi:10.4161/cc.7.6.5834
- Fletcher, C. E., Dart, D. A., Sita-Lumsden, A., Cheng, H., Rennie, P. S., and Bevan, C. L. (2012). Androgen-regulated Processing of the Oncomir miR-27a, Which Targets Prohibitin in Prostate Cancer. *Hum. Mol. Genet.* 21, 3112–3127. doi:10.1093/hmg/ddsl39
- Fontana, L., Fiori, M. E., Albini, S., Cifaldi, L., Giovannazzi, S., Forloni, M., et al. (2008). Antagomir-17-5p Abolishes the Growth of Therapy-Resistant Neuroblastoma through P21 and BIM. *PLoS one* 3, e2236. doi:10.1371/journal.pone.0002236
- Fortunato, O., and Iorio, M. V. (2020). The Therapeutic Potential of MicroRNAs in Cancer: Illusion or Opportunity? *Pharmaceuticals (Basel)* 13, 438. doi:10.3390/ph13120438
- Foss, F. M., Quersfeld, C., Kim, Y. H., Pinter-Brown, L. C., William, B. M., Porcu, P., et al. (2018). Ph 1 Study of MRG-106, an Inhibitor of miR-155, in CTCL. *Jco* 36, 2511. doi:10.1200/jco.2018.36.15_suppl.2511
- Fujita, Y., Kojima, K., Hamada, N., Ohhashi, R., Akao, Y., Nozawa, Y., et al. (2008). Effects of miR-34a on Cell Growth and Chemoresistance in Prostate Cancer PC3 Cells. *Biochem. Biophys. Res. Commun.* 377, 114–119. doi:10.1016/j.bbrc.2008.09.086
- Fuziwar, C. S., and Kimura, E. T. (2015). Insights into Regulation of the miR-17-92 Cluster of miRNAs in Cancer. *Front. Med. (Lausanne)* 2, 64. doi:10.3389/fmed.2015.00064
- Galm, O., Herman, J. G., and Baylin, S. B. (2006). The Fundamental Role of Epigenetics in Hematopoietic Malignancies. *Blood Rev.* 20, 1–13. doi:10.1016/j.blre.2005.01.006
- Gambari, R., Brognara, E., Spandidos, D. A., and Fabbri, E. (2016). Targeting oncomiRNAs and Mimicking Tumor Suppressor miRNAs: New Trends in the Development of miRNA Therapeutic Strategies in Oncology (Review). *Int. J. Oncol.* 49, 5–32. doi:10.3892/ijo.2016.3503
- Gandellini, P., Folini, M., Longoni, N., Pennati, M., Binda, M., Colecchia, M., et al. (2009). miR-205 Exerts Tumor-Suppressive Functions in Human Prostate through Down-Regulation of Protein Kinase Cepsilon. *Cancer Res.* 69, 2287–2295. doi:10.1158/0008-5472.CAN-08-2894
- Gao, C., Zhou, C., Zhuang, J., Liu, L., Liu, C., Li, H., et al. (2018). MicroRNA Expression in Cervical Cancer: Novel Diagnostic and Prognostic Biomarkers. *J. Cel Biochem* 119, 7080–7090. doi:10.1002/jcb.27029
- Gao, P., Xing, A. Y., Zhou, G. Y., Zhang, T. G., Zhang, J. P., Gao, C., et al. (2013). The Molecular Mechanism of microRNA-145 to Suppress Invasion-Metastasis cascade in Gastric Cancer. *Oncogene* 32, 491–501. doi:10.1038/onc.2012.61
- Garbett, K. A., Horváth, S., Ebert, P. J., Schmidt, M. J., Lwin, K., Mitchell, A., et al. (2010). Novel Animal Models for Studying Complex Brain Disorders: BAC-Driven miRNA-Mediated *In Vivo* Silencing of Gene Expression. *Mol. Psychiatry* 15, 987–995. doi:10.1038/mp.2010.1
- Garzon, R., Heaphy, C. E., Havelange, V., Fabbri, M., Volinia, S., Tsao, T., et al. (2009). MicroRNA 29b Functions in Acute Myeloid Leukemia. *Blood* 114, 5331–5341. doi:10.1182/blood-2009-03-211938

- Gaur, A., Jewell, D. A., Liang, Y., Ridzon, D., Moore, J. H., Chen, C., et al. (2007). Characterization of microRNA Expression Levels and Their Biological Correlates in Human Cancer Cell Lines. *Cancer Res.* 67, 2456–2468. doi:10.1158/0008-5472.CAN-06-2698
- Girard, M., Jacquemin, E., Munnich, A., Lyonnet, S., and Henrion-Caude, A. (2008). miR-122, a Paradigm for the Role of microRNAs in the Liver. *J. Hepatol.* 48, 648–656. doi:10.1016/j.jhep.2008.01.019
- Gong, C., Yang, Z., Wu, F., Han, L., Liu, Y., and Gong, W. (2016). miR-17 Inhibits Ovarian Cancer Cell Peritoneal Metastasis by Targeting ITGA5 and ITGB1. *Oncol. Rep.* 36, 2177–2183. doi:10.3892/or.2016.4985
- Gruszka, R., and Zakrzewska, M. (2018). The Oncogenic Relevance of miR-17-92 Cluster and its Paralogous miR-106b-25 and miR-106a-363 Clusters in Brain Tumors. *Int. J. Mol. Sci.* 19, 879. doi:10.3390/ijms19030879
- Gu, Y., Cheng, Y., Song, Y., Zhang, Z., Deng, M., Wang, C., et al. (2014). MicroRNA-493 Suppresses Tumor Growth, Invasion and Metastasis of Lung Cancer by Regulating E2F1. *PLoS one* 9, e102602. doi:10.1371/journal.pone.0102602
- Guessous, F., Alvarado-Velez, M., Marcinkiewicz, L., Zhang, Y., Kim, J., Heister, S., et al. (2013). Oncogenic Effects of miR-10b in Glioblastoma Stem Cells. *J. Neurooncol.* 112, 153–163. doi:10.1007/s11060-013-1047-0
- Gumireddy, K., Young, D. D., Xiong, X., Hogenesch, J. B., Huang, Q., and Deiters, A. (2008). Small-molecule Inhibitors of MicroRNA miR-21 Function. *Angew. Chem. Int. Ed. Engl.* 47, 7482–7484. doi:10.1002/anie.200801555
- Han, C., Shen, J. K., Hornicek, F. J., Kan, Q., and Duan, Z. (2017). Regulation of microRNA-1 (miR-1) Expression in Human Cancer. *Biochim. Biophys. Acta Gene Regul. Mech.* 1860, 227–232. doi:10.1016/j.bbagr.2016.12.004
- He, B., Zhao, Z., Cai, Q., Zhang, Y., Zhang, P., Shi, S., et al. (2020). miRNA-Based Biomarkers, Therapies, and Resistance in Cancer. *Int. J. Biol. Sci.* 16, 2628–2647. doi:10.7150/ijbs.47203
- He, L., He, X., Lim, L. P., De Stanchina, E., Xuan, Z., Liang, Y., et al. (2007). A microRNA Component of the P53 Tumour Suppressor Network. *Nature* 447, 1130–1134. doi:10.1038/nature05939
- He, Z., Yu, L., Luo, S., Li, M., Li, J., Li, Q., et al. (2017). miR-296 Inhibits the Metastasis and Epithelial-Mesenchymal Transition of Colorectal Cancer by Targeting S100A4. *BMC cancer* 17, 1–10. doi:10.1186/s12885-017-3121-z
- Hermeking, H. (2010). The miR-34 Family in Cancer and Apoptosis. *Cel Death Differ* 17, 193–199. doi:10.1038/cdd.2009.56
- Hou, C., Sun, B., Jiang, Y., Zheng, J., Yang, N., Ji, C., et al. (2016). MicroRNA-31 Inhibits Lung Adenocarcinoma Stem-like Cells via Down-Regulation of MET-Pi3k-Akt Signaling Pathway. *Anticancer Agents Med. Chem.* 16, 501–518. doi:10.2174/1871520615666150824152353
- Huang, L., Wang, L., Wang, L., Wu, Z., Jiang, F., Li, Q., et al. (2020). MicroRNA Let-7b Inhibits Proliferation and Induces Apoptosis of Castration-Resistant Prostate Cancer Cells by Blocking the Ras/Rho Signaling Pathway via NRAS. *Clin. translational Sci.*
- Huang, T. C., Chang, H. Y., Chen, C. Y., Wu, P. Y., Lee, H., Liao, Y. F., et al. (2011). Silencing of miR-124 Induces Neuroblastoma SK-N-SH Cell Differentiation, Cell Cycle Arrest and Apoptosis through Promoting AHR. *FEBS Lett.* 585, 3582–3586. doi:10.1016/j.febslet.2011.10.025
- Hudson, R. S., Yi, M., Esposito, D., Watkins, S. K., Hurwitz, A. A., Yfantis, H. G., et al. (2012). MicroRNA-1 Is a Candidate Tumor Suppressor and Prognostic Marker in Human Prostate Cancer. *Nucleic Acids Res.* 40, 3689–3703. doi:10.1093/nar/gkr1222
- Humphreys, K. J., McKinnon, R. A., and Michael, M. Z. (2014). miR-18a Inhibits CDC42 and Plays a Tumour Suppressor Role in Colorectal Cancer Cells. *PLoS one* 9, e112288. doi:10.1371/journal.pone.0112288
- Ibrahim, A. F., Weirauch, U., Thomas, M., Grünweller, A., Hartmann, R. K., and Aigner, A. (2011). MicroRNA Replacement Therapy for miR-145 and miR-33a Is Efficacious in a Model of colon Carcinoma. *Cancer Res.* 71, 5214–5224. doi:10.1158/0008-5472.CAN-10-4645
- Javanmard, S. H., Vaseghi, G., Ghasemi, A., Rafiee, L., Ferns, G. A., Esfahani, H. N., et al. (2020). Therapeutic Inhibition of microRNA-21 (miR-21) Using Locked-Nucleic Acid (LNA)-anti-miR and its Effects on the Biological Behaviors of Melanoma Cancer Cells in Preclinical Studies. *Cancer Cel Int* 20, 1–12. doi:10.1186/s12935-020-01394-6
- Ji, J., Shi, J., Budhu, A., Yu, Z., Forgues, M., Roessler, S., et al. (2009). MicroRNA Expression, Survival, and Response to Interferon in Liver Cancer. *N. Engl. J. Med.* 361, 1437–1447. doi:10.1056/NEJMoa0901282
- Jiang, C. S., Wang, X. M., Zhang, S. Q., Meng, L. S., Zhu, W. H., Xu, J., et al. (2015). Discovery of 4-Benzoylamino-N-(prop-2-Yn-1-Yl)benzamides as Novel microRNA-21 Inhibitors. *Bioorg. Med. Chem.* 23, 6510–6519. doi:10.1016/j.bmc.2015.08.007
- Jiang, S., Zhang, H. W., Lu, M. H., He, X. H., Li, Y., Gu, H., et al. (2010). MicroRNA-155 Functions as an OncomiR in Breast Cancer by Targeting the Suppressor of Cytokine Signaling 1 Gene. *Cancer Res.* 70, 3119–3127. doi:10.1158/0008-5472.CAN-09-4250
- Johnson, S. M., Grosshans, H., Shingara, J., Byrom, M., Jarvis, R., Cheng, A., et al. (2005). RAS Is Regulated by the Let-7 microRNA Family. *Cell* 120, 635–647. doi:10.1016/j.cell.2005.01.014
- Jopling, C. L., Yi, M., Lancaster, A. M., Lemon, S. M., and Sarnow, P. (2005). Modulation of Hepatitis C Virus RNA Abundance by a Liver-specific MicroRNA. *Science* 309, 1577–1581. doi:10.1126/science.1113329
- Kang, W., Tong, J. H., Lung, R. W., Dong, Y., Zhao, J., Liang, Q., et al. (2015). Targeting of YAP1 by microRNA-15a and microRNA-16-1 Exerts Tumor Suppressor Function in Gastric Adenocarcinoma. *Mol. Cancer* 14, 52–10. doi:10.1186/s12943-015-0323-3
- Kano, M., Seki, N., Kikkawa, N., Fujimura, L., Hoshino, I., Akutsu, Y., et al. (2010). miR-145, miR-133a and miR-133b: Tumor-Suppressive miRNAs Target FSCN1 in Esophageal Squamous Cell Carcinoma. *Int. J. Cancer* 127, 2804–2814. doi:10.1002/ijc.25284
- Kapoor, I., Bodo, J., Hill, B. T., Hsi, E. D., and Almasan, A. (2020). Targeting BCL-2 in B-Cell Malignancies and Overcoming Therapeutic Resistance. *Cell Death Dis* 11, 1–11. doi:10.1038/s41419-020-03144-y
- Kardani, A., Yaghoobi, H., Alibakhshi, A., and Khatami, M. (2020). Inhibition of miR-155 in MCF-7 Breast Cancer Cell Line by Gold Nanoparticles Functionalized with Antagomir and AS1411 Aptamer. *J. Cel Physiol* 235, 6887–6895. doi:10.1002/jcp.29584
- Kato, T., Enomoto, A., Watanabe, T., Haga, H., Ishida, S., Kondo, Y., et al. (2014). TRIM27/MRTF-B-dependent Integrin β 1 Expression Defines Leading Cells in Cancer Cell Collectives. *Cell Rep* 7, 1156–1167. doi:10.1016/j.celrep.2014.03.068
- Kikkawa, N., Kinoshita, T., Nohata, N., Hanazawa, T., Yamamoto, N., Fukumoto, I., et al. (2014). microRNA-504 Inhibits Cancer Cell Proliferation via Targeting CDK6 in Hypopharyngeal Squamous Cell Carcinoma. *Int. J. Oncol.* 44, 2085–2092. doi:10.3892/ijo.2014.2349
- Kluiver, J., Slezak-Prochazka, I., Smigielska-Czepiel, K., Halsema, N., Kroesen, B. J., and van den Berg, A. (2012). Generation of miRNA Sponge Constructs. *Methods* 58, 113–117. doi:10.1016/j.jymeth.2012.07.019
- Kota, J., Chivukula, R. R., O'Donnell, K. A., Wentzel, E. A., Montgomery, C. L., Hwang, H. W., et al. (2009). Therapeutic microRNA Delivery Suppresses Tumorigenesis in a Murine Liver Cancer Model. *Cell* 137, 1005–1017. doi:10.1016/j.cell.2009.04.021
- Lee, D. Y., Deng, Z., Wang, C. H., and Yang, B. B. (2007). MicroRNA-378 Promotes Cell Survival, Tumor Growth, and Angiogenesis by Targeting SuFu and Fus-1 Expression. *Proc. Natl. Acad. Sci. U S A.* 104, 20350–20355. doi:10.1073/pnas.0706901104
- Lee, E. J., Baek, M., Gusev, Y., Brackett, D. J., Nuovo, G. J., and Schmittgen, T. D. (2008). Systematic Evaluation of microRNA Processing Patterns in Tissues, Cell Lines, and Tumors. *RNA* 14, 35–42. doi:10.1261/rna.804508
- Lee, R. C., Feinbaum, R. L., and Ambros, V. (1993). The *C. elegans* Heterochronic Gene Lin-4 Encodes Small RNAs with Antisense Complementarity to Lin-14. *Cell* 75, 843–854. doi:10.1016/0092-8674(93)90529-y
- Li, K. K., Pang, J. C., Lau, K. M., Zhou, L., Mao, Y., Wang, Y., et al. (2013). MiR-383 Is Downregulated in Medulloblastoma and Targets Peroxiredoxin 3 (PRDX3). *Brain Pathol.* 23, 413–425. doi:10.1111/bpa.12014
- Li, L., and Wang, B. (2014). Overexpression of microRNA-30b Improves Adenovirus-Mediated P53 Cancer Gene Therapy for Laryngeal Carcinoma. *Int. J. Mol. Sci.* 15, 19729–19740. doi:10.3390/ijms151119729
- Li, Y., Zu, L., Wang, Y., Wang, M., Chen, P., and Zhou, Q. (2015). miR-132 Inhibits Lung Cancer Cell Migration and Invasion by Targeting SOX4. *J. Thorac. Dis.* 7, 1563–1569. doi:10.3978/j.issn.2072-1439.2015.09.06
- Liang, Z., Ahn, J., Guo, D., Votaw, J. R., and Shim, H. (2013). MicroRNA-302 Replacement Therapy Sensitizes Breast Cancer Cells to Ionizing Radiation. *Pharm. Res.* 30, 1008–1016. doi:10.1007/s11095-012-0936-9
- Lichner, S., Saleh, C., Subramaniam, V., Seivwright, A., Prud'homme, G. J., and Yousef, G. M. (2015). miR-17 Inhibition Enhances the Formation of Kidney Cancer Spheres with Stem Cell/Tumor Initiating Cell Properties. *Oncotarget* 6, 5567–5581. doi:10.18632/oncotarget.1901

- Lin, Y., Liu, A. Y., Fan, C., Zheng, H., Li, Y., Zhang, C., et al. (2015). MicroRNA-33b Inhibits Breast Cancer Metastasis by Targeting HMGA2, SALL4 and Twist1. *Sci. Rep.* 5, 1–12. doi:10.1038/srep09995
- Ling, N., Gu, J., Lei, Z., Li, M., Zhao, J., Zhang, H. T., et al. (2013). microRNA-155 Regulates Cell Proliferation and Invasion by Targeting FOXO3a in Glioma. *Oncol. Rep.* 30, 2111–2118. doi:10.3892/or.2013.2685
- Liu, K., Li, X., Cao, Y., Ge, Y., Wang, J., and Shi, B. (2015). MiR-132 Inhibits Cell Proliferation, Invasion and Migration of Hepatocellular Carcinoma by Targeting PIK3R3. *Int. J. Oncol.* 47, 1585–1593. doi:10.3892/ijo.2015.3112
- Liu, Q., Fu, H., Sun, F., Zhang, H., Tie, Y., Zhu, J., et al. (2008). miR-16 Family Induces Cell Cycle Arrest by Regulating Multiple Cell Cycle Genes. *Nucleic Acids Res.* 36, 5391–5404. doi:10.1093/nar/gkn522
- Liu, T., Hu, K., Zhao, Z., Chen, G., Ou, X., Zhang, H., et al. (2015). MicroRNA-1 Down-Regulates Proliferation and Migration of Breast Cancer Stem Cells by Inhibiting the Wnt/ β -Catenin Pathway. *Oncotarget* 6, 41638–41649. doi:10.18632/oncotarget.5873
- Liu, W., Zabirnyk, O., Wang, H., Shiao, Y. H., Nickerson, M. L., Khalil, S., et al. (2010). miR-23b Targets Proline Oxidase, a Novel Tumor Suppressor Protein in Renal Cancer. *Oncogene* 29, 4914–4924. doi:10.1038/nc.2010.237
- Lou, S., Sun, T., Li, H., and Hu, Z. (2018). Mechanisms of microRNA-Mediated Gene Regulation in Unicellular Model Alga *Chlamydomonas Reinhardtii*. *Biotechnol. Biofuels* 11, 1–12. doi:10.1186/s13068-018-1249-y
- Lujambio, A., Roperio, S., Ballestar, E., Fraga, M. F., Cerrato, C., Setièn, F., et al. (2007). Genetic Unmasking of an Epigenetically Silenced microRNA in Human Cancer Cells. *Cancer Res.* 67, 1424–1429. doi:10.1158/0008-5472.CAN-06-4218
- Luo, W., Huang, B., Li, Z., Li, H., Sun, L., Zhang, Q., et al. (2013). MicroRNA-449a Is Downregulated in Non-small Cell Lung Cancer and Inhibits Migration and Invasion by Targeting C-Met. *PLoS one* 8, e64759. doi:10.1371/journal.pone.0064759
- Ma, J., Hong, L., Xu, G., Hao, J., Wang, R., Guo, H., et al. (2016). miR-483-3p Plays an Oncogenic Role in Esophageal Squamous Cell Carcinoma by Targeting Tumor Suppressor E124. *Cell Biol Int* 40, 448–455. doi:10.1002/cbin.10585
- Makarova, J. A., and Kramerov, D. A. (2007). Noncoding RNAs. *Biochemistry (Mosc)* 72, 1161–1178. doi:10.1134/s0006297907110016
- Matsuzaki, J., and Suzuki, H. (2015). Role of MicroRNAs-221/222 in Digestive Systems. *J. Clin. Med.* 4, 1566–1577. doi:10.3390/jcm4081566
- Melo, S., Villanueva, A., Moutinho, C., Davalos, V., Spizzo, R., Ivan, C., et al. (2011). Small Molecule Enoxacin Is a Cancer-specific Growth Inhibitor that Acts by Enhancing TAR RNA-Binding Protein 2-mediated microRNA Processing. *Proc. Natl. Acad. Sci. U S A.* 108, 4394–4399. doi:10.1073/pnas.1014720108
- Meq, V. O. (2013). The Oncogenic MicroRNA OncomiR-21. *J. Virol.* 87, 80.
- Mihailovich, M., Bremang, M., Spadotto, V., Musiani, D., Vitale, E., Varano, G., et al. (2015). miR-17-92 fine-tunes MYC Expression and Function to Ensure Optimal B Cell Lymphoma Growth. *Nat. Commun.* 6, 1–15. doi:10.1038/ncomms9725
- Naro, Y., Thomas, M., Stephens, M. D., Connelly, C. M., and Deiters, A. (2015). Aryl Amide Small-Molecule Inhibitors of microRNA miR-21 Function. *Bioorg. Med. Chem. Lett.* 25, 4793–4796. doi:10.1016/j.bmcl.2015.07.016
- Ng, W. L., Yan, D., Zhang, X., Mo, Y. Y., and Wang, Y. (2010). Over-expression of miR-100 Is Responsible for the Low-Expression of ATM in the Human Glioma Cell Line: M059J. *DNA Repair (Amst)* 9, 1170–1175. doi:10.1016/j.dnarep.2010.08.007
- Okamoto, K., Ishiguro, T., Midorikawa, Y., Ohata, H., Izumiya, M., Tsuchiya, N., et al. (2012). miR-493 Induction during Carcinogenesis Blocks Metastatic Settlement of colon Cancer Cells in Liver. *EMBO J.* 31, 1752–1763. doi:10.1038/emboj.2012.25
- Otokesh, B., Abbasi, M., Gorgani, H. O., Farahini, H., Moghtadaei, M., Boddouhi, B., et al. (2020). MicroRNAs Signatures, Bioinformatics Analysis of miRNAs, miRNA Mimics and Antagonists, and miRNA Therapeutics in Osteosarcoma. *Cancer Cell Int* 20, 1–20. doi:10.1186/s12935-020-01342-4
- Pan, X., Wang, Z. X., and Wang, R. (2010). MicroRNA-21: a Novel Therapeutic Target in Human Cancer. *Cancer Biol. Ther.* 10, 1224–1232. doi:10.4161/cbt.10.12.14252
- Papargyri, N., Pontoppidan, M., Andersen, M. R., Koch, T., and Hagedorn, P. H. (2020). Chemical Diversity of Locked Nucleic Acid-Modified Antisense Oligonucleotides Allows Optimization of Pharmaceutical Properties. *Mol. Ther. Nucleic Acids* 19, 706–717. doi:10.1016/j.omtn.2019.12.011
- Parkin, A., Man, J., Timpson, P., and Pajic, M. (2019). Targeting the Complexity of Src Signalling in the Tumour Microenvironment of Pancreatic Cancer: from Mechanism to Therapy. *FEBS J.* 286, 3510–3539. doi:10.1111/febs.15011
- Pekarsky, Y., and Croce, C. M. (2015). Role of miR-15/16 in CLL. *Cel Death Differ* 22, 6–11. doi:10.1038/cdd.2014.87
- Peng, Y., and Croce, C. M. (2016). The Role of MicroRNAs in Human Cancer. *Signal. Transduct. Target. Ther.* 1, 15004–15009. doi:10.1038/sigtrans.2015.4
- Poltronieri, P., D'Urso, P. I., Mezzolla, V., and D'Urso, O. F. (2013). Potential of Anti-cancer Therapy Based on Anti-miR-155 Oligonucleotides in Glioma and Brain Tumours. *Chem. Biol. Drug Des.* 81, 79–84. doi:10.1111/cbdd.12002
- Pu, M., Chen, J., Tao, Z., Miao, L., Qi, X., Wang, Y., et al. (2019). Regulatory Network of miRNA on its Target: Coordination between Transcriptional and post-transcriptional Regulation of Gene Expression. *Cell Mol Life Sci* 76, 441–451. doi:10.1007/s00018-018-2940-7
- Quintavalle, C., Garofalo, M., Zanca, C., Romano, G., Iaboni, M., del Basso De Caro, M., et al. (2012). miR-221/222 Overexpression in Human Glioblastoma Increases Invasiveness by Targeting the Protein Phosphate PTP μ . *Oncogene* 31, 858–868. doi:10.1038/nc.2011.280
- Reid, G., Kao, S. C., Pavlakis, N., Brahmabhatt, H., MacDiarmid, J., Clarke, S., et al. (2016). Clinical Development of TargomiRs, a miRNA Mimic-Based Treatment for Patients with Recurrent Thoracic Cancer. *Epigenomics* 8, 1079–1085. doi:10.2217/epi-2016-0035
- Reid, J. F., Sokolova, V., Zoni, E., Lampis, A., Pizzamiglio, S., Bertan, C., et al. (2012). miRNA Profiling in Colorectal Cancer Highlights miR-1 Involvement in MET-dependent Proliferation. *Mol. Cancer Res.* 10, 504–515. doi:10.1158/1541-7786.MCR-11-0342
- Reinhart, B. J., Slack, F. J., Basson, M., Pasquinelli, A. E., Bettinger, J. C., Rougvie, A. E., et al. (2000). The 21-nucleotide Let-7 RNA Regulates Developmental Timing in *Caenorhabditis elegans*. *Nature* 403, 901–906. doi:10.1038/35002607
- Roberts, T. C., Langer, R., and Wood, M. J. A. (2020). Advances in Oligonucleotide Drug Delivery. *Nat. Rev. Drug Discov.* 19, 673–694. doi:10.1038/s41573-020-0075-7
- Roma-Rodrigues, C., Rivas-García, L., Baptista, P. V., and Fernandes, A. R. (2020). Gene Therapy in Cancer Treatment: Why Go Nano? *Pharmaceutics* 12, 233. doi:10.3390/pharmaceutics12030233
- Saito, Y., Nakaoka, T., and Saito, H. (2015). microRNA-34a as a Therapeutic Agent against Human Cancer. *J. Clin. Med.* 4, 1951–1959. doi:10.3390/jcm4111951
- Savi, F., Forno, I., Favarsani, A., Luciani, A., Caldiera, S., Gatti, S., et al. (2014). miR-296/Scribble axis Is Dysregulated in Human Breast Cancer and miR-296 Restoration Reduces Tumour Growth In Vivo. *Clin. Sci. (Lond)* 127, 233–242. doi:10.1042/CS20130580
- Scheibner, K. A., Teaboldt, B., Hauer, M. C., Chen, X., Cherukuri, S., Guo, Y., et al. (2012). MiR-27a Functions as a Tumor Suppressor in Acute Leukemia by Regulating 14-3-3 σ . *PLoS one* 7, e50895. doi:10.1371/journal.pone.0050895
- Scherr, M., Venturini, L., Battmer, K., Schaller-Schoenitz, M., Schaefer, D., Dallmann, I., et al. (2007). Lentivirus-mediated Antagomir Expression for Specific Inhibition of miRNA Function. *Nucleic Acids Res.* 35, e149. doi:10.1093/nar/gkm971
- Schmidt, M. F. (2014). Drug Target miRNAs: Chances and Challenges. *Trends Biotechnol.* 32, 578–585. doi:10.1016/j.tibtech.2014.09.002
- Segura, M. F., Hanniford, D., Menendez, S., Reavie, L., Zou, X., Alvarez-Diaz, S., et al. (2009). Aberrant miR-182 Expression Promotes Melanoma Metastasis by Repressing FOXO3 and Microphthalmia-Associated Transcription Factor. *Proc. Natl. Acad. Sci. U S A.* 106, 1814–1819. doi:10.1073/pnas.0808263106
- Selcuklu, S. D., Donoghue, M. T., Rehmet, K., de Souza Gomes, M., Fort, A., Kovvuru, P., et al. (2012). MicroRNA-9 Inhibition of Cell Proliferation and Identification of Novel miR-9 Targets by Transcriptome Profiling in Breast Cancer Cells. *J. Biol. Chem.* 287, 29516–29528. doi:10.1074/jbc.M111.335943
- Sengupta, S., den Boon, J. A., Chen, I. H., Newton, M. A., Stanhope, S. A., Cheng, Y. J., et al. (2008). MicroRNA 29c Is Down-Regulated in Nasopharyngeal Carcinomas, Up-Regulating mRNAs Encoding Extracellular Matrix Proteins. *Proc. Natl. Acad. Sci. U S A.* 105, 5874–5878. doi:10.1073/pnas.0801130105
- Shakeri, A., Ghanbari, M., Tasbandi, A., and Sahebkar, A. (2021). Regulation of microRNA-21 Expression by Natural Products in Cancer. *Phytotherapy Res.*
- Shao, J., Cao, J., Liu, Y., Mei, H., Zhang, Y., and Xu, W. (2015). MicroRNA-519a Promotes Proliferation and Inhibits Apoptosis of Hepatocellular Carcinoma Cells by Targeting FOXF2. *FEBS Open Bio* 5, 893–899. doi:10.1016/j.fob.2015.10.009

- Shen, H., Wang, D., Li, L., Yang, S., Chen, X., Zhou, S., et al. (2017). MiR-222 Promotes Drug-Resistance of Breast Cancer Cells to Adriamycin via Modulation of PTEN/Akt/FOXO1 Pathway. *Gene* 596, 110–118. doi:10.1016/j.gene.2016.10.016
- Shi, W., Gerster, K., Alajez, N. M., Tsang, J., Waldron, L., Pintilie, M., et al. (2011). MicroRNA-301 Mediates Proliferation and Invasion in Human Breast Cancer. *Cancer Res.* 71, 2926–2937. doi:10.1158/0008-5472.CAN-10-3369
- Shi, Z., Zhang, J., Qian, X., Han, L., Zhang, K., Chen, L., et al. (2013). AC1MMYR2, an Inhibitor of Dicer-Mediated Biogenesis of Oncomir miR-21, Reverses Epithelial-Mesenchymal Transition and Suppresses Tumor Growth and Progression. *Cancer Res.* 73, 5519–5531. doi:10.1158/0008-5472.CAN-13-0280
- Shi, Z. M., Wang, J., Yan, Z., You, Y. P., Li, C. Y., Qian, X., et al. (2012). MiR-128 Inhibits Tumor Growth and Angiogenesis by Targeting p70S6K1. *PLoS one* 7, e32709. doi:10.1371/journal.pone.0032709
- Shu, Y., Wu, K., Zeng, Z., Huang, S., Ji, X., Yuan, C., et al. (2018). A Simplified System to Express Circularized Inhibitors of miRNA for Stable and Potent Suppression of miRNA Functions. *Mol. Ther. Nucleic Acids* 13, 556–567. doi:10.1016/j.omtn.2018.09.025
- Si, M. L., Zhu, S., Wu, H., Lu, Z., Wu, F., and Mo, Y. Y. (2007). miR-21-mediated Tumor Growth. *Oncogene* 26, 2799–2803. doi:10.1038/sj.onc.1210083
- Singh, S., Narang, A. S., and Mahato, R. I. (2011). Subcellular Fate and Off-Target Effects of siRNA, shRNA, and miRNA. *Pharm. Res.* 28, 2996–3015. doi:10.1007/s11095-011-0608-1
- Song, B., Ji, W., Guo, S., Liu, A., Jing, W., Shao, C., et al. (2014). miR-545 Inhibited Pancreatic Ductal Adenocarcinoma Growth by Targeting RIG-I. *FEBS Lett.* 588, 4375–4381. doi:10.1016/j.febslet.2014.10.004
- Song, J. H., and Meltzer, S. J. (2012). MicroRNAs in Pathogenesis, Diagnosis, and Treatment of Gastroesophageal Cancers. *Gastroenterology* 143, 35–e2. doi:10.1053/j.gastro.2012.05.003
- Song, J. J., and Li, W. (2019). MiR-10b Suppresses the Growth and Metastasis of Colorectal Cancer Cell by Targeting FGF13. *Eur. Rev. Med. Pharmacol. Sci.* 23, 576–587. doi:10.26355/eurrev_201901_16870
- Sun, X. J., Liu, H., Zhang, P., Zhang, X. D., Jiang, Z. W., and Jiang, C. C. (2013). miR-10b Promotes Migration and Invasion in Nasopharyngeal Carcinoma Cells. *Asian Pac. J. Cancer Prev.* 14, 5533–5537. doi:10.7314/apjcp.2013.14.9.5533
- Sun, Y., Bai, Y., Zhang, F., Wang, Y., Guo, Y., and Guo, L. (2010). miR-126 Inhibits Non-small Cell Lung Cancer Cells Proliferation by Targeting EGFL7. *Biochem. Biophys. Res. Commun.* 391, 1483–1489. doi:10.1016/j.bbrc.2009.12.098
- Takagi, S., Nakajima, M., Kida, K., Yamaura, Y., Fukami, T., and Yokoi, T. (2010). MicroRNAs Regulate Human Hepatocyte Nuclear Factor 4alpha, Modulating the Expression of Metabolic Enzymes and Cell Cycle. *J. Biol. Chem.* 285, 4415–4422. doi:10.1074/jbc.M109.085431
- Takamizawa, J., Konishi, H., Yanagisawa, K., Tomida, S., Osada, H., Endoh, H., et al. (2004). Reduced Expression of the Let-7 microRNAs in Human Lung Cancers in Association with Shortened Postoperative Survival. *Cancer Res.* 64, 3753–3756. doi:10.1158/0008-5472.CAN-04-0637
- Takasaki, S. (2015). Roles of microRNAs in Cancers and Development. *Methods Mol. Biol.* 1218, 375–413. doi:10.1007/978-1-4939-1538-5_24
- Takeshita, F., Patrawala, L., Osaki, M., Takahashi, R. U., Yamamoto, Y., Kosaka, N., et al. (2010). Systemic Delivery of Synthetic microRNA-16 Inhibits the Growth of Metastatic Prostate Tumors via Downregulation of Multiple Cell-Cycle Genes. *Mol. Ther.* 18, 181–187. doi:10.1038/mt.2009.207
- Tan, S., Li, R., Ding, K., Lobie, P. E., and Zhu, T. (2011). miR-198 Inhibits Migration and Invasion of Hepatocellular Carcinoma Cells by Targeting the HGF/c-MET Pathway. *FEBS Lett.* 585, 2229–2234. doi:10.1016/j.febslet.2011.05.042
- Tan, S. B., Huang, C., Chen, X., Wu, Y., Zhou, M., Zhang, C., et al. (2013). Small Molecular Inhibitors of miR-1 Identified from Photocycloadducts of Acetylenes with 2-Methoxy-1,4-Naphthalenequinone. *Bioorg. Med. Chem.* 21, 6124–6131. doi:10.1016/j.bmc.2013.04.058
- Tang, H., Yao, L., Tao, X., Yu, Y., Chen, M., Zhang, R., et al. (2013). miR-9 Functions as a Tumor Suppressor in Ovarian Serous Carcinoma by Targeting TLN1. *Int. J. Mol. Med.* 32, 381–388. doi:10.3892/ijmm.2013.1400
- Taniguchi, K., Sugito, N., Kumazaki, M., Shinohara, H., Yamada, N., Nakagawa, Y., et al. (2015). MicroRNA-124 Inhibits Cancer Cell Growth through PTB1/PKM1/PKM2 Feedback cascade in Colorectal Cancer. *Cancer Lett.* 363, 17–27. doi:10.1016/j.canlet.2015.03.026
- Tavazoie, S. F., Alarcón, C., Oskarsson, T., Padua, D., Wang, Q., Bos, P. D., et al. (2008). Endogenous Human microRNAs that Suppress Breast Cancer Metastasis. *Nature* 451, 147–152. doi:10.1038/nature06487
- Tetzlaff, M. T., Liu, A., Xu, X., Master, S. R., Baldwin, D. A., Tobias, J. W., et al. (2007). Differential Expression of miRNAs in Papillary Thyroid Carcinoma Compared to Multinodular Goiter Using Formalin Fixed Paraffin Embedded Tissues. *Endocr. Pathol.* 18, 163–173. doi:10.1007/s12022-007-0023-7
- Thomas, M., Lange-Grünweller, K., Weirauch, U., Gutsch, D., Aigner, A., Grünweller, A., et al. (2012). The Proto-Oncogene Pim-1 Is a Target of miR-33a. *Oncogene* 31, 918–928. doi:10.1038/nc.2011.278
- Thum, T., Catalucci, D., and Bauersachs, J. (2008). MicroRNAs: Novel Regulators in Cardiac Development and Disease. *Cardiovasc. Res.* 79, 562–570. doi:10.1093/cvr/cvn137
- Tian, Y., Luo, A., Cai, Y., Su, Q., Ding, F., Chen, H., et al. (2010). MicroRNA-10b Promotes Migration and Invasion through KLF4 in Human Esophageal Cancer Cell Lines. *J. Biol. Chem.* 285, 7986–7994. doi:10.1074/jbc.M109.062877
- To, K. K. W., Fong, W., Tong, C. W. S., Wu, M., Yan, W., and Cho, W. C. S. (2020). Advances in the Discovery of microRNA-Based Anticancer Therapeutics: Latest Tools and Developments. *Expert Opin. Drug Discov.* 15, 63–83. doi:10.1080/17460441.2020.1690449
- Trang, P., Medina, P. P., Wiggins, J. F., Ruffino, L., Kelnar, K., Omotola, M., et al. (2010). Regression of Murine Lung Tumors by the Let-7 microRNA. *Oncogene* 29, 1580–1587. doi:10.1038/nc.2009.445
- Trang, P., Wiggins, J. F., Daige, C. L., Cho, C., Omotola, M., Brown, D., et al. (2011). Systemic Delivery of Tumor Suppressor microRNA Mimics Using a Neutral Lipid Emulsion Inhibits Lung Tumors in Mice. *Mol. Ther.* 19, 1116–1122. doi:10.1038/mt.2011.48
- Tsang, W. P., Ng, E. K., Ng, S. S., Jin, H., Yu, J., Sung, J. J., et al. (2010). Oncofetal H19-Derived miR-675 Regulates Tumor Suppressor RB in Human Colorectal Cancer. *Carcinogenesis* 31, 350–358. doi:10.1093/carcin/bgp181
- Tu, K., Liu, Z., Yao, B., Han, S., and Yang, W. (2016). MicroRNA-519a Promotes Tumor Growth by Targeting PTEN/PI3K/AKT Signaling in Hepatocellular Carcinoma. *Int. J. Oncol.* 48, 965–974. doi:10.3892/ijo.2015.3309
- Ugalde, A. P., Ramsay, A. J., De La Rosa, J., Varela, I., Mariño, G., Cadiñanos, J., et al. (2011). Aging and Chronic DNA Damage Response Activate a Regulatory Pathway Involving miR-29 and P53. *EMBO J.* 30, 2219–2232. doi:10.1038/emboj.2011.124
- van Zandwijk, N., Pavlakakis, N., Kao, S. C., Linton, A., Boyer, M. J., Clarke, S., et al. (2017). Safety and Activity of microRNA-Loaded Minicells in Patients with Recurrent Malignant Pleural Mesothelioma: a First-In-Man, Phase 1, Open-Label, Dose-Escalation Study. *Lancet Oncol.* 18, 1386–1396. doi:10.1016/S1470-2045(17)30621-6
- Velagapudi, S. P., Gallo, S. M., and Disney, M. D. (2014). Sequence-based Design of Bioactive Small Molecules that Target Precursor microRNAs. *Nat. Chem. Biol.* 10, 291–297. doi:10.1038/nchembio.1452
- Vishnoi, A., and Rani, S. (2017). MiRNA Biogenesis and Regulation of Diseases: an Overview. *Methods Mol. Biol.* 1509, 1–10. doi:10.1007/978-1-4939-6524-3_1
- Viteri, S., and Rosell, R. (2018). An Innovative Mesothelioma Treatment Based on miR-16 Mimic Loaded EGFR Targeted Minicells (TargomiRs). *Transl. Lung Cancer Res.* 7, S1. doi:10.21037/tlcr.2017.12.01
- Volinia, S., Calin, G. A., Liu, C. G., Ambros, S., Cimmino, A., Petrocca, F., et al. (2006). A microRNA Expression Signature of Human Solid Tumors Defines Cancer Gene Targets. *Proc. Natl. Acad. Sci. U.S.A.* 103, 2257–2261. doi:10.1073/pnas.0510565103
- Voorhoeve, P. M., Le Sage, C., Schrier, M., Gillis, A. J., Stoop, H., Nagel, R., et al. (2006). A Genetic Screen Implicates miRNA-372 and miRNA-373 as Oncogenes in Testicular Germ Cell Tumors. *Cell* 124, 1169–1181. doi:10.1016/j.cell.2006.02.037
- Wang, C. Z., Yuan, P., and Li, Y. (2015). MiR-126 Regulated Breast Cancer Cell Invasion by Targeting ADAM9. *Int. J. Clin. Exp. Pathol.* 8, 6547–6553.
- Wang, L., Qu, J., Zhou, L., Liao, F., and Wang, J. (2018). MicroRNA-373 Inhibits Cell Proliferation and Invasion via Targeting BRF2 in Human Non-small Cell Lung Cancer A549 Cell Line. *Cancer Res. Treat.* 50, 936–949. doi:10.4143/crt.2017.302
- Wang, L., Yao, J., Shi, X., Hu, L., Li, Z., Song, T., et al. (2013). MicroRNA-302b Suppresses Cell Proliferation by Targeting EGFR in Human Hepatocellular Carcinoma SMMC-7721 Cells. *BMC cancer* 13, 448–449. doi:10.1186/1471-2407-13-448

- Wang, S., Yan, Y., Cheng, Z., Hu, Y., and Liu, T. (2018). Sotetsuflavone Suppresses Invasion and Metastasis in Non-small-cell Lung Cancer A549 Cells by Reversing EMT via the TNF- α /nf- κ B and PI3K/AKT Signaling Pathway. *Cell Death Discov* 4, 26–11. doi:10.1038/s41420-018-0026-9
- Wang, Y. Y., Ye, Z. Y., Zhao, Z. S., Li, L., Wang, Y. X., Tao, H. Q., et al. (2013). Clinicopathologic Significance of miR-10b Expression in Gastric Carcinoma. *Hum. Pathol.* 44, 1278–1285. doi:10.1016/j.humpath.2012.10.014
- Wang, Z. (2011). *The Concept of Multiple-Target Anti-miRNA Antisense Oligonucleotide Technology, MicroRNA and Cancer*. Springer, 51–57. doi:10.1007/978-1-60761-863-8_4
- Wang, Z. (2011). *The Guideline of the Design and Validation of MiRNA Mimics, MicroRNA and Cancer*. Springer, 211–223. doi:10.1007/978-1-60761-863-8_15
- Warren, C. F. A., Wong-Brown, M. W., and Bowden, N. A. (2019). BCL-2 Family Isoforms in Apoptosis and Cancer. *Cel Death Dis* 10, 1–12. doi:10.1038/s41419-019-1407-6
- Watashi, K., Yeung, M. L., Starost, M. F., Hosmane, R. S., and Jeang, K. T. (2010). Identification of Small Molecules that Suppress microRNA Function and Reverse Tumorigenesis. *J. Biol. Chem.* 285, 24707–24716. doi:10.1074/jbc.M109.062976
- Weiler, J., Hunziker, J., and Hall, J. (2006). Anti-miRNA Oligonucleotides (AMOs): Ammunition to Target miRNAs Implicated in Human Disease? *Gene Ther.* 13, 496–502. doi:10.1038/sj.gt.3302654
- Welch, C., Chen, Y., and Stallings, R. L. (2007). MicroRNA-34a Functions as a Potential Tumor Suppressor by Inducing Apoptosis in Neuroblastoma Cells. *Oncogene* 26, 5017–5022. doi:10.1038/sj.onc.1210293
- Wen, Q., Zhao, J., Bai, L., Wang, T., Zhang, H., and Ma, Q. (2015). miR-126 Inhibits Papillary Thyroid Carcinoma Growth by Targeting LRP6. *Oncol. Rep.* 34, 2202–2210. doi:10.3892/or.2015.4165
- Wickramasinghe, N. S., Manavalan, T. T., Dougherty, S. M., Riggs, K. A., Li, Y., and Klinge, C. M. (2009). Estradiol Downregulates miR-21 Expression and Increases miR-21 Target Gene Expression in MCF-7 Breast Cancer Cells. *Nucleic Acids Res.* 37, 2584–2595. doi:10.1093/nar/gkp117
- Wiggins, J. F., Ruffino, L., Kelnar, K., Omotola, M., Patrawala, L., Brown, D., et al. (2010). Development of a Lung Cancer Therapeutic Based on the Tumor Suppressor microRNA-34. *Cancer Res.* 70, 5923–5930. doi:10.1158/0008-5472.CAN-10-0655
- Wu, K. J. (2020). The Role of miRNA Biogenesis and DDX17 in Tumorigenesis and Cancer Stemness. *Biomed. J.* 43, 107–114. doi:10.1016/j.bj.2020.03.001
- Wu, P. (2020). Inhibition of RNA-Binding Proteins with Small Molecules. *Nat. Rev. Chem.* 4, 441–458. doi:10.1038/s41570-020-0201-4
- Wuchty, S., Arjona, D., Li, A., Kotliarov, Y., Walling, J., Ahn, S., et al. (2011). Prediction of Associations between microRNAs and Gene Expression in Glioma Biology. *PLoS one* 6, e14681. doi:10.1371/journal.pone.0014681
- Würdinger, T., Tannous, B. A., Saydam, O., Skog, J., Grau, S., Soutschek, J., et al. (2008). miR-296 Regulates Growth Factor Receptor Overexpression in Angiogenic Endothelial Cells. *Cancer cell* 14, 382–393. doi:10.1016/j.ccr.2008.10.005
- Wystub, K., Besser, J., Bachmann, A., Boettger, T., and Braun, T. (2013). miR-1/133a Clusters Cooperatively Specify the Cardiomyogenic Lineage by Adjustment of Myocardin Levels during Embryonic Heart Development. *PLoS Genet.* 9, e1003793. doi:10.1371/journal.pgen.1003793
- Xia, J., Cao, T., Ma, C., Shi, Y., Sun, Y., Wang, Z. P., et al. (2018). miR-7 Suppresses Tumor Progression by Directly Targeting MAP3K9 in Pancreatic Cancer. *Mol. Ther. Nucleic Acids* 13, 121–132. doi:10.1016/j.omtn.2018.08.012
- Xia, Z., Liu, F., Zhang, J., and Liu, L. (2015). Decreased Expression of MiRNA-204-5p Contributes to Glioma Progression and Promotes Glioma Cell Growth, Migration and Invasion. *PLoS one* 10, e0132399. doi:10.1371/journal.pone.0132399
- Xiong, Y., Kotian, S., Zeiger, M. A., Zhang, L., and Kebebew, E. (2015). miR-126-3p Inhibits Thyroid Cancer Cell Growth and Metastasis, and Is Associated with Aggressive Thyroid Cancer. *PLoS one* 10, e0130496. doi:10.1371/journal.pone.0130496
- Xu, K., Chen, Z., Qin, C., and Song, X. (2014). miR-7 Inhibits Colorectal Cancer Cell Proliferation and Induces Apoptosis by Targeting XRCC2. *Onco Targets Ther.* 7, 325–332. doi:10.2147/OTT.S59364
- Xu, Y., Jin, J., Liu, Y., Huang, Z., Deng, Y., You, T., et al. (2014). Snail-regulated MiR-375 Inhibits Migration and Invasion of Gastric Cancer Cells by Targeting JAK2. *PLoS one* 9, e99516. doi:10.1371/journal.pone.0099516
- Yamashita, R., Sato, M., Kakumu, T., Hase, T., Yogo, N., Maruyama, E., et al. (2015). Growth Inhibitory Effects of miR-221 and miR-222 in Non-small Cell Lung Cancer Cells. *Cancer Med.* 4, 551–564. doi:10.1002/cam4.412
- Yang, H., Liu, P., Zhang, J., Peng, X., Lu, Z., Yu, S., et al. (2016). Long Noncoding RNA MIR31HG Exhibits Oncogenic Property in Pancreatic Ductal Adenocarcinoma and Is Negatively Regulated by miR-193b. *Oncogene* 35, 3647–3657. doi:10.1038/onc.2015.430
- Yang, Z. G., Ma, X. D., He, Z. H., and Guo, Y. X. (2017). miR-483-5p Promotes Prostate Cancer Cell Proliferation and Invasion by Targeting RBM5. *Int. Braz. J. Urol.* 43, 1060–1067. doi:10.1590/S1677-5538.IBJU.2016.0595
- Yoshino, H., Chiyomaru, T., Enokida, H., Kawakami, K., Tatarano, S., Nishiyama, K., et al. (2011). The Tumour-Suppressive Function of miR-1 and miR-133a Targeting TAGLN2 in Bladder Cancer. *Br. J. Cancer* 104, 808–818. doi:10.1038/bjc.2011.23
- Young, D. D., Connelly, C. M., Grohmann, C., and Deiters, A. (2010). Small Molecule Modifiers of microRNA miR-122 Function for the Treatment of Hepatitis C Virus Infection and Hepatocellular Carcinoma. *J. Am. Chem. Soc.* 132, 7976–7981. doi:10.1021/ja910275u
- Yu, A. M., Choi, Y. H., and Tu, M. J. (2020). RNA Drugs and RNA Targets for Small Molecules: Principles, Progress, and Challenges. *Pharmacol. Rev.* 72, 862–898. doi:10.1124/pr.120.019554
- Yu, G., Li, H., Wang, J., Gumireddy, K., Li, A., Yao, W., et al. (2014). miRNA-34a Suppresses Cell Proliferation and Metastasis by Targeting CD44 in Human Renal Carcinoma Cells. *J. Urol.* 192, 1229–1237. doi:10.1016/j.juro.2014.05.094
- Zhang, B. G., Liu, B. Y., Yan, M., Chen, X. H., Yu, P. T., and Zhu, Z. G. (2011). Biological Behaviour and PTEN Expression Change after MicroRNA-21 Down-Regulation in Gastric Cancer Cells. *J. Surg. Concepts Pract.* 16, 562–567.
- Zhang, S., Ma, C., Pang, H., Zeng, F., Cheng, L., Fang, B., et al. (2016). Arsenic Trioxide Suppresses Cell Growth and Migration via Inhibition of miR-27a in Breast Cancer Cells. *Biochem. Biophys. Res. Commun.* 469, 55–61. doi:10.1016/j.bbrc.2015.11.071
- Zhang, Y., Chao, T., Li, R., Liu, W., Chen, Y., Yan, X., et al. (2009). MicroRNA-128 Inhibits Glioma Cells Proliferation by Targeting Transcription Factor E2F3a. *J. Mol. Med. (Berl)* 87, 43–51. doi:10.1007/s00109-008-0403-6
- Zhang, Z., Liu, S., Shi, R., and Zhao, G. (2011). miR-27 Promotes Human Gastric Cancer Cell Metastasis by Inducing Epithelial-To-Mesenchymal Transition. *Cancer Genet.* 204, 486–491. doi:10.1016/j.cancergen.2011.07.004
- Zhang, Z. G., Chen, W. X., Wu, Y. H., Liang, H. F., and Zhang, B. X. (2014). MiR-132 Prohibits Proliferation, Invasion, Migration, and Metastasis in Breast Cancer by Targeting HN1. *Biochem. Biophys. Res. Commun.* 454, 109–114. doi:10.1016/j.bbrc.2014.10.049
- Zhou, L. Y., Qin, Z., Zhu, Y. H., He, Z. Y., and Xu, T. (2019). Current RNA-Based Therapeutics in Clinical Trials. *Curr. Gene Ther.* 19, 172–196. doi:10.2174/1566523219666190719100526
- Zhu, S., Si, M. L., Wu, H., and Mo, Y. Y. (2007). MicroRNA-21 Targets the Tumor Suppressor Gene Tropomyosin 1 (TPM1). *J. Biol. Chem.* 282, 14328–14336. doi:10.1074/jbc.M611393200
- Zoni, E., van der Horst, G., van de Merbel, A. F., Chen, L., Rane, J. K., Pelger, R. C., et al. (2015). miR-25 Modulates Invasiveness and Dissemination of Human Prostate Cancer Cells via Regulation of α v- and α 6-Integrin Expression. *Cancer Res.* 75, 2326–2336. doi:10.1158/0008-5472.CAN-14-2155

Conflict of Interest: The authors declare that the research was conducted in the absence of any commercial or financial relationships that could be construed as a potential conflict of interest.

Publisher's Note: All claims expressed in this article are solely those of the authors and do not necessarily represent those of their affiliated organizations, or those of the publisher, the editors and the reviewers. Any product that may be evaluated in this article, or claim that may be made by its manufacturer, is not guaranteed or endorsed by the publisher.

Copyright © 2021 Fu, Wang, Li, Chen, Au-Yeung and Shi. This is an open-access article distributed under the terms of the Creative Commons Attribution License (CC BY). The use, distribution or reproduction in other forums is permitted, provided the original author(s) and the copyright owner(s) are credited and that the original publication in this journal is cited, in accordance with accepted academic practice. No use, distribution or reproduction is permitted which does not comply with these terms.



Ginsenoside Rb1 Lessens Gastric Precancerous Lesions by Interfering With β -Catenin/TCF4 Interaction

Jinhao Zeng^{1,2}, Xiao Ma³, Ziyi Zhao², Yu Chen², Jundong Wang², Yanwei Hao¹, Junrong Yu¹, Zhongzhen Zeng¹, Nianzhi Chen¹, Maoyuan Zhao¹, Jianyuan Tang^{2*} and Daoyin Gong^{4*}

¹Department of Chinese Internal Medicine, Hospital of Chengdu University of Traditional Chinese Medicine, Chengdu, China,

²TCM Regulating Metabolic Diseases Key Laboratory of Sichuan Province, Hospital of Chengdu University of Traditional Chinese Medicine, Chengdu, China, ³School of Pharmacy, Chengdu University of Traditional Chinese Medicine, Chengdu, China,

⁴Department of Pathology, Hospital of Chengdu University of Traditional Chinese Medicine, Chengdu, China

OPEN ACCESS

Edited by:

Zhi-Xiang Yuan,
Southwest Minzu University, China

Reviewed by:

Montserrat Reyes,
University of Chile, Chile
Yang Bi,
Children's Hospital of Chongqing
Medical University, China

*Correspondence:

Jianyuan Tang
tangjy@cdutcm.edu.cn
Daoyin Gong
daoyingong@163.com

Specialty section:

This article was submitted to
Pharmacology of Anti-Cancer Drugs,
a section of the journal
Frontiers in Pharmacology

Received: 19 March 2021

Accepted: 09 July 2021

Published: 14 September 2021

Citation:

Zeng J, Ma X, Zhao Z, Chen Y, Wang J,
Hao Y, Yu J, Zeng Z, Chen N, Zhao M,
Tang J and Gong D (2021)
Ginsenoside Rb1 Lessens Gastric
Precancerous Lesions by Interfering
With β -Catenin/TCF4 Interaction.
Front. Pharmacol. 12:682713.
doi: 10.3389/fphar.2021.682713

Background: Seeking novel and effective therapies for gastric precancerous lesions (GPL) is crucial to reducing the incidence of gastric cancer. Ginsenoside Rb1 (GRb1) is a major ginsenoside in ginseng and has been proved to possess multiple bioactivities. However, whether GRb1 could protect against GPL and the underlying mechanisms have not been explored.

Methods: We evaluated the effects of GRb1 on gastric precancerous lesions in rats on macroscopic, microscopic and ultramicroscopic levels. Then, an antibody array was employed to screen differential expression proteins (DEPs). Validation for the targeting DEP and investigation for the possible mechanism was conducted using immunohistochemistry, qRT-PCR, TUNEL apoptosis assay, immunoprecipitation and immunoblotting.

Results: GRb1 was found to reverse intestinal metaplasia and a portion of dysplasia in the MNNG-induced GPL rats. The antibody array assay revealed seven DEPs in GPL rats as compared to control rats (5 DEPs were up-regulated, while two DEPs were down-regulated). Among the DEPs, β -catenin, beta-NGF and FSTL1 were significantly down-regulated after GRb1 administration. Our validation results revealed that enhanced protein expression and nuclear translocation of β -catenin were present in animal GPL samples. In addition, analysis of human gastric specimens demonstrated that β -catenin up-regulation and nuclear translocation were significantly associated with advanced GPL pathology. GRb1 intervention not only decreased protein expression and nuclear translocation of β -catenin, but interfered with β -catenin/TCF4 interaction. Along with this, declined transcriptional and protein expression levels of downstream target genes including c-myc, cyclin D1 and Birc5 were observed in GRb1-treated GPL rats.

Conclusion: GRb1 is capable of preventing the occurrence and progression of GPL, which might be contributed by diminishing protein expression and nuclear translocation of β -catenin and interfering with β -catenin/TCF4 interaction.

Keywords: ginsenoside Rb1, gastric precancerous lesions, intestinal metaplasia, dysplasia, β -catenin/TCF4 interaction

INTRODUCTION

Gastric cancer still remains a major cancer worldwide, ranking fifth for incidence and fourth for mortality globally in the latest published global cancer statistics (Sung et al., 2021). Gastric carcinogenesis is a multistep process, in which gastric intestinal metaplasia (IM) and dysplasia (DYS) precedes most gastric adenocarcinomas and hence they are widely recognized as precancerous lesions (GPL). It is well established that the risk of gastric cancer increases with the severity of precancerous lesions (Akbari et al., 2019). This underscores the importance of screening, surveillance and treatment of patients harboring precancerous lesions. Preventing and even reversing the progression of GPL would definitely provide tangible benefits in reduction of gastric cancer incidence (De Vries et al., 2008; Akbari et al., 2019). For the therapy of GPL, it is recognized at present that endoscopic mucosal dissection was recommended for severe dysplasia and early gastric cancer (Pimentel-Nunes et al., 2019); however, no specific treatment for a majority of GPL available in clinical practice. Some vitamin and mineral supplements, particularly folic acid (Zhu et al., 2003), may be beneficial in reducing risk of progression to gastric cancer, but their therapeutic effect against GPL has not been verified (Jacobs et al., 2002; Dawsey et al., 2014). Seeking novel and effective therapies for patients with GPL has fueled a huge concern.

Ginsenoside Rb1 (known as one of the main bioactive components of *ginseng*) is the major constituent screened from Weipixiao (Zeng et al., 2016), a Chinese herbal prescription showing therapeutic effect against GPL, as revealed by previous clinical and animal studies (He et al., 2017; Zhang, 2017; Zeng et al., 2018). Previously, GRb1 has been proved to be a safe extraction and possess antineoplastic (Liu et al., 2017), antioxidative (Miao et al., 2017), anti-inflammatory (Liu et al., 2020) and anti-angiogenesis (Lu et al., 2017) bioactivities. In addition, an earlier study identified the gastroprotective activity of GRb1 in an ethanol-induced gastric lesion model, and demonstrated that the anti-ulcer effect is produced through an increase in mucus secretion (Jeong et al., 2003). GRb1 was recently found to reduce intestinal histological injury, and suppress inflammatory responses and oxidative stress (Chen et al., 2019). Moreover, GRb1 promote intestinal epithelial wound healing in a colitis rat model through regulating extracellular signal-regulated kinase and Rho signaling (Toyokawa et al., 2019). However, heretofore, whether GRb1 is capable of halting and even reversing GPL still remains unknown.

The Wnt/ β -catenin signaling pathway plays a key role in the regulation of cell proliferation, differentiation, embryogenesis and tumorigenesis. The contribution of aberrant Wnt/ β -catenin pathway to development of gastric cancer has been established (Clevers, 2006; Hanaki et al., 2012). Wnt/ β -catenin pathway has become the new targets for anti-tumor therapy, for instance, disruption of the pathway could suppress metastatic activity in gastric cancer cells (Hanaki et al., 2012). β -catenin serves as the key downstream effector of the canonical pathway. When Wnt ligands binds to its membrane receptor complex, β -catenin becomes stabilized and accumulates in cytoplasm, and then enters to nucleus with the TCF, thereby driving the

transcription of multiple proliferation- and apoptosis-associated genes (Nusse and Clevers, 2007). In this process, β -catenin/TCF4 interaction is a central variable. The downstream target genes of Wnt/ β -catenin, such as c-Jun, c-Myc and cyclin D1, Birc5 and Wisp1, have a significant relevance to multiple cellular biological behaviors including proliferation and apoptosis. Studies have shown that when the expression of β -catenin is reduced, the expressions of its activation targets including c-Jun, c-Myc and cyclin D1 are also decreased (Qin et al., 2019). Up-regulation of Birc5, which would promote cell proliferation, is activated by Wnt/ β -catenin signaling pathway (Fujiya et al., 2020). Additionally, activated Wnt/ β -catenin signaling promotes cancer metastasis through paracrine Wisp1 (Tai et al., 2014).

We verified the hypothesis in the present study that GRb1 could protect against gastric precancerous lesions. Next, we employed an antibody array to screen differential expression proteins and then carried out validation experiments. Finally, we sought to investigate the possible underlying mechanism regarding regulation on nuclear translocation of β -catenin and β -catenin/TCF4 interaction. Our work may provide experimental evidence for potential clinical use of GRb1 in GPL treatment.

MATERIALS AND METHODS

Animals

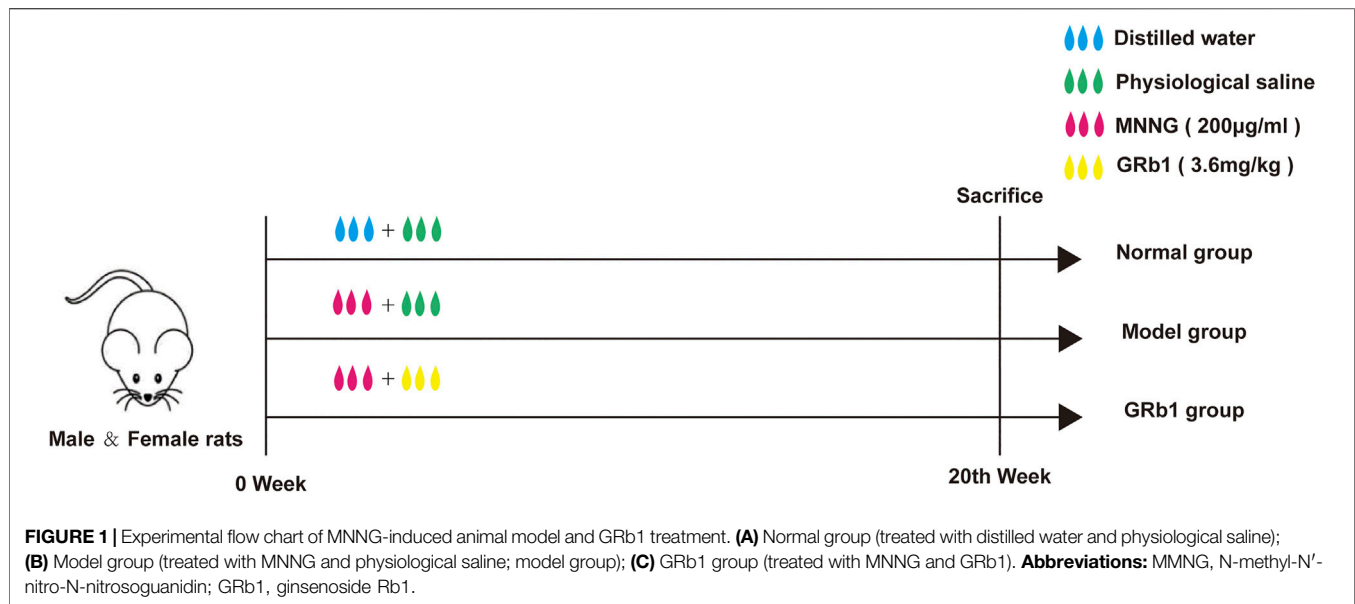
Sprague-Dawley rats weighing 160–180 g (half male and half female) were obtained from Chengdu Dashuo Experimental Animal Co., Ltd., Chengdu, China (SCXK-2020-030). This experiment was conducted in TCM Regulating Metabolic Diseases Key Laboratory of Sichuan Province, Hospital of Chengdu University of Traditional Chinese Medicine. Animal welfare considerations taken and all procedures were approved by the Institutional Animal Care and Use Committee (approval no. 2019-17).

Clinical Tissue Samples

Formalin-fixed, paraffin-embedded samples of GPL gastric mucosa (94 cases) and normal gastric mucosa (85 cases) were provided from the Hospital of Chengdu University of TCM (Chengdu, China), and retrospectively analyzed. The pathological diagnosis of each sample was performed by two independent senior pathological staffs in the Department of Pathology. This study was approved by the Institutional Review Board of the Teaching Hospital of Chengdu University of TCM (Chengdu, China) (approval no. 2018KL-023) and written informed consent was obtained from all participants for being included in the study.

Drugs and Reagents

N-methyl-N'-nitro-N-nitrosoguanidine (MNNG) was purchased from Tokyo Chemical Industry CO., LTD., Japan (cat. no. M0527); Ginsenoside Rb1 was supplied by Hefei Bomei Biotechnology CO., LTD., China (cat. no. BZP0234); Rat antibody array 90 glass slide kit was supplied by RayBiotech, United States (cat. no. AAR-BLG-1); β -catenin antibody was



purchased from Thermo Fisher Scientific, Inc., United States (cat. no. MA1-301); Transcription factor 7-like 2 (TCF-4/TCF7L2) antibody, c-myc antibody, cyclin D1 antibody, baculoviral IAP repeat containing 5 (Birc5) antibody and proliferating cell nuclear antigen (PCNA) antibody were purchased from abcam, United Kingdom (cat. nos. ab134275; ab32072; ab134175; ab76424; ab18197); Wnt1-inducible signaling pathway protein 1 (Wisp1) antibody, and c-jun antibody were obtained from Bioss, Inc., China (cat. nos. bs-6321R; bs-0670R). Ki67 antibody was supplied by Novus Biologicals, LLC, United States (cat. no. NB500-170). TdT-mediated dUTP Nick-End Labeling (TUNEL) apoptosis assay kit was supplied by Boster Biological Technology CO., LTD., China (cat. no. MK1025).

GPL Model and GRb1 Treatment

Animals were randomly assigned to three groups as follows ($n = 10$): 1) Normal (treated with distilled water and physiological saline, normal group); 2) Model (treated with MNNG and physiological saline; model group); 3) Model + GRb1 (treated with MNNG and GRb1; GRb1 group). MNNG is a carcinogen, which can induce the occurrence of gastric precancerous lesions (Saito et al., 1970; Tatematsu et al., 1988). To establish GPL model, the animals, except the normal controls, were allowed to drink MNNG solution (200 µg/ml) *ad libitum*, and underwent hunger-satiety shift every other day. The modeling procedure lasted for 20 consecutive weeks. Simultaneously, from the first day of MNNG treatment to the 20th week, GRb1 at 3.6 mg/kg was intragastrically administered to the rats in the GRb1 group once a day, while rats in normal group and model group received vehicle physiological saline by gastrogavage (10 ml/kg) once daily. At the end of 20th week, all animals were humanely anesthetized with sodium pentobarbital (140 mg/kg i. p.) after 12 h fasting. Following sacrifice by cervical dislocation, stomachs were harvested immediately. The flow chart of the experiment is shown in **Figure 1**.

Hematoxylin and Eosin Staining

Gastric tissues were fixed in 4% paraformaldehyde overnight at room temperature, dehydrated in graded ethanol series (30, 50, 70, 95 and 100%) and then embedded in paraffin. To examine pathological morphology, paraffin-embedded samples were cut into 5 µm-thick sections and then stained with hematoxylin and eosin. Each slide was monitored under microscopy (IX71; Olympus Corporation) and images were captured. The magnifications used were $\times 400$. These slides were evaluated by two independent pathologists in a blinded manner.

Transmission Electron Microscope

Fresh gastric mucosa was cut into 1 mm³ blocks and fixed in 2.5% glutaraldehyde in cacodylate buffer (pH 7.4) at 4°C for 4 h, and then post-fixed in 1% osmium tetroxide, also in phosphate buffer for 2 h. Next, samples were routinely dehydrated in graded ethanol series (50, 70, 80, 90, 95 and 100%) and transferred to acetone solution for 20 min. For infiltration, the samples were immersed in a mixture of acetone and epoxy resin twice (2:1 for 3 h at the first time, 1:2 for overnight at the second time), and then embedded in epoxy resin-filled capsules. Finally, 70 nm ultrathin sections were counterstained with 2% aqueous uranyl acetate and 0.8% lead citrate. Ultrastructure of gastric epithelial cells was observed and photographed using a transmission electron microscope (H-7650; Hitachi Ltd.). The magnification was $\times 10,000$.

Alcian Blue-Periodic Acid Schiff and High Iron Diamine Staining

AB-PAS staining was performed to evaluate the severity of IM lesion. Neutral mucins present in normal mucosa were stained magenta, while acidic mucins present in IM lesion were stained blue. Then, HID-PAS staining was conducted to

further assess small intestinal-type metaplasia (S-IM) and colonic-type metaplasia (C-IM), in which sulfomucins expressed only in C-IM lesion were stained brown. Images were captured under microscopy (IX71; Olympus Corporation) with magnification of $\times 100$.

Antibody Array Assay

Biotin label-based rat antibody array was conducted to determine the expression levels of 90 rat proteins, according to the manufacturer's instructions. Briefly, gastric epithelium was collected and homogenized in pre-cooled lysis buffer containing protease inhibitor cocktail at 4°C. Homogenates were then centrifuged at 12,000 rpm for 15 min twice. Next, supernatants were dialyzed in separate dialysis tubes, followed by determination of the total protein concentration using the bicinchoninic acid (BCA) assay (cat. no. 23227, Pierce Scientific Rockford, United States). After biotin-labeling the samples and blocking process, 400 μ l of diluted samples was added into each well for incubation overnight at 4°C. Then, each sub-array was incubated with Cy3-Conjugated Streptavidin at room temperature for 2 h (avoid exposure to light). Finally, the glass slides were scanned to detect the fluorescent signals of microarrays using an InnoScan 300 Microarray Scanner (Innopsys, France) at a wavelength of 532 nm.

Immunohistochemistry

Paraffin-embedded gastric tissues were cut into 3 μ m-thick sections, and dewaxed with xylene at room temperature and rehydrated in a descending ethanol series (100, 95, 85 and 75%). For antigen retrieval, sections were heated at 97°C for 20 min. Following a peroxidase blocking with 3% hydrogen peroxide for 15 min and 5% bovine serum albumin blocking for 30 min, the sections were incubated with primary antibodies against β -catenin (1:500), TCF-4 (1:1,000), PCNA (1:500) and Ki67 (1:100) overnight at 4°C. The sections were then exposed to HRP/Fab polymer conjugate at room temperature for 30 min (cat. no. PV-6000-D, Zhongshan Goldenbridge Biotechnology Co., Ltd.), following which they were stained with 3,3'-diaminobenzidine solution for 5 min and counterstained with hematoxylin for 20 s at room temperature. Three random visual fields were selected and photographed from each section. Quantification of expression levels was determined by mean of integrated optical density (IOD) using Image Pro Plus 6.0 software (Media Cybernetics, Inc.). Moreover, the expression pattern of β -catenin and its relationships with clinicopathological characteristics of GPL patients were evaluated. The sections were assessed by two independent investigators, without prior knowledge of the clinicopathological data, in a blinded manner. The immunoreactivity scores (IRS) were determined by the sum total of the percentage of positive cells (0 points, 0–5% positive cells; 1 point, 6–25%; 2 points, 26–50%; 3 points, 51–75% and 4 points, 76–100%), and staining intensity scores (0 points, no staining; 1 point, weak staining; 2 points, moderate staining and 3 points, strong staining). A final

IRS ≥ 4 indicated strong positivity, while scores < 4 indicated weak positivity.

TUNEL Apoptosis Assay

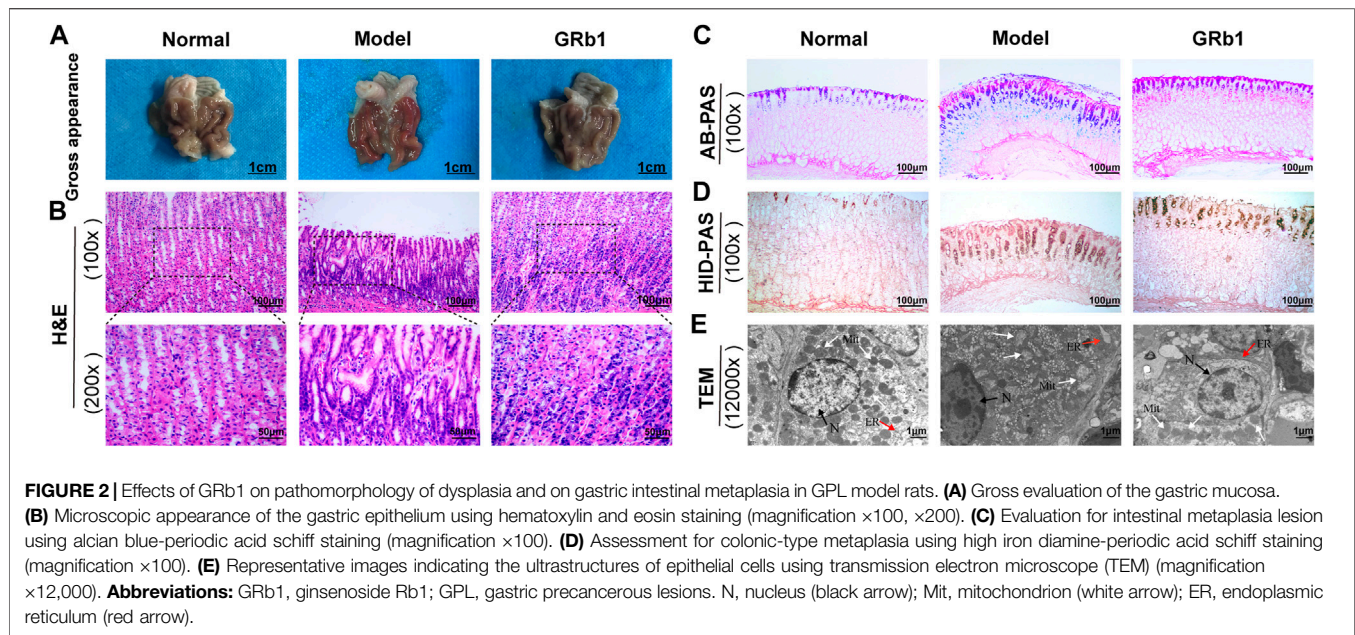
TUNEL apoptosis assay was carried out according to the manufacturer's instructions. Briefly, 3 μ m-thick sections, sliced from paraffin-embedded gastric tissues, were routinely dewaxed and rehydrated. The sections were incubated with proteinase K working solution at 37°C for 15 min, followed by incubation with labeling buffer containing Terminal deoxynucleotidyl Transferase (TdT) and digoxin labeled deoxyuridine triphosphate (dUTP). Next, proceed with blocking reagent prior to incubation with biotinylated anti-digoxin antibody at 37°C for 30 min. Finally, samples were exposed to strept avidin-biotin complex (SABC), followed by staining with 3, 3'-diaminobenzidine solution and counterstaining with hematoxylin. Apoptotic cells were shown as nuclear staining. Counting for apoptotic cells was performed using light microscopy (IX71; Olympus Corporation) with magnification of $\times 200$. Three randomly selected fields were captured for each section, in which apoptosis index was calculated.

Immunoprecipitation and Immunoblotting

Frozen gastric epithelium was collected, and homogenates and supernatants were prepared as described above. Total protein concentration was determined using the BCA assay (cat. no. 23227, Pierce Scientific Rockford, United States). Then, 480 μ g of total protein were incubated with 20 μ l of protein A/G beads (cat. no. sc-2003; Santa Cruz Biotechnology, Inc.) at 4°C for 1 h (the negative controls were incubated with 20 μ l of protein A/G beads and 2 μ l IgG). After centrifugation, 2 μ l β -catenin antibody (1:200) was added in lysate supernatants for incubation overnight at 4°C, and, next, 20 μ l of protein A/G beads was mixed, followed by gentle rotation at 4°C for 2 h. Following centrifugation and removal of supernatants, the beads were collected. The immunoprecipitation complex was washed 4 times, mixed with reduced loading buffer, boiled, and centrifuged. Finally, western blotting was performed to detect the abundance of both β -catenin and TCF-4 proteins in the immunoprecipitation complex. To determine the protein expression levels of c-myc, cyclin D1, Wisp1 and Birc5, western blotting was also performed as described previously (Li et al., 2021).

Reverse Transcription and Quantitative Real-Time PCR

Total RNA from gastric epithelium was extracted using a TRIzol kit (G3013; Servicebio). RNA concentration and quality were determined using the spectrophotometer (NanoDrop 2000; Thermo Fisher Scientific Inc.) and 1% agarose gels. Complementary DNA was synthesized using the RevertAid First Strand cDNA Synthesis Kit (K1621; Thermo Fisher Scientific Inc.). Subsequently, mRNA levels of *c-myc*, *c-jun*, *cyclin D1*, *Wisp1* and *Birc5* were determined using StepOne



Plus real-time PCR System (Applied Biosystems Inc.). Thermal conditions were as follows: 10 min at 95°C, 40 cycles of 15 s at 95°C and 60 s at 60°C, with 0.3°C rise per 15 s from 60°C to 95°C. *Gapdh* was applied as an endogenous control for RNA input. Differences in amplification were calculated using the $2^{-\Delta\Delta Ct}$ method. The primer sequences used were as follows: *c-myc* forward 5'-AAAACCCGACAGTCACGACG-3' and reverse 5'-GTAGCGACCGCAACATAGGAC-3'; *cyclin D1* forward 5'-TTCATCGAACACTTCTCTCCA-3' and reverse 5'-GAGGGTGGGTTGGAAA TGAA-3'; *c-jun* forward 5'-GCA ATGGGCACATCACCCTAC-3' and reverse 5'-GTGACA CTGGGCAGCGTATTCT-3'; *Wisp1* forward 5'-ACATCAAGGCAGG GAAGAAATG-3' and reverse 5'-CCT CTGGACACTGGAAATCAAC-3'; *Birc5* forward 5'-GACCAC CGGATCTACACCTTC-3' and reverse 5'-CTCGGTAGGGCA GTGGATGAA-3'; *Gapdh* forward 5'-CTGGAGAAACCTGCC AAGTATG-3' and reverse 5'-GGTGAAGAATGGGAGTT GCT-3'.

Statistical Analysis

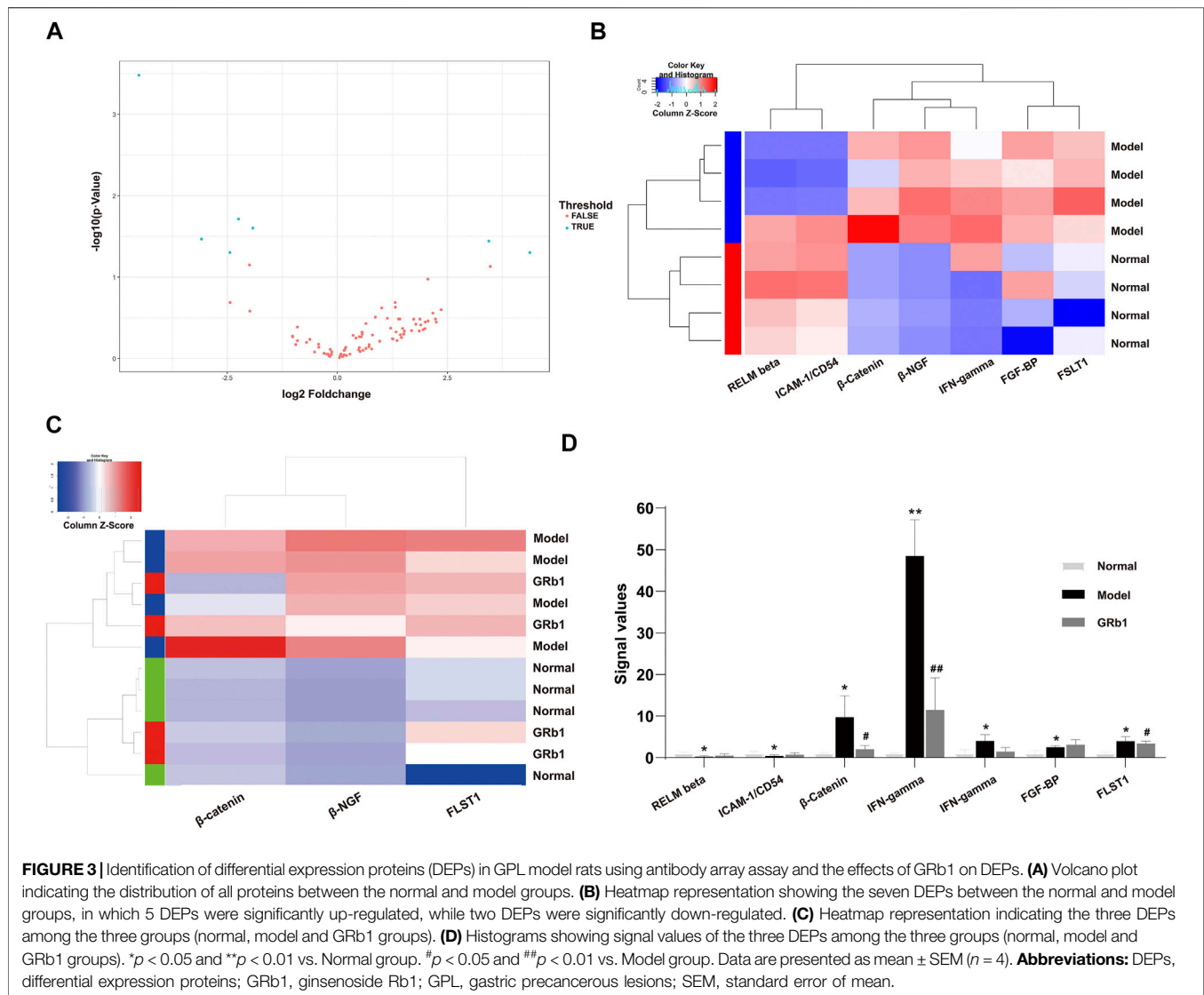
For antibody array assay, R software (version 3.6.3) package “limma” was employed to analyze the differential expression proteins using a linear model of empirical Bayesian method. When p value < 0.05, differential expression is considered. The other statistical data was analyzed using SPSS 23.0 software (IBM Inc.). Differences between groups were evaluated using one-way analysis of variance, followed by Tukey method for homogeneous data and Dunnett's T3 method for non-homogeneous data. Data are expressed as the mean \pm standard deviation. p < 0.05 was considered to indicate a statistically significant difference. Unpaired Student's t-test was used to assess the differences in β -catenin expression levels between gastric precancerous lesions group and control group. Pearson's χ^2 test and Fisher's exact test

were used to assess the association between nuclear localization of β -catenin, β -catenin expression and clinicopathological characteristics.

RESULTS

GRb1 Ameliorates Pathomorphology of Dysplasia

We test the effects of GRb1 on pathomorphology of gastric epithelium in GPL rats on macroscopic, microscopic and ultramicroscopic levels. As shown in **Figures 2A,B,E**, normal control rats exhibited normal macroscopic appearance of gastric mucosa, intact arrangement and morphology of gland and cells under light microscope, as well as intact and clear ultrastructure of epithelial cells revealed by TEM. By contrast, gastric mucosa from GPL model rats appeared as dark red, poor lustrousness, and, often, rough-surfaced. Light microscope revealed distorted, crowded glands in which cellular atypia characterized by enlarged and hyperchromatic nuclei, increased nuclear-cytoplasmic ratio and loss of polarity was noted. In addition, TEM provided evidence of pleomorphic nuclei, prominent chromatin condensation and nuclear membrane invagination in the GPL model rats. Swollen mitochondria with broken cristae, and expanded endoplasmic reticulum with sharp decreased numbers of ribosomes were also present. These observations were suggestive of DYS lesion. In most cases of GRb1-treated rats, the appearances of these aberrant morphologic alterations were less pronounced than those in GPL model rats. Therefore, GRb1 efficiently ameliorated the pathological morphologies of DYS lesion in GPL rats.



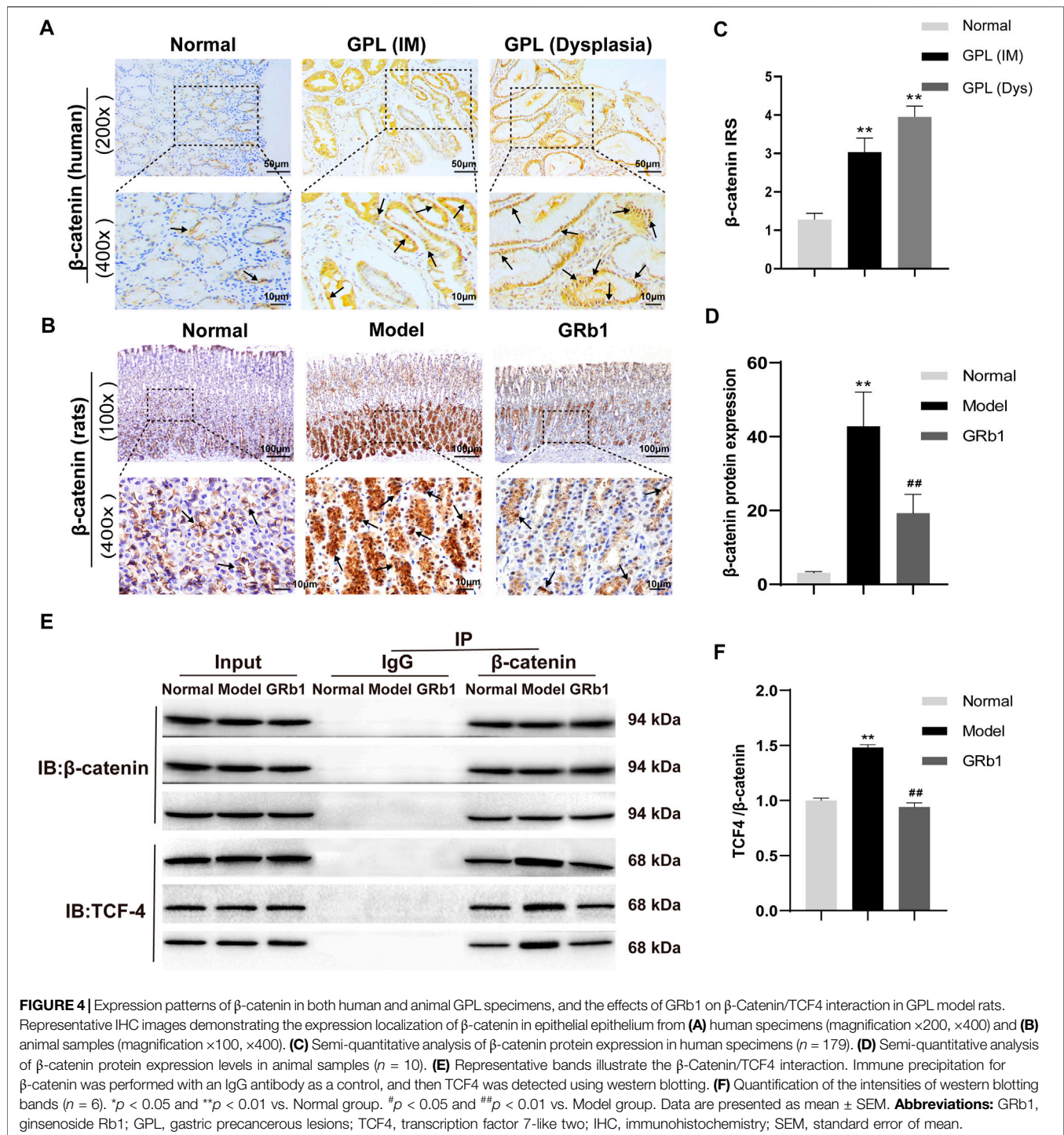
GRb1 Effectively Halts and Even Reverses Gastric Intestinal Metaplasia

We then examined the degree of IM lesion in gastric epithelium using AB-PAS staining. Neutral mucins present in normal gastric epithelium were stained magenta, while acidic mucins present in IM lesion were stained blue (or purple when combined with neutral). As depicted in **Figure 2C**, blue- or purple-stained foci were found in gastric epithelium from model rats, suggesting that extensive IM lesion appeared. Acidic mucins can be, in turn, sialic or sulfated; the latter stain brown with HID (19). We thus combined HID-PAS staining to further assess small intestinal-type metaplasia (S-IM) and colonic-type metaplasia (C-IM). In model rats, brown-stained sulfomucins appeared and, in approximately two-thirds, became the predominant mucin, indicating the presence of C-IM lesion, as shown in **Figure 2D**. Comparatively, both types of sulfomucins and sialomucins were becoming less abundant in GRb1-treated

rats. These findings indicated that GRb1 effectively halted and even reversed both S-IM and C-IM lesions.

Differential Expression Proteins in GPL Model Group and Effect of GRb1 on DEPs

To screen differential expression proteins (DEPs) in the GPL rats relative to normal controls, we carried out antibody array assay. Statistical analysis results unveiled that, compared to the normal group, seven DEPs were screened out in the GPL model group (**Figure 3A**). Among the seven DEPs, five proteins (beta-nerve growth factor (NGF), interferon (IFN)-gamma, fibroblast growth factor-binding protein (FGF-BP), follistatin-like 1 (FSTL1) and β -catenin) were significantly up-regulated; while two proteins (resistin-like molecule (RELM) beta and intercellular adhesion molecule-1 (ICAM-1)/CD54) were remarkably down-regulated (**Figure 3B**). It is noteworthy that, among the five proteins up-regulated in the GPL model group, β -catenin, beta-NGF and FSTL1



were significantly down-regulated after GRb1 administration (Figures 3C,D). Intriguingly, the result was in tune with our earlier study showing that an herbal formula Weipixiao, of which GRb1 is the major bioactive constituent (Zeng et al., 2016) could down-regulate β -catenin expression in GPL rats. Thus, this strongly implies that β -catenin may be a potential therapeutic target in GRb1-induced therapeutic effects on GPL.

Verification of β -Catenin Up-Regulation and Nuclear Translocation in Human GPL Specimens

In order to verify the role of β -catenin in precursors of gastric cancer, we investigate the expression and subcellular localization of β -catenin in 94 cases of human GPL specimens and in 85 cases

TABLE 1 | Correlation between nuclear localization of β -catenin and clinical characteristics.

Variable	Case	Membrane/cytoplasm	Nucleus	p-value, nucleus vs. membrane/cytoplasm
Age				
<60	49	19	30	0.867
≥60	27	11	16	
Gender				
Male	42	17	25	0.842
Female	34	13	21	
Location of lesion				
Body	10	3	7	0.850
Angle	16	7	9	
Antrum	38	16	22	
Multiple	12	4	8	
Hp infection				
Negative	31	11	20	0.555
Positive	45	19	26	
Histopathological category				
Normal gastric epithelium	62	59	3	<0.001
Gastric precancerous lesions	76	30	46	
Small intestinal-type metaplasia	22	15	7	
Colonic-type metaplasia	20	8	12	
Mild dysplasia	19	5	14	0.010
Moderate dysplasia	7	1	6	
Severe dysplasia	8	1	7	

TABLE 2 | Correlation between β -catenin positivity and clinicopathological characteristics of patients with gastric precancerous lesions.

Variable	Case	β -catenin strong positivity	β -catenin weak positivity/absent	p-value, strong vs. weak/absent
Age				
<60	61	39	22	0.545
≥60	33	19	14	
Gender				
Male	49	32	17	0.453
Female	45	26	19	
Location of lesion				
Body	13	6	7	0.068
Angle	19	16	3	
Antrum	48	26	22	
Multiple	14	10	4	
Hp infection				
Negative	40	25	15	0.891
Positive	54	33	21	
Histopathological category				
Normal gastric epithelium	85	39	46	0.034
Gastric precancerous lesions	94	58	36	
Small intestinal-type metaplasia	30	17	13	
Colonic-type metaplasia	24	11	13	
Mild dysplasia	23	19	4	0.096
Moderate dysplasia	8	6	2	
Severe dysplasia	9	5	4	

of gastric specimens from the healthy. β -catenin expression was identified in 80.9% (76/94) of the GPL specimens and 72.9% (62/85) of the normal specimens. The β -catenin immunoreactivity was notably stronger in the human GPL specimens than in the healthy controls (**Figures 4A,C**). In the normal specimens from the healthy, moreover, the proportions of β -catenin localization at cell membrane/cytoplasm and nucleus were 95.2% (59/62) and

4.8% (3/62), respectively. By contrast, incidence of β -catenin localization at cell membrane/cytoplasm decreased (30/76, 39.5%) but significantly increased at the nucleus (46/76, 60.5%) in the human GPL specimens.

Association between clinical characteristics and β -catenin positivity/subcellular localization in patients with GPL was investigated. Our analysis demonstrated that rate of nuclear

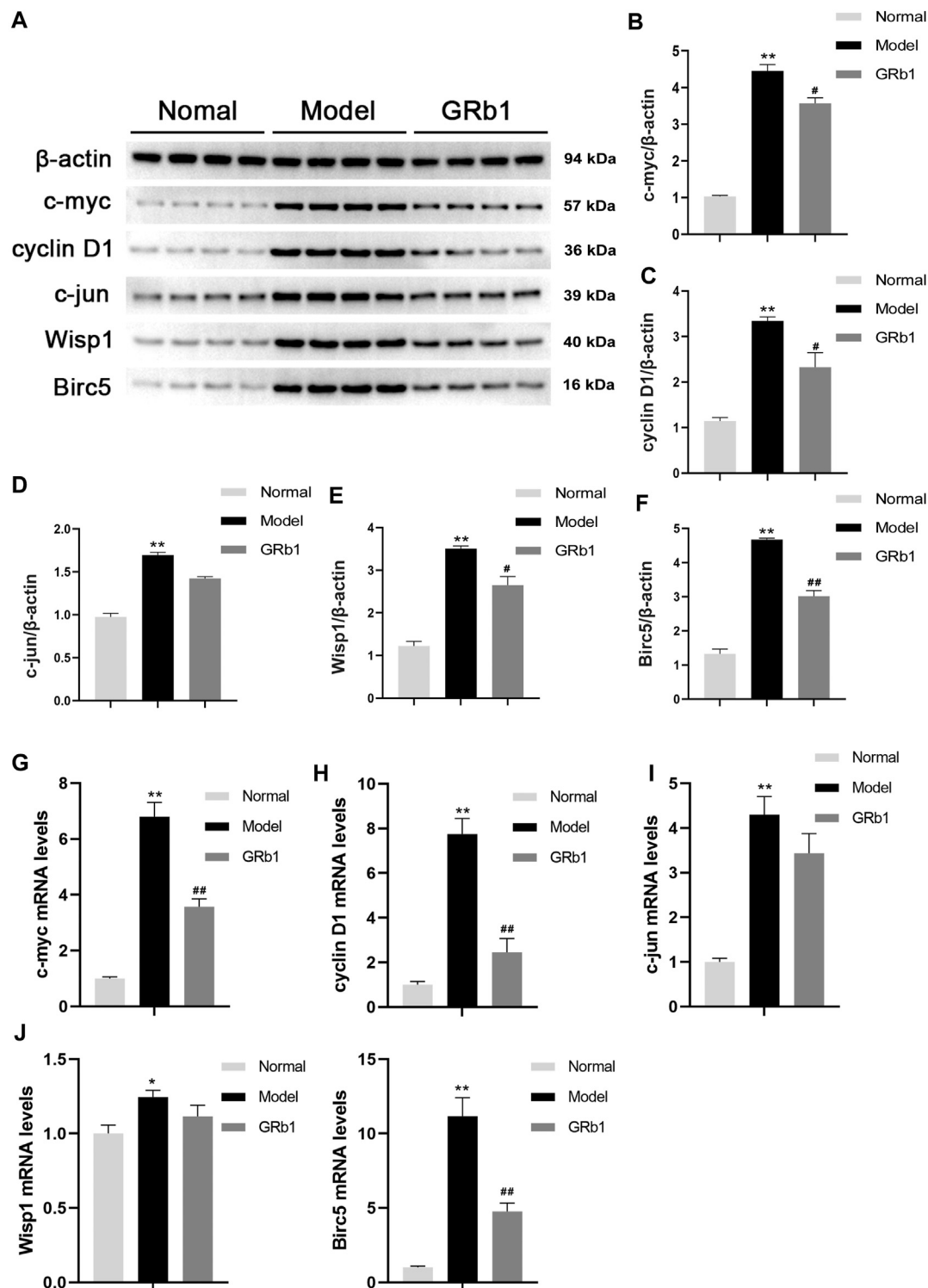


FIGURE 5 | (A) Effects of GRb1 on the protein expression levels of c-myc, cyclin D1, c-jun, Wisp1 and Birc5 in GPL model rats. **(A)** Representative western blotting bands of c-myc, cyclin D1, c-jun, Wisp1 and Birc5. Quantitative analysis of **(B)** c-myc, **(C)** cyclin D1, **(D)** c-jun, **(E)** Wisp1, and **(F)** Birc5 in western blotting bands ($n = 4$). Effects of GRb1 on mRNA levels of c-myc, cyclin D1, c-jun, Wisp1 and Birc5 in GPL model rats. Quantization for mRNA levels of **(G)** c-myc, **(H)** cyclin D1, **(I)** c-jun, **(J)** Wisp1, and **(K)** Birc5 in gastric epithelium from each group ($n = 6$). * $p < 0.05$ and ** $p < 0.01$ vs. Normal group. # $p < 0.05$ and ## $p < 0.01$ vs. Model group. Data are presented as mean \pm SEM. **Abbreviations:** GRb1, ginsenoside Rb1; GPL, gastric precancerous lesions; SEM, standard error of mean.

localization of β -catenin was significantly different between normal gastric epithelium and GPL samples. Moreover, nuclear expression of β -catenin in gastric epithelium increased depending on the pathological grade of GPL (From small intestinal-type metaplasia to severe dysplasia). In the GPL specimens assessed, high percentage of nuclear staining with β -catenin was not significantly associated with age, sex and location of lesion (Table 1). Analysis of the association between β -catenin expression levels (strong positivity vs. weak positivity/absent) and clinicopathological characteristics demonstrated that strong β -catenin positivity was significantly associated with advanced GPL pathology. In the 94 cases of gastric precancerous lesions assessed, high β -catenin expression was not associated with gender, location of lesion and Hp infection (Table 2).

GRb1 not Only Decreases Protein Expression and Nuclear Translocation of β -Catenin, but Interferes With β -Catenin/TCF4 Interaction

Our verification results in the present animal study showed that β -catenin protein expression was increased and β -catenin preferentially accumulated in the cytoplasm and, in some cases, translocated into the nucleus in GPL model rats (Figure 4B). In accordance with the results of the antibody array, GRb1 decreased protein expression and nuclear translocation of β -catenin (Figure 4D). β -catenin has been widely acknowledged as a key mediator in Wnt pathway in human gastric cancer (Flanagan et al., 2017). Following by cytosol accumulation and nuclear translocation, β -catenin binds to transcriptional factors the T-cell factor (TCF) to induce the transcription of Wnt target genes (Nusse and Clevers, 2007). To check whether GRb1 affected the β -catenin/TCF4 interaction, gastric epithelium was subjected to immunoprecipitation for β -catenin with IgG antibody as a control, and the resulting immunocomplexes were immunoblotted for TCF4. The results revealed that GRb1 effectively diminished the binding of β -catenin to TCF4 (Figures 4E,F), suggesting that GRb1 was able to disrupt the interaction of β -catenin with TCF4.

GRb1 Lowers Transcriptional and Protein Expression Levels of Downstream Target Genes, Including c-Myc, Cyclin D1 and Birc5

To further confirm the effects of GRb1 on the downstream target genes of β -catenin, such as c-myc, cyclin D1, c-jun, Wisp1 and Birc5 that are closely associated with cellular proliferation and apoptosis, RT-PCR was employed to define the transcriptional levels of these target genes. The protein levels of these target genes were determined by Western blot. It appeared that mRNA and protein levels of the genes detected were significantly higher in the GPL rats than in the normal controls. When compared with the GPL rats, mRNA levels of c-myc, cyclin D1 and Birc5 were significantly down-regulated in the GRb1-treated GPL rats (Figures 5G–K), and protein expression levels of c-myc, cyclin

D1, Wisp1 and Birc5 were markedly down-regulated in the GRb1-treated GPL rats (Figures 5A–F). Thus, our findings indicated that GRb1 repressed the transcriptional activity of the target genes of β -catenin/TCF4 activation, especially c-myc, cyclin D1 and Birc5.

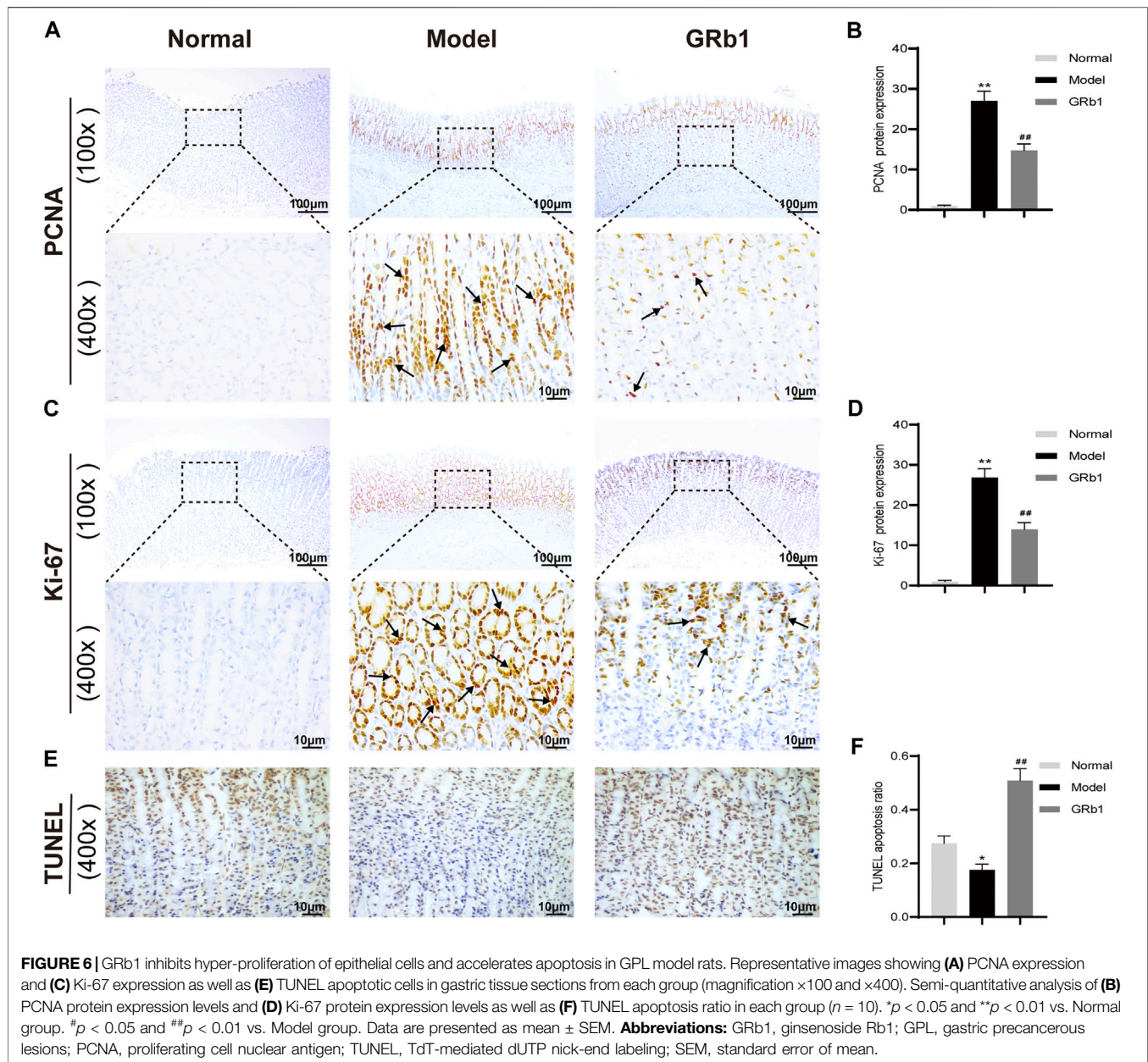
GRb1 Inhibits the Hyper-Proliferation of Epithelial Cells and Accelerates Apoptosis

The proliferation and apoptosis of gastric epithelial cells was further evaluated. Firstly, the protein expression of PCNA and Ki-67, which are widely considered as the specific reporters for cell proliferation, were determined. Our IHC analysis demonstrated that the expression of PCNA and Ki-67 was significantly higher in GPL model rats than in the normal controls, suggesting that GPL rats were experiencing hyper-proliferative state of epithelial cells relative to normal rats; while GPL rats treated with GRb1 achieved a significant decrease in the expression of PCNA and Ki-67 proteins (Figures 6A–D). We then attempted to probe the apoptosis ratio of epithelial cells. From the TUNEL assay analysis, it is evident that GPL model rats displayed a lower percentage of apoptotic cells than normal rats. The apoptosis ratio was increased following GRb1 treatment (Figures 6E,F). Collectively, these findings suggested that GRb1 was able to inhibit the hyper-proliferation of epithelial cells and accelerate apoptosis in GPL rats.

DISCUSSION

In the present study, we found that GRb1 administration reverse intestinal metaplasia and a portion of dysplasia in the MNNG-induced GPL rats. To screen targeting DEPs and investigate the possible mechanism, we applied antibody array assay and screened out seven DEPs in GPL model group relative to normal group, in which three DEPs (β -catenin, beta-NGF and FSTL1) were significantly down-regulated after GRb1 administration. Among the three DEPs, β -catenin was the therapeutic target we were most interested in, because our earlier study showed that an herbal formula Weipixiao, of which GRb1 is the major bioactive constituent (Zeng et al., 2016), could also down-regulate β -catenin expression in GPL rats.

β -catenin is an integral structural component of cell adherens junctions and a key downstream effector of canonical Wnt pathway (Valenta et al., 2012). It has been reported that positive rate of β -catenin expression was higher in precancerous gastric tissues than and chronic non-atrophic gastritis tissues (Sun et al., 2012). Activation of β -catenin signaling by Trefoil factor 1 (TFF1) loss was proved to promote cell proliferation and gastric tumorigenesis (Soutto et al., 2015). It is worth noting that nuclear localization of β -catenin is involved in tumorigenesis. A study focusing on precancerous change in oral leukoplakia revealed that β -catenin was primarily expressed at the cell membrane in normal oral epithelium, whereas nuclear expression of β -catenin was found in 92% of oral leukoplakia with



dysplasia (Ishida et al., 2007). In line with the above findings, we demonstrated that the rate of nuclear translocation of β -catenin was significantly higher in the human GPL specimens than in the healthy controls. Similar results were observed in our animal study. These lines of evidence indicate that nuclear accumulation of β -catenin plays a crucial role during malignant transition of gastric epithelium. In this study, we showed that GRb1 decreased β -catenin accumulation and localization to the nucleus in GPL rats. Similar results were reported in a recent study that GRb1 suppressed β -catenin nuclear translocation in vascular smooth muscle cells, thereby contributing to the relief of vascular calcification associated to chronic kidney disease (Zhou et al., 2019).

It has been recognized that Wnt/ β -catenin/TCF-4 pathway is often aberrantly activated in gastric cancer (Zhuang et al., 2016), in which β -catenin/TCF-4 interaction occupies an important role. Upon activation of the Wnt/ β -catenin signaling pathway, Wnt binds to the receptor family of curly proteins, resulting in the dissociation and accumulation of β -catenin in the cytoplasm. Free β -catenin in the nucleus binds to TCF and regulates the transcription of target genes (Pai et al., 2017). We thus interested in how GRb1 administration influenced the β -catenin/TCF-4 complex, which remain largely unexplored. We found in this research that β -catenin/TCF-4 complex was aberrantly activated in precursors of gastric cancer, and that GRb1 treatment disrupted the interaction of β -catenin with TCF-4.

Previously, increased transcription levels of c-myc, cyclin D1, c-jun, Wisp1 and Birc5 in the development and progression of gastric cancer were reported (Valenta et al., 2012; Gurbuz and Chiquet-Ehrismann, 2015; Peng et al., 2016; Liu et al., 2019). As expected, transcriptional levels of the five target genes were up-regulated in GPL model rats. GRb1 treatment down-regulated the transcription levels of c-myc, cyclin D1 and Birc5. Moreover, GRb1 treatment was found to inhibit the hyper-proliferation of epithelial cells and accelerate apoptosis in GPL rats. However, GRb1 administration showed no significant regulatory effects on c-jun and Wisp1 mRNA levels. One possible contributor is that c-jun and Wisp1 may not be the potential therapeutic targets for GPL treated with GRb1. Overall, our work demonstrated the benefits of GRb1 treatment for the management of gastric precancerous lesions, which is encouraging. However, only a single dose of GRb1 was administered, and the detailed pharmacodynamics of GRb1, such as dose-effect relationships, will be researched soon.

In summary, we showed the novel finding that GRb1 prevented the occurrence and progression of gastric precancerous lesions. The therapeutic effects might be contributed by decreasing protein expression and nuclear translocation of β -catenin and interfering with β -catenin/TCF4 interaction, and by repressing the transcriptional activity of downstream genes including c-myc, cyclin D1 and Birc5.

DATA AVAILABILITY STATEMENT

The original contributions presented in the study are included in the article/supplementary material, further inquiries can be directed to the corresponding authors.

REFERENCES

- Akbari, M., Tabrizi, R., Kardeh, S., Lankarani, K. B., Zhang, B. P., Zhao, X. Y., et al. (2019a). Gastric Cancer in Patients with Gastric Atrophy and Intestinal Metaplasia: A Systematic Review and Meta-Analysis. *PLoS One* 14, e0219865. doi:10.1371/journal.pone.0219865
- Akbari, M., Kardeh, B., Tabrizi, R., Ahmadizar, F., and Lankarani, K. B. (2019b). Incidence Rate of Gastric Cancer Adenocarcinoma in Patients with Gastric Dysplasia. *J. Clin. Gastroenterol.* 53, 703–710. doi:10.1097/mcg.0000000000001257
- Chen, S., Li, X., Wang, Y., Mu, P., Chen, C., Huang, P., et al. (2019). Ginsenoside Rb1 Attenuates Intestinal Ischemia/reperfusion induced Inflammation and Oxidative Stress via Activation of the PI3K/Akt/Nrf2 Signaling Pathway. *Mol. Med. Rep.* 19, 3633–3641. doi:10.3892/mmr.2019.10018
- Clevers, H. (2006). Wnt/ β -Catenin Signaling in Development and Disease. *Cell* 127 (3), 469–480. doi:10.1016/j.cell.2006.10.018
- Dawsey, S. P., Hollenbeck, A., Schatzkin, A., and Abnet, C. C. (2014). A Prospective Study of Vitamin and mineral Supplement Use and the Risk of Upper Gastrointestinal Cancers. *PLoS On* 9, e88774. doi:10.1371/journal.pone.0088774
- De, Vries, A. C., van Grieken, N. C. T., Looman, C. W. N., Casparie, M. K., de Vries, E., Meijer, G. A., et al. (2008). Gastric Cancer Risk in Patients with Premalignant Gastric Lesions: a Nationwide Cohort Study in the Netherlands. *Gastroenterology* 134, 945–952. doi:10.1053/j.gastro.2008.01.071

ETHICS STATEMENT

The animal study was reviewed and approved by Animal experiments were performed under the approval of the Institutional Animal Care and Use Committee (approval no. R201901); This study was also approved by the Institutional Review Board of the Teaching Hospital of Chengdu University of TCM (Chengdu, China) (approval no. 2018KL-023) and written informed consent was obtained from all participants for being included in the study.

AUTHOR CONTRIBUTIONS

DG, JT, and JZ conceived and designed the study. JY, MZ, ZhZ, and ZiZ carried out the experiments. YC, NC, and YH collected the data. XM and JW organized the database and performed the statistical analysis. JZ and DG drafted the manuscript and revised it. All authors have read and approved the final manuscript.

FUNDING

This work was funded by the National Natural Science Foundation of China (Grant Nos. 81804066 and 81904178), the Project of “Xing-lin Scholars” of Chengdu University of Traditional Chinese Medicine (Grant Nos. QNXZ2019017 and QNXZ2020003), the “Hundred Talents Program” of the Hospital of Chengdu University of TCM (Grant Nos. 20-Q03, 20-Q05, 20-Q18 and 20-L01) and the Science and Technology Developmental Foundation of the Hospital of Chengdu University of TCM (Grant Nos. 19TS03, 19LW05 and 19LW06), and Research Project of Sichuan Provincial Administration of TCM (Grant No. 2021MS104).

- Flanagan, D. J., Vincan, E., and Phesse, T. J. (2017). Winding Back Wnt Signalling: Potential Therapeutic Targets for Treating Gastric Cancers. *Br. J. Pharmacol.* 174, 4666–4683. doi:10.1111/bph.13890
- Fujiya, K., Ohshima, K., Kitagawa, Y., Hatakeyama, K., Nagashima, T., Aizawa, D., et al. (2020). Aberrant Expression of Wnt/ β -Catenin Signaling Pathway Genes in Aggressive Malignant Gastric Gastrointestinal Stromal Tumors. *Eur. J. Surg. Oncol.* 46 (6), 1080–1087. doi:10.1016/j.ejso.2020.02.036
- Gurbuz, I., and Chiquet-Ehrismann, R. (2015). CCN4/WISP1 (WNT1 Inducible Signaling Pathway Protein 1): A Focus on its Role in Cancer. *Int. J. Biochem. Cel. Biol.* 62, 142–146. doi:10.1016/j.biocel.2015.03.007
- Hanaki, H., Yamamoto, H., Sakane, H., Matsumoto, S., Ohdan, H., Sato, A., et al. (2012). An Anti-wnt5a Antibody Suppresses Metastasis of Gastric Cancer Cells *In Vivo* by Inhibiting Receptor-Mediated Endocytosis. *Mol. Cancer Ther.* 11 (2), 298–307. doi:10.1158/1535-7163.mct-11-0682
- He, J. J., et al. (2017). The Clinical Efficacy of Weipixiao to Treat Chronic Atrophic Gastritis. *J. Guangzhou Univ. TCM* 34, 823–827.
- Ishida, K., Ito, S., Wada, N., Deguchi, H., Hata, T., Hosoda, M., et al. (2007). Nuclear Localization of Beta-Catenin Involved in Precancerous Change in Oral Leukoplakia. *Mol. Cancer* 6, 62. doi:10.1186/1476-4598-6-62
- Jacobs, E. J., Connell, C. J., McCullough, M. L., Chao, A., Jonas, C. R., Rodriguez, C., et al. (2002). Vitamin C, Vitamin E, and Multivitamin Supplement Use and Stomach Cancer Mortality in the Cancer Prevention Study II Cohort. *Cancer Epidemiol. Biomarkers Prev.* 11, 35–41.

- Jeong, C. S., Hyun, J. E., Kim, Y. S., and Lee, E.-S. (2003). Ginsenoside Rb1 the Anti-ulcer Constituent from the Head of *Panax Ginseng*. *Arch. Pharm. Res.* 26, 906–911. doi:10.1007/bf02980198
- Li, B., Xie, P. J., Hao, Y. W., Guo, Y., Yu, J. R., Gong, D. Y., et al. (2021). Yuan-zhi-san Inhibits Tau Protein Aggregation in an $A\beta_{1-40}$ -Induced Alzheimer's Disease Rat Model via the Ubiquitin-Proteasome System. *Mol. Med. Rep.* 23 (4), 279. doi:10.3892/mmr.2021.11918
- Liu, D., Liu, T., Teng, Y., Chen, W., Zhao, L., and Li, X. (2017). Ginsenoside Rb1 Inhibits Hypoxia-Induced Epithelial-Mesenchymal Transition in Ovarian Cancer Cells by Regulating microRNA-25. *Exp. Ther. Med.* 14, 2895–2902. doi:10.3892/etm.2017.4889
- Liu, G., Liu, S., Cao, G., Luo, W., Li, P., Wang, S., et al. (2019). SPAG5 Contributes to the Progression of Gastric Cancer by Upregulation of Survivin Depend on Activating the Wnt/ β -Catenin Pathway. *Exp. Cel. Res.* 379, 83–91. doi:10.1016/j.yexcr.2019.03.024
- Liu, Y., Zhu, H., Zhou, W., and Ye, Q. (2020). Anti-inflammatory and Anti-gouty-arthritis Effect of Free Ginsenoside Rb1 and Nano Ginsenoside Rb1 against MSU Induced Gouty Arthritis in Experimental Animals. *Chemico-Biological Interactions* 332, 109285. doi:10.1016/j.cbi.2020.109285
- Lu, H., Zhou, X., Kwok, H.-H., Dong, M., Liu, Z., Poon, P.-Y., et al. (2017). Ginsenoside-Rb1-Mediated Anti-angiogenesis via Regulating PEDF and miR-33a through the Activation of PPAR-Gamma Pathway. *Front. Pharmacol.* 8, 783. doi:10.3389/fphar.2017.00783
- Miao, H. H., Zhang, Y., Ding, G. N., Hong, F. X., Dong, P., and Tian, M. (2017). Ginsenoside Rb1 Attenuates Isoflurane/surgery-Induced Cognitive Dysfunction via Inhibiting Neuroinflammation and Oxidative Stress. *Biomed. Environ. Sci.* 30, 363–372. doi:10.3967/bes2017.047
- Nusse, R., and Clevers, H. (2017). Wnt/ β -Catenin Signaling, Disease, and Emerging Therapeutic Modalities. *Cell* 169, 985–999. doi:10.1016/j.cell.2017.05.016
- Pai, S. G., Carneiro, B. A., Mota, J. M., Costa, R., Leite, C. A., Barroso-Sousa, R., et al. (2017). Wnt/ β -catenin Pathway: Modulating Anticancer Immune Response. *J. Hematol. Oncol.* 10 (1), 101. doi:10.1186/s13045-017-0471-6
- Peng, Y., Zhang, P., Huang, X., Yan, Q., Wu, M., Xie, R., et al. (2016). Direct Regulation of FOXK1 by C-Jun Promotes Proliferation, Invasion and Metastasis in Gastric Cancer Cells. *Cell Death Dis.* 7, e2480. doi:10.1038/cddis.2016.225
- Pimentel-Nunes, P., Libanio, D., Marcos-Pinto, R., Areia, M., Leja, M., Esposito, G., et al. (2019). Management of epithelial precancerous conditions and lesions in the stomach (MAPS II): European Society of Gastrointestinal Endoscopy (ESGE), European Helicobacter and Microbiota Study Group (EHMSG), European Society of Pathology (ESP), and Sociedade Portuguesa de Endoscopia Digestiva (SPED) guideline update 2019. *Endoscopy* 51 (4), 365–388. doi:10.1055/a-0859-1883
- Qin, G., Li, Y., Xu, X., Wang, X., Zhang, K., Tang, Y., et al. (2019). Panobinostat (LBH589) Inhibits Wnt/ β -Catenin Signaling Pathway via Upregulating APC Expression in Breast Cancer. *Cell Signal.* 59, 62–75. doi:10.1016/j.cellsig.2019.03.014
- Saito, T., Inokuchi, K., Takayama, S., and Sugimura, T. (1970). Sequential Morphological Changes in N-methyl-N'-nitro-N-nitrosoguanidine Carcinogenesis in the Glandular Stomach of Rats. *J. Natl. Cancer Inst.* 44 (4), 769–783.
- Soutto, M., Peng, D., Katsha, A., Chen, Z., Piazzuelo, M. B., Washington, M. K., et al. (2015). Activation of β -catenin Signalling by TFF1 Loss Promotes Cell Proliferation and Gastric Tumorigenesis. *Gut* 64, 1028–1039. doi:10.1136/gutjnl-2014-307191
- Sun, G. Y., Wu, J. X., Wu, J. S., Pan, Y. T., and Jin, R. (2012). Caveolin-1, E-Cadherin and β -catenin in Gastric Carcinoma, Precancerous Tissues and Chronic Non-atrophic Gastritis. *Chin. J. Cancer Res.* 24, 23–28. doi:10.1007/s11670-012-0023-0
- Sung, H., Ferlay, J., Siegel, R. L., Laversanne, M., Soerjomataram, I., Jemal, A., et al. (2021). Global Cancer Statistics 2020: GLOBOCAN Estimates of Incidence and Mortality Worldwide for 36 Cancers in 185 Countries. *CA A. Cancer J. Clin.* 71 (3), 209–249. doi:10.3322/caac.21660
- Tai, H.-C., Chang, A.-C., Yu, H.-J., Huang, C.-Y., Tsai, Y.-C., Lai, Y.-W., et al. (2014). Osteoblast-derived WISP-1 Increases VCAM-1 Expression and Enhances Prostate Cancer Metastasis by Down-Regulating miR-126. *Oncotarget* 5 (17), 7589–7598. doi:10.18632/oncotarget.2280
- Tatematsu, M., Aoki, T., Inoue, T., Mutai, M., Furihata, C., and Ito, N. (1988). Coefficient Induction of Pepsinogen 1-decreased Pyloric Glands and Gastric Cancers in Five Different Strains of Rats Treated with N-methyl-N'-nitro-N-nitrosoguanidine. *Carcinogenesis* 9 (3), 495–498. doi:10.1093/carcin/9.3.495
- Toyokawa, Y., Takagi, T., Uchiyama, K., Mizushima, K., Inoue, K., Ushiroda, C., et al. (2019). Ginsenoside Rb1 Promotes Intestinal Epithelial Wound Healing through Extracellular Signal-regulated Kinase and Rho Signaling. *J. Gastroenterol. Hepatol.* 34, 1193–1200. doi:10.1111/jgh.14532
- Valenta, T., Hausmann, G., and Basler, K. (2012). The many Faces and Functions of β -catenin. *EMBO J.* 31, 2714–2736. doi:10.1038/emboj.2012.150
- Zeng, J., Guo, J., Gong, D., Zhang, Y., You, F., Liang, C., et al. (2018). Weipixiao Ameliorates Gastric Precancerous Lesions in a Rat's Model by Regulating GSK3 β and C-Myc. *J. Tradit. Chin. Med.* 38, 705–713.
- Zeng, J.-h., Pan, H.-f., Liu, Y.-z., Xu, H.-b., Zhao, Z.-m., Li, H.-w., et al. (2016). Effects of Weipixiao (胃痞消) on Wnt Pathway-Associated Proteins in Gastric Mucosal Epithelial Cells from Rats with Gastric Precancerous Lesions. *Chin. J. Integr. Med.* 22, 267–275. doi:10.1007/s11655-015-2131-4
- Zeng, J. H., Yan, R., Pan, H., You, F., Cai, T., Liu, W., et al. (2018). Weipixiao Attenuate Early Angiogenesis in Rats with Gastric Precancerous Lesions. *BMC Complement. Altern. Med.* 18, 250. doi:10.1186/s12906-018-2309-3
- Zhang, S. L. (2017). Weipixiao in the Treatment of Chronic Atrophic Gastritis: A Random Parallel Control Study. *J. Pract. Traditional Chin. Intern. Med.* 31, 12–14.
- Zhou, P., Zhang, X., Guo, M., Guo, R., Wang, L., Zhang, Z., et al. (2019). Ginsenoside Rb1 Ameliorates CKD-associated Vascular Calcification by Inhibiting the Wnt/ β -catenin Pathway. *J. Cel. Mol. Med.* 23, 7088–7098. doi:10.1111/jcmm.14611
- Zhu, S., Mason, J., Shi, Y., Hu, Y., Li, R., Wahg, M., et al. (2003). The Effect of Folic Acid on the Development of Stomach and Other Gastrointestinal Cancers. *Chin. Med. J. (Engl)* 116, 15–19.
- Zhuang, K., Yan, Y., Zhang, X., Zhang, J., Zhang, L., and Han, K. (2016). Gastrin Promotes the Metastasis of Gastric Carcinoma through the β -catenin/TCF-4 Pathway. *Oncol. Rep.* 36, 1369–1376. doi:10.3892/or.2016.4943

Conflict of Interest: The authors declare that the research was conducted in the absence of any commercial or financial relationships that could be construed as a potential conflict of interest.

Publisher's Note: All claims expressed in this article are solely those of the authors and do not necessarily represent those of their affiliated organizations, or those of the publisher, the editors and the reviewers. Any product that may be evaluated in this article, or claim that may be made by its manufacturer, is not guaranteed or endorsed by the publisher.

Copyright © 2021 Zeng, Ma, Zhao, Chen, Wang, Hao, Yu, Zeng, Chen, Zhao, Tang and Gong. This is an open-access article distributed under the terms of the Creative Commons Attribution License (CC BY). The use, distribution or reproduction in other forums is permitted, provided the original author(s) and the copyright owner(s) are credited and that the original publication in this journal is cited, in accordance with accepted academic practice. No use, distribution or reproduction is permitted which does not comply with these terms.



Small-Molecule Inhibitors Overcome Epigenetic Reprogramming for Cancer Therapy

Wenjing Xiao^{1,2†}, Qiaodan Zhou^{3†}, Xudong Wen^{4†}, Rui Wang⁵, Ruijie Liu¹, Tingting Wang¹, Jianyou Shi^{6*}, Yonghe Hu^{1,2*} and Jun Hou^{1,2*}

¹School of Materials Science and Engineering, Southwest Jiaotong University, Chengdu, China, ²Department of Pharmacy, The General Hospital of Western Theater Command of PLA, Chengdu, China, ³Department of Ultrasonic, Sichuan Academy of Medical Sciences and Sichuan Provincial People's Hospital, School of Medicine, University of Electronic Science and Technology of China, Chengdu, China, ⁴Department of Gastroenterology and Hepatology, Chengdu First People's Hospital, Chengdu, China, ⁵Information Department of Medical Security Center, The General Hospital of Western Theater Command of PLA, Chengdu, China, ⁶Personalized Drug Therapy Key Laboratory of Sichuan Province, Department of Pharmacy, Sichuan Academy of Medical Sciences and Sichuan Provincial People's Hospital, School of Medicine, University of Electronic Science and Technology of China, Chengdu, China

OPEN ACCESS

Edited by:

Sanjun Shi,

Chengdu University of Traditional Chinese Medicine, China

Reviewed by:

Guowei Yin,

Sun Yat-sen University, China

Daniel Neureiter,

Salzburger Landeskliniken, Austria

*Correspondence:

Jianyou Shi

shijianyoude@126.com

Jun Hou

jun_hou@yeah.net

Yonghe Hu

huyonghezy@163.com

[†]These authors have contributed equally to this work

Specialty section:

This article was submitted to Pharmacology of Anti-Cancer Drugs, a section of the journal Frontiers in Pharmacology

Received: 29 April 2021

Accepted: 02 August 2021

Published: 17 September 2021

Citation:

Xiao W, Zhou Q, Wen X, Wang R, Liu R, Wang T, Shi J, Hu Y and Hou J (2021) Small-Molecule Inhibitors Overcome Epigenetic Reprogramming for Cancer Therapy. *Front. Pharmacol.* 12:702360. doi: 10.3389/fphar.2021.702360

Cancer treatment is a significant challenge for the global health system, although various pharmacological and therapeutic discoveries have been made. It has been widely established that cancer is associated with epigenetic modification, which is reversible and becomes an attractive target for drug development. Adding chemical groups to the DNA backbone and modifying histone proteins impart distinct characteristics on chromatin architecture. This process is mediated by various enzymes modifying chromatin structures to achieve the diversity of epigenetic space and the intricacy in gene expression files. After decades of effort, epigenetic modification has represented the hallmarks of different cancer types, and the enzymes involved in this process have provided novel targets for antitumor therapy development. Epigenetic drugs show significant effects on both preclinical and clinical studies in which the target development and research offer a promising direction for cancer therapy. Here, we summarize the different types of epigenetic enzymes which target corresponding protein domains, emphasize DNA methylation, histone modifications, and microRNA-mediated cooperation with epigenetic modification, and highlight recent achievements in developing targets for epigenetic inhibitor therapy. This article reviews current anticancer small-molecule inhibitors targeting epigenetic modified enzymes and displays their performances in different stages of clinical trials. Future studies are further needed to address their off-target effects and cytotoxicity to improve their clinical translation.

Keywords: small-molecule inhibitors, epigenetic drugs, epigenetic reprogramming, cancer biomarker, histone modification, microRNA

Abbreviations: AML, acute myeloid leukemia; CGIs, cytosine–guanine base islands; CpG, cytosine–guanine base; DNMTi, DNA methyl transferases inhibitors; DNMTs, DNA methyltransferases; DOT1L, disruptor of telomeric silencing 1-like; HATi, HAT inhibitors; HATs, histone acetyltransferases; 5mC, 5-carbon on cytosine residues; MDS, myelodysplastic syndrome; PRMT, protein arginine methyltransferase; and SMIRs, specific microRNAs.

INTRODUCTION

Epigenetics is rising to prominence in molecular cell biology as an evolutionary mechanism by which external factors have intermediate-term effects on gene expression without changing the underlying genetic sequence (Rodenhiser and Mann, 2006; Handel et al., 2010). The epigenetic modification includes, but does not limit to, DNA methylation of cytosine–guanine base (CpG) motif and a wide range of histone modifications, including methylation, acetylation, phosphorylation, sumoylation, and ubiquitination (Esteller, 2007; Herranz and Esteller, 2007). Epigenetics is a significant driver of biological complexity and has a role in developing many diseases (Feinberg and Irizarry, 2010; Flavahan et al., 2017; Feinberg, 2018). For example, silencing of tumor suppressor genes or activation of oncogenes by DNA methylation or histone modifications contributes to the onset of a diversity of cancers (Gronbaek et al., 2007). To date, the most well-established therapeutic field of epigenetics is cancer, in which DNA methylation, histone modification, and abnormal expression of microRNA have all been linked to tumor development (Shi et al., 2003; Yen et al., 2016). In this review, we summarize the basic principles manipulating the abovementioned epigenetic pathways and highlight the evidence of the promising clinical and preclinical results using small-molecule inhibitors against chromatin regulators for cancer treatment.

Epigenetic Modifications and Human Diseases

Epigenetics is one of the fastest developing fields in biology (Nepali and Liou, 2021). Recent achievements highlight the accelerated development of epigenetics, such as the definition of a human DNA methylome at single-nucleotide resolution, the various discoveries of histone variants and modifications, the study of the CpG island in the genome, and the progress of genome-wide nucleosome positioning maps (Baldi, 2019). It is necessary for the same genotype to raise numerous different phenotypes so that epigenetic marks can persist during the development and can be passed on to the offspring. The potential location of epigenetic marks includes DNA methylation, histone modification, and nucleosome location. They are the key to regulating gene and noncoding RNA expression (Miranda Furtado et al., 2019). As a result, the research of these mutations in epigenetic markers and epigenetic mechanisms associated with diseases has been launched. A comprehensive understanding of the epigenetic mechanisms, their interactions, and changes in health and disease has become an important research topic. The importance of epigenetics in maintaining normal development is reflected in that many diseases occur when the wrong epigenetic markers are introduced or added at the wrong time or place (Ganesan et al., 2019). It is displayed by searching the keyword “epigenetics” on PubMed; it displays that there were around 200 articles published in 1999, but more than 54, 00 in 2021. Thus far, efforts in epigenetic research have mainly focused on cancer, but as the field has grown, it has provided new insights

into other types of diseases (Angarica and Del Sol, 2017; Wu et al., 2019). Considering the global incidence of obesity, it cannot be explained only by genetic factors, environmental factors are more likely to be the driving factors. Epigenetics is one of the essential mechanisms which link environmental factors with gene expression changes. Since the year of 2008, research on the role of epigenetics in T2D has begun to develop (Ling and Rönn, 2019). In 2013, an epigenetic association study of obesity indicated that the DNA methylation difference of obese subjects was greater than that of lean subjects. Moreover, this study identified some CpG sites associated with obesity. Also, it showed that both differential methylation and differential variability could predict obesity and the reliability is about 70% (Xu et al., 2013). With the breakthrough in technology, it is possible to initiate epigenomic analysis on a large scale (Li et al., 2016; Azangou-Khyavy et al., 2020). Dayeh et al. found altered DNA methylation of 1,649 CpG sites annotated to 843 genes in islets from 15 T2D cases versus 34 controls. Out of these genes, other 102 exhibited differential gene expression in the islets from T2D donors (Dayeh et al., 2014). CDKN1A, PDE7B, and SEPT9 belong to the genes with decreased DNA methylation and increased gene expression in T2D islets (Dayeh et al., 2014). Therefore, the development of epigenetics would provide an open field for the discovery of targets for prediction and therapeutics in human diseases (Portela and Esteller, 2010).

Epigenetics and Cancer

Epigenetics participates in all stages of cancer development (Bates, 2020). Achievements of the Human Genome Project (HGP) have provided thousands of new targets in cancer treatment (International Cancer Genome et al., 2010). However, the HGP did not explain the difference in gene expression during cancer development. The effect of epigenetics in cancer has raised the attention of scientists (Park and Han, 2019). Genetic and epigenetic mutations participate in tumorigenesis and metastasis by controlling the interaction between tumor suppressor genes with oncogenes. In contrast to genetic mutations, epigenetic mutations regulated gene expression without changing the genome sequence (Nebbioso et al., 2018). The development of epigenetic research provides insight for cancer diagnosis, treatment, and improvement of drug resistance (Verma, 2015; Ponnusamy et al., 2020). For instance, the promoter containing CpG islands of breast cancer cells was selectively hypermethylated to inactivation of tumor suppressor gene expression, such as cell cycle regulator ($p16^{INK4a}$ and $p14^{ARF}$), apoptotic regulator (*APC*, *HIC1*, and *Twist*), and DNA repair genes (*GSTP1*, *BRCA1*, and *MGMT*). These well-known tumor suppressor genes promote the development of breast cancer by changing various physiological functions of the cell due to promoter hypermethylated (Shukla et al., 2019). The nature of epigenetic modification is dynamic and reversible, which ensures a new epigenetic program and reprograms cells according to different conditions and provides other targets for designing antitumor drugs. Current animal models can only reflect the advanced stage of tumor growth but cannot reflect the early events. The breakthrough of epigenetics indicates that the dynamic and

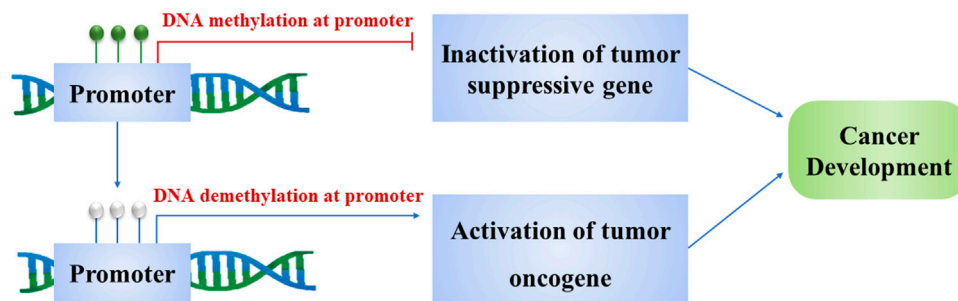


FIGURE 1 | Methylation and demethylation of the gene promoter turn on tumorigenesis. Methylation of promoters inactivates tumor suppressor genes and induces cancer development. Demethylation of promoters activates oncogenes and results in the cancer cell proliferation.

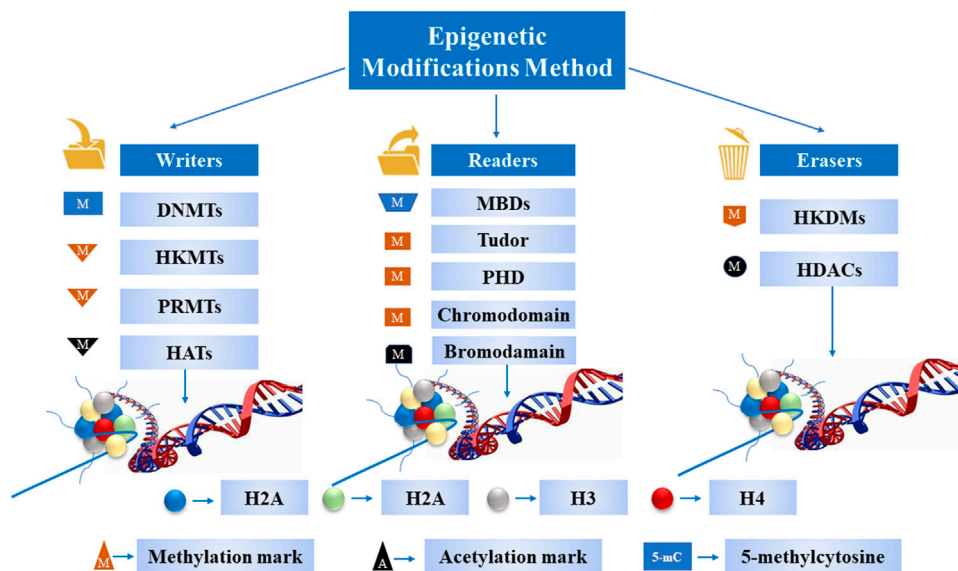


FIGURE 2 | A schematic diagram of epigenetic tools. These enzymes and protein domains carry out most of the epigenetic modifications on DNA and histone tails.

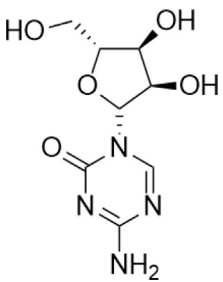
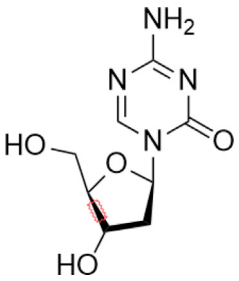
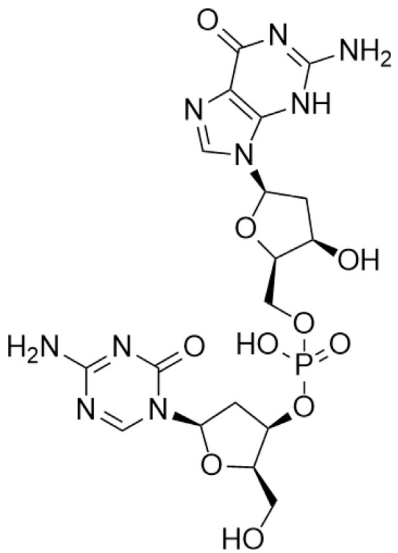
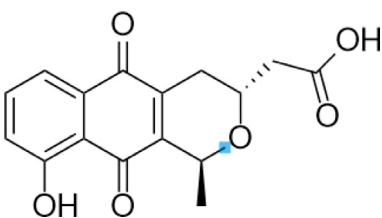
reversible nature of epigenetic plays a vital role in the early development of cancer. Common epigenetic factors induce tumor cells to reprogram and, thus, have pluripotency. Elucidating the relationship between reprogramming-related transcription factors and tumor epigenomes may help understand the molecular basis of regulating the cancer phenotype (Kim, 2020). In addition to cancer therapy, epigenetics also can serve as biomarkers for cancer diagnosis and risk assessment due to epigenetic changes before histopathological changes (Verma, 2015). Pancreatic ductal adenocarcinoma is usually diagnosed in the advanced stage without a little effective treatment strategy. The development of epigenetic markers is helpful for the early diagnosis of this tumor. Various methylation markers have been reported in pancreatic ductal adenocarcinoma, such as *p16*, *hMLH1* and *hMLH2*, and *cyclin D2* (Matsubayashi et al., 2003; Kumari et al., 2009; Kisiel et al., 2012). In the following sections, the

main events involved in epigenetic regulation in cancer are discussed.

DNA Methylation

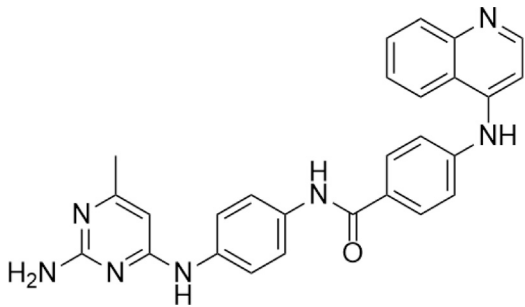
DNA methylation is molecularly defined as a process that adds a methyl group to 5-carbon on cytosine residues (5mC) in CpG dinucleotides by DNA methyltransferase enzymes, which primarily exists in centromeres, telomeres, inactive X-chromosomes, and repeat sequences (Ning et al., 2016). The number of epigenetic modifications substantially outnumbers that of somatic mutations in human cancers. Also, individual tumor types can be stratified into subgroups based on different DNA methylation profiles (Pan et al., 2018). Consequently, DNA methylation has been regarded as a hallmark of cancer development and is characterized by global DNA hypomethylation of repetitive elements and CpG-poor regions concomitant with gene-specific DNA hypermethylation (Estecio

TABLE 1 | A list of DNA methyltransferase inhibitors under different phases of clinical trial and their indication.**DNA methyltransferase inhibitors**

Classification	Compounds	Structure	Clinical stage	References
Nucleoside analogue	Azacytidine		Phase III	Derissen et al. (2013)
	Decitabine		Phase II	Dhillon (2020)
	SGI-110		Phase II	(Daher-Reyes et al., 2019)
Nonnucleoside analogue	Nanaomycin A		Preclinical	Nakamae et al. (2018)

(Continued on following page)

TABLE 1 | (Continued) A list of DNA methyltransferase inhibitors under different phases of clinical trial and their indication.

DNA methyltransferase inhibitors				
Classification	Compounds	Structure	Clinical stage	References
	SGI-1027		Preclinical	Sun et al. (2018)
	MG98	uncovered	Phase II	Linnekamp et al. (2017)

and Issa, 2011; Liang and Weisenberger, 2017). Molecularly, DNA methylation alterations may lead to gene silencing due to DNA hypermethylation of CpG island promoter and gene activation owing to DNA hypomethylation of CpG-poor gene promoters, the process which is executed by DNA methyltransferases (DNMTs) (**Figure 1**) (Bestor and Verdine, 1994). DNMT1, DNMT3A, and DNMT3B are three well-established types of DNMTs responsible for maintaining chromosomal homeostasis (Zhang and Xu, 2017). Defective DNMTs may induce imbalance in DNA, which leads to the onset of chromatin remodeling, genomic instability, and gene inactivation (Nephew and Huang, 2003; Esteller, 2007). Gaudet et al. have established that either deletion or reduction of DNMT1 can result in substantial genome-wide hypomethylation and chromosomal instability (Gaudet et al., 2003); Qu et al. have reported that hypomethylated CpG islands (CGIs) of the HOXB cluster found in acute myelocytic leukemia are highly associated with DNMT3A mutations (Qu et al., 2014). These discoveries shed light on cancer diagnosis and treatment, realizing the enormous potential of genomic methylation abnormalities in tumorigenesis.

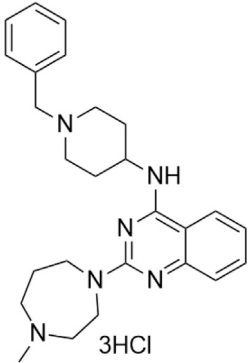
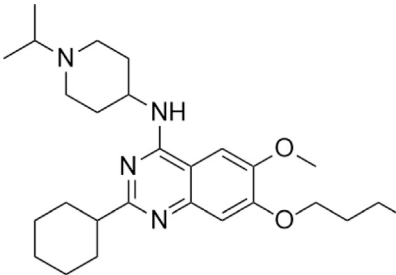
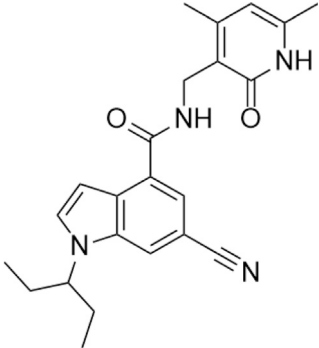
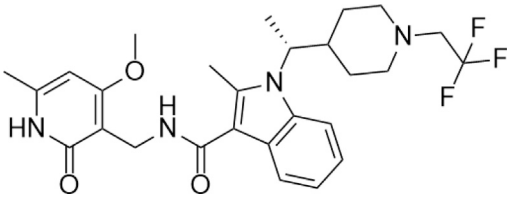
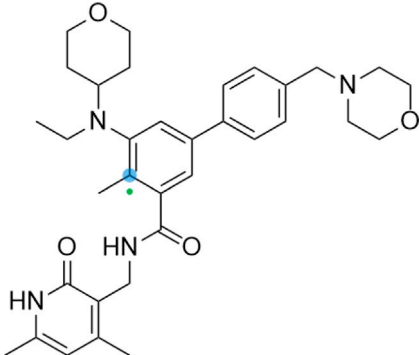
Covalent Histone Modifications

Modulation of chromatin *via* covalent histone modification is one of the most fundamental ways to regulate DNA accessibility during physiological processes, including gene transcription, DNA replication, and DNA damage repair (Chi et al., 2010). To date, over ten different types of histone modifications have been identified to be involved in the process as mentioned above. The key modulators manipulating these modifications have been deciphered progressively with the better understanding of epigenetics. These modifications fall into three categories: 1) writers: the enzymes are proficient in adding a nucleotide base and specific amino acid residues on histones; 2) erasers: the enzymes are capable of removing a nucleotide base and specific amino acid

residues; and 3) readers: the proteins possess specialized domains that can recognize specific epigenetic marks in a locus. All these enzymes and protein domains are defined as epigenetic tools (**Figure 2**). The N-terminal tails of histones are usually the targets of covalent histone modification, which undergo a variety of posttranslational modifications, including methylation, acetylation, ubiquitylation, sumoylation, and phosphorylation on specific residues (Th'ng et al., 2005; Bhaumik et al., 2007). The establishment of an appropriate pattern of histone modifications is crucial for normal development and differentiation. On the contrary, the disorganized pattern of histone modification is associated with tumor initiation and development (Bannister and Kouzarides, 2011).

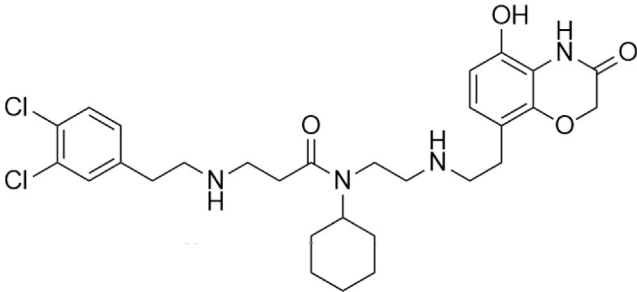
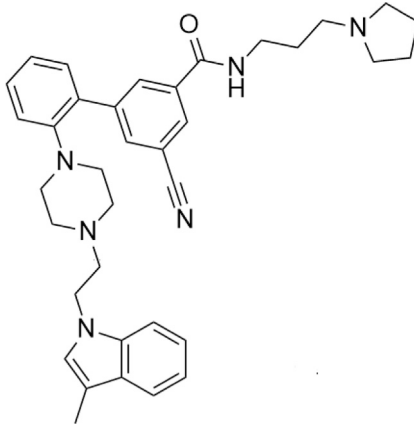
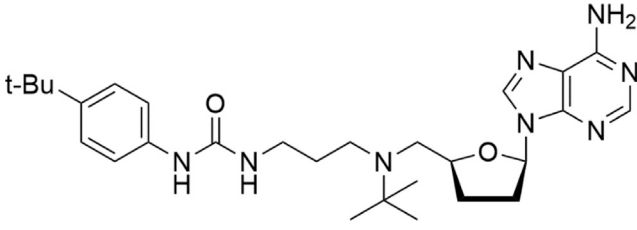
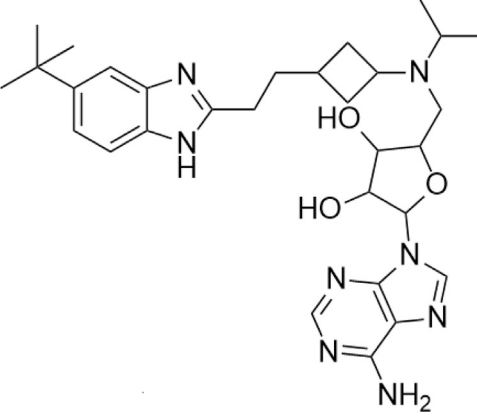
miRNAs are defined as small single-stranded noncoding RNA molecules (containing ~22 nucleotides) found in mammals that function in gene silencing and posttranscriptional gene regulation (Hutvagner and Simard, 2008). Mechanically, miRNAs negatively regulate the gene expression of target mRNAs *via* the sequence-specific base pairing of miRNAs with 3' untranslated regions of target messenger RNAs, followed by the cleavage of the mRNA strand (Hutvagner and Simard, 2008). Given the nature that miRNAs are expressed in a cell-specific manner and are involved in the safeguarding biological processes that include cell proliferation, differentiation, and apoptosis, aberrant miRNAs expression is involved in the cancers of different origins that include breast, colon, gastric, lung, prostate, and thyroid (Di Leva and Croce, 2013; Reddy, 2015). Unlike normal mRNAs regulated by epigenetic mechanisms, a tight connection occurs between miRNAs and epigenetic modification. On the one hand, epigenetic modification could result in the aberrancies of the miRNome (Valeri et al., 2009). The dysregulation of miRNome is defined as the hallmark of cancer initiation and metastasis. The majority of epigenetic regulation events are involved in the dysregulation of miRNome (Humphries et al., 2019). On the other hand, a specific group of miRNAs that is called epi-miRNAs

TABLE 2 | A list of histone lysine methyltransferase inhibitors under different phases of clinical trial and their indication.**Histone lysine methyltransferase inhibitors**

Classification	Compounds	Structure	Clinical stage	References
G9a (H3K9)	BIX-01294		Preclinical	Deng et al. (2020a)
	UNC0638		Preclinical	Nuakaw et al. (2020)
EZH2 (H3K27)	EI1		Preclinical	Fioravanti et al. (2018)
	CPI-1205		Clinical	Gulati et al. (2018)
	EPZ6438		Clinical	Zhou et al. (2020)

(Continued on following page)

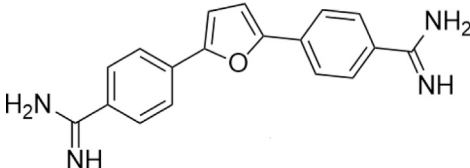
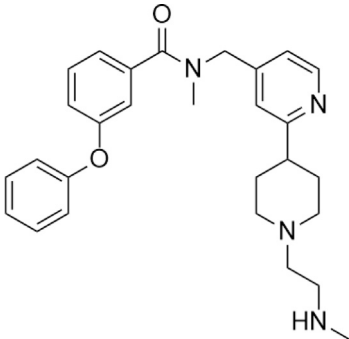
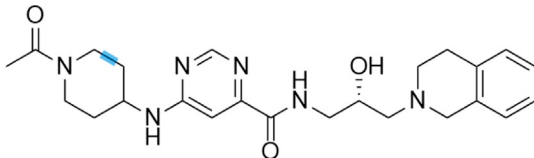
TABLE 2 | (Continued) A list of histone lysine methyltransferase inhibitors under different phases of clinical trial and their indication.**Histone lysine methyltransferase inhibitors**

SMYD2 (H3K36)	AZ-505		Preclinical	de Grass et al. (2014)
	LLY-507		Preclinical	Kukita et al. (2019)
DOT1L (H3K79)	SYC-522		Preclinical	Liu et al. (2014)
	EPZ-5676		Clinical	

can manipulate epigenetic regulatory mechanisms inside a cell by targeting enzymes that are responsible for DNA methylation (DNMT3A and DNMT3B) and histone modifications (EZH2) (Liu et al., 2013). MiRNA and epigenetics are feedback loops rather than liners (Yao et al., 2019). A primary theory has been established that miRNAs modulate epigenetics *via* regulating

epigenetic modifier enzymes, which facilitate a trilateral regulatory “epi-miR-epi” feedback circuit in pathological and physiological processes. The result of this “epi-miR-epi” interaction has emerged as a new layer of complexity in gene regulation, whose comprehension sheds light on understanding human cancerogenesis.

TABLE 3 | A list of histone arginine methyltransferase inhibitors under different phases of clinical trial and their indication.

Histone arginine methyltransferase inhibitor				
Classification	Compounds	Structure	Clinical stage	References
PRMT1	DB75		Preclinical	Oudard et al. (2017)
PRMT4	TP064		Preclinical	Loe et al. (2021)
PRMT5	EPZ015938 (GSK3326595)		Clinical	Li et al. (2019)

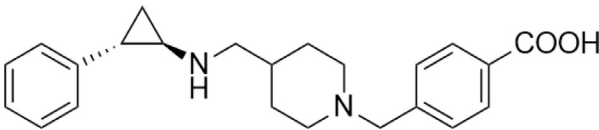
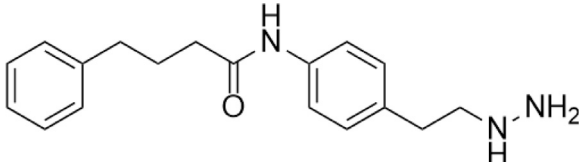
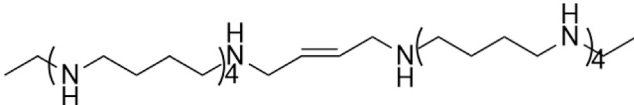
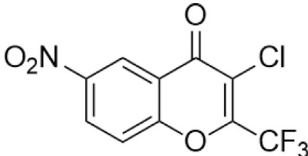
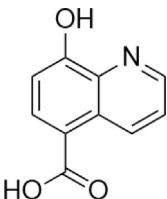
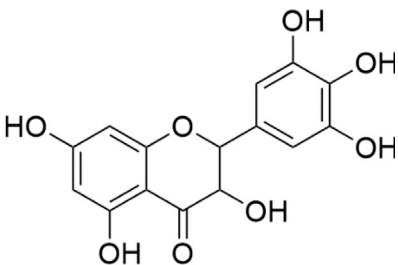
Epigenetic Therapy of Cancer

The reversible nature of the profound epigenetic modification in cancer has raised the possibility of “epigenetic therapy” as a treatment option against refractory cancers. Several small-molecule inhibitors working as chromatin regulators have been at advanced stages of clinical trials, and the US Food and Drug Administration (FDA) has approved azanucleosides targeting DNMTs, vorinostat targeting HDACs, and fedratinib targeting JAK2 for clinical treatment (Dzobo, 2019). This success indicates that the rationale of developing small-molecule inhibitors targeting epigenetic pathways may represent a novel therapeutic approach in the clinical setting. A successful clinical introduction of epigenetic inhibitors such as DNA methyltransferase inhibitors (DNMTis) and histone deacetylase inhibitors (HDACis) has been well established in treating hematological malignancies. These discoveries have opened new unexplored areas to understand the pathogenesis of cancer development and provided new targets for antitumor therapy development (Prachayasittikul et al., 2017; Gambacorta et al., 2019).

DNA Methyltransferase Inhibitors

Tumor suppressor genes function mainly to either repress or inhibit the cell cycle or promote apoptosis (Joyce et al., 2021). The better-known tumor suppressor gene includes gene cyclin-dependent kinase inhibitor 2A (CDKN2A) (Zhao et al., 2016), breast cancer susceptibility gene breast cancer 1 (BRCA1) (Krais and Johnson, 2020), and adenomatous polyposis coli (APC) (Schrock et al., 2020). Global DNA hypomethylation and hypermethylation of the promoter regions of the tumor suppressor gene manipulated by DNMTs have been widely found in the malignant cells, which provide a promising target to develop drugs against DNMTs (Subramaniam et al., 2014). DNMTi includes two categories: nucleoside and nonnucleoside inhibitors (Singh et al., 2013). Among these small-molecule inhibitors, cytosine analogs azacytidine (5-azacytidine) and decitabine (5-aza-2'-deoxycytidine) are the two best known nucleosides DNMTis (Fahy et al., 2012). Molecularly, 5-azacytidine is an inducer of chromosome breakage and a mutagen by demonstrating its ability to incorporate itself into the human genome *via* various mechanisms (Imanishi et al.,

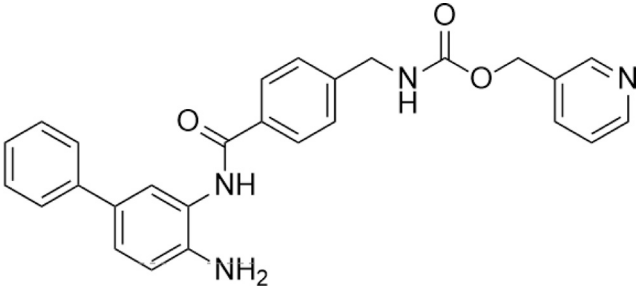
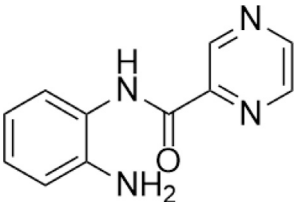
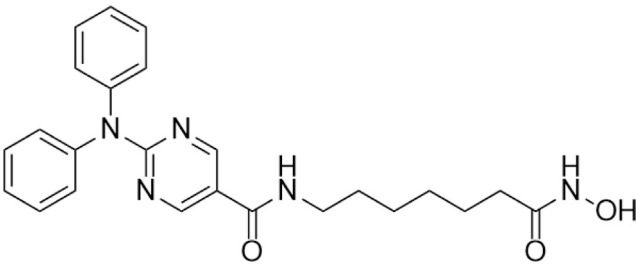
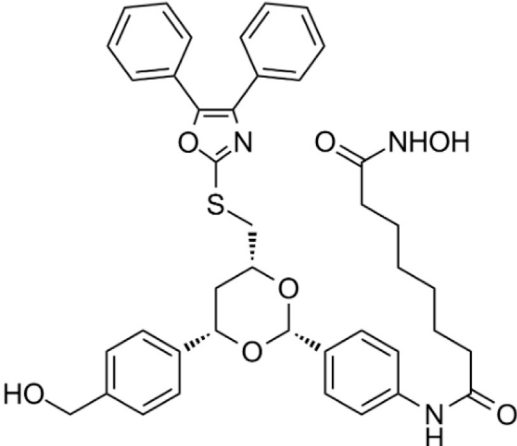
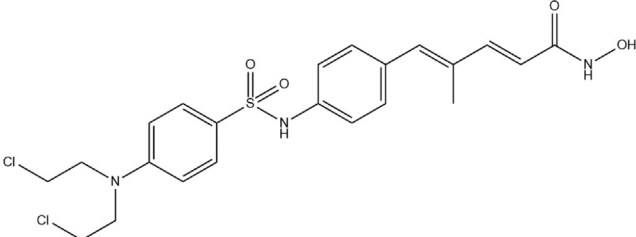
TABLE 4 | A list of histone demethylase inhibitors under different phases of clinical trial and their indication.

Histone demethylase inhibitor				
Classification	Compounds	Structure	Clinical stage	References
LSD1 inhibitors	Tranylcypromine analogue (GSK2879552)		Clinical	Kalin et al. (2018)
	Bizine		Preclinical	Kim et al. (2020)
	PG11144		Preclinical	Zhu et al. (2012)
	Namoline		Preclinical	Sewry et al. (2019)
	IOX1		Preclinical	Hoyle et al. (2021)
KDM6B			Preclinical	Basu Mallik et al. (2017)

2014). Its strategies include inhibition of tRNA methyltransferases, interference with tRNA methylation, and interruption of ribosomal RNA processing (Lu and Randerath, 1980; Grosso and Pitot, 1984; Mohana Kumar et al., 2006). In addition, 5-azacytidine can also interfere with de novo thymidylate synthesis, empowering its cytotoxicity effect (Osorio-Montalvo et al., 2018). Pharmacologically, 5-azacytidine and 5-aza-2'-deoxycytidine form an irreversible complex with the DNMTs, which results in the degradation of DNMTs (Valdez et al., 2010). To date, both drugs have been approved for the treatment of myelodysplastic syndrome (MDS) and AML in the clinical setting (Soriano et al., 2007). However,

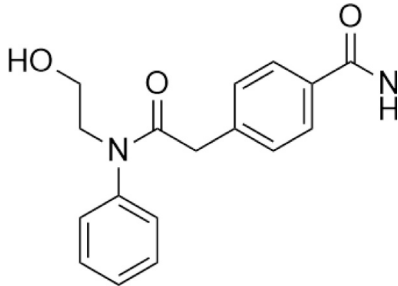
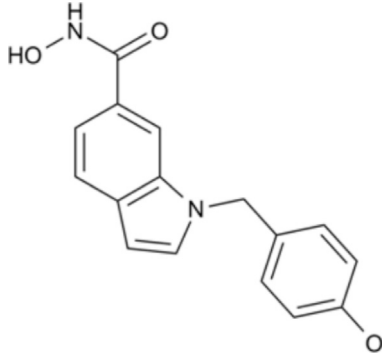
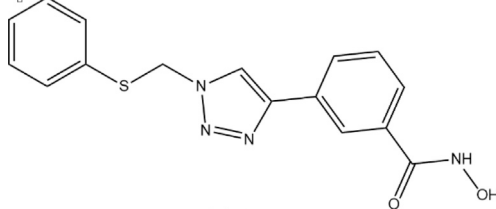
recognized by the pleiotropic effects of 5-azacytidine, 5-aza-2'-deoxycytidine, and their targets as mentioned above, researchers have confronted enormous challenges discovering novel inhibitors that are somewhat held back. To alleviate the toxic profiles of 5-azacytidine and 5-aza-2'-deoxycytidine, a less poisonous cytidine analog was developed, called zebularine. It exerts demethylation activity by stabilizing the binding of DNMTs to DNA, hindering the methylation and decreasing the dissociation, thereby trapping the enzyme and preventing turnover even at other sites (Sanaei and Kavooosi, 2020). It also enhances tumor cell chemo- and radiosensitivity and has antimitogenic and angiostatic activities (Balch et al., 2005; Hellebrekers et al., 2006;

TABLE 5 | A list of histone deacetylase inhibitors under different phases of clinical trial and their indication.**Histone acetyltransferase inhibitors**

Classification	Compounds	Structure	Clinical stage	References
HDAC1/2i	MRLB-223		Preclinical	Newbold et al. (2013)
HDAC3i	BG45		Preclinical	Tang et al. (2018)
HDAC6i	Rocilinostat (ACY-1215)		clinical	Yang et al. (2020)
	Tubacin		Preclinical	Liang et al. (2019)
HDAC8i	C1A		Preclinical	Kaliszczak et al. (2013)

(Continued on following page)

TABLE 5 | (Continued) A list of histone deacetylase inhibitors under different phases of clinical trial and their indication.**Histone acetyltransferase inhibitors**

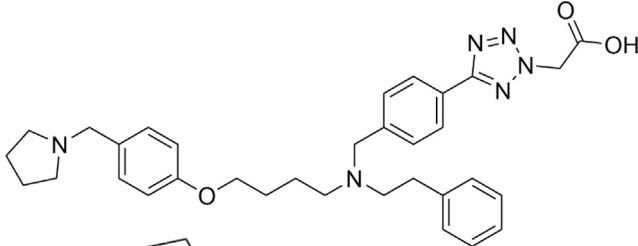
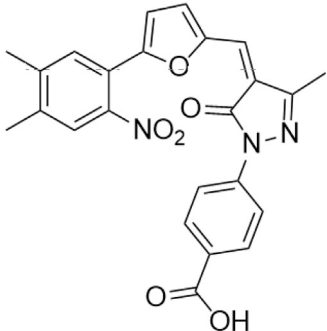
HPOB		Preclinical	Liu et al. (2018)
PCI-34051		Preclinical	Morgen et al. (2020)
C149		Preclinical	Suzuki et al. (2012)

Greer et al., 2017). Zebularine inhibits DNA methylation and reactivates a gene previously silenced by methylation (Cheng et al., 2003). The mechanism of action of Zebularine is concentration dependent. High doses of Zebularine can induce cell cytotoxicity through double-strand breaks, cell cycle arrest, and causing DNA damage (Orta et al., 2017). Unfortunately, the high dose required for therapeutic value excluded Zebularine for its clinical application. Nowadays, there are three candidates from second-generation nucleoside DNMTi under clinical trials. SGI-110 is designed for the treatment of advanced hepatocellular carcinoma (NCT01752933), MDS and AML (NCT01261312), while 4'-thio-2'-deoxycytidine and RX-3117 are still under investigation against advanced solid tumors (NCT02423057) and metastatic pancreatic cancer (NCT03189914), respectively (Issa et al., 2015; Lu et al., 2020) (Campbell and Tummino, 2014).

Unlike the nucleoside analogs, nonnucleoside DNMTi directly bind to the catalytic region of DNMTs instead of incorporation into DNA. Consequently, the cytotoxicity of 5-azacytidine and 5-aza-2'-deoxycytidine is less than that of nucleoside DNMTi (Rondelet et al., 2017). 5-Azacytidine and 5-aza-2'-deoxycytidine are potent inhibitors of DNA methyltransferase. Its cytotoxicity has been attributed to

several possible mechanisms, including reexpression of growth suppressor genes and formation of covalent adducts between DNA methyltransferase and 5-aza-2'-deoxycytidine-substituted DNA which may lead to steric inhibition of DNA function (Christman et al., 1985; Kiianitsa et al., 2020; Nunes et al., 2020). They include procainamide, procaine, epigallocatechin-3-gallate (EGCG), SGI-1027, nanaomycin A, flavonoid, and compound 5. Pharmacologically, procainamide and procaine can modify the CpG regions of DNA, resulting in blocking DNMTs activities (Li et al., 2018); Morris et al. reported that flavonoid and EGCG could inhibit DNMT1 enzyme activity from restoring RXRa expression in human colon cancer cells (Li et al., 2018). Datta et al. found that SGI-1027 (a quinoline derivative) could make the MLH1 and P16 promoter region in colon cancer cells reactive *via* inhibiting all three DNMTs (Datta et al., 2009). Similarly, it is documented that nanaomycin A can selectively target DNMT3a to induce the activation of tumor suppressor genes in cancer cell lines (Kuck et al., 2010). Compound 5 derived from a chemical modification of SGI-1027 is the first nonnucleoside DNMTi that has been investigated in cancer cell lines. It can display potent antiproliferative effects against histiocytic lymphoma, breast cancer, Burkitt's lymphoma, and

TABLE 6 | A list of histone acetyltransferase inhibitors under different phases of clinical trial and their indication.

Histone acetyltransferase inhibitors				
Classify	Compounds	Structure	Clinical stage	References
Tip60	TH1834		Preclinical	Idrissou et al. (2020)
p300	C646		Preclinical	Ono et al. (2016)

prostate cancer at micromolar doses (Zhou et al., 2018). However, few of these inhibitors have been used in the clinical setting owing to their dissatisfactory clinical safety and efficacy. **Table 1** summarizes several drugs that are in the different stages of clinical trials.

Lysine can be monomethylated, demethylated, or trimethylated by lysine methyltransferases (KMTs). Suv39h1 is the first histone KMT, and its main methylation site is H3K9. However, it was found that the site of H3K9 was almost no longer enzymatically active after the modification and its trimethylated peptide was no longer used as the substrate of methylase. In addition, the acetylation of H3K9 can inhibit the methylation of this site, and the dephosphorylation of H3S10 is the prerequisite for the methylation of H3K9. Thus, the phosphorylation of H3S10 can inhibit the methylation of adjacent site K9.

According to the types of amino acids at the modification sites, histone methylation can activate or inhibit gene transcription. For example, the methylation of histone H3K4, H3K36, and H3K79 sites can effectively activate the expression of corresponding genes, while the demethylation or trimethylation of H3K9, H3K27, and h4k20 is usually associated with gene silencing.

Histone lysine methylation plays an important role in the construction and maintenance of heterochromatin and euchromatin regions. In summary, lysine methylation regulates protein function mainly through two mechanisms: on the one hand, it can interact with other forms of PTMs; on the other hand, it can regulate protein function by influencing protein-protein interaction. Given that specific lysine residues on histone protein

are prone to methylation, which subsequently leads to tumor development, researchers developed specific inhibitors to interfere with the catalytic activity of methyltransferases on histone protein methylation (Rea et al., 2000). These methyltransferases specific for H3K4 include SET1, MLL, and SMYD1&3 families of proteins (Biswas and Rao, 2018). Cao et al. reported that a small molecule (MM-401) could disrupt the methyltransferase activity of MLL1 (Cao et al., 2014). Methylation of H3K9 was executed by G9a, GLP, SETDB1/2, and SUV39H1/2 (Torrano et al., 2019). Chaetocin was initially designed as an HKMT inhibitor under this category (Sak et al., 2021). Since then, several modified inhibitors were developed. BIX-01294, the first selective inhibitor of G9a, and its advanced alternative UNC0638 are potential candidates as antitumor agents (Pirola et al., 2018). Pappano et al. reported that A-366, a peptide-competitive inhibitor of G9a and GLP, plays a key role in inhibiting leukemic cells (Pappano et al., 2015). Coincidentally, Yuan et al. also documented that BRD4770, an inhibitor of G9a, could induce pancreatic cancer cell death combined with gossypol (Yuan et al., 2013). As a well-established hallmark of cancer initiation, methylation of H3K27 is catalyzed by EZH1/2 (Dai et al., 2017). As a result, the inhibitors that target EZH1/2 have demonstrated promising effects on tumor shrinkage in the preclinical setting (Dai et al., 2017). It was reported that UNC 1999, a SAM-competitive dual inhibitor of EZH1/2, inhibited cell proliferation of MLL-rearranged acute leukemia (Yamagishi et al., 2019). Recently, constellation pharmaceuticals initiated a clinical trial for testing the safety and efficacy of CPI-1205, an EZH2 inhibitor against B-cell lymphoma (NCT02395601) (Gehling et al., 2015). Also, tazemetostat (an EZH2 inhibitor)

is under clinical investigation (NCT03010982 and NCT03028103) (Kuntz et al., 2016). Methylation of H3K36 is another widely studied target for developing small-molecule inhibitors. Astra Zeneca identified AZ-505 as a specific inhibitor of methylation of H3K36 delayed cyst growth in a mouse model of polycystic kidney disease (Nguyen and Zhang, 2011). Nguyen et al. also reported that LLY-507, a selective inhibitor of SET and MYND domain-containing protein 2 (SMYD2) for methylation of H3K36, could abolish cell proliferation of several cancerous cell lines (Nguyen and Zhang, 2011). Besides, a disruptor of telomeric silencing 1-like (DOT1L), a histone H3K79 methyltransferase, has also been targeted to disrupt histone modification (Liu et al., 2014). Preclinical studies have demonstrated that DOT1L inhibitors that include EPZ004777, EPZ-5676, and SYC-522 can inhibit hematopoietic malignancies in different stages of clinical trials (Liu et al., 2014). Although most of the inhibitors mentioned above are still under clinical investigation, the recent accelerated approval of tazemetostat for metastatic or locally advanced epithelioid sarcoma sheds light on a promising direction towards further developing such compounds for cancer treatment. **Table 2** lists several drugs that are currently in the preclinical and clinical trials.

Methylation of histones can also occur in arginine residues, enabling the cell another layer of regulatory options (Cuthbert et al., 2004). Given the nature that arginine can be mono-, di-, or methylated modified, the modifications extend the complexity of gene regulation and are associated with transcriptional activation or suppression according to the location of the arginine residues (Wysocka et al., 2006; Jain and Clarke, 2019). Like the development of KDM inhibitors, the search for an arginine demethylase is also under active investigation. Physiologically, protein arginine methyltransferase (PRMT) can catalyze methylation of arginine residues on histones (Thompson and Fast, 2006; Jain and Clarke, 2019). PRMT family proteins and their arginine methylation are closely related to the occurrence and development of cancer. PRMT has nine members from PRMT1 to 9. Arginine methylation can be divided into monomethylation, symmetrical dimethylation, and asymmetrical dimethylation. According to arginine methylation, PRMT family members can be divided into three types: I, II, and III. Type I includes PRMT1, 2, 3, 4, 6, and 8, which can catalyze monomethylation and asymmetric dimethylation; type II includes Prmt5 and 9, which can catalyze monomethylation and symmetrical dimethylation; and type III includes prmt7 that can only catalyze monomethylation. Dysfunction of PRMT has been associated with different cancers, which leads to the efforts to developing specific inhibitors targeting this protein (Mohammad et al., 2019). Drew et al. reported that TP-064 and EZM2302, two inhibitors against PRMT4, inhibited the growth of multiple myeloma in the preclinical setting (Drew et al., 2017). EPZ015938, a selective inhibitor against PRMT5, is now under clinical investigation for patients with solid tumors and non-Hodgkin's lymphoma (Siu et al., 2019). Bonday et al. also demonstrated that LLY-283, an inhibitor against PRMT5, can reduce tumor cell growth *in vitro* (Bonday et al., 2018). PRMT family members are often

coexpressed and highly expressed in cancer, but its clinical significance is not clear. Liu Wen et al. confirmed that PRMT4, PRMT5, and PRMT7 were highly expressed in breast cancer, colorectal cancer, and prostate cancer, and the high expression of PRMTs was highly correlated with the enrichment of arginine methylation and abnormal alternative splicing of hnRNPA1. In breast cancer, colorectal cancer, and prostate cancer cells, PRMT4, PRMT5, and PRMT7 and their mediated hnRNPA1 methylation and splicing isomerism can effectively promote the growth of cancer cells. This provides a new direction and approach for cancer treatment. **Table 3** highlights some PRMTs in the preclinical and clinical settings.

Demethylation of lysine residues on histone proteins *via* targeting histone lysine demethylase KDM1 (LSD1/2) and KDM2-8 (JmjC domain proteins) represents another strategy of developing small-molecule inhibitors (Rotili and Mai, 2011; Hoffmann et al., 2012). Both families have been investigated for the development of inhibitors owing to their crucial role in tumorigenesis. Prusevich et al. found that bizine, the second generation of LSD1/2, significantly inhibited cancer cell proliferation *in vitro* (Prusevich et al., 2014). Zhu et al. reported that the inhibition of LSD1 reduced the growth of human breast cancer cell lines (Zhu et al., 2012). Willmann et al. demonstrated that LSD1 inhibition could also be used for androgen-dependent prostate cancer treatment (Willmann et al., 2012). Gupta recently identified that an irreversible LSD1 inhibitor, HCI-2509, was beneficial against MYCN-amplified neuroblastoma cells (Gupta et al., 2018). On the other hand, the development of specific inhibitors of JmjC-KDM also has come a long way. It was established that hydroxamic acid scaffold, hydroxyquinoline analogs, and cyclic peptides showed potential effectiveness as JmjC-KDM inhibitors (Rose et al., 2008). Though these inhibitors are still at the early stages of development, Hopkinson et al. and Thinnes et al. have initiated two preclinical studies to test the effectiveness of IOX1 and flavonoids against cancer cells (Hopkinson et al., 2013; Thinnes et al., 2014). Current drug development is summarized in **Table 4**.

Acetylation is a very common posttranslational modification (Drazic et al., 2016). In human cells, more than 1,750 proteins can be acetylated at lysine residues. Histone deacetylases (HDACs), as epigenetic modifiers, play an important role in gene transcription (Autin et al., 2019). Changes, mutations, and/or inappropriate recruitment of HDACs have been widely found, which are involved in tumorigenesis through a series of biological pathways (Hadley et al., 2019). Therefore, HDACs are considered a promising tumor therapeutic target, and their inhibitors are developing rapidly (Luparello et al., 2020). The application of HDAC inhibitors (HDACis) as anticancer drugs in cancer has been confirmed in cell lines and animal models (Falkenberg and Johnstone, 2014). The first generation of HDACi was developed based on screening by experience for some agents whose potential targets were HDACs. These agents originated from the tumor cell differentiation inducer, including butyrate, trichostatin A (TSA), and vorinostat (Leder and Leder, 1975; Riggs et al., 1977). Then, more HDACis were discovered from natural products, which

have different properties and clinical settings (Johnstone, 2002; West and Johnstone, 2014). However, the traditional HDACi was targeting multiple HDACs, which led to the difficulty of verifying the biological consequences and toxicities from inhibition of a specific HDAC or/and combined effect of multiprotein HDAC complexes (Bantscheff et al., 2011). Therefore, researchers need to identify more molecules as a new HDACi generation with an improved activity and specificity. HDACi has four major classic structures, including hydroxamic acid derivatives, aminobenzamide, cyclic peptide, and short-chain fatty acids (Cappellacci et al., 2020). Then, we sum up the HDACi which has been approved by the FDA of USA in **Table 5**. More interestingly, advantages of multitargeting antitumor drugs have been presented due to the multifactorial nature of tumor etiology in this respect because histone deacetylase inhibitors play an important role in many anticancer activities and have become a privileged tool for the development of mixed drugs. EGFR/HER2/HDAC hybrid inhibitor CUDC-101 is the first success of multitargeting drugs, which is one of the HDAC/kinase dual-acting compounds family (Luan et al., 2019). The other excellent “hybrid drug” is PI3Ks/HDAC hybrid inhibitor CUDC-907, which entered a phase 2 clinical trial (Hesham et al., 2018). GUDC-101 and CUDC-907 exhibit improved synergistic effects than the single-targeted drugs and overcome resistance to receptor tyrosine kinase inhibitors *via* multiple signaling. HDAC/CDK-4/JAK1i and LSD1/HDACi are the novel multitargets to develop “hybrid drug.” Preclinical data of Roxyl-zhc-84 (HDAC/CDK-4/JAK1i) and corin (LSD1/HDACi) also show better therapeutic effect than single acting compounds alone or in combination (Huang et al., 2018; Kalin et al., 2018). The clinical and preclinical results of the abovementioned agents show that the development of high-efficiency multitarget hybrid drugs is worthy of further research. The design guideline of hybrid HDACi should keep the potency and drug similarity of single target compounds to their respective targets and have an acceptable ADMET spectrum, while avoiding the increased toxicity and targeting effect due to the decreased targeting selectivity.

Histone acetylation is considered as the best-studied histone modification, which occurs at the ϵ amino groups of evolutionarily conserved lysine residues on tail domains (Hake et al., 2004). From a functional perspective, histone acetylation is primarily associated with the activation of transcription. It mainly occurs at the regions of enhancers, promoters, and the gene body (Wang et al., 2009). Altered global levels of histone acetylation, such as acetylation of H4 at lysine (K), have been linked to tumor development in various cancers, which have also been found to be of potential prognostic value (Elsheikh et al., 2009). When hyperacetylation of proto-oncogenes occurs, the expression of the target genes will be activated. On the contrary, when hypoacetylation of tumor suppressors occurs, co-occurring with DNA methylation, the tumor suppressors will be inactivated. These two mechanisms collectively contribute to the onset of tumor initiation and development. The enzymes that catalyze the addition of acetyl groups to histone lysine residues are histone acetyltransferases

(HATs) (Seto and Yoshida, 2014). Numerous chemical compounds have been tested for their potential as HAT inhibitors (HATis) (Carrozza et al., 2003; Eliseeva et al., 2007; Arif et al., 2010). Stimson et al. reported that PCAF and p300 inhibitors, two isothiazolinone-based compounds, could inhibit cell proliferation of colon cancer cells (Stimson et al., 2005). More recently, Modak et al. found that embelin, a natural compound of hydroxybenzoquinone class, could block the activity of PCAF (Modak et al., 2013). Sun et al. reported that HAT Tip60 could sensitize tumor cells against ionizing radiation (Sun et al., 2006). Gao et al. reported that TH 1834, a novel version of Tip60 inhibitor, can induce cancer cell apoptosis (Gao et al., 2014). However, the questions are that these chemical compounds are moderately toxic towards humans (Bruserud et al., 2007; Subramanian et al., 2010; Deng H. et al., 2020). As a result, researchers are still working on screening the better candidates with low toxicity but high effectiveness. **Table 6** summarized two drugs that are in the preclinical stage.

Small Molecules Targeting miRNAs

Given the well-documented nature that miRNAs play central roles in tumor development and because of the challenges of using nucleotide analogs for regulating miRNAs expression, it has been realized that the development of small-molecule drugs targeting specific miRNAs (SMIRs) would be a novel avenue for cancer treatment (Zhang et al., 2010). SMIRs are small synthetic organic molecules that can irreversibly bind to miRNAs. Mechanically, they bind to the grooves and pockets on the surface of miRNAs and interfere with the biological functions of targeted miRNAs (Mohammad et al., 2019). However, due to the structural flexibility and highly electronegative surfaces of SMIRs, RNA molecules have been excluded as drug target candidates for a long period. However, from the perspective of miRNA spatial structures, miRNAs appear to be “druggable” because the formation of stem loops in pre-miRNAs and the bulges in miRNAs can facilitate targeting by small molecules (Velagapudi et al., 2014). Of interest, Gumireddy et al. reported that diazobenzene and its derivatives could serve as specific inhibitors of pri-miR-21 formation (Gumireddy et al., 2008). Besides, it is documented that small-molecule enoxacin (Penetrex) can enhance small-interfering RNA-mediated mRNA silencing and facilitate the biogenesis of endogenous miRNAs (Shan et al., 2008). Though these mechanisms remain unclear, these findings undoubtedly provide proof of the modulation of miRNA activity by small-inhibitory molecules.

Recently, a novel strategy of developing a novel combined treatment therapy has been found. The rationale is rooted in the concept that many cancers share common gene or/and protein regulation pathways by chromatin regulators and miRNAs. For example, Swierczynski et al. comprised data from mirbase.org and DIANA-MICROT to find the overlap of HDAC-miRNA combinations. Then, they indicated HDACs and miRNAs shared some gene or/and protein regulation pathways (Swierczynski et al., 2015). Though detailed mechanisms remain to be elucidated, the complex linkage between miRNA and HDAC has emerged as a potential drug target, which might provide

possible novel therapeutic approaches in the near future. It is reported that complete inhibition of HDAC2 can increase histone H4 pan-acetylation of the miR-183 promoter region and subsequently upregulate the transcriptional activity of miR-183, which leads to miR-183-mediated tumor suppression in neuroblastoma (Swierczynski et al., 2015; Zhu and Wang, 2021). Similarly, inhibition of HDAC3 with specific inhibitors can result in an increased hyperacetylation of the Dleu/miR-15a/16-1 promoter region. This upregulation increases the expression of miR-15a/16-1, which suppresses lung cancer cell growth. Besides, silencing of HDAC9 can stop sprouting *in vitro* and reduce vessel growth in a zebrafish model *in vivo* via the repression of the miR-17-92 cluster, indicating a possible common therapeutic target for cancer vasculogenesis (Hernandez-Romero et al., 2019). These could lead to personalized cancer therapies, which employ HDACs and simultaneously modify miRNAs. But, their mechanism of action remains to be addressed (Dawson and Kouzarides, 2012).

Epigenetic Therapy (EpiDrugs) in Acquired Chemoresistance

Chemoresistance is a major obstacle to successful chemotherapy in clinic. Acquired drug resistance was controlled by multiple genetic and/or epigenetic ways (Ponnusamy et al., 2020). Unlike genetic mutations, epigenetic modulation in chemoresistance presents the characteristics of plasticity and reversibility, which puts a new insight into overcoming the acquired chemoresistance *via* epigenetic reprogramming (Miranda Furtado et al., 2019). Recurrent tumors may still be sensitive to second-line chemotherapy because of the heterogeneity and poised epigenetics. However, during chemotherapy, the temporal epigenetic changes would induce acquired chemoresistance and lead to sensitive tumor no longer responding to second-line chemotherapy (Brown et al., 2014). The possible ways by which epigenetic dysregulation contribute to acquired chemoresistance are listed in detail as follows: 1) Chemotherapy induces abnormalities in cell energy metabolism that regulate the generation/source of epigenetic factors and alter the cellular epigenetic spectrum, thereby promoting acquired chemoresistance (Wang et al., 2018); 2) various efflux transporters, including p-glycoprotein, multidrug-resistant protein, and breast cancer resistance protein associated with acquired drug resistance showed epigenetic dysregulation during chemotherapy (Kim et al., 2014); 3) epigenetic events such as DNA methylation and histone modification induce apoptotic tolerance and autophagy contributing to the development of acquired drug resistance (Hervouet et al., 2013; Sui et al., 2013); 4) epigenetic dysregulation-mediated regulation of major tumor growth signaling and altered chemotherapeutic target expression may contribute to acquired chemoresistance; 5) epigenetics also improves acquired chemoresistance by regulating genes involved in the formation of tumor microenvironments, such as tumor-associated fibroblasts and HIF-1 α (Marks et al., 2016); 6) cellular reprogramming regulated by epigenetic events was established and developed with acquired chemoresistance (Phi et al., 2018); 7) epigenetic dysregulation and subsequent aberrant cellular energetics promote drug resistance by

silencing genes involved in DNA repair or directly altering their structure (House et al., 2014). 8) epigenetic dysregulation is a key pathway for ROS and its related oxidative stress to induce acquired chemoresistance (Shrishrimal et al., 2019). Therefore, it is not sufficient to target genetic abnormalities alone as a method to overcome acquired chemoresistance. Due to epigenetic heterogeneity in different patients and tumors, understanding the epigenetic dynamic landscape response to chemotherapy is necessary for EpiDrug discovery. Recently, clinical and preclinical studies have been conducted to evaluate the effect of EpiDrugs in overcoming drug resistance (Ediriweera et al., 2019). However, the results showed the double edges of EpiDrugs in chemoresistance. Due to the lack of specificity, despite EpiDrugs silencing tumor suppressors, they also hypomethylated microsatellite regions and activated oncogenes, promoting chemoresistance (Ley et al., 2010). Taking together, developing EpiDrugs with a specific target and selectivity is critical and challenging. Meanwhile, dose adjustment and scheduling may be an important issue in EpiDrugs used to overcome chemoresistance (Ediriweera et al., 2019).

CONCLUSION

Since the discovery of epigenetics by C. Waddington, tremendous development has been achieved in the field of epigenetics. Various enzymes and specialized proteins have been established for remodeling chromatin organization. Though cancer is a polygenic disease, studies have established a tight association of epigenetics with tumorigenesis. The profile of epigenetic alteration has provided novel targets for the development of antitumor agents as indicated by the US-FDA approval of HDAC inhibitors to treat a form of lymphoma (Giannini et al., 2012). However, enormous challenges remain to be overcome to accelerate the transition from bench to bedside. First of all, several substrates synergistically taking part in chromatin remodeling have been identified. In addition, most enzymes work as a part of a multiprotein complex, which increases the difficulty for active enzyme production and screening. These successful cases verify the hypothesis that it is possible to regulate the epigenetic process of treating diseases, and the therapeutic window of this new drug can be realized in the clinic. Although there are some ongoing clinical trials for a wide range of neoplastic and nonneoplastic diseases, the application of epigenetic drugs in clinical practice is mostly limited to hematological malignancies. The potential of epigenetic drugs is expanding to other diseases, from infectious diseases to brain diseases, cardiovascular diseases, and metabolic disorders. It seems promising, and more interesting results are expectant within a few years. However, the development of clinical trials needs to identify biomarkers that can predict drug response and avoid complications and unnecessary side effects in patients with nonsensitive tumors. Epigenetic mutations (hypermethylation of the tumor suppressor gene promoter) and epigenetic enzyme mutations (loss or gain of function) can be used as predictors of chemotherapy response in several cancers. For instance, epigenetic silencing of MGMT has been used as a biomarker to predict response to temozolomide in

patients with glioblastoma. With the development of next-generation sequencing technology, it is possible to explore more unknown fields for the world. Therefore, further efforts will focus on increasing drug selectivity and expanding the spectrum towards solid tumors, since most of the clinically available epigenetic drugs are pan-HDAC inhibitors that are only effective against hematological malignancies. Appropriate patient selection and optimizing trial design and dosing schedules may also improve clinical efficacy.

AUTHOR CONTRIBUTIONS

WX, QZ, and XW wrote the review. RW designed the figures and tables. RL and TW collected the information. WX, JS, JH, and YH

supervised the whole work, contributed to writing, and critically revised the article.

FUNDING

This work was supported by the Natural Science Foundation of China (81402507, 81900339, and 82073311), Health Commission of Sichuan Province (19ZDXM0016), Science & Technology Department of Sichuan Province (2018SZ0033 and 2018JY0542), the Key Research and Development Projects in Chengdu (2020-YF05-00058-SN), the Key Research and Development Projects in Sichuan Province (2020YFS0399), and the Fundamental Research Funds for the Central Universities (2682021TPY031).

REFERENCES

- Angarica, V. E., and Del Sol, A. (2017). Bioinformatics Tools for Genome-wide Epigenetic Research. *Adv. Exp. Med. Biol.* 978, 489–512. doi:10.1007/978-3-319-53889-1_25
- Arif, M., Vadamurthy, B. M., Choudhary, R., Ostwal, Y. B., Mantelingu, K., Kodaganur, G. S., et al. (2010). Nitric Oxide-Mediated Histone Hyperacetylation in Oral Cancer: Target for a Water-Soluble HAT Inhibitor, CTK7A. *Chem. Biol.* 17 (8), 903–913. doi:10.1016/j.chembiol.2010.06.014
- Autin, P., Blanquart, C., and Fradin, D. (2019). Epigenetic Drugs for Cancer and microRNAs: A Focus on Histone Deacetylase Inhibitors. *Cancers* 11 (10), 1530. doi:10.3390/cancers11101530
- Azangou-Khyavy, M., Ghasemi, M., Khanali, J., Boroomand-Saboor, M., Jamalkhah, M., Soleimani, M., et al. (2020). CRISPR/Cas: From Tumor Gene Editing to T Cell-Based Immunotherapy of Cancer. *Front. Immunol.* 11, 2062. doi:10.3389/fimmu.2020.02062
- Balch, C., Yan, P., Craft, T., Young, S., Skalik, D. G., Huang, T. H.-M., et al. (2005). Antimitogenic and Chemosensitizing Effects of the Methylation Inhibitor Zebularine in Ovarian Cancer. *Mol. Cancer Ther.* 4 (10), 1505–1514. doi:10.1158/1535-7163.MCT-05-0216
- Baldi, S. (2019). Nucleosome Positioning and Spacing: from Genome-wide Maps to Single Arrays. *Essays Biochem.* 63 (1), 5–14. doi:10.1042/EBC20180058
- Bannister, A. J., and Kouzarides, T. (2011). Regulation of Chromatin by Histone Modifications. *Cell Res* 21 (3), 381–395. doi:10.1038/cr.2011.22
- Bantscheff, M., Hopf, C., Savitski, M. M., Dittmann, A., Grandi, P., Michon, A.-M., et al. (2011). Chemoproteomics Profiling of HDAC Inhibitors Reveals Selective Targeting of HDAC Complexes. *Nat. Biotechnol.* 29 (3), 255–265. doi:10.1038/nbt.1759
- Basu Mallik, S., Pai, A., Shenoy, R. R., and Jayashree, B. S. (2017). Novel Flavonol Analogues as Potential Inhibitors of JMJD3 Histone Demethylase-A Study Based on Molecular Modelling. *J. Mol. Graphics Model.* 72, 81–87. doi:10.1016/j.jmgm.2016.12.002
- Bates, S. E. (2020). Epigenetic Therapies for Cancer. *N. Engl. J. Med.* 383 (7), 650–663. doi:10.1056/NEJMra1805035
- Bestor, T. H., and Verdine, G. L. (1994). DNA Methyltransferases. *Curr. Opin. Cel Biol.* 6 (3), 380–389. doi:10.1016/0955-0674(94)90030-2
- Bhaumik, S. R., Smith, E., and Shilatfard, A. (2007). Covalent Modifications of Histones During Development and Disease Pathogenesis. *Nat. Struct. Mol. Biol.* 14 (11), 1008–1016. doi:10.1038/nsmb1337
- Biswas, S., and Rao, C. M. (2018). Epigenetic Tools (The Writers, the Readers and the Erasers) and Their Implications in Cancer Therapy. *Eur. J. Pharmacol.* 837, 8–24. doi:10.1016/j.ejphar.2018.08.021
- Bonday, Z. Q., Cortez, G. S., Grogan, M. J., Antonysamy, S., Weichert, K., Bocchinfuso, W. P., et al. (2018). LLY-283, A Potent and Selective Inhibitor of Arginine Methyltransferase 5, PRMT5, with Antitumor Activity. *ACS Med. Chem. Lett.* 9 (7), 612–617. doi:10.1021/acsmchemlett.8b00014
- Brown, R., Curry, E., Magnani, L., Wilhelm-Benartzi, C. S., and Borley, J. (2014). Poised Epigenetic States and Acquired Drug Resistance in Cancer. *Nat. Rev. Cancer* 14 (11), 747–753. doi:10.1038/nrc3819
- Bruserud, O., Stapnes, C., Ersvæ, E., Gjertsen, B., and Rynningen, A. (2007). Histone Deacetylase Inhibitors in Cancer Treatment: A Review of the Clinical Toxicity and the Modulation of Gene Expression in Cancer Cells. *Cpb* 8 (6), 388–400. doi:10.2174/138920107783018417
- Campbell, R. M., and Tummino, P. J. (2014). Cancer Epigenetics Drug Discovery and Development: The Challenge of Hitting the Mark. *J. Clin. Invest.* 124 (1), 64–69. doi:10.1172/JCI71605
- Cao, F., Townsend, E. C., Karatas, H., Xu, J., Li, L., Lee, S., et al. (2014). Targeting MLL1 H3K4 Methyltransferase Activity in Mixed-Lineage Leukemia. *Mol. Cell* 53 (2), 247–261. doi:10.1016/j.molcel.2013.12.001
- Cappellacci, L., Perinelli, D. R., Maggi, F., Grifantini, M., and Petrelli, R. (2020). Recent Progress in Histone Deacetylase Inhibitors as Anticancer Agents. *Cmc* 27 (15), 2449–2493. doi:10.2174/0929867325666181016163110
- Carrozza, M. J., Utley, R. T., Workman, J. L., and Côté, J. (2003). The Diverse Functions of Histone Acetyltransferase Complexes. *Trends Genet.* 19 (6), 321–329. doi:10.1016/S0168-9525(03)00115-X
- Cheng, J. C., Matsen, C. B., Gonzales, F. A., Ye, W., Greer, S., Marquez, V. E., et al. (2003). Inhibition of DNA Methylation and Reactivation of Silenced Genes by Zebularine. *JNCI J. Natl. Cancer Inst.* 95 (5), 399–409. doi:10.1093/jnci/95.5.399
- Chi, P., Allis, C. D., and Wang, G. G. (2010). Covalent Histone Modifications - Miswritten, Misinterpreted and Mis-Erased in Human Cancers. *Nat. Rev. Cancer* 10 (7), 457–469. doi:10.1038/nrc2876
- Christman, J. K., Schneiderman, N., and Acs, G. (1985). Formation of Highly Stable Complexes Between 5-Azacytosine-Substituted DNA and Specific Non-histone Nuclear Proteins. Implications for 5-Azacytidine-Mediated Effects on DNA Methylation and Gene Expression. *J. Biol. Chem.* 260 (7), 4059–4068. doi:10.1016/s0021-9258(18)89231-6
- Cuthbert, G. L., Daujat, S., Snowden, A. W., Erdjument-Bromage, H., Hagiwara, T., Yamada, M., et al. (2004). Histone Deimination Antagonizes Arginine Methylation. *Cell* 118 (5), 545–553. doi:10.1016/j.cell.2004.08.020
- Daher-Reyes, G. S., Merchan, B. M., and Yee, K. W. L. (2019). Guadecitabine (SGI-110): An Investigational Drug for the Treatment of Myelodysplastic Syndrome and Acute Myeloid Leukemia. *Expert Opin. Investig. Drugs* 28 (10), 835–849. doi:10.1080/13543784.2019.1667331
- Dai, M., Tobinai, K., Makita, S., Ishida, T., Kusumoto, S., Ishitsuka, K., et al. (2017). First-in-Human Study of the EZH1/2 Dual Inhibitor DS-3201b in Patients with Relapsed or Refractory Non-hodgkin Lymphomas — Preliminary Results. *Blood* 130, 4070. doi:10.1182/blood.V130.Suppl_1.4070.4070
- Datta, J., Ghoshal, K., Denny, W. A., Gamage, S. A., Brooke, D. G., Phiasivongsa, P., et al. (2009). A New Class of Quinoline-Based DNA Hypomethylating Agents Reactivates Tumor Suppressor Genes by Blocking DNA Methyltransferase 1 Activity and Inducing its Degradation. *Cancer Res.* 69 (10), 4277–4285. doi:10.1158/0008-5472.CAN-08-3669
- Dawson, M. A., and Kouzarides, T. (2012). Cancer Epigenetics: From Mechanism to Therapy. *Cell* 150 (1), 12–27. doi:10.1016/j.cell.2012.06.013
- Dayeh, T., Volkov, P., Saló, S., Hall, E., Nilsson, E., Olsson, A. H., et al. (2014). Genome-wide DNA Methylation Analysis of Human Pancreatic Islets From

- Type 2 Diabetic and Non-diabetic Donors Identifies Candidate Genes that Influence Insulin Secretion. *Plos Genet.* 10 (3), e1004160. doi:10.1371/journal.pgen.1004160
- de Grass, D., Manie, S., and Amosum, S. (2014). Effectiveness of a Home-based Pulmonary Rehabilitation Programme in Pulmonary Function and Health Related Quality of Life for Patients with Pulmonary Tuberculosis: A Pilot Study. *Afr. H. Sci.* 14 (4), 866–872. doi:10.4314/ahs.v14i4.14
- Deng, B. B., Jiao, B. P., Liu, Y. J., Li, Y. R., and Wang, G. J. (2020a). BIX-01294 Enhanced Chemotherapy Effect in Gastric Cancer by Inducing GSDME-mediated Pyroptosis. *Cell Biol Int* 44 (9), 1890–1899. doi:10.1002/cbin.11395
- Deng, H., Fujiwara, N., Cui, H., Whitford, G. M., Bartlett, J. D., and Suzuki, M. (2020b). Histone Acetyltransferase Promotes Fluoride Toxicity in LS8 Cells. *Chemosphere* 247, 125825. doi:10.1016/j.chemosphere.2020.125825
- Derissen, E. J. B., Beijnen, J. H., and Schellens, J. H. M. (2013). Concise Drug Review: Azacitidine and Decitabine. *The Oncologist* 18 (5), 619–624. doi:10.1634/theoncologist.2012-0465
- Dhillon, S. (2020). Decitabine/Cedazuridine: First Approval. *Drugs* 80 (13), 1373–1378. doi:10.1007/s40265-020-01389-7
- Di Leva, G., and Croce, C. M. (2013). miRNA Profiling of Cancer. *Curr. Opin. Genet. Develop.* 23 (1), 3–11. doi:10.1016/j.gde.2013.01.004
- Drazic, A., Myklebust, L. M., Ree, R., and Arnesen, T. (2016). The World of Protein Acetylation. *Biochim. Biophys. Acta (Bba) - Proteins Proteomics* 1864 (10), 1372–1401. doi:10.1016/j.bbapap.2016.06.007
- Drew, A. E., Moradei, O., Jacques, S. L., Rioux, N., Boriack-Sjodin, A. P., Allain, C., et al. (2017). Identification of a CARM1 Inhibitor with Potent In Vitro and In Vivo Activity in Preclinical Models of Multiple Myeloma. *Sci. Rep.* 7 (1), 17993. doi:10.1038/s41598-017-18446-z
- Dzobo, K. (2019). Epigenomics-Guided Drug Development: Recent Advances in Solving the Cancer Treatment "jigsaw Puzzle". *OMICS: A J. Integr. Biol.* 23 (2), 70–85. doi:10.1089/omi.2018.0206
- Ediriweera, M. K., Tennekoon, K. H., and Samarakoon, S. R. (2019). Emerging Role of Histone Deacetylase Inhibitors as Anti-breast-cancer Agents. *Drug Discov. Today* 24 (3), 685–702. doi:10.1016/j.drudis.2019.02.003
- Eliseeva, E. D., Valkov, V., Jung, M., and Jung, M. O. (2007). Characterization of Novel Inhibitors of Histone Acetyltransferases. *Mol. Cancer Ther.* 6 (9), 2391–2398. doi:10.1158/1535-7163.MCT-07-0159
- Elsheikh, S. E., Green, A. R., Rakha, E. A., Powe, D. G., Ahmed, R. A., Collins, H. M., et al. (2009). Global Histone Modifications in Breast Cancer Correlate with Tumor Phenotypes, Prognostic Factors, and Patient Outcome. *Cancer Res.* 69 (9), 3802–3809. doi:10.1158/0008-5472.CAN-08-3907
- Estécio, M. R. H., and Issa, J.-P. J. (2011). Dissecting DNA Hypermethylation in Cancer. *FEBS Lett.* 585 (13), 2078–2086. doi:10.1016/j.febslet.2010.12.001
- Esteller, M. (2007). Cancer Epigenomics: DNA Methylomes and Histone-Modification Maps. *Nat. Rev. Genet.* 8 (4), 286–298. doi:10.1038/nrg2005
- Fahy, J., Jeltsch, A., and Arimondo, P. B. (2012). DNA Methyltransferase Inhibitors in Cancer: A Chemical and Therapeutic Patent Overview and Selected Clinical Studies. *Expert Opin. Ther. Patents* 22 (12), 1427–1442. doi:10.1517/13543776.2012.729579
- Falkenberg, K. J., and Johnstone, R. W. (2014). Histone Deacetylases and Their Inhibitors in Cancer, Neurological Diseases and Immune Disorders. *Nat. Rev. Drug Discov.* 13 (9), 673–691. doi:10.1038/nrd4360
- Feinberg, A. P., and Irizarry, R. A. (2010). Stochastic Epigenetic Variation as a Driving Force of Development, Evolutionary Adaptation, and Disease. *Proc. Natl. Acad. Sci.* 107 (Suppl. 1), 1757–1764. doi:10.1073/pnas.0906183107
- Feinberg, A. P. (2018). The Key Role of Epigenetics in Human Disease Prevention and Mitigation. *N. Engl. J. Med.* 378 (14), 1323–1334. doi:10.1056/NEJMr1402513
- Fioravanti, R., Stazi, G., Zwergel, C., Valente, S., and Mai, A. (2018). Six Years (2012–2018) of Researches on Catalytic EZH2 Inhibitors: The Boom of the 2-Pyridone Compounds. *Chem. Rec.* 18 (12), 1818–1832. doi:10.1002/tcr.201800091
- Flavahan, W. A., Gaskell, E., and Bernstein, B. E. (2017). Epigenetic Plasticity and the Hallmarks of Cancer. *Science* 357 (6348), eaal2380. doi:10.1126/science.aal2380
- Gambacorta, V., Gnani, D., Vago, L., and Di Micco, R. (2019). Epigenetic Therapies for Acute Myeloid Leukemia and Their Immune-Related Effects. *Front. Cel Dev. Biol.* 7, 207. doi:10.3389/fcell.2019.00207
- Ganesan, A., Arimondo, P. B., Rots, M. G., Jeronimo, C., and Berdasco, M. (2019). The Timeline of Epigenetic Drug Discovery: From Reality to Dreams. *Clin. Epigenet* 11 (1), 174. doi:10.1186/s13148-019-0776-0
- Gao, C., Bourke, E., Scobie, M., Famme, M. A., Koolmeister, T., Helleday, T., et al. (2014). Rational Design and Validation of a Tip60 Histone Acetyltransferase Inhibitor. *Sci. Rep.* 4, 5372. doi:10.1038/srep05372
- Gaudet, F., Hodgson, J. G., Eden, A., Jackson-Grusby, L., Dausman, J., Gray, J. W., et al. (2003). Induction of Tumors in Mice by Genomic Hypomethylation. *Science* 300 (5618), 489–492. doi:10.1126/science.1083558
- Gehling, V. S., Vaswani, R. G., Nasveschuk, C. G., Duplessis, M., Iyer, P., Balasubramanian, S., et al. (2015). Discovery, Design, and Synthesis of Indole-Based EZH2 Inhibitors. *Bioorg. Med. Chem. Lett.* 25 (17), 3644–3649. doi:10.1016/j.bmcl.2015.06.056
- Giannini, G., Cabri, W., Fattorusso, C., and Rodriquez, M. (2012). Histone Deacetylase Inhibitors in the Treatment of Cancer: Overview and Perspectives. *Future Med. Chem.* 4 (11), 1439–1460. doi:10.4155/fmc.12.80
- Greer, S., Han, T., Dieguez, C., McLean, N., Saer, R., Reis, I., et al. (2017). Enzyme-Driven Chemo-And Radiation-Therapy with 12 Pyrimidine Nucleoside Analogs Not yet in the Clinic. *Acamc* 17 (2), 250–264. doi:10.2174/1871520616666161013145853
- Grønbaek, K., Hother, C., and Jones, P. A. (2007). Epigenetic Changes in Cancer. *APMIS* 115 (10), 1039–1059. doi:10.1111/j.1600-0463.2007.apm_636.xml.x
- Grosso, L. E., and Pitot, H. C. (1984). Alterations in the Maturation and Structure of Ribosomal Precursor RNA in Novikoff Hepatoma Cells Induced by 5-fluorocytidine. *Biochemistry* 23 (12), 2651–2656. doi:10.1021/bi00307a017
- Gulati, N., Béguelin, W., and Giulino-Roth, L. (2018). Enhancer of Zeste Homolog 2 (EZH2) Inhibitors. *Leuk. Lymphoma* 59 (7), 1574–1585. doi:10.1080/10428194.2018.1430795
- Gumireddy, K., Young, D. D., Xiong, X., Hogenesch, J. B., Huang, Q., and Deiters, A. (2008). Small-Molecule Inhibitors of MicroRNA miR-21 Function. *Angew. Chem. Int. Ed.* 47 (39), 7482–7484. doi:10.1002/anie.200801555
- Gupta, S., Doyle, K., Mosbrugger, T. L., Butterfield, A., Weston, A., Ast, A., et al. (2018). Reversible LSD1 Inhibition with HCl-2509 Induces the P53 Gene Expression Signature and Disrupts the MYCN Signature in High-Risk Neuroblastoma Cells. *Oncotarget* 9 (11), 9907–9924. doi:10.18632/oncotarget.24035
- Hadley, M., Noonepalle, S., Banik, D., and Villagra, A. (2019). Functional Analysis of HDACs in Tumorigenesis. *Methods Mol. Biol.* 1983, 279–307. doi:10.1007/978-1-4939-9434-2_17
- Hake, S. B., Xiao, A., and Allis, C. D. (2004). Linking the Epigenetic 'language' of Covalent Histone Modifications to Cancer. *Br. J. Cancer* 90 (4), 761–769. doi:10.1038/sj.bjc.6601575
- Handel, A. E., Ebers, G. C., and Ramagopalan, S. V. (2010). Epigenetics: Molecular Mechanisms and Implications for Disease. *Trends Mol. Med.* 16 (1), 7–16. doi:10.1016/j.molmed.2009.11.003
- Hellebrekers, D. M. E. I., Jair, K.-W., Viré, E., Eguchi, S., Hoebers, N. T. H., Fraga, M. F., et al. (2006). Angiostatic Activity of DNA Methyltransferase Inhibitors. *Mol. Cancer Ther.* 5 (2), 467–475. doi:10.1158/1535-7163.MCT-05-0417
- Hernández-Romero, I. A., Guerra-Calderas, L., Salgado-Albarrán, M., Maldonado-Huerta, T., and Soto-Reyes, E. (2019). The Regulatory Roles of Non-coding RNAs in Angiogenesis and Neovascularization From an Epigenetic Perspective. *Front. Oncol.* 9, 1091. doi:10.3389/fonc.2019.01091
- Herranz, M., and Esteller, M. (2007). DNA Methylation and Histone Modifications in Patients with Cancer: Potential Prognostic and Therapeutic Targets. *Methods Mol. Biol.* 361, 25–62. doi:10.1385/1-59745-208-4:25
- Hervouet, E., Cheray, M., Vallette, F., and Cartron, P.-F. (2013). DNA Methylation and Apoptosis Resistance in Cancer Cells. *Cells* 2 (3), 545–573. doi:10.3390/cells2030545
- Hesham, H. M., Lasheen, D. S., and Abouzid, K. A. M. (2018). Chimeric HDAC Inhibitors: Comprehensive Review on the HDAC-Based Strategies Developed to Combat Cancer. *Med. Res. Rev.* 38 (6), 2058–2109. doi:10.1002/med.21505
- Hoffmann, I., Roatsch, M., Schmitt, M. L., Carlino, L., Pippel, M., Sippl, W., et al. (2012). The Role of Histone Demethylases in Cancer Therapy. *Mol. Oncol.* 6 (6), 683–703. doi:10.1016/j.molonc.2012.07.004
- Hopkinson, R. J., Tumber, A., Yapp, C., Chowdhury, R., Aik, W., Che, K. H., et al. (2013). 5-Carboxy-8-hydroxyquinoline Is a Broad Spectrum 2-Oxoglutarate Oxygenase Inhibitor Which Causes Iron Translocation. *Chem. Sci.* 4 (8), 3110–3117. doi:10.1039/C3SC51122G
- House, N. C. M., Koch, M. R., and Freudenreich, C. H. (2014). Chromatin Modifications and DNA Repair: Beyond Double-Strand Breaks. *Front. Genet.* 5, 296. doi:10.3389/fgene.2014.00296

- Hoyle, R. G., Wang, H., Cen, Y., Zhang, Y., and Li, J. (2021). IOX1 Suppresses Wnt Target Gene Transcription and Colorectal Cancer Tumorigenesis Through Inhibition of KDM3 Histone Demethylases. *Mol. Cancer Ther.* 20 (1), 191–202. doi:10.1158/1535-7163.MCT-20-0328
- Huang, Z., Zhou, W., Li, Y., Cao, M., Wang, T., Ma, Y., et al. (2018). Novel Hybrid Molecule Overcomes the Limited Response of Solid Tumours to HDAC Inhibitors via Suppressing JAK1-STAT3-BCL2 Signalling. *Theranostics* 8 (18), 4995–5011. doi:10.7150/thno.26627
- Humphries, B., Wang, Z., and Yang, C. (2019). MicroRNA Regulation of Epigenetic Modifiers in Breast Cancer. *Cancers* 11 (7), 897. doi:10.3390/cancers11070897
- Hutvagner, G., and Simard, M. J. (2008). Argonaute Proteins: Key Players in RNA Silencing. *Nat. Rev. Mol. Cell Biol.* 9 (1), 22–32. doi:10.1038/nrm2321
- Idrissi, M., Lebert, A., Boissier, T., Sanchez, A., Houf, F. Z., Penault-Llorca, F., et al. (2020). Digging Deeper into Breast Cancer Epigenetics: Insights from Chemical Inhibition of Histone Acetyltransferase TIP60 In Vitro. *OMICS: A J. Integr. Biol.* 24 (10), 581–591. doi:10.1089/omi.2020.0104
- Imanishi, S., Umez, T., Ohtsuki, K., Kobayashi, C., Ohyashiki, K., and Ohyashiki, J. H. (2014). Constitutive Activation of the ATM/BRCA1 Pathway Prevents DNA Damage-Induced Apoptosis in 5-Azacytidine-Resistant Cell Lines. *Biochem. Pharmacol.* 89 (3), 361–369. doi:10.1016/j.bcp.2014.03.008
- International Cancer Genome, C., Hudson, T. J., Anderson, W., Artez, A., Barker, A. D., Bell, C., et al. (2010). International Network of Cancer Genome Projects. *Nature* 464 (7291), 993–998. doi:10.1038/nature08987
- Issa, J.-P. J., Roboz, G., Rizzieri, D., Jabbour, E., Stock, W., O'Connell, C., et al. (2015). Safety and Tolerability of Guadecitabine (SGI-110) in Patients with Myelodysplastic Syndrome and Acute Myeloid Leukemia: A Multicentre, Randomised, Dose-Escalation Phase 1 Study. *Lancet Oncol.* 16 (9), 1099–1110. doi:10.1016/S1470-2045(15)00038-8
- Jain, K., and Clarke, S. G. (2019). PRMT7 as a Unique Member of the Protein Arginine Methyltransferase Family: A Review. *Arch. Biochem. Biophys.* 665, 36–45. doi:10.1016/j.abb.2019.02.014
- Johnstone, R. W. (2002). Histone-deacetylase Inhibitors: Novel Drugs for the Treatment of Cancer. *Nat. Rev. Drug Discov.* 1 (4), 287–299. doi:10.1038/nrd772
- Joyce, C., Rayi, A., and Kasi, A. (2021). *Tumor-Suppressor Genes*. Treasure Island, FL: StatPearls.
- Kalin, J. H., Wu, M., Gomez, A. V., Song, Y., Das, J., Hayward, D., et al. (2018). Targeting the CoREST Complex with Dual Histone Deacetylase and Demethylase Inhibitors. *Nat. Commun.* 9 (1), 53. doi:10.1038/s41467-017-02242-4
- Kaliszczak, M., Trousil, S., Åberg, O., Perumal, M., Nguyen, Q.-D., and Aboagye, E. O. (2013). A Novel Small Molecule Hydroxamate Preferentially Inhibits HDAC6 Activity and Tumour Growth. *Br. J. Cancer* 108 (2), 342–350. doi:10.1038/bjc.2012.576
- Kiianitsa, K., Zhang, Y., and Maizels, N. (2020). Treatment of Human Cells with 5-Aza-dC Induces Formation of PARP1-DNA Covalent Adducts at Genomic Regions Targeted by DNMT1. *DNA Repair* 96, 102977. doi:10.1016/j.dnarep.2020.102977
- Kim, H. Y., Lee, H., Lee, J. K., Kim, H. V., Kim, K.-S., and Kim, Y. (2020). Bicine Promotes Rapid Formation of β -sheet-rich Amyloid- β Fibrils. *PLoS One* 15 (10), e0240608. doi:10.1371/journal.pone.0240608
- Kim, I.-W., Han, N., Burckart, G. J., and Oh, J. M. (2014). Epigenetic Changes in Gene Expression for Drug-Metabolizing Enzymes and Transporters. *Pharmacotherapy* 34 (2), 140–150. doi:10.1002/phar.1362
- Kim, J. (2020). Cellular Reprogramming to Model and Study Epigenetic Alterations in Cancer. *Stem Cell Res.* 49, 102062. doi:10.1016/j.scr.2020.102062
- Kisiel, J. B., Yab, T. C., Taylor, W. R., Chari, S. T., Petersen, G. M., Mahoney, D. W., et al. (2012). Stool DNA Testing for the Detection of Pancreatic Cancer. *Cancer* 118 (10), 2623–2631. doi:10.1002/cncr.26558
- Krais, J. J., and Johnson, N. (2020). BRCA1 Mutations in Cancer: Coordinating Deficiencies in Homologous Recombination with Tumorigenesis. *Cancer Res.* 80 (21), 4601–4609. doi:10.1158/0008-5472.CAN-20-1830
- Kuck, D., Caulfield, T., Lyko, F., and Medina-Franco, J. L. (2010). Nanaomycin A Selectively Inhibits DNMT3B and Reactivates Silenced Tumor Suppressor Genes in Human Cancer Cells. *Mol. Cancer Ther.* 9 (11), 3015–3023. doi:10.1158/1535-7163.MCT-10-0609
- Kukita, A., Sone, K., Oda, K., Hamamoto, R., Kaneko, S., Komatsu, M., et al. (2019). Histone Methyltransferase SMYD2 Selective Inhibitor LLY-507 in Combination with Poly ADP Ribose Polymerase Inhibitor Has Therapeutic Potential against High-Grade Serous Ovarian Carcinomas. *Biochem. Biophys. Res. Commun.* 513 (2), 340–346. doi:10.1016/j.bbrc.2019.03.155
- Kumari, A., Srinivasan, R., Vasishta, R. K., and Wig, J. D. (2009). Positive Regulation of Human Telomerase Reverse Transcriptase Gene Expression and Telomerase Activity by DNA Methylation in Pancreatic Cancer. *Ann. Surg. Oncol.* 16 (4), 1051–1059. doi:10.1245/s10434-009-0333-8
- Kuntz, K. W., Campbell, J. E., Keilhack, H., Pollock, R. M., Knutson, S. K., Porter-Scott, M., et al. (2016). The Importance of Being Me: Magic Methyls, Methyltransferase Inhibitors, and the Discovery of Tazemetostat. *J. Med. Chem.* 59 (4), 1556–1564. doi:10.1021/acs.jmedchem.5b01501
- Leder, A., and Leder, P. (1975). Butyric Acid, A Potent Inducer of Erythroid Differentiation in Cultured Erythroleukemic Cells. *Cell* 5 (3), 319–322. doi:10.1016/0092-8674(75)90107-5
- Ley, T. J., Ding, L., Walter, M. J., McLellan, M. D., Lamprecht, T., Larson, D. E., et al. (2010). DNMT3A Mutations in Acute Myeloid Leukemia. *N. Engl. J. Med.* 363 (25), 2424–2433. doi:10.1056/NEJMoa1005143
- Li, X., Wang, C., Jiang, H., and Luo, C. (2019). A Patent Review of Arginine Methyltransferase Inhibitors (2010–2018). *Expert Opin. Ther. Patents* 29 (2), 97–114. doi:10.1080/13543776.2019.1567711
- Li, X., Xiong, X., and Yi, C. (2016). Epitranscriptome Sequencing Technologies: Decoding RNA Modifications. *Nat. Methods* 14 (1), 23–31. doi:10.1038/nmeth.4110
- Li, Y. C., Wang, Y., Li, D. D., Zhang, Y., Zhao, T. C., and Li, C. F. (2018). Procaine Is a Specific DNA Methylation Inhibitor with Anti-tumor Effect for Human Gastric Cancer. *J. Cel. Biochem.* 119 (2), 2440–2449. doi:10.1002/jcb.26407
- Liang, G., and Weisenberger, D. J. (2017). DNA Methylation Aberrancies as a Guide for Surveillance and Treatment of Human Cancers. *Epigenetics* 12 (6), 416–432. doi:10.1080/15592294.2017.1311434
- Liang, J. Q., Lu, F., Gan, B., Wen, Y. Y., Chen, J., Wang, H. G., et al. (2019). Low-dose Tubacin Promotes BMSCs Proliferation and Morphological Changes Through the ERK Pathway. *Am. J. Transl. Res.* 11 (3), 1446–1459.
- Ling, C., and Rönn, T. (2019). Epigenetics in Human Obesity and Type 2 Diabetes. *Cel. Metab.* 29 (5), 1028–1044. doi:10.1016/j.cmet.2019.03.00929
- Linnekamp, J. F., Butter, R., Spijker, R., Medema, J. P., and van Laarhoven, H. W. M. (2017). Clinical and Biological Effects of Demethylating Agents on Solid Tumours - A Systematic Review. *Cancer Treat. Rev.* 54, 10–23. doi:10.1016/j.ctrv.2017.01.004
- Liu, L., Sun, X., Xie, Y., Zhuang, Y., Yao, R., and Xu, K. (2018). Anti-Proliferative Activity of HPOB Against Multiple Myeloma Cells via P21 Transcriptional Activation. *Molecules* 23 (5), 1044. doi:10.3390/molecules23051044
- Liu, W., Deng, L., Song, Y., and Redell, M. (2014). DOT1L Inhibition Sensitizes MLL-Rearranged AML to Chemotherapy. *PLoS One* 9 (5), e98270. doi:10.1371/journal.pone.0098270
- Liu, X., Chen, X., Yu, X., Tao, Y., Bode, A. M., Dong, Z., et al. (2013). Regulation of MicroRNAs by Epigenetics and Their Interplay Involved in Cancer. *J. Exp. Clin. Cancer Res.* 32, 96. doi:10.1186/1756-9966-32-96
- Loe, A. K. H., Francis, R., Seo, J., Du, L., Wang, Y., Kim, J.-E., et al. (2021). Uncovering the Dosage-dependent Roles of Arid1a in Gastric Tumorigenesis for Combinatorial Drug Therapy. *J. Exp. Med.* 218 (6), e20200219. doi:10.1084/jem.20200219
- Lu, L. J., and Randerath, K. (1980). Mechanism of 5-Azacytidine-Induced Transfer RNA Cytosine-5-Methyltransferase Deficiency. *Cancer Res.* 40 (8 Pt 1), 2701–2705.
- Lu, Y., Chan, Y.-T., Tan, H.-Y., Li, S., Wang, N., and Feng, Y. (2020). Epigenetic Regulation in Human Cancer: The Potential Role of Epi-Drug in Cancer Therapy. *Mol. Cancer* 19 (1), 79. doi:10.1186/s12943-020-01197-3
- Luan, Y., Li, J., Bernatchez, J. A., and Li, R. (2019). Kinase and Histone Deacetylase Hybrid Inhibitors for Cancer Therapy. *J. Med. Chem.* 62 (7), 3171–3183. doi:10.1021/acs.jmedchem.8b00189
- Luparello, C., Mauro, M., Arizza, V., and Vazzana, M. (2020). Histone Deacetylase Inhibitors from Marine Invertebrates. *Biology* 9 (12), 429. doi:10.3390/biology9120429
- Marks, D. L., Olson, R. L., and Fernandez-Zapico, M. E. (2016). Epigenetic Control of the Tumor Microenvironment. *Epigenomics* 8 (12), 1671–1687. doi:10.2217/epi-2016-0110

- Matsubayashi, H., Sato, N., Fukushima, N., Yeo, C. J., Walter, K. M., Brune, K., et al. (2003). Methylation of Cyclin D2 Is Observed Frequently in Pancreatic Cancer But Is Also an Age-Related Phenomenon in Gastrointestinal Tissues. *Clin. Cancer Res.* 9 (4), 1446–1452.
- Miranda Furtado, C. L., Dos Santos Luciano, M. C., Silva Santos, R. D., Furtado, G. P., Moraes, M. O., and Pessoa, C. (2019). Epidrugs: Targeting Epigenetic Marks in Cancer Treatment. *Epigenetics* 14 (12), 1164–1176. doi:10.1080/15592294.2019.1640546
- Modak, R., Basha, J., Bharathy, N., Maity, K., Mizar, P., Bhat, A. V., et al. (2013). Probing P300/CBP Associated Factor (PCAF)-dependent Pathways with a Small Molecule Inhibitor. *ACS Chem. Biol.* 8 (6), 1311–1323. doi:10.1021/cb4000597
- Mohammad, H. P., Barbash, O., and Creasy, C. L. (2019). Targeting Epigenetic Modifications in Cancer Therapy: Erasing the Roadmap to Cancer. *Nat. Med.* 25 (3), 403–418. doi:10.1038/s41591-019-0376-8
- Mohana Kumar, B., Jin, H.-F., Kim, J.-G., Song, H.-J., Hong, Y., Balasubramanian, S., et al. (2006). DNA Methylation Levels in Porcine Fetal Fibroblasts Induced by an Inhibitor of Methylation, 5-azacytidine. *Cell Tissue Res* 325 (3), 445–454. doi:10.1007/s00441-006-0201-9
- Morgen, M., Steimbach, R. R., G  rally, M., Hellweg, L., Sehr, P., Ridinger, J., et al. (2020). Design and Synthesis of Dihydroxamic Acids as HDAC6/8/10 Inhibitors. *ChemMedChem* 15 (13), 1163–1174. doi:10.1002/cmdc.202000149
- Nakamae, S., Toba, Y., Takayama, K., Sakurai, F., and Mizuguchi, H. (2018). Nanaomycin A Treatment Promotes Hepatoblast Differentiation From Human iPS Cells. *Stem Cell Develop.* 27 (6), 405–414. doi:10.1089/scd.2017.0251
- Nebbioso, A., Tambaro, F. P., Dell'Aversana, C., and Altucci, L. (2018). Cancer Epigenetics: Moving Forward. *Plos Genet.* 14 (6), e1007362. doi:10.1371/journal.pgen.1007362
- Nepali, K., and Liou, J.-P. (2021). Recent Developments in Epigenetic Cancer Therapeutics: Clinical Advancement and Emerging Trends. *J. Biomed. Sci.* 28 (1), 27. doi:10.1186/s12929-021-00721-x
- Nephew, K. P., and Huang, T. H.-M. (2003). Epigenetic Gene Silencing in Cancer Initiation and Progression. *Cancer Lett.* 190 (2), 125–133. doi:10.1016/s0304-3835(02)00511-6
- Newbold, A., Matthews, G. M., Bots, M., Cluse, L. A., Clarke, C. J. P., Banks, K.-M., et al. (2013). Molecular and Biologic Analysis of Histone Deacetylase Inhibitors with Diverse Specificities. *Mol. Cancer Ther.* 12 (12), 2709–2721. doi:10.1158/1535-7163.MCT-13-0626
- Nguyen, A. T., and Zhang, Y. (2011). The Diverse Functions of Dot1 and H3K79 Methylation. *Genes Develop.* 25 (13), 1345–1358. doi:10.1101/gad.2057811
- Ning, B., Li, W., Zhao, W., and Wang, R. (2016). Targeting Epigenetic Regulations in Cancer. *Acta Biochim. Biophys. Sin. (Shanghai)* 48 (1), 97–109. doi:10.1093/abbs/gmv116
- Nualkaew, T., Khamphikham, P., Pongpaksupasin, P., Kaewsakulthong, W., Songdej, D., Paiboonsukwong, K., et al. (2020). UNC0638 Induces High Levels of Fetal Hemoglobin Expression in β -thalassemia/HbE Erythroid Progenitor Cells. *Ann. Hematol.* 99 (9), 2027–2036. doi:10.1007/s00277-020-04136-w
- Nunes, S. P., Henrique, R., Jer  nimo, C., and Paramio, J. M. (2020). DNA Methylation as a Therapeutic Target for Bladder Cancer. *Cells* 9 (8), 1850. doi:10.3390/cells9081850
- Ono, H., Basson, M. D., and Ito, H. (2016). P300 Inhibition Enhances Gemcitabine-Induced Apoptosis of Pancreatic Cancer. *Oncotarget* 7 (32), 51301–51310. doi:10.18632/oncotarget.10117
- Orta, M. L., Pastor, N., Burgos-Mor  n, E., Dom  nguez, I., Calder  n-Monta  o, J. M., Huertas Casta  o, C., et al. (2017). Zebularine Induces Replication-dependent Double-Strand Breaks Which Are Preferentially Repaired by Homologous Recombination. *DNA Repair* 57, 116–124. doi:10.1016/j.dnarep.2017.07.002
- Osorio-Montalvo, P., S  nchez-Carbonell, L., and De-la-Pe  a, C. (2018). 5-Azacytidine: A Promoter of Epigenetic Changes in the Quest to Improve Plant Somatic Embryogenesis. *Ijms* 19 (10), 3182. doi:10.3390/ijms19103182
- Oudard, S., Fizazi, K., Sengelov, L., Dugaard, G., Saad, F., Hansen, S., et al. (2017). Cabazitaxel Versus Docetaxel as First-Line Therapy for Patients with Metastatic Castration-Resistant Prostate Cancer: A Randomized Phase III Trial—FIRSTANA. *Jco* 35 (28), 3189–3197. doi:10.1200/JCO.2016.72.1068
- Pan, Y., Liu, G., Zhou, F., Su, B., and Li, Y. (2018). DNA Methylation Profiles in Cancer Diagnosis and Therapeutics. *Clin. Exp. Med.* 18 (1), 1–14. doi:10.1007/s10238-017-0467-0
- Pappano, W. N., Guo, J., He, Y., Ferguson, D., Jagadeeswaran, S., Osterling, D. J., et al. (2015). The Histone Methyltransferase Inhibitor A-366 Uncovers a Role for G9a/GLP in the Epigenetics of Leukemia. *PLoS One* 10 (7), e0131716. doi:10.1371/journal.pone.0131716
- Park, J. W., and Han, J.-W. (2019). Targeting Epigenetics for Cancer Therapy. *Arch. Pharm. Res.* 42 (2), 159–170. doi:10.1007/s12272-019-01126-z
- Phi, L. T. H., Sari, I. N., Yang, Y.-G., Lee, S.-H., Jun, N., Kim, K. S., et al. (2018). Cancer Stem Cells (CSCs) in Drug Resistance and Their Therapeutic Implications in Cancer Treatment. *Stem Cell Int.* 2018, 1–16. doi:10.1155/2018/5416923
- Pirola, L., Ciesielski, O., and Balcerczyk, A. (2018). The Methylation Status of the Epigenome: Its Emerging Role in the Regulation of Tumor Angiogenesis and Tumor Growth, and Potential for Drug Targeting. *Cancers* 10 (8), 268. doi:10.3390/cancers10080268
- Ponnusamy, L., Mahalingaiah, P. K. S., and Singh, K. P. (2020). Epigenetic Reprogramming and Potential Application of Epigenetic-Modifying Drugs in Acquired Chemotherapeutic Resistance. *Adv. Clin. Chem.* 94, 219–259. doi:10.1016/bs.acc.2019.07.011
- Portela, A., and Esteller, M. (2010). Epigenetic Modifications and Human Disease. *Nat. Biotechnol.* 28 (10), 1057–1068. doi:10.1038/nbt.1685
- Prachayasittikul, V., Prathipati, P., Pratiwi, R., Phanus-Umporn, C., Malik, A. A., Schaduagratt, N., et al. (2017). Exploring the Epigenetic Drug Discovery Landscape. *Expert Opin. Drug Discov.* 12 (4), 345–362. doi:10.1080/17460441.2017.1295954
- Prusevich, P., Kalin, J. H., Ming, S. A., Basso, M., Givens, J., Li, X., et al. (2014). A Selective Phenelzine Analogue Inhibitor of Histone Demethylase LSD1. *ACS Chem. Biol.* 9 (6), 1284–1293. doi:10.1021/cb500018s
- Qu, Y., Lennartsson, A., Gaidzik, V. I., Deneberg, S., Karimi, M., Bengt  n, S., et al. (2014). Differential Methylation in CN-AML Preferentially Targets Non-CGI Regions and Is Dictated by DNMT3A Mutational Status and Associated with Predominant Hypomethylation of HOX Genes. *Epigenetics* 9 (8), 1108–1119. doi:10.4161/epi.29315
- Rea, S., Eisenhaber, F., O'Carroll, D., Strahl, B. D., Sun, Z.-W., Schmid, M., et al. (2000). Regulation of Chromatin Structure by Site-specific Histone H3 Methyltransferases. *Nature* 406 (6796), 593–599. doi:10.1038/35020506
- Reddy, K. B. (2015). MicroRNA (miRNA) in Cancer. *Cancer Cel Int* 15, 38. doi:10.1186/s12935-015-0185-1
- Riggs, M. G., Whittaker, R. G., Neumann, J. R., and Ingram, V. M. (1977). n-Butyrate Causes Histone Modification in HeLa and Friend Erythroleukaemia Cells. *Nature* 268 (5619), 462–464. doi:10.1038/268462a0
- Rodenhiser, D., and Mann, M. (2006). Epigenetics and Human Disease: Translating Basic Biology into Clinical Applications. *Can. Med. Assoc. J.* 174 (3), 341–348. doi:10.1503/cmaj.050774
- Rondelet, G., Fleury, L., Faux, C., Masson, V., Dubois, J., Arimondo, P. B., et al. (2017). Inhibition Studies of DNA Methyltransferases by Maleimide Derivatives of RG108 as Non-nucleoside Inhibitors. *Future Med. Chem.* 9 (13), 1465–1481. doi:10.4155/fmc-2017-0074
- Rose, N. R., Ng, S. S., Mecinovi  , J., Li  nard, B. M. R., Bello, S. H., Sun, Z., et al. (2008). Inhibitor Scaffolds for 2-oxoglutarate-dependent Histone Lysine Demethylases. *J. Med. Chem.* 51 (22), 7053–7056. doi:10.1021/jm800936s
- Rotili, D., and Mai, A. (2011). Targeting Histone Demethylases: A New Avenue for the Fight against Cancer. *Genes & Cancer* 2 (6), 663–679. doi:10.1177/1947601911417976
- Sak, A., Bannik, K., Groneberg, M., and Stuschke, M. (2021). Chaetocin Induced Chromatin Condensation: Effect on DNA Repair Signaling and Survival. *Int. J. Radiat. Biol.* 97 (4), 494–506. doi:10.1080/09553002.2021.1872813
- Sanaei, M., and Kavosi, F. (2020). Effect of Zebularine in Comparison to and in Combination with Trichostatin A on CIP/KIP Family (p21Cip1/Waf1/Sdi1, p27Kip1, and p57Kip2), DNMTs (DNMT1, DNMT3a, and DNMT3b), Class I HDACs (HDACs 1, 2, 3) and Class II HDACs (HDACs 4, 5, 6) Gene Expression, Cell Growth Inhibition and Apoptosis Induction in Colon Cancer LS 174T Cell Line. *Asian Pac. J. Cancer Prev.* 21 (7), 2131–2139. doi:10.31557/APJCP.2020.21.7.2131

- Schrock, M. S., Stromberg, B. R., Scarberry, L., and Summers, M. K. (2020). APC/C Ubiquitin Ligase: Functions and Mechanisms in Tumorigenesis. *Semin. Cancer Biol.* 67 (Pt 2), 80–91. doi:10.1016/j.semcancer.2020.03.001
- Seto, E., and Yoshida, M. (2014). Erasers of Histone Acetylation: The Histone Deacetylase Enzymes. *Cold Spring Harbor Perspect. Biol.* 6 (4), a018713. doi:10.1101/cshperspect.a018713
- Sewry, C. A., Laitila, J. M., and Wallgren-Pettersson, C. (2019). Nemaline Myopathies: A Current View. *J. Muscle Res. Cell Motil* 40 (2), 111–126. doi:10.1007/s10974-019-09519-9
- Shan, G., Li, Y., Zhang, J., Li, W., Szulwach, K. E., Duan, R., et al. (2008). A Small Molecule Enhances RNA Interference and Promotes MicroRNA Processing. *Nat. Biotechnol.* 26 (8), 933–940. doi:10.1038/nbt.1481
- Shi, H., Wei, S. H., Leu, Y. W., Rahmatpanah, F., Liu, J. C., Yan, P. S., et al. (2003). Triple Analysis of the Cancer Epigenome: An Integrated Microarray System for Assessing Gene Expression, DNA Methylation, and Histone Acetylation. *Cancer Res.* 63 (9), 2164–2171.
- Shrishrimal, S., Kosmacek, E. A., and Oberley-Deegan, R. E. (2019). Reactive Oxygen Species Drive Epigenetic Changes in Radiation-Induced Fibrosis. *Oxidative Med. Cell Longevity* 2019, 1–27. doi:10.1155/2019/4278658
- Shukla, S., Penta, D., Mondal, P., and Meeran, S. M. (2019). Epigenetics of Breast Cancer: Clinical Status of Epi-Drugs and Phytochemicals. *Adv. Exp. Med. Biol.* 1152, 293–310. doi:10.1007/978-3-030-20301-6_16
- Singh, V., Sharma, P., and Capalash, N. (2013). DNA Methyltransferase-1 Inhibitors as Epigenetic Therapy for Cancer. *Ccdt* 13 (4), 379–399. doi:10.2174/15680096113139990077
- Siu, L. L., Rasco, D. W., Vinay, S. P., Romano, P. M., and Gounder, M. M. J. A. o. O. (2019). 438OMETEOR-1: A Phase I Study of GSK3326595, A First-In-Class Protein Arginine Methyltransferase 5 (PRMT5) Inhibitor. *Ann. Oncol.* 30 (5), v159–v193. doi:10.1093/annonc/mdz244
- Soriano, A. O., Yang, H., Faderl, S., Estrov, Z., Giles, F., Ravandi, F., et al. (2007). Safety and Clinical Activity of the Combination of 5-azacytidine, Valproic Acid, and All-Trans Retinoic Acid in Acute Myeloid Leukemia and Myelodysplastic Syndrome. *Blood* 110 (7), 2302–2308. doi:10.1182/blood-2007-03-078576
- Stimson, L., Rowlands, M. G., Newbatt, Y. M., Smith, N. F., Raynaud, F. I., Rogers, P., et al. (2005). Isothiazolones as Inhibitors of PCAF and P300 Histone Acetyltransferase Activity. *Mol. Cancer Ther.* 4 (10), 1521–1532. doi:10.1158/1535-7163.MCT-05-0135
- Subramaniam, D., Thombre, R., Dhar, A., and Anant, S. (2014). DNA Methyltransferases: A Novel Target for Prevention and Therapy. *Front. Oncol.* 4, 80. doi:10.3389/fonc.2014.00080
- Subramanian, S., Bates, S. E., Wright, J. J., Espinoza-Delgado, I., and Piekarczyk, R. L. (2010). Clinical Toxicities of Histone Deacetylase Inhibitors. *Pharmaceuticals* 3 (9), 2751–2767. doi:10.3390/ph3092751
- Sui, X., Chen, R., Wang, Z., Huang, Z., Kong, N., Zhang, M., et al. (2013). Autophagy and Chemotherapy Resistance: A Promising Therapeutic Target for Cancer Treatment. *Cell Death Dis* 4, e838. doi:10.1038/cddis.2013.350
- Sun, N., Zhang, J., Zhang, C., Zhao, B., and Jiao, A. (2018). DNMTs Inhibitor SGI-1027 I-nduces A-poptosis in Huh7 H-uman H-epatocellular C-arcinoma C-ells. *Oncol. Lett.* 16 (5), 5799–5806. doi:10.3892/ol.2018.9390
- Sun, Y., Jiang, X., Chen, S., and Price, B. D. (2006). Inhibition of Histone Acetyltransferase Activity by Anacardic Acid Sensitizes Tumor Cells to Ionizing Radiation. *FEBS Lett.* 580 (18), 4353–4356. doi:10.1016/j.febslet.2006.06.092
- Suzuki, T., Ota, Y., Ri, M., Bando, M., Gotoh, A., Itoh, Y., et al. (2012). Rapid Discovery of Highly Potent and Selective Inhibitors of Histone Deacetylase 8 Using Click Chemistry to Generate Candidate Libraries. *J. Med. Chem.* 55 (22), 9562–9575. doi:10.1021/jm300837y
- Swierczynski, S., Klier, E., Illig, R., Alinger-Scharinger, B., Kiesslich, T., and Neureiter, D. (2015). Histone Deacetylation Meets miRNA: Epigenetics and Post-transcriptional Regulation in Cancer and Chronic Diseases. *Expert Opin. Biol. Ther.* 15 (5), 651–664. doi:10.1517/14712598.2015.1025047
- Tang, S., Cheng, B., Zhe, N., Ma, D., Xu, J., Li, X., et al. (2018). Histone Deacetylase Inhibitor BG45-Mediated HO-1 Expression Induces Apoptosis of Multiple Myeloma Cells by the JAK2/STAT3 Pathway. *Anticancer Drugs* 29 (1), 61–74. doi:10.1097/CAD.0000000000000568
- Th'ng, J. P. H., Sung, R., Ye, M., and Hendzel, M. J. (2005). H1 Family Histones in the Nucleus. *J. Biol. Chem.* 280 (30), 27809–27814. doi:10.1074/jbc.M501627200
- Thinness, C. C., England, K. S., Kawamura, A., Chowdhury, R., Schofield, C. J., and Hopkinson, R. J. (2014). Targeting Histone Lysine Demethylases - Progress, Challenges, and the Future. *Biochim. Biophys. Acta (Bba) - Gene Regul. Mech.* 1839 (12), 1416–1432. doi:10.1016/j.bbaggm.2014.05.009
- Thompson, P. R., and Fast, W. (2006). Histone Citrullination by Protein Arginine Deiminase: Is Arginine Methylation a Green Light or a Roadblock?. *ACS Chem. Biol.* 1 (7), 433–441. doi:10.1021/cb6002306
- Torrano, J., Al Emran, A., Hammerlindl, H., and Schaidler, H. (2019). Emerging Roles of H3K9me3, SETDB1 and SETDB2 in Therapy-Induced Cellular Reprogramming. *Clin. Epigenet* 11 (1), 43. doi:10.1186/s13148-019-0644-y
- Valdez, B. C., Li, Y., Murray, D., Corn, P., Champlin, R. E., and Andersson, B. S. (2010). 5-Aza-2'-deoxycytidine Sensitizes Busulfan-Resistant Myeloid Leukemia Cells by Regulating Expression of Genes Involved in Cell Cycle Checkpoint and Apoptosis. *Leuk. Res.* 34 (3), 364–372. doi:10.1016/j.leukres.2009.08.014
- Valeri, N., Vannini, I., Fanini, F., Calore, F., Adair, B., and Fabbri, M. (2009). Epigenetics, miRNAs, and Human Cancer: A New Chapter in Human Gene Regulation. *Mamm. Genome* 20 (9-10), 573–580. doi:10.1007/s00335-009-9206-5
- Velagapudi, S. P., Gallo, S. M., and Disney, M. D. (2014). Sequence-based Design of Bioactive Small Molecules That Target Precursor MicroRNAs. *Nat. Chem. Biol.* 10 (4), 291–297. doi:10.1038/nchembio.1452
- Verma, M. (2015). The Role of Epigenomics in the Study of Cancer Biomarkers and in the Development of Diagnostic Tools. *Adv. Exp. Med. Biol.* 867, 59–80. doi:10.1007/978-94-017-7215-0_5
- Wang, T., Fahrman, J. F., Lee, H., Li, Y.-J., Tripathi, S. C., Yue, C., et al. (2018). JAK/STAT3-Regulated Fatty Acid β -Oxidation Is Critical for Breast Cancer Stem Cell Self-Renewal and Chemoresistance. *Cel Metab.* 27 (1), 136–150. doi:10.1016/j.cmet.2017.11.001
- Wang, Z., Zang, C., Cui, K., Schones, D. E., Barski, A., Peng, W., et al. (2009). Genome-wide Mapping of HATs and HDACs Reveals Distinct Functions in Active and Inactive Genes. *Cell* 138 (5), 1019–1031. doi:10.1016/j.cell.2009.06.049
- West, A. C., and Johnstone, R. W. (2014). New and Emerging HDAC Inhibitors for Cancer Treatment. *J. Clin. Invest.* 124 (1), 30–39. doi:10.1172/JCI69738
- Willmann, D., Lim, S., Wetzel, S., Metzger, E., Jandausch, A., Wilk, W., et al. (2012). Impairment of Prostate Cancer Cell Growth by a Selective and Reversible Lysine-specific Demethylase 1 Inhibitor. *Int. J. Cancer* 131 (11), 2704–2709. doi:10.1002/ijc.27555
- Wu, H., Chen, Y., Zhu, H., Zhao, M., and Lu, Q. (2019). The Pathogenic Role of Dysregulated Epigenetic Modifications in Autoimmune Diseases. *Front. Immunol.* 10, 2305. doi:10.3389/fimmu.2019.02305
- Wysocki, J., Allis, C. D., and Coonrod, S. (2006). Histone Arginine Methylation and its Dynamic Regulation. *Front. Biosci.* 11, 344–355. doi:10.2741/1802
- Xu, X., Su, S., Barnes, V. A., De Miguel, C., Pollock, J., Ownby, D., et al. (2013). A Genome-wide Methylation Study on Obesity. *Epigenetics* 8 (5), 522–533. doi:10.4161/epi.24506
- Yamagishi, M., Hori, M., Fujikawa, D., Ohsugi, T., Honma, D., Adachi, N., et al. (2019). Targeting Excessive EZH1 and EZH2 Activities for Abnormal Histone Methylation and Transcription Network in Malignant Lymphomas. *Cel Rep.* 29 (8), 2321–2337. doi:10.1016/j.celrep.2019.10.083
- Yang, Y., Li, Y., Gu, H., Dong, M., and Cai, Z. (2020). Emerging Agents and Regimens for Multiple Myeloma. *J. Hematol. Oncol.* 13 (1), 150. doi:10.1186/s13045-020-00980-5
- Yao, Q., Chen, Y., and Zhou, X. (2019). The Roles of microRNAs in Epigenetic Regulation. *Curr. Opin. Chem. Biol.* 51, 11–17. doi:10.1016/j.cbpa.2019.01.024
- Yen, C.-Y., Huang, H.-W., Shu, C.-W., Hou, M.-F., Yuan, S.-S. F., Wang, H.-R., et al. (2016). DNA Methylation, Histone Acetylation and Methylation of Epigenetic Modifications as a Therapeutic Approach for Cancers. *Cancer Lett.* 373 (2), 185–192. doi:10.1016/j.canlet.2016.01.036
- Yuan, Y., Tang, A. J., Castoreno, A. B., Kuo, S.-Y., Wang, Q., Kuballa, P., et al. (2013). Gossypol and an HMT G9a Inhibitor Act in Synergy to Induce Cell Death in Pancreatic Cancer Cells. *Cell Death Dis* 4, e690. doi:10.1038/cddis.2013.191
- Zhang, S., Chen, L., Jung, E. J., and Calin, G. A. (2010). Targeting MicroRNAs with Small Molecules: From Dream to Reality. *Clin. Pharmacol. Ther.* 87 (6), 754–758. doi:10.1038/clpt.2010.46
- Zhang, W., and Xu, J. (2017). DNA Methyltransferases and Their Roles in Tumorigenesis. *Biomark Res.* 5, 1. doi:10.1186/s40364-017-0081-z

- Zhao, R., Choi, B. Y., Lee, M.-H., Bode, A. M., and Dong, Z. (2016). Implications of Genetic and Epigenetic Alterations of CDKN2A (P16 INK4a) in Cancer. *EBioMedicine* 8, 30–39. doi:10.1016/j.ebiom.2016.04.017
- Zhou, L., Mudianto, T., Ma, X., Riley, R., and Uppaluri, R. (2020). Targeting EZH2 Enhances Antigen Presentation, Antitumor Immunity, and Circumvents Anti-PD-1 Resistance in Head and Neck Cancer. *Clin. Cancer Res.* 26 (1), 290–300. doi:10.1158/1078-0432.CCR-19-1351
- Zhou, Z., Li, H.-Q., and Liu, F. (2019). DNA Methyltransferase Inhibitors and Their Therapeutic Potential. *Ctmc* 18 (28), 2448–2457. doi:10.2174/1568026619666181120150122
- Zhu, H., and Wang, C. (2021). HDAC2 -mediated Proliferation of Trophoblast Cells Requires the miR-183/FOXA1/IL-8 Signaling Pathway. *J. Cel Physiol* 236 (4), 2544–2558. doi:10.1002/jcp.30026
- Zhu, Q., Huang, Y., Marton, L. J., Woster, P. M., Davidson, N. E., and Casero, R. A., Jr. (2012). Polyamine Analogs Modulate Gene Expression by Inhibiting Lysine-specific Demethylase 1 (LSD1) and Altering Chromatin Structure in Human Breast Cancer Cells. *Amino Acids* 42 (2-3), 887–898. doi:10.1007/s00726-011-1004-1

Conflict of Interest: The authors declare that the research was conducted in the absence of any commercial or financial relationships that could be construed as a potential conflict of interest.

Publisher's Note: All claims expressed in this article are solely those of the authors and do not necessarily represent those of their affiliated organizations, or those of the publisher, the editors and the reviewers. Any product that may be evaluated in this article, or claim that may be made by its manufacturer, is not guaranteed or endorsed by the publisher.

Copyright © 2021 Xiao, Zhou, Wen, Wang, Liu, Wang, Shi, Hu and Hou. This is an open-access article distributed under the terms of the Creative Commons Attribution License (CC BY). The use, distribution or reproduction in other forums is permitted, provided the original author(s) and the copyright owner(s) are credited and that the original publication in this journal is cited, in accordance with accepted academic practice. No use, distribution or reproduction is permitted which does not comply with these terms.



OPEN ACCESS

Edited by:

Jianxun Ding,
Changchun Institute of Applied
Chemistry (CAS), China

Reviewed by:

Tongkai Chen,
Guangzhou University of Chinese
Medicine, China
Xianglong Hu,
South China Normal University, China
Yi Cao,
Xiangtan University, China
Kunyi Yu,
The Affiliated Hospital of Southern
Medical University, China
Zhigang He,
Zhejiang University, China

*Correspondence:

Xifeng Liu
xifengliu@126.com
Shijun Zhang
zhshjun@mail.sysu.edu.cn
Ling Yu
994242527@qq.com

[†]These authors have contributed
equally to this work

Specialty section:

This article was submitted to
Pharmacology of Anti-Cancer Drugs,
a section of the journal
Frontiers in Pharmacology

Received: 11 August 2021

Accepted: 09 September 2021

Published: 20 October 2021

Citation:

Wang Y, Li P, Mao S, Mo Z, Cao Z,
Luo J, Zhou M, Liu X, Zhang S and Yu L
(2021) Exosome CTLA-4 Regulates
PTEN/CD44 Signal Pathway in Spleen
Deficiency Internal Environment to
Promote Invasion and Metastasis of
Hepatocellular Carcinoma.
Front. Pharmacol. 12:757194.
doi: 10.3389/fphar.2021.757194

Exosome CTLA-4 Regulates PTEN/CD44 Signal Pathway in Spleen Deficiency Internal Environment to Promote Invasion and Metastasis of Hepatocellular Carcinoma

Yongdan Wang^{1†}, Pan Li^{1†}, Shuai Mao^{2,3†}, Zhuomao Mo¹, Zhirui Cao¹, Jin Luo¹,
Meiling Zhou¹, Xifeng Liu^{4*}, Shijun Zhang^{1*} and Ling Yu^{2,3*}

¹Department of Traditional Chinese Medicine, The First Affiliated Hospital, Sun Yat-sen University, Guangzhou, China, ²Second Clinical College, Guangzhou University of Chinese Medicine, Guangzhou, China, ³AMI Key Laboratory of Chinese Medicine in Guangzhou, Guangdong Provincial Hospital of Chinese Medicine, Guangzhou, China, ⁴School of Life Sciences, Xiangya Medical College, Central South University, Changsha, China

Hepatocellular carcinoma (HCC) is one of the most common primary cancers, and its pathogenesis is complicated and difficult to screen. Currently, there is no effective treatment. In traditional Chinese medicine, a large proportion of patients with HCC have been diagnosed with spleen deficiency (SD) syndrome and treated with tonifying traditional Chinese medicine, which has significant clinical efficacy. However, the role and molecular mechanism of SD in HCC remain unclear. In this study, 40 mice were randomly divided into four groups: control, SD, HCC, and SD-HCC groups. The liver cancer model of SD was established by reserpine induction and orthotopic transplantation. The effects of SD on the proliferation, apoptosis, invasion, and metastasis of HCC cells were studied by cell proliferation, cell apoptosis, cell scratch, and transwell assay. We found that compared with the HCC group, the protein expressions of cytotoxic T lymphocyte antigen 4 (CTLA-4), programmed cell death protein 1 (PD-1), phosphatase and tensin homolog (PTEN), and AKT (also known as protein kinase B or PKB) in the exosomes of the SD-HCC group were upregulated. In addition, the metastases and self-renewal of exosomes in the SD-HCC group were more aggressive than those in the HCC group, which could be partially reversed with the addition of CTLA-4 inhibitors. Further studies showed that in the internal environment of SD, CTLA-4 promoted tumor invasion and metastasis by regulating the PTEN/CD44 pathway. In conclusion, our findings suggest that during SD in the internal environment, exosome CTLA-4 regulates the PTEN/CD44 signal pathway to promote the proliferation, self-renewal, and metastasis of liver cancer.

Keywords: hepatocellular carcinoma, spleen deficiency, exosome, CTLA-4, PTEN

INTRODUCTION

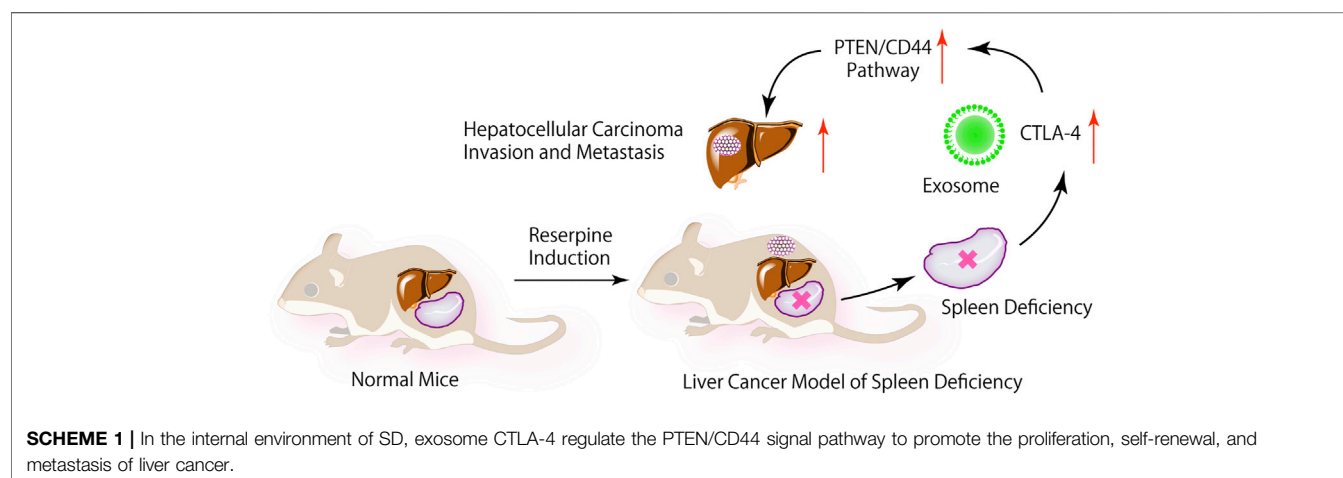
Hepatocellular carcinoma (HCC) is a highly prevalent and lethal cancer, ranking the fifth most commonly diagnosed cancer and the third leading cause of cancer-associated deaths worldwide (Chen et al., 2016). The incidence of HCC has increased significantly recently, with about 840,000 new cases each year (Bray et al., 2018). It has been reported that the incidence and mortality of HCC in China account for 50% of HCC in the world (Feng et al., 2019). Hepatitis B virus (HBV) infection is the main cause of HCC in East Asia, especially in China (Bray et al., 2018). The rapid development and high recurrence are major challenges in the treatment of HCC due to its highly metastatic nature (Gish et al., 2007; Hu et al., 2020). Therefore, it is urgent to seek valuable biomarkers and potential therapeutic targets to improve the clinical curative effect on HCC patients.

The imbalance of the internal environment is closely related to the occurrence and development of tumors (Craig et al., 2020; Llovet et al., 2021). Generally, only about 5% of tumors could be explained by genetic factors alone, whereas most tumors are the result of a combination of environmental and genetic factors (Bhattacharjee et al., 2013). In the TCM (traditional Chinese medicine) therapy systems, “Bian Zheng Lun Zhi” is the core, that is, a treatment based on syndrome differentiation, which prioritizes to adjust the internal environment (Zhang et al., 2020). TCM syndromes are the characteristics of all syndromes in a patient’s clinical manifestations essentially and help guide the design of individualized treatments (Ji et al., 2016). In TCM theory, symptoms such as loose stools, abdominal distension after meals, loss of appetite, sallow complexion, weight loss, general weakness, and/or low disease resistance could be summarized as spleen deficiency (SD) (Luo et al., 2017). Interestingly, the majority of patients with cancer cachexia have been diagnosed with SD in China (Sun et al., 2016a; Zhang et al., 2020). According to the literature, SD may lead to dysfunction in T cell recognition by disordering the expression of TCRV β in rats (Chen et al., 2014). In addition, another study reported that immunoregulatory traditional Chinese medicine is beneficial to liver cancer and induces cell

apoptosis through the Caspase-3/PARP signaling pathway (Yu et al., 2021). The above studies suggest the importance of the internal environment of SD in the occurrence and development of immune recognition disorders of HCC.

The barrier to successful cancer immunotherapy is the capability of tumors to escape from the host’s immune system (Whiteside et al., 2011). Exosomes, small membranous sacs of endocytic origin (30–150 nm), are considered as intercellular messengers that can carry a large number of macromolecular cargos, including proteins, mRNA, lipids, and miRNA (Wen et al., 2016; Bach et al., 2017; Ruivo et al., 2017; Su et al., 2021). Studies have found that exosomes derived from tumors carry immunosuppressive proteins, including PD-1, CTLA-4, FasL, TRAIL, CD39, and CD73, which induce apoptosis and depletion of T lymphocytes to achieve tumor immune escape (Whiteside, 2013; Ukrainskaya et al., 2019; Benecke et al., 2021). Cytotoxic T lymphocyte antigen 4 (CTLA-4), a member of the immune protein superfamily, competes with the T cell co-stimulator CD28 for binding to CD80 and CD86 with a higher affinity to antigen-presenting cells during the priming phase in the lymph nodes and conveys inhibitory signals within the T cells (Van Coillie et al., 2020; Goenka et al., 2021). Clinical evidence has shown that anti-CTLA-4 therapy can enhance the activation of effector T cells (Maker et al., 2005), increase the ratio of effector T cells to Treg (Quezada et al., 2006; Curran et al., 2010; Ou et al., 2018), and promote the transport of activated T cells to tumor tissues (Quezada et al., 2006). Our previous study found that traditional Chinese medicine could improve the tumor microenvironment of patients to treat liver cancer and speculated that the immune checkpoints CTLA-4, LAG-3, and BIRC5 are the key targets for activating immune cells to treat liver cancer (Mo et al., 2020). However, only a minority of people can respond to immunotherapy (Mahoney et al., 2015). Consequently, it is still a critical challenge to explore the molecular mechanisms of immunotherapy for HCC.

PTEN is known as a tumor suppressor protein in most tumors, which is located in Chromosome 10 (Su et al., 2016; Luongo et al., 2019). The loss of PTEN function due to epigenetic silencing or genetic aberration has been associated with malignant



transformation, progression, chemotherapy response, and survival of a variety of cancers (Wang et al., 2018a; Raffone et al., 2019). PTEN regulates PI3K/Akt/mTOR by its phosphatase activity, which is one of the most important signaling pathways for cell growth and survival in cancer (Su et al., 2016; Lee et al., 2018; Luongo et al., 2019). It has been reported that CD44 is one of the biomarkers and a key regulator of cancer stem cells (CSCs), including self-renewal, tumor initiation, and metastasis (Wang et al., 2018b). PTEN plays a critical role in the immobility and regulation of the cell cycle entry of transforming stem cells (SCs), and the loss of PTEN tends to promote cancerous phenotypes (Luongo et al., 2019). It has been found that miR-21, a gene known to target PTEN, significantly regulates the growth and/or differentiation of CSCs in colon cancer (Yu et al., 2015). The imbalance of the PTEN/CD44 signaling pathway plays a vital role in maintaining the characteristics of CSC (Luongo et al., 2019; Cetintas and Batada, 2020). Nevertheless, the link between CTLA-4 and PTEN/CD44 signaling pathway has not been reported.

Based on the above studies, we proposed the hypothesis that the change of CTLA-4 expression in exosomes of SD internal environment is related to the PTEN/CD44 signaling pathway, as demonstrated in **Scheme 1**. Exosome CTLA-4 is an important factor in HCC. Therefore, we aimed to explore the underlying mechanism of exosome CTLA-4 in HCC progression. We have tried our best to seek a new therapeutic target for patients with liver cancer.

MATERIALS AND METHODS

Chemicals and Materials

Reserpine powder (R817202), purity greater than 98.0%, was purchased from Jiusuo Technology Co. Ltd. (Guangzhou, China). Glacial acetic acid (B018) was purchased from Feng Wei Technology Co. Ltd. (Guangzhou, China). The preparation process of the reserpine solution is as follows: 10 mg of reserpine powder was added with 10 ml acetic acid to obtain 1 mg/ml reserpine solution A and stored at 4°C. Before each experiment, 0.1 ml reserpine solution A and 9.9 ml sodium chloride as injection were added to obtain 0.01 mg/ml reserpine solution B. In addition to special labeling, other chemicals were purchased from UZhiYi Biotechnology Co. Ltd. (Guangzhou, China).

Cell Line and Cell Culture

Mouse HCC cell line hep1-6 was obtained from the Institute of Biochemistry and Cell Biology (Shanghai, China). The cell line was cultured in RPMI-1640 medium (Hy Clone, Los Angeles, CA, United States), which contained 10% fetal bovine serum (FBS) and 5% carbon dioxide. The ambient temperature was controlled at about 37°C. HCC cell lines were identified by microsatellite analysis, in which the cells were cultured for no more than 2 months.

Animals and Groups

Forty male SPF C57BL/6 mice (4 weeks old, 18–20 g) and three male SPF BALB/C-Nu (4 weeks old, 16–18 g) were purchased

from GemPharmatech Co. Ltd. (Jiangsu, China). Laboratory animal quality certificate no: SCXK(SU)2018-0008. The animals were kept in a specific pathogen-free environment with a temperature of 25°C, relative humidity of 60–80%, free eating, and drinking water. All experiments were conducted in the SPF laboratory of the animal center of the first affiliated hospital, Sun Yat-Sen University (Guangzhou, China). The license number was SYXK (Guangdong) 2020-0108. Experimental animals were used in accordance with the 3R principle for humane care. The animal experiments were approved by the clinical research and animals ethics committee of the first affiliated hospital, Sun Yat-Sen University. In the SPF barrier environment, 40 C57BL/6 male mice were randomly divided into the normal group, SD group, liver cancer group, and SD liver cancer group. There were 10 mice in each group and 40 mice were labeled.

The Establishment of Spleen Deficiency Model

A mouse model of SD was established by reserpine. Mice in the SD group and SD liver cancer group were subcutaneously injected with reserpine solution B, one time per day at a dose of 0.1 ml/10 g. At the same time, the normal and liver cancer groups were subcutaneously injected with sodium chloride once per day at the same dose of 0.1 ml/10 g for 14 consecutive days. The weight of all the mice was measured daily, and the amount of food they ate in each cage was recorded. At the same time, the odor, mental state, body cold and heat, respiratory status, hair color, food intake, and stool of all mice in the four groups were observed. At the end of the 14th day, the severity of SD in mice was evaluated by using the SD rating scale (**Table 1**).

The mice were forced to swim, and the time from the beginning of swimming to the first stop swimming was recorded, which is helpful to judge the effect of the SD model in mice. In this case, a water tank with a smooth sidewall and a suitable size was prepared with water temperature kept at 25°C. First, the mice were put into a water tank for 30 s, and then the mice were acclimated to the water tank environment. The mice that could not swim or could not swim very well were excluded, and the order of the mice that were put into the water tank was recorded. After the mice returned to their normal state, they were placed in the tank again in the same order as before, and the total duration of swimming–struggling–floating immobility was recorded and a statistical analysis of the results performed.

BALB/C-Nu Mice Tumorigenesis Experiment

When C57BL/6 mice were induced with SD for 1 week, precultured hep1-6 cell suspension (1×10^7 /ml) was subcutaneously injected into the armpit of BALB/C nude mice at 0.1 ml. Each mouse was inoculated with 1×10^6 cells. The mental status and tumorigenesis of the nude mice were observed every day. When the diameter of the subcutaneous tumor was

TABLE 1 | Spleen deficiency rating scale.

Item	One point	Two-point	Three-point	Four-point
Odor	No unusual	Faint odor	Serious odor	Extremely odor
Mental state	Normal	Tiredness	Drowsy	Irritability
Body cold and heat	Normal	Crouch	Serious cold	Extremely cold
Respiratory status	Normal	Pant	Shortness of breath	Faint breath
Hair color	Normal	No bright	Shaggy hair	Rarer and yellow
Stool	Normal	Slight wettability	Serious wettability	Extreme wettability
Food intake	Normal	Reduce food intake by 50%	Reduce food intake by 75%	Barely food intake

The calculated sum of the scores of each item (total score ≤ 6 , no SD; $7 \leq$ total scores ≤ 12 , mild SD; $13 \leq$ total scores ≤ 18 , typical SD; $19 \leq$ total scores ≤ 24 , severe SD).

about 1 cm at 2 weeks, the tumor could be used to establish the liver cancer model.

Establishment of Liver Cancer Model

One week after the SD model was established, the orthotopic liver cancer models were established in the liver cancer group and the spleen liver cancer group. Mice were anesthetized with 1% pentobarbital sodium solution (50 mg/kg). At the same time, the BALB/C nude mice were killed by cervical dislocation, the tumor was quickly removed under aseptic conditions, the necrotic tissue was removed, and the flesh-like tissue was cut into 1-mm³-sized pieces in PBS solution. The skin was incised at the xiphoid process and the left lobe of the liver pulled out of the abdominal cavity. The 1-mm³-sized tumor tissue was placed in the cannula (5 mm from the tip of the cannula), and the cannula was inserted into the liver surface at an angle of 10 degrees, then the tumor tissue was implanted under the liver capsule. Absorbable gelatin sponge was applied to the bleeding area, and the liver lobe was sent back to the abdominal cavity. Penicillin solution was used to flush the abdominal cavity, and absorbable suture was used to close the abdominal cavity. The mice were closely monitored for survival and weighed daily. After the liver cancer model was established for 28 days, blood and tissue samples were collected.

Extraction of Exosomes

The serum exosomes of mice were extracted by ultracentrifugation. The blood (500 μ L) was collected in a centrifuge tube, then centrifuged at 4°C for 5 min at 3,000 r/min after the blood had coagulated. The supernatant serum was transferred to a new centrifuge tube and centrifuged at 4°C for 10 min at 300 $\times g$. The supernatant was centrifuged at 4°C for 10 min at 2000 $\times g$, then the precipitates were discarded, and the supernatant was further centrifuged for 70 min at 10000 $\times g$. After this step, the supernatant was transferred to a new high speed centrifuge tube, centrifuged at 4°C for 70 min at 100,000 $\times g$. The supernatant was discarded and added with the appropriate amount of PBS buffer to make the exosomes suspended in the PBS buffer. The suspension was centrifuged at 4°C for 70 min at 100,000 $\times g$, and the supernatant was discarded. The bottom precipitated exosomes were suspended in 200 μ L of 4°C precooled PBS buffer and kept at -80°C for future usage.

MTT Assay

HepG2 cells were digested with 0.25% trypsin at the logarithmic growth stage, digestion was stopped with serum-containing

medium, and these were then beaten into a single-cell suspension, stained using trypan blue stain, and counted. The cells were inoculated into a 96-well plate, and another blank control well was set up, which was only adding a complete culture medium, and cultured in the incubator (37°C, 5% CO₂, saturation humidity) for 24 h. The cells were cultured to form a monolayer covering the bottom of the well. The culture solution was then removed and added with 10 μ L PBS (control group), serum exosomes of liver cancer, serum exosome of liver cancer with SD, and serum exosome of liver cancer with SD that combined with 50 ng/ml CTLA-4, 100 ng/ml CTLA-4, or 200 ng/ml CTLA-4 inhibitor. After culturing at 37°C for 72 h, 50 μ L (1 mg/ml) of MTT was added and cocultured for 4 h, then the supernatant was discarded and replaced with 150 μ L DMSO solution. The plate was placed in the microwell plate oscillator to oscillate for 15 min, and the blue-purple crystal dissolved completely. The OD values of each well were measured at 570 nm wavelength by enzyme-linked immunosorbent assay. Each group was tested with 12 repeating wells.

Apoptosis Assay

Apoptosis of HepG2 cells was detected by Annexin V-FITC/PI double-labeled flow detector. The cells were cultured in a DMEM medium containing 10% fetal bovine serum (FBS) at 37°C, 5% CO₂, and saturated humidity for the logarithmic phase. The cell concentration was adjusted to 1×10^4 /ml. The cells were inoculated into a six-well cell plate with each well about 2 ml. Then, added with 10 μ L PBS (control group), serum exosomes of liver cancer, serum exosome of liver cancer with SD, and serum exosome of liver cancer with SD that combined with 200 ng/ml CTLA-4 inhibitor. According to the instructions of the Annexin V-FITC/PI double staining kit, the cells were collected 24 h later, digested by trypsin, then centrifuged to collect the cells. After resuspending the cells with 1 ml precooled PBS, 100 μ L of cell suspension solution was transferred to a 5-ml culture tube and added with 5 μ L Annexin V-FITC and 5 μ L PI. After incubation at room temperature for 15 min in the dark, the cells were added with 400 μ L of combined buffer and analyzed by flow cytometry.

Cell Migration Assay

HepG2 cells (HepG2, HepG2 + HCC exosome, HepG2 + SD-HCC exosome, HepG2 + SD-HCC exosome + CTLA-4 inhibitor) were selected in the logarithmic phase. The cells were digested with trypsin, centrifuged, and washed twice with PBS. The concentration of cells was adjusted to 2×10^5 /ml in a serum-

free medium. The transwell chamber was placed in a 24-well plate, 100 μ L cell suspension was added in the transwell chamber, then along with 5 μ L PBS (control group), serum exosomes of liver cancer, serum exosome of liver cancer with SD, and serum exosome of liver cancer with SD that combined with 200 ng/ml CTLA-4 inhibitor were added. 600 μ L medium containing 10% FBS was added in the lower chamber and incubated for 24 h at 37°C in 5% CO₂. After removing the transwell chamber and discarding the culture fluid from the well, it was rinsed with PBS and 4% paraformaldehyde for 30 min. The chamber was dried properly and dyed with crystal violet for 30 min, using a cotton swab to gently remove the non-penetrating cells from the surface of the membrane, and washed twice with PBS. Under the microscope, five high-power ($\times 400$) views were randomly selected to observe the cells in each group. The number of transmembrane cells was used to express the ability of locomotion. Cells of each group were set into three double wells.

Cell Invasion Assay

A serum-free medium containing fibronectin was added to the lower chamber of the transwell cell membrane. At 4°C, Matrigel was melted overnight, diluted in the serum-free medium, and applied to the upper surface of the transwell chamber at an amount of 100 μ L Matrigel (1 mg/ml) per well. This was set in a 37°C incubator for 30 min. The other experimental steps and cell processing methods were the same as the Cell Migration Assay. The invasive ability was expressed by the number of transmembrane cells. The experiment was repeated three times.

Wound-Healing Assays

Lines were drawn across the back of the six-well plate, and 5×10^5 cells were inoculated into each well. The cell processing methods are the same as the Apoptosis Assay. On the next day, the back of the six-well plate was scratched using the tip of a pipette. The wells were then washed three times with sterile PBS to remove the cells below the underline to ensure that the remaining space was clearly visible. Then, the serum-free medium was replaced, and the cells were cultured in a 5% CO₂ incubator at 37°C. At 0, 24 h, and 48 h, the wounds were observed and photographed under a microscope. The width of the wounds at each time was recorded.

H&E Staining of Tissue Sections

The liver tissues of the normal group, SD group, liver cancer group, and SD liver cancer group were selected. After the tissue was fixed with 10% formaldehyde, it was put into alcohol ranging from low-concentration alcohol to high-concentration alcohol for dehydration treatment. The tissue block was immersed in xylene for transparency and then embedded in paraffin. The paraffin wax was removed with xylene before staining. Then the slides were washed through the high concentration to low concentration of alcohol, and finally immersed into distilled water. The slices were dyed in hematoxylin solution for 5 min, flushed with water for 1 hour, then dehydrated with 70 and 90% alcohol for 10 min and stained by eosin for 2 minutes. After staining, the slides were dehydrated with alcohol from low concentration to high concentration and then made transparent by using xylene. Finally, the slices are sealed,

labeled, and set aside. The histomorphological structure was observed under the microscope.

Immunohistochemical Assay

The tissue was fixed using 10% formaldehyde, dehydrated from low concentration alcohol to high concentration alcohol, made transparent using xylene, embedded in paraffin, and sectioned. The tissue slices were placed in the oven at 60°C for 30 min, and then were taken out, cooled, dewaxed, and hydrated with high concentration alcohol to low concentration alcohol, which were then was incubated with 3% hydrogen peroxide at room temperature for 5–10 min. The slices were repaired by microwave in 0.01 mol/L citric acid buffer (pH = 6.0) for 30 min and sealed with 5% normal sheep serum for 30 min at room temperature. The sheep serum was removed from the section and added to the diluted primary antibody (1:250). Then, this was incubated overnight at 4°C. The diluted secondary antibody was added and incubated at 37°C for 30 min. This was then rinsed with PBS for 2 min (three times). A moderate amount of *Streptomyces* antibiotic protein peroxidase was added and was then incubated at 37°C for 30 min and rinsed with PBS for 3 min (two times). These were then stained with DAB color for 5 min and rinsed thoroughly with distilled water. Restaining, dehydration, transparency, and sealing were performed. Five high-power microscopic views were randomly selected from each section to observe the staining of the cells.

Western Blotting Assay

Firstly, liver tissue of the normal group and SD group, and liver cancer tissue of the liver cancer group and SD liver cancer group were extracted. The tissues were split with RIPA for 30 min, and then the split solution was transferred to a centrifuge tube and centrifuged for 10 min at 4°C, 12,000 rpm. The supernatant (protein sample) was packed in a 0.5-ml centrifuge tube and stored at –20°C. The concentration of protein was determined by the BCA (bicinchoninic acid) method.

After the addition of 20 g of the sample, the protein was separated by 10% SDS-PAGE and transferred to the PVDF membrane by the wet transfer membrane. When the membrane transfer is completed, the membrane is cut into different bands according to the target protein molecule of the target protein. Sealing fluid containing 5% skimmed milk powder was used to seal this for 2 h at room temperature. The diluted (1:1000) primary antibody (CTLA-4, CD80, CD86, PD-1, PD-L1, PTEN, CD44, and β -Actin) was added and rested at 4°C overnight. It was then rinsed with TBST three times (10 min/time). An HRP-labeled anti-rabbit or anti-rat IgG was used as the secondary antibody (1:10000) and incubated at room temperature for 1 hour. This was rinsed again with TBST for three times (10 min/time). Finally, chemiluminescence detection (light-proof operation) was performed, and β -actin was used as the internal control. The ratio of various proteins to β -actin indicates the relative expression level of each protein.

Real-Time Quantitative PCR Analysis

For liver tissue of the normal group and SD group, liver cancer tissue of liver cancer group and SD liver cancer group, the total RNA was extracted according to the instructions of the TRIzol RNA extraction kit. RNA concentrations were measured using an

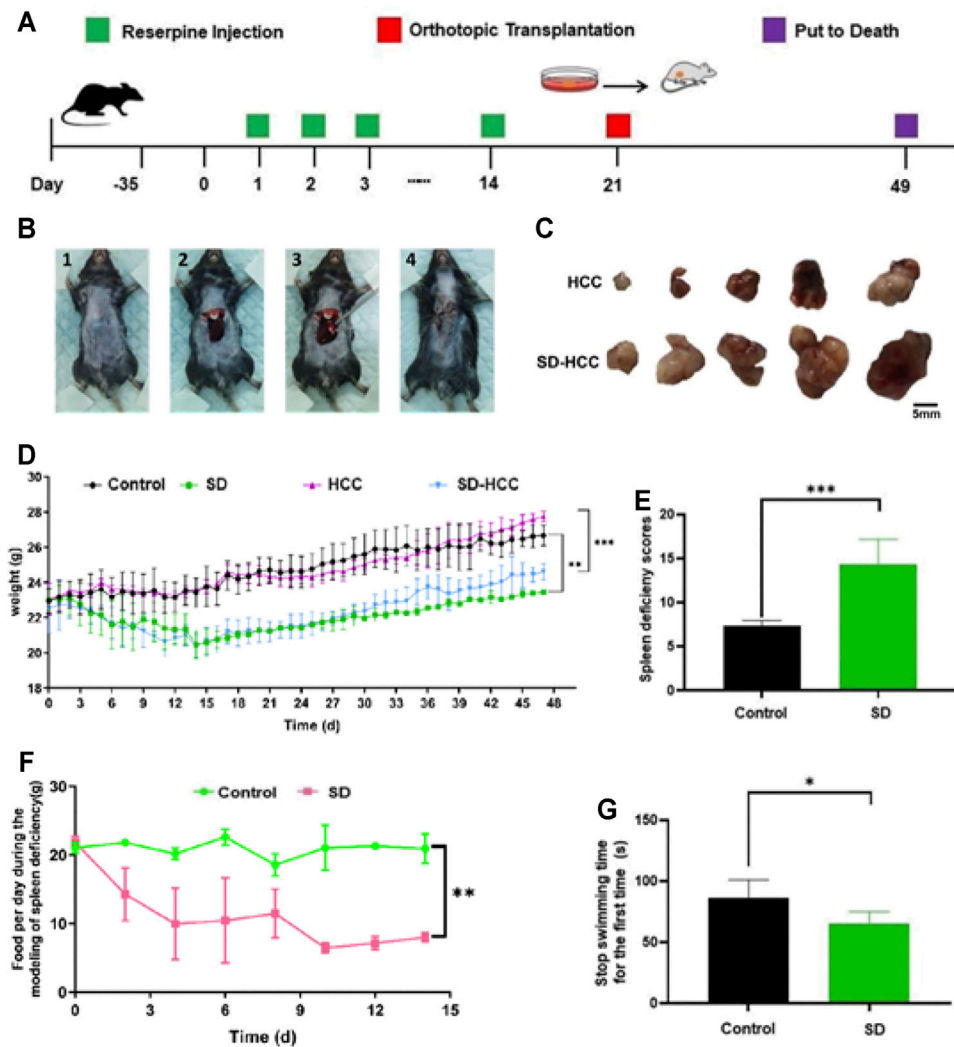


FIGURE 1 | Preparation of orthotopic transplantation liver cancer model with SD. (A) Flow chart; (B) transplantation process: 1) shave and disinfect the surgical area, 2) squeeze out the liver lobe, 3) inoculate the tumor mass, 4) suture the wound; (C) comparison of tumor size; (D) bodyweight change curve; (E) SD score statistics; (F) changes in the diet of mice during the preparation of SD model; (G) stop swimming time statistics. $n = 3$, $^*p < 0.05$, $^{**}p < 0.01$, $^{***}p < 0.001$.

ultraviolet photometer, and mRNA was reverse-transcribed into cDNA by reverse transcription kit then stored at -20°C after the reaction. GAPDH was used as the internal control for the relative quantitative analysis. Then, PCR amplification was performed using cDNA as a template. The total reaction system of real-time PCR was 20 L. The amplification procedures were pre-denaturation in 95°C , 2 min; denaturation in 95°C , 20 s; annealing in 60°C , 20 s; and extension in 72°C , 30 s, altogether 40 cycles. At 72°C for 10 min after the last cycle, the relative expression levels of CTLA-4, PD-1, PD-L1, PTEN, and CD44 mRNA were analyzed by the $2^{-\Delta\Delta\text{Ct}}$ analytical method. The experiment was repeated three times independently. Genespecific primers are listed at supplementary material.

Statistical Analysis

SPSS 26.0 software was used for data analysis and Prism GraphPad 5.0 software was used for mapping and

measurement. The data are expressed as mean \pm standard deviation. The differences between the two groups were tested by Student's t-test, and the differences among many groups were compared by variance analysis. Groups tested with $p < 0.05$ showed that the difference was statistically significant. All the tests were repeated three times independently.

RESULTS

Establishment of the SD-HCC Model With Reserpine

After passing the quarantine period, the mice were treated with reserpine (0.1 mg/kg) daily for 14 days. Orthotopic liver cancer transplantation was performed 14 days later, and the specimens were collected after 49 days. The flow chart is shown in

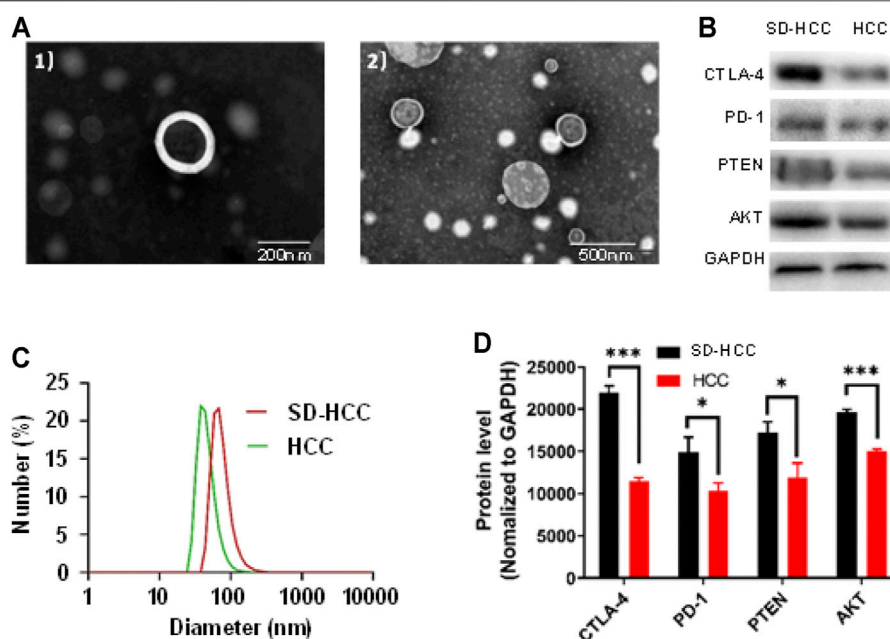


FIGURE 2 | Exosome verification. **(A)** TEM images of 1) HCC exosomes, 2) SD-HCC exosomes; **(B)** exosomal protein level detection band chart; **(C)** size distribution of exosomes; **(D)** histogram of exosomal protein levels. $n = 3$, $*p < 0.05$, $***p < 0.001$.

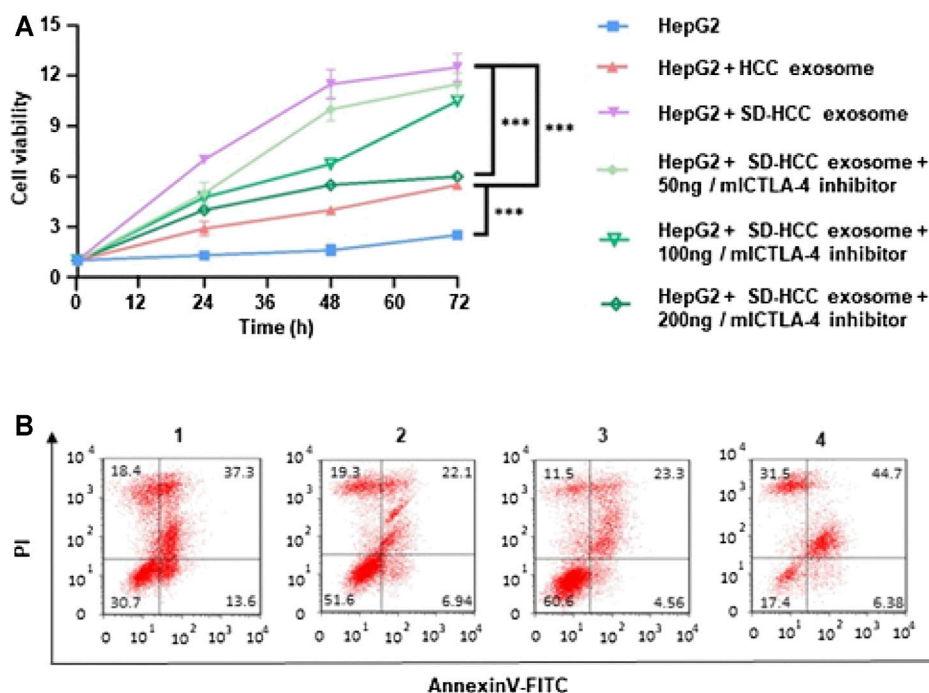


FIGURE 3 | *In vitro* evaluation of cell proliferation of exosomes. **(A)** Relative cell viability of HepG2 after 72 h incubation of HCC exosomes and SD-HCC exosomes; **(B)** the Annexin V/PI apoptosis assay was measured by FCM analysis of HepG2 cells after being treated with each group for 24 h. $n = 3$, $***p < 0.001$. 1) HepG2, 2) HepG2 + HCC exosome, 3) HepG2 + SD-HCC exosome, 4) HepG2 + SD-HCC exosome + CTLA-4 inhibitor.

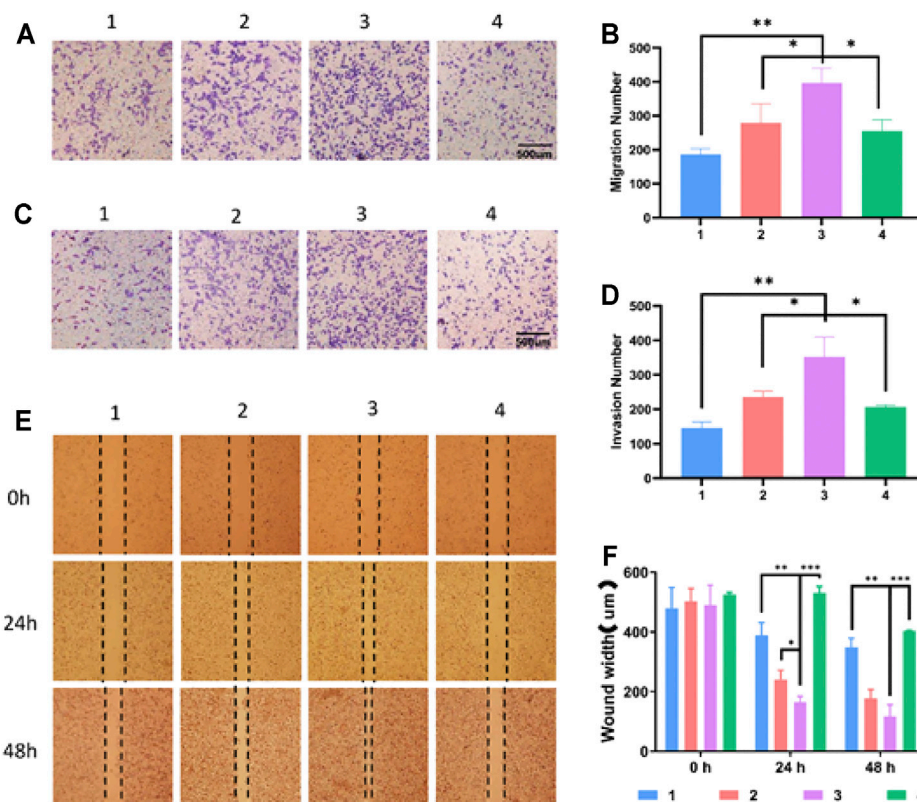


FIGURE 4 | Effect of exosomes of SD on growth and invasion of HCC cells. **(A)** Cell migration experiment, **(B)** histogram of migration experiment statistics, **(C)** cell invasion test, **(D)** invasion experiment statistics histogram, **(E)** cell scratch test, **(F)** scratch experiment statistics histogram. $n = 3$, * $p < 0.05$, ** $p < 0.01$, *** $p < 0.001$, 1) HepG2, 2) HepG2 + HCC exosome, 3) HepG2 + SD-HCC exosome, 4) HepG2 + SD-HCC exosome + CTLA-4 inhibitor.

Figure 1A. The SD score (Luo et al., 2017) is an important method for assessing SD by evaluating scores for factors including body odor, mental state, chill and fever, respiration, fur, feces, and appetite. The SD scores assessment showed that the SD group had lower scores than the control group ($p < 0.001$) (**Figure 1E**). Compared with the control group and HCC group, the weight of the mice in the SD-HCC and SD groups was lower and significantly different ($p < 0.01$) during 5–49 days (**Figure 1D**). The SD group consumed less food per day than the control group (**Figure 1F**). The forced swim test revealed that the stop swimming time of the SD group was shorter for the first time (**Figure 1G**). The preparation process of orthotopic transplantation liver cancer model is as follows: first, mouse HCC hepa1-6 cells were inoculated subcutaneously into nude mice. When a 1 cm^3 tumor was formed, the tumor was taken out and cut into 1-mm^3 -sized pieces for use. The operation area in the C57BL/6 black mouse was shaved and disinfected. A $0.5\text{--}0.8 \text{ mm}$ incision was made near the breastbone, and the liver was extruded. The spare tumor tissue was inoculated into the liver lobe with a trocar. After pressing the hemostatic, the liver lobe was returned to the body, and the incision was sutured. The animals were dissected 28 days after the operation. The liver tumor grew well, and the tumor size of the mice in the HCC group was significantly smaller than that in the SD-HCC group, which demonstrated that the orthotopic transplantation model was

successfully prepared. The transplantation process and tumor size comparison pictures are shown in **Figures 1B,C**.

Exosomes Extraction and Verification

We chose mice from the HCC group and the SD-HCC group. After the preparation of the model was completed, blood was taken, and exosomes were extracted. We examined the morphology of HCC exosomes and SD-HCC exosomes by using transmission electron microscopy (TEM). The results displayed exosomes as spherical, membrane-bound vesicles (**Figure 2A**). The hydrodynamic diameter of the HCC and SD-HCC exosomes was measured to be 43 and 68 nm by dynamic light scattering (**Figure 2C**). Detecting the components of exosomes, we found that the levels of CTLA-4 and AKT in serum exosomes in SD-HCC were higher than those in the HCC group ($p < 0.001$). The contents of PD-1 and PTEN were higher than those in the HCC group, and the difference was significant ($p < 0.05$), suggesting that the exosomes were successfully extracted, and SD could affect the expression of CTLA-4 and other proteins in the exosomes (**Figures 2B,D**).

Proliferation Inhibition

To explore the relationship between SD and cell proliferation *in vitro*, we generated cell growth curves evaluated by MTT.

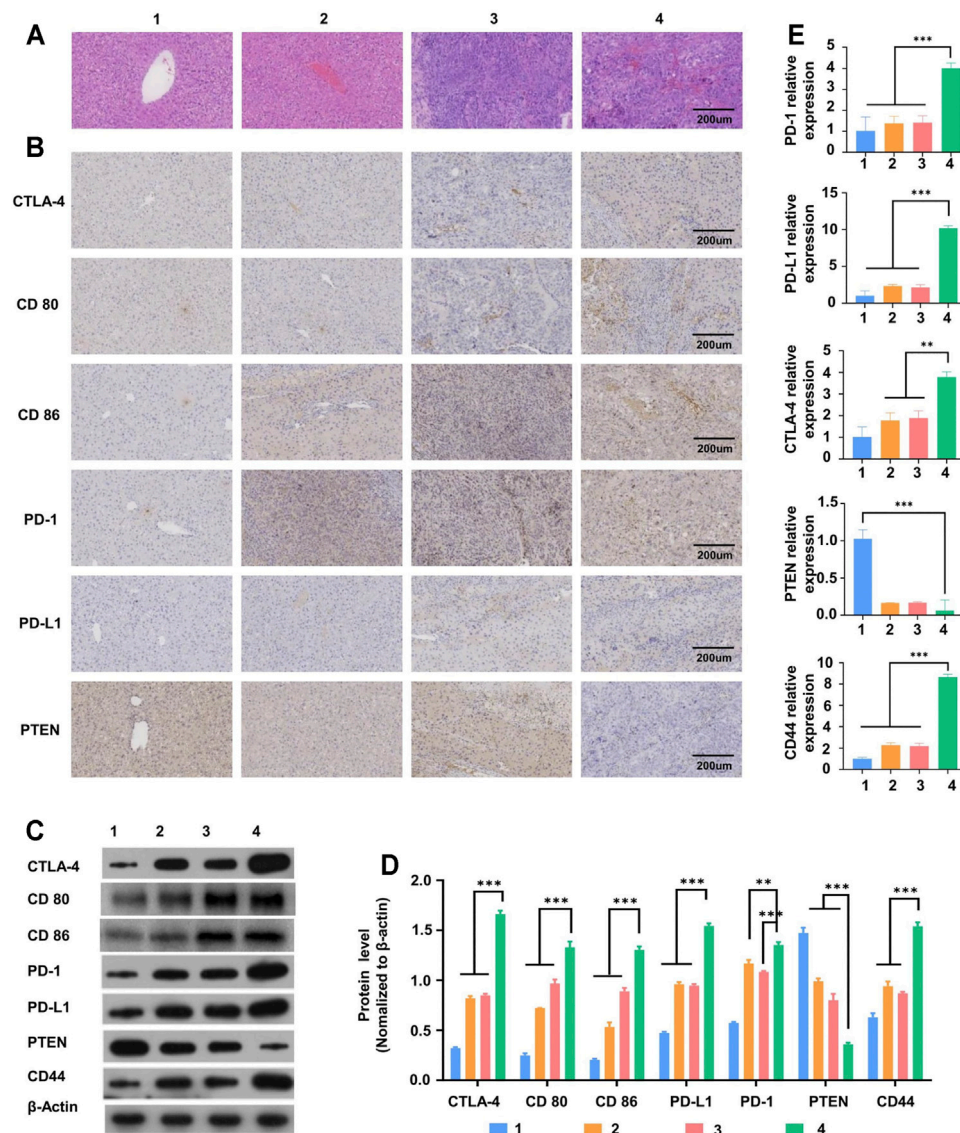


FIGURE 5 | Liver tissue slice morphology and molecular mechanism of liver tumor occurrence and development. **(A)** H&E staining observation of morphological changes of liver tissue sections of mice in different treatment groups, **(B)** immunohistochemical detection of CTLA-4 and other immune checkpoint protein distribution, **(C)** Western blot detection of CTLA-4 and other immune checkpoint-related protein band diagram, **(D)** histogram, **(E)** RT-PCR detects the expression of mRNA related to immune checkpoints. $n = 3$, $^{**}p < 0.01$, $^{***}p < 0.001$, 1) control group, 2) SD group, 3) HCC group, 4) SD-HCC group.

Briefly, 10 μ l of PBS, liver cancer mouse serum, SD liver cancer mouse serum, SD liver cancer mouse serum plus CTLA-4 inhibitors were added separately into a 96-well plate with HepG2 cells. The results revealed that HCC cell proliferation was promoted by SD liver cancer mouse serum compared with liver cancer mouse serum in 48 and 72 h. The addition of CTLA-4 inhibitors could partially reverse this change (**Figure 3A**). Apoptosis study of HepG2 cells tested by flow cytometry showed that SD liver cancer mouse serum could induce least miniature cells apoptosis compared with liver cancer mouse serum. The addition of CTLA-4 inhibitors could partially reverse cell apoptosis (**Figure 3B**).

Cell Migration and Invasion

To study the effect of SD on the migration and invasion of liver cancer cells, the HepG2 cells were treated with SD liver cancer mouse serum or liver cancer mouse serum for 48 h. The cell scratch method and transwell test were used to detect the migration and invasion ability of HepG2 cells after drug treatment. We found that compared with the HCC group and the SD-HCC add CTLA-4 inhibitor groups, the SD-HCC group had a stronger migration ability (**Figures 4A,B**) and stronger invasion ability (**Figures 4C,D**). In the scratch experiment, we observed that the diameter of the scratches in the SD-HCC group was narrower than in the other three groups at 24 and 48 h after

the scratches were made. The differences are statistically significant ($p < 0.001$) (Figures 4E,F).

H&E Staining of Liver Tumor

Hematoxylin and eosin (H&E) staining of the liver tissues from the HCC and SD-HCC groups showed all sizes of carcinoma cells with some multinucleated giant tumor cells, and the funicular slices were distributed and accumulated irregularly without normal hepatocyte construction (Figure 5A). To some extent, the results indicated that the degree of malignancy of the tumor tissue was higher in the SD-HCC group than in the HCC group.

Molecular Mechanism of Liver Tumor Occurrence and Development

In order to verify the influence of the internal environment of SD on liver tumor occurrence and development, we established liver cancer models and SD liver cancer models in the early stage. The results of immunohistochemistry and WB (Western Blot) showed that both the SD group and liver cancer group mice had significantly higher ($p < 0.01$) levels of CTLA-4 and PD-1 compared with the normal group. In addition, the liver cancer mice with SD had significantly higher levels of CTLA-4 and PD-1 proteins than those in the liver cancer group only ($p < 0.01$) (Figures 5B–D). The mRNA expression in tissues as analyzed by the RT-PCR test showed a similar trend (Figure 5E). All these results suggest that the internal environment of SD may affect liver tumor occurrence and development by disturbing CTLA-4 and other series of proteins and genes.

DISCUSSION

HCC is one of the most malignant cancers and is the third leading cause of cancer-related death due to its high recurrence and poor prognosis (Chen et al., 2016). HBV infection is a major risk factor for HCC, and Chinese HCC patients account for 50% of HCC patients in the world (Bray et al., 2018; Feng et al., 2019). Currently, treatment strategies for HCC patients include surgery, liver transplantation, chemotherapy, radiotherapy, biological therapy, and targeted molecular therapy, but the overall effect is not satisfactory due to the highly metastatic nature of HCC (Couri and Pillai, 2019). Therefore, it is necessary to search for reliable biomarkers and therapeutic targets to monitor the progress of HCC. The imbalance of the body's internal environment is closely related to the occurrence and development of cancer, and genetic inheritance can only explain 5% of the occurrence of cancer (Bhattacharjee et al., 2013; Craig et al., 2020; Llovet et al., 2021). Eventually, changes in the body's internal environment are unfavorable to the survival of normal cells but appropriate to the survival of tumor cells. “Bian Zheng Lun Zhi,” the core of TCM therapy systems, is based on syndrome differentiation, which helps to guide the design of individualized treatments (Ji et al., 2016; Zhang et al., 2020). Syndromes such as loose stools, abdominal distension after meals, loss of appetite, sallow complexion, weight loss, general weakness, and/or low disease resistance could be summarized as SD in TCM

theoretical system. In the clinical investigation of 767 cases of gastric cancer patients, 32.86% of patients showed the syndrome of SD and stomach cold syndrome (Sun et al., 2010). SD syndrome is also considered to be the key pathogenesis of colorectal cancer (Sun et al., 2016a). It has been reported that traditional Chinese medicine for invigorating the spleen helps in delaying the pathological process of HCC cachexia induced by ascites by reducing the levels of IL-1 α , IL-6, and TNF α and inhibiting the activation of the ubiquitin–proteasome pathway (Sun et al., 2016b). Meanwhile, traditional Chinese medicine in invigorating the spleen could prolong the survival time and decrease tumor metastasis in the liver in mice, which may be associated with enhancing the expression of PTEN in the liver (Yin et al., 2008). Therefore, the internal environment of SD is especially vital for the occurrence and development of immune recognition disorders of HCC.

In our study, reserpine was used to establish a model of SD syndrome referring to the previous researches (Zhao et al., 2011; Luo et al., 2017). Chronic rather than acute doses of reserpine were used to induce the syndrome of SD in the mice in this study. In our analysis, we referred to each factor in the SD scores assessment (Luo et al., 2017) and found that the score of the SD group was higher than that of the control group. During the establishment of the model of SD syndrome, there were also significant differences between the SD group and the control group in the amount of daily food intake and the time to stop swimming. In addition, compared with the control group, the weight of the mice in the SD group decreased significantly, and this effect continued throughout the modeling process. The results of H&E staining showed that the malignant degree of tumor in the SD-HCC group was higher than that in the HCC group. These results indicated that the SD model was successfully established, and the factor of SD indeed affected the growth of the HCC mice.

In recent years, tumor immunotherapy has been the focus of research which has brought great benefits to cancer patients. However, due to a variety of complex factors, it is easy for tumors to escape from the host immune system during the treatment process, leading to treatment failure (Whiteside et al., 2011). Moreover, tumor immunotherapy also induces some serious toxic events and autoimmune diseases, such as pituitary hypophysitis, autoimmune hepatitis, pneumonia, and so on (Cogdill et al., 2017; Couzin-Frankel, 2017). Therefore, it is very necessary to find out the cancer-related immune mechanism. Exosomes (30–150 nm) are considered as messengers between cells, carrying a large number of macromolecules, including proteins, mRNAs, lipids, and miRNAs, which constitutes an important part of the tumor immune microenvironment (Wen et al., 2016; Bach et al., 2017; Ruivo et al., 2017; Su et al., 2021). Exosomes are nanoscale membranous vesicles secreted from intracellular multivesicular bodies (MVBs) or late endosomes into the extracellular space through extracellular action (Su et al., 2021). CD81, CD63, and TSG101 have become the most commonly used exosomal labeling proteins (Pegtel and Gould, 2019). In our study, after the establishment of the model, we selected the serum of the HCC group and SD-HCC group mice

for separation of the exosomes. Exosomes were observed as spherical, membrane-bound vesicles by using TEM. The hydrodynamic diameter of the exosomes was measured as 43 and 68 nm by dynamic light scattering. These characteristics of exosomes are consistent with the results of other studies, which demonstrates that we successfully extracted exosomes of HCC. Studies have found that tumor-derived exosomes carry immunosuppressive proteins, such as PD-1, CTLA-4, FasL, TRAIL, etc. (Whiteside, 2013; Ukrainskaya et al., 2019; Benecke et al., 2021). Detecting the components of exosomes, we found the presence of PD-1, CTLA-4, PTEN, and AKT. Interestingly, the level of CTLA-4 of the SD-HCC group was the highest, which may indicate that CTLA-4 plays an important role in exosome HCC with SD syndrome.

CTLA-4 is highly expressed in lymphocytes CD4 + and CD8 + T (Phung et al., 2020), competing with the T-cell costimulator CD28 for binding to CD80 and CD86 with a higher affinity, which conveys inhibitory signals within the T cells (Van Coillie et al., 2020; Goenka et al., 2021). We examined liver tumor tissues to verify this relationship between CTLA-4 and T cells in the internal environment of SD. The results of immunohistochemistry and WB showed that CTLA-4, CD80, and CD86 were higher in the HCC and SD-HCC groups than in the other groups, and it was significantly higher in the SD-HCC group. The mRNA expression showed the same results. These data may indicate that T-cell activation and function were restricted. It has been reported that mutations in the CTLA-4 gene are associated with an increased risk of human autoimmune disorders (Ueda et al., 2003; Schubert et al., 2014). In immunotherapy of cancer, the use of blocking anti-CTLA-4 and anti-PD-1 antibodies have yielded promising results, and the 2018 Nobel Prize was granted to Jim P. Allison and Tasuku Honjo, who are the pioneers in this field (Wolchok, 2018). In the cell proliferation experiment, compared with the serum of HCC mice at 48 and 72 h, the serum of SD-HCC mice promoted the proliferation of HCC cells and the addition of CTLA-4 inhibitor could partially reverse this change. Detecting apoptosis on HepG2 cells showed that SD-HCC mice serum can induce the least cell apoptosis compared with liver cancer mouse serum and when added into CTLA-4 inhibitors could partially reverse cells apoptosis. In order to study the effect of SD on the migration and invasion of HCC cells, cell scratch assay and transwell test were used after drug treatment. Compared with the HCC group and the CTLA-4 inhibitor group, the SD-HCC group had stronger migration ability and stronger invasion ability. These results suggest that SD may boost the occurrence and development of liver cancer through exosome CTLA-4.

PTEN is an important tumor suppressor protein, and a loss in its function is associated with malignant transformation, progression, chemotherapy response, and survival of a variety of cancers (Su et al., 2016; Wang et al., 2018a; Luongo et al., 2019; Raffone et al., 2019). PTEN has an important effect on regulating the PI3K/Akt/mTOR signaling pathway, which plays an important role in the proliferation and maintenance of CSC self-renewal, according to reports (Su et al., 2016; Yang et al., 2016; Luongo et al., 2019). The relationship between PTEN and PI3K/Akt/mTOR can be partly illustrated in our study according

to the result of detecting exosome components, which displayed the presence of PTEN and Akt in the exosomes and was higher in the SD-HCC group than in the HCC group. Growing evidence has indicated that PTEN has specific functions to interfere with stem/progenitor cells, including regulating the differentiation of neural SCs, promoting the differentiation of mesenchymal SCs, and maintaining the balance between proliferation and differentiation of hematopoietic SCs (Su et al., 2016). It is well known that CSCs have the characteristics of self-renewal and differentiation (Luongo et al., 2019; Nero et al., 2019; Cetintas and Batada, 2020). There are multiple biomarkers of CSCs, including CD133, SOX2, BMI1, CD44, Nanog, and ABCG2 (Hu et al., 2020). The PTEN/CD44 signaling pathway plays an important role in maintaining the characteristics of CSCs, involved in tumorigenesis, invasion and metastasis, and immune escape (Luongo et al., 2019; Nero et al., 2019; Cetintas and Batada, 2020). In this study, the expression of PTEN and CD44 is the highest in the SD-HCC group than in the other groups according to the results of immunohistochemistry, WB, and mRNA. We inferred that the SD factor could promote the expression of PTEN and CD44 and thus has a positive effect on the differentiation of CSCs. Besides liver cancer, the current treatments of various types of other cancers are also waiting for better outcomes. Although there are multiple forms of technologies those were explored, e.g., photoacoustic technology, reactive oxygen species, and cytotoxic peroxynitrite (ONOO⁻), the efficiency of cancer treatments is still far from satisfactory (Wang et al., 2021; Zhang et al., 2021). Here, our findings from exosomes may provide some hints from a new angle for high efficiency of treatment of various cancers.

In conclusion, in the HCC mouse model, we found that SD plays a key role in the occurrence and development of immune recognition disorders of HCC. In addition, at the molecular level, the exosome CTLA-4 expression in the SD-HCC group was upregulated, which played a powerful role in regulating the growth, self-renewal, and metastasis of HCC. SD also promoted the PTEN/CD44 pathway process. These important findings suggest that the internal environment of SD exosome CTLA-4 promotes the metastasis of liver cancer by regulating the PTEN/CD44 pathway. However, the molecular mechanism of how CTLA-4 regulates the PTEN/CD44 pathway remains unclear and needs further study.

DATA AVAILABILITY STATEMENT

The original contributions presented in the study are included in the article/**Supplementary Material**, further inquiries can be directed to the corresponding authors.

ETHICS STATEMENT

The animal study was reviewed and approved by the clinical research and animals ethics committee of the first affiliated hospital, Sun Yat-Sen University.

AUTHOR CONTRIBUTIONS

YW, PL, XL, SZ, and LY: conceptualization, methodology, data collection, data analysis, manuscript writing and revision; ZM, ZC, JL, MZ and SM: methodology, data collection. All authors approved the final version of the manuscript.

FUNDING

This study was supported by the China Postdoctoral Science Foundation (Nos 2020M673026, 2021T140778), the National Natural Science Foundation of China (Nos 8210153649,

81903967, 81873248), Project of Inheriting Famous TCM Masters of Guangdong Provincial Administration of Traditional Chinese Medicine (No. (2020)1), the Scientific Research Project of Guangdong Provincial Administration of Traditional Chinese Medicine (No. 20211070).

SUPPLEMENTARY MATERIAL

The Supplementary Material for this article can be found online at: <https://www.frontiersin.org/articles/10.3389/fphar.2021.757194/full#supplementary-material>

REFERENCES

- Bach, D. H., Hong, J. Y., Park, H. J., and Lee, S. K. (2017). The Role of Exosomes and miRNAs in Drug-Resistance of Cancer Cells. *Int. J. Cancer* 141 (2), 220–230. doi:10.1002/ijc.30669
- Benecke, L., Coray, M., Umbricht, S., Chiang, D., Figueiró, F., and Muller, L. (2021). Exosomes: Small EVs with Large Immunomodulatory Effect in Glioblastoma. *Int. J. Mol. Sci.* 22 (7). doi:10.3390/ijms22073600
- Bhattacharjee, P., Banerjee, M., and Giri, A. K. (2013). Role of Genomic Instability in Arsenic-Induced Carcinogenicity. A Review. *Environ. Int.* 53, 29–40. doi:10.1016/j.envint.2012.12.004
- Bray, F., Ferlay, J., Soerjomataram, I., Siegel, R. L., Torre, L. A., and Jemal, A. (2018). Global Cancer Statistics 2018: GLOBOCAN Estimates of Incidence and Mortality Worldwide for 36 Cancers in 185 Countries. *CA Cancer J. Clin.* 68 (6), 394–424. doi:10.3322/caac.21492
- Cetintas, V. B., and Batada, N. N. (2020). Is There a Causal Link between PTEN Deficient Tumors and Immunosuppressive Tumor Microenvironment? *J. Transl. Med.* 18 (1), 45. doi:10.1186/s12967-020-02219-w
- Chen, W., Zheng, R., Baade, P. D., Zhang, S., Zeng, H., Bray, F., et al. (2016). Cancer Statistics in China, 2015. *CA Cancer J. Clin.* 66 (2), 115–132. doi:10.3322/caac.21338
- Chen, Y., Sun, B. G., Zhang, S. J., Chen, Z. X., Hardi, C. F., and Xiang, T. (2014). Observations of TCRV β Gene Expression in Rats with Dampness Syndrome. *Evid. Based Complement. Alternat Med.* 2014, 373608. doi:10.1155/2014/373608
- Cogdill, A. P., Andrews, M. C., and Wargo, J. A. (2017). Hallmarks of Response to Immune Checkpoint Blockade. *Br. J. Cancer* 117 (1), 1–7. doi:10.1038/bjc.2017.136
- Couri, T., and Pillai, A. (2019). Goals and Targets for Personalized Therapy for HCC. *Hepatol. Int.* 13 (2), 125–137. doi:10.1007/s12072-018-9919-1
- Couzin-Frankel, J. (2017). Autoimmune Diseases Surface after Cancer Treatment. *Science* 358 (6365), 852. doi:10.1126/science.358.6365.852
- Craig, A. J., von Felden, J., Garcia-Lezana, T., Sarcognato, S., and Villanueva, A. (2020). Tumour Evolution in Hepatocellular Carcinoma. *Nat. Rev. Gastroenterol. Hepatol.* 17 (3), 139–152. doi:10.1038/s41575-019-0229-4
- Curran, M. A., Montalvo, W., Yagita, H., and Allison, J. P. (2010). PD-1 and CTLA-4 Combination Blockade Expands Infiltrating T Cells and Reduces Regulatory T and Myeloid Cells within B16 Melanoma Tumors. *Proc. Natl. Acad. Sci. U.S.A.* 107 (9), 4275–4280. doi:10.1073/pnas.0915174107
- Feng, R. M., Zong, Y. N., Cao, S. M., and Xu, R. H. (2019). Current Cancer Situation in China: Good or Bad News from the 2018 Global Cancer Statistics? *Cancer Commun. (Lond)* 39 (1), 22. doi:10.1186/s40880-019-0368-6
- Gish, R. G., Porta, C., Lazar, L., Ruff, P., Feld, R., Croitoru, A., et al. (2007). Phase III Randomized Controlled Trial Comparing the Survival of Patients with Unresectable Hepatocellular Carcinoma Treated with Nilotrex or Doxorubicin. *J. Clin. Oncol.* 25 (21), 3069–3075. doi:10.1200/JCO.2006.08.4046
- Goenka, R., Xu, Z., Samayoa, J., Banach, D., Beam, C., Bose, S., et al. (2021). CTLA4-Ig-Based Bifunctional Costimulation Inhibitor Blocks CD28 and ICOS Signaling to Prevent T Cell Priming and Effector Function. *J. Immunol.* 206 (5), 1102–1113. doi:10.4049/jimmunol.2001100
- Hu, H., Luo, S. J., Cao, Z. R., Wu, Y., Mo, Z., Wang, Y., et al. (2020). Depressive Disorder Promotes Hepatocellular Carcinoma Metastasis via Upregulation of ABCG2 Gene Expression and Maintenance of Self-Renewal. *J. Cancer* 11 (18), 5309–5317. doi:10.7150/jca.45712
- Ji, Q., Luo, Y. Q., Wang, W. H., Liu, X., Li, Q., and Su, S. B. (2016). Research Advances in Traditional Chinese Medicine Syndromes in Cancer Patients. *J. Integr. Med.* 14 (1), 12–21. doi:10.1016/S2095-4964(16)60237-6
- Lee, Y. R., Chen, M., and Pandolfi, P. P. (2018). The Functions and Regulation of the PTEN Tumour Suppressor: New Modes and Prospects. *Nat. Rev. Mol. Cell Biol.* 19 (9), 547–562. doi:10.1038/s41580-018-0015-0
- Llovet, J. M., De Baere, T., Kulik, L., Haber, P. K., Greten, T. F., Meyer, T., et al. (2021). Locoregional Therapies in the Era of Molecular and Immune Treatments for Hepatocellular Carcinoma. *Nat. Rev. Gastroenterol. Hepatol.* 18 (5), 293–313. doi:10.1038/s41575-020-00395-0
- Luo, H., Chen, Y., Sun, B., Xiang, T., and Zhang, S. (2017). Establishment and Evaluation of Orthotopic Hepatocellular Carcinoma and Drug-Induced Hepatocellular Carcinoma in Mice with Spleen-Deficiency Syndrome in Traditional Chinese Medicine. *Afr. J. Tradit. Complement. Altern. Med.* 14 (1), 165–173. doi:10.21010/ajtcam.v14i1.18
- Luongo, F., Colonna, F., Calapà, F., Vitale, S., Fiori, M. E., and De Maria, R. (2019). PTEN Tumor-Suppressor: The Dam of Stemness in Cancer. *Cancers (Basel)* 11 (8). doi:10.3390/cancers11081076
- Mahoney, K. M., Rennert, P. D., and Freeman, G. J. (2015). Combination Cancer Immunotherapy and New Immunomodulatory Targets. *Nat. Rev. Drug Discov.* 14 (8), 561–584. doi:10.1038/nrd4591
- Maker, A. V., Attia, P., and Rosenberg, S. A. (2005). Analysis of the Cellular Mechanism of Antitumor Responses and Autoimmunity in Patients Treated with CTLA-4 Blockade. *J. Immunol.* 175 (11), 7746–7754. doi:10.4049/jimmunol.175.11.7746
- Mo, Z., Cao, Z., Yu, L., Wang, Y., Li, P., Lin, Y., et al. (2020). An Integrative Analysis Reveals the Potential Mechanism between Herbal Medicine Yinchen and Immunoregulation in Hepatocellular Carcinoma. *Biomed. Res. Int.* 2020, 8886914. doi:10.1155/2020/8886914
- Nero, C., Ciccarone, F., Pietragalla, A., and Scambia, G. (2019). PTEN and Gynecological Cancers. *Cancers (Basel)* 11 (10). doi:10.3390/cancers11101458
- Ou, W., Thapa, R. K., Jiang, L., Soe, Z. C., Gautam, M., Chang, J. H., et al. (2018). Regulatory T Cell-Targeted Hybrid Nanoparticles Combined with Immuno-Checkpoint Blockage for Cancer Immunotherapy. *J. Control. Release* 281, 84–96. doi:10.1016/j.jconrel.2018.05.018
- Pegtel, D. M., and Gould, S. J. (2019). Exosomes. *Annu. Rev. Biochem.* 88, 487–514. doi:10.1146/annurev-biochem-013118-111902
- Phung, C. D., Pham, T. T., Nguyen, H. T., Nguyen, T. T., Ou, W., Jeong, J. H., et al. (2020). Anti-CTLA-4 Antibody-Functionalized Dendritic Cell-Derived Exosomes Targeting Tumor-Draining Lymph Nodes for Effective Induction of Antitumor T-Cell Responses. *Acta Biomater.* 115, 371–382. doi:10.1016/j.actbio.2020.08.008
- Quezada, S. A., Peggs, K. S., Curran, M. A., and Allison, J. P. (2006). CTLA4 Blockade and GM-CSF Combination Immunotherapy Alters the Intratumor Balance of Effector and Regulatory T Cells. *J. Clin. Invest.* 116 (7), 1935–1945. doi:10.1172/JCI27745

- Raffone, A., Travaglini, A., Saccone, G., Campanino, M. R., Mollo, A., De Placido, G., et al. (2019). Loss of PTEN Expression as Diagnostic Marker of Endometrial Precancer: A Systematic Review and Meta-Analysis. *Acta Obstet. Gynecol. Scand.* 98 (3), 275–286. doi:10.1111/aogs.13513
- Ruivo, C. F., Adem, B., Silva, M., and Melo, S. A. (2017). The Biology of Cancer Exosomes: Insights and New Perspectives. *Cancer Res.* 77 (23), 6480–6488. doi:10.1158/0008-5472.CAN-17-0994
- Schubert, D., Bode, C., Kenefack, R., Hou, T. Z., Wing, J. B., Kennedy, A., et al. (2014). Autosomal Dominant Immune Dysregulation Syndrome in Humans with CTLA4 Mutations. *Nat. Med.* 20 (12), 1410–1416. doi:10.1038/nm.3746
- Su, R., Nan, H., Guo, H., Ruan, Z., Jiang, L., Song, Y., et al. (2016). Associations of Components of PTEN/AKT/mTOR Pathway with Cancer Stem Cell Markers and Prognostic Value of These Biomarkers in Hepatocellular Carcinoma. *Hepatol. Res.* 46 (13), 1380–1391. doi:10.1111/hepr.12687
- Su, T., Zhang, P., Zhao, F., and Zhang, S. (2021). Exosomal MicroRNAs Mediating Crosstalk between Cancer Cells with Cancer-Associated Fibroblasts and Tumor-Associated Macrophages in the Tumor Microenvironment. *Front. Oncol.* 11, 631703. doi:10.3389/fonc.2021.631703
- Sun, B., Luo, H., Deng, L., Zhang, S., and Chen, Z. (2016). The Study on Mechanism of the Modified Chinese Herbal Compound, Jianpijiedu, on a Mouse Model of Hepatic Carcinoma Cachexia. *Mol. Med. Rep.* 14 (4), 3113–3121. doi:10.3892/mmr.2016.5602
- Sun, D. Z., Liu, L., Jiao, J. P., Wei, P. K., Jiang, L. D., and Xu, L. (2010). Syndrome Characteristics of Traditional Chinese Medicine: Summary of a Clinical Survey in 767 Patients with Gastric Cancer. *Zhong Xi Yi Jie He Xue Bao* 8 (4), 332–340. doi:10.3736/jcim20100406
- Sun, X. G., Lin, X. C., Diao, J. X., Yu, Z. L., and Li, K. (2016). Pi (Spleen)-Deficiency Syndrome in Tumor Microenvironment Is the Pivotal Pathogenesis of Colorectal Cancer Immune Escape. *Chin. J. Integr. Med.* 22 (10), 789–794. doi:10.1007/s11655-015-2086-5
- Ueda, H., Howson, J. M., Esposito, L., Heward, J., Snook, H., Chamberlain, G., et al. (2003). Association of the T-Cell Regulatory Gene CTLA4 with Susceptibility to Autoimmune Disease. *Nature* 423 (6939), 506–511. doi:10.1038/nature01621
- Ukrainskaya, V. M., Rubtsov, Y. P., Knorre, V. D., Maschan, M. A., Gabibov, A. G., and Stepanov, A. V. (2019). The Role of Tumor-Derived Vesicles in the Regulation of Antitumor Immunity. *Acta Naturae* 11 (4), 33–41. doi:10.32607/20758251-2019-11-4-33-41
- Van Coillie, S., Wiernicki, B., and Xu, J. (2020). “Molecular and Cellular Functions of CTLA-4,” in *Regulation of Cancer Immune Checkpoints: Molecular and Cellular Mechanisms and Therapy*. Editor J. Xu (Singapore: Springer Singapore), 7–32. doi:10.1007/978-981-15-3266-5_2
- Wang, L., Zuo, X., Xie, K., and Wei, D. (2018). The Role of CD44 and Cancer Stem Cells. *Methods Mol. Biol.* 1692, 31–42. doi:10.1007/978-1-4939-7401-6_3
- Wang, X., Cao, X., Sun, R., Tang, C., Tzankov, A., Zhang, J., et al. (2018). Clinical Significance of PTEN Deletion, Mutation, and Loss of PTEN Expression in De Novo Diffuse Large B-Cell Lymphoma. *Neoplasia* 20 (6), 574–593. doi:10.1016/j.neo.2018.03.002
- Wang, Z., Zhan, M., Li, W., Chu, C., Xing, D., Lu, S., et al. (2021). Photoacoustic Cavitation-Ignited Reactive Oxygen Species to Amplify Peroxynitrite Burst by Photosensitization-free Polymeric Nanocapsules. *Angew. Chem. Int. Ed. Engl.* 60 (9), 4720–4731. doi:10.1002/anie.202013301
- Wen, S. W., Sceneay, J., Lima, L. G., Wong, C. S., Becker, M., Krumeich, S., et al. (2016). The Biodistribution and Immune Suppressive Effects of Breast Cancer-Derived Exosomes. *Cancer Res.* 76 (23), 6816–6827. doi:10.1158/0008-5472.CAN-16-0868
- Whiteside, T. L. (2013). Immune Modulation of T-Cell and NK (Natural Killer) Cell Activities by TEXs (Tumour-derived Exosomes). *Biochem. Soc. Trans.* 41 (1), 245–251. doi:10.1042/BST20120265
- Whiteside, T. L., Mandapathil, M., Szczepanski, M., and Szajnik, M. (2011). Mechanisms of Tumor Escape from the Immune System: Adenosine-Producing Treg, Exosomes and Tumor-Associated TLRs. *Bull. Cancer* 98 (2), E25–E31. doi:10.1684/bdc.2010.1294
- Wolchok, J. (2018). Putting the Immunologic Brakes on Cancer. *Cell* 175 (6), 1452–1454. doi:10.1016/j.cell.2018.11.006
- Yang, C. F., Yang, G. D., Huang, T. J., Li, R., Chu, Q. Q., Xu, L., et al. (2016). EB-virus Latent Membrane Protein 1 Potentiates the Stemness of Nasopharyngeal Carcinoma via Preferential Activation of PI3K/AKT Pathway by a Positive Feedback Loop. *Oncogene* 35 (26), 3419–3431. doi:10.1038/onc.2015.402
- Yin, L. R., Chen, Z. X., Zhang, S. J., Sun, B. G., Liu, Y. D., and Huang, H. Z. (2008). Expression of Phosphatase and Tensin Homolog Deleted on Chromosome Ten in Liver of Athymic Mice with Hepatocellular Carcinoma and the Effect of Fuzheng Jiedu Decoction. *World J. Gastroenterol.* 14 (1), 108–113. doi:10.3748/wjg.14.108
- Yu, L., Wang, Z., Mo, Z., Zou, B., Yang, Y., Sun, R., et al. (2021). Synergetic Delivery of Triptolide and Ce6 with Light-Activatable Liposomes for Efficient Hepatocellular Carcinoma Therapy. *Acta Pharmaceutica Sinica B.* doi:10.1016/j.apsb.2021.02.001
- Yu, Y., Nangia-Makker, P., Farhana, L., G Rajendra, S., Levi, E., and Majumdar, A. P. (2015). miR-21 and miR-145 Cooperation in Regulation of colon Cancer Stem Cells. *Mol. Cancer* 14, 98. doi:10.1186/s12943-015-0372-7
- Zhang, W. L., Li, N., Shen, Q., Fan, M., Guo, X. D., Zhang, X. W., et al. (2020). Establishment of a Mouse Model of Cancer Cachexia with Spleen Deficiency Syndrome and the Effects of Atractylenolide I. *Acta Pharmacol. Sin* 41 (2), 237–248. doi:10.1038/s41401-019-0275-z
- Zhang, Y., He, X., Zhang, Y., Zhao, Y., Lu, S., Peng, Y., et al. (2021). Native Mitochondria-Targeting Polymeric Nanoparticles for Mild Photothermal Therapy Rationally Potentiated with Immune Checkpoints Blockade to Inhibit Tumor Recurrence and Metastasis. *Chem. Eng. J.* 424, 130171. doi:10.1016/j.cej.2021.130171
- Zhao, N., Zhang, W., Guo, Y., Jia, H., Zha, Q., Liu, Z., et al. (2011). Effects on Neuroendocrinoimmune Network of Lizhong Pill in the Reserpine Induced Rats with Spleen Deficiency in Traditional Chinese Medicine. *J. Ethnopharmacol* 133 (2), 454–459. doi:10.1016/j.jep.2010.10.016

Conflict of Interest: The authors declare that the research was conducted in the absence of any commercial or financial relationships that could be construed as a potential conflict of interest.

Publisher's Note: All claims expressed in this article are solely those of the authors and do not necessarily represent those of their affiliated organizations, or those of the publisher, the editors, and the reviewers. Any product that may be evaluated in this article, or claim that may be made by its manufacturer, is not guaranteed or endorsed by the publisher.

Copyright © 2021 Wang, Li, Mao, Mo, Cao, Luo, Zhou, Liu, Zhang and Yu. This is an open-access article distributed under the terms of the Creative Commons Attribution License (CC BY). The use, distribution or reproduction in other forums is permitted, provided the original author(s) and the copyright owner(s) are credited and that the original publication in this journal is cited, in accordance with accepted academic practice. No use, distribution or reproduction is permitted which does not comply with these terms.



Tumor Microenvironment-Responsive Polypeptide Nanogels for Controlled Antitumor Drug Delivery

Yanhong Liu¹, Linjiao Chen¹, Qingyang Shi¹, Qing Zhao² and Hongshuang Ma^{3*}

¹Center for Reproductive Medicine, Center for Prenatal Diagnosis, First Hospital, Jilin University, Changchun, China, ²Department of Obstetrics, First Hospital, Jilin University, Changchun, China, ³Department of Rheumatology and Immunology, The First Hospital of Jilin University, Changchun, China

Tumor microenvironment-responsive polypeptide nanogels belong to a biomaterial with excellent biocompatibility, easily adjustable performance, biodegradability, and non-toxic properties. They are developed for selective delivery of antitumor drugs into target organs to promote tumor cell uptake, which has become an effective measure of tumor treatment. Endogenous (such as reduction, reactive oxygen species, pH, and enzyme) and exogenous (such as light and temperature) responsive nanogels can release drugs in response to tumor tissues or cells to improve drug distribution and reduce drug side effects. This article systematically introduces the research progress in tumor microenvironment-responsive polypeptide nanogels to deliver antitumor drugs and provides a reference for the development of antitumor nanoformulations.

OPEN ACCESS

Edited by:

Sanjun Shi,
Chengdu University of Traditional
Chinese Medicine, China

Reviewed by:

Lesan Yan,
Wuhan University of Technology,
China
Peisheng Xu,
University of South Carolina,
Columbia, United States

*Correspondence:

Hongshuang Ma
mahongshuang@jlu.edu.cn

Received: 27 July 2021

Accepted: 21 September 2021

Published: 27 October 2021

Citation:

Liu Y, Chen L, Shi Q, Zhao Q and Ma H
(2021) Tumor
Microenvironment-Responsive
Polypeptide Nanogels for Controlled
Antitumor Drug Delivery.
Front. Pharmacol. 12:748102.
doi: 10.3389/fphar.2021.748102

Keywords: nanogels, stimulus-responsive, drug delivery, polypeptide, nanoparticle, copolymer

INTRODUCTION

Cancer is a kind of disease with the highest mortality rate in the world. Although a variety of cancer treatments have been developed, such as gene therapy (O'Connor and Crystal, 2006), photodynamic therapy (Chen et al., 2002), photothermal ablation (Lal et al., 2008), immunotherapy (Riddell, 2001), and radiation therapy (Stupp et al., 2005), chemotherapy combined with surgical treatment is one of the most effective ways to cure cancers. Chemotherapy to cure cancers mainly rises to the challenge to selectively eliminate tumor cells without affecting normal tissues. Ideally, an antitumor drug will target tumor cells and be kept within a range expected to achieve the therapeutic effect for a long time. To this end, researchers have conducted a lot of research in the field of nanomedicine (Wei et al., 2021; Zheng et al., 2021) and developed a series of nanocarrier materials, such as dendrimers (Liu et al., 2011), micelles (Zheng et al., 2020), nanogels (Ma et al., 2021), mesoporous silica (Zhang L. et al., 2016), and carbon dots (Zeng et al., 2016).

The ideal drug delivery system should maintain enhanced tumor accumulation, effective cell uptake, and a controlled drug release rate, thereby improving the efficacy of drug delivery and minimizing the side effects of drugs. Nanogels are nanoscale gel particles with a stable three-dimensional swelling polymer chain cross-linked network (Gonçalves et al., 2014; Merino et al., 2015), and the inclusion of drugs in them can effectively avoid enzymatic degradation. Nanogels have high hydrogel water content, can shrink or swell according to changes in the external environment, have good passive targeting, and have the characteristics of long blood circulation time. Due to the enhanced permeability and retention (EPR) effect, nanosized particles are more likely to accumulate in the interstices of tumors, and sizes less than 100 nm are ideal for cancer drug delivery (Ramasamy et al., 2014; Sundaramoorthy et al., 2016). In the tumor microenvironment, factors such as low pH, a

TABLE 1 | Tumor microenvironment-responsive polypeptide nanogels for controlled antitumor drug delivery.

Material type	Material	Payload	Results	References
pH-responsive	poly (L-glutamic acid)/chitosan (PLGA/CS)	mitoxantrone	The nanogel has very good biocompatibility, and the drug-loaded nanogel has a significant inhibitory effect on tumor cells compared with free drugs	Yan et al. (2017)
	mPEG-b-PLG	DOX	Compared with the free drug, it increases the apoptosis of tumor tissues, shows an enhanced therapeutic effect, reduces systemic toxicity, and also improves the biodistribution, pharmacokinetics, and efficacy of the drug	Li et al. (2013)
	poly (MEO2MA-OEGMA-mBISS)	DOX	The nanogel has good biocompatibility, and the cytotoxicity is similar to that of the free drug after loading the drug	Mackiewicz et al. (2019)
	PEG-PASP-DOX	DOX	It exhibits obvious phototoxicity and synergistic toxicity to tumor cells and accumulates for a long time in tumors	Lu et al. (2014)
	PGA	DOX	Optimal impact on primary tumor growth, lung metastasis, and toxicologic properties	Arroyo-Crespo et al. (2018)
	Methoxy poly (ethylene glycol)-b-poly [N-[N-(2-aminoethyl)-2-aminoethyl] -L-glutamic acid]	DOX	The lethality of DOX in nanoparticles to cells is also higher than that of free DOX	Li et al. (2018b)
	MPEG-PEI-PBLL	DOX	Reduces systemic toxicity, has little effect on healthy cells, prolongs the circulation time, and improves the viability of mice	Yan et al. (2020)
Reduction-responsive	PEG ₁₁₃ -b-PPAL	DOX	The nanogel has good biocompatibility and has a better inhibitory effect on tumor cells	Yao et al. (2019)
	STP-NG	SHK	Good safety and can enhance tumor-specific affinity	Li et al. (2018a)
	mPEG-P(LP-co-LC)	DOX	Shows enhanced antitumor efficacy and safety, limits the recruitment of regulatory T cells and myeloid suppressor cells, and enhances the antitumor activity of CD8 + T cells	Liu et al. (2015) He et al. (2016) Feng et al. (2021)
	PLL-P(LP-co-LC)	HCPT	Enhanced apoptosis	Guo et al. (2017)
	R ₉ -PEG-P(LP-co-LC)	HCPT	Extend retention time and enhance drug penetration	Guo et al. (2020)
	PMNG	DOX	Good targeting and great advantages in inhibiting the growth of primary and metastatic tumors	Chen et al. (2017b)
	NIRF nanogel	DOX	Good accumulation in tumor cells	Xing et al. (2012)
ROS-responsive	PEG-PCys-Pphe	DOX	Reduce the loss of drugs and quickly release drugs in response to intracellular GSH levels	Wang et al. (2012)
	DCM	DOX	Reduce drug efflux, significantly reduce tumor volume, and cause no damage to major organs	Deepagan et al. (2016)
	PEG-b-PPGA	DOX	The structure is stable, the antitumor activity is better than that of free drugs, and the treatment tolerance is good	Kim et al. (2013)
Enzyme-responsive	mPEG-Peptide-PCL	DOX	Good targeting	Guo et al. (2018)
	Hep-F127	hydrated cisplatin and curcumins	High drug-loading efficiency and good slow and controlled release effect	Nguyen et al. (2018)
Temperature-responsive	PEG-PK-PA/HA	FITC-BSA	The nanogel can be tightened by heat shrinkage and high internalization efficiency	Ko et al. (2015)
	poly (N-isopropylacrylamide), poly (l-lactic acid), and poly (l-lysine)	NGF	It has no cytotoxicity to neuron-like PC12 cells for at least 1 month	Kim et al. (2018)
Light-responsive	SIPING	DOX	It has high delivery efficiency to prevent cell efflux and can release large amounts of drugs through near-infrared light	Chen et al. (2019)
	poly (Cys-PCL)	paclitaxel	It has excellent tumor suppression ability, good drug tolerance, and biological safety	Zhang et al. (2019)
	mPEG-b-P(LGA-co -CELG-dTbDEA)	DOX	It has good delivery effect, improved antitumor activity, and safety	Ding et al. (2013)
	Methoxy poly (ethylene glycol)-poly (L-glutamic acid-co-L-cystine)	DOX	It releases fast and shows excellent tumor suppression and safety	Shi et al. (2017)
	FD-NP	DOX	It can significantly improve cell binding and terminal/lysosome escape and high delivery efficiency <i>in vivo</i>	Yi et al. (2016)
	sPEG/GLC	miR155	Immunosuppressive TAM effectively repolarizes into antitumor M1 macrophages, increasing the activated T lymphocytes and NK cells in the tumor	Liu et al. (2017b)
	PC-g-PEG-LAC	DOX and 6-mercaptopurine	It has a targeting effect on the HepG2 cell line and has enhanced cytotoxicity compared to a single free drug	Wu et al. (2016)

(Continued on following page)

TABLE 1 | (Continued) Tumor microenvironment-responsive polypeptide nanogels for controlled antitumor drug delivery.

Material type	Material	Payload	Results	References
SNP		CA4P and BTZ	It reversed the drug resistance caused by the overexpression of ABCG2 and significantly inhibited tumor growth	Chen et al. (2020)

high reactive oxygen species (ROS) level, high glutathione (GSH) concentration, and high enzyme expression in the environment will cause the linker to break and release the drug. As a result, a nanogel with the characteristics of pH, active oxygen, reduction sensitivity, enzyme, temperature, and light response was designed (Figure 1).

Compared with traditional polymer nanogels, peptide nanogels have excellent characteristics, such as good biocompatibility, easy adjustment of performance, and release of safe and non-toxic products after degradation. Compared with polyester nanogels (Bahadur and Xu, 2012; He et al., 2014), the acidity increases due to the accumulation of carboxyl-containing molecules after degradation. The degradation products of polypeptide nanogels are mainly amino acids, which will not cause further side effects (Ding et al., 2011a; Tian et al., 2012; Zhang et al., 2015). In addition, due to the rich variety of amino acids, a variety of monomers can be selected to adjust the properties of the polypeptide nanogels. At the same time, the side chain of the polypeptide can further modify other functional groups through reactions such as transesterification, condensation, click chemistry, or aminolysis to prepare polyamino acids with different reactivities and biological activities. Therefore, in all drug delivery systems, the use of environmentally responsive polypeptide nanogels as a promising method to deliver antitumor drugs has attracted widespread attention. In this article, the environmentally responsive nanogels are divided into three categories: endogenous response, exogenous response, and multiple responses, and elaborated on the research progress in this area that has been made in recent years (Table 1).

NANOGE L SYNTHESIS METHOD

The preparation method of the polyamino acid nanogel is relatively simple and is usually divided into three kinds: 1) chemical cross-linking, 2) monomer polymerization, and 3) template method.

Chemical cross-linking refers to the formation of a cross-linked structure by connecting a polypeptide containing necessary side groups to a molecule with a multifunctional group and finally forming a nanogel. This is one of the most extensive methods used for preparing peptide nanogels. The side chain of the polypeptide can be further modified with other functional groups through reactions such as transesterification, condensation, click chemistry, or aminolysis to prepare polyamino acids with different reactivities and biological activities.

Monomer polymerization refers to the one-step ring opening polymerization (ROP) of amino acid monomers with two N-internal carboxylic anhydride groups (NCA) through a one-step polymerization method to obtain polyamino acid nanogels. There are not many amino acids that can be used in this method, and they are mainly used in reduction-responsive polypeptide nanogels.

The template method is used to construct a template so that the nanogel can form a shell on the surface and then eliminate the template to obtain a polypeptide nanogel. This method uses fewer, commonly used templates including gold nanoparticles, mesoporous silica, and so on.

These three methods have opened a broad spectrum for the synthesis of peptide nanogels and made the usage of responsive peptide nanogels possible.

SINGLE STIMULUS-RESPONSIVE NANOGE L S

Endogenous Tumor Microenvironment-Responsive Nanogels

Endogenous tumor microenvironment-responsive nanogels are a group of nanogels that selectively respond to the difference between the internal tumor environment and normal tissues and then release the loaded drug to avoid poor water solubility, poor distribution, and high toxicity of chemotherapeutic drugs to normal tissues. The common ones are mainly classified as follows:

pH-Responsive Nanogels

The upregulation of glycolysis, a near-universal trait of primary and metastatic cancers indicated based on clinical tumor imaging can give rise to glucose consumption and the production of metabolite lactic acid, which in turn leads to microenvironmental acidosis. Significantly different pH values between plasma (pH = 7.4) and the tumor extracellular microenvironment (pH = 6.5–7.2) and between lysosomes (pH = 4.5–5.5) and endosomes (pH = 5.5–6.8) (Kuppusamy et al., 2002; Wojtkowiak et al., 2011) provide a good trigger for drug release. From this observation, a pH-responsive drug delivery system has been developed and deeply explored. The existing preparation strategies mainly include hydrophilic–hydrophobic conversion and the introduction of pH-sensitive bonds.

The tumor extracellular microenvironment is weakly acidic due to the combination of acidic byproducts produced via tumor metabolism and high glycolytic activity due to impaired acid clearance, where the pH-responsive groups are protonated to trigger hydrophilic–hydrophobic conversion, separating drug

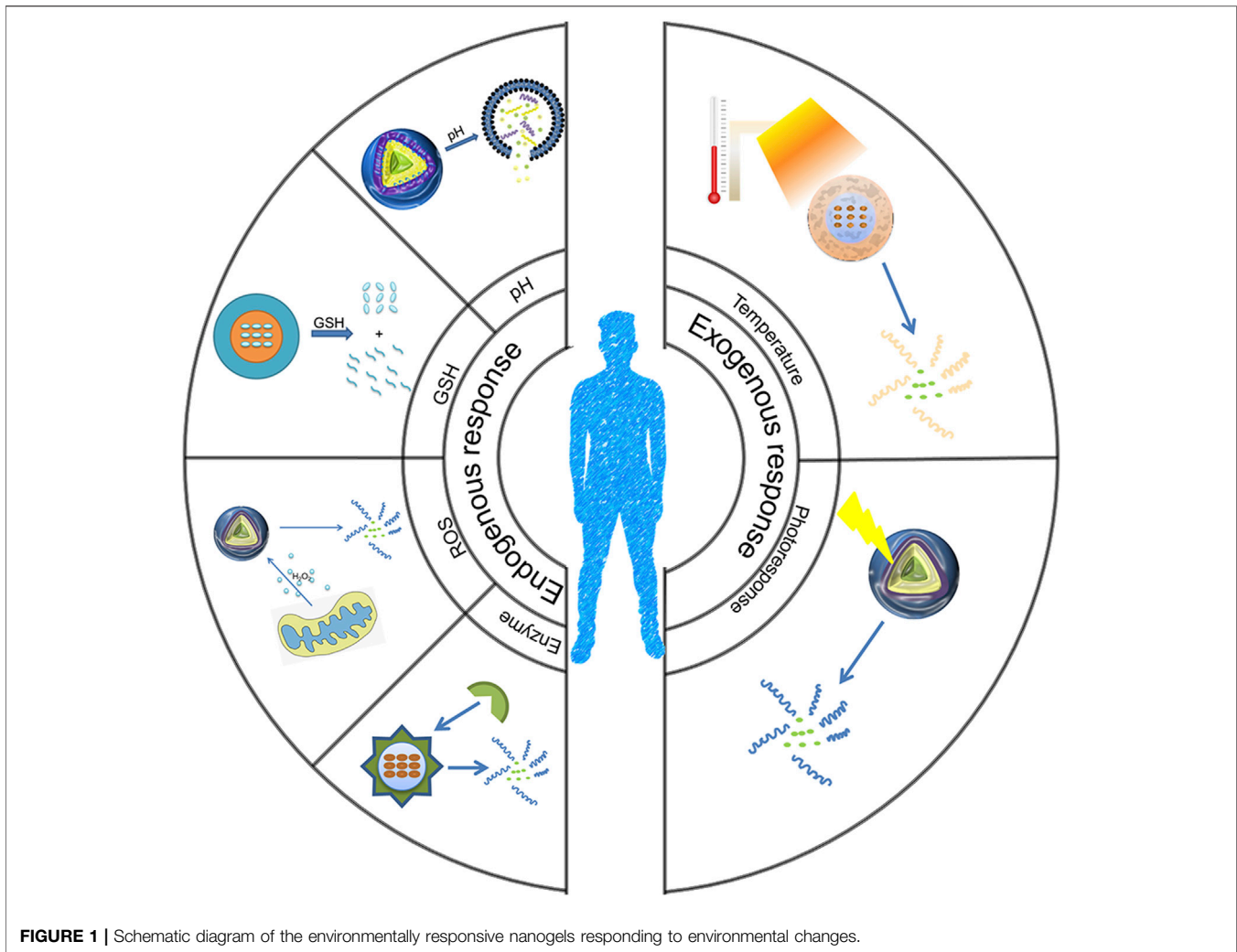


FIGURE 1 | Schematic diagram of the environmentally responsive nanogels responding to environmental changes.

molecules from the carrier and releasing them in the tumor tissue, thereby improving the efficiency of nanoparticle delivery.

Yan et al. (Yan et al., 2017) reported a method to synthesize a hollow nanogel poly (L-glutamic acid)/chitosan (PLGA/CS) loaded with the water-soluble antitumor drug mitoxantrone using a nanotemplate method with good biocompatibility. As shown in **Figure 2A**, the author grafted PLGA onto silica nanoparticles and then used CS as a cross-linking agent to finally remove the template silica. As shown in **Figure 2B**, the nanogel has a particle size of 189.3 nm under neutral conditions, and the size of the nanogel is significantly reduced when the pH value is 5–9. As shown in **Figure 2C**, the use of the MTT assay to study the cytotoxicity of PLGA/CS nanogels and drug-loaded nanogels *in vitro* shows that the biocompatibility of nanogels is very good, and the MTX-loaded nanogels perform well on tumor cells compared with free MTX, which shows a significant inhibitory effect. As shown in **Figure 2D**, the endocytosis of nanogels was evaluated using a fluorescence microscope. Rhodamine B (RB) was used as a model dye. The fluorescence signal of cells incubated with RB-loaded nanogels was much stronger than that of RB-treated cells. This is because CS

decorated on the surface of the nanogel can promote cell internalization. This will deliver higher concentrations of drugs into the cells (Wang et al., 2016). Therefore, this pH-sensitive nanogel synthesized by the nanotemplate method has great potential in smart drug delivery systems (Weigel and Yik, 2002).

Li et al. (Li et al., 2013) developed a polypeptide-based block ionomer complex composed of anionic methoxy(polyethylene glycol)-b-poly-L-glutamic acid and cationic doxorubicin hydrochloride for treating non-small cell lung cancer.

Compared with normal biological tissues, solid tumors can cause cell acidosis. Therefore, it is a current hotspot for introducing pH-sensitive bonds into nanogels.

Mackiewicz et al. (Mackiewicz et al., 2019) synthesized biocompatible degradable nanogels based on polyethylene glycol methyl methacrylate (OEGMA) and diethylene glycol methyl methacrylate cross-linked with redox-sensitive linker N,N-bis (methacryloyl) cystine to synthesize biocompatible and degradable nanogels. With the aid of the carboxyl group in N,N-bis (methacryloyl) cystine, the nanogels had become sensitive to pH, became more stable in the physiological

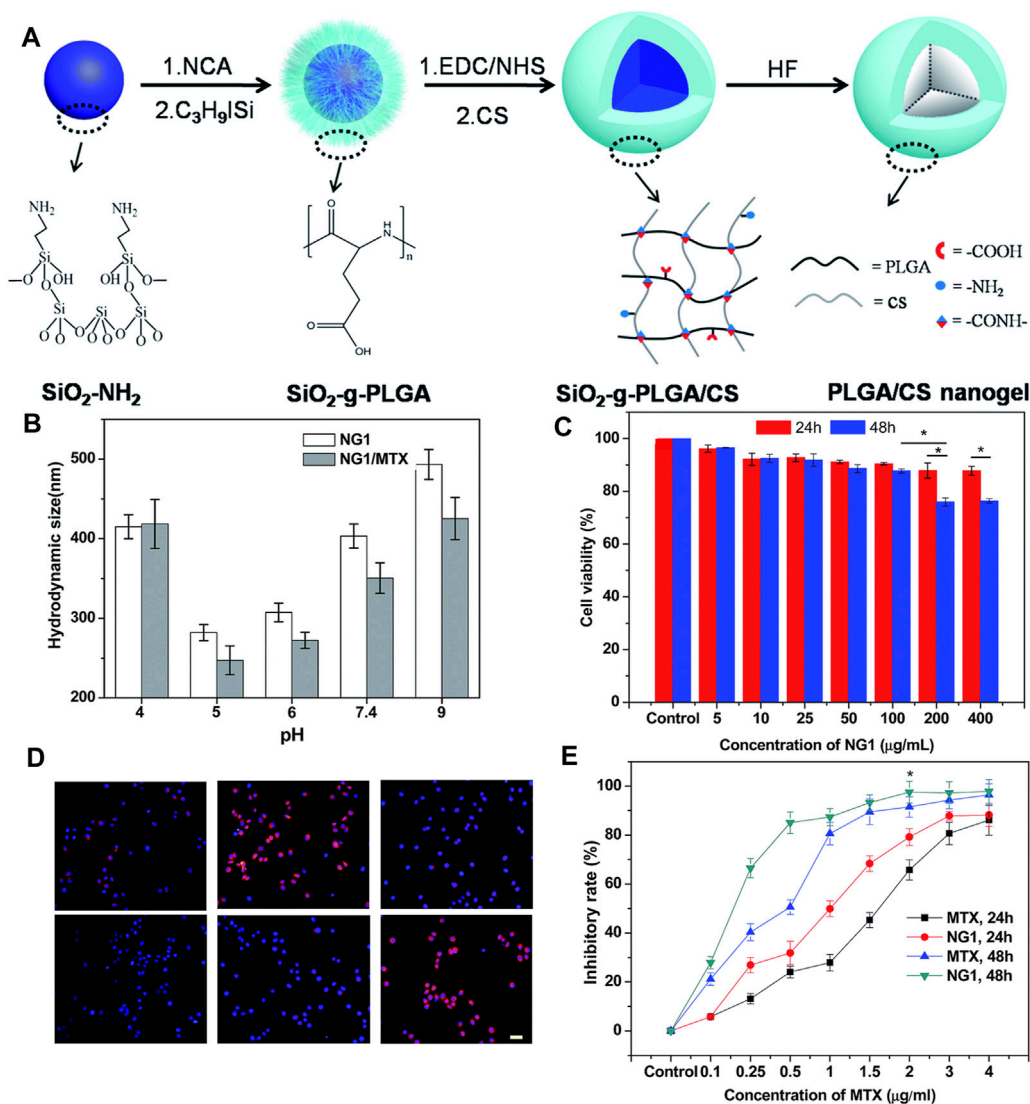


FIGURE 2 | Physical properties of PLGA/CS and the action of drugs (Yan et al., 2017). **(A)** Synthesis method of nanogels. **(B)** Change in particle size of nanogels at different pH. **(C)** Endocytosis effect of nanogels. **(D)** Inhibition rate of MTX-loaded nanogel and MTX on tumor cells. **(E)** Inhibition rate of MTX-loaded nanogel and MTX on tumor cells.

environment, and binded 8% DOX loaded through electrostatic interaction. This degradable nanogel was non-toxic to cells; however, the drug-loaded nanogel has a killing effect on cancer cells, similar to free DOX.

Lu et al. (Lu et al., 2014) formed a pH-responsive peptide nanogel by the hydrazone self-cross-linking of poly (asparagine sultaine-co-aspartyl hydrazide) and poly (asparagine sultaine-co-2-oxyethyl aspartame) under mild conditions. Hydrazone has been extensively studied in biomedical research due to its preparation under mild conditions and hydrolysis under acidic conditions (Bae and Kataoka, 2009). This nanogel has excellent stability and anti-protein adsorption ability. The nanogel has been stable in the PBS solution for 3 weeks and in the protein solution for at least 12 h. When the pH drops to 4.0, the size of the PAsp nanogel will change rapidly. With 18% drug loading rate, doxorubicin (DOX) as a model drug has been loaded onto the

nanogel, and the potential of the nanogel as a pH-sensitive drug delivery system was evaluated. When pH = 5.0, the nanogel released more than 70% of the drug in 12 h, and only about 25% of the drug was released at a pH of 7.4. In the *in vitro* cytotoxicity test, the nanogel showed good biocompatibility. Confocal microscopy results show that the loaded DOX can be successfully released and transported to the nucleus of the tumor cells. Therefore, this easily prepared nanogel is a promising, intelligent drug delivery system.

Arroyo-Crespo et al. (Arroyo-Crespo et al., 2018) developed a family of biodegradable poly (L-glutamic acid) (PGA) conjugates based on pH response, to optimize anticancer effects. DOX-loaded conjugates prepared using different pH-sensitive linkers to connect DOX and amino glutamine could promote specific drug release from the main polymer chain in the tumor microenvironment (TME). In a preclinical metastatic triple-

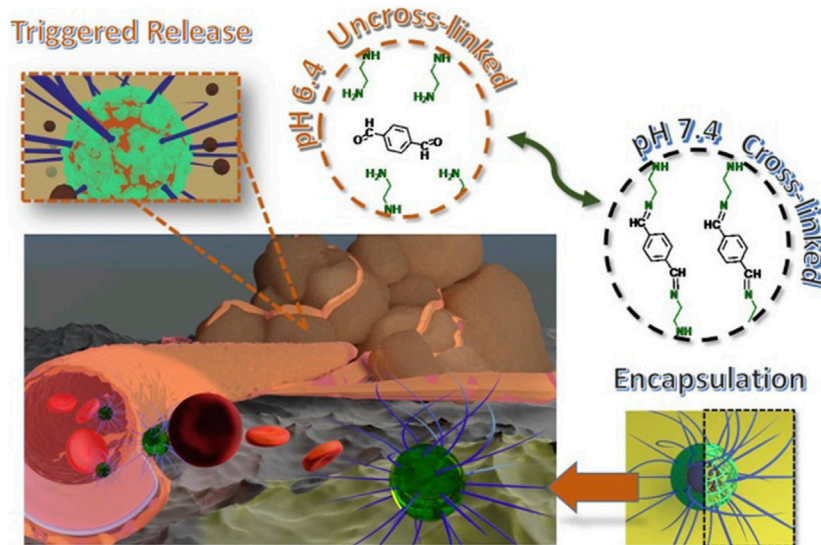


FIGURE 3 | Formation of pH-responsive mPEG-b-PNLG nanogels and the mechanism underlying drug delivery (Li Y. et al., 2018).

negative breast cancer (TNBC) mouse model, low DOX load and short linkers have the best effects on primary tumor growth, lung metastasis, and toxicologic properties. Juan et al. (Arroyo-Crespo et al., 2018) also determined the relevant molecular mechanisms through transcriptomics analysis, including differential immunomodulation between the conjugates and cell death pathways. Their efforts focus on the advantages of the targeted TME, the therapeutic value of polymer-based combined methods, and methods based on omics analysis that can enhance the anticancer performance of drug delivery materials.

Li et al. (Li Y. et al., 2018) proposed a new method to prepare pH-responsive nanogels by a simple one-step method. They used hydrophilic methoxy poly (ethylene glycol)-b-poly {N-[N-(2-aminoethyl)-2-aminoethyl]-L-glutamic acid} to construct a pH-responsive nanogel by a pH-sensitive benzimine bond. The acid-labile benzimine bond could be cleaved under weak acidic conditions (pH = 6.4) (Figure 3), and then the prepared nanogel could physically encapsulate the therapeutic molecules with high stability with the help of the mPEG shell, whereas, the core of the nanogel at physiological pH could minimize the non-specific absorption of its payloads and side effects. Once the drug-loaded nanogel system accumulated at the tumor site was exposed to the acidic conditions of the tumor, the core part could be quickly destroyed because of the rupture of the benzimine bond, resulting in enhanced drug accumulation at the tumor site. Compared with other pH-responsive nanogels, this nanogel has advantages in three aspects: 1) Preparation and drug loading of the nanogel can be completed in one step; 2) the polymer used is biodegradable and biocompatible, and the nanogel responds to subtle pH changes; and 3) a decrease in pH will trigger the release of the loaded drug and the dissociation of the nanogel, which makes it possible to remove the nanogel that has completed its mission.

Yan et al. (Yan et al., 2020) successfully synthesized a pH-responsive nanomaterial methoxy poly (ethylene

glycol)-b-polyethyleneimine-poly (N_ε-Cbz-L-lysine) (mPEG-PEI-PBLL), further improving its controlled release ability and drug loading efficiency. Schiff's base introduced into the polymer allowed the material to be responsive to changes in pH. mPEG-PEI-PBLL was degraded at pH = 5.0 and stabilized at pH = 7.4. mPEG-PEI-PBLL could self-assemble due to its amphiphilic property and effectively encapsulates the therapeutic agent by introducing PEI (hyperbranched copolymer). The drug loading index of the nanogel was about 25.8%. The PBLL block as a hydrophobic block can obtain a good degree of polymerization, and the polymer structure which was similar to the protein has very good biocompatibility. Moreover, therapeutic agents such as DOX and DiD, a near-infrared dye, were effectively contained in the pH-responsive nanogels. In this study, the biological properties of mPEG-PEI-PBLL nanogels were also evaluated by investigating *in vivo* cell absorption, biocompatibility, and pharmacokinetics. Cell uptake studies indicated that the absorption rate of DOX which was wrapped in the nanogels was much slower than free DOX, subsequently reducing systemic toxicity in the body. The biodistribution of the drug shows that nanogels can reduce excessive damage to healthy cells and tissues. Moreover, *in vivo* treatment and pharmacokinetic studies indicated that the nanogels could accumulate at the tumor tissue to inhibit the growth of the tumor while improving the survival of mice. These findings reveal that the drug delivery system prolongs the circulation of the drug in the blood and allows the drug to effectively accumulate at the tumor tissue.

Therefore, the nanogels prepared by these two strategies have very broad application prospects.

Reduction-Responsive Nanogels

GSH is an important chemical substance to determine the redox environment in the body. The concentration of GSH in normal

tissue cells (2–10 mmol/L) is 100–1,000 times that of the extracellular concentration. Because tumor cells are often deprived of oxygen, the concentration of GSH in tumor cells is at least four times higher than that in normal tissues and cells. Therefore, the tumor cell microenvironment has strong reducibility (Meng et al., 2009; Park et al., 2010; Sun et al., 2013; Huo et al., 2014; Phillips and Gibson, 2014). To this end, numerous studies have been conducted.

Cross-linking is the main component to prepare reduction-responsive nanogels. These kinds of agents are active units that contain disulfide bonds that can be reduced and form a 3D cross-linked redox-responsive network through the disulfide bond to load therapeutic drugs. These nanogels can be reduced by the reducing environment, thereby releasing their payload followed by biodegradation. Many redox reactive crosslinkers used in the synthesis of nanogels contain cystine and cystamine as reductive reactive components, terminal acrylates are involved in free radical polymerization reactions, and PEG was used as the functional backbone of the nanogels (Ma et al., 2010; Yu et al., 2011; Dispınar et al., 2012; Zhang Q. et al., 2013). Disulfide bonds are the main reporting structural units and important structural unit of reduction-reactive materials, which have excellent activity. When GSH or dithiothreitol are present, disulfide bonds will be broken to provide biodegradability and rapid drug release. To this end, disulfide bonds have been used to develop many reduction-responsive nanogels (Wu et al., 2009; Abdullah Al et al., 2013). This section mainly focuses on disulfide-bonded cross-linked nanogels from the perspective of cross-linking agents.

The first strategy is to prepare a disulfide bond cross-linked polypeptide nanogel by the addition of a disulfide bond-containing cross-linking agent into the polypeptide.

Yao et al. (Yao et al., 2019) developed a polypeptide nanogel, poly (ethylene glycol)-block-poly (ϵ -propargyloxycarbonyl-L-lysine) (PEG₁₁₃-b-PPAL) coupled with reducible side chains to deliver antitumor drugs. PEG₁₁₃-b-PPAL was synthesized by ROP of alkyne-containing NCA. Then, they introduced the disulfide bond-containing side chain into the PEGylated polypeptide by the click reaction. The obtained polymer self-assembled to form a nanogel and exhibited a reduction reaction when treated with 10 mmol/L GSH (Figure 4A). Then, DOX was loaded onto the nanogel at a percentage of 6.73wt and a loading efficiency of 40.3%. The average diameters of the blank and polylysine-derived polymer nanogel loaded with DOX (LMs/DOX) were about 48.0 and 63.8 nm, respectively (Figure 4B). *In vitro* drug release shows that doxorubicin can be released much quickly in the presence of GSH. CLSM and flow cytometry analysis further proved the sensitive release behavior of LMs/DOX to GSH and its ability to enhance the intracellular delivery of DOX. MTT results showed negligible cytotoxicity of the polymer to normal cells L929 or cancer cells MCF-7 (Figure 4C). With the increase of DOX concentration, there was a better anti-proliferative activity in MCF-7 cells in LMs/DOX, LMs/DOX/GSH, and DOX HCl groups. When the concentration of DOX was lower than 2.5 mg/L, the cell viability of the nanogel group was lower than the free-drug group, and the cell viability of LMs/DOX with GSH was lower than LMs/DOX. This may be due to the fact that GSH

pretreatment triggers faster release of DOX, resulting in a stronger inhibition of proliferation in MCF-7 cells (Figure 4D). These findings indicate that LMs/DOX have broad prospects in cancer treatment.

The second strategy is to use cystine with a disulfide bond to polymerize and to prepare cross-linked polypeptide nanogels.

Li et al. (Li S. et al., 2018) attempted to reinforce the inhibition of osteosarcoma and lung metastasis by drug-induced necrosis. As shown in Figure 5A, they used a sarcoma-targeting peptide-modified disulfide-bonded cross-linked polypeptide nanogels (STP-NG) to enhance the intracellular delivery of shikonin (SHK), thereby inhibiting the progression of osteosarcoma with minimal systemic toxicity. This study confirmed the ability of STP to target 143B cells. As shown in Figures 5B–D, STP could specifically bind to cell surface vimentin in osteosarcoma, but does not bind to cell surface vimentin-deficient hFOB1.19 cells and blood cells (Satelli et al., 2014). Due to this difference, an ideal efficacy and minimal toxicity can be obtained. In addition, due to the targeting effect of STP-NG/SHK, higher membrane binding force has been observed, thereby increasing the cellular uptake of NG/SHK that could selectively accumulate in 143B osteosarcoma *in situ* (Figure 5E). RIP1- and RIP3-dependent necrosis *in vitro* proved that the inhibitory effect of STP-NG/SHK on cell proliferation was enhanced (Figures 5F,G). This animal experiment showed excellent antitumor efficacy of STP-NG/SHK (Figures 6A–E), and metastatic osteosarcoma in the STP-NG/SHK group was mostly suppressed (Figures 6F,G). These data prove that STP-NG/SHK profoundly inhibits osteosarcoma metastasis to the lungs. This excellent anti-metastatic effect was caused by intracellular drug release and tumor targeting. STP-NG/SHK targeting cell surface vimentin was related to epithelial-to-mesenchymal transition, and it is critical for metastasis (Satelli and Li, 2011). As shown in Figure 6H, SHK mainly damages the myocardium, whereas the abnormalities in other organs were minimal. H and E staining showed that compared with free SHK, NG/SHK and STP-NG/SHK showed much lower myocardial damage. These results indicate that coating drugs with nanogels can reduce systemic toxicity and improve biological safety, and STP can further effectively enhance tumor-specific affinity. Therefore, the intelligent drug delivery system equipped with SHK has great significance for VIM-targeted malignant tumor chemotherapy.

Feng et al. (Feng et al., 2021) synthesized three kinds of mPEG-P (LP-co-LC) nanogels with different L-cysteine scales, including mPEG-P (LP₁₀-co-LC₁₅) (NG₁₀₋₁₅), mPEG-P (LP₁₀-co-LC₁₀) (NG₁₀₋₁₀), and mPEG-P (LP₁₀-co-LC₅) (NG₁₀₋₅). They evaluated the pharmacokinetic properties, tissue distribution, and antitumor efficiency of these nanogels with similar surface charge, morphology, and reductive reaction characteristics. As the degree of polymerization of L-cysteine in the nanogels increased from five to 15, the size of the nanogels also increased from 105 to 256 nm. Researchers found that NG₁₀₋₅ has the best stability in physiological environments. Compared with other two nanogels, NG₁₀₋₅ could migrate to the tumor faster and accumulate for a longer time after intravenous injection. These results indicate that the size of the nanoparticles was more

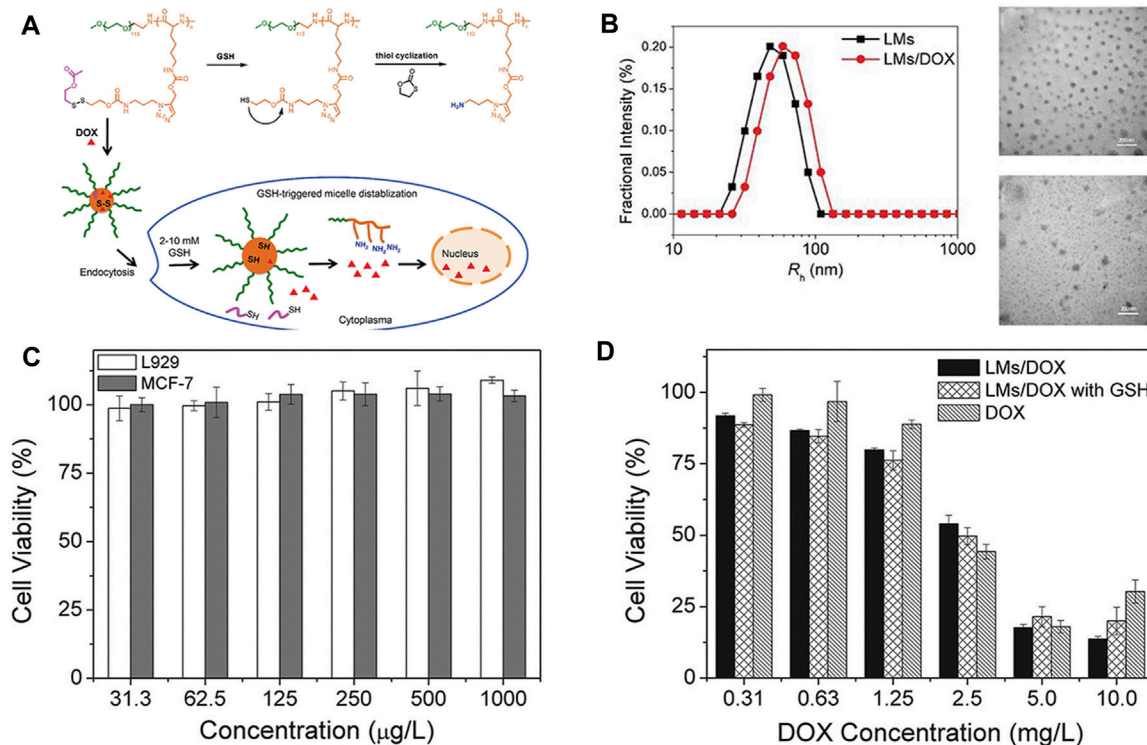


FIGURE 4 | Chemical structure of the PEG₁₁₃-bP (Lys-DSA) polymer thiol reaction and *in vitro* and *in vivo* experimental characterizations (Yao et al., 2019). **(A)** Schematic diagram of the chemical structure of the polymer thiol reaction and the reduction-sensitive DOX release behavior after LMs/DOX endocytosis. **(B)** Hydrodynamic radius and TEM images of blank and drug-loaded nanogels. **(C)** Cytotoxicity of nanogels on L929 cells and MCF-7 cells *in vitro*. **(D)** Cytotoxicity of DOX-loaded nanogels and free DOX.

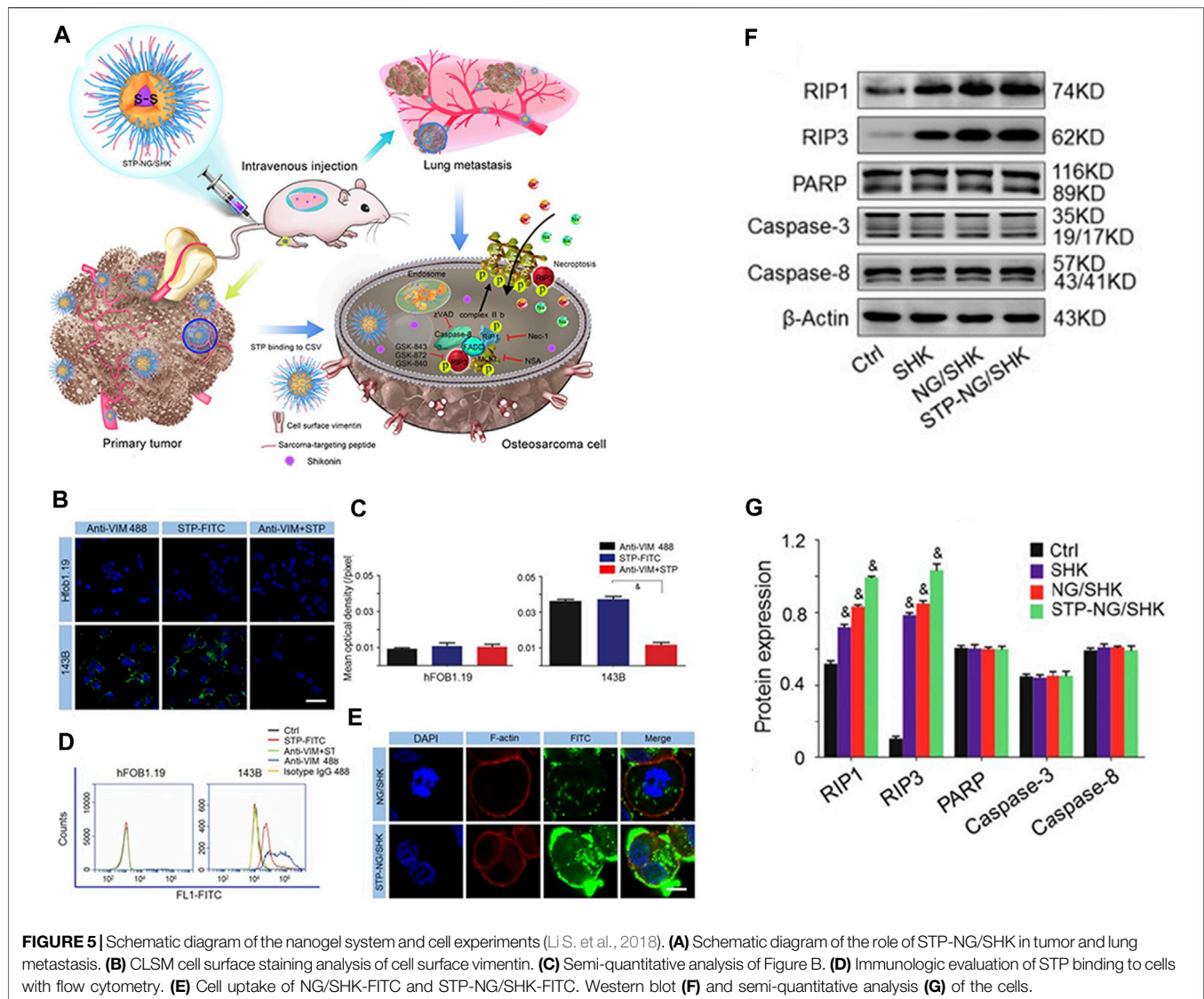
influential than that of polymers. Compared with the other two nanogels, NG_{10.5}/DOX maintained a higher blood concentration and retained more drugs in the tumor. The improvement in the pharmacokinetics of NG_{10.5}/DOX may result from slower liver clearance and more accumulation in the tumor. In addition, among these three preparations, NG_{10.5}/DOX has optimal antitumor efficacy on 4T1 breast cancer. On this basis, Feng et al. (Feng et al., 2021) used mPEG-P (LP-co-LC) to co-encapsulate DOX and 1-methyl-DL-tryptophan (1 MT) referred as NG/(DOX + 1 MT) for 4T1 breast cancer treatment. By reducing the dose of DOX required to induce immunogenic cell death-inducing (ICD), the author achieved the goal of reducing the toxicity of mice and inducing the ICD of cancer cells at the same time. The drugs in NG/(DOX + 1 MT) were released in the tumor cells at the same time, and they have a synergistic antitumor effect. Nanogels exhibit excellent performance by downregulating the expression and activity of indoleamine 2,3-dioxygenase, limiting the recruitment of regulatory T cells and myeloid suppressor cells, and enhancing the antitumor activity of CD8⁺ T cells (Holmgaard et al., 2015; Peng et al., 2018; Huang et al., 2019).

Liu et al. (Liu et al., 2015) prepared a reduction-reactive nanogel methoxy poly (ethylene glycol)-poly (L-phenylalanine-co-L-cystine) (mPEG-P (LP-co-LC)) with a medium drug loading of 10.2 wt% and a diameter of less than 110 nm. DOX was used as

a model antitumor drug loaded onto the nanogels to treat liver cancer in rodent models. The drug-loaded nanogels accumulated in the tumor tissues and released their payload rapidly due to the redox environment in tumor cells after the nanogels entered the cells. The toxicity of the loaded drug was mitigated because of stable encapsulation with the nanogels, and less drug leakage enhanced the retention and permeability effect. Compared with free drugs, the selective intratumoral release of DOX targeting intracellular reduction enhanced the antitumor efficacy of the drug-loaded nanogels.

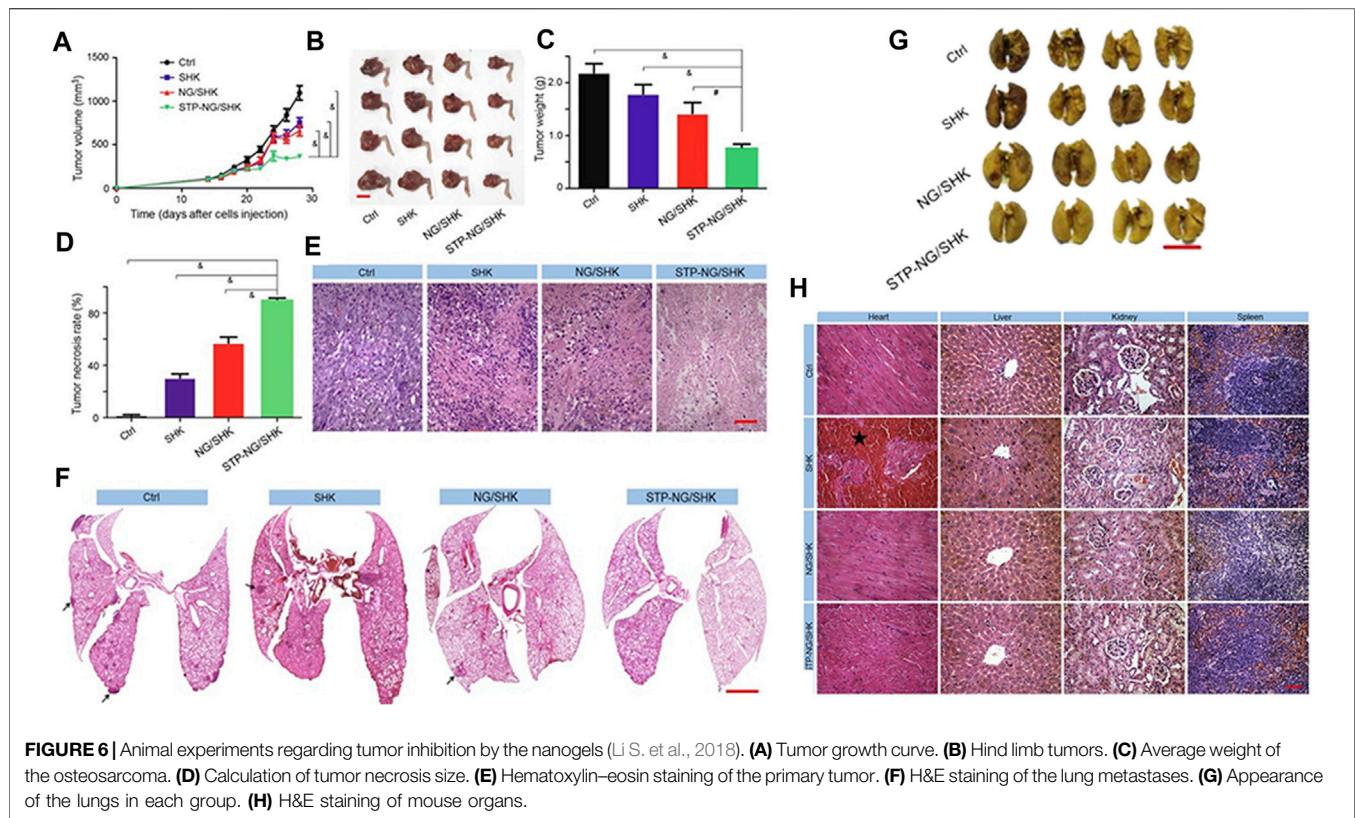
He et al. (He et al., 2016) used mPEG-P (LP-co-LC) nanogels for RM-1 prostate cancer chemotherapy. DOX acted as a conventional chemotherapeutic drug to be embedded in the nanogels. Based on the drug-loaded nanogels labeled as NG/DOX, GSH induced cell swelling and promoted the release of DOX. Subsequently, NG/DOX presented with effective cell uptake and proliferative inhibition. In addition, NG/DOX showed enhanced antitumor efficacy and safety in the mouse model of RM-1 prostate cancer transplantation, indicating that it has a huge therapeutic potential in clinical practice.

In the study by Guo et al. (Guo et al., 2017), poly (L-lysine)-poly (L-phenylalanine-co-L-cystine), delivered 10-hydroxycamptothecin (HCPT) into BC cells *in situ*. The drug-loaded nanogel was labeled as NG/HCPT. NG/HCPT increases retention time and improves tissue permeability, thereby



promoting cancer cell uptake and intracellular activation of HCPT. Positively charged poly (α -lysine) allows the nanogel to bind to the negatively charged bladder mucosa. Thereby, NG/HCPT was given a mucosal adhesion. In addition, the amphiphilic nanogel with α -lysine residues will allow HCPT to enter cells similarly to amphiphilic cell-penetrating peptides (CPPs) (Shin et al., 2014). Cystine offers an opportunity that the disulfide bonds in the NG/HCPT core can be selectively degraded by intracellular GSH, which further accelerates the release of HCPT, thereby enhancing cell apoptosis (Wang J. et al., 2014; Lin TY. et al., 2016). This feature can reduce the dosage and avoid the potential risk of drug resistance due to high-dose administration. Based on this, Guo et al. (Guo et al., 2020) prepared a positively charged disulfide bond cross-linked nanogel, oligoarginine-PEG-P (LP-co-LC) (R9-PEG-P (LP-co-LC)), which further increases the residence time and enhanced the penetration ability of chemotherapeutics into the bladder wall. CPPs were less cytotoxic and can penetrate through the cell

membrane to transport the “cargo” (Douat et al., 2015; Meloni et al., 2015). The combination of CPPs and antitumor drugs is becoming an attractive opinion to enhance the treatment effect (Shi and Qi, 2017). Arginine-rich CPPs have been confirmed with a high-efficient cellular uptake, especially the oligoarginine which contains nine arginine residues (Li et al., 2015; Zhang N. et al., 2016). Therefore, R9 upregulates the mucosal adhesion of the HCPT-loaded R9-PEG-P (LP-co-LC) (R9 NG/HCPT) through an electrostatic interaction with the negatively charged bladder, further promoting the permeability of the drug-loaded nanogel in the bladder wall. In addition, as a CPP, R9 effectively penetrates the cell membrane and transports the drugs. The disulfide bond gives the nanogel the function of selectively delivering HCPT in the cell through the reducing microenvironment. R9 NG/HCPT exhibits excellent cytotoxicity to human BC 5637 cells *in vitro* and significantly enhances the antitumor activity in mouse and rat orthotopic BC models *in vivo*.



Chen et al. (Chen et al., 2017b) synthesized morpholine and phenylboronic acid dual-modified polypeptide nanogels (PMNG) to conform receptor-mediated targeting and microenvironment-mediated targeting into a drug delivery system. Phenylboronic acid was used for selective receptor-mediated targeting in the highly metastatic cells, overexpressing sialyl on the membrane (Matsumoto et al., 2010; Sanjoh et al., 2014). Charge-transformable morpholine was neutral at physiological pH, and it has a positive charge in tumor tissues, which can be used to enhance cellular internalization in the tumor microenvironment (Zhang Y. et al., 2013; Guo et al., 2015). The nanogels were cross-linked by the core of disulfide bonds, which can be disassembled by intracellular GSH to selectively release DOX. PMNG has an excellent ability to target primary and metastatic B16F10 tumors, overexpressing sialyl *in vitro* and *in vivo*. In addition, PMNG/DOX has shown great advantages in inhibiting the growth of primary and metastatic tumors.

Xing et al. (Xing et al., 2012) prepared reduction-sensitive polymer nanocarriers with near-infrared fluorescent probes. They first synthesized a disulfide bond cross-linked polypeptide nanogel (NIRF nanogels) with near-infrared fluorescence properties and then encapsulated DOX in the core of the nanogels to prepare a near-infrared fluorescent drug carrier (NIRF prodrug). *In vitro* drug release studies of NIRF prodrugs have shown that there was an accelerated release in the environment where exists 10 mmol/L GSH. Studies on cell uptake of NIRF nanogels and NIRF prodrugs have indicated that

they can enter cells through cellular endocytosis. NIRF labeling can directly describe the drug release from the NIRF nanogels using imaging methods, and subsequently the released drug molecules migrate to the nuclei, while the NIRF nanogel remains in the cytoplasm. The *in vivo* distribution of NIRF nanogels and NIRF prodrugs on tumor-bearing mice indicates that they all accumulate at the tumor site 24 h after injection through enhanced retention effect and permeability. This accumulation may be attributed to the highly permeable vascular structure of the tumor, which leads to the accumulation of nanomaterials (Ichikawa et al., 2004). The NIRF prodrugs that were prepared in these studies have antitumor potential.

The third strategy is to oxidize polypeptides containing sulfhydryl groups to prepare disulfide bond cross-linked polypeptide nanogels.

Wang et al. (Wang et al., 2012) prepared poly (ethylene glycol)-b-poly (L-cysteine)-b-poly (L-phenylalanine) (PEG-PCys-PPhe) by ROP. As shown in **Figure 7A**, self-assembled into a micelle with a core shell structure in an aqueous solution, the shell has self-crosslinked by the oxidation of the thiol group, and finally a disulfide-bonded cross-linked nanogel with reduction responsiveness was obtained. Glue, even in harsh environments can maintain the stability of the nanogels. As shown in **Figure 7B**, the hydrodynamic radius measured by DLS was about 150 nm, whereas the average diameter measured by TEM was about 50 nm. As shown in **Figure 7C**, *in vitro* drug release studies have shown that nanogels can reduce

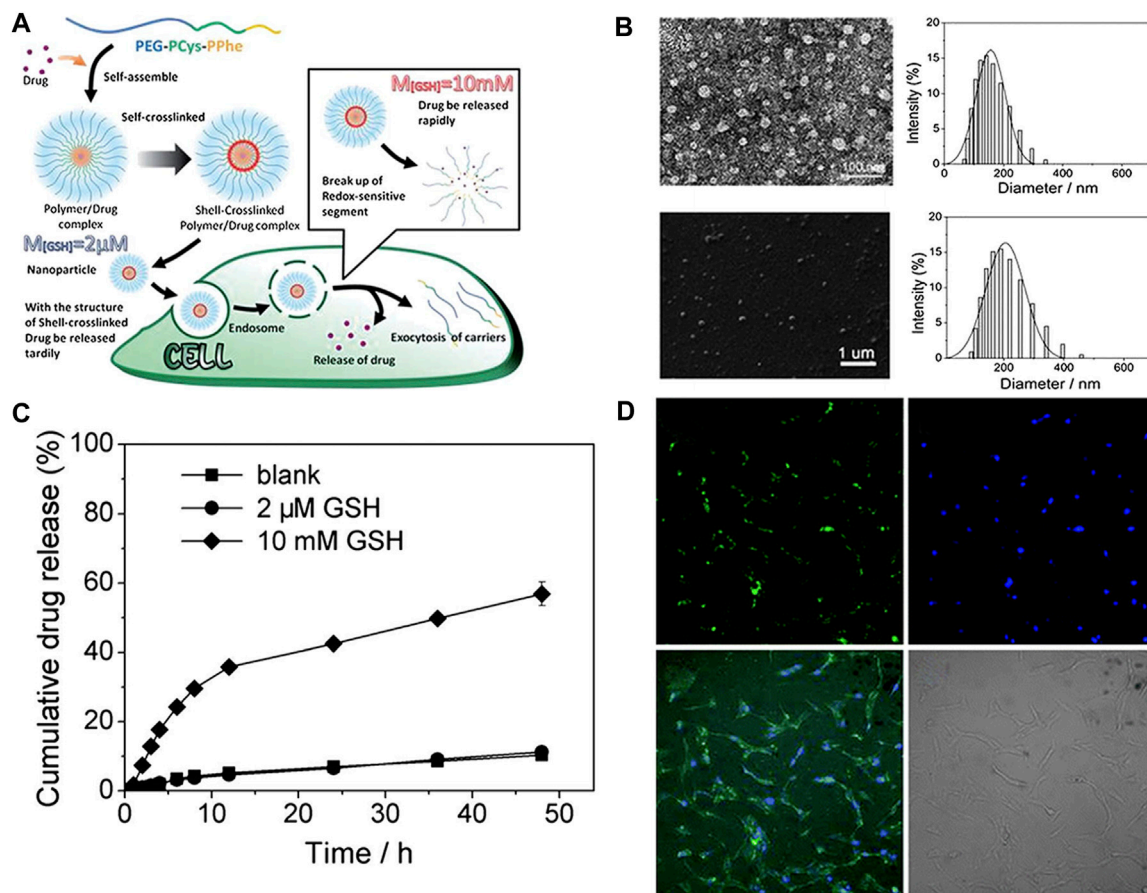


FIGURE 7 | Characterization of self-assembly process and drug release of the nanogels (Wang et al., 2012). **(A)** Self-assembly process and drug release of the nanogels. **(B)** TEM image and particle size distribution of nanogels and the scanning electron microscope image and particle size of nanogels in the tetrahydrofuran solution. **(C)** Drug release of PEG-PCys-PPhe. **(D)** Confocal laser scanning microscopy (CLSM) image regarding co-incubation of HeLa cells and PEG-PCys-PPhe.

drug loss and accelerate drug release due to high GSH levels in the cell. As shown in **Figure 7D**, the cell uptake experiment results showed that the nanogels can be successfully internalized into HeLa cells because all cells exhibited green fluorescence.

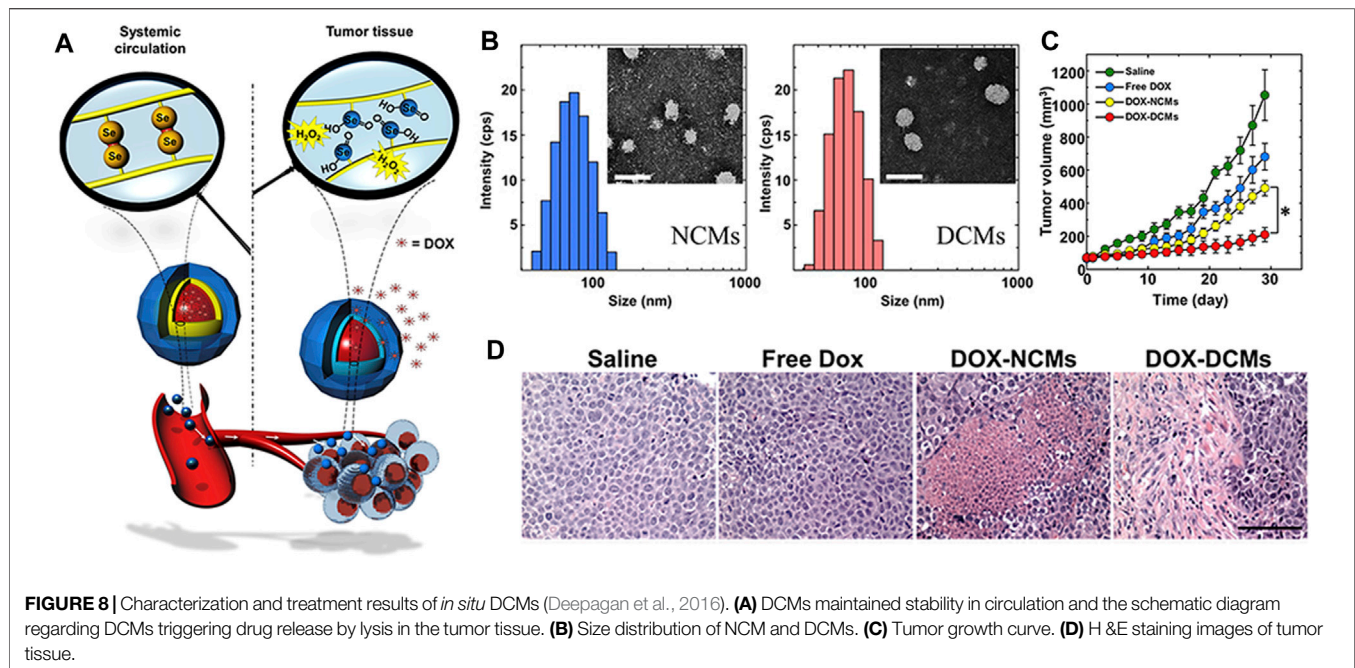
In summary, because the disulfide bond contained in cystine can be quickly broken under a high GSH environment, thereby releasing a large amount of drug, this method can greatly improve the therapeutic efficiency of the drug.

Reactive Oxygen Species-Responsive Nanogels

ROS play an important role in cell signal transduction. They are involved in various signal paths, such as mediating inflammation, cell growth and differentiation, and regulating enzyme activity. Reactive oxygen species mainly exist in hydrogen peroxide, superoxide, and hydroxyl radicals (Lee et al., 2013) and are highly reactive. It is worth noting that normal cells have a stable redox environment and have a series of systems to remove and balance ROS levels. An increase in the ROS level may destroy intracellular homeostasis and cause oxidative damage to lipase and DNA, thereby leading to a series of diseases. Cancer cells with abnormal regulation of redox homeostasis and stress adaptability are more susceptible to

oxidative stress induced by ROS generators, which is a significant basis for ROS therapy to work. ROS-responsive drugs can kill cancer cells selectively and reduce the damage to normal cells. At present, ROS-responsive nanodrugs, microspheres, and polymers have been well-studied. However, there are only a few reports on ROS-responsive nanogels (Liu JN. et al., 2017; Bawa and Oh, 2017; Dharmaraja, 2017).

Deepagan et al. (Deepagan et al., 2016) developed *in situ* diselenide-cross-linked nanogels (DCMs) that, as anticancer drug carriers, can respond to abnormal ROS levels in tumor areas. The DCMs were derived spontaneously from selenol-loading triblock copolymers that were composed of polyethylene glycol and polypeptide derivatives. As shown in **Figure 8A**, DOX was effectively encapsulated in the hydrophobic core during the formation of nanogels. The DCMs maintained their stability in blood. However, when DCMs enter into ROS-rich tumor tissues, the hydrophobic diselenide bond of the DCMs was broken into hydrophilic selenic acid derivatives, which triggers the drug release from DOX-encapsulating DCMs (DOX-DCMs). As shown in **Figure 8B**, both DCMs and non-crosslinked micelles (NCMs) were spherical with the feature of a single peak size distribution. The average diameter of NCM and



DCMs was about 65.48 and 85.10 nm, respectively. Least absorption of these nanoparticles by the reticuloendothelial system was observed (Blanco et al., 2015). The DCMs have great structural stability, even in the presence of destabilizing agents, and the DCMs maintained structural stability for at least 6 days under physiologic conditions. The diselenide cross-linking of DOX-DCMs, as a diffusion barrier, can effectively control the release of DOX. However, more DOX was released from DOX-DCMs within 3 days in the presence of H_2O_2 (100 μM). Moreover, enhanced drug release inhibited the efflux of p-glycoprotein (Wang et al., 2011). As shown in **Figure 8C**, compared with other treatments, DOX-DCM treatment greatly reduced tumor volume. As shown in **Figure 8D**, the hematoxylin–eosin staining images confirmed that DOX-DCM treatment resulted in the presence of a larger amount of dead cells in tumors, but the damage to the main organs can be ignored.

Enzyme-Responsive Nanogels

The enzyme is a kind of biological-related stimulant that can be overexpressed at the edge of tumor invasion and can also be used as a trigger to control the release of the drug. Currently, the main targets are matrix metalloproteinase and cathepsin B.

Kim et al. (Kim et al., 2013) synthesized partially hydrophobically modified polypeptide poly (ethylene glycol)-b-poly (l-glutamic acid) (PEG-b-PPGA) with L-phenylalanine methyl ester moieties and then used it for the synthesis of the template of nanogels. Then, Ca^{2+} was added to make it condense (**Figure 9A**). The resultant nanogels exhibited features that were similar to those of the hydrogels due to the protonation of the carboxyl group and the pH-dependent helical performance of the PPGA segment. Then, they loaded DOX onto the nanogel at high drug capacity. Under strong destabilization conditions (urea), nanogels maintained their firm structure, but they can be

destroyed rapidly by enzymatic degradation. As shown in **Figure 9B**, the DOX-loaded nanogel can regulate the release of drugs and control the of the nanogel by lysosomal capture. DOX-loaded cross-linked nanogels show lower cytotoxic activity than free DOX. The reduction of cytotoxicity was consistent with the degradation of the nanogels. In addition, as shown in **Figure 9C**, biodegradable PEG nanogels provided sufficient DOX concentration to inhibit tumor growth in xenograft mouse models of ovarian cancer. Due to the retention effect and enhanced permeability, nanogel particles accumulated in solid tumors. The increase in the circulation time of nanogels (Oberoi et al., 2012) also increases the contact between the tumor and drug. Nanogels have stronger antitumor activity than free adriamycin. In addition, as shown in **Figure 9D**, there was no significant change between the body weight of the control and treatment groups, suggesting that all treatments were well tolerated.

Guo et al. (Guo et al., 2018) successfully synthesized a tri-block copolymer mPEG-Peptide-PCL, a kind of novel enzyme-responsive nanoparticle. The copolymer can respond to matrix metalloproteinase which is active and overexpressed in cancer, and, therefore, it can be used to guide targeted therapy. In this copolymer, the role of PCL was to load drugs. The peptide was used to target the tumor. The peptide GPLGIAGQ was designed to be degraded by matrix metalloproteinase-2 (Kratz et al., 2001). Cell-penetrating peptide R9 could promote the cellular uptake of nanoparticles (Wang HX. et al., 2014). PEGylation can improve the stability of the nanogel and extend its circulation time *in vivo*. *In vitro*, these scholars also evaluated the cumulative release rate of curcumin, as a model drug, under different pH conditions. In addition, they also assessed the cytotoxicity and cellular uptake in L929 and NSCLC A549 cells. *In vivo*, Guo et al. (Guo et al., 2018) characterized the selective targeting and biodistribution of

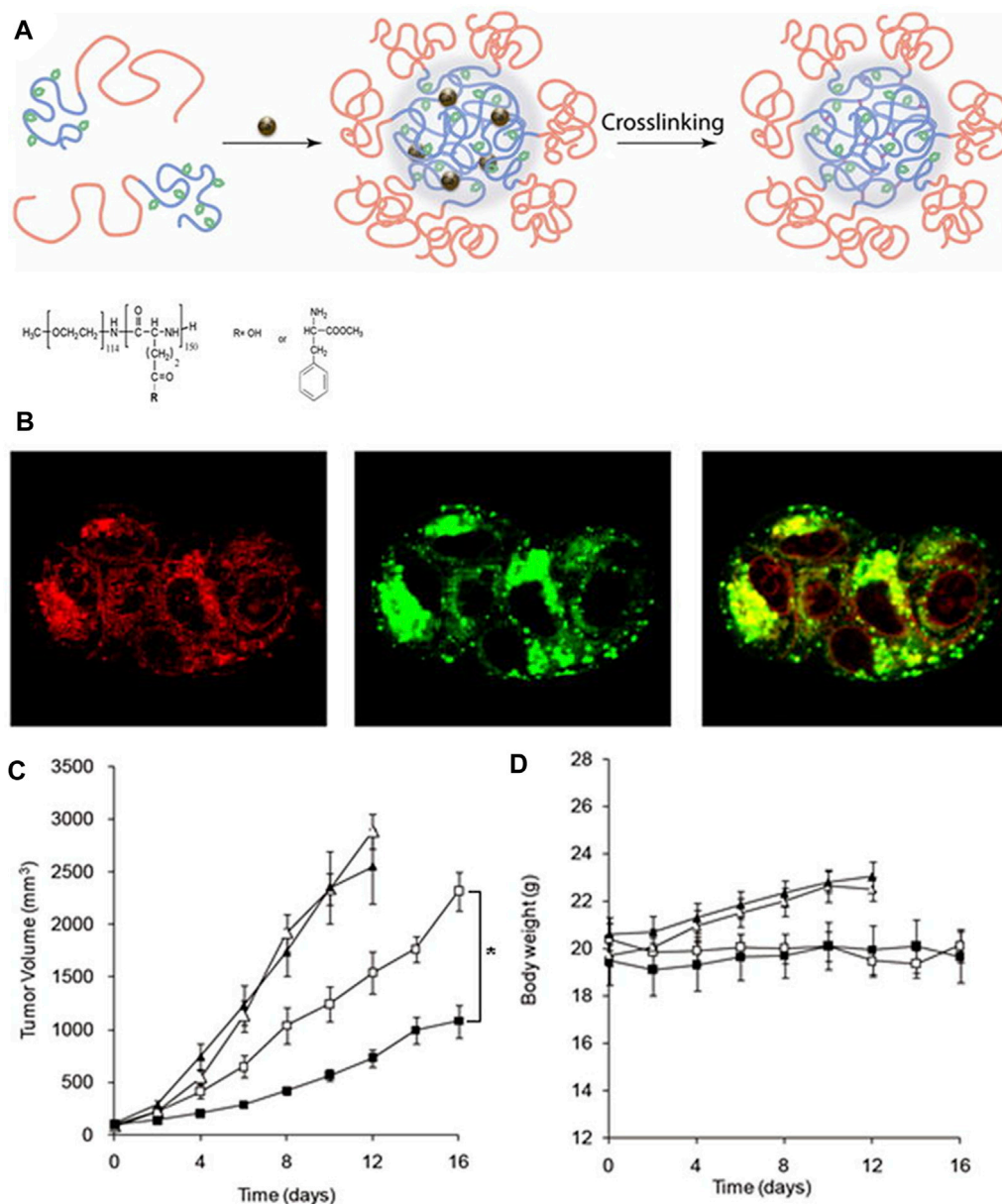


FIGURE 9 | Synthesis and biological characterization of nanogels (Kim et al., 2013). **(A)** Schematic diagram of nanoparticle self-assembly. **(B)** Localization of DOX-loaded nanogels in cells. Effects of DOX-loaded nanogels on the tumor volume **(C)** and body weight **(D)**.

mPEG-peptide-PCL using an *in vivo* imaging system because of the strong fluorescence effect of curcumin.

In summary, the enzyme-responsive nanogel is released in response to biological enzymes, which has very good biological targeting and safety properties.

Exogenous Stimuli-Responsive Nanogels

Exogenous stimuli can also influence the structure of nanogels and promote the release of nanogels in a responsive manner. Compared with endogenous stimuli-responsive nanogels, exogenous stimuli-responsive nanogels can be better controlled, and, therefore, exogenous stimuli-responsive

nanogels release drugs more accurately. Exogenous stimuli-responsive nanogels mainly consisted of temperature-responsive and photoresponsive nanogels. Similar to endogenous stimuli-responsive nanogels, the mechanism of exogenous stimuli-responsive nanogels is that the exogenous stimuli promote the drug release rapidly by disrupting the internal cross-linking network of polypeptide nanogels, which results in expansion or chemical bond breakage.

Temperature-responsive Nanogels

Nanogels can also be designed to release drugs under exogenous stimulation (especially temperature) (Gao and Dong, 2017). The

molecular structure of temperature-responsive nanogels usually contains functional groups, such as amides, ether bonds, and hydroxyl groups. Nanogels can respond to changes in external temperature through rapid volume changes, and a discontinuous volume phase transition occurs at a specific temperature, leading to the controlled release of drugs from these nanogels (Lin J.-Y. et al., 2016). This temperature is called lower critical solution temperature (LCST). When the temperature is below the LCST, nanogels are in a swollen state. When the temperature is above the LCST, the nanogels rapidly lose water and shrink, thereby exhibiting a response to temperature (Kujawa and Winnik, 2001).

Nguyen et al. (Nguyen et al., 2018) synthesized a thermosensitive copolymer heparin-Pluronic F127 to co-encapsulate cisplatin and curcumins to form a dual-drug delivery system. The interaction between hydrated cisplatin and curcumins and the properties of amphiphilic heparin-Pluronic F127 greatly improved not only the working efficacy of the controlled release system but also the drug loading efficiency. The anti-proliferative activity determined by *in vitro* and xenograft tumor tests revealed that in-depth studies were needed to investigate the uses of this delivery system against various cancers and drug-resistant cancers because of the synergistic activity of bioactive phytochemical and anticancer drugs in nanocarriers.

To deliver fluorescein isothiocyanate-conjugated bovine serum albumin, Ko et al. (Ko et al., 2015) designed temperature-sensitive tri-block nanogels using ionic complexes of hyaluronic acid (HA) and poly (ethylene glycol)-poly (L-lysine)-poly (L-alanine) which are called PEG-PK-PA. The PA block formed a hydrophobic nanocore. The positively charged PK block was compounded with the negatively charged HA block. PEG formed the outer shell of nanogels and prevented random aggregation of nanogels during the formation of ionic complexes. As shown in **Figures 10A–C**, nanogels have unique reversible temperature sensitivity. Therefore, nanogels shrink when heated. The internalization efficiency of nanogels could be controlled by adjusting the Zeta potential and size of nanogels and by greatly reducing the cytotoxicity of positively charged nanogels through the formation of ionic complexes with negatively charged HA. As shown in **Figure 10D**, the internalization of the model drug increased greatly if the ζ^+ and ζ^0 systems were used, and it was very low if the ζ^- system was used. Moreover, the use of the ζ^0 system led to the most excellent internalization efficacy. As shown in **Figure 10E**, the MTT assay showed that the ζ^0 and ζ^- systems have a significant improvement in cell compatibility compared with the ζ^+ system. This occurred because the ionic interaction between the positively charged ζ^+ system and the negatively charged cell membrane damages the cell membrane and induces cytotoxicity (Hunter, 2006; Kurosaki et al., 2009). Therefore, the negatively charged HA shield was combined with the positively charged PEG-PK-PA nanogel to reduce cytotoxicity. Filipin, rottlerin, and chlorpromazine are specific inhibitors of caveolae-mediated endocytosis, micropinocytosis, and clathrin-mediated endocytosis, respectively (Xiang et al., 2012; Saha et al., 2013). As shown in **Figure 10F**, flow cytometry results have confirmed that fluorescence was greatly

reduced by the chlorpromazine-treated ζ^0 system. This suggests that clathrin-mediated endocytosis led to the internalization of the ζ^0 system.

Kim et al. (Kim et al., 2018) designed a biodegradable and thermoresponsive linear-dendritic nanogel containing poly (L-lysine), poly (L-lactic acid), and poly (N-isopropylacrylamide). The LCST of the nanogel was very low when it is in water at temperatures of 30–37°C. When the concentration is between 0.05 and 1 mg/ml (Kim et al., 2006), the integration of the poly (L-lactic acid) component provides the necessary hydrophobicity, and the drug reservoir was loaded with lipophilic reagents through hydrophobic–hydrophobic interactions. The nanogel has good biocompatibility. The nanogel itself and its degradative products were non-cytotoxic to neuron-like PC12 cells for at least 1 month. The nerve growth factors were added to the nanoparticles via aqueous phase mediation, which were slowly released from the nanogel for about 12 and 33 days at 25 and 37°C, respectively. The released nerve growth factor exhibits biological activity by promoting the neurite growth of PC12 cells. This study reveals a new concept that using biodegradable and thermoresponsive nanogels for the treatment of neurologic diseases through thermal targeting and sustained release of nerve growth factors and other protein drugs.

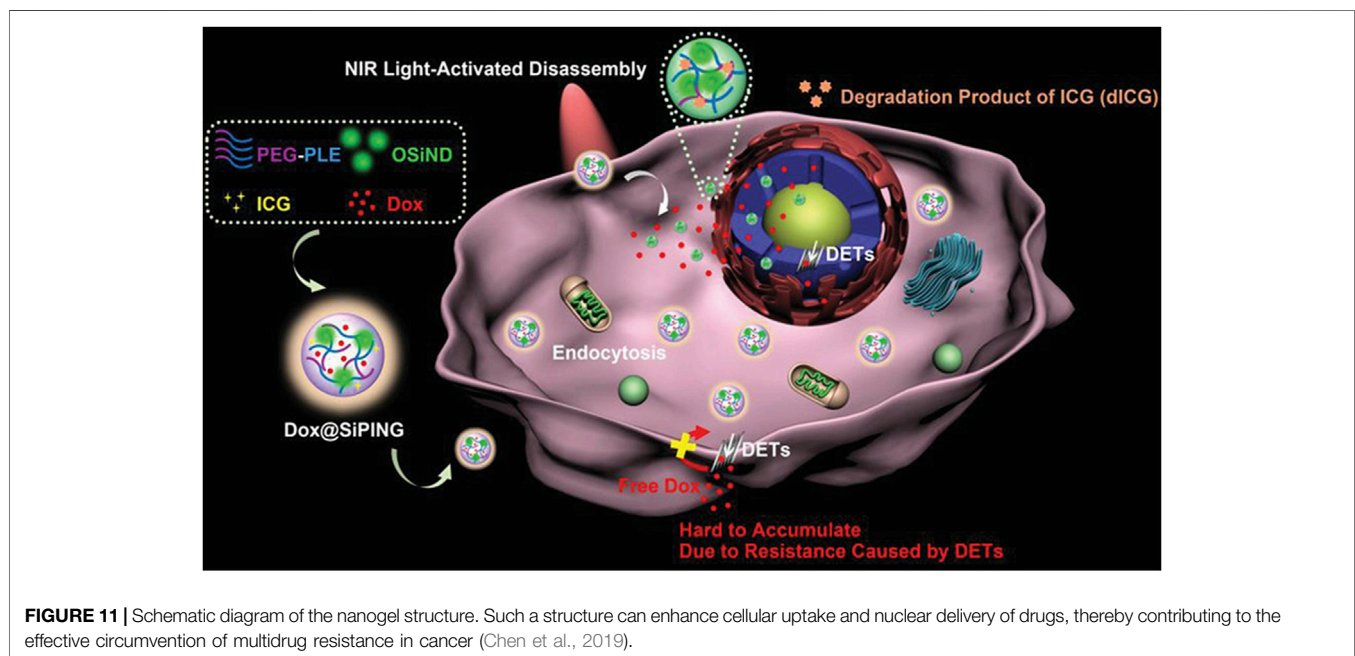
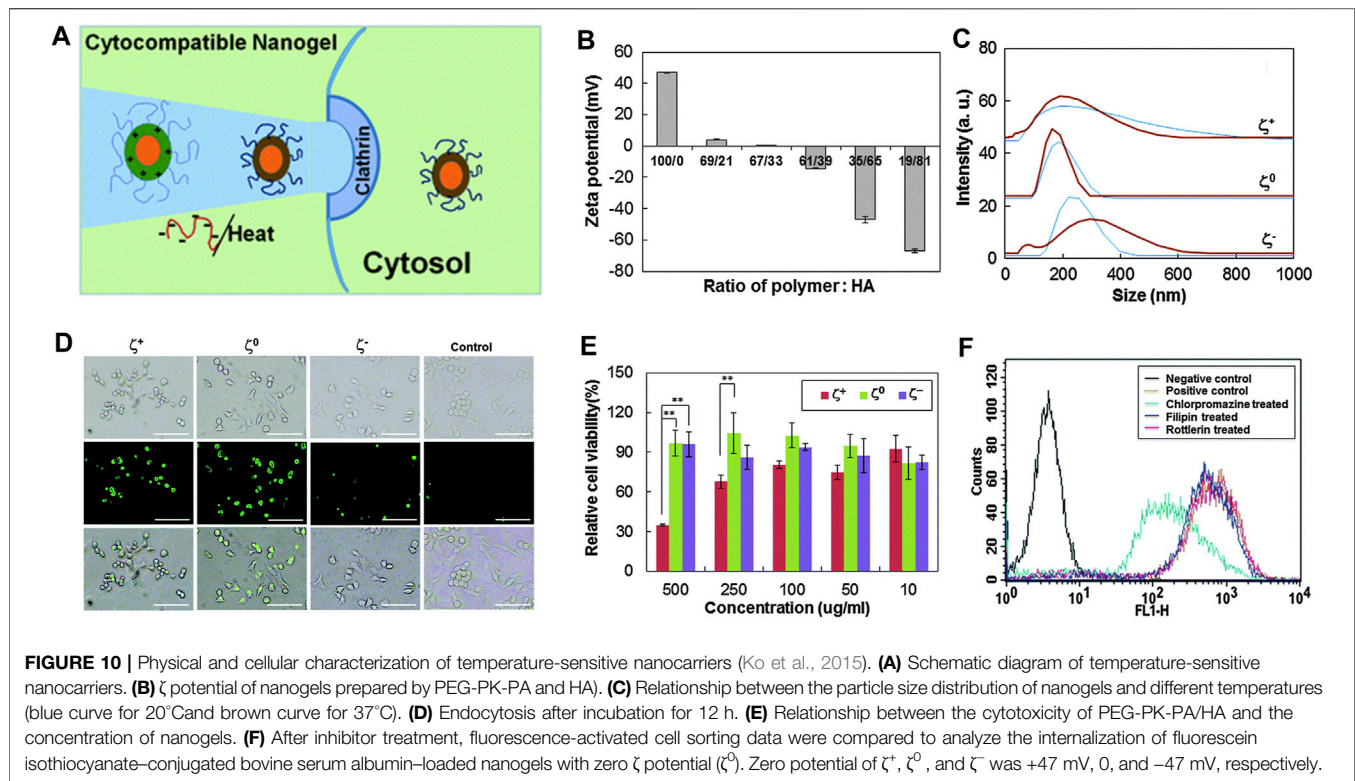
In summary, the temperature-sensitive nanogel is stimulated by external factors to achieve the purpose of the release and has better controllability.

Light-Responsive Nanogels

Light has become a stimulus that has attracted a lot of attention, is particularly suitable for the design of advanced biomedical platforms, improves the spatiotemporal control of the behavior of biomaterials, and dynamically adjusts their performance (Rapp and DeForest, 2020). In addition, the light-responsive platform also provides numerous opportunities for sequential degradation of implanted devices or remotely controlled drug delivery in a safe and non-invasive manner (Li et al., 2019).

Inspired by the design of a “Trojan horse”, Chen et al. (Chen et al., 2019) developed a photocontrollable nanogel, which is called SiPING, through simple self-assembly of three functional materials. The SiPING was composed of three functional components, including 1) long-circulating biocompatible polymer poly (ethylene glycol)-b-poly (L-glutamic acid), which prevents the nanogels from being detected by drug efflux transporters (DETs) on the membrane to enhance the accumulation and circulation of the nanogels; 2) photodegradable indocyanine green, which enables the photoactivatable disassembly for photo-controllable drug release; and 3) green fluorescent organosilica nanodot, which can be used as the bridge connecting the other two components and bioimaging probes. The traceable “SiPING” plays the role of a “Trojan horse” and has a very broad application prospect as a multifunctional nanoplatform. As shown in **Figure 11**, due to the existence of DET, the plasma membrane acts as the gate of the cell, making it difficult for DOX to cross.

By hiding inside the nanogel with a suitable surface coating to avoid the recognition of DETs, lots of DOX molecules were



transported into multidrug-resistant cells via endocytosis pathways. This allows DOX to form a high local concentration near the nucleus to prepare for further transport to the nucleus. Under the condition of photo-triggered degradation of the nanogels, a large amount of “auxiliaries” were released from the nanogels, allowing the drug to quickly occupy the nucleus

under the condition of DETs and were still on present on the nuclear membrane; thus, multidrug resistance can be effectively circumvented. Therefore, the multidrug-resistant cells could be killed by DOX-loaded nanogels in two steps: 1) DOX-loaded nanogels’ behavior like a “Trojan horse” and escape from DETs on the plasma membrane, effectively transporting DOX into the

cytoplasm and preventing drug efflux 2) Irradiation with near-infrared light leads to the decomposition of the nanogel, releasing a large number of DOX that can escape from DETs on the plasma membrane, thereby exerting its nuclear effect in multidrug-resistant cells.

There are few studies on light-responsive nanogels. Generally, photo responsiveness and thermal responsiveness are used in combination to achieve better results.

MULTI-STIMULI-RESPONSIVE NANOGENS

To better use complex microenvironments in the tumor for drug delivery and release, more attention has been paid to multi-stimuli-responsive nanogels. The introduction of stimulus-responsive nanogels greatly improves the controllable degree and range of polymers, which can better deliver drugs to the tumor site and release drugs more accurately. Therefore, multiresponsive polymers have become the research area of most interest in recent years.

Zhang et al. (Zhang et al., 2019) prepared a polymer with disulfide bond-containing dimethyl L-cystinate and polycaprolactone oligomer using polycondensation via a pH-responsive imine bond. Then, they processed the polymer into nanoparticles (diameter <100 nm) using the nanoprecipitation method. The nanoparticles can release paclitaxel faster at mildly acidic pH and in the presence of high concentrations of GSH. They hardly exhibit release under physiological conditions. Compared with free paclitaxel, the nanoparticles were more cytotoxic to 4T1 cancer cells. *In vivo* test results show that the nanoparticles exhibit excellent anti-tumor ability and good biosafety.

Ding et al. (Ding et al., 2013) prepared reduction and pH dual-responsive polypeptide nanogels using the two-step strategy. First, using mPEG-NH₂ as a macromolecule inducer, they synthesized mPEG-b-P (LGA-co-CELG) through the ROP of γ -benzyl-L-glutamate NCA (BLG-NCA) and γ -2-chloroethyl-L-glutamate NCA (CELG-NCA). Then, the benzyl group was deprotected (Ding et al., 2011b). Subsequently, the CELG unit was quaternized with 2,2'-dithiobis (N,N-dimethylethylamine) to prepare a polypeptide nanogel. DOX was added to the nanogels as an antitumor drug. Under normal physiologic conditions, DOX-loaded nanogels have a stable core cross-linking structure. However, in the simulated *in vivo* environment, tumor tissue, and intracellular redox microenvironment (10.0 nM GSH), carboxyl protonation reduces the interaction between the LGA unit in the core of nanoparticles and DOX and the breaking of the disulfide bond caused by GSH, which promotes the rapid release of effective load (Sanson et al., 2010). Confocal fluorescence microscopy results showed that compared with maternal DOX micelles and free DOX, DOX-loaded nanogels can deliver DOX to HepG2 cells more effectively. Quaternary ammonium group-induced improvement in cell internalization and low intracellular pH and high-level GSH triggered the enhancement of intracellular DOX release, ensuring the effective anti-proliferative activity of DOX-labeled nanogels *in vitro*. In addition, compared with

DOX-loaded micelles and free DOX, DOX-loaded nanogels improved both *in vivo* and *in vivo* antitumor activity and *in vivo* safety.

Shi et al. (Shi et al., 2017) prepared a reduction and pH dual-responsive nanogel methoxy poly (ethylene glycol)-poly (L-glutamic acid-co-L-cystine). This nanogel has the advantage of simple preparation, high drug loading, and good response to different stimuli. These nanogels can be effectively synthesized by the ROP of amino acid NCA. The model antitumor drug DOX was added to the nanogels at the drug loading efficiency of 96.7 wt%. The particle size of NG/DOX was about 117.6 nm, which helps prolong the circulation time in the body and increases the accumulation in tumor tissues (Li et al., 2016). In addition, after intravenous injection, NG/DOX maintained structural integrity and minimal drug release in circulation *in vivo*. Due to the EPR effect, NG/DOX can be enriched in tumor tissues and enters the cell through endocytosis. NG/DOX releases effective load due to low intracellular pH and high-level GSH. Taken together, NG/DOX exhibits excellent antitumor properties and high biosafety *in vivo*. Some other antitumor drugs containing amino acids can be highly delivered as required by the smart nanogels. All these findings confirm that reduction and pH dual-responsive nanogels have bright application prospects to treat tumors.

Yi et al. (Yi et al., 2016) synthesized a smart peptide nanogel based on n-butylamine-poly (L-lysine)-b-poly (L-cystine) (PLL-PLC) with 1,2-dicarboxylic acid-cyclohexene anhydride (DCA) and folic acid (FA) for the delivery of multistage-responsive tumor-targeted drugs. The copolymer was spontaneously crosslinked with polymers to form pH and the redox nanoparticle FD-NP. The FD-NP has a reversible zeta potential of about 30 mV and +15 mV at pH 7.4 and 5.0, respectively. Moreover, the drug loading capacity of DOX in FD-NP was 15.7 wt%. It released approximately 24.5% DOX within 60 h at pH 7.4. However, at pH 5.0, the presence of 10 mM dithiothreitol significantly accelerated the release of DOX. FD-NP enhances the uptake of DOX in FA receptor-positive cancer cells only at pH 7.4, but it promotes the uptake of DOX by FA receptor-positive HeLa and FA receptor-negative A549 cells in the weak acidic environment and greatly improves the cellular binding and lysosomal escapes. The *in vivo* study in a HeLa cancer model revealed that compared with charge-irreversible FD-NPs, charge-reversible FD-NPs deliver DOX to the tumor more effectively. Therefore, the multistage-responsive FD-NPs can be used as highly efficient drug vectors for tumor-targeted chemotherapy.

Liu et al. (Liu L. et al., 2017) prepared self-crosslinked redox-responsive nanogels by coating DCA-grafted PEG-PLL (sPEG) with galactose-functionalized n-butylamine-poly (L-lysine)-b-poly (L-cysteine) polypeptides (GCL) and used them for TAM-targeted miR delivery and anticancer therapy. The *in vitro* study of Liu et al. (Liu L. et al., 2017) revealed that the cationic GLC core can be shielded by sPEG under physiologic pH conditions, but it was re-exposed because of rapid sPEG falling caused by reversible charge. The encapsulation of sPEG/GLC effectively promotes the delivery of macrophage-targeted miR under acidic conditions, but it reduced miR uptake at neutral pH.

miR155-loaded sPEG/GLC (sPEG/GLC/155) nanocomplexes can increase miR155 expression in TAM both *in vivo* and *in vitro*. sPEG/GLC/155 can also increase the M1 macrophage markers and inhibit the M2 macrophage markers in TAM, effectively repolarizing the immunosuppressive TAM into antitumor M1 macrophages. In addition, sPEG/GLC/155 treatment greatly increases the number of activated T lymphocytes and natural killer cells in tumors, leading to tumor regression.

Wu et al. (Wu et al., 2016) successfully prepared plasmonic glyco-PEGylated polypeptide nanoparticles lactose (LAC) and PEG-grafted polycysteine terpolymer (PC-g-PEG-LAC) under mild conditions by integrating cocktail therapy and photothermal therapy into biodegradable and biocompatible nanocarriers. The polypeptide composite nanoparticles have strong near-infrared absorption and excellent photothermal properties. They have reductive responsiveness because their disulfide bonds can be degraded by GSH. They are also responsive to near-infrared light and can also release drugs. Irradiation heating can completely kill HepG2 cancer cells *in vitro*, showing excellent photothermal properties. The scholars loaded DOX and 6-mercaptopurine, two anticancer drugs, to nanoparticles through the Au-S bond and physical interaction, respectively. The composite nanoparticles loaded with both 6-mercaptopurine and DOX exhibit a reduction-sensitive and near-infrared light-triggered drug release profile and enhance cytotoxicity. The half-maximal inhibitory concentration produced by the cocktail chemo-photothermal therapy was lower than that of cocktail chemotherapy or photothermal therapy alone. Therefore, the cocktail chemo-photothermal therapy has a good synergistic antitumor effect. These findings provide evidence for establishing a simple strategy for the preparation of lactose-targeted, plasmonic, and dual drug-loaded polypeptide nanogels and open up a new way for developing a combined therapy of cocktail chemotherapy and photothermal therapy.

To realize spatiotemporal transmission and reverse hypoxia-induced drug resistance, Chen et al. (Chen et al., 2020) designed a shell-stacked nanoparticle (SNP) to co-encapsulate a proteasome inhibitor bortezomib (BTZ) and a vascular disrupting agent combretastatin A-4 phosphate (CA4P). The SNP is an ideal carrier for spatiotemporal transmission of BTZ and CA4P because it can rapidly detach the shell and penetrate tumor tissues (Chen et al., 2017a). First, BTZ was loaded onto the nanogel poly (L-lysine)-poly (L-phenylalanine-co-L-cystine) through hydrophobic interaction (NP_{BTZ}), and then CA4P was electrostatically loaded on NP ($\text{CA4PNP}_{\text{BTZ}}$). Finally, methoxy poly (ethylene glycol)-b-poly (L-lysine) modified with dimethylmaleic anhydride was coated on $\text{CA4PNP}_{\text{BTZ}}$ to form a shell-stacked

nanoparticle ($\text{S}_{\text{CA4PNP}_{\text{BTZ}}}$). After embedding CA4P and covering by the shell, the size of the composite increases to 150 nm due to the shell-stacking effect (Chen et al., 2017a). At high intracellular GSH concentrations, $\text{S}_{\text{CA4PNP}_{\text{BTZ}}}$ can spatiotemporally transport CA4P and BTZ to tumor blood vessels and tumor cells, respectively. Moreover, deeply penetrated NP can transport BTZ to tumor cells far away from the exudation site. In addition, the SNP can also reverse drug resistance caused by the overexpression of ABCG2 under the CA4P-induced hypoxia condition. Although the use of these nanoparticles can induce hypoxia in tumors, NP can reverse drug resistance by enhancing endocytosis and accelerating intracellular drug release. The spatiotemporal-targeted combination therapy significantly inhibits the progress of lung cancer and colon cancer. This provides a new strategy for the treatment of advanced cancer.

Multiresponsive nanogels are currently a hot topic of research. Compared with single-response nanogels, it has better responsiveness and a better drug release effect.

PROSPECTS

To achieve more accurate and intelligent drug delivery to tumor tissues and improve multidrug resistance, scholars have made unremitting efforts in studying tumor microenvironment response. Although nanogels have advantages, including small particle size, long circulating time, good biocompatibility, biodegradability, and high drug loading capacity, there is still room for the optimization of nanoparticles in terms of single and multiple tumor microenvironment responses. Many study teams have performed *in vivo* and *in vitro* tests and confirmed that tumor microenvironment-responsive nanogels exhibit good therapeutic effects and have few adverse reactions. However, tumor microenvironment-responsive nanoparticles are easy to be eliminated by the immune system or accumulate toxicity. Therefore, they pose many challenges for the transition of tumor microenvironment-responsive nanoparticles from preclinical research to clinical application. With interdisciplinary development among materials science, molecular biology, tumor pharmacology, pharmaceuticals, and other disciplines, future research studies should focus on nanogels with highly reversible, highly sensitive, and multiple responses.

AUTHOR CONTRIBUTIONS

HM provided the thoughts of the entire article and revised the outline. YL collected the information and wrote the entire article. LC, QS, and QZ reviewed and corrected the article.

REFERENCES

- Abdullah-Al-Nahain, N., Nam, J. A., Mok, H., Lee, Y.-k., and Park, S. Y. (2013). Dual-responsive Crosslinked Pluronic Micelles as a Carrier to Deliver Anticancer Drug Taxol. *Macromol. Res.* 21 (1), 92–99. doi:10.1007/s13233-013-1011-z
- Arroyo-Crespo, J. J., Armiñán, A., Charbonnier, D., Balzano-Nogueira, L., Huertas-López, F., Martí, C., et al. (2018). Tumor Microenvironment-Targeted Poly-L-Glutamic Acid-Based Combination Conjugate for Enhanced Triple Negative Breast Cancer Treatment. *Biomaterials* 186, 8–21. doi:10.1016/j.biomaterials.2018.09.023
- Bae, Y., and Kataoka, K. (2009). Intelligent Polymeric Micelles from Functional Poly(ethylene Glycol)-Poly(amino Acid) Block Copolymers. *Adv. Drug Deliv. Rev.* 61 (10), 768–784. doi:10.1016/j.addr.2009.04.016

- Bahadur K C, R., and Xu, P. (2012). Multicompartment Intracellular Self-Expanding Nanogel for Targeted Delivery of Drug Cocktail. *Adv. Mater.* 24 (48), 6479–6483. doi:10.1002/adma.201202687
- Bawa, K. K., and Oh, J. K. (2017). Stimulus-Responsive Degradable Polylactide-Based Block Copolymer Nanoassemblies for Controlled/Enhanced Drug Delivery. *Mol. Pharm.* 14 (8), 2460–2474. doi:10.1021/acs.molpharmaceut.7b00284
- Blanco, E., Shen, H., and Ferrari, M. (2015). Principles of Nanoparticle Design for Overcoming Biological Barriers to Drug Delivery. *Nat. Biotechnol.* 33 (9), 941–951. doi:10.1038/nbt.3330
- Chen, J., Ding, J., Wang, Y., Cheng, J., Ji, S., Zhuang, X., et al. (2017a). Sequentially Responsive Shell-Stacked Nanoparticles for Deep Penetration into Solid Tumors. *Adv. Mater.* 29 (32), 1701170. doi:10.1002/adma.201701170
- Chen, J., Ding, J., Xu, W., Sun, T., Xiao, H., Zhuang, X., et al. (2017b). Receptor and Microenvironment Dual-Recognizable Nanogel for Targeted Chemotherapy of Highly Metastatic Malignancy. *Nano Lett.* 17 (7), 4526–4533. doi:10.1021/acs.nanolett.7b02129
- Chen, J., Jiang, Z., Xu, W., Sun, T., Zhuang, X., Ding, J., et al. (2020). Spatiotemporally Targeted Nanomedicine Overcomes Hypoxia-Induced Drug Resistance of Tumor Cells after Disrupting Neovasculature. *Nano Lett.* 20 (8), 6191–6198. doi:10.1021/acs.nanolett.0c02515
- Chen, J., Keltner, L., Christophersen, J., Zheng, F., Krouse, M., Singhal, A., et al. (2002). New Technology for Deep Light Distribution in Tissue for Phototherapy. *Cancer J.* 8 (2), 154–163. doi:10.1097/00130404-200203000-00009
- Chen, X., Zhang, X., Guo, Y., Zhu, Y. X., Liu, X., Chen, Z., et al. (2019). Smart Supramolecular "Trojan Horse"-Inspired Nanogels for Realizing Light-Triggered Nuclear Drug Influx in Drug-Resistant Cancer Cells. *Adv. Funct. Mater.* 29 (13), 1807772. doi:10.1002/adfm.201807772
- Deepagan, V. G., Kwon, S., You, D. G., Nguyen, V. Q., Um, W., Ko, H., et al. (2016). *In Situ* diselenide-crosslinked Polymeric Micelles for ROS-Mediated Anticancer Drug Delivery. *Biomaterials* 103, 56–66. doi:10.1016/j.biomaterials.2016.06.044
- Dharmaraja, A. T. (2017). Role of Reactive Oxygen Species (ROS) in Therapeutics and Drug Resistance in Cancer and Bacteria. *J. Med. Chem.* 60 (8), 3221–3240. doi:10.1021/acs.jmedchem.6b01243
- Ding, J., Xiao, C., Tang, Z., Zhuang, X., and Chen, X. (2011a). Highly Efficient "grafting from" an α -helical Polypeptide Backbone by Atom Transfer Radical Polymerization. *Macromol. Biosci.* 11 (2), 192–198. doi:10.1002/mabi.201000238
- Ding, J., Xu, W., Zhang, Y., Sun, D., Xiao, C., Liu, D., et al. (2013). Self-reinforced Endocytosis of Smart Polypeptide Nanogels for "On-Demand" Drug Delivery. *J. Control. Release* 172 (2), 444–455. doi:10.1016/j.jconrel.2013.05.029
- Ding, J., Xiao, C., Zhao, L., Cheng, Y., Ma, L., Tang, Z., et al. (2011b). Poly(L-glutamic Acid) Grafted with Oligo(2-(2-(2-Methoxyethoxy)ethoxy)ethyl Methacrylate): Thermal Phase Transition, Secondary Structure, and Self-Assembly. *J. Polym. Sci. A. Polym. Chem.* 49 (12), 2665–2676. doi:10.1002/pola.24698
- Dispinar, T., Van Camp, W., De Cock, L. J., De Geest, B. G., and Du Prez, F. E. (2012). Redox-responsive Degradable PEG Cryogels as Potential Cell Scaffolds in Tissue Engineering. *Macromol. Biosci.* 12 (3), 383–394. doi:10.1002/mabi.201100396
- Douat, C., Aisenbrey, C., Antunes, S., Decossas, M., Lambert, O., Bechinger, B., et al. (2015). A Cell-Penetrating Foldamer with a Bioreducible Linkage for Intracellular Delivery of DNA. *Angew. Chem. Int. Ed. Engl.* 54 (38), 11133–11137. doi:10.1002/anie.201504884
- Feng, X., Xu, W., Xu, X., Li, G., Ding, J., and Chen, X. (2021). Cystine Proportion Regulates Fate of Polypeptide Nanogel as Nanocarrier for Chemotherapeutics. *Sci. China Chem.* 64 (2), 293–301. doi:10.1007/s11426-020-9884-6
- Gao, Y., and Dong, C.-M. (2017). Reduction- and Thermo-Sensitive Core-Cross-Linked Polypeptide Hybrid Micelles for Triggered and Intracellular Drug Release. *Polym. Chem.* 8 (7), 1223–1232. doi:10.1039/C6PY01929C
- Gonçalves, M., Maciel, D., Capelo, D., Xiao, S., Sun, W., Shi, X., et al. (2014). Dendrimer-Assisted Formation of Fluorescent Nanogels for Drug Delivery and Intracellular Imaging. *Biomacromolecules* 15 (2), 492–499. doi:10.1021/bm401400r
- Guo, F., Wu, J., Wu, W., Huang, D., Yan, Q., Yang, Q., et al. (2018). PEGylated Self-Assembled Enzyme-Responsive Nanoparticles for Effective Targeted Therapy against Lung Tumors. *J. Nanobiotechnology* 16 (1), 57. doi:10.1186/s12951-018-0384-8
- Guo, H., Li, F., Qiu, H., Xu, W., Li, P., Hou, Y., et al. (2020). Synergistically Enhanced Mucoadhesive and Penetrable Polypeptide Nanogel for Efficient Drug Delivery to Orthotopic Bladder Cancer. *Research (Wash D C)* 2020, 8970135. doi:10.34133/2020/8970135
- Guo, H., Xu, W., Chen, J., Yan, L., Ding, J., Hou, Y., et al. (2017). Positively Charged Polypeptide Nanogel Enhances Mucoadhesion and Penetrability of 10-hydroxycamptothecin in Orthotopic Bladder Carcinoma. *J. Control. Release* 259, 136–148. doi:10.1016/j.jconrel.2016.12.041
- Guo, X., Wei, X., Jing, Y., and Zhou, S. (2015). Size Changeable Nanocarriers with Nuclear Targeting for Effectively Overcoming Multidrug Resistance in Cancer Therapy. *Adv. Mater.* 27 (41), 6450–6456. doi:10.1002/adma.201502865
- He, H., Cattran, A. W., Nguyen, T., Nieminen, A. L., and Xu, P. (2014). Triple-responsive Expansile Nanogel for Tumor and Mitochondria Targeted Photosensitizer Delivery. *Biomaterials* 35 (35), 9546–9553. doi:10.1016/j.biomaterials.2014.08.004
- He, L., Li, D., Wang, Z., Xu, W., Wang, J., Guo, H., et al. (2016). L-Cystine-Crosslinked Polypeptide Nanogel as a Reduction-Responsive Excipient for Prostate Cancer Chemotherapy. *Polymers (Basel)* 8 (2). doi:10.3390/polym8020036
- Holmgard, R. B., Zamarin, D., Li, Y., Gasmi, B., Munn, D. H., Allison, J. P., et al. (2015). Tumor-Expressed Ido Recruits and Activates MDSCs in a Treg-dependent Manner. *Cell Rep* 13 (2), 412–424. doi:10.1016/j.celrep.2015.08.077
- Huang, H., Jiang, C. T., Shen, S., Liu, A., Gan, Y. J., Tong, Q. S., et al. (2019). Nanoenabled Reversal of Ido1-Mediated Immunosuppression Synergizes with Immunogenic Chemotherapy for Improved Cancer Therapy. *Nano Lett.* 19 (8), 5356–5365. doi:10.1021/acs.nanolett.9b01807
- Hunter, A. C. (2006). Molecular Hurdles in Polyfectin Design and Mechanistic Background to Polycation Induced Cytotoxicity. *Adv. Drug Deliv. Rev.* 58 (14), 1523–1531. doi:10.1016/j.addr.2006.09.008
- Huo, M., Yuan, J., Tao, L., and Wei, Y. (2014). Redox-responsive Polymers for Drug Delivery: from Molecular Design to Applications. *Polym. Chem.* 5 (5), 1519–1528. doi:10.1039/c3py01192e
- Ichikawa, K., Hikita, T., Maeda, N., Takeuchi, Y., Namba, Y., and Oku, N. (2004). PEGylation of Liposome Decreases the Susceptibility of Liposomal Drug in Cancer Photodynamic Therapy. *Biol. Pharm. Bull.* 27 (3), 443–444. doi:10.1248/bpb.27.443
- Kim, J. O., Oberoi, H. S., Desale, S., Kabanov, A. V., and Bronich, T. K. (2013). Polypeptide Nanogels with Hydrophobic Moieties in the Cross-Linked Ionic Cores: Synthesis, Characterization and Implications for Anticancer Drug Delivery. *J. Drug Target.* 21 (10), 981–993. doi:10.3109/1061186X.2013.831421
- Kim, Y. S., Gulfam, M., and Lowe, T. L. (2018). Thermoresponsive- Co-biodegradable Linear-Dendritic Nanoparticles for Sustained Release of Nerve Growth Factor to Promote Neurite Outgrowth. *Mol. Pharm.* 15 (4), 1467–1475. doi:10.1021/acs.molpharmaceut.7b01044
- Kim, Y. S., Gil, E. S., and Lowe, T. L. (2006). Synthesis and Characterization of Thermoresponsive-Co-Biodegradable Linear-Dendritic Copolymers. *Macromolecules* 39 (23), 7805–7811. doi:10.1021/ma0602730
- Ko, D. Y., Moon, H. J., and Jeong, B. (2015). Temperature-sensitive Polypeptide Nanogels for Intracellular Delivery of a Biomacromolecular Drug. *J. Mater. Chem. B* 3 (17), 3525–3530. doi:10.1039/C5TB00366K
- Kratz, F., Drevs, J., Bing, G., Stockmar, C., Scheuermann, K., Lazar, P., et al. (2001). Development and *In Vitro* Efficacy of Novel MMP2 and MMP9 Specific Doxorubicin Albumin Conjugates. *Bioorg. Med. Chem. Lett.* 11 (15), 2001–2006. doi:10.1016/S0960-894X(01)00354-7
- Kujawa, P., and Winnik, F. M. (2001). Volumetric Studies of Aqueous Polymer Solutions Using Pressure Perturbation Calorimetry: A New Look at the Temperature-Induced Phase Transition of poly(N-Isopropylacrylamide) in Water and D₂O. *Macromolecules* 34 (12), 4130–4135. doi:10.1021/ma002082h
- Kuppusamy, P., Li, H., Ilango, G., Cardounel, A. J., Zweier, J. L., Yamada, K., et al. (2002). Noninvasive Imaging of Tumor Redox Status and its Modification by Tissue Glutathione Levels. *Cancer Res.* 62 (1), 307–312.
- Kurosaki, T., Kitahara, T., Fumoto, S., Nishida, K., Nakamura, J., Niidome, T., et al. (2009). Ternary Complexes of pDNA, Polythyleneimine, and Gamma-Polyglutamic Acid for Gene Delivery Systems. *Biomaterials* 30 (14), 2846–2853. doi:10.1016/j.biomaterials.2009.01.055

- Lal, S., Clare, S. E., and Halas, N. J. (2008). Nanoshell-Enabled Photothermal Cancer Therapy: Impending Clinical Impact. *Acc. Chem. Res.* 41 (12), 1842–1851. doi:10.1021/ar800150g
- Lee, S. H., Gupta, M. K., Bang, J. B., Bae, H., and Sung, H. J. (2013). Current Progress in Reactive Oxygen Species (ROS)-Responsive Materials for Biomedical Applications. *Adv. Healthc. Mater.* 2 (6), 908–915. doi:10.1002/adhm.201200423
- Li, H. J., Du, J. Z., Du, X. J., Xu, C. F., Sun, C. Y., Wang, H. X., et al. (2016). Stimuli-responsive Clustered Nanoparticles for Improved Tumor Penetration and Therapeutic Efficacy. *Proc. Natl. Acad. Sci. U S A.* 113 (15), 4164–4169. doi:10.1073/pnas.1522080113
- Li, L., Scheiger, J. M., and Levkin, P. A. (2019). Design and Applications of Photoresponsive Hydrogels. *Adv. Mater.* 31 (26), e1807333. doi:10.1002/adma.201807333
- Li, M., Schlesiger, S., Knauer, S. K., and Schmuck, C. (2015). A Tailor-Made Specific Anion-Binding Motif in the Side Chain Transforms a Tetrapeptide into an Efficient Vector for Gene Delivery. *Angew. Chem. Int. Ed. Engl.* 54 (10), 2941–2944. doi:10.1002/anie.201410429
- Li, M., Song, W., Tang, Z., Lv, S., Lin, L., Sun, H., et al. (2013). Nanoscaled poly(L-Glutamic Acid)/doxorubicin-Amphiphile Complex as pH-Responsive Drug Delivery System for Effective Treatment of Nonsmall Cell Lung Cancer. *ACS Appl. Mater. Inter.* 5 (5), 1781–1792. doi:10.1021/am303073u
- Li, S., Zhang, T., Xu, W., Ding, J., Yin, F., Xu, J., et al. (2018a). Sarcoma-Targeting Peptide-Decorated Polypeptide Nanogel Intracellularly Delivers Shikonin for Upregulated Osteosarcoma Necroptosis and Diminished Pulmonary Metastasis. *Theranostics* 8 (5), 1361–1375. doi:10.7150/thno.18299
- Li, Y., Bui, Q. N., Duy, L. T. M., Yang, H. Y., and Lee, D. S. (2018b). One-Step Preparation of pH-Responsive Polymeric Nanogels as Intelligent Drug Delivery Systems for Tumor Therapy. *Biomacromolecules* 19 (6), 2062–2070. doi:10.1021/acs.biomac.8b00195
- Lin, J.-Y., Lai, P.-L., Lin, Y.-K., Peng, S., Lee, L.-Y., Chen, C.-N., et al. (2016a). A Poloxamer-Polypeptide Thermosensitive Hydrogel as a Cell Scaffold and Sustained Release Depot. *Polym. Chem.* 7 (17), 2976–2985. doi:10.1039/C5PY02067K
- Lin, T. Y., Li, Y., Liu, Q., Chen, J. L., Zhang, H., Lac, D., et al. (2016b). Novel Theranostic Nanoporphyrins for Photodynamic Diagnosis and Trimodal Therapy for Bladder Cancer. *Biomaterials* 104, 339–351. doi:10.1016/j.biomaterials.2016.07.026
- Liu, J., Pang, Y., Huang, W., Zhu, Z., Zhu, X., Zhou, Y., et al. (2011). Redox-responsive Polyphosphate Nanosized Assemblies: a Smart Drug Delivery Platform for Cancer Therapy. *Biomacromolecules* 12 (6), 2407–2415. doi:10.1021/bm2005164
- Liu, J. N., Bu, W., and Shi, J. (2017a). Chemical Design and Synthesis of Functionalized Probes for Imaging and Treating Tumor Hypoxia. *Chem. Rev.* 117 (9), 6160–6224. doi:10.1021/acs.chemrev.6b00525
- Liu, L., Yi, H., He, H., Pan, H., Cai, L., and Ma, Y. (2017b). Tumor Associated Macrophage-Targeted microRNA Delivery with Dual-Responsive Polypeptide Nanovectors for Anti-cancer Therapy. *Biomaterials* 134, 166–179. doi:10.1016/j.biomaterials.2017.04.043
- Liu, X., Wang, J., Xu, W., Ding, J., Shi, B., Huang, K., et al. (2015). Glutathione-degradable Drug-Loaded Nanogel Effectively and Securely Suppresses Hepatoma in Mouse Model. *Int. J. Nanomedicine* 10, 6587–6602. doi:10.2147/IJN.S90000
- Lu, C., Li, B., Liu, N., Wu, G., Gao, H., and Ma, J. (2014). A Hydrazone Crosslinked Zwitterionic Polypeptide Nanogel as a Platform for Controlled Drug Delivery. *RSC Adv.* 4 (92), 50301–50311. doi:10.1039/C4RA08871A
- Ma, N., Li, Y., Xu, H., Wang, Z., and Zhang, X. (2010). Dual Redox Responsive Assemblies Formed from Diselenide Block Copolymers. *J. Am. Chem. Soc.* 132 (2), 442–443. doi:10.1021/ja908124g
- Ma, W., Chen, Q., Xu, W., Yu, M., Yang, Y., Zou, B., et al. (2021). Self-targeting Visualizable Hyaluronate Nanogel for Synchronized Intracellular Release of Doxorubicin and Cisplatin in Combating Multidrug-Resistant Breast Cancer. *Nano Res.* 14 (3), 846–857. doi:10.1007/s12274-020-3124-y
- Mackiewicz, M., Romanski, J., Krug, P., Mazur, M., Stojek, Z., and Karbarz, M. (2019). Tunable Environmental Sensitivity and Degradability of Nanogels Based on Derivatives of Cystine and Poly(ethylene Glycols) of Various Length for Biocompatible Drug Carrier. *Eur. Polym. J.* 118, 606–613. doi:10.1016/j.eurpolymj.2019.06.031
- Matsumoto, A., Cabral, H., Sato, N., Kataoka, K., and Miyahara, Y. (2010). Assessment of Tumor Metastasis by the Direct Determination of Cell-Membrane Sialic Acid Expression. *Angew. Chem. Int. Ed. Engl.* 49 (32), 5494–5497. doi:10.1002/anie.201001220
- Meloni, B. P., Milani, D., Edwards, A. B., Anderton, R. S., O'Hare Doig, R. L., Fitzgerald, M., et al. (2015). Neuroprotective Peptides Fused to Arginine-Rich Cell Penetrating Peptides: Neuroprotective Mechanism Likely Mediated by Peptide Endocytic Properties. *Pharmacol. Ther.* 153, 36–54. doi:10.1016/j.pharmthera.2015.06.002
- Meng, F., Hennink, W. E., and Zhong, Z. (2009). Reduction-sensitive Polymers and Bioconjugates for Biomedical Applications. *Biomaterials* 30 (12), 2180–2198. doi:10.1016/j.biomaterials.2009.01.026
- Merino, S., Martín, C., Kostarelos, K., Prato, M., and Vázquez, E. (2015). Nanocomposite Hydrogels: 3D Polymer-Nanoparticle Synergies for On-Demand Drug Delivery. *ACS Nano* 9 (5), 4686–4697. doi:10.1021/acsnano.5b01433
- Nguyen, N. T., Nguyen, N. N. T., Tran, N. T. N., Le, P. N., Nguyen, T. B. T., Nguyen, N. H., et al. (2018). Synergic Activity against MCF-7 Breast Cancer Cell Growth of Nanocurcumin-Encapsulated and Cisplatin-Complexed Nanogels. *Molecules* 23 (12), 12. doi:10.3390/molecules23123347
- O'Connor, T. P., and Crystal, R. G. (2006). Genetic Medicines: Treatment Strategies for Hereditary Disorders. *Nat. Rev. Genet.* 7 (4), 261–276. doi:10.1038/nrg1829
- Oberoi, H. S., Nukolova, N. V., Laquer, F. C., Poluektova, L. Y., Huang, J., Alnouti, Y., et al. (2012). Cisplatin-loaded Core Cross-Linked Micelles: Comparative Pharmacokinetics, Antitumor Activity, and Toxicity in Mice. *Int. J. Nanomedicine* 7, 2557–2571. doi:10.2147/IJN.S29145
- Park, K. M., Lee, D. W., Sarkar, B., Jung, H., Kim, J., Ko, Y. H., et al. (2010). Reduction-sensitive, Robust Vesicles with a Non-covalently Modifiable Surface as a Multifunctional Drug-Delivery Platform. *Small* 6 (13), 1430–1441. doi:10.1002/sml.201000293
- Peng, J., Xiao, Y., Li, W., Yang, Q., Tan, L., Jia, Y., et al. (2018). Photosensitizer Micelles Together with Ido Inhibitor Enhance Cancer Photothermal Therapy and Immunotherapy. *Adv. Sci. (Weinh)* 5 (5), 1700891. doi:10.1002/advs.201700891
- Phillips, D. J., and Gibson, M. I. (2014). Redox-Sensitive Materials for Drug Delivery: Targeting the Correct Intracellular Environment, Tuning Release Rates, and Appropriate Predictive Systems. *Antioxid. Redox Signal.* 21 (5), 786–803. doi:10.1089/ars.2013.5728
- Ramasamy, T., Haidar, Z. S., Tran, T. H., Choi, J. Y., Jeong, J. H., Shin, B. S., et al. (2014). Layer-by-layer Assembly of Liposomal Nanoparticles with PEGylated Polyelectrolytes Enhances Systemic Delivery of Multiple Anticancer Drugs. *Acta Biomater.* 10 (12), 5116–5127. doi:10.1016/j.actbio.2014.08.021
- Rapp, T. L., and DeForest, C. A. (2020). Visible Light-Responsive Dynamic Biomaterials: Going Deeper and Triggering More. *Adv. Healthc. Mater.* 9 (7), e1901553. doi:10.1002/adhm.201901553
- Riddell, S. R. (2001). Progress in Cancer Vaccines by Enhanced Self-Presentation. *Proc. Natl. Acad. Sci. U S A.* 98 (16), 8933–8935. doi:10.1073/pnas.171326398
- Saha, K., Kim, S. T., Yan, B., Miranda, O. R., Alfonso, F. S., Shlosman, D., et al. (2013). Surface Functionality of Nanoparticles Determines Cellular Uptake Mechanisms in Mammalian Cells. *Small* 9 (2), 300–305. doi:10.1002/sml.201201129
- Sanjoh, M., Miyahara, Y., Kataoka, K., and Matsumoto, A. (2014). Phenylboronic Acids-Based Diagnostic and Therapeutic Applications. *Anal. Sci.* 30 (1), 111–117. doi:10.2116/analsci.30.111
- Sanson, C., Schatz, C., Le Meins, J. F., Soum, A., Thévenot, J., Garanger, E., et al. (2010). A Simple Method to Achieve High Doxorubicin Loading in Biodegradable Polymersomes. *J. Control. Release* 147 (3), 428–435. doi:10.1016/j.jconrel.2010.07.123
- Satelli, A., and Li, S. (2011). Vimentin in Cancer and its Potential as a Molecular Target for Cancer Therapy. *Cell Mol Life Sci* 68 (18), 3033–3046. doi:10.1007/s00018-011-0735-1
- Satelli, A., Mitra, A., Cutrera, J. J., Devarie, M., Xia, X., Ingram, D. R., et al. (2014). Universal Marker and Detection Tool for Human Sarcoma Circulating Tumor Cells. *Cancer Res.* 74 (6), 1645–1650. doi:10.1158/0008-5472.Can-13-1739
- Shi, B., Huang, K., Ding, J., Xu, W., Yang, Y., Liu, H., et al. (2017). Intracellularly Swollen Polypeptide Nanogel Assists Hepatoma Chemotherapy. *Theranostics* 7 (3), 703–716. doi:10.7150/thno.16794
- Shi, N. Q., and Qi, X. R. (2017). Taming the Wildness of "Trojan-Horse" Peptides by Charge-Guided Masking and Protease-Triggered Demasking for the

- Controlled Delivery of Antitumor Agents. *ACS Appl. Mater. Inter.* 9 (12), 10519–10529. doi:10.1021/acsami.7b01056
- Shin, M. C., Zhang, J., Min, K. A., Lee, K., Byun, Y., David, A. E., et al. (2014). Cell-penetrating Peptides: Achievements and Challenges in Application for Cancer Treatment. *J. Biomed. Mater. Res. A* 102 (2), 575–587. doi:10.1002/jbma.a.34859
- Stupp, R., Mason, W. P., van den Bent, M. J., Weller, M., Fisher, B., Taphoorn, M. J., et al. (2005). Radiotherapy Plus Concomitant and Adjuvant Temozolomide for Glioblastoma. *N. Engl. J. Med.* 352 (10), 987–996. doi:10.1056/NEJMoa043330
- Sun, H., Meng, F., Cheng, R., Deng, C., and Zhong, Z. (2013). Reduction-sensitive Degradable Micellar Nanoparticles as Smart and Intuitive Delivery Systems for Cancer Chemotherapy. *Expert Opin. Drug Deliv.* 10 (8), 1109–1122. doi:10.1517/17425247.2013.783009
- Sundaramoorthy, P., Ramasamy, T., Mishra, S. K., Jeong, K. Y., Yong, C. S., Kim, J. O., et al. (2016). Engineering of Caveolae-specific Self-Micellizing Anticancer Lipid Nanoparticles to Enhance the Chemotherapeutic Efficacy of Oxaliplatin in Colorectal Cancer Cells. *Acta Biomater.* 42, 220–231. doi:10.1016/j.actbio.2016.07.006
- Tian, H., Tang, Z., Zhuang, X., Chen, X., and Jing, X. (2012). Biodegradable Synthetic Polymers: Preparation, Functionalization and Biomedical Application. *Prog. Polym. Sci.* 37 (2), 237–280. doi:10.1016/j.progpolymsci.2011.06.004
- Wang, F., Wang, Y. C., Dou, S., Xiong, M. H., Sun, T. M., and Wang, J. (2011). Doxorubicin-Tethered Responsive Gold Nanoparticles Facilitate Intracellular Drug Delivery for Overcoming Multidrug Resistance in Cancer Cells. *ACS Nano* 5 (5), 3679–3692. doi:10.1021/nn200007z
- Wang, H. X., Yang, X. Z., Sun, C. Y., Mao, C. Q., Zhu, Y. H., and Wang, J. (2014a). Matrix Metalloproteinase 2-responsive Micelle for siRNA Delivery. *Biomaterials* 35 (26), 7622–7634. doi:10.1016/j.biomaterials.2014.05.050
- Wang, J., Yang, G., Guo, X., Tang, Z., Zhong, Z., and Zhou, S. (2014b). Redox-responsive Polyanhydride Micelles for Cancer Therapy. *Biomaterials* 35 (9), 3080–3090. doi:10.1016/j.biomaterials.2013.12.025
- Wang, K., Luo, G.-F., Liu, Y., Li, C., Cheng, S.-X., Zhuo, R.-X., et al. (2012). Redox-sensitive Shell Cross-Linked PEG-Polypeptide Hybrid Micelles for Controlled Drug Release. *Polym. Chem.* 4 (4), 1084–1090. doi:10.1039/C2PY00600F
- Wang, Y., Xu, S., Xiong, W., Pei, Y., Li, B., and Chen, Y. (2016). Nanogels Fabricated from Bovine Serum Albumin and Chitosan via Self-Assembly for Delivery of Anticancer Drug. *Colloids Surf. B Biointerfaces* 146, 107–113. doi:10.1016/j.colsurfb.2016.05.043
- Wei, L., Chen, J., and Ding, J. (2021). Sequentially Stimuli-Responsive Anticancer Nanomedicines. *Nanomedicine (Lond)* 16 (4), 261–264. doi:10.2217/nnm-2021-0019
- Weigel, P. H., and Yik, J. H. (2002). Glycans as Endocytosis Signals: the Cases of the Asialoglycoprotein and Hyaluronan/chondroitin Sulfate Receptors. *Biochim. Biophys. Acta* 1572 (2), 341–363. doi:10.1016/S0304-4165(02)00318-5
- Wojtkowiak, J. W., Verduzco, D., Schramm, K. J., and Gillies, R. J. (2011). Drug Resistance and Cellular Adaptation to Tumor Acidic pH Microenvironment. *Mol. Pharm.* 8 (6), 2032–2038. doi:10.1021/mp200292c
- Wu, J., Liu, X.-Q., Wang, Y.-C., and Wang, J. (2009). Template-free Synthesis of Biodegradable Nanogels with Tunable Sizes as Potential Carriers for Drug Delivery. *J. Mater. Chem.* 19 (42), 7856–7863. doi:10.1039/B908768K
- Wu, X., Zhou, L., Su, Y., and Dong, C. M. (2016). Plasmonic, Targeted, and Dual Drugs-Loaded Polypeptide Composite Nanoparticles for Synergistic Cocktail Chemotherapy with Photothermal Therapy. *Biomacromolecules* 17 (7), 2489–2501. doi:10.1021/acs.biomac.6b00721
- Xiang, S., Tong, H., Shi, Q., Fernandes, J. C., Jin, T., Dai, K., et al. (2012). Uptake Mechanisms of Non-viral Gene Delivery. *J. Control. Release* 158 (3), 371–378. doi:10.1016/j.jconrel.2011.09.093
- Xing, T., Mao, C., Lai, B., and Yan, L. (2012). Synthesis of Disulfide-Cross-Linked Polypeptide Nanogel Conjugated with a Near-Infrared Fluorescence Probe for Direct Imaging of Reduction-Induced Drug Release. *ACS Appl. Mater. Inter.* 4 (10), 5662–5672. doi:10.1021/am301600u
- Yan, R., Liu, X., Xiong, J., Feng, Q., Xu, J., Wang, H., et al. (2020). pH-Responsive Hyperbranched Polypeptides Based on Schiff Bases as Drug Carriers for Reducing Toxicity of Chemotherapy. *RSC Adv.* 10 (23), 13889–13899. doi:10.1039/d0ra01241f
- Yan, S., Sun, Y., Chen, A., Liu, L., Zhang, K., Li, G., et al. (2017). Templated Fabrication of pH-Responsive Poly(L-Glutamic Acid) Based Nanogels via Surface-Grafting and Macromolecular Crosslinking. *RSC Adv.* 7 (24), 14888–14901. doi:10.1039/C7RA00631D
- Yao, J., He, P., Zhang, Y., Zhang, H., Zhang, P., Deng, M., et al. (2019). PEGylated Polylysine Derived Copolymers with Reduction-responsive Side Chains for Anticancer Drug Delivery. *Polym. Int.* 68 (10), 1817–1825. doi:10.1002/pi.5892
- Yi, H., Liu, P., Sheng, N., Gong, P., Ma, Y., and Cai, L. (2016). *In Situ* crosslinked Smart Polypeptide Nanoparticles for Multistage Responsive Tumor-Targeted Drug Delivery. *Nanoscale* 8 (11), 5985–5995. doi:10.1039/c5nr07348k
- Yu, J., Fan, H., Huang, J., and Chen, J. (2011). Fabrication and Evaluation of Reduction-Sensitive Supramolecular Hydrogel Based on Cyclodextrin/polymer Inclusion for Injectable Drug-Carrier Application. *Soft Matter* 7 (16), 7386–7394. doi:10.1039/C1SM05426K
- Zeng, Q., Shao, D., He, X., Ren, Z., Ji, W., Shan, C., et al. (2016). Carbon Dots as a Trackable Drug Delivery Carrier for Localized Cancer Therapy *In Vivo*. *J. Mater. Chem. B* 4 (30), 5119–5126. doi:10.1039/C6TB01259K
- Zhang, L., Chen, Y., Li, Z., Li, L., Saint-Cricq, P., Li, C., et al. (2016a). Tailored Synthesis of Octopus-type Janus Nanoparticles for Synergistic Actively-Targeted and Chemo-Photothermal Therapy. *Angew. Chem. Int. Ed. Engl.* 55 (6), 2118–2121. doi:10.1002/anie.201510409
- Zhang, N., Yan, Z., Zhao, X., Chen, Q., and Ma, M. (2016b). Efficient Mini-Transporter for Cytosolic Protein Delivery. *ACS Appl. Mater. Inter.* 8 (39), 25725–25732. doi:10.1021/acsami.6b08202
- Zhang, Q., Aleksanian, S., Noh, S. M., and Oh, J. K. (2013a). Thiol-responsive Block Copolymer Nanocarriers Exhibiting Tunable Release with Morphology Changes. *Polym. Chem.* 4 (2), 351–359. doi:10.1039/C2PY20582C
- Zhang, Q., Ding, J., Lv, C., Xu, W., Sun, X., and Meng, X. (2015). Epirubicin-Complexed Polypeptide Micelle Effectively and Safely Treats Hepatocellular Carcinoma. *Polymers* 7 (11), 2410–2430. doi:10.3390/polym7111521
- Zhang, X., Kang, Y., Liu, G. T., Li, D. D., Zhang, J. Y., Gu, Z. P., et al. (2019). Poly(cystine-PCL) Based pH/redox Dual-Responsive Nanocarriers for Enhanced Tumor Therapy. *Biomater. Sci.* 7 (5), 1962–1972. doi:10.1039/c9bm00009g
- Zhang, Y., Wang, C., Xu, C., Yang, C., Zhang, Z., Yan, H., et al. (2013b). Morpholino-decorated Long Circulating Polymeric Micelles with the Function of Surface Charge Transition Triggered by pH Changes. *Chem. Commun. (Camb)* 49 (66), 7286–7288. doi:10.1039/C3CC43334J
- Zheng, C., Li, M., and Ding, J. (2021). Challenges and Opportunities of Nanomedicines in Clinical Translation. *BIO Integration* 2 (2), 57–60. doi:10.15212/bioi-2021-0016
- Zheng, P., Liu, Y., Chen, J., Xu, W., Li, G., and Ding, J. (2020). Targeted pH-Responsive Polyion Complex Micelle for Controlled Intracellular Drug Delivery. *Chin. Chem. Lett.* 31 (5), 1178–1182. doi:10.1016/j.ccl.2019.12.001

Conflict of Interest: The authors declare that the research was conducted in the absence of any commercial or financial relationships that could be construed as a potential conflict of interest.

Publisher's Note: All claims expressed in this article are solely those of the authors and do not necessarily represent those of their affiliated organizations, or those of the publisher, the editors, and the reviewers. Any product that may be evaluated in this article, or claim that may be made by its manufacturer, is not guaranteed or endorsed by the publisher.

Copyright © 2021 Liu, Chen, Shi, Zhao and Ma. This is an open-access article distributed under the terms of the Creative Commons Attribution License (CC BY). The use, distribution or reproduction in other forums is permitted, provided the original author(s) and the copyright owner(s) are credited and that the original publication in this journal is cited, in accordance with accepted academic practice. No use, distribution or reproduction is permitted which does not comply with these terms.



Functional Nanomedicines for Targeted Therapy of Bladder Cancer

Chao Tang¹, Heng Liu¹, Yanpeng Fan¹, Jiahao He², Fuqiu Li³, Jin Wang^{1*} and Yuchuan Hou^{1*}

¹Department of Urology, the First Hospital of Jilin University, Changchun, China, ²School of Chemical Engineering, Changchun University of Technology, Changchun, China, ³Department of Dermatology, the Second Hospital of Jilin University, Changchun, China

OPEN ACCESS

Edited by:

Sanjun Shi,
Chengdu University of Traditional
Chinese Medicine, China

Reviewed by:

Kaiyuan Ni,
Koch Institute for Integrative Cancer
Research at MIT, United States
Mohd Ahmar Rauf,
University of Miami Hospital,
United States

*Correspondence:

Jin Wang
jinglewang@jlu.edu.cn
Yuchuan Hou
hou63@163.com

Specialty section:

This article was submitted to
Pharmacology of Anti-Cancer Drugs,
a section of the journal
Frontiers in Pharmacology

Received: 17 September 2021

Accepted: 29 October 2021

Published: 16 November 2021

Citation:

Tang C, Liu H, Fan Y, He J, Li F,
Wang J and Hou Y (2021) Functional
Nanomedicines for Targeted Therapy
of Bladder Cancer.
Front. Pharmacol. 12:778973.
doi: 10.3389/fphar.2021.778973

Bladder cancer is one of most common malignant urinary tract tumor types with high incidence worldwide. In general, transurethral resection of non-muscle-invasive bladder cancer followed by intravesical instillation of chemotherapy is the standard treatment approach to minimize recurrence and delay progression of bladder cancer. However, conventional intravesical chemotherapy lacks selectivity for tumor tissues and the concentration of drug is reduced with the excretion of urine, leading to frequent administration and heavy local irritation symptoms. While nanomedicines can overcome all the above shortcomings and adhere to the surface of bladder tumors for a long time, and continuously and efficiently release drugs to bladder cancers. The rapid advances in targeted therapy have led to significant improvements in drug efficacy and precision of targeted drug delivery to eradicate tumor cells, with reduced side-effects. This review summarizes the different available nano-systems of targeted drug delivery to bladder cancer tissues. The challenges and prospects of targeted therapy for bladder cancer are additionally discussed.

Keywords: bladder cancer, targeted therapy, nanoparticle, intravesical instillation, chemotherapy

1 INTRODUCTION

Bladder cancer (BC) is the ninth most common urinary tract cancer type worldwide. In Western countries, the incidence of bladder cancer is different between genders, and the life time risk of bladder cancer is approximately 1.1 and 0.27% in men and women, respectively (Lenis et al., 2020). BC is reported to be the ninth leading cause of cancer-related mortality in men. In 2020, according to the American Cancer Society, 81,400 new BC cases and about 17,980 bladder cancer-related deaths were predicted in the United States alone (2020). In Europe, the incidence and mortality of BC are estimated as 27.1 and 8.9% respectively (Taskovska et al., 2020). Based on clinicopathological results, BC is classified into muscle-invasive bladder cancer (MIBC) and non-muscle-invasive bladder cancer (NMIBC, staged as Ta, T1, or carcinoma *in situ*) (Zhuo et al., 2016), the latter accounting for more than 75% cases (Babjuk et al., 2021). Transurethral resection procedures can effectively save the human bladder and enhance patient quality of life. However, studies have shown that without therapeutic drug interventions, the 5-years recurrence rate of NMIBC is ~60–75% and about 15–25% of the recurrent tumor would progress into MIBC (Martinez et al., 2019; Seidl, 2020). Owing to its high recurrence rates, BC is a long-term disease that poses a heavy financial burden compared to other cancer types.

Thus, reducing the recurrence rate and preventing tumor progression remain significant challenges in the field of BC research. The gold standard treatment for superficial BC is complete transurethral resection and postoperative adjuvant intravesical instillation of

chemotherapy to reduce recurrence and delay or even prevent progression to muscle-invasive disease. Clinical experience supports the utility of intravesical instillation therapy as an auxiliary method to prevent postoperative tumor recurrence. The drug contacts the bladder mucosa via this system to directly or indirectly kill the remaining tumor cells in the bladder, prevent tumor cell planting and reduce the recurrence rate.

Chemotherapy drugs and immune agents can be intravesically instilled into bladder directly via dissolving in saline. Chemotherapeutic agents for BC mainly include epirubicin (EPI), tetrahydropyran-yl-adriamycin (THP) (Chen et al., 2012), gemcitabine (GEM) (Bohle et al., 2009), and mitomycin C (MMC) (Schmidt et al., 2020), which exert their effects through inhibiting tumor cell nucleic acid synthesis and influencing the cell cycle to induce cell death. *Bacillus Calmette-Guérin* (BCG) has long been approved as an immunotherapeutic agent (Guallar-Garrido and Julian, 2020) and its potential mechanism of action of BCG is that the absorption, internalization and subsequent induction of cytokines produced by BCG after intravesical instillation induce adaptive immunity and anti-tumor effects, thereby reducing the recurrence and progression of bladder cancer (Pettenati and Ingersoll, 2018; Han et al., 2020).

Clinically, intravesical drugs can reduce tumor recurrence rates to some extent. However, the treatment effect is significantly lower than expected, which may be attributed the following factors: 1) the drugs lack selectivity for tumor cells, leading to limitation of the tumor-killing effect, and exert significant toxic effects on normal bladder mucosa (Vasir and Labhasetwar, 2005); 2) due to the continuous production of urine, the concentration of drug within bladder cancer tissue is reduced, and with the continuous excretion of urine, the drug is excreted from the body, shortening its retention time in the bladder (GuhaSarkar et al., 2017); 3) drug efficacy is limited by the biological barrier of the bladder urothelium (Li et al., 2019); 4) owing to frequent administration and heavy local irritation symptoms, some patients cannot tolerate continual intravesical instillation. Therefore, the optimal strategy for therapy may be to enhance the ability of the drug to recognize bladder cancer tissue and extend its retention time on the target surface. Additionally, drugs could be efficiently internalized and taken up by tumor cells to achieve precise targeted cell killing, maximally inhibiting progression of tumor recurrence and reducing local side-effects.

Targeted therapy has received considerable research attention for further development. Targeted drug delivery systems present significant advantages in the treatment of bladder cancer by facilitating selective delivery of chemotherapy to tissues. However, achievement of therapeutic drug delivery specifically to tumor cells or tissues through the membrane and subsequent release of the drug into target tumors without damage to normal cells remains a significant challenge (Zheng et al., 2021c). Researchers have attempted to resolve this issue by using nanoparticles as delivery vehicles (Pridgen et al., 2007; Sarah C.; Andrew et al., 2012; Baetke et al., 2015). Numerous studies to date have developed nanotechnology with multiple features and functions for accomplishing efficient drug delivery and release.

Nanotechnology mainly deals with materials between 1 and 200 nm in size (Azocar et al., 2019). Since the concept of nanotechnology was first introduced in 1959 by Richard Feynman, rapid developments have occurred over several decades with considerable success in multiple fields, including chemistry, physics, biology and medicine (Bayda et al., 2019). In the field of medicine, nanotechnology has been successfully applied to diagnose and treat diseases using the properties (Zhang et al., 2020) and physical characteristics of nanomaterials at the molecular level (Betty et al., 2010). Nanomaterials have the characteristics of large specific surface area, strong adsorption capacity, high bioavailability, precise targeting characteristics and controlled release rate of drugs (Sibuyi et al., 2019). Nanotechnology has been used to effectively design and develop targeted vehicles providing drug delivery systems that transport therapeutic drugs into cancer cells through biological barriers. Relative to conventional drug therapy, nano-drugs have a higher surface area to volume ratio. Simultaneously, with advances in tunable optical, magnetic, electronic, and biological properties, nanomaterials can be developed with different sizes, shapes, chemical compositions, and surface chemical characteristics (Peer et al., 2007; Xia et al., 2009). Based on their multiple beneficial features, nanomaterials have significant potential as a new generation of drug delivery vehicles. To date, the FDA has approved 51 nanomedicines for clinical use and 77 products for clinical trials (Bobo et al., 2016).

Nanoparticles used as chemotherapy drug carriers are submicron-sized particles (3–200 nm), devices or systems generated using different materials including polymers, such as micelles, dendrimers, liposomes, viral nanoparticles, and even organometallic compounds (Cho et al., 2008). The nanomaterial surface is usually coated with a variety of polymers or specific biorecognition molecules for improved biocompatibility and targeting. For BC therapy systems, nanoparticles are divided into two types: non-specific and specific targeted therapy (Figure 1). The former type acts through interaction forces on the cell membrane surface to achieve specific targeted release of drugs, including surface charge, and besides, reduction-responsive nanoparticle is also one type of non-specific targeted nanoparticles. After being endocytosed into cells, under the action of high GSH, the disulfide bonds in reduction-responsive nanoparticles carrying therapeutic drugs are degraded, thereby releasing the therapeutic drugs and increasing the concentration of the drug in the cell, while the latter system binds cells through peptides or proteins and so on to achieve efficient cancer-targeted therapy (Table 1). The challenges and prospects of targeted therapy for BC are extensively discussed in this review.

2 NON-SPECIFIC TARGETED THERAPEUTIC NANOCARRIERS FOR TREATMENT OF BLADDER CANCER

The efficacy of conventional instilled chemotherapy for bladder cancer is adversely affected by limitations in the ability of drugs to reach tumors (Arranja et al., 2017). During the treatment process, repeated instillation of drugs into the bladder is often necessary, which reduces the quality of life of BC patients and poses a serious burden to their families. To overcome the drawbacks of

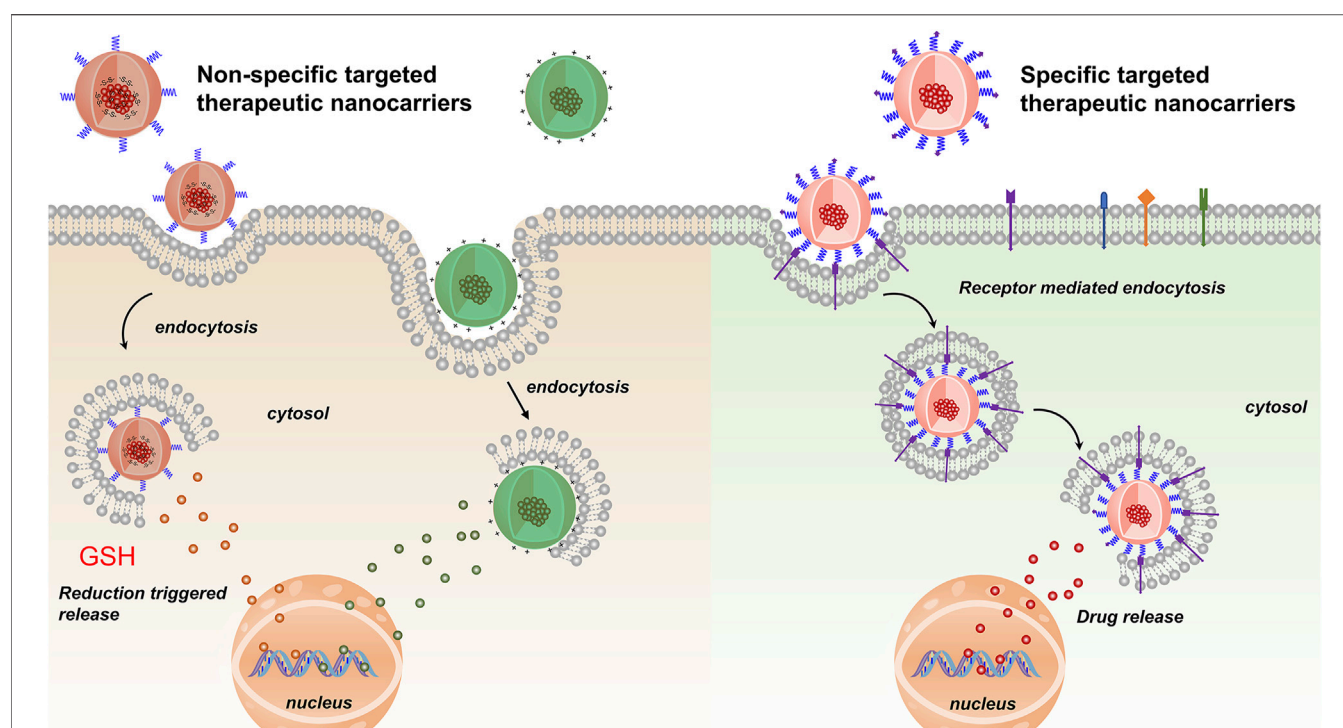


FIGURE 1 | Non-specific and specific targeted therapeutic nanocarriers for treatment of BC.

TABLE 1 | The mechanism of non-specific and specific targeted therapeutic nanocarriers for treatment of cancer.

Nanocarriers type	Nanocarriers properties	Material type	References
Non-specific targeted NPs	Positively NPs	CAT-TCPP/FCS CS-PCL (PLL-P (LP-co-LC) P (LP-co-LC)	Li et al. (2020) Bilensoy et al. (2009) (Guo et al., 2018; Guo et al. (2017) Guo et al. (2020b)
Specific targeted NPs	Reduction responsive NPs Small molecules-modified Peptides-modified	FA-conjugated Au@TNA/MB Bld-1-KLA MSNs@PDA-PEP PLZ4-PNP PLZ4-DNR/PTX MPI/F-PEI PCL-b-PEO C225 antibody siRNA@CS-HAD	Hsu et al. (2020) Jung et al. (2016) Wei et al. (2017) Lin et al. (2016) Pan et al. (2016) Wang et al. (2008) Zhou et al. (2013) Cho et al. (2019) Liang et al. (2021)
	Protein-modified Hyaluronic acid-modified		

conventional chemotherapeutic agents, achievement of targeted effects on tumors is necessary. Recent studies have validated the potential of nanotechnology-based drug targeted delivery systems in achieving targeted drug release. The so-called targeted release of drugs refers to the delivery and release of chemotherapeutic drugs into target tumor sites, which should help reduce accumulation in non-tumor sites and improve their utilization and therapeutic effects (Moses. et al., 2003; Maeda et al., 2013; Bertrand et al., 2014).

Nanocarriers are commonly used to enhance the targeted release of drugs (Dadwal et al., 2018) but can encounter several obstacles in the process of drug delivery, such as the barrier effect of biological mucosa and non-targeted uptake of

drugs. Therefore, nano-drug carrier system designs are generally based on the characteristics of the carrier to enhance targeted drug delivery. For example, a number of positively charged drug carriers (Choi et al., 2016; Young et al., 2016) and nanocarriers with reductive responsiveness (Hadi et al., 2021; Kuang et al., 2021; Oluwasanmi and Hoskins, 2021) are frequently used as non-specific drug delivery carriers.

2.1 Positive Nanoparticle Carriers for Bladder Cancer

Several types of nanoparticles have been investigated in clinical medicine applications including disease diagnosis and treatment.

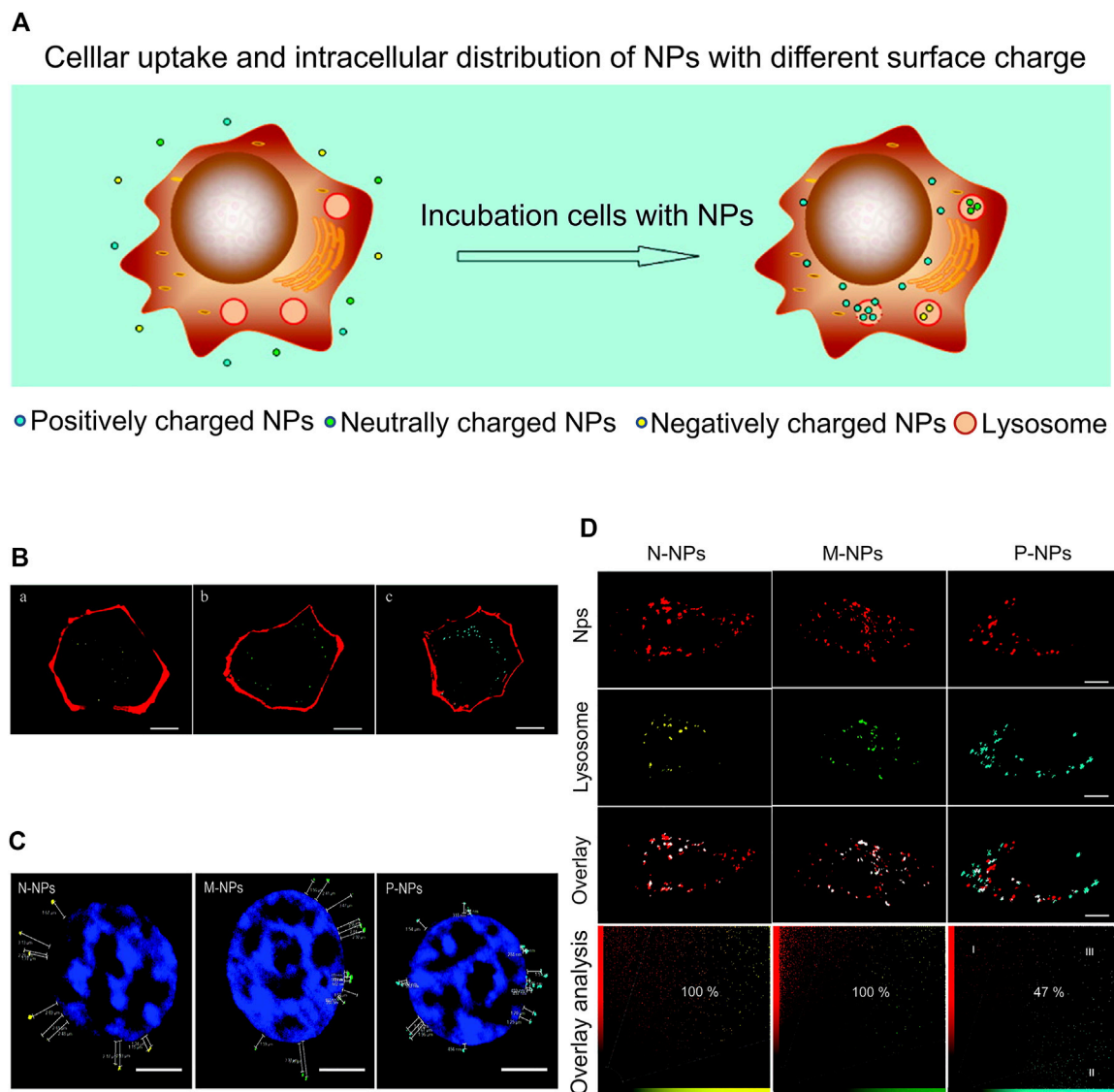
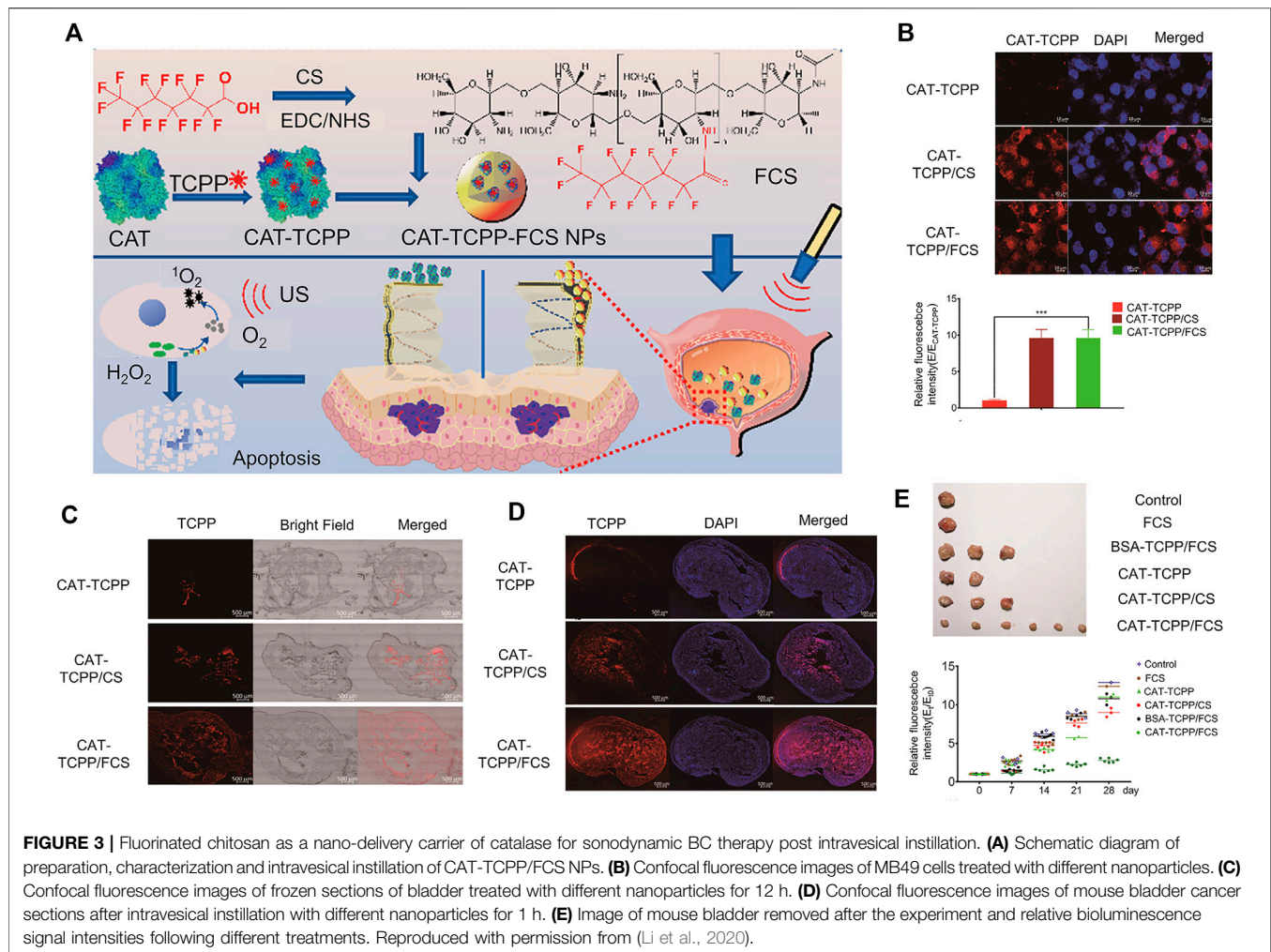


FIGURE 2 | Surface charges affect cellular uptake. **(A)** Cellular uptake and intracellular distribution of NPs with different surface charges. **(B)** CLSM images of HKC cells incubated with NPs of different charges: **(A)** negatively charged, **(B)** neutrally charged, and **(C)** positively charged. **(C)** CLSM images of HKC cells after treatment with NPs of different charges. **(D)** CLSM images of lysosomes of HKC cells treated with different nanoparticles for 6 h. Reproduced with permission from (Yue et al., 2011).

The carrier function of nanoparticles for drug delivery is a considerable focus of research. All nanoparticle applications are based on the uptake and utilization of nanomedicines by cells, with surface charge determined as an important factor affecting cellular uptake (Frohlich, 2012). According to differences in the nature of the surface charge, nanocarriers are divided into positively, neutrally and negatively charged nanoparticles. The BC cell surface has a large number of negative charges (Thomas et al., 2009; Marquez-Miranda et al., 2016). Two main ways for cells to take up positively charged nanoparticles have been identified, specifically, endocytosis (Hong et al., 2006; Xiang et al., 2012) and cell membrane perforation (Hong et al., 2006; Leroueil et al., 2007). Positive

nanocarriers facilitate endocytosis of drugs by cells and overcome impermeability of cell membranes. For example, hydrophobic drugs are released from endosomes and move to targeted locations (Ramos et al., 2014). Positively charged nanoparticles thus have a higher affinity for cells relative to the other two nanoparticle types and enter cells more efficiently (Wu et al., 2016).

Chitosan (polyglucosamine (1-4)-2-amino-BD glucose) is a product of deacetylation of chitin. Chitosan is the only polycationic polysaccharide in nature with unique biological properties amenable for clinical use, such as non-toxicity, good biocompatibility, and easy degradation (Zhang et al., 2016). This linear polyamine contains three active functional groups



comprising hydroxyl groups that are easy to modify and graft. Based on its cationic properties (Guo et al., 2019; Guo et al., 2020a; Qiu et al., 2020), chitosan can be cross-linked with multivalent anions. Chitosan nanoparticles are one of the commonly used carriers for targeted delivery of anti-cancer drugs, including DNA or proteins that induce local genetic immunity. To exploit the unique beneficial properties of chitosan, different chemical modifications have been generated, providing a range of derivatives with properties useful for multiple applications (Yue et al., 2011). Based on chitosan modifications, several derivatives with distinct properties have been obtained to date, including o-carboxymethyl chitosan (Saranya et al., 2011), glycol chitosan (Koo et al., 2013), graft copolymerized chitosan (Prabaharan, 2015), and cross-linking chitosan derivatives (Amidi et al., 2010). In an earlier study, Yue and co-workers prepared three chitosan-based nanoparticles with distinct surface charges through SPG membrane emulsification and precipitation technology to assess surface charge effects on cellular uptake and intracellular transport. As shown in Figure 2, surface charge affected the uptake of cells and a positive charge could improve the rate of cell internalization.

The inner bladder surface has a biological barrier that prevents drug penetration. The bladder permeability barrier is caused by the thick mucus gel layer coating the bladder mucosa aligned with glycosaminoglycan chains dispersed in a viscous hydrogel (Erdoglar et al., 2015).

Li and co-workers designed and synthesized a sonodynamic therapy (SDT) mucosal platform that autonomously generates transmucosal oxygen. In this system, fluorinated chitosan was used as an efficient and non-toxic transmucosal delivery carrier loaded with meso-tetra(4-carboxyphenyl) porphine-conjugated catalase. CAT-TCPP/FCS nanoparticles (NP) instilled into the bladder showed excellent transmucosal and tumor penetration ability. Simultaneously, CAT-TCPP/FCS nanoparticles effectively alleviated hypoxia in the tumor by catalyzing H_2O_2 in the targeted tumor sites to generate O_2 through catalase and improved the therapeutic effect of SDT in ablation of bladder cancer under ultrasound (Li et al., 2020) (Figure 3A). Compared with bladder cancer cells treated with free CAT-TCPP, stronger CAT-TCPP fluorescence was observed in cells treated with CAT-TCPP/FCS nanoparticles, validating nanoparticle-enhanced cellular uptake (Figure 3B). As shown in Figures 3C–E, in the *in vivo* intravesical instillation experiment, bladder instilled with CAT-TCPP/FCS

NPs showed stronger CAT-TPP fluorescence and deeper fluorescence penetration (Li et al., 2020). In this study, synthetic fluorinated chitosan was used as a protein carrier to achieve efficient transmucosal and intratumor delivery in the bladder. Fluorinated chitosan is considered a promising platform for intravesical instillation of drugs in addition to chitosan-based nanoparticles.

In a study by Bilensoy et al., positively charged polycaprolactone coated with chitosan (CS-PCL) was used to load the intravesical chemotherapeutic drug mitomycin C (MMC). Notably, CS-PLC nanocarriers remained in the bladder for a long time, accumulated in bladder tumors, and prevented drug loss during urine excretion (Bilensoy et al., 2009).

In addition to positively charged chitosan-based nanoparticles, polyamino acid nanoparticles, such as poly-L-lysine (PLL), are commonly used as a positively charged drug delivery vehicle (Guo et al., 2017; Guo et al., 2018).

PLL is a water-soluble positive biopolymer that contains the monomeric lysine unit. Due to its inherent natural characteristics, such as non-antigenicity, biocompatibility and biodegradability, PLL is widely applied in multiple biomedical and pharmaceutical fields (Zheng M. et al., 2021). PLL has typical properties of polymeric nanoparticles. The amine group can be chemically conjugated with hydrophobic substances with carboxyl groups so that lipophilic drugs are effectively encapsulated during NP formation (Zhou et al., 2015). In addition to the advantages of conjugation, another important feature of the amino group of PLL is that its properties change under specific conditions. Specifically, in an acidic environment, the amino group is converted into a positively charged hydrophilic amino group that can interact with BC cell membranes through electrostatic interactions (Vasir and Labhasetwar, 2008). In a study by Guo et al., a cationic peptide nanogel (PLL-P (LP-co-LC) was designed to successfully deliver 10-hydroxycamptothecin (10-HCPT) (NP/HCPT) for intravesical instillation therapy to bladder cancer *in situ*. *In vitro*, NP/HCPT promoted endocytosis of drugs by cells and exerted obvious cytotoxicity, while *in vivo*, NP/HCPT displayed adhesion to bladder mucosa and strong penetration ability (Guo et al., 2017; Guo et al., 2018).

2.2 Reduction Responsive Nanoparticle Carriers for Bladder Cancer

Several studies have reported that the intracellular environment of numerous tumor tissues is reductive. Under the same conditions, tumor tissues have high stability compared with normal tissues (Karimi et al., 2016), mainly due to the presence of a higher concentration of glutathione (GSH) (Asantewaa and Harris, 2021; Bansal and Simon, 2018). GSH is a common internal environmental stimulus in cells that rapidly destroys the stability of intracellular nanocarriers to achieve effective drug release (Cheng et al., 2011) (Figure 4A). Several researchers have focused on developing functional carriers with reduction responsiveness based on two strategies: insertion of disulfide bonds in the polymer backbone or using reduction-sensitive cross-linking molecules (Gulfam et al., 2017; Conte et al., 2018; Deng et al., 2018; Monteiro et al., 2020). Glutathione (GSH)

levels inside and outside cancer cells are markedly different (Lai et al., 2021; Liu et al., 2021). Nanocarriers with reducing properties can achieve drug release more accurately and rapidly. After endocytosis of nanomedicine by cancer cells, under conditions of high GSH, disulfide bonds are reduced to a sulfhydryl group as a reduction response, causing the polymer to decompose and release the loaded drug (Zhao et al., 2017; Hu et al., 2018; Yang et al., 2021). With the rapid development of reduction-sensitive and reversible cross-linked polymers in the past few years, various reduction-sensitive systems have shown significant activity against different malignant tumors (Meng et al., 2009; Cheng et al., 2011; Feng et al., 2020). Bladder cancer cells contain a high concentration of GSH that can restore the microenvironment.

Guo and co-workers designed a disulfide bond cross-linked nanogel based on poly (L-phenylalanine-co-L-cystine) (Figure 4B). As shown in Figures 4C–F, the nanogel exerted obvious cytotoxicity in the human BC cell line 5,637. The longer residence time of the chemotherapy drug 10-HCPT in the bladder enhanced penetration ability into the bladder wall, leading to a significant inhibitory effect on tumors in animal models (Guo et al., 2020b).

3 SPECIFIC TARGETED THERAPEUTIC NANOCARRIERS FOR BLADDER CANCER

Compared with the traditional method of administration, namely, direct intravesical drug instillation therapy, nanocarriers or biological materials exert greater effects on eliminating tumors and inhibiting tumor growth. However, ordinary nanomaterials have a number of drawbacks (Wei et al., 2021). The principle of action of nanocarriers is to extend the retention time of drugs and enhance penetration ability into bladder walls (Ding et al., 2019). However, no obvious advantages in active targeting of cancer cells have been observed, thus limiting the maximum therapeutic effect of drugs. Although a better curative effect could be achieved, a number of associated side-effects are reported. For treatment of BC, in addition to the use of nanocarriers with strong mucosal adhesion for delivery of drugs or passively targeted therapy, another potential strategy is active nanocarrier-mediated targeting of the tumor. This section introduces in detail nano-delivery vehicles that can specifically identify bladder cancer and reduce the toxicity of drugs to normal cells and tissues to enhance targeted treatment (Xu et al., 2020).

3.1 Small Molecule-Modified Targeted Therapeutic Nanocarriers for Bladder Cancer

Folic acid (FA, also known as vitamin B9) is a critical nutrient for growth and development of organisms that plays an indispensable role in DNA methylation, biosynthesis and repair. In nature, folic acid is widely distributed in various fruits and vegetables (Tu et al., 2018). Two mechanisms of FA uptake have been identified: 1) reduced folate carrier (RFC1)

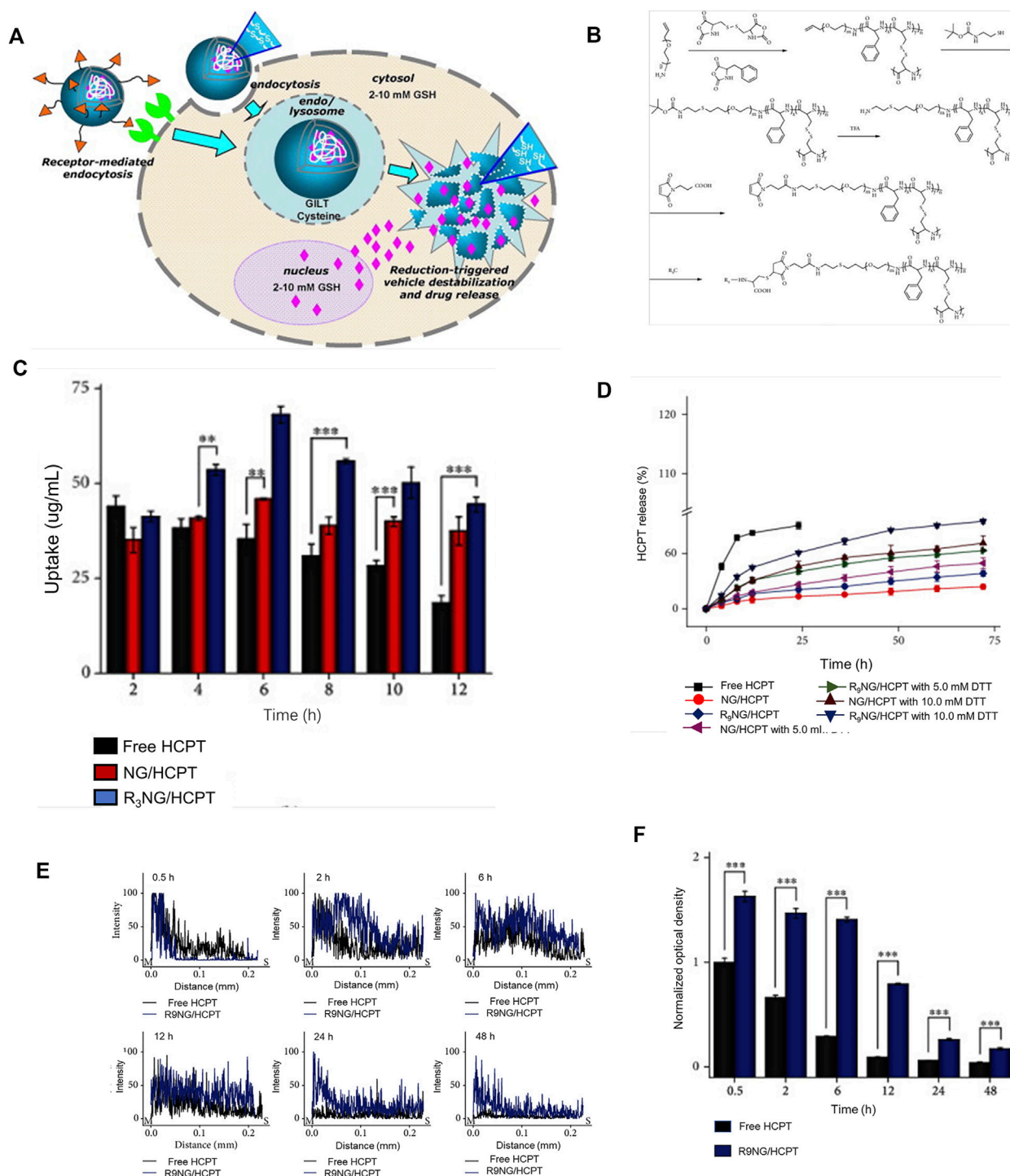
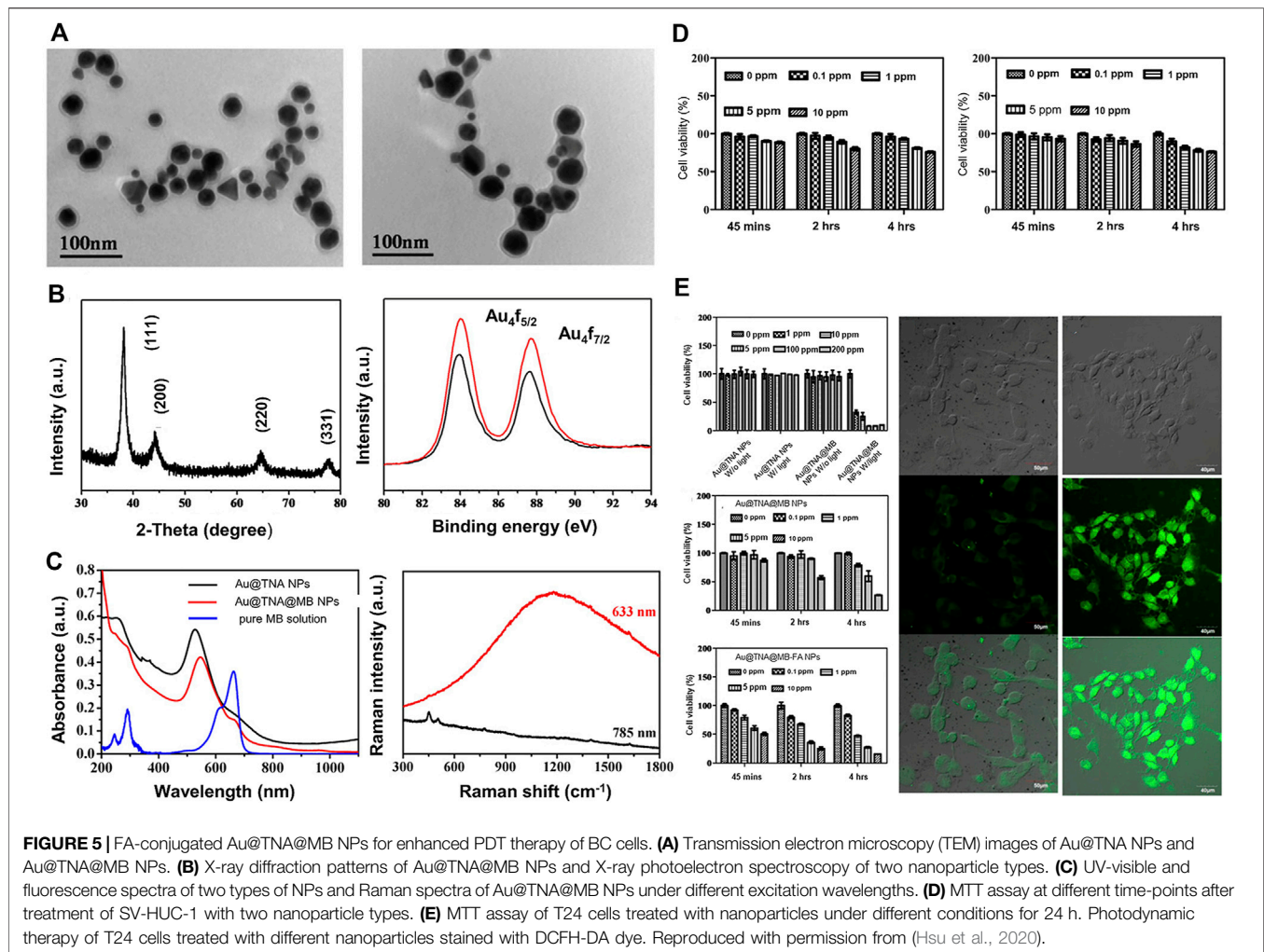


FIGURE 4 | Reduced responsive nanoparticles as carriers for intracellular drug release. **(A)** Schematic illustration of reduced responsive nanoparticle carriers for intracellular drug release (Cheng et al., 2011). **(B)** Synthesis route of R9-PEG-P (LP-co-LC). **(C)** Intracellular HCPT release in human BC 5637 cells treated with different formulations of HCPT. **(D)** In vitro release profiles of R9NG/HCPT. **(E)** Quantification of bladder penetration of HCPT based on fluorescence intensity. **(F)** Quantitative analysis of fluorescence intensity of HCPT. Reproduced with permission from (Guo et al., 2020).

promotes endocytosis of folic acid in a reduced form by cells and 2) high-affinity folate receptor recognizes folic acid and promotes its oxidation by cells through receptor mediation. Folic acid that

enters the cell through this pathway is released into the cytoplasm through endosomal acidification (Godeshala et al., 2016). FR has been shown to be overexpressed in a number of human tumor



types, including triple-negative breast cancer, ovarian cancer, and non-small cell lung cancer. Additionally, the receptor is overexpressed in bladder cancer relative to normal bladder cells (Godeshala et al., 2016). The differential expression of FR between normal bladder and bladder cancer cells provides a significant research direction for targeted therapy.

Based on the above findings, Hsu et al. designed and prepared Au@TNA core-shell nanoparticles via tannic acid (TNA)-assisted reduction of HAuCl_4 . Next, the photosensitizer methylene blue (MB) was combined on the surface of Au@TNA to generate Au@TNA@MB nanoparticles. Subsequently, nanoparticles were modified with folic acid (FA) to obtain FA-Au@TNA/MB NPs. The newly generated nanocarrier was composed of two types of nanoparticles (spherical and triangular) with an average size of 26.43 ± 3.7 nm (Figures 5A–C). *In vitro*, the photosensitizer exerted slight toxicity on the normal urothelial cell line SV-HUC-1 (Figure 5D) but aggregated significantly in the bladder cancer cell line T24, leading to reduced survival of cancer cells (Figure 5E). Therefore, FA-conjugated Au@TNA/MB NPs present a promising PS nanomaterial for treatment of NMIBC. Further animal experiments are required to confirm the therapeutic

effects and adverse effects of these nanomaterials on bladder cancer (Hsu et al., 2020).

3.2 Peptide-Modified Specific Targeted Therapeutic Nanocarriers for Bladder Cancer

Compared with other targeted therapy, peptide-modified nanocarriers offer several advantages including lower production costs, relative stability, effortless commercialization, simple operation, and reduction of the immune response. At the same time, binding of peptides to receptors can achieve precise targeted therapy through design of specific reactive groups. In addition, particle size is relatively low, which has little effect on the physical and chemical properties of the synthesized nanoparticles (Zhong et al., 2014).

3.2.1 Bld-1-Modified Specific Targeted Therapeutic Nanocarriers for Bladder Cancer

Recent studies have focused on screening of specific organs. The majority of tumor-specific peptides have been identified from phage display libraries. As many as 10^{10} known peptides exist in

the phage library (Koivunen et al., 1999; Smith, 1985; H. MICHAEL; Ellerby et al., 1999; ohanna A.; Joyce, 2003). One notable example is the RGD motif comprising three amino acids, which binds tumor vascular endothelial cells through $\alpha v \beta 3$ integrin (expressed specifically in vascular endothelial cells). Compared with their normal counterparts, tumor cells display upregulation of a number of growth factor receptors that can serve as molecular markers. For instance, epidermal growth factor receptor, urinary glycoprotein and $\alpha 6 \beta 4$ integrin are highly expressed in bladder cancer.

Lee et al. used a phage display peptide library to identify peptides specifically targeting BC cells. Several peptide sequences with a common motif, CXNXDXRX/RC, were selected. As discussed above, the inner wall of the bladder has a special protective layer composed of glycosaminoglycans and mucin. Although this layer can protect urothelium from adhesion of chemicals and microorganisms in concentrated urine, it also hinders intravesical instillation therapy. Effective penetration of the drug at this time shortens the action time. One of the peptides screened (CSNRDARRC) showed strong selective binding to bladder cancer cells. Fluorescent labeling experiments further revealed that CSNRDARRC co-localized with cytokeratin in bladder cancer tissues. Importantly, the peptide was not detected in normal bladder tissues and other organs. The tumor cell selectivity of CSNRDARRC and its specific targeting of bladder cancer strongly support the utility of this peptide as a BC-targeted therapeutic agent (Lee et al., 2007).

Jung et al. utilized the CSNRDARRC peptide (Bld-1) as a targeting ligand to selectively deliver KLA to bladder cancer and examined the activity of Bld-1-KLA hybrid peptide as targeted therapy for bladder tumors with pro-apoptotic peptides. The hybrid peptide effectively targeted bladder cancer cells and induced apoptosis, and could therefore serve as an excellent bladder tumor-targeting pro-apoptotic peptide (Jung et al., 2016).

In addition, the Bld-1 peptide itself may be applied as a targeting ligand in combination with nanocarriers loaded with conventional chemotherapeutics for drug delivery to bladder tumors. Wei et al. (Wei et al., 2017) described a simple surface modification method based on polydopamine (PDA). The group prepared a novel mesoporous silica as a doxorubicin-loaded nanocarrier and used peptide (CSNRDARRC)-coupled targeted delivery for bladder cancer nanotherapy. The synthesis process is shown in **Figure 6A**. Further characterization of the synthesized drug-loaded nanoparticles revealed a nanoparticle size of 168.3 ± 8.1 nm for DOX-loaded MSNs@PDA and 170.2 ± 7.5 nm for DOX-loaded MSN@PDA-PEP, respectively (**Figure 6B**). Cell experiments were developed to verify endocytosis of the peptide-modified drug-loaded DOX-loaded MSN@PDA-PEP and its killing effect (**Figures 6C,D**). As shown in **Figure 6E**, DOX-loaded MSN@PDA-PEP significantly inhibited tumor growth in animal experiments. In conclusion, DOX-loaded MSN@PDA-PEP could specifically recognize BC cells, increase drug toxicity and suppress growth of BC.

3.2.2 PLZ4-Modified Specific Targeted Therapeutic Nanocarriers for Bladder Cancer

The phage display library was screened for peptides that could be used in bladder cancer therapy (Lee et al., 2007). *In vivo* targeting

of human primary bladder cancer cells was a subsequent focus of a study by Zhang et al. A one-bead one-compound combinatorial peptide library technology (OBOC) was applied to identify several bladder-specific ligands with the same DGR motif showing potential utility in targeted bladder cancer therapy. However, only the cyclic PLZ4 peptide with the amino acid sequence cQDGRMGFc was specific for bladder cancer. PLZ4 could specifically bind $\alpha v \beta 3$ integrin on BC cells but not normal urothelial cells (Zhang et al., 2012).

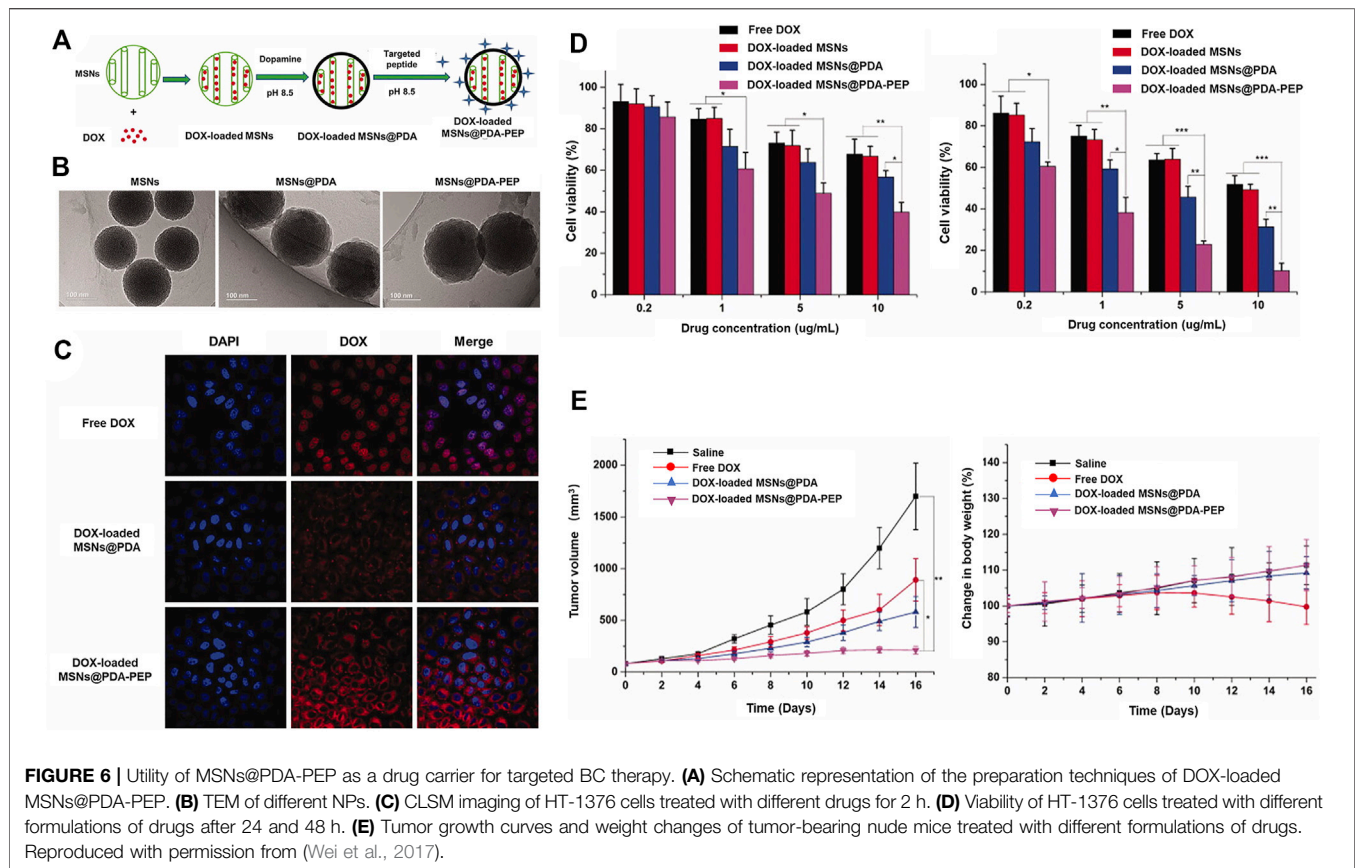
Lin and co-workers developed a multifunctional nanoporphyin platform modified with PLZ4 ligand. PLZ4-nanoporphyin (PNP) has multiple applications in photodynamic diagnosis, photothermal therapy and targeted chemotherapy. PNP is a nanosphere that emits fluorescence/heat/reactive oxygen species upon irradiation with near-infrared. Compared with free Dox, the PLZ4-PNP platform significantly prolonged overall survival of mice. The three effective modes (photodynamic/photothermal/chemistry) of the platform could be easily applied for individualized treatment and have significant potential in the targeted management of bladder cancer (Lin et al., 2016).

The group of Lin further combined one end of polyethylene glycol with a cholic acid cluster and modified the other end with PLZ4. Daunorubicin (DNR) and paclitaxel (PTX) were loaded into the prepared micelles to form PLZ4-modified PLZ4-DNR/PTX nanoparticles with a particle size of about 23.2 ± 8.1 nm and their efficacy in dog bladder cancer examined *in vivo* and *in vitro*. As shown in **Figure 7**, compared with non-targeted nanomicelles, PLZ4-modified nanomicelles could deliver drugs to bladder cancer tissues more effectively and promote nanomicelle absorption from the bladder (Lin et al., 2012). Pan and co-workers developed bladder cancer-specific nanomicelles loaded with the chemotherapeutic drug paclitaxel (PTX). The micelles were gradually combined with polyethylene glycol, cholic acid and PLZ4. PTX and micelles were mixed and encased in the core, finally forming disulfide-crosslinked PLZ4 nanomicelles (DC-PNM-PTX). The drug loading rate of PTX was 25% and drug loading efficiency was >99%. The nanomicelles were spherical with a particle size of about 25 nm. Notably, upon intravenous administration *in vivo*, DC-PNM-PTX targeted bladder cancer but had no specificity for lung cancer in the same animal (Pan et al., 2016).

PLZ4 has therefore been identified as a target peptide for bladder cancer and effectively utilized as a modified vehicle for accurate delivery of drugs to achieve the maximum therapeutic effect.

3.2.3 MPI-Modified Specific Targeted Therapeutic Nanocarriers for Bladder Cancer

Polybia mastoparans are novel mastoparan peptides purified from venom of the neotropical social wasp *Polybia paulista* (de Souza et al., 2009). Polybia mastoparan I (MPI), a member of the Polybia mastoparan family, is a tetradeca peptide with an amidated carbon terminal and three lysine residues in the fourth, fifth and 11th positions (Souza et al., 2005). The amino acid sequence of MPI is IDWKKLLDAAKQIL and its α -helical conformation promotes cell apoptosis and lysis. MPI selectively inhibits proliferation of bladder cancer cells with negligible toxicity to normal cells and has the



advantages of high efficiency, specific targeting, biological safety, and excellent biological tolerance that are not observed with conventional chemotherapy drugs. However, the high molecular weight and high hydrophilicity of MPI cause insufficient bladder wall permeability, which limits the widespread promotion and application of this polypeptide (Wang et al., 2008; Orsolic, 2012; Li et al., 2019). Previous studies by Li et al. indicate that polymers with a higher degree of fluorination can improve the delivery efficiency of biomolecules. Recently, the delivery potential of F-PEI was examined as a new generation of transmucosal drug carriers through intravesical perfusion. After mixing, MPI polypeptides self-assembled with F-PEI to form MPI/F-PEI via the fluoride effect, hydrogen bonding and electrostatic interactions. The authors constructed a subcutaneous tumor model and administered free MPI, MMC, and MPI nanoparticles. Notably, MPI nanoparticles had an obvious inhibitory effect on tumor growth relative to free MPI and MMC. Based on these earlier studies, we infer that fluorinated polymers can be effectively used as transmucosal drug delivery vehicles with good application prospects for bladder cancer management, thus providing a new avenue for diversification of bladder cancer treatment in the future (Wang et al., 2008).

3.2.4 c(RGDfK)-Modified Specific Targeted Therapeutic Nanocarriers for Bladder Cancer

The arginine-glycine-aspartic acid (RGD) peptide sequence with remarkable targeting ability specifically interacts with cells

overexpressing $\alpha v \beta 3$ integrin and plays a critical regulatory role in tumor growth, metastasis and angiogenesis (Zheng et al., 2020). High-affinity interactions between RGD peptides and tumor-associated integrins have led to their wide usage in construction of active targeting systems for anti-cancer drug delivery (Xiong et al., 2007; Zhan et al., 2010; Tian et al., 2011; Chen et al., 2015).

Zhou et al. (2013) developed a potential targeted drug delivery system for intravesical instilled chemotherapy for superficial bladder cancer. In this study, amphiphilic diblock copolymer polycaprolactone-b-polyethylene oxide (PCL-b-PEO), cyclic (arginine-glycine-aspartic acid-D-phenylalanine-lysine) (c(RGDfK)) and FITC were conjugated through specific end groups of the hydrophilic block and assembled into micelles. Interactions between micelles and various model cells were analyzed using confocal laser scanning microscopy and flow cytometry. The c(RGDfK) on the micelle surface was confirmed via $^1\text{H-NMR}$ analysis and affinity for human glioblastoma-astrocytoma cells (U87MG). The *in vitro* cytotoxicity assay was used to evaluate the viability of bladder cancer cells (T-24) after incubation with doxorubicin (DOX) polymer micelles. The results showed strong affinity of c(RGDfK)-modified micelles for T-24 cells and significant inhibitory effect on cell proliferation when loaded with doxorubicin drugs, supporting a significant effect of c(RGDfK) on bladder cancer. The c(RGDfK)-modified micelles assembled by PCL-b-PEO diblock copolymer developed in this

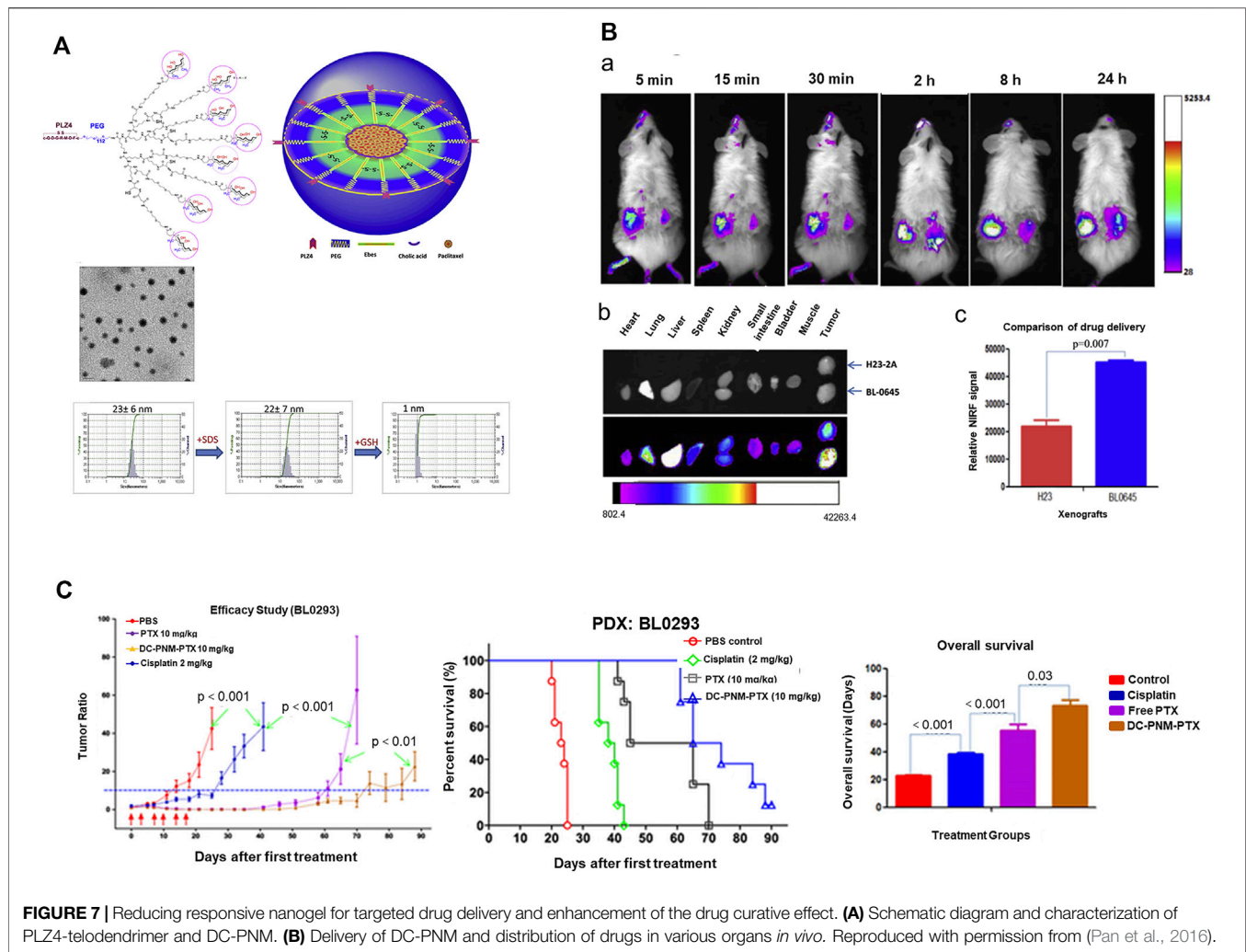


FIGURE 7 | Reducing responsive nanogel for targeted drug delivery and enhancement of the drug curative effect. **(A)** Schematic diagram and characterization of PLZ4-telodendrimer and DC-PNM. **(B)** Delivery of DC-PNM and distribution of drugs in various organs *in vivo*. Reproduced with permission from (Pan et al., 2016).

study displayed remarkable potential as a nano-drug system for superficial bladder cancer bladder perfusion chemotherapy (Figure 8).

3.2.5 Protein-Modified Specific Targeted Therapeutic Nanocarriers for Bladder Cancer

The epidermal growth factor receptor (EGFR) is a focus of increasing research attention in the field of cancer treatment. EGFR is a member of the tyrosine kinase receptor family and its abnormal expression is associated with excessive cell proliferation. In addition, EGFR is reported to promote angiogenesis in tumors and inhibit growth and development of tumor cells (Yewale et al., 2013). EGFR is also overexpressed in bladder cancer and shown to be related to tumor stage, progression and clinical results. Two main EGFR inhibitors have been identified, specifically, monoclonal antibodies (Sartore-Bianchi et al., 2009) and small-molecule tyrosine kinase inhibitors (MAARTEN L. Janmaat, 2003). C225, a monoclonal antibody also known as cetuximab, mainly acts on the extracellular domain of EGFR. C225 competes with ligands for binding to EGFR, thereby blocking

activation of the receptor and achieving treatment effects (Yao et al., 2019).

In terms of nanotherapy, Cho and co-workers synthesized multifunctional nanoclusters of upconversion nanoparticles (UCNP) and gold nanorod (AuNR) through PEGylation. The UCNP-AuNR multifunctional nanoclusters generated could be effectively applied to treat bladder cancer. Subsequently, these nanoclusters were further modified with antibodies to generate functionalized UCNP-AuNR with C225 antibody. In cell experiments, functionalized nanoclusters exerted obvious cytotoxic effects relative to those without antibody modifications. The use of monoclonal antibodies to modify nanocarriers is proposed to effectively reduce the dosage and maximize the therapeutic effects of drugs (Cho et al., 2019).

3.3 Hyaluronic Acid-Modified Specific Targeted Therapeutic Nanocarriers for Bladder Cancer

Owing to its multiple biological properties, such as high hydrophilicity and swelling capacity, hyaluronic acid (HA)

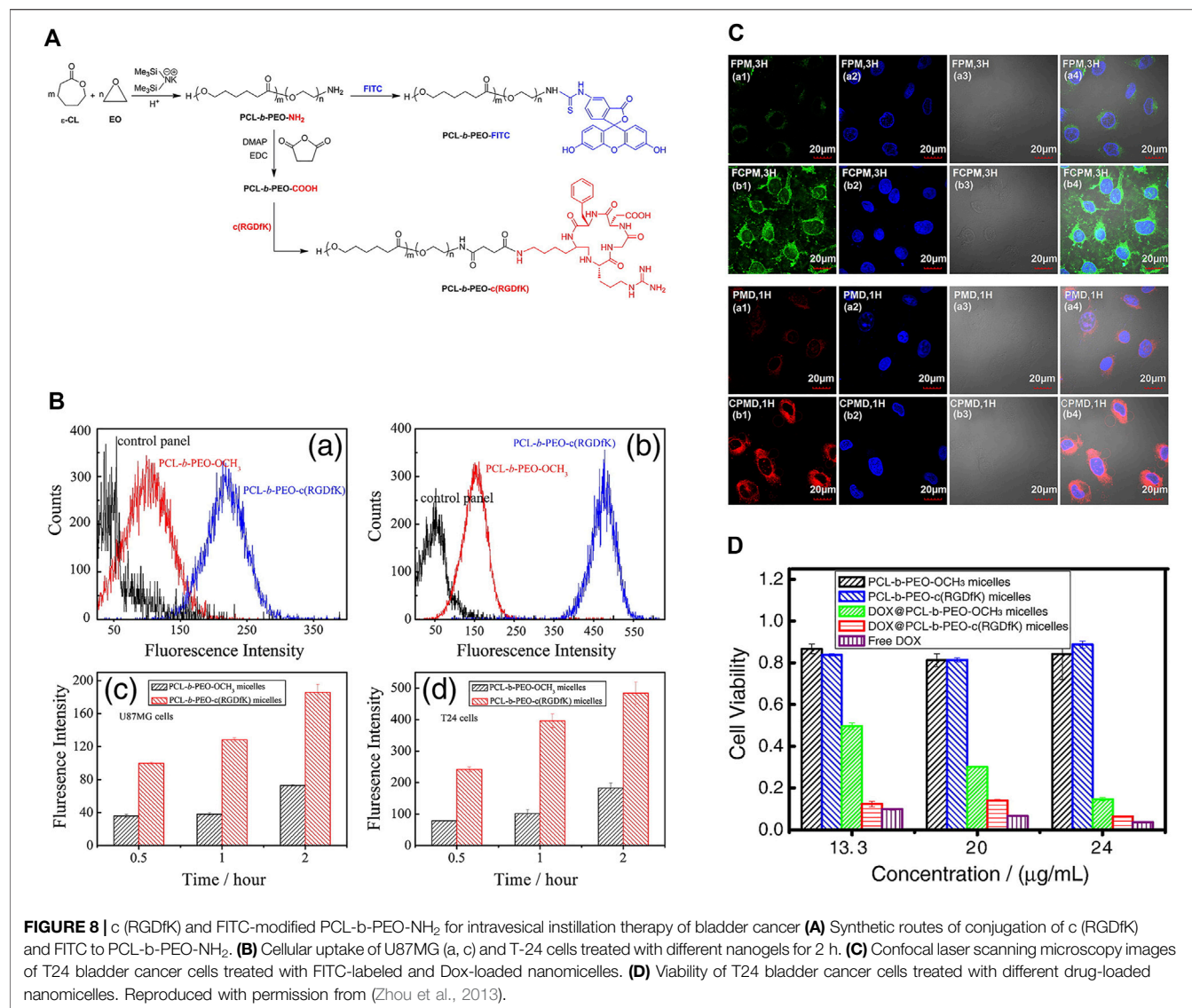
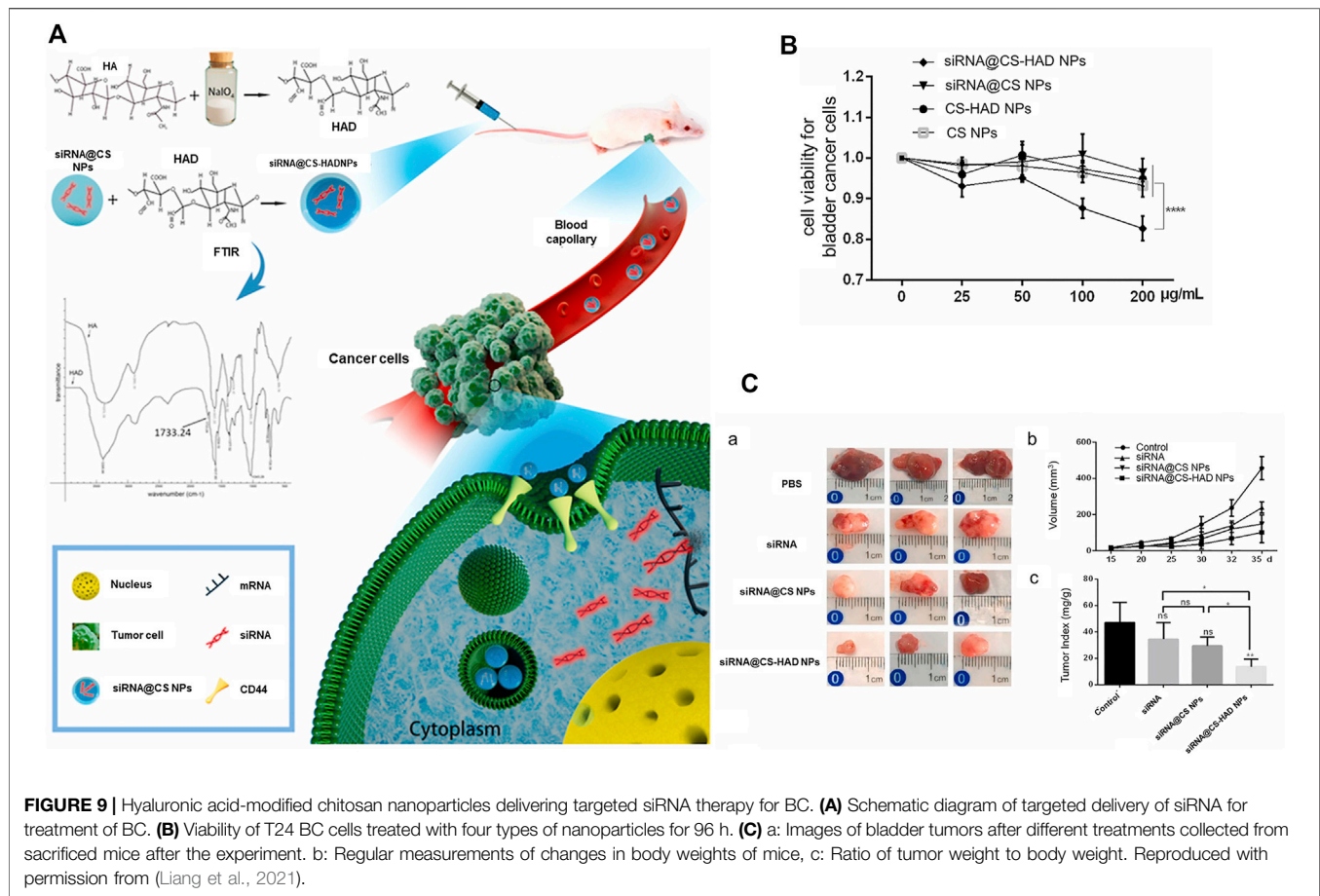


FIGURE 8 | ϵ (RGDFK) and FITC-modified PCL-b-PEO-NH₂ for intravesical instillation therapy of bladder cancer (A) Synthetic routes of conjugation of ϵ (RGDFK) and FITC to PCL-b-PEO-NH₂. (B) Cellular uptake of U87MG (a, c) and T-24 cells treated with different nanogels for 2 h. (C) Confocal laser scanning microscopy images of T24 bladder cancer cells treated with FITC-labeled and Dox-loaded nanomicelles. (D) Viability of T24 bladder cancer cells treated with different drug-loaded nanomicelles. Reproduced with permission from (Zhou et al., 2013).

is utilized in various drug carrier systems (Turcsanyi et al., 2020). HA is enriched in the extracellular matrix and secreted by cancer cells (Banerjee et al., 2016). In bladder cancer, tumor stroma and tumor cells can synthesize HA. CD44, a multifunctional cell surface transglycoprotein and a member of the cell adhesion molecule family overexpressed in various tumor cells, is involved in the growth, metastasis and apoptosis of several cancer cell types.

Liang and co-workers confirmed markedly higher expression of CD44 in bladder cancer relative to normal bladder. CD44 was further identified as a specific receptor for HA. Combination of HA and CD44 could induce conformational changes and allow adaptor proteins or cytoskeleton elements to bind intracellular domains, thereby activating multiple signaling pathways for cell proliferation, adhesion and metastasis (Ponta et al., 2003; Zoller, 2011). The authors designed and screened siRNAs that could interfere

with the Bcl2 gene and subsequently prepared CS-HAD nanoparticles targeting CD44 for siRNA delivery in an ethanol-water mixture. This system delivered siRNA to T24 bladder cancer cells through a ligand receptor-mediated targeting mechanism, ultimately interfering with expression of the apoptosis gene Bcl2. The siRNA@CS-HAD NP nanosystem had a particle size of 100–200 nm, good stability, and strong siRNA encapsulation ability. The results of *in vivo* and *in vitro* experiments showed that siRNA@CS-HAD nanoparticles effectively suppressed bladder cancer growth without exerting significant biological toxicity. The delivery of cy3-siRNA promoted targeted gene silencing. *In vivo*, siRNA@CS-HAD NPs accumulated in BC tissues and exerted a strong inhibitory effect on target oncogenes and tumor growth. This novel nanosystem may therefore present an effective method for targeted treatment of BC with high CD44 expression (Liang et al., 2021) (Figure 9).



4 CONCLUSION AND FUTURE PERSPECTIVES

Bladder cancer is a global disease with high incidence worldwide. Treatment of bladder cancer generally entails surgical removal followed by intravesical instillation of chemotherapy into the bladder to prevent recurrence. However, conventional chemotherapeutic drugs are not selective for normal tissue cells and trigger numerous side-effects when frequently instilled. For example, instillation of conventional chemotherapeutics into the bladder is associated with chemical cystitis and hematuria, with the severity being significantly dependent on the dose and frequency of instillation. Moreover, the majority of adverse effects can be improved after termination of drug treatment. Due to the higher recurrence and progression rate of BC, patients require long-term and repeated intravesical instillation after surgery. However, frequent intravesical instillation of chemotherapy is associated with several problems, such as high cost and excessive family burden. In recent years, nanotechnology has been applied to resolve these issues and shown to be feasible and efficient for diagnosis and therapy of bladder cancer.

According to their characteristics, nanoparticles are divided into actively targeted and passively targeted therapeutic carriers. The fundamental principle of passive targeted therapy is the EPR

effect while the active targeted drug delivery system uses specific ligands for attachment to vehicles or modification of the nanocarrier surface. Using the above mechanisms, nanoparticles can overcome the limitations of current traditional drug treatments for tumors, leading to significant improvement of therapeutic activity along with reduction of the side-effects of drugs. For instance, the nanoparticle surface induces significant changes in nanocarrier properties and interactions with the surrounding environment. At the same time, nanoparticles carry charges and non-specifically bind tumors through electrostatic interactions. As described above, positively charged nano-drug delivery carriers formed by chitosan bind non-specifically to the negatively charged inner wall of the bladder, leading to enhanced drug pairing. Adhesion to the bladder wall prolongs contact time with the tumor and enhances drug effects to an extent. Increasing attention has focused on tumor-specific targeted therapy and further research is ongoing.

Targeting ligands bound to the surface of nanoparticles can efficiently recognize receptors expressed on cancer cells, significantly improving the selectivity and killing effects of chemotherapeutics on bladder cancer cells. Targeting ligands generally include protein/peptide, hyaluronic acid, folic acid, and polysaccharides. Numerous *in vivo* and *in vitro* experiments on nanoparticles modified with targeting ligands and encapsulating chemotherapeutic drugs have

confirmed that receptor-mediated endocytosis increases chemotherapeutic drug uptake by cancer cells. Targeted nanoparticle delivery carriers have several advantages over general nanocarriers. Firstly, these carriers are selective for bladder cancer cells, reducing their combination with normal bladder tissues and cells, and decreasing the side-effects caused by drug perfusion in the bladder. Secondly, drug-loaded nano-systems accumulate at tumor targets and release the drug, increasing therapeutic drug concentrations at the tumor tissue sites. Thirdly, specific ligand-receptor binding can extend the drug retention time in the bladder and prevent its excretion with urine. Fourthly, the release time and speed of the drug can be controlled to reduce or even avoid irritation to the bladder caused by multiple infusions of the drug.

Despite the numerous benefits of targeted nanoparticles in tumor treatment, several problems need to be resolved before clinical application, for example, between the experimental stage of nanomedicine and its transformation into a clinical agent, the technical problems of large-scale production of nanomedicines, and cost control during the manufacturing process. Moreover, immunotherapy has also made major clinical breakthroughs and it may be applied to bladder cancer in the future, which will greatly improve the therapeutic effect of bladder cancer (Zheng et al., 2021b; Feng et al., 2021; Sun et al., 2021).

REFERENCES

- Amidi, M., Mastrobattista, E., Jiskoot, W., and Hennink, W. E. (2010). Chitosan-based Delivery Systems for Protein Therapeutics and Antigens. *Adv. Drug Deliv. Rev.* 62, 59–82. doi:10.1016/j.addr.2009.11.009
- Andrew, Z., Wang, R. L., and Farokhzad, O. C. (2012). Nanoparticle Delivery of Cancer Drugs. *Annu. Rev. Med.* doi:10.1146/annurev-med-040210-162544
- Arranja, A. G., Pathak, V., Lammers, T., and Shi, Y. (2017). Tumor-targeted Nanomedicines for Cancer Theranostics. *Pharmacol. Res.* 115, 87–95. doi:10.1016/j.phrs.2016.11.014
- Asantewaa, G., and Harris, I. S. (2021). Glutathione and its Precursors in Cancer. *Curr. Opin. Biotechnol.* 68, 292–299. doi:10.1016/j.copbio.2021.03.001
- Azócar, M. I., Alarcón, R., Castillo, A., Blamey, J. M., Walter, M., and Paez, M. (2019). Capping of Silver Nanoparticles by Anti-inflammatory Ligands: Antibacterial Activity and Superoxide Anion Generation. *J. Photochem. Photobiol. B* 193, 100–108. doi:10.1016/j.jphotobiol.2019.02.005
- Babjuk, M., Burger, M., Capoun, O., Cohen, D., Comperat, E. M., Dominguez Escrig, J. L., et al. (2021). European Association of Urology Guidelines on Non-muscle-invasive Bladder Cancer (Ta, T1, and Carcinoma In Situ). *Eur. Urol.* s0302, 01978. doi:10.1016/j.eururo.2021.08.010
- Baetke, Sarah. C., Lammers, T., and Kiessling, Fabian. (2015). *Applications of Nanoparticles for Diagnosis and Therapy of Cancer*.
- Banerjee, S., Modi, S., McGinn, O., Zhao, X., Dudeja, V., Ramakrishnan, S., et al. (2016). Impaired Synthesis of Stromal Components in Response to Minnelide Improves Vascular Function, Drug Delivery, and Survival in Pancreatic Cancer. *Clin. Cancer Res.* 22, 415–425. doi:10.1158/1078-0432.CCR-15-1155
- Bansal, A., and Simon, M. C. (2018). Glutathione Metabolism in Cancer Progression and Treatment Resistance. *J. Cell Biol.* 217, 2291–2298. doi:10.1083/jcb.201804161
- Bayda, S., Adeel, M., Tuccinardi, T., Cordani, M., and Rizzolio, F. (2019). The History of Nanoscience and Nanotechnology: From Chemical-Physical Applications to Nanomedicine. *Molecules* 25, 112. doi:10.3390/molecules25010112
- Bertrand, N., Wu, J., Xu, X., Kamaly, N., and Farokhzad, O. C. (2014). Cancer Nanotechnology: the Impact of Passive and Active Targeting in the Era of Modern Cancer Biology. *Adv. Drug Deliv. Rev.* 66, 2–25. doi:10.1016/j.addr.2013.11.009
- Betty, Y. S., Kim, M. D., Ph, D., Rutka, James. T., M, D., Ph, D., et al. (2010). *Nanomedicine. The New Engl. Journal of Medicine*.
- Bilensoy, E., Sarisozen, C., Esendağlı, G., Doğan, A. L., Aktaş, Y., Sen, M., et al. (2009). Intravesical Cationic Nanoparticles of Chitosan and Polycaprolactone for the Delivery of Mitomycin C to Bladder Tumors. *Int. J. Pharm.* 371, 170–176. doi:10.1016/j.ijpharm.2008.12.015
- Bobo, D., Robinson, K. J., Islam, J., Thurecht, K. J., and Corrie, S. R. (2016). Nanoparticle-Based Medicines: A Review of FDA-Approved Materials and Clinical Trials to Date. *Pharm. Res.* 33, 2373–2387. doi:10.1007/s1095-016-1958-5
- Böhle, A., Leyh, H., Frei, C., Kühn, M., Tschada, R., Potte, T., et al. (2009). Single Postoperative Instillation of Gemcitabine in Patients with Non-muscle-invasive Transitional Cell Carcinoma of the Bladder: a Randomised, Double-Blind, Placebo-Controlled Phase III Multicentre Study. *Eur. Urol.* 56, 495–503. doi:10.1016/j.eururo.2009.06.010
- Chen, G., He, Y., Wu, X., Zhang, Y., Luo, C., and Jing, P. (2012). *In Vitro and In Vivo* Studies of Pirarubicin-Loaded SWNT for the Treatment of Bladder Cancer. *Braz. J. Med. Biol. Res.* 45, 771–776. doi:10.1590/s0100-879x2012007500111
- Chen, Q., Wang, X., Wang, C., Feng, L., Li, Y., and Liu, Z. (2015). Drug-Induced Self-Assembly of Modified Albumins as Nano-Theranostics for Tumor-Targeted Combination Therapy. *ACS Nano* 9, 5223–5233. doi:10.1021/acsnano.5b00640
- Cheng, R., Feng, F., Meng, F., Deng, C., Feijen, J., and Zhong, Z. (2011). Glutathione-responsive Nano-Vehicles as a Promising Platform for Targeted Intracellular Drug and Gene Delivery. *J. Control. Release* 152, 2–12. doi:10.1016/j.jconrel.2011.01.030
- Cho, K., Wang, X., Nie, S., Chen, Z. G., and Shin, D. M. (2008). Therapeutic Nanoparticles for Drug Delivery in Cancer. *Clin. Cancer Res.* 14, 1310–1316. doi:10.1158/1078-0432.CCR-07-1441
- Cho, S. K., Su, L. J., Mao, C., Wolenski, C. D., Flaig, T. W., and Park, W. (2019). Multifunctional Nanoclusters of NaYF₄:Yb³⁺,Er³⁺ Upconversion Nanoparticle and Gold Nanorod for Simultaneous Imaging and Targeted Chemotherapy of Bladder Cancer. *Mater. Sci. Eng. C Mater. Biol. Appl.* 97, 784–792. doi:10.1016/j.msec.2018.12.113
- Choi, K. O., Choe, J., Suh, S., and Ko, S. (2016). Positively Charged Nanostructured Lipid Carriers and Their Effect on the Dissolution of Poorly Soluble Drugs. *Molecules* 21, 672. doi:10.3390/molecules21050672

AUTHOR CONTRIBUTIONS

CT wrote the manuscript. HL, YF, JH, and FL revised the manuscript. YH and JW designed the structure of the review and revised the manuscript. All authors contributed to the article and approved the submitted version.

FUNDING

This work was supported by the National Natural Science Foundation of China (Grant No. 52173281) Provincial Industrial Innovation Special Fund Project of Jilin Province (Grant No. 2018C052-3) the Science and Technology Development Program of Jilin Province (Grant No. 20200404182YY).

- Conte, C., Mastrotto, F., Taresco, V., Tchoryk, A., Quaglia, F., Stolnik, S., et al. (2018). Enhanced Uptake in 2D- and 3D- Lung Cancer Cell Models of Redox Responsive PEGylated Nanoparticles with Sensitivity to Reducing Extra- and Intracellular Environments. *J. Control. Release* 277, 126–141. doi:10.1016/j.jconrel.2018.03.011
- Dadwal, A., Baldi, A., and Kumar Narang, R. (2018). Nanoparticles as Carriers for Drug Delivery in Cancer. *Artif. Cell Nanomed Biotechnol* 46, 295–305. doi:10.1080/21691401.2018.1457039
- de Souza, B. M., da Silva, A. V., Resende, V. M., Arcuri, H. A., Dos Santos Cabrera, M. P., Ruggiero Neto, J., et al. (2009). Characterization of Two Novel Polyfunctional Mastoparan Peptides from the Venom of the Social Wasp *Polybia Paulista*. *Peptides* 30, 1387–1395. doi:10.1016/j.peptides.2009.05.008
- Deng, Z., Yuan, S., Xu, R. X., Liang, H., and Liu, S. (2018). Reduction-Triggered Transformation of Disulfide-Containing Micelles at Chemically Tunable Rates. *Angew. Chem. Int. Ed. Engl.* 57, 8896–8900. doi:10.1002/anie.201802909
- Ding, J., Chen, J., Gao, L., Jiang, Z., Zhang, Y., Li, M., et al. (2019). Engineered Nanomedicines with Enhanced Tumor Penetration. *Nano Today* 29, 800. doi:10.1016/j.nantod.2019.100800
- Ellerby, H. M., LisaEllerby, M., Renate, Kain., Gabriel, Del. Rio., Stanislaw, Krajewski., ChristianLombardo, R., et al. (1999). Anti-cancer Activity of Targeted Pro-apoptotic Peptides. *Nat. Med.* 5, 1032. doi:10.1038/12469
- Erdogan, N., Iskit, A. B., Eroglu, H., Sargon, M. F., Mungan, N. A., and Bilensoy, E. (2015). Antitumor Efficacy of *Bacillus Calmette-Guerin* Loaded Cationic Nanoparticles for Intravesical Immunotherapy of Bladder Tumor Induced Rat Model. *J. Nanosci Nanotechnol* 15, 10156–10164.
- Feng, X., Xu, W., Liu, J., Li, D., Li, G., Ding, J., et al. (2021). Polypeptide Nanoformulation-Induced Immunogenic Cell Death and Remission of Immunosuppression for Enhanced Chemoimmunotherapy. *Sci. Bull.* 66, 362–373. doi:10.1016/j.scib.2020.07.013
- Feng, X., Xu, W., Xu, X., Li, G., Ding, J., and Chen, X. (2020). Cystine Proportion Regulates Fate of Polypeptide Nanogel as Nanocarrier for Chemotherapeutics. *Sci. China Chem.* 64, 293–301. doi:10.1007/s11426-020-9884-6
- Fröhlich, E. (2012). The Role of Surface Charge in Cellular Uptake and Cytotoxicity of Medical Nanoparticles. *Int. J. Nanomedicine* 7, 5577–5591. doi:10.2147/IJN.S36111
- Godeshala, S., Nitiyanandan, R., Thompson, B., Goklany, S., Nielsen, D. R., and Rege, K. (2016). Folate Receptor-Targeted Aminoglycoside-Derived Polymers for Transgene Expression in Cancer Cells. *Bioeng. Transl. Med.* 1, 220–231. doi:10.1002/btm2.10038
- Guallar-Garrido, S., and Julián, E. (2020). *Bacillus Calmette-Guérin* (BCG) Therapy for Bladder Cancer: An Update. *Immunotargets Ther.* 9, 1–11. doi:10.2147/ITT.S202006
- GuhaSarkar, S., More, P., and Banerjee, R. (2017). Urothelium-adherent, Ion-Triggered Liposome-In-Gel System as a Platform for Intravesical Drug Delivery. *J. Control. Release* 245, 147–156. doi:10.1016/j.jconrel.2016.11.031
- Gulfam, M., Matini, T., Monteiro, P. F., Riva, R., Collins, H., Spriggs, K., et al. (2017). Bioreducible Cross-Linked Core Polymer Micelles Enhance *In Vitro* Activity of Methotrexate in Breast Cancer Cells. *Biomater. Sci.* 5, 532–550. doi:10.1039/c6bm00888g
- Guo, H., Li, F., Qiu, H., Liu, J., Qin, S., Hou, Y., et al. (2020a). Preparation and Characterization of Chitosan Nanoparticles for Chemotherapy of Melanoma through Enhancing Tumor Penetration. *Front. Pharmacol.* 11, 317. doi:10.3389/fphar.2020.00317
- Guo, H., Li, F., Qiu, H., Xu, W., Li, P., Hou, Y., et al. (2020b). Synergistically Enhanced Mucoadhesive and Penetrable Polypeptide Nanogel for Efficient Drug Delivery to Orthotopic Bladder Cancer. *Research* 2020, 8970135. doi:10.34133/2020/8970135
- Guo, H., Li, F., Xu, W., Chen, J., Hou, Y., Wang, C., et al. (2018). Mucoadhesive Cationic Polypeptide Nanogel with Enhanced Penetration for Efficient Intravesical Chemotherapy of Bladder Cancer. *Adv. Sci. (Weinh)* 5, 1800004. doi:10.1002/advs.201800004
- Guo, H., Xu, W., Chen, J., Yan, L., Ding, J., Hou, Y., et al. (2017). Positively Charged Polypeptide Nanogel Enhances Mucoadhesion and Penetrability of 10-hydroxycamptothecin in Orthotopic Bladder Carcinoma. *J. Control. Release* 259, 136–148. doi:10.1016/j.jconrel.2016.12.041
- Guo, H., Li, F., Qiu, H., Zheng, Q., Yang, C., Tang, C., et al. (2019). Chitosan-Based Nanogel Enhances Chemotherapeutic Efficacy of 10-Hydroxycamptothecin against Human Breast Cancer Cells. *Int. J. Polym. Sci.* 2019, 1–6. doi:10.1155/2019/1914976
- Hadi, M. M., Nesbitt, H., Masood, H., Sciscione, F., Patel, S., Ramesh, B. S., et al. (2021). Investigating the Performance of a Novel pH and Cathepsin B Sensitive, Stimulus-Responsive Nanoparticle for Optimised Sonodynamic Therapy in Prostate Cancer. *J. Control. Release* 329, 76–86. doi:10.1016/j.jconrel.2020.11.040
- Han, J., Gu, X., Li, Y., and Wu, Q. (2020). Mechanisms of BCG in the Treatment of Bladder Cancer-Current Understanding and the prospect. *Biomed. Pharmacother.* 129, 110393. doi:10.1016/j.biopha.2020.110393
- Hong, S., Leroueil, P. R., Janus, E. K., Peters, J. L., Kober, M. M., Islam, M. T., et al. (2006). Interaction of Polycationic Polymers with Supported Lipid Bilayers and Cells: Nanoscale Hole Formation and Enhanced Membrane Permeability. *Bioconjug. Chem.* 17, 728–734. doi:10.1021/bc060077y
- Hsu, C. W., Cheng, N. C., Liao, M. Y., Cheng, T. Y., and Chiu, Y. C. (2020). Development of Folic Acid-Conjugated and Methylene Blue-Adsorbed Au@TNA Nanoparticles for Enhanced Photodynamic Therapy of Bladder Cancer Cells. *Nanomaterials (Basel)* 10. doi:10.3390/nano10071351
- Hu, J., Zhuang, W., Ma, B., Su, X., Yu, T., Li, G., et al. (2018). Redox-Responsive Biomimetic Polymeric Micelle for Simultaneous Anticancer Drug Delivery and Aggregation-Induced Emission Active Imaging. *Bioconjug. Chem.* 29, 1897–1910. doi:10.1021/acs.bioconjchem.8b00119
- Janmaat, M. L., and Giaccone, G. (2003). Small-Molecule Epidermal Growth Factor Receptor Tyrosine Kinase Inhibitors. *Oncologist* 8, 576–586. doi:10.1634/theoncologist.8-6-576
- Joyce, J. A., Laakkonen, P., Bernasconi, M., Bergers, G., Ruoslahti, E., and Hanahan, D. (2003). Stage-specific Vascular Markers Revealed by Phage Display in a Mouse Model of Pancreatic Islet Tumorigenesis. *Cancer Cell* 4, 393–403. doi:10.1016/s1535-6108(03)00271-x
- Jung, H. K., Kim, S., Park, R. W., Park, J. Y., Kim, I. S., and Lee, B. (2016). Bladder Tumor-Targeted Delivery of Pro-apoptotic Peptide for Cancer Therapy. *J. Control. Release* 235, 259–267. doi:10.1016/j.jconrel.2016.06.008
- Karimi, M., Ghasemi, A., Sahandi Zangabad, P., Rahighi, R., Moosavi Basri, S. M., Mirshekari, H., et al. (2016). Smart Micro/nanoparticles in Stimulus-Responsive Drug/gene Delivery Systems. *Chem. Soc. Rev.* 45, 1457–1501. doi:10.1039/c5cs00798d
- Koivunen, E., Arap, W., Valtanen, H., RainisaloMedina, A., Medina, O. P., Heikkilä, P., et al. (1999). Tumor Targeting with a Selective Gelatinase Inhibitor. *Nat. Biotechnol.* 17, 768–774. doi:10.1038/11703
- Koo, H., Min, K. H., Lee, S. C., Park, J. H., Park, K., Jeong, S. Y., et al. (2013). Enhanced Drug-Loading and Therapeutic Efficacy of Hydrotropic Oligomer-Conjugated Glycol Chitosan Nanoparticles for Tumor-Targeted Paclitaxel Delivery. *J. Control. Release* 172, 823–831. doi:10.1016/j.jconrel.2013.08.297
- Kuang, X., Chi, D., Li, J., Guo, C., Yang, Y., Zhou, S., et al. (2021). Disulfide Bond Based cascade Reduction-Responsive Pt(IV) Nanoassemblies for Improved Anti-tumor Efficiency and Biosafety. *Colloids Surf. B Biointerfaces* 203, 111766. doi:10.1016/j.colsurfb.2021.111766
- Lai, X., Geng, X., Li, M., Tang, M., Liu, Q., Yang, M., et al. (2021). Glutathione-responsive PLGA Nanocomplex for Dual Delivery of Doxorubicin and Curcumin to Overcome Tumor Multidrug Resistance. *Nanomedicine (Lond)* 16, 1411–1427. doi:10.2217/nnm-2021-0100
- Lee, S. M., Lee, E. J., Hong, H. Y., Kwon, M. K., Kwon, T. H., Choi, J. Y., et al. (2007). Targeting Bladder Tumor Cells *In Vivo* and in the Urine with a Peptide Identified by Phage Display. *Mol. Cancer Res.* 5, 11–19. doi:10.1158/1541-7786.MCR-06-0069
- Lenis, A. T., Lec, P. M., Chamie, K., and Mshs, M. D. (2020). Bladder Cancer: A Review. *JAMA* 324, 1980–1991. doi:10.1001/jama.2020.17598
- Leroueil, P. R., Hong, S., Mecke, A., Baker, J. R., Orr, B. G., and Banaszak Holl, M. M. (2007). Nanoparticle Interaction with Biological Membranes: Does Nanotechnology Present a Janus Face? *Acc. Chem. Res.* 40, 335–342. doi:10.1021/ar600012y
- Li, G., Lei, Q., Wang, F., Deng, D., Wang, S., Tian, L., et al. (2019). Fluorinated Polymer Mediated Transmucosal Peptide Delivery for Intravesical Instillation Therapy of Bladder Cancer. *Small* 15, e1900936. doi:10.1002/smll.201900936
- Li, G., Wang, S., Deng, D., Xiao, Z., Dong, Z., Wang, Z., et al. (2020). Fluorinated Chitosan to Enhance Transmucosal Delivery of Sonosensitizer-Conjugated Catalase for Sonodynamic Bladder Cancer Treatment Post-intravesical Instillation. *ACS Nano* 14, 1586–1599. doi:10.1021/acsnano.9b06689

- Liang, Y., Wang, Y., Wang, L., Liang, Z., Li, D., Xu, X., et al. (2021). Self-crosslinkable Chitosan-Hyaluronic Acid Dialdehyde Nanoparticles for CD44-Targeted siRNA Delivery to Treat Bladder Cancer. *Bioact Mater.* 6, 433–446. doi:10.1016/j.bioactmat.2020.08.019
- Lin, T. Y., Li, Y., Liu, Q., Chen, J. L., Zhang, H., Lac, D., et al. (2016). Novel Theranostic Nanoporphyrins for Photodynamic Diagnosis and Trimodal Therapy for Bladder Cancer. *Biomaterials* 104, 339–351. doi:10.1016/j.biomaterials.2016.07.026
- Lin, T. Y., Zhang, H., Luo, J., Li, Y., Gao, T., Lara, P. N., et al. (2012). Multifunctional Targeting Micelle Nanocarriers with Both Imaging and Therapeutic Potential for Bladder Cancer. *Int. J. Nanomedicine* 7, 2793–2804. doi:10.2147/IJN.S27734
- Liu, X., Li, Y., Wang, K., Chen, Y., Shi, M., Zhang, X., et al. (2021). GSH-responsive Nanoporous Drug to Inhibit Glycolysis and Alleviate Immunosuppression for Cancer Therapy. *Nano Lett.* 21, 7862–7869. doi:10.1021/acs.nanolett.1c03089
- Maeda, H., Nakamura, H., and Fang, J. (2013). The EPR Effect for Macromolecular Drug Delivery to Solid Tumors: Improvement of Tumor Uptake, Lowering of Systemic Toxicity, and Distinct Tumor Imaging *In Vivo*. *Adv. Drug Deliv. Rev.* 65, 71–79. doi:10.1016/j.addr.2012.10.002
- Márquez-Miranda, V., Peñaloza, J. P., Araya-Durán, I., Reyes, R., Vidaurre, S., Romero, V., et al. (2016). Effect of Terminal Groups of Dendrimers in the Complexation with Antisense Oligonucleotides and Cell Uptake. *Nanoscale Res. Lett.* 11, 66. doi:10.1186/s11671-016-1260-9
- Martinez, V. G., Munera-Maravilla, E., Bernardini, A., Rubio, C., Suarez-Cabrera, C., Segovia, C., et al. (2019). Epigenetics of Bladder Cancer: Where Biomarkers and Therapeutic Targets Meet. *Front. Genet.* 10, 1125. doi:10.3389/fgene.2019.01125
- Meng, F., Hennink, W. E., and Zhong, Z. (2009). Reduction-sensitive Polymers and Bioconjugates for Biomedical Applications. *Biomaterials* 30, 2180–2198. doi:10.1016/j.biomaterials.2009.01.026
- Monteiro, P. F., Gulfam, M., Monteiro, C. J., Travanut, A., Abelha, T. F., Pearce, A. K., et al. (2020). Synthesis of Micellar-like Terpolymer Nanoparticles with Reductively-Cleavable Cross-Links and Evaluation of Efficacy in 2D and 3D Models of Triple Negative Breast Cancer. *J. Control. Release* 323, 549–564. doi:10.1016/j.jconrel.2020.04.049
- Moses, M. A., Brem, H., and Langer, R. (2003). Advancing the Field of Drug Delivery: Taking Aim at Cancer. *CANCER CELL* 4, 337–341. doi:10.1016/s1535-6108(03)00276-9
- Oluwasanmi, A., and Hoskins, C. (2021). Potential Use of the Diels-Alder Reaction in Biomedical and Nanomedicine Applications. *Int. J. Pharm.* 604, 120727. doi:10.1016/j.ijpharm.2021.120727
- Orsolic, N. (2012). Bee Venom in Cancer Therapy. *Cancer Metastasis Rev.* 31 (1), 173–194. doi:10.1007/s10555-011-9339-3
- Pan, A., Zhang, H., Li, Y., Lin, T. Y., Wang, F., Lee, J., et al. (2016). Disulfide-crosslinked Nanomicelles Confer Cancer-specific Drug Delivery and Improve Efficacy of Paclitaxel in Bladder Cancer. *Nanotechnology* 27, 425103. doi:10.1088/0957-4484/27/42/425103
- Peer, D., Karp, J. M., Hong, S., Farokhzad, O. C., Margalit, R., and Langer, R. (2007). Nanocarriers as an Emerging Platform for Cancer Therapy. *Nat. Nanotechnol.* 2, 751–760. doi:10.1038/nnano.2007.387
- Pettenati, C., and Ingersoll, M. A. (2018). Mechanisms of BCG Immunotherapy and its Outlook for Bladder Cancer. *Nat. Rev. Urol.* 15, 615–625. doi:10.1038/s41585-018-0055-4
- Ponta, H., Sherman, L., and Herrlich, P. A. (2003). CD44: from Adhesion Molecules to Signalling Regulators. *Nat. Rev. Mol. Cell Biol.* 4, 33–45. doi:10.1038/nrm1004
- Prabaharan, M. (2015). Chitosan-based Nanoparticles for Tumor-Targeted Drug Delivery. *Int. J. Biol. Macromol.* 72, 1313–1322. doi:10.1016/j.jbiomac.2014.10.052
- Pridgen, E. M., Langer, R., and Farokhzad, O. C. (2007). Biodegradable, Polymeric Nanoparticle Delivery Systems for Cancer Therapy. *Nanomedicine (Lond)* 2, 669–680. doi:10.2217/17435889.2.5.669
- Qiu, H., Guo, H., Li, D., Hou, Y., Kuang, T., and Ding, J. (2020). Intravesical Hydrogels as Drug Reservoirs. *Trends Biotechnol.* 38, 579–583. doi:10.1016/j.tibtech.2019.12.012
- Ramos, J., Forcada, J., and Hidalgo-Alvarez, R. (2014). Cationic Polymer Nanoparticles and Nanogels: from Synthesis to Biotechnological Applications. *Chem. Rev.* 114, 367–428. doi:10.1021/cr3002643
- Saranya, N., Moorthi, A., Saravanan, S., Devi, M. P., and Selvamurugan, N. (2011). Chitosan and its Derivatives for Gene Delivery. *Int. J. Biol. Macromol.* 48, 234–238. doi:10.1016/j.jbiomac.2010.11.013
- Sartore-Bianchi, A., Martini, M., Molinari, F., Veronese, S., Nichelatti, M., Artale, S., et al. (2009). PIK3CA Mutations in Colorectal Cancer Are Associated with Clinical Resistance to EGFR-Targeted Monoclonal Antibodies. *Cancer Res.* 69, 1851–1857. doi:10.1158/0008-5472.CAN-08-2466
- Schmidt, S., Kunath, F., Coles, B., Draeger, D. L., Krabbe, L. M., Dersch, R., et al. (2020). Intravesical Bacillus Calmette-Guérin versus Mitomycin C for Ta and T1 Bladder Cancer. *Cochrane Database Syst. Rev.* 1, CD011935. doi:10.1002/14651858.CD011935.pub2
- Seidl, C. (2020). Targets for Therapy of Bladder Cancer. *Semin. Nucl. Med.* 50, 162–170. doi:10.1053/j.semnucmed.2020.02.006
- Sibuyi, N. R. S., Moabelo, K. L., Meyer, M., Onani, M. O., Dube, A., and Madiehe, A. M. (2019). Nanotechnology Advances towards Development of Targeted-Treatment for Obesity. *J. Nanobiotechnology* 17, 122. doi:10.1186/s12951-019-0554-3
- Smith, G. P. (1985). Filamentous Fusion Phage_ Novel Expression Vectors that Display Cloned Antigens on the Virion Surface. *Science (Wash)* 228, 1315–1317.
- Souza, B. M., Mendes, M. A., Santos, L. D., Marques, M. R., César, L. M., Almeida, R. N., et al. (2005). Structural and Functional Characterization of Two Novel Peptide Toxins Isolated from the Venom of the Social Wasp *Polybia Paulista*. *Peptides* 26, 2157–2164. doi:10.1016/j.peptides.2005.04.026
- Sun, Y., Feng, X., Wan, C., Lovell, J. F., Jin, H., and Ding, J. (2021). Role of Nanoparticle-Mediated Immunogenic Cell Death in Cancer Immunotherapy. *Asian J. Pharm. Sci.* 16, 129–132. doi:10.1016/j.ajps.2020.05.004
- Taskovska, M., Kreft, M. E., and Smrkolj, T. (2020). Current and Innovative Approaches in the Treatment of Non-muscle Invasive Bladder Cancer: the Role of Transurethral Resection of Bladder Tumor and Organoids. *Radiol. Oncol.* 54, 135. doi:10.2478/raon-2020-0025
- Thomas, T. P., Majoros, I., Kotlyar, A., Mullen, D., Holl, M. M., and Baker, J. R. (2009). Cationic Poly(amidoamine) Dendrimer Induces Lysosomal Apoptotic Pathway at Therapeutically Relevant Concentrations. *Biomacromolecules* 10, 3207–3214. doi:10.1021/bm900683r
- Tian, H., Lin, L., Chen, J., Chen, X., Park, T. G., and Maruyama, A. (2011). RGD Targeting Hyaluronic Acid Coating System for PEI-PBLG Polycation Gene Carriers. *J. Control. Release* 155, 47–53. doi:10.1016/j.jconrel.2011.01.025
- Tu, H., Dinney, C. P., Ye, Y., Grossman, H. B., Lerner, S. P., and Wu, X. (2018). Is Folic Acid Safe for Non-muscle-invasive Bladder Cancer Patients? an Evidence-Based Cohort Study. *Am. J. Clin. Nutr.* 107, 208–216. doi:10.1093/ajcn/nqx019
- Turcsányi, Á., Varga, N., and Csapó, E. (2020). Chitosan-modified Hyaluronic Acid-Based Nanosized Drug Carriers. *Int. J. Biol. Macromol.* 148, 218–225. doi:10.1016/j.jbiomac.2020.01.118
- Vasir, J. K., and Labhasetwar, V. (2008). Quantification of the Force of Nanoparticle-Cell Membrane Interactions and its Influence on Intracellular Trafficking of Nanoparticles. *Biomaterials* 29, 4244–4252. doi:10.1016/j.biomaterials.2008.07.020
- Vasir, J. K., and Labhasetwar, V. (2005). Targeted Drug Delivery in Cancer Therapy. *Technol. Cancer Res. Treat.* 4, 363–374. doi:10.1177/153303460500400405
- Wang, K. R., Zhang, B. Z., Zhang, W., Yan, J. X., Li, J., and Wang, R. (2008). Antitumor Effects, Cell Selectivity and Structure-Activity Relationship of a Novel Antimicrobial Peptide Polybia-MPI. *Peptides* 29, 963–968. doi:10.1016/j.peptides.2008.01.015
- Wei, L., Chen, J., and Ding, J. (2021). Sequentially Stimuli-Responsive Anticancer Nanomedicines. *Nanomedicine* 16, 261–264. doi:10.2217/nnm-2021-0019
- Wei, Y., Gao, L., Wang, L., Shi, L., Wei, E., Zhou, B., et al. (2017). Polydopamine and Peptide Decorated Doxorubicin-Loaded Mesoporous Silica Nanoparticles as a Targeted Drug Delivery System for Bladder Cancer Therapy. *Drug Deliv.* 24, 681–691. doi:10.1080/10717544.2017.1309475
- Wu, L., Ni, C., Zhang, L., Shi, G., Bai, X., Zhou, Y., et al. (2016). Surface Charge Convertible and Biodegradable Synthetic Zwitterionic Nanoparticles for Enhancing Cellular Drug Uptake. *Macromol. Biosci.* 16, 308–313. doi:10.1002/mabi.201500299
- Xia, Y., Xiong, Y., Lim, B., and Skrabalak, S. E. (2009). Shape-controlled Synthesis of Metal Nanocrystals: Simple Chemistry Meets Complex Physics? *Angew. Chem. Int. Ed. Engl.* 48, 60–103. doi:10.1002/anie.200802248

- Xiang, S., Tong, H., Shi, Q., Fernandes, J. C., Jin, T., Dai, K., et al. (2012). Uptake Mechanisms of Non-viral Gene Delivery. *J. Control. Release* 158, 371–378. doi:10.1016/j.jconrel.2011.09.093
- Xiong, X. B., Mahmud, A., and Lavasanifar, H. A. (2007). Conjugation of Arginine-Glycine-Aspartic Acid Peptides to Poly(ethylene Oxide)-B-Poly(epsilon-Caprolactone) Micelles for Enhanced Intracellular Drug Delivery to Metastatic Tumor Cells. *Biomacromolecules* 8, 874–884. doi:10.1021/bm060967g
- Xu, X., Liu, K., Jiao, B., Luo, K., Ren, J., Zhang, G., et al. (2020). Mucoadhesive Nanoparticles Based on ROS Activated Gambogic Acid Prodrug for Safe and Efficient Intravesical Instillation Chemotherapy of Bladder Cancer. *J. Control. Release* 324, 493–504. doi:10.1016/j.jconrel.2020.03.028
- Yang, J. Z., Zou, H. Y., Ding, J. X., and Chen, X. S. (2021). Controlled Synthesis and Biomedical Applications of Cystine-Based Polypeptide Nanomaterials. *Acta Polym. Sin* 52, 960–977.
- Yao, Z., Peng, P., Xu, D., Zhou, X., Pan, Z., Li, Z., et al. (2019). EGFR Inhibitor C225 Increases the Radio-Sensitivity of Human Breast Cancer Cells. *Asian Pac. J. Cancer Prev.* 20, 311–319. doi:10.31557/APJCP.2019.20.1.311
- Yewale, C., Baradia, D., Vhora, I., Patil, S., and Misra, A. (2013). Epidermal Growth Factor Receptor Targeting in Cancer: A Review of Trends and Strategies. *Biomaterials* 34, 8690–8707. doi:10.1016/j.biomaterials.2013.07.100
- Young, J. J., Chen, C. C., Chen, Y. C., Cheng, K. M., Yen, H. J., Huang, Y. C., et al. (2016). Positively and Negatively Surface-Charged Chondroitin Sulfate-Trimethylchitosan Nanoparticles as Protein Carriers. *Carbohydr. Polym.* 137, 532–540. doi:10.1016/j.carbpol.2015.10.095
- Yue, Z. G., Wei, W., Lv, P. P., Yue, H., Wang, L. Y., Su, Z. G., et al. (2011). Surface Charge Affects Cellular Uptake and Intracellular Trafficking of Chitosan-Based Nanoparticles. *Biomacromolecules* 12, 2440–2446. doi:10.1021/bm101482r
- Zhan, C., Gu, B., Xie, C., Li, J., Liu, Y., and Lu, W. (2010). Cyclic RGD Conjugated Poly(ethylene Glycol)-Co-Poly(lactic Acid) Micelle Enhances Paclitaxel Anti-glioblastoma Effect. *J. Control. Release* 143, 136–142. doi:10.1016/j.jconrel.2009.12.020
- Zhang, H., Aina, O. H., Lam, K. S., de Vere White, R., Evans, C., Henderson, P., et al. (2012). Identification of a Bladder Cancer-specific Ligand Using a Combinatorial Chemistry Approach. *Urol. Oncol.* 30, 635–645. doi:10.1016/j.urolonc.2010.06.011
- Zhang, H., Dong, S., Li, Z., Feng, X., Xu, W., Tulinao, C. M. S., et al. (2020). Biointerface Engineering Nanoplatfroms for Cancer-Targeted Drug Delivery. *Asian J. Pharm. Sci.* 15, 397–415. doi:10.1016/j.ajps.2019.11.004
- Zhang, X., Yang, X., Ji, J., Liu, A., and Zhai, G. (2016). Tumor Targeting Strategies for Chitosan-Based Nanoparticles. *Colloids Surf. B Biointerfaces* 148, 460–473. doi:10.1016/j.colsurfb.2016.09.020
- Zhao, D., Wu, J., Li, C., Zhang, H., Li, Z., and Luan, Y. (2017). Precise Ratiometric Loading of PTX and DOX Based on Redox-Sensitive Mixed Micelles for Cancer Therapy. *Colloids Surf. B Biointerfaces* 155, 51–60. doi:10.1016/j.colsurfb.2017.03.056
- Zheng, M., Pan, M., Zhang, W., Lin, H., Wu, S., Lu, C., et al. (2021a). Poly(α -lysine)-based Nanomaterials for Versatile Biomedical Applications: Current Advances and Perspectives. *Bioact. Mater.* 6, 1878–1909. doi:10.1016/j.bioactmat.2020.12.001
- Zheng, P., Ding, B., Jiang, Z., Xu, W., Li, G., Ding, J., et al. (2021b). Ultrasound-Augmented Mitochondrial Calcium Ion Overload by Calcium Nanomodulator to Induce Immunogenic Cell Death. *Nano Lett.* 21, 2088–2093. doi:10.1021/acs.nanolett.0c04778
- Zheng, P., Ding, B., Shi, R., Jiang, Z., Xu, W., Li, G., et al. (2021c). A Multichannel Ca(2+) Nanomodulator for Multilevel Mitochondrial Destruction-Mediated Cancer Therapy. *Adv. Mater.* 33, e2007426. doi:10.1002/adma.202007426
- Zheng, P., Liu, Y., Chen, J., Xu, W., Li, G., and Ding, J. (2020). Targeted pH-Responsive Polyion Complex Micelle for Controlled Intracellular Drug Delivery. *Chin. Chem. Lett.* 31, 1178–1182. doi:10.1016/j.cclet.2019.12.001
- Zhong, Y., Meng, F., Deng, C., and Zhong, Z. (2014). Ligand-directed Active Tumor-Targeting Polymeric Nanoparticles for Cancer Chemotherapy. *Biomacromolecules* 15, 1955–1969. doi:10.1021/bm5003009
- Zhou, D., Zhang, G., and Gan, Z. (2013). c(RGDfK) Decorated Micellar Drug Delivery System for Intravesical Instilled Chemotherapy of Superficial Bladder Cancer. *J. Control. Release* 169, 204–210. doi:10.1016/j.jconrel.2013.01.025
- Zhou, Z., Tang, J., Sun, Q., Murdoch, W. J., and Shen, Y. (2015). A Multifunctional PEG-PLL Drug Conjugate Forming Redox-Responsive Nanoparticles for Intracellular Drug Delivery. *J. Mater. Chem. B* 3, 7594–7603. doi:10.1039/c5tb01027f
- Zhuo, C., Li, X., Zhuang, H., Tian, S., Cui, H., Jiang, R., et al. (2016). Evaluating the Efficacy and Safety of Intravesical Chemotherapies for Non-muscle Invasive Bladder Cancer: a Network Meta-Analysis. *Oncotarget* 7, 82567–82579. doi:10.18632/oncotarget.12856
- Zöller, M. (2011). CD44: Can a Cancer-Initiating Cell Profit from an Abundantly Expressed Molecule? *Nat. Rev. Cancer* 11, 254–267. doi:10.1038/nrc3023

Conflict of Interest: The authors declare that the research was conducted in the absence of any commercial or financial relationships that could be construed as a potential conflict of interest.

Publisher's Note: All claims expressed in this article are solely those of the authors and do not necessarily represent those of their affiliated organizations, or those of the publisher, the editors, and the reviewers. Any product that may be evaluated in this article, or claim that may be made by its manufacturer, is not guaranteed or endorsed by the publisher.

Copyright © 2021 Tang, Liu, Fan, He, Li, Wang and Hou. This is an open-access article distributed under the terms of the Creative Commons Attribution License (CC BY). The use, distribution or reproduction in other forums is permitted, provided the original author(s) and the copyright owner(s) are credited and that the original publication in this journal is cited, in accordance with accepted academic practice. No use, distribution or reproduction is permitted which does not comply with these terms.



The Inhibitory Effects of 6-Thioguanine and 6-Mercaptopurine on the USP2a Target Fatty Acid Synthase in Human Submaxillary Carcinoma Cells

Chiao-Pei Cheng¹, Shu-Ting Liu², Yi-Lin Chiu², Shih-Ming Huang^{2*} and Ching-Liang Ho^{3*}

OPEN ACCESS

Edited by:

Sanjun Shi,
Chengdu University of Traditional
Chinese Medicine, China

Reviewed by:

Hongmei Cui,
Lanzhou University, China
Inamul Hasan Madar,
Korea University, South Korea

*Correspondence:

Shih-Ming Huang
shihming@ndmctsg.hk.edu.tw
Ching-Liang Ho
02241@mail.ndmctsg.hk.edu.tw

Specialty section:

This article was submitted to
Pharmacology of Anti-Cancer Drugs,
a section of the journal
Frontiers in Oncology

Received: 13 September 2021

Accepted: 22 November 2021

Published: 10 December 2021

Citation:

Cheng C-P, Liu S-T, Chiu Y-L,
Huang S-M and Ho C-L (2021) The
Inhibitory Effects of 6-Thioguanine and
6-Mercaptopurine on the USP2a
Target Fatty Acid Synthase in Human
Submaxillary Carcinoma Cells.
Front. Oncol. 11:749661.
doi: 10.3389/fonc.2021.749661

Overexpression of the deubiquitinase USP2a leads to stabilization of fatty acid synthase (FAS), the levels of which are often elevated in aggressive human cancers. Consequently, there is an urgent need for inhibitors to suppress the deubiquitination activity of USP2a so as to upregulate FAS protein degradation. We first analyzed the relationship between the expression level of USP2a and survival using The Cancer Genome Atlas Head-Neck Squamous Cell Carcinoma (HNSC) data collection. Our results suggested survival rates were lower among HNSC patients expressing higher levels of USP2a. We then investigated two thiopurine drugs, 6-thioguanine (6-TG) and 6-mercaptopurine (6-MP), to determine whether they could potentially serve as inhibitors of USP2a. Western blot analysis showed that levels of two USP2a target proteins, FAS and Mdm2, were dose-dependently decreased in A253 submaxillary carcinoma cells treated with 6-TG or 6-MP. Responding to the degradation of Mdm2, levels of p53 were increased. We found that 6-TG and 6-MP also suppressed levels of both USP2a mRNA and protein, suggesting these two thiopurines do not act solely through direct inhibition of USP2a. The effects of 6-TG and 6-MP were not cell type-specific, as they elicited similar decreases in FAS protein in leukemia, prostate and cervical cancer cell lines. 6-TG and 6-MP had effects on several cell cycle proteins, including another USP2a target protein, cyclin D1. The populations of cells in subG1 and S phase were increased by 6-TG and 6-MP, which was accompanied by reductions in G1 phase cells. In untreated cells, USP2a transfection increased FAS and cyclin D1 levels compared to an enzyme-dead USP2a C276A mutant, which lacked deubiquitinating activity. However, USP2a transfection failed to reverse the suppressive effects of 6-TG and 6-MP on FAS levels. In summary, these findings suggest 6-TG and 6-MP reduce the stability of some USP2a targets, including FAS and Mdm2, by inhibiting

USP2a-catalyzed deubiquitination in some cancer cells. Our work also provides repurposing evidence supporting 6-TG and 6-MP as target therapeutic drugs, such as USP2a/FAS in this study.

Keywords: ubiquitin, USP2a, fatty acid synthase, cyclin D1, thiopurine

INTRODUCTION

By mediating the degradation of short-lived and abnormal proteins, ubiquitination plays critical roles in the growth, environmental adaptation, development, and stress responses of eukaryotic cells. Indeed, the ubiquitin/26S proteasome proteolytic pathway plays important roles in virtually all aspects of cell biology (1, 2). Reversal of ubiquitination is accomplished through deubiquitinases (DUBs) (3, 4). Within the DUB family, ubiquitin-specific proteases (USPs) constitute the largest subgroup, with more than 60 members. USPs may help regulate the ubiquitin-dependent 26S proteasome degradation pathway by generating free ubiquitin monomers, recycling ubiquitin, and/or removing ubiquitin from specific targets, thereby preventing target degradation. Moreover, increasing evidence now indicates that alterations in DUB expression frequency alterations as well as DUB gene mutations correlate with human diseases, ranging from immune system diseases to human cancers.

USP2a is an androgen-regulated DUB reportedly overexpressed in prostate tumors, where it exerts an anti-apoptotic effect (5–7). In addition, in biologically aggressive human tumors, overexpressed USP2a interacts with and stabilizes fatty acid synthase (FAS) (5, 8, 9), which is now recognized as a potentially therapeutic target in cancers of the breast, colon, endometrium, ovary, prostate, and thyroid (10–15). In LNCaP human prostate carcinoma cells, USP2a knockdown using targeted siRNA increases levels of poly-ubiquitinated FAS, reduces levels of FAS protein, and promotes induction of apoptosis (5, 7, 9).

The thiopurine analogues 6-mercaptopurine (6-MP) and 6-thioguanine (6-TG) have long been used in the treatment of acute lymphoblastic leukemia, the most common type of childhood cancer (16, 17). In addition to their anticancer effects, they have been used as clinically effective anti-inflammatory and immunosuppressive agents for over 50 years (18). Studies of 6-TG and 6-MP have revealed that although their therapeutic efficacies are similar, the two drugs differ in their mechanisms of action (16, 19, 20). The prodrug forms of 6-TG and 6-MP are enzymatically converted into cytotoxic nucleotides by hypoxanthine-guanine phosphoribosyl transferase. In addition, both drugs appear to have deubiquitinating and deISGylation activities, which enable them to inhibit coronavirus papain-like protease activity in cases of severe acute respiratory syndrome (21, 22). Thiopurines may thus belong to a new class of nonselective isopeptidase inhibitors with the ability to inhibit various isopeptidases and elicit accumulation of poly-ubiquitinated proteins (20). Recently, Dr. Chou's laboratory demonstrated that a noncompetitive

inhibition pattern best describes the inhibition of USP2a enzyme activity by 6-TG and 6-MP (23). This work also provided direct evidence of the functional impact of USP2a C276S mutation on its deubiquitinating activity.

Scientists are currently focusing on pharmacological disruption of DUB activity as a rationale for cancer therapy (24). In the present study, we sought to clarify the relationship between thiopurine analogs and USP2a, as both USP2a and USP14 will bind 6-MP and 6-TG (21, 22). We also examined the effects of 6-MP and 6-TG on USP2a target proteins to elucidate its functional roles. Our data suggest 6-MP and 6-TG may reduce the stability of some USP2a targets, including FAS and Mdm2, by inhibiting USP2a-catalyzed deubiquitination. These findings provide new insight into the anti-tumor functions of thiopurines.

MATERIALS AND METHODS

TCGA-HNSC Data Mining

Gene expression profiles, clinical data and pathway activation scores in The Cancer Genome Atlas Head-Neck Squamous Cell Carcinoma (TCGA-HNSC) data collection were downloaded from UCSC XENA (<https://xenabrowser.net/heatmap/>). In the present study, we used gene expression, survival and pathway activity data. Briefly, patients in TCGA-HNSC were divided into a USP2 High group (30% from the patient with highest USP2 expression) and USP2 Low group (30% from the patient with lowest USP2 expression). For pathway activity, we downloaded “z scores of 1387 constituent PARADIGM pathways”, grouped based on USP2 expression and then analyzed for intergroup differences using GraphPAD (Version 9.1.2). Details of how these data were processed can be found on the UCSC Xena website.

Cell Culture and Chemicals

A253 submaxillary carcinoma cells were cultured in McCoy's 5a medium supplemented with 10% fetal bovine serum and 1% penicillin-streptomycin (Invitrogen, USA). The HeLa human cervical cancer cell line, DU-145 prostate cancer cell line, and Reh and SupB15 leukemia cell lines were cultured in Dulbecco's modified Eagle's medium supplemented with 10% phosphate buffered saline (PBS) and 1% penicillin-streptomycin (Invitrogen, USA). 6-MP and 6-TG were purchased from Sigma Aldrich (St. Louis, MO, USA).

Western Blot Analysis

Cell lysates were prepared in lysis buffer (100 mM Tris-HCl [pH 8.0], 150 mM NaCl, 0.1% SDS, and 1% Triton X-100) at 4°C. Proteins in the cell extracts were separated by SDS-PAGE, transferred onto polyvinylidene difluoride membranes

(Millipore, USA) and detected using antibodies against α -actinin (ACTN), ATF3, COX-2, cyclin D1, FAS, Mdm2, p21, p53, proliferating cell nuclear antigen (PCNA), USP2a (Santa Cruz Biotechnology, USA), Cdc2, cyclin B1, and p-Cdc2 (Cell Signaling, USA).

Reverse Transcription-Polymerase Chain Reaction

Total RNA was isolated using TRIzol (Thermo Fisher Scientific) reagent according to the manufacturer's instructions. One microgram of total RNA was subjected to reverse transcription using MMLV reverse transcriptase (Epicentre Biotechnologies, USA) for 60 min at 37°C. The PCR reactions were run on a Veriti Thermal Cycler (Applied Biosystems, USA). The following PCR primers were used for ATF3: forward primer 5'-GAGG ATTTTGCTAACCTGAC-3' and reverse primer 5'-TAGCTCTG CAATGTTTCCTTC-3'; COX-2: forward primer 5'-TGGCGCTC AGCCATACAGCAA-3' and reverse primer 5'-GGTGAAAGC TGGCCCTCGCT-3'; cyclin D1: forward primer 5'-ATGGAACA CCAGTCCTGTGCTGC-3' and reverse primer 5'-TCAGAT GTCCACGTCCCGCAGCTCGG-3'; FAS: forward primer 5'-TG AGCCTCATGCGCTGGAC-3' and reverse primer 5'-CGCA CCTCCTTGCAAACAC-3'; GAPDH: forward primer 5'-CTT CATTGACCTCAACTAC-3' and reverse primer 5'-GCCA TCCACAGTCTTCTG-3'; Mdm2: forward primer 5'-CTTGA TGCTGGTGTAAGTGA-3' and reverse primer 5'-GTTGAT GGCTGAGAATAGTC-3'; p21: forward primer 5'-CTGAG CCGCGACTGTGATGCG-3' and reverse primer 5'-GGTCT GCCGCCGTTTTTCGACC-3'; p53: forward primer 5'-GATGA AGCTCCCAGAATGCCAGAG-3' and reverse primer 5'-GAG TTCCAAGGCCTCATTGAGCTC-3'; and USP2a: forward primer 5'-CGAGGTGAACCGAGTGACAC-3' and reverse primer 5'-TGTTGTGAGCTTGCTGGTTCG-3'.

Fluorescence-Activated Cell Sorting and Cell Cycle Profiling

The cell cycle distribution was determined by measuring DNA content using the FACS after staining with propidium iodide (PI). The cells were fixed in 70% ice-cold ethanol and kept at -20°C overnight. Before analysis, the harvested cells were washed twice with ice-cold PBS and stained with PI solution (5 μ g/ml PI in PBS, 0.5% Triton X-100, and 0.5 μ g/ml RNase A) for 30 min at 37°C in the dark. All the samples were analyzed using a FACSCalibur flow cytometer (BD Biosciences). Data were analyzed using Cell Quest Pro software (BD Biosciences).

Plasmids and Transfection

USP2a wild-type expression vector was constructed by inserting the full-length PCR fragments into the pSG5.HA vectors *via* the *EcoRI*-*XhoI* restriction sites. A vector encoding a USP2a C267A mutant [pSG5.HA.USP2a (C267A)] was constructed using site-directed mutagenesis with a Promega Gene Edit kit (Promega, Madison, MI, USA). Cells plated in 6-well plates were transfected using jetPEI (PolyPlus-transfection, France) according to the manufacturer's protocol; total DNA was adjusted to 1.0 μ g by addition of the empty vector.

RESULTS

Evaluating the Impact and Potential Mechanisms of USP2a Expression in HNSC Patients

In biologically aggressive human tumors, overexpressed USP2a interacts with and stabilizes FAS, Mdm2, and cell cycle-related proteins (5–7). We first analyzed the relationship between the level of USP2a expression and survival using TCGA-HNSC data collection (**Figure 1A**). Our results indicated that the survival rate was lower among HNSC patients expressing higher levels of USP2a. The Z scores for fatty acyl-CoA biosynthesis and conversion of palmitic acid to very long chain fatty acyl-CoAs were higher in the USP2a High group, whereas the Z score of mitochondrial fatty acid beta-oxidation of unsaturated fatty acids was lower in the USP2a High group (**Figure 1B**). In the USP2a High group, we observed that Z scores for the p53 signaling pathway, stabilization of p53, p53-dependent G1 DNA damage response, direct p53 effectors (**Figure 1C**), cyclin B2-mediated events, cyclin B1-associated events during G2/M transition, the cell cycle G1/S check point, and cell cycle G2/M check point were all lower (**Figure 1D**).

Multiple Pathways Used by 6-MP and 6-TG in the Regulation of USP2a Target Proteins in A253 Cells

FAS and Mdm2 are well-known target proteins for USP2a deubiquitinating activity (5, 25). Inhibition of USP2a could therefore result in their ubiquitin-dependent degradation. Consistent with that idea, in A253 cells treated with 100 μ M 6-TG or 6-MP, Western blot analyses revealed time-dependent reductions in the levels of FAS and Mdm2 (**Figure 2A**). Moreover, the degradation of Mdm2 led to increases in the levels of p53 (26). The effects of 6-TG and 6-MP on levels of p21, a p53 target gene (27), were inconsistent, especially with 6-MP treatment (**Figure 2A**, compare lanes 7–12). RT-PCR analysis showed that neither 6-TG nor 6-MP affected Mdm2 mRNA expression, which is consistent with them acting through USP2a inhibition. Both 6-TG and 6-MP suppressed expression of FAS mRNA (**Figure 2B**) while inducing expression of p53 mRNA and its splicing variant. On the other hand, they had no effect on expression of p21 mRNA.

A member of ATF/CREB transcriptional factor family, activating transcription factor 3 (ATF3) is a direct target of p53 that is rapidly induced by a wide range of cellular stresses (28, 29). Thus, increases in p53 elicited by treating A253 cells with 6-TG or 6-MP led to increases in both ATF3 mRNA and protein (**Figure 2**). A previous study demonstrated that ATF3 negatively regulates COX-2 during acute inflammation (30). We observed that the higher levels of ATF3 seen in 6-TG-treated A253 cells led to downregulation of COX-2 mRNA and protein; however, the effect of 6-MP on COX-2 expression was inconsistent (**Figures 2A, B**, compare lanes 7–12).

To confirm the importance of USP2a inhibition in FAS regulation by 6-TG and 6-MP, we examined their dose-dependent effects (**Figure 3**). We first observed that 6-TG was

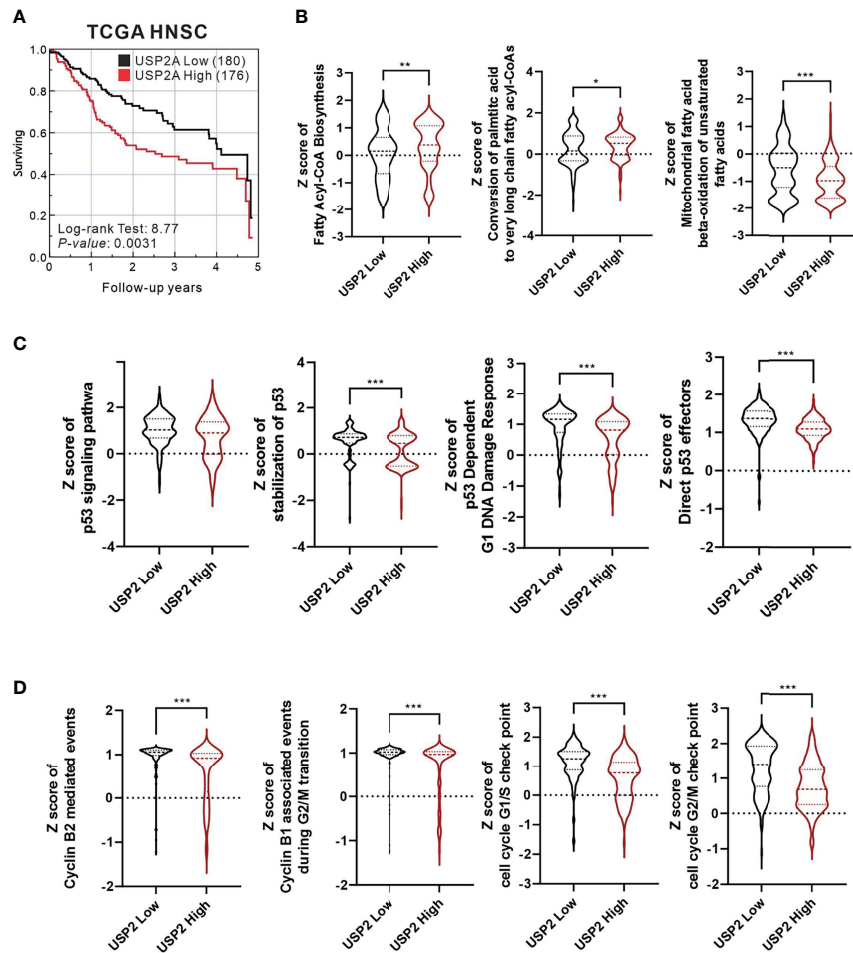


FIGURE 1 | Analysis of The Cancer Genome Atlas Head-Neck Squamous Cell Carcinoma (TCGA-HNSC) data collection. The relationship between USP2a expression levels and **(A)** survival rate analyzed using the log-rank test; **(B)** fatty acid synthesis; **(C)** p53 function; **(D)** cell cycle progression. For all statistical analyses, unpaired t-tests were used, and results were considered significant at $p < 0.05$. * $p < 0.05$, ** $p < 0.01$, and *** $p < 0.001$.

able upregulate levels of USP2a protein while suppressing its mRNA expression (**Figures 3A, B**). Suppression of both USP2a mRNA and protein was observed with 6-MP (**Figures 3C, D**). Both 6-TG and 6-MP suppress levels of FAS protein, which is consistent with their dose-dependent suppression of FAS mRNA (**Figure 3**). These findings suggest that in A253 cells, 6-TG and 6-MP may modulate levels of USP2a target proteins, including FAS and Mdm2, through inhibition of USP2a's deubiquitination activity or by directly suppressing mRNA expression of USP2a or its targets.

To determine whether the observed suppression of FAS protein by 6-TG and 6-MP in A253 cells was cell type-specific, we also tested their effects in the Reh and SupB15 leukemia cell lines, the DU-145 prostate cancer cell line, and the HeLa human cervical cancer cell line. Western blot analyses showed that 6-TG and 6-MP reduced the levels of FAS protein in Reh, SupB15, and HeLa cells (**Figures 4A, B, D**), but had no effect in DU-145 cells (**Figure 4C**). The effects of 6-TG and 6-MP on levels of USP2a protein varied among these four cell lines.

6-MP and 6-TG Regulate Cell-Cycle Progression-Related Proteins in A253 Cells

In addition to FAS and Mdm2, cyclin D1 is a well-known target of USP2a deubiquitinating activity (31). Cyclin D1 plays a key role in G1 progression during the cell cycle. Our results indicate that 6-TG or 6-MP (100 μ M) time-dependently suppressed levels of cyclin D1 protein (**Figures 5A, B**). The thiopurine-induced decline of cyclin D1 was accompanied by upregulation of ATF3. We also observed activation of the cdc2-cyclin B1 axis for transition from G2 to the mitotic phase in 6-TG- and 6-MP-treated A253 cells. These effects of 6-TG and 6-MP on cyclin D1 and the cdc2-cyclin B1 axis were dose-dependent (**Figures 5C, D**). The effects on cyclin D1 protein were not reflected by the corresponding mRNA levels (**Figures 5E, F**). This cell cycle profiling demonstrates that 6-TG and 6-MP increase cell populations in subG1 and S phase by time-dependently decreasing the G1 phase population (**Figures 6A, B**).

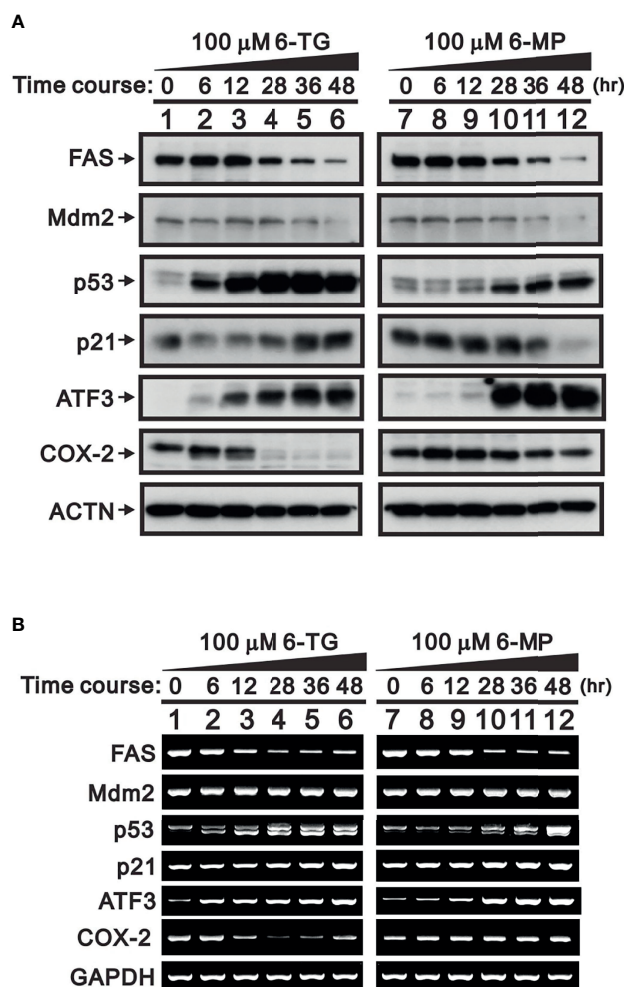


FIGURE 2 | Time-course of the effects of 6-TG and 6-MP in A253 cells. Cells were treated for the indicated times with vehicle or 100 μ M 6-TG or 6-MP, after which cell lysates were subject to **(A)** Western blotting analysis with antibodies against FAS, Mdm2, p53, p21, ATF3, and COX-2; or **(B)** RT-PCR analysis for FAS, Mdm2, p53, p21, ATF3, and COX-2 mRNAs. ACTN is a protein loading control; GAPDH is an mRNA loading control.

Exogenously Expressed USP2a Fails to Reverse the Effects of 6-TG and 6-MP in A253 Cells

The catalytic amino acid in the USP2a active site is Cys276, and substituting an Ala residue at that site eliminates the enzyme's catalytic activity (23, 32). We tested whether the catalytic function of USP2a is involved in stabilizing target proteins using a USP2 C276A mutant (7). We observed that levels of both FAS and cyclin D1 proteins were dose-dependently increased in A253 cells transiently transfected with wild-type USP2a, but that increase was less evident in cells transfected with the USP2a C276A mutant (**Figure 7**). This suggests the deubiquitination activity of USP2a is important for stabilization of its target proteins, including FAS and cyclin D1. Similarly, we observed that transfection of wild-type USP2a dose-dependently increased levels of p53, p21, and ATF3 proteins (**Figure 7**). However, in cells treated with 6-

MP, transfection of USP2a did not effectively inhibit the drug-induced cyclin D1 degradation (**Figure 8**, compare panels A and B or C), suggesting USP2a is not the only target of 6-MP. Induction of p53 protein was enhanced in USP2a transfectants treated with 6-MP (**Figure 8**, compare panels A and B or C).

DISCUSSION

Our results demonstrate that levels of FAS, cyclin D1, and Mdm2 proteins are reduced in cells treated with 6-TG or 6-MP. They further suggest this effect of 6-TG and 6-MP reflects their ability to inhibit USP2a and, thus, increase ubiquitination and proteasomal degradation. By inhibiting ubiquitination, DUBs play a crucial role in determining the cellular fate of numerous proteins (2). USP2a is member of the DUB family and may function in the removal of ubiquitin from specific targets to

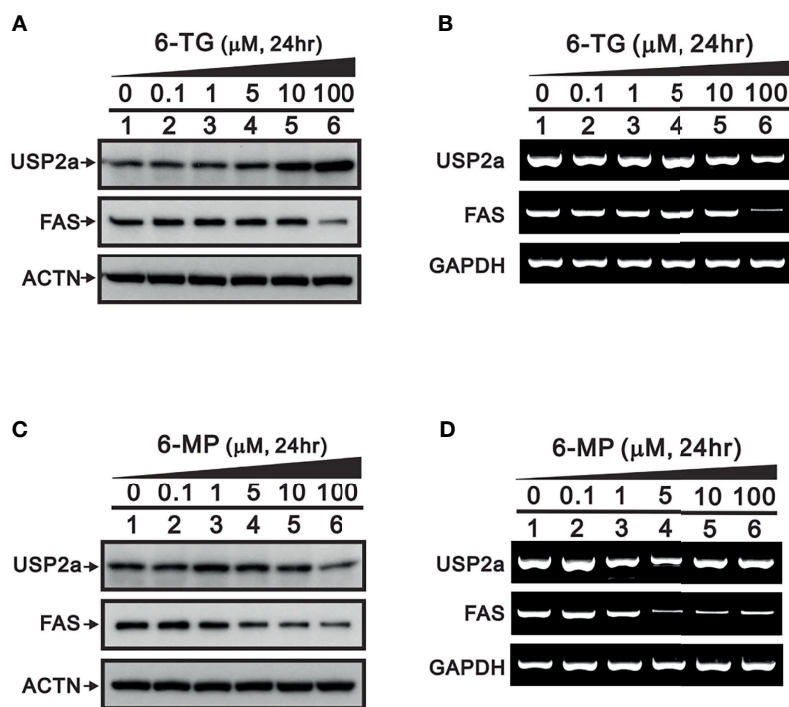


FIGURE 3 | Dose-dependent effects of 6-TG and 6-MP on expression of USP2a protein and mRNA in A253 cells. Cells were treated for 24 h with the indicated concentration of 6-TG (**A, B**) or 6-MP (**C, D**), after which cell lysates were subjected to (**A, C**) Western blotting analysis with antibodies against USP2a and FAS; or (**B, D**) RT-PCR analysis for USP2a and FAS mRNAs. ACTN is a protein loading control; GAPDH is an mRNA loading control.

prevent their degradation (3). In addition to the reported discovery of two small-molecule inhibitors of USP2a (33, 34), the noncompetitive inhibition of USP2a enzyme activity by 6-TG was recently reported, and the kinetic and catalytic mechanism was confirmed by X-ray crystallography (23). In the present study, we examined whether 6-TG or 6-MP could serve as an effective USP2a inhibitor in cells. Our findings suggest that 6-TG or 6-MP could serve as an effective USP2a inhibitor in cells and stabilize USP2a's target proteins, including FAS, Mdm2, and cyclin D1. However, the inability of exogenous USP2a to offset the inhibitory effect of 6-TG and 6-MP on USP2a activity suggests 6-TG and 6-MP exert other effects that predominate in A253 cells. In addition to inhibiting USP2a enzyme activity, our data suggest 6-TG and 6-MP may directly regulate USP2a mRNA and protein expression, though we detected differences in the cellular responses to the two drugs. This may reflect, in part, a difference in the susceptibility of 6-TG and 6-MP to S-methylation catalyzed by thiopurine methyltransferase, an enzyme involved in their metabolism (19). However, the detailed mechanisms of 6-TG and 6-MP remain to be investigated in the future.

Proteins known to be targets of USP2a include FAS, CRY1, cyclin A1, cyclin D1, EGFR, Mdm2, Aurora-A, and RIP kinase 1 (5, 25, 31, 32, 35–38). The impact of USP2a activity will depend on the function its target proteins and the effect of their stabilization on the activities of relevant signaling networks.

FAS is often overexpressed in aggressive human tumors, including prostate cancer and glioma. In addition, p53 is not a direct target of USP2a, but Mdm2 is a target. Destabilization of Mdm2 decreases the degradation of p53 and, in turn, leads to induction of p53 target genes, including stress proteins such as p21 and ATF3. The Mdm2-p53-ATF3-COX-2 axis provides a case in which an indirect effect of USP2a may play an important role mediated through p53, ATF3, or COX-2 protein. Thus, the indirect effects of 6-TG and 6-MP may open new avenues in the treatment of various cancers. In that context, although the use of 6-TG and 6-MP in the treatment of leukemia is well established, their modes of action remain controversial (39). The combined direct and indirect effects of these thiopurine drugs, which likely involve protein-protein interactions that are not well defined, may underlie the controversial findings from the present working models.

6-TG and 6-MP are well-studied thiopurine analogs that have both anticancer and immunosuppressive activities (18, 40). All thiopurines are prodrugs, and their cytotoxic activities are regulated by endogenous enzymes in different metabolic pathways (16, 40). In general, the cytotoxicity of 6-TG is believed to mainly reflect incorporation of 6-thioguanine nucleotides into DNA, whereas 6-MP exerts its effects mainly through inhibition of purine biosynthesis. The observation that thiopurine analogues inhibit coronavirus papain-like protease in severe acute respiratory syndrome, prompted us to test whether

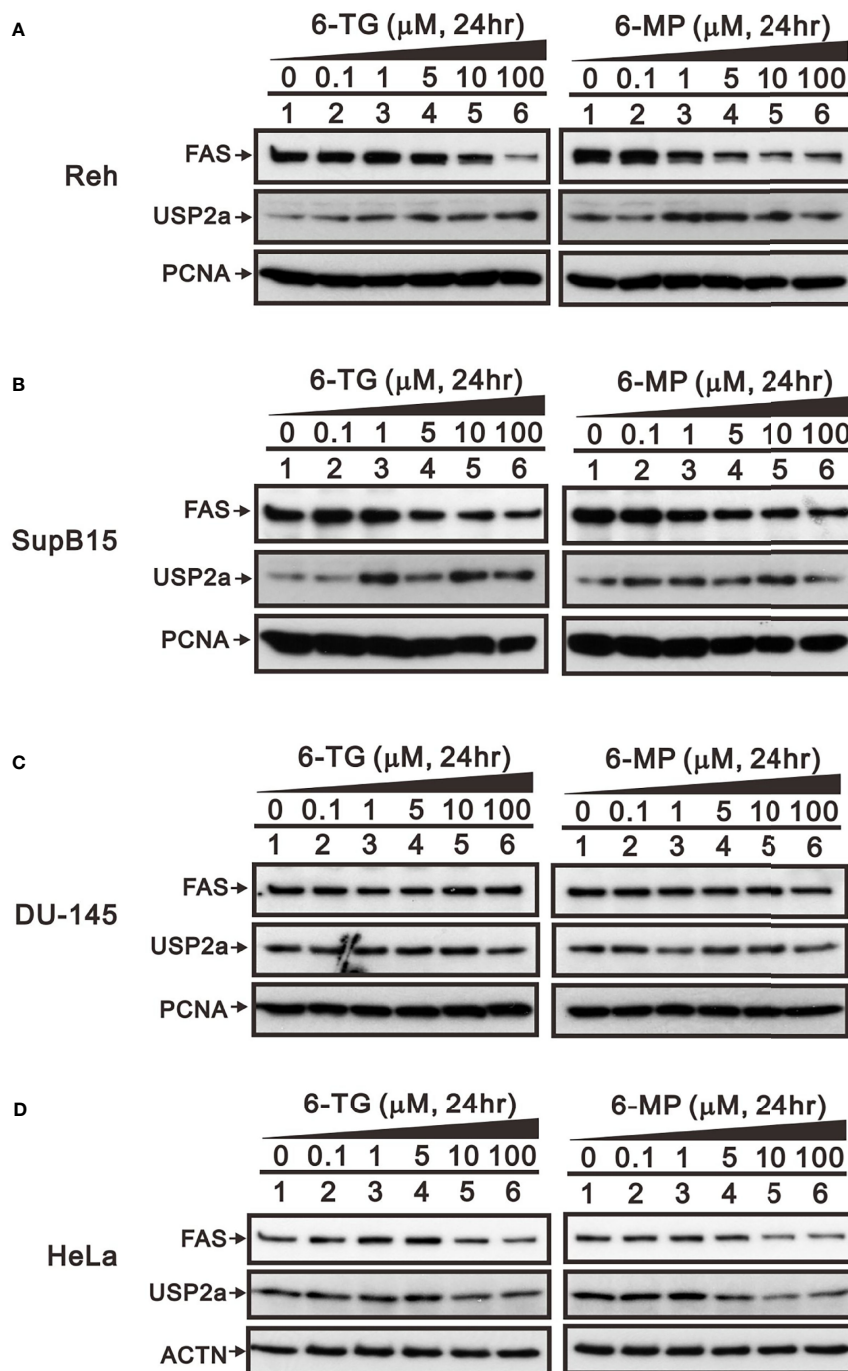


FIGURE 4 | Effects of 6-TG and 6-MP on expression of FAS protein in several cell types. **(A)** Reh, **(B)** SupB15, **(C)** DU-145, and **(D)** HeLa cells were treated for 24 h with the indicated concentrations of 6-TG or 6-MP, after which cell lysates were subjected to Western blotting analysis with antibodies against FAS and USP2a. PCNA or ACTN are protein loading controls.

6-TG and 6-MP would act as inhibitors of USP2a. We observed that 6-TG and 6-MP differentially inhibit the deubiquitination activity of USP2a and modulate the mRNA and protein expression of USP2a and FAS. Although multiple working mechanisms for antitumor functions of 6-TG and 6-MP have

been reported (18, 41, 42), the clinical responses suggest that combining thiopurines with a natural compound or other agent, such as methylthioadenosine or methotrexate, might enhance therapeutic efficacy in methylthioadenosine phosphorylase-deficient tumors (16).

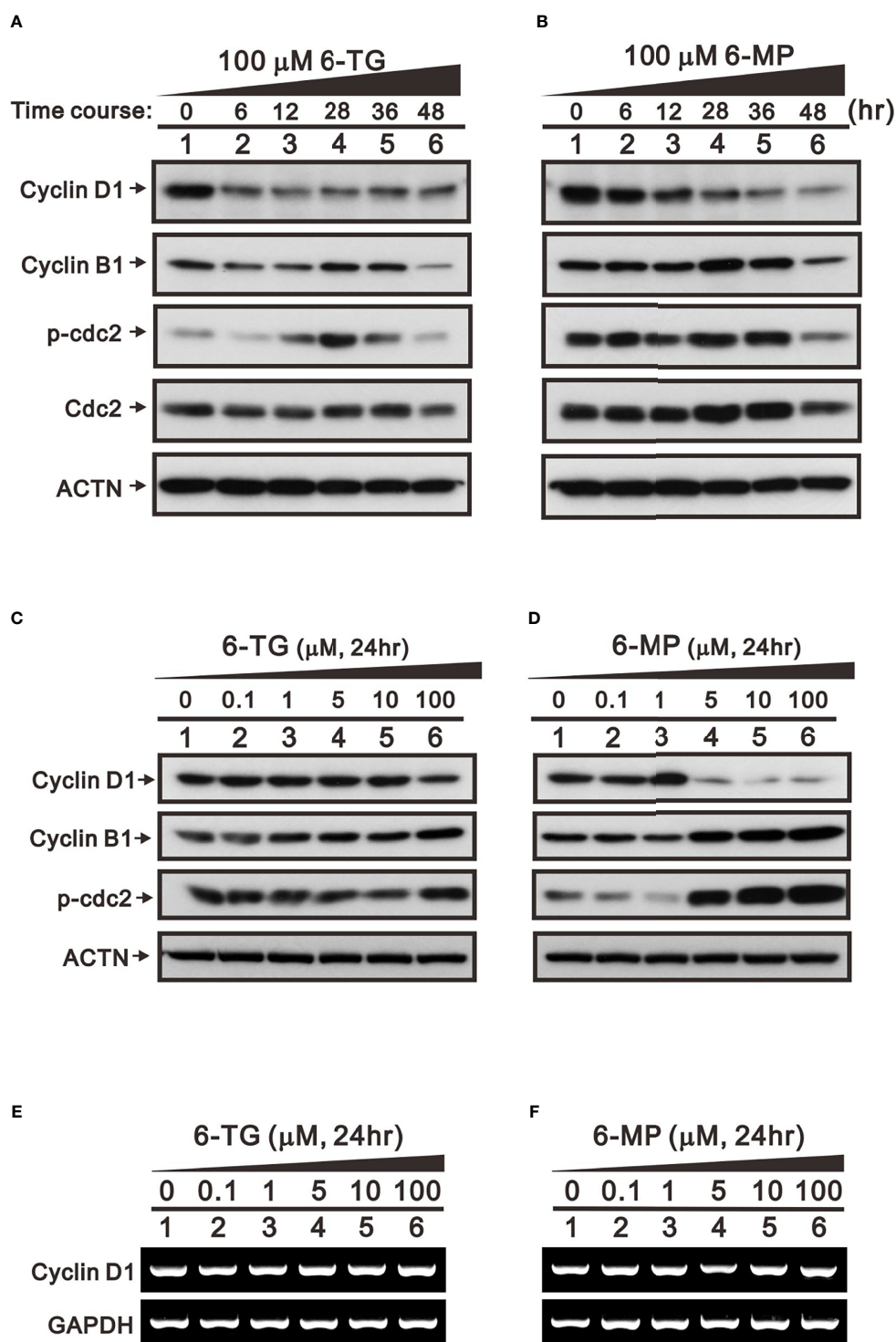


FIGURE 5 | Time- and dose-dependent effects of 6-TG and 6-MP on expression of cell cycle-related proteins in A253 cells. Cells were treated for the indicated times (**A, B**) with 100 μ M 6-TG or 6-MP or for 24 h (**C–F**) with the indicated concentration of 6-TG or 6-MP. (**A–D**) Cell lysates were then subjected Western blotting analysis with antibodies against the indicated proteins. ACTN is a protein loading control. (**E, F**) Cell lysates were subjected to the RT-PCR analysis for cyclin D1 mRNA. GAPDH is an mRNA loading control.

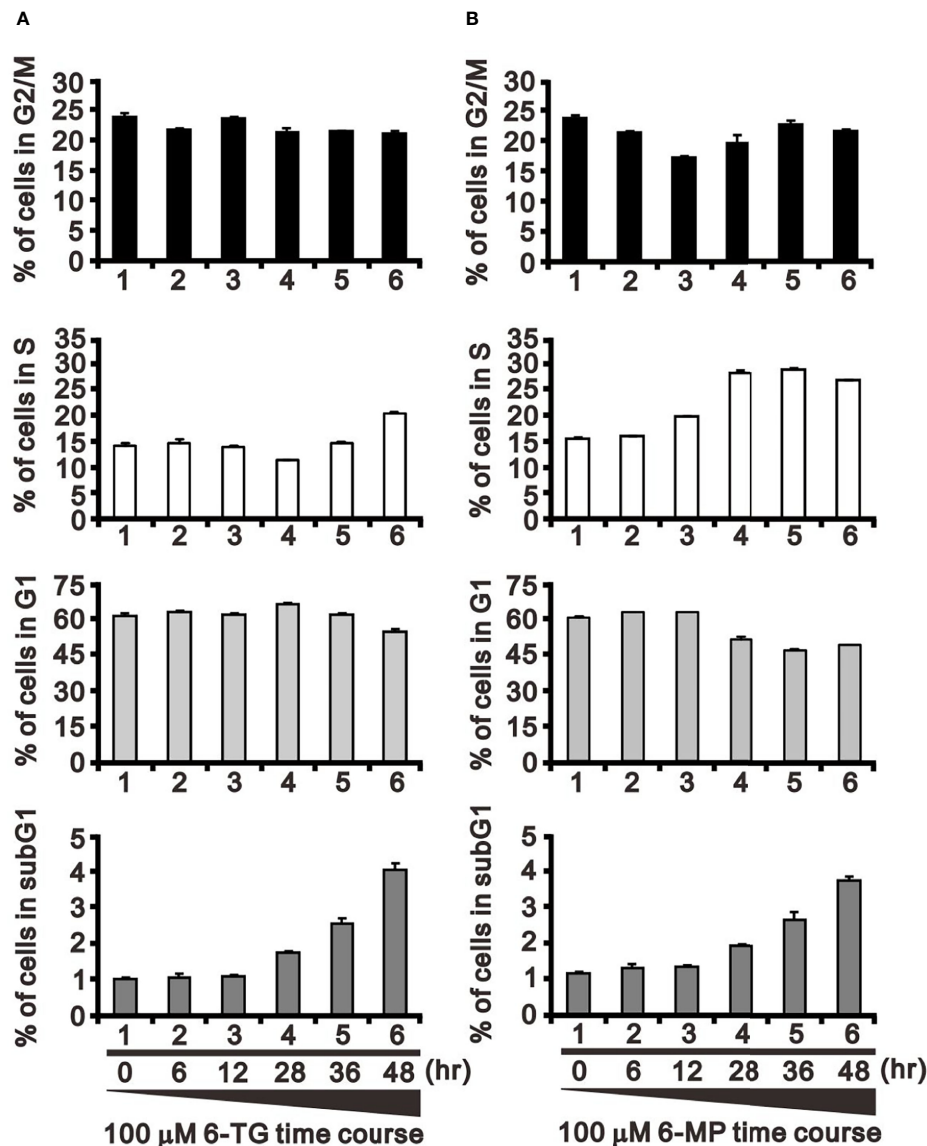


FIGURE 6 | Effects of 6-TG and 6-MP on the cell cycle profile in A253 cells. Cells were treated for the indicated times with 100 μ M 6-TG (A) or 6-MP (B), after which the populations at the indicated cell cycle phases were quantified using flow cytometry. Dead cells were detected based on PI uptake.

FAS is present at high levels in many human cancers, including colon, endometrial, ovarian, prostate, and thyroid cancer (10–15). FAS is well-known to catalyze the NADPH-dependent condensation of malonyl-CoA and acetyl-CoA to produce the 16-carbon saturated free fatty acid palmitate. The association of FAS expression with tumor virulence suggests FAS activity is vital to human cancer cells. Several studies have shown that FAS inhibition using siRNAs or small-molecule inhibitors induces tumor cell apoptosis (43–45). By inhibiting USP2a, 6-TG and 6-MP destabilize FAS. Treatment with 6-TG and 6-MP also leads to increases in the population of cells in subG1 phase, which may be related to the induction of apoptosis mediated through FAS degradation. In addition to inducing apoptosis, the

effects of thiopurines on FAS have other profound and complicated implications for the synthesis of nucleotide analogs in cancer cells. Those interesting issues will be addressed in the future.

CONCLUSIONS

In summary, our findings verify the impact 6-TG- and 6-MP-mediated inhibition of USP2a on its target proteins, including FAS, Mdm2, and cyclin D1. 6-TG and 6-MP also suppressed levels of both USP2a mRNA and protein. The effects of 6-TG and 6-MP were not cell type-specific, as they elicited similar decreases in FAS

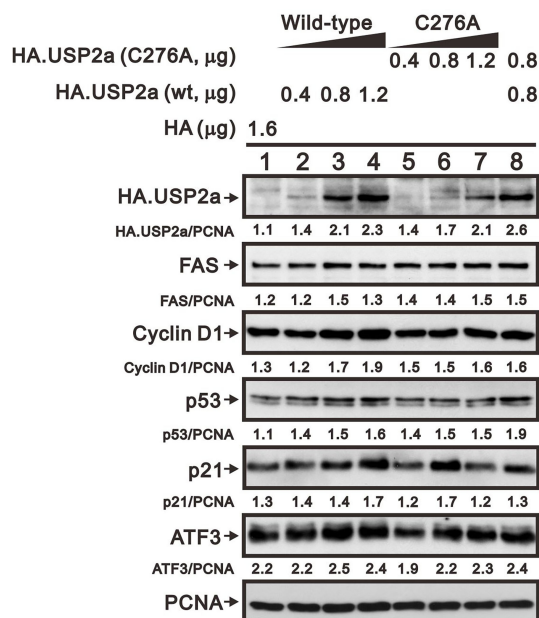


FIGURE 7 | Levels of USP2a target proteins in A253 cells expressing wild-type USP2a or its C276A mutant. Cells were transiently transfected for 36 h with the indicated amount of pSG5.HA.USP2a (wild-type) or pSG5.HA.USP2a (C276A) vector, after which cell lysates were subject to Western blotting analysis with antibodies against HA, FAS, cyclin D1, p53, p21, and ATF3. PCNA is a loading control. Protein bands were quantified through pixel density scanning and evaluated using ImageJ software, version 1.44a (<http://imagej.nih.gov/ij/>).

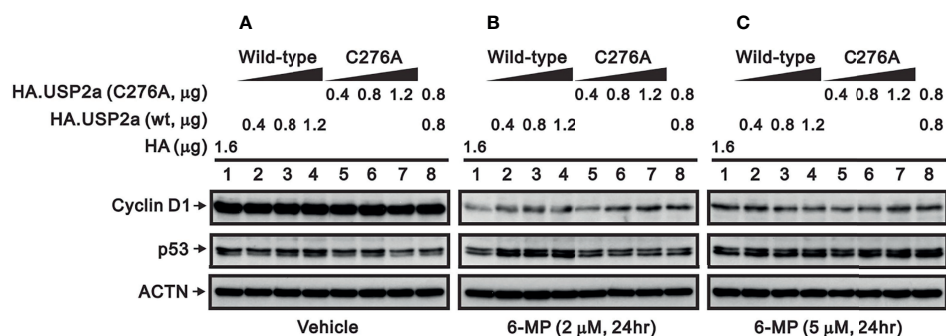


FIGURE 8 | Effect of 6-MP on levels of USP2a target proteins in A253 cells expressing wild-type USP2a or its C276A mutant. Cells were transiently transfected for 16 h with the indicated amount of pSG5.HA.USP2a (wild-type) or pSG5.HA.USP2a (C276A) and then treated for 24 h with (A) vehicle, (B) 2 μM 6-MP, or (C) 5 μM 6-MP. Cell lysates were the subjected to Western blotting analysis with antibodies against cyclin D1 and p53. ACTN is a loading control.

protein in leukemia, prostate and cervical cancer cell lines. 6-TG and 6-MP had effects on several cell cycle proteins, including another USP2a target protein, cyclin D1. The cell populations in subG1 or S phase were increased by 6-TG and 6-MP, which was accompanied by reductions in G1 phase cells. Notably, exogenous overexpression of USP2a failed to offset the effects of 6-TG and 6-MP on levels of USP2a target proteins, suggesting 6-TG and 6-MP do not act solely through inhibition of USP2a. Examination of the interplay among cancer biology, metabolism, and small

molecule drug may open avenues to devise new diagnostic and treatment strategies for cancer patients.

DATA AVAILABILITY STATEMENT

The original contributions presented in the study are included in the article/supplementary material. Further inquiries can be directed to the corresponding author.

AUTHOR CONTRIBUTIONS

C-PC conceived, analyzed data, and wrote the paper. S-TL and Y-LC carried out experiments and analyzed data. S-MH and C-LH conceived the study, participated in its design, and helped draft the manuscript. All authors contributed to the article and approved the submitted version.

REFERENCES

- Smalle J, Vierstra RD. The Ubiquitin 26S Proteasome Proteolytic Pathway. *Annu Rev Plant Biol* (2004) 55:555–90. doi: 10.1146/annurev.arplant.55.031903.141801
- Shi D, Grossman SR. Ubiquitin Becomes Ubiquitous in Cancer: Emerging Roles of Ubiquitin Ligases and Deubiquitinases in Tumorigenesis and as Therapeutic Targets. *Cancer Biol Ther* (2010) 10(8):737–47. doi: 10.4161/cbt.10.8.13417
- Meivissen TET, Komander D. Mechanisms of Deubiquitinase Specificity and Regulation. *Annu Rev Biochem* (2017) 86:159–92. doi: 10.1146/annurev-biochem-061516-044916
- Bonacci T, Emanuele MJ. Dissenting Degradation: Deubiquitinases in Cell Cycle and Cancer. *Semin Cancer Biol* (2020) 67(Pt 2):145–58. doi: 10.1016/j.semcancer.2020.03.008
- Graner E, Tang D, Rossi S, Baron A, Migita T, Weinstein LJ, et al. The Isopeptidase USP2a Regulates the Stability of Fatty Acid Synthase in Prostate Cancer. *Cancer Cell* (2004) 5(3):253–61. doi: 10.1016/S1535-6108(04)00055-8
- Nicholson B, Marblestone JG, Butt TR, Mattern MR. Deubiquitinating Enzymes as Novel Anticancer Targets. *Future Oncol* (2007) 3(2):191–9. doi: 10.2217/14796694.3.2.191
- Priolo C, Tang D, Brahmamandan M, Benassi B, Sicinska E, Ogino S, et al. The Isopeptidase USP2a Protects Human Prostate Cancer From Apoptosis. *Cancer Res* (2006) 66(17):8625–32. doi: 10.1158/0008-5472.CAN-06-1374
- Tao BB, He H, Shi XH, Wang CL, Li WQ, Li B, et al. Up-Regulation of USP2a and FASN in Gliomas Correlates Strongly With Glioma Grade. *J Clin Neurosci* (2013) 20:717–20. doi: 10.1016/j.jocn.2012.03.050
- da Silva SD, Cunha IW, Nishimoto IN, Soares FA, Carraro DM, Kowalski LP, et al. Clinicopathological Significance of Ubiquitin-Specific Protease 2a (USP2a), Fatty Acid Synthase (FASN), and ErbB2 Expression in Oral Squamous Cell Carcinomas. *Oral Oncol* (2009) 45(10):e134–9. doi: 10.1016/j.oraloncology.2009.02.004
- Ogino S, Noshio K, Meyerhardt JA, Kirkner GJ, Chan AT, Kawasaki T, et al. Cohort Study of Fatty Acid Synthase Expression and Patient Survival in Colon Cancer. *J Clin Oncol* (2008) 26(35):5713–20. doi: 10.1200/JCO.2008.18.2675
- Pizer ES, Wood FD, Heine HS, Romantsev FE, Pasternack GR, Kuhajda FP. Inhibition of Fatty Acid Synthesis Delays Disease Progression in a Xenograft Model of Ovarian Cancer. *Cancer Res* (1996) 56(6):1189–93.
- Pizer ES, Jackisch C, Wood FD, Pasternack GR, Davidson NE, Kuhajda FP. Inhibition of Fatty Acid Synthesis Induces Programmed Cell Death in Human Breast Cancer Cells. *Cancer Res* (1996) 56(12):2745–7.
- Pizer ES, Lax SF, Kuhajda FP, Pasternack GR, Kurman RJ. Fatty Acid Synthase Expression in Endometrial Carcinoma: Correlation With Cell Proliferation and Hormone Receptors. *Cancer* (1998) 83(3):528–37. doi: 10.1002/(SICI)1097-0142(19980801)83:3<528::AID-CNCR22>3.0.CO;2-X
- Swinen JV, Vanderhoydonc F, Elgamel AA, Eelen M, Vercaeren I, Joniau S, et al. Selective Activation of the Fatty Acid Synthesis Pathway in Human Prostate Cancer. *Int J Cancer* (2000) 88(2):176–9. doi: 10.1002/1097-0215(20001015)88:2<176::AID-IJC5>3.0.CO;2-3
- Liu J, Brown RE. Immunohistochemical Expressions of Fatty Acid Synthase and Phosphorylated C-Met in Thyroid Carcinomas of Follicular Origin. *Int J Clin Exp Pathol* (2011) 4(8):755–64.
- Munshi PN, Lubin M, Bertino JR. 6-Thioguanine: A Drug With Unrealized Potential for Cancer Therapy. *Oncologist* (2014) 19(7):760–5. doi: 10.1634/theoncologist.2014-0178
- Karimi-Maleh H, Shojaei AF, Tabatabaiean K, Karimi F, Shakeri S, Moradi R. Simultaneous Determination of 6-Mercaptopurine, 6-Thioguanine and Dasatinib as Three Important Anticancer Drugs Using Nanostructure Voltammetric Sensor Employing Pt/MWCNTs and 1-Butyl-3-Methylimidazolium Hexafluoro Phosphate. *Biosens Bioelectron* (2016) 86:879–84. doi: 10.1016/j.bios.2016.07.086
- Karran P, Attard N. Thiopurines in Current Medical Practice: Molecular Mechanisms and Contributions to Therapy-Related Cancer. *Nat Rev Cancer* (2008) 8(1):24–36. doi: 10.1038/nrc2292
- Hogarth LA, Redfern CP, Teodoridis JM, Hall AG, Anderson H, Case MC, et al. The Effect of Thiopurine Drugs on DNA Methylation in Relation to TPMT Expression. *Biochem Pharmacol* (2008) 76(8):1024–35. doi: 10.1016/j.bcp.2008.07.026
- Sgorbissa A, Potu H, Brancolini C. Isopeptidases in Anticancer Therapy: Looking for Inhibitors. *Am J Transl Res* (2010) 2(3):235–47.
- Chou CY, Chien CH, Han YS, Prebanda MT, Hsieh HP, Turk B, et al. Thiopurine Analogues Inhibit Papain-Like Protease of Severe Acute Respiratory Syndrome Coronavirus. *Biochem Pharmacol* (2008) 75(8):1601–9. doi: 10.1016/j.bcp.2008.01.005
- Chen X, Chou CY, Chang GG. Thiopurine Analogue Inhibitors of Severe Acute Respiratory Syndrome-Coronavirus Papain-Like Protease, a Deubiquitinating and Deisylating Enzyme. *Antivir Chem Chemother* (2009) 19(4):151–6. doi: 10.1177/095632020901900402
- Chuang SJ, Cheng SC, Tang HC, Sun CY, Chou CY. 6-Thioguanine Is a Noncompetitive and Slow Binding Inhibitor of Human Deubiquitinating Protease USP2. *Sci Rep* (2018) 8(1):3102. doi: 10.1038/s41598-018-21476-w
- Antao AM, Tyagi A, Kim KS, Ramakrishna S. Advances in Deubiquitinating Enzyme Inhibition and Applications in Cancer Therapeutics. *Cancers (Basel)* (2020) 12(6):1579. doi: 10.3390/cancers12061579
- Stevenson LF, Sparks A, Allende-Vega N, Xirodimas DP, Lane DP, Saville MK. The Deubiquitinating Enzyme USP2a Regulates the P53 Pathway by Targeting Mdm2. *EMBO J* (2007) 26(4):976–86. doi: 10.1038/sj.emboj.7601567
- Wu X, Bayle JH, Olson D, Levine AJ. The P53-Mdm-2 Autoregulatory Feedback Loop. *Genes Dev* (1993) 7(7A):1126–32. doi: 10.1101/gad.7.7a.1126
- el-Deiry WS, Harper JW, O'Connor PM, Velculescu VE, Canman CE, Jackman J, et al. WAF1/CIP1 Is Induced in P53-Mediated G1 Arrest and Apoptosis. *Cancer Res* (1994) 54(5):1169–74.
- Hai T, Wolfgang CD, Marsee DK, Allen AE, Sivaprasad U. ATF3 and Stress Responses. *Gene Expr* (1999) 7(4-6):321–35.
- Thompson MR, Xu D, Williams BR. ATF3 Transcription Factor and Its Emerging Roles in Immunity and Cancer. *J Mol Med (Berl)* (2009) 87(11):1053–60. doi: 10.1007/s00109-009-0520-x
- Hellmann J, Tang Y, Zhang MJ, Hai T, Bhatnagar A, Srivastava S, et al. Atf3 Negatively Regulates Ptg2/Cox2 Expression During Acute Inflammation. *Prostaglandins Other Lipid Mediat* (2015) 116–117:49–56. doi: 10.1016/j.prostaglandins.2015.01.001
- Shan J, Zhao W, Gu W. Suppression of Cancer Cell Growth by Promoting Cyclin D1 Degradation. *Mol Cell* (2009) 36(3):469–76. doi: 10.1016/j.molcel.2009.10.018
- Mahul-Mellier AL, Datler C, Pazarentzos E, Lin B, Chaisaklert W, Abuali G, et al. De-Ubiquitinating Proteases USP2a and USP2c Cause Apoptosis by Stabilising RIP1. *Biochim Biophys Acta* (2012) 1823(8):1353–65. doi: 10.1016/j.bbamer.2012.05.022
- Magiera K, Tomala M, Kubica K, De Cesare V, Trost M, Zieba BJ, et al. Lithocholic Acid Hydroxyamide Destabilizes Cyclin D1 and Induces G0/G1 Arrest by Inhibiting Deubiquitinase USP2a. *Cell Chem Biol* (2017) 24(4):458–70.e418 doi: 10.1016/j.chembiol.2017.03.002
- Tomala MD, Magiera-Mularz K, Kubica K, Krzanik S, Zieba B, Musielak B, et al. Identification of Small-Molecule Inhibitors of USP2a. *Eur J Med Chem* (2018) 150:261–7. doi: 10.1016/j.ejmech.2018.03.009

FUNDING

This work was supported by grants from the Ministry of National Defense-Medical Affairs Bureau [MND-MAB-109-084 and MND-MAB-110-089 to S-MH], the Ministry of Science and Technology [MOST 105-2314-B-016-047, 106-2314-B-016-039, and 110-2314-B-016-056 to C-LH], Taiwan, ROC.

35. Tong X, Buelow K, Guha A, Rausch R, Yin L. USP2a Protein Deubiquitinates and Stabilizes the Circadian Protein CRY1 in Response to Inflammatory Signals. *J Biol Chem* (2012) 287(30):25280–91. doi: 10.1074/jbc.M112.340786
36. Liu Z, Zanata SM, Kim J, Peterson MA, Di Vizio D, Chiriac LR, et al. The Ubiquitin-Specific Protease USP2a Prevents Endocytosis-Mediated EGFR Degradation. *Oncogene* (2013) 32:1660–9. doi: 10.1038/ncr.2012.188
37. Kim J, Kim WJ, Liu Z, Loda M, Freeman MR. The Ubiquitin-Specific Protease USP2a Enhances Tumor Progression by Targeting Cyclin A1 in Bladder Cancer. *Cell Cycle* (2012) 11(6):1123–30. doi: 10.4161/cc.11.6.19550
38. Shi Y, Solomon LR, Pereda-Lopez A, Giranda VL, Luo Y, Johnson EF, et al. Ubiquitin-Specific Cysteine Protease 2a (USP2a) Regulates the Stability of Aurora-A. *J Biol Chem* (2011) 286(45):38960–8. doi: 10.1074/jbc.M111.231498
39. Estlin EJ. Continuing Therapy for Childhood Acute Lymphoblastic Leukaemia: Clinical and Cellular Pharmacology of Methotrexate, 6-Mercaptopurine and 6-Thioguanine. *Cancer Treat Rev* (2001) 27(6):351–63. doi: 10.1053/ctrv.2002.0245
40. Swann PF, Waters TR, Moulton DC, Xu YZ, Zheng Q, Edwards M, et al. Role of Postreplicative DNA Mismatch Repair in the Cytotoxic Action of Thioguanine. *Science* (1996) 273(5278):1109–11. doi: 10.1126/science.273.5278.1109
41. Ren X, Li F, Jeffs G, Zhang X, Xu YZ, Karran P. Guanine Sulphinic Acid is a Major Stable Product of Photochemical Oxidation of DNA 6-Thioguanine by UVA Irradiation. *Nucleic Acids Res* (2010) 38(6):1832–40. doi: 10.1093/nar/gkp1165
42. Daehn I, Karran P. Immune Effector Cells Produce Lethal DNA Damage in Cells Treated With a Thiopurine. *Cancer Res* (2009) 69(6):2393–9. doi: 10.1158/0008-5472.CAN-08-4264
43. Ventura R, Mordec K, Waszczuk J, Wang Z, Lai J, Fridlib M, et al. Inhibition of *De Novo* Palmitate Synthesis by Fatty Acid Synthase Induces Apoptosis in Tumor Cells by Remodeling Cell Membranes, Inhibiting Signaling Pathways, and Reprogramming Gene Expression. *EBioMedicine* (2015) 2(8):808–24. doi: 10.1016/j.ebiom.2015.06.020
44. Agostini M, Almeida LY, Bastos DC, Ortega RM, Moreira FS, Seguin F, et al. The Fatty Acid Synthase Inhibitor Orlistat Reduces the Growth and Metastasis of Orthotopic Tongue Oral Squamous Cell Carcinomas. *Mol Cancer Ther* (2014) 13(3):585–95. doi: 10.1158/1535-7163.MCT-12-1136
45. Rossato FA, Zecchin KG, La Guardia PG, Ortega RM, Alberici LC, Costa RA, et al. Fatty Acid Synthase Inhibitors Induce Apoptosis in Non-Tumorigenic Melan-a Cells Associated With Inhibition of Mitochondrial Respiration. *PLoS One* (2014) 9(6):e101060. doi: 10.1371/journal.pone.0101060

Conflict of Interest: The authors declare that the research was conducted in the absence of any commercial or financial relationships that could be construed as a potential conflict of interest.

Publisher's Note: All claims expressed in this article are solely those of the authors and do not necessarily represent those of their affiliated organizations, or those of the publisher, the editors and the reviewers. Any product that may be evaluated in this article, or claim that may be made by its manufacturer, is not guaranteed or endorsed by the publisher.

Copyright © 2021 Cheng, Liu, Chiu, Huang and Ho. This is an open-access article distributed under the terms of the Creative Commons Attribution License (CC BY). The use, distribution or reproduction in other forums is permitted, provided the original author(s) and the copyright owner(s) are credited and that the original publication in this journal is cited, in accordance with accepted academic practice. No use, distribution or reproduction is permitted which does not comply with these terms.



From AVATAR Mice to Patients: RC48-ADC Exerted Promising Efficacy in Advanced Gastric Cancer With HER2 Expression

OPEN ACCESS

Edited by:

Jingxin Mo,
University of New South Wales,
Australia

Reviewed by:

Manisha Kumari,
Thomas Jefferson University,
United States
Mark Barok,
University of Helsinki, Finland

*Correspondence:

Lin Shen
shenlin@bjmu.edu.cn
Jing Gao
gaojing_pumc@163.com

[†]Present Address:

Lin Shen,
Key Laboratory of Carcinogenesis and
Translational Research (Ministry of
Education/Beijing), Department of
Gastrointestinal Oncology, Peking
University Cancer Hospital and
Institute, Beijing, China

[†]These authors have contributed
equally to this work

Specialty section:

This article was submitted to
Pharmacology of Anti-Cancer Drugs,
a section of the journal
Frontiers in Pharmacology

Received: 13 August 2021

Accepted: 19 November 2021

Published: 05 January 2022

Citation:

Chen Z, Yuan J, Xu Y, Zhang C, Li Z,
Gong J, Li Y, Shen L and Gao J (2022)
From AVATAR Mice to Patients: RC48-
ADC Exerted Promising Efficacy in
Advanced Gastric Cancer With
HER2 Expression.
Front. Pharmacol. 12:757994.
doi: 10.3389/fphar.2021.757994

Zuhua Chen^{1,2†}, Jiajia Yuan^{1†}, Yingying Xu¹, Cheng Zhang¹, Zhongwu Li³, Jifang Gong¹,
Yanyan Li¹, Lin Shen^{1*†} and Jing Gao^{4*}

¹Key Laboratory of Carcinogenesis and Translational Research (Ministry of Education/Beijing), Department of Gastrointestinal Oncology, Peking University Cancer Hospital and Institute, Beijing, China, ²Department of Oncology, Tongji Hospital, Tongji Medical College, Huazhong University of Science and Technology, Wuhan, China, ³Key Laboratory of Carcinogenesis and Translational Research (Ministry of Education/Beijing), Department of Pathology, Peking University Cancer Hospital and Institute, Beijing, China, ⁴National Cancer Center/National Clinical Research Center for Cancer/Cancer Hospital and Shenzhen Hospital, Chinese Academy of Medical Sciences and Peking Union Medical College, Shenzhen, China

RC48-ADC is a novel humanized antibody specific for human epidermal growth factor receptor 2 (HER2) in conjugation with a microtubule inhibitor via a cleavable linker. This study was to evaluate the antitumor activity and mechanism of RC48-ADC in gastric cancer (GC) and explore the population that may benefit from RC48-ADC treatment. Four human GC cell lines and nine patient-derived xenograft (PDX) models were exploited to evaluate the antitumor effect of RC48-ADC or trastuzumab treatment *in vitro* and *in vivo*. The expression and phosphorylation of HER2 were assessed by immunohistochemistry (IHC) staining. Critical molecules of downstream PI3K/AKT and cell cycle and apoptosis signaling pathways were detected and quantified by immunoblotting. Combined with preliminary results of preclinical research, three patients with IHC3+, IHC2+/FISH+, and IHC2+/FISH- of HER2 were enrolled to verify the efficacy of RC48-ADC treatment in advanced GC. *In vitro*, RC48-ADC had superior antiproliferative effects in a dose-dependent manner on GC cells, especially on HER2-positive cells. *In vivo*, RC48-ADC exceeded trastuzumab in GC PDX models with HER2 expression, even in models with moderate to low expression of HER2. Further exploration of mechanism showed that RC48-ADC exerted the antitumor effect by inhibiting phosphorylation of HER2, inducing G2/M phase arrest and cell apoptosis in HER2-expressed PDX models. In clinical practice, RC48-ADC had satisfactory efficacy in HER2-positive and HER2 moderately expressed GC patients and demonstrated promising efficacy in HER2-positive patients who have progressed after anti-HER2 therapy. In conclusion, RC48-ADC exerted promising antitumor activity in HER2-positive as well as score of 2+ in IHC and ISH-negative AGC patients after progression of systematic treatment.

Keywords: RC48-ADC, gastric cancer, HER2 expression, PDX model, targeted therapeutic agents

INTRODUCTION

Antibody–drug conjugates (ADCs), a conjugation of a monoclonal antibody, a payload cytotoxic agent, and chemical linkers, have emerged as a promising anticancer strategy for the past decades (Abdollahpour-Alitappeh et al., 2019). ADCs have tumor specificity and antitumor potency not achievable with traditional drugs, through the cellular process of antibody–antigen binding on cancer cell surface, endocytosis into the cell, and releasing of cytotoxin (Hafeez et al., 2020). To date, ADCs including Adcetris®, Akalux®, Besponsa®, Blenrep®, Enhertu®, Lumoxiti®, Mylotarg®, Polivy®, Trodelvy®, and Kadcyla® have been approved for cancer therapy by the US Food and Drug Administration.

Trastuzumab is a monoclonal antibody targeting human epidermal growth factor receptor 2 (HER2) that exerts antitumor activity by mediating antibody-dependent cellular cytotoxicity (ADCC), inhibiting of HER2-mediated signal transduction, and shedding of HER2-extracellular domain (ECD) (Hudis, 2007). Trastuzumab has been approved in the treatment of HER2-positive patients with breast cancer (BC) (Slamon et al., 2001; Piccart-Gebhart et al., 2005) and advanced gastric cancer (AGC) (Bang et al., 2010). T-DM1 (Kadcyla®), an ADC comprising trastuzumab and the tubulin inhibitor emtansine, which achieves significantly longer median overall survival (OS) and progression-free survival (PFS) in EMILIA (Verma et al., 2012) and TH3RESA (Krop et al., 2017) trials, has been approved for the treatment of HER2-positive metastatic BC patients who previously received trastuzumab. Although T-DM1 was highly effective in HER2-positive gastric cancer (GC) cells and xenografts, the GATSBY study conferred that T-DM1 was not superior to taxane in patients with previously treated HER2-positive AGC (Thuss-Patience et al., 2017). The treatment of patients with HER2-positive AGC resistant to trastuzumab remains an unmet need.

Trastuzumab deruxtecan (DS-8201a) is a novel HER2-ADC composed of trastuzumab and a topoisomerase I inhibitor payload that has been recently approved by the FDA for the treatment of patients with previously treated HER2-positive AGC (Ogitani et al., 2016). The DESTINY-Gastric01 study demonstrated the significant improvements in response and OS of DS-8201a among HER2-positive AGC (Shitara et al., 2020). The objective response rate (ORR) of DS-8201a in patients with immunohistochemistry (IHC)3+ (58%, 53/91) was higher than that in patients with IHC2+ and ISH+ (29%, 8/28), which sparked additional interest of ADCs in therapeutic development of AGC. RC48-ADC is a humanized anti-HER2 monoclonal antibody (hertuzumab) conjugated to microtubule inhibitor monomethyl auristatin E (MMAE) *via* a cleavable linker. A phase 2 study reported that RC48-ADC was well tolerated and demonstrated an ORR of 51.2% in patients with previously treated HER2-positive locally advanced or metastatic urothelial carcinoma (Sheng et al., 2021). This study explored the antitumor effect and mechanism of the RC48-ADC in GC cells and AVATAR models and evaluated its efficacy on three AGC patients with different statuses of HER2.

MATERIALS AND METHODS

Patients and Tumor Samples

This study included three patients with AGC who received systematic treatment from 2017 to 2021 at Peking University Cancer Hospital, Beijing, China. Histopathology confirmation and HER2 detection were determined by two pathologists. This study was approved by the institutional review board at Peking University Cancer Hospital. The clinical response of treatment was evaluated by computed tomography (CT) and was categorized as a complete response (CR), partial response (PR), stable disease (SD), or progressive disease (PD), according to the RECIST 1.1 criteria.

This study was approved by the Medical Ethics Committee of Peking University Cancer Hospital. All animal studies complied with the ARRIVE guidelines and were conducted in accordance with the National Institutes of Health Guide for the Care and Use of Laboratory Animals (NIH Publications No. 8023, revised 1978). Experiments involving human were in accordance with the ethical standards of committees (institutional and national) and with The Code of Ethics of the World Medical Association (Declaration of Helsinki). All patients completed written informed consent prior to study entry.

Reagents and Antibodies

RC48-ADC was provided by RemeGenCo, Ltd., and dissolved in normal saline. Trastuzumab was purchased from Shanghai Roche Pharmaceutical Ltd. Antibodies specific for HER2, pHER2, AKT, pAKT, S6, pS6, ERK, pERK, pCDK1, CDK2, cyclin E1, p53, Bcl-2, and Bax were purchased from Cell Signaling Technology (Boston, MA, USA). The antibody specific for β -actin was purchased from Sigma-Aldrich (St. Louis, MO, USA).

Cell Lines and Cell Culture

Two HER2-positive GC cell lines (NCI-N87 and SNU-216) and two HER2-negative GC cell lines (NUGC-4 and HGC-27) were used in this study. NCI-N87 was kindly provided by professor You-yong Lv (Peking University Cancer Hospital and Institute, China); SNU-216 and NUGC-4 cell lines were purchased from Cobioer Biological Technology (Nanjing, China). HGC-27 was purchased from the cell bank of Peking Union Medical College (Beijing, China). GC cells were cultured in RPMI 1640 (Gibco, MD, USA) supplemented with 10% fetal bovine serum (Gibco) and then incubated in a humidified incubator (37°C) with 5% CO₂. All cell lines were confirmed by short-tandem repeat (STR) analysis.

Cell Viability Assay

A total of 5,000 cells per well were plated onto 96-well plates and incubated with complete medium overnight. Cells were exposed to RC48-ADC (0–10,000 nM) and trastuzumab (0–10,000 nM) for 72 h. The cell viability was assessed by Cell Counting Kit-8 assay (Dojindo, Kumamoto, Japan). The absorbance at 450 nm was measured by a microplate spectrophotometer. All of the experiments were repeated three times. The IC₅₀ was calculated using GraphPad Prism 7.0.

The Antitumor Activity of RC48-ADC in AVATAR Mice

The establishment and molecular characteristics of AVATAR models for AGC patients were previously reported (Zhu et al., 2015; Chen et al., 2018). Tumor tissues of nine PDX models were subcutaneously inoculated into the flank of 6-week-old non-obese diabetic/severe combined immunodeficiency (NOD/SCID) mice. When the tumor volume reached 750 mm³, we separated the tumors, sliced into small fragments, and then reinoculated into other NOD/SCID mice. Mice with tumors of 150–250 mm³ were randomized to RC48-ADC group (5 mg/kg), trastuzumab group (5 mg/kg), and vehicle group (physiological saline). All animals were administrated *via* weekly vein injection for 3 weeks. The length and width of tumor tissues and body weights of mice were measured twice a week, and the tumor volume was calculated as $(\text{Length} \times \text{Width}^2)/2$. Mice were sacrificed after the administration cycle or when the tumor volume reached 2,000 mm³. Tumor growth inhibition (TGI) was determined as $[1 - \Delta T/\Delta C] \times 100\%$ (ΔT and ΔC presented changes in tumor volume of the treatment group and vehicle group over the course of the treatment).

Western Blotting Analysis

Total protein was extracted from tumor tissues and the concentration was measured *via* BCA Protein Assay Kit (Beyotime, Shanghai, China). Here, 50 µg protein samples were separated by 10% sodium dodecyl sulfate polyacrylamide gel electrophoresis (SDS-PAGE) and transferred onto nitrocellulose membranes (GE Healthcare, Piscataway, NJ). After incubation with corresponding primary antibodies diluted in 5% bovine serum albumin (BSA) overnight at 4°C and incubation with secondary antibodies for 1 h at room temperature, protein samples were visualized using ECL-plus Western Blotting Detection Reagents (GE Healthcare Life Sciences, Chalfont, UK). Protein bands were quantified and normalized with ImageJ software.

Immunohistochemistry Staining

Tumor tissues were isolated from euthanized mice, and then formalin-fixed paraffin-embedded (FFPE) tissue blocks were prepared. IHC staining for HER2 was performed according to the manufacturer's instructions and interpreted by two independent pathologists. IHC scores for HER2 were interpreted as follows: 0, no staining; 1+, weak or focal staining; 2+, moderate staining; and 3+, strong staining.

Statistical Analysis

The differences between/among groups were analyzed using unpaired two-tailed t-tests, one-way ANOVAs, or factorial analysis by GraphPad Prism version 7.0 (GraphPad Software Inc., CA, USA).

RESULTS

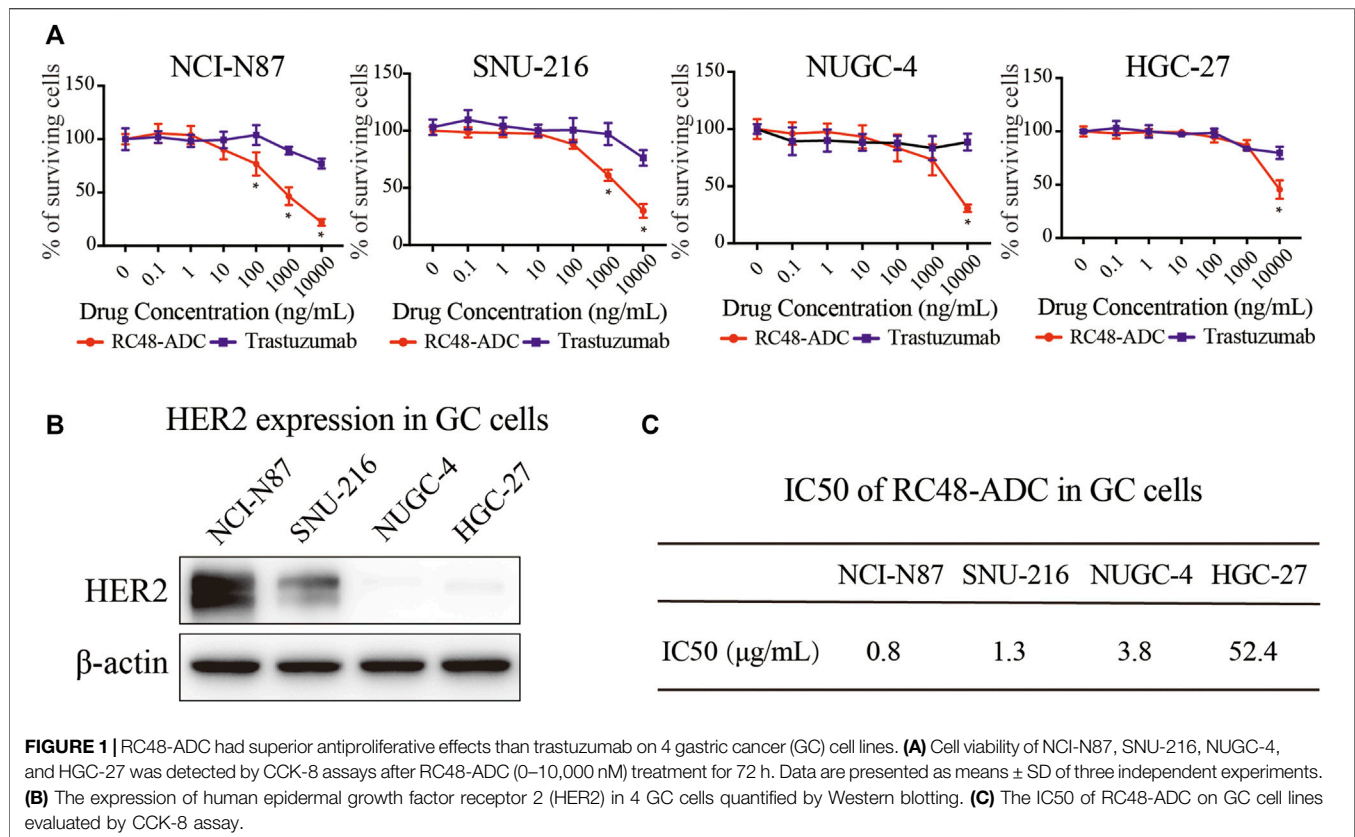
RC48-ADC Exerted Selective Antitumor Activity in Gastric Cancer Cells and Patient-Derived Xenograft Models

Cell viability tests were conducted to evaluate the antitumor activity of RC48-ADC on 4 GC cell lines, followed by protein expression analysis to clarify the profiling of those cells. Compared with trastuzumab, RC48-ADC had superior antiproliferative effects in a dose-dependent manner on 4 cell lines (Figure 1A). NCI-N87 and SNU-216 cells were more sensitive to RC48-ADC treatment, resulting from the superior expression of HER2 (Figures 1B, C).

Nine GC PDX models were exploited to evaluate the TGI of RC48-ADC and trastuzumab *in vivo*. In general, RC48-ADC showed excellent antitumor activity in PDX models with different expression levels of HER2 (TGI: 82%–134%, $p < 0.05$; Figure 2A, Table 1). In PDX models with high expression (IHC3+) and amplification (FISH+) of HER2 (Figure 2B, Table 1), the antitumor activity of RC48-ADC was significantly superior to trastuzumab in PDX1 (TGI: 134% vs. 68%, $p < 0.001$) and equivalent to trastuzumab in three other models (TGI: 94%–126% vs. 82%–125%). As to PDX models with moderate and low expression of HER2, RC48-ADC exerted significantly stronger antitumor efficacy than trastuzumab (TGI: 82%–105% vs. 32%–63%, $p < 0.001$). The dynamic changes in body weight of mice during treatment were presented as Supplementary Figure S1. In addition, one PDX model with moderate expression of HER2 was chosen to further explore the antitumor activity under different drug concentrations of RC48-ADC. The antitumor effect of 5 mg/kg group exceeded that of the 2.5 mg/kg group, whereas it equaled that of the 10 mg/kg group, which suggested that the efficacy of RC48-ADC was dose-dependent (Figures 2C, D).

RC48-ADC Decreased the Phosphorylation of HER2 and Induced Cell Cycle Arrest in G2/M Phase and Apoptosis in Gastric Cancer Patient-Derived Xenograft Models

RC48-ADC was a humanized monoclonal antibody specific for HER2 (hertuzumab) conjugated with MMAE. It exerted an antiproliferative effect *via* blocking HER2-driven signaling such as the PI3K/AKT/mTOR and MAPK pathways and inducing cell cycle arrest in G2/M phase through microtubule depolymerization. We detected the protein expression and phosphorylation of HER2 as well as its downstream AKT, S6, and ERK in five PDX models with moderate to high expression of HER2. Both trastuzumab and RC48-ADC could decrease the phosphorylation of HER2, and the inhibitory effect of RC48-ADC was stronger (Figure 3A). In addition, the phosphorylation of downstream AKT and S6 was significantly increased after RC48-ADC treatment in the three PDX models (Figures 3A, B).



As a key regulator in the transition from G2 phase to M phase, CDK1 was found to be involved in modulating the cell cycle by forming the CDK1/cyclin B1 complex. The critical regulatory step in activating cdc2 during progression into mitosis appears to be dephosphorylation of cdc2 at Thr14 and Tyr15. After 3 weeks of RC48-ADC treatment, the phosphorylated CDK1 (Thr14) was downregulated when compared with the vehicle group. Meanwhile, the expression of CDK2 and CyclinE1 also decreased to a certain extent (Figures 3C, D), which further suggested the G2/M cycle block induced by MMAE.

RC48-ADC could also exert its antitumor effect by inducing apoptosis. After treatment with RC48-ADC, the expression of antiapoptotic protein Bcl-2 decreased, accompanied by the upregulation of proapoptotic protein Bax in PDX models (Figures 3E, F).

RC48-ADC Demonstrated Promising Efficacy in Advanced Gastric Cancer Patients With HER2 Expression

Three AGC patients with HER2 overexpression were enrolled to receive RC48-ADC treatment after disease progression with systematic therapies. The characteristics of these patients were shown in Table 2. All of them were administered intravenously with 2.5 mg/kg of RC48-ADC every 2 weeks during a treatment cycle of 6 weeks. Patient 1, a 56-year-old man, was diagnosed as HER2-positive (IHC3+/FISH+) GC with multiple liver

metastases. Previously, he was administered five cycles of XELOX regimen in combination with trastuzumab and one cycle of paclitaxel. After two cycles of RC48-ADC treatment, he achieved a clinical response of PR accompanied by decreased CA199 (Figures 4A, B). Treatment-related adverse events (TRAEs) including fatigue (grade 2), diarrhea (grade 1), and neurotoxicity (grade 1) were observed. The disease progressed after five cycles of treatment, and the PFS was 258 days.

Patient 2 was a 54-year-old woman who was initially diagnosed with HER2-positive (IHC2+/FISH+) GC at stage IIB. She received four cycles of adjuvant chemotherapy with SOX regimen and subsequently underwent gastrectomy. The disease progressed with liver metastasis during the first-line treatment of TS regimen, then she received lapatinib combined with capecitabine for four cycles and apatinib in combination with trastuzumab for seven cycles. After two cycles of treatment with RC48-ADC, the liver lesion obviously reduced in size and resulted in the clinical response of PR (Figures 4C, D). Due to a grade 2 neurotoxicity, the dosage of RC48-ADC was reduced to 2 mg/kg from the fourth treatment cycle. This patient achieved a maintained PR until the last follow-up on June 11, 2021.

Patient 3 was a 62-year-old woman diagnosed with HER2-moderate expressed and FISH-negative GC with peritoneum and ovary metastases. She previously received multiple chemotherapy without anti-HER2 treatment, and the disease progressed during the maintenance therapy of S-1. After one cycle of RC48-ADC treatment, the thickness of the stomach wall obviously decreased

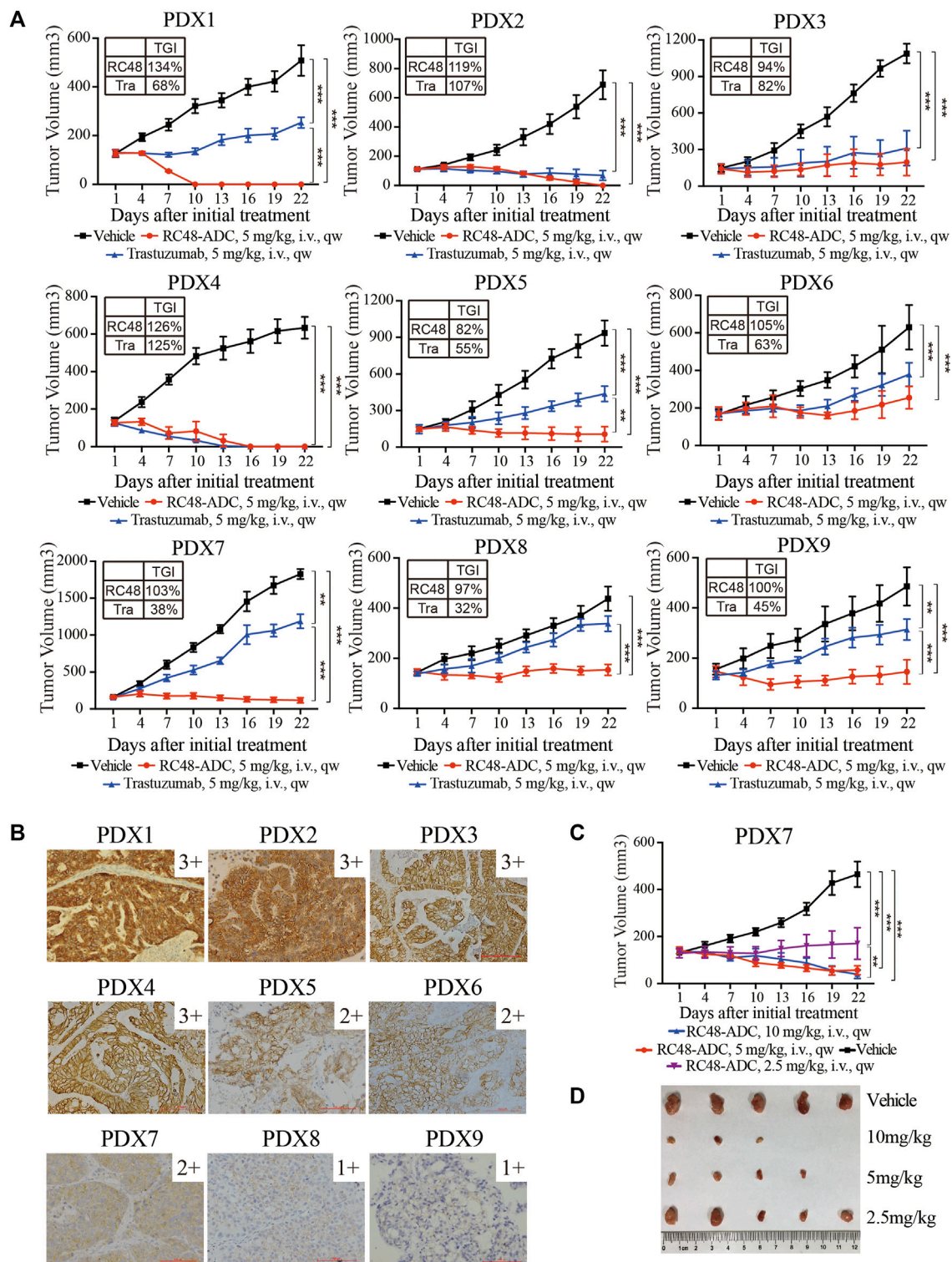


FIGURE 2 | RC48-ADC exerted selective antitumor activity in gastric cancer (GC) patient-derived xenograft (PDX) models with human epidermal growth factor receptor 2 (HER2) expression. **(A)** The antitumor activity of RC48-ADC and trastuzumab treatment in nine PDX models with different expression levels of HER2. Data are presented as means \pm SD ($n = 5$ mice per group). TGI, tumor growth inhibition; i.v., intravenous injection. ** $p < 0.005$, *** $p < 0.001$ according to repeated-measures ANOVAs. Tra, trastuzumab. **(B)** The expression of HER2 evaluated by immunohistochemistry in PDX models. Scores were interpreted as 3+, 2+, 1+, and 0 ($\times 200$ magnification; scale bar represents 100 μ m). **(C)** The antitumor activity of RC48-ADC under different concentrations in a PDX model with moderate expression of HER2. ** $p < 0.005$, *** $p < 0.001$ according to repeated-measures ANOVAs. **(D)** Tumor size of xenografts in the four groups.

TABLE 1 | The molecular characteristics and tumor growth inhibition of RC48-ADC in PDX models.

PDX ID	HER2 IHC	HER2 FISH	TGI (%)	
			Trastuzumab	RC48-ADC
1	3+	+ (cluster)	68	134
2	3+	+ (cluster)	107	119
3	3+	+ (cluster)	82	94
4	3+	+ (cluster)	125	126
5	2+	– (3:2)	55	82
6	2+	– (1:1)	63	105
7	2+	– (3:2)	38	103
8	1+	– (1:1)	32	97
9	1+	– (1:1)	45	100

in abdominal CT scan accompanied by the decrease of CA125. She achieved PR as the best response and experienced TRAEs including grade 2 fatigue and grade 1 neurotoxicity (Figures 4E, F). She died due to gastrointestinal hemorrhage during the fourth cycle of treatment, and the PFS was 177 days.

The preliminary results show that RC48-ADC has satisfactory efficacy in HER2-positive or HER2-moderate expressed GC patients, and the adverse effects are tolerable. In addition, RC48-ADC has also shown promising antitumor effects in HER2-positive patients who have progressed after receiving anti-HER2 therapy. Among these three patients, the adverse events were fatigue (grade 2), diarrhea (grade 1), and neurotoxicity (grades 1–2).

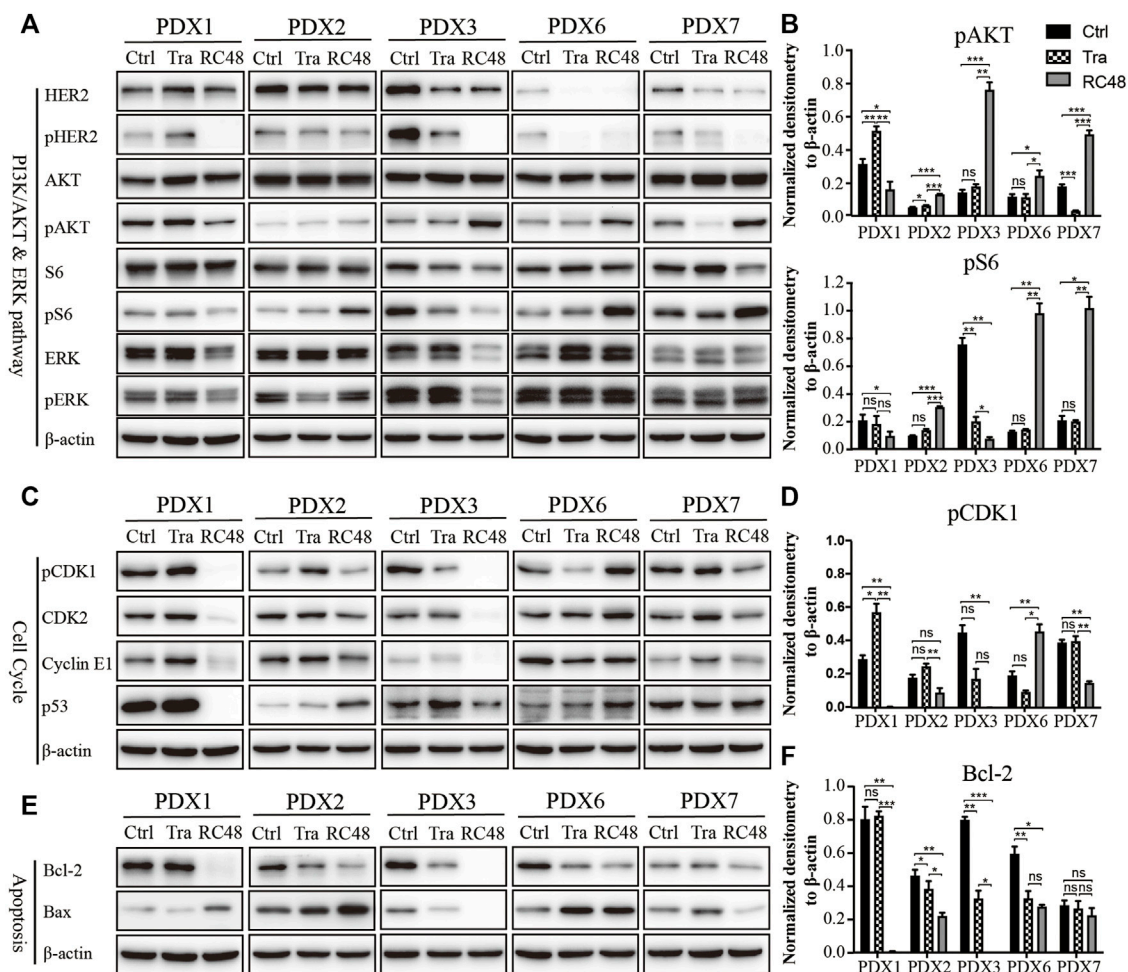
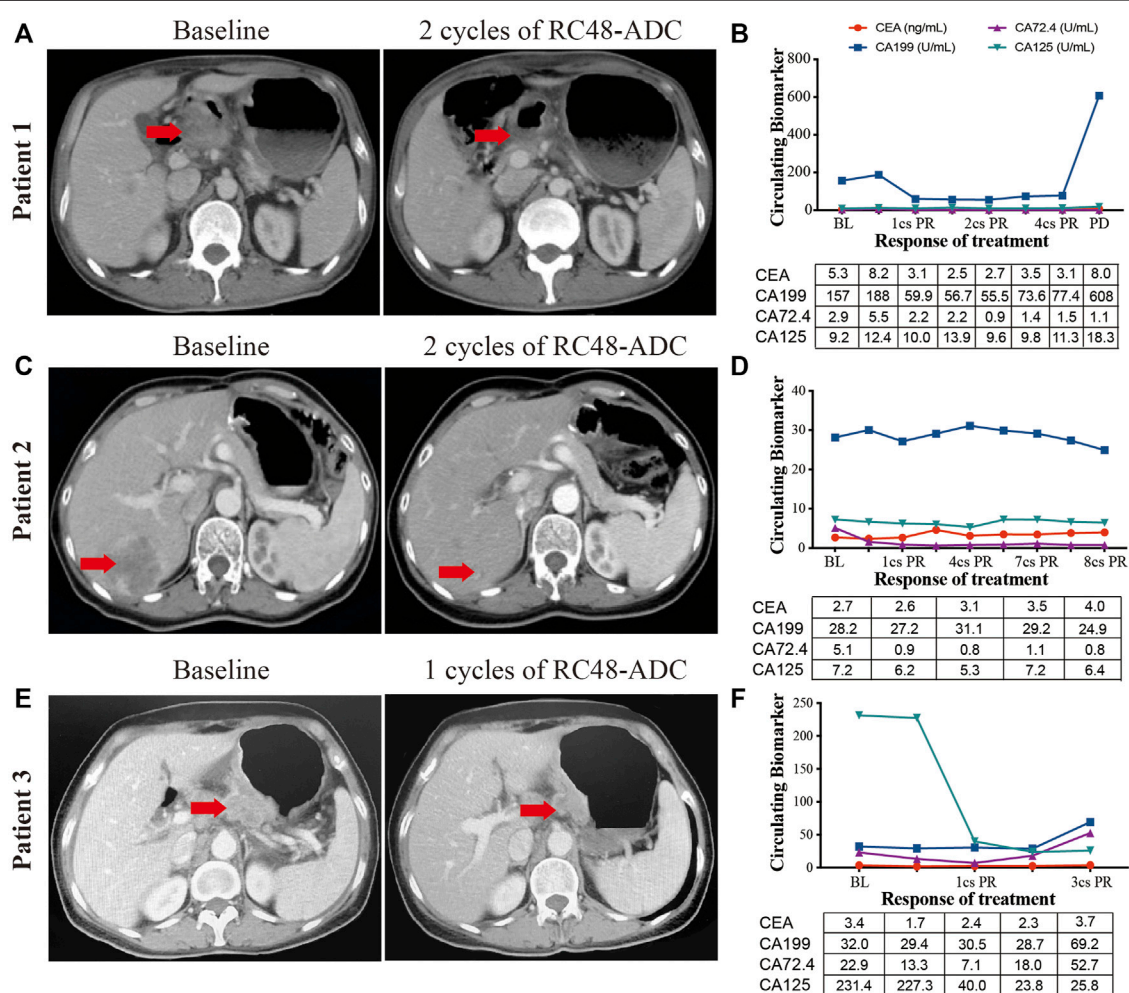


FIGURE 3 | RC48-ADC decreased the phosphorylation of human epidermal growth factor receptor 2 (HER2) and induced cell cycle arrest in G2/M phase and apoptosis in gastric cancer (GC) patient-derived xenograft (PDX) models. (A, B) Expression and quantification of critical molecules in the PI3K/AKT/S6 and ERK signaling pathway. (C, D) Expression and quantification of critical molecules in the cell cycle pathway. (E, F) Expression and quantification of antiapoptotic protein Bcl-2 and Bax. ns, no significance; * $p < 0.05$; ** $p < 0.01$; *** $p < 0.001$ according to repeated-measures ANOVAs. Data are presented as means \pm SDs of three independent experiments.

TABLE 2 | The clinical characteristics of the enrolled AGC patients.

Patient	Gender	Age	TNM	Primary site	Metastatic Site	Differentiation	Lauren classification	HER2 IHC	HER2 FISH	Prior therapies
1	Male	56	pT3N2M1	Antrum	Liver	Medium	Mixed	3+	+	1st: XELOX + trastuzumab*5cs 2nd: Paclitaxel*1cs 3rd: RC48-ADC*4cs
2	Female	54	ypT4aN0M0→M1	Antrum	Liver	Medium	Intestinal	2+	+	Neoadjuvant: SOX*4cs 1st: TS*4cs 2nd: lapatinib + capecitabine*4cs 3rd: apatinib + trastuzumab*7cs 4th: RC48-ADC*8cs
3	Female	62	cT + N + M1	Corpus	Peritoneum Ovary	Low	Mixed	2+	–	1st: DP*5cs 2nd: TS*8 cs, S-1 maintained 3rd: RC48-ADC*4cs

**FIGURE 4 |** The clinical responses of three human epidermal growth factor receptor 2 (HER2)-expressed advanced gastric cancer (AGC) patients treated with RC48-ADC. **(A, C, E)** Abdominal CT scans of tumor lesions before and after one or two cycles of RC48-ADC treatment in three patients. **(B, D, F)** The dynamic change of CEA, CA199, CA72.4, and CA125 during RC48-ADC treatment in three patients. BL, baseline; PR, partial response; SD, stable disease; PD, progressive disease.

DISCUSSION

In the present study, we evaluated the antitumor activity and mechanism of RC48-ADC in GC cells and PDX models and explored its efficacy on three AGC patients with different statuses of HER2. We found that 1) RC48-ADC exceeded trastuzumab in GC PDX models with HER2 expression, even in models with moderate to low expression of HER2; 2) RC48-ADC exerted an antitumor effect by inhibiting the phosphorylation of HER2, inducing G2/M phase arrest and cell apoptosis in HER2-expressed PDX models; 3) RC48-ADC had satisfactory efficacy in HER2-positive and HER2-moderate expressed GC patients and demonstrated promising efficacy in HER2-positive patients who have progressed after anti-HER2 therapy.

Although T-DM1 showed promising efficacy in preclinical research, the GATSBY study conferred that T-DM1 was not superior to taxane in patients with previously treated HER2-positive AGC (Thuss-Patience et al., 2017). Unlike the conjugation of trastuzumab and the tubulin inhibitor erlotinib in T-DM1, RC48-ADC is composed of hertuzumab and the microtubule inhibitor MMAE. Compared with trastuzumab, hertuzumab was reported to have a higher affinity to HER2 and capacity of antibody-dependent cell-mediated cytotoxicity (ADCC) *in vitro* (Li et al., 2016). After conjugation with MMAE, the cytotoxicity of hertuzumab was significantly enhanced, whereas the binding specificity for HER2 was not affected (Li et al., 2016). Furthermore, unlike T-DM1 with minimal bystander effect on nearby cells due to poor membrane permeability, RC48-ADC has a bystander effect that can reverse T-DM1 resistance by acting on populations of cells not overexpressing HER2 (Staudacher and Brown, 2017). Preclinical study showed that RC48-ADC exerted much stronger antitumor activity than monotherapy of trastuzumab, hertuzumab, MMAE, and combination treatment of hertuzumab and MMAE in NCI-N87 xenograft models (Li et al., 2016). Based on these published results, we evaluated the efficacy of RC48-ADC on GC cells, AVATAR mice, and patients in the present study.

Consistent with previous studies, we observed the superior antitumor activity of RC48-ADC than trastuzumab in GC cells and PDX models. Recently, the series of DESTINY study revealed that the ORR of DS-8201a was higher among patients with IHC3+ than those with IHC2+ and ISH-positive patients (Shitara et al., 2020; Siena et al., 2021), which suggests higher levels of HER2 expression seem to result in a better response. In the present study, all the four HER2-positive PDX models were confirmed with score of 3+ on IHC analysis. Due to the lack of model with 2+ of IHC and positive result on ISH, we could not evaluate the efficacy of RC48-ADC on those PDX models. Previous research reported that higher HER2 expression was associated with enhanced uptake and intracellular release of conjugated MMAE (Li et al., 2020), which might explain the difference in efficacy among HER2-positive patients with different expression levels.

Another finding of this study was that RC48-ADC exerted a promising antitumor activity in models with moderate to low expression of HER2 and achieved the clinical response of

PR in a previously treated patient with 2+ of IHC and negative result on ISH. According to literature, patients with HER2 IHC2+/FISH- account for about 40%–60% of GC (Liu et al., 2016), which is expected to expand the targeted population of RC48-ADC. Actually, in a phase I study of RC48-ADC that we conducted in advanced solid tumors, patients with HER2 IHC2+/FISH- (ORR: 5/14, 35.7%) responded similarly to those with IHC2+/FISH+ (ORR: 2/10, 20%) and IHC3+ (ORR: 3/22, 13.6%) (Xu et al., 2021). In addition, a phase II study of RC48-ADC also reported that eight urothelial carcinoma patients with IHC2+ and FISH-negative experienced PR (ORR: 40%) (Sheng et al., 2021). Combined with these preliminary results in preclinical and early clinical research, we further designed and conducted a single-arm phase II study to explore the efficacy and safety of RC48-ADC for patients with HER2-overexpressed AGC (NCT03556345). In 125 enrolled patients, the ORR of RC48 was 24.8% (31/125). The median PFS and OS were 4.1 months (95% CI: 3.7–4.9 months) and 7.9 months (95% CI: 6.7–9.9 months), respectively. Furthermore, the ORR of RC48-ADC in patients with HER2 IHC2+/FISH- (1/6, 16.7%) is lower than that in HER2-positive patients (20/76, 26.3%) (Peng et al., 2021). In June 10, 2021, RC48-ADC was approved by the National Medical Products Administration for the treatment of locally advanced or metastatic GC with HER2 overexpression who had received at least second-line treatment of systemic chemotherapy. A randomized controlled phase III trial is ongoing to compare the efficacy and safety of RC48-ADC with those of the current third-line treatment of AGC patients (NCT04714190).

There are some limitations in this study. On one hand, the efficacy comparison of RC48-ADC, T-DM1, and DS-8201 in cell lines and PDXs was not conducted. From the results of phase II studies (NCT03556345 and NCT03329690), the ORR of RC48 (24.8%, 31/125) is relatively lower than that of DS-8201 (51%, 61/119) (Shitara et al., 2020; Peng et al., 2021). Considering the differences in the baseline characteristics of the enrolled patients in the two studies, the difference in efficacy between RC48 and DS-8201a needs to be further explored. On the other hand, due to the lack of model with IHC2+/ISH+ of HER2, we could not compare the efficacy of RC48-ADC in these models with HER2 IHC3+ models.

CONCLUSION

RC48-ADC exerted promising antitumor activity in HER2-positive as well as IHC2+ and ISH-negative AGC patients after progression of systematic treatment.

DATA AVAILABILITY STATEMENT

The original contributions presented in the study are included in the article/**Supplementary Material**, further inquiries can be directed to the corresponding authors.

ETHICS STATEMENT

The studies involving human participants were reviewed and approved by the Medical Ethics Committee of Peking University Cancer Hospital. The patients/participants provided their written informed consent to participate in this study. The animal study was reviewed and approved by the Medical Ethics Committee of Peking University Cancer Hospital. Written informed consent was obtained from the individual(s) for the publication of any potentially identifiable images or data included in this article.

AUTHOR CONTRIBUTIONS

LS and JG conceived and designed the study. ZC and JY performed *in vitro* experiments. CZ and YL contributed reagents and materials. ZL contributed to data analysis. JY, YX, and JG conducted the clinical study. ZC, JG, and LS wrote and revised the article. All of the authors read and approved the final article.

REFERENCES

- Abdollahpour-Alitappeh, M., Lotfinia, M., Gharibi, T., Mardaneh, J., Farhadihosseiniabadi, B., Larki, P., et al. (2019). Antibody-drug Conjugates (ADCs) for Cancer Therapy: Strategies, Challenges, and Successes. *J. Cel Physiol* 234, 5628–5642. doi:10.1002/jcp.27419
- Bang, Y. J., Van Cutsem, E., Feyereislova, A., Chung, H. C., Shen, L., Sawaki, A., et al. (2010). Trastuzumab in Combination with Chemotherapy versus Chemotherapy Alone for Treatment of HER2-Positive Advanced Gastric or Gastro-Oesophageal junction Cancer (ToGA): a Phase 3, Open-Label, Randomised Controlled Trial. *Lancet* 376, 687–697. doi:10.1016/S0140-6736(10)61121-X
- Chen, Z., Huang, W., Tian, T., Zang, W., Wang, J., Liu, Z., et al. (2018). Characterization and Validation of Potential Therapeutic Targets Based on the Molecular Signature of Patient-Derived Xenografts in Gastric Cancer. *J. Hematol. Oncol.* 11, 20. doi:10.1186/s13045-018-0563-y
- Hafeez, U., Parakh, S., Gan, H. K., and Scott, A. M. (2020). Antibody-Drug Conjugates for Cancer Therapy. *Molecules* 25, 4764. doi:10.3390/molecules25204764
- Hudis, C. A. (2007). Trastuzumab--mechanism of Action and Use in Clinical Practice. *N. Engl. J. Med.* 357, 39–51. doi:10.1056/NEJMra043186
- Krop, I. E., Kim, S. B., Martin, A. G., Lorusso, P. M., Ferrero, J. M., Badovinac-Crnjevic, T., et al. (2017). Trastuzumab Emtansine versus Treatment of Physician's Choice in Patients with Previously Treated HER2-Positive Metastatic Breast Cancer (TH3RESA): Final Overall Survival Results from a Randomised Open-Label Phase 3 Trial. *Lancet Oncol.* 18, 743–754. doi:10.1016/S1470-2045(17)30313-3
- Li, H., Yu, C., Jiang, J., Huang, C., Yao, X., Xu, Q., et al. (2016). An Anti-HER2 Antibody Conjugated with Monomethyl Auristatin E Is Highly Effective in HER2-Positive Human Gastric Cancer. *Cancer Biol. Ther.* 17, 346–354. doi:10.1080/15384047.2016.1139248
- Li, L., Xu, M. Z., Wang, L., Jiang, J., Dong, L. H., Chen, F., et al. (2020). Conjugating MMAE to a Novel Anti-HER2 Antibody for Selective Targeted Delivery. *Eur. Rev. Med. Pharmacol. Sci.* 24, 12929–12937. doi:10.26355/eurev_202012_24196
- Liu, X., Wang, X., Wang, B., Ren, G., and Ding, W. (2016). HER2 Gene Amplification by Fluorescence *In Situ* Hybridization (FISH) Compared with Immunohistochemistry (IHC) in 122 Equivocal Gastric Cancer Cases. *Appl. Immunohistochem. Mol. Morphol.* 24, 459–464. doi:10.1097/PAI.0000000000000219
- Ogitani, Y., Aida, T., Hagihara, K., Yamaguchi, J., Ishii, C., Harada, N., et al. (2016). DS-8201a, A Novel HER2-Targeting ADC with a Novel DNA Topoisomerase I

FUNDING

This work was supported by the National Key Research and Development Program of China (No. 2017YFC1308900) and the National Natural Science Foundation of China (No. 82002602).

ACKNOWLEDGMENTS

We acknowledge RemeGenCo., Ltd., for providing RC48-ADC in this study.

SUPPLEMENTARY MATERIAL

The Supplementary Material for this article can be found online at: <https://www.frontiersin.org/articles/10.3389/fphar.2021.757994/full#supplementary-material>

- Inhibitor, Demonstrates a Promising Antitumor Efficacy with Differentiation from T-DM1. *Clin. Cancer Res.* 22, 5097–5108. doi:10.1158/1078-0432.CCR-15-2822
- Peng, Z., Liu, T., Wei, J., Wang, A., He, Y., Yang, L., et al. (2021). Efficacy and Safety of a Novel Anti-HER2 Therapeutic Antibody RC48 in Patients With HER2-Overexpressing, Locally Advanced or Metastatic Gastric or Gastroesophageal Junction Cancer: A Single-Arm Phase II Study. *Cancer Commun. (Lond)* 41, 1173–1182. doi:10.1002/cac2.12214
- Piccart-Gebhart, M. J., Procter, M., Leyland-Jones, B., Goldhirsch, A., Untch, M., Smith, I., et al. (2005). Trastuzumab after Adjuvant Chemotherapy in HER2-Positive Breast Cancer. *N. Engl. J. Med.* 353, 1659–1672. doi:10.1056/NEJMoa052306
- Sheng, X., Yan, X., Wang, L., Shi, Y., Yao, X., Luo, H., et al. (2021). Open-label, Multicenter, Phase II Study of RC48-ADC, a HER2-Targeting Antibody-Drug Conjugate, in Patients with Locally Advanced or Metastatic Urothelial Carcinoma. *Clin. Cancer Res.* 27, 43–51. doi:10.1158/1078-0432.CCR-20-2488
- Shitara, K., Bang, Y. J., Iwasa, S., Sugimoto, N., Ryu, M. H., Sakai, D., et al. (2020). Trastuzumab Deruxtecan in Previously Treated HER2-Positive Gastric Cancer. *N. Engl. J. Med.* 382, 2419–2430. doi:10.1056/NEJMoa2004413
- Siena, S., Di Bartolomeo, M., Raghav, K., Masuishi, T., Loupakis, F., Kawakami, H., et al. (2021). Trastuzumab Deruxtecan (DS-8201) in Patients with HER2-Expressing Metastatic Colorectal Cancer (DESTINY-CRC01): a Multicentre, Open-Label, Phase 2 Trial. *Lancet Oncol.* 22, 779–789. doi:10.1016/S1470-2045(21)00086-3
- Slamon, D. J., Leyland-Jones, B., Shak, S., Fuchs, H., Paton, V., Bajamonde, A., et al. (2001). Use of Chemotherapy Plus a Monoclonal Antibody against HER2 for Metastatic Breast Cancer that Overexpresses HER2. *N. Engl. J. Med.* 344, 783–792. doi:10.1056/NEJM200103153441101
- Staudacher, A. H., and Brown, M. P. (2017). Antibody Drug Conjugates and Bystander Killing: Is Antigen-dependent Internalisation Required? *Br. J. Cancer* 117, 1736–1742. doi:10.1038/bjc.2017.367
- Thuss-Patience, P. C., Shah, M. A., Ohtsu, A., Van Cutsem, E., Ajani, J. A., Castro, H., et al. (2017). Trastuzumab Emtansine versus Taxane Use for Previously Treated HER2-Positive Locally Advanced or Metastatic Gastric or Gastro-Oesophageal junction Adenocarcinoma (GATSBY): an International Randomised, Open-Label, Adaptive, Phase 2/3 Study. *Lancet Oncol.* 18, 640–653. doi:10.1016/S1470-2045(17)30111-0
- Verma, S., Miles, D., Gianni, L., Krop, I. E., Welslau, M., Baselga, J., et al. (2012). Trastuzumab Emtansine for HER2-Positive Advanced Breast Cancer. *N. Engl. J. Med.* 367, 1783–1791. doi:10.1056/NEJMoa1209124

- Xu, Y., Wang, Y., Gong, J., Zhang, X., Peng, Z., Sheng, X., et al. (2021). Phase I Study of the Recombinant Humanized Anti-HER2 Monoclonal Antibody-MMAE Conjugate RC48-ADC in Patients with HER2-Positive Advanced Solid Tumors. *Gastric Cancer* 24, 913–925. doi:10.1007/s10120-021-01168-7
- Zhu, Y., Tian, T., Li, Z., Tang, Z., Wang, L., Wu, J., et al. (2015). Establishment and Characterization of Patient-Derived Tumor Xenograft Using Gastroscopic Biopsies in Gastric Cancer. *Sci. Rep.* 5, 8542. doi:10.1038/srep08542

Conflict of Interest: The authors declare that the research was conducted in the absence of any commercial or financial relationships that could be construed as a potential conflict of interest.

Publisher's Note: All claims expressed in this article are solely those of the authors and do not necessarily represent those of their affiliated organizations or those of the publisher, the editors, and the reviewers. Any product that may be evaluated in this article, or claim that may be made by its manufacturer, is not guaranteed or endorsed by the publisher.

Copyright © 2022 Chen, Yuan, Xu, Zhang, Li, Gong, Li, Shen and Gao. This is an open-access article distributed under the terms of the Creative Commons Attribution License (CC BY). The use, distribution or reproduction in other forums is permitted, provided the original author(s) and the copyright owner(s) are credited and that the original publication in this journal is cited, in accordance with accepted academic practice. No use, distribution or reproduction is permitted which does not comply with these terms.



Transmembrane 4L Six Family Member 1 Suppresses Hormone Receptor--Positive, HER2-Negative Breast Cancer Cell Proliferation

Jie Chen^{1†}, Jin Zhu^{2†}, Shuai-Jun Xu^{3†}, Jun Zhou¹, Xiao-Fei Ding¹, Yong Liang¹, Guang Chen^{1*} and Hong-Sheng Lu^{4*}

¹Department of Experimental and Clinical Medicine, Taizhou Central Hospital (Taizhou University Hospital), Taizhou University, Taizhou, China, ²Department of Breast Surgical Oncology, Jiangxi Cancer Hospital, Nanchang, China, ³Graduate School of Medicine, Hebei North University, Zhangjiakou, China, ⁴Department of Pathology, Taizhou Central Hospital (Taizhou University Hospital), Taizhou University, Taizhou, China

OPEN ACCESS

Edited by:

Sanjun Shi,
Chengdu University of Traditional
Chinese Medicine, China

Reviewed by:

Marwa Abdelhaq,
Tanta University, Egypt
Joshi Stephen,
Baylor College of Medicine,
United States
Anatoliy Samoylenko,
University of Oulu, Finland

*Correspondence:

Guang Chen
gchen@tzc.edu.cn
Hong-Sheng Lu
luhs@tzc.edu.cn

[†]These authors have contributed
equally to this work

Specialty section:

This article was submitted to
Pharmacology of Anti-Cancer Drugs,
a section of the journal
Frontiers in Pharmacology

Received: 05 September 2021

Accepted: 10 January 2022

Published: 27 January 2022

Citation:

Chen J, Zhu J, Xu S-J, Zhou J,
Ding X-F, Liang Y, Chen G and Lu H-S
(2022) Transmembrane 4L Six Family
Member 1 Suppresses Hormone
Receptor--Positive, HER2-Negative
Breast Cancer Cell Proliferation.
Front. Pharmacol. 13:770993.
doi: 10.3389/fphar.2022.770993

Background: The prognosis of breast cancer varies according to the molecular subtype. Transmembrane 4L six family 1 (TM4SF1) exhibits different expression patterns among the molecular subtypes of breast cancer. However, the expression profile of TM4SF1 in hormone receptor HR⁺HER2⁻ breast cancer remains unclear.

Methods: TM4SF1 mRNA levels were examined in major subclasses of breast cancer by analyzing The Cancer Genome Atlas (TCGA) datasets. In addition, TM4SF1 protein and mRNA levels in HR⁺HER2⁻ breast cancer tissue samples were determined by immunohistochemistry and Western blot assay. The effect of TM4SF1 on cell proliferation was evaluated using MTT, colony formation, 3D organoid, and xenograft models, following the TM4SF1 overexpression or knockdown.

Results: TCGA database analysis demonstrated that TM4SF1 was downregulated in breast cancer compared with the healthy adjacent breast tissue. In addition, the expression of TM4SF1 in basal-like one and the mesenchymal TNBC tissue was higher than that of the healthy adjacent breast tissue. Other types, including the luminal androgen receptor-positive TNBC tissue, expressed lower levels of TM4SF1. Immunohistochemistry and real-time quantitative PCR assays demonstrated that the TM4SF1 protein and mRNA levels were downregulated in the HR⁺HER2⁻ breast cancer tissue compared with the healthy adjacent tissue. Moreover, the TM4SF1 overexpression reduced the viability of MCF-7 and ZR-75-1 breast cancer cells, whilst reducing the number of colonies and 3D-organoids formed by these cell lines. By contrast, TM4SF1 knockdown led to an increased MCF-7 cell proliferation. However, in the TNBC cell line, MDA-MB-231, TM4SF1 silencing reduced cell proliferation. *In vivo*, the TM4SF1 overexpression inhibited MCF-7 xenograft growth in a nude mouse model, which was associated with the downregulation of the Ki-67 expression, apoptosis induction, and inhibition of the mTOR pathway.

Conclusion: TM4SF1 is downregulated in HR + HER2-breast cancer, and the overexpression of TM4SF1 suppresses cell proliferation in this cancer subtype.

Keywords: transmembrane 4 L six family 1, breast cancer, hormone receptor-positive, HER2-negative, tumor suppressor

INTRODUCTION

Breast cancer is the most common cancer among women worldwide, with variable prognosis depending on the molecular subtype. There are five main molecular subtypes of breast cancer that are based on the genes a cancer expresses: luminal A, luminal B, triple-negative/basal-like, HER2-enriched, and normal-like breast cancer (Harbeck and Gnant, 2017). Triple-negative breast cancer (TNBC) is hormone receptor (HR)-negative (estrogen receptor (ER)- and progesterone receptor (PR)-negative) and HER2-negative. This type of cancer is more common in women with BRCA1 gene mutations, grows and spreads faster, has limited treatment options, and is associated with poor prognosis (Nath et al., 2021). HER2-enriched breast cancer is HR-negative and HER2-positive. Anti-HER2 therapies are used to treat all stages of HER2-positive breast cancer, from the early stage to metastasis (Ocaña et al., 2020). Luminal B breast cancer is HR-positive and either HER2-positive or HER2-negative with high levels of Ki-67. This kind of cancer usually grows faster than luminal A breast cancers, which is HR-positive, HER2-negative, and has low levels of the protein Ki-67. Luminal A cancers are low-grade, tend to grow slowly, and have the best prognosis. Normal-like breast cancer is similar to luminal A disease. Endocrine therapy is usually indicated for ER⁺ breast cancer (Spring et al., 2016). However, resistance to this form of therapy is common and may lead to disease recurrence, metastasis, and eventually death (Xiao et al., 2018). Hormone receptor (HR)⁺HER2⁻ breast cancer remains the dominant contributor to annual breast cancer deaths worldwide (Cuyún Carter et al., 2021).

Transmembrane 4 L six family 1 (TM4SF1) is a 202-amino-acid protein of the TM4 superfamily, with four hydrophobic transmembrane domains (Fu et al., 2020). TM4SF1 mediates signal transduction events that play a role in the regulation of cell development, activation, growth, and motility. It is a cell surface antigen and is highly expressed in different carcinomas (Fu et al., 2020). TM4SF1 was initially observed to be upregulated in malignant melanoma in response to activated HERmrk kinase, a chimeric protein consisting of the extracellular part of EGFR (HER) and the cytoplasmic part of *Xiphophorus* melanoma receptor kinase (Teutschbein et al., 2010). TM4SF1 is also highly expressed in other cancer types, including prostate (Allioli et al., 2011), ovarian (Gao et al., 2019), glioma (Wang et al., 2015), colorectal (Park et al., 2017), liver (Zhu et al., 2021), thyroid (Lee et al., 2019), lung (Ma et al., 2018), pancreatic (Cao et al., 2016), and breast cancers (Tu et al., 2012; Xing et al., 2017; Fan et al., 2019). However, TM4SF1 also can be downregulated in gastric cancer (Peng et al., 2018) and mammary ductal carcinoma *in situ* (Abba et al., 2004).

The expression and function of TM4SF1 in breast cancer development are unclear and may depend on the molecular subtype. Indeed, it has been demonstrated that TM4SF1 is

downregulated in mammary ductal carcinoma *in situ* (Abba et al., 2004). In addition, the overexpression of p23 in the MCF-7 breast cancer cell line results in increased invasion, which is associated with TM4SF1 downregulation (Simpson et al., 2010). These aforementioned studies indicate that TM4SF1 may act as a tumor suppressor in breast cancer. However, TM4SF1 is also positively correlated with cell migration, plays a major role in metastatic reactivation, and promotes relapse in TNBC (Gao et al., 2016).

Hormone receptor (HR)⁺HER2⁻ breast cancer contributes to most breast cancer deaths (Spring et al., 2016). Clarifying the expression profiles of TM4SF1 in HR⁺HER2⁻ breast cancer and its role in this specific cancer progression is important for developing a potential therapeutic strategy for HR⁺HER2⁻ breast cancer. In the present study, The Cancer Genome Atlas (TCGA) database was used to characterize TM4SF1 expression profiles between different types of breast cancer. TM4SF1 expression profiles in HR⁺HER2⁻ breast cancer tissues were tested by immunohistochemistry and qRT-PCR assay; its roles in HR⁺HER2⁻ breast cancer development were investigated upon TM4SF1 overexpression or knockdown.

MATERIALS AND METHODS

Cell Culture

MCF-7 was cultured in the MEM supplemented with 10% FBS and antibiotics. ZR-75-1 cells were cultured in the DMEM supplemented with 10% FBS and antibiotics. MDA-MB-231 cells were cultured in the RPMI-1640 medium supplemented with 10% FBS and antibiotics. 293T was cultured in the DMEM supplemented with 10% FBS and antibiotics. All cells were purchased from the Chinese Academy of Sciences Type Culture Collection. Cells were maintained at 37°C in a humidified atmosphere with 5% CO₂.

Immunohistochemistry

Human hormone receptor (HR)⁺HER2⁻ breast cancer tissue samples were obtained from Taizhou Central Hospital with the consent of all patients. The tissue samples were fixed in formalin and embedded in paraffin. Each slide containing both healthy adjacent breast tissue and tumor breast tissue samples was used for immunohistochemistry. The present study was approved by the Medical Ethics Committee of Taizhou Central Hospital (approval no. F-YXLL-004).

Tissue sections were rehydrated using xylene and graded concentrations of ethanol, incubated in sodium citrate (10 mM; pH 6.0) for 10 min, and then cooled down to room temperature. Endogenous peroxidase activity was then blocked with 3% hydrogen peroxide for 30 min at room temperature. The sections were permeabilized with 0.1% Triton and blocked in 10% goat serum for 30 min. The following primary antibodies were used: anti-TM4SF1 (1:400, Abcam), anti-Ki-67 (1:200, Cell

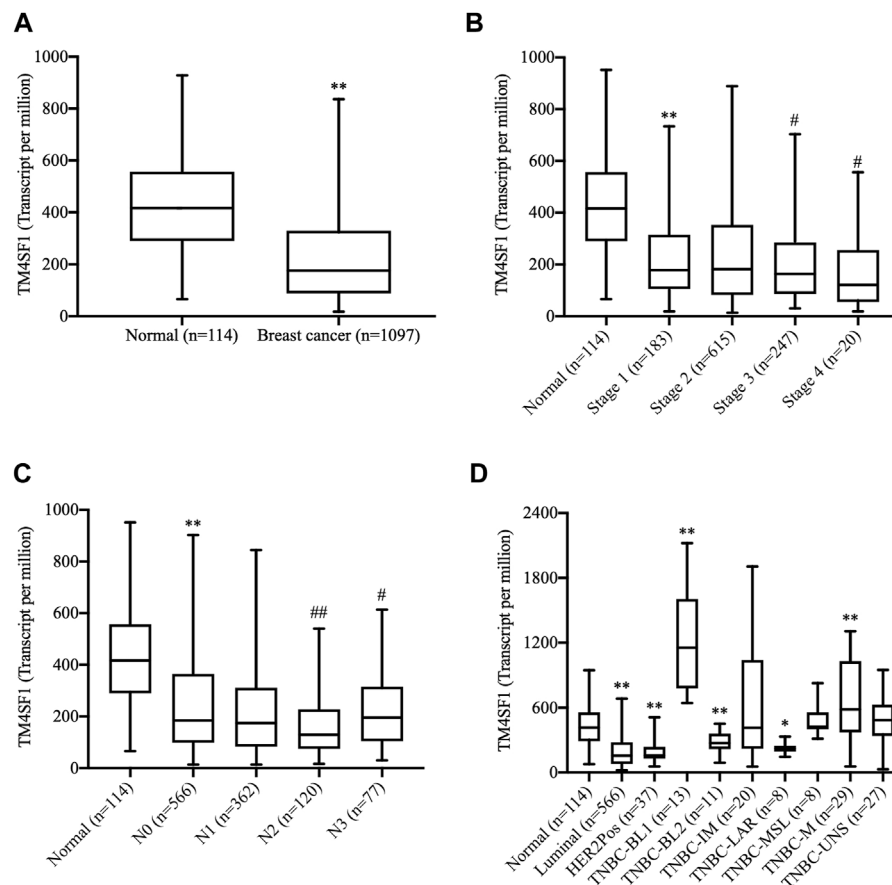


FIGURE 1 | Analysis of the TM4SF1 expression in breast cancer using data from The Cancer Genome Atlas. **(A)** Unpaired analysis showed a significant decrease of TM4SF1 expression levels in the breast cancer tissue compared with the normal breast tissue. ** $p < 0.01$ vs. the normal tissue. **(B)** Expression of TM4SF1 in BRCA based on individual cancer stages. ** $p < 0.01$ vs. the normal tissue. ## $p < 0.01$, # $p < 0.05$ vs. Stage 1. **(C)** Expression of TM4SF1 in BRCA based on the nodal metastasis status. ** $p < 0.01$ vs. Normal, ## $p < 0.01$, # $p < 0.05$ vs. N0. N0: No regional lymph node metastasis, N1: Metastases in 1–3 axillary lymph nodes, N2: Metastases in 4–9 axillary lymph nodes, N3: Metastases in 10 or more axillary lymph nodes. **(D)** Paired analysis revealed that TM4SF1 expression profiles in various molecular subtypes of breast cancer. * $p < 0.05$, ** $p < 0.01$ vs. the normal tissue (ANOVA). TM4SF1, transmembrane 4 L six family 1; TNBC, triple-negative breast cancer; BL1, basal-like 1; BL2, basal-like 2; IM, immunomodulatory; M, mesenchymal; MSL, mesenchymal stem-like; LAR, luminal androgen receptor; UNS, unspecified.

Signaling Technology, Inc.), and anti-FLIP (1:400, Cell Signaling Technology, Inc.). All primary antibodies were diluted in 5% goat serum and added to the sections at 4°C overnight. The sections were then incubated with a biotinylated goat anti-rabbit antibody (1:200; BD Pharmingen; BD Biosciences). For detection, streptavidin–horseradish peroxidase and a DAB substrate kit (BD Pharmingen; BD Biosciences) were used. Counterstaining was carried out using hematoxylin.

Lentiviral Plasmid Transduction

The pLenti-EF1a-EGFP-P2A-Puro-CMV-TM4SF13-Flag plasmid was designed and synthesized by OBiO Biotechnology Corp., Ltd. The GenBank accession number for the TM4SF1 gene is NM_014220.3. The pMDG2.G and psPAX2 plasmids for the lentivirus assembly were obtained from Addgene, Inc. The 293T cells stably expressing the TM4SF1 plasmid and a control vector were prepared by lentiviral transduction. Briefly, co-transfection was performed by combining the lentiviral plasmid (2.5 µg) with the packaging plasmids (0.75 µg pMD2.

and 1.90 µg psPAX2). The 293T cells were then infected with viral supernatants containing 8 µg/ml polybrene (MedChemExpress). Transduced cells were selected using 1 µg/ml puromycin.

Small interfering RNA (siRNA) transfection. Synthetic siRNAs targeting TM4SF1 were purchased from Shanghai GenePharma Co., Ltd. The sequences were as follows: siRNA-1, 5'-GCACGA TGCATCGGACATTCT-3'; siRNA-2, 5'-GCTATGGGAAGT GTGCACGAT-3'; and control-siRNA, 5'-UUCUCCGAACGU GUCACGUTT-3'. siRNA was transfected using Lipofectamine®-RNAiMAX (Invitrogen; Thermo Fisher Scientific, Inc.).

Reverse Transcription-Quantitative PCR

Total RNA was extracted using Trizol® and then reverse-transcribed with the Prime Script™ RT reagent kit (Takara Biotechnology Co., Ltd.). The cDNA templates were amplified by qPCR using the PowerUp™ SYBR™ Green Master Mix (Thermo Fisher Scientific, Inc.). The primer sequences were as follows: TM4SF1 forward, 5'-TGCAGGATCTGGCTACTGTG-3' and reverse, 5'-CAGAAGGTACTGGCCCTCAG-3'; and

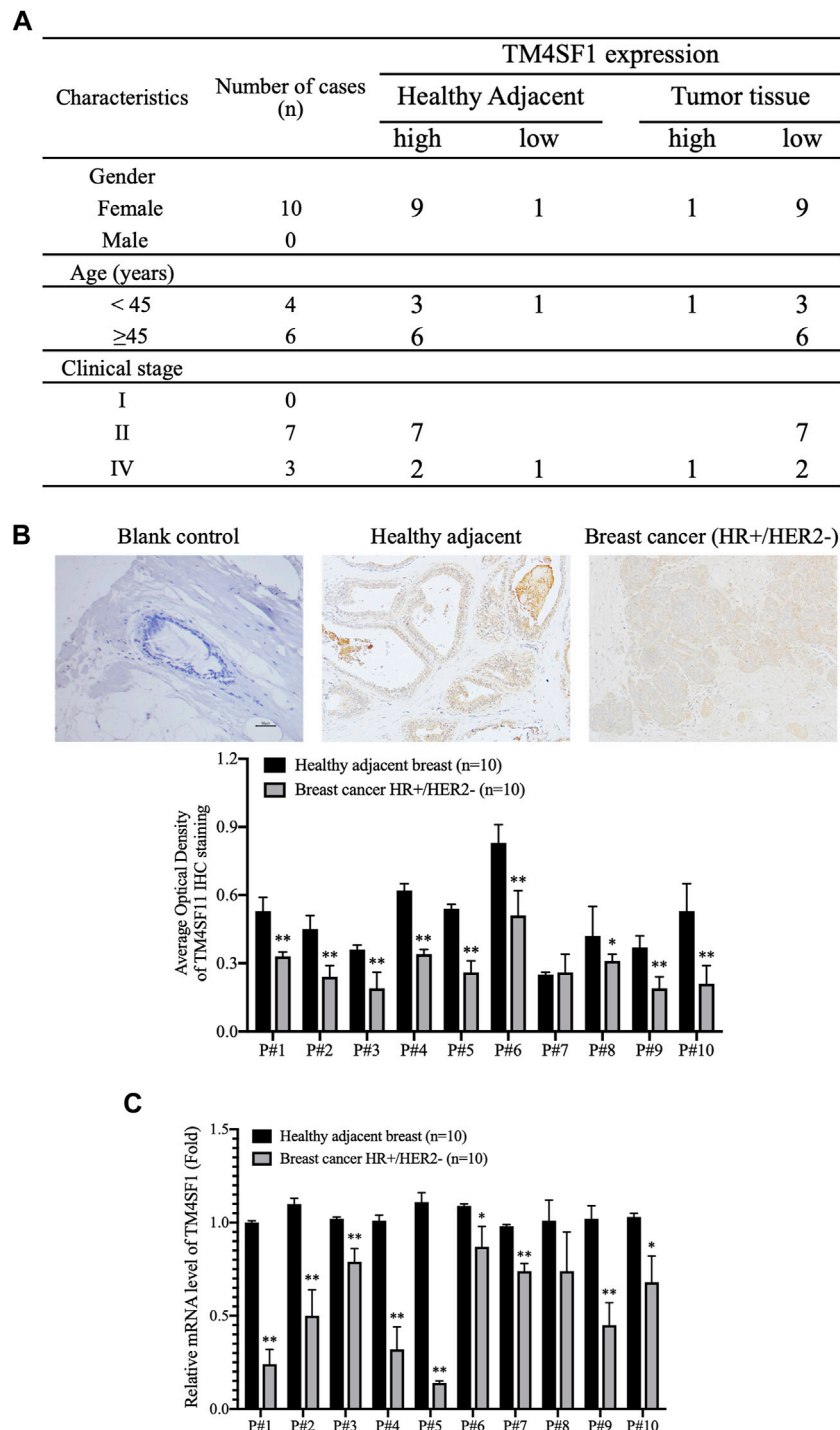


FIGURE 2 | TM4SF1 expression profile in hormone receptor-positive, HER2-negative invasive breast cancer. **(A)** Clinicopathological characteristics of patients with breast cancer. $n = 10$. **(B)** Representative immunohistochemical staining images of TM4SF11 in breast cancer and healthy adjacent tissue sample (upper panel). Semi-quantification of TM4SF1 staining using the average optical density measured by ImageJ d 1.47 software (lower panel). mean \pm SD, $n = 10$, $**p < 0.01$ compared with the healthy adjacent breast tissue by t -test analysis. **(C)** Data are presented as a fold change relative to the TM4SF1 mRNA levels in the healthy adjacent breast tissue (mean \pm SD, $n = 10$). $**p < 0.01$ compared with the healthy adjacent breast tissue by t -test analysis. TM4SF1, transmembrane 4 L six family 1.

GAPDH forward, 5'-GCACCGTCAAGGCTGAGAAC-3' and reverse, 5'-GCCTTCTCCATGGTGGTGA-3'. The thermocycling conditions were as follows: 1) 50°C for 120 s, 2)

95°C for 120 s, 3) 40 cycles of 95°C for 15 s and 60°C for 60 s, 4) 95°C for 15 s, 5) 60°C for 60 s, and 6) 95°C for 15 s. Gene expression levels were calculated using the ΔC_q method. The

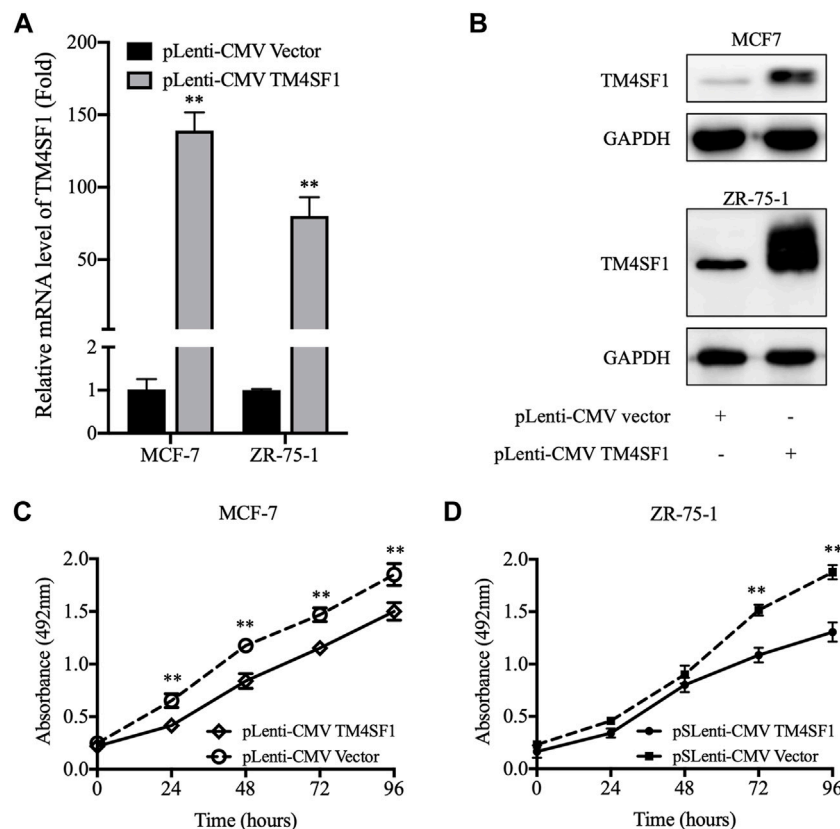


FIGURE 3 | pLenti-CMV TM4SF1 transfection-mediated upregulation of TM4SF1 reduces cell viability. **(A)** TM4SF1 overexpression efficiency was evaluated using real-time quantitative PCR (normalized to GAPDH). Data are presented as fold changes relative to the TM4SF1 levels in control cells (mean \pm SD, $n = 3$). ** $p < 0.01$ compared with the pLenti-vector transfected group by *t*-test analysis. **(B)** TM4SF1 protein levels were significantly upregulated following with the TM4SF1 plasmid. GAPDH was used a loading control. **(C, D)** MTT assays were performed to detect the MCF-7 and ZR-75-1 cell viability (mean \pm SD), * $p < 0.05$, ** $p < 0.01$ compared with the pLenti-vector transfected group by *t*-test analysis. Data shown are representative of at least two independent experiments. TM4SF1, transmembrane 4 L six family 1.

mRNA levels of TM4SF1 were normalized to those of GAPDH mRNA.

Immunoblotting

Immunoblotting was conducted using standard procedures. Briefly, the cells were resuspended in the RIPA lysis buffer (Beyotime Institute of Biotechnology). The sample was transferred to a 1.5-ml centrifuge tube and then centrifuged at 10,000 \times g for 5 min at 4°C to pellet the cell and tissue debris and collect the protein lysates. Equal masses of protein (50 μ g) were analyzed by SDS-PAGE. Antibodies against TM4SF1 (#ab113504, Polyclonal, Abcam, Cambridge, United States), AKT (#9272, Polyclonal), phosphorylated AKT (#9275, Polyclonal), and β -actin (#5125s, Polyclonal) (Cell Signaling Technology, Boston, United States) were obtained. Antibodies against Bax (BA0315), Bcl-2 (BA0412), caspase 3 (BM4340), caspase 9 (BM4619), and FLIP (M01295, Monoclonal, 7F10) were obtained from Boster Biological Technology (Wuhan, China). Antibodies against GAPDH (0411, Polyclonal), LC3 (G-4, sc-398822), and Beclin-1 (E-8, sc-48341) from Santa Cruz Biotechnology (Santa Cruz, CA) were used. All primary antibodies were polyclonal. Proteins

were visualized using a peroxidase-conjugated secondary antibody (Sigma-Aldrich; Merck KGaA) using ECL solution (Thermo Fisher Scientific, Inc.) for detection.

MTT Assay

Cell proliferation was evaluated using MTT assays. Briefly, 1×10^3 cells were plated in a 96-well plate using a complete culture medium. After 4, 24, 48, or 72 h, MTT was added to each well at a final concentration of 0.5 mg/ml. The reaction was allowed to proceed for 4 h at 37°C. The formazan crystals were then dissolved in 100 μ L DMSO. The plates were incubated in an orbital shaker at room temperature for 15 min, and the absorbance was then read at 490 nm. All assays were performed in triplicates.

3D Organoid Formation

Briefly (Chen et al., 2020), a total of 1×10^3 cells were gently mixed with 30 μ L Matrigel and plated as a droplet containing the single cells onto a prewarmed (in a 37°C incubator) 24-well ultra-low attachment plate. The droplets were allowed to solidify at 37°C for 15 min, then covered with 500 μ L complete cell culture

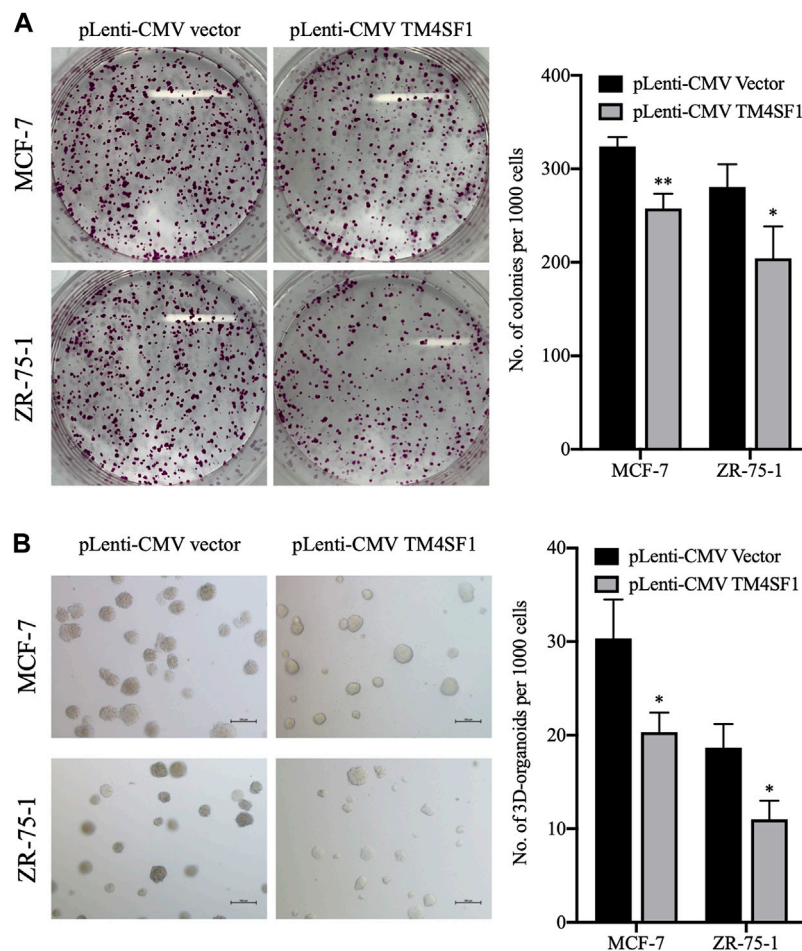


FIGURE 4 | TM4SF1 overexpression inhibits colony and 3D spheroid formation in MCF-7 and ZR-75-1 cells. **(A)** Representative images of the colonies at least three independent experiments (left). Quantification data counting numbers (right; mean \pm SD). * $p < 0.05$, ** $p < 0.01$ compared with the pLenti-vector transfected group by *t*-test analysis. **(B)** Representative images of invasive extensions from the 3D spheroids from least three independent experiments. Objective, $\times 20$. Quantification data counting numbers (right; mean \pm SD). * $p < 0.05$ compared with the pLenti-vector transfected group by *t*-test analysis.

medium, and incubated at 37°C for 15 days 3D organoid images were examined under a microscope.

Colony Formation Assay

For colony formation assays, 1×10^3 cells were seeded into 6-well plates and incubated for 10 days at 37°C with 5% CO₂. The colonies were fixed in 100% methanol, then stained for 30 min in crystal violet, and washed in ddH₂O. The clones were counted under a microscope.

Annexin V/Propidium Iodide Staining

Cell apoptosis was analyzed by flow cytometry. Following different treatments, cells were trypsinized and washed with PBS twice. The cells were then stained with Annexin V-FITC/propidium iodide (Beyotime Institute of Biotechnology) according to the manufacturer's instructions. Apoptosis was analyzed by MultiCycle software.

In Vivo Xenograft Model and Tumorigenicity

All animal experiments were approved by the Medical Ethics Committee of the Taizhou University College of Medicine (approval no. TZYXY 2020). A total of 24 male BALB/C-nu/nu mice (age, 6–8 weeks; average weight, ~25 g) were obtained from Changzhou Cavens Animal Co., Ltd. The mice were housed in sterile cages under laminar airflow hoods at 20°C in a specific pathogen-free environment with a 12-h light/dark cycle and provided with autoclaved chow and water *ad libitum*. A total of 10^7 parallel-controlled or TM4SF1-overexpressing MCF-7 cells were injected subcutaneously into the flank of the mice, respectively. Tumor dimensions were measured with calipers twice a week, and the volumes were calculated as (width)² \times length/2. After 12 weeks, the animals were sacrificed by cervical dissociation, and the tumors were removed and weighed. The largest tumor diameter was 1.434 cm, and none of the animals developed multiple tumors.

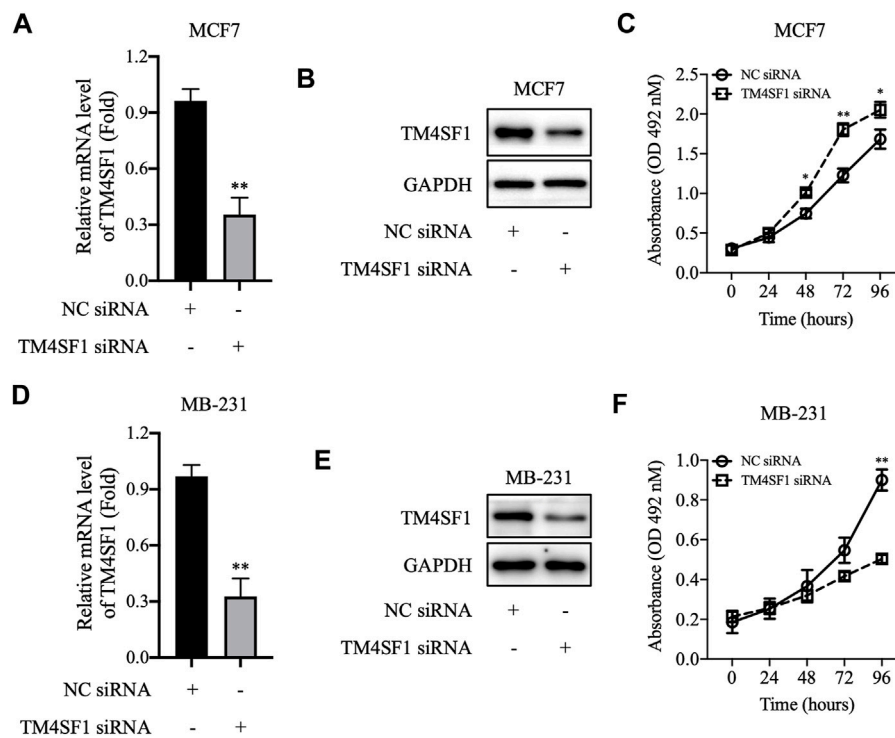


FIGURE 5 | TM4SF1 knockdown in breast cancer cells. **(A–C)** TM4SF1 knockdown efficiency was evaluated using quantitative PCR (normalized to GAPDH). Data are presented as fold changes relative to the TM4SF1 levels in control cells, mean \pm SD. ** $p < 0.01$ compared with the negative control siRNA-transfected group by *t*-test analysis. **(B–E)** TM4SF1 protein levels were significantly downregulated following transfection with TM4SF1 siRNA. GAPDH was used as a loading control. **(D–F)** Effect of TM4SF1 siRNA transfection on cell proliferation, mean \pm SD, ** $p < 0.05$, ** $p < 0.01$ compared with the negative control siRNA-transfected group by *t*-test analysis. Data shown are representative of at least two independent experiments. TM4SF1, transmembrane 4 L six family one; siRNA, small interfering RNA.

Statistical Analysis

The data are presented as the mean \pm standard deviation and were analyzed using Student's unpaired *t*-test or one way ANOVA by GraphPad Prism software (GraphPad Software). A *p*-value < 0.05 was considered significant.

RESULTS

TM4SF1 Expression Profiles in Breast Cancer by TCGA Database Analysis

The expression of TM4SF1 was first examined in breast cancer ($n = 1,097$) and normal breast ($n = 114$) TCGA data. TM4SF1 mRNA was expressed at lower levels in breast cancer than in normal tissue samples (Figure 1A). Moreover, TM4SF1 exhibited a lower expression along with the tumor stage (Figure 1B) and lower in lymph node-positive tissue specimens than that in lymph node-negative tissue specimens (Figure 1C). In addition, the expression levels of TM4SF1 were also analyzed in TNBC subclasses. Basal-like one and mesenchymal TNBC tissue expressed higher levels of TM4SF than the normal breast tissue. However, other types of breast cancer, including luminal androgen receptor-positive TNBC, expressed lower levels of TM4SF (Figure 1D). These findings indicated that the expression profiles of TM4SF1 in breast cancer varied with breast cancer subtypes.

Downregulation of TM4SF1 in HR⁺HER2⁻ Breast Cancer

The expression of TM4SF1 was subsequently examined in HR⁺HER2⁻ patients with breast cancer by immunohistochemistry ($n = 7$; Figure 2A). TM4SF1 staining was semi-quantified by measuring the average optical density by ImageJ software. The results demonstrated that TM4SF1 protein levels were downregulated in the HR⁺HER2⁻ breast cancer tissue compared with the healthy adjacent breast tissue (Figure 2B). Moreover, total RNA was extracted from those above 7 samples, and the mRNA levels of TM4SF1 were determined using RT-qPCR. The TM4SF1 mRNA expression level was downregulated in the HR⁺HER2⁻ breast cancer tissue compared with that of the healthy adjacent breast tissue (Figure 2C).

TM4SF1 Overexpression Inhibits MCF-7 and ZR-75-1 Cell Viability and Proliferation

The next experiments were designed to examine whether TM4SF1 acted as a tumor suppressor in HR⁺HER2⁻ breast cancer. TM4SF1-overexpressing cells were generated using the pLenti-CMV TM4SF1 lentiviral transduction system in the HR⁺HER2⁻ MCF-7 and ZR-75-1 breast cancer cell lines. As shown in Figures 3A,B, TM4SF1 mRNA and protein levels were markedly increased in MCF-7 and ZR-75-1 cells

transfected with pLenti-CMV TM4SF1. Moreover, TM4SF1-overexpressing cells displayed reduced viability in an MTT assay compared with pLenti-CMV vector transfected cells (Figures 3C,D).

As the repopulation of residual tumor cells can lead to cancer recurrence, which depends on the ability of cells to divide (Matsuda et al., 2021), the effect of TM4SF1 on clonogenicity was evaluated using a colony formation assay. As shown in Figure 4A, the TM4SF1 overexpression significantly decreased the plating efficiency (colonies number from 1000 cells) after 10 days of incubation compared with the pLenti-CMV vector group (32 vs. 26% in MCF-7 cells; 27.5 vs. 19.5% in ZR-75-1 cells).

3D organoid models allow the understanding of complex biology in cancer development, whereas 2D models have not proven as successful. When performing 3D cell culture experiments, the cell environment can be manipulated to mimic that of a cell *in vivo* and provide more accurate data about cell-to-cell interactions, tumor characteristics, drug discovery, metabolic profiling, stem cell research, and other types of diseases (Jensen and Teng, 2020). Thus, the effect of TM4SF1 on breast cancer cell 3D organoid formation was then evaluated. MCF-7 and ZR-75-1 cells transfected with the pLenti-CMV vector could form ~30 and ~18 3D organoid structures per 1,000 cells, respectively. By contrast, TM4SF1-overexpressing MCF-7 and ZR-75-1 cells formed only ~20 and 10 3D organoids per 1,000 cells, respectively (Figure 4B).

TM4SF1 Knockdown Promoted MCF-7 Cell Proliferation *In Vitro*

We further downregulated the TM4SF1 expression level by siRNA transfection in MCF-7 cells and tested whether disruption of TM4SF1 in HR⁺/HER2⁻ breast cancer cells affects the cell proliferation. As shown in Figures 5A,B, TM4SF1 mRNA and protein levels decreased obviously in MCF-7 after being transfected with TM4SF1-siRNA. Consequently, cells transfected with TM4SF1-siRNA grow slower than control cells in the MTT assay (Figure 5C). However, TM4SF1-siRNA transfection results in the opposite phenomenon in the triple-negative breast cancer (ER⁻/PH⁻/HER2⁻) cell line MDA-MB-231 (Figures 5D–F).

TM4SF1 Overexpression MCF-7 and ZR-75-1 Regulates Tumor Growth *In Vivo*

Because the TM4SF1 expression was downregulated in HR⁺HER2⁻ breast cancer and the TM4SF1-overexpression inhibited MCF-7 and ZR-75-1 cell viability and proliferation *in vitro*, the roles of TM4SF1 in the HR⁺HER2⁻ breast tumor growth were examined in a murine model. As shown in Figure 6A, TM4SF1-overexpressing MCF-7 xenografts grew slower than those in the pLenti-CMV vector control group. Immunohistochemical staining data showed that the frequency of Ki-67⁺ cells was markedly reduced following the TM4SF1 overexpression (Figure 6B), indicating reduced proliferation. Furthermore, TUNEL immunofluorescence staining demonstrated that the TM4SF1 overexpression induced apoptosis *in vivo* (Figure 6C).

In addition, as shown in Figure 6D, the TM4SF1 overexpression downregulated the levels of phosphorylated AKT and phosphorylated p70s6k1, which indicated that TM4SF1 may inhibit the AKT/mTOR pathway. Consistent with TUNEL staining, cleaved caspase 3/9 and Bax protein levels were upregulated, while those of BCL-2 and FLIP were downregulated following the TM4SF1 overexpression. These results indicated that the TM4SF1 overexpression promoted apoptosis.

DISCUSSION

Breast cancer is the most common invasive cancer in women and the second leading cause of cancer death in women, after lung cancer (Parada et al., 2019). Moreover, although breast cancer is perhaps the most studied malignancy to date, the heterogeneity of this disease represents a major challenge for treatment (Piccart et al., 2021). Breast cancer is divided into different types depending on its origin, and the prognosis and treatment options for each type are generally based on the tumor-node-metastasis staging, lymphovascular spread, histological grade, HR status, ERBB2 (formerly HER2 or HER2/neu) overexpression, comorbidities, menopausal status, and age (Onitilo et al., 2009). In the present study, TM4SF1 was showed to be downregulated in HR⁺HER2⁻ breast cancer tissue samples, which suggested that it might act as a tumor suppressor for this breast cancer subtype.

However, most studies indicated that the high expression of TM4SF1 is correlated with the T stage, TNM stage, and lymph node metastasis in various cancer types, including prostate (Allioli et al., 2011), ovarian (Gao et al., 2019), glioma (Wang et al., 2015), colorectal (Park et al., 2017), liver (Zhu et al., 2021), thyroid (Lee et al., 2019), lung (Ma et al., 2018), pancreatic (Cao et al., 2016), and breast cancers (Tu et al., 2012; Xing et al., 2017; Fan et al., 2019). However, the low expression of TM4SF1 has been found to be associated with carcinogenesis and development, tumor progression, and invasion of gastric cancer (Peng et al., 2018), which indicates TM4SF1 is a tumor suppressor for gastric cancer and a novel prognostic marker for patients with gastric cancer. Thus, the role of TM4SF1 in cancer progression and invasion may also be tissue-specific.

The previous studies about TM4SF1 in breast cancer progression and development were also controversial cause utilizing different cell lines randomly (Abba et al., 2004; Simpson et al., 2010; Gao et al., 2016). A comparative SAGE analysis of mammary ductal carcinoma *in situ* (DCIS) versus normal breast epithelium revealed that the expression of TM4SF1 is significantly downregulated in DCIS (Abba et al., 2004). In the MCF-7 breast cancer cell line, the overexpression of p23 results in increased invasion, which is associated with TM4SF1 downregulation (Simpson et al., 2010). However, in TNBC cell lines 4T1 and MDA-MB-231 cells, TM4SF1 promotes cancer stem cell traits mechanistically by coupling DDR1 to PKC α and augmenting JAK-STAT signaling. In the present study, MCF-7 and ZR-75-1 cells (which are ER⁺PR⁺HER2⁻ cell lines) were used to investigate the role of TM4SF1 in HR⁺HER2⁻ breast cancer. The results demonstrated that the overexpression of TM4SF1 in

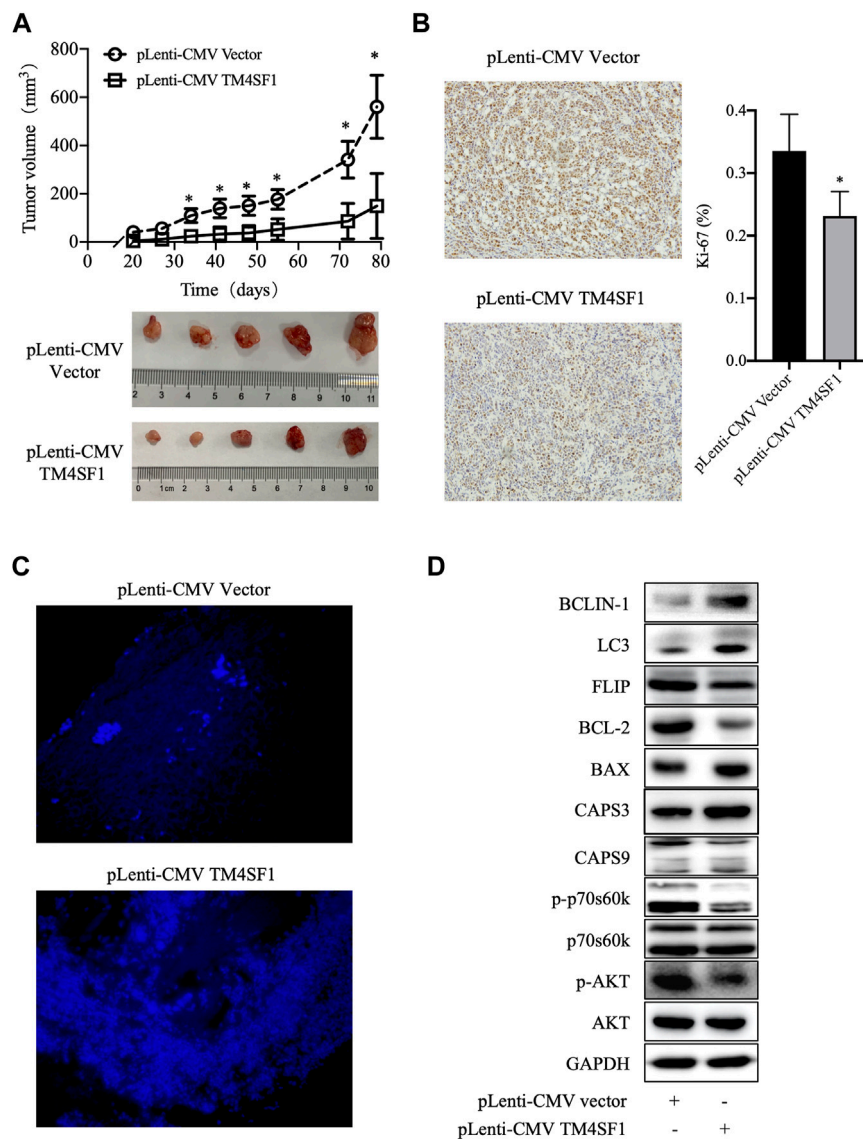


FIGURE 6 | TM4SF1 overexpression inhibits the growth of MCF-7 xenografts. **(A)** Tumor growth curve of MCF-7 cells transfected with pLenti-CMV TM4SF1 or pLenti-CMV vectors (upper panel). Tumor images (lower panel). **(B)** Representative Ki-67 immunohistochemical staining image (left). Frequency of Ki-67⁺ cells (right, mean \pm SD). * $p < 0.05$ compared with the pLenti-vector transfected group by *t*-test analysis. **(C)** TM4SF1 overexpression induces apoptosis in MCF-7 xenografts. Representative TUNEL staining images of apoptotic cancer cells are shown. **(D)** Effect of the TM4SF1 overexpression on the mTOR pathway, apoptosis, and autophagy in MCF-7 cells. GAPDH was used as a loading control. Data shown are representative of at least two independent experiments. TM4SF1, transmembrane 4 L six family 1.

these cell lines resulted in a decrease in their viability, 3D organoid formation, and colony formation. Conversely, TM4SF1 siRNA transfection increased the MCF-7 cell proliferation. By contrast, in the MDA-MB-231 TNBC cell line where TM4SF1 is overexpressed, TM4SF1 siRNA decreased the MDA-MB-231 cell proliferation. *In vitro*, TM4SF1-overexpressing MCF-7 xenografts grew at a slower rate than the control group. In tumor xenograft tissue, the frequency of Ki-67⁺ cells was significantly reduced following the TM4SF1 overexpression, whereas TUNEL staining was increased. Consistent with these findings, cleaved caspase 3/9 and Bax protein levels were

upregulated, while those of BCL-2 and FLIP were downregulated following the TM4SF1 overexpression. These results suggested that the TM4SF1 overexpression could inhibit cell proliferation and induces apoptosis.

Moreover, it was also shown that the phosphorylation of AKT and p70S6K1 levels was reduced following the TM4SF1 overexpression. By contrast, the levels of the autophagy markers Beclin one and LC3 were increased (Figure 6D). Excessive autophagy can result in cell death (Lupinacci et al., 2021). Increased apoptosis was also observed in TM4SF1-overexpressing cells. These findings indicate that TM4SF1 may

be involved in HR⁺HER2⁻ breast cancer development *via* the mTOR pathway.

In conclusion, TM4SF1 mRNA and protein levels were downregulated in HR⁺HER2⁻ breast cancer compared with noncancerous tissue samples. The overexpression of TM4SF1 inhibited breast cancer growth *in vivo*, as well as breast cancer cell viability and proliferation *in vitro*. Thus, TM4SF1 suppresses the HR⁺HER2⁻ breast cancer cell proliferation, but the exact role of this molecule remains unclear and deserves further investigation.

DATA AVAILABILITY STATEMENT

The raw data supporting the conclusion of this article will be made available by the authors, without undue reservation.

ETHICS STATEMENT

The studies involving human participants were reviewed and approved by the Medical Ethics Committee of Taizhou Central hospital (approval, No. F-YXLL-004; Taizhou, China). The patients/participants provided their written informed consent to participate in this study. The animal study was reviewed and approved by the Medical Ethics Committee of Taizhou University College of Medicine (approval, No.TZXYX2020; Taizhou, China).

REFERENCES

- Abba, M. C., Drake, J. A., Hawkins, K. A., Hu, Y., Sun, H., Notcovich, C., et al. (2004). Transcriptomic Changes in Human Breast Cancer Progression as Determined by Serial Analysis of Gene Expression. *Breast Cancer Res.* 6 (5), R499–R513. doi:10.1186/bcr899
- Allioli, N., Vincent, S., Vlaeminck-Guillem, V., Decaussin-Petrucci, M., Ragage, F., Ruffion, A., et al. (2011). TM4SF1, a Novel Primary Androgen Receptor Target Gene Over-expressed in Human Prostate Cancer and Involved in Cell Migration. *Prostate* 71 (11), 1239–1250. doi:10.1002/pros.21340
- Cao, J., Yang, J. C., Ramachandran, V., Arumugam, T., Deng, D. F., Li, Z. S., et al. (2016). TM4SF1 Regulates Pancreatic Cancer Migration and Invasion *In Vitro* and *In Vivo*. *Cell Physiol Biochem* 39 (2), 740–750. doi:10.1159/000445664
- Chen, G., Ding, X. F., Pressley, K., Bouamar, H., Wang, B., Zheng, G., et al. (2020). Everolimus Inhibits the Progression of Ductal Carcinoma *In Situ* to Invasive Breast Cancer *via* Downregulation of MMP9 Expression. *Clin. Cancer Res.* 26 (6), 1486–1496. doi:10.1158/1078-0432.CCR-19-2478
- Cuyún Carter, G., Stephenson, J. J., Gable, J. C., Zincavage, R., Price, G. L., Churchill, C., et al. (2021). Prognostic Factors in Hormone Receptor-Positive/Human Epidermal Growth Factor Receptor 2-Negative (HR+/HER2-) Advanced Breast Cancer: A Systematic Literature Review. *Cancer Manag. Res.* 13, 6537–6566. doi:10.2147/CMAR.S300869
- Fan, C., Liu, N., Zheng, D., Du, J., and Wang, K. (2019). MicroRNA-206 Inhibits Metastasis of Triple-Negative Breast Cancer by Targeting Transmembrane 4 L6 Family Member 1. *Cancer Manag. Res.* 11, 6755–6764. doi:10.2147/CMAR.S199027
- Fu, F., Yang, X., Zheng, M., Zhao, Q., Zhang, K., Li, Z., et al. (2020). Role of Transmembrane 4 L Six Family 1 in the Development and Progression of Cancer. *Front. Mol. Biosci.* 7, 202. doi:10.3389/fmolb.2020.00202
- Gao, C., Yao, H., Liu, H., Feng, Y., and Yang, Z. (2019). TM4SF1 Is a Potential Target for Anti-invasion and Metastasis in Ovarian Cancer. *BMC Cancer* 19 (1), 237. doi:10.1186/s12885-019-5417-7

AUTHOR CONTRIBUTIONS

GC and H-SL conceived and designed the study; GC, X-FD, JC, JZ, and S-JX developed the methodology; GC, X-FD, JC, JZ, and S-JX helped with the acquisition of data (provided animals, acquired, and managed patients, provided facilities, etc.); JZ, X-FD, YL, GC, and H-SL contributed to the analysis and interpretation of data (e.g., statistical analysis, biostatistics, and computational analysis).

FUNDING

This study was, in part, funded by the Public Technology Research Projects of the Science Technology Department of Zhejiang Province (Nos. LY20H310003, LGF19H050004 and LGD20H310001), the National Natural Science Foundation of China (No. 81802657 and 81201530), the Scientific Research Foundation of the Education Department of Zhejiang Province (Y2019A1713), the Medical Health Science and Technology Project of Zhejiang Provincial Health Commission (2020385091), and the Technology Research Projects of the Science Technology Department of Taizhou (Nos. 20ywb97, 1901ky77, 1901ky54, and 1902ky45), the Medical and Health Technology of Zhejiang Province (No. 2020RC147), and the Medical Health Science and Technology Project of Jiangxi Provincial Health Commission (202130717).

- Gao, H., Chakraborty, G., Zhang, Z., Akalay, I., Gadiya, M., Gao, Y., et al. (2016). Multi-organ Site Metastatic Reactivation Mediated by Non-canonical Discoidin Domain Receptor 1 Signaling. *Cell* 166 (1), 47–62. doi:10.1016/j.cell.2016.06.009
- Harbeck, N., and Gnant, M. (2017). Breast Cancer. *Lancet* 389 (10074), 1134–1150. doi:10.1016/S0140-6736(16)31891-8
- Jensen, C., and Teng, Y. (2020). Is it Time to Start Transitioning from 2D to 3D Cell Culture. *Front. Mol. Biosci.* 7, 33. doi:10.3389/fmolb.2020.00033
- Lee, S., Bae, J. S., Jung, C. K., and Chung, W. Y. (2019). Extensive Lymphatic Spread of Papillary Thyroid Microcarcinoma Is Associated with an Increase in Expression of Genes Involved in Epithelial-Mesenchymal Transition and Cancer Stem Cell-like Properties. *Cancer Med.* 8 (15), 6528–6537. doi:10.1002/cam4.2544
- Lupinacci, S., Perri, A., Totada, G., Vizza, D., Lofaro, D., Pontrelli, P., et al. (2021). Rapamycin Promotes Autophagy Cell Death of Kaposi's Sarcoma Cells through P75NTR Activation. *Exp. Dermatol.* doi:10.1111/exd.14438
- Ma, Y. S., Yu, F., Zhong, X. M., Lu, G. X., Cong, X. L., Xue, S. B., et al. (2018). miR-30 Family Reduction Maintains Self-Renewal and Promotes Tumorigenesis in NSCLC-Initiating Cells by Targeting Oncogene TM4SF1. *Mol. Ther.* 26 (12), 2751–2765. doi:10.1016/j.ymthe.2018.09.006
- Matsuda, S., Kimoto, M., Higashi, C., Imai, N., Noro, A., Yamashita, M., et al. (2021). Clinical Significance of Endoscopic Response Evaluation to Predict the Distribution of Residual Tumor after Neoadjuvant Chemotherapy for Esophageal Squamous Cell Carcinoma. *Ann. Surg. Oncol.* 23. doi:10.1245/s10434-021-11009-7
- Nath, A., Mitra, S., Mistry, T., Pal, R., and Nasare, V. D. (2021). Molecular Targets and Therapeutics in Chemoresistance of Triple-Negative Breast Cancer. *Med. Oncol.* 39 (1), 14. doi:10.1007/s12032-021-01610-x
- Ocaña, A., Amir, E., and Pandiella, A. (2020). HER2 Heterogeneity and Resistance to Anti-HER2 Antibody-Drug Conjugates. *Breast Cancer Res.* 22 (1), 15.
- Onitilo, A. A., Engel, J. M., Greenlee, R. T., and Mukesh, B. N. (2009). Breast Cancer Subtypes Based on ER/PR and Her2 Expression: Comparison of Clinicopathologic Features and Survival. *Clin. Med. Res.* 7 (1-2), 4–13. doi:10.3121/cmr.2009.825

- Parada, H., Sun, X., Tse, C. K., Olshan, A. F., and Troester, M. A. (2019). Lifestyle Patterns and Survival Following Breast Cancer in the Carolina Breast Cancer Study. *Epidemiology* 30 (1), 83–92. doi:10.1097/EDE.0000000000000933
- Park, Y. R., Kim, S. L., Lee, M. R., Seo, S. Y., Lee, J. H., Kim, S. H., et al. (2017). MicroRNA-30a-5p (miR-30a) Regulates Cell Motility and EMT by Directly Targeting Oncogenic TM4SF1 in Colorectal Cancer. *J. Cancer Res. Clin. Oncol.* 143 (10), 1915–1927. doi:10.1007/s00432-017-2440-4
- Peng, X. C., Zeng, Z., Huang, Y. N., Deng, Y. C., and Fu, G. H. (2018). Clinical Significance of TM4SF1 as a Tumor Suppressor Gene in Gastric Cancer. *Cancer Med.* 7 (6), 2592–2600. doi:10.1002/cam4.1494
- Piccart, M., van 't Veer, L. J., Poncet, C., Lopes Cardozo, J. M. N., Delaloge, S., Pierga, J. Y., et al. (2021). 70-gene Signature as an Aid for Treatment Decisions in Early Breast Cancer: Updated Results of the Phase 3 Randomised MINDACT Trial with an Exploratory Analysis by Age. *Lancet Oncol.* 22 (4), 476–488. doi:10.1016/S1470-2045(21)00007-3
- Simpson, N. E., Lambert, W. M., Watkins, R., Giashuddin, S., Huang, S. J., Oxelmark, E., et al. (2010). High Levels of Hsp90 Cochaperone P23 Promote Tumor Progression and Poor Prognosis in Breast Cancer by Increasing Lymph Node Metastases and Drug Resistance. *Cancer Res.* 70 (21), 8446–8456. doi:10.1158/0008-5472.CAN-10-1590
- Spring, L. M., Gupta, A., Reynolds, K. L., Gadd, M. A., Ellisen, L. W., Isakoff, S. J., et al. (2016). Neoadjuvant Endocrine Therapy for Estrogen Receptor-Positive Breast Cancer: A Systematic Review and Meta-Analysis. *JAMA Oncol.* 2 (11), 1477–1486. doi:10.1001/jamaoncol.2016.1897
- Teutschbein, J., Haydn, J. M., Samans, B., Krause, M., Eilers, M., Scharl, M., et al. (2010). Gene Expression Analysis after Receptor Tyrosine Kinase Activation Reveals New Potential Melanoma Proteins. *BMC Cancer* 10, 386. doi:10.1186/1471-2407-10-386
- Tu, S. H., Huang, H. I., Lin, S. I., Liu, H. Y., Sher, Y. P., Chiang, S. K., et al. (2012). A Novel HLA-A2-Restricted CTL Epitope of Tumor-Associated Antigen L6 Can Inhibit Tumor Growth *In Vivo*. *J. Immunother.* 35 (3), 235–244. doi:10.1097/CJI.0b013e318248f2ae
- Wang, P., Bao, W., Zhang, G., Cui, H., and Shi, G. (2015). Transmembrane-4-L-six-family-1, a Potential Predictor for Poor Prognosis, Overexpressed in Human Glioma. *Neuroreport* 26 (8), 455–461. doi:10.1097/WNR.0000000000000370
- Xiao, T., Li, W., Wang, X., Xu, H., Yang, J., Wu, Q., et al. (2018). Estrogen-regulated Feedback Loop Limits the Efficacy of Estrogen Receptor-Targeted Breast Cancer Therapy. *Proc. Natl. Acad. Sci. U S A.* 115 (31), 7869–7878. doi:10.1073/pnas.1722617115
- Xing, P., Dong, H., Liu, Q., Zhao, T., Yao, F., Xu, Y., et al. (2017). Upregulation of Transmembrane 4 L6 Family Member 1 Predicts Poor Prognosis in Invasive Breast Cancer: A STROBE-Compliant Article. *Medicine (Baltimore)* 96 (52), e9476. doi:10.1097/MD.00000000000009476
- Zhu, C., Luo, X., Wu, J., Liu, Y., Liu, L., Ma, S., et al. (2021). TM4SF1, a Binding Protein of DVL2 in Hepatocellular Carcinoma, Positively Regulates Beta-Catenin/TCF Signalling. *J. Cel Mol Med* 25 (5), 2356–2364. doi:10.1111/jcmm.14787

Conflict of Interest: The authors declare that the research was conducted in the absence of any commercial or financial relationships that could be construed as a potential conflict of interest.

Publisher's Note: All claims expressed in this article are solely those of the authors and do not necessarily represent those of their affiliated organizations, or those of the publisher, the editors, and the reviewers. Any product that may be evaluated in this article, or claim that may be made by its manufacturer, is not guaranteed or endorsed by the publisher.

Copyright © 2022 Chen, Zhu, Xu, Zhou, Ding, Liang, Chen and Lu. This is an open-access article distributed under the terms of the Creative Commons Attribution License (CC BY). The use, distribution or reproduction in other forums is permitted, provided the original author(s) and the copyright owner(s) are credited and that the original publication in this journal is cited, in accordance with accepted academic practice. No use, distribution or reproduction is permitted which does not comply with these terms.

Advantages of publishing in Frontiers



OPEN ACCESS

Articles are free to read
for greatest visibility
and readership



FAST PUBLICATION

Around 90 days
from submission
to decision



HIGH QUALITY PEER-REVIEW

Rigorous, collaborative,
and constructive
peer-review



TRANSPARENT PEER-REVIEW

Editors and reviewers
acknowledged by name
on published articles

Frontiers

Avenue du Tribunal-Fédéral 34
1005 Lausanne | Switzerland

Visit us: www.frontiersin.org

Contact us: frontiersin.org/about/contact



REPRODUCIBILITY OF RESEARCH

Support open data
and methods to enhance
research reproducibility



DIGITAL PUBLISHING

Articles designed
for optimal readership
across devices



FOLLOW US

@frontiersin



IMPACT METRICS

Advanced article metrics
track visibility across
digital media



EXTENSIVE PROMOTION

Marketing
and promotion
of impactful research



LOOP RESEARCH NETWORK

Our network
increases your
article's readership